

Humboldt Bay Independent Spent Fuel Storage Installation



Pacific Gas and Electric Company
Final Safety Analysis Report Update

NRC Docket No. 72-27

HUMBOLDT BAY ISFSI FSAR UPDATE

LIST OF CURRENT PAGES

Page No.	Revision	Page No.	Revision	Page No.	Revision
<u>CONTENTS</u>		Table 2.5-2	0	Figure 2.3-5	0
i thru iii	5	Table 2.5-3, 2 Sheets	0	Figure 2.3-6	0
		Table 2.6-1	0	Figure 2.3-7	0
		Table 2.6-2	0	Figure 2.3-8, 3 Sheets	0
<u>GLOSSARY</u>		Table 2.6-3, 2 Sheets	0	Figure 2.3-9	0
1 thru 7	4	Table 2.6-4, 14 Sheets	0	Figure 2.4-1	0
		Table 2.6-5, 3 Sheets	0	Figure 2.4-2	0
		Table 2.6-6, 4 Sheets	0	Figure 2.5-1	0
<u>CHAPTER 1</u>		Table 2.6-7	0	Figure 2.5-2	0
i	1	Table 2.6-8	0	Figure 2.5-3	0
1.1-1 thru 1.1-3	1	Table 2.6-9	0	Figure 2.5-4	0
1.2-1	0	Table 2.6-10	0	Figure 2.5-5	0
1.3-1 thru 1.3-2	1	Table 2.6-11	0	Figure 2.5-6	0
1.4-1	0	Table 2.6-12	0	Figure 2.5-7	0
1.5-1	0	Table 2.6-13	0	Figure 2.5-8	0
		Table 2.6-14	0	Figure 2.5-9	0
		Table 2.6-15	0	Figure 2.5-10	0
<u>CHAPTER 2</u>		Table 2.6-16	0	Figure 2.5-11	0
i thru xviii	3	Table 2.6-17	0	Figure 2.5-12	0
2.1-1 thru 2.1-8	0	Table 2.6-18	0	Figure 2.5-13	0
2.2-1 thru 2.2-28	5	Table 2.6-19	0	Figure 2.5-14	0
2.3-1 thru 2.3-6	0	Table 2.6-20	0	Figure 2.6-1	0
2.4-1 thru 2.4-5	0	Table 2.6-21	0	Figure 2.6-2	0
2.5-1 thru 2.5-16	0	Table 2.6-22	0	Figure 2.6-3	0
2.6-1 thru 2.6-150	1	Table 2.6-23, 2 Sheets	0	Figure 2.6-4	0
Table 2.1-1	0	Table 2.6-24	0	Figure 2.6-5	0
Table 2.1-2	0	Table 2.6-25	0	Figure 2.6-6	0
Table 2.1-3	0	Table 2.6-26	0	Figure 2.6-7	0
Table 2.1-4	0	Table 2.6-27	0	Figure 2.6-8	0
Table 2.1-5	0	Table 2.6-28	0	Figure 2.6-9	0
Table 2.2-1, 6 Sheets	4	Figure 2.1-1	0	Figure 2.6-10	0
Table 2.3-1	0	Figure 2.1-2	0	Figure 2.6-11	0
Table 2.3-2	0	Figure 2.1-3	0	Figure 2.6-12	0
Table 2.3-3	0	Figure 2.1-4	0	Figure 2.6-13	0
Table 2.3-4	0	Figure 2.1-5	0	Figure 2.6-14	0
Table 2.3-5	0	Figure 2.1-6	0	Figure 2.6-15	0
Table 2.3-6, 7 Sheets	0	Figure 2.1-7	0	Figure 2.6-16	0
Table 2.3-7	0	Figure 2.1-8	0	Figure 2.6-17	0
Table 2.3-8	0	Figure 2.1-9	0	Figure 2.6-18	0
Table 2.3-9	0	Figure 2.1-10	0	Figure 2.6-19	0
Table 2.4-1	0	Figure 2.1-11	0	Figure 2.6-20	0
Table 2.4-2	0	Figure 2.2-1	0	Figure 2.6-21	0
Table 2.4-3	0	Figure 2.2-2	0	Figure 2.6-22	0
Table 2.4-4	0	Figure 2.3-1	0	Figure 2.6-23	0
Table 2.4-5	0	Figure 2.3-2	0	Figure 2.6-24	0
Table 2.5-1, 5 Sheets	0	Figure 2.3-3	0	Figure 2.6-25	0
		Figure 2.3-4	0	Figure 2.6-26	0

HUMBOLDT BAY ISFSI FSAR UPDATE

LIST OF CURRENT PAGES

<u>Page No.</u>	<u>Revision</u>	<u>Page No.</u>	<u>Revision</u>	<u>Page No.</u>	<u>Revision</u>
Figure 2.6-27	0	Figure 2.6-74	0	<u>CHAPTER 3</u>	
Figure 2.6-28	0	Figure 2.6-75	0		
Figure 2.6-29	0	Figure 2.6-76	0	i thru iii	5
Figure 2.6-30	0	Figure 2.6-77	0	3.1-1 thru 3.1-4	5
Figure 2.6-31	0	Figure 2.6-78	0	3.2-1 thru 3.2-11	2
Figure 2.6-32	0	Figure 2.6-79	0	3.3-1 thru 3.3-16	4
Figure 2.6-33	0	Figure 2.6-80	0	3.4-1	0
Figure 2.6-34	0	Figure 2.6-81	0	Table 3.1-1, 2 Sheets	1
Figure 2.6-35	0	Figure 2.6-82	0	Table 3.1-2	1
Figure 2.6-36	0	Figure 2.6-83	0	Table 3.1-3, 3 Sheets	5
Figure 2.6-37	0	Figure 2.6-84	0	Table 3.2-1	0
Figure 2.6-38	0	Figure 2.6-85	0	Table 3.2-2	0
Figure 2.6-39	0	Figure 2.6-86	0	Table 3.2-3	0
Figure 2.6-40	0	Figure 2.6-87	0	Table 3.4-1, 2 Sheets	0
Figure 2.6-41	0	Figure 2.6-88	0	Table 3.4-2, 4 Sheets	4
Figure 2.6-42	0	Figure 2.6-89	0	Table 3.4-3	1
Figure 2.6-43	0	Figure 2.6-90	0	Table 3.4-4	2
Figure 2.6-44	0	Figure 2.6-91	0	Table 3.4-5, 11 Sheets	0
Figure 2.6-45	0	Figure 2.6-92	0	Figure 3.2-1, 5 Sheets	1
Figure 2.6-46	0	Figure 2.6-93	0	Figure 3.3-1, 4 Sheets	1
Figure 2.6-47	0	Figure 2.6-94	0	Figure 3.3-2, 3 Sheets	1
Figure 2.6-48	0	Figure 2.6-95	0	Figure 3.3-3, 7 Sheets	1
Figure 2.6-49	0	Figure 2.6-96	0	Figure 3.3-4	1
Figure 2.6-50	0	Figure 2.6-97	0	Figure 3.3-5	1
Figure 2.6-51	0	Figure 2.6-98	0		
Figure 2.6-52	0	Figure 2.6-99	0	<u>CHAPTER 4</u>	
Figure 2.6-53	0	Figure 2.6-100	0		
Figure 2.6-54	0	Figure 2.6-101	0	i thru iv	3
Figure 2.6-55	0	Figure 2.6-102	0	4.1-1	4
Figure 2.6-56	0	Figure 2.6-103	0	4.2-1 thru 4.2-34	4
Figure 2.6-57	0	Figure 2.6-104	0	4.3-1 thru 4.3-6	1
Figure 2.6-58	0	Figure 2.6-105	0	4.4-1 thru 4.4-10	3
Figure 2.6-59	0	Figure 2.6-106	0	4.5-1 thru 4.5-4	1
Figure 2.6-60	0	Figure 2.6-107	0	4.6-1 thru 4.6-8	0
Figure 2.6-61	0	Figure 2.6-108	0	4.7-1 thru 4.7-3	1
Figure 2.6-62	0	Figure 2.6-109	0	Table 4.2-1	0
Figure 2.6-63	0	Figure 2.6-110	0	Table 4.2-2	0
Figure 2.6-64	0	Figure 2.6-111	0	Table 4.2-3	0
Figure 2.6-65	0	Figure 2.6-112	0	Table 4.2-4	0
Figure 2.6-66	0	Figure 2.6-113	0	Table 4.2-5	0
Figure 2.6-67	0	Figure 2.6-114	0	Table 4.2-6	0
Figure 2.6-68	0	Figure 2.6-115	0	Table 4.2-7	0
Figure 2.6-69	0	Figure 2.6-116	0	Table 4.2-8	2
Figure 2.6-70	0	Figure 2.6-117	0	Table 4.2-9	0
Figure 2.6-71	0	Figure 2.6-118	0	Table 4.2-10	0
Figure 2.6-72	0	Figure 2.6-119	0	Table 4.2-11, 7 Sheets	0
Figure 2.6-73	0	Figure 2.6-120	0	Table 4.2-12, 4 Sheets	0

HUMBOLDT BAY ISFSI FSAR UPDATE

LIST OF CURRENT PAGES

Page No.	Revision	Page No.	Revision	Page No.	Revision
Table 4.3-1	0	Table 7.3-1	0	<u>CHAPTER 10</u>	
Table 4.5-1	6	Table 7.5-1	0		
Table 4.6-1, 4 Sheets	1	Table 7.5-2	2	i thru iii	3
Figure 4.1-1	0	Table 7.5-3	2	10.1-1	0
Figure 4.2-1	0	Figure 7.3-1	0	10.2-1 thru 10.2-12	6
Figure 4.2-2	0	Figure 7.3-2	0	Table 10.1-1	0
Figure 4.2-3, 2 Sheets	0	Figure 7.3-3	0	Table 10.2-1	3
Figure 4.2-4	0	Figure 7.3-4	0	Table 10.2-2	0
Figure 4.2-5	0			Figure 10.2-1	0
Figure 4.2-6	0	<u>CHAPTER 8</u>		Figure 10.2-2	0
Figure 4.2-7	0			Figure 10.2-3	0
Figure 4.3-1	0	i thru iii	3		
Figure 4.3-2	0	8.1-1 thru 8.1-8	0	<u>CHAPTER 11</u>	
Figure 4.3-3	0	8.2-1 thru 8.2-49	4		
		8.3-1	0	i	5
<u>CHAPTER 5</u>		Table 8.2-1	1	11.1-1	5
		Table 8.2-2	0	11.1-2	5
i thru iii	5	Table 8.2-3	0		
5.1-1 thru 5.1-11	5	Table 8.2-4	0		
5.2-1	0	Table 8.2-5	0		
5.3-1	0	Table 8.2-6	0		
5.4-1	0	Table 8.2-7	0		
Table 5.1-1	0	Table 8.2-8	0		
		Table 8.2-11	0		
<u>CHAPTER 6</u>		Table 8.2-12	0		
		Table 8.2-13	0		
i	2	Table 8.2-14	0		
6.1-1	0	Table 8.3-1	0		
6.2-1	3	Figure 8.2-1	0		
6.3-1	3	Figure 8.2-2	0		
		Figure 8.2-3	0		
<u>CHAPTER 7</u>		Figure 8.2-4	0		
		Figure 8.2-5	0		
i thru iii	5				
7.1-1 thru 7.1-5	6	<u>CHAPTER 9</u>			
7.2-1 thru 7.2-6	5				
7.3-1 thru 7.3-4	7	i	5		
7.4-1 thru 7.4-2	2	9.1-1 thru 9.1-4	6		
7.5-1 thru 7.5-3	1	9.2-1 thru 9.2-4	6		
7.6-1 thru 7.6-5	6	9.3-1 thru 9.3-4	6		
7.7-1	4	9.4-1 thru 9.4-3	6		
Table 7.2-1	3	9.5-1	2		
Table 7.2-2	0	9.6-1 thru 9.6-2	2		
Table 7.2-3	0				
Table 7.2-4	0				
Table 7.2-5	0				
Table 7.2-6	0				

HUMBOLDT BAY ISFSI FSAR UPDATE

CONTENTS

GLOSSARY

Chapter 1 - INTRODUCTION AND GENERAL DESCRIPTION

- 1.1 Introduction
- 1.2 General Description of Location
- 1.3 General Storage System Description
- 1.4 Identification of Agents and Contractors
- 1.5 Material Incorporated by Reference

Chapter 2 - SITE CHARACTERISTICS

- 2.1 Geography and Demography of Site Selected
- 2.2 Nearby Industrial, Transportation, and Military Facilities
- 2.3 Climatology and Meteorology
- 2.4 Surface Hydrology
- 2.5 Subsurface Hydrology
- 2.6 Geology and Seismology

Tables for Chapter 2
Figures for Chapter 2

Chapter 3 - PRINCIPAL DESIGN CRITERIA

- 3.1 Purposes of Installation
- 3.2 Design Criteria for Environmental Conditions and Natural Phenomena
- 3.3 Design Criteria for Safety Protection Systems
- 3.4 Summary of Design Criteria

Tables for Chapter 3
Figures for Chapter 3

HUMBOLDT BAY ISFSI FSAR UPDATE

CONTENTS

Chapter 4 - ISFSI DESIGN

- 4.1 Location and Layout
- 4.2 Storage System
- 4.3 Transport System
- 4.4 Operating Systems
- 4.5 Classification of Structures, Systems, and Components
- 4.6 Materials Evaluation
- 4.7 Decommissioning Plan

Tables for Chapter 4

Figures for Chapter 4

Chapter 5 - ISFSI OPERATIONS

- 5.1 Operation Description
- 5.2 Control Room and Control Areas
- 5.3 Spent Fuel Accountability Program
- 5.4 Spent Fuel Transport

Tables for Chapter 5

Chapter 6 - WASTE MANAGEMENT

- 6.1 MPC Confinement Boundary Design
- 6.2 Radioactive Wastes
- 6.3 References

Chapter 7 - RADIATION PROTECTION

- 7.1 Ensuring that Occupational Radiation Exposures are As Low As Is Reasonably Achievable
- 7.2 Radiation Sources
- 7.3 Radiation Protection Design Features
- 7.4 Estimated Onsite Collective Dose Assessments
- 7.5 Offsite Collective Dose
- 7.6 Health Physics Program
- 7.7 Environmental Monitoring Program

Tables for Chapter 7

Figures for Chapter 7

HUMBOLDT BAY ISFSI FSAR UPDATE

CONTENTS

Chapter 8 - ACCIDENT ANALYSES

- 8.1 Off-Normal Operations
- 8.2 Accidents
- 8.3 Site Characteristics Affecting Safety Analysis

Tables for Chapter 8
Figures for Chapter 8

Chapter 9 - CONDUCT OF OPERATIONS

- 9.1 Organizational Structure
- 9.2 ISFSI Test Program
- 9.3 Training Program
- 9.4 Normal Operations
- 9.5 Emergency Planning
- 9.6 Physical Security Program

Chapter 10 - OPERATING CONTROLS AND LIMITS

- 10.1 Proposed Operating Controls and Limits
- 10.2 Development of Operating Controls and Limits

Tables for Chapter 10
Figures for Chapter 10

Chapter 11 - QUALITY ASSURANCE

- 11.1 Quality Assurance
- 11.2 References

GLOSSARY

A glossary of most of the terms and acronyms used in this final safety analysis report report, including their frequently used variations, is presented in this section as an aid to readers and reviewers.

Accident Events means events that are considered to occur infrequently, if ever, during the lifetime of the facility. Natural phenomena, such as earthquakes, tornadoes, floods, and tsunamis, are considered to be accident events.

ALARA means as low as is reasonably achievable.

ADE means annual dose equivalent.

APCD means Air Pollution Control District.

AREOR means Annual Radiological Environmental Operating Report.

Best Management Practices (BMPs) means schedules of activities, prohibitions of practices, maintenance procedures, and other management practices to prevent or reduce the pollution of “waters of the United States.” BMPs also include treatment requirements, operating procedures, and practices to control plant site runoff, spillage or leaks, sludge or waste disposal, or drainage from raw material storage.

Boral® is the trademark name to denote an aluminum-boron carbide cermet manufactured in accordance with U.S. Patent No. 4027377. Another individual material supplier may use another trade name to refer to the same product.

CAL OSHA means California Occupational Safety and Health Administration.

Cask Transporter (or Transporter) is a U-shaped tracked vehicle used for lifting, handling, and onsite transport of loaded casks.

CCC means California Coastal Commission.

CDFG means California Department of Fish and Game.

CDP means coastal development permit.

CEDE means committed effective dose equivalent.

CEQA means California Environmental Quality Act.

CFR means Code of Federal Regulations.

CoC means a certificate of compliance issued by the NRC that approves the design of a spent fuel storage cask design in accordance with Subpart L of 10 CFR 72.

GLOSSARY

Confinement Boundary means the outline formed by the sealed, cylindrical enclosure of the multi-purpose canister (MPC) shell welded to a solid baseplate, a lid welded around the top circumference of the shell wall, the port cover plates welded to the lid, and the closure ring welded to the lid and MPC shell providing the redundant sealing.

Confinement System means the MPC that encloses and confines the spent nuclear fuel during storage.

Controlled Area (for RP purposes) means the area, outside the restricted area but inside the site boundary, for which access can be limited by PG&E to meet the requirements of 10 CFR 20.1301, 72.104, and the physical security plan.

Cooling Time for a spent fuel assembly is the time between its discharge from the reactor (reactor shutdown) and the time the spent fuel assembly is loaded into the MPC.

CWHR means the California Wildlife Habitat Relationships Program.

CZLUD means coastal zone land use ordinance.

dB(A) means decibels (on the A-weighted scale).

DBE means design basis earthquake.

DCSS means dry cask storage system.

Damaged Fuel Assembly is a fuel assembly with known or suspected cladding defects, as determined by review of records, greater than pinhole leaks or hairline cracks; empty fuel rod locations that are not replaced with dummy fuel rods; or those that cannot be handled by normal means. Fuel assemblies that cannot be handled by normal means due to fuel cladding damage are considered fuel debris.

Damaged Fuel Container (or Damaged Fuel Canister or DFC) means a specially designed enclosure for damaged fuel or fuel debris that permits gaseous and liquid media to escape from the container to the MPC while minimizing dispersal of gross particulates. The damaged fuel container/canister (DFC) features a lifting location that is suitable for remote handling of a loaded or unloaded DFC.

Davit Crane is a specially designed 95-ton rated crane that will be installed in the refueling building for cask handling operations. The davit crane is a floor-mounted, removeable device specifically designed for use at HBPP Unit 3.

HBPP DSAR means the HBPP Defueled Safety Analysis Report for HBPP Unit 3 SAFSTOR 10 CFR Part 50 license.

DE means design earthquake.

HUMBOLDT BAY ISFSI FSAR UPDATE

GLOSSARY

DHS means Department of Health Services.

Humboldt Bay ISFSI (or ISFSI) means the total Humboldt Bay fuel storage system and includes the HI-STAR HB System, transporter, storage vault, and ancillary equipment.

DOE means the US Department of Energy.

EIR means environmental impact report.

ER means environmental report.

Enclosure Vessel (EV) means the pressure vessel defined by the cylindrical shell, baseplate, port cover plates, lid, and closure ring that provides confinement for the helium gas contained within the MPC. The enclosure vessel and the fuel basket together constitute the MPC.

Forced Helium Dehydration (or FHD) is one of the two possible drying systems used to dry the inside of the MPC and can be used to backfill the MPC with the inert gas (helium).

FSAR means final safety analysis report.

Fuel Basket means a honeycombed structural weldment with square openings that can accept a fuel assembly of the type for which it is designed.

Fuel Debris is a subset of damaged fuel, and refers to ruptured fuel rods, severed rods, loose fuel pellets, or fuel assemblies with known or suspected defects that cannot be handled by normal means due to fuel cladding damage.

GET means general employee training.

HI-STAR HB Overpack (or Loaded Overpack or Storage Cask) means the cask that receives and contains the sealed MPCs (containing spent nuclear fuel) for final storage in the storage vault. It provides the gamma and neutron shielding, missile protection, and protection against natural phenomena and accidents for the MPC.

HI-STAR HB System consists of, for the Humboldt Bay ISFSI, the Holtec International MPC, and HI-STAR HB cask.

Holtite is a trademarked Holtec International neutron shield material.

HBPP means Humboldt Bay Power Plant.

GLOSSARY

Important to Safety (ITS) means a function or condition required to store spent nuclear fuel safely; to prevent damage to spent nuclear fuel during handling and storage; and to provide reasonable assurance that spent nuclear fuel can be received, handled, packaged, stored, and retrieved without undue risk to the health and safety of the public. This definition is used to classify structures, systems, and components of the ISFSI as important to safety (ITS) or not important to safety (NITS).

Independent Spent Fuel Storage Installation (ISFSI) means a facility designed, constructed, and licensed for the interim storage of spent nuclear fuel and other radioactive materials associated with spent fuel storage in accordance with 10 CFR 72. For Humboldt Bay, this term is clarified to mean the total storage system and includes the HI-STAR HB System, transporter, storage vault, and ancillary equipment.

Insolation means incident solar radiation.

Intact Fuel Assembly is defined as a fuel assembly without known or suspected cladding defects greater than pinhole leaks and hairline cracks, and which can be handled by normal means. Partial fuel assemblies, that is fuel assemblies from which fuel rods are missing, shall not be classified as intact fuel assemblies unless dummy fuel rods are used to displace an amount of water greater than or equal to that displaced by the original fuel rod(s).

Keystone Species means a species capable of having a major influence on community structure, often in excess of that expected from its relative abundance.

LAR means license amendment request.

LDE means lens dose equivalent.

License Life means the duration that the HI-STAR HB System and the Humboldt Bay ISFSI are authorized by virtue of certification by the US NRC.

Metamic™ is a trademarked neutron absorber material.

Maximum Reactivity means the highest possible k-effective including bias, uncertainties, and calculational statistics evaluated for the worst-case combination of fuel basket manufacturing tolerances.

MLLW means Mean Lower Low Water and is the average of the two daily low tide levels.

Moderate Burnup Fuel is a spent fuel assembly with an average burnup less than or equal to 45,000 MWD/MTU.

MTU means metric tons of uranium.

GLOSSARY

Multi-Purpose Canister (MPC) means the sealed canister that consists of a honeycombed fuel basket contained in a cylindrical canister shell that is welded to a baseplate, lid with welded port cover plates, and closure ring. The MPC is the confinement boundary for storage conditions.

MWD/MTU means megawatt-days per metric ton of uranium.

NEPA means the National Environmental Policy Act of 1969 including any amendments thereto.

Neutron Shielding means a material used to thermalize and capture neutrons emanating from the radioactive spent nuclear fuel.

NFPA means National Fire Protection Association.

NPDES means national pollutant discharge elimination system.

NRC means the US Nuclear Regulatory Commission.

NRHP means National Register of Historic Places.

NWPA means the Nuclear Waste Policy Act of 1982 and any amendments thereto.

Owner- Controlled Area means inside the site boundary, for which access can be limited by PG&E.

PFSF means Private Fuel Storage Facility.

PFSLLC means Private Fuel Storage Limited Liability Corporation.

PMF means probable maximum flood.

Protected Area (or ISFSI Protected Area) means the area within the storage vault.

Reactivity is used synonymously with effective neutron multiplication factor or k-effective.

RFB means Refueling Building.

REMP means radiological environmental monitoring program.

Restricted Area means the area to which access is limited by PG&E for the purpose of protecting individuals against undue risks from exposure to radiation and radioactive materials in accordance with 10 CFR 20. The Restricted Area is determined based on a dose assessment for activities being performed in accordance with radiological

GLOSSARY

protection procedures to ensure compliance with 10 CFR 20 and 72.104. The Restricted Area for normal storage operations is in accordance with 10 CFR 72.180 and 73.51. For maintenance activities that require removal of the vault lid, removal of a cask from the vault, or transport activities to transfer spent fuel and GTCC waste offsite, the Restricted Area will be determined based on a dose assessment for these activities in accordance with radiological protection procedures to ensure compliance with 10 CFR 20 and 72.104 and compensatory measures will be taken in accordance with the ISFSI security plan.

RWQCB means Regional Water Quality Control Board.

SDE means shallow dose equivalent.

Security Area consists of the vault structure and an isolation zone (a minimum 20 ft. distance between the vault and the security area fence).

Security Area Fence circumscribes the Security Area.

SFP means spent fuel pool.

SNF or Spent Fuel means spent nuclear fuel. Per 10 CFR 72.3, spent fuel includes the special nuclear material, byproduct material, source material, and other radioactive materials associated with fuel assemblies.

SSC means structures, systems, and components.

TEDE means total effective dose equivalent.

Thermosiphon is the term used to describe the buoyancy-driven natural convection circulation of helium within the MPC fuel basket.

TLD means thermoluminescent dosimeters.

TODE means total organ dose equivalent.

Transport route means the route to be used by the cask transporter for onsite transfer of the loaded HI-STAR HB cask from the RFB via the oil supply road to the ISFSI storage vault.

USGS means the US Geological Survey.

UTM means Universal Transverse Mercator and is used to define topographic locations in metric coordinates.

GLOSSARY

Vacuum drying system is one of the two possible drying systems used to dry both the inside of the MPC and Overpack water annulus.

χ/Q means site-specific atmospheric dispersion factors used in radiological dose calculations for normal and accidental releases.

ZPA means zero period acceleration.

ZR means any zirconium-based fuel cladding material authorized for use in a commercial nuclear power plant reactor.

HUMBOLDT BAY ISFSI FSAR UPDATE

CHAPTER 1

INTRODUCTION AND GENERAL DESCRIPTION

CONTENTS

<u>Section</u>	<u>Title</u>	<u>Page</u>
1.1	INTRODUCTION	1.1-1
1.2	GENERAL DESCRIPTION OF LOCATION	1.2-1
1.3	GENERAL STORAGE SYSTEM DESCRIPTION	1.3-1
1.4	IDENTIFICATION OF AGENTS AND CONTRACTORS	1.4-1
1.5	MATERIAL INCORPORATED BY REFERENCE	1.5-1

HUMBOLDT BAY ISFSI FSAR UPDATE

CHAPTER 1

INTRODUCTION AND GENERAL DESCRIPTION

Pursuant to 10 CFR 72, the Nuclear Regulatory Commission (NRC) issued Materials License SNM-2514 to Pacific Gas and Electric Company (PG&E) on November 17, 2005, to build and operate the Humboldt Bay Independent Spent Fuel Storage Installation (ISFSI). The license was issued for a period of 20 years in accordance with 10 CFR 72.42. This Final Safety Analysis Report (FSAR) Update is issued by PG&E and will be updated periodically in accordance with the provisions of 10 CFR 72.70.

This chapter explains the need for the Humboldt Bay ISFSI, and provides general descriptions of the co-located Humboldt Bay Power Plant (HBPP) and the ISFSI. Also, agents and contractors are identified, as well as material incorporated by reference. Some of the information pertaining to HBPP and the ISFSI site was taken from the Defueled Safety Analysis Report for HBPP Unit 3 (Reference 1). Information pertaining to the Humboldt Bay ISFSI and its dry cask storage system was taken from the storage system vendor documents cited in Section 1.5.

1.1 INTRODUCTION

HBPP consists of five electric generation units. Unit 3, a boiling water reactor (BWR), operated for approximately 13 years before being shut down in July 1976. The reactor has remained inactive since that time. Units 1 and 2 are co-located conventional 53 megawatt-electric (MWe) units capable of operating on fuel oil or natural gas. Unit 3 is located in a separate building, but is adjacent to Unit 2. There are also two gas turbines, rated at 15 MWe each, located nearby the Unit 1, 2, and 3 structures. The five generating units, as well as the plant site, are owned by PG&E.

HBPP Unit 3 received a construction permit on October 17, 1960. Provisional Operating License DPR-7 was issued in August 1962 and commercial operation began in August 1963. On May 17, 1976, the Nuclear Regulatory Commission (NRC) issued an order that required the satisfactory completion of a specified seismic design upgrade program and resolution of specified geologic and seismic concerns prior to power operation following the 1976 shutdown. In 1983, PG&E concluded that the seismic modifications and other modifications required (in response to the Three Mile Island accident in 1979) were not economical and opted to decommission the plant. In 1988, the NRC approved the SAFSTOR Plan for Unit 3 and revised the operating license to a possess-but-not-operate license that expires on November 9, 2015.

The Humboldt Bay ISFSI is designed to store up to 400 spent fuel assemblies in 5 casks, with a sixth cask to store greater than class C (GTCC) waste. The maximum average fuel burn-up per assembly of any fuel that is stored at the ISFSI is less than 23,000 MWD/MTU. The maximum average initial fuel assembly enrichment is equal to

HUMBOLDT BAY ISFSI FSAR UPDATE

or less than 2.51 percent. A listing of potential GTCC waste for the ISFSI storage at HBPP is provided in Table 3.1-3.

The Nuclear Waste Policy Act (NWPAct) of 1982, as amended, mandated that the Department of Energy (DOE) assume responsibility for the permanent disposal of spent nuclear fuel from the nation's commercial nuclear power plants beginning in January 1998, pending the availability of a permanent DOE repository. Nuclear power plant operators such as PG&E have been given the responsibility under the NWPAct to provide for the interim onsite storage of spent fuel until it is accepted by DOE. DOE has not met its NWPAct mandate to have a repository in operation commencing in January 1998, and no interim spent fuel storage facility has been established. Thus, spent fuel stored at HBPP will need to remain at HBPP until a DOE or other facility is available. An ISFSI will facilitate the dismantling of the existing Unit 3 structures; thereby, providing for earlier termination of the SAFSTOR 10 CFR 50 license. In contrast with the current wet storage method, dry storage of spent fuel is a passive storage process that does not require extensive operating equipment or personnel to maintain. There are essentially no effluents, liquids, or gases from the operation of an ISFSI, as compared to the allowable effluents in SAFSTOR.

The Humboldt Bay ISFSI consists of an ISFSI storage vault, onsite cask transporter, and the dry cask storage system. PG&E has decided to use the Holtec International HI-STAR 100 dry cask system, as modified for the HBPP spent fuel. The physical characteristics of the spent fuel assemblies and GTCC waste to be stored are described in Section 3.1. The HB-specific design is referred to as the HI-STAR HB. The HI-STAR HB is both a storage and transport cask that provides structural protection and radiation shielding for the multi-purpose canister (MPC-HB) (containing the spent fuel). The handling of the HI-STAR HB onsite will be accomplished using a tracked transporter. The HB ISFSI will use the transporter developed for the Diablo Canyon ISFSI. The HI-STAR HB will be licensed under 10 CFR 71 for transport of the spent fuel offsite to a federal repository.

The ISFSI is located on the same property as the existing HBPP facility. The ISFSI storage vault is an interim facility consisting of an in-ground concrete vault structure with storage capacity for six shielded casks, five containing spent nuclear fuel and one containing GTCC waste. The spent fuel will be stored there until the DOE takes possession of the spent fuel and transports it to a long-term repository.

Licensing of the Humboldt Bay ISFSI also involved NRC review of a number of site-specific issues. These included the site-specific environmental review, geotechnical issues related to the site, natural phenomena, and other site-specific matters. Holtec developed a modified HI-STAR overpack and MPC for use at Humboldt Bay due to the HBPP smaller fuel assembly (length and width). The modified HI-STAR HB design and associated analyses were performed in accordance with the analyses methodologies previously licensed by the NRC for the HI-STAR 100 System. This FSAR Update references the Holtec HI-STAR 100 Final Safety Analysis Report

HUMBOLDT BAY ISFSI FSAR UPDATE

(Reference 2) for description of the generic HI-STAR analyses and certain HI-STORM FSAR analyses (Reference 3) that are applicable to the HI-STAR HB and also provides supplemental analyses for these site-specific issues that are applicable to Humboldt Bay ISFSI site and the HI-STAR HB.

As discussed in Section 9.4.2, PG&E requested and was granted an exemption from 10 CFR 72.72(d), which requires that spent fuel and high level radioactive waste records in storage be kept in duplicate. As specified in License Condition 16 of the Humboldt Bay ISFSI License SNM-2514, the exemption allows PG&E to maintain records of spent fuel and high-level radioactive waste in storage either in duplicate, as required by 10 CFR 72.72(d), or, alternatively, a single set of records may be maintained at a records storage facility that satisfies the standards of ANSI N45.2.9-1974. All other requirements of 10 CFR 72.72(d) must be met. Pursuant to 10 CFR 72.140(d), PG&E will use an NRC-approved QA program that satisfies the criteria of 10 CFR 50, Appendix B, to implement the QA requirements for the ISFSI. Refer to Chapter 11. An exemption from the record storage requirements of 10 CFR 72.72(d) allows records of spent fuel storage to be maintained in the same manner as the HBPP QA records.

In accordance with 10 CFR 72.42, the Humboldt Bay ISFSI license was issued for a term of 20 years. If near the end of the initial license term, permanent or interim DOE High Level Waste facilities are unavailable for acceptance of commercial nuclear spent fuel, PG&E expects to submit an application for ISFSI license renewal pursuant to 10 CFR 72.42(b).

The Humboldt Bay ISFSI is designed to protect the stored fuel and prevent release of radioactive material under all normal, off-normal, and accident conditions of storage in accordance with all applicable regulatory requirements contained in 10 CFR 72. This FSAR was prepared in compliance with the requirements of 10 CFR 72 and using the guidance contained in Regulatory Guide 3.62, "Standard Format and Content for the Safety Analysis Report for Onsite Storage of Spent Fuel Storage Casks," (February 1989); and NUREG-1567, "Standard Review Plan for Spent Fuel Dry Storage Facilities," (March 2000).

Additionally, the NRC has issued a license amendment allowing PG&E to permit cask handling activities in the HBPP Unit 3 refueling building (Reference 5).

1.2 GENERAL DESCRIPTION OF LOCATION

The Humboldt Bay Independent Spent Fuel Storage Installation (ISFSI) is located within the Pacific Gas and Electric (PG&E) owner-controlled area at the Humboldt Bay Power Plant (HBPP). The HBPP is located near the coastal community of King Salmon on the shore of Humboldt Bay in Humboldt County, in northwestern California. Eureka, the largest city in Humboldt County, is located approximately 3 miles north of the ISFSI site.

PG&E owns approximately 143 acres on the shore of Humboldt Bay opposite the bay entrance. PG&E also owns the water areas extending approximately 500 ft into Humboldt Bay from the land area.

There are several small residential communities within 5 miles of the ISFSI site, including King Salmon, Humboldt Hill, Fields Landing, and the suburban communities surrounding the City of Eureka.

The terrain in the vicinity of the HBPP rises rapidly from the bay on the north side to an elevation of approximately 65 ft mean lower low water (MLLW) at Buhne Point peninsula. Terrain to the north and east of the site is generally flat. To the south and east, the terrain rises rapidly forming Humboldt Hill, which reaches an elevation of over 500 ft MLLW within 2 miles of the ISFSI and is the site of several small neighborhoods. Humboldt County is mostly mountainous except for the level plain that surrounds Humboldt Bay. The coastal mountains extend to the central valley. The owner-controlled area is not traversed by public highway or railroad. The only access to the ISFSI site is from the south via King Salmon Avenue, which also serves the community of King Salmon situated on the western part of the peninsula. Public trails run along the shoreline and along the fence to the northwest of the owner-controlled area.

PG&E has full authority to control all activities within the ISFSI site, ISFSI-controlled area, and owner-controlled area boundaries.

The major access in the vicinity of the ISFSI and other communities of Humboldt County is via US Highway 101, which generally traverses north-south through Humboldt County. This highway passes about 0.3 mile east of the ISFSI site and is accessible at approximately 0.35 mile to the southeast of the site.

There are several landings in the community of King Salmon, located just west of the entrance gate to the owner-controlled area. The community of King Salmon serves frequent commercial and recreational boat traffic.

The ISFSI is located within the PG&E owner-controlled area at HBPP. Figure 2.1-1 shows the location of the plant and ISFSI. Figure 2.1-2 shows a plan drawing of the ISFSI site. There are no important-to-safety structures, systems, or components that are shared between the ISFSI and HBPP. A more detailed description of the ISFSI site is provided in Section 2.1.

1.3 **GENERAL STORAGE SYSTEM DESCRIPTION**

The Humboldt Bay Independent Spent Fuel Storage Installation (ISFSI) includes the following major structures, systems, and components (SSCs): the storage vault, onsite transporter, and dry cask storage system. The dry cask storage system selected by Pacific Gas and Electric Company (PG&E) is the Holtec International HI-STAR HB System. This is a variation of the HI-STAR 100 System, which has been certified by the Nuclear Regulatory Commission (NRC) for use by general licensees as well as site-specific licensees. The HI-STAR HB System is comprised of the MPC-HB, DFC(s), and the HI-STAR HB storage/transport overpack. The design and operation of these components are generically described in detail in the HI-STAR 100 System FSAR. Holtec developed the modified (shorter) HI-STAR and MPC for use at Humboldt Bay due to the Humboldt Bay Power Plant (HBPP) smaller fuel assembly (length and width). The modified HI-STAR HB design and associated analyses were performed in accordance with the analyses methodologies previously licensed by the NRC for the HI-STAR 100 System. This FSAR references the Holtec HI-STAR 100 Final Safety Analysis Report (Reference 2) for description of the generic HI-STAR analyses and certain HI-STORM FSAR analyses (Reference 3) that are applicable to the HI-STAR HB and also provides supplemental analyses for the site-specific issues that are applicable to Humboldt Bay site and the HI-STAR HB.

A general description of major SSCs is provided herein. More detailed descriptions of the HI-STAR HB System are contained in Section 4.2 of this FSAR and in the Holtec International documents cited in Reference 2. More details on the storage vault and transporter are provided in Sections 4.2 through 4.4 of this FSAR.

Figure 4.2-2 shows a cut-away view of the MPC-HB and the storage overpack. The MPC-HB, shown partially withdrawn from the overpack, provides the confinement boundary for the spent fuel and associated nonfuel hardware. It is an integrally-welded pressure vessel that holds up to 80 HBPP spent fuel assemblies and meets the stress limits of the ASME Boiler and Pressure Vessel Code, Section III, Subsection NB. The MPCs are welded cylindrical structures consisting of a honeycomb fuel basket, a baseplate, canister shell, a lid, and a closure ring. The honeycomb fuel basket uses geometric spacing and fixed neutron absorbers for criticality control. The MPC is made entirely of stainless steel, except for the neutron absorbers and an aluminum seal washer in the vent and drain ports.

The HI-STAR HB storage/transport cask provides an internal, cylindrical cavity of sufficient size to house an MPC during loading, unloading, and movement of the MPC from the spent fuel pool (SFP) to the storage vault. It is a rugged, heavy-walled cylindrical container constructed of carbon steel. The overpack provides gamma and neutron shielding, and protects the MPC from missiles and natural phenomena during both transport and storage. Figure 3.3-3 shows the HI-STAR HB cask.

The loaded overpacks are stored vertically in a multi-cell vault constructed of reinforced concrete. It provides additional shielding and defense-in-depth of the casks from

HUMBOLDT BAY ISFSI FSAR UPDATE

missiles and natural phenomena. The vault is sized to hold five fuel casks and one GTCC certified cask. Figure 4.1-1 shows the ISFSI vault. As shown in Figure 4.1-1, the storage vault is about 600 ft from the refueling building (RFB).

A transporter is used to move the HI-STAR HB cask from outside the RFB to the vault. The transporter is a U-shaped tracked vehicle consisting of the vehicle main frame, hydraulic lifting towers, an overhead beam system that connects between the lifting towers, a cask restraint system, the drive and control systems, and a series of cask lifting attachments. The transporter design permits the HI-STAR HB cask to be handled vertically. Figure 4.3-1 shows the transporter with the HI-STAR cask in the vertical orientation.

The transporter is also used to lower the HI-STAR HB into the storage vault. Each loaded overpack is approximately 8 ft in diameter, 10.5 ft high, and weighs about 160,000 pounds. The Security Area Fence has applicable barrier, access, and surveillance controls as described in TAC No. L23683. The Security Area Fence is approximately 70 ft by 112 ft.

The preparation and loading of the MPCs take place in the RFB. These activities are described in Sections 4.4 and 5.1.

The important-to-safety SSCs of the ISFSI are identified in Section 4.5.

1.4 IDENTIFICATION OF AGENTS AND CONTRACTORS

Engineering, site preparation, and construction of the Independent Spent Fuel Storage Installation (ISFSI) storage vault will be performed by Pacific Gas and Electric Company (PG&E), Holtec, Enercon and additional specialty contractors as necessary.

Holtec International will provide the spent fuel storage system, consisting of the HI-STAR HB overpack, multi-purpose canister-HB, transporter; and design for the ISFSI storage vault.

Enercon will provide design of ancillary facilities including the transport route and security system.

PG&E will be responsible for the operation of the ISFSI.

All of these activities involving important-to-safety structures, systems, and components are subject to Nuclear Regulatory Commission-approved QA programs as discussed in Chapter 11 and in the Holtec references cited in Section 1.5.

HUMBOLDT BAY ISFSI FSAR UPDATE

1.5 MATERIAL INCORPORATED BY REFERENCE

1. Defueled Safety Analysis Report for Humboldt Bay Power Plant Unit 3, Revision 4, August 2002.
2. Final Safety Analysis Report for the HI-STAR 100 System, Holtec International Report No. HI-210610, Revision 1, December 2002.
3. Final Safety Analysis Report for the HI-STORM 100 System, Holtec International Report No. HI-2002444, Revision 1, September 2002.
4. License Amendment Request 04-02, Spent Fuel Cask Handling, PG&E Letter HBL-04-016, July 9, 2004.
5. License Amendment 37 to DPR-7, Spent Fuel Cask Handling, Issued by the NRC, December 15, 2005.

HUMBOLDT BAY ISFSI FSAR UPDATE

CHAPTER 2

SITE CHARACTERISTICS

CONTENTS

Section	Title	Page	
2.1	GEOGRAPHY AND DEMOGRAPHY OF SITE SELECTED	2.1-1	
2.1.1	Site Location	2.1-1	
2.1.2	Site Description	2.1-1	
2.1.3	Population Distribution and Trends	2.1-3	
2.1.4	Use of Nearby Lands and Waters	2.1-5	
2.1.5	References	2.1-8	9-01
2.2	NEARBY INDUSTRIAL, TRANSPORTATION, AND MILITARY FACILITIES	2.2-1	
2.2.1	Offsite Potential Hazards	2.2-1	
2.2.2	Onsite Potential Hazards	2.2-11	
2.2.3	Summary	2.2-27	9-01
2.2.4	References	2.2-27	
2.3	CLIMATOLOGY AND METEOROLOGY	2.3-1	
2.3.1	Regional Climatology	2.3-1	
2.3.2	Local Meteorology	2.3-4	
2.3.3	Onsite Meteorological Measurement Program	2.3-4	
2.3.4	Diffusion Estimates	2.3-5	
2.3.5	References	2.3-6	
2.4	SURFACE HYDROLOGY	2.4-1	
2.4.1	Hydrologic Description	2.4-1	
2.4.2	Floods	2.4-3	
2.4.3	Potential Dam Failures	2.4-4	
2.4.4	Probable Maximum Surge and Seiche Flooding	2.4-4	
2.4.5	Probable Maximum Tsunami Flooding	2.4-4	
2.4.6	Ice Flooding	2.4-5	
2.4.7	Flooding Protection Requirements	2.4-5	
2.4.8	Environmental Acceptance of Effluents	2.4-5	
2.4.9	References	2.4-5	
2.5	SUBSURFACE HYDROLOGY	2.5-1	
2.5.1	Stratigraphy	2.5-1	
2.5.2	Aquifers	2.5-3	
2.5.3	Groundwater Recharge, Gradients, and Discharge	2.5-8	

HUMBOLDT BAY ISFSI FSAR UPDATE

CHAPTER 2

SITE CHARACTERISTICS

CONTENTS (Continued)

Section	Title	Page
2.5.4	Hydraulic Properties of Aquifers	2.5-11
2.5.5	Groundwater Use	2.5-13
2.5.6	Groundwater Quality	2.5-13
2.5.7	Contaminant Transport Analysis	2.5-15
2.5.8	References	2.5-15
2.6	GEOLOGY AND SEISMOLOGY	2.6-1
2.6.1	Introduction	2.6-1
2.6.2	Tectonic Framework	2.6-3
2.6.3	Regional Geology and Seismicity	2.6-16
2.6.4	Site Geology	2.6-43
2.6.5	Seismic Source Characterization	2.6-56
2.6.6	Earthquake Ground Motions	2.6-62
2.6.7	Liquefaction and Landslide Potential	2.6-69
2.6.8	Surface-Faulting Potential	2.6-75
2.6.9	Probable Maximum Tsunami Flooding	2.6-84
2.6.10	References	2.6-125

HUMBOLDT BAY ISFSI FSAR UPDATE

CHAPTER 2

SITE CHARACTERISTICS

TABLES

Table	Title
2.1-1	Population Trends of the State of California and of Humboldt and Trinity Counties
2.1-2	Population Centers Within 50 miles of ISFSI Site
2.1-3	Age and Sex of Total Population: 2000 Humboldt County, California
2.1-4	Percent of Population by Race for the State of California and for Humboldt and Trinity Counties
2.1-5	State and County Parks and Public Lands Within 50 miles of ISFSI Site
2.2-1	Fire/Explosive Hazards
2.3-1	Temperature, Dew Point Temperature, and Relative Humidity
2.3-2	Eureka Maximum Rainfall Statistics and Several Calculated Return Periods
2.3-3	Design Basis Snowfall Parameters
2.3-4	Peak Winds Gusts Recorded at Eureka Between 1887 and 1996
2.3-5	Mean Frequency of Meteorology Phenomena
2.3-6	Joint Frequency Distributions of Wind Speed and Atmospheric Stability Class
2.3-7	Eureka Mixing Heights – Meters
2.3-8	Input data Used in Diffusion Modeling
2.3-9	Results of Diffusion Modeling, (χ/Q) Factors

HUMBOLDT BAY ISFSI FSAR UPDATE

CHAPTER 2

SITE CHARACTERISTICS

TABLES (Continued)

Table	Title
2.4-1	Normal Monthly Precipitation and Temperatures at Eureka WSO (No. 04-2910) Latitude 40°48'N, Longitude 124°10'W Elevation 43 FT (NGVD)
2.4-2	Annual maximum Peak Discharges
2.4-3	Annual Highest Tide Level
2.4-4	Probable Maximum Flood Peaks and Levels Humboldt Bay
2.4-5	Estimates of Wave Runup
2.5-1	Piezometers Used in 1999 Groundwater Measurements in the Humboldt Bay ISFSI Site Area
2.5-2	Selected Water Quality Data for Wells in the Humboldt Bay ISFSI Site Vicinity
2.5-3	Groundwater Wells Within Two Miles of the Humboldt Bay ISFSI
2.6-1	Geologic Time Scale and Subdivisions of the Mesozoic and Cenozoic Eras
2.6-2	Comparison of the Timing of Events on the Main Segment of the Cascadia Subduction Zone with Events on the Eel River Segment
2.6-3	Geologic History of the Humboldt Bay ISFSI Site
2.6-4	Magnitude 5 and Larger Earthquakes within 160 kilometers (100 miles) of the HB-ISFSI Site, 1850 through April 2002
2.6-5	Earthquakes that Produced Ground Motions Greater than 0.10g at Humboldt Bay Power Plant, 1975 through 1994
2.6-6	Descriptions of Soil Profiles
2.6-7	Alternative Segment Lengths and Weights for the Cascadia Interface Using the Carver Model (Carver, 2002c, Page 5A-3)

CHAPTER 2

SITE CHARACTERISTICSTABLES (Continued)

Table	Title
2.6-8	Distance (km) from U. S. Coastline to 4 Updip Reference Boundaries of the Cascadia Subduction Zone
2.6-9	Horizontal Extent (km) of the Cascadia Interface Using the Change in Fold Trends (Figure 2-16) as the Updip Interface Boundary
2.6-10	Downdip Width (km) of the Cascadia Interface
2.6-11	Maximum Rupture Downdip Width (km) of the Cascadia Interface Averaged Along the Rupture Length
2.6-12	Mean Characteristic Magnitudes for the Cascadia Interface Using the Carver Segmentation Model
2.6-13	Mean Characteristic Magnitudes for the Little Salmon Fault System
2.6-14	MCE for Cascadia Interface and Little Salmon Fault
2.6-15	84th Percentile MCE Design Spectra for the Fault Normal Component
2.6-16	84th Percentile MCE Design Spectra for the Fault Parallel Component
2.6-17	84th Percentile MCE Design Spectra for the Vertical Component
2.6-18	Equal Hazard Spectra (g) for the Fault Normal Component for Soil Site Conditions
2.6-19	Equal Hazard Spectra (g) for the Fault Parallel Component for Soil Site Conditions
2.6-20	Equal Hazard Spectra for the Vertical Component
2.6-21	Well-Studied Historical Thrust Earthquakes Associated with Surface Fault Ruptures

HUMBOLDT BAY ISFSI FSAR UPDATE

CHAPTER 2

SITE CHARACTERISTICS

TABLES (Continued)

Table	Title
2.6-22	Observations of Runup Elevations at Humboldt Bay and Other Locations in Northern California from the 27-28 March 1964 Alaska Earthquake (PG&E, 1966)
2.6-23	Evidence of Past Tsunamis at Marsh Sites in Northern California
2.6-24	Cascadia Subduction Zone Events
2.6-25	Open Coast Runup Estimates from Paleoseismic Sites along the Northern California Coast and World Wide Data
2.6-26	Estimated Runup Heights at Lagoon Creek from the Sediment Transport Model
2.6-27	Wiegel's Estimates of Tsunami Runups and Their Probability at Humboldt Bay Power Plant
2.6-28	Estimates of Maximum Runup Elevations at the ISFSI Site

CHAPTER 2

SITE CHARACTERISTICS

FIGURES

Figure	Title
2.1-1	Site Location
2.1-2	Property Plan
2.1-3	Regional Topography
2.1-4	Aerial View of ISFSI Site Vicinity
2.1-5	Sensitive Land Uses
2.1-6	Population Distribution 0 to 10 Miles, 2000 Census
2.1-7	Population Distribution 0 to 10 Miles, 2010 Projected
2.1-8	Population Distribution 0 to 10 Miles, 2025 Projected
2.1-9	Population Distribution 10 to 50 Miles, 2000 Census
2.1-10	Population Distribution 10 to 50 Miles, 2010 Projected
2.1-11	Population Distribution 10 to 50 Miles, 2025 Projected
2.2-1	Potential Hazards Within a 5-Mile Radius
2.2-2A	Site Plan Historical
2.2-2B	Site Plan Current
2.3-1	Wind Directional Distribution 1905 Through 1996
2.3-2	Average Monthly Rainfall 1887-1996
2.3-3	Maximum Monthly Rainfall 1887-1996
2.3-4	Average Monthly Temperatures 1887-1996
2.3-5	Maximum and Minimum Temperatures by Month 1887-1996
2.3-6	Topographical Features to 8 Km

9-01

CHAPTER 2

SITE CHARACTERISTICS

FIGURES (Continued)

Figure	Title
2.3-7	Topographical Features to 16 Km
2.3-8	Topographical Cross Sections
2.3-9	Windrose of Humboldt Bay Meteorology Data 1966-1967
2.4-1	Watersheds of Humboldt Bay
2.4-2	Mean Annual Precipitation at Eureka
2.5-1	Geologic Map of the Humboldt Bay ISFSI Site Vicinity Showing Water Wells Within 2 Miles of the ISFSI Site
2.5-2	Generalized Stratigraphic Column in the Humboldt Bay ISFSI Site Area
2.5-3	Geologic Map Showing Borings and Monitoring Wells in the Humboldt Bay ISFSI Site Area
2.5-4	Generalized Model of Aquifers in the Humboldt Bay ISFSI Site Area
2.5-5	Geologic Cross Section X-X' from Buhne Point to Unit No. 3 Power Plant, Humboldt Bay ISFSI Site Area
2.5-6	Geologic Cross Section Y-Y' Through the Humboldt Bay ISFSI Site
2.5-7	Cross Section A-A' Through Unit 3, Humboldt Bay ISFSI Site Area
2.5-8	Cross Section C-C' of Unit 3, Humboldt Bay ISFSI Site Area
2.5-9	Piezometric Surface on Upper Hookton Aquifer, Humboldt Bay ISFSI Site Area
2.5-10	Relationship Between Tide Levels in Humboldt Bay and Piezometric Levels from Wells MW-1, MW-2, MW-6, MW-7, and MW-9 (Bechtel) Near Unit 3 Humboldt Bay ISFSI Site Area

CHAPTER 2

SITE CHARACTERISTICS

FIGURES (Continued)

Figure	Title
2.5-11	Relationship Between Tide Levels in Humboldt Bay and Piezometric Levels from Well Clusters 16-A, 16-B, 16-C, and 16-D9 (TES) in Wastewater Ponds Area, Humboldt Bay ISFSI Site Area
2.5-12	Perched Water Tables from Upper Parts (A) of the Hookton Silt and Clay Deposits and of the Holocene Bay Deposits, Humboldt Bay ISFSI Site Area
2.5-13	Perched Water Tables from Lower Part (B) of the Hookton Silt and Clay Deposits and of the Holocene Bay Deposits, Humboldt Bay ISFSI Site Area
2.5-14	Generalized Model Showing Aquifer Recharge and Discharge in the Humboldt Bay ISFSI Site Area
2.6-1	Topographic Map of Humboldt Bay Showing Location of the Humboldt Bay ISFSI Site
2.6-2	South Humboldt Bay, View Is Southeast
2.6-3	Color Shaded-Relief Map (Oblique Mercator Projection) of the Cascadia Subduction Zone Along the Northwest Coast of the United States and Canada (from R.A. Haugerud, 1988, USGS Open-File Report 98-140).
2.6-4	General Plate Tectonic Setting of the Western United States
2.6-5	Tectonic Evolution of the West Coast United States During Past 50 Million Years (From National Geographic Society, 1995)
2.6-6	Map of Subplates in the North American Plate and Major Faults in Northwestern California
2.6-7	Tectonics of the Gorda Plate (Modified from Wilson, 1989, Figure 3)
2.6-8	Schematic Maps Showing the Components of the Little Salmon Fault System

CHAPTER 2

SITE CHARACTERISTICS

FIGURES (Continued)

Figure	Title
2.6-9	Major Active Faults and Known or Inferred Earthquake Rupture Areas (Line Pattern) in the Mendocino Triple Junction Region (Stippled Area)
2.6-10	Schematic Cross Section Showing the Suggested Mechanisms for the 1964 Alaska Earthquake (Plafker, 1972), and Postulated Cascadia Subduction Zone Earthquake Sources
2.6-11	Generalized Regional Geologic Map Showing Principal Faults and Folds, Area of Active Mendocino Uplift (Stippled Pattern), and Major Plates (after McLaughlin and Others, 2000)
2.6-12	Generalized Regional Structure Section A-A' Showing Depth Distribution of Epicenters (Open Circles) and Selected Focal Mechanisms (Beach Balls) of Earthquakes from M. Magee (Stanford University and USGS), 1994 (after McLaughlin and Others, 2000)
2.6-13	Geologic Map of the Humboldt Bay Region
2.6-14	Geologic Cross Section of the Humboldt Bay Region
2.6-15	Composite Stratigraphic Column, Onshore Eel River Basin (after Clarke, 1992)
2.6-16	Oblique Aerial Views Looking North Along the Humboldt Hill Anticline and the Little Salmon Fault Zone
2.6-17	Marine Terrace Map of the Humboldt Bay Region
2.6-18	Surface Traces of the Little Salmon Fault Zone South of the ISFSI Site
2.6-19	Cross Section A-A' Across the Little Salmon Fault Zone at Humboldt Hill (after Woodward-Clyde Consultants, 1980, Figure C-15)
2.6-20	Geologic Cross Section A-A' Across a Trace of the Little Salmon Fault Zone at College of the Redwoods, 5 Kilometers South of Humboldt Bay ISFSI Site (after LACO Associates, 1999, Figure 5)

HUMBOLDT BAY ISFSI FSAR UPDATE

CHAPTER 2

SITE CHARACTERISTICS

FIGURES (Continued)

Figure	Title
2.6-21	Geologic Cross Section B-B' Across a Trace of the Little Salmon Fault Zone at College of the Redwoods, 5 Kilometers South of Humboldt Bay ISFSI Site (after LACO Associates, 1999, Figure 6)
2.6-22	Geologic Cross Section C-C' Across a Trace of the Little Salmon Fault Zone at College of the Redwoods, 5 Kilometers South of Humboldt Bay ISFSI Site (after LACO Associates, 1999, Figure 7)
2.6-23	Geologic Cross Section D-D' Across a Trace of the Little Salmon Fault Zone at College of the Redwoods, 5 Kilometers South of Humboldt Bay ISFSI Site (after LACO Associates, 1999, Figure 8)
2.6-24	Magnitude 5 and Larger Earthquakes for the Period 1850 through April 2002 within 160 Kilometers (100 Miles) of the Site
2.6-25	Magnitude 3 and Larger Earthquakes from the Period 1974 through April 2002 within 160 Kilometers (100 miles) of the Site
2.6-26	Seismic Cross Sections of Magnitude 3 and Larger Earthquakes from the Period 1974 through April 2002
2.6-27	Magnitude 2 and Larger Earthquakes from the Period 1974 through April 2002, Within 40 Kilometers (25 Miles) of the Site, and Earthquakes of Magnitude 5 and Larger from 1850 through 1973 Within the Map Boundary
2.6-28	Seismic Cross Section of Magnitude 2 and Larger Earthquakes from the Period 1974 through April 2002
2.6-29	Oblique Aerial View of the Humboldt Bay ISFSI Site
2.6-30	Locations of Borings, Cross Sections, and Seismic Reflection Lines Used in the 1980 Woodward-Clyde Consultants Report
2.6-31	Geologic Map of the ISFSI Site
2.6-32	Locations of Geologic Trenches and Borings Near the ISFSI Site

CHAPTER 2

SITE CHARACTERISTICS

FIGURES (Continued)

Figure	Title
2.6-33	Oblique Aerial View Looking Northwest from Above Humboldt Hill Toward the Entrance of Humboldt Bay
2.6-34	Comparison of the Shoreline Shown on 1858 and 1959 Surveys
2.6-35	View Looking West from Buhne Point Showing the Escarpment Along the North Side of the Buhne Point Terrace and Riprap Along the Shoreline of Humboldt Bay
2.6-36	Geologic Cross Section X-X ⁵
2.6-37	View to East of Buhne Point Terrace Surface and ISFSI Site
2.6-38	Oblique Aerial Photographs Showing Disturbance of Buhne Point Terrace During Trenching Activities by Earth Sciences Associates (circa 1975)
2.6-39	Generalized Stratigraphic Section at the ISFSI Site
2.6-40	Stratigraphic Section of the Uppermost Lower Hookton and Upper Hookton Formation Exposed in Woodward-Clyde Consultants' Trenches 11-T6a, 11-T6b, and 11-T6c (after Woodward-Clyde Consultants, 1980, Figure C-28)
2.6-41	Outcrop of Sand with Interbedded Silt (Light Layers) in Sea Cliff North of ISFSI Site
2.6-42	Composite Log of Trenches WCC-11T6a and GMX-T1
2.6-43	Log of Trench GMX-72
2.6-44	Geologic Cross Section Y-Y
2.6-45	Relict Soil and Upper Hookton Formation Deposits Exposed in Trench GMX-72 (NW Wall at Station 180 ft.)
2.6-46	Structure Contour Map of the Little Salmon Fault North of Humboldt Hill (after Woodward-Clyde Consultants, 1980, Figure C-14)

CHAPTER 2

SITE CHARACTERISTICS

FIGURES (Continued)

Figure	Title
2.6-47	Structure Contour Map of the Bay Entrance Fault
2.6-48	Structure Contour Map of the Buhne Point Fault (Reinterpretation of Data Presented on Woodward-Clyde Consultants, 1980, Figure C-25)
2.6-49	Cross Section A-A' Across the Little Salmon Fault Zone at Humboldt Hill (Modified from Woodward-Clyde Consultants, 1980, Figure C-15)
2.6-50	Cross Section B-B' Across the Bay Entrance and Buhne Point Faults
2.6-51	Structure Contour Map of Top of Unit F
2.6-52	Log of Trench 11-T6b Showing Small Faults of the Buhne Point Fault in the Lower Hookton Formation (from Woodward-Clyde Consultants, 1980, Figure C-35)
2.6-53	Log of Trench 11-T6c Showing Small Faults of the Buhne Point Fault in the Lower Hookton Formation (from Woodward-Clyde Consultants, 1980, Figure C-35)
2.6-54	Mckinleyville Trench (from Woodward-Clyde Consultants, 1980, Figure b-19a). Location of Trench Shown on Figure 2.6-13.
2.6-55	Geologic Cross Section W-W ¹
2.6-56	Exposure of Discharge Canal Fault in Sea Cliff West of Discharge Canal
2.6-57	Log of ESA (1977) Trench BP-2
2.6-58	Log of ESA (1977) Trench BP-3
2.6-59	Alternative Interpretations of the Irregularities in the Top of the Unit F Clay Between Boreholes WCC80-CH4 and WCC80-CH5
2.6-60	Trench GMX-T1, View East-Southeast

CHAPTER 2

SITE CHARACTERISTICS

FIGURES (Continued)

Figure	Title
2.6-61	Surveying Geologic Contacts in Trench GMX-T2. View is Toward the South.
2.6-62	Artificial Fill Overlying Sand and Silt Layers of the Upper Hookton Formation in Northwest Wall of Trench GMX-T2 Between Station 36 ft. and Station 44 ft
2.6-63	Clay Fractures in Upper Hookton Formation in Trench GMX-T2
2.6-64	Fracture Lined with Black Compressed Rootlets in Clayey-Silt Bed in Trench GMX-T2
2.6-65	Continuous Bedding Across Bleached Fracture in Silty Clay in Trench GMX-T2
2.6-66	Fault Normal Design Spectrum for Damping Values of 2%, 4%, 5%, and 7%
2.6-67	Fault Parallel Design Spectrum for Damping Values of 2%, 4%, 5%, and 7%
2.6-68	Vertical Spectrum for Damping Values of 2%, 4%, 5%, and 7%
2.6-69	Equal Hazard Spectra for the FN Component, Soil Site Conditions
2.6-70	Equal Hazard Spectra for the FP Component, Soil Site Conditions
2.6-71	Equal Hazard Spectra for the Vertical Component for Soil
2.6-72	Comparison of Deterministic Spectra with 2000-Year Probabilistic Spectra
2.6-73	Typical Types of Surface Deformation Associated with Thrust Faulting
2.6-74	Collapsed Fault Scarp in Alluvium on the Hanning Bay Fault, Montague Island, Alaska

CHAPTER 2

SITE CHARACTERISTICS

FIGURES (Continued)

Figure	Title
2.6-75	This trench exposure near Trinidad, approximately 36 kilometers north of the ISFSI site, is an example of surface deformation produced by a displacement on a low-angle thrust fault (from Woodward-Clyde Consultants, 1980, Figure B-14). The style of deformation corresponds to Type b on Figure 2.6-73
2.6-76	Fault Scarp on the Chelungpu Fault at the Kuang Fu Middle School, Taiwan
2.6-77	Comparison of Faulting Near the Humboldt Bay ISFSI Site with Deformation Mapped in the Hanging Wall of the Little Salmon Fault Zone at College of the Redwoods, About 5 Kilometers South of the Site
2.6-78	Complex Zones of Deformation Where Crustal Shortening is Accommodated by Numerous Small-Displacement Conjugate Faults
2.6-79	Schematic Progressive Development of Fault Bend and Fault Propagation Folds (<i>from Suppe, 1983</i>)
2.6-80	Log of Trench Across a Trace of the Mad River Fault Zone
2.6-81	Fault Bend Fold and Associated Shears and Fractures of the Chelungpu Fault, Fengyuan, Taiwan
2.6-82	Fractures and Faults in the Hanging Wall of the Oued Fodda Fault, Algeria
2.6-83	Comparison of Faulting Near the Humboldt Bay ISFSI Site with 1999 Surface Rupture Along the Chelungpu Fault, Taiwan
2.6-84	Schematic Diagrams of Major Tsunami Sources
2.6-85	Illustration of Tsunami Terms
2.6-86	Diagrams Illustrating Progression of Tsunamis at the Coast, and Stratigraphic Columns in the Quiet Water of Bays and Ponds

CHAPTER 2

SITE CHARACTERISTICS

FIGURES (Continued)

Figure	Title
2.6-87	North Spit, Humboldt Bay (Foreground), and Arcata Bay (Background)
2.6-88	Coastal Sites Investigated for Evidence of Paleotsunamis in Northwestern California
2.6-89	Cross Section of a Typical Intertidal Marsh
2.6-90	Cross Section of a Typical Coastal Freshwater Marsh
2.6-91	Idealized Detailed Section Showing Multiple Graded Sands in a Tsunami Deposit
2.6-92	Gouge Coring at Crescent City Marsh
2.6-93	Typical Gouge Core
2.6-94	Drilling Using the Vibracore at Lagoon Creek
2.6-95	Typical Drive Cores
2.6-96	Comparison of Ages for Cascadia Earthquakes from Tsunami Data Between Northern California and Washington
2.6-97	Location of Cores in Crescent City Marsh
2.6-98	Crescent City, View to West
2.6-99	Crescent City Marsh
2.6-100	Correlation of Tsunami Sands in Selected Cores Across Crescent City Marsh
2.6-101	Location of Cores in the Lagoon Creek Marsh
2.6-102	Lagoon Creek Pond and Marsh
2.6-103	Wilson Creek and Lagoon Creek

CHAPTER 2

SITE CHARACTERISTICS

FIGURES (Continued)

Figure	Title
2.6-104	Beach Berm at Lagoon Creek 23 Feet Above MLLW
2.6-105	Correlation of Tsunami Sands in Selected Cores Across the Lagoon Creek Marsh
2.6-106	Detailed Stratigraphy of Core LC-16 from the Lagoon Creek Marsh
2.6-107	Detailed Stratigraphy of Core LC-2 from the Lagoon Creek Marsh
2.6-108	Townsite of Orekw (Oreck) and Location of Cores in Orick Marsh
2.6-109	Townsite of Orick and the Orick Marsh at the Mouth of Redwood Creek
2.6-110	Geomorphology of the North and South Spits of Humboldt Bay
2.6-111	South Spit
2.6-112	Mouth of Humboldt Bay, and the South Bay Hookton Slough Sites
2.6-113	Lag Pebbles at Elevation 27 Feet (MLLW) on the Sand Dunes on the North Spit Believed to be Deposited by a Tsunami that Inundated the Dunes
2.6-114	Map of the North Spit Site, South Bay, and Other Humboldt Bay Marsh Sites
2.6-115	South Bay Site
2.6-116	Correlation of Tsunami Sands in Selected Cores Across the South Bay Marsh
2.6-117	Present Coastline Superimposed on the 1858 Map of Mouth of Humboldt Bay
2.6-118	The 1806 Map of Humboldt Bay (Bay of Rezanov) Made by Russian Explorers

SITE CHARACTERISTICS

FIGURES (Continued)

Figure	Title
2.6-119	Plot of Moment Magnitude Versus Average Maximum Tsunami Runup for the Better-Documented Tsunamigenic Earthquakes
2.6-120	Schematic Diagram Showing Estimated Tsunami Runup Heights at the Humboldt Bay ISFSI Site

CHAPTER 2

SITE CHARACTERISTICS

This chapter provides information on the location of the Humboldt Bay Independent Spent Fuel Storage Installation (ISFSI) and descriptions of the geographical, demographical, meteorological, hydrological, seismological, and geological characteristics of the storage site and surrounding vicinity.

2.1 GEOGRAPHY AND DEMOGRAPHY OF SITE SELECTED

2.1.1 SITE LOCATION

The ISFSI is located within the Pacific Gas and Electric (PG&E) owner-controlled area at the Humboldt Bay Power Plant (HBPP). The HBPP is located near the coastal community of Fields Landing on the eastern shore of Humboldt Bay in Humboldt County, in northwestern California. Eureka, the largest city in Humboldt County, is located approximately 3 miles north of the ISFSI site (Figure 2.1-1).

PG&E owns approximately 143 acres on the northeastern part of Buhne Point of Humboldt Bay opposite the bay entrance. PG&E also owns the water areas extending approximately 500 ft into Humboldt Bay from the land area (see Figure 2.1-2). The ISFSI **is** located approximately 700 ft west of **the Unit 3 historical location** at an elevation of approximately 44 ft above mean lower low water (MLLW) (Figure 2.1-2). The coordinates of the ISFSI site are 40°44'30.6" North, 124°12'39" West (UTM Zone 10, 4,510,592.5 meters North, 397,761.3 meters East). Figure 2.1-3 shows the topography of the site and surrounding areas. An aerial view of the ISFSI site vicinity is shown in Figure 2.1-4.

| 9-01

There are several small residential communities within 5 miles of the ISFSI site, including King Salmon, Humboldt Hill, Fields Landing, and the suburban communities surrounding the City of Eureka. Figure 2.1-5 identifies the location of the nearest residence within each of 16 segments centered on the major compass points. Most of these residences are within 1 mile of the site.

2.1.2 SITE DESCRIPTION

The terrain in the vicinity of the HBPP rises rapidly from the bay on the north side to an elevation of approximately 69 ft MLLW at Buhne Point. Terrain to the north and east of the site is generally flat. To the south and east, the terrain rises rapidly forming Humboldt Hill, which reaches an elevation of over 500 ft MLLW within 2 miles of the ISFSI and is the site of several small neighborhoods. Humboldt County is mostly mountainous except for the level plain that surrounds Humboldt Bay. The coastal mountains extend to the central valley. The ISFSI **is** located near the top of a small hill surrounded by wetlands to the east and Humboldt Bay to the west.

| 9-01

HUMBOLDT BAY ISFSI FSAR UPDATE

The owner-controlled area is shown in Figure 2.1-2. The Buhne Point peninsula ranges in elevation from sea level to approximately 69 ft MLLW. The ISFSI controlled area varies between sea level and 64 ft MLLW and is approximately 700 ft in width formed by the regulatory 100 meter boundary condition. The PG&E owner-controlled area is not traversed by public highway or railroad. The only access to the ISFSI site is from the south off of King Salmon Avenue, which also serves the community of King Salmon situated on the western part of the peninsula. Public trails run along the shoreline in the ISFSI 100-meter controlled area.

9-01

9-01

PG&E has full authority to control all activities within the ISFSI site and owner-controlled area boundaries. The mineral rights within the site are owned by PG&E; there is no information suggesting that the land contains commercially valuable minerals.

9-01

Begin Historical information - HBPP consisted of five electric generation units. Unit 3, a boiling water reactor, operated for approximately 13 years before being shut down in July 1976. Units 1 and 2 were collocated conventional 53 megawatt-electric (MWe) units capable of operating on fuel oil or natural gas. Unit 3 was located in a separate building, but was adjacent to Unit 2. There were also 2 gas turbines, rated at 15 MWe each, located in the vicinity of the Units 1, 2, and 3 structures. The five generating units, as well as the plant site, were owned by PG&E as shown on Figure 2.2-2A. **End Historical information.**

9-01

The above described fossil units and Unit 3 have been removed and the Humboldt Bay Generating Station (HBGS) has been built on the site. The HBGS consists of 10 gas fired internal combustion units of approximately 16MWe each. The current configuration of the Humboldt Bay Site which includes the HBPP (currently decommissioning), the HBGS, and the Humboldt Bay ISFSI (HB ISFSI) is shown on Figure 2.2-2B

9-01

In accordance with 10 CFR 72.106, a 100-meter controlled area has been established around the ISFSI, as shown in Figures 2.1-2, 2.2-2A, and 2.2-2B. A public trail to access a breakwater for fishing traverses the ISFSI 100-meter controlled area (see Figures 2.1-2, 2.2-2A, and 2.2-2B), a condition allowed by 10 CFR 72.106, so long as appropriate and effective arrangements are made to control traffic and to protect public health and safety. The public trail crossing the PG&E property to the north of the ISFSI is controlled when required by fencing, gates, or personnel. Figures 2.2-2A and 2.2-2B indicate the approximate location of the fences, gates, or posted individuals (when required). The gates (if present) will normally be open to allow access to the public trail during normal ISFSI operation. If an accident should occur within the 100-meter controlled area during normal ISFSI operation, PG&E will assess radiological conditions. If radiation levels exceed the allowable levels for public health and safety, PG&E will close and lock the gates or otherwise control access to prevent public access within the 100-meter controlled area until actions are completed to return radiation levels to allowable levels. During loaded cask movements or handling evolutions, the gates will be locked or otherwise controlled to prevent public access within the 100-meter controlled area until the cask transfer activities and any corrective actions are completed. Loaded cask movements or handling evolutions have occurred primarily

9-01

9-01

9-01

9-01

HUMBOLDT BAY ISFSI FSAR UPDATE

during the initial transport of storage casks to the ISFSI and **probably will not occur** again until the casks are transported offsite to the U.S. Department of Energy permanent **or temporary** storage repository.

| 9-01

| 9-01

The major access in the vicinity of the ISFSI and other communities of Humboldt County is via US Highway 101, which generally traverses north-south through Humboldt County. This highway passes about 0.3 mile east of the ISFSI site and is accessible at approximately 0.35 mile to the southeast of the site.

There are several landings in the community of King Salmon, located just west of the entrance gate to the owner-controlled area. King Salmon serves frequent commercial and recreational boat traffic. Commercial air traffic into and out of Humboldt County is primarily through Eureka/Arcata Airport, located in McKinleyville, approximately 20 miles north of the ISFSI site.

A set of Northwestern Pacific railroad tracks runs generally north-south along the southeastern PG&E property line. Presently, there are no existing plans to rehabilitate and reuse the tracks.

| 9-01

Two small streams discharge into Humboldt Bay near the site. Salmon Creek and Elk River are located within a mile south and north of the site, respectively. These streams are used for watering livestock, but are not used for potable drinking water supply.

2.1.3 POPULATION DISTRIBUTION AND TRENDS

The population distribution and projections for areas around the ISFSI site are based on the 2000 census and on estimates prepared by the California Department of Finance. The population data presented in this section for the ISFSI are based on distances from the ISFSI site.

The population data are provided for areas within a 50-mile radius of the ISFSI. Population distributions are provided for areas within specific radii and sectors, and include the 2000 census data as well as projections for the years 2010 and 2025. Census data was analyzed at the census block level within the 1-mile radius and at the block group level outside of 1 mile. Population projections were based on California Department of Finance projected growth rates for Humboldt County between 1990 and 2040.

The area within 50 miles of the ISFSI includes most of Humboldt County, and a small sparsely populated portion of Trinity County (see Figure 2.1-9). Approximately 50 percent of the area within the radius is on land, with the balance being Humboldt Bay and the Pacific Ocean. In general, the portion of California that lies within 50 miles of the ISFSI is relatively sparsely populated, with the exception of a few urbanized areas along the coast.

HUMBOLDT BAY ISFSI FSAR UPDATE

According to the 2000 census, the population of Humboldt County was 126,518 and the population of Trinity County was 13,022 in 2000. Table 2.1-1 shows the population trends of the state of California and Humboldt and Trinity Counties from 1940 to 2000. Humboldt County has seven incorporated cities ranging in size from approximately 300 to 26,000 persons. Approximately one half of Humboldt County's residents live in incorporated communities, and 59 percent of the county population lives in the area surrounding Humboldt Bay. This area includes the cities of Arcata, Ferndale, Fortuna, and Eureka and the unincorporated community of McKinleyville (Reference 1).

According to the State Department of Finance, the cities of Eureka and Arcata together contain about 35 percent of Humboldt County's population, while 13 percent of the population is scattered among five other incorporated cities. Approximately 67,000 of county residents reside in unincorporated communities. Table 2.1-2 shows the growth since 1970 of the incorporated cities and other major communities within 50 miles of the ISFSI site and provides distance and direction from the site (Reference 2).

Table 2.1-3 provides the age and sex of the total population for Humboldt County in 2000. Table 2.1-4 provides the distribution of population by race as reported in the 2000 census.

2.1.3.1 Population within 10 Miles

The 2000 census counted approximately 49,740 residents within 10 miles of the ISFSI site. The nearest residence is about 0.15 mile southwest of the ISFSI site. There are approximately 35,790 residents within 5 miles of the ISFSI site.

Figure 2.1-6 shows the 2000 census population distribution within a 10-mile radius wherein the area is divided into 22.5-degree sectors and part circles with radii of 1, 2, 3, 4, 5, and 10 miles. Figures 2.1-7 and 2.1-8 show projected population distribution for 2010 and 2025, respectively, and are based primarily on population projections published by the California Department of Finance (Reference 3). The distributions are based on the assumption that the land usage will not change in character during the next 25 years, and that the population growth within 10 miles will be proportional to growth in Humboldt County as a whole (0.61 percent annual growth rate) (Reference 3).

The nearest population center is the City of Eureka located approximately 3 miles north-northeast of the ISFSI site. The 2000 census shows the city to have a population of 26,128.

2.1.3.2 Population Between 10 and 50 Miles

Figure 2.1-9 shows the 2000 census population distribution between 10 and 50 miles, within the sectors of 22.5 degrees, with part circles of radii of 10, 20, 30, 40, and 50 miles. The 2000 U.S. Census reported 123,938 people living within 50 miles of the ISFSI site. In 2000, some 76 percent of Humboldt County's total population resided in the population centers listed in Table 2.1-2.

Figures 2.1-10 and 2.1-11 show projected population distributions for 2010 and 2025, respectively, and are based primarily on population projections published by the California Department of Finance (Reference 3).

2.1.3.3 Transient Population

In addition to the resident population presented in the tables and population distribution figures, there is a seasonal influx of vacation and weekend visitors within a 50-mile radius, especially during the summer months. The influx is heaviest in the area around Humboldt Redwoods State Park and along the Pacific Ocean coast to the north of the site in the area around the City of Trinidad.

The Humboldt County Convention and Visitors Bureau estimated that the County receives between 2.1 and 2.2 million visitors per year (Reference 4). Table 2.1-5 lists state and county recreation areas and public lands within 50 miles of the site.

2.1.3.4 Public Facilities and Institutions

There are numerous schools located within 10 miles of the ISFSI site, particularly in the population centers listed in Table 2.1-2. Several K-12 schools are located within 5 miles of the site, serving the City of Eureka and neighboring communities. Humboldt State University, with an enrollment of approximately 7,500 students, is located in the City of Arcata approximately 15 miles northeast of the ISFSI site. The College of the Redwoods is located within 5 miles of the site just south of the City of Eureka and has an enrollment of approximately 5,000 full and part-time students.

Several parks and recreation areas are located within 10 miles of the ISFSI site. The beaches around Humboldt Bay and the Pacific Ocean are popular with local residents as well as visitors from outside the local area. The City of Eureka has several municipal parks and there is a municipal golf course located approximately 3 miles northeast of the ISFSI site.

2.1.4 USE OF NEARBY LANDS AND WATERS

Humboldt Bay and the surrounding lowlands dominate the region north, south, and west of the site. The lowland areas around the site are primarily vacant land and are used to a limited extent for grazing beef cattle. The small community of Fields Landing is located adjacent to a lumber shipyard approximately 0.4 mile south of the ISFSI site. Humboldt Hill is the dominant feature southeast of the site. Most of the mountainous area east and southeast of the site is inaccessible; however, there are several small communities located on Humboldt Hill and in the larger valleys. The City of Eureka is the largest population center in Humboldt County and is located approximately 3 miles north of the ISFSI site.

2.1.4.1 Agriculture

Humboldt County has relatively little level land, except along the coast of the Pacific Ocean. Overall, land use in Humboldt County is 74 percent forests, 10 percent agriculture, 6 percent public use, 4 percent residential, 3 percent water resources, 2 percent industrial and 1 percent commercial. Logging and recreation are the most significant land uses in the county. The county ranks 35 out of 58 in total agricultural production in the state of California. The county's primary agricultural products in 2000 were dairy (\$33.5 million), nursery and greenhouse crops (\$32.9 million), and cattle and calves (\$17.2 million). The total farm acreage in the county was approximately 584,000 in 1997 (Reference 5).

9-01

2.1.4.2 Dairy

Most of the dairies are located along the Elk River while the coastal lowlands are used primarily for cattle grazing and ranching. The nearest dairy is 1.8 miles east of the site. This dairy produces approximately 800 gallons of milk per day.

2.1.4.3 Fisheries

The ISFSI site is located in the vicinity of several ports that support commercial and sport fishing activities. Humboldt Bay, inland waterways, and the coastal waters of the Pacific Ocean are used for recreational fishing. The California Department of Fish and Game (DFG) calculates sport fishing activity by the number of fish landed and commercial fishing activity by poundage of landings. According to data provided by DFG, the combined sport catch for Eureka, King Salmon, Shelter Cove, and Trinidad in 2001 totaled approximately 10,260 rockfish, 4,465 crabs, 1,640 salmon, and 728 fish of other species.

Commercial landings are calculated by poundage of landings. In 2001, at Eureka, King Salmon, Shelter Cove, and Trinidad, the landings were estimated by DFG to be as follows: 2,619,534 pounds of sole, 1,397,057 pounds of shrimp and prawns, 1,056,681 pounds of rockfish, 879,357 pounds of tuna, 615,259 pounds of crab, and 766,399 pounds of other fish species.

2.1.4.4 Water Use

The Humboldt Bay Municipal Water District (HBMWD) provides water to residential and industrial users in the Humboldt Bay area. The district operates two separate water systems. Drinking water is supplied through the domestic water system. Raw water, used only for industrial purposes, is taken directly from the surface of the Mad River and delivered, untreated, to industrial customers. HBMWD produces a capacity of 20 million gallons per day of water from five Ranney wells in the Mad River near Essex. The City of Eureka General Plan Background Report identifies three groundwater wells located within 1 mile of the ISFSI site. These wells are shown in Figure 2.1-5 (Reference 6).

2.1.4.5 Land Usage Within 5 Miles

HUMBOLDT BAY ISFSI FSAR UPDATE

Figure 2.1-5 shows the location of sensitive land uses (nearest residences, farms, gardens, and groundwater wells) within 5 miles of the ISFSI site. The Humboldt County Department of Agriculture identified a total of nine farms and ranches and one community vegetable garden within 5 miles of the ISFSI site. The primary local farming products are dairy products, cattle, goats, and llamas. The nearest vegetable garden is the Wiyot Tribe community vegetable garden located approximately 4.2 miles southwest of the site.

The primary industry in the area, and in Humboldt County, is lumber and lumber/paper manufacturing. Lumber production in Humboldt County in 2000 was valued at \$285.5 million. A lumber-loading shipyard is located less than 1 mile south of the ISFSI site. Lumber mills are located in the nearby communities of Eureka and Arcata and farther inland in the communities of Scotia, Korb, and Redcrest.

2.1.4.6 Other Nearby Usage

While the fishing and lumber industries are in decline, service industries and recreation are becoming increasingly important parts of the county's economic base. The primary service employers in the Humboldt Bay area include medical services, education, and government. Visitors are attracted to the area by the numerous state and county parks both along the coast and in the inland forests.

There are public beaches located along Humboldt Bay and the Pacific Ocean coast that are popular with local residents as well as tourists. Much of the coastal area on the inside of the bay falls within the Humboldt Bay National Wildlife Refuge, which is within 5 miles of the ISFSI site.

HBPP is located in unincorporated Humboldt County, and lies within the City of Eureka sphere of influence. This area is subject to the provisions of the City of Eureka Zoning Ordinance. Additionally, HBPP is located in the coastal zone. In 1984, the City of Eureka adopted a Local Coastal Program (LCP) in accordance with the California Coastal Act. The LCP superceded the City of Eureka's 1977 General Plan and governed land use and development within the coastal zone until it was superceded by the city's 1997 General Plan (Reference 6).

The PG&E-owned land around the ISFSI site is zoned Coastal-Dependent Industrial. The areas immediately south and east of the site are zoned Waterfront Commercial. The community of King Salmon, located immediately southwest of the site, is zoned Low-Density Residential. The Humboldt Hill area to the south and east of the site has a variety of residential zoning designations and is surrounded by land zoned for agriculture. No major new developments are planned for the area within 5 miles of the ISFSI site. Areas near the ISFSI site experiencing significant growth are generally situated to the south of the City of Eureka and include the communities of Bayview, Cutten, and Humboldt Hill (see Table 2.1-2).

2.1.5 REFERENCES

1. Humboldt County Profile, Humboldt County, 2002.
2. Historical Census Populations of California State, Counties, Cities, Places, and Towns, 1850-2000, California State Department of Finance, 2002.
3. Population Projections, 1990-2040, California State Department of Finance, 1998.
4. D. Leonard, Executive Director, Humboldt County Visitor Bureau, Telephone Conversation, November 14, 2002.
5. 1997 Census of Agriculture, County Profile, Humboldt California, USDA National Agricultural Statistics Service.
6. City of Eureka General Plan Background Report, J. Lawrence Mintier and Associates, 1997.

2.2 NEARBY INDUSTRIAL, TRANSPORTATION, AND MILITARY FACILITIES

2.2.1 OFFSITE POTENTIAL HAZARDS

During the original licensing of the Independent Spent Fuel Storage Installation (ISFSI), there were fossil-fueled units (Humboldt Bay Power Plant (HBPP) Units 1 and 2, and mobile emergency power plants) and one shutdown nuclear unit (HBPP Unit 3) within the HBPP owner-controlled area. The original licensing analyses evaluated potential fire and explosion hazards associated with these units. The fossil-fueled Units were removed and replaced with the new Humboldt Bay Generating Station (HBGS) subsequent to the completion of the original licensing. In addition, decommissioning activities commenced and are still in progress. The ISFSI FSAR was updated to reflect the revised fire and explosion hazards and additional evaluations were performed for the new hazards associated with new HBGS and decommissioning activities. The fire and explosion hazards associated with Unit 1, 2, and 3 were labeled with numeric event identifiers. The fire and explosion hazards for the new HBGS were identified with alphabetical identifiers. The descriptions of the Units 1, 2, and 3 and mobile emergency power plant fire and explosion hazard evaluations are identified as historical in Section 2.2.2.1 since they are no longer present on site. However, the evaluations for the Units 1, 2, and 3 fire and explosion hazards are still valid and were determined to be bounding for the new HBGS hazards. FSAR Chapters 2 and 8 fire and explosion hazards and their associated evaluations are identified as historical if they are no longer present.

2.2.1.1 Description of Location and Routes

The primary industry in Humboldt County, including areas surrounding the ISFSI site, is lumber and forest products, including paper manufacturing. Approximately 1,740,000 acres of land, or 75 percent of Humboldt County, is covered with forests of commercial value, principally Douglas fir and redwood. There are major lumber companies on the north peninsula of Humboldt Bay (Samoa Peninsula) as well as to the south and north of the ISFSI site on the mainland. Several lumber mills, including lumber storage yards, are located within 25 miles of the ISFSI site. The nearest major mill is located on the Samoa Peninsula approximately 3 miles north of the site, and there are small facilities in the city of Eureka approximately 3 miles north of the site.

All of the lumber companies are accessible from US Highway 101 via local roadways, with the majority located adjacent to the highway. There is also a lumber railroad that traverses much of Samoa Peninsula, and connects to the main railroad that traverses next to US Highway 101 in this area of Humboldt County. This railway had served as a major lumber shipping route on land until the late 1970s. However, this railroad has been non-operational since 1997 and lumber freight is currently shipped principally by truck, supplemented with cargo ships.

The major land transportation route in the area is US Highway 101, which traverses in a north-south direction in this area of Humboldt County. In the vicinity of the ISFSI site,

HUMBOLDT BAY ISFSI FSAR UPDATE

this highway is 4 lanes and passes within approximately 2,000 ft to the east of the ISFSI site.

The ISFSI site is located within 200 ft of the shoreline of Humboldt Bay. Humboldt Bay is a land bound bay that is open to the Pacific Ocean through a maintained shipping entrance channel northwest of the ISFSI site. The bay has two main channels, a North Channel and a South Channel. The North Channel was dredged to a minimum depth of 40 ft in 2001 and is used mostly by private yachts and recreational vessels. However, it is also used by large cargo vessels and passenger vessel cruise ships having gross tonnage of approximately 45,000 tons (up to 650 ft in length). The South Channel is a smaller channel, which was also dredged to a minimum of 40 ft in 2001 and the vessels using this South Channel are limited to mostly private yachts, recreational vessels, and occasionally barges off loading lumber or logs. The edge of the South Channel at its closes point is approximately 850 yards from the ISFSI site.

The Eureka-Arcata Airport, located adjacent to US Highway 101 approximately 20 miles to the north of the ISFSI site, is the primary airport for commercial air traffic in Humboldt County. This airport serves on average 207 flight operations per day (Refer to www.airnav.com/airport/KACV). Of those, 34 operations are commercial, primarily via turbo-prop aircraft that seat no more than 30 people, and 2 operations are air taxi. These aircraft have a gross weight of no more than 30,000 pounds. The remaining average daily operations include 87 local general aviation, 58 transient general aviation and 28 military aircraft operations. The general aviation operations consist mostly of aircraft that seat no more than 8 people, with an average gross weight of less than 12,500 pounds. The military operations involve the US Coast Guard Air Station, which is located at the airport. Flight operations include training activities as well as actual events involving coastal surveillance and air-sea rescue missions. The military aircraft used are mostly helicopters and some small non-armed training aircraft.

The Eureka Municipal Airport is located on the Samoa Peninsula at approximately 2 miles north of the ISFSI site. Direct access to this airport is via local roadways connected to the north of the airport with State Highway 255, which connects the Samoa Peninsula with US Highway 101. This airport serves on average 96 flight operations per week (Refer to www.airnav.com/airport/033) of which all are general aviation flights involving 54 local and 42 transient general aviation operations. The general aviation operations consist mostly of aircraft that seat no more than 8 people, with an average gross weight of less than 12,500 pounds.

The Murray Field Airport is located at the northern edge of Eureka immediately adjacent to US Highway 101, approximately 7 miles northeast of the ISFSI site. This airport serves on average 179 flight operations per day (Refer to www.airnav.com/airport/EKA). Of those an average of less than 1 operation is air taxi. The remaining average daily operations include 123 local general aviation, 54 transient general aviation and 1 military aircraft operations. These operations consist mostly of aircraft that seat no more than 8 people, with an average gross weight of less than 12,500 pounds. The military operations involve small non-armed training aircraft.

HUMBOLDT BAY ISFSI FSAR UPDATE

The Kneeland Airport is located approximately 14 miles east of the ISFSI site. This airport serves on average 27 flight operations per day (Refer to www.airnav.com/airport/019). Of these flight operations, 3 are local general aviation and 24 are transient general aviation aircraft operations. These operations consist of aircraft that seat no more than 8 people, with an average gross weight of less than 12,500 pounds and California Department of Forestry helicopters.

The Rohnerville Airport is located approximately 3 miles southeast of Fortuna, California and 15 miles southeast of the ISFSI site. This airport serves on average 75 flight operations per day (Refer to www.airnav.com/airport/KFOT) of which all are general aviation flights involving 45 local and 30 transient general aviation operations. The general aviation operations consist mostly of aircraft that seat no more than 8 people, with an average gross weight of less than 12,500 pounds and small to medium size helicopters.

There are three federal flight corridors, which fly almost directly over the ISFSI facility; these are V27, V195, and V494. These corridors converge on the Fortuna transponder. Per the Federal Aviation Administration (FAA) Northwest Mountain Region (Reference 1), the estimated traffic on these corridors is 18 flights per day and the majority of the aircraft using these routes are above 10,000 ft and below 18,000 ft. In addition, there are some high altitude airways that pass over the general area with approximately 52 flights per day. These flights are almost exclusively at 33,000 ft and are classified as direct flights by the FAA.

There is also federal flight corridor V607, which is the main flight approach corridor into the Eureka-Arcata Airport. The center of this corridor passes approximately 13 miles east of the ISFSI. The estimated traffic on this corridor is 207 flight operations per day.

For all of the above airports and flight corridors, the assumption is that 50 percent of the general aviation operations are by piston driven aircraft and 50 percent by turboprop driven aircraft. This is considered conservative based on the type of aircraft maintained at the airports in the area.

There is also a military training route (VR 1251), which passes the ISFSI facility to the east at an approximate distance of 18 miles. The use of this route is limited to transport through the area, as there are no major military bases or facilities in the region within 50 miles of the ISFSI site.

There is a US Coast Guard Reservation and Lifeboat Station located near the end of Samoa Peninsula, which is approximately 1.5 miles north of the ISFSI site, where a Coast Guard Cutter is stationed. The station is accessible via the waters of Humboldt Bay as well as local access roadways connected with State Highway 255. The US Coast Guard Air Station is located at the Eureka-Arcata Airport, approximately 20 miles north of the ISFSI site. Training activities as well as actual events involving coastal

surveillance and air-sea rescue missions along the Humboldt County coastline are conducted from both locations year round.

2.2.1.2 Hazards from Facilities and Ground Transportation

Figure 2.2-1 identifies the major (historical and existing) facilities and ground transportation routes within 5 miles of the ISFSI, which could be a potential hazard. The major land transportation route in the area is US Highway 101, which traverses in a north-south direction in this area of Humboldt County. In the vicinity of the ISFSI site, this highway is four lanes and passes within approximately 2,000 ft to the east of the ISFSI site. The traffic loading on this highway based on 1999 data from the “Traffic Volumes on the California State Highway System” report (Refer to www.dot.ca.gov/hq/traffops/saferesr/trafdata/1999all.htm) on average is approximately 24,500 vehicles per day, with a peak daily average of 27,000 vehicles per day. This traffic is a mixture of cars, light trucks and larger commercial vehicles, including a substantial number of lumber trucks.

Regulatory Guide (RG) 1.91 (Reference 2) states that conservatively the maximum probable hazardous solid cargo for a single highway truck is approximately 50,000 TNT-pounds. RG 1.91 provides a formula for determining setback distance based on a maximum 1 psi pressure wave resulting from an explosion, $R > kW^{1/3}$. In this formula, R equals distance in ft from an exploding charge of W pounds of TNT and factor k is 45. Based on this formula and the maximum probable charge of 50,000 pounds, the required setback distance R would be greater than 1,658 ft. As noted above, US Highway 101 is approximately 2,000 ft from the ISFSI facility, which exceeds the minimum setback and will require no further evaluation for the ISFSI facility.

However, there are sections of the historical transport route for the spent fuel from the HBPP refueling building (RFB) to the ISFSI facility that is within approximately 1,500 ft of US Highway 101 and will require further assessment. When looking at these potential hazards a determination was made that they are an explosion hazard but do not constitute a fire hazard. They are not considered fire hazards, since the terrain and distance between the highway and the historical ISFSI transport route is mostly swamp of a lower elevation, and the owner-controlled plant areas have very limited vegetation. This offsite explosion hazard for the historical transport route was identified and its evaluation is discussed in Section 8.2.6.

The ISFSI site and historical transport route to the ISFSI is located within approximately 200 ft of the shoreline of North Channel of Humboldt Bay. The North Channel is primarily used by private yachts and recreational vessels. However, it also has some large cargo vessel traffic having gross tonnage of approximately 45,000 tons (up to 650 ft in length). Most of the vessels and all of the cargo vessels that use the North Channel remain in the actual channel. The edge of that channel is approximately 1,500 yards from the ISFSI facility and spent fuel historical transport route. Outside of that channel the water depth reduces very quickly and will not allow the larger vessels to

HUMBOLDT BAY ISFSI FSAR UPDATE

operate. In addition to the vessels in the channel, there are a number of piers available for ship docking along the shorelines of the north channel, including Eureka and along the Samoa Peninsula. The main berthing areas for small boats are at a public marina on Woodley Island in the North Bay, which is approximately 4 miles from the ISFSI site. Of the vessels using the North Channel the largest explosive or fire hazardous cargo is from a barge delivering diesel fuel oil and gasoline to the Chevron terminal approximately once every eight days. That barge carries up to a maximum of 87,000 barrels to the Chevron fuel terminal, which is approximately 2 miles north of the ISFSI site.

The South Channel is a smaller channel mostly used by private yachts, recreational vessels, and occasionally a barge off loading lumber or logs. Only a few docking areas are available in Humboldt Bay to the south of the ISFSI site, primarily at Fields Landing, which also contains a dry dock and boat repair facilities. Fields Landing is occasionally used for ship loading and off-loading of lumber. The edge of the South Channel at its closest point is approximately 850 yards from the ISFSI site. As a result of the limited vessel use of this channel, the size of the vessels, the type of cargo, and the distance to the edge of the channel from the ISFSI, the hazard from this traffic is considered limited.

In the summer, boat traffic and related activities in Humboldt Bay, including recreational fishing, can increase noticeably because of incoming vessels from other areas as well as additional local sailing. There are sufficient docking facilities in the public marina and other piers to accommodate approximately 100 small vessels. However, the actual number of boats docked in the bay at any time typically totals no more than several dozen.

Although there are various types of vessels and cargos moving in the channels past the ISFSI, the largest is the 87,000 barrel barge, which is delivered to the Chevron Fuel Terminal. This barge holds a maximum of 87,000 barrels of liquid fuels. This barge has a total of 12 separate tank compartments and usually carries gasoline in 8 compartments and diesel fuel in the other 4 compartments. Since the waters of the bay come within 200 ft of the ISFSI site and the fact that gasoline floats, this hazard was identified as both a fire and explosion hazard. The offsite potential of fire and explosion is discussed in Sections 8.2.5 and 8.2.6, respectively, and is considered to bound all other hazards from vessel traffic for the ISFSI facility for both the North and South Channels of Humboldt Bay. During historical transport of the spent fuel to the ISFSI, transport of the spent fuel and GTCC waste casks to an authorized offsite storage facility, removal of a cask from the vault for maintenance activities, or removal of a vault cell lid for maintenance/inspections, the 87,000-barrel barge is not considered to be a credible hazard for fire or explosion. This is based on administrative controls implemented through the Humboldt Bay ISFSI Technical Specification 5.1.5 Cask Transportation Evaluation Program (CTEP) or Vault Lid Opening Hazard Control Program, which is part of the Humboldt Bay ISFSI Technical Specification 5.1.4 ISFSI Operations Program, as applicable, that ensures no cask handling activities will take place while the barge is moving through the bay. In addition, prior to the transport of any spent fuel (historical), transport of the spent fuel and GTCC waste casks to an

HUMBOLDT BAY ISFSI FSAR UPDATE

authorized offsite storage facility, removal of a cask from the vault for maintenance activities, or removal of a vault cell lid for maintenance/inspections, the Coast Guard will be notified of the spent fuel movement and will be requested to assist in monitoring vessel traffic in the vicinity of the ISFSI facility.

The 87,000-barrel barge delivers its cargo to the Chevron Fuel Terminal in Eureka approximately 2 miles from the ISFSI facility. This fuel terminal stores a maximum of 50,000 barrels of gasoline and 45,000 barrels of diesel fuel oil. On average, there are approximately 35,000 barrels of gasoline and 22,000 barrels of diesel fuel oil stored at the facility. The capacity of the largest single gasoline storage tank at the facility is 20,600 barrels and the capacity of the largest single diesel fuel oil storage tank at the facility is 30,000 barrels. The Chevron Fuel Terminal has fire suppression at the terminal docks and in the pipe racks to the tanks. Although this facility does house significant amounts of fuel, the limited maximum single tank capacity and the distance from the ISFSI facility, preclude it from being considered a credible explosive or fire hazard to either the transport (historical) of spent fuel or to the ISFSI facility itself.

The Northwestern Pacific Railroad traverses adjacent to US Highway 101 in the vicinity of the ISFSI site at a distance of approximately 1,200 ft. This line was used to connect Humboldt Bay with the coastal areas of central California. Currently there is no passenger or freight traffic on this line in Humboldt County and major renovations would be required to restore that service. However, several locomotives remain in the area and occasionally are used to move heavy equipment locally, such as industrial cranes. For these locomotives the main hazard would be the diesel fuel they carry. Because of the properties of diesel fuel, its limited volume, and the distance between the ISFSI and these locomotives, it is not considered as a credible explosion hazard. The fire potential is also considered not to be significant because of the lower swampy terrain between the ISFSI and the rail lines.

There has been some consideration by the Northwestern Pacific Railroad Company to renovate the rail lines and reinitiate some limited freight and passenger rail traffic in the area. However, no definitive plans have been identified for such renovation, and there are no indications from regulatory agencies, such as the California Department of Transportation or the Federal Emergency Management Administration, that such plans would be feasible. Therefore, the availability of rail service in Humboldt County at any future time is unlikely. However, if some rail service is reestablished in the future, a RG 1.91 hazards evaluation will be performed to ensure no unacceptable risk will result. Because of the highway and shipping in the area, there is a possibility of a release of toxic chemicals from transportation accidents, which may have some effect on the administration of ISFSI operations. The storage casks are passive systems and do not require fresh air or other mechanisms for cooling, therefore a toxic chemical release in the area would not affect their safe operation.

In the consideration of offsite explosions or fire events involving transportation accidents where chemical hazards are involved, the duration of the events is generally on the order of one day, since these hazards typically burn severely but quickly even if they

cannot be extinguished immediately. The primary concerns in such events involve cleanup activities and remedial actions following the event. Thus these events can typically be managed with no significant adverse impact to the ISFSI storage casks, and any effect on the ISFSI site is expected to be less serious than events that may occur onsite.

2.2.1.3 Hazards from Air Crashes

The ISFSI facility is in an area where there are five airports and several federal aviation corridors. Accordingly, an analysis was performed of aircraft hazards for the ISFSI site. The analysis followed the guidance of NUREG-0800, (Reference 3) Section 3.5.1.6, Aircraft Hazards. While this guidance applies to power reactor sites, the analysis of aircraft crash probabilities on a site is not dependent on the nature of the site other than size and, thus, the guidance of NUREG-0800 can be applied to the ISFSI.

As specified in NUREG-0800, the probability of aircraft crashes is considered to be negligibly low by inspection and does not require further analysis if the three criteria specified in Item II.1 of Section 3.5.1.6 are met. In particular, Criterion 1 specifies that the plant-to-airport distance, D , is between 5 and 10 statute miles, and the projected annual number of is less than $500D^2$, or the plant-to-airport distance, D , is greater than 10 statute miles, and the projected annual number of operations is less than $1000D^2$, then, the probability of aircraft crashes is negligibly low. Of the five airports in the area of the ISFSI facility, the Eureka Arcata, Kneeland and Rohnerville Airports meet Criterion 1 of the NUREG-0800 as follows:

The Eureka-Arcata Airport is approximately 20 miles to the north of the ISFSI site with annual flight operations totals of approximately 75,600, which is less than $1,000(20)^2$ or 400,000.

The Kneeland Airport is approximately 14 miles southeast of the ISFSI site with annual flight operations totals of approximately 9,855, which is less than $1,000(14)^2$ or 196,000.

The Rohnerville Airport is approximately 15 miles southeast of the ISFSI site with annual flight operations totals of approximately 27,375, which is less than $1,000(15)^2$ or 225,000.

The Eureka Municipal Airport is located approximately 3 miles north of the ISFSI site, which is less than 5 miles from the ISFSI site. This does not meet Criterion 1 of NUREG-0800 and required further evaluation.

The Murray Field Airport located approximately 7 miles northeast of the ISFSI site with annual flight operations totals of approximately 65,335, which is more than $1000(7)^2$ or 49,000, does not meet Criterion 1 of NUREG-0800 and required further evaluation.

HUMBOLDT BAY ISFSI FSAR UPDATE

Criterion 2 specifies that the facility must be at least 5 statute miles from the edge of military training routes. There is no military training route within 5 statute miles of the ISFSI facility (the edge of VR 1251 is approximately 14 miles). Therefore, further evaluation under this criterion is not required.

Criterion 3 specifies that a facility must be at least 2 statute miles beyond the nearest edge of a federal airway, holding pattern, or approach pattern. Federal flight corridor V607, the edge of which passes approximately 9 miles northeast of the ISFSI site, is one of the main flight approach corridors into the Eureka-Arcata Airport. This corridor meets Criterion 3 of NUREG-0800 and does not require further evaluation. However, several other approach and departure corridors for the Eureka-Arcata Airport are located directly over the ISFSI or would be within 2 statute miles to the nearest edge of those corridors and do not meet Criterion 3 of NUREG-0800. Therefore, a further evaluation is required.

There are 3 other federal flight corridors, V27, V195, and V494, which are located almost directly over the ISFSI facility. These three air corridors do not meet Criterion 3 of NUREG-0800. Therefore, a further evaluation is required.

Evaluation of Airways, Landing and Takeoff Operations

To determine the probability of an aircraft crashing into the ISFSI site per year, an evaluation of the various airways, landing and departure patterns, and air traffic in the vicinity of the ISFSI was performed (Reference 4). This evaluation was performed based on the guidance and acceptance criteria in NUREG-0800.

For local traffic at the Eureka-Arcata, Eureka Municipal and the Murray Field Airports

To determine the probability of a crash involving air traffic in or out of these three airports, several assumptions were made as follows:

- (1) In the case of the Eureka Municipal and Murray Field Airports, there are no control towers and the traffic is less precise for approaches and departures. As a result, 100 percent of all arrivals and departures for the Eureka Municipal Airport and the Murray Field Airport are assumed to fly directly over the ISFSI (Reference 4).
- (2) For the Eureka-Arcata Airport the traffic patterns are very controlled and precise. The distance to the airport is over 20 miles and the distance to the edge of normal approach and departure route (V607) for this airport is more than 9 miles away, which per NUREG-0800 criteria would not require further review for the ISFSI. However, a few secondary approaches and departure routes potentially either pass directly over the ISFSI or very close to it. However, based on the configuration of the airport runways and the prevailing winds in the area, it is conservatively

HUMBOLDT BAY ISFSI FSAR UPDATE

assumed that 95 percent of all arrivals and departures follow the normal (V607) route and would not be considered a threat to the ISFSI.

Details of the information relied upon in Reference 4 to arrive at the assumption that military air taxis and helicopters that use the Eureka-Arcata Airport are bounded by turbine-powered helicopters and why this assumption is conservative is provided in PG&E Response to NRC Question 15-7 in Reference 10.

Based on the above assumptions the following probabilities were determined for the three airports (Reference 4)

- Total probability for the Eureka-Arcata Airport is 1.2×10^{-7}
- Total probability for the Murray Field Airport is 8.72×10^{-8}
- Total probability for the Eureka Municipal Airport is 1.02×10^{-7}

Federal Air Route Non-Local Traffic

The above probability evaluations take into consideration all local traffic on the federal air routes including V27, V195 and V494. However, per a FAA traffic review (Reference 1), the total non-local traffic on these airways per day includes 15 commercial and 3 general aviation operations. These operations pass through the area at between 10,000 and 18,000 ft. Per the evaluation (Reference 4), the probability of a crash at the ISFSI per year from these operations was determined to be 5.48×10^{-8} .

High Altitude Traffic

There is some additional traffic in the area that takes place almost exclusively at altitudes greater than 33,000 ft. Per the evaluation in Reference 4, the probability of a crash at the ISFSI per year from these operations is $2.60\text{E-}7$.

Holding Patterns

There are no holding patterns in the area that would require evaluation per NUREG-0800 with the exception of one instrument approach occasionally used to the Eureka-Arcata Airport. It has a 1 minute holding pattern on approach over the vicinity of the ISFSI site. Traffic on this pattern has been included in the estimated traffic for that airport in the probability values provided above.

Total Aircraft Crash Probability

The total probability of aircraft crashes in the ISFSI site area is 6.24×10^{-7} (Reference 4), which is the sum of all of the above probabilities. This is less than the threshold of 1×10^{-6} approved by the NRC (Reference 5) for acceptable frequency of aircraft impact into a facility from all types of aircraft. Therefore, there is no credible affect on the ISFSI site from an aircraft crash.

As described in the Safety Evaluation Report for the Humboldt Bay ISFSI (Reference 11), the NRC performed various sensitivity and confirmatory analyses to develop reasonable assurance that the annual frequency of accidental aircraft crashes onto the proposed ISFSI is low and will be acceptable. The estimated crash probability values determined by the NRC are different from those determined by PG&E in Reference 4 because of different scenarios and assumptions made. However, both the NRC's and PG&E's crash estimates are in general agreement and are below the acceptance criterion of 1×10^{-6} . Therefore, the NRC concluded that the annual frequency of crashes for both civilian and military aircraft at the Humboldt Bay ISFSI is acceptable.

2.2.1.3.1 Future Potential Aircraft Hazards

Pacific Gas and Electric Company (PG&E) estimates the projected growth of civilian flights based on FAA long-range forecast (Reference 6). Commercial aircraft operations include air carriers and commuter/air taxi takeoff and landings at all US towered and non-towered airports. The FAA has forecasted that commercial aircraft operations are projected to increase from 28.6 million in 1998 to 47.6 million in 2025. This is a projected increase of 66 percent by 2025.

General aviation operations at all towered and non-towered airports in the US are projected by the FAA to increase from 87.4 million in 1998 to 99.2 million in 2025. This is a projected increase of 14 percent by 2025.

The FAA also predicts that the military traffic will not increase appreciably, if at all, in the foreseeable future.

Based on the above FAA projections, the cumulative aircraft probabilities for the ISFSI will increase to 7.024×10^{-7} in 2025 (Reference 4). This increase remains below the threshold of 1×10^{-6} approved by the NRC (Reference 5) as an acceptable frequency for impact into the facility from all types of aircraft

2.2.1.4 Hazards from Military Facilities

There are no major military bases or facilities in the region within 50 miles of the ISFSI site. However, there is a US Coast Guard Reservation and Lifeboat Station located at the tip of Samoa Peninsula, which is approximately 1.5 miles north of the ISFSI site, where a Coast Guard Cutter is stationed. The station is accessible via the waters of Humboldt Bay as well as local access roadways connected with State Highway 255. The US Coast Guard Air Station is located at the Eureka-Arcata Airport, approximately 20 miles north of the ISFSI site. Training activities as well as actual events involving coastal surveillance and air-sea rescue missions along the Humboldt County coastline are conducted from both locations year round. The potential for military aircraft used by the Coast Guard in the area of the ISFSI has been included in the hazards for aircraft evaluation above.

2.2.1.5 Mining

There are no mining facilities within 5 miles of the ISFSI site. Generally, mining activity is minimal in Humboldt County.

2.2.2 ONSITE POTENTIAL HAZARDS

2.2.2.1 Onsite Structures and Facilities - Historical

As discussed in Section 2.2, the following is a historical discussion of two fossil-fueled units (HBPP Units 1 and 2), one shutdown nuclear unit (HBPP Unit 3), and two mobile emergency power plants (MEPPs) within the HBPP owner-controlled area that existed during the original ISFSI licensing. The original licensing analyses evaluated potential fire hazards associated with these units. Fossil-fueled Units 1 and 2 and the two MEPPs were removed and replaced with the new HBGS subsequent to the completion of the original licensing.

Figure 2.2-2A shows that the nearest industrial facilities to the ISFSI are two fossil-fueled units (Units 1 and 2) located at the HBPP site, which are approximately 100 yards east of the ISFSI and immediately adjacent to Unit 3. Units 1 and 2 are rated at approximately 50 MWe each. Each of these units is contained within individual structures and has an exhaust vent stack whose top is 120 ft above grade. The Unit 3 structure, including the spent fuel storage pool and its current vent stack whose top is 50 ft above grade, is planned to be dismantled following the transfer of all spent fuel to the ISFSI. None of the three exhaust vent stacks are close enough to the ISFSI facility or the transport route to have any potential to affect the transport operation or the storage of spent fuel in the ISFSI.

| 9-01

In addition, as shown on Figure 2.2-2A, there are two MEPPs located at the HBPP site that are rated at 15 MWe each and operate on an as-needed basis. These two plants are located approximately 300 yards east of the ISFSI, at the HBPP switchyard, and will remain in place to provide power when needed.

| 9-01

There are also several fuel oil storage tanks located in the HBPP site. The tanks include one large fuel oil storage tank (with a 2,760,169-gallon capacity), two smaller fuel oil service tanks (each with a 120,120-gallon capacity), one diesel oil storage tank (84,940 gallon capacity), and one small 120-gallon gasoline storage tank. The large tank is designated Unit 1 Fuel Oil Storage Tank. All of the tanks are used to store fuel or diesel oil in support of operation of HBPP Units 1 and 2. Table 2.2-1 lists all of the various site tank sizes and the approximate distance of each tank from the ISFSI and the historical ISFSI transport route.

Typically, the smaller fuel tanks are full, and the large tank maintains a supply of fuel oil sufficient to operate either Unit 1 or Unit 2 for 3 days in the event that natural gas supplies to HBPP are lost. Administrative controls exist at HBPP to ensure that a

sufficient fuel oil level in the large tanks is maintained, and to restrict the total quantity of oil to no greater than 1 million gallons.

The two fossil-fueled units at HBPP have the capability to be powered by either natural gas or fuel oil. However, because of California emission limitations and financial considerations, natural gas is used as the primary fuel to generate electricity from these two units on a routine basis, and fuel oil is used only when natural gas becomes unavailable. The two MEPPs at HBPP are powered by diesel fuel only.

PG&E supplies natural gas for the two fossil-fueled units via an underground pipeline, which is connected to a main line running parallel with Highway Route 101. The line into the boilers is routed underground from the offsite main around the north side of the power plants and up to the west side of the boilers. The onsite natural gas line is 12 inches in diameter and most of this gas line is below grade. The gas line is above grade: (1) at the point where the line feeds the Unit 1 and Unit 2 boilers, which is approximately 377 ft to the ISFSI, and (2) at the regulation facility on the east edge of the owner controlled area at approximately 1,100 ft from the ISFSI. This facility regulates the main gas line pressure from approximately 400 psi to 30 psi for use by the HBPP fossil fuel units.

Various facilities at HBPP also store a limited quantity of compressed gas cylinders, such as oxygen, nitrogen, and acetylene for use in various maintenance and construction activities. These compressed gas cylinders are over 200 ft from the ISFSI facility with no direct line of sight to the ISFSI or the transport route (historical).

There are no power lines, towers, or other facilities in the vicinity of the ISFSI, which could have an adverse impact on the ISFSI or the ISFSI transportation route.

2.2.2.2 Hazards from Fires and Explosions – Existing and Historical Structures and Facilities

The following sections discuss the identified potential hazards from fire and explosions for the transportation of the spent fuel to the ISFSI facility (historical), the ISFSI facility with all the vault lids in place, transport of the spent fuel and GTCC casks to an authorized offsite storage facility, maintenance activities that involve removal and reinstallation of a cask from the vault, or a vault cell lid removal for maintenance/inspections. The potential hazards discussed in these sections were identified through evaluation of both the offsite and onsite sources. Table 2.2-1 provides a summary of the various potential fires and explosive sources that were identified and evaluated. Potential hazards in the table that were deemed not credible based on meeting acceptable risk criteria from RG 1.91 were not evaluated further. The events that were found to require further evaluation were assigned event numbers and are discussed in more detail in the following sections and in Sections 8.2.5 and 8.2.6.

2.2.2.2.1 Hazards from Fires – Existing and Historical Structures and Facilities

As discussed in the previous sections there are no offsite land-based transportation accidents, pipelines, or manufacturing facilities that provide a credible exposure from fires to the ISFSI facility or the transportation route (historical). This is based on the distance to these transportation routes, the lack of facilities in the proximity of the site, the potential size of the hazards, and the terrain between any potential hazards and the ISFSI or ISFSI transport route (historical). However, there are some potential onsite sources and one offsite marine-based source that were identified and required further evaluation.

Fires are classified as human-induced or natural phenomena design events in accordance with ANSI/ANS 57.9, Design Events III and IV (Reference 8). To identify sources and to establish a conservative design basis for onsite exposure, a review was performed of the ISFSI storage site, and the complete transport route from the RFB to the ISFSI storage site (historical). The various onsite sources that were identified are discussed below and summarized in Table 2.2-1. Based on evaluation of these potential sources, the onsite events listed below were determined to require further review. Also included in this event list is the one off-site marine-based event which requires further evaluation. Unless noted, each of these events are currently applicable to the ISFSI.

- F1 Onsite transporter fuel tank fire
 - F1.1 Mobile crane or forklift
- F2 Other onsite vehicle fuel tank fires
- F3 Combustion of local stationary fuel oil and diesel oil tanks (historical)
- F4 Combustion of 7,500 gallon fuel or diesel oil tanker truck
- F5 Combustion of 3,000 gallon gasoline tanker truck and 120 gallon gasoline storage tank (historical)
- F6 Combustion of propane storage tank (historical)
- F7 Combustion of propane tanker truck (historical)
- F8 Fire from mineral oil from the Unit 3 main bank transformers (historical)
- F9 Fire from natural gas pipeline
- F10 Fire in the surrounding vegetation
- F11 Fire from 87,000 barrel-barge in bay

F12 Combustion of other local combustible materials

Locations where the potential for fire hazards occur include the ISFSI storage vault; the area immediately surrounding the ISFSI storage vault, and along the transport route between the RFB and the ISFSI storage vault (historical). Figure 2.2-2A shows the locations of the local stationary fuel oil (historical) and diesel oil tanks. Design-bases fires and their associated evaluations are discussed in Section 8.2.5. This section and Section 8.2.5 discuss various administrative controls to ensure that any fire cannot exceed a design basis for the cask.

9-01

Events F1 and F2

For the evaluation of the onsite transporter and other onsite vehicle fuel tank fires (Events F1 and F2), it is postulated that the fuel tank is ruptured, spilling all the contained fuel, and the fuel is ignited. The hydraulic oil used in the onsite transporter is non-flammable, and is therefore not a concern in the fire evaluation. The fuel tank capacity of the onsite transporter (Event F1) is limited to a maximum of 50 gallons of diesel fuel. The maximum fuel tank capacity for other onsite vehicles (Event F2) in proximity to the transport route (historical) and the ISFSI storage vault is also assumed to be 20 gallons. As discussed in Section 8.2.5, the results of Event F1 analyses indicate that the HI-STAR HB cask undergoes no structural degradation and that only a small amount of shielding material (Holtite) is damaged or lost. This Event F1 analysis bounds the 20-gallon onsite vehicle fuel tank fire (Event F2).

Event F1 is an applicable hazard in the event of a cask being removed from the vault during maintenance or during spent fuel and GTCC waste casks transfer to an authorized offsite storage facility. Administrative controls will be used consistent with the Humboldt Bay ISFSI Technical Specification CTEP.

Event F2 is an applicable hazard for the ISFSI storage mode, in the event of a vault lid being removed for inspection/maintenance, a cask being removed from the vault during maintenance, or during spent fuel and GTCC waste casks transfer to an authorized offsite storage facility. Administrative controls will be used consistent with the Humboldt Bay ISFSI Technical Specification CTEP or Vault Lid Opening Hazard Control Program, as applicable.

Event F1.1

Event F1.1 is a variation of F1 and evaluated a fire associated with a diesel-powered mobile crane that may be used to remove or reinstall a vault lid. Event F1.1 also includes a fire associated with related equipment needed to mobilize the crane in the ISFSI area, such as a diesel-powered forklift. Event F1.1 is an existing hazard for the ISFSI vault during storage, in the event of a vault lid being removed for inspection/maintenance, a cask being removed from the vault during maintenance, or

during transfer of spent fuel and GTCC waste casks to an authorized offsite storage facility.

Administrative controls will be used consistent with the Humboldt Bay ISFSI Technical Specification CTEP to ensure an engineering evaluation is completed for these items to ensure they are bounded by the HI-STAR HB design limits provided in Section 8.2 during a cask being removed from the vault during maintenance or transfer of spent fuel and GTCC waste casks to an authorized offsite storage facility. The administrative controls of the Vault Lid Opening Hazard Control Program will be utilized to ensure an engineering evaluation is completed for these items to ensure they are bounded by the HI-STAR HB design limits provided in Section 8.2 whenever a vault lid is removed for maintenance/inspections so it is not considered a hazard to these activities and is only a hazard to the ISFSI storage vault. Based on the use of the administrative controls, Event F1.1 is bounded by the F1 event for a 50-gallon onsite transporter diesel fuel tank fire.

Event F3 (historical)

Event F3 evaluated the onsite stationary fuel oil tanks associated with HBPP Units 1, 2, and 3 (which have been removed and are listed in Table 2.2-1 as historical) and the ISFSI backup diesel generator fuel tank. Descriptions of the Event F3 fuel oil and diesel tanks and associated fire evaluations are provided below. The Event F3 evaluation methodology and hazard analysis are relied upon as a bounding evaluation for the onsite stationary diesel tanks associated with the HBGS and the ISFSI as discussed below.

The ISFSI vault is embedded in a hill that is approximately 44 ft in elevation and at least 20 ft above the elevation of the various fuel and diesel oil tanks except for the ISFSI backup diesel generator fuel tank (which will not exceed 200 gallons). The backup diesel generator tank is positioned so that any liquid spilled from a breach in its fuel tank and environmental containment would not run toward the cask area. Thus, there is no chance that a liquid fuel type fire from a hazard would move toward the ISFSI facility from its origin.

All onsite stationary fuel oil or diesel tanks (Event F3) are at least 198 ft from the ISFSI facility, and (historical) transport route (Figure 2.2-2A), and are surrounded by berms, except for the ISFSI backup diesel generator fuel tank, which will not exceed 200 gallons and which is surrounded by a containment, and is over 100 feet from the nearest cask. Although ignition of fuel oil or diesel fuel oil is not considered a credible event because of their high flash point, the existing stationary fuel oil and diesel tanks have been evaluated as discussed in Section 8.2.5. That evaluation found that because of the tank distances to the transport route (historical) or the storage facility, the total energy potentially received from these hazards is insignificant compared to the design basis fire event.

Event F4

9-01

HUMBOLDT BAY ISFSI FSAR UPDATE

The onsite fuel and diesel oil tanks are periodically filled by standard tanker trucks with a capacity of up to 7,500 gallons. The trucks can pass by the ISFSI facility. Although ignition of the fuel in these tanker trucks is not considered credible based on the high flash point of their contents, an analysis was performed for a ruptured 7,500 gallon fuel oil tanker truck (Event F4) at 80 ft from the ISFSI and is discussed in Section 8.2.5. The diesel fuel oil tanker truck passes the ISFSI at a similar distance and the evaluation of the fuel oil tanker truck is considered to bound the diesel oil truck.

Administrative controls will be used consistent with the Humboldt Bay ISFSI Technical Specification CTEP to ensure the tanker trucks are not allowed in the ISFSI vicinity during a cask being removed from the vault during maintenance or transfer of spent fuel and GTCC waste casks to an authorized offsite storage facility. The administrative controls of the Vault Lid Opening Hazard Control Program will be utilized to ensure these hazards do not adversely impact the ISFSI whenever a vault lid is removed for maintenance/inspections and is only a hazard to the ISFSI storage vault.

Event F5 (historical)

Event F5 evaluated a small 120-gallon storage tank located on the west side of the HBPP site and an associated 3,000-gallon capacity tanker truck. This tank was associated with HBPP Units 1, 2, and 3, has since been removed, and is listed in Table 2.2-1 as historical. Historical administrative controls were used to ensure the tanker truck was not allowed on the site during transport operations so it was not considered a hazard to the transport operation and was only a hazard to the ISFSI. These events are evaluated in Section 8.2.5 and their resulting fires are acceptable and bounded by the Event F1 fire.

Events F6-F8 (historical)

Events F6-F8 have been deleted since the hazard source is no longer present. The evaluation of events F6-F8 are no longer relied upon.

Event F9

Event F9 evaluated the natural gas pipeline fire hazard associated with Humboldt Units 1 and 2. The low pressure portion of the natural gas pipeline (30 psi) has been removed and is listed in Table 2.2-1 as historical. The high pressure portion of the natural gas pipeline (400 psi, upstream of the regulating station) supplies the new HBGS natural gas pipeline and is an existing hazard.

The following is a description and evaluation of the natural gas pipeline for Units 1 and 2. Those descriptions associated with the low pressure portion of the natural gas pipeline are historical. There is a 12-inch natural gas line that enters the HBPP site from the west and supplies fuel to Units 1 and 2. This gas line has a regulating station at the edge of the owner-controlled area of the site that reduces the line pressure from above

HUMBOLDT BAY ISFSI FSAR UPDATE

400 psi to the service pressure of 30 psi. The 30 psi portion of the line is shutoff and depressurized during transport operations and is therefore not a hazard to the transporter and is only a concern to the ISFSI when it is pressurized. However, the high pressure side of the regulating station is a concern to both the transporter and the ISFSI. In Section 8.2.5 these hazards are evaluated and the results are acceptable and bounded by the Event F1 fire.

The natural gas pipeline supplying the HBGS is discussed as Event FH in Section 2.2.2.6.1.

Event F10

Event F10 concerns the native vegetation surrounding the ISFSI storage vault, which is primarily grass, with some small brush and trees. Maintenance programs will prevent uncontrolled growth of the vegetation in the area immediately outside the ISFSI **Security Area Fence**, out to a distance of 50 feet from the **Security Area Fence**.

9-01

As discussed in Section 8.2.5, a conservative fire model was established for evaluation of grass fires, which has demonstrated that grass fires are bounded by the 50-gallon transporter fuel tank fire evaluation.

For the ISFSI site, the Security Area not covered by the storage vault will be covered with crushed rock approximately 12 inches deep. The Security Area consists of the vault structure and an isolation zone (a minimum 20 ft distance between the vault and the fence). A maintenance program will control any significant growth of vegetation through the crushed rock. Therefore, the surface of the Security Area will be noncombustible.

Event F11

The one offsite marine-based fire hazard is from an 87,000 barrel gasoline barge in Humboldt Bay (Event F11). This event has been evaluated as discussed in Section 8.2.5.

Event F12

No combustible materials will be stored within the Security Area around the ISFSI storage vault at any time. In addition, prior to a vault lid being removed for inspection/maintenance, a cask being removed from the vault during maintenance, or during transfer of spent fuel and GTCC waste casks to an authorized offsite storage facility, a walkdown of the general area and transportation route will be performed to ensure all local combustible materials (Event F12), including all transient combustibles, are controlled in accordance with administrative procedures.

9-01

In summary, as discussed in above and in Section 8.2.5, the potential effects of any of these postulated fires from Events F1-F12 have been found to be insignificant or

acceptable. The physical layout of the Humboldt Bay ISFSI and the administrative controls on fuel sources ensures that the general design criteria related to fire protection specified in 10 CFR 72.122(c) are met (Reference 9).

2.2.2.2.2 Explosion Hazards – Existing and Historical Structures and Facilities

As discussed in the previous sections, there are no offsite land-based transportation accidents, pipelines, or manufacturing facilities that provide a credible exposure from explosions to the ISFSI facility. However, there is one potential offsite land-based hazard that could affect the transportation route (historical) and is discussed in this section. In addition, there are various onsite hazards and one offsite marine-based hazard that are discussed below.

As discussed in Section 2.2, some of the hazards discussed below are related to the original licensing analyses evaluated for potential explosion hazards associated with the fossil-fueled HBPP Units 1 and 2, shutdown nuclear unit (HBPP Unit 3) and mobile emergency power plants (MEPPs). Fossil-fueled Units 1 and 2 and MEPPs were removed and replaced with the new HBGS subsequent to the completion of the original licensing. Historical events are annotated as such.

Explosions are classified as human-induced or natural phenomena design events in accordance with ANSI/ANS 57.9 Design Events III and IV. To determine the potential explosive hazards, which could affect the ISFSI or the spent fuel during transport (historical), a review of the ISFSI storage area and the transportation route from the Unit 3 RFB was completed. The various onsite sources that were identified are discussed below and summarized in Table 2.2-1. Based on evaluation of these potential sources, the events listed below were determined to require further review:

- E1 Detonation of the bulk propane storage facility (historical)
- E2 Detonation of onsite natural gas line
- E3 Propane tanker truck (historical)
- E4 Detonation of the gasoline tanker and the 120-gallon gasoline storage tank (historical)
- E5 Detonation of a transporter or other onsite vehicle fuel tank
- E5.1 Detonation of a mobile crane or forklift fuel tank
- E6 Detonation of vehicles on Route 101
- E7 Fossil power plant explosion (fixed or mobile units) (historical)
- E8 Detonation of 87,000 barrels fuel barge

E9 Explosive decompression of compressed gas bottles

Figures 2.2-2A and 2.2-2B show the location of the stationary potential explosion sources. Events E1, E2, E4, E6, and E7 are assumed to occur in the vicinity of the ISFSI storage vault or transport route (historical) and potentially affect the loaded overpack in transport (historical) or in storage. Events E3, E5, E5.1, E8, and E9 occur in the vicinity of the ISFSI vault and will only potentially affect the storage system. This section also discusses various administrative controls to ensure that any potential explosion hazards will meet the RG 1.91 criteria. These administrative controls are further discussed in Section 8.2.6.

9-01

Event E1 (historical)

Event E1 was precluded by the removal of the onsite propane storage tank in 2010.

Event E2

Event E2 evaluated the natural gas pipeline explosion hazards associated with Humboldt Units 1, 2, and 3. The low pressure portion of the natural gas pipeline (30 psi) has been removed and is listed in Table 2.2-1 as historical. The high pressure portion of the natural gas pipeline (400 psi, upstream of the regulating station) supplies the new HBGS natural gas pipeline and is an existing hazard. The natural gas pipeline explosion evaluation for the HBGS is discussed in Section 2.2.2.6.2 as Event EA.

The following is a description and evaluation of the natural gas pipeline for Units 1 and 2. Those descriptions associated with the low pressure portion of the natural gas pipeline are historical. For Event E2 there are four credible explosive scenarios that involve the detonation of the onsite 12-inch gas line. The first involves an immediate detonation at a point on the low pressure onsite pipeline between regulating station at the edge of the owner-controlled area and Units 1 and 2 boilers (historical). This could be from a leak or break in the line anywhere along its length. The second is the detonation of a vapor cloud from a leak or break as it moves across the HBPP site (historical). Neither of these scenarios is considered credible for the transport of spent fuel (historical), as administrative controls will require the gas line from the regulating station to the boilers be shut off and depressurized during transport. The third scenario involves a leak or break and local detonation of the high pressure side of the regulating station. The fourth scenario is the detonation of a vapor cloud from the high pressure leak or break as it moves across the site. Section 8.2.6 evaluates the effect of these explosive scenarios on both the transportation to and storage at the ISFSI facility.

Event E3 (historical)

Event E3 was precluded by the removal of the onsite propane storage tank in 2010.

Event E4 (historical)

The following is a historical description and evaluation of the 120-gallon gasoline storage tank and the gasoline tanker truck for HBPP Units 1, 2, and 3. Event E4 concerns the detonation of a 120-gallon gasoline storage tank and the gasoline tanker truck that periodically fills this tank. This event was historically evaluated for both the transportation and storage. Historical administrative controls did not allow the tanker onsite during transport operations.

9-01

Event E5

In Event E5, the transporter uses diesel fuel. Detonation of diesel fuel used in any onsite vehicle is not considered credible because of its high flash point. As a result, the evaluation of Event E5 is limited to a gasoline-powered vehicle with a maximum fuel tank size of 20 gallons. This evaluation is discussed further in Section 8.2.6.

Event E5.1

Event E5.1 is a variation of E5 and evaluated a diesel-powered mobile crane that may be used to remove or reinstall a vault lid. Event F1.1 also includes a fire associated with related equipment needed to mobilize the crane in the ISFSI area, such as a diesel-powered forklift. Detonation of diesel fuel used in any onsite vehicle is not considered credible because of its high flash point.

Event E6

Event E6 involves a vehicle crash on Route 101 and its potential affect on the ISFSI transport route (historical) or during transfer of the spent fuel and GTCC waste casks to an authorized offsite storage facility. This is not a concern for the ISFSI facility itself because the distance exceeds the acceptance criteria in RG 1.91. However, it is a concern for the historical transport route and during transfer of the spent fuel and GTCC waste casks to an authorized offsite storage facility and is discussed in Section 8.2.6.

Event E7 (historical)

Event E7 involves a fossil power plant explosion (fixed or mobile units). There are built-in safety provisions at HBPP Units 1 and 2, as well as in the mobile generators, that are designed to prevent explosions and fires and to avoid undetected leakage. Similarly, explosions of steam boilers at the power plants are precluded by design requirements as required by codes and standards. However, there have been industry events of this type and therefore this was evaluated as discussed in Section 8.2.6.

Event E8

Event E8 involves the detonation of an 87,000-barrel gasoline barge in the bay adjacent to the ISFSI facility. This event is not considered to be a credible event for the transport of spent fuel (historical), as administrative controls under the Humboldt Bay ISFSI Technical Specification CTEP will ensure that no transport of fuel takes place when this barge is moving through the bay. Section 8.2.6 discusses an evaluation of this hazard for the ISFSI.

There are several other large stationary fuel oil and diesel fuel oil tanks in the vicinity of the ISFSI vault. These are not considered a credible explosion source because of their high flash point and the lack of local ignition sources. In addition, the fuel oil or diesel fuel oil delivery tankers which travel in the vicinity of the ISFSI vault are also not considered a credible detonation source because of the high flash points of their content. For these tankers, administrative controls will preclude these trucks being within the owner-controlled area during the vault lid being removed for inspection/maintenance, a cask being removed from the vault during maintenance, or during transfer of spent fuel and GTCC waste casks to an authorized offsite storage facility.

Event E9

Various buildings at the HBPP site also store a limited quantity of compressed gas cylinders, such as oxygen, nitrogen, and acetylene for use in various maintenance activities. Event E9 involves the missile created by the explosive decompression of a gas cylinder assuming that a compressed gas cylinder under high-pressure is damaged such that the valve assembly located at the top of the cylinder breaks off. Section 8.2.6 discusses an evaluation of this hazard for the ISFSI.

In summary, there are no onsite hazards in the area of the ISFSI facility that will have a significant impact on the transport (historical) or storage of spent fuel. During a cask being removed from the vault during maintenance or during transfer of spent fuel and GTCC waste casks to an authorized offsite storage facility, all activities will be controlled under a Humboldt Bay ISFSI Technical Specification CTEP. In addition, the Vault Lid Opening Hazard Control Program administrative controls will be utilized to ensure these hazards do not adversely impact the ISFSI whenever a vault lid is removed for maintenance/inspections.

2.2.2.3 Turbine Missiles – Historical

There is an onsite potential for a turbine missile event from either HBPP Unit 1 or 2. Although these types of events are rare, they do occur. This event is not considered to be credible for effect on the ISFSI facility because the turbines for these units are configured to be perpendicular to the ISFSI and more than 400 ft away. Since these types of events cause damage radially from the centerline of the turbine there will be no affect on the ISFSI facility. However, the configuration of the turbines could potentially affect the transport of spent fuel as the transport route runs parallel with the turbines. As a result, this potential for this event has been evaluated and found acceptable as discussed in Section 8.2.13.

2.2.2.4 Chemical Hazards – Historical

A walkdown of all chemical hazards was performed in the area of the ISFSI and along the transport route. Although there were some chemical hazards identified that could potentially have an effect on the ISFSI or the transport system, none were found to be significant. To ensure minimum potential for any chemical hazards, administrative controls provided to control fire and explosive hazards above will also include identification, control, and evaluation of hazardous chemicals.

2.2.2.5 Onsite Structures and Facilities – New HBGS Facility

Figure 2.2-2B shows the location of a new fossil-fueled power plant at the HBPP site, named the Humboldt Bay Generating Station (HBGS). The HBGS is a load following plant consisting of 10 natural gas-fired reciprocating engine-generator sets and associated equipment with a combined generating capacity of 163 MWe (nominal). Much of the information presented in this section describing HBGS design, operation, and potential hazards has been derived from PG&E's Application for Certification to construct the HBGS made to the California Energy Commission on September 29, 2006 (Reference 12).

| 9-01

The HBGS is located approximately 450 ft east of the ISFSI and, at its nearest boundary, is approximately 20 ft from historical Unit 3 and the beginning of the historical cask transport route from the Unit 3 RFB. The HBGS has the capability to be powered by either natural gas or diesel fuel oil. Primary operation will be with natural gas, with low-sulphur diesel fuel used only as a backup during times of natural gas curtailment. Natural gas for the HBGS is supplied via an underground pipeline, which is connected to a main line running parallel with Highway Route 101. The line into the HBGS is routed through a regulation facility on the east edge of the owner-controlled area at approximately 1100 ft from the ISFSI. The onsite natural gas line for the HBGS is 10 inches in diameter and runs into the eastern side of the power building, where it is distributed to the reciprocating engines.

Major storage tanks that provide support to the HBGS and are potential fire and explosion hazards include:

- Two 27,000 gal aqueous ammonia storage tanks
- A 5,500 gal corrosion inhibitor storage tank
- A 634,000 gal diesel fuel oil tank
- Ten 3,300 gal hydraulic oil tanks, one for each engine
- A 21,100 gal clean lube oil tank and a 9,200 gal dirty lube oil tank

- A 15,870 gal mineral insulating oil tank
- A 12,000 gal lubrication oil tank

2.2.2.6 Hazards from Fires and Explosions – New Structures and Facilities

The following sections discuss the identified potential hazards from fires and explosions associated with the HBGS that could affect the ISFSI facility during storage and other activities such as the vault lid being removed for inspection/maintenance, a cask being removed from the vault during maintenance, or during transfer of spent fuel and GTCC waste casks to an authorized offsite storage facility. Table 2.2-1 provides a summary of both historical and existing potential fires and explosive sources that were identified and evaluated. Potential hazards in the table that were deemed not credible based on meeting acceptable risk criteria from RG 1.91 were not evaluated further. The HBGS events that were found to require further evaluation were assigned event designations A through H for fire hazards and designation A for an explosion hazard and are discussed below.

2.2.2.6.1 Hazards from Fires – New Structures and Facilities

Fires are classified as human-induced or natural phenomena design events in accordance with ANSI/ANS 57.9, Design Events III and IV (Reference 8). To determine the potential fire hazards at the HBPP that could affect the ISFSI in the storage mode, or other activities such as the vault lid being removed for inspection/maintenance, a cask being removed from the vault during maintenance, or during transfer of spent fuel and GTCC waste casks to an authorized offsite storage facility, a review was performed of the potential fire hazards. The fire sources associated with the HBGS that were identified are summarized in Table 2.2-1.

Based on evaluation of these potential fire sources, several were bounded by evaluations performed for the historical onsite structures and facilities (see Table 2.2-1). Those HBGS events bounded by previously evaluated events and those determined to require further review are listed below:

- | | |
|----|--|
| FA | Aqueous ammonia tank fire |
| FB | Corrosion inhibitor tank fire |
| FC | Combustion of diesel oil tanks |
| FD | Combustion of hydraulic oil tanks |
| FE | Combustion of lube oil tank |
| FF | Combustion of mineral insulating oil and lubricating oil tanks |

HUMBOLDT BAY ISFSI FSAR UPDATE

- FG Truck transport to supply any of the HBGS fire sources listed above
- FH Fire from natural gas pipeline

Event FA

Event FA involves aqueous ammonia which is incombustible in its liquid state. Under normal storage conditions, ammonia would not evaporate to the atmosphere because it will be contained within two totally enclosed, 27,000 gal tanks, each equipped with ventilation as required by Article 80 of the California Fire Code. In the unlikely event that a release were to occur, the ammonia spilled into the catch basin or bermed area beneath the tank could evaporate and form a vapor cloud. Ammonia vapor is combustible only within a narrow range of concentrations in air. The potential effects from the burning vapor are bounded by evaluations performed for other existing onsite fuels (Events F3 and F4) based on volume and distance from the ISFSI storage vault. There is also no credible threat from explosion of the aqueous ammonia, as the evaporation rate of aqueous ammonia is similar to water, which is sufficiently low that the lower explosion limit of 15 percent (or 15 ppm) would not be reached. In addition, the potential for a vapor cloud from a leak in the tank is not considered credible based on the low potential of a tank leak or break, the short duration of cask exposure, and the prevailing winds being from west to east away from the ISFSI.

Of more significance, the aqueous ammonia is classified as a regulated substance, and an accidental release of the 19 percent aqueous solution would present a significant health hazard. The ammonia is subject to the requirements of the California Fire Code, Article 80, as well as the California Accidental Release Program (CalARP). The facility has prepared a Risk Management Plan in accordance with CalARP regulations, further specifying safe handling procedures for the ammonia as well as emergency response procedures in the event of an accidental release. This Plan shows that plant and security personnel are protected from the health effects of an accidental release of the ammonia.

Event FB

Event FB involves a corrosion inhibitor which is inserted into the cooling water for the radiator array and jacket water circuit of the reciprocating engines. The corrosion inhibitor is contained in the radiator array and the jacket water circuit for the engines. The closest point to the ISFSI is greater than 600 ft and greater than 90 ft from the historical transport route. The inhibitor is combustible, but has a high flash point. The corrosion inhibitor is not considered to be a significant fire hazard because its flash point is greater than the average ambient temperature for the site. The effect on the ISFSI vault is bounded by Event F3 based on volume and distance.

Event FC

HUMBOLDT BAY ISFSI FSAR UPDATE

Event FC involves Diesel No. 2 fuel oil stored in a 634,000 gal tank as a backup fuel for operation of the reciprocating engines and in a 600 gal tank for a black start and fire pump operation. The diesel tanks are located greater than 900 ft from the ISFSI vault and greater than 350 ft from the historical transport route; both tanks are bermed. Diesel No. 2 is combustible, but has a high flash point. The effects of a fire in these tanks on the ISFSI vault during storage, or other activities such as the vault lid being removed for inspection/maintenance, a cask being removed from the vault during maintenance, or during transfer of spent fuel and GTCC waste casks to an authorized offsite storage facility, is bounded by Event F3 evaluation for other fuels based on volume and distance.

Event FD

Event FD involves hydraulic oil which is contained in ten 3,300 gal tanks, one for each engine. The tanks/engines are located greater than 900 ft from the ISFSI vault and greater than 20 ft from the historical transport route. The hydraulic oil can be combustible, but it has a high flash point. The effects of a fire in these tanks on the ISFSI vault during storage, or other activities such as the vault lid being removed for inspection/maintenance, a cask being removed from the vault during maintenance, or during transfer of spent fuel and GTCC waste casks to an authorized offsite storage facility, is bounded by Event F3 evaluation for other fuels based on volume and distance.

Event FE

Event FE involves lubricating oil for operation of the reciprocating engines which is stored in a 21,100 gal clean lube oil tank and in a 9,200 gal dirty lube oil tank, both of which are bermed. The total amount of lube oil onsite, including that in the engines, is 34,500 gal. The storage tanks are located on the east side of the HBGS, greater than 800 ft from the ISFSI vault and greater than 200 ft from the historical transport route. The lube oil is flammable. The ISFSI and cask have been analyzed and determined to be unaffected for over 120,000 gal of fuel oil burning at a distance of 198 ft (Event F3). As a result, this event is considered bounded by the previous evaluation of Event F3. The effects of a fire in these tanks on the ISFSI vault during storage, or other activities such as the vault lid being removed for inspection/maintenance, a cask being removed from the vault during maintenance, or during transfer of spent fuel and GTCC waste casks to an authorized offsite storage facility, is bounded by Event F3 evaluation for other fuels based on volume and distance.

Event FF

Event FF involves mineral insulating oil which is contained within the transformers for a total of 15,870 gallons on site. The closest transformer is greater than 550 ft from the ISFSI vault and greater than 20 ft from the historical transport route; and mineral lubrication oil which is contained in each of the engine generators within the engine hall. There is a total of 12,000 gallons onsite. The closest engine generator is greater than

600 ft from the ISFSI vault and greater than 20 ft from the historical transport route. Mineral oil can be combustible, depending on the manufacturer, but has a high flash point. The effects of a fire in these tanks on the ISFSI vault during storage, or other activities such as the vault lid being removed for inspection/maintenance, a cask being removed from the vault during maintenance, or during transfer of spent fuel and GTCC waste casks to an authorized offsite storage facility, is bounded by Event F3 evaluation for other fuels based on volume and distance.

Event FG

Event FG involves trucks that are used to transport the hazardous materials onsite to refill the HBGS tanks described above. . . All trucks transporting hazardous materials to the HBGS are normally greater than 400 ft from the ISFSI vault. During a cask being removed from the vault during maintenance, or during transfer of spent fuel and GTCC waste casks to an authorized offsite storage facility, the Humboldt Bay ISFSI Technical Specification CTEP will prohibit HBGS trucks use of the roads near the ISFSI. In addition, the Vault Lid Opening Hazard Control Program administrative controls will be utilized to prohibit HBGS trucks use of the roads near the ISFSI whenever a vault lid is removed.

As a result of the distance of these vehicles from the ISFSI vault and the fact that the ISFSI is elevated above the potential path of these vehicles and any potential spills, this event is considered bounded by the Event F4 evaluation.

Event FH

Event FH involves the location and operation of the onsite natural gas pipeline supply to the HBGS reciprocating engines, which is described in Section 2.2.2.5. The potential effect of a natural gas fire on the ISFSI vault is bounded by the Event F1 analysis provided in Section 8.2.5.2.2.6. In addition, the new HBGS natural gas pipeline is equipped with automatic gas shutoff valves.

2.2.2.6.2 Explosion Hazards – New Structures and Facilities

Explosions are classified as human-induced or natural phenomena design events in accordance with ANSI/ANS Design Events III and IV. To determine the potential explosive hazards at the HBGS that could affect the ISFSI or the spent fuel during transport (historical), a review of the ISFSI storage area and the historical transportation route from the Unit 3 RFB was completed. The various onsite explosion sources that were identified are discussed below and summarized in Table 2.2-1. Those determined to require further review are listed below:

EA Detonation of onsite natural gas pipeline

Event EA involves the location and operation of the onsite natural gas pipeline supplying the HBGS reciprocating engines which is described in Section 2.2.2.5.

The potential effect of a natural gas explosion on the ISFSI vault during long-term storage is bounded by the Event E2 analysis provided in Section 8.2.6.2.2. The potential effect of a natural gas explosion during a vault lid removal event for maintenance/inspections, a cask being removed from the vault during maintenance, or during transfer of spent fuel and GTCC waste casks to an authorized offsite storage facility is not credible due to the new HBGS gas pipeline being equipped with automatic gas shutoff valves, distance from the ISFSI vault, and the prevailing winds being from west to east away from the ISFSI vault, as discussed in Section 8.2.6.2.2.

2.2.2.6.3 Turbine Missiles – New Structures and Facilities

High-speed turbines are not a part of the HBGS; therefore, turbine missiles from the HBGS are not a credible threat to the activities occurring at the ISFSI vault, the historical spent fuel transport route, or the future transport of spent fuel and GTCC waste casks to an authorized offsite storage facility.

2.2.2.7 Chemical Hazards – New Structures and Facilities

Potential chemical hazards associated with the HBGS that could affect the ISFSI or the historical spent fuel transport route have been evaluated.

2.2.3 SUMMARY

In summary, there is no credible accident scenario involving any industrial, transportation, or military facilities in the area around the ISFSI site that will have any significant adverse impact on the transportation and storage of fuel in the ISFSI.

2.2.4 REFERENCES

1. FAA Speed Memo dated 04/25/03 from Michael Rae Cooke, FOIA Officer ANM-505.4, subject: FOIA 2003-073-3, 2003-005018NM; federal airways.
2. Regulatory Guide 1.91, Evaluations of Explosions Postulated to Occur on Transportation Routes near Nuclear Power Plants, US Nuclear Regulatory Commission, February 1978.
3. Standard Review Plan for the Review of Safety Analysis Reports for Nuclear Power Plants, USNRC, NUREG-0800, July 1981.
4. Calculation PRA-03-14, Risk Assessment of Aircraft Hazard for Dry Cask/Spent Fuel Transportation and Storage for Humboldt Bay ISFSI, Revision 1, July 2004.
5. Memorandum for John F. Cordes, Director, Office of Commission Appellate Adjudication, dated November 14, 2001, Subject: Staff Requirements – Affirmation Session, 8:55 A.M., Wednesday, November 14, 2001, Commissioners' Conference Room, One White Flint North, Rockville, Maryland (Open to Public Attendance), Reference M011114A.

HUMBOLDT BAY ISFSI FSAR UPDATE

6. Federal Aviation Administration Long-Range Forecast, 1999.
7. DOE-STD-3014-96 Accident Analysis for Aircraft Crash Into Hazardous Facilities, US Department of Energy, October 1996.
8. ANSI/ANS 57.9, 1992, Design Criteria for an Independent Spent Fuel Storage Installation (Dry Storage Type), American National Standards Institute.
9. 10 CFR 72, Licensing Requirements for the Independent Storage of Spent Nuclear Fuel and High-Level Radioactive Waste.
10. PG&E Letter HIL-04-007, Response to NRC Request for Additional Information for the Humboldt Bay Independent Spent Fuel Storage Installation Application, October 1, 2004.
11. Safety Evaluation Report for the Humboldt Bay Independent Spent Fuel Storage Installation, Materials License SNM-2514, November 2005.
12. PG&E Submittal to the California Energy Commission, Application for Certification to Construct the Humboldt Bay Repowering Project, September 29, 2006.

2.3 CLIMATOLOGY AND METEOROLOGY

2.3.1 REGIONAL CLIMATOLOGY

The climate of the greater Humboldt Bay region, including Eureka and the immediate coastal strip where the project site is located, is characterized as Mediterranean. Summers have little or no rainfall and low overcast and fog are frequently observed. Winters are wet, with frequent passage of Pacific storms, and temperatures are mild.

Because of close proximity to the ocean and bay, the region experiences high relative humidity throughout the year. The humidity is generally highest in the late night and early morning hours when the coastal stratus and fog are most prevalent. At these times the humidity averages 87 percent. During the late morning and early evening hours, the humidity decreases to an average of 78 percent.

The coastal range mountains extend south from the State of Washington to near San Francisco, passing around the Humboldt Bay region. The coastal hills surrounding Humboldt Bay begin with Patrick's Point, 30 miles to the north, then extend to the southeast, then to the southwest, ending in Cape Mendocino, 23 miles from the site. The tops of these hills range from 1,500 to 2,500 ft, with the highest point (Kings Peak) reaching 4,087 ft, 40 miles directly south of Eureka. These hills greatly modify the rainfall and temperatures of the region by creating a rain shadow and sheltering the region from the brunt of the heavier rainfall and temperature extremes.

As winter storms move in from the Pacific and Gulf of Alaska, the prefrontal winds are generally from the southeast to southwest. Over the Humboldt Bay region, the hills generally deflect these winds south to southeast. After frontal passage, the winds are generally from the north to northwest.

The cold and unstable air that follows many of the winter systems causes Eureka to experience most of its thunderstorm activity. This is also when the region receives most of its hail and/or ice pellets (note that thunderstorms in the summer are extremely rare).

In the adjacent ocean water, the California current flows south along the coast constantly modifying the colder air behind any frontal activity. The sea surface temperature averages 50 to 52°F in the winter and protects Eureka from the frigid temperatures that accompany winter storms.

The ring of hills surrounding the area also contributes to the marine effects in the summer. Sea surface temperatures average 55 to 57°F in the summer and this strongly influences air temperature. Extensive fog and low clouds are a frequent occurrence during the summer. The fog and stratus usually retreat offshore late in the morning and early afternoon and returns during the night.

The marine layer is typically 800 to 1,500 ft thick. There are also periods when the day to night cycle is broken, and the entire area remains under continuous low clouds and fog for days on end.

2.3.1.1 Temperature, Dew Point Temperature, and Relative Humidity

Temperatures in Eureka and much of the surrounding bay experience relatively small change in the daily and seasonal ranges. In the summer, the daily average range of temperatures is within 10°F, but with fog and stratus over the area, the daily range can be as low as 2°F. In the winter, the average daily range is larger with an average 14°F spread.

Most summertime record high temperatures occur when offshore flow develops when the inland valleys are under the influence of a thermal low-pressure trough. As the thermal low moves west towards the coast, the stratus and fog disappear and clear weather prevails over much of the region. The ambient temperature range has varied from a low of 20°F recorded on January 14, 1888, to a high of 87°F recorded on October 26, 1993 (Reference 1).

Other temperature statistics include:

- | | |
|---|---|
| • Coldest Maximum Temperature | 33°F on Feb. 08, 1900 |
| • Highest Daily Average Temperature | 73°F on Sept. 21, 1939 |
| • Warmest Minimum Temperature | 63°F on Aug. 27, 1894,
Feb. 26, 1980, Jan.14, 1981 |
| • Lowest Daily Average Temperature | 28°F on Jan. 14, 1888 |
| • Number of days per year when high
or low Temperature is: | |
| ⇒ Greater than 90°F | 0 (Period of record 1941 - 1992) |
| ⇒ Less than 32°F | 5 (Period of record 1941 - 1992) |

Based on hourly observations at Arcata/Eureka National Weather Service Station during 1949 to through 2001, daily and monthly averages of temperatures, dew point temperature, and relative humidity representative of the ISFSI project area are presented in Table 2.3-1. Within that data period, the maximum and minimum observed dew point temperature was 68 and 3°F, respectively, and the maximum and minimum observed relative humidity was 100 and 9 percent, respectively (Reference 2).

2.3.1.2 Precipitation

Precipitation records at Eureka are representative of the ISFSI site. During the rainy season, generally November through March, Eureka receives about 75 percent of its average annual rainfall, with greatest monthly totals in December and January. The average annual rainfall over the 110 year period at Eureka is 38.87 inches. This is one of the lowest averages in northwest California and is caused by a rain shadow due to the surrounding hills and minimal uplifting along the immediate west facing beaches.

HUMBOLDT BAY ISFSI FSAR UPDATE

The rain shadow effect can be seen by comparing Eureka's average rainfall with nearby sites surrounding the area. For example, at Patrick's Point State Park, 24 miles north of Eureka, the average rainfall is 60.79 inches and at Scotia, 23 miles south, the rainfall averages 47.20 inches and at Willow Creek, 29 miles east of Eureka, the average is 48.34 inches (Reference 1). There is clearly substantial variation within relatively small distances. Table 2.3-2 shows a list of maximum rainfall statistics and several calculated return periods (Reference 3). Annually, there is an average of 117 days with precipitation greater than or equal to 0.01 inch and 8 days with precipitation greater than or equal to 1.00 inch, based on the 1971 to 2000 period (Reference 4).

In general, frozen precipitation falls as small hail or ice pellets. This occurs after the passage of a moderate to strong cold front, with its cold, unstable air mass. Eureka has received snow on rare occasions, and because it is so rare, annual normal snowfall is just a trace (0.3 inches). The record storm of 1907 produced most of Eureka's snowfall records. There are 12 other snowfalls of note during the 110-year data base. All other snowfall events have been less than 1 inch, and the majority of those have been reported just as a "Trace" (Reference 1). Table 2.3-3 shows the design basis snowfall parameters applicable for the Humboldt Bay Power Plant (HBPP). No published statistics were available for the frequency of ice storms in the Eureka area.

2.3.1.3 Winds

The wind direction and speeds in Eureka are governed by the seasonal location of the eastern Pacific high pressure system and the low pressure systems that bring the winter storms to the northwest coast. For about three quarters of the year, the region experiences prevailing winds from the north to northwest as the semi-permanent high pressure settles over the Pacific Ocean to the west of Eureka. During the winter, the winds are generally from the south to southeast as the weather is largely influenced by low-pressure systems that originate in the Gulf of Alaska. Figure 2.3-1 shows the directional distribution based on the period 1905 through 1996.

The lack of an easterly wind component is caused by the hills surrounding the region blocking the east winds from reaching the coast. When east winds do occur, they occur in the late night or early morning and are due to down slope flows from the surrounding hills. Eureka's highest daily wind speed is 38.2 mph for the 24-hour period on April 29, 1915. The highest peak gust is 69 mph and was recorded twice, both in 1981. The first occurred on January 21 and the second on November 13. Table 2.3-4 shows peak gusts recorded at Eureka between 1887 and 1996 (Reference 1). The 50-year, return period for a 1-minute average wind speed is 58 mph with an expected 50-year, peak gust of 71 mph (Reference 5).

2.3.1.4 Tornadoes and Thunderstorms

The Eureka area experiences relatively few tornadoes. Over the period 1950 through 1995 there was one tornado recorded in the Eureka area. It occurred on

HUMBOLDT BAY ISFSI FSAR UPDATE

March 29, 1958, and was reported as an F2 in force (winds 113-157 mph) on the 7 point Fujita scale F0 to F6 (Reference 6).

During the wet season, the thunderstorm frequency is one day per month (Table 2.3-5). Only infrequent (less than one per day per month) thunderstorm activity occurs during the dry season. There is no published information on the frequency of lightning strikes.

2.3.1.5 Solar Radiation

Solar radiation data considered representative of the Humboldt Bay Independent Spent Fuel Storage Installation (ISFSI) site are available from the Renewable Resources Data Center's website <http://rredc.nrel.gov/>. Statistics of measurements made at Arcata Airport during 1961 through -1990 are available. Arcata Airport is located approximately 17 miles north-northeast of the ISFSI site. Maximum flat-plate solar radiation measured at the Arcata site was 7.0 kwh/m²/day in May. This is equivalent to 602 g-cal/cm²/day.

2.3.2 LOCAL METEOROLOGY

Meteorology for the HBPP was reviewed as part of the Environmental Report for Decommissioning in July 1984 (Reference 7). Data acquired by the National Weather Service (NWS) and other sources are summarized below. The first Eureka weather station was established by the U. S. Army Signal Service on December 1, 1886. Since that date there has been continuous weather observations within the region. The current NWS Office is located on Woodley Island about 6 miles northeast of HBPP. All of the data described in Section 2.3.1, except the tornado data, were compiled from local meteorology. Figure 2.3-2 shows the average monthly rainfall recorded at Eureka and Figure 2.3-3 shows the maximum rainfall for each month over the 110-year period of record. Figure 2.3-4 shows the average temperature by month over the period of record and Figure 2.3-5 shows the maximum and minimum temperatures at Eureka (Reference 1). A map showing the detailed topographic features within 8 km is shown in Figure 2.3-6 and a smaller scale map of topographic features out to 16 km is shown in Figure 2.3-7. Profiles of maximum elevation versus distance from the ISFISI site, out to 16 km, for each 22.5 degree compass point sectors are shown in Figures 2.3-8, a-i. Note that sectors 247.5 through 067.5 degrees are over the ocean and are not shown.

2.3.3 ONSITE METEOROLOGICAL MEASUREMENT PROGRAM

Table 2.3-6 shows the joint frequency distributions of wind speed, direction, and atmospheric stability class for data collected onsite. The distributions are for stability Classes A through G as defined in Regulatory Guide (RG) 1.23. Figure 2.3-9 shows the wind rose for the data collected at the project site during the 1966 to 1967 period. Specifications of those measurements are given in the Final Hazards Summary Report (Reference 8). Table 2.3-7 shows the average mixing height for the Eureka area by season for morning and afternoon (Reference 9).

HUMBOLDT BAY ISFSI FSAR UPDATE

There is no ongoing meteorological measurement program at HBPP because no offsite releases are required to be postulated in accordance with ISG-18. Meteorological measurements are made by the NWS at their Woodley Island offices. In support of ongoing ISFSI operations, Pacific Gas and Electric will use the data measured at NWS Woodley Island in lieu of an onsite measurement program at HBPP. The Woodley Island location is about 6 miles northeast of HBPP. The general topography at Woodley Island is flat, which is similar to the ISFSI site, and the regional topography involving the coast line and hills/mountains are similar for the two areas as well. The intervening area between the Woodley Island site and HBPP is a relatively flat plain that lies adjacent to the water edge in the Humboldt Bay. Based on proximity and these regional topography factors, winds measured at Woodley Island are considered representative of winds at the ISFSI site.

2.3.4 DIFFUSION ESTIMATES

2.3.4.1 Basis

No routine or accidental releases are planned or postulated as a result of ISFSI operation in accordance with ISG-18. Nevertheless, χ/Q values have been calculated that can be used to estimate radiological doses from any accidental release in accordance with RG 1.145 (Reference 10).

2.3.4.2 Calculations – Worst Case Short Term Event

A worst case assessment required by 10 CFR 72.106 was determined based on the minimum distance between the ISFSI vault and the nearest exclusion zone boundary. That distance was measured to be about 100 meters. A release at the surface ($H=0$) was assumed. Following the steps of the procedure presented in Figure A-1 of RG 1.145 to account for the combined effects of increased plume meander and building wake on diffusion during light winds and stable or neutral atmospheric conditions, the resulting maximum 1-hour average diffusion factor, $\chi U_{10}/Q$, was estimated to be $1.3 \times 10^{-2} \text{ m}^{-2}$, where U_{10} is the 10 meter wind speed and χ/Q is the dispersion factor. This value was estimated from RG 1.145, Figure A-1, based on atmospheric stability class G and a meander factor, M , equal to 6 during wind speeds less than 2 m/sec. Assuming the 10 meter wind speed equals 1 m/sec, the worst case 1-hour dispersion factor χ/Q would be $1.3 \times 10^{-2} \text{ sec/m}^3$.

2.3.4.3 Diffusion Modeling for Normal Operations and Anticipated Occurrences

Atmospheric dispersion factors (χ/Q) were modeled for receptor points at the site boundary, nearby residences, and nearest school. The results of this modeling analysis can be used for dose calculations. The Industrial Source Complex Long Term – Version 96113 model (Reference 11) was used to calculate the maximum annual (χ/Q) factors for the ISFSI facility. The onsite meteorological data given in Table 2.3-6 and the mixing height data given in Table 2.3-7 were used in the model analysis. An area source with the approximate dimensions of the ISFSI containment structure was

HUMBOLDT BAY ISFSI FSAR UPDATE

modeled. Other input data used in the model are shown in Table 2.3-8. A map showing the ISFSI source location, other features of the HBPP, and the owner-controlled area is shown in Figure 2.2-2. The modeled annual (χ/Q) factor results are shown in Table 2.3-9.

2.3.5 REFERENCES

1. NOAA Technical Memorandum, NWS WR-252, Climate of Eureka, CA, February 1998.
2. EarthInfo Inc, Boulder Colorado, www.earthinfo.com, NCDC Surface Airways, Hourly Observations for Arcata/Eureka National Weather Service, 1949-2001.
3. Return Periods from 'Rainfall Analyses for Drainage Design', Cal. DWR, Bulletin 195, 1988 revision.
4. 2001 Local Climatological Data, Annual Summary with Comparative Data, Eureka, Publication of National Oceanic and Atmospheric Administration, California; National Climatic Data Center, Ashville, N.C.
5. Holets, Extreme Wind Speed Estimates Along PG&E Transmission Line Corridors, PG&E R&D Report 006.4-90.6, May 1990.
6. California Tornadoes 1950-1995,
(<http://www.tornadoproject.com/alltorns/astorn.htm>).
7. Environmental Report for HBPP Decommissioning, July 1984.
8. HBPP Unit 3 Final Hazards Summary Report, September 1, 1961.
9. Holzworth, Mixing Heights, Wind Speeds, and Potential for Urban Air Pollution Throughout the Contiguous United States, EPA, 1972.
10. Regulatory Guide 1.145, Atmospheric Dispersion Models for Potential Accident Consequence Assessments at Nuclear Power Plants, US NRC, 1983.
11. Users Guide for the Industrial Source Complex (ISC3) Dispersion Models, Volume 1 – User instructions, EPA-454/B-95-003a, 1995.

2.4 SURFACE HYDROLOGY

The data and analysis in this section were obtained from the material presented in the "Memorandum Report: Flood Hydrology for the Decommissioning of HBPP Unit No. 3," dated June 1985 (Reference 1), supplemented where appropriate with information contained in the "HBPP Final Hazards Summary Report" (Reference 2) and the "SAFSTOR Environmental Report" (Reference 3).

2.4.1 HYDROLOGIC DESCRIPTION

The Humboldt Bay Independent Spent Fuel Storage Installation (ISFSI) lies in the Eureka Plain Sub-basin of the North Coast Basin. The Eureka plain drainage basin is within the hydrologic unit defined as the Redwood Creek-Mad River-Humboldt Bay Unit. This unit can supply water to an area with a projected population of 80,000. Redwood Creek discharges directly into the Pacific Ocean 38 miles north of the ISFSI site, independent of Humboldt Bay. The Mad River flows west approximately 13-15 miles northeast of the site. The only major surface water storage in the area is provided by the 2.7-billion gallon capacity Ruth Reservoir on the Mad River, which regulates municipal and industrial water supply for the Arcata-Eureka area. The Mad River Sub-basin presently exports water to the Eureka Plain Sub-basin, which enters the Pacific Ocean independent of Humboldt Bay. The mouth of the Eel River lies some 8 miles south of the site. The Eel River also discharges directly into the Pacific Ocean. This river is not used for potable water supply within 25 miles of the site.

With respect to the ISFSI site, the watersheds of Humboldt Bay and the bay itself are the most relevant surface water bodies (see Figure 2.4-1). The four major creeks that drain into Humboldt Bay are Freshwater Creek, Elk River, Salmon Creek, and Jacoby Creek. Several smaller tributaries also drain into the Bay. Salmon Creek and Elk River are the nearest streams to the site; both within a mile south and north of the ISFSI site, respectively. Salmon Creek and Elk River are used for watering livestock, but are not used as a potable water supply.

Freshwater Creek is the largest drainage basin in the drainage system; it drains an area of 61.73 square miles. It rises in the north-central part of T.4N, R.2E; flows west 5 miles, then northwest into the north end of Humboldt Bay. The creek has a length of 13 miles.

Elk River drains an area of 51.3 square miles. It rises in the central part of T.3N, R.1E; flows northwest and discharges into Humboldt Bay near the town of Elk River. The river has a length of 12 miles with North and South Forks as principle tributaries.

Salmon Creek drains a total area of 28.30 square miles. It rises in the central part of T.3N, R.1E, Humboldt base and meridian. It flows west 9 miles, then northwest about 4 miles to the western part of T.4N, R.1W, where it enters the south end of Humboldt Bay. The lower course of the creek is marshy.

HUMBOLDT BAY ISFSI FSAR UPDATE

Jacoby Creek drains an area of 16.40 square miles. It rises in the northern part of T.4N, R.2E; flows northwestward to the northern part of T.5N, R.1E, where it enters the north end of Humboldt Bay. The creek has a length of about 8 miles.

Other small tributaries in the watershed that drain into the bay are called sloughs.

2.4.1.1 Humboldt Bay

Humboldt Bay is a tidal bay receiving and discharging ocean water through its inlet. Figure 2.4-1 shows Humboldt Bay divided into an Entrance Bay extending from Buhne Point to the mouth of the Elk River; a South Bay, south of Buhne Point; and a North Bay, north of the mouth of the Elk River and including Arcata Bay. Very little fresh water discharges into Humboldt Bay.

Humboldt Bay is a large, shallow body of water with deep channels. It is separated from the ocean by two long, narrow spits. The middle portion of the bay is joined to the ocean by a narrow channel passing between the north and south spits. The bay is approximately 14 miles long, its width ranges from 0.5 miles near its middle to over 2 miles at the south end and 4 miles at the north end, with an average depth of 12 ft mean lower low water (MLLW).

Humboldt Bay can be separated into three distinct units: South Bay, extending from Table Bluff to Buhne Point; Entrance Bay, extending from Buhne Point to the mouth of the Elk River; and North Bay, extending from the river mouth to the Arcata Bottoms. South Bay is a broad, shallow area approximately 4 miles long and 2 miles wide. Southport and Hookton channels, draining the west and east sides of South Bay, respectively, are long, narrow, fairly deep channels. Entrance Bay is an oval-shaped area directly inshore from the entrance channel. Except for the west side, where the main channels flow north and south, there is a broad shoal area. Its area is 2.9 square miles. The area exposed at low tide is nearly all sand beach. North of Humboldt Bay is a broad, shallow area drained by three channel systems which combine northwest of the Eureka waterfront into a narrow deep-water channel communicating with Entrance Bay. Eureka Channel drains the southern edge of North Bay, a large area of flat farmland, and receives runoff from the Freshwater Creek watershed. Arcata Channel drains the large central portion of North Bay and receives the runoff from Jacoby Creek and minor tributaries flowing through Arcata.

North and South Bays have mud bottoms for the most part, although there is one exception in each bay. Sand Island in North Bay is a sandy hummock surrounded by mud flats. A flat near the junction of Hookton and Southport channels in South Bay is made up of firm black sand. Entrance Bay, however, has a sand bottom, with abundant broken clam shells in some areas.

The tides of Humboldt Bay are of moderate height. The mean and diurnal tide ranges are 4.3 ft and 6.2 ft at the entrance, 4.8 ft and 6.6 ft at Hookton Slough, and 5.0 ft and 7.0 ft at Arcata Wharf. Because the bay is so shallow, its tidal prism is large in

comparison to its low-tide volume. The average volume of the tidal exchange from a higher high to a lower low tide amounts to approximately 61,000 acre-ft, or 44 percent of the mean higher high tide volume. Since this water is replaced by the subsequent tide, water quality conditions in the ocean have a considerable influence on water quality and ecological characteristics of the bay.

2.4.1.2 ISFSI Site

The ISFSI site is located on a relatively flat area on Buhne Point at elevation 44 ft MLLW. Surface drainage around the ISFSI area flows naturally into the existing plant drainage system. By way of the plant drain system, the surface water then discharges into the cooling water intake canal, flows through the plant, and discharges into Humboldt Bay via the cooling water discharge canal. Outside the area served by the plant drainage system, most of the surface runoff drains to the east and into the discharge canal. The remainder drains into Buhne Slough, a natural drainage for the area, which drains directly into both the intake canal and Humboldt Bay.

2.4.2 FLOODS

2.4.2.1 Site Flooding

The elevation of the ISFSI area is approximately 44 ft above MLLW. This elevation is approximately 32 ft higher than the main power plant level. Thus any drainage will be away from the ISFSI area, and flooding is not a concern.

2.4.2.2 Probable Maximum Flood (PMF) on Streams, Rivers, and Bay

The climate of the ISFSI site and vicinity, characteristic of most of California, is divided into a wet and a dry season. Most of the rainfall occurs from storms during the wet season, which extends from November through March. About 75 percent of the annual precipitation occurs during this season. The dry season extends from May through September, and only 10 percent of the average annual precipitation is contributed during this period. The rest of the annual precipitation is contributed during the transitional months of October and April.

The mean annual precipitation at the site is approximately 40 inches. The mean annual precipitation at Eureka from 1948 through 2002 as published by the National Climactic Center (Reference 4) is shown in Figure 2.4-2. The normal monthly precipitation data for Eureka are shown in Table 2.4-1.

Major floods in the study area have all occurred during the winter months, as a combination of rainfloods and high tides.

The rainfloods have sharp high peaks and are usually of short duration and comparatively small volume. Because of the relatively low elevation of the area, snowfall and snowmelt are not considerations for flooding in the area.

HUMBOLDT BAY ISFSI FSAR UPDATE

Table 2.4-2 shows historic annual instantaneous peak flows measured at two stream gages in the basin for rainfloods. The Elk River station, 11-4797, is located near Falk and the Jacoby Creek station, 11-4800, is located near Freshwater.

Water surface profiles were run through sub-basin 15 to determine the elevations under various conditions of the probable maximum flood (PMF). The U.S. Army Corps of Engineers computer program, HEC-2 (Reference 5) was used to develop the profiles. Initially, the flood profiles were run through the bay under the antecedent bay level at a level of 6.7 ft above MLLW. A water level of 6.7 ft represents a mean value from all historic high tides. For the study, a more conservative approach was used to assign the antecedent bay level, representing reasonably probable highest tide level. Based on the 38 years of data (from 1920 to 1958), and applying a 95 percent exceedance criterion, the 2nd highest tide data point should be used. Therefore, the antecedent value of 9.96 ft MLLW, is applied to the determination of probable maximum flood impact to the sites (Table 2.4-3).

Table 2.4-4 shows the water surface elevation at the bay near the ISFSI site during the various probable maximum floods. It can be seen that the incremental increase in water levels by the PMF are insignificant, at less than 0.1 ft. The freeboard estimated for the ISFSI site is about 34 ft, as shown in Table 2.4-4.

2.4.3 POTENTIAL DAM FAILURES

The only major surface water storage is provided by Ruth reservoir on the Mad River, which regulates municipal and industrial water supply for the Arcata-Eureka area. The Mad River Sub-basin presently exports water to the Eureka Plain Sub-basin. The Mad River discharges directly into the Pacific Ocean, about 14 miles to the north of the ISFSI. Because the floods resulting from the breaching of this dam would not be a threat to the proposed facilities, no analysis is needed.

2.4.4 PROBABLE MAXIMUM SURGE AND SEICHE FLOODING

Wave heights and runup on the embankment along the shoreline near the ISFSI have been evaluated for peak winds associated with maximum flooding events. According to information from Reference 6, which contains wind data for the Eureka area from 1887 to 1996, the highest measured peak wind gusts in Eureka were 69 mph in January and November of 1981. Estimates of wave runup for several wind and flooding scenarios are presented in Table 2.4-5. As shown, the freeboard for the ISFSI remains greater than 25 ft for all scenarios considered.

2.4.5 PROBABLE MAXIMUM TSUNAMI FLOODING

The probable maximum tsunami flooding is evaluated in detail in Section 2.6.9, which concluded that the tsunami hazard at the Humboldt Bay ISFSI site is dominated by a local tsunami generated by a magnitude ~9 earthquake on the Cascadia subduction zone. This tsunami is expected to flow strongly through the mouth of Humboldt Bay, as

well as wash over the South Spit and the southern part of the North Spit. Using the estimate of 30 to 40 feet above MLLW for the runup height of the tsunami at the bay entrance, and an attenuation factor of 0.7 to 0.9, the inundation height would be 21 to 36 feet above MLLW if the tsunami occurred at low tide. Incorporating wave runup for storms from Table 2.4-5, gives a maximum value of 49.86 ft (including high tide and wave runup for storms). The maximum tsunami occurring coincident with a design basis storm wave runup and high tide is not considered credible.

2.4.6 ICE FLOODING

Because of the climatic conditions of the site, ice flooding is not applicable.

2.4.7 FLOODING PROTECTION REQUIREMENTS

Surface drainage around the ISFSI area flows naturally into the existing plant drainage system. By way of the plant drain system, the surface water then discharges into the cooling water intake canal, flows through the plant, and discharges into Humboldt Bay via the cooling water discharge canal. Outside the area served by the plant drainage system, most of the surface runoff drains to the east and into the discharge canal. The remainder drains into Buhne Slough, a natural drainage for the area, which drains directly into both the intake canal and Humboldt Bay. Thus, the drainage system at the site is efficient, and flooding of the ISFSI is not a concern.

2.4.8 ENVIRONMENTAL ACCEPTANCE OF EFFLUENTS

Best management practices for effluent management are discussed in Sections 4.1 and 4.2 of the Environmental Report. Surface runoff from the ISFSI has no radioactive contamination and will not adversely affect the surrounding ecosystem.

2.4.9 REFERENCES

1. Memorandum Report: Flood Hydrology for the Decommissioning of HBPP Unit No. 3, Civil Engineering Department, PG&E, June 1985.
2. HBPP Unit 3 Final Hazards Summary Report, September 1961 Humboldt Bay Power Plant, PG&E.
3. SAFSTOR Environmental Report, Humboldt Bay Power Plant, PG&E.
4. Interim Report, Probable Maximum Precipitation in California, Weather Bureau, Hydrometeorological Report No. 36, Washington, D. C., October 1961 with revisions dated October 1969.
5. Water Surface Profiles, 723-X6-L202A, HEC-2, U.S. Army Corps of Engineers, The Hydrologic Engineering Center, Davis, California.
6. NOAA Technical Memorandum, NWSWR-252, Climate of Eureka, CA, February 1988.

2.5 SUBSURFACE HYDROLOGY

Groundwater level and flow direction at the Humboldt Bay Independent Spent Fuel Storage Installation (ISFSI) is influenced by several factors, including topography, proximity to Humboldt Bay, and stratigraphy. The ISFSI is sited west of the power plant on a low hill east of Buhne Point (Figure 2.6-1) as illustrated in the oblique aerial photos of the Humboldt Bay ISFSI site (Figure 2.6-2). The hill is bounded on the north by Humboldt Bay, on the east by the discharge canal and marshes, on the south by the intake canal and remnant marshes that existed around Buhne Slough prior to their filling for construction of the power plant, roads and so forth, and on the west by filled marshes at King Salmon (Figure 2.5-1). About a half mile to the southeast is Humboldt Hill.

In this section of the Final Safety Analysis Report Update, the ISFSI site area is defined as the area within 1500 ft of the ISFSI and includes Buhne Point Hill, the adjacent marshes and the bordering tidal zone in Humboldt Bay. The larger ISFSI site vicinity is the area within 2 miles of the ISFSI (Figure 2.5-1). The ISFSI region for the groundwater analysis is within about 10 miles of the ISFSI and extends from the Eel River north to Eureka.

2.5.1 STRATIGRAPHY

The geology in the ISFSI Region is presented in Section 2.6.3 and for the ISFSI site area in Section 2.6.4. Several figures from these sections provide background information for the groundwater analysis, including the regional and local geologic maps (Figures 2.6-13, 2.6-14, 2.6-32 and 2.6-51), stratigraphic sections (Figures 2.6-15, 2.6-39 and 2.6-40), terraces (Figure 2.6-17), map showing geographic features of area in 1858 (Figure 2.6-34), and cross sections (Figures 2.6-36 and 2.6-44)

The geology and aquifer characteristics that are important to understanding the groundwater at and near the ISFSI site are summarized in this section. The main geologic formation in this area is the Pleistocene Hookton Formation that is about 1,100 ft thick beneath the ISFSI site area. Its sediments hold several of the important groundwater aquifers in the ISFSI site area as well as in the ISFSI region. The Hookton Formation unconformably overlies the Pleistocene Scotia Bluffs Formation. The Pleistocene marine terrace deposits that cap the Hookton (Figure 2.6-17) are generally included as part of the formation. The Hookton Formation locally is overlain by Holocene Bay deposits of Humboldt Bay and by Holocene alluvial deposits along the streams in the region (Figure 2.5-1).

The generalized stratigraphic section of the Hookton Formation at the ISFSI site area is illustrated in Figure 2.5-2 and briefly described below.

Hookton Formation

The Hookton Formation in the ISFSI region consists of interbedded shallow-water marine, estuarine, and fluvial deposits of sand, silty sand, chert-rich gravel, and clay that is about 1100 ft thick below the ISFSI. The formation is divided into upper and lower Hookton (Figure 2.5-2). The upper unit is 60 to 80 ft thick and consists of laterally discontinuous beds of clay and silt, and sand and gravel that change laterally with interfingering, cut-and-fill, and gradational facies changes. The clay beds that are ancient bay sediments have more lateral persistence than interbedded sandy and silty layers.

The Hookton strata beneath Buhne Point Hill have been tectonically tilted to the east a few degrees toward the intake and discharge canals as described in Section 2.6.4 and shown in cross sections (Figures 2.6-36, 2.6-44 and 2.6-55). The Discharge Canal fault has displaced the Hookton Formation, the south side up-thrown compared to the north side as described in Section 2.6.4 (Figures 2.6-51 and 2.6-55).

Lower Hookton Formation - The lower Hookton Formation consists of laterally persistent beds of alternating sand, silty sand, gravel, gravely sand, silty clay, and clay. The upper 26 ft to 150 ft consists of sand and gravel that overlies the Unit F clay. The Unit F clay, which is about 50 ft thick, is a distinctive marker bed (Section 2.6.4) with relatively low permeability that functions as a regional aquitard. Beneath the Unit F clay are alternating layers of clean, well-sorted sand and clay that extend from 200 to about 1,100 ft deep.

Upper Hookton Formation - The upper Hookton Formation in the ISFSI site area can be divided into two informal lithologic units 'upper Hookton silt and clay beds' and the 'upper Hookton sand beds.' The upper Hookton sand beds overlie a discontinuous clay bed (the 'second bay clay') that underlies the Unit 3 power plant area and the waste disposal ponds where it is 8 to 13 ft thick and is present in much of the site area. The upper Hookton sand beds are 25 to 40 ft thick and consist of sand and gravel layers with lesser silt and clay beds.

Under Buhne Point Hill the upper Hookton sand beds are overlain by the upper Hookton silt, clay and silty sand beds, which extend from the surface to a depth of about 30 ft. Included in the upper part of this unit are late Pleistocene estuarine/marine terrace deposits that consist of silty sand and silt beds with lenses of sand. The lower part consists of clay and silt beds referred to as the 'first bay clay' that is present in the subsurface across beneath Buhne Point Hill.

2.5.1.1 Bay and Estuarine Deposits

In the ISFSI site vicinity surrounding Buhne Point Hill, the Hookton Formation is overlain by bay and marsh deposits. These consist of the several different deposits: the tidal flat sands to the northwest, thicker bay deposits to the southwest at King Salmon, and estuarine and marsh deposits to the east and southeast. Figure 2.6-34 illustrates these

conditions in 1858. Since 1858 the creation of the broad tidal flats northwest of Buhne Point Hill by wave erosion since about 1900 have truncated the Hookton Formation and expose it directly to the bay waters; the bay deposits there are thin sand sheets. Many of the marshes and tidal channels to the south east have been filled or modified for construction of the Humboldt Bay Power Plant (HBPP), the development of the village of King Salmon, building of highways and railroads, and other uses.

The Holocene bay deposits have been investigated at the former waste-disposal surface impoundments (waste disposal ponds) that are about 1000 ft east of the ISFSI site (Figure 2.5-3). In this area the bay deposits consist of interfingering silt and clay layers and local sand lenses that extend from the surface to 25 to 40 ft deep.

2.5.2 AQUIFERS

2.5.2.1 Regional Aquifers

The U.S. Geological Survey (Reference 1) describes the groundwater conditions in the Eel River-Humboldt Bay area. This information is summarized in this section of the report.

Groundwater in the region is contained primarily in two zones. The first zone is in the loosely consolidated surficial deposits. These deposits form several separate aquifers including alluvial sand and gravel, terrace deposits, and dune sand. Shallow, unconfined water table conditions characterize these aquifers. The second zone is in the poorly to moderately consolidated sediments of the Hookton and Carlotta formations. These formations have thick sand beds that contain several widespread, confined groundwater aquifers in the region.

Aquifers in Alluvium - Alluvium underlies the various floodplains of the major rivers, and also occurs as stringers within estuarine and marsh deposits. This freshwater bearing zone consists of shallow, poorly sorted layers of sand and gravel that makes it the most productive aquifer in the region. Beneath the Mad River and Eel River floodplains this aquifer is as much as 100 ft and 200 ft thick, respectively. However, because of the high well yields, most wells tapping the alluvium are less than 70 ft in depth with many less than 30 ft deep. The alluvial aquifer of the Elk River Valley (Figure 2.5-1), southeast of the ISFSI, is the main water bearing body in the ISFSI site vicinity.

Aquifers in Terrace Deposits - Terrace deposits are also an important source of water in the region. They occur on the hillsides bordering the large river valleys and the coast. The maximum thickness of the terrace deposits is about 100 ft. Most wells tapping the terrace deposits are less than 60 ft deep. Marine and estuarine terrace deposits capping the Hookton Formation occur on the top and flanks of Humboldt Hill south of the ISFSI and on Buhne Point Hill, but these deposits are discontinuous from terrace to terrace (Figures 2.6-17 and 2.5-1) and generally have not been developed as aquifers.

HUMBOLDT BAY ISFSI FSAR UPDATE

Aquifers in Dune Sand - Dune sand on the North spit of Humboldt Bay, where they are locally more than 100 ft thick, are important local sources of fresh water (Figure 2.5-1). However, this aquifer is separated from the ISFSI site area by Humboldt Bay and is not connected to any of the aquifers in the ISFSI site area. Potential fresh water aquifers in the dune sands on the South Spit have not been tested, but the sand dunes above sea level are much thinner and more limited than on the North Spit.

Aquifers in the Hookton Formation - The Hookton Formation is second to alluvium as a groundwater reservoir and water supply source in the region. Wells north of Eureka produce artesian water from confined layers of sand or gravel in the formation. In the Eureka area, the Hookton Formation supplies unconfined water to many domestic wells. In parts of the Eel River Valley and Eureka Plain, the strata supporting this aquifer are as much as 400 feet thick. Although regionally the Hookton is an important source of water, the yield from individual wells is generally small. Silting has been a problem in many wells.

Other Aquifers - Although the aquifers in the Carlotta Formation are developed south of the Eel River, these are not an important source of water north of the Eel River. The formation is not present beneath the ISFSI site area. The underlying consolidated rocks of the Wildcat Group, Yager Formation, and Franciscan Assemblage do not yield appreciable amounts of water to wells and are not a source of water near the ISFSI.

2.5.2.2 Aquifers in the ISFSI Site Area

The groundwater in the ISFSI Site Area has been investigated over a several year period by Pacific Gas and Electric (PG&E). The results of these studies are reported in Bechtel Inter-office memorandum, dated July 31, 1984 (Reference 2); PG&E Department of Engineering Research (DER) Report No. 402.331-85.11, 1985 (Reference 3), Woodward-Clyde Consultants (WCC), dated November 1985 (Reference 4), and PG&E Department of Technical and Ecological Services (TES) Reports, dated January 1987, November 1988 and December 1989 (References 5, 6, and 7). Two areas have been investigated in detail, one near the Unit 3 Power Plant and one near the former wastewater pond site that is east of Unit 3. The various borings used to establish the stratigraphy, including those that held piezometers and monitoring wells, are shown in Figure 2.5-3. Table 2.5-1 summarizes the basic information about the 67 borings and monitoring wells used to measure the piezometric levels taken on May 6, 1999. Of these, only the 10 Bechtel wells have been left open. The others were destroyed in September 1999.

Based on the information from these borings and analysis of the stratigraphy and aquifer characteristics, several aquifers and zones of perched groundwater in the ISFSI site area are evident. The current interpretation of the groundwater aquifers and zones varies significantly from earlier interpretations because the strata within the Hookton Formation are better understood. Also, in the earlier interpretations the Holocene bay deposits were lumped with the Hookton, but are now separated and shown to unconformably overlie the upper Hookton Formation. In addition, the tectonic tilting and

HUMBOLDT BAY ISFSI FSAR UPDATE

faulting of the Hookton Formation in part controls water movement and piezometric levels.

The identified aquifers and groundwater zones are listed below. For reference, the earlier interpretations are noted in parentheses as well as illustrated on the generalized model of aquifers shown in Figure 2.5-4. The zones are described in the following section from deeper to shallower and illustrated in Figures 2.5-5 to 2.5-9.

- (1) 'Lower Hookton aquifer' - The lower Hookton aquifer is the freshwater aquifer in the sands and gravels below the Unit F clay in the lower Hookton Formation (second aquifer of Bower, 1988; in TES, 1988, Reference 6).
- (2) 'Aquifer between Unit F and 2nd bay clays' - The sand and gravel beds of lower Hookton Formation above the Unit F Clay and below the 2nd bay clay are probably also an aquifer that connects hydraulically to the upper Hookton aquifer. However, little is known of this aquifer and is not discussed further in this report.
- (3) 'Upper Hookton aquifer' - The upper Hookton aquifer is the brackish water aquifer in the upper Hookton sand beds above the 2nd bay clay and below the overlying silt and clay beds of the upper Hookton Formation. (This aquifer is the zone C and D of the semi-unconfined second water bearing zone of Bower, 1988; in TES, 1988, Reference 6; upper sand zone of Dames and Moore as reported in WCC, Reference 4).
- (4) 'Zone of perched groundwater in the upper Hookton silt and claybeds' - The zone of perched groundwater in the upper Hookton silt and clay beds includes several perched water tables in the upper Hookton fine-grained deposits. The upper part of this zone consists of sandy silt, silt and clay beds, and the lower part consists of silt and clay beds (zones A and B of first water bearing zone of Bower, 1988; in TES, 1988, Reference 6).
- (5) 'Zone of perched groundwater in the Holocene bay silts and clays' - The zone of perched groundwater in the Holocene bay silt and clay deposit is the unconfined groundwater zone (zones A and B of first water bearing zone of Bower, 1988; in TES, 1988, Reference 6).

Lower Hookton Aquifer – The lower Hookton aquifer lies below the 50 ft thick, regional aquitard known as the Unit F clay. Beneath this impermeable layer, the aquifer is defined as the freshwater bearing zone of clean, sorted sands that are deeper than about 200 ft below the ISFSI. Although the sand layers extend deeper, they are utilized in wells above 450 ft depth, which defines the boundary of interest for the groundwater flow directions and gradients at the ISFSI. This confined aquifer is artesian in places.

The conductivity of the aquifer ranges from 140 to 200 micromhos/cm (Table 2.5-2).

HUMBOLDT BAY ISFSI FSAR UPDATE

Upper Hookton Aquifer – Above the Unit F clay aquitard and below the upper Hookton silt and clay beds (comprising permeable beds in both the lower and upper Hookton Formation) is the shallow, brackish-water aquifer that is called for convenience in this report as the upper Hookton aquifer. The aquifer, which is over 100 ft thick, is semi-confined by the upper silt and clay bed aquitard. The unit is comprised of sand and gravel lenses, including some clean sand strata. A clay bed of varying thickness and extent is about 20 ft below the top of the aquifer. This clay bed is shown as the second bay clay in the geologic sections and has been referred to as a site-wide aquitard (clay layer of Bower, 1988; in TES, 1998, Reference 6). An analysis, however, shows that it is discontinuous; in Figure 2.5-8, the clay bed bifurcates: the upper part pinches out and the lower part appears to be pinched out to the west of the western most boring; in Figure 2.5-7 the upper bifurcation of the clay bed pinches out. The lower part of the bifurcation is below the borings; however, it is not present in the deeper borings (D&M 59-1A and D&M73-3) on the up-dip projection of the clay bed. The 2nd bay clay is present beneath the ISFSI site as illustrated in Figures 2.5-5 and 2.5-6.

The character of the upper Hookton aquifer is known from several piezometers and monitoring wells in the wastewater pond area and in the Unit 3 area (Table 2.5-1). The monitoring wells were screened at two intervals: the C-level monitoring wells were screened in the upper portion of the aquifer and the D-level monitoring wells were screened at a deeper level in the aquifer but above the second bay clay “aquitard.” Several other wells also record the piezometric surface of the upper Hookton aquifer on Buhne Point Hill.

The piezometric surface in May 1999 from the upper Hookton aquifer is shown in the cross sections (Figures 2.5-5 to 2.5-8) and as contours in Figure 2.5-9. Analysis of the figures shows that the piezometric levels for both the C and D zones are essentially identical, indicating good vertical communication in the aquifer above the second bay clay bed. The piezometric surface beneath Buhne Point Hill is nearly horizontal, and slopes gradually to the north toward Humboldt Bay. North of the Discharge Canal fault the piezometric surface slopes northwest. The difference in the amount and direction of slope of the piezometric surface on either side of the fault indicates that the fault is an aquitard, with higher water levels on the north side than the south.

As evident on the cross sections, the upper Hookton aquifer is confined by the upper Hookton silt and clay beds in the Unit 3 and wastewater ponds area, but is unconfined beneath the higher part of Buhne Point Hill, making it a semi-confined aquifer.

The depth to the piezometric surface on the upper Hookton aquifer below the ISFSI site is estimated from information interpreted in Borehole GMX99-2 that was drilled in February during the wet season (Figure 2.5-9). The shear and compression wave velocity profile from this boring (February 18, 1999; Reference 8) indicates that saturated deposits occur at 34 ft below ground, placing it at about elevation 6 ft mean lower low water (MLLW) within the lowermost deposits of the upper Hookton aquifer. Considering the three-month time difference between the measurements of the other wells in May, the estimate of 6 ft during the wet season is consistent with the other data,

HUMBOLDT BAY ISFSI FSAR UPDATE

and it is estimated that the groundwater level in early part of the dry season would be lower, at about 5 ft (MLLW).

The tides have a strong influence on the upper Hookton piezometric surfaces. This is illustrated in wells at the wastewater pond site and near Unit 3 (Figures 2.5-10 and 2.5-11). The piezometric surface lags the tidal changes by a few hours and has up to about a 3 ft elevation change during a tidal cycle. This indicates that water in Humboldt Bay and in this aquifer at the ISFSI site area is connected in the outcrops below the bay, as illustrated in Figures 2.5-6 and 2.5-14. The salinity in the upper Hookton aquifer is discussed in Section 2.5.7.

Zone of Perched Groundwater in the Upper Hookton Silt and Clay Beds – The zone of perched groundwater in the upper Hookton deposits is in the silt and clay beds between the surface and the upper Hookton aquifer. These silt and clay beds are approximately 30 ft thick in the ISFSI site area. The groundwater in this zone occurs as discontinuous zones of perched water tables. The piezometers were placed in the upper and lower parts of this zone, indicated as A and B, respectively (Table 2.5-1), and these show somewhat different piezometric levels. The piezometric surface in 1999 from the A and B levels is shown in cross sections A-A and C-C (Figures 2.5-7 and 2.5-8) and as contours in Figures 2.5-12 and 2.5-13.

Analysis of Figures 2.5-12 and 2.5-13 shows that the piezometric surface in the lower part (B) of the groundwater zone slopes to the north south of Unit 3 (where the wells are).

The upper part (A) of the zone of perched groundwater in the upper Hookton silt and clay beds shows a perched table at Boring MW-8 (BEC84-8) on Buhne Point Hill north of Unit 3 that is at elevation 17.92 ft, only 6 ft below the surface. South of Unit 3 a different perched surface is near horizontal at about 8.5 ft, as evident in five wells, 1 to 3 ft above the piezometric surface of the B zone.

At the ISFSI site, perched water is interpreted from the Borehole GMX99-2 (Figure 2.5-9). The shear and compression wave velocity profile from this boring (February 18, 1999) (Reference 9) indicates that saturated deposits occurred between depths of 10 to 15 ft (elevation 25 to 30 ft) (Reference 8). In addition when the trenches were excavated at the site, groundwater flowed into the trench for a few hours from local groundwater zones, but had stopped by the next day.

Zone of Perched Groundwater in the Holocene Bay Silt and Clay Beds - The zone of perched groundwater in the Holocene bay silt and clay beds is in the tidal marsh deposits and bay mud that underlie the former wastewater pond site and is believed to be similar to other locations in bay deposits near the ISFSI. This groundwater zone is in unconsolidated silt and clay beds that unconformably overlie the upper Hookton sand beds that are 23 to 26 ft below the surface.

Monitoring wells in the Holocene bay silt and clay beds at the pond site help characterize the water table and piezometric surfaces in this unit. The A-level monitoring wells were screened to bracket the surface of the water table and the B-level monitoring wells were screened in the middle and lower portions of the deposit. The cross section through the area (Figure 2.5-8) illustrates these conditions. The general piezometric surface for the B part of the zone ranges between the 6 and 10 ft elevation, a foot or two below the water table in the A part of the zone. Contours on the B part of the zone (Figure 2.5-13) show a northwest trending trough to the northwest of the ponds site with highs on either side, indicating that flow directions are toward Humboldt Bay and away from the bay toward the marsh to the southeast. The figure also illustrates that the B piezometric surface in the Holocene bay deposits is separate from the B piezometric surface in the upper Hookton groundwater zone by the unconformity between them.

The A part of the zone appears to record a perched water table or various localized water tables. Two such groundwater levels are at boring WWC-9A on the south side of the ponds (Figure 2.5-8) and a high to the north of the closed ponds (Figure 2.5-12). The surface indicates that the A part of the groundwater flows to the northwest toward the discharge canal and southeast toward the marsh.

The piezometric surfaces for the A part of the zone at the pond site fluctuates about 3 ft seasonally. The tides have almost no influence on any of the A or B perched water tables in the Holocene bay deposits as illustrated in well cluster 6 (WCC85-6A and B, and DER85-6) (Figure 2.5-11).

2.5.3 GROUNDWATER RECHARGE, GRADIENTS, AND DISCHARGE

2.5.3.1 Regional Area

As discussed by the U.S. Geological Survey (Reference 1) and in PG&E's environmental report (Reference 10), groundwater in the Humboldt Bay region generally flows west and northwest toward the coast. Water level contours for the alluvial aquifer in the Eel River Valley and the Elk River Valley show that the groundwater flows west to northwest, down the valleys, and toward the coast in these alluvial aquifers.

Recharge of fresh groundwater resources is generally from direct precipitation and by direct seepage from rivers and streams. Some water also moves laterally into the various water bearing zones from adjacent formations and some moves upward from leakage due to differences in head between the shallow and deeper water bearing formations. The confined aquifers in the Carlotta and Hookton Formations primarily receive recharge from precipitation and stream seepage in their outcrop areas that are considerable distances away from the ISFSI site.

Groundwater discharge in the Humboldt Bay region is both natural and artificial. Natural discharge occurs by subsurface flow to streams, tidal estuaries on the coastal plains and to the ocean; by evaporation and transpiration; and by discharge through springs.

Artificial discharge of groundwater occurs by pumping or artesian flow from wells. The discharge of groundwater along the coastal plains is partly controlled by tidal conditions.

2.5.3.2 ISFSI Site Vicinity

The two shallow groundwater tables in the ISFSI site vicinity are the alluvial aquifer in the Elk River Valley and the alluvial aquifer in the 'Buhne Slough valley.' These were investigated by E.C. Marliave (References 11, and 12) in 1959 and 1960. Analysis of data from seven shallow 'test holes' drilled in the area east of and south of Buhne Point as presented by E.C. Marliave and the geomorphic and stratigraphic information provided in Sections 2.6.3 and 2.6.4 provides the following understanding regarding constraints on the groundwater conditions in this area.

The three test holes (wells) in the alluvial aquifer along the Elk River Valley (Figure 2.5-1) showed that the water table slopes down valley has a gradient of about 12 ft/mile (about 0.002 ft/ft). Regardless of the effect of tides near the mouth of the Elk River Valley, the alluvial aquifer is flushed each year by high flows during winter and spring runoff.

The groundwater divide that follows the low ridge at Spruce Point and extends north from there separates the Elk River alluvial aquifer and the ISFSI site area from the alluvial aquifer in the much smaller 'Buhne Slough Valley' that is west and southwest of Spruce Point. Thus, groundwater flow east of this area is to the northeast toward Elk River and then to Humboldt Bay and groundwater flow west and south of this area is to the west toward the now mostly buried Buhne Slough (Buhne Slough, but not Spruce Point, is shown in Figure 2.5-3). It is also shown as an unnamed slough in the 1858 map as winding east of Buhne Point into the short valley southwest of Spruce Point. Buhne Slough and nearby marshes have been filled by development in the area and only exist in part; the intake canal for the HBPP has diverted most of the water that used to enter Buhne Slough; only the intake canal is shown in Figure 2.5-1.

Information from the four test holes (wells) around Buhne Slough Valley as analyzed by E.C. Marliave (Reference 12) shows that shallow groundwater flows toward the remnants of Buhne Slough. The water table slopes west at 3 to 5 ft/mi (0.001 to 0.0006 ft/ft) from the slopes of the northern end of Humboldt hill (0.005 ft/ft to the upper part of Buhne Slough area, but a lesser gradient of 0.001 ft/ft from the divide area westward toward the lower reach of Buhne Slough). The topographic high of Buhne Point Hill has a water table that slopes east toward the remnants of Buhne Slough at 2.5 to 5 ft/mi (0.001 to 0.0005 ft/ft) from the southern flank of Buhne Point Hill.

2.5.3.3 ISFSI Site Area

Recharge and discharge of the aquifers and groundwater zones in the ISFSI site area varies as illustrated in Figure 2.5-14 and is described below.

HUMBOLDT BAY ISFSI FSAR UPDATE

Lower Hookton Aquifer - Recharge of the lower Hookton confined aquifer beneath the regionally contiguous Unit F clay bed is believed to be through deep percolation of rainfall into formation outcrops in the Humboldt Hill area, beneath the terraces on the hill, and from alluvium along the Elk River Valley (Figure 2.5-1). Subsequent lateral flow beneath confining beds transports the water beneath the ISFSI site and to areas of discharge in Humboldt Bay and probably into the Pacific Ocean beyond Humboldt Bay.

Upper Hookton Aquifer - Recharge of the upper Hookton aquifer in the ISFSI site vicinity comes from three sources. The first consists of freshwater from the nearby, topographically higher Humboldt Hill area where percolation of rainfall enters the formation outcrops and from beneath the terraces on the hill (Figure 2.5-1). Lateral flow brings it into the site area. A second potential area of recharge is brackish water from the Buhne Slough area east of Buhne Point Hill, including cooling water intake and discharge canals. The third area of recharge is from seepage of seawater into the aquifer from Humboldt Bay.

Little vertical flow occurs within the upper Hookton aquifer. Vertical gradients range from 10 to 20 ft/mile (0.002 to 0.004 ft/ft) (Reference 6).

Tidal fluctuations in Humboldt Bay have significant short-term (hours) effects on the groundwater flow directions and rates within the upper Hookton aquifer at Buhne Point Hill. During rising tides, bay water flows into the formation near Buhne Point Hill in a generally southerly direction; during falling tides, the flow is out of the formation into the bay, generally in a northerly direction. However, the upper Hookton aquifer is believed to have a net discharge of groundwater into Humboldt Bay and possibly offshore into the Pacific Ocean. Net horizontal flow velocities within the upper Hookton aquifer range from 2×10^{-7} to 1×10^{-5} cm/s (Reference 6).

Zone of Perched Groundwater in the Upper Hookton Silt and Clay Beds – Recharge into the zone of perched groundwater in the upper Hookton silt and clay beds beneath Buhne Point Hill at the ISFSI site is primarily from direct precipitation and percolation into the interfingering layers of silt, clay and lesser sand lenses that characterize the deposits. Local perched water tables occur in these beds, but the southeast tilting of these layers tends to direct groundwater flow toward the intake and discharge canals. Near Unit 3, the perched water table is at about 8.5 ft elevation (Figures 2.5-7 and 2.5-12). This water is somewhat brackish (salinity about 2600 to 2800 micromhos/cm) reflecting a mixing with some bay water from the nearby marshes and the intake and discharge canals, or from upward migration of water into these beds from the underlying upper Hookton aquifer. The recharge potential on Buhne Point Hill is low because the silty sand, silt and clay deposits directly below ground are relatively impermeable.

Based on the definite piezometric head separation between the zone of perched groundwater and the upper Hookton aquifer (Figures 2.5-7 and 2.5-8) and the 1st bay clay that separates them, hydraulic communication between the two aquifers is poor; hence, minimal flow are believed to occur between these two zones. The perched

groundwater in the upper Hookton Formation appears to discharge into the nearby marshes and into the intake and discharge canals. Little discharge is expected to reach the underlying upper Hookton aquifer because the 1st bay clay that is at the base of the deposit restricts vertical flows. Moreover, in the Unit 3 area the piezometric surface of the underlying upper Hookton aquifer is higher than the base of the 1st bay clay providing upward piezometric pressure into the perched groundwater zone.

Zone of perched groundwater in the Holocene bay silt and clay beds- Recharge of the zone of perched groundwater in the Holocene bay silt and clay beds in the wastewater pond area and nearby marshes is primarily from direct precipitation and percolation into the interfingering layers of silt, clay and lesser sand lenses that characterize the deposits. Local perched water occurs in these beds. The lower parts of the beds are recharged in part by inflows of bay water at high tides from the tidal marshes, Humboldt Bay, and the intake and discharge canals, particularly at high tides.

Groundwater flow within the zone of perched groundwater in the Holocene bay silt and clay beds is primarily horizontal. Estimated horizontal flow velocities (5×10^{-8} to 7×10^{-5} cm/s) are one to two orders of magnitude greater than estimated vertical velocities (3×10^{-9} to 6×10^{-7} cm/s) (Reference 6).

Based on the lack of response within the zone of perched groundwater in the Holocene bay silt and clay beds to tidal fluctuations (Figure 2.5-11) and the definite piezometric head separation between the two zones (Figure 2.5-8), hydraulic communication between the zone of perched groundwater and upper Hookton aquifer is poor; hence, minimal flow occurs between these two zones.

Discharge is into the adjacent tidal marshes, Humboldt Bay, and the intake and discharge canals. This is probably highest when the tides are low.

2.5.4 HYDRAULIC PROPERTIES OF AQUIFERS

2.5.4.1 Regional Well Yields

Information on wells in the region comes from References 1 and 10. Specific capacities of wells tapping the regional alluvial aquifers range from 20 to 350 gpm/ft of drawdown. The terrace deposits commonly yield more than 150 gpm with specific capacities of up to 90 gpm/ft of drawdown.

Although regionally the Hookton Formation is an important source of water, the yield from individual wells is generally small, commonly less than 10 gpm from flowing wells (artesian) to 30 gpm from pumped wells. Specific capacity is on the order of 0.5 gpm/ft of drawdown. PG&E Well No. 2, which draws water from the lower Hookton aquifer, produces 75 gpm, the capacity of the pump.

Yields from wells tapping aquifers in the Carlotta Formation vary, but are generally less than those in the alluvium and terrace deposits, and more than those tapping aquifers in

the Hookton Formation. Most Carlotta wells have specific capacities ranging from 15 to 100 gpm/ft of drawdown.

2.5.4.2 Hydraulic Properties of Aquifers in the ISFSI Site Area

In the wastewater ponds area (Reference 6), the transmissivity, hydraulic conductivity (permeability), and storage coefficients for the perched water zone in the Holocene bay deposits and the upper Hookton aquifer were estimated by several methods. Laboratory permeability tests were performed on soil samples collected from both the zone and the aquifer to estimate the vertical hydraulic conductivity of the respective water-bearing zones. Slug test data were analyzed according to the method reported in Reference 6 to provide an estimate of the horizontal hydraulic conductivity in the vicinity of each well tested. A tidal fluctuation analysis method was applied to water level data collected from wells completed in the upper Hookton aquifer to provide estimates of the transmissivity, hydraulic conductivity, and storativity of that zone. The tidal method was not appropriate for the perched groundwater zone because tidally induced fluctuations in this zone were negligible. Copies of test data and methodology are provided in the appendices for Reference 6.

Zone of perched groundwater in the Holocene bay deposits - During the 1988 study period (Reference 6), the horizontal groundwater gradients within the zone of perched groundwater in the Holocene bay deposits ranged from 0.007 to 0.025 ft/ft, while the vertical gradients ranged from zero (no vertical flow) to 0.146 ft/ft. Estimated horizontal permeability for this zone ranged from 2×10^{-6} to 8×10^{-4} cm/s. Estimated vertical permeability values for soil samples collected from the zone ranged from 2×10^{-7} to 5×10^{-6} cm/s. Estimated horizontal flow velocities (5×10^{-8} to 7×10^{-5} cm/s) are one to two orders of magnitude greater than estimated vertical velocities (3×10^{-9} to 6×10^{-7} cm/s).

Based on a saturated thickness of approximately 20 ft, the range of transmissivity values for the zone of perched groundwater in the Holocene bay deposits is 1×10^{-3} to 5×10^{-1} cm²/s (Reference 6).

Upper Hookton Aquifer - During the 1988 study period, horizontal groundwater gradients (Reference 6) within the upper Hookton aquifer in the vicinity of the former wastewater ponds ranged from 0.001 to 0.002 ft/ft, while the vertical gradients ranged from 0.002 to 0.004 ft/ft. The range of horizontal permeability values for this aquifer, estimated by the tidal method, was 7×10^{-5} to 2×10^{-3} cm/s, with most values being close to 1×10^{-3} cm/s. The range of vertical permeability was estimated as 1×10^{-5} to 4×10^{-4} cm/s. Net horizontal flow velocities within the upper Hookton aquifer range from 2×10^{-7} to 1×10^{-5} cm/s, while estimated vertical flow velocities ranged from 2×10^{-6} to 4×10^{-6} cm/s.

Based on a saturated thickness of approximately 25 ft for the upper Hookton aquifer, the range of transmissivity values is 0.04 cm²/s to 1.21 cm²/s. Estimated storativity values were all in the 10^{-5} range.

HUMBOLDT BAY ISFSI FSAR UPDATE

Based on down-hole flow meter measurements in the upper Hookton aquifer in the Unit 3 area (Reference 2) for wells MW-1 through MW-11 and calculated permeability using the tidal method, a flow velocity range of 3,100 to 10,400 ft/yr (3×10^{-3} to 3×10^{-2} cm/sec) was calculated. This range is higher than that calculated for the aquifer beneath the wastewater ponds area (described above) and on the high side of those values calculated for References 6 and 10 (2,000 ft/yr or 1.9×10^{-3} cm/s). The differences most likely reflect different local stratigraphic characteristics in the aquifer.

2.5.5 GROUNDWATER USE

Regional Area

Groundwater in the region is used for irrigation, industrial water supply, public and domestic water supplies. Some wells are used for environmental monitoring. Except for the water supply for the City of Eureka, which is supplied by surface water from the Mad River, all of the domestic, industrial and agricultural water needs in Humboldt County are met by groundwater. In the area extending from the Eel River Valley north to the Mad River Valley, the quantity of groundwater that was pumped for all purposes was nearly 9 billion gallons in 1975. This water is extracted mainly from shallow wells in alluvium and terrace deposits of the Eel, Mad and Van Duzen River Valleys. Sands of the Hookton and Carlotta Formations are also important sources of groundwater, but well yields are generally less than from the alluvium.

ISFSI Site Vicinity

Table 2.5-3 lists the wells within a radius of slightly more than 2 miles from the ISFSI site. Of the 39 active wells, two are industrial, seven are municipal, water companies or commercial, seven are used for irrigation, 19 are individual domestic wells, three are monitoring (generally with more than one well), and one is a test well. These wells are located as shown in Figure 2.5-1.

2.5.6 GROUNDWATER QUALITY

Regional Area

The quality of the groundwater in regional aquifers is generally good, most of it being moderately hard, calcium-magnesium-bicarbonate water. Typically, chloride concentrations from wells completed in the alluvial aquifers that are generally less than 50 ft deep are below 100 mg/l. The only well (16 ft deep) completed in the dune sand for which there are data showed a chloride concentration of 24 mg/l. Chloride concentrations from wells less than 100 ft to several hundred feet deep completed in the Hookton Formation generally are less than 100 mg/l and often less than 50 mg/l. Wells completed in the Carlotta Formation are typically several hundred ft deep, and generally have chloride concentrations less than 50 mg/l. One 268 ft deep well had a chloride concentration of 230 mg/l. Concentrations in some wells have been reported at 28 parts per million (ppm) and chloride concentrations in shallow aquifers near the tidal

HUMBOLDT BAY ISFSI FSAR UPDATE

reaches of the rivers range from 500 to 1,000 ppm (Reference 1). In these areas along the coast, a concentration of 100 mg/l chloride indicates the landward edge of the freshwater-seawater transition zone, although it does not necessarily represent the landward limit of brackish or unusable groundwater.

ISFSI Site Area

The quality of the groundwater in the aquifers in the ISFSI Site Area is summarized in Table 2.5-2.

The quality of the water in the lower Hookton aquifer at the ISFSI is known from the former PG&E Well No. 1 (Table 2.5-2; Figure 2.5-1) that was destroyed in September 2000. It was freshwater that had 12 to 26 ppm chloride and total conductivity of 140 to 200 micromhos/cm.

The salinity in the upper Hookton aquifer as measured by the conductivity ranges between 1,100 and 26,000 micromhos/cm and chloride ranges from 200 to 9,000 ppm (Table 2.5-2). The lowest conductivity readings, 1,000 to 2,500, are south of Unit 3; the conductivity is higher around the wastewater pond site where the conductivity is 5,500 to 26,000 (Figure 2.5-9), probably reflecting salt water intrusion from the marshes in this area.

The water in the upper part (A) of the zone of perched groundwater in the upper Hookton silt and clay beds is brackish. South of Unit 3, the water in the A part of the zone is brackish with conductivity ranging from 2,500 to 2,800 micromhos/cm and chloride ranges from 450 to 800 ppm (Table 2.5-2; Figure 2.5-12).

The water in the upper part (A) of the zone of perched groundwater in the Holocene silt and clay beds is brackish. The conductivity of the A part of the zone ranges from 5,000 to 7,000 micromhos/cm and chloride from 1500 to 5,000 ppm (Table 2.5-2, Figure 2.5-12). The lower conductivity, when compared to the B zone, reflects the higher elevation of the perched water table where salt water intrusion is less.

The quality of water in the lower part (B) of the zone of perched groundwater in the Holocene bay silt and clay beds is brackish. The conductivity of the B part of the zone ranges from 9,000 to 17,500 micromhos/cm and chloride ranges from 1,800 to 4,500 ppm (Table 2.5-2). The highest reading is south of the wastewater ponds area near the marsh (Figure 2.5-13). The high conductivity reflects salt water intrusion into the lower aquifer from the marshes and discharge canal.

The confined nature of the deeper, lower Hookton aquifer (the two PG&E industrial wells were artesian at the time of installation) also serves to protect this zone by preventing downward vertical migration of brackish water. Aside from the brackish nature of the water, there are no currently known areas of groundwater contamination beneath the ISFSI site. Clean closure of both the oil water separator and former evaporation pond areas related to Unit 3 was obtained from the California North Coast

HUMBOLDT BAY ISFSI FSAR UPDATE

Regional Water Quality Control Board in October 1997. The monitoring wells used to assess the aquifer were destroyed in September 1999.

2.5.7 CONTAMINANT TRANSPORT ANALYSIS

The spent fuel at the ISFSI will be maintained in dry storage casks. There will not be any routine effluent releases or any credible off-normal events or accidents that result in liquid effluents. Therefore, the ISFSI will have no effect on surface water or groundwater.

2.5.8 REFERENCES

1. Ground-Water Conditions in the Eureka Area, Humboldt County, California, U.S. Geological Survey, Water-Resources Investigations 78-127, Prepared in cooperation with the Humboldt County Department of Public Works, 1975.
2. Inter-office Memorandum from B.L. Turner to P.A. Mote Concerning the Humboldt Bay Power Plant Unit No. 3 Ground-Water Studies, Bechtel Civil & Minerals, Inc., Job No. 16620, July 31, 1984.
3. Construction, Development, and Sampling of Humboldt Bay Power Plant Groundwater Monitoring Wells, PG&E Department of Engineering Research (DER), 1985, DER Report No. 402.331-85.11.
4. Resource Conservation and Recovery Act (RCRA) Part B Permit Application, Hydrogeologic Assessment Report, Impoundment Integrity Report, and Proposed Groundwater Monitoring Program, Woodward-Clyde Consultants (WCC), 1985, November 1985, Appendix A.
5. Tidal Influence on Groundwater Flow Direction Beneath Unit No. 3 at Humboldt Bay Power Plant, PG&E TES Report No.402.331-87.2, January 1987.
6. Humboldt Bay Power Plant Wastewater Treatment Impoundments Hydrogeologic Characterization Study, PG&E TES Report No.402.331-88.39, November 1988.
7. Summary of March 1989 Monitoring Well Installation and Development Activities in the Surface Impoundment Area at Humboldt Bay Power Plant, December 1989, PG&E Department of Technical and Ecological Services (TES) Report No. 402.331-89.22.
8. Humboldt Bay Power Plant Data Report C, Downhole Geophysics in the ISFSI Site Area, Humboldt Bay Power Plant ISFSI, Narayanan, Kathek, 2002, 220p.
9. Determination of Liquefaction Potential at HBPP ISFSI Site, PG&E Geosciences Department, Calculation Document No.GEO.HBIP.02.02, May 22, 2002.4. HBPP Final Hazards Summary Report, Humboldt Bay Power Plant, PG&E.

HUMBOLDT BAY ISFSI FSAR UPDATE

10. SAFSTOR Environmental Report, Humboldt Bay Power Plant, PG&E.
11. Geologic reconnaissance of groundwater conditions, Buhne Point, Eureka, Marliave, E.C., 1959, 9 p. plus figures: in Appendix II of the HBPP Final Hazards Summary Report (in Reference 4).
12. Letter to J.F Bonner, re: Unit No. 3, Eureka Plant, from Marliave, E.C., 1960, 6p. plus figures: in Appendix II of the Final Hazards Summary Report (in Reference 4).

2.6 GEOLOGY AND SEISMOLOGY

2.6.1 INTRODUCTION

This section provides information to update the tectonic setting of the Humboldt Bay region, and the evaluation of the seismic hazards that could affect the proposed site for an Independent Spent Fuel Storage Installation (ISFSI) on the Humboldt Bay Power Plant (HBPP) property. This section also provides earth sciences data, earthquake hazards assessments, and geotechnical foundation data and analyses in support of the Humboldt Bay ISFSI.

2.6.1.1 Background

Humboldt Bay Power Plant and the ISFSI site lie on the east flank of Buhne Point, a small headland on the eastern shore of Humboldt Bay (Figures 2.6-1, 2.6-2). Units 1 and 2 are fossil-fueled generating plants built in 1954 and 1956, respectively, and operate today.

Unit 3, a small (62 MW) nuclear power plant, was constructed in 1962. It was initially designed for a peak ground acceleration of 0.2 g. On June 7, 1975, the local magnitude 5.3 Ferndale earthquake, 14 miles (22 km) distant (at a depth of 23.6 km) resulted in a free-field peak ground acceleration of 0.3g at the plant site. In 1976, when Unit 3 was shut down for refueling, the seismic criteria were reevaluated. A preliminary analysis indicated that a free-field peak ground acceleration of 0.5g would be appropriate, and consequently some of the plant facilities were retrofitted to withstand this larger ground motion. Concurrently, a detailed reevaluation of seismic sources was conducted (Reference 1). This reevaluation led to the discovery of the Little Salmon fault zone within a mile of Unit 3. Because of the potential for a large-magnitude earthquake on the Little Salmon fault zone, the application to restart the plant was withdrawn, and, in 1988, Unit 3 was put into a SAFSTOR mode. Seismic strong-motion monitoring has continued to the present.

On December 26, 1994, a moment magnitude 5.4 earthquake occurred 9 miles (14 km) west of the HBPP site at a depth of 23.5 kilometers. The earthquake resulted in a free-field peak ground acceleration of 0.55g at the plant site, slightly higher than the 0.5g used during evaluations of Unit 3 from 1976 to 1982. The event prompted NRC staff to inspect the site in February 1995. During the site visit, the NRC requested PG&E to reevaluate the seismic hazards at the plant site. The reevaluations were to include an analysis of potential ground motions, incorporating new near-source data from recent earthquakes in Northridge (1994) and in Kobe (1995).

In 1998, PG&E began studies for dry cask storage at the plant, and the reevaluation requested by the NRC was expanded to include assessment of seismic hazards at the proposed ISFSI site. The reevaluation was also expanded to include data and relevant research from the 1999 earthquakes in Turkey and Taiwan, which have provided valuable new data that contribute to our understanding of the tectonics in the Humboldt Bay region.

2.6.1.2 Definition of the Study Area

This review considered the seismic hazards to the Humboldt Bay ISFSI site, which is located within the HBPP site area (called “plant site”), enclosed by the outer farm fence that also envelops Units 1, 2, and 3, and associated structures (Figure 2.6-1). Because of the extensive previous studies for the nuclear power plant, Unit 3 occasionally is mentioned in this evaluation as a geographic reference point.

2.6.1.3 Scope of Seismic Hazard Studies

The Humboldt Bay ISFSI site is on the western edge of the North American plate, near the southern end of the Cascadia subduction zone (Figure 2.6-3). Since the evaluation of seismic sources conducted for the plant site in 1980, knowledge about the Cascadia subduction zone has changed significantly. In the early 1980s, it was widely thought that the interface part of the Cascadia subduction zone was aseismic. During the past 10 years, studies of tectonic subsidence, paleotsunamis, and paleoliquefaction along the Pacific Northwest coast have shown that the Cascadia interface has generated several large earthquakes during the past few thousand years.

A comprehensive model of the tectonic framework of the region to better understand the seismic potential of the Cascadia subduction zone was developed. Section 2.6.2 of this evaluation summarizes the latest thinking on the tectonic framework of the ISFSI site region. In Section 2.6.3, earlier studies of the regional geology and seismicity were updated, including recent evaluations of the Little Salmon fault zone. The geology of the ISFSI site is presented in Section 2.6.4. The seismic potential of the Cascadia interface and the characterization of other seismic sources in the Humboldt Bay region that could affect the site are discussed in Section 2.6.5. There have been major improvements in the evaluation of ground motions caused by large earthquakes since the 1980 evaluations. Due to the large increase in strong-motion recordings, for both shallow crustal earthquakes in active tectonic regions and subduction zone earthquakes, ground motion attenuation relations have been revised significantly as described in References 2 - 9. Attenuation relations and the ground motions for the ISFSI site are discussed in Section 2.6.6.

Based on recent drilling and trenching investigations, the hazards of liquefaction and landsliding, and surface faulting were evaluated and are discussed in Section 2.6.7 and Section 2.6.8, respectively.

Section 2.6.9 presents new data, based on an active Cascadia subduction zone, that are used to evaluate the hazard of tsunamis at the Humboldt Bay ISFSI site.

2.6.1.4 Definition Of Terms

Units of measure - These studies use both English and metric measurements. Metric measurements were used because they are the professional standard in seismicity and seismic geology evaluations. However, site geotechnical investigations typically use English measurements. Both measurements may be given, as necessary.

HUMBOLDT BAY ISFSI FSAR UPDATE

Reference elevation - Mean lower low water (MLLW) is the reference elevation for bathymetry and topography at the site. Hence, all elevation measurements at the site are referenced to mean lower low water, which is set at 0. The tidal range is 6.9 feet to mean higher high water (MHHW), and mean sea level is 3.7 feet. The top of the ISFSI site is at elevation 44 feet above MLLW.

Magnitude scale - All earthquake magnitudes are moment magnitudes, M , (Reference 10) unless stated otherwise.

Geologic time scale - A geologic time chart that shows the subdivisions of the Mesozoic and Cenozoic Eras as used in these studies is presented in Table 2.6-1.

2.6.2 TECTONIC FRAMEWORK

2.6.2.1 Introduction

The Humboldt Bay ISFSI site is on the western edge of the North American plate, near the southern end of the Cascadia subduction zone, and a short distance north of the Mendocino triple junction region (Figure 2.6-4). The region is traversed by many active faults, which form the complex structural and tectonic architecture of the southern part of the subduction zone and the triple junction. Although the region is among the most seismically active of any in western North America, the seismicity observed over the relatively short historical period (the past 150 years or so) undoubtedly does not reflect the full seismic potential of the region. The largest earthquakes include very large subduction-zone earthquakes that are not represented by the historically observed seismicity, but evidence of these earthquakes is preserved in the paleoseismic record.

This record was studied along the coast of northern California, Oregon, and Washington, especially in the Humboldt Bay region, to better understand the tectonic framework and, thus, the seismic potential of the Cascadia subduction zone. This data base, which has undergone dramatic changes during the past two decades, is crucial to assessing the seismic hazards at the ISFSI site. The tectonic model used here is based on today's knowledge, and is consistent with worldwide observations of subduction zones and their earthquake potential. This produces a comprehensive model of the tectonic framework that is reasonable, and results in a conservative seismic hazard assessment for the Humboldt Bay ISFSI site.

The tectonics of coastal northwestern California are dominated by plate boundary interactions among the North American plate, the Pacific plate, and the combined Gorda-Juan de Fuca plates (Figure 2.6-4). North of the triple junction, the Gorda-Juan de Fuca plates are being subducted beneath the North American plate along the Cascadia subduction zone, whereas south of this junction, the Pacific plate moves northward relative to the North American plate along the San Andreas fault zone. The Mendocino fault marks the right lateral transform boundary between the Pacific plate and the Gorda-Juan de Fuca plates. On a global-plate-tectonics scale, these three plates meet at the Mendocino triple junction: the intersection of the San Andreas and Mendocino transform fault zones with the Cascadia subduction zone. Although it is

commonly depicted as a point slightly offshore and south of Cape Mendocino, the junction is actually a broad region of complex structure.

Both transform faults have been seismically active historically. The San Andreas fault slipped as much as 6 meters in northern California in the magnitude 7.8 (earthquake magnitudes are moment magnitudes (M), unless stated otherwise) San Francisco earthquake in 1906; the fault rupture extended at least as far north as Point Arena, and possibly north to Point Delgada, a short distance south of the triple junction (References 11-13). The Mendocino fault zone has produced earthquakes up to magnitude 7.25, which have occurred at different locations along much of its length. In contrast, the Cascadia subduction zone leg of the triple junction has been nearly aseismic historically. The April 25, 1992, magnitude 7.1 Petrolia earthquake is the only recorded large seismic event associated with the subduction zone (Reference 14).

Field studies in the triple junction region show that the transform and subduction zone boundaries of the three principal plates are broad zones containing elaborate systems of individual faults and fault-bounded crustal blocks tens of kilometers wide. Thus, on a more detailed scale, the Mendocino triple junction is a large, structurally complex region encompassing the intersection of these wide plate boundaries and is best characterized by distinct subplates. To provide a better understanding of this complicated region, a brief discussion of the three plate-boundary elements of the triple junction will be presented first, followed by a description of the triple junction region itself. Details of the geology of the Humboldt Bay ISFSI region are presented in Section 2.6.3.

2.6.2.2 North American Plate Boundary

The present plate configuration in northern California was initiated during the early Miocene, about 20 million years ago, when the former Farallon and Kula plates (Figure 2.6-5) were consumed by subduction beneath the western edge of North America, and contact was made between the Pacific plate and the North American plate (Reference 15). The first Pacific/North American plate contact occurred in southwestern California, and produced the Mendocino triple junction and proto San Andreas fault system. The unsubducted remnant of the former Farallon plate became the predecessor to the modern Juan de Fuca plate. Throughout the late Cenozoic, (past 5 million years) the Juan de Fuca plate continued to subduct obliquely to the northeast beneath the western edge of North America, as the Mendocino triple junction migrated northward through central and into northwestern California, extending the San Andreas fault system into northern California. Thus, the San Andreas fault system decreases in age and total net slip from south to north. In the northernmost part of California, near the triple junction region, the fault system has experienced relatively little net displacement, and is no older than Quaternary (1.6 million years).

As the Mendocino triple junction migrated northward through western California, and the San Andreas transform system increased its length, large crustal slivers were broken off from the North American plate (Reference 16). Several of these detached blocks of continental crust, including the continental Salinian block in central and northern California and the oceanic Vizcaino block at the northern end of the San

HUMBOLDT BAY ISFSI FSAR UPDATE

Andreas fault system (Reference 17), were attached to the eastern edge of the Pacific plate as the San Andreas fault motions were transferred eastward (Reference 18).

Other detached pieces of the North American plate were entrained between east-stepping branches of the San Andreas fault zone. Two of these fault-bounded crustal slivers in northwestern California are interpreted by Kelsey and Carver (Reference 19) to have persisted through the latest Cenozoic to the present. According to these authors, the western crustal sliver, herein designated the Petrolia subplate, is in contact with the Pacific plate on its western side along the San Andreas fault zone. The Petrolia subplate is bordered on the east by the Bear River shear zone and a zone of right-slip faults including, from northwest to southeast, the Garberville fault, the Maacama fault, the Rogers Creek fault, and the Hayward fault (Figure 2.6-6). The second fault-bounded crustal block, the Eel River subplate, is interpreted to lie between the Petrolia subplate and the North American plate (Figure 2.6-6). This sliver of North American plate crust is bounded on the west by the Bear River shear zone and the Garberville/Maacama/Rogers Creek/Hayward fault zone, and on the east by a similar system of predominately right-slip faults, including, from northwest to southeast, the Lake Mountain fault, the Bartlett Springs fault, the Green Valley fault, and the Calaveras fault. These right-slip fault zones are part of the San Andreas fault system, which separates the Pacific and North American plates south of the Mendocino fault zone.

North of the Mendocino fault zone, the western side of the North American plate is bounded by the Cascadia subduction zone, which includes the plate boundary megathrust and a broad west-vergent, overlapping system of thrust faults along the plate margin. In northwestern California, this imbricate system includes two major fault zones: the Mad River fault zone, and the Little Salmon fault zone, which we interpret to accommodate a large part of the convergence between the North American plate and subducting Gorda plate. Where the southern part of the Gorda plate is subducting beneath the Eel River and Petrolia subplates, there are two subduction zone segments, called the Eel River and Petrolia segments. Historical seismicity and paleoseismic evidence indicate these segments have slip histories that are independent of the main Cascadia subduction zone, as discussed in Section 2.6.2.4.

In contrast to the San Andreas fault zone in northern California, which has been nearly aseismic since the 1906 earthquake, both the Garberville/Maacama/Rogers Creek/Hayward and the Lake Mountain/Bartlett Springs/Green Valley/Calaveras fault zones are well-defined seismically, and have been the source of many predominately right-slip to right-oblique or reverse-slip earthquakes (regional faults are shown on Figure 2.6-6, except for the Rogers Creek, Hayward, Green Valley and Calaveras faults, which are south of the mapped area). Reference 20). The seismicity reflects right-slip transform motion, resulting from northwest movement of the Pacific plate relative to the western North American plate margin. Focal mechanisms show these faults to have steep northeasterly dips. Focal depths range from a few kilometers to the base of the crust in this region, which is about 20 kilometers (Reference 20-21). The depth distribution of seismicity associated with the Garberville/Maacama/ Rogers Creek/ Hayward and the Lake Mountain/Bartlett Springs/Green Valley/Calaveras fault zones shows the crustal blocks bounded by these fault zones are detached from the

North American plate and are moving within the San Andreas transform system as small subplates.

This interpretation of the interplate structure of the Garberville/ Maacama/Rogers Creek/ Hayward fault zone and the Lake Mountain/Bartlett Springs/Green Valley/Calaveras fault zone is supported by the results of deep-crustal and upper-mantle seismic imaging studies that show apparent offset of prominent lower-crustal and upper-mantle reflectors across these faults (Reference 21). Trilateration, triangulation, and Global Positioning Satellite geodetic measurements of strain across northwestern California south of the Mendocino triple junction show that much of the right-slip motion between the Pacific plate and the North American plate currently is localized along these two fault zones (References 22-23).

2.6.2.3 Pacific/Gorda-Juan De Fuca Plate Boundary

The plate boundary between the Pacific and Gorda-Juan de Fuca plates has traditionally been defined as the Mendocino transform fault zone, a nearly west trending, right-slip fault zone that extends about 1,400 kilometers across the sea floor from Punta Gorda, 15 to 25 kilometers south of Cape Mendocino, to the southern end of the Gorda rise. The landward end of the fault zone is well expressed topographically and bathymetrically by the Mendocino escarpment, a prominent sea floor escarpment having more than 900 meters of relief. The escarpment separates the anomalously shallow continental marine margin underlain by the Vizcaino block of the Pacific plate south of the Mendocino fault zone (Figure 2.6-4) from the deep Gorda basin to the north (Reference 17). The Mendocino fault zone is highly seismic, and has produced many moderate to large earthquakes during the historical period, including several in the magnitude range of 7 to 7.25 (References 24-25).

There is considerable evidence of north/south compression across the eastern part of the Mendocino fault zone. Many of the earthquakes along this part of the zone have oblique compressional focal mechanisms. Additionally, the topographic relief of the Mendocino escarpment is attributed to compression-driven uplift of the northern edge of the Vizcaino block. Rounded cobbles dredged from the crest of the Mendocino ridge, a prominent fault-parallel ridge on the sea floor along the northern edge of the Vizcaino block, suggest the ridge was emergent during the late Cenozoic, and has since subsided below sea level (References 17, 26, and 27). The elevation of the thicker and older crust of the Vizcaino block above the thinner and younger Gorda plate oceanic crust north of the transform fault zone is the opposite of what would be predicted from isostatic effects. The elevation of the northern edge of the Vizcaino block has been attributed to dynamically supported uplift driven by the north/south compression between the Pacific and Gorda plates (Reference 17).

The southern half of the Gorda plate, north of the Mendocino fault zone and west of the Cascadia subduction zone, is strongly deformed and highly seismic. Northeast-trending, high-angle, left-slip faults distributed across this part of the plate have produced many historical earthquakes having magnitudes as large as 7.2 (References 24-25) (Figure 2.6-7). Near the triple junction, some of the seismicity also yields north/south compressional focal mechanisms (References 28-29). Magnetic

anomalies in the southern part of the Gorda plate have been rotated clockwise relative to the Gorda rise; older anomalies have progressively greater rotation. In the triple junction region, this apparent rotation approaches 60 degrees for anomaly 3 (isochrons 3.86 to 4.79 million years old, Figure 2.6-7). Additionally, the length of the deformed anomalies is less than the length of the parent Gorda rise; older anomalies have progressively more shortening. Wilson (Reference 30) called the deforming southern part of the plate the “Gorda deformation zone,” and questioned whether it could be considered part of an internally rigid crustal plate.

The northern boundary of the Gorda deformation zone is a relatively sharp transition from rotated oceanic crust on the south to rigid crust having sparse seismicity and magnetic anomalies that are generally parallel to the Gorda rise to the north. This transition strikes N60°W, and intersects the subduction zone offshore of the coast a short distance north of the latitude of Humboldt Bay. Although no discernible offset of magnetic anomalies or rise-generated structural fabric in the Gorda plate is evident along this transition, Wilson (Reference 30) attributes the boundary to right shear at depth, possibly localized along faults in a narrow zone in the lower part of the oceanic plate. The transition is generally coincident with the northern limit of concentrated Gorda plate seismicity (Reference 31).

Two kinematic models have been proposed to explain the deformation within the Gorda deformation zone. Riddihough (Reference 32) postulated the southern part of the Gorda plate has behaved as an internally rigid block that has undergone clockwise rotation around a nearby pole. He postulated shortening along the southern margin of the block by obduction of the Pacific plate along the eastern end of the Mendocino transform fault zone. However, the lack of evidence of thrusting of the Vizcaino block over the southern margin of the Gorda plate, and the evidence of widely distributed faulting within the plate do not support this interpretation.

A preferred alternative explanation for the deformation of the southern part of the Gorda plate includes asymmetrical spreading at the Gorda rise, and pervasive left shear distributed on many vertical faults aligned along the original structural fabric of the Gorda crust (References 30-31). More rapid spreading to the north along the rise is apparent in the rotation of the magnetic anomalies. Left shear along zones of structural weakness inherited from the rise results from the plate rotation, as long, narrow, fault-bounded blocks slide past one another, analogous to a toppling stack of books.

2.6.2.4 Cascadia Subduction Zone

The Cascadia subduction zone extends from northern California 1,100 kilometers north to southern British Columbia. The oblique convergence of the Gorda-Juan de Fuca plate with the North American plate is accommodated by subduction along this zone. The zone is characterized by the very young age of the subducting Gorda-Juan de Fuca plate (less than 10 million years at the trench), a shallow angle of subduction of the down-going oceanic plate (dip less than 10 degrees), a moderate rate of convergence (3 to 4 cm/yr), a moderate rate of the oblique component of the convergence (1 to 2 cm/yr), and a relatively shallow trench. Based on these properties, when compared to other subduction zones worldwide, Cascadia belongs to a class of

HUMBOLDT BAY ISFSI FSAR UPDATE

strongly coupled (Chilean-type) subduction zones, compared with subduction zones where the plates are weakly coupled (Mariana-type) (Reference 33). Examples of other Chilean-type subduction zones include those in Alaska, the eastern and central Aleutians, southern Chile, northwestern South America, southeastern Russia, and southwestern Japan (Reference 33). Chilean-type subduction zones have produced the largest earthquakes (magnitude 7.7 to 9.5; average magnitude, 8.7) and longest rupture lengths (150 to 1,000 km; average rupture length, 540 km), compared with weakly coupled subduction zones (average magnitude, 7.7; average rupture length, 110 km) (based on a summary of 53 worldwide subduction zone events between 1938 and 1991) (Reference 34, Table 2-2).

Within the Mendocino triple junction region, three Cascadia subduction zone segments can be defined (Figure 2.6-6). The main segment is the 1,000-kilometer-long Cascadia subduction zone segment that extends north from Humboldt Bay. The interpretation was made that South of Humboldt Bay the Eel River segment, an approximately 80-kilometer-long segment along which the northern part of the Gorda deformation zone is obliquely subducting beneath the Eel River subplate. The southern segment, designated the Petrolia segment, reflects convergence of the southern part of the Gorda deformation zone and the Petrolia subplate. The Petrolia segment has a mapped length of 25 to 30 kilometers. These three segments have different seismic histories.

Although the main Cascadia subduction zone segment has been seismically quiet during recorded history, paleoseismic and tsunami evidence has led to wide acceptance that the zone has produced great earthquakes in the past, most recently about 300 years ago, and has the potential to generate great earthquakes in the future (Reference 35). High-precision radiocarbon ages have been obtained from tree ring series from trees interpreted to have been killed by saltwater incursion due to coseismic subsidence along the Washington (Reference 36) and Oregon coasts (Reference 37) and in the Mad River Slough at Humboldt Bay (References 38-39). These ages indicate the most recent great Cascadia earthquake occurred during a 10- to 20-year interval around AD 1700. Additionally, high-precision radiocarbon ages for herbaceous salt marsh plants, also interpreted as having been killed by flood water due to earthquake-generated coastal subsidence, were derived from nine coastal locations along the main Cascadia subduction zone segment in northern California, Oregon, and Washington (Reference 40). These ages also indicate the most recent great earthquake on the main Cascadia subduction zone segment occurred during a 10- to 20-year interval around AD 1700.

The date of this earthquake can be further pinpointed by observations of a trans-Pacific tsunami that destroyed houses in Kuwagasaki and was recorded at four other locations in Japan on January 27, 1700. This wave is interpreted to have been caused by the most recent large slip event on the Cascadia subduction zone (Reference 41). Satake and his colleagues (Reference 41) modeled both segmented (magnitude ~8) and long (magnitude ~9) rupture lengths on the Cascadia subduction zone. They found the long rupture was necessary to produce a tsunami large enough to cause the damage reported in the Japanese literature. Additionally, because the stratigraphy in many of the coastal marshes in North America (from California to British Columbia) shows only

HUMBOLDT BAY ISFSI FSAR UPDATE

one sand deposit from the 1700 tsunami, not several, the paleoseismic evidence also suggests the most recent Cascadia earthquake resulted from a long, single rupture of the subduction zone, causing an earthquake near magnitude 9.

The April 25, 1992, magnitude 7.1 Petrolia earthquake was a thrust event that broke along the southernmost segment of the Cascadia subduction zone (Reference 14). The earthquake resulted from rupture of the plate interface along the northwestern end of the Petrolia subplate (Humboldt plate of Reference 42). This earthquake demonstrated the seismic potential of the southernmost part of the subduction zone, and the segmentation associated with the subplates, defined by the branches of the San Andreas fault system (Figures 2.6-4 and 2.6-6). As discussed in Section 2.6.5, although the Petrolia segment has a mapped length of 25 to 30 kilometers, only the eastern part of the subplate, which has a north to south width of 18 kilometers, is considered to be seismogenic.

The third segment of the Cascadia subduction zone in the triple junction region is between the 1992 rupture and the main Cascadia subduction zone segment north of Humboldt Bay. This segment is the convergent margin between the deforming Gorda plate (Gorda deformation zone) and the Eel River subplate. It has not generated a notable earthquake in more than 150 years, but the paleoseismic record for this part of the subduction zone demonstrates the segment is tectonically active. Fossil tree stumps in the lower Eel River Valley are presently below sea level, and tree ring analyses show these trees died suddenly (References 43-45). The submergence was associated with subsidence in the Eel River Valley, presumably during a prehistoric earthquake.

The Eel River Valley is located in the core of a syncline filled with a thick sequence of late Cenozoic sediments. The syncline is interpreted to represent the structural depression formed in the backstop region of elastic relaxation behind a large northwest-striking, northeast-dipping thrust fault, possibly the Russ fault (Reference 46), which reaches the surface to the southwest near the southern edge of the Eel River subplate.

The timing of the late Holocene paleoseismic events in northwestern California cannot be differentiated on the basis of conventional radiocarbon ages from the Cascadia events farther north, suggesting most of the subduction zone may have been unsegmented during most seismic cycles (Reference 47). Li (Reference 44) used conventional radiocarbon dating to estimate the ages of a series of subsidence events in the Eel River syncline based on detailed analysis of the marsh stratigraphy. Several of the subsidence events, which are interpreted to have been caused by coseismic subsidence associated with earthquakes on the Cascadia subduction zone, have ages similar to events on the Little Salmon fault zone and to events on the main segment of the Cascadia subduction zone farther north. Data from References 44, and 48 – 53 are used to develop Table 2.6-2. (See also Section 2.6.9, and Figure 2.6-96). However, high-precision carbon-14 ages for tree ring series from submerged trees in the lower Eel River Valley indicate the most recent large earthquake on the Eel River segment of the Cascadia subduction zone occurred during the early 1800s (Reference 48 - copies of the original data records for these carbon-14 ages are in the PG&E files). This is significantly younger than the most recent event on the main segment of the subduction

HUMBOLDT BAY ISFSI FSAR UPDATE

zone to the north, which occurred in 1700 AD. Therefore, it has been concluded that the Eel River and main segments of the Cascadia subduction zone ruptured independently during the most recent event on each of these segments.

Nelson and others (Reference 54) correlate turbidite deposits in the offshore channels from Vancouver Island to the Noyo Channel, south of Cape Mendocino, to regional earthquakes. They postulate that the 13 turbidites since about 7,200 years ago in the Cascadia, Astoria, and Rogue channel systems were caused by earthquakes on the Cascadia subduction zone (average recurrence of 600 years). South of the Rogue River, the number of turbidites progressively increases; there are 50 Holocene turbidites in the Eel River channel. They ascribe 20 of these to Cascadia events and 30 to San Andreas events. We believe some of these may have been triggered by events on the Petrolia and Eel River subplates at the southern end of the Cascadia subduction zone.

The structure of the main Cascadia subduction zone segment in the study region is interpreted to include a 65- to 100-km-wide active fold and thrust belt in the North American plate margin that extends onshore in northern California (Figure 2.6-8). The fold and thrust belt is composed mainly of two distinct groups of thrust faults: the Mad River fault zone, and the Little Salmon fault system (Reference 50). Both groups are composed of right-stepping, en echelon, seaward-vergent imbricate thrust faults. Although the groups are subparallel to the trench, their component faults are oriented normal to the direction of oblique convergence between the Gorda-Juan de Fuca and North American plates.

The Mad River fault zone and Little Salmon fault system are separated by the Freshwater syncline (Figures 2.6-8 and 2.6-9), a long flat-floored synclinal structure filled with young sediment that extends onshore through the northern part of Humboldt Bay. This structure is adjacent and parallel to the Little Salmon fault system offshore for more than 200 kilometers. It is interpreted to represent the zone of elastic extension and subsidence associated with the Little Salmon fault zone and other faults within the Little Salmon fault system. The high-precision radiocarbon ages from trees at Mad River Slough, which indicate coseismic subsidence of this syncline in 1700 (References 38 and 39), supports an interpretation that the Little Salmon fault zone and the main Cascadia subduction zone experience coseismic slip during great Cascadia subduction zone earthquakes. It is possible that the subsidence in Mad River Slough in 1700 is primarily the result of slip on the underlying subduction zone and that vertical deformation caused by the Little Salmon fault in northern Humboldt Bay is secondary deformation and superimposed on top of the subduction zone (megathrust) related deformation.

The interpretation of coseismic slip on the Little Salmon fault zone and the main Cascadia subduction zone, however, is supported by two types of evidence. First, most of the coast from Big Lagoon south to the triple junction (Figure 2.6-9), a distance of 50 kilometers, exhibits evidence of late Holocene uplift. This area is underlain by the plate interface at a typically shallow depth of 10 to 20 kilometers (about 12 ± 1 km below Eureka). Second, in the Humboldt Bay region, field evidence of coseismic subsidence is localized in the Freshwater, South Bay, and Eel River synclines. Each of these

HUMBOLDT BAY ISFSI FSAR UPDATE

synclines trends parallel to and is in the hanging wall of a major fault: the Russ and Table Bluff faults with the Eel River and South Bay synclines, respectively, and the Little Salmon fault which is bordered by the Freshwater syncline from Humboldt Bay north into southern Oregon (Reference 55-56). Each of these three faults has a high slip rate and large amount of net vertical displacement. Dislocation modeling for this region was conducted as part of the NOAA Cascadia tsunami inundation study (Reference 57) and the CDMG Northern California Cascadia Earthquake Scenario (Reference 58). The modeling suggests slip on the Little Salmon fault during a megathrust event would result in regional uplift along the coast and subsidence of the axis of the Freshwater syncline. Results of the dislocation modeling presented in the NOAA publication (Reference 57) illustrate the form of the surface elevation changes along the coast.

The close proximity of the syncline axis to the surface trace of the Little Salmon fault zone (~10 kilometers) places constraints on the dip of the Little Salmon fault zone. Assuming the fault joins the subduction zone megathrust at the base of the accretionary wedge, about 14 ± 1 kilometers below the surface at the coast at Humboldt Bay (Reference 59), the dip of thrusts in the Little Salmon fault zone must be greater than 40 degrees. Much shallower dips have been observed on the near-surface traces of the fault zone at the coast (Reference 50). Isopach maps of the Little Salmon fault based on measured depths of intercepts of the fault in gas wells at the Tompkins Hill gas field, about 16 kilometers southeast of the plant site, show the fault steepens from less than 12 degrees at the surface to more than 28 degrees at a depth of about 1,800 meters. Large anticlines on the hanging wall of the fault, including the Humboldt Hill anticline, also indicate the dip of the fault increases with depth.

The outer 15 to 25 kilometers of the accretionary margin is cut by thrusts that are parallel to the subduction front and are both seaward- and landward-vergent (Reference 60). The part of the accretionary margin containing the subduction-front-parallel thrusts and the landward part cut by the en echelon thrust zones are separated by a structural discontinuity (Figure 2.6-9) (Reference 50 and 56). Seismic reflection profiles across the structural discontinuity show the eastern part of the accretionary margin, the part cut by the en echelon faults, is floored with older basement rocks (Franciscan Formation), whereas seaward of the structural discontinuity, the accretionary prism is composed of recently scraped-off Gorda plate sediments (References 56 and 60). We interpret the difference in orientation of thrusts on either side of the structural discontinuity as reflecting the limit of strong interseismic coupling between the subducting oceanic plate and the accretionary margin.

Active thrusting on the Little Salmon fault system also is inferred from the evidence of large, locally generated tsunamis that has been found along the Cascadia subduction zone from Vancouver Island to northern California (Reference 35; Section 2.6.9). Radiocarbon ages for the seven most recent tsunamis along the northern California coast are indistinguishable from the ages for subduction earthquakes from coastal subsidence data in Washington State (Reference 49; Section 2.6.9). Both the Japanese records of the trans-Pacific Cascadia tsunami (Reference 41) and runup-height estimates from paleotsunami evidence in northern California (see Section 2.6.9) indicate the tsunamis were too large to be generated by slip on the shallowly dipping megathrust only. This assessment is supported by the results of attempts to model

tsunami generation on the southern part of the Cascadia subduction zone (Reference 57). However, if a large part of the slip on the plate boundary were taken up on thrusts in the Little Salmon fault system, the resulting large vertical sea-floor deformations would be capable of producing tsunamis large enough to produce the evidence found in the paleotsunami record along the northern California coast and reported in early 18th century Japanese literature. The paleotsunami evidence of large tsunami runup heights for previous tsunamis along the northern California coast (Section 2.6.9) also implies that intraplate slip during the most recent seven subduction earthquakes largely has been transferred to the Little Salmon fault system, and the outer 15 to 25 kilometers of the megathrust has experienced relatively less displacement.

A steep, strike-slip fault with flower-structure-like splays can be inferred approximately 10 kilometers offshore along the projected seaward trend of the Little Salmon fault (Figure 10A of Reference 61). As shown on a multichannel seismic reflection profile, this offshore fault is associated with little vertical separation of the basement offshore and little evidence of offset of the Pliocene through Holocene strata (Reference 61, unit A). A strike-slip interpretation for offshore faults would not support the interpretation, proposed in the discussion directly above, that a large part of the slip on the plate boundary is taken up on thrusts in the Little Salmon fault system. The offshore profile of Gulick and others (Reference 61), however, is not consistent with cross sections of the Little Salmon fault onshore. Specifically, onshore cross sections show that the Little Salmon fault is associated with large near-surface displacements on moderate to low angle imbricate thrusts and large vertical separation of the basement/Wildcat contact. Abundant evidence for reverse/thrust displacement on the Little Salmon and Mad River fault zones onshore is found in exposures, trenches, gas wells, and borings. Additionally, the large-scale morphology of the Little Salmon fault includes prominent upper plate anticlines, providing clear evidence of predominantly dip-slip movement.

2.6.2.5 Mendocino Triple Junction Region

As stated previously, the Mendocino triple junction is the intersection of three plate boundaries, each of which is a wide zone of deformation composed of multiple faults. Several previous investigators have recognized this complex and broad architecture (Reference 42 and 60). However, most previous analyses of tectonics and seismic sources in the northwestern California region have generalized the intersecting plate boundaries into discrete narrow zones, and have treated the triple junction as a point, or they have avoided detailed treatment of the triple junction region altogether, considering only the major plate-bounding faults and seismically active areas outside the triple junction region.

New information useful for developing a detailed tectonic model for the Mendocino triple junction region comes from offshore and onshore geologic mapping, identification and characterization of active tectonic structures, seismic refraction and reflection studies of shallow and deep crustal structure, seismicity and seismological investigations, and paleoseismic studies conducted during the past decade. The updated tectonic framework used for assessing seismic sources in the northwestern California region

HUMBOLDT BAY ISFSI FSAR UPDATE

considers the seismotectonic interactions of the subplates and the individual faults within the triple junction region. The triple junction is treated as a broad region at the intersection of the three, wide, plate-boundary deformation zones.

The northwestern extent of the triple junction region is marked by the deformation front of the subduction zone south of the intersection with the transition between the Gorda deformation zone and the undeformed Gorda plate. This point coincides in general with a change in the architecture of the accretionary margin of the Cascadia subduction zone. Along this part of the convergent margin, the internally deforming Gorda deformation zone is subducting at a highly oblique angle beneath the northwestern ends of the Eel River and Petrolia subplates. North of the intersection of the Gorda plate/Gorda deformation zone transition and the subduction zone, the rigid Gorda-Juan de Fuca plate is subducting beneath the North American plate along the main Cascadia subduction zone segment.

The southern part of the accretionary margin, south of the intersection of the subduction front and the transition in the Gorda plate, has a distinctly different architecture than the margin to the north of this intersection (Figure 2.6-9). The structural discontinuity that is prominent northeast of the rigid Gorda plate/Gorda deformation zone transition is absent to the south; instead, west-northwest-trending thrust faults extend from the coast to near the deformation front (Reference 55). These faults and associated folds are generally parallel to large, young, onshore structures, including the Eel River syncline, the Russ fault, and the Bear River shear zone, and appear to reflect tectonics driven by the northward movement of the Pacific plate in the triple junction region (Reference 62).

The northeastern limit of the triple junction region was placed along the landward projection of the transition zone in the subducted Gorda plate. It is interpreted to be along the southern part of the Little Salmon and Table Bluff fault zones in the overlying continental crust. Within this triple junction region, the subplates within the San Andreas transform zone and the fault-bounded blocks of the Gorda deformation zone converge. Their rates and directions of convergence differ from those along the main Cascadia subduction zone segment to the north, where the internally rigid oceanic plate is subducting beneath the North American plate.

The eastern extent of the triple junction region is interpreted to be along the Lake Mountain fault along the eastern edge of the Eel River subplate (Figures 2.6-6 and 2.6-9), and conforms to the eastern limit of the San Andreas transform fault zone. At depth, west of this eastern boundary of the triple junction, the Mendocino transform is represented by the southern edge of the seismically active subducted Gorda plate (Figure 2.6-7) (References 59 and 63). Both the Eel River subplate and the Petrolia subplate overlie the subducted southern Gorda plate edge.

The southern extent of the triple junction region is interpreted to be at the extreme eastern end of the Mendocino fault zone, near Punta Gorda (Figure 2.6-9), and is defined by the northern edge of the rigid Pacific plate. The Mendocino fault zone is very well expressed offshore and to the west of the subduction zone deformation front; however, the location of the fault zone near the coast is not well known. A linear

projection of the fault zone from its well-defined trace offshore to the shoreline places the plate boundary in the Mendocino Canyon as it crosses the continental shelf, and under the coastline near Mussel Rocks and McNutt Gulch, west of Petrolia (Reference 56). However, aftershocks following the 1992 Petrolia earthquake defined a strike-slip fault trending beneath the Mattole submarine canyon and extending under the coast near the mouth of the Mattole River (Reference 14), implying a slight southward bend in the fault around the northeast corner of the Pacific plate (Figure 2.6-9). Coastal uplift during the 1992 Petrolia earthquake extended several kilometers farther south to Punta Gorda (Reference 64), and may represent obduction of the southwestern edge of the Petrolia subplate over the Mendocino fault zone during the Petrolia earthquake.

2.6.2.6 Aleutian Subduction Zone Analog

The eastern Aleutian subduction zone has many characteristics similar to those of the Cascadia subduction zone. Analysis of the 1964 Alaska earthquake provides a useful analog to better understand the potential earthquake and tsunami hazards associated with the Cascadia subduction zone.

The 1964 magnitude 9.2 Alaska earthquake was caused by rupture on the eastern part of the Aleutian subduction zone, and by displacements on intraplate faults. These combined displacements uplifted part of the accretionary continental margin, creating the large tsunami associated with this earthquake. This Alaskan structural setting is comparable to the Cascadia subduction zone, with the Little Salmon fault system cutting through the accretionary prism, and provides an analog for northern California (Figure 2.6-10). The details of this earthquake are presented in Appendix 2A of Reference 65; the important points are summarized below.

The 1964 Alaska earthquake deformation involved a segment of the eastern Aleutian arc 800 kilometers long and 275 to 400 kilometers wide. This major tectonic event was characterized by seismicity less than 30 kilometers deep, regional vertical displacements in a broad asymmetric downwarp to 2 meters, and flanking zones of marked uplift to 11.3 meters on the seaward side (References 66-67).

Subordinate northwest-dipping reverse faults, the Patton Bay and Hanning Bay faults, displaced the surface on Montague Island. The Patton Bay fault, which experienced at least 7.9 meters of dip-slip, extends offshore to the southwest onto the continental shelf, and intraplate fault displacement seaward of Middleton Island near the continental shelf edge is suggested by 3.5-meter coseismic uplift and northeastward tilting of the island. The intraplate thrust faults at Montague and Middleton Islands alone accommodated at least 23 meters of the total slip on the Aleutian megathrust, assuming average fault dips of about 30 degrees (Figure 2.6-10).

Arrival times on the Alaskan coast show the source area for a major train of destructive sea waves (tsunamis) generated on the continental shelf corresponds closely to the zone of major uplift on the Patton Bay fault and subsidiary faults on the continental shelf and slope. The waves clearly resulted from sudden coseismic upheaval of the sea floor (References 66 and 68).

These data show that a major fraction of the slip may be partitioned among intraplate thrust faults that break relatively steeply to the surface and consequently can result in greater seafloor uplift than an equivalent displacement entirely on the megathrust. In Cascadia, the zones of active faults and related folds of the Little Salmon fault zone appear analogous in tectonic behavior to the intraplate faults observed or inferred within the focal regions of the 1964 Alaska earthquake, which generated a major tsunami.

2.6.2.7 Summary Of Tectonic Framework

- The Humboldt Bay ISFSI site is situated near the southern end of the Cascadia subduction zone, at the northern margin of the complex and highly seismic Mendocino triple junction region.
- Within the Mendocino triple junction region, three distinct Cascadia subduction zone segments were delineated. The southernmost, about 25 to 30 kilometers long, represents the part of the subduction zone where the deforming southern margin of the Gorda plate is converging with the Petrolia subplate at the northern end of the San Andreas transform fault zone. The April 25, 1992, magnitude 7.1 Petrolia earthquake demonstrated the seismic potential of this segment. The second segment of the subduction zone, about 80 kilometers long, is defined by convergence of the deforming southern part of the Gorda plate with the Eel River subplate at the northern end of the San Andreas transform zone. It has not produced an historical earthquake, but paleoseismic evidence indicates the segment last ruptured about 1820, and caused subsidence of the lower Eel River valley. These subduction-zone segments constitute independent seismic sources for large earthquakes in the Humboldt Bay region. The main Cascadia subduction zone segment extends north from Humboldt Bay for about 1,000 kilometers. This zone last ruptured causing a great earthquake in 1700, and has the potential to generate great earthquakes in the future.
- Along the Cascadia subduction zone, the northwestern limit of the Mendocino triple junction region is interpreted to be where a transition from deformed to internally rigid Gorda oceanic crust intersects the subduction zone. This northwestern limit to the triple junction region is considered to mark the southern extent of plate-boundary rupture during great earthquakes on the main Cascadia subduction zone.
- The structure of the main Cascadia subduction zone segment includes a prominent fold and thrust belt, roughly parallel to the leading edge of the North American plate, that includes the Little Salmon fault system. Faults within the Little Salmon fault system are interpreted to be steeply dipping (more than 40 degrees) and, together with the Table Bluff fault and Mad River fault zone, to accommodate a large part of the slip generated during great subduction earthquakes. Data from the Aleutian and Cascadia

subduction zones indicate that intraplate deformation can take up much or all of the plate convergence, and that this deformation can extend landward to areas where the megathrust is as much as 17 kilometers deep.

- Offshore vertical displacements of the sea floor related to secondary faulting within the upper plate have been shown to be effective mechanisms for tsunami generation during the 1964 Alaska earthquake, and are suspected in other great tsunamigenic subduction-zone events. For Cascadia, a comparable mechanism, involving rupture on intraplate faults in the Little Salmon fault system, is considered to be responsible for generating the robust local tsunamis observed in the paleotsunami record.

2.6.3 REGIONAL GEOLOGY AND SEISMICITY

2.6.3.1 Introduction

Because the seismic hazard at the Humboldt Bay ISFSI site is controlled, to a large extent, by nearby active faults, this discussion of the regional geologic setting and seismicity for the Humboldt Bay ISFSI site focuses primarily on the region within about 30 kilometers of the site. More distant sources were considered as part of the regional tectonic framework (Section 2.6.2), and are also considered in the seismic source characterization (Section 2.6.5). Regional seismicity data within 160 kilometers (100 miles) of the site also are considered in this section, with an emphasis on earthquakes that have occurred within 40 kilometers (25 miles) of the site. The details and analysis of the site geology are presented in Section 2.6.4, Site Geology.

2.6.3.2 Regional Geology

Figures 2.6-11 (faults in the vicinity of Humboldt Bay are more accurately depicted on Figures 2.6-13 and 2.6-18) and 2.6-12 are a generalized geologic map and cross section that show the major geologic terranes (the term terrane refers to a rock or group of rocks and the area in which it outcrops) and geologic structure of the Mendocino triple junction region. Figures 2.6-13 and 2.6-14 provide a more detailed geologic map and cross section that show the main structural features of the Humboldt Bay region. Table 2.6-3 contains a summary of the geologic history of the Humboldt Bay ISFSI site.

2.6.3.2.1 Regional Stratigraphy

The Humboldt Bay ISFSI site is in a broad depositional basin (the Eel River basin), which is underlain by a thick sequence of late Cenozoic (the geologic time scale is presented in Table 2.6-1) marine sedimentary rocks of the Wildcat Group (QTW on Figure 2.6-11). A composite stratigraphic column of the onshore part of the Eel River basin is presented in Figure 2.6-15. The late Cenozoic deposits unconformably overlie basement rocks of the Late Jurassic to late Tertiary Franciscan Complex. Ogle (Reference 69) divides the Wildcat Group into five formations (lithostratigraphic units) and defines a sixth, the Hookton Formation, which unconformably overlies the Wildcat

Group. Woodward-Clyde Consultants (Reference 1) conducted detailed stratigraphic and structural investigations of the site region, refining Ogle's map and clearly demonstrating the time-transgressive nature of the upper Tertiary and Quaternary formations. The following discussion is based primarily on the Woodward-Clyde work (Reference 1, Appendix A), augmented by subsequent studies in the region.

Franciscan Complex (Pre-Wildcat Accreted Basement Rocks)

The Central Belt and Coastal Belt terranes of the Franciscan Complex form the basement rocks in the Humboldt Bay region. These terranes were accreted to the western margin of North America by plate convergence prior to development of the present Cascadia subduction zone.

The Late Jurassic and Cretaceous Central Belt Franciscan Complex, which crops out north and east of the Freshwater fault and the Coastal Belt thrust (Figures 2.6-11 and 2.6-13), consists of weakly to moderately metamorphosed sandy and silty turbidities, pillow basalt, thinly bedded chert, and interbedded shale. In many places the Central Belt rocks are intensely sheared, are tectonically mixed, and form a *mélange* in which more resistant basalt, sandstone, chert, and higher-grade metamorphic rocks including blueschist constitute tectonic blocks in a shaley matrix. The Central Belt Franciscan Complex, which was accreted to the northern California coastal region during the Late Jurassic to Cretaceous, makes up the pre-late Cenozoic basement along much of the northern California coast. These rocks (Figure 2.6-13) underlie the sedimentary rocks of the late Cenozoic Wildcat Group to the north and northeast of Humboldt Bay, east of the Freshwater fault (Reference 70).

The Coastal Belt Franciscan Complex is distinctly different from the Central Belt. Coastal Belt rocks consist mostly of lower to upper Tertiary marine sandstone (graywacke), siltstone, and shale that crop out to the southeast and south of Humboldt Bay (Reference 71). The Coastal Belt Franciscan Complex is subdivided into four terranes: (1) Coast Ranges terrane (sometimes referred to as the Coastal terrane); (2) King Range terrane; (3) False Cape terrane; and (4) Yager terrane (Figure 2.6-11) (Reference 72). All of these, except the King Range terrane, occur within the Humboldt Bay region (Figure 2.6-13). These sedimentary rock sequences consist largely of turbidites that were accreted to the western margin of the Central Belt. The Coastal Belt terranes are unconformably overlain by the late Cenozoic sediments of the Wildcat Group.

The Yager terrane, which is the oldest unit within the Coastal Belt Franciscan Complex, includes sandy and silty turbidites of the early Tertiary Yager Formation. The Yager Formation is strongly folded and cut by numerous early and middle Tertiary faults. During the middle Tertiary, the Yager Formation was accreted to the western margin of North America and juxtaposed against rocks of the Central Belt *mélange* along the Freshwater fault and Coastal Belt thrust (Figures 2.6-11 and 2.6-13) (References 46 and 56). The Yager Formation underlies the Wildcat Group and younger sediments southeast of Humboldt Bay, from the vicinity of the Russ fault in the south to the Freshwater fault and Coastal Belt thrust on the north (Figure 2.6-13) in the lower Elk, Van Duzen, and Eel River drainages.

The youngest accreted basement rocks of the Coastal Belt Complex in the Humboldt Bay region make up the False Cape and the Coast Ranges terranes (Reference 73). These units consist of highly sheared Miocene to early Pliocene sandstone, siltstone, and shale that reflect tectonic offscraping and shallow underplating of Farallon plate sediments in the proto-Cascadia subduction zone.

The Coast Ranges terrane, exposed south of the Russ fault and west of the Yager terrane, is a highly sheared *mélange* composed predominantly of sandstone, argillite, and minor conglomerate. The False Cape terrane is exposed along the coast south of the Russ fault between False Cape and Cape Mendocino (Reference 46). The False Cape fault includes strongly deformed turbidite sediments locally sheared into *mélange* containing blocks of lower Wildcat Group sediments. Except for the active accretionary prism offshore, the False Cape and Coast Ranges terranes are the most recent sediments to be accreted on the edge of the North American plate, and are in part coeval with lower Wildcat Group sediments.

Wildcat Group and Falor Formation (Late Tertiary and Quaternary)

Franciscan basement rocks in the onshore Humboldt Bay region are unconformably overlain by a sequence of late Tertiary and Quaternary onlap deposits as much as 3,600 meters thick that were deposited on the upper plate of the modern Cascadia subduction zone. Their depositional history includes sedimentation in deep-trench and lower-slope basin environments during the Miocene, and progressive shoaling through the late Pliocene to shelf and marginal marine depositional settings during the early Pleistocene. Collectively, these sediments are named the Wildcat Group (Reference 69) and are interpreted to have been deposited in a large, evolving forearc basin called the Eel River basin (Reference 74). Lower Wildcat Group sediments reflect deposition in a locally quiescent tectonic environment, as indicated by the lack of significant regional unconformities and relatively uniform lithofacies with parallel bedding that covered large areas.

In contrast, the lithologies of upper Wildcat Group sediments are laterally variable, reflecting depositional environments that ranged from deep marine on the west margin of the Eel River basin to fluvial on the east margin. Coarsening of sediments with increasing age toward the east indicates the westward shoaling of the basin. Macro- and microfossils, sedimentary structures, and other paleoenvironmental characteristics of the upper Wildcat Group sediments record northeast-to-southwest shallowing of the basin in response to the rapidly developed fold-and-thrust system associated with the evolution of the Cascadia subduction margin. The initiation of the contractional tectonics that followed deposition of the Rio Dell Formation drastically changed sedimentation patterns within the Eel River basin. Localized uplift due to anticlinal fold growth over active thrust faults divided the subsiding basin into several small depocenters or subbasins. These subbasins, located in the synclinal regions of the fold-and-thrust belt, contain growth strata that record both basin subsidence and adjacent anticlinal uplift. This fold-and-thrust tectonics, coeval fore arc subsidence, and related patterns of sedimentation have continued through the Quaternary and dominate the geology of the region today.

HUMBOLDT BAY ISFSI FSAR UPDATE

In ascending order, Ogle's (Reference 69) subdivision of the Wildcat Group consists of the Pullen, Eel River, Rio Dell, Scotia Bluffs, and Carlotta formations. In the lower Eel River Valley/Wildcat Ridge area, the three lower formations consist predominantly of fine-grained sediments, whereas the two upper formations are made up of coarse-grained clastic sediments. In addition to these formations, Manning and Ogle (Reference 75) delineate another formation in the Mad River Valley northeast of Humboldt Bay, the Falor Formation, which is now geographically separate from the Wildcat Group (Figure 2.6-13), but formed as the marginal marine and adjacent terrestrial facies of the upper Rio Dell sediments.

Pullen Formation - As described by Ogle (Reference 69), the Pullen Formation consists mostly of diatomaceous siltstone and mudstone, with some ferruginous limestone nodules and a few thin glauconitic sandstone beds.

Eel River Formation - The Eel River Formation is composed of dark gray to black mudstone, siltstone, and interbedded sandstone. Most of the sandstone and some of the finer-grained sediments are reported to be glauconitic (Reference 69).

Rio Dell Formation - The Rio Dell Formation consists of predominantly massive marine siltstone, lesser amounts of claystone, and fine- to very fine grained, poorly sorted sandstone. Water depths, inferred from microfossils at Centerville Beach (Reference 76), ranged from about 1,800 meters near the base of the formation to about 90 meters at the top.

Scotia Bluffs Formation - The Scotia Bluffs Formation overlies and interfingers with the upper Rio Dell Formation in the Eel River area. The Scotia Bluffs Formation consists predominantly of massive fine- to medium-grained shallow marine sandstone and lesser amounts of pebbly conglomerate and siltstone that indicate deposition in a fluvial environment (Reference 69). Marine fossils at its type locality in Scotia Bluffs indicate that at least part of the formation was deposited in water having depths of 30 meters or less (Reference 77). The alternating marine and fluvial facies probably reflect glacio-eustatic sea-level-driven transgressions and regressions of the early to middle Pleistocene coastline.

Carlotta Formation - The Carlotta Formation overlies and interfingers with the Scotia Bluffs Formation. East of the Eel River and Fortuna, this formation consists of massive coarse-grained conglomerate, poorly sorted sandstone, bedded and massive blue-gray siltstone, and blue-gray mudstone. The presence of coarse, poorly sorted conglomerate, the absence of marine fossils, and the presence of fossil redwood logs all suggest the Carlotta Formation was deposited in a predominantly continental environment. South of Ferndale, along Wildcat Ridge, the formation consists mostly of massive sandstone containing thin pebbly conglomerate. Coarse, massive conglomerate is limited to near the base of the formation.

Age and Correlation of Wildcat Group - The formations within the Wildcat Group are defined primarily based on lithology, and are time-transgressive. That is, the age of the stratigraphic units as defined by Ogle (Reference 69) varies in different areas,

HUMBOLDT BAY ISFSI FSAR UPDATE

particularly for the upper Wildcat units. Detailed geologic mapping by Woodward-Clyde Consultants (Reference 1, Appendix A) shows that the base of the Scotia Bluffs and Carlotta formations step progressively higher in the stratigraphic section from east to west. The ages of the upper Wildcat formations in the vicinity of the Humboldt Bay ISFSI site are discussed further in Section 2.6.4.

Falor Formation - The Falor Formation in the upper Mad River Valley is more than 1 kilometer thick and consists of onshore and marginal marine facies in thrust-bounded slices across the Mad River fault zone (Reference 75-78). The basal part of the Falor deposits contains the Huckleberry Ridge tephra (Reference 78), which is 1.8 to 2.0 million years old (Reference 79). Therefore, the basal Falor deposits are roughly correlative to the upper Rio Dell Formation at Centerville beach, which is dated by the 1.2- to 1.5-million-year-old Rio Dell ash (Reference 79).

Hookton Formation (Middle to Late Quaternary)

Based on exposures in the Table Bluff area, just south of Humboldt Bay, Ogle (Reference 69) describes the Hookton Formation as yellow-orange gravel, sand, silt, and clay that unconformably overlie the Wildcat Group. Aware that the Hookton Formation is difficult to define as a regional stratigraphic unit, he stated, "No adequate type section can be given because of the extreme variability of these beds." Without a clear stratigraphic context, the Hookton Formation is difficult to distinguish from weathered sediments of the Carlotta and Scotia Bluffs formations. In the southeast part of the area, the Hookton Formation generally consists of silt, sand, and coarse conglomerate. West and north of Tompkins Hill, it consists of fine-grained, well-sorted sand interbedded with pebbly conglomerate and thin silt and clay beds. The lithology of the Hookton Formation in the vicinity of the ISFSI site is described in more detail in Section 2.6.4.

Age and Correlation of Hookton Formation - It is difficult to distinguish between some sediments in the Hookton Formation and the upper part of the Wildcat Group at the outcrop or local scale. At the regional scale, strongly localized lateral and vertical variability of sediment type within the Hookton Formation reflects strong local tectonic influences on sedimentation. In contrast to the Wildcat Group, the Hookton and other post-Wildcat Group sediments and geomorphic surfaces, including marine terraces, show consistent east-to-west migration of the coastline and decreasing age of lithofacies toward the west. Paleomagnetic data, correlation of volcanic ashes, and radiometric dates also indicate that these upper deposits are progressively younger from east to west.

Woodward-Clyde Consultants (Reference 1) recognized that the sediments that unconformably overlie the Wildcat Group near the HBPP probably are not the same age as deposits mapped as Hookton Formation in other areas. Therefore, they restricted use of the term Hookton Formation to deposits that unconformably overlie the Wildcat Group in the Tompkins Hill/Table Bluff/Humboldt Hill area and in the subsurface in the Buhne Point area at the ISFSI site, excluding Holocene alluvium, marine terrace and bay deposits. This division is followed in this evaluation.

Hookton deposits in this area contain dated and correlative volcanic ash layers that are useful in assessing the structural history of the area. These tephras, which have normal magnetic polarity, are interpreted to be younger than the transition between the Matuyama and Bruhnes magnetic polarity epochs (Reference 1), which occurred 780,000 years ago. (Paleomagnetic data, radiometric dates, and correlation of volcanic ashes in the lower part of the unit indicate the base of the Hookton Formation is less than about 780,000 years and older than about 400,000 years old. The maximum age is based on the age of the Bruhnes/Matuyama boundary, which occurs either near the base of the Hookton Formation, or within the time span encompassed by the unconformity at the base of the Hookton Formation. The minimum age is based on K-Ar and fission track dates obtained on an ash bed, the Railroad Gulch Ash, in the lower part of the Hookton Formation. Based on these data, Woodward-Clyde Consultants (Reference 1) estimated that deposition of the Hookton Formation in the Tomkins Hill area, 10 to 15 kilometers south of the site, began 600,000 \pm 100,000 years ago.) (Reference 80). The base of the Hookton Formation is older than the Railroad Gulch ash. The Railroad Gulch ash correlates to the Rockland ash from the Lassen Peak area, California (Reference 81). Although the Rockland ash has been difficult to date and its age is still debated (Reference 82), it is at least 400,000 years old (Reference 81) and may be as old as 600,000 years (Reference 83). The age of the Hookton deposits beneath the ISFSI site is discussed in detail in Section 2.6.4.

Marine Terraces (Late Quaternary)

Although originally included as part of the Hookton Formation shown by Ogle (Reference 69) and followed by Woodward-Clyde Consultants (Reference 1), the sequence of uplifted marine terraces along the margins of hills and coastal bluffs in the Humboldt Bay region can be separated into distinct units. This sequence records late Pleistocene uplift and deformation associated with the growth of faults and folds in the upper plate of the Cascadia subduction zone (Reference 84). Marine terrace sequences in the Humboldt Bay region are associated with uplift and growth along the Table Bluff anticline and fault, the Humboldt Hill anticline and Little Salmon fault zone (Figure 2.6-16, item a), and the Eureka anticline (Figure 2.6-16). Intervening synclines, such as the South Bay and Freshwater synclines, are areas of active, episodic subsidence (Reference 85).

The ages of marine terraces in the Humboldt Bay region and in other parts of northern California have been estimated by application of global sea level curves to flights of terraces, numerical dating, correlation of volcanic ash, and correlation based on relative soil profile development. The ages of the sequences of marine terraces north of the site near Trinidad and McKinleyville (Reference 84) and south of the site near Cape Mendocino (References 86-88) have been estimated by correlation of the global sea level curve, following the practices applied elsewhere in the world (for example, References 89-91). Carver and Burke (Reference 84) stated, "Terrace age assignments are based on the best matches between: (1) altitude sequences of local terrace remnants, and (2) unique terrace altitude sets produced by applying uniform average uplift rates to known ages and altitude of formation of New Guinea terraces." In the Humboldt Bay region, soil profile development was used to correlate terraces in the Trinidad and McKinleyville flights with terraces at Table Bluff (and elsewhere).

Independent age dates, including limiting age estimates, also were used in developing age estimates for marine terraces.

The numerical dates from terraces in the Humboldt Bay area include thermoluminescence dates of silts (References 92-94) and correlation of the Loleta ash in a terrace deposit at the top of Table Bluff with the Bend Pumice tuff (References 79 and 83). These ages are consistent with those assigned to the terraces in the Humboldt Bay area (Figure 2.6-16); however, age assignments for the terraces at Humboldt Hill and in the Eureka area are more uncertain than are the ages for the terraces in the Table Bluff, McKinleyville and Trinidad areas. Correlations of the terrace sequences and the assigned ages of the local terraces are based primarily on the characteristics of their paleosols, rather than the soil chronosequences that have been developed for the dated terrace sequences at Trinidad, McKinleyville, and Cape Mendocino (Reference 84).

The marine terrace sequence developed in the region surrounding the ISFSI site has been well established by multiple lines of evidence. Nonetheless, alternative explanations for these features can be proposed. One alternative is that some of the topographically differentiated terraces, inferred to have distinct underlying platforms, could be combined because the underlying wave-cut platform is the same age. Another alternative is that some terraces are faulted, creating additional surfaces that have been interpreted as terraces of different ages. If faulting has produced vertically displaced terrace sections of the same age, however, these faults have not been recognized in the field. An alternative explanation for the high rates of uplift recorded by the lowest marine terrace (roughly 1 millimeter per year) adjacent to Eureka is that this uplift is driven by a local intraplate structure (e.g., a blind, active thrust, or reverse fault), as has been observed at other coastal sites in Northern California and southern Oregon (References 95-97). However, no specific evidence of such blind fault structures has been noted in previous mapping (e.g., Reference 69 and 73); nor has any evidence been mapped in the offshore that could trend onshore under the Eureka area (Reference 55). Also, key stratigraphic contacts directly inland from Eureka are at nearly the same elevation throughout the region.

2.6.3.2.2 Regional Geologic Structure

The structural geology of the Humboldt Bay region is dominated by north-northwest-trending contractional structures formed during several phases of plate convergence that have affected the region since the Late Jurassic. Three classes of structures are evident at the regional scale:

- (1) faults, folds, and tectonic mélanges formed during multiple episodes of accretion of the Franciscan Complex basement rocks during the late Mesozoic and early Tertiary;
- (2) early and mid-Tertiary structures formed in the accreted continental margin prior to the plate tectonic organization of the modern Cascadia subduction zone; and

- (3) late Cenozoic structures (basin subsidence and localized anticlinal uplift) related to the tectonics of the modern Cascadia subduction zone
Figure 2.6-14 is a northeast-southwest geologic section across the Humboldt Bay region.

Franciscan Complex Basement Structures

The accretion of Franciscan Complex rocks in the Humboldt Bay region occurred during a long and complex deformational phase in the structural development of northwestern California that has included repeated episodes of tectonism (Reference 98). As a result, the Franciscan rocks are strongly folded and faulted and locally are pervasively sheared. The various Franciscan Complex terranes are bounded by major faults that have large cumulative displacements.

The Central Belt contains the oldest Franciscan Complex rocks exposed in the Humboldt Bay region. Structures within the Central Belt include large-displacement faults that juxtapose different lithologic assemblages, and bodies of rock having different metamorphic grades. The Coastal Belt Franciscan Complex rocks are younger and have a lower grade of metamorphism. Locally, the Coastal Belt rocks are strongly folded and cut by many faults. The principal basement structures in the Humboldt Bay area are the Freshwater and Russ faults, which form the northeast and south tectonic boundaries of the Coastal Belt, respectively (Figure 2.6-13).

Freshwater fault - The Freshwater fault separates Franciscan rocks of the Central Belt on the east from the Coastal Belt on the west. The structural boundary between the Central Belt and the Coastal Belt continues south of the Humboldt Bay region in the northern and central California Coast Ranges (Reference 73 and 99). Onshore, the Freshwater fault is a steep, easterly dipping, high-angle reverse fault that also may have accommodated large amounts of right slip. Offshore, the Freshwater fault is overlain by sediments deposited in the Eel River basin; most of the deformation on the Freshwater fault pre-dates deposition of the Wildcat Group (Reference 69). The Freshwater fault is displaced by, and therefore predates, the Greenwood Heights fault in the Mad River fault zone (Figure 2.6-14).

Russ fault - The Russ fault extends for 33 kilometers from the coast east-southeast along the crest of Wildcat Ridge to the Eel River (Figures 2.6-11). The fault extends offshore another 24 kilometers to the northwest. The Russ fault forms the tectonic contact between the Yager terrane on the north and the Coast Ranges terrane on the south (Figures 2.6-11 and 2.6-13). Locally, the fault also lies along the contact between the Wildcat Group and basement of the Coast Ranges terrane. Based on bedrock mapping, McLaughlin and others (Reference 73) interpret the Russ fault to be a steep, south-dipping major bedrock structure that extends to the top of the subducting Gorda Plate. As shown on their cross section (Figure 2.6-12), the fault is displaced down to the north, and appears to be associated with microseismicity.

At False Cape (Figure 2.6-11) the fault is exposed in the sea cliff, where it dips at a high angle to the north, and displaces two marine terraces vertically 22 meters and 36 meters (References 100-101). The apparent displacement is down to the south, which is opposite to the sense of the bedrock displacement. Based on the sea cliff

exposure, the Russ fault is interpreted to be a north-dipping reverse fault that displaces lower Wildcat Group sediments and Coast Ranges terrane over rocks of the False Cape terrane, consistent with the interpretation of Aalto and others (Reference 46). The inconsistency in the apparent vertical displacement may indicate a component of strike-slip motion (Reference 102), or may reflect reactivation of the upper part of the fault during the current stress regime as a north-dipping reverse fault that bounds the southern margin of the Eel River syncline. Because of the uncertainties in the slip direction, the slip rate on the Russ fault is poorly constrained. Based on the displaced late Pleistocene marine terraces, the rate of vertical separation across the fault is 0.2 millimeters per year (References 101-102).

Late Cenozoic Faults and Folds

Thrust faults and fault-related folds that make up the active Cascadia fold-and-thrust belt have strongly deformed lower Wildcat Group sediments, influenced the deposition of post-Rio Dell sediments, and affected the geomorphic development of the modern landscapes (References 19 and 56). The interaction of subsidence and fold-thrust deformation has resulted in a clear tectonic distinction between the uplifting regions that overlie active thrust faults and fault-related anticlines, and subsiding basins that are coincident with the intervening synclinal regions.

The Quaternary anticlines in the Humboldt Bay region are interpreted to be active fault-related folds associated with thrusts in the Cascadia fold-and-thrust belt. These folds include the Table Bluff, Humboldt Hill, and Fickle Hill anticlines (Figures 2.6-14 and 2.6-16). These anticlines, which have as much as 1.5 kilometers of structural relief, record significant crustal contraction related to faulting. The anticlines are asymmetrical, having longer northeast limbs that dip between 20 and 40 degrees. The shorter southwest limbs dip steeply, and locally are overturned (References 19 and 78).

Two major zones of thrust faults and related folding have been mapped in the Humboldt Bay region: the Mad River fault zone (Reference 50 and 78), and the Little Salmon fault zone (References 1, 50, 69, and 103) (Figures 2.6-13 and 2.6-14). At the regional scale, these thrust zones trend north and northwest, dip east and northeast, and displace Franciscan Complex basement and lower Wildcat Group rocks over the upper Wildcat Group and younger sediments (Figure 2.6-14).

The late Cenozoic thrusts in the Humboldt Bay region have generally shallow dips in the near surface. Measurements of the dips of thrust faults exposed in trenches, sea cliffs, road cuts, and other shallow exposures range from about 40 degrees to nearly horizontal, averaging about 25 degrees. Although most of the thrusts dip to the northeast, southwest dips also occur.

Changes in dip at depth on the thrusts in the Humboldt Bay region are indicated by exposures of the faults, by fault intersections in boreholes, and by the presence of large anticlines in the hanging walls of most of the major faults. The increase in dip at relatively shallow depths (<1 kilometer) on the thrusts is indicated by fault intersections in the deep wells at the Tompkins Hill gas field and from mapping of deeply eroded

HUMBOLDT BAY ISFSI FSAR UPDATE

Wildcat sediments (Falor Formation) in the upper Mad River Valley (References 19 and 78).

Mad River fault zone - At its closest point, the Mad River fault zone is approximately 23 kilometers north of the Humboldt Bay ISFSI site. The onshore part of the fault zone includes the Trinidad, Blue Lake, McKinleyville, Mad River, Fickle Hill, and Greenwood Heights faults (Figures 2.6-13 and 2.6-14). The surface traces of these faults are generally parallel, northwest-trending, and 2 to 5 kilometers apart. At the coast, the fault zone is about 20 kilometers wide. The offshore part of the Mad River fault zone trends north-northwest along the inner continental shelf as a 15- to 25-kilometer-wide belt of en echelon thrust faults and fault-generated folds (Figures 2.6-6, 2.6-8, and 2.6-13). The total length of the fault zone, including the offshore traces mapped by Clarke (Reference 56), is about 80 kilometers. The thrust faults in the Mad River fault zone are interpreted to coalesce at depth, forming a southwest-vergent imbricate fan thrust system (Figure 2.6-14). The imbricate fan thrust system is inferred to root at depth into the Cascadia megathrust.

Individual faults within the Mad River fault zone juxtapose the basal contact of the Falor Formation (about 2 million years old) with the underlying Franciscan Complex in a series of northeast-tilted fault slices (Figure 2.6-14). Displacements on these faults range from about 1 to 3 kilometers. These displacements are based on measurement of the Franciscan/Falor contact and the stratigraphic thickness of faulted Falor Formation sediments across the Mad River fault zone in the upper Mad River Valley area.

Near the coast, the Mad River fault zone intersects a series of late Pleistocene shorelines represented by uplifted and faulted marine terraces (References 1 and 101). Slip rates estimated for individual thrust faults in the Mad River fault zone, based on dating of the terraces and the amount of uplift, are generally 1 to 2 millimeters per year. Across the zone, the cumulative rate indicated by the marine terrace deformation is about 5 to 9 millimeters per year (References 19, 78, 102, 103, and 104).

Little Salmon fault system and Little Salmon fault zone - The Little Salmon fault zone is part of a system of active folds and reverse faults that extends for 330 kilometers from its intersection with the Freshwater fault/Coastal Belt thrust near Bridgeville, California, northwestward to its intersection with the Thompson Ridge fault off the coast of southern Oregon (Figure 2.6-6). Offshore, this system is composed of north-northwest-trending en echelon anticlines and thrust faults. The fault system trends parallel to the deformation front associated with the leading edge of the Cascadia subduction zone. The southern and central part of the zone is bounded on the west by a well-defined structural discontinuity between northwest-trending structures within the Little Salmon fault system and the more north-south structures along the accretionary margin; on the east, it is bounded by large synclines (Figure 2.6-9). The northern boundaries of the system are not as well defined, but the system clearly does not extend beyond the west-northwest-trending Thompson Ridge fault, which truncates the more northerly trending structures of the Little Salmon fault system. The width of the fault system varies, but typically is about 20 kilometers. Near the site, the fault zone is about 25 kilometers wide, extending from the Table Bluff fault on the

HUMBOLDT BAY ISFSI FSAR UPDATE

southwest, across the Little Salmon fault zone, to the axis of the Freshwater syncline (Figure 2.6-13).

The Little Salmon fault zone, which is the nearest capable fault to the site, has a total length of 95 kilometers, including the offshore traces as mapped by Clark (Reference 56), and the Yager fault to the southeast (Figures 2.6-8 and 2.6-13). The fault zone was identified as a major late Cenozoic thrust first by Ogle (Reference 69). The southeastern end of the Little Salmon fault zone is coincident with the end of the Little Salmon fault system (at its intersection with the Freshwater fault near the town of Bridgeville) (Reference 19). It trends northwest along the Van Duzen River Valley to Humboldt Bay (Reference 69), then continues offshore from the coast obliquely across the continental shelf west and northwest of Eureka (Reference 55-56). Detailed studies during the past 20 years along the margin of South Bay and Little Salmon Creek indicate the fault zone consists of several imbricate branches that are well defined in the geomorphology (Figure 2.6-17). Along the southwestern flank of Humboldt Hill (about 6 kilometers south of the Humboldt Bay ISFSI site), the Little Salmon fault zone includes at least three southwest-vergent imbricate faults that have been active during the Holocene (References 105-108). The westernmost trace, which lies along Little Salmon Creek (south of Salmon Creek), is the fault trace that has the largest Holocene displacement in this area, but the adjacent eastern trace has the greatest total displacement. Northwest of Salmon Creek, the western trace extends beneath and is hidden by modern sediments on the margin of Humboldt Bay west of Humboldt Hill. The middle trace (Little Salmon fault trace on Figure 2.6-17) traverses the western part of the College of the Redwoods campus (Reference 109-110), and can be identified in borings southwest of the plant site. The east trace has been mapped from near Salmon Creek northwestward along the base of Humboldt Hill, traversing the eastern part of the College of the Redwoods campus. North of Humboldt Hill, the eastern trace, which passes southwest of Buhne Point and the ISFSI site, is called the Bay Entrance fault.

The Table Bluff fault is a 23-kilometer-long, west-northwest-trending imbricate thrust within the Little Salmon fault zone in the Little Salmon fault system (Figure 2.6-13). Although the Table Bluff fault is poorly exposed at the surface, Quaternary uplift and folding associated with it is apparent in the geomorphic expression and near-surface structure of the Table Bluff anticline. Interpretation of seismic profiles (ARCO seismic profiles, in PG&E files) and the outcropping structure of the Table Bluff anticline suggest that the fault forms a south-vergent thrust wedge beneath the anticline, with the upper several kilometers of the fault dipping to the south and southwest, and the deeper part of the fault dipping to the northeast (Figure 2.6-14). The deep geometry of the Table Bluff blind-thrust wedge is uncertain. The apparent merging or overlapping with the Little Salmon fault zone along strike suggests it probably splays off of the Little Salmon fault zone at depth. However, where the faults diverge and become widely separated, they are depicted as independent structures (Figure 2.6-14), and are assumed to extend down dip to the plate interface at the top of the Gorda Plate. Analogous “splay faults” which branch upward from the megathrust and cut through the upper plate have recently been imaged on the Nankai subduction zone, a shallow dipping subduction zone similar to Cascadia in southwest Japan (Reference 111).

HUMBOLDT BAY ISFSI FSAR UPDATE

Near the coast, the vertical separation of the base of the Wildcat sediments across the Little Salmon fault zone and the Table Bluff fault (Little Salmon fault system) is more than 3,400 meters (Reference 69, & ARCO seismic profiles, in PG&E files), and the total dip-slip separation may be as much as 7 kilometers (Reference 19). The faulting of the Rio Dell Formation and other units of the Wildcat Group began about 700,000 years ago (during or soon after deposition of the Scotia Bluffs Formation about 800,000 years ago, and before the beginning of deposition of the Hookton Formation about 600,000 years ago) (Reference 1, 19, and 112). Depending on the fault dip, estimates of long-term slip rate range from 6 to 10 millimeters per year for the Little Salmon fault zone at Humboldt Bay, and from about 2 to 3 millimeters per year for the Table Bluff fault. Slip rates from trench studies for the east and west traces of the Little Salmon fault zone during the late Holocene on the east side of the South Bay produce similar estimates (References 50 and 105). The total slip rate across the Table Bluff fault and the Little Salmon fault zone is between 8 and 13 millimeters per year (References 50, 78, and 102).

At the northern end of Humboldt Hill, the Little Salmon fault displaces the entire lower Hookton section, and places Rio Dell Formation over the Hookton sediments (Figure 2.6-18). The amount of vertical separation of the older units is progressively larger. In the vicinity of Humboldt Hill, the vertical displacement of the top of the Rio Dell Formation is 880 to 1,400 meters. The base of the Hookton Formation is displaced 319 to 564 meters, and the top of the unit F clay in the upper part of the lower Hookton Formation is displaced 210 to 247 meters. Using vertical displacement data from boring WCC-12 and a dip of 30 degrees, Woodward-Clyde Consultants (Reference 1) calculated long-term average slip rates on the Little Salmon fault in the range of 1 to 3 millimeters per year. The vertical separation across the fault decreases north of Humboldt Hill, perhaps indicating that slip on the Little Salmon trace has transferred mostly to the Bay Entrance trace northwest of Humboldt Hill.

The style of deformation associated with late Quaternary slip on the Little Salmon fault zone at College of the Redwoods, about 5 kilometers south of the Humboldt Bay ISFSI site (Figure 2.6-17), has been reconstructed based on geotechnical borings and trenches (References 110 and 113). Trenches exposed 25- to 30-meter-wide zones of deformation containing multiple faults, fractures, and discrete fault-bend-fold axial surfaces in the hanging wall (Figures 2.6-19, 2.6-20, 2.6-21, 2.6-22). The structure varies along strike. Typical fault patterns consist of subparallel low- and high-angle faults having reverse and normal displacements. Southwest-dipping reverse faults are interpreted to be secondary backthrusts that increase in number and dip toward the main thrust tip, suggesting increasing proximity to the northeast-dipping master thrust (Reference 113). Graben structures having about 1 meter of cumulative vertical separation also were mapped (Figure 2.6-20). The normal faults, which decrease in slip and terminate downward, record extension in the hanging wall as it rides over bends in the underlying thrust ramp. Folding of strata occurs across discrete axial surfaces that are interpreted to coincide with changes in dip of the underlying thrust ramp (for example, Figure 2.6-19). Fault-generated folding in the overriding thrust sheet results in differential displacement of the ground surface across active axial surfaces (Reference 113). Because the Holocene sediments and soils had been

removed by grading prior to construction of the campus buildings, the Holocene activity of the fault could not be assessed based on the trenches at College of the Redwoods.

Paleoseismic investigations along the Little Salmon fault zone by Carver and Burke (Reference 114), Carver (Reference 115), Carver and Aalto (Reference 116), and Clarke and Carver (Reference 50) constrain the size and the approximate timing of the most recent surface-faulting events. At the Little Salmon Creek exploration locality (Figure 2.6-17), at least three events during the past 1,700 years are interpreted from trench exposures across the western trace. By reconstructing the components of folding and faulting, the displacement per event was estimated to be between 3.6 and 4.5 meters. Displacements of 1 to 2 meters were identified along the eastern trace, which is a few hundred meters east of the western trace. Radiocarbon ages for the events on the western trace indicate that faulting occurred about 300, 800, and 1,600 years ago (Reference 50). The ages of the displacements on the eastern trace could not be determined, but they probably were synchronous with events on the western trace. The results of the detailed paleoseismic studies demonstrate that the location, style, and pattern of deformation have been replicated during successive surface-faulting events on the Little Salmon fault zone.

A late Holocene history of earthquake-related deformation linked to displacement along the western trace of the Little Salmon fault has been reported by Witter and others (Reference 51). At the Swiss Hall site (Figure 2.6-17, 2.6-2a and 2b), a 1- to 1.5-meter-high moletrack scarp projects into Humboldt Bay and deforms late Holocene intertidal sediment. Complex folding of interbedded estuarine and tidal marsh deposits was identified in trenches and sediment cores excavated across the moletrack scarp, indicating that growth of the scarp was produced by coseismic folding. Stratigraphic and structural relations, radiocarbon age data, and diatom paleoecology provide evidence for three to four episodes of surface deformation related to earthquakes on the fault trace within the past 2,300 years. On the basis of radiocarbon age constraints, these earthquakes occurred sometime during the following intervals: event 4 between 2,300 and 1,840 years ago; event 3 between 1,710 and 1,530 years ago; event 2 between 1,230 and 540 years ago; and event 1 less than 460 years ago. At Hookton Slough, 1 to 2 kilometers west of the Swiss Hall site, buried tidal marsh soils provide evidence that episodes of sudden local sea-level rise occurred over extensive areas in southern Humboldt Bay. At least three and as many as five subsidence events are inferred based on stratigraphic analyses of cores near Hookton Slough. At least three of the subsidence events were accompanied by tsunamis that deposited sand on top of the buried marsh soils. The data suggest that submergence in the footwall of the Little Salmon fault occurred during upper-plate earthquakes. This study concludes that, where slip events on the Little Salmon fault were coincident with regional subsidence, the evidence supports an interpretation that the upper-plate faulting could have been triggered by coseismic rupture on the southern Cascadia plate interface.

Synclines - The regions between the major zones of fold-thrust deformation and uplift are characterized by broad, flat-floored Quaternary synclines that are active. These synclines, which include the Freshwater, South Bay, and Eel River synclines (Figure 2.6-13), are underlain by a thick section of Wildcat Group and younger sediments. The synclines, flanked by anticlinal uplifts and thrust generated uplifts, are

isolated basins that formed in response to localized folding. A tectonic explanation for the synclines is not as apparent as for the anticlines. Elastic thinning of the backstop region of the crustal thrust faults and interseismic sedimentation probably contribute to their growth. Isostatic adjustment from loading of the footwall by overthrusting of the upper plate is also a possible mechanism for growth of the synclines.

Holocene salt marsh sediments in the core of each syncline contain sequences of peat layers buried under intertidal mud. In the area of the broad Freshwater syncline, buried peat sequences are distributed throughout a 12-kilometer-wide zone. These sequences are interpreted as the stratigraphic record of coseismic subsidence during large thrust earthquakes along the plate interface (References 39, 40, and 50). The similarity in radiocarbon ages of paleoseismic subsidence events in the Freshwater syncline along the Mad River Slough (References 38 and 40) and adjacent to the Little Salmon fault on the south side of Humboldt Hill (Reference 50) support the hypothesis that the two structures are kinematically and structurally related.

2.6.3.3 Regional Seismicity

The region of the southernmost Cascadia subduction zone and the easternmost Mendocino fracture zone is one of the most seismically active areas in California. As per NUREG-1567 (2.4.6.2), this study considered seismicity in the area within 160 kilometers (100 miles). Additional seismicity was evaluated within 40 kilometers (25 miles) of the ISFSI site. Also included is a discussion of earthquake strong-motion data recorded by the HBPP strong-motion recording system, and effects observed at the plant.

2.6.3.3.1 Seismicity Catalog

The seismicity catalog used for this evaluation covers the period 1850 through April 2002, divided into historical data for the period 1850 through 1973, and more modern data for the period 1974 through April 2002. The historical data consist of magnitude 5 and larger events within 160 kilometers of the ISFSI site. The 1974 and later data are subdivided into magnitude 3 and larger earthquakes within the 160-kilometer radius, and magnitude 2 and larger within 40 kilometers of the site. References 24, 25, 34, 41 and 118 – 133 were used to develop Table 2.6-4, which lists the sources from which location and magnitude data for the magnitude 5 and larger events were derived. The source of the 1974 and later data for magnitude 2.0 to 4.9 earthquakes is the U.S. Geological Survey (Reference 117).

As shown in Table 2.6-4, the locations and magnitudes of magnitude 5 and larger events often were derived from several sources, including recent work by Bakun (Reference 118) and Toppozada and others (Reference 119) for pre-1900 earthquakes. For pre-1900 earthquakes Toppozada and others (Reference 120) estimated intensity magnitudes calibrated to Richter local magnitudes. The intensity magnitudes reported by Bakun (Reference 118) are estimated using the method from Bakun and Wentworth (Reference 121) and are calibrated to moment magnitude as defined by Hanks and Kanamori (Reference 10). The catalog used for this evaluation may not be complete at the magnitude 5 level, because it does not include events for which only maximum

HUMBOLDT BAY ISFSI FSAR UPDATE

intensity is reported, and not magnitude. The lower limit of modified Mercalli intensity (MMI) is about VI for damaging earthquakes, which corresponds to about magnitude 5.5 (Reference 25). Generally, the earthquakes not included in the catalog have maximum intensities (MMI values) of V or VI. The various magnitude symbols (e.g., M_L , M_S , M) are defined in the notes at the end of Table 2.6-4. Special magnitude symbols, such as $[ML]$ or \underline{M} , are also defined in there. These special symbols represent variations of magnitudes from specific sources.

Except for the 1700 Cascadia and 1906 San Francisco earthquakes, earthquake locations in Table 2.6-4 are plotted in Figures 2.6-23 and 2.6-24. When more than one location and/or magnitude is listed for an earthquake, the first listed is used in the figures. Figure 2.6-23 shows magnitude 5 and larger earthquakes from 1850 through 2000, and Figure 2.6-24 shows magnitude 3 and greater events from 1974 through April 2002, within the 160-kilometer radius. Preferred locations and magnitude values generally are taken from the most recently published evaluations. The oldest earthquake in the record dates from 1853, and the period 1853 through 1909 contains predominantly pre-instrument locations. 1910 was the start of the University of California, Berkeley, catalog (Reference 24), which was the principal source of data for the period 1910 through 1973. 1974 marks the Pacific Gas and Electric Company's (PG&E's) installation of their first local network. Data from the PG&E network are now part of the seismicity database at the U. S. Geological Survey's Northern California Data Center.

Earthquakes in the historical record contain substantial uncertainties, which have also changed over time. Toppozada and others (Reference 120) estimated epicentral locations for pre-1900 earthquakes in the area. Many locations were based solely on personal reports and local newspapers, and could be mislocated by 100 kilometers or more (Reference 25 and 120). Between 1887 and 1932, earthquakes in the Humboldt region were located primarily using instruments at the University of California, Berkeley, campus (UCB) and at Mt. Hamilton (both installed in 1887) (Reference 24), along with intensity observations. Dengler and others (Reference 25) suggest the location uncertainty for these events in this time range is about 100 kilometers.

The first seismographic station in the Humboldt region was installed in 1932 at Ferndale (Reference 24 and 25). This station was transferred to the City of Ferndale in 1962; post-1962 data from this station has not been used by the UCB network (Reference 134). Following installation of stations at Arcata in 1948 and Fickle Hill (east of Eureka) in 1968, location uncertainties dropped to about 50 kilometers (Reference 25). Although the Arcata station is still in operation, the Fickle Hill station was removed in April 1994 (Reference 134). By 1994, however, as described below, the U. S. Geological Survey's local seismographic network provided enough coverage to constrain uncertainties to significantly less than 50 kilometers.

The first local seismographic network at the HBPP was installed for PG&E in mid-1974 by TERA Corporation (Reference 1). The network, which operated for 12 years, consisted of 16 stations centered around the power plant (Reference 132). UCB continued to operate two of the stations from 1986 to 1994 (Reference 132). Between 1979 and 1982, the USGS installed a dozen more stations, partly in response to the

HUMBOLDT BAY ISFSI FSAR UPDATE

offshore Trinidad earthquake of November 1980. Following the large earthquakes in August 1991, the USGS installed a few more stations, bringing the total to eighteen. The USGS stations continue to operate to the present.

Hypocentral uncertainty of onshore events, particularly for events of magnitude 3 and greater, is about 2 kilometers (Reference 135). The uncertainties in offshore hypocentral locations are greater because these events occur outside the local seismic networks. The scatter of offshore hypocenters at depths greater than 30 kilometers on cross section C-C' (Figure 2.6-25) is interpreted to indicate large uncertainties in depth location. Most offshore earthquakes in the region are assumed to be in the Gorda plate down to about 30 kilometers.

The threshold for magnitude detection is also an issue in earthquake records. The record of damaging ($M > 5.5$) earthquakes in the Humboldt region since 1850 likely is complete, because the area has been inhabited since that time, and more than one newspaper has been in continuous operation that would report such events (Reference 25). Figure 2.6-22 shows that magnitude 5 earthquakes are fairly evenly distributed across the offshore region to the 160-kilometer (100-mile) radius for the period of 1910 and later. The lack of offshore magnitude 5 events during the earlier period probably reflects limitations in the magnitude detection limit, rather than lack of offshore activity at the magnitude 5 level.

Events of magnitude 2 and greater within 40 kilometers (25 miles) of the ISFSI site are plotted on Figure 2.6-26. Most of the seismicity within the 40-kilometer radius likely is represented here. Estimates of the current thresholds for magnitude completion with distance from the coast are: magnitude 1.8 for onshore events; magnitude 2.3 for offshore events within about 30 kilometers of the coast; magnitude 3.0 out to about 75 kilometers; and magnitude 4.25 out to about 160 kilometers (Reference 135). Consequently, some magnitude 3 to 4 earthquakes that occurred beyond about 75 kilometers may not be represented.

2.6.3.3.2 Magnitude 5 and Larger Earthquakes

The earthquake record for the past 150 years indicates that at least 120 earthquakes of magnitude 5 and larger occurred from 1850 through April 2002 within 160 kilometers of the Humboldt Bay ISFSI site (Figure 2.6-23; Table 2.6-4); 20 occurred within 40 kilometers of the site (Figure 2.6-26). Of magnitude 7 earthquakes, nine occurred between 1850 and 1994, three between 1873 and 1899, two in the early 1920s, and four between 1980 and 1994. The closest magnitude 7 earthquake to the ISFSI site is the 1923 event, about 30 kilometers to the southwest. The great ($M \sim 9$) 1700 Cascadia earthquake was reported prior to the local historical record, but was observed by the Japanese.

Bakun (Reference 118) reanalyzed the locations of selected north coast earthquakes by considering that some moderate-sized events previously located on or near shore may actually be larger earthquakes located farther offshore. Several of the earthquakes he studied were in the Humboldt region, and are described below,

HUMBOLDT BAY ISFSI FSAR UPDATE

including the magnitude 7 earthquake in 1873. This study generally relies on Bakun's (Reference 118) revised locations and preferred magnitudes.

Described below are the magnitude 7 earthquakes and other selected events listed in Table 2.6-4, including the magnitude 9 Cascadia subduction zone earthquake of 1700 and the magnitude 7.8 San Francisco earthquake of 1906. For events after 1974, descriptions note whether the earthquakes triggered the Humboldt Bay Strong Motion Network (described in Section 2.6.3.3.4).

27 January 1700 - The occurrence of a great Cascadia subduction zone earthquake on this date has been documented using evidence of a major trans-Pacific tsunami that inundated the Northern California, Oregon, and Washington coastal regions and destroyed homes in Japan. Evidence of a tsunami along the western United States coastline includes tree ring information from submerged trees that were killed by salt water inundation along the main subduction zone, oral histories from local Native American tribes, and sudden subsidence of the Eel River syncline and Mad River Slough (see Section 2.6.2.4). Written records from Japan indicate the time of the earthquake was the evening of 27 January 1700, at 9:45 local time in the Pacific Northwest. Satake and others (References 41 and 136) found that a long rupture length (magnitude ~9) would have been necessary to produce a tsunami that would produce damage in Japan.

23 October 1853 - Toppozada and others (Reference 120) locate this earthquake east of Humboldt Bay. Bakun (Reference 118) estimates an intensity magnitude of 5.5, as did Toppozada and others (Reference 119). Bakun also believes this may represent a magnitude 6 to 7 earthquake located offshore. Stover and Coffman (Reference 137) report that houses in Eureka "undulated like ships at sea," and people were thrown from their beds.

23 November 1873 - Toppozada and others (Reference 120) locate this earthquake onshore, north of Crescent City at the Oregon/California border. The earthquake was widely felt in Oregon and to Tacoma, Washington, as well as south to San Francisco and Sacramento (Toppozada and others (Reference 120). Bakun (Reference 118) prefers an onshore epicenter just north of the 160-kilometer radius, with a hypocenter either within the subduction zone, no deeper than about 15 kilometers, or within the shallower thrust faults of the North American plate. His location is based on MMI intensities of VIII reported near the coast. Toppozada and others (Reference 120) estimate an intensity magnitude of 6.7. Bakun (Reference 118) estimates an intensity magnitude 7.3. Wong (Reference 138) re-examines the event, estimating a focal depth of <25 to 30 kilometers within the Gorda Plate. He also believes there was possible strike-slip motion based on intensity patterns. The earthquake was felt as far south as San Francisco and north to Portland, Oregon; many chimneys were toppled in the region (Reference 137).

9 May 1878 - Toppozada and others (Reference 120) report this earthquake as an intensity magnitude 5.8 event onshore near Shelter Cove. Based on a review of felt reports in the Point Arena area and comparisons to the twentieth century intensity patterns of other magnitude 7 earthquakes, Bakun (Reference 118) believes this was a

HUMBOLDT BAY ISFSI FSAR UPDATE

magnitude 7+ earthquake that occurred about 75 kilometers offshore along the Mendocino fault zone. This earthquake and the 1 September 1994 earthquake of magnitude 7 are the largest earthquakes associated with the Mendocino fault zone in the historical record. Damage included chimneys knocked down near Petrolia and landslides triggered along the coast in southern Humboldt County (Reference 137).

16 April 1899 - Several locations and magnitudes have been proposed for this event. The difference in locations are largest concerning longitudinal coordinates (Table 2.6-4). Topozada and others (Reference 120) list this as an intensity magnitude 5.7 off the Eureka coast. Ellsworth (Reference 122) prefers a location 150 kilometers offshore, and a magnitude of 7.0. The largest MMI value for this event is VI (Reference 120). Bakun (Reference 118) believes this earthquake may be either a magnitude 5 to 6 event near the coast, or a magnitude 7 event farther offshore. Bakun (Reference 118) does not believe the four reported intensities constrain the location. His distant location agrees with Ellsworth's (Reference 122) location, as does his magnitude of 7. Stover and Coffman (Reference 137) report that this earthquake was described "as one of the most severe shocks ever experienced," although it also caused only minor damage to a mill in Eureka.

18 April 1906 - The San Francisco earthquake of 1906 (moment magnitude 7.8) is included in this study because it ruptured from San Juan Bautista to near Cape Mendocino (Reference 122), causing substantial damage in the Humboldt region. Topozada and Parke (Reference 139) show Modified Mercalli Intensity values of VIII near Eureka, VI+ near Humboldt Bay, and IX near Petrolia and Ferndale. IX was the highest intensity based on damage (Reference 137). Nearly every chimney in Ferndale collapsed following the earthquake, and liquefaction was observed in the Eel River Valley and near Humboldt Bay (Reference 140).

23 April 1906 - Meltzner and Wald (Reference 123) consider this earthquake, which occurred 5 days after the 18 April 1906 main shock, to be an aftershock of the previous earthquake. The earthquake was felt widely throughout northern California and southern Oregon, with the strongest shaking along the Humboldt County coast. Stover and Coffman (Reference 137) report that chimneys were toppled in Ferndale and clocks were stopped at Cape Mendocino, Eureka, and Trinidad Head. Topozada and others (Reference 119) assign a magnitude of 6.4 to this event. Meltzner and Wald (Reference 123) constrain the magnitude to between magnitude 6-1/2 and 7. This study uses the Topozada and others (Reference 119) location of 41°N, 124°W30, about 50 kilometers northwest of Eureka; Meltzner and Wald (Reference 123) prefer a location centered farther west at about 40.8°N, 125.3°W.

31 January 1922 - This earthquake is considered the largest historical north coast earthquake; felt reports extended from San Francisco to Eugene, Oregon (References 131 and 137). Recent catalogs report magnitudes of from 7.0 to 7.3 (Table 2.6-4). Smith and Knapp (Reference 31) locate this earthquake about 45 kilometers offshore, west-northwest from Eureka, but the similarity of intensity patterns to those of the 1994 earthquake suggest it might have occurred farther offshore (Reference 131).

HUMBOLDT BAY ISFSI FSAR UPDATE

22 January 1923 - This earthquake caused major damage in the Cape Mendocino area (Reference 131), including many houses damaged at Ferndale, Petrolia, and Upper Mattole; broken water lines; and a house shaken from its foundation in Pepperwood (Reference 137). The UCB catalog reports a local magnitude 7.2 for the earthquake. Intensity VII and VIII values constrain the location to near the Cape Mendocino area, consistent with Smith and Knapp's (Reference 31) offshore location about 13 miles northwest of Cape Mendocino (Reference 131). The intensity data, however, do not indicate whether the earthquake occurred along the Mendocino fault or slightly farther north, either within the southern part of the Gorda plate or along the Cascadia subduction zone, similar to the 1992 earthquake (discussed below). Using teleseismic data for the 7 June 1975 Ferndale earthquake (M_L 5.3) as a calibration event, Smith and Knapp (Reference 31) relocate the 1923 event onshore, 20 kilometers east of Eureka. They acknowledge that their location is suspect, however, because errors in the P-wave arrival times were not compensated for in the relocation procedure.

20 August 1927 - This earthquake occurred offshore, about 50 kilometers northwest of Eureka. Although it was a moderate earthquake (M_L 5.0), it was felt sharply and caused fairly substantial local damage. Stover and Coffman (Reference 137) report destroyed chimneys, broken windows and water pipes, and cracked walls in Eureka and Arcata and downed chimneys in Fortuna. They also report cracks in mud and moderate landsliding in Redwood Park (Eureka).

6 June 1932 - One person was killed and several more injured in Eureka (Reference 137) as a result of this magnitude 6.4 earthquake (Reference 127), about 50 kilometers west-southwest of Eureka. There was substantial property damage in Eureka and Arcata, and nearly all of the chimneys in Fields Landing were destroyed (Reference 137). Ground cracking and blowholes were observed on Cock Robin Island, at the mouth of the Eel River (Reference 137).

21 December 1954 - This earthquake occurred on land, 40 kilometers east of Eureka (Reference 122). Magnitude estimates include local magnitude 6.5 and Gutenberg Richter magnitude 6.6. One person was killed and several were injured; property damage was estimated at \$2.2 million (Reference 137). It was felt widely, from Oregon to San Francisco, suggesting a shallow depth within the North American plate along the Mad River fault zone (Reference 25). The lack of documented surface rupture, however, makes the depth difficult to confirm (Reference 25). A local magnitude 4.7 aftershock occurred on 30 December 1954, causing minor damage, including further damage to Eureka's water supply pipeline (Reference 137).

7 June 1975 - Called the Ferndale earthquake, this local magnitude 5.3 event occurred at a depth of 23 kilometers beneath Ferndale (Reference 126), within the Gorda plate. Stover and Coffman (Reference 137) report damage to chimneys in Fortuna and surrounding towns, including Ferndale; a water main broke at Rio Dell; and landslides were observed in the Fortuna-Rio Dell area. Aftershock activity was confined to the Gorda plate (Reference 141). The focal mechanism shows strike slip on north-northwest- and east-northeast-striking planes (Reference 1). Tera Corporation (Reference 141) prefers a N70°E-striking, nearly vertical fault plane undergoing left-lateral motion. Pacific Gas and Electric Company (Reference 142) assigns a focal

HUMBOLDT BAY ISFSI FSAR UPDATE

mechanism of N75°E, dipping 72°SE. They also report minor damage at the HBPP site; minor cracking in the blacktop of the plant entrance, a small crack in a newly poured concrete floor, and three small objects falling. The main shock triggered the HBPP strong-motion network. The largest peak acceleration recorded was 0.3g on the free-field horizontal component, oriented east-west (References 143 – 152 were used to develop Table 2.6-5; Section 2.6.3.3.4).

8 November 1980 - Called the Trinidad earthquake, this surface wave magnitude 7.2 earthquake occurred offshore, 50 kilometers northwest of the plant site within the Gorda Plate. No foreshocks were reported; however, two magnitude 5 aftershocks occurred to the southwest (Table 2.6-4) within the aftershock trend. Aftershock patterns show a northeasterly fault rupture (Reference 130) trending about N50°E (Reference 137). Reported depths for this earthquake range from about 6 to 20 kilometers (see Table 2.6-4), exemplifying the hypocentral uncertainty for offshore regions. Tera Corporation (Reference 130) and Eaton (Reference 153) report a strike-slip focal mechanism with a preference for left slip on a N50°E-trending fault plane. There was substantial damage to structures, including a collapsed overpass across Highway 101 east of Fields Landing; two houses that were displaced from their foundations; and broken gas, water, and sewer lines (Reference 137). The main shock triggered the HBPP strong-motion network. Terra Technology Services (Reference 144) reports a maximum free-field peak acceleration of 0.50g on the east-west horizontal component (Table 2.6-5, Section 2.6.3.3.4). However, they also report that these measurements are suspect because of instrument malfunctions prior to the earthquake.

16 August 1991 - This was the second of four large earthquakes that occurred within about a month along the coast of northern California and southern Oregon, and one of three that occurred within the Gorda plate. The short time between the four apparently independent events is unprecedented in the historical record for this area (Reference 30). The surface wave magnitude of this earthquake was 6.3; it was located about 95 kilometers offshore, west of Crescent City, and 120 kilometers west-southwest, within the Gorda plate. The event was preceded by a surface wave magnitude 6.9 earthquake on 12 July that occurred about 70 kilometers farther north (outside the study area) and 95 kilometers west-southwest from Gold Beach, Oregon, also within the Gorda plate (Reference 30). Although the earthquake was felt widely in northern California and southern Oregon, it did not trigger the HBPP strong-motion network.

17 August 1991 (12:29 PM) - Called the Honeydew earthquake, this surface wave magnitude 6.2 event occurred 21 hours after the 16 August event described above. It was located on land, about 7 miles south of Petrolia and west of Honeydew, and 50 kilometers south of the HBPP, at a depth of 12 kilometers (Reference 154). The earthquake caused minor damage in the towns of Petrolia and Honeydew. Some aftershocks were felt locally. It is the largest earthquake on land in the Mendocino triple junction region in this century (Reference 154). The proposed fault motion is thrust along a northeast-vergent fault plane, based on the focal mechanism and a zone of northwest-trending surface cracks up-dip from the hypocenter (Reference 155). The hypocenter is within the Petrolia subplate, a detached sliver of the North American plate (Section 2.6.2.2). The largest intensity values (MMI) of VIII were reported near

HUMBOLDT BAY ISFSI FSAR UPDATE

Honeydew, also up-dip from the hypocenter; values of IV were reported in the Eureka area and near the plant site (Reference 154). The earthquake triggered the strong motion network at the HBPP site. The largest peak acceleration recorded was 0.064g on the horizontal component (orientation not specified) of the free-field sensor (Reference 156). This event is not included in Table 2.6-5 because peak ground motion was less than 10%g, which generally is below the damage threshold for structures.

17 August 1991 (3:17 PM) - This surface wave magnitude 7.1 earthquake was the third and largest of the Gorda plate earthquakes that occurred following the event of 12 July 1991. Occurring three hours after the 17 August event, it was located about 62 kilometers northwest of the plant site. The earthquake did not trigger the HBPP strong-motion network.

25 and 26 April 1992 - This earthquake sequence, called the Petrolia sequence, included an onshore main shock of surface wave magnitude 7.1 on 25 April 1992 and two offshore aftershocks of surface wave magnitude 6.6 the following day. The 1992 main shock, at a depth of 10 kilometers, is considered evidence of fault rupture along the Gorda/North American plate interface (Reference 14); the aftershocks were Gorda intraplate earthquakes. Damage from these earthquakes was extensive. The region was declared a major disaster area by President Bush based on damage estimates of \$48 million to \$66 million (Reference 14). Although much of the damage was caused by the main shock, fires were triggered by the first large aftershock, nearly destroying a shopping center in Scotia (Reference 14). The focal mechanism for the main shock shows thrust motion along a N10°W-trending fault plane; mechanisms for both aftershocks show right slip along northwest-oriented planes (Reference 14). All three earthquakes triggered the HBPP strong-motion network. Free-field horizontal peak accelerations of 0.22g, 0.25g, and 0.13g, respectively, were recorded (Table 2.6-5, Section 2.6.3.3.4). All were recorded on the east-west horizontal component; the maximum 0.22g (main shock) was recorded on both horizontal components.

1 September 1994 - This moment magnitude 7.0 (Reference 118) earthquake was felt throughout a wide area from San Francisco to southwest Oregon (Reference 131). Yet because the earthquake occurred about 150 kilometers offshore, it caused no reported damage. The location for this earthquake varies considerably, depending on which catalog is used. The catalog for this study incorporates the NEIC location using the Worldwide Network, per D. Oppenheimer (Reference 135), as opposed to the USGS location that uses arrival times from only the local seismic network. This and the 1878 earthquakes are the largest historical earthquakes associated with the Mendocino fault zone. Focal mechanisms for the 1994 main shock and five of the largest aftershocks (none larger than magnitude 4.5) are strike slip, consistent with the strike of the Mendocino fault zone (Reference 131). The combination of strike-slip focal mechanisms and east-northeast displacements measured at onshore stations indicates that the preferred motion is right slip along the fault zone (Reference 131). These earthquakes did not trigger the HBPP strong-motion network.

26 December 1994 - This moment magnitude 5.4 earthquake occurred 8 kilometers west of the Humboldt Bay ISFSI site. Although it was moderate in size, it was felt

strongly at the plant site; the strong-motion system recorded horizontal peak accelerations of 0.55g (north-south component) (Table 2.6-5). Although no damage was reported at the site (Section 2.6.3.3.4), preliminary damage estimates in the Eureka area exceeded \$2.7 million (Reference 131). This event occurred within the Gorda plate at 23 kilometers depth, caused by strike-slip motion along northwest- or northeast-oriented fault planes.

2.6.3.3.3 Association of Earthquakes with Tectonic and Geologic Structures

The magnitude 5 and larger historical data and the post-1973 data (Figures 2.6-23 and 2.6-24) show that most regional earthquake activity has been concentrated along the Mendocino fault zone and scattered to the north across the southern part of the Gorda plate in the Gorda deformation zone. A lower level of activity has occurred in the onshore North American plate. The Pacific plate west of the San Andreas fault zone and south of the Mendocino fault zone is relatively aseismic. Following is a summary of the association of earthquakes with the primary seismically active structures of the Humboldt Bay region: the Mendocino fault zone, the Gorda plate and Gorda deformation zone, the Petrolia subplate (location of the Petrolia earthquake sequence), and the North American plate.

Mendocino fault zone -The Mendocino fault zone is highly active, as reflected by the occurrence of magnitude 5 and greater earthquakes within about 20 kilometers of the fault zone since at least the late 1870s (Figure 2.6-24). Although there is uncertainty in locations of offshore events, the narrow, west-trending pattern of the earthquakes along the mapped fault trace (Figure 2.6-24) is consistent with the well-expressed topography and bathymetry of the Mendocino triple junction region (Section 2.6.2.3).

The 1878 and 1994 earthquakes are the largest associated with the Mendocino fault zone. Focal mechanisms for the 1994 main shock and five of the largest aftershocks show that fault motion is predominantly right slip (Reference 131), consistent with previous focal mechanisms (References 157-158). The more accurately located magnitude 3 and larger events from the post-1973 data set (Figure 2.6-24) suggest that the diffuse historical earthquakes shown south of the Mendocino fault zone on Figure 2.6-23 may be somewhat mislocated, and probably occurred farther north within the fault zone.

Gorda plate and Gorda deformation zone - The offshore region of the Gorda plate is highly seismically active. Some of the larger Gorda plate earthquakes are the 1922, 1980, and three 1991 earthquakes described in Section 2.6.3.3.2. Smaller Gorda plate earthquakes were the 7 June 1975 Ferndale event (M_L 5.3), the 26 December 1994 event (M 5.4), and the 31 July 1987 event (M 5.2) (Figure 2.6-27). Bakun (Reference 118) postulates that the 1873 earthquake, previously located by UCB onshore near the 42nd parallel, likely occurred slightly farther north (Figure 2.6-23) within the Gorda plate.

Most earthquakes within the Gorda plate are located in the Gorda deformation zone (GDZ) (Figures 2.6-6, 2.6-23, and 2.6-24). This trend is consistent with a change from a rigid to deforming Gorda plate southward across the GDZ. This pattern is evident in both larger ($M \geq 5$) and smaller ($M \geq 3$) earthquakes. Cross section C-C' (Figure 2.6-25)

illustrates the Gorda slab plunging under the North American plate. The angle of subduction increases with depth to the east. The northeast cross section D-D' (Figure 2.6-25), across the southern part of the Mendocino triple junction region, shows a vertical pattern of events between about 18 and 30 kilometers horizontal distance, and then a steeply northeast-dipping pattern to about 30 kilometers depth. The change in dip at 15 kilometers is coincident with the interface between the Gorda and Pacific plates.

Cross section C-C' also shows that, at the magnitude 3 threshold, most activity has been within the Gorda plate. Magnitude 2 and larger earthquakes (Figure 2.6-27) within 40 kilometers of the site also indicate that most of the events are within the Gorda plate and near the Mendocino triple junction region. Earthquake activity within both the Gorda and North American plates dies out to the north, as seen on cross section E-E' (Figure 2.6-27).

The 1980 Trinidad earthquake and prolific aftershock sequence provided evidence of shearing in the southern part of the GDZ. Most of the focal mechanisms west of the Mendocino triple junction and north of the Mendocino fault zone indicate left slip along northeast trends (Reference 30).

North American plate - The North American plate (including the Petrolia and Eel River subplates) has been characterized by occasional moderate earthquakes that occur onshore, to the east and northeast, within the study area. Examples are the 1954 (M_{G-R} 6.6) earthquake near Mad River, and the 1991 Honeydew earthquake (M_S 6.2). Based primarily on felt reports, Dengler and others (Reference 25) conclude that the 1954 earthquake likely was associated with the Mad River fault zone. The 1991 Honeydew earthquake occurred along a northeast-vergent thrust fault within the Petrolia subplate. North American plate focal mechanisms from McPherson (Reference 30) show primarily reverse and strike slip along northwest trends.

Post-1973 microseismic activity within the North American plate, within a 40-kilometer radius of the site, shows isolated events and diffuse clusters along the coast near the Little Salmon fault zone, the Eel River syncline, and the Russ fault (Figure 2.6-26). Similar to seismicity patterns for the subducted Gorda plate, earthquake activity within the North American plate dies out to the north and east, as seen on cross section E-E' (Figure 2.6-27). Except for the activity near the Russ fault, seismicity patterns do not appear to be associated with specific faults. Cross section E-E' shows that most of the activity near the Eel River syncline occurs in the Gorda plate; activity near the Little Salmon fault zone occurs in the Gorda and North American plates. The small clusters between about 5 and 10 kilometers depth may be associated with the Table Bluff fault zone.

The shallow (2- to 6-kilometer-deep) activity beneath the surface trace of the Russ fault (cross section E-E' on Figure 2.6-27) is consistent with McLaughlin and others' (Reference 73) cross section (Figure 2.6-12) that is oriented parallel to and southeast of E-E'. The events shown in McLaughlin and others' (Reference 73) cross section suggest a steep southerly dip of the Russ fault, which is opposite from the interpretation of a northerly dip shown on Figure 2.6-27. McLaughlin and others' (Reference 73)

locations were obtained from a detailed velocity analysis filtered to show the most precise locations (Reference 159).

Petrolia subplate - The 1992 M_S 7.1 Petrolia earthquake helped define the Petrolia subplate. With the exception of the 1700 Cascadia event, this is the only event in the catalog that is interpreted to be an interplate earthquake, occurring at the interface between the Gorda and North American plates. The low-angle thrust motion is consistent with subduction along the interface of the Gorda and North American plates (Petrolia subplate), at the southernmost end of the Cascadia subduction zone. The dense concentration of events near Cape Mendocino includes aftershocks from the 1992 Petrolia earthquake, some of which are shown in Figure 2.6-27. The spatial gap in activity beneath the 1992 aftershocks, between about 12 and 16 kilometers depth, as seen in both cross sections, is coincident with the plate interface region, as interpreted from Figure 2.6-11 and Geomatrix (Reference 160). Oppenheimer and others (Reference 14) suggest the gap may be a ductile aseismic zone.

2.6.3.3.4 Earthquake Ground Motions Recorded at Humboldt Bay Power Plant

Pacific Gas and Electric Company (PG&E) has operated a strong-motion recording network at the HBPP continuously since September 1971 (Reference 143). The network has gone through several upgrades in the past 30+ years. The first instruments consisted of a Teledyne MTS-100 strong-motion recording system and three FB-103 triaxial force-balance accelerometers, one in the refueling building at elevation +12 feet (4 meters), one in the Reactor Caisson at elevation -66 feet (-20 meters), and one in the storage building at +12 feet (4 meters) (Reference 142). These instruments were replaced in 1977 with sensors and recorders from Terra Technology. This new network also consisted of three three-component forced-balance accelerometer sensors and a central recording system, in this case a DCA-300-P9. This system used the same Unit 3 locations for the sensors, except that the sensor in the outside storage building was moved to a better free-field site in the north yard. The DCA-300-P9 recorded on cassette tapes, similar to the Teledyne/Terrametrics system. In 1991 the system was upgraded to use DOS-based Ramdeck software to communicate with the recorder and to download and analyze data more efficiently. In 1997 the recorder was upgraded again to a GNC-R recorder. The communication software for this latest upgrade is DOS-based but can be used with Windows OS.

A stand-alone three-component accelerometer (model SSA-2 by Kinometrics) also has been in operation at the plant site since 1991. It was located in the administration building until 2001; it now resides in the main building communications room. To provide for continuous coverage, this recorder is used primarily as an alternate recorder when the central recording system is down for maintenance or replacement. For example, the records from the 26 December 1994 earthquake (Table 2.6-5) were recorded only on the SSA-2 instrument because the Terra Technology system was down for maintenance at the time of the earthquake.

Since 1975, the strong-motion instruments at the HBPP have recorded six earthquakes having peak horizontal accelerations greater than 0.10g. These were the 1975 Ferndale (M_L 5.3) earthquake, the 1980 Trinidad (M_S 7.2) earthquake, the 1992

Petrolia main shock (M_S 7.1) and two aftershocks (both M_S 6.6), and the 1994 (M_L 5.4) earthquake. Table 2.6-5 lists these events, their recorded free-field ground motions, the effects observed at the plant, and the tectonic source of each event. The events are labeled on Figure 2.6-23 using numbers that correspond to those in the table.

The largest peak horizontal acceleration recorded by PG&E's network (0.55g) was from the 26 December 1994 earthquake, 8 kilometers from the plant. The event was felt strongly at the plant (Table 2.6-5). The second-largest reported acceleration was 0.50g on the east-west horizontal component from the November 1980 Trinidad earthquake, located 50 kilometers northwest of the plant. However, Terra Technology Services (Reference 144) reports that an instrument malfunction occurred prior to the earthquake. A blown fuse on the battery charger produced insufficient battery power to obtain a good record of the event. Despite their efforts to recover the data, they report that the amplitudes of the waveforms may be incorrect, which means that the recorded peak accelerations may also be incorrect.

The 1975 Ferndale earthquake, located 22 kilometers southeast of the plant, produced a peak horizontal acceleration of 0.30g. Both this and the 1994 events were located at about 23 kilometers depth (Figure 2.6-27). The 1992 earthquakes, located between 55 and 70 kilometers from the plant, produced peak accelerations of 0.13g to 0.25g.

No structural damage was reported at the HBPP from any of the events described above. After the 1992 main shock, however, new hairline cracks were observed in the walls of the refueling building. Other effects were water sloshing in the spent fuel pool following the 1975 and 1992 (main shock) earthquakes, tools falling from racks after the 1980 event, and fuses falling from the startup transformer during the 1994 earthquake.

2.6.3.4 Summary Of Regional Geology And Seismicity

Regional Stratigraphy

- The Humboldt Bay ISFSI site is in a broad depositional basin, the Eel River basin, that is underlain by a thick sequence of late Cenozoic marine sedimentary rocks. The late Cenozoic deposits unconformably overlie basement rocks of the Cretaceous to late Tertiary Franciscan Complex that were accreted to the western margin of North America by plate convergence prior to the development of the present Cascadia subduction zone about 20 million years ago.
- The thick (as much as 3,600 meters) sequence of late Tertiary and Quaternary deposits, which are referred to collectively as the Wildcat Group, was deposited on the upper plate of the modern Cascadia subduction zone. The lower Wildcat Group sediments reflect deposition in a locally quiescent tectonic environment. In contrast, the upper Wildcat Group sediments are laterally variable, recording northeast-to-southwest shortening of the basin by a rapidly developed system of folds and thrust faults. Contractional tectonics initiated about 700,000 years ago, following

HUMBOLDT BAY ISFSI FSAR UPDATE

deposition of the Rio Dell Formation, when localized uplift due to anticlinal folding over active thrust faults divided the subsiding Eel River basin into several small subbasins.

- The late Pleistocene Hookton Formation and other post-Wildcat Group sediments and geomorphic surfaces, including uplifted marine terraces, record continued uplift of the hills and subsidence of the basins associated with the growth of faults and folds in the upper plate of the Cascadia subduction zone.

Regional Geologic Structure

- The Humboldt Bay region is dominated by north-northwest-trending contractional structures formed during several phases of plate convergence that have affected the region since the Late Jurassic. Three ages of structures are evident at the regional scale.
 - (1) Faults, folds, and tectonic mélanges formed during multiple episodes of accretion of the Franciscan Complex basement rocks during the late Mesozoic and early Tertiary.
 - (2) Early and mid Tertiary structures formed in the accreted continental margin prior to the development of the present plate tectonic structure of the Cascadia subduction zone.
 - (3) Late Cenozoic structures (basin subsidence and localized anticlinal uplift) have been created by the tectonics of the modern Cascadia subduction zone
- The interaction of subsidence and fold-thrust deformation during the past approximately 700,000 years has resulted in a clear tectonic distinction between the uplifting areas that overlie active thrust faults and fault-related anticlines (for example, the Table Bluff, Humboldt Hill, and Fickle Hill anticlines), and subsiding local basins that are coincident with intervening synclines.
- Two major zones of thrust faults and related folding have been mapped in the Humboldt Bay region: the Mad River fault zone and the Little Salmon fault system.
- The Mad River fault zone is an approximately 80-kilometer-long, 15- to 25--kilometer-wide belt of en echelon thrust faults and fault-generated folds that trend north-northwest and dip predominantly northeast. The onshore part of the fault zone includes the Trinidad, Blue Lake, McKinleyville, Mad River, Fickle Hill, and Greenwood Heights faults. Late Quaternary slip rates on individual faults within the zone, based on dating

HUMBOLDT BAY ISFSI FSAR UPDATE

of uplifted marine terraces, are generally 1 to 2 millimeters per year. The cumulative slip rate across the zone is about 5 to 9 millimeters per year.

- The Little Salmon fault system is a 15- to 25-kilometer-wide belt of en echelon anticlines and active thrust faults that extends for 330 kilometers parallel to the deformation front associated with the leading edge of the Cascadia subduction zone. Onshore, near the site, the Little Salmon fault system includes the Table Bluff fault and the Little Salmon fault zone. The slip rate for the Little Salmon fault zone is estimated to be between 6 and 10 millimeters per year, and 2 to 3 millimeters per year for the Table Bluff fault.
- The Little Salmon fault zone is the nearest capable fault to the site. Including the Yager fault to the southeast and offshore traces to the northwest, it has a total length of 95 kilometers. The fault zone consists of multiple imbricate traces that are well defined in the geomorphology, deforming Holocene geomorphic surfaces and sediments. Near the Humboldt Bay ISFSI site, the fault zone consists of two main faults (the Little Salmon fault and the Bay Entrance fault), and two subsidiary faults (the Buhne Point and Discharge Canal faults). Paleoseismic investigations along the fault zone southeast of the site (at the Little Salmon Creek exploration locality) indicate that at least three surface-faulting events occurred along the western trace of the fault zone during the past 1,700 years. Radiocarbon dates indicate that these events occurred about 1,600, 800, and 300 years ago. The results of the detailed paleoseismic studies demonstrate that the location, style, and pattern of deformation have been replicated during successive surface-faulting events on the Little Salmon fault zone.
- The Table Bluff fault is a 23-kilometer-long thrust in the Little Salmon fault system. Seismic profiles and surface mapping indicate the fault consists of a south-vergent thrust wedge beneath the actively deforming Table Bluff anticline.

Regional Seismicity

- The Humboldt region (within 160 kilometers [100 miles] of the ISFSI site) is an area of high seismic activity in which 121 earthquakes of magnitude 5 and greater have been recorded during the past 150 years, including nine magnitude 7 events. Most of these earthquakes have occurred in the offshore region within and along the southern margin of the Gorda plate on the Mendocino fault zone.
- In general, the regional pattern of modern magnitude 3 and larger earthquakes shows the Gorda plate subducting beneath the North American plate, and the Mendocino fault zone as a distinct boundary between the rigid Pacific plate and the deforming Gorda plate.

HUMBOLDT BAY ISFSI FSAR UPDATE

- Moderate to large earthquakes have been recorded within or on the shared boundaries of all three primary tectonic structures within 160 kilometers of the ISFSI site. The April 1992 Petrolia earthquake occurred on the interface of the Gorda and North American plates (Petrolia subplate) on the Petrolia segment of the Cascadia subduction zone, and the January 1700 event appears to have ruptured the main segment of the Cascadia subduction zone. Gorda plate earthquakes include the 1975, 1980, and 1991 offshore events; the December 1994 main shocks; and two 1992 aftershocks. The 1991 Honeydew earthquake occurred within the Petrolia subplate, a detached sliver of the North American plate. The September 1994 earthquake, and likely the 1878 earthquake, occurred on the Mendocino fault zone.
- Seismic activity in both the Gorda and North American plates decreases significantly north of the Mendocino triple junction region and east of the offshore Gorda plate. Within the triple junction region, the Gorda plate is more seismically active than is the North American plate.
- The Pacific plate south of the Mendocino fault zone and west of the San Andreas fault zone has few earthquakes.
- Except possibly for microearthquakes beneath the Russ fault, seismic activity cannot be associated confidently with specific faults within 40 kilometers (25 miles) of the ISFSI site.
- Two moderate Gorda plate earthquakes within 20 kilometers of the ISFSI site produced relatively large ground motions at the HBPP. The ML 5.3 event of November 1975 produced peak horizontal accelerations of 0.30g, and the ML 5.4 event of December 1994 produced peak accelerations of 0.55g.

2.6.4 SITE GEOLOGY

2.6.4.1 Introduction

Humboldt Bay Power Plant and the ISFSI site lie on the east flank of Buhne Point, a small headland on the eastern shore of Humboldt Bay (Figures 2.6-1, 2.6-2 and 2.6-29). The site is underlain by a thick sequence of late Tertiary (the geologic time scale is presented in Table 2.6-1) and Quaternary sedimentary rocks capped by a late Pleistocene terrace. Buhne Point, which is situated within the Little Salmon fault zone, has been uplifted and tilted to the northeast by displacement on the fault. The results of mapping, borehole, trenching, and dating studies at and near the site are used in the current study to characterize site geology.

Trenches and borehole data developed by Earth Sciences Associates (References 161 and 162) and Woodward-Clyde Consultants (Reference 1) (Figure 2.6-30) are used to

demonstrate the continuity of strata beneath the Humboldt Bay ISFSI site, and to document the locations of tectonic and nontectonic deformation in the site vicinity. Also analyzed and incorporated are data from two new trenches and borehole data from the recent geotechnical study performed to evaluate liquefaction susceptibility and slope stability at the ISFSI site (Section 2.6.7).

Figure 2.6-31 is a geologic map that shows the locations of the previous and new trenches and borings near the ISFSI site. Data from these investigations were used to demonstrate the continuity of individual stratigraphic horizons across the site and to identify stratigraphic and structural discontinuities that may indicate active faults near the site. For the current evaluation, the stratigraphic and structural data obtained during the extensive investigations for the HBPP in the late 1970s (Reference 1, 161, and 162) were reexamined, along with the results of subsequent studies that included trenching investigations of the Little Salmon fault for College of the Redwoods (References 109, 110, and 163) and for the U.S. Geological Survey (Reference 50 and 105).

Field mapping was conducted in March 2000 at and near the ISFSI site to identify geologic features, such as unstable slopes, deformational zones, soil/weathering profiles, and other features that may be important to assessing the potential for ground deformation or fault rupture at the ISFSI site. As part of that work, the lithostratigraphy, soil stratigraphy, structure, and slope features associated with the terrace on Buhne Point and the hillslopes along the periphery of the terrace were mapped (Figure 2.6-30). Topographic profiles were measured, and the deposits and soils exposed in the escarpments on the north and south sides of the uplifted terrace at Buhne Point were described in detail. In August 2000, Geomatrix excavated two new trenches, which have a combined length of 75 meters. These trenches, and trenching conducted by Woodward-Clyde Consultants (Reference 1), provided continuous exposure of the near-surface Quaternary deposits at the site (Figure 2.6-31).

Section 2.6.4.2 describes the physiographic setting of the ISFSI site. Section 2.6.4.3 describes site stratigraphy. Particular attention is paid to the nature of the deposits that underlie the ISFSI site and the soil profiles developed on the Buhne Point terrace. The well-bedded middle to late Pleistocene estuarine and fluvial deposits that underlie the site provide the means for identifying late Quaternary faulting and related deformation. The soils on the terrace surface were used to assess the minimum age of near-surface deposits.

Section 2.6.4.4 describes faulting related to the Little Salmon fault zone, including the Bay Entrance and Buhne Point fault traces. Because the site is on the hanging wall of the Buhne Point fault, particular attention was paid to the potential for hanging-wall deformation (secondary faulting, folding, and tilting) related to slip on the Bay Entrance, Buhne Point, and Discharge Canal faults. Section 2.6.4.5 addresses the continuity of the middle to late Pleistocene deposits beneath and directly adjacent to the ISFSI site.

2.6.4.2 Physiographic Setting

The ISFSI site is located on a low hill, referred to in this report as Buhne Point hill, on the eastern side of Humboldt Bay opposite the entrance of the bay (Figure 2.6-29a). The hill, which has a maximum elevation of about 23 meters, extends east of Buhne

HUMBOLDT BAY ISFSI FSAR UPDATE

Point for about 480 meters, and is 50 to 180 meters wide (Figure 2.6-31). The hill, capped by an erosional remnant of an uplifted terrace, is an outlier of Humboldt Hill, a northwest-trending ridge that extends southeast of the site (Figure 2.6-33). Humboldt Hill is a large fault-ramp anticline situated along the leading edge of the hanging wall of the Little Salmon fault zone. Buhne Point hill, where the ISFSI site is located, is bordered on the north by a coastal bluff that drops off steeply (graded slope of about 1:1) to the shore of Humboldt Bay. The eastern and southern sides of the hill are bordered by a low tidal marsh. The western side of the hill is bordered by the village of King Salmon, which is built on fill over tidal marsh and beach deposits that extend more than 500 meters into the bay. The westernmost part of the hill forms Buhne Point. Comparison of historical and modern maps indicates that the present hill is only a remnant of a much larger hill that existed in 1850 when Buhne Point was first described as a navigational aid into the entrance of the bay. The first detailed map of the area, made in 1858 (Figure 2.6-34), shows a flat-iron-shaped hill having steep bluffs along its northern and southwestern sides. The flat terrace surface slopes gently away from the bluffs to the southeast. The present shoreline is about 400 meters southeast of the 1858 shoreline (Figure 2.6-34). The dramatic coastal retreat and loss of most of Buhne Point hill to wave erosion began when the entrance to the bay was deepened, and jetties (Figure 2.6-33) were placed adjacent to the entrance to provide a permanent deep-water access for ships during the late 1800s. The bluff retreat was arrested when riprap was placed along the base of the bluff in the early 1950s to prevent further wave erosion (Figure 2.6-35).

Buhne Point hill was formed by tectonic uplift associated with the Little Salmon fault zone combined with wave erosion. The escarpment along the southwest side of the hill is interpreted to be the eroded fault scarp produced by down-on-the-southwest displacement along the Buhne Point trace of the Little Salmon fault zone. The northeast margin of the hill that is apparent on the 1858 map (Figure 2.6-34) appears to be related, at least in part, to down-to-the-northeast displacement on a small secondary fault, the Discharge Canal fault. The bluff that existed on the northwest side of Buhne Point hill in 1858 was the eroded sea cliff that faced the ocean across from the natural entrance to the bay. This bluff has since retreated to its present position at the northern side of the plant area.

An approximately east-west topographic profile and geologic cross section along Buhne Point hill parallel to the coast (Figure 2.6-36) indicates two distinct terrace surfaces along this profile. The higher terrace, the Buhne Point terrace (Qpht on Figure 2.6-31), is a planar geomorphic surface having a gentle (2 to 4 degrees) southeast tilt (Figure 2.6-37). The small inset terrace below this surface on the western end of the hill (Figure 2.6-36) appears to have been man made, because it is not evident on the 1858 survey map. Also, the strata at the present ground surface are not weathered, indicating that the soils were removed.

The surface of the Buhne Point terrace was modified in several places during construction of the power plant. For example, low-angle oblique aerial photographs in PG&E's archives (Figures 2.6-38, items a and b) show grading activities from south of the old security fence to the edge of the bluff on the north side of the terrace. Parts of the Buhne Point terrace surface (Qpht on Figure 2.6-31) in the vicinity of the ISFSI site

may have been lowered by as much as 2 to 3 meters; the most significant lowering occurred along the edge of the bluff, decreasing toward the security fence. In several places, the disturbed areas are underlain by about a meter of fill. The ISFSI site is located near the old security fence in the area of disturbed ground.

2.6.4.3 Stratigraphy

As described in Section 2.6.3.2.1, the ISFSI site is underlain by more than 900 meters of late Pliocene and Quaternary deposits. Three lithostratigraphic formations separated by unconformities were encountered at the site, as shown on Figure 2.6-39. From oldest to youngest, these are the Rio Dell Formation, the Scotia Bluffs Formation and the Hookton Formation, which is divided into lower and upper members. The following descriptions of the Rio Dell, Scotia Bluffs, and lower Hookton formations are based on Woodward-Clyde Consultants (Reference 1). In addition to data from the Woodward-Clyde study, the description of the upper member of the Hookton Formation includes information obtained from geotechnical borings and trenches at the ISFSI site and from surface outcrops in the Buhne Point area.

At Buhne Point, a coastal terrace surface is formed in the upper Hookton sediments; this surface appears to be conformable with the upper Hookton sediments. Remnants of a relict paleosol described in Section 2.6.4.3.4 are preserved in undisturbed areas on the terrace surface. The characteristics of this paleosol enable correlation with the regional soil chronosequence (References 84, 101, and 164) and assignment of an age for the terrace. Around Buhne Point hill, the Hookton deposits are unconformably overlain by Holocene colluvial, landslide, alluvial, and estuarine deposits. Extensive areas of the site have been graded, and in most places the natural soils/surface weathering profile have been removed or buried by man-made fill.

2.6.4.3.1 Rio Dell Formation (Late Pliocene to Early Pleistocene)

The Rio Dell Formation is a homogeneous marine mudstone that is encountered in boreholes at 520 meters beneath the site. The formation is about 600 meters thick. Regionally, the Rio Dell Formation is time-transgressive - marine fossils indicate age ranges from late Pliocene to Pleistocene. Near the site, the uppermost Rio Dell Formation is estimated to be 1.1 ± 0.2 million years old (Reference 1), making its age early Pleistocene.

2.6.4.3.2 Scotia Bluffs Formation (Early Pleistocene)

At the site, the Rio Dell Formation is unconformably overlain by more than 340 meters of shallow-water sandy marine sediments that probably are correlative with the Scotia Bluffs Formation (following the nomenclature used by Woodward-Clyde Consultants (Reference 1), a query is used after Scotia Bluffs to indicate that correlation of this unit, where it is encountered in borings, to Ogle's (Reference 69) type locality for the Scotia Bluffs Formation is uncertain. The query is not used on geologic maps, where the deposits are exposed at the surface and the correlation is more reliable) of Ogle (Reference 69). The deposits consist mostly of silty sand and sandy silt interbedded with clayey sediment. The clay beds provide excellent marker horizons that can be

recognized on geophysical logs, particularly the natural gamma-ray logs. In the site area, Woodward-Clyde Consultants (Reference 1) subdivided the formation into eight units, labeled O through V (from youngest to oldest). The precise age of the Scotia Bluffs Formation has not been determined, but it probably was deposited between about 1.1 million years ago (the estimated age of the upper Rio Del Formation) and about 780,000 years ago (older than the Brunhes/Matuyama magnetic reversal (Woodward-Clyde Consultants (Reference 1) used an age of about 700,000 years for the polarity transition between the Matuyama and Brunhes polarity epochs. Based on recent dating using advanced potassium-argon techniques, the date of this transition is now placed at 780,000 years (Reference 80)) that was identified by Woodward-Clyde Consultants (Reference 1) from borehole and outcrop samples at Centerville Beach). Therefore, the Scotia Bluffs Formation is early Pleistocene in age.

2.6.4.3.3 Hookton Formation (Middle to Late Pleistocene)

As described in Section 2.6.3.2.1, (the Hookton Formation consists of middle to late Pleistocene interbedded shallow marine, estuarine, and fluvial deposits that unconformably overlie Scotia Bluffs and older formations. In the vicinity of Buhne Point, the Hookton Formation is divided into a lower and an upper unit (Figures 2.6-39 and 2.6-40). The lower Hookton Formation deposits consist of alternating sand, silty sand, gravelly sand, silty clay, and clay about 265 to 275 meters thick. The thickness of the Hookton Formation varies near the site because of active faulting and folding during deposition of the unit. For example, deep boreholes and cross sections in Woodward-Clyde Consultants (Reference 1) show that the thickness of the lower Hookton beds increases from the hanging-wall blocks (upthrown sides) to the footwall blocks (downthrown sides) across the Buhne Point, Bay Entrance, and Little Salmon faults, indicating that folding and faulting occurred during deposition of the lower Hookton Formation. In addition, tectonic thickening (i.e., duplication/stacking of stratigraphic section by superposition of older units over younger units by reverse faulting) accounts for apparent stratigraphic thickening near the site.

Laterally persistent clay beds, typically overlain by gravelly sands, provide useful marker horizons. A distinctive clay bed, Unit F, near the top of the lower Hookton Formation is a particularly useful marker horizon that has been identified in borings across the site and in the western end of Trench 11-T6c at the northwest end of Buhne Point. The age of the uppermost part of the lower Hookton Formation is about $160,000 \pm 40,000$ years, based on amino acid racemization dates on fossil shell material collected from clayey sediment in a Caltrans road cut near the northern end of Humboldt Hill about 900 meters south of the site (Reference 1). The age of the Unit F clay is estimated to be $310,000 \pm 70,000$ years, based on average rates of deposition between the dated clay (top of the lower Hookton Formation) above Unit F and the basal sediments of the Hookton Formation that are estimated to have been deposited between $600,000 \pm 100,000$ years ago (Reference 1).

Upper Hookton Formation deposits consist primarily of silt and clay alternating with thinner sand and gravel lenses. No distinctive marker horizons were identified in the upper Hookton Formation that could be correlated across the Little Salmon and Bay Entrance faults, but the deposits are significantly thicker on the downthrown sides of

these faults. As exposed in trenches and in the sea cliff along the north side of the Buhne Point terrace, the deposits underlying the terrace commonly contain distinctive layers having sharp contacts (Figure 2.6-41). The textures of the strata vary somewhat laterally, but individual layers commonly can be traced for several meters. The clayey bay mud deposits tend to be more laterally persistent than the interbedded sandy and silty layers. However, both sandy and clayey marker horizons in the upper Hookton Formation deposits exposed in trenches were traceable across the ISFSI site. Lithologic contacts could be mapped with sufficient resolution to preclude any fault displacements larger than a few centimeters (typically 2 centimeters or less), as shown on the logs of trench walls (Figures 2.6-42 and 2.6-43).

Correlation of the stratigraphy in boreholes to the strata exposed in the sea cliff and local trenches indicates that the boundary between the lower and upper members of the Hookton Formation is at the base of the very dense sandy gravel 16 to 23 meters below the ISFSI site. Geologic cross sections X-X⁵ and Y-Y¹ (Figures 2.6-36 and 2.6-44) depict the position of this contact beneath the site, as well as the correlation of two distinctive estuarine mud units in the upper Hookton Formation. The upper part of the lower Hookton Formation consists of very dense, poorly to well-graded sand and silty sand with occasional gravel overlying the Unit F clay bed, which occurs at a depth of 46 meters in borehole GMX-99-2. The two layers of bay mud (clay and silt) in the upper Hookton Formation are separated by a 9- to 10-meter-thick sandy and silty deposit, the texture of which ranges laterally from silty sand to low- to high-plasticity silt. These lateral variations are interpreted to be facies changes. Deposits overlying the uppermost clay bed are predominately sandy and silty clay, well to poorly graded sand, and silty and clayey sand. These deposits, as well as the upper part of the highest bay mud clay and silt beds, were exposed in trenches WCC-11-T6a, GMX-T1, and GMX-T2 (Figures 2.6-32, 2.6-42, and 2.6-43). A layer of clayey man-made fill overlies the upper Hookton Formation across most of the ISFSI site. The fill ranges from 0 to 3.2 meters thick, but typically is 0.6 to 1 meter thick.

2.6.4.3.4 Buhne Point Terrace and Paleosol (Late Pleistocene)

The uppermost Hookton deposits are conformable with a planar geomorphic surface, the Buhne Point terrace (Qpht on Figure 2.6-31), which dips gently (2 to 4 degrees) to the southeast. A strongly developed soil has formed in the near-surface deposits. This paleosol crops out in exposures on the steep slopes northeast and southwest of the ISFSI site, and in the southwest end of trench GMX-T2. Based on these exposures, the paleosol appears to be concordant with the tilted terrace surface. It has a well-developed argillic horizon, reddish brown (7.5YR hue) color, clay films, and strong structure (Figure 2.6-45 and Table 2.6-6). The presence of a relatively thick, strongly developed argillic horizon (Bt horizon) and the reddish color indicate that the soil on the Buhne Point terrace is correlative with Class II (80,000- and 105,000-year-old) soils developed on marine terraces in the Humboldt Bay area (Reference 84). In particular, the degree of soil development on the terrace surface at Buhne Point is similar to the soil at the South Port Landing quarry on Table Bluff, where a thermoluminescence age of 103,000 years was obtained for sediments underlying the terrace (Reference 92).

The Buhne Point terrace is interpreted to have formed during a high stand of sea level in the late Pleistocene, most likely during marine oxygen-isotope Stage 5c or 5a. The ages of oxygen-isotope Stage 5 marine terraces along the California coast are well documented (for example, Reference 91); Stage 5e marine terraces are dated at 120,000 to 125,000 years, Stage 5c terraces are approximately 105,000 years old, and Stage 5a formed approximately 80,000 years ago. The soils data described above suggest that the terrace has been emergent since at least Stage 5a and possibly longer. This conclusion is consistent with previous estimates of the age of the Buhne Point terrace by Woodward-Clyde Consultants (Reference 1), who interpreted it as post-upper Hookton Formation sediment deposited after deposition of a clay bed containing shell material having a $160,000 \pm 40,000$ -year-old amino acid racemization age, and prior to 37,000 years ago, as determined from radiocarbon dating of wood samples from Trench 11-T6a. This date is older than the effective range of radiocarbon dating in 1980. A wood sample from upper Hookton deposits collected from trench GMX T2 (Figure 2.6-43) yielded a radiocarbon age of >45,730 radiocarbon years B.P., confirming that the upper Hookton deposits are older than the effective age range for radiocarbon dating (Reference 167). The strongly developed soil on the Buhne Point terrace supports an age of more than 80,000 years.

2.6.4.3.5 Surficial Deposits (Holocene)

Holocene surficial deposits in the Buhne Point area include alluvial/estuarine marsh sediments, colluvium on the slopes, and shallow landslides (Figure 2.6-31). The alluvial/estuarine deposits underlie the flat area southwest of the Buhne Point terrace in the King Salmon Avenue area and east of the Discharge Canal. Colluvium derived from the eroded fault scarp along the southwest side of Buhne Point terrace probably interfingers with the alluvial/estuarine sediments.

Small landslides along the bluffs that border the Buhne Point terrace (Figure 2.6-31) are most abundant on the sea cliff adjacent to Humboldt Bay on the north side of the terrace. Most of the landslides are shallow (< 2 meters thick), translational landslides. However, the two northwesternmost landslides along the sea cliff appear to be somewhat deeper (5 to 7 meters) and to have rotational movement. This landsliding postdates the grading of the sea cliff and placement of riprap along the shoreline, which were completed during the late 1950s. No large landslides were observed along the bluff and, based on geologic conditions underlying the bluff, no large, deep-seated landslides are expected.

2.6.4.4 Faulting In The Site Vicinity Associated With The Little Salmon Fault Zone

As described in Section 2.6.3.2.2 and shown on Figure 2.6-18, four traces of the Little Salmon fault zone are mapped in the vicinity of the Humboldt Bay ISFSI site. These include two primary fault traces, the Little Salmon and Bay Entrance faults, and two subsidiary faults in the hanging wall of the Bay Entrance fault, the Buhne Point and Discharge Canal faults. The Little Salmon fault corresponds to the middle trace of the Little Salmon fault zone to the southeast, and the Bay Entrance fault corresponds to the eastern trace of the Little Salmon fault zone to the southeast. The Little Salmon, Bay Entrance, and Buhne Point faults all dip to the northeast and displace the late

Pleistocene Hookton Formation down to the southwest (Figures 2.6-46, 2.6-47, and 2.6-48). The Discharge Canal fault dips steeply to the southwest and has down-to-the-northeast displacement.

2.6.4.4.1 Little Salmon Fault

The location of the Little Salmon fault near the site is based on borings and seismic lines conducted by Woodward-Clyde Consultants (Reference 1) (Figure 2.6-30). The fault strikes about N45°W and dips about 25°NE (Figure 2.6-46). The fault projects to the surface about 2.2 kilometers southwest of the ISFSI site. Projection of the structure contours shown on Figure 2.6-46 to the northwest places the fault about 1,300 meters beneath the western boundary of the HBPP site. However, the fault was not encountered in boring WCC-4 (Figure 2.6-46), indicating that this trace either dies out south of the site, or its dip steepens at depth, placing the fault more than 1,600 meters below the ISFSI site. In either case, the Little Salmon fault was not encountered in site area borings or trenches. As described in Section 2.6.3.2.2, the Little Salmon fault displaces the entire lower Hookton section at the northern end of Humboldt Hill, placing Rio Dell Formation over Hookton sediments (Figure 2.6-49). It appears that, north of Humboldt Hill, slip on the Little Salmon trace of the Little Salmon fault zone is transferred to the Bay Entrance fault.

2.6.4.4.2 Bay Entrance Fault

The Bay Entrance fault is the closest of the main traces of the Little Salmon fault zone to the ISFSI site. As inferred from borings, the fault strikes N5-10°W and dips approximately 50° to 60°E (Figure 2.6-47). The fault projects to the surface about 500 meters west of the ISFSI site (Figure 2.6-50). The closest distance to the fault (fault-normal distance measured to the center of the site) is between about 410 and 470 meters. The fault appears to have a right-slip component that is about 50 percent of the dip-slip separation, based on analysis of boring and geophysical data (Reference 1).

The base of the Hookton Formation is displaced about 440 meters (dip-slip), and the upper Hookton Formation is displaced about 270 meters (Reference 1, Figure C-10 and Table 2). Progressive separation of the older beds in the Hookton Formation indicates the fault was active during deposition of the Hookton Formation. The long-term, dip-slip displacement rate on the Bay Entrance fault southwest of the ISFSI site is believed to be 1 to 2 millimeters per year.

South of the plant site, the Bay Entrance fault corresponds to the east trace of the Little Salmon fault zone (Figure 2.6-18). In a quarry exposure directly south of College of the Redwoods, this trace displaces lower Wildcat sedimentary rocks (Pullen Formation) over late Pleistocene and Holocene sediments (Reference 105). To the south, at Salmon Creek, this trace deforms a late Holocene alluvial terrace. Based on the displaced terraces, Carver and Burke (Reference 114) estimate the late Holocene slip rate to be 2 to 3 millimeters per year.

2.6.4.4.3 Buhne Point Fault

The location of the Buhne Point fault is based on analysis of site borings (Figures 2.6-48 and 2.6-50). The fault strikes about N45-70°W. The fault dips about 35°NE down to elevation -900 feet (-275 meters), where the dip flattens to less than 20° (Figure 2.6-50). Below elevation -300 meters (-1,000 feet), the dip of the fault steepens to about 45° and probably continues to steepen until the fault merges with the Bay Entrance fault. The fault plane lies about 140 to 160 meters beneath the ISFSI site.

The projected surface trace of the Buhne Point fault is parallel to and southwest of the southwest margin of the Buhne Point terrace, about 180 meters southwest of the ISFSI site (Figure 2.6-48). The 5- to 15-meter-high scarp along the southwest side of the Buhne Point terrace is interpreted to be a wave-eroded fault scarp associated with the Buhne Point fault. Although erosion and grading during plant construction modified the scarp, it reflects the general trend of the surface trace.

The Buhne Point fault shows progressively greater vertical separation of older horizons. It displaces the Scotia Bluffs Formation 71 meters (vertical separation on Unit Q); the base of the Hookton Formation 49 meters; and the Unit L clay in the lower part of the Hookton 21 meters (Reference 1 Figure C-8). Structure contours on the top of Unit F in the vicinity of the ISFSI site (Figure 2.6-51) indicate the vertical displacement on the top of this unit in the upper part of the lower Hookton Formation ranges from 6 to 10 meters.

The upper Hookton underlying the terrace at Buhne Point is tilted 2 to 4 degrees to the southeast, indicating continued deformation and faulting on the Bay Entrance and Buhne Point faults during the late Pleistocene (the past 80,000 years). Based on the displacement of Unit F (160,000 ± 40,000 years old), the long-term-average slip rate on the Buhne Point fault (dip slip) is about 0.1 millimeter per year. This slip rate is an order of magnitude lower than the slip rate for the Little Salmon and Bay Entrance traces of the fault zone.

Woodward-Clyde Consultants (Reference 1) excavated trenches 11-T6b and 11-T6c across the scarp that borders the Buhne Point terrace (Figures 2.6-31, 2.6-52, and 2.6-53). Both trenches exposed zones of fractures and small-displacement faults in the upper part of the lower Hookton Formation. The fractures and small faults are similar to those observed in the hanging wall of other reverse faults that were investigated during regional fault studies (Reference 1 and 103). For example, Woodward-Clyde Consultants (Reference 1) mapped similar features in the hanging wall of the McKinleyville fault, about 25 kilometers north of the plant site (Figure 2.6-54). The fractures and small-displacement faults are inferred to represent deformation in the hanging wall along the leading edge of a reverse fault, suggesting that a fault lies within a few tens of meters of the present topographic scarp. Based on the structure contours on the top of the Unit F clay (Figure 2.6-51), a small splay branches from the main trace of the Buhne Point fault to the northwest toward Buhne Point. The vertical displacement on the splay fault is about 3 meters.

Interpretation of the structure contour map of the top of the Unit F clay (Figure 2.6-51) and geologic cross section W-W¹ (Figure 2.6-55) indicate this marker horizon is displaced 6 to 10 meters down on the southwest across the Buhne Point fault. The relatively small displacement on this fault is not enough to account for the total uplift of the Buhne Point terrace, which, at its highest point, is about 20 meters above mean lower low water. Faulting on the Bay Entrance fault must accommodate part of the uplift.

2.6.4.4.4 Discharge Canal Fault

A small fault, informally referred to as the Discharge Canal fault, displaces the upper Hookton Formation with a vertical separation of three meters or more. The fault is partly exposed in a hand-dug pit in the sea cliff about 75 meters west of the discharge canal for the power plant (outcrop JW-7; Figures 2.6-31 and 2.6-56). In this exposure, a sand layer is clearly displaced down on the northeast by numerous closely spaced, steeply dipping to near-vertical (70°S to 90°) faults that generally strike $\text{N}50^{\circ}\text{W}$. The fault is associated with a monoclinical flexure exposed in trenches BP-2 and BP-3, east of the ISFSI site and directly west of the discharge canal (Figure 2.6-31). Logs of these trenches (Reference 159) show a sand layer in the upper Hookton Formation that is deformed into a steep “monocline” (down on the northeast) that trends $\text{N}70^{\circ}\text{W}$ (Figures 2.6-57 and 2.6-58). The vertical separation across the feature is greater than or about equal to 3 meters (the limit of the exposure in trench BP-2). The surface trace defined by these exposures corresponds to a 3-meter down-to-the-northeast step in the top of Unit F (Figure 2.6-44). Based on the location of the offset in Unit F relative to the surface trace, the fault dips 70° to 80° to the southwest. The Discharge Canal fault is interpreted to be a backthrust on the hanging wall of the Buhne Point fault (Figure 2.6-50). The “monocline” represents either folding above the tip of a blind reverse fault, or hanging-wall deformation above a backthrust that daylights (or is covered by young bay sediments) to the northeast. Another small fault crops out in the sea cliff about 45 meters east of the mapped trace of the Discharge Canal fault (Figure 2.6-31), where a 10- to 20-centimeter-thick sand layer in the upper Hookton Formation is abruptly truncated by a zone of faint, closely spaced shears. The fault strikes $\text{N}32^{\circ}\text{W}$ and dips 77°SW . Assuming reverse slip, the displacement exceeds about 1.5 meters (and exceeds the height of the exposure).

2.6.4.4.5 Other Minor Faults

As shown on Figure 2.6-31, the only stratigraphic displacements observed near the site were exposed in trench WCC-11-T6a, more than 30 meters west of the ISFSI site, where a small, rootless, graben-shaped feature is located in bedded silts (Reference 65, Appendix 4A, Figure C-12, Sheet 3, Station 160 m). Two narrow zones of antithetic faults that are spaced about 30 centimeters apart form a depression about 15 centimeters deep in the silt bed; there is no apparent vertical separation across the feature. Woodward-Clyde Consultants (Reference 1) attributes the feature to soft-sediment deformation during deposition of the Hookton sediments, because the underlying and overlying sediments were not similarly disturbed. The bounding shears, however, have characteristics that are similar to the “monocline” exposed in trenches BP-2 and BP-3 and in the sea cliff exposure (Figure 2.6-31). Therefore, the feature probably represents minor secondary deformation (bending-moment normal faulting) in

the hanging-wall block of the Buhne Point fault. As described above, zones of small faults and fractures also are evident in trenches WCC-11-T6b and WCC-11-T6c (Figures 2.6-31, 2.6-52, and 2.6-53).

2.6.4.5 Continuity Of Strata Beneath The Site

This section discusses the continuity of the strata beneath the ISFSI site, both the Unit F clay of the upper lower Hookton Formation, and upper Hookton strata.

2.6.4.5.1 Unit F Clay (Upper Lower Hookton Formation)

The potential for detecting small faults in the Unit F marker horizon is affected by: (1) which varies, as shown on Figure 2.6-51); (3) the possibility of erosional irregularities in the top of Unit F; and (4) the possibility of broad folding (non-brittle deformation) of Unit F. Considering these factors, the limit of resolution for detecting faults in Unit F beneath the ISFSI site is estimated to be about 2 meters.

Figure 2.6-51 shows a structure contour map based on the lithologic picks for the elevation of the top of Unit F encountered in site area boreholes and in trench WCC-11-T6c (Reference 168-169). Unit F is about 40 meters below the ISFSI site, where the contact between Unit F and the overlying sand and gravel generally strikes N30-40°E and dips 5°SE. The dip is shallower to the east adjacent to the Discharge Canal fault; southeast of the site, the strike rotates to trend more eastward. This rotation in strike may reflect erosion of the upper contact of Unit F, the presence of a southwest-verging thrust fault at depth, or broad folding of Unit F. The available data indicate that erosion and/or broad synclinal folding probably account for the swing in structure contours, although faulting at depth cannot be ruled out. If a southwest-verging reverse fault was present at depth, its subsurface trace would project to the northeast of the site, and the up-dip projection of the fault plane would be approximately toward the site. However, slip on this hypothetical fault would die out along strike to the northwest, based on the decreased to no deflection in the structure contour at and northeast of the site. As described below, the absence of faulting in near-surface sediments (i.e., strata of the upper Hookton Formation) at and near the ISFSI site is documented in trenches of this and previous studies. For comparison, the deformation of the upper Hookton Formation strata by the Discharge Canal fault is readily identifiable in trenches and test pits. The absence of significant faulting in the trenches indicates that the fault does not exist, does not project through the site, or has not been active for more than 80,000 years.

Evidence of erosion on the top of Unit F is indicated in an alignment of five closely spaced boreholes that are from 2.4 to 3.6 meters apart. These boreholes were drilled about 200 meters east-southeast of the ISFSI site as part of a cross-hole shear-wave-velocity experiment (boreholes WCC80-CH-1 through WCC80-CH-5 on Figure 2.6-51). The lithologic logs for these boreholes indicate 1.5 meters of local relief in the top of the Unit F clay. Figures 2.6-59a and b are geologic cross sections at the top of Unit F that show two alternative interpretations of the CH series boreholes. As shown, the variability in the elevation of the top of Unit F could be due to either a small fault (Figure 2.6-59a), or a cut-and-fill channel (Figure 2.6-52b). If it were a fault, the vertical

separation between boreholes WCC80-CH4 and WCC80-CH3 would be between 1.2 and 1.7 meters down to the east. However, given the negligible (~0.3 meter) net vertical separation across the series of boreholes, and the anomalous apparent west dip of the top of Unit F between boreholes WCC80-CH3 and WCC80-CH5 compared to the trend of the Unit F surface (Figure 2.6-51), the relief probably reflects a cut-and-fill channel.

Geologic cross section W-W¹ (Figure 2.6-55) trends northeast/southwest, approximately perpendicular to the strike of the northeastern splay of the Buhne Point and the Discharge Canal faults. Unit F can be traced continuously across the uplifted block between these faults, which displace the Unit F clay 6 to 10 meters and 3 to 5 meters (vertical separation), respectively. There are no discernable faults (faults having a vertical separation greater than 2 meters) in this 310,000-year-old clay marker horizon beneath the ISFSI site.

2.6.4.5.2 Upper Hookton Strata

Geologic cross section Y-Y¹ (Figure 2.6-44), which extends north/south through the ISFSI site, illustrates the stratigraphic relations in the upper Hookton deposits beneath the site. Based on the borings and observations made in the sea cliff exposure, the upper Hookton deposits are continuous; there is no evidence these deposits, which are at least 80,000 year old, are faulted beneath the site.

Trenches WCC-11-T6a and GMX-T1 cross the ISFSI site in a N75°W direction (see Figures 2.6-32, 2.6-42 and 2.6-60, and Reference 65, Appendix 4A). Trench GMX-T2 crosses the site in a N24-37°E direction, which is approximately perpendicular to the trend of the Buhne Point and Discharge Canal faults (Figure 2.6-61). These trenches provided continuous exposure in upper Hookton Formation bay mud deposits across the ISFSI site. Trench WCC-11-T6a extended for more than 200 meters along the uplifted block (Buhne Point terrace) that lies between the northeast-dipping Buhne Point fault and the southwest-dipping backthrust near the Discharge Canal (Figure 2.6-31). The trench exposures provide direct evidence for the absence of faulting beneath the ISFSI site with a high degree of resolution (typically less than 2 centimeters) in the exposed deposits, which are at least 80,000 years old (Figure 2.6-62).

Several thin fractures lined with roots and fine sand were observed in trenches GMX-T1 and GMX-T2 (Figures 2.6-42, 2.6-43, 2.6-63, 2.6-64 and 2.6-65). The fractures, which cut thinly laminated silt, clayey silt, and fine sand, show no discernable displacement, and prominent marker horizons in the upper Hookton Formation deposits can be traced across the upward (and downward) projections of the fractures with no displacement.

The strata exposed in trenches WCC-11-T6a, GMX-T1, and GMX-T2 provide direct evidence for no significant faulting (more than about 2 centimeters) in strata at the foundation level of the ISFSI site since the late Pleistocene (during at least the past 80,000 years). No displacements were observed, and the stratigraphic contacts exposed in trench walls are sharp enough to preclude vertical fault displacements greater than about 2 centimeters.

2.6.4.6 SUMMARY OF SITE GEOLOGY

Knowledge of site geology is based on extensive studies of the stratigraphy beneath the site, regional mapping of the Little Salmon fault zone, trenching at the site, analysis of the geomorphology of the Buhne Point terrace, and review of recent studies of the Little Salmon fault. The primary elements of site geology are summarized below.

- The ISFSI site is underlain by a well-bedded sequence of Tertiary and Quaternary sedimentary rocks that contain excellent planar datums that record deformation on the Little Salmon fault zone and allow for estimation of deformation rates.
- Based on its relative topographic position and the presence of a strongly developed relict paleosol, the raised and tilted terrace surface (the Buhne Point terrace) at the ISFSI site formed during an interglacial high stand of sea level, and is correlated to either the 80,000- or the 105,000-year-old (Stage 5a or 5c) marine terraces that are well preserved at other places along the northern California coast.
- The ISFSI site is on the hanging wall of the Little Salmon fault zone. Three branches of this fault zone - the Little Salmon, Bay Entrance, and Buhne Point faults - dip to the northeast beneath the site.
- The Little Salmon fault projects to the surface about 2.2 kilometers southwest of the ISFSI site. This fault either dies out south of, or is more than 1,600 meters below, the site.
- The Bay Entrance fault is the closest main splay of the Little Salmon fault zone to the Humboldt Bay ISFSI site. The fault projects to the surface about 500 meters west of the ISFSI site, and is about 410 to 470 meters from the site at its closest approach (fault-normal distance measured to the center of the site).
- The Buhne Point fault, a secondary splay in the hanging wall of the Bay Entrance fault, projects to the surface about 180 meters southwest of the ISFSI site and lies about 140 to 160 meters below the site. The southwest-dipping Discharge Canal fault splays off the Buhne Point fault daylighting near the Discharge Canal about 150 meters northeast of the site.
- Displacement on the Bay Entrance and Buhne Point faults uplifted the hanging-wall block between the main trace of the Buhne Point and Discharge Canal faults, tilting the Buhne Point terrace 2 to 4 degrees to the southeast. The tilted terrace surface reflects the tectonic deformation on the hanging wall of the Little Salmon fault zone, including ruptures associated with multiple earthquakes on the Cascadia subduction zone during the past 80,000 years.

- Despite the close proximity of the ISFSI site to active traces of the Little Salmon fault zone, the upper part of the lower Hookton Formation (about 310,000 years old) and the upper Hookton Formation deposits (>80,000 years old) are not faulted, as evidenced by continuous, unbroken upper Hookton strata in the near surface beneath the ISFSI site. These strata can be traced continuously across the ISFSI site with a high degree of resolution.

2.6.5 SEISMIC SOURCE CHARACTERIZATION

2.6.5.1 INTRODUCTION

Interpretations of the tectonic framework of the Mendocino triple junction region have evolved rapidly during the past few decades as new geologic, seismologic, and crustal structure information has become available. In particular, the characterization of the Cascadia subduction zone has changed dramatically (see Section 2.6.2). Prior to the mid 1980s, the Cascadia subduction zone was judged not to be seismically active by the majority of seismologists and geologists, and was interpreted not to have the capability of producing significant earthquakes. As new geologic evidence was identified during the mid and late 1980s, the perception of the capability of the subduction zone changed, and by the mid 1990s, a new scientific consensus that the subduction zone is capable of generating great earthquakes had evolved (Reference 35).

Because the scientific community increasingly accepted the Cascadia subduction zone as a potential source for earthquakes, the California Seismic Safety Commission, along with the California Department of Transportation (Caltrans) and the Oregon Department of Transportation, sponsored studies to define the characteristics and assess the consequences of a Cascadia subduction earthquake. In California, the California Division of Mines and Geology (CDMG) prepared a Cascadia earthquake scenario analysis (Reference 58). The CDMG scenario earthquake was defined as a “Gorda segment” rupture, involving slip on the southern 240 kilometers of the Cascadia interface and generating a magnitude 8.4 earthquake. Additionally, the CDMG scenario event included slip on the Little Salmon fault zone that was triggered by slip on the subduction interface. The Little Salmon fault zone was interpreted to be a crustal thrust fault above the Cascadia interface. The scenario earthquake was also considered to be a source for generating a local tsunami.

2.6.5.2 DESIGN INPUTS

2.6.5.2.1 Width Approaches for Cascadia Interface

The width of the Cascadia interface depends on the location of the updip (shallowest point) and downdip (deepest point) limits of potential seismogenic rupture. Geomatrix (Reference 34, page 2-21) gives two alternative models for the location of the updip limit and two alternative models for the location of the downdip limit.

The updip extent is defined by either the location of the deformation front or the location of the change in structural trends near the slope break (change in fold trends).

Geomatrix (Reference 34, p 2-21) estimates that fault width using the change in fold trends boundary is 25 km less than using the deformation front boundary. Geomatrix (Reference 34, page 2-21) gives relative weights of 0.7 to the change in fold trends model and 0.3 to the deformation front model.

The downdip extent is defined by either the location of the zero isobase line or the midpoint of the transition zone defined by the thermal and geodetic modeling.

Geomatrix (Reference 34, page 2-21) gives relative weights of 0.6 to the zero isobase model and 0.4 to the thermal-geodetic model.

On page 2-21 of Geomatrix (Reference 34), the width of the Cascadia interface is given for the four combinations of the locations of the updip and down-dip limits, but the values are not correct. It appears that they incorrectly used the location of the change in fold trends as the location of the deformation front and the change in the fold trends was placed 25 km east of the misplaced deformation front. The result of this error is that interface widths listed in Geomatrix (Reference 34) are too small. New calculations of the width of the interface are made in section 2.6.5.4.1 below.

2.6.5.2.2 Dimensions of the Cascadia Interface

Rupture Lengths

Carver (Reference 170) models the Cascadia interface as a combination of the Cascadia interface, Little Salmon fault zone, and Table Bluff fault. The alternative models for the lengths of the Cascadia interface ruptures and the weights for the alternatives given by Carver (Reference 170) are listed in Table 2.6-7.

Dip

Cohee et al. (Reference 171, p. 37, caption to Figure 3) give the dip of the interface of 11° in Washington and 21° in Oregon. The average value of 16° is used for the fault rupture.

2.6.5.2.3 Little Salmon Fault Zone

Rupture Length

Carver (Reference 170) defines the Little Salmon fault zone as extending from the Yager fault to the Thompson Ridge fault (Reference 170, Figure 2-5). The length of the zone is 310 km (Reference 170, pg 5A-6).

Dip

Carver (Reference 170) gives three possible dips of the fault of 40, 45, and 50 degrees; weights on each are 0.2, 0.6 and 0.2, respectively.

Crustal Thickness

The thickness of the crust in the Humboldt Bay ISFSI region is given as 15 km (Reference 170).

Displacement per Event

The fault displacement is given as 7m or 9.3m (equally likely) (Reference 170).

Style of Faulting

The Little Salmon fault is a reverse slip fault (Reference 170).

2.6.5.3 METHOD AND EQUATION SUMMARY

2.6.5.3.1 Method

The magnitude of the Maximum Credible Earthquake is computed based on the mean magnitude determined for the maximum rupture area or fault displacement

2.6.5.3.2 Equations

Magnitude-Area Relations

The Wells and Coppersmith (Reference 172; Table 2A, p. 990) scaling relation for magnitude as a function of rupture area for crustal faults (using all fault types) is given by

$$M = 0.98 \log(A) + 4.07 \quad (\text{Eq 2.6-1})$$

where A is the rupture area in km^2 and M is moment magnitude.

The Abe (Reference 173-174) relation for magnitude as a function of rupture area for subduction zones is given by (Reference 34, p. 2-29)

$$M = \log(A) + 3.99. \quad (\text{Eq 2.6-2})$$

The Geomatrix (Reference 175) relation for magnitude as a function of rupture area for subduction zones is given by (Reference 34, p. 2-29)

$$M = 0.81 \log(A) + 4.7 \quad (\text{Eq 2.6-3})$$

Magnitude-Displacement Relations

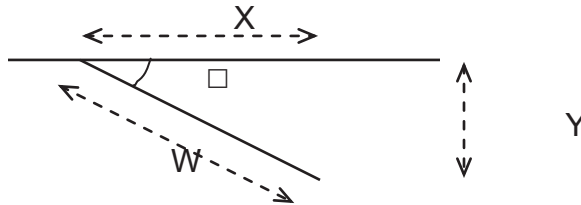
The Wells and Coppersmith (Reference 172; Table 2B, p. 991) scaling relation for magnitude as a function of average fault displacement for crustal faults (using all fault types) is given by

$$M = 0.82 \log(D) + 6.93 \quad (\text{Eq 2.6-4})$$

where D is the average displacement over the rupture surface in m.

Downdip Width

The following illustration is used for Eqns. 2.6-5 and 2.6-6.



For a fault with dip δ and horizontal extent X , the downdip width, W , is given by

$$W = \frac{X}{\cos(\delta)} \quad (\text{Eq 2.6-5})$$

For a fault with dip δ and vertical extent Y , the downdip width, W , is given by

$$W = \frac{Y}{\sin(\delta)} \quad (\text{Eq 2.6-6})$$

Eq. (2.6-5) and (2.6-6) are well known trigonometric relations.

Weighted Average

Given N values X_i with weights wt_i , the weighted mean is (Reference 176, p. 73)

$$Mean = \frac{\sum_{i=1}^N X_i wt_i}{\sum_{i=1}^N wt_i} \quad (\text{Eq 2.6-7})$$

2.6.5.4 CALCULATION OF MAGNITUDE

2.6.5.4.1 Magnitude for the Cascadia Interface

Horizontal Extent of Updip Boundary

The downdip widths of the interface given by Geomatrix (Reference 34, p. 2-21) are not consistent with the plots on Figure 2-17. To resolve this inconsistency, other sources of this information were reviewed.

HUMBOLDT BAY ISFSI FSAR UPDATE

The locations of the Cascadia subduction zone's Deformation Front (Reference 34, Figure 2-16 and Plate 1) were compared to the location of the Cascadia Subduction Zone mapped by the National Geographic Society (Reference 177). Geomatrix (Reference 34, Figure 2-16) shows locations from California to north of the Explorer plate (about 40° to 52° N); Geomatrix (Reference 34, Plate 1) extends only along the Oregon coast (about 42° to 46° N); NGS (Reference 177) plots the zone only along the U. S. coastline and ends at the Canadian border (south of Eureka to about 48.5° N)

All three sets of distances were measured as distances due west of the U. S. coastline and are shown in Table 2.6-8. Additionally, the location of the Change in Fold Trends (Reference 34, Plate 1) is included in Table 2.6-8.

The distance to the updip subduction zone boundary measured from NGS agrees well with the deformation front boundary plotted in Geomatrix Plate 1 but not at all with the deformation front plotted in Geomatrix Figure 2-16. The distance to the deformation front plotted in Geomatrix Figure 2-16 agrees well with the change in fold trends plotted in Geomatrix Plate 1. Because the NGS is a data source independent of Geomatrix (Reference 34), the boundaries in Geomatrix Plate 1 appear correct. The boundary plotted in Geomatrix's Figure 2-16 should be labeled as the change in fold trends boundary, and not as the deformation front.

Width

The horizontal extent of the Cascadia interface was measured from Geomatrix (Reference 34, Figure 2-16) using the change in fold trends boundary (identified incorrectly in their Figure 2-16 as the deformation front) as the updip margin and both the zero isobase and transition zone boundaries as the downdip margins (Table 2.6-9). The Transition Zone plotted in Geomatrix's Figure 2-16 is used by Geomatrix (Reference 34) as the Thermal/Geodetic boundary (p. 2-21). The distances measured were along lines approximately normal to the updip and downdip margins and intersected the coastline at the latitudes listed in Table 2.6-9.

The horizontal extent using the deformation front as the updip boundary is computed by adding 30 km to the extent using the change in fold trends as the updip boundary. Geomatrix (Reference 34, p. 2-14) states that the change in fold trends is located 30 km landward of the deformation front. Later (p. 2-21) they show the downdip width of the rupture is 25 km less using the change in fold trends as compared to the deformation front. Based on this, the location of the deformation front is assumed to be 30 km seaward of the change in fold trends.

The downdip width of the Cascadia interface between the change in fold trends and the zero isobase and the transition zone boundaries was computed from the horizontal extent (Table 2.6-9) using eq. 2.6-5 and the dip of 16°. The resulting downdip widths are shown in Table 2.6-10.

HUMBOLDT BAY ISFSI FSAR UPDATE

The interface widths were averaged over latitudes corresponding to the segment rupture length models (Table 2.6-7) - between Eureka and the middle of Washington (41° to 47°) and between Eureka and the Explorer plate (41° to 49°). These averaged values were then rounded to the nearest 5 km to reflect the accuracy of the measurements. The resulting widths are listed in Table 2.6-11.

Magnitude

The magnitude of the characteristic earthquake for the main Cascadia interface is estimated using the two alternative relations between magnitude and rupture area for subduction events (eq. 2.6-2 and 2.6-3) with equal weights. The rupture area is computed by multiplying the segment lengths given in Table 2.6-7 and the downdip widths listed in Table 2.6-11. All possible combinations of widths and segment lengths are considered; the 16 permutations are listed in Table 2.6-12. The total weight is the product of the weights for the updip extent, downdip extent, length, and magnitude-area (M(A) model) relation. The mean magnitude listed at the bottom of Table 2.6-12 is computed by summing the $wt \cdot Mag$ values (eq. 2.6-7).

Distance

The updip location of the Cascadia interface in the region near the Humboldt Bay ISFSI, as described by Carver (Reference 170), is given by the Table Bluff fault. Using Figure 2.6-13, the horizontal distance between the Humboldt Bay ISFSI site and the surface expression of the Table Bluff fault is measured as 5.5 km. The Table Bluff fault has a change in dip direction as shown in Figure 2.6-14. In the top 2 km, the fault has a shallow dip to the southwest, whereas below 2 km, the fault has a shallow dip to the northeast. The part of the fault below 2 km dipping to the northeast is consistent with the dip direction of the subduction zone. Therefore, the distance to the fault is measured to the part of the fault dipping to the northeast. Using the cross-section (Figure 2.6-14), the closest distance between the site and the northeast dipping part of the fault is measured to be 7 km.

2.6.5.4.2 Magnitude for the Little Salmon Fault System

Magnitude

The magnitude of the characteristic earthquake for the Little Salmon fault zone is estimated using the relations between magnitude and rupture area for crustal faults (eq. 2.6-1) and between magnitude and fault displacement (eq. 2.6-4). The two alternative approaches (area or distance) are given equal weight.

Inputs from Section 2.6.5.2.3 are used in Table 2.6-13 to compute magnitude.

Distance

The Bay Entrance fault is the closest strand of the Little Salmon fault to the Humboldt Bay ISFSI site. The approximate location of the Bay Entrance fault is shown in the

cross section in Figure 2.6-55. Based on this figure, the shortest distance between the Humboldt Bay ISFSI site and the Bay Entrance Fault is measured to be 0.5 km.

2.6.5.5 Results and Conclusions

The Little Salmon fault zone and the Cascadia interface are assumed to rupture synchronously. The source types, magnitudes, and rupture distances listed in Table 2.6-14 represent the Maximum Credible Earthquake (MCE) for these two subsources, and are used for deterministic evaluations of the ground motion at Humboldt Bay ISFSI.

2.6.6 EARTHQUAKE GROUND MOTIONS

2.6.6.1 Approach

The approach used for developing the ground motion characteristics to be used for design and analyses of the ISFSI SSCs is discussed below. The seismic design criteria are presented in Section 3.2.4.

There are two basic approaches to develop design basis vibratory ground motions: deterministic and probabilistic. 10 CFR Part 100 Appendix A requires the use of deterministic approaches in the development of a single set of earthquake sources. Appendix A requires: (1) development for each source a postulated earthquake to be used to determine the ground motion that can affect the site; (2) locating the postulated earthquake according to prescribed rules; and (3) calculating ground motion at the site. 10 CFR 72.102 previously required the development of a Design Earthquake in accordance with 10 CFR Part 100 Appendix A. A final rule was published in the Federal Register (68FR54143) on September 16, 2003 that revised the ISFSI seismic siting and design criteria. This rule change requires that a new specific-license applicant for a dry cask storage facility located in either the western United States or in areas of known seismic activity in the eastern U.S., and not co-located with an operating reactor such as the Humboldt Bay ISFSI, address uncertainties in seismic hazard analysis by using appropriate analyses, such as probabilistic seismic hazard analysis (PSHA) or suitable sensitivity analyses, for determining the design earthquake ground motion (DE). The final rule allows the selection of a DE appropriate for, and commensurate with, the risk associated with an ISFSI. PG&E's Response to NRC Question 2-5 (Reference 279) provides additional information on detailed analysis of uncertainties in earthquake ground motions assessments.

Regulatory Guide 3.73 (Reference 178) was developed to provide general guidance on procedures acceptable to the NRC staff for: 1) conducting a detailed evaluation of site area geology and foundation stability; 2) conducting investigations to identify and characterize uncertainty in seismic sources in the site region important for the PSHA; 3) evaluating and characterizing uncertainty in the parameters of seismic sources; 4) conducting PSHA for the site; and 5) determining the DE to satisfy the requirements of 10 CFR Part 72. Regulatory Guide 3.73 indicates that the controlling earthquakes are to be developed for the ground motion level corresponding to the reference probability of $5E-4/\text{yr}$.

HUMBOLDT BAY ISFSI FSAR UPDATE

In the Regulatory Guide 3.73 PSHA approach, all potential earthquakes are considered (all magnitudes and locations on all seismic sources). That is, the probabilistic approach does not consider just one scenario, but all possible scenarios. In addition, the rate of earthquakes (how often each scenario earthquake occurs) is also considered. Finally, rather than just considering a median or 84th percentile ground motion, the probabilistic approach considers all possible ground motions for each earthquake and their associated probabilities of occurring based on the variability of the ground motion attenuation relationship. The probabilistic approach yields a probabilistic description of how likely it is to observe different levels of ground motion at the site. Typically, this is given in terms of the annual probability that a given level of ground motion will be exceeded at the site. The inverse of the annual rate at which the ground motion is exceeded is called the return period. For a specified return period, the controlling earthquake scenarios are identified by deaggregation.

Under the 10 CFR Part 100 Appendix A deterministic approach, a governing scenario earthquake is specified (magnitude and location) and the ground motion is computed using the appropriate attenuation relationships. However, even when the design earthquake is given in terms of its specific magnitude and distance to the site, there is still a range of potential ground motions that could occur at the site. This variability of the ground motions is characterized by the standard deviation of the attenuation relationship. Traditionally, in deterministic analyses, either the median (50th percentile) or median plus one standard deviation (84th percentile) ground motions are selected for use as design ground motions.

The site conditions at the HBPP consist of more than 400 feet of firm alluvial soils (References 1 and 179). There are two approaches that can be used to incorporate the site response effects into the ground motion estimates, a site-specific geotechnical model, and an empirical model. In the site-specific geotechnical model approach, the ground motions are first developed for outcrop rock conditions, then the soil ground motions are computed by propagating the rock ground motions through the overlying site-specific soil profile using an analytical model of the site response. Alternatively, in the empirical model approach, empirical attenuation relationships developed for a generic soil category that is similar to the soil conditions at the site are used directly to estimate the ground motions at the site.

As discussed in Sections 2.6.3 and 2.6.5, faults in the Little Salmon Fault Zone are very close to the site and are capable of generating large-magnitude earthquakes. The ground motions from these events could be very large, and the non-linear response under high strain levels of the soils could significantly alter the frequency characteristics of the horizontal ground motions from those developed for the rock outcrop motions. The expected level of shaking is well outside the range of the available empirical data and extrapolation of the non-linear effects contained in empirical soil attenuation relations to very high ground motion levels may not be applicable nor appropriate. Therefore, this study used the site-specific geotechnical model approach to develop the horizontal components of the ground motion on the top of the soil. Vertical ground motions are controlled by compression waves, which typically do not exhibit strong non-linear effects as they propagate through the overlying soil deposits. Consequently, the

empirical model was used to develop the vertical component of the ground motions. Additional information describing the significance of the vertical ground motion component in structural and geotechnical analyses is provided in PG&E's Response to NRC Question 2-8 (Reference 279) and in a geotechnical report assessing vertical ground motion on slope stability (Reference 278).

In this chapter, a brief description of development of the licensing basis ground motions is given. A probabilistic analysis was performed to determine the uniform hazard spectrum (UHS) with a 2000-year return period. The details of this PSHA are given in Calculation GEO.HBIP.03.04 (Reference 188). While the 2000-year return period UHS defines the licensing basis for the ground motions, more conservative spectra were used for the design basis based on a deterministic approach. A detailed description of the site response analysis for the deterministic is given in Calculation GEO.HBIP.02.06 (Reference 181). A detailed description of the development of the design basis response spectra for the ISFSI ground motion is provided in calculation GEO.HBIP.02.04 (Reference 180). Development of 4 sets of spectrum compatible ground motions is documented in detail in calculation GEO.HBIP.02.05 (Reference 182).

2.6.6.2 Attenuation Relations

Attenuation relationships describe the amplitude (and spectral ordinates) of the ground motion for a given earthquake magnitude, distance to the site, style-of-faulting, and gross site condition. All attenuation relationships were developed based on recordings from past earthquakes and most attenuation relationships assume the ground motion parameters to be lognormally distributed. The uncertainty in the ground motion prediction is typically incorporated into the design by the standard deviation of the attenuation relationships. For critical structures, conservatism is obtained by using a median plus one standard deviation (or 84th percentile) prediction; that is, the ground motion will have only a 16 percent chance of being larger than the design value for the given magnitude and site distance.

Different tectonic environments give rise to different ground motion attenuation relationships (Reference 183). Three categories of regional ground motion attenuation relations are typically used in seismic hazard assessments: shallow crustal earthquakes in active tectonic regions, shallow crustal earthquakes in stable continental regions, and earthquakes in subduction zones. In the Humboldt region, both shallow crustal earthquakes in active tectonic regions and subduction zone earthquakes occur, so two categories of attenuation relationships will need to be considered in characterizing the ground motions for the region.

Standard attenuation relationships were selected from the published literature. For application to the HBPP, results from the standard attenuation relationships were further modified to account for directivity effects, synchronous rupture, and outcrop rock conditions. These modifications are described following the selection of representative attenuation relationships.

2.6.6.2.1 Shallow Crustal Earthquakes

For shallow crustal earthquakes in active tectonic regions, four sets of up-to-date empirical attenuation relationships for horizontal response spectral values on rock site conditions were selected. These are the attenuation relations developed by Abrahamson and Silva (Reference 184), Campbell (Reference 7) (for soft-rock), Sadigh and others (Reference 8), and Idriss (References 2-4). These attenuation relationships are based primarily on California strong motion data, and are representative of the current state of knowledge about ground motion attenuation relationships for rock sites for shallow crustal earthquakes in active tectonic regions. These models include a style-of-faulting factor that distinguishes between strike-slip and reverse earthquakes, and include a standard deviation that is dependent on the earthquake magnitude. The model by Boore and others (Reference 6), often used in seismic hazard studies, was excluded because it is based on very few data on rock at short distances, and results in rock ground motions at short distances that were judged to be not reliable (and not conservative).

The median peak acceleration attenuation models are compared for a magnitude 7.5 reverse mechanism earthquake using the four attenuation relationships to demonstrate the reasonableness and consistency between the four models. In general, the peak accelerations derived from the four models are fairly consistent. At short distances, which are critical for the Humboldt site, the median ground motions for the four models differ by about 30 percent. The magnitude dependence of the standard deviation for peak acceleration for the models is then compared. The standard deviations are fairly similar for the four models, and differ by less than 0.1 natural log units. The mathematical forms and coefficients of the attenuation relationships are listed in calculation GEO.HBIP.02.04 (Reference 180).

2.6.6.2.2 Subduction Zone Earthquakes

There are two types of subduction zone earthquakes: interface earthquakes, and intraslab earthquakes. Although the ground motions can be significantly different for these two types of earthquakes, most attenuation studies for subduction zone earthquakes have not distinguished between these two types. The exception is the Youngs and others (Reference 9) model. By separating the two earthquake types, Youngs and others found a significant difference in the ground motions between the two types of subduction earthquakes. Because this difference between interface and intraslab earthquakes is judged to be significant, the Youngs and others (Reference 9) attenuation relation for subduction earthquakes was used. The mathematical forms and coefficients of the Youngs and others (Reference 9) attenuation relation are listed in calculation GEO.HBIP.02.04 (Reference 180). Additional information describing the significance of the attenuation modeling is provided in PG&E's Response to NRC Question 2-3 (Reference 279).

2.6.6.2.3 Directivity

The selected shallow crustal and subduction attenuation relationships described above predict the average of the two horizontal components for average directivity conditions. Recent studies have shown that for sites located close to the causative fault, rupture

directivity can have significant effect on horizontal spectra at long periods (Reference 181). There are two parts to the directivity effect. First, the average horizontal spectral acceleration at long periods ($T > 1$ sec) of forward directivity recordings are generally higher than those predicted by the attenuation relations. Second, directivity leads to a systematic difference in the long period spectral accelerations on the two horizontal components: the component oriented perpendicular (normal) to the fault strike is systematically larger than the component oriented parallel to the fault strike. This difference is due to the constructive interference of the S-waves generated by the part of the rupture located between the hypocenter and the site. Directivity effects are strongest when the slip direction is aligned with the rupture direction (Reference 185). For reverse faults, the slip direction and rupture direction are aligned when the rupture direction is updip, rather than along strike, which is the case for strike-slip faults.

Somerville and others (Reference 185) developed empirical relations describing the magnitude, distance, and period dependence of these directivity effects. A modified form of these models was used to supplement the empirical attenuation relationships to account for directivity effects. Because directivity effects lead to different horizontal ground motions in the fault-normal and fault-parallel directions, two horizontal spectra were developed, one for the fault-normal component and one for the fault-parallel component.

2.6.6.2.4 Fling

A second near fault effect is fling. Fling is caused by the permanent tectonic deformation that occurs at the site. For sites close to the fault, the tectonic displacement usually takes place over a time period of a few seconds. The fling affects the long period motions. In most engineering applications, fling has not been included in the design ground motions. Fling effects have not been well observed until recent large earthquakes, particularly the 1999 Turkey and Taiwan earthquakes. Because the site is located close to Little Salmon Fault zone and a large slip (e.g. 8 m) is expected on this fault, the fling effects are included for the ISFSI.

Current response spectral attenuation relations do not represent fling effects. The fling is therefore in addition to the ground motion computed for the response spectral attenuation relations. It is incorporated by adding the fling in to the time histories. This process is described in Calculation GEO.HBIP.02.05 (Reference 182).

2.6.6.2.5 Synchronous Rupture

In the source characterization model used in the PSHA, the Little Salmon Fault is considered to be part of the rupture of the Cascadia interface event so the ground motion estimate needs to account for synchronous rupture of the Little Salmon fault and the Cascadia interface. The standard attenuation relationships used in this study do not consider the case of synchronous rupture of multiple faults. Therefore, random vibration theory (square root of sum of squares, or SRSS) was used to calculate the response spectral values for synchronous rupture. The synchronous rupture effects both the median and the variability of the ground motion. Additional justification for this approach was provided in the PG&E Response to NRC Question 2-7 (Reference 278).

2.6.6.2.6 Outcrop Rock Site Condition

There are very few empirical data for hard rock site conditions. Therefore, the empirical attenuation relations for rock sites are based on data that includes weathered rock and some thin soils (less than 20 m thick). On average, the shear-wave velocity at the surface of sites that are classified as “rock” is about 1,000 feet per second. The shear wave velocity for the outcrop rock used in the site response study is 4,000 feet per second. As a result, the generic “rock” attenuation relations are not directly applicable to the outcrop rock site condition.

The effect of the weathered rock and thin soils that are included in generic “rock” sites has been evaluated by Idriss (Reference 186) and Silva (Reference 187). Idriss used recorded ground motion with available shear-wave velocity profiles to deconvolve the shallow site response from the recorded ground motions, and then estimated outcrop ground motions for a surface shear-wave velocity of 4,000 feet per second. Silva (Reference 187) used simulated ground motions to compare surface ground motions for hard rock (outcrop rock) with those from generic rock. The results of these two studies are summarized in terms of response spectral scale factors that can be applied to ground motions from generic rock attenuation relations to produce outcrop rock ground motions. These scale factors were applied to the median rock attenuation relations. The variability of the ground motions may also be affected by the weathered rock and thin soils. It is expected the variability of the outcrop rock motion would be less than for the weathered rock motion; however, this reduction in variability has not been considered in this study, resulting in some conservatism in the UHS at longer return periods.

2.6.6.3 Ground Motions

In accordance with 10 CFR 72.103, a probabilistic seismic analysis was developed using the guidance of Regulatory Guide 3.73, “Site Evaluations and Design Earthquake Ground Motion for Dry Cask Independent Spent Fuel Storage and Monitored Retrievable Storage Installations” (formerly DG-3021).

Standard PSHA methodology was modified to include the effects of rupture directivity. The variability of the hypocenter location on the fault is included using a uniform distribution over the lower half of the fault plane.

Results of the PSHA were developed for various return periods of 25 years to 10,000 years. The design basis ground motion for the ISFSI is the 2000 year return period (corresponding to a reference annual probability of exceedance of 5E-4). Tabular results of the PSHA spectrum are contained in Tables 2.6-18, 2.6-19, and 2.6-20. The UHS for the fault normal, fault parallel, and vertical components are shown in Figures 2.6-69, 2.6-70, and 2.6-71, respectively. For a 2000-year return period, the deaggregation shows that the hazard is dominated by the synchronous rupture of the main Cascadia Interface and the Little Salmon Fault. Complete details of the PSHA evaluation methodology including deaggregation plots are contained in calculation GEO.HBIP.03.04 (Reference 188)

Determination of ground motions at other return periods is done by using linear interpolation on the log annual probability (AP) of exceedance and log spectral acceleration values. Given the annual probability of exceedance values AP_1 and AP_2 at spectral acceleration values SA_1 and SA_2 , respectively, then using linear interpolation on the log-log values, the spectral acceleration SA at annual probability AP is given by:

$$\ln(SA) = \ln(SA_1) + (\ln(AP) - \ln(AP_1)) \frac{[\ln(SA_2) - \ln(SA_1)]}{[\ln(AP_2) - \ln(AP_1)]}$$

2.6.6.3.1 Design Ground Motions

A deterministic ground motion for the controlling earthquake scenario, was developed for use in the evaluation of the ISFSI. The earthquake consists of two subsources: a magnitude 8.8 earthquake on the main Cascadia Interface at a distance of 8 km and a magnitude 7.7 reverse slip earthquake on the Little Salmon Fault at a distance of 0 km. The 84th percentile spectral acceleration based on the attenuation relations is used. For the Little Salmon subsurface, the effects of rupture directivity and fling are included. The plant site is located directly updip from the Bay Entrance branch of the Little Salmon Fault Zone, which is a reverse fault. The directivity effect is computed assuming that the rupture starts at the bottom of the fault and ruptures updip toward the site. This leads to the maximum directivity effect.

As noted earlier, the spectrum of the synchronous rupture from these two subsources is computed using random vibration theory. The rock site spectrum for the synchronous rupture is then scaled to account for the site response using the site-specific amplification factors described in calculation GEO.HBIP.02.06 (Reference 181). This results in a soil surface spectrum. Additional information on soil properties used to derive soil amplification factors for the ISFSI site is provided in the PG&E Response to NRC Question 2-9 in Reference 279.

The 84th percentile response spectra on the fault-normal component for the combined rupture are shown in Figure 2.6-65. The ground motion for the synchronous rupture is dominated by the Little Salmon subsurface. The Cascadia interface subsurface increases the amplitude of the ground motion by only about 10 percent. The main effect of the Cascadia interface subsurface is to increase the duration of the shaking. Figure 2.6-66 shows the response spectra for the fault-parallel component. At long periods, the fault-normal component is a factor of 2 to 3 larger than the fault-parallel component, reflecting the effect of rupture directivity. Figure 2.6-67 shows the response spectra for the vertical component. Tables 2.6-15 through 2.6-17 show the digital values of the spectra.

A comparison of the deterministic spectra with the 2000-year UHS is shown in Figure 2.6-72. The deterministic spectra equal or exceed the 2000-year return period UHS at all spectral periods for all three components. At long spectral periods, the difference is large for the fault normal component. Therefore, the deterministic spectra include significant conservatism relative to the license basis.

2.6.6.3.2 Time Histories

The spectra discussed above describe the amplitude of shaking, but not the time trace of the shaking. Individual realizations of the ground shaking can be fully described by a time history that gives the acceleration as a function of time throughout the earthquake; however, there are an infinite number of the time histories that have the response spectral amplitudes enveloping the target spectrum. The appropriate phasing of the ground motion can be given by empirical or simulated time histories for the appropriate magnitude and distance range, and directivity conditions.

Because the target spectrum for the rock motions is based on the superposition of two subsources (Little Salmon and main Cascadia interface), the initial time histories should also reflect this superposition. There are no empirical recordings available that are appropriate for such a synchronous rupture. The time histories were first developed for the individual sub-sources and the added together (in the time domain) to give the initial time histories for the spectral matching to the maximum earthquake target spectrum. The steps in developing the time histories for the individual subsources and how they were then combined are given in calculation GEO.HBIP.02.05 (Reference 182). The time histories were modified to match the deterministic design spectra using a time domain spectral matching procedure. This procedure preserves the overall non-stationary characteristics of the acceleration, velocity, and displacement waveforms of the initial time history, while matching the target spectrum. The target spectrum was defined over the frequency range of 0.1 to 100 Hz with 104 frequencies. After matching to the target design spectra, the vertical and fault normal time histories were further modified to include the effects of fling. This is done by adding the fling to the time history in the time domain based on a fault displacement of 8m. This process of adding fling is described in calculation GEO.HBIP.02.05 (Reference 182). The resulting time histories met the Standard Review Plan 3.7.1 criteria for enveloping the design spectra, and the ASCE-4 criterion for statistical independence between the 3 components.

These spectrum-compatible time histories are contained in calculation GEO.HBIP.02.05, Figures 7-47 through 7-50 (Reference 182).

2.6.7 LIQUEFACTION AND LANDSLIDE POTENTIAL

2.6.7.1 Introduction

To assess liquefaction and landslide potential at the proposed ISFSI site (hereinafter, "the site") and along the proposed transport route during earthquake loading, a series of borings were drilled at the site, and laboratory tests on soil samples obtained from the borings were conducted to define soil properties. Liquefaction potential was assessed using field blowcounts and standard liquefaction susceptibility charts relating blowcounts to earthquake-induced cyclic stress ratios (calculation GEO.HBIP.02.02 (Reference 189)). Slope stability and potential earthquake-induced displacements were analyzed using field and laboratory data, postulated design ground motions, and a Newmark-type procedure incorporating a finite element model of the site and a critical

section along the transport route (calculations GEO.HBIP.02.07 and GEO.HBIP.02.08 (References 190 and 191), respectively).

2.6.7.2 Field Exploration And Laboratory Testing At The ISFSI Site

Subsurface conditions at the site were characterized by drilling three exploratory borings, GMX99-3, GMX99-4, and GMX99-5 (Figure 7-1 of GEO.HBIP.02.07). Borings were drilled and sampled to depths ranging from 61.9 to 77.3 feet. Two additional borings, GMX99-1 and GMX99-2, were drilled to depths of 95 and 402 feet, respectively, somewhat south of the site, to investigate other potential sites, obtain in situ geophysical properties, and evaluate the continuity of soils underlying Buhne Point hill. Borings were drilled using mud-rotary drilling techniques. A more detailed description of the field exploration program appears in Data Report B (Reference 192).

Selected soil samples retrieved from the exploratory borings were delivered to the laboratory for examination and testing to evaluate their physical characteristics and engineering properties. Samples were tested to derive their moisture content, unit weight, plasticity, grain-size distribution, and undrained shear strength using both unconsolidated- and consolidated-undrained triaxial compression tests. The laboratory tests performed are discussed in more detail in Data Report E (Reference 193). Test results are presented in Data Report E, and also are summarized at the corresponding sample locations on the boring logs in Data Report B.

2.6.7.3 Site and Subsurface Conditions at the ISFSI Site

The ISFSI site is located on a relatively flat area of the Buhne Point hill, approximately 300 feet northeast of the Unit 2 Fuel Oil Tank, and approximately 70 feet south of the bluff cut into the hill that overlooks Humboldt Bay (Figure 2.6-31). The ground surface slopes gently southeast (the elevation drops by 4 to 6 feet across the site), and has been altered only slightly since plant construction.

Clayey sand and clay underlie the site to a depth of approximately 23 feet. Trenches excavated at the site indicate these strata are relatively continuous laterally, and dip 2 to 4 degrees to the southeast (Section 2.6.4). For the purposes of these analyses, however, it was assumed that these and the underlying layers lie horizontally. Very dense sand and silty sand underlie these upper cohesive materials, to a depth of 50 to 53 feet. In boring GMX99-5, the sand grades to very stiff to hard sandy silt and silt. A relatively thin layer (less than 10 feet thick) of hard silt and silty clay having a thin stratum of very stiff peat was encountered in all borings at a depth of approximately 55 feet. The borings were terminated in the dense to very dense sand and gravel below this layer. A generalized soil profile used for engineering analyses is presented on Figure 7-2 of GEO.HBIP.02.07.

Standard penetration test (SPT) blowcounts were obtained in the borings to analyze the potential for liquefaction of sandy soils. The depth to groundwater was not recorded in the field because drilling fluid was used to remove cuttings during drilling. However, geophysical data obtained in two of the borings indicate soils are saturated to an elevation of approximately 6 feet above mean lower low water (MLLW) as documented

in Data Report C (Reference 194). This places the groundwater level at a depth of about 37 feet below the existing ground surface at the ISFSI site. SPT blowcounts from the borings were normalized to $(N_1)_{60}$ blowcounts as described in GEO.HBIP.02.02. The liquefaction susceptibility curve developed by Seed and others (Reference 195) shows that at very high earthquake-induced cyclic stress ratios, values of $(N_1)_{60}$ asymptotically approach a limiting value of 30 blows per foot. The curve developed by Seed and others (Reference 195) was reviewed and adopted, with minor modifications, in a workshop on the evaluation of liquefaction resistance of soils (Reference 196) as published in Youd and others (Reference 197) and shown in Figure 3 of GEO.HBIP.02.02. The modifications did not affect this limiting blowcount value. Data from borings drilled during previous studies in the vicinity of Unit 3 (Reference 1) were also analyzed to assess liquefaction susceptibility. The $(N_1)_{60-cs}$ blowcounts from previous studies and this study are presented on Figure 2 of GEO.HBIP.02.02. Because nearly all the $(N_1)_{60-cs}$ blowcounts are greater than 30, the site and nearby transport route are judged not susceptible to liquefaction. Additional information related to the potential for liquifaction at the ISFSI site in the vicinity of the concrete vault is provided in the PG&E Response to NRC Question 2-14 in Reference 279.

2.6.7.4 Slope Stability Analyses At The ISFSI Site

Slope stability analyses were performed to evaluate the factor of safety against sliding at the site.

Two cross sections were analyzed in this study (Figure 7-1 of GEO.HBIP.02.07). Cross section A-A' is on the bluff side of the hill. The front edge of the proposed ISFSI site is about 70 feet from the slope break at elevation 44 feet above mean lower low water. A 20-foot-wide pressure load of 3,000 pounds per square foot (psf) was placed at a depth of about 15 feet below the ground surface to represent the ISFSI vault load. The two-dimensional slope stability analysis conservatively assumed an infinite pad length.

The second cross section, B-B', is on the plant side of the hill. The proposed site is about 150 feet from the top of the cut slope near the Unit 2 fuel oil tank. A generalized soil profile is presented on Figure 7-2 of GEO.HBIP.02.07. The water table was assumed to be at elevation 6 feet above MLLW.

Soil strengths were assigned to the various units as described in GEO.HBIP.02.07. Subsurface layers and soil properties used in the stability analyses are presented in Table 7-1 of GEO.HBIP.02.07.

Searches were conducted for the minimum factor of safety using the general limit equilibrium method and the long-term (effective stress) soil-strength parameters described above for circular slide masses daylighting beneath the pad. The results of the stability analyses are shown on Figures 7-6 and 7-7 of GEO.HBIP.02.07 for the two cross sections analyzed. The minimum factors of safety computed range between 2.7 and 4.9, which are sufficiently high to preclude unlimited slope displacements (slope failure) during earthquake shaking.

2.6.7.5 Slope Displacement Analyses At The ISFSI Site

The slopes were further analyzed for their potential to undergo limited earthquake-induced displacements. Using the slide masses having the lowest factor of safety, the potential for permanent displacements were evaluated using the concept of yield acceleration proposed by Newmark (Reference 198) and modified by Makdisi and Seed (Reference 199).

The slope stability computations were repeated for the slide mass having the lowest static factor of safety by incrementally increasing the horizontal pseudostatic acceleration to derive the yield acceleration, k_y , that reduced the factor of safety of the slip surface to one. For the critical slide masses at the site, computed values of k_y are about 0.69g and 0.66g for the bluff-side and plant-side slopes, respectively.

The earthquake-induced seismic coefficient time histories (and their peak values k_{max}) for the critical slide masses were computed using two-dimensional dynamic finite element analyses. Soil properties required for the analyses were derived as described in GEO.HBIP.02.07. Properties are presented in Table 7-3 of GEO.HBIP.02.07. A finite element representation of the site is shown on Figure 7-13 of GEO.HBIP.02.07. Two separate horizontal motions (sets 1 and 3 from Section 2.6.6) were rotated to the direction of each section and input at the base of the model. The seismic coefficient time history for each critical slide mass was output from the analyses. Plots of the seismic coefficient time histories for each input ground motion are shown in Figures 7-14 through 7-17 of GEO.HBIP.02.07. Information provided in Reference 278 demonstrates that vertical ground motion does not significantly affect slope stability at the ISFSI facility.

Newmark-type displacement analyses were performed to determine the earthquake-induced permanent displacements of each critical slide mass. The analyses utilized the seismic coefficient time histories and the yield accelerations calculated as described above.

For a yield acceleration of 0.69g, the earthquake-induced downslope displacements for the critical bluff-side slide mass are calculated to range from 0.2 to 0.5 feet. Permanent displacements for the slide mass on the plant-side slope range from 0.3 to 4.7 feet for a yield acceleration of 0.66g. The average displacement for the full range of displacements is 1.4 feet.

The four sets of design ground motions developed for the Humboldt Bay ISFSI correspond to the median plus one standard deviation or 84th percentile spectrum. In performing the Newmark displacement analysis, only two of the four sets of the ground motions were used because the selected two are expected to produce larger displacement estimates as documented in calculation GEO.HBIP.02.07 (Reference 190). The 84th percentile seismic induced displacements can be estimated using the median (or average) values of the 4 cases analyzed using the 84th percentile ground motions. The maximum displacement of 4.7 ft would correspond to a percentile that is significantly over the 84th percentile criteria used for seismic design of the facility. However, as a conservative measure, PG&E has evaluated the acceptability of

the maximum displacement of 4.7 ft. Details of the evaluation are provided in the PG&E Response to NRC Question 2-11 in Reference 279.

2.6.7.6 Site And Subsurface Conditions Along The Transport Route

The most critical location along the transport route in terms of slope stability is denoted by Section C-C' on Figure 8-1 of GEO.HBIP.02.08. The selected cross section shown on Figure 8-1 meets the following two criteria simultaneously: a) closest approach of transporter to slope (in this case, the bank of the Discharge Canal) and b) greatest height of slope. Beyond this location, the distance between the transport route and the Discharge Canal bank increases as the route continues up the hill, thereby reducing the effect of the transporter load on the bank.

The subsurface stratigraphy at the selected location is determined based on nearby borings. Logs from nearby borings were reviewed and stratigraphy from the logs summarized as shown on Figure 8-2 of GEO.HBIP.02.08. Soil stratigraphy as determined from nearby borings consists of the same sequence of stiff clays overlying dense sands and gravels as found in boring 99-2 near the proposed ISFSI site further up the hill, as summarized in Table 8-1 of GEO.HBIP.02.08.

2.6.7.7 Slope Stability Analyses At The Transport Route Critical Cross Section

Because available data indicate soil stratigraphy and properties are consistent with those determined at the ISFSI site, static and dynamic properties of the subsurface soils at the critical transport route cross section are selected to be the same as at the ISFSI site as presented in GEO.HBIP.02.07, as summarized in Tables 8-1 and 8-2 of GEO.HBIP.02.08.

A static slope stability analysis was performed at the most critical location along the transport route to obtain the short term static factor of safety with transporter loading. It was conservatively assumed that there is no water in the adjacent Discharge Canal but that clay and sand layers are saturated to elevation 6. The results of the stability analyses are shown on Figure 8-3 of GEO.HBIP.02.08. The minimum factor of safety computed is 1.7.

2.6.7.8 Slope Displacement Analyses at the Transport Route Critical Cross Section

The slope was further analyzed for its potential to undergo limited earthquake-induced displacements. As for the ISFSI site, the potential for permanent displacement at the transport route critical section was evaluated using the concept of yield acceleration proposed by Newmark (Reference 198) and modified by Makdisi and Seed (Reference 199).

The slope stability computations were repeated by incrementally increasing the horizontal pseudostatic acceleration to determine the yield acceleration, k_y , that reduced the factor of safety of the slide mass to 1.0. The resulting yield acceleration is 0.84.

analyses. The analyses were performed at the cross section analyzed using the dynamic properties summarized in Table 8-2 of GEO.HBIP.02.08. A finite element representation of the site is shown on Figure 8-4 of GEO.HBIP.02.08. Ground motion sets 1 and 3 from Section 2.6.6 were rotated to the direction of the section and input at the base of the model. The seismic coefficient time histories of the critical slide mass were output from the analyses. Plots of the seismic coefficient time histories for each input ground motion are shown in Figures 8-5 and 8-6 of GEO.HBIP.02.08.

Newmark-type displacement analyses were performed to determine the earthquake-induced permanent displacements of the critical section. The analyses utilized the seismic coefficient time histories and the yield accelerations calculated as described above.

For ground motion set 1 and a yield acceleration of 0.84, displacements range from 2.6 to 4.7 feet. For ground motion set 3, displacements range from 2.6 to 9.0 feet. The average displacement for the full range of displacements is 4.7 feet. The displacement for the transport earthquake would be negligible as the ground motion is less than the yield acceleration.

2.6.7.9 Summary of Liquefaction and Landslide Potential

- Geologic assessments described in Section 2.6.4 indicate that wave-induced erosion along the bluff has been largely eliminated by the placement of riprap at the base of the bluff in the 1950s, although shallow landslides along the bluff have occurred infrequently since then. The PG&E Response to NRC Question 2-1 in Reference 279 refers to an assessment of erosion at Buhne Hill. This evaluation demonstrates that the riprap is suitable to provide bluff stability for all expected conditions for the life of the ISFSI. Any significant bluff instability or impairments of the riprap will be corrected.
- Analyses of slope stability indicate that static factors of safety for circular failure surfaces daylighting beneath the ISFSI site are 2.7 or greater. The static factor of safety beneath the critical section of the transport route is 1.7.
- During the postulated design ground motions, analyses indicate displacements of the failure surface beneath the ISFSI site average about 1 foot. Displacements of the critical section along the transport route average about 5 feet.
- Very high blowcounts in sands underlying the site indicate that the site is not susceptible to liquefaction.

2.6.8 SURFACE-FAULTING POTENTIAL

2.6.8.1 Introduction

The assessment of the potential for surface faulting at the Humboldt Bay ISFSI site is based on many studies of the geology of the site and vicinity conducted throughout the past 50 years, particularly the detailed investigations performed during the 1970s and in 1999 and 2000 for the HBPP and the ISFSI. The earliest major study that recognized the Little Salmon fault was Ogle's work in 1953 (Reference 69). Pertinent data from this and other investigations are presented in Sections 2.6.3 and 2.6.4, which describe regional and site geology, respectively.

The following factors were considered in assessing the potential for surface fault rupture at the ISFSI site:

- (1). The proximity of the site to known active faults, based on regional mapping of the Little Salmon fault zone and interpretations of faulting near the site developed from borings, trenches, and geologic mapping
- (2). Comparison of the geologic structure in the vicinity of the Humboldt Bay ISFSI site with the characteristics of surface faulting associated with historical thrust-faulting earthquakes and with well-documented Quaternary thrust faults in the Humboldt Bay region
- (3). The age and continuity of strata beneath the site, based on data from borings and continuous exposures in trenches excavated at the site
- (4). The recurrence of surface faulting on the Little Salmon fault zone relative to the ages of unfaulted strata beneath the site, and
- (5). Comparison of the hanging-wall deformation at Buhne Point fault with the 1999 surface rupture on the Chelungpu fault in Taiwan

2.6.8.2 Proximity Of Site To Known Active Faults

As described in Sections 2.6.3.2.2 and 2.6.4.4, the ISFSI site sits on the hanging wall of a capable thrust fault, the Little Salmon fault zone. In the vicinity of the site, the fault zone has two primary traces and two subsidiary traces (Figure 2.6-18). These traces are referred to as the Little Salmon, Bay Entrance, Buhne Point, and Discharge Canal faults. The first three strike northwest and dip to the northeast beneath the site. The Little Salmon fault projects to the surface about 2.2 kilometers southwest of the ISFSI site (Figure 2.6-46), and either dies out south of, or is more than 1,600 meters below, the site (Section 2.6.4.4.1). The Bay Entrance fault is the closest of the main fault traces of the Little Salmon fault zone to the ISFSI site. The fault projects to the surface about 500 meters west of the site, and the closest distance (fault-normal distance measured to the center of the site) is between about 410 and 470 meters (Figures 2.6-46 and 2.6-49). The Buhne Point fault, a secondary fault in the Little Salmon fault zone, projects to the surface about 200 meters southwest of the ISFSI site

and lies about 140 to 160 meters beneath the site (Figures 2.6-48 and 2.6-50). The fourth fault, the Discharge Canal fault, is a southwest-dipping backthrust splay of the Buhne Point fault that intersects the surface about 125 to 150 meters northeast of the site (Figures 2.6-31, 2.6-50, and 2.6-51).

2.6.8.3 Surface Deformation Associated With Thrust Faults

The characteristics of surface deformation from earlier episodes of fault rupture commonly are replicated during subsequent faulting events. Descriptions of surface faulting associated with historical earthquakes, therefore, can help to characterize the geometry and style of surface deformation that may be associated with a future surface-faulting event. Well-documented thrust-faulting events (Table 2.6-21) comprise a variety of types of surface deformation that commonly include both fault displacement and folding. The style of faulting and related surface deformation, width of the deformed area, amount of surface displacement, and relative contributions of fault displacement and folding to the total slip on a fault commonly change within short distances along strike. Assessments of historical thrust-faulting earthquakes worldwide, and detailed studies of late Quaternary faulting in northern California, support characterization of the nature and extent of surface deformation (faulting and folding) that may be associated with future displacements on the Little Salmon fault zone near the ISFSI site.

2.6.8.3.1 Characteristics of Thrust Faults

The near-surface structures of thrust faults range from a single low-dip-angle fault plane to complex systems that contain many branching reverse faults, backthrusts, secondary normal, strike-slip, or oblique-slip faults and folds (Figure 2.6-73). A single, narrow surface trace represents one end-member of the range of near-surface thrust fault structures (Figure 2.6-73, item a). Such a structure accommodates all displacement on a single fault plane, or on a few closely spaced imbricate faults that intersect the ground surface along a narrow, generally well-defined scarp. The scarp, which commonly is at or near the angle of repose of the sediment or broken rock along the fault, represents the collapsed tip of the hanging wall that was thrust upward during the faulting event. The 1964 scarp along much of the length of the Patton Bay and Hanning Bay faults on Montague Island in Alaska is of this type (Figure 2.6-74) (Reference 200). In general, thrust faults made up of single or multiple imbricate thrust surfaces are more likely in more competent rocks and well-consolidated sediments and where the geometry of the fault is simple (not changing dip or strike and not at a stepover or ramp).

Where near-surface sediments are unconsolidated and weak, the overthrust fault tip may roll over and follow the ground surface during thrusting. The result is an anticlinal flexure and a rounded scarp in which the thrust intersects the ground surface near the base of the scarp slope (Figures 2.6-73, items b through d). Such surface displacements produce a fault plane that has inherited the slope of the former ground surface on the footwall and commonly results in a nearly horizontal fault beneath the scarp. This style of surface displacement was characteristic of the 1968 Meckering earthquake in Australia (Reference 201); examples from northern California include the scarp and trench exposure of the Trinidad fault near Trinidad, California (Figure 2.6-75).

Many examples of this style of surface deformation also were generated by the Chi-Chi earthquake in Taiwan (Figure 2.6-76) (References 202-203).

Both synthetic thrust and antithetic backthrust faults are common along large thrusts near the surface. Backthrusts represent reversals in dip of the fault plane, in which slip is accommodated in the conjugate shear direction (Figure 2.6-73, item e). Where secondary backthrust faults break through the hanging wall of a main thrust, an uplifted wedge-shaped block bounded by thrusts having opposing dip angles is produced in the hanging wall. In some places, all the slip is accommodated on backthrusts, resulting in thrust-wedge structures (Figure 2.6-73, item f). Backthrusts have been found along the Little Salmon fault zone at several places, including College of the Redwoods (Figures 2.6-20 through 2.6-23) and near the HBPP (Figure 2.6-50). The ISFSI site sits on the internally coherent, uplifted wedge-shaped block defined by the Buhne Point fault (a synthetic main thrust) and the Discharge Canal fault (an antithetic back thrust) (Figures 2.6-50 and 2.6-77, item a).

Another end-member of the thrust fault structural style is a system of many (hundreds or even thousands) of small, closely spaced synthetic and antithetic conjugate thrust and backthrust fault planes that intersect the ground surface across a broad zone of deformation that is tens to hundreds of meters wide, producing the geomorphic appearance of an anticlinal flexure or monocline. These faults form conjugate fault sets (Figure 2.6-73, item h) that represent coulomb shear failure of the near-surface sediments under nearly horizontal compression (Reference 204). The synthetic and antithetic faults intersect at the shear angle of the faulted material. One of the best-exposed local examples of conjugate faulting is in the sea cliff where the McKinleyville fault crosses the coastline north of Eureka (Figure 2.6-78) (Reference 205). This faulting pattern also was found in trenches across a trace of the Mad River fault zone at the Humboldt County Airport, southeast of Clam Beach near McKinleyville (Figure 2.6-54). Several examples of this type of faulting have been identified on the Little Salmon fault system near the site, such as at the quarry exposure in Humboldt Hill that is across US Highway 101 from the power plant (Reference 1). Displacement on this type of thrust is distributed on many fault surfaces, each accommodating a small part of the total. This type of shallow thrust fault commonly results in a wide, gently sloping scarp that geomorphically is poorly defined. Conjugate microfaults also are common adjacent to larger-displacement thrust faults. The numerous small-displacement faults in the hanging wall of the Buhne Point fault exposed in trenches WCC-11-T6b and WCC-11-T6c are of this type (Figures 2.6-53 and 2.6-54).

Some or all of the displacement on many thrust faults may be expressed at the surface by folding (Figures 2.6-73, items d, g, i). Several kinds of surface-folding processes have been recognized. Where the fault is made up of one or a few well-defined fault planes that end before reaching the surface, fault-propagation anticlines (Reference 1), can be produced at the fault tip (Figures 2.6-73, item i and 2.6-79). If surface sediments are highly plastic, such as wet, compact, clayey sediments, the anticline can be very sharp and even overturned. Such a fault-propagation fold was found in trenches across one of several traces of the Mad River fault at McKinleyville (Figure 2.6-80). However, this type of faulting has not been seen in the vicinity of the Humboldt Bay ISFSI site.

Fault bend folds are common along the surface traces of many thrust faults. Such folds result from horizontal rotation of the hanging wall above segments of the fault plane having different dip angles (Figures 2.6-73, items c, d, g). The dip angles of many thrusts decrease as the fault approaches the surface and are “blind” (do not reach the surface). This type of folding was described extensively for large, deep-seated thrusts (Reference 206), but also is common in the near surface associated with low-angle, dip-slip thrust faults. Fault bend folds are characterized by limbs that have planar panels separated by relatively sharp hinge lines (Figures 2.6-73, items d, g). The panels lie above planar segments of the underlying fault, and the hinges form above bends in the fault plane. Where horizontal geomorphic or stratigraphic datums such as marine terraces overlie shallow thrusts, the effects of underlying fault bends commonly are expressed by tilting of the originally horizontal surface. This process forms two types of hinges: permanent hinges that migrate up-dip, away from the underlying fault bend, and stationary hinges, which remain above the underlying fault bend. During fault displacement, the hanging wall migrates through the axial plane of the stationary hinges and rotates to a new dip angle by shearing. Surface deformation and damage associated with this type of hanging-wall shearing were observed in Taiwan along the Chelungpu fault during the 1999 Chi-Chi earthquake (Figure 2.6-81) (Reference 203). Fault bend folds having hinge-line deformations of this type have been described in trench exposures and boreholes across the Little Salmon fault zone at College of the Redwoods, about 5 kilometers south of the Humboldt Bay ISFSI site (Reference 110; Figures 2.6-20 through 2.6-23). Figure 2.6-72 compares the faulting observed at College of the Redwoods with faults near the ISFSI site.

Secondary normal faults produced by extension of the upper surface of the hanging wall above fault-generated folds are common on some thrusts. These faults, called bending-moment faults (Reference 207), generally are parallel to the strike of the underlying thrusts and associated fold axes. They commonly include both antithetic and synthetic normal faults bounding graben localized in the hanging wall near the tip of the thrust. Slip on such secondary normal faults occurred along the Chelungpu fault during the 1999 Chi-Chi earthquake (References 202-203). Another dramatic example is seen on the hanging wall of the fault from the 1980 El Asnam, Algeria, earthquake (Figure 2.6-82) (Reference 208). The small, rootless graben exposed in trench WCC-11-T6a (see Reference 65, Appendix 4A, Figure C-12, Sheet 3, Station 160 m), about 35 meters west of the ISFSI site, may represent minor bending-moment, normal faulting in the hanging wall of the Buhne Point fault (Section 2.6.4.4.5).

The geometry and deformation characteristics of surface rupture on thrust faults in the Humboldt Bay region fit the above-described faulting types as reconstructed from scarp morphology and from shallow subsurface fault structures observed in trenches and other near-surface exposures (Reference 1, 50, 84, and 110). Each of the various styles of thrust-fault-generated surface deformation has produced distinctive geomorphic and shallow subsurface structures that have persisted as enduring evidence of the deformation style of the generating fault.

2.6.8.3.2 Hanging-Wall Deformation on the Buhne Point Fault

The Humboldt Bay ISFSI site occupies a relatively stable wedge-shaped block of a raised, tilted, and faulted late Pleistocene (the geologic time scale is presented in Table 2.6-1) marine terrace with underlying marine sediments. The Buhne Point fault displaces the terrace block along the south boundary of the power plant property. Trenches across part of this fault exposed closely spaced conjugate thrusts having small (a few millimeters to centimeters) displacements. A small backthrust, the Discharge Canal fault, has been mapped cutting the terrace on the north side of the property. Between the backthrust and the Buhne Point fault, the marine terrace is uplifted and gently tilted to the northeast, indicating the presence of a fault bend ramp at depth beneath the site. This ramp probably is on the Bay Entrance fault. Trenches across the site area between the backthrust and the Buhne Point fault revealed unfaulted, tilted planar bedding consistent with the tilted terrace surface. The single exception is the small graben-like structure that was interpreted by Woodward-Clyde Consultants (Reference 1) as soft-sediment deformation unrelated to the underlying fault. Alternatively, as discussed in Sections 2.6.4.4.5 and 2.6.8.3.1, this feature may represent secondary, bending-moment deformation related to folding. However, neither axial hinges associated with fault bend folds nor secondary bending-moment faults were found in the late Pleistocene strata exposed in trenches at the ISFSI site.

2.6.8.4 Age, Continuity, and Stability of Strata Beneath the Site

The strata beneath the ISFSI site consist of late Pleistocene interbedded estuarine and alluvial sand, silt, and clay of the Hookton Formation (Section 2.6.4.3.3). A distinctive marker horizon in the lower Hookton Formation, the top of the Unit F clay, is about 40 meters below the ISFSI site, where the contact between Unit F and the overlying sand and gravel strikes N30°-40°E and dips about 5°SE (Figures 2.6-36, 2.6-44, 2.6-51 and 2.6-55). This marker horizon, which is known from borings in the uplifted block, is bounded by the Buhne Point and Discharge Canal faults (Figure 2.6-55). Analysis of borehole data regarding the elevation of the top of the Unit F clay, along with projections between borings, indicates that the clay has no major displacements. There is a small (less than 2.5-meter) vertical displacement of Unit F in the hanging wall of the Buhne Point fault about 170 meters southwest of the ISFSI site (the Buhne Point splay fault on Figures 2.6-31, 2.6-51, and 2.6-55). There also may be a small (1.2 to 1.5 meter) vertical displacement of the top of the Unit F clay 220 meters east of the ISFSI site (between borings WCC80-CH3 and WCC80-CH4; see Figures 2.6-31 and 2.6-59). The Unit F marker horizon beneath the site does not appear to have been displaced significantly (within the limits of interpretation of the boring data), even though numerous displacements have occurred on the nearby Buhne Point and Little Salmon faults.

The Unit F clay marker horizon, which is in the upper part of the lower Hookton Formation, is unconformably overlain by the upper Hookton Formation and the Buhne Point terrace surface. These deposits and the terrace surface predate formation of a well-developed paleosol (Table 2.6-6) that is at least 83,000 years old (equivalent to or older than Oxygen Isotope Stage 5a). Geologic cross section Y-Y¹ (Figures 2.6-31 and 2.6-44) illustrates the stratigraphic relations in the near-surface (upper Hookton

Formation) deposits beneath the ISFSI site. Based on observations of borings, trenches, and the sea cliff exposure, upper Hookton deposits are continuous, providing direct evidence that these deposits are not faulted beneath the site.

Deposits of the upper Hookton Formation were continuously exposed in trenches that trend almost east/west and north-northeast/south-southwest across the ISFSI site (Figures 2.6-32, 2.6-42 and 2.6-43). Trench exposures provide the most direct means of detecting faults and assessing the continuity of bedding in the near-surface strata beneath and adjacent to the site (see Section 2.6.4.5.2 and Reference 65, Appendix 4A). The well-bedded sediments exposed in trench walls made it possible to detect faults having very small (a few millimeters to a few centimeters) displacements. Figures 2.6-31 and 2.6-32 show the locations of fractures and small displacements mapped in the trench exposures. Except for the Discharge Canal fault, nearly all the deformation observed in the trenches was in the western part of Buhne Point hill, and is interpreted to be deformation in the hanging wall close to the Buhne Point fault (within 100 to 150 meters of the projected surface trace). The only stratigraphic displacements observed near the ISFSI site bound a small graben in a silt bed about 35 meters west of the site (Figure 2.6-31 and Reference 65, Appendix 4A, Figure 4A-12, Sheet 3, Station 160 m). The graben consists of two narrow zones of antithetic faults about 30 centimeters apart that form a depression in the silt bed about 15 centimeters deep; there is no apparent vertical separation across the feature. Woodward-Clyde Consultants (Reference 1) attributed the feature to soft-sediment deformation during deposition of the Hookton sediments, because the underlying and overlying sediments are not similarly disturbed. However, it is possible that the small normal faults represent bending-moment faults above a fault bend fold in the hanging-wall of the Buhne Point fault. Other discontinuous fractures exposed in trenches GMX-T1 and GMX-T2 and in the other trenches near the ISFSI site displace none of the prominent lithologic contacts within the upper Hookton Formation. No displacements were observed in any of the site area trenches within about 30 meters of the site. The generally well-bedded strata exposed in these trenches provide confidence that no faults are present having offsets greater than a few millimeters in most places and not greater than 2 centimeters in areas where bedding is less well defined. The trench exposures provide direct evidence for no faulting in the upper Hookton Formation deposits beneath the site during the past 83,000 years at a minimum.

2.6.8.5 Recurrence of Surface Faulting Relative to Ages of Strata Beneath the Site

Paleoseismic investigations along the Little Salmon fault zone by Carver (Reference 115), Clarke and Carver (Reference 50), and Witter and others (Reference 51), and at the edge of South Bay by Patton and others (Reference 209) constrain the approximate timing of individual surface-faulting events. Radiocarbon ages for events on the western trace indicate that faulting occurred about 300; 800; 1,600; 2,150; and 3,500 years ago (Reference 50). The timing of events identified in trenches across the eastern trace is unknown, but they may have been synchronous with events on the western trace.

Estimates of the late Holocene (past approximately 6,000 years) slip rate on the Little Salmon fault zone, based on trenching studies, are 6 to 12 millimeters per year (Reference 50 and 78) and 2.9 to 6.9 millimeters per year (Reference 51), rates that are in general agreement with the long-term (past 700,000 years) slip rate across all three main fault traces (Reference 160). Estimates of the frequency of large-magnitude earthquakes based on the geologic slip rate (Reference 160) are similar to those based on paleoseismic evidence. Despite uncertainties in the size and interval between events, the data indicate that during the late Holocene, surface-faulting earthquakes occurred every few hundred to a thousand years or so. The similarity between the long-term and short-term slip rates suggests that surface-faulting events have occurred with the same frequency for hundreds of thousands of years.

There are no data on the timing of individual events on the Bay Entrance trace of the Little Salmon fault zone west of the ISFSI site. The estimated 1- to 2-millimeter-per-year slip rate on the Bay Entrance trace (Section 2.6.4.4.2) is about one-third to one-twelfth the slip rate on the Little Salmon fault zone to the south. This slower rate indicates that slip on the Bay Entrance fault trace has been transferred to other branches of the fault, or surface-faulting events along this section of the fault either are less frequent or are characterized by smaller displacements. In either case, tens to hundreds of rupture events have occurred on the fault zone near the ISFSI site during the past 83,000 years. (Calculated by dividing the range of estimates of the recurrence of late Holocene faulting from trenching data [Section 2.6.3] into the minimum age of the Buhne Point terrace [Section 2.6.4]).

The repeated faulting events have produced deformation in the hanging wall of the Bay Entrance fault. This deformation is evident as 6 to 10 meters of post-Unit F displacement on the Buhne Point fault, at least 4.5 meters of displacement on the Discharge Canal fault, distributed faulting near the leading edge of the Buhne Point fault, and at least 20 meters of uplift and 2 to 4 degrees of tilting of the Buhne Point terrace. No displacements have been found in the late Pleistocene deposits that underlie the proposed ISFSI site.

2.6.8.6 Comparison of Deformation at Buhne Point With 1999 Surface Fault Rupture on the Chelungpu Fault, Taiwan

The Chelungpu fault in Taiwan shares several general structural and tectonic characteristics with the Little Salmon fault zone, including its subduction-zone setting, long length, relatively large amount of slip per event, and high slip rate. Surface faulting along the Chelungpu fault during the 1999 magnitude 7.6 Chi-Chi earthquake produced vertical displacements of 2 to 9 meters along an 80-kilometer-long rupture (References 202-203).

Kelson and others (Reference 202) provide well-documented examples of the various styles of surface deformation associated with this large thrust earthquake, giving numerous examples of the response of building foundations and reinforced-concrete structures along the Chelungpu fault to the permanent ground deformations produced by tectonic faulting and folding. There is a direct correlation between the pattern and

HUMBOLDT BAY ISFSI FSAR UPDATE

style of surface deformation and the damage to engineered structures. The following general observations were made.

- Building collapses and extensive damage caused by surface faulting were concentrated on the hanging-wall side of the fault. Most damage was concentrated along the primary trace, where displacements were the largest and where rollover of the hanging wall was most pronounced. Locally significant damage was also concentrated along the larger secondary faults.
- Permanent ground deformation and associated damage to buildings were relatively minor to absent on the footwall side of the surface rupture, even for buildings located very close to the fault scarp.
- Tilting and secondary faulting occurred in the hanging wall as much as 350 meters from the primary fault trace. Secondary faults that generated local damage included synthetic thrusts, backthrusts, and normal faults (bending-moment faults). Away from the main trace, reinforced-concrete structures, such as swimming pools and large building foundations, were tilted and intersected by small secondary faults (bending-moment faults and synthetic and antithetic thrust faults), but did not sustain significant damage.
- The zone of hanging-wall deformation contained extensive areas between surface traces where deformation was limited to uplift and minor tilting of the near-surface deposits. Building damage in these areas generally was limited to the effects of strong ground shaking.
- Faults commonly were deflected around large reinforced-concrete structures founded on weak, unconsolidated deposits.
- The location and style of deformation from the 1999 Chi-Chi earthquake generally replicated the deformation produced during previous surface-faulting events, as manifested in the geomorphology, stratigraphy, and near-surface geology.

Figure 2.6-83 shows a comparison of faulting near the Humboldt Bay ISFSI site with the style of faulting observed along the 1999 surface rupture on the Chelungpu fault. The ISFSI site is situated near the center of a wedge-shaped block approximately midway between, and about 150 meters from, a synthetic thrust fault (the Buhne Point fault) and an antithetic backthrust (the Discharge Canal fault) on the hanging wall of the Little Salmon fault zone (Bay Entrance fault trace) (Figures 2.6-31 and 2.6-83, item a). The closest primary fault trace, the Bay Entrance fault, is about 500 meters west of the site. Tilted, but otherwise undeformed, late Pleistocene sediments underlie the site. By analogy to the Chelungpu fault (Figures 2.6-83, item b through d), one might expect slip on the Buhne Point and Discharge Canal faults in response to a moderate- to large-magnitude surface-faulting event on the Little Salmon fault zone. However, the ISFSI

site is on the part of the hanging wall where only some uplift and minor tilting (less than 1 degree) is expected.

2.6.8.7 Summary Of Surface-Faulting Potential At The Site

- During at least the past 83,000 years (the minimum age of the Buhne Point terrace), multiple displacements (tens to hundreds of events) on the Little Salmon fault zone have uplifted the hanging-wall block between the Buhne Point fault and the Discharge Canal backthrust and have tilted the Buhne Point terrace a total of 2 to 4 degrees to the southeast. The present terrace surface reflects cumulative tilting; any one event represents a small fraction of the total. The long history (> 83,000 years) of recurrent faulting in localized areas indicates that future displacements likely will recur on and be restricted to the Buhne Point and Discharge Canal faults.
- The Bay Entrance, Buhne Point, and Discharge Canal faults have been the locus of repeated displacement events during the late Quaternary. The total vertical displacement of the Unit F clay across these faults is about 270 meters, 6 to 9, and 3 meters, respectively. The Buhne Point terrace has been uplifted more than 20 meters. Repeated faulting events have produced a zone of fractures and small faults in the hanging wall that is concentrated near (within 100 to 150 meters of) the projected surface trace of the Buhne Point fault.
- Detailed mapping of trenches at the ISFSI site provide direct evidence for no surface faulting at or within 30 meters of the ISFSI site with a very high degree of resolution (millimeters to a few centimeters). The late Pleistocene strata beneath the site have not been faulted during at least the past 83,000 years, and there are no abrupt changes in the dip of those late Pleistocene strata that would indicate the presence of a hinge line or shallow fault bend fold at or near the site. Therefore, no new faults are expected to form at the site during future surface-faulting events on the Little Salmon fault zone.
- The style of faulting near the ISFSI site is similar to well-documented examples of active thrust faults elsewhere in the Humboldt Bay region, and to the 1999 thrust-faulting earthquake in Taiwan. Detailed fault mapping and paleoseismic studies demonstrate that the pattern of faulting associated with these thrust faults is replicated during successive surface-faulting events. Therefore, the potential for surface faulting (including the potential for secondary faulting and folding) at the Humboldt Bay ISFSI site, where the Quaternary stratigraphic record spans numerous earthquake cycles, can be assessed with a very high degree of confidence.

- One cannot preclude the possibility that fractures and small displacements may occur in the foundation materials beneath the ISFSI site during future earthquakes (i.e., less than about 2 centimeters, which is the limit of resolution of trench-wall mapping at the ISFSI site). However, such small displacements do not constitute a significant hazard. For example, reinforced-concrete structures, such as swimming pools and large building foundations, on the hanging wall of the Chelungpu fault were tilted and intersected by small secondary faults (bending-moment faults and synthetic and antithetic reverse faults) without sustaining any significant damage. This experience demonstrates that the ISFSI's reinforced foundation can be designed and constructed to resist minor surface displacements from secondary faulting and tilting, similar to that observed along the Chelungpu fault in Taiwan and on the Little Salmon fault at College of the Redwoods.

The structure and style of deformation at and near the ISFSI site indicate that future activity on the Little Salmon fault zone will not produce surface faulting at the site. Fault displacement along the Buhne Point fault southwest of the ISFSI site probably will result in small amounts of slip on many conjugate faults, and perhaps additional small displacements within the existing zone of conjugate faulting on the hanging wall near the primary trace of the Buhne Point fault. Minor displacements also may accrue on the backthrust northeast of the site (the Discharge Canal fault). The terrace underlying the site can be expected to be elevated up to a few meters during future faulting events on the Little Salmon fault zone, but the angle of tilt is not likely to change much, if at all (less than 1 degree), and no significant secondary faults are expected to form in the hanging wall that passes through the ISFSI site. The possibility cannot be precluded that small fractures and faults having as much as about 2 centimeters of vertical displacement may occur in the strata that underlie the site during future great earthquakes along the Little Salmon fault zone, but these are not considered to pose a significant hazard. Based on this analysis of the geologic data, surface fault rupture does not pose a hazard to the Humboldt Bay ISFSI site.

2.6.9 PROBABLE MAXIMUM TSUNAMI FLOODING

2.6.9.1 Introduction

Tsunami hazards along the coast of northern California have been recognized for many decades. The tsunami associated with the 1964 Alaska earthquake was very destructive in Crescent City, and caused minor runups within Humboldt Bay (Figure 2.6-1). Following this event, at the request of the Atomic Energy Commission, PG&E prepared a report that reviewed the historic occurrence of far-field tsunamis in northern California, the exposure of the HBPP site to past tsunamis, and estimated the likelihood of future tsunami flooding at the site (Reference 210).

During the past 15 years, tsunami hazards along the coast of northern California have received increased attention by scientists, engineers, and public safety agencies because of new findings and interpretations of the tsunamigenic potential of the Cascadia subduction zone, (The reference is to rupture of a large part or the entire

1,100-kilometer long Cascadia subduction zone. For the tsunami evaluation, tsunami generation from rupture of short segments (less than 100 km long) at the south end of the subduction zone, or segments less than several hundred km long at the northern part of the zone is not important. Although earthquakes on the Petrolia or Eel River segments may cause small tsunamis, it is rupture of a long segment of the Cascadia subduction zone that has the potential to produce the large tsunamis that are being considered in this section.) and their implications for near-field tsunami generation (References 57, 58, 211-214). This section first summarizes the recent tsunami history of Humboldt Bay, and then present the results of current geologic studies of prehistoric tsunamis (paleotsunamis) along the northern California coast, including Humboldt Bay. Finally, a review is made for several analytic estimates of tsunami inundation at Humboldt Bay and in the vicinity of the ISFSI site, which are compared to those estimates with the geologic estimates of past tsunami flooding in the region.

2.6.9.2 Definition of Tsunamis

A tsunami is a gravitational sea wave or swell, or train of waves or swells produced by any large-scale, short-duration, disturbance of the ocean floor. Such disturbances are often due to sudden vertical displacement of the sea floor during an earthquake, but are also caused by submarine landslides (Figure 2.6-84) or, less commonly, by explosive volcanic activity or subaerial landslides (Reference 215). A local tsunami is one that originated at or near the coast that is inundated by the tsunami. A distant tsunami is one that originates beyond the felt limits of the causative earthquake, sometimes from across the ocean. In the deep open ocean tsunami waves are characterized by great speed of propagation (more than 400 mi./hr), long wave length (more than 500 mi.), long period (varying from 5 minutes to a few hours, but typically 10 to 60 minutes), and low observable wave height or amplitude. When tsunamis enter shallow coastal waters the wave slows, wave length decreases, and amplitude increases. Due to the long length of the waves in the open ocean, the sea surface slopes so gently the waves can pass unnoticed, then appear as destructively high waves in shallow coastal waters (Reference 216). The waves are not sinusoidal, but have irregular shapes, best illustrated by the detailed record of the 1964 tsunami at Women's Bay, Kodiak Island, Alaska. There the highest wave was the fifth to arrive; it rose to 19 feet above the post earthquake datum (MLLW), but receded to approximately 30 feet below the datum (Reference 217).

As indicated in the definition, tsunamis have several origins. A seismic sea wave is a long-period tsunami that is caused by displacement of the sea floor during an earthquake; it may propagate hundreds to thousands of miles across oceans. A tsunamigenic earthquake is any earthquake that generates a tsunami. A landslide-generated tsunami is caused by a submarine landslide or a coastal landslide, commonly triggered by an earthquake, entering the ocean. Typically, landslide-generated tsunamis have locally high runups on the nearby shores, higher than the runups elsewhere from the associated seismic sea wave.

Tsunami runup or wave inundation is the horizontal component of the slope distance traveled by the onshore surge, as measured from the shoreline (Figure 2.6-85). Tsunami runup height at a particular location is the vertical component of the slope

HUMBOLDT BAY ISFSI FSAR UPDATE

distance traveled by the surge. The runup height from tsunamis is dependent upon several factors: the characteristics of the tsunami itself, the submarine topography offshore, the topography onshore, coseismic elevation changes of the shoreline, and the tidal stage at the time of tsunami arrival. Runup height may be referenced to mean sea level (MSL), which is the reference “0” elevation for most surface maps, including the U. S. Geological Survey maps. However, field investigations following tsunami events commonly use field characteristics that are then related to elevation. For example, mean sea level is recognizable in the intertidal zone because it approximately corresponds to the upper limit of barnacle and seaweed growth. Another measure is the “extreme high tide shoreline”, which is marked by the highest tidal debris and the seaward limit of terrestrial vegetation. This shoreline is a little higher than the common tidal measure of mean higher high water (MHHW) that is the mean of the higher of the two daily high tides, as measured over a period of time (usually 19 years). Similarly the tidal measure of mean lower low water (MLLW) is the mean of the lower of the two daily low tides. These means are not the highest nor the lowest tides recorded at a site.

Mean lower low water historically has been the reference elevation for bathymetry and topography at the HBPP and, hence is selected for use in the analysis of the ISFSI site. For consistency, unless otherwise noted, all elevation measurements in this section are referenced to mean lower low water, which is set at 0 in this evaluation. At the Coast Guard Station on Humboldt Bay at the southern end of the North Spit (40°46.0 N; 124°13.0 W) mean sea level is at 3.7 feet and the tidal range between MLLW and MHHW is 6.9 feet (Reference 218). The highest reported tide above mean lower low water measured in the plant site vicinity since 1920 is 12.5 feet (Reference 219). Waves from tectonic sea-floor displacements have produced runups as high as 50 feet or so (Reference 65, Appendix 9A), and can cause much damage along the exposed coast near the source. Wave runup heights from some submarine landslides have been much greater, for example, 170 feet in Prince William Sound, Alaska in 1964 (Reference 65, Appendix 9A), but have been restricted to relatively short reaches of the coast near their origin. Lander and others (Reference 220) conclude that most local tsunamis following earthquakes along the west coast of the United States since 1812 have involved submarine landsliding. Similarly, Plafker (Reference 65, Appendix 9A) considers that landslide-generated waves are more common than generally is recognized in studies of historic tsunamis, particularly many of the older ones that were not investigated in detail.

Based on eyewitness reports and tide-gauge recordings at the coast, large tectonically-generated tsunamis commonly begin with gradual withdrawal of the sea, which exposes the seabed in front of the shore, in some places for a thousand feet or more. Some tsunamis have been observed to begin with a rise of water level followed by drawdown of the sea (Figure 2.6-86). The arrival of a tsunami wave crest at the coast is usually preceded by a steady rise of the sea, like a flood tide, but much more rapid. As the wave crest approaches the coast, it may or may not form a breaking wave front as it spills across the beach and floods inland. When the crest reaches the coast the water level commonly remains high for some minutes before receding. Tsunamis characteristically consist of wave trains that produce several successive episodes of rising water level that inundate the coast, with intervening withdrawal that exposes the sea floor. The first wave is often smaller than later waves.

Tsunamis can transport near-shore and beach sand, gravel, woody debris, marine life, vegetation, and man-made objects well inland from the normal high-tide line. They can alter natural geologic conditions significantly, and can damage or destroy man-made structures. In remote areas, and in the case of prehistoric tsunamis, the damage and deposits of sand, gravel, and woody debris may be the only evidence of a tsunami inundation.

2.6.9.3 Historical Tsunamis in the Humboldt Bay Area

A detailed catalog of tsunamis affecting the west coast of the United States since 1806 was prepared by Lander and others (Reference 220), which is considered the most current and most detailed compilation available. The authors of this catalog used earlier national and international compilations, including the 1965 study by Professor R. L. Wiegel, which was the basis of the PG&E (Reference 210) report to the Atomic Energy Commission. Lander and others (Reference 220) augmented the data base by review of contemporary newspapers and other original and derivative literature, including tide-gauge records.

Lander and others (Reference 220) evaluated the validity of each of the tsunami reports using a scale ranging from “0 - not a valid tsunami report,” to “3 - probably a valid report,” and “4 - certainly a valid report.” They noted that some waves reported as tsunamis might have been caused by meteorological conditions (very low air pressure during a storm) or unusually high astronomical tides. They felt validity 3 and 4 tsunami reports could be used “with a fair degree of confidence” (p. 12).

The catalog is separated into local tsunamis and distant tsunamis. For the U.S. west coast, Lander and others (Reference 220) rate 18 local tsunamis as validity 3 or 4. Only one of these reports was a tsunami whose origin was from the coast between Cape Mendocino and the Oregon border; it is associated with the April 25, 1992, Petrolia earthquake, a shallow thrust event of magnitude 7.1, interpreted to be a subduction zone earthquake (Figure 2.6-96) (Reference 14; Section 2.6.22). The earthquake caused uplift of up to 4.6 feet at the adjacent coast (Reference 64); this uplift of the sea-floor is interpreted to have generated the small tsunami observed as far away as Crescent City, where the tidal gauge measured the maximum wave height at 3.9 feet. A maximum runup height of 3 feet was reported north of Humboldt Bay at Trinidad. At the Coast Guard Station inside Humboldt Bay at the North Spit (Figure 2.6-87), the maximum-recorded wave height was 3.1 feet (Reference 220).

No historic accounts are known of storm surges (a tide-like rise of water driven ashore by strong sustained wind and usually accompanied by a rising tide) across the Humboldt Bay spits, but storm waves have over-topped the South Spit on various occasions. These include the 1997-98 El Nino winter, which had very large storm waves that accompanied about a 1.5 foot increase in sea level relative to normal. These overtopping waves did not modify the overall spit morphology or lower its height, but rather drained down the bay side of the spit locally, as passive, gravity-driven sheet wash, or as weakly channeled flow where the spit crest was already relatively low. These overtopping waves may have transported some sand into the bay, to form local

HUMBOLDT BAY ISFSI FSAR UPDATE

sand deposits along the shoreline on the bay side of the spit. These deposits are not similar to the widespread sand sheets on eroded marsh surfaces found in the paleo-marsh stratigraphy at the southwest corner of the bay.

Lander and others (Reference 220) list 47 distant tsunamis having validity 3 or 4, based on tide-gauge data. Only 15 of these were directly observed on the west coast, suggesting the other 32 were rather small. Only seven distant tsunamis caused damage; the 1964 Alaska earthquake tsunami was the most severe. Of the seven, only events in 1964 and 1960 were observed at Humboldt Bay. The 1946 event was reported at Crescent City, but not at Humboldt Bay. Information on the 1964, 1960, and 1946 events follows.

28 March 1964, Prince William Sound, Alaska, magnitude 9.2 - The tsunami from this earthquake arrived at Humboldt Bay at high tide (Reference 220). Although there was no tide gauge in the bay at the time, the U.S. Army, Engineer District, San Francisco, compiled visual observations of maximum wave elevations at three points inside the bay and at four locations along the northern California coast.

PG&E personnel made the two observations at the HBPP. These data are presented in Table 2.6-22, taken from PG&E (Reference 210). Sites within Humboldt Bay were somewhat protected from tsunami effects compared to points on the open coast. Nonetheless, "The Eureka Boat Basin suffered little damage, but the water rose over the 10-foot sea wall and flowed 8 feet into the street at the height of the rise. The tide was 6 feet. The bay was filled with logs and debris. Half of the sea and channel markers were moved off their stations by the surge" (Reference 220, p. 107). The tsunami in Humboldt Bay was attenuated by a factor of 3 to 5 compared to Crescent City.

22 May 1960, South-central Chile, magnitude 9.5 - Noted by Lander and others (Reference 220) as the most damaging tsunami recorded anywhere in the world, the effects in Humboldt Bay were limited to reported strong currents at the bay entrance and the Eureka small-boat harbor. No damage was observed. For comparison, the run-up height of 12.5 feet (7.4 feet above the predicted tide) was reported at Crescent City, where extensive flooding and some damage occurred.

1 April 1946, Aleutian Islands, magnitude 7.4 - This earthquake resulted in the creation of the Pacific Tsunami Warning Service, due to its spectacular destructiveness in Hilo, Hawaii. Although a 3-foot wave was reported in Crescent City, and some damage was reported at Fort Bragg and to the south, the Humboldt County coast was "virtually untouched" (Reference 220).

There are no other reports of known tsunami effects in Humboldt Bay mentioned either by Professor Wiegel (Reference 210) or Lander and others (Reference 220). Other major Pacific Rim earthquakes (magnitude 8.0 or larger) occurred in Peru, Chile, Japan, Kamchatka, and the Aleutian Islands during the past 150 years of reporting. Runups above tide level ranging from about 4 inches to as much as 4.7 feet (from the November 4, 1952, Kamchatka earthquake and tsunami) were reported at Crescent

City due to these earthquakes, but there were no reports of these tsunamis at Humboldt Bay.

As Professor Wiegel noted (Reference 210, page 6), “There is little information available on tsunamis within Humboldt Bay.” This is the case because distant tsunamis from great Pacific Rim earthquakes usually are too small at the Humboldt Bay coast to create noticeable effects inside the bay. Lander and others (Reference 220, p. 23) note that the orientation of the eastern Aleutian source region and its optimal propagation direction to northern California and the Pacific Northwest suggest the 1964 Alaska earthquake “probably represents the maximum possible” distant tsunami to affect this region.

2.6.9.4 Geologic Study Of Past Tsunamis Along The Northern California Coast

As noted in Section 2.6.22, the geologic record of tsunamis for the past several thousand years along the coasts of Oregon and Washington has contributed to the identification of the earthquake potential of the Cascadia subduction zone (Reference 35). Beginning in 1996, PG&E initiated a program of similar investigations along the northern California coast opposite the southern end of the Cascadia subduction zone (Figure 2.6-88). This project was carried out by Gary A. Carver, Professor Emeritus of Geology at Humboldt State University, and three of his graduate students, and was completed in late 1998 (Reference 222-225). The results of this work are summarized in this section.

The PG&E-supported tsunami investigation had several objectives:

- Evaluate the Cascadia subduction zone and other possible sources that could generate local tsunamis large enough to potentially cause damage along the coast near Humboldt Bay
- Document the timing of prehistoric tsunamis along the coast of northern California
- Estimate the heights of the runups of past tsunamis
- Evaluate whether or not past tsunamis entered Humboldt Bay, and if they did, whether they reached the proposed ISFSI site

2.6.9.4.1 Characteristics of Tsunami Deposits

Although geologic evidence of tsunami inundation can take many forms, the most enduring evidence is stratigraphic. Hence, the studies for PG&E focused on stratigraphic, sedimentologic, and paleontologic evidence of tsunamis preserved in intertidal bay marshes (Figure 2.6-89) and coastal freshwater marshes and ponds (Figure 2.6-90) and stratigraphic evidence in coastal sand dunes. Shallow freshwater marshes and ponds are very low energy depositional environments that accumulate organic-rich sediments at relatively slow rates. Continuously submerged beneath

HUMBOLDT BAY ISFSI FSAR UPDATE

shallow, anoxic water, these sediments are typically undisturbed, and even fine details of the stratigraphy are commonly well preserved. Intertidal marshes are low- to moderate-energy depositional environments where finely bedded muddy and peaty sediments are preserved - relatively undisturbed.

In contrast, tsunami deposits are high-energy, clastic sediments, typified as layers of sand and deposits of mixed mud, peat, and exotic debris. Where coastal marshes and ponds are in the runup zone of a tsunami, they are excellent traps for accumulating and preserving these high-energy sandy sediments transported by the landward surge of marine water. Tsunami deposits are easily recognized in the otherwise quiet-water, peaty, and muddy marsh sediments. Where tsunamis inundate freshwater ponds or marshes, post-tsunami deposits often reflect tsunami disturbance to the adjacent area that drains into the pond or marsh as a change from predominately peaty sediments below the tsunami layer to muddy deposits immediately above the tsunami horizon. Sedimentary features that reflect turbulence associated with the rapid landward surge of the tsunami, such as rip-up clasts, vegetation “flopovers”, and erosional unconformities, followed by quiet water deposition when the wave crest reaches the shoreline, typified by graded bedding, also characterize tsunami deposits (Figures 2.6-89, 2.6-90, 2.6-91).

Sedimentologic and stratigraphic evidence of tsunami runup has been described for such deposits in freshwater marshes and ponds in Washington and Oregon and on western Vancouver Island (References 35, 221, 226-230). These authors have interpreted these deposits to have originated from large tsunamis caused by earthquakes on the Cascadia subduction zone. The PG&E investigations found similar deposits in the freshwater marshes and ponds on the northern California coast. The characteristics of these deposits are used to assess whether they were deposited by tsunamis or by other processes.

Sand layers can be introduced into marshes and ponds by several processes other than tsunamis, including storm waves and storm surges, wind, streams, and unchanneled surface runoff. However, sedimentologic characteristics of the sand layers generated by tsunamis differ from sand layers deposited by other processes. The following characteristics were used to establish a tsunami origin for sand layers interbedded with marsh deposits in Northern California:

- Landward thinning and fining of the sand layers indicate that the water flow transporting the sand lost energy in the landward direction, and was therefore moving inland. Landward transport of coarse, angular particles derived from local sources, such as minor landslides into the marsh, shows the surges were moving in the inland direction, as well.
- The presence of marine diatoms in onshore sand layers shows they were deposited from a flow of ocean water. A diatom is a microscopic, single-celled plant that grows in both marine and fresh water. Diatoms secrete shells of silica, called frustules, which are deposited and preserved in sediments. Frustules from diatoms living in freshwater marshes, salt-water marshes, tidal flats, and the offshore ocean are easily differentiated;

HUMBOLDT BAY ISFSI FSAR UPDATE

thus, the diatoms contained in sediment are indicative of the source of water that transported and deposited the sediment.

- An energetic depositional mode is manifested by several physical characteristics of the sand layers. Eroded basal contacts and rip-up fragments of local marsh sediments incorporated in the sand demonstrate the inundating surges had enough energy to pluck chunks of peat and mud from the substrate. Large numbers of broken diatom frustules suggest a high degree of turbulence, with grains crashing against each other.
- Where the coastal topography is low lying, tsunami sand layers commonly extend far inland, more than a kilometer at some places in northern California. The sand layers gradually thin landward and are very well sorted and normally graded indicating the sand was deposited from suspension. This implies the water maintained enough velocity to carry sand-sized particles in suspension far inland and deposition occurred as the tsunami surge stopped. The absence of cross bedding indicates the sand was not continually reworked by wave action, as would be expected for sand deposited by storm waves. Grain-size distributions, diatoms, and sand-layer lithologies that match those found on the adjacent beach demonstrate the source of the sand was the beach.
- Multiple, normally graded beds within the same sand sheet show that the disturbance event included multiple distinct surges that each deposited a separate normally graded bed of sand from suspension. In some places, the stems or leaves of fragile marsh plants growing on the depositional surface are preserved entombed upright in sand deposited during the earliest one or two pulses, only to be "flopped over" and buried by sand from a stronger later pulse. Silt partings between layers provide evidence for quiet-water deposition from very turbid water between episodes of high-energy sand transport and deposition from suspension. These interpretations are consistent with inundation during multiple surges typical of a local tsunami.
- The presence of woody debris and forest litter capping sand layers suggests the surges flowed into forests on the fringes of the marsh and forest debris was carried back to the marsh as the water receded. This detrital material is typically concentrated in a "trash layer" with mixed mud, peat, and sand at the top of the sand layers. Woody debris is a common component of historic tsunami deposits (Reference 231).
- Coincidence of characteristic sand layers with other evidence of local earthquakes also forms a strong argument for tsunami deposition. Subsidence during subduction zone earthquakes can leave distinctive traces in coastal marsh stratigraphy (Reference 35). Salt-marsh peat and subaerial soil form near and above the high tide level and after they have rapidly subsided into the intertidal zone during subduction earthquakes,

they are commonly preserved as buried peat layers having gradational lower contacts and sharp upper contacts with intertidal mud. The presence of high-marsh or freshwater diatoms in peat or soils underlying mud containing intertidal diatoms strengthens the argument for coseismic subsidence. A sand layer having sedimentologic characteristics of tsunami deposition that mantles the buried marsh surface is most likely a tsunami deposit. A sand layer that directly mantles a landslide deposit in a coastal marsh sequence suggests the sand was deposited by a tsunami, and that the landslide was triggered by the same earthquake that caused the tsunami. In marshes that do not have evidence of subsidence, frequently the sediments immediately above the sand layer commonly contain detrital wood and higher mud content. This "post-tsunami disturbance pattern" is interpreted to represent the increased clastic sedimentation from the disturbed area around the marsh following the tsunami.

2.6.9.4.2 Methods Used for Tsunami Investigation

The methods used for the PG&E tsunami investigation included gouge coring, the collection of vibracores, radiocarbon dating, diatom identification, and grain-size analysis.

Gouge Coring - Gouge cores were collected from marsh and bay sediments to assess the stratigraphy of sites likely to contain sedimentary evidence of past tsunamis along the northern California coast. Gouge coring was the technique used for reconnaissance investigations, because this type of sample collection can be done rapidly with easily used, highly portable equipment. A gouge corer is a 1-inch-diameter, half-cylinder steel core barrel 1 meter long attached to threaded rod sections. The core barrel is pushed into the subsurface by hand (Figure 2.6-92). The resulting sample is slightly less than 1 inch in diameter and usually is slightly disturbed, but it is adequate to assess the stratigraphy and allow identification of sand layers that may represent tsunami deposits (Figure 2.6-93). The gouge coring technique has the advantages of allowing examination of the sample in the field, and the rapid collection and assessment of many samples in a short time. The disadvantages of using this type of corer are a very small sample volume, some distortion and disturbance of the sample during collection, and a maximum sample length of about 1 meter, requiring multiple overlapping cores to sample stratigraphic sections deeper than 1 meter.

Vibracores - Vibracores were collected at sites where the gouge coring showed that detailed studies of paleotsunami deposits would be fruitful. Vibracores are 3-inch diameter, nearly undisturbed samples of sediment collected in full-cylinder core tubes. The core tube (thin-walled aluminum pipe) is driven into the sediments using the vibratory motion of an attached power head (Figure 2.6-94). The cores are continuous to lengths of up to about 5 meters, and of relatively large volume, providing larger samples for sedimentologic and radiometric analysis. Forty-four vibracores were collected and analyzed from three sites: 13 from Crescent City, 21 from Lagoon Creek, and 10 from South Bay. In addition at Crescent City and Orick, drive cores (vibracore sampling tubes driven into the sediments using a sledgehammer) were collected and

HUMBOLDT BAY ISFSI FSAR UPDATE

analyzed, one from Crescent City, and two from Orick (Figure 2.6-95). Both vibracores and drive cores produce high-quality sediment samples. The disadvantages of vibracoring include the large size and weight of the apparatus, which make it difficult to use, and restricts the number of cores that can be collected. Additionally the aluminum casing used to collect a vibracore sample must be cut with a saw to expose the sample, making it impractical to examine the cores in the field.

Radiocarbon Dating - Radiocarbon ages for tsunami deposits were obtained for 46 samples from 5 sites along the northern California coast. Forty-two of the samples were from three sites: Crescent City (13 samples), Lagoon Creek (19 samples), and South Bay (10 samples). Carbon-14 ages for three samples from the dune complex on the North Spit of Humboldt Bay and one sample from the Orick marsh also were obtained during this study. At Lagoon Creek, the presence of the well-dated Little Glass Mountain tephra in the marsh stratigraphy provided additional age control for the tsunami record.

Most (38) samples were analyzed using accelerator mass spectrometry methods on carefully selected small twigs and herbaceous plant parts, and small pieces of detrital wood, charcoal, and spruce cones that were in stratigraphic context with the tsunami sands. Most of the wood and charcoal samples were from tsunami sand layers or trash layers capping sands. Peat samples and herbaceous plant parts were collected from the uppermost peat layers immediately below the sand layers. Seven large wood and peat samples were analyzed by standard radiometric methods.

Radiocarbon analyses for this study were performed by Beta Analytic, Incorporated. The laboratory's carbon-14 ages were calibrated using a carbon-13 correction, and the calibration program of Stuiver and Reimer (Reference 53), using a lab error multiplier of 1.6. The ages reflect the 95-percent confidence level (2 sigma), and are reported as calibrated radiocarbon years before present, which, by convention, are calendar years before AD 1950.

Diatom Identification - Diatom samples were processed by treating the sediment with 35-percent hydrogen peroxide solution to remove organic material. The sample was rinsed, and a slurry was prepared using distilled water. A two-drop sample of the slurry was settled onto a coverslip, and the sample on the coverslip air-dried. Permanent slides were prepared by mounting the sample with a fixative on microscope slides. These slides were examined using a deep-field zoom microscope at 400X to 1000X, as necessary for identifications.

Grain-size Analysis - Sand samples were analyzed for grain-size distribution to characterize the textures and measure the grain size for modeling the flow parameters during deposition. Sand samples were wet-sieved in a 0.062-millimeter microsieve. The sand fraction was treated with a 30-percent hydrogen peroxide solution to remove organic material, and oven-dried. The dried samples were mechanically screened through selected phi-size microsieve columns, and the size fractions weighed.

Runup Heights - At most locations in northern California where field evidence of paleotsunami inundation was found no surveyed elevation datum was available for elevation reference. Field measurements of heights of marshes, beach berms, pebble

layers in the dunes, tsunami sand layers, and other indicators used to indicate or calculate runup height were made by measuring the vertical distance to the tsunami indicators from debris deposited by previous high tides in sheltered locations on the adjacent shoreline. The high tide line debris is assumed to approximate mean higher high water (MHHW). These values in this report are adjusted to mean lower low water (MLLW) by adding 7 feet (the mean tide range for the northern California coast) to the field measurements.

2.6.9.4.3 Evidence for Past Tsunamis in Northern California

Stratigraphic evidence of past tsunamis - thin sand sheets and associated marine diatoms and other diagnostic features - is abundant in bays, lakes, and marshes along the Pacific Coast in Oregon, Washington, and on western Vancouver Island. The current investigations have focused on finding and assessing similar geologic evidence of large historical and prehistoric tsunamis in the coastal wetlands between Cape Mendocino and the Oregon/California border. The tsunami investigation included:

- Surveying the wetlands along the northern California coast to identify sites that could act as sediment traps that could potentially record past tsunami inundation.
- Evaluating the marsh stratigraphy near Crescent City, where tsunamis from distant sources are known to have inundated the coast in 1960 and 1964, to establish diagnostic characteristics of these tsunami events, and to search for evidence of previous tsunami inundation.
- Investigating the stratigraphy in freshwater marshes and ponds at Crescent City and Lagoon Creek, where the most complete stratigraphic record of tsunamis appeared to be preserved. At these sites, detailed stratigraphic, sedimentologic, paleontologic, and geochronologic analyses were conducted to assess the late Holocene history of tsunami inundation.
- Investigating the sediments in Humboldt Bay for evidence of past tsunamis. One site, a marsh along the South Spit in southwestern Humboldt Bay (South Bay), contained stratigraphic evidence of past tsunamis and was investigated in detail. Subsequent investigation of southeastern Humboldt Bay by Patton and others (Reference 209) has identified a second site at Hookton Slough that has stratigraphic evidence of paleotsunamis. This site has also been extensively investigated.
- Mapping the spits and dune fields that serve as barriers and partial barriers to tsunamis entering Humboldt Bay to find erosional features and sediments left by past tsunamis. The paleomorphology of the spits was also assessed because it is important to the interpretation of paleotsunami evidence in the bay.

HUMBOLDT BAY ISFSI FSAR UPDATE

- Assessing the height of past tsunami waves from the evidence of past tsunami runup and the sediment characteristics of the tsunami deposits.
- Studying the local Native American oral histories, which include stories interpreted to describe ancient earthquakes and flooding by tsunamis on the northern coast of California prior to the arrival of white settlers in the 1850s.
- Reviewing the empirical data on tsunami runups elsewhere in the world and correlating the data with earthquake source parameters, triggered landslides, and secondary faulting (Reference 65, Appendix 9A).

Evidence for tsunami inundation was found in the stratigraphy at nine of the sixteen sites surveyed (Figure 2.6-88): eight of the fifteen coastal marsh sites (Table 2.6-23) and one site in the dunes of the North Spit. The marsh sites at Crescent City and Lagoon Creek provide the most compelling evidence for tsunami inundation and were studied in greatest detail. Strong evidence of paleotsunamis was also found at Orick and in the South Bay; these sites were also carefully studied. Evidence of for past tsunamis was also found at marsh sites at East Creek, Major Creek, and Big Lagoon but initial investigation indicated the information from these sites was limited and they were not studied in detail. A summary of the types of evidence of past tsunami inundation at each of the coastal marsh sites is presented in Table 2.6-23. Evidence of paleotsunamis is also evident in the sand dunes on the North Spit. No evidence of past tsunami inundation was found at High Prairie Creek, or at six sites investigated around the north and east sides of Humboldt Bay.

The stratigraphic position and radiocarbon ages for the major tsunami layers in the northern California marshes are very similar in stratigraphic position and radiocarbon ages to Cascadia subduction zone earthquakes derived from coastal deposits from British Columbia to California (References 35, 49, 52, 108, 230, and 232). Therefore, a one-to-one correlation is assumed, and uses the event nomenclature of Atwater and Hemphill-Haley (Reference 49) for the tsunami horizons at northern California marshes (Figure 2.6-96; Table 2.6-24).

Crescent City - The marsh at Crescent City, which lies behind a wide beach and low beach berm, was investigated for historic and paleotsunami deposits by Carver and others (Reference 222) (Figure 2.6-97; 2.6-98 and 2.6-99). Radiocarbon ages for samples at the base of the marsh sediments at Crescent City show the marsh was formed about 3,000 years ago. Two types of sand layers are present: thin sand layers limited to the seaward part of the marsh and interpreted as deposits from distant-source tsunamis (or from small regional tsunamis generated by sources other than a long rupture of the Cascadia subduction zone); and thick sand layers that can be traced across the marsh to the inland edge, interpreted to have been deposited by local tsunamis generated by long ruptures of the Cascadia subduction zone. Sand deposits from overtopping storm waves were not encountered at the Crescent City marsh site.

HUMBOLDT BAY ISFSI FSAR UPDATE

The stratigraphy at the Crescent City marsh (Figure 2.6-100) contains at least seven sand layers that have the characteristics of far-traveled tsunamis. The 1960 tsunami that originated from the Chilean earthquake and the 1964 tsunami from the Alaskan earthquake deposited the upper two of these sand layers. These tsunamis were generated by the two largest earthquakes of the past century. The earthquakes were near maximum for the Pacific region, and the 1964 earthquake had an optimum wave path to northern California; thus, they probably represent the maximum size for far-traveled tsunamis (Reference 220). This is the only place along the southern Cascadia margin where sand deposited by these well-documented modern tsunamis can be compared with paleotsunami sands at the same site, thus allowing direct comparison of geologic deposits and historical observations. At least five similar prehistoric sands were found in the seaward part of the marsh stratigraphy. These also are interpreted to represent the stratigraphic evidence of tsunamis from distant sources, similar to the Chilean and Alaskan tsunamis. It is likely that many more far-traveled tsunamis reached this site but the evidence is not preserved.

At least five thick, extensive, sand layers are preserved in the stratigraphy at Crescent City. These possess most of the characteristics of tsunami deposition and are interpreted to have originated from local Cascadia subduction zone events (Figure 2.6 100). Each of these sand layers uncomfortably overlies older marsh sediments and reflects tsunami erosion of the seaward part of the marsh. Several show - excellent examples of multiple graded beds from repeated wave inundation indicative of a typical local tsunami wave train (Figure 2.6-90).

Lagoon Creek - The Lagoon Creek marsh (Figures 2.6-101; 2.6-102 and 2.6-98) is a freshwater pond and marsh situated 17 feet above mean lower low water in a narrow valley behind a 23-foot-high beach berm (Figure 2.6-104). During the past 3,000 years, the Lagoon Creek site has been relatively stable when compared to sea level. The site appears to have undergone only a small amount of long-term uplift (References 222 and 224) that appears to have matched the eustatic rise in sea level during the late Holocene. The geomorphology of the region around the site suggests the late Holocene tectonic elevation change has been minimal: there are no raised terraces, older dunes or prograding beaches indicating uplift at or near the site. In addition, the beach berm that impounds the shallow pond, which gives the name to Lagoon Creek, appears to have been relatively stable for the past 3000 years because the freshwater marsh sediments have radiocarbon ages for samples near the base of the marsh sediments of that age; this indicates no late Holocene subsidence at the site. Hence, the Lagoon Creek site has experienced rather constant relative sea level during the late Holocene.

During investigations of this favorably situated marsh, several paleotsunami deposits were discovered (References 222-224). Freshwater lacustrine and wetland sediments underlying the marsh include at least eight interbeds of coastal sand that have characteristics of a tsunami origin (Figures 2.6-105, 2.6-106, 2.6-107). Six of the sand layers are thick and widespread; several extend about a mile inland. Most core samples of these sand layers are normally graded, and some of the sand layers consist of several fining-upward sequences. In the seaward part of the marsh, the sands contain ripped-up clasts of marsh sediments. The sands also contain marine diatoms,

including many that are broken, but well preserved. Marine diatoms were found in all the sand layers and, in one layer, the diatoms were traceable in the marsh stratigraphy inland for about one-quarter mile beyond the landward extent of the sand. All the sand layers thin and fine landward and the mineral composition of the sand in the lagoon and marsh stratigraphy is similar to that of the modern beach. Combined, these characteristics indicate the sands at Lagoon Creek were transported from offshore and carried inland across the marsh by landward surges of seawater that eroded the seaward part of the marsh. The sands were rapidly deposited from suspension as a sheet on the marsh surface. Calibrated radiocarbon ages indicate a separate sand layer correlates with each of the most recent six Cascadia subduction zone events based on the earthquake history documented by Atwater and Hemphill-Haley (Reference 49) (Table 2.6-24). These sand layers are interpreted to be deposits from large local tsunamis produced during ruptures on the Cascadia subduction zone.

Two additional thin sand layers, which also appear to be tsunami deposits, were found in several cores from the seaward part of the Lagoon Creek marsh. The upper of the two thin sand layers is above the “Y” layer, and thus less than about 300 years old. The other is between the “Y” and “W” sands. Both are traceable inland only about 1,300 feet from the modern beach berm. These two sand layers could have been deposited by far-traveled tsunamis, or tsunamis generated by local faulting or submarine landsliding offshore, or nearby ruptures on short segments of the Cascadia subduction zone, such as the Eel River segment. These do not have the characteristics of sand deposits from storm waves or storm surges that over topped the berm (Reference 222).

East Creek, Major Creek, Orick, and Big Lagoon - East Creek and Major Creek are adjacent watersheds in the Gold Bluffs Beach State Park (Figure 2.6-88). Their coastal marshes contain sand layers having some characteristics indicative of tsunami deposition (Reference 222). East Creek contains at least two sand layers similar in grain size to the adjacent beach; they have sharp basal and upper contacts and are capped by woody debris. One of these two layers contains marine diatoms, whereas the underlying peat contains only freshwater diatoms. Major Creek contains at least five thin sand layers, one of which possesses the characteristics of a tsunami sand, and is normally graded.

Orick and Big Lagoon are specifically mentioned as having been flooded by the sea in detailed Native American oral histories that depict a great earthquake followed by a tsunami one night long before the arrival of white settlers (References 233-234). The Yurok story, *The Flood*, describes a flood from the ocean inundating a small village near Orick (Orekw) (Figures 2.6-108 and 2.6-109). The stratigraphy in a marsh immediately downhill from the Orekw village site contains three, separate sand layers, two of which lie atop peat containing freshwater diatoms and are overlain by mud having intertidal diatom species (Reference 222). This lithologic and diatom evidence for subsidence, along with several additional sand-layer characteristics (Table 2.6-23) strongly suggests deposition by a local tsunami at this site. The middle layer contains a triplet of fining upward sand layers and has a Carbon 14 date of 180 ± 40 years BP (AD 1665-1950) and is interpreted to be the “Y” event in 1700 AD.

HUMBOLDT BAY ISFSI FSAR UPDATE

Two thin (~1 inch) undated sand layers in gouge cores taken from a freshwater marsh approximately 600 to 1300 feet from the beach at the south end of Big Lagoon may be tsunami deposits as well. This site is also identified as having been flooded in the Yurok story, *The Flood* (References 233-234).

North and South Spits - The North and South spits of Humboldt Bay act as barriers that partially block tsunamis from entering the bay (Figure 2.6-110, 2.6-1, 2.6-87, 2.6-111, and 2.6-112). The spits are covered by extensive dune fields composed exclusively of well-sorted aeolian sand derived from the beaches on the western side of the spits. In addition to sand, sediments in the active littoral and beach zones also include significant components of gravel, pebbles, and cobbles. The cobbles and pebbles extend to an elevation of 38 feet above mean lower low water (Reference 235). Carver (Reference 235) interprets the scattered cobbles and pebbles mantling eroded dunes on the seaward face of the North Spit to have been deposited by landward directed high-velocity surges of water that rose above the level of modern high storm tides (Figure 2.6-113). Stratigraphic position indicates these cobbles and pebbles were deposited after the formation of the oldest dunes about 1,100 years ago and before the formation of the intermediate-age dunes that formed less than 300 years ago.

The dunes on the northern part of the North Spit range from 53 to 72 feet above mean lower low water. These old dunes are tree covered and have a soil with an incipient A/C horizon developed on them. This soil is uneroded above the limit of pebble scatter, which indicates the spit has not been overtopped or eroded by tsunamis or storm waves (Reference 225). In addition, no tsunami deposits are present in marshes at the north end of Humboldt Bay and along the Mad River Slough behind this part of the spit (Section 2.6.9.4.4). These dune features place an upper limit of past tsunami runup height at the coast at Humboldt Bay in the late Holocene.

The height, width, and length of the South Spit (Figure 2.6-111) are considerably less than the North Spit. Geologic evidence suggests the South Spit has been in approximately the same position and at about the same height for the past 1,000 years. Leroy (Reference 225) reports that the average height of the South Spit dunes is about 18 feet above mean lower low water and the maximum south spit dune height is 23 feet above mean lower low water. Morphology of the dunes and degree of soil development on the South Spit are similar to those on the youngest parts of the North Spit, which have been dated at about 300 years old, or younger.

South Bay - One site in the southwestern part of Humboldt Bay, referred to as the South Bay site, is just east of the south end of the South Spit (Figures 2.6-114, 2.6-111, 2.6-112, and 2.6-115). The stratigraphy beneath a weakly developed salt marsh at this site contains distinct evidence for local tsunamis (Reference 222) (Figure 2.6-116). At least two buried peat units capped by sand layers record earthquake-induced subsidence immediately followed by tsunami inundation that eroded the marsh and deposited the sand sheets containing rip-up clasts of marsh peat. Radiocarbon dates indicate the sands were deposited about 1,200 and 300 years ago. These tsunami deposits indicate the South Spit must have been substantially overtopped during these events. One, and possibly two, additional sand layers have several characteristics typical of tsunami deposits, but they are not associated with buried marsh soils. Cores

from this marsh recovered strata that only date back about 2,000 years.

Unconformities within the bay stratigraphy and the presence of sandy tidal channel deposits make correlation of sand layers between cores more difficult at this site than at the other more protected sites.

Non-tsunami sand layers also are present in the sediments at the South Bay site (Reference 222). These sands, deposited as small sandbars on the tidal flats and tidal channel deposits, have cross-bedding, wide ranges in particle size, and other sedimentologic and compositional characteristics that are not typical of tsunami deposits. They are interpreted to be deposited either by storm waves that overtopped the South Spit and washed sand from the spit into the bay margin or by erosion and re-deposition of sandy channel deposits by currents within the bay. No sand deposits that have the characteristics of storm surges were found at the other marsh sites, including Crescent City.

Hookton Slough - The Hookton Slough marsh is at the southeast margin of South Bay about 6 kilometers from South Spit (Figure 2.6-114 and 2.6-112). At this site four buried marsh soils are interpreted to record abrupt subsidence from large earthquakes on the nearby Little Salmon fault, the southern Cascadia subduction zone, or both (References 51 and 209). Diatoms from the buried soils and overlying mud confirm the abrupt subsidence. The three older buried marsh soils are mantled by sand sheets that exhibit characteristics of tsunami origin including multiple normally graded beds and textures similar to the beach and dune sands at the coast. Coseismic subsidence of these soils occurred about 1600, 2150, and 3500 years BP based on radiocarbon ages from delicate detrital plant fossils (Reference 51). Of these the event at 1600 years and possibly the event at 3500 years correlate to Cascadia events "S" and "L". The event at 2150 is a separate event thought to be associated with displacement on the nearby Little Salmon fault. The event also may correlate with a subsidence and tsunami event about 2000 years ago recorded at Sixes Rivers (Reference 52).

2.6.9.4.4 Humboldt Bay Sites Having No Evidence of Past Tsunamis

Sand layers interpreted to be deposits from past tsunamis in Humboldt Bay are restricted to the southwestern and southeastern margins of the South Bay (South Bay and Hookton Slough sites) as described above. No evidence of past tsunamis was found at other sites examined during the investigation of the bay (Figure 2.6-88), including the eastern side of the South Bay, the area near the HBPP, and Arcata Bay including the Mad River Slough (Figure 2.6-87).

On the eastern side of the bay, the stratigraphy at four marshes, the Jacoby Creek marsh, the Eureka Slough marsh, the Railroad site, and marshes in the Humboldt Bay National Wildlife Refuge near the College of the Redwoods (Reference 222) (Figure 2.6-114), were found to contain a buried and subsided soil interpreted to be stratigraphic evidence of the most recent large Cascadia subduction zone earthquake (event "Y"). This buried soil horizon provided a guide to the stratigraphic position of potential evidence of the most recent tsunami generated by a Cascadia earthquake, and allowed assessment of the presence or absence of tsunamigenic sediments correlative with those found at open-ocean sites on the northern California coast. At all

HUMBOLDT BAY ISFSI FSAR UPDATE

four of these sites, the buried soil was directly overlain by well-stratified intertidal mud. The soil/mud contacts were sharp, and had no evidence of scour or erosion, as would be expected if the subsidence had been followed by rapidly flowing water from tsunami inundation. In addition, no sand was observed at the soil/mud contact at any of these sites. Sand might be expected on the contact between the subsided soil and the overlying mud if significant tsunami inundation by water carrying suspended sand had occurred.

Mad River Slough - Evidence for the absence of tsunami-deposited sand is particularly strong at the northern end of Arcata Bay in the area of the Mad River Slough where the marsh stratigraphy has been extensively studied in great detail (References 39 and 236). The uppermost buried soil and its overlying sediment are remarkably well preserved, and at many places include entombed marsh plant assemblages that were growing on the marsh surface at the time the marsh subsided. The above-ground stems and leaves of the fragile marsh plants are buried in their original upright growth position in overlying intertidal mud. The mud is very fine grained, micro-laminated, and the contact between the overlying mud and the underlying peaty marsh soil is very sharp. In outcrop, the contact can be resolved to within a few millimeters. No sand or other evidence of tsunami disturbance has been found along this contact at the many locations where it has been studied. The most likely interpretation of these contact relationships is that no significant tsunami inundation by water carrying suspended sand or with erosive flow occurred in the Mad River Slough area of Arcata Bay following the most recent Cascadia subduction zone earthquake (event “Y”). Contacts of bay mud over salt marsh peat that have carbon-14 dates correlative to Cascadia events “W,” “U,” and “S” also are present in the Mad River Slough area, and these contacts also do not have tsunami sand layers (Reference 39).

HBPP Area - Several sites whose geologic setting make them suitable for assessing the presence or absence of tsunami evidence were investigated near the HBPP and the ISFSI site (Reference 222). These included relict tidal channels and low-lying marshlands a few hundred meters north, east, and southeast of the ISFSI site. Several cores from the tidal channels contained thin sandy layers composed of poorly sorted sandy mud and muddy sand having abundant shell fragments. The sandy layers are thinly laminated. The poor sorting, macrofossil fragment content, and laminated structure of these sandy layers is in contrast to the well-sorted, normally graded and shell-fragment-free character of tsunami-generated sand layers. Interpretation of the sandy layers found in the relict tidal channels were viewed as normal channel lag sediments resulting from tidal current scour and deposition in the channel bottoms. No tsunami sand layers were found in the marsh sediments near the ISFSI site.

Although the absence of diagnostic tsunamigenic sediments along the north and east margins of Humboldt Bay, including the area near the Humboldt Bay ISFSI site, does not prove conclusively that tsunami inundation has not occurred in these areas, the absence of evidence of tsunamis indicates the areas were not significantly affected by the tsunamis that produced the sedimentary record of inundation at open-ocean sites in northern California and along the extreme southern end of the South Bay.

2.6.9.4.5 Correlation of Tsunami Deposits

Comparison of tsunami histories from the Crescent City, Lagoon Creek, Orick, South Bay, and Hookton Slough marshes shows that no single site contains a complete record of all the tsunamis that have inundated the northern California coast during the past several thousand years (dated events are shown on Figure 2.6-96) (Reference 222). The very low lying and exposed Crescent City marsh is the most sensitive of the sites evaluated; it records the relatively low waves from distant-source tsunamis, including sands from the 7.4- and 16-foot-high runups (above predicted tidal level, Table 2.6-22) from the 1960 Chile and 1964 Alaska waves, respectively. However, several large tsunamis that left stratigraphic records at Lagoon Creek and South Bay are not as well preserved as sand sheets in the Crescent City marsh. Instead, erosion during subsequent tsunamis has likely removed these deposits from the marsh stratigraphy (Reference 222). In contrast, Lagoon Creek contains the most complete record of large tsunami inundations, but has only limited evidence from smaller, distant tsunamis. Presumably the higher berm fronting the Lagoon Creek site prevented small runup height waves from entering the marsh, and reduced the flow of the large local tsunamis sufficiently to limit erosional reworking of earlier deposits to the seaward most part of the marsh, allowing better preservation of evidence from large local tsunamis.

The combined tsunami record from Crescent City and Lagoon Creek indicates the presence of an additional major tsunami deposit that is not evident in the Cascadia subduction zone sequence in Washington and northern Oregon (Table 2.6-24). Although some of the calibrated 2-sigma ages of the “W” layer at Crescent City and the “W” layer at Lagoon Creek both overlap (Figure 2.6-96) the “W” event age from Washington, the California layers probably do not correlate with the Washington event. The “W” layer at Crescent City appears to be deposited by a local or distant tsunami about 850 years ago (the mean of the four most likely dates for this deposit) that strongly affected the Crescent City marsh, eroding much of the previous record, including most of the deposits from the ~1,150-year old “W” layer preserved in the Lagoon Creek stratigraphy. The deposit from the Crescent City “W” event in the Lagoon Creek sediments may appear as the small sand deposit in the seaward portion of the Lagoon Creek marsh that lies stratigraphically above the “W” layer and below the “Y” layer there. This deposit could have been caused by an unusually robust far-traveled tsunami, or by submarine landsliding, but it was more likely caused by a tsunami generated by local faulting offshore on the southern part of the Cascadia subduction zone. A tsunami with similar ages is also known from the Sixes River site in southern Oregon (Reference 52) and elsewhere in northern California: possibly from the cores at Orick, from sand sheet overlying a subsided marsh soil in the Eel River Estuary (References 43-44), and may correlate with a similarly dated displacement event on the Little Salmon fault at the Little Salmon site (References 50 and 105) and the Swiss Hall site east of South Bay (Reference 51). It appears that this event only ruptured the southern part (Eel River segment) of the Cascadia subduction zone, or alternatively was the result of a large event on the Little Salmon fault system.

The stratigraphic signature of coseismic subsidence associated with a tsunami deposit is particularly well developed for the “Y” event at Orick, and for the horizons identified in South Bay (Reference 222) and Hookton Slough sites (Reference 209). Coseismic subsidence coincident with the deposition of tsunami sands is indicated by the

HUMBOLDT BAY ISFSI FSAR UPDATE

stratigraphy, sedimentology, diatoms, and macrofossils found at these sites. At these sites tsunami sand dated to the last approximately 300 years and subsequent mud containing lower intertidal marine or brackish-water diatoms overlie the salt marsh and freshwater peaty sediments. Other studies identified subsidence horizons that are correlated to earthquakes on the Cascadia subduction zone at Mad River Slough (References 50, 51, and 236), the South Bay (Reference 85) and possibly coincident with faulting on the Little Salmon fault at the Swiss Hall site east of South Bay (Reference 235). The association of tsunami evidence with evidence for coseismic subsidence indicates the tsunamis were locally generated.

At the Lagoon Creek marsh, a small local landslide deposit derived from distinctive Franciscan Formation lithologies is interbedded in the marsh stratigraphy about one-half mile inland from the coast. Several gouge cores and three vibracores (LC-9, LC-10, and LC-13) sampled the leading edge of this landslide, which came from a conspicuous scar on the steep slope adjacent to the marsh (Reference 222-223). The landslide appears to have been active at least twice, each time a distinctive diamicton was deposited across the marsh surface: once immediately before deposition of sand layer "U," and once immediately before sand layer "S." Each of these sand layers lies directly on the diamicton with no evidence of marsh vegetation or fine grained marsh sediments at the sharp basal contact of the overlying sands. Up-valley both sand layers contain abundant angular clasts of landslide lithologies that were entrained and transported only landward. No other landslide that could have been the source for the distinctive Franciscan material was found in the marsh. It is believed that the seismic shaking triggered the landslides. The entrainment and up-valley redeposition of the slide material in the tsunami sand layers is interpreted to represent the reworking of the slide by rapid up-valley tsunami flow immediately after the slide debris was deposited on the marsh surface. This evidence of strong shaking coincident with tsunami generation re-enforces the interpretation that the large tsunamis found in the paleotsunami record in northern California were locally generated by slip on the subduction zone.

Small sand dikes and sand tubes are intruded into the marsh sediments at Crescent City, Lagoon Creek, and South Bay sites (Reference 222). Most of these intrusive sand bodies have grain sizes and compositions similar to the tsunami sands. They were interpreted to be derived from the tsunami sand layers deeper in the marsh sequence and to have been injected into the overlying marsh deposits when the sand liquefied and vented to the surface due to strong seismic shaking. Many of the dikes and tubes terminate at the top of a buried marsh and are overlain by a separate tsunami sand layer. Strong shaking that produced the sand dikes and tubes indicates that a local earthquake generated the tsunamis.

An interpretation was also made for several types of micro-sedimentary structures and stratigraphic characteristics of the more extensive tsunami sands in northern California marshes at Crescent City, Lagoon Creek, Orick, South Bay, and Hookton Slough to be the result of locally generated tsunamis. In particular, the multiple fining-upward sand sequences, separated by marsh grass "flopovers," and a trash layer capping the sequence are interpreted to be caused by several high-runup inundations that were closely spaced in time. These features are rare or absent from deposits of far-traveled

tsunamis. Such multiple waves are known to be characteristic of large tsunamis on coasts adjacent to tsunami sources elsewhere in the world.

Radiocarbon ages (Dates in this report are all expressed as calibrated radiocarbon years BP (before 1950, considered “present”). Calibrated radiocarbon date is one that indicates that the date is the result of radiocarbon calibration using tree ring data. These values should correspond exactly to normal historical years BC and AD. The term means the number of years before 1950 and can be directly compared to calendar years.) for large tsunami events in northern California are the same, within the precision range of the carbon-14 ages, as the estimates of the rupture chronology for the last six major events on the Cascadia subduction zone recognized on the southern Washington coast (“Y,” “W,” “U,” “S,” “N,” and “L”) (Reference 49) (Table 2.6-21; Figure 2.6-96). In particular the radiocarbon ages at Lagoon Creek for each of the sand layers correlate, at the 2-sigma confidence level, with each of these Cascadia subduction zone events (References 222 and 224).

The most recent major earthquake on the Cascadia subduction zone was the “Y” event that occurred about 300 years ago, as dated by high precision tree-ring series and radiocarbon analysis in Washington that shows the earthquake occurred in the winter of 1699-1700 (Reference 237). Whether several segments ruptured or this was a single very large event was not known until the records of tsunamis in Japan were examined. Historical documents record only one tsunami wave sequence in Japan for the time interval indicated by the carbon-14 and tree-ring analyses. The wave sequence had to have come from a distant source, because it was not associated with an earthquake in Japan. Modeling tsunami propagation from Kamchatka and the Aleutians indicates these are unlikely sources for the wave recorded in Japan. People who would have recorded such an event locally inhabited other circum-Pacific sources but none is reported. Back-calculating from the arrival times recorded for the wave at five locations in Japan, the earthquake that caused the wave occurred about 9:00 PM on January 26, 1700 (Reference 41). This is supported by the Yurok oral history from Orick, and at least six other traditional stories from coastal Indians in northern California and several from Washington and Vancouver Island (Reference 234), that describe the earthquake as happening at night. The reported damage in Japan indicates the tsunami was large. Model studies (References 41 and 136) of segmented and long-rupture Cascadia sources show that only long ruptures generate tsunamis large enough to have produced the damage-causing run-ups observed and recorded in Japan. The interpretation of a single long rupture for the 1700 AD event is supported by the “Y” paleotsunami record in marsh deposits from Vancouver Island to northern California. These marshes have only one sand sheet deposited during the “Y” time interval.

Similarly the tsunami sands that record the five previous major subduction earthquakes from Cascadia have single event deposits (one tsunami sand) indicating that a single robust tsunami was generated by each Cascadia event from Canada to northern California. If Cascadia ruptured as segments closely spaced in time (a cycle of events as each segment ruptured a few tens of years apart) then the paleotsunami record for late Holocene events would record several less robust tsunamis for each cycle, and some or perhaps most sites where tsunami sands were deposited would exhibit several

closely spaced sand sheets of similar age. However, only single sand sheets have been found for each of these major events.

Nonetheless, some sites on the coast between Vancouver Island and Eureka record other, local paleotsunamis in addition to the major event tsunami sands. As discussed earlier the tsunami sand at Crescent City that dates to 800 to 1000 years BP (mean 850 years) is not correlative with the chronology of major events on Cascadia. This event appears also be recorded at Lagoon Creek by a thin sand that is between the thick well dated and well developed tsunami sand layers “Y” and “W” and in the Orick marsh as a thin sand below the ~300 year horizon. This event is permissively the same event dated about 800 years ago on the Little Salmon fault from the Little Salmon Creek site (Reference 114), the Swiss Hall site (Reference 51) and also may correlate with a subsidence horizon and tsunami sand found in the Eel River Valley (References 43-44) and is about the same time as an event in the Sixes River area in southern Oregon (Figure 2.6-96). Kelsey and others (Reference 52) propose another southern Cascadia segment rupture from stratigraphic evidence in southern Oregon that is dated at about 2010 to 2300 years BP. This age for an event has no known equivalent as a subduction zone earthquake or tsunami anywhere else in Cascadia; however, a possible slip event on Little Salmon fault in this same time range is suggested from the paleoseismic studies at the margin of South Bay at the Swiss Hall site (Reference 51) and in the marsh stratigraphy at the Hookton Slough site (Reference 209).

The average recurrence interval of large, near-source tsunamis from Cascadia over the ~3,000-year record is less than 500 years. However, the ages for individual events show the recurrence rate for the most recent six events is not uniform (Section 2.6.2.4, Table 2.6-2; Table 2.6-24) (Reference 49). Intervals between events “W,” “U,” and “S” are less than 300 years, whereas the intervals between “Y” and “W” and between “S” and “N” are 700 years or more, possibly reflecting “earthquake clustering” that is known on other seismic sources in the world. More than 300 years have elapsed since the most recent event.

2.6.9.4.6 Runup Estimates for Past Tsunamis

Estimates were made for the height of runups and inundation distances for several past Cascadia subduction zone tsunamis in northern California using several different approaches: comparison with historical tsunamis at Crescent City (Reference 222); analysis of the distribution of sand, diatoms, and particle-size of sand layers at Lagoon Creek (References 222-224, and 238); consideration of Native American oral histories at Orick (References 222 and 234); and analysis of pebble distribution and erosion on dunes and spits at Humboldt Bay (References 48, 170, 222, 225, and 235).

Crescent City - At Crescent City, a direct comparison of the extent, thickness, and structure of paleotsunami sand layers deposited by local tsunamis with the characteristics of the sand layers deposited by the far-traveled 1960 and 1964 tsunamis (Reference 222) provides a basis for estimating the elevation for larger wave runup heights from a local source. The Crescent City marsh is about 13 feet above mean lower low water (6 feet above MHHW), and Highway 101 that is built on the beach berm is several feet above that. The 1964 tsunami coincided with a high spring tide

HUMBOLDT BAY ISFSI FSAR UPDATE

(Reference 239), so the runup was higher than it would have been if the tide had been low. Tidal records show wave height as 20 to 21 feet (MLLW at Crescent City (Table 2.6-22), but local runup heights, as recorded by damage to structures on and near the beach at Sand Mine Road, were 7 to 10 feet above Highway 101 (10 to 13 feet above the marsh). Thus, at Sand Mine Road the wave runup height in 1964 was about 23 to 26 feet above mean lower low water (16 to 19 feet above MHHW). The sand layers from the 1960 and 1964 tsunamis in the Crescent City marsh near Sand Mine Road are just under one-half inch thick in the most seaward part of the marsh; neither sand layer extends more than 600 feet inland from the beach. No marsh erosion occurred during these events.

By contrast, thicker sand layers (>3.5 in. thick) lower in the stratigraphic section at the Crescent City marsh extend 1300 feet inland, to the back edge of the marsh (Reference 222). The inland extent of flooding during these tsunamis probably was significantly greater than the 1300-foot distance from the beach to the back edge of the marsh where sand deposits are preserved, but further inland no marsh existed to collect and preserve sand. These thicker sand layers commonly contain multiple fining-upward sequences, reflecting repeated inundation by successive surges of the near-field tsunami wave train. This evidence is especially well developed in sand on the seaward side of the marsh. Only at the back edge of the marsh do the thick and extensive sand layers resemble the thin 1964 deposits. Using the tsunami flow parameters (depth and velocity) that are indicated by the characteristics of the sand layer at the seaward side of the Crescent City marsh, then the 10 to 13-foot water depth in the marsh in 1964 could be considered similar to the depth of the tsunami at the inland-most part of the marsh during the “Y” and some of the earlier large, local events. Hence the runups from the local paleotsunamis were clearly much higher at the beach than 23 to 26 feet (above MLLW) attained in 1964.

As a comparison, the 1964 Alaska earthquake produced near-field tsunami on Kodiak Island that are characterized by multiple fining-upward sand sequences in marshes at Women’s, Middle, and Kalsen bays. The 1964 sand in the Kodiak tsunami deposits consists of both Katmai ash, which is a medium to coarse sand size pumice, and similar size black lithic sand derived from shale, slate, and sandstone. At most sites these two components are in roughly equal amounts, but at some sites one or the other of the two sand types predominate. Where multiple sand layers from successive wave pulses are preserved the denser lithic sand forms the lower part of a couplet with the Katmai ash sand at the top of each layer (Reference 204). The Kodiak sand layers were deposited by runup that crested about 10 to 18 feet above the marsh surfaces. No erosion of the marsh surface occurred at Women’s Bay where water was 10 feet above the marsh, but erosion of the Myrtle Creek marsh at Kalsen Bay occurred where water depth was 12 feet above the marsh.

The characteristics of sand sequences at Kodiak are remarkably similar to the prehistoric tsunami deposits in the Crescent City marsh at Sand Mine Road. Based on comparison with sand sheets deposited in marshes in Kodiak in 1964, it is estimated that they must have been at least as deep as 12 feet because they eroded the marshes. Considering that the 1964 tsunami that was 23 to 26 feet (MLLW) did not erode the marsh, the paleotsunamis that crossed the marsh must have been at least 5

HUMBOLDT BAY ISFSI FSAR UPDATE

feet deeper, more than 28 to 31 feet above mean lower low water for event “Y,” and possibly higher for event “W,” where waves crossed the beach at Crescent City (Table 2.6-22).

Mofjeld and others (Reference 240) have used the precise timing of the last Cascadia subduction earthquake (event “Y”) derived from the documented historic observations in Japan (Reference 41) to reconstruct the tide stage along the Pacific Northwest coast during the earthquake. Satake and coworkers back-calculate the time of the earthquake from arrival times of the tsunamis reported in Japan to be about 0500 UT on January 27, 1700 (9:00 PM PST on January 26, 1700). Mofjeld and coworkers calculated the tide stages in Cascadia for that date indicate the earthquake occurred during a low, neap tide. They report the tide level reached a minimum of about 1.4 feet at 0541 UT (9:41 PM PST) at Humboldt Bay, about the time of the earthquake. The following high tide at Humboldt Bay was at about 1230 UT (4:30 AM PST) and was about 5.9 feet. Since near field tsunamis from great subduction earthquakes produce tsunami wave trains that arrive at intervals over many hours, the initial tsunami pulses probably arrived during low water and contrast with the 1964 distant tsunami that arrived on the northern California coast at high tide. However, later waves in the tsunami wave train could have come ashore during the subsequent high tide stage, comparable to the 1964 tsunami. The tide stage during earlier Cascadia tsunamis is unknown.

Lagoon Creek - At Lagoon Creek, particle-size distribution, extent, structure, and the elevation of sand sheets help constrain wave runup height, inundation distance, and unit discharge for the “Y,” “W,” “U,” and “S” events (Reference 223). Flow parameters at Lagoon Creek were estimated by analysis of the particle-size distribution for the coarse-sand fraction of tsunami layers across the marsh as done elsewhere by Atwater and Moore (Reference 241) and Moore (Reference 242). Abramson and Carver and others (Reference 222-223) estimated the water depth for inundating flows that deposited sand at Lagoon Creek was 11 to 46 feet above the marsh surface using a range of wave velocities from 6.5 to 16.5 feet per second (Table 2.6-26). The analyses resulted in estimates of unit discharge for flows carrying sand above the marsh surface at the time of inundation. This unit discharge, calculated for the “Y,” “W,” “U,” and “S” events, places limits on flow parameters for these inundation events. Runup-height estimates (above MLLW) at the beach berm of between 18 feet (minimum, event “U,” using a velocity of 16.5 ft/s, and assuming complete berm erosion) and 52 feet (maximum, event “S,” using a velocity of 6.5 ft/s assuming no berm erosion) resulted from these analyses. Elevation of the marsh surface was interpreted as the base of the sand layer in Core 4, approximately 2,000 feet inland from the coast. Core 4 is the approximate location at which sand grain size begins to fine away from the beach. The calculations selecting an intermediate velocity value of 10 feet per second that is believed to be representative or “best estimate” of water depths are shown on Table 2.6-26; using this velocity, runup height estimates range between 26 and 33 feet (MLLW). Runup estimates for event “Y” range from 24 to 44 feet (MLLW), and the preferred estimate is 33 feet above mean lower low water.

Orick - At Orick and Big Lagoon, Yurok oral histories provide several accounts of inundation levels (Reference 234). These stories identify house sites and other

HUMBOLDT BAY ISFSI FSAR UPDATE

landmarks as flooded by an ancient tsunami (event “Y”). Runup heights indicated by these stories at Orick are in the range of 66 to 69 feet above mean lower low water (Figure 2.6-108). These unusually high runup heights, if accurate, may reflect the effects of a nearby submarine landslide, or tsunami focusing and constructive wave interference that caused an unusual high runup at this location.

Humboldt Bay - Runup estimates at Humboldt Bay are based on the evidence of overtopping of the South Spit during each of the Cascadia subduction zone events. The lack of pre-event-“Y” morphology or soil development on the South Spit, and sand sheets having basal unconformities in the bay margin stratigraphy at the south end of the spit at the South Bay site reflect substantial landward flows across the spit. However, the absence of sand on the same paleoseismic horizons in the wildlife refuge on the east side of South Bay, some 2.5 to 3 miles southeast of the spit, suggests that these waves may not have transported sand all the way across the bay. The tsunami sands found at Hookton Slough, which is south of the South Bay National Wildlife Refuge site, are believed to be sand that was incorporated from the readily available sand in the tidal channels and sand flats in South Bay northwest of Hookton Slough (Reference 209).

Overtopping of the South Spit by the most recent three or more Cascadia subduction zone tsunamis shows the runup height of each of these tsunamis had to be higher than 18 to 23 feet above mean lower low water, the average and maximum height of the spit dunes (MLLW) for about the past millennium (Reference 235). The characteristics of the tsunami sand layers, including extensive tsunami erosion of the salt marshes adjacent to the spit, indicate flows over the marsh were greater than the historical inundation levels (21 to 25 feet) at Crescent City from distant-source tsunamis (discussed above). The tsunami runup at the South Spit had to be significantly higher than the top of the narrow dune field because the tsunami eroded the spit and had enough velocity to rip up and erode the highly vegetated marsh surface on the bay margin. The sand sheet deposited in the South Bay by event “Y” thins more rapidly than the correlative sand sheet at Lagoon Creek, suggesting that the depth of the tsunami above the marsh decreased rapidly as it spread into the bay and was less than 13 to 33 feet (Table 2.6-26), the depth of estimated runup flows at Lagoon Creek for event “Y”, as discussed above (Reference 223). It was found that the depths that correspond to runup heights are less than 20 to 40 feet for event “Y” at the south spit.

The absence of tsunami sand sheets on the same paleoseismic horizons in the stratigraphy in the northern part of Humboldt Bay and the Mad River Slough, and the presence of an uneroded soil capping old dunes on the North Spit indicate the dunes on the northern part of the North Spit have not been overtopped, thus, runups have been less than 53 to 72 feet, the average and maximum elevation of the dunes (MLLW) at the North Spit.

Radiocarbon-dated strata are mantled by concentrations of scattered-pebbles and cobbles within the dune stratigraphy on the seaward side of the North Spit, but landward of the high tide mark (Reference 225) (Figure 2.6-113). These pebbles extend to an elevation of 38 feet above mean lower low water (Reference 235). These pebbles and cobbles are interpreted by Leroy (Reference 225) to be from erosion within

the dunes during extreme tides. However, because they are 30 feet higher than mean higher high water, Carver (Reference 235) interprets them to be from transport of clasts onto the dunes during inundation by a large tsunami, probably the “Y” event, or possibly the “W” event. The inundation event that deposited them must have been higher than 38 feet, the present elevation of the clasts. Comparison to tsunami transported pebbles and small cobbles, similar to those on the North Spit, from the 1964 Alaska earthquake at the Myrtle Creek marsh at Kalsen Bay, Kodiak Island, provides an insight to potential runups. The Myrtle Creek marsh was littered with similar but larger rocks where water depth was less than 12 feet above the marsh. This suggests that the tsunami surge at the North Spit was several feet higher than 38 feet, but less than 50 feet above mean lower low water. Carver (Reference 235) estimates that the runup was between 35 and 40 feet.

Given the observations at the South Spit, and the constraint that the water did not top the northern part of the North Spit, the estimate of runups at Lagoon Creek, and the analysis of the historical tsunamis at Crescent City and on Kodiak Island (Table 2.6-25) it is estimated that past Cascadia-generated tsunami had runup heights of about 30 to 40 feet above mean lower low water at the sand spits facing the open coast at Humboldt Bay.

2.6.9.4.7 Potential for Local Landslide-Generated Tsunamis

Landslide-generated tsunamis can contribute to the wave train of a seismic generated tsunami and can cause locally higher runups on the affected coast. The compilation by Lander and others (Reference 220) notes that of fifteen high-quality tsunami reports associated with earthquakes along the west coast of the U.S. since 1812, eight to thirteen were caused by or included submarine landslides. Five of the landslide-related tsunamis affected the coast of southern California; four affected the central California coast or San Francisco Bay. Only one affected the northern California coast, at Crescent City; it was due to an 1873 earthquake north of the Oregon border.

Submarine landsliding is a common and ongoing process off the California coast. Clarke and others (Reference 243) note its prevalence in the broad, southern California continental borderland, possibly the reason for the large fraction of landslide-related tsunamis in southern California reported by Lander and others (Reference 220). Offshore northern California, high sedimentation rates and steep sea-floor topography are conditions that produce instability and promote submarine landslides. Particularly steep slopes are present along the Mendocino escarpment, along part of the outer continental slope, and in the Eel and Trinity submarine canyons. Mapping of the continental margin offshore of northern California has identified many ancient landslides on the sea floor (Reference 244). Most of these probably were seismically generated. Given the frequent occurrence of strong earthquakes in historical time in the offshore area north of Cape Mendocino, it is surprising there is only one report (1873, Crescent City) of a landslide-related tsunami in this region. This apparent dichotomy may be because the infrequent large long-duration megathrust earthquakes in this area may have already caused failure of any marginally stable slopes leaving few slopes susceptible to additional large landslides and there have been none historically.

Another potential offshore landslide area is the Eel River basin where seismic reflection profiles show an area of ridge and swale topography along the continental slope and gully-type topography (the Humboldt slide) (Reference 245-246). The Humboldt slide was originally been interpreted as a shallow sediment failure along rotated blocks (e.g., submarine landslide) by Field and others (Reference 244) but Gardner and others (Reference 245) has been recently reinterpreted as a series of sediment waves caused by turbidity currents (Reference 246) or internal tidal waves (References 247 - 248). It is also possible that several of the 50 turbidite deposits reported from in the Eel River basin by Nelson and others (Reference 54) were triggered by earthquakes on the Cascadia subduction zone. The landslides that caused the turbidities were probably far enough away and not large enough to cause a large landslide generated tsunami at the coast.

Analysis of the paleotsunamis in northern California suggests possible locally high tsunami runup during event “Y” (January 26, 1700) at Orick, where the estimated runup height from native oral histories of 66 to 69 feet (above MLLW) (Figure 2.6-115) exceeds the estimates at Crescent City (higher than 28 to 31 feet MLLW) and Lagoon Creek (26 to 33) to the north and Humboldt Bay (30 to 40 feet) to the south. The Clarke and Field (Reference 249) geologic map shows several regions of unstable sediment deposits on the continental shelf between 12 and 31 miles to the northwest and west of Orick. However, the continental slope in this area is generally shallow and not conducive to landslides.

If a landslide originated at one of these locations, it is likely that its tsunami would have affected other areas, as well as Orick. Unfortunately, there are too few locations along the coast where reliable runup-height estimates for the 1700 tsunami have been measured to allow testing of the landslide hypothesis for the anomalous wave height at Orick. Another explanation for this apparently high runup may be a combination of the azimuth of wave arrival, wave amplification, and focusing of the waves caused by local effects from seafloor topography.

Recent high-resolution sea-bottom imaging by Goldfinger and Watts (Reference 250) indicates the presence of very large landslide masses along the Cascadia continental margin, but their subdued geomorphic appearance indicates that they are old, estimated at ~110,000 yrs, 450,000 yrs, and 1.2 million yrs (Reference 65, Appendix 9A). Although huge slide masses, such as these, could generate very large local tsunamis, no such events, other than possibly Orick, have been preserved in the geologic record for at least the past approximately 3,000 years at the sites studied. Such catastrophic events appear to be infrequent compared with the occurrence of tectonically generated tsunamis from ruptures of the Cascadia subduction zone, even though the long duration of such large events should be effective in triggering large landslides.

2.6.9.4.8 Summary of Results of the Paleotsunami Study

The key results of our geologic study of past tsunamis in northern California can be summarized as follows:

HUMBOLDT BAY ISFSI FSAR UPDATE

- The stratigraphic evidence from Crescent City, Lagoon Creek, and South Bay (Figure 2.6-96) shows the northern California coast has experienced at least eight large-runup tsunamis during the past 3,600 years. Six of these correlate with those of the Cascadia subduction zone events recognized in Oregon and Washington. The record includes events (“Y”, “W”, “U”, “S”, “N”, “L”) at about 300, 1,150, 1,350, 1,650, 2,550, and 2,950 years ago. Regional distribution of these events suggests that most of the northern California tsunamis have been generated by large earthquakes (magnitude ~9) on the Cascadia subduction zone from long fault ruptures along the northern California, Oregon, and Washington coast. The stratigraphic evidence also indicates at least two local tsunami events. One is recorded at Crescent City, Lagoon Creek, and in the lower Eel River Valley at about 850 years BP. The other is at Hookton Slough at about 3600 years BP. Only at the South Bay site is there evidence of storm waves over topping of the beach berm, and these have distinctive characteristics that differentiate them from tsunami deposits.
- Potential tsunamis from the Cascadia subduction zone could generate / wave runups along the open coast at Humboldt Bay. The height would probably be greater if the earthquake also triggered one or more large submarine landslides off the adjacent coast; however, no evidence of such larger, landslide-generated tsunamis in the past 2,000 and probably the past 3,600 years has been found in Humboldt Bay.
- At Crescent City, evidence for at least five smaller, distant-source tsunamis was found. These events were similar in general to the 1960 Chilean and 1964 Alaskan tsunamis. Although runups as high as 21 to 25 feet above mean lower low water based on geological evidence (tidal records were 20 to 21 feet) were observed in Crescent City during the 1964 event, the runups in Humboldt Bay were only about 10 feet above mean lower low water (4.4 feet above the tide level at the time). The runups for the 1964 tsunami are the largest in recorded history for distant tsunamis striking the Humboldt Bay area. No geologic evidence (sand deposits) of distant-source tsunamis was found inside Humboldt Bay.
- No indication was found that a significant (sand-carrying) tsunami runup has ever reached the area around the HBPP. The northern North Spit directly blocked tsunamis from reaching the northern part of Humboldt Bay; however, tsunami runups more than 18 to 23 feet above mean lower low water would cross the South Spit and the southern end of the North Spit and we paleotsunamis are estimated to have had heights of 30 to 40 feet as they reached the spits. Tsunamis with lower runups could have crossed the sandbars that partially blocked the entrance channel to Humboldt Bay (Figures 2.6-117 and 2.6-118) prior to dredging the channel in 1860, but these would have dissipated rapidly as they spread out into Humboldt Bay. In any case, the marsh deposits at and near the Humboldt

Bay ISFSI site contain no evidence of sand being deposited from tsunami inundation.

2.6.9.5 Additional Assessments of Tsunami Hazard

To augment and support the interpretation of the tsunami evidence discussed above, two additional types of data were considered: well-documented historical tsunami records worldwide to estimate the possible tsunami runups appropriate for the Cascadia subduction zone, and tsunami inundation analyses performed by others for the Humboldt Bay area.

2.6.9.5.1 Empirical Comparisons of Worldwide Tsunami Runup Heights

George Plafker, retired expert from the U. S. Geological Survey, reviewed the empirical worldwide data regarding tsunamis for PG&E (Reference 251) to help constrain the wave runup height for a plausible tsunami source along the Cascadia subduction zone by comparison with other large historical tsunamigenic earthquakes worldwide (Figure 2.6-119). Included in this group are those events for which source mechanism, moment magnitude, and fault slip have been calculated and for which there are relatively complete observational data, such as local tsunami runup height, arrival times, and coseismic shoreline displacement. The data are presented in Appendix 9A of Reference 65.

For most tsunamigenic earthquakes, the associated tsunamis are generated primarily by regional coseismic vertical tectonic displacement of the sea floor. In some subduction zone environments, such as Cascadia, the associated tsunamis primarily are generated by seaward thrusting along the subduction zone megathrust and subsidiary faults that splay off the subduction zone and break to the sea floor through the upper thrust plate (Reference 252, contained in Appendix 2A to Reference 65 and discussed in Section 2.6.2). Within this category are the three largest tsunamigenic earthquakes that have occurred in convergent continental margin environments during the 20th century: the 1960 Chile, the 1964 Alaska, and the 1979 Colombia earthquakes. As illustrated in Figure 2.6-119, the average maximum runups of tectonically-generated tsunamis increase approximately linearly with moment magnitude.

Some tsunamigenic earthquakes have waves generated by both tectonic displacements and earthquake-triggered submarine landslides in coastal areas. These include the 1964 Alaska, the 1992 Flores Island, the 1998 Aitape, the 1946 Aleutian, and possibly the 1993 Hokkaido events (Reference 65, Appendix 2A). As shown on Figure 2.6-119, slide-augmented waves may be as much as four times higher than the waves generated tectonically by the same earthquake. In other earthquakes, such as the 1994 Mindoro strike-slip earthquake, waves having maximum runups of 23 feet appear to be generated entirely by near-shore submarine landslides (Figure 2.6-119).

For some tsunamigenic earthquakes, maximum runups are locally as much as 2-1/2 times larger than would be expected for their magnitudes (Figure 2.6-119). These include the 1992 Nicaragua and the 1994 Java events. For some of these

earthquakes, some of the relatively high runups may be attributed to peculiarities of wave build-up due to interaction of the tsunami with the sea floor and shoreline topography. However, it is more probable that these generally higher runups resulted from a contribution to the wave train by unrecognized offshore landslides, rather than from a fundamental difference in earthquake mechanism, wave interactions, or bottom and shoreline configurations. The effect of near shore and off shore landslides is well documented for the 1964 Alaska earthquake and the 1998 Aitape earthquake, respectively (Reference 65, Appendix 9A).

The 1946 Aleutian earthquake is unique in that it generated both a very high near-source runup of 42.7 m (137 feet) (Reference 65, Appendix 9A), and a high far-field runup of more than 16 m (52 feet) in Hawaii (Figure 2.6-119). Distribution and arrival times of the near-field tsunami strongly suggest a near-field source. Comparison of this tsunami to others shows that the near-source runup is more than six times higher than that expected for tectonically generated tsunamis from comparable-magnitude earthquakes (Figure 2.6-119). Origin of the far-field tsunami is unknown.

With regard to the Cascadia subduction zone, earthquake-triggered submarine landsliding on a very large scale might account for the waves generated by those events for which the tsunami is too large for the earthquake magnitude. As previously discussed (Section 2.6.9.4.7) large submarine landslides have been mapped on the sea floor offshore of northern California. The anomalous high runups reported at Orick possibly resulted from a tsunami that was enhanced by an offshore landslide. Recent detailed bathymetric mapping of the Cascadia continental margin (Reference 250) has revealed several enormous landslide masses off shore of Oregon that have features interpreted as indicative of large and sudden movements of thousands of square miles of the lower continental slope. These appear to have occurred at infrequent intervals and inferred to be hundreds of thousands of years old by the thickness of the overlying sediment and the inferred sedimentation rates. The presence of these large offshore submarine landslides suggests a mechanism for generating anomalously large tsunamis at infrequent intervals. However, no geologic evidence for such tsunamis has been found in the late Holocene coastal stratigraphy in northwestern California or other places along the Cascadia coast.

For a magnitude 8.8 tsunamigenic earthquake on the Cascadia subduction zone (Section 2.6.5), empirical worldwide tsunami data indicate such an earthquake would generate average maximum runup heights along the northern California coast of 31 feet (mean sea level [35 feet MLLW]). The runup range for magnitude 8.5 to 9.2 is 28 to 37 feet [32 to 41 feet MLLW] (Figure 2.6-119; Table 2.6-25). This generally agrees with the findings and estimate of 30 to 40 feet for the wave height offshore of Humboldt Bay for paleotsunami studies in northern California.

2.6.9.5.2 Analytical Models of Potential Tsunami Inundation

Six analytical studies of potential tsunami inundation have addressed the potential tsunami hazard to Humboldt Bay. These studies span the period since 1965, and use a variety of approaches to assess potential tsunami effects on the Humboldt Bay coast, inside the bay, and in the vicinity of the HBPP. In each study, the runup height at the

HUMBOLDT BAY ISFSI FSAR UPDATE

coast at Humboldt Bay has been estimated, and in several cases, the runup height at the power plant has been assessed. Each study's approach has been summarized below using the estimates as they pertain to the evaluation of the ISFSI site

As discussed in Section 2.6.9.2, the reference level of mean lower low water is used to facilitate comparison of the results of each study to the topographic setting of the ISFSI site (Figure 2.6-120). The elevation of mean lower low water is set at 0, which is 3.7 feet below mean sea level, and the tidal range between mean lower low water and mean higher high water is 6.9 feet. The highest reported tide in the ISFSI site vicinity since 1920 was 12.5 feet (MLLW) (Reference 219). The yard elevation of the HBPP is 12 feet (MLLW), the reference level for all surveys at the HBPP (elevation 8.3 feet above mean sea level). As sketched on Figure 2.6-120, the proposed ISFSI site is approximately elevation 44 feet, and the Buhne Point hill varies in height along the bluff facing Humboldt Bay from 75 feet on the northwest to 24 feet on the southeast (MLLW).

Wiegel (Reference 210) - Shortly after the occurrence of tsunami inundation at Crescent City and elsewhere along the northern California Coast due to the 1964 Alaska earthquake, PG&E was asked by the U.S. Atomic Energy Commission to assess the protection of the Humboldt Bay nuclear power plant against tsunamis. PG&E retained civil engineering Professor R. L. Wiegel of the University of California at Berkeley, a widely recognized expert on tsunamis and their engineering impact, to evaluate the likelihood of tsunami flooding at the power plant.

Wiegel (Reference 210) reviewed the data on historic tsunami waves in Humboldt Bay, noting that the largest were associated with the March 1964 Alaskan earthquake, which had a maximum runup height of 4.4 feet above the tide level (9.6 feet above MLLW) at the power plant intake (Table 2.6-22). To augment the observations at Humboldt Bay, Wiegel used frequency distribution functions of observations at localities that had more data: Crescent City harbor and The Presidio in San Francisco, California; Hilo, Hawaii; and a compilation of Japanese runup data. He assumed a Poisson distribution of runup height occurrences, anchored by the maximum runup of 4.4 feet above the tide stage reported at the HBPP intake in 1964, and extrapolated using the general shape of the tsunami runup heights versus frequency for the other localities. Table 2.6-27 illustrates Wiegel's calculated probability levels and associated runup heights above mean lower low water level.

In addition to distant tsunamis, Wiegel also considered the probability of locally generated tsunamis. He extrapolated the frequency of occurrence of offshore earthquakes north of the Mendocino escarpment based on historic seismicity. For a magnitude 8 earthquake having an approximate recurrence of 800 years, he estimated a tsunami having a runup of about 25 feet on the open coast, and about one-half this value at Buhne Point. He concluded, "Based upon present evidence, there appears to be little likelihood of the generation of a large tsunami in a region near Humboldt Bay." At the time of his analysis, in late 1964, the existence of the Cascadia subduction zone as a potential local tsunami source was yet to be recognized.

PG&E (Reference 219) - In June 1985, PG&E prepared a Memorandum Report to respond to a Nuclear Regulatory Commission question on flood hydrology pertaining to

HUMBOLDT BAY ISFSI FSAR UPDATE

the decommissioning of Unit 3 at the HBPP. Potential tsunamis were calculated in two ways.

The evaluation of tsunami flooding levels performed by Wiegel (Reference 210) was augmented using a report prepared by Brandsma and others (Reference 253) for the NRC, in which offshore wave heights and time histories are presented for coastal segments of the United States due to distantly generated tsunamis. Using a Corps of Engineers procedure (Reference 254) and Brandsma and others' maximum tsunami wave of ± 5.2 feet at a point offshore in water of moderate depth (600 feet), PG&E (Reference 219) computed the wave runup at the mouth of Humboldt Bay to be 16.1 feet above mean lower low water. This runup height would decrease as the wave propagated through the bay to the power plant site, although no quantitative analysis of the attenuation was done.

In the second approach, PG&E (Reference 219) used information from a study by Houston and Garcia (Reference 255) that predicted tsunamis for the west coast of the U.S. for flood insurance purposes. Houston and Garcia's (Reference 255) 100-year tsunami runup at the entrance to Humboldt Bay was estimated to be 10.6 feet above mean lower low water, and the 500-year tsunami runup was estimated to be 20.7 feet above mean lower low water. Similar to the above procedure, no specific analysis was performed to predict water levels at the power plant site itself.

Whitmore (Reference 256) - In the numerical analysis by Whitmore (Reference 256), Cascadia subduction zone source parameters were used to compute inundation wave amplitudes along the coast of Washington, Oregon, northern California, and adjacent areas to the north and south. The largest event analyzed was magnitude 8.8 that ruptured from central Washington to between Eureka and Crescent City. The fault rupture was 400 miles long, dipped 13 degrees, and the maximum sea-floor uplift was 12 feet. At points along the coast opposite the modeled earthquake, the maximum computed tsunami amplitude was 19 feet, with an average maximum amplitude of about 15 feet. Maximum amplitudes were computed at three locations within Humboldt Bay (Eureka: 1.7 feet, Fields Landing: 0.66 feet, and Bucksport, between Eureka and Fields Landing: 2.8 feet). The maximum amplitude of 8.7 feet was calculated on the ocean side of the North Spit, just to the south of the end of the modeled fault rupture. The Bucksport location is considered to be the most similar to the Humboldt Bay ISFSI site. Although technically the wave half-amplitudes are the predicted height of the potential runup, the full amplitude is considered to be closer to actual runup elevation (MLLW) because of the wide grid spacing used in the model and to account for asymmetry of the tsunami waves in this report.

National Oceanic and Atmospheric Administration (Reference 57) - Following the occurrence of the April 25, 1992, Cape Mendocino shallow thrust earthquake, the National Oceanic and Atmospheric Administration evaluated potential tsunami inundation along the northern California coast associated with possible Cascadia subduction zone events. The results of the study were intended to be used for emergency planning purposes and, as such, are generalized.

HUMBOLDT BAY ISFSI FSAR UPDATE

The planned approach for the study (Reference 57), included application of seismic source models for the Cascadia subduction zone to predict the generation of significant tsunami waves impinging on Humboldt Bay and Crescent City, followed by numerical modeling of inundation in these two areas of interest. The initial results of the seismic source modeling indicated the Cascadia subduction zone produced tsunami wave amplitudes that were judged to be unreasonably small. Therefore, Bernard and others (Reference 57) evaluated the complexities of recent tsunamis generated by earthquakes in Nicaragua (1992), Indonesia (1992), and Japan (1993), and used an empirical approach to estimate the incident wave amplitudes at Humboldt Bay. Using tsunami observations associated with the 1964 Alaska and 1993 Hokkaido earthquakes, they judgmentally derived a 10-meter (33-foot) incident wave at a 50-meter (164-foot) water depth to be used in inundation models.

The inundation modeling for Humboldt Bay is described in Appendix H of Bernard and others (Reference 57) in terms of the computer modeling input, procedures, and output, and is accompanied by a small-scale map of the inundation area and the 100-meter grid used for the modeling. A 1:24,000-scale map of the Humboldt Bay region that shows the inundation boundary also is provided. Bernard and others state (Reference 57, Appendix H, page 67), "The inundation levels inside the harbor reached 3 meters at some locations..." (10 feet referenced to mean sea level). Because the small-scale map and 1:24,000-scale map are somewhat disparate, a conservative consideration of 10 feet as the Bernard and others (Reference 57) runup estimate for the ISFSI site vicinity was made.

Bernard and others (Reference 57) state (page 67), "All the Humboldt Spit was flooded." The South Spit has a maximum elevation of about 23 feet above mean lower low water. The southern end of the North Spit is similar to the South Spit in elevation, but the central part and northern end of the North Spit ranges from 56 to a maximum of about 73 feet in elevation above mean lower low water. For an input wave of 33 feet in the near offshore, the statement in Appendix H seems problematical regarding the higher portions of the North Spit.

Lamberson and others (Reference 257) - Roland Lamberson, Professor at Humboldt State University, has developed, along with his students, a numerical tidal model calibrated for Humboldt Bay. During 1997, they performed a pilot study (Reference 257) to assess the feasibility of using their current finite-difference tidal model to simulate tsunami wave amplitudes and water velocities inside Humboldt Bay. They tested their model at low tide (0 set at mean lower low water), using an arbitrary input set of three large (4 to 6 meter amplitude) waves at the mouth of Humboldt Bay, having a period of 15 minutes. At the entrance to Humboldt Bay the third wave had the maximum wave height of 8 meters (26 feet MLLW). A wave overtopping the spits was not included in their model, although the input wave clearly would have washed over the South Spit and the southern portion of the North Spit.

In their model, the maximum flooding at the ISFSI site occurred during the second wave, and had an elevation of 5 meters (16.4 feet) above mean lower low water. Current velocities at the ISFSI site were a maximum of 2 meters (6.6 feet) per second. Lamberson and others (Reference 285) concluded their model performed well.

Myers and others (Reference 213) – Edward Myers, a Ph.D. student, and a team of researchers from the Oregon Graduate Institute developed a finite element model for propagation of Cascadia subduction zone tsunami waves from their source near the plate interface off the coast of the Pacific northwest, to the coast. To generate the tsunamis, they used various rupture models for the Cascadia subduction zone as presented in Priest and others (Reference 214). These models assume a geometry of the plate interface and vary the rupture dimensions by adjusting the locations and amounts of slip on the seaward and landward transition zones around a central locked zone. They estimated regions and amounts of seafloor uplift corresponding with each of these rupture scenarios, assumed the sea floor uplift was directly transferred to the sea surface as the initial conditions for their model. They then propagated the tsunami wave trains through their finite element grid toward the coast, and reported the estimated wave heights and run-up velocities associated with each of the scenarios.

In their study, the authors reported their results for a number of locations along the coast from Cape Mendocino to the northern Olympic Peninsula. These results depend on a relatively coarse finite element grid, and are most useful to estimate tsunami-focusing mechanisms offshore, but are considered approximate for estimation of runup at the coast (Reference 258). The authors chose two sites for detailed estimation of runup characteristics: Seaside and Newport, Oregon. The finite element grid was much denser than the regional grid at these two sites to permit detailed estimation of runup routes, flow velocities, and runup heights. The authors report that predicted wave heights and runup velocities are very sensitive to grid density, reinforcing the notion that estimates of run-up outside of Seaside and Newport should be considered approximate. Furthermore, Dr. Baptista (Reference 258) reports that runup velocities predicted by these models are much less accurate than wave heights.

This model predicts wave heights at the coast at Humboldt Bay between 17 and 30 feet (MLLW) and flow velocities between 3 and 13 ft/s, but they did not model runups within Humboldt Bay. At Klamath, near Lagoon Creek, they predict wave heights between 17 and 46.5 feet (MLLW) and flow velocities between 6.5 and 15 ft/s, but preferably around 10 ft/s.

Discussion – Table 2.6-28 summarizes the results of the various studies. For each study, the runup height of the wave at the mouth of Humboldt Bay is listed; in cases where an offshore wave in shallow water was specified, the runup was taken to be equivalent to the offshore wave height (Figure 2.6-85). The estimated runup heights at the Humboldt Bay ISFSI site are shown at mean lower low water and at mean higher high water (Table 2.6-28; Figure 2.6-120). The latter value was obtained by adding the tide differential (6.9 feet) to the tsunami runup height.

The Wiegel (Reference 210) and PG&E (Reference 219) studies were based on distant tsunamis only, and were performed prior to the knowledge that the Cascadia subduction zone could produce a very large earthquake, and that such earthquakes could produce significant tsunamis. Even so, their maximum tsunami inundation estimates greatly exceed those of the 1964 earthquake (Table 2.6-22), which is considered by Lander and others (Reference 220) to be the largest potential distant tsunami on the northern California coast. The geologic record at Crescent City

HUMBOLDT BAY ISFSI FSAR UPDATE

(Reference 222) shows no evidence of significantly larger distant tsunamis during the past several thousand years, unless the circa 850 years BP event (Crescent City “W”) is an unusually large distant event. Our preferred interpretation is that it is local, possibly related to the event that caused subsidence of the Eel River valley. The conservatism used in the 1966 and 1985 studies resulted in maximum values of 21 feet (MLLW) and 27 feet (MHHW) (Reference 254) that are somewhat lower than to those derived from consideration of local tsunamis caused by Cascadia subduction zone earthquakes, but considering the knowledge at the time are considered remarkable.

The computer model studies have progressed markedly in the past 20 years, but the results should be taken as a guide to how tsunamis may impact a coast and spread inland. Most use sinusoidal waves for the analysis, but clearly this is not what occurs (discussed in 9.2). Importantly the models need to have a fine grid that adequately characterizes the subocean and shore topography (Reference 213 and 258). Nonetheless, the modeling results to date provide useful information and insights that help limit the estimates of runup at the coast off Humboldt Bay and in the ISFSI site area.

In analyzing a large Cascadia earthquake, the input tsunami wave height of 10 meters (MSL) at an offshore water depth of 50 meters (167 feet), as selected judgmentally in the Bernard and others (Reference 57) study, is comparable to the 30- to 40-foot (above MLLW) paleotsunami runup wave height we have estimated at the Humboldt Bay North and South spits. These values are significantly greater than the values computed by Whitmore (Reference 256) for various locations along the coast. Even his maximum amplitude value of 6 meters (19 feet) appears to be unacceptably low, considering the evidence for tsunamis crossing the South Spit during the past several thousand years. Lamberson and others (Reference 258) selected an arbitrary value of about 26 feet (8 meters) as model input, but they easily could have chosen a larger value. As mentioned above, the model from Myers and others (Reference 213) produced maximum coastal wave height estimates (which were also labeled “Maximum Runup”) at Humboldt Bay between 17 and 30 feet above MLLW, depending on the model for rupture of the Cascadia subduction zone. The authors emphasize that Humboldt Bay is at the periphery of their grid, and that these values are much less reliable than those from central Oregon, particularly Seaside and Newport. Nonetheless, they describe these estimates as “reasonable” (Reference 258).

Thus the lack of paleotsunami sand deposits in the vicinity of the plant and at other places around the bay may reflect the absence of a significant wave or a lack of a source of sand near the site. If it is assumed a source of sand is available, then the lack of tsunami sands near the ISFSI site provides a possible height constraint for paleotsunamis at the site. The analysis to constrain water depth and velocity of the inundating flows that deposited paleotsunami sands at Lagoon Creek (Table 2.6-26) (Reference 223) provides insights to this issue. If paleotsunamis entered Humboldt Bay and induced inundating flows of similar depths on marshes and mud flats, it could reasonably be expected for them to deposit sand layers as well, provided there was a source of sand near the marsh. The elevation of the tidal marshes near the ISFSI site is 5 to 7 feet above mean lower low water; these marshes extended for about one-half mile north of the ISFSI site (Figure 2.6-34, Section 2.6.9.4) prior to the construction of

jetties in about 1900 to stabilize the entrance to Humboldt Bay, and were 3 to 4 kilometers from the sand spits at the coast. Any tsunami entering the bay had to cross 500 meters of spit, traverse 1 kilometer of bay and 1 ½ to 2 kilometers of marsh to reach the ISFSI area. It is unlikely that sand from the spits would reach the ISFSI area because the tsunami sands from Lagoon Creek had settled out beyond about a kilometer inland from the beach berm. Any tsunami sand near the ISFSI would have to be from a local source, such as a beach along Buhne Point or tidal channels in the bay. Nonetheless it is assumed that a source of sand existed for the following calculation: when the marsh elevation (5 to 7 feet) is added to the minimum depth of flow expected to transport and deposit a sand layer, the value is less than 24 to more likely 34 feet above mean lower low water. Any runups higher than this are presumed to have been large enough to have deposited sand layers in the marshes near the ISFSI site. Thus, the evidence for no sand deposits near the ISFSI site suggests that the maximum estimated runup at the ISFSI site was less than 24 to 34 feet (MLLW), which is slightly higher than the estimated runup elevations at the coast based on the several models (Table 2.6-28).

2.6.9.6 Additional Factors Influencing The Tsunami Hazard At The ISFSI Site

Several additional factors need to be considered in order to understand the uncertainties in the estimates of the tsunami hazard at the Humboldt Bay ISFSI site.

2.6.9.6.1 Estimated Runup At The Open Coast At Humboldt Bay

The range of maximum estimates of runup height for the Cascadia paleotsunamis along the open coast of northern California at the five sites where paleotsunami information is available varies between 18 to 52 feet, or to 69 feet if the data for Orick is included, but is more likely between 26 to 33 feet above mean lower low water from the analysis of the events at Lagoon Creek marsh (Table 2.6-25).

For the “Y” event, which has the most data for a single event, runup estimates vary at different sites along the coast. At Lagoon Creek, runup estimates for this event range from 24 to 44 feet (MLLW). The maximum runup of 69 feet at Orick (based on Yurok oral histories) is presumed to describe the “Y” event, as it likely represents the most recent very large tsunami at that site. At the North Spit, deposition of gravel and cobbles within the sand dunes constrains runup to be somewhat higher than 38 feet above MLLW (Section 2.6.9.4.6). The maximum open-ocean tsunami runup height at the mouth of Humboldt Bay from a local subduction-generated tsunami is constrained by the 53- to 72-foot elevation (i.e., less than 53 to 72 feet above MLLW) of the uneroded dunes on the North Spit, which have not been overtopped. As mentioned in Section 2.6.9.4.6, preferred estimates for tsunami wave height at the mouth of Humboldt Bay based on evidence from the North and South Spits are between 30 and 40 feet above mean lower low water.

This variability in run up heights is well within the observed range of variability in runup heights observed at different locations along coasts adjacent to historical great

subduction earthquakes, including Chile in 1960, and Alaska in 1964 (Figure 2.6-114, Reference 65, Appendix 9A)

Berm Erosion - the runup height estimates at the lagoon creek beach berm and the south spit are based on the assumption that the sand berms used as the elevation baselines for the calculations were not eroded by the initial rise in water level, and persisted as high barriers during the successive tsunami pulses. However, observations of similar sites in Chile show barriers composed of sand erode rapidly, and do not persist during the tsunami. Because tsunamis are dispersive wave trains and do not completely drain before the next wave arrives, and the highest inland runups usually occur after the initial wave in the wave train, the erosion of the barrier by initial wave pulses leads to more rapid inundation and more extensive runups inland by later waves. However, the presence of a relatively continuous stratigraphic sequence spanning at least the past 3000 years and the lack of significant unconformities in the marsh sediments behind the berm at lagoon creek indicate that if the berm was eroded by past tsunamis its elevation was not reduced below that of the marsh impounded behind it.

Velocity - The finite-element modeling of a Cascadia tsunami by Meyer and others (Reference 220; Section 2.6.9.5.2) indicates the runup height above tide level ranges from about 3 to 9 meters (10 to 30 feet) at Crescent City, and about 3 to 12 meters (10 to 39 feet) at Klamath. If maximum high tide coincides with maximum runup at these sites predicted runup heights would be 17 to 37 feet at Crescent City and 17 to 46 feet at Lagoon Creek. Modeled wave velocities for the tsunamis at these locations are about 3 meters per second (10 ft/sec).

The sediment transport model that relates particle deposition to water velocity used by Abramson (Reference 223) and Carver and others (Reference 222) at Lagoon Creek to estimate the maximum water depth of past tsunamis (Section 2.6.9.4.6) was calculated using a range of 2 to 5 meters per second (6.5 to 16.5 feet per second). The minimum inundation velocity was estimated from the probable time and distance of tsunami runup. In this case, assuming a tsunami wave period of one hour, the time during which flows are actually flooding the marsh would be somewhat less than 15 minutes (one quarter of the period, minus the time of sea level rise required to overtop the beach berm). The minimum distances the waves traveled inland for events Y, W, U, and S ranged between 1260 and 1330 meters (approximately 4,130 and 4,360 feet) inland based on the presence of sand layers and marine diatoms in cores (Reference 222). Dividing this minimum distance by the estimated time of flooding yields approximate rates of 1.4 -1.5 meters per second (4.5-5 feet per second). Considering that a 1-hour wave period is conservatively long (Section 2.6.9.2), the time of inundation is somewhat less than one-quarter of the period, and the runup distances documented in cores are minimum distances, it is estimated that a reasonable minimum runup flow velocity of 2 meters per second (6.5 feet per second) at Lagoon Creek (References 222-223). The maximum runup velocity of 5 meters per second (16.5 feet per second) is averaged over the distance of particle transport, and is based on comparison to velocities measured in large rivers and tidal bores worldwide (References 222-223). For example the tidal bore at the Amazon River is 16 feet (5 meters) high, and attains speed of 20 feet/second (6.2 m/s) (Reference 259).

HUMBOLDT BAY ISFSI FSAR UPDATE

Because the velocity value of 6.5 feet per second is believed to be low and because runup height calculated from the particle size model is inversely proportional to the velocity, the maximum runup heights are somewhat overestimated at this low velocity. Table 2.6-26 shows the water depths (consistent with the particle-size distributions observed in the Lagoon Creek marsh) and associated runup heights at Lagoon Creek derived using three velocities: 6.5 feet per second (minimum), 16.5 feet per second (maximum), and 10 feet per second (the velocities believed to be reasonable as predicted by Myers and others, (Reference 213). The preferred values for runup heights at Lagoon Creek are 26 to 33 feet above mean lower low water, based on a flow velocity of 10 feet per second (3 meters per second) as the most reasonable estimate of runup heights.

Flow depths reported in Table 2.6-26 refer to the depth of flow over the marsh surface. The marsh elevation for each event is taken to be the elevation of the sand layer on the marsh surface in the stratigraphy at core location 4 (Figure 2.6-2.6-96), which is about 2000 feet inland, the distance inland where the coarse fraction sand-size begins to decrease. All runup estimates reported in Table 2.6-26 are relative to modern MLLW. It is assumed that the elevation of the Lagoon Creek site remains tectonically stable and does not change in the analysis of tsunami events, i.e. no net uplift or subsidence.

Tide Stage - The tsunami wave height required to produce the water depths and runup heights observed for paleotsunamis depends on the stage of the tide at the time of the tsunamis. Because the tide stage is unknown for all but the most recent (event "Y") of the paleotsunamis along the northern California coast, only a range and limiting bounds can be estimated. (However, there is some evidence that large earthquakes preferentially occur at low tides (Reference 260). At low tide, the wave amplitude must increase to generate the runup heights estimated at the site, and conversely, a higher tide stage requires a lower wave height.

Because a high or low tide lasts only a few hours each day, the probability of any of the largest wave pulses of paleotsunamis arriving during high tide levels is small (about 1 in 6 for either a high or low water stage), and the probability that the maximum height wave pulses from all of the six Cascadia tsunamis in the stratigraphic record of northern California occurred during a high tide is very small (about 1 in 1,296). The normal semi-diurnal tide range along this part of the coast is about 6.9 feet. The most likely tide stage would be near mean sea level, about 3 feet. An example of the influence of tides on tsunami runup is on Kodiak Island in 1964 (Reference 217 and 261). There the highest wave heights were generally associated with one of the first three waves in the tsunami wave train, but, because these waves arrived at relatively low tide stages, they did not result in the highest runup heights on the coast. Later, smaller waves arriving during high tide reached higher on the coast at some locations. At Crescent City the 1964 tsunami coincided with a high spring tide (Reference 239) and hence the runup was near maximum there. These examples illustrate that the tidal factor is important, both in interpreting the paleotsunami wave heights, and estimating future runups.

Open-Coast Runup Estimate - It is estimated that future runup on the open coast at the mouth of Humboldt Bay due to a local Cascadia tsunami will be about 30 to 40 feet

HUMBOLDT BAY ISFSI FSAR UPDATE

above mean lower low water. This estimate is based on six separate analyses of potential runup height values summarized in Table 2.6-25:

- (1). Geologic and stratigraphic evidence from marshes along the northern California coast
- (2). Topographic constraints and geologic evidence of paleotsunamis at the North and South spits
- (3). Calculations of the water depth at Lagoon Creek, using the intermediate flow velocity of 10 feet per second
- (4). Empirically predicted runup height from worldwide data of tsunami runup heights from subduction-generated tsunamis, particularly continental margin areas, such as those in Alaska, Chile, Peru and Colombia (Figure 2.6-119)
- (5). Oral history accounts of the 1700 AD earthquake, and
- (6). The results of the tsunami modeling of the northwest coast and Humboldt Bay

2.6.9.6.2 Runup Heights at the ISFSI Site

Although the estimated tsunami runups at the North and South spits and the mouth of Humboldt Bay are 30 to 40 feet (above MLLW), the runup after entering the bay will be significantly lower on the eastern shore of the bay than on the open coast. Two factors need to be considered to understand the uncertainties in the estimates of the tsunami hazard at the Humboldt Bay ISFSI site: the change in bathymetry and shoreline since 1850, and tectonic uplift and coseismic downwarping that accompanies an earthquake on the Cascadia Subduction zone and the Little Salmon fault.

The shoreline and channel at the entrance to Humboldt Bay have changed dramatically since the early 1800's. The earliest maps show that the North and South spits partially blocked Humboldt Bay prior to about 1860 (Figures 2.6-117 and 2.6-118), so the effects of the excavated Humboldt Bay shipping channel and post-1860 erosion in the Buhne Point area on future tsunami runup in the bay and at the ISFSI site is uncertain. The bay entrance and shoreline at Buhne Point has changed in several ways the since the last subduction event:

- (1). Modification of the entrance of the bay
- (2). Changes in the depth of the bay between the mouth and the plant site, and
- (3). Regression of the shoreline at Buhne Point

HUMBOLDT BAY ISFSI FSAR UPDATE

When the first map was made in the early 1800's by the Russian explorers (Figure 2.6-118) and later in the 1850's (Figure 2.6-117) the Bay entrance was very narrow and shallow with the channel confined between two overlapping spits, all factors that would dampen the effect of a tsunami reaching the ISFSI site area. With the artificially wide and deep open entrance to today's bay, waves are much more likely to enter the bay through the mouth and retain much more energy than before the mouth was modified. The deep dredged ship channels in the bay between the mouth and Buhne Point have replaced the much shallower, muddy-bottomed reach between the mouth and the site, allowing a wave to move from the mouth to the site with less attenuation. Buhne Point hill, however, would continue to protect the ISFSI site from the direct impact of the tsunami runup front (Figure 2.6-120), and tend to reduce runup heights at the ISFSI site because it is on the lee side of Buhne Point.

Tectonic uplift and subsidence near the ISFSI site is probable during major Cascadia subduction zone earthquakes that are accompanied by large displacements on the Little Salmon fault system (Section 2.6.9.2). The paleoseismic record in the Humboldt Bay area shows subduction zone events are associated with coseismic subsidence of synclines at Arcata Bay on the footwall of the Mad River fault zone and South Bay on the footwall of the Little Salmon and Table Bluff faults. Between these synclines is an area, including Humboldt Hill, Buhne Point and the part of North Spit opposite Eureka, that is being uplifted on the hanging wall of the Little Salmon fault. Bay margin sediments at locations above the hanging wall of the Little Salmon fault, including the Eureka anticline, which is considered a hanging wall structure, have no evidence (salt marsh peat abruptly overlain by intertidal mud) of coseismic subsidence. In contrast, coseismic subsidence stratigraphy is found in the cores of the large synclines at Arcata Bay-Mad River Slough and the South Bay syncline (South Bay and Hookton Slough sites) (References 85, 209, 222, and 262).

Because the ISFSI site is located on the upthrown block of the Little Salmon fault system, it appears reasonable to assume that future large local tsunamis impinging on Humboldt Bay would be influenced by displacement on the Little Salmon fault. The investigations in Humboldt Bay at the Swiss Hall (Reference 51) and Hookton Slough (Reference 209) sites, which are in the marshes bordering South Bay, and at other locations in the south Bay (Reference 262) indicates a small amount of coseismic emergence on the hanging wall of the fault and a larger amount of subsidence of the footwall associated with past slip events. The amount of coseismic subsidence is reflected by the abrupt changes in sedimentary and paleontology indicators of intertidal zonation (Reference 262-263) in the bay margin sediments. The net tectonic elevation change over seismic cycles is approximated by the thickness of intertidal mud overlying marsh peat and soils (Reference 209 and 262) and ranges up to 6 feet of subsidence (this ignores eustatic rise in sea level, which may approach 2 mm/yr according to Douglas (Reference 264)). The long-term record of cumulative displacement on the Little Salmon fault shows the same relationship: predominate subsidence of the footwall and lesser emergence of the hanging wall. Thus, the down side of the fault is underlain by thousands of feet of relatively young (Quaternary) sediments and a thick Neogene Wildcat Group section is preserved (if the Table Bluff fault is included, about 12,000 feet of Neogene section in the Eel River Valley lies below sea level), while on the upthrown side (hanging wall) only a small part of the Wildcat section is preserved,

HUMBOLDT BAY ISFSI FSAR UPDATE

suggesting many thousands of feet of net uplift. During a tsunamigenic subduction earthquake involving the Little Salmon fault the vertical land level changes in the vicinity of the ISFSI site would have two effects. Uplift of the hanging wall would raise the ISFSI site slightly, possibly a foot or two, and tend to reduce the level of tsunami flooding in the aftermath of large tsunamigenic earthquakes near the coast. This may help explain the lack of observed paleotsunami sand deposits in the area of the HBPP. However, subsidence of up to 6 feet would tend to increase the runup in Humboldt Bay because South Spit would be coseismically lowered and increase the tsunami flooding in South Bay.

Attenuation of Runup Heights in Humboldt Bay - the values for the attenuation factor for tsunami wave height in Humboldt Bay can be approached in several ways. Plafker and Kachadoorian (Reference 261) report that on Kodiak Island, “the highest recorded runups were along exposed beaches and bluffs, whereas the runup heights in adjacent sheltered embayments and segments of the coast protected by offshore reefs were substantially lower.” Comparisons of runup heights on open coasts and nearby bays along the northeast shore of Kodiak Island show that the 1964 maximum runup heights at Cape Chiniak and narrow cape were about 10 meters (33.3 feet) above tide level. At Cape Chiniak, trees along the shoreline were destroyed up to an elevation of 31.5 feet above the highest tide level on the night of the tsunami (Reference 261). The highest runup heights for these same waves were 18.4 feet in Kelsen Bay, and 12.8 feet at the naval station at woman’s bay. Kalsen bay is large, deep, and open to the ocean, whereas the naval station at woman’s bay is more protected, and the bay has a narrow and relatively shallow entrance. Both bays are significantly less sheltered than Humboldt bay. The attenuation of the tsunami runup heights at these two bays relative to the open coast in 1964 was 0.6 and 0.4, respectively.

Although runup is expected to be lower in the ISFSI site area than on the open coast, the amount is uncertain. There is no measurement of the runup at the open coast at the mouth of Humboldt Bay during the 1964 Alaska tsunami, the tsunami produced a maximum wave height of 21 to 25 feet at Crescent City and of 12.6 ± 0.5 feet on the coast at Trinidad, about 30 miles north of the bay entrance (Table 2.6-22). At the ISFSI site, the wave height was 3.8 feet. If the open-ocean value at Trinidad is representative of the runup at the mouth of the bay, the attenuation factor was about 0.3, but the sand spits were not overtopped, so this attenuation is certainly low. Previous tsunami inundation studies for modeled tsunami wave heights in Humboldt Bay also have estimated attenuation amounts. Those range from 30% to 63 % (Table 2.6-28). The analysis of Lagoon Creek data suggests that if inundating flows reached 24 to 34 feet (above MLLW) at the marsh around the ISFSI, they would deposit sand, at the site, assuming that a nearby source of sand from within the bay was available to supply sediment. Because there is no sand or other evidence that tsunami runup has ever reached the site, past runups in the late Holocene are assumed to be less than that elevation.

Based on the above range of the attenuation factors, and because of the proximity of the ISFSI site area to the mouth of the Humboldt Bay channel, it is estimated that for the analysis of the ISFSI site, an attenuation value between 0.7 to 0.9 is appropriate to characterize the expected reduction in runup height from the seaward side of the bay

entrance to the site. Applying this to the estimated maximum of 30 to 40 feet (MLLW) at the coast, the estimated runup at the ISFSI site is between 21 and 36 feet (MLLW) and 23 and 38 (MHHW). As a check, back calculating the runup height using the estimated attenuation of 0.7 to 0.9 applied to the maximum estimate of 24 to 34 feet above the marsh near the ISFSI (from the Lagoon Creek analysis), the runup at the open coast at Humboldt Bay would likely have to be 27 to 38 and 34 to 49 feet (MLLW), respectively, to carry sand into the ISFSI site area (Table 2.6-28).

2.6.9.7 Summary of Tsunami Hazard at the Humboldt Bay ISFSI Site

- The tsunami hazard at the Humboldt Bay ISFSI site is dominated by a local tsunami generated by a magnitude ~9 earthquake on the Cascadia subduction zone, resulting from rupture of the zone from the Humboldt Bay area north to Canada. This tsunami is expected to flow strongly through the mouth of Humboldt Bay, as well as wash over the South Spit and the southern part of the North Spit.
- The runup height from a local Cascadia-generated tsunami on the open coast at the mouth of Humboldt Bay is estimated to be as much as 30 to 40 feet above mean lower low water at the bay entrance. This estimate considers evidence of paleotsunamis at the North Spit, and assumes overtopping and erosion of the sand barriers and marsh at the South Spit. It compares well with the predicted runup height estimates from historical tsunamis in continental margin settings in Alaska, Chile, Peru, and Colombia, as well as runup estimates for paleotsunamis at Lagoon Creek and Crescent City.
- The vault for the placement of the dry casks at the ISFSI facility is near the top of Buhne Point hill (Figures 2.6-1 and 2.6-120). The top of the vault is at an elevation of 44 feet above mean lower low water. This elevation is higher than the tsunami height estimates at mean lower low water considered in this study (Table 2.6-28), which include bounding estimates for distant tsunamis, modeling of locally generated tsunamis associated with the Cascadia subduction zone, and tsunami heights from geologic evidence of no sand-transporting tsunamis inundating the region around the ISFSI site.
- Using the estimate of 30 to 40 feet above mean lower low water for the runup height of the tsunami at the bay entrance, and an attenuation factor of 0.7 to 0.9, the inundation height would be 21 to 36 feet above mean lower low water if the tsunami occurred at low tide, or 28 to 43 feet above mean lower low water at the ISFSI site area if the tsunami occurred at high tide. The offshore bathymetry at Humboldt Bay is smooth and wide, and topographic enhancement of tsunamis is not expected at the ISFSI site.
- Incorporating wave run-up for storms from Table 2.4-5, gives maximum value of 49.86 ft (including high tide and wave run-up for storms). The

HUMBOLDT BAY ISFSI FSAR UPDATE

maximum tsunami occurring coincident with a design basis storm wave run-up and high tide is not considered credible

- Even if a tsunami runup flowed above the ISFSI elevation, the tsunami hazard at the proposed ISFSI site is negligible, because the casks can be temporarily wetted without harm and they will be contained in underground vaults which protect them from damage by flowing water and damage from water-born debris.

2.6.10 REFERENCES

1. Woodward-Clyde Consultants, 1980, Evaluation of the potential for resolving the geologic and seismic issues at the HBPP Unit No. 3: Summary to Pacific Gas and Electric Company, San Francisco, 74 p. plus appendix volume.
2. Idriss, I. M., 1991, Selection of earthquake ground motions at rock sites: Report Prepared for the Structures Division, Building and Fire Research Laboratory, National Institute of Standards and Technology, Department of Civil Engineering, University of California, Davis, September.
3. Idriss, I. M., 1994, Updated standard errors: personal communication, April 17, 1994.
4. Idriss, I. M., 1995, An overview of earthquake ground motions pertinent to seismic zonation: Proceedings Fifth International Conference on Seismic Zonation, Nice, France, p. 2111-2124.
5. Abrahamson, N. A., and Silva, W., 1997, Empirical response spectral attenuation relations for shallow crustal earthquakes: Seismological Research Letters, v. 68, p. 94-127.
6. Boore, D. M., Joyner, W. B. and Fumal, T. E., 1997, Equations for estimating horizontal response spectra and peak acceleration from Western North American earthquakes: A summary of recent work: Seismological Research Letters, v. 68, p. 128-153.
7. Campbell, K. W., 1997, Empirical near-source attenuation relationships for horizontal and vertical components of peak acceleration, peak ground velocity, and pseudo-absolute acceleration response spectra, Seismological Research Letters, v. 68, p. 154-179.
8. Sadigh, K., Chang, C.-Y., Egan, J. A., Makdisi, F., and Youngs, R. R., 1997, Attenuation relationships for shallow crustal earthquakes based on California strong motion data: Seismological Research Letters, v. 68, p. 180-189.
9. Youngs, R. R., Chiou, S. J., Silva, W. J., and Humphrey, J.R., 1997, Strong ground motion attenuation relationships for subduction zone earthquakes

HUMBOLDT BAY ISFSI FSAR UPDATE

based on empirical data and numerical modeling: *Seismological Research Letters*, v. 68, p. 58-73.

10. Hanks, T. C., and Kanamori, H., 1979, A moment magnitude scale, *Journal of Geophysical Research*, v. 84, p. 2348-2350.
11. Lawson, A. C., 1908, The California earthquake of April 18, 1906: Carnegie Institute of Washington Publication 1, p. 54-59 and 165-170.
12. Brown, R. D., and Wolf, E. W., 1972, Map showing recently active breaks along the San Andreas fault between Point Delgada and Bolinas Bay, California: U. S. Geological Survey Miscellaneous Geological Investigations Map I-692, 2 sheets.
13. Prentice, C., 1989, The northern San Andreas fault - Russian River to Point Arena, *in* Sylvester, A. G., and Crowell, J. C. (eds.), *The San Andreas Transform Belt: American Geophysical Union Field Trip Guidebook T309*, p. 49-51.
14. Oppenheimer, D., Beroza, G., Carver, G., Dengler, L., Eaton, J., Gee, L., Gonzalez, F., Jayko, A., Li, W. H., Lisowski, M., Magee, M., Marshall, G., Murry, M., McPherson, R., Romanowicz, B., Satake, K., Simpson, R., Somerville, P., Stein, R., and Valentine, D., 1993, The Cape Mendocino, California, earthquakes of April 1992—subduction at the triple junction: *Science*, v. 261, p. 433-438.
15. Atwater, T., 1970, Implications of plate tectonics for the tectonic evolution of western North America: *Geological Society of America Bulletin*, v. 81, p. 3513-3536.
16. Dickenson, W. R., and Snyder, W. S., 1979, Geometry of triple junctions related to the San Andreas transform: *Journal of Geophysical Research*, v. 84, p. 561-572.
17. Leitner, B., Trehu, A. M., and Godfry, N. J., 1998, Crustal structure of the northwest Vizcaino block and Gorda escarpment, offshore northern California - implications for postsubduction deformation of a paleoaccretionary margin: *Journal of Geophysical Research*, v. 103, no. B10, p. 23795-23812.
18. Griscom, A., and Jachens, R. C., 1989, Tectonic history of the northern portion of the San Andreas fault system, California, inferred from gravity and magnetic anomalies: *Journal of Geophysical Research*, v. 94, no. B3, p. 3089-3099.
19. Kelsey, H. M., and Carver, G. A., 1988, Late Neogene and Quaternary tectonics associated with the northward growth of the San Andreas transform fault, northern California: *Journal of Geophysical Research*, v. 93, no. B5, p. 4797-4819.

HUMBOLDT BAY ISFSI FSAR UPDATE

20. Castillo, D. A., and Ellsworth, W. L., 1993, Seismotectonics of the San Andreas fault system between Point Arena and Cape Mendocino in northern California - implications for the development of a young transform: *Journal of Geophysical Research*, v. 98, no. B4, p. 6543-6560.
21. Trehu, A. M., and the Mendocino Working Group, 1995, Pulling the rug out from under California: seismic images of the Mendocino triple junction region: *EOS, Transactions of the American Geophysical Union*, v. 76, no. 38, 369, p. 380-381.
22. Freymueller, J. T., Murray, M.H., Segall, P. and Castillo, D., 1999, Kinematics of the Pacific-North America plate boundary zone, northern California, *Journal of Geophysical Research*, 104, p. 7419-7442.
23. Lisowski, M., and Prescott, W. H., 1989, Strain accumulation near the Mendocino triple junction, California (abs.): *EOS, Transactions of the American Geophysical Union*, v. 70, p. 1332.
24. Bolt, B. A., and Miller, R., 1975, Catalogue of earthquakes in northern California, Jan 1, 1910- Dec 31, 1972: *Seismographic Stations*, University of California, Berkeley, 567 p.
25. Dengler, L., Carver, G., and McPherson, R., 1992a, Sources of North Coast seismicity: *California Geology*, v. 45, no. 2, p. 40-53.
26. Krause, D. C., Menard, H. W., and Smith, S. M., 1964, Topography and lithology of the Mendocino Ridge: *Journal of Marine Research*, v. 22, p. 236-249.
27. Duncan, R. A., Fisk, M. R., Carey, A. G. Jr., Lund, D., Douglas, L., Wilson, D. S., Stewart, R., and Fox, C. G., 1994, Origin and emergence of the Mendocino Ridge (abs): *EOS, Transactions of the American Geophysical Union*, v. 75, no. 44, Supplement to Fall Meeting, p. 475.
28. McPherson, R. C., 1989, Seismicity and focal mechanisms near Cape Mendocino, northern California: M. S. Thesis, Humboldt State University, Arcata, California, 75 p.
29. McPherson, R., 1992, Style of faulting at the southern end of the Cascadia subduction zone, *in* R. M. Burke and G. A. Carver (eds.), *Pacific Cell, Friends of the Pleistocene guidebook for the field trip to northern coastal California*, June 5-7, 1992, p. 97-111
30. Wilson, D., 1989, Deformation of the so-called Gorda Plate: *Journal of Geophysical Research*, v. 94, no. B3, p. 3065-3075.
31. Smith, S. W., and Knapp, J. S., 1980, The northern termination of the San Andreas fault, *in* Streitz, R., and Sherburne, R. (eds.), *Studies of the San*

HUMBOLDT BAY ISFSI FSAR UPDATE

Andreas Fault Zone in Northern California: California Division of Mines and Geology Special Report 140, p. 153-164.

32. Riddihough, R., 1984, Recent movement of the Juan de Fuca plate system: *Journal of Geophysical Research*, v. 89, p. 6980-6994.
33. Heaton, T. H., and Kanamori, H., 1984, Seismic potential associated with subduction in the northwest United States: *Bulletin of the Seismological Society of America*, v. 74, p. 933-941.
34. Geomatrix Consultants, Inc. (Geomatrix), 1995, Seismic design mapping, State of Oregon: Final Report Prepared for Oregon Department of Transportation, Salem, Oregon, Personal Services Contract 11688, January.
35. Atwater, B. F., Nelson, A. R., Clague, J. J., Carver, G. A., Yamaguchi, D. K., Bobrowsky, P. T., Bourgeois, J., Darienzo, M. E., Grant, W. C., Hemple-Haley, E., Kelsey, H. M., Jacoby, G. C., Nishenko, S. P., Palmer, S. P., Peterson, C. D., and Reinhart, M. A., 1995, Summary of coastal geologic evidence for past great earthquakes at the Cascadia subduction zone: *Earthquake Spectra*, v. 11, no. 1, p. 1-18.
36. Atwater, B. F., and Yamaguchi, D. K., 1991, Sudden, probably coseismic submergence of Holocene trees and grass in coastal Washington State: *Geology*, v. 19, no. 7, p. 706-709.
37. Atwater, B. F., Stuiver, M., and Yamaguchi, D. K., 1991, Radiocarbon test of earthquake magnitude at the Cascadia subduction zone: *Nature*, v. 353, p. 156-158.
38. Carver, G. A., Stuiver, M., and Atwater, B. F., 1992, Radiocarbon ages of earthquake-killed trees at Humboldt Bay, California (abs.): *Eos* v. 73. no. 43, p. 398.
39. Jacoby, G. C., Carver, G. A., and Wagner, W., 1995, Trees and herbs killed by an earthquake ~300 years ago at Humboldt Bay, California: *Geology*, v. 23, p. 77-80.
40. Nelson, A., Atwater, B., Benson, B., Bobrowsky, P., Bradley, L., Clague, J., Carver, G., Darienzo, M., Grant, W., Krueger, H., Sparks, R., Stafford, T., and Stuiver, M., 1995, Radiocarbon evidence for extensive plate-boundary rupture about 300 years ago at the Cascadia subduction zone: *Nature*, v. 378, no. 6555, p. 371-374.
41. Satake, K., Shimazaki, K., Tsuji, Y., and Ueda, K., 1996, Time and size of a giant earthquake in Cascadia inferred from Japanese tsunami records of January 1700: *Nature*, v. 379, p. 246-249.

HUMBOLDT BAY ISFSI FSAR UPDATE

42. Tanioka, Y., Satake, K., and Ruff, L., 1995, Seismotectonic of the April 25, 1992, Petrolia earthquake and the Mendocino triple junction region: *Tectonics*, v. 14, no. 5, p. 1095-1103.
43. Li, W.-H., 1992, The late Holocene subsidence stratigraphy in the Eel River syncline, northern California: in Burke, R.M., and Carver, G.A., (eds.), *Guidebook for the Pacific Cell Friends of the Pleistocene Field Trip to Coastal Northern California*, June 5-7, 1992, p. 235-239.
44. Li, W.-H., 1992, Evidence for late Holocene coseismic subsidence in the lower Eel River Valley, Humboldt County, northern California - an application of foraminiferal zonation to indicate tectonic submergence: M. S. Thesis, Humboldt State University, Arcata, California, 92 p.
45. Jacoby, G.C. 1998. Personal Communications.
46. Aalto, K. R., McLaughlin, R. J., Carver, G. A., Barron, J. A., Sliter, W. V., and McDougall, K., 1995, Uplifted Neogene margin, southernmost Cascadia-Mendocino triple junction region, California: *Tectonics*, v. 14, no. 5, p. 1104-1116.
47. Carver, G. A., 2000, Paleoseismic geology of the southern part of the Cascadia subduction zone, in Clague, J., Atwater, B., Wang, K., Wang, M. M., and Wong, I. (eds.): *Proceedings of the Geological Society of America Penrose Conference, Great Cascadia Earthquake Tricentennial, 4-8 June 2000*, Seaside, Oregon, p. 26-27.
48. Carver, G. A., 2002, Written communication providing documentation for the radiocarbon analysis of tree ring series samples from fossil trees in the lower Eel River Valley: letter from Gary Carver to William Page (PG&E Geosciences) dated December 26, 2002; 1 p. plus 3 attachments (4 pp. total).
49. Atwater, B. F., and Hemphill-Haley, E., 1997, Recurrence intervals for great earthquakes of the past 3,500 years at northeastern Willapa Bay, Washington: *U. S. Geological Survey Professional Paper 1576*, 108 p.
50. Clarke, S. H. Jr., and Carver, G. A., 1992, Late Holocene tectonics and paleoseismicity, southern Cascadia subduction zone: *Science*, v. 255, p. 188-192.
51. Witter, R.C., Patton, J., Carver, G.A., Kelsey, H.M., Garrison-Laney, C., Koehler, R.D., and Hemphill Haley, E., 2002, Upper plate earthquakes on the western Little Salmon fault and contemporaneous subsidence of southern Humboldt Bay over the past 3,600 years, northwestern California: *U.S. Geological survey, National Earthquake Hazards Reduction Program Final Technical Report*, Award number 01HQGR0125, 44 p.

HUMBOLDT BAY ISFSI FSAR UPDATE

52. Kelsey, H.M., Witter, R.C., and Hemphill-Haley, E., 2002, Plate-boundary earthquakes and tsunamis of the past 5500 yr, Sixes River estuary, southern Oregon: Geological Society of America Bulletin, v. 114, no. 3, p. 298-314.
53. Stuiver, M., and Reimer, P. J., 1993, Extended 14C data base and revised CALIB 3.0 14C age calibration program: Radiocarbon, v. 35, p. 215-230.
54. Nelson, C. H., Goldfinger, C., and Johnson, J. E., 2000 (in press), Turbidites event stratigraphy - implications for Holocene paleoseismicity of the Cascadia subduction zone and northern San Andreas faults, (abs.): Eos, Transactions American Geophysical Union, v. 81, no. 48, p. F851.
55. Clarke, S. H. Jr., 1990, Map showing geologic structures of the northern California continental margin: U. S. Geological Survey Miscellaneous Field Studies Map MF-2130.
56. Clarke, S. H. Jr., 1992, Geology of the Eel River basin and adjacent region - implications for late Cenozoic tectonics of the southern Cascadia subduction zone and Mendocino triple junction: American Association of Petroleum Geologists Bulletin, v. 76, p. 199-224.
57. Bernard, E., Madher, C., Curtis, G., and Satake, K., 1994, Tsunami inundation model study of Eureka and Crescent City, California: National Oceanic and Atmospheric Administration Technical Memorandum ERL PMEL-103, 80 p.
58. Topozada, T., Borchardt, G., Haydon, W., and Peterson, M., 1995, Planning scenario in Humboldt and Del Norte counties, California, for a great earthquake on the Cascadia subduction zone: California Division of Mines and Geology Special Publication 115 , 151 p. plus appendices.
59. Beaudoin, B. C., Godfrey, N. J., Kiemperer, S. L., Lendl, C., Trehu, A. M., Henstock, T. J., Levander, A., Holl, J. E., Meltzer, A. S., Luetgert, J. H., and Moony, W. D., 1996, Transition from slab to slabless - results from the 1993 Mendocino triple junction seismic experiment: Geology, v. 24, no. 3, p. 195-199.
60. Gulick, P. S., Meltzer, A. M., and Clarke, S. H., 1998, Seismic structure of the southern Cascadia subduction zone and accretionary prism north of the Mendocino triple junction: Journal of Geophysical Research, v. 103, no. B11, p. 27207-27222.
61. Gulick, S.P.S., Meltzer, A.S., and Clarke, S.H., 2002, Effect of the northward-migrating Mendocino triple junction on the Eel River forearc basin, California: Stratigraphic development, Geological Society of America Bulletin 114, p. 178-191.

HUMBOLDT BAY ISFSI FSAR UPDATE

62. Wang, K., Jiangheng, H., and Davis, E. E., 1997, Transform push, oblique subduction resistance, and interplate stress of the Juan de Fuca plate: *Journal of Geophysical Research*, v. 102, no. B1, p. 661-674.
63. Jachens, R. C., and Griscom, A., 1983, Three-dimensional geometry of the Gorda plate beneath northern California: *Journal of Geophysical Research*, v. 88, p. 9375-9392.
64. Carver, G. A., Jayko, A. S., Valentine, D. W., and Li, W. H., 1994, Coastal uplift associated with the 1992 Cape Mendocino earthquake, northern California: *Geology*, v. 22, p. 195-198.
65. PG&E technical Report TR2002-01, December 2002
66. Plafker, G., 1969, Tectonics of the March 27, 1964, Alaska Earthquake, Regional Effects: U. S. Geological Survey Professional Paper 543-I, 74 p.
67. Plafker, G., 1972, The Alaskan earthquake of 1964 and Chilean earthquake of 1960—implications for arc tectonics: *Journal of Geophysical Research*, v. 77, no. 5, p. 901-925
68. Plafker, G., and Rubin, M., 1967, Vertical tectonic displacements in south-central Alaska during and prior to the great 1964 earthquake: *Journal Geosciences, Osaka City University*, v. 10, art. 1-7, p. 1-14.
69. Ogle, B. A., 1953, Geology of the Eel River Valley area, Humboldt County, California: Division of Mines, Department of Natural Resources, State of California, Bulletin 164, 128 p.
70. Irwin, W. P., 1960, Geologic reconnaissance of the northern Coast Ranges and Klamath Mountains, California, with a summary of the mineral resources: California Division of Mines Bulletin 179, 80 p.
71. Evitt, W. R., and Pierce, S. T., 1975, Early Tertiary ages from the Coastal Belt of the Franciscan Complex, northern California: *Geology*, v. 3, no. 3, p. 433-436.
72. McLaughlin, R. J., Kling, S. A., Poore, R. Z., McDougall, K., Beutner, E. C., and Ohlin, H. N., 1979, Post-middle Miocene microplate accretion of Franciscan coastal belt rocks to northern California (abs.): *Geological Society of America Abstracts with Programs*, v. 11, no. 7, p. 476.
73. McLaughlin, R. J., Ellen, S. D., Blake, M. C. Jr., Jayko, A. S., Irwin, W. P., Aalto, K. R., Carver, G. A., and Clarke, S. H. Jr., 2000, Geology of the Cape Mendocino, Eureka, Garberville, and southwestern part of the Hayfork 30 x 60 minute quadrangles and adjacent offshore area, northern California: U. S. Geological Survey Miscellaneous Field Studies Map MF-2336.

HUMBOLDT BAY ISFSI FSAR UPDATE

74. Nilson, T. H., and Clarke, S. H. Jr., 1987, Geologic evolution of the late Cenozoic basins of northern California, *in* Schymiczek, H., and Suchland, R. (eds.), *Tectonics, Sedimentation and Evolution of the Eel River and Other Coastal Basins of Northern California*: San Joaquin Geological Society Miscellaneous Publication 37, p. 15-29.
75. Manning, G. A., and Ogle, B. A., 1950, Geology of the Blue Lake quadrangle, California: California Division of Mines Bulletin 148, 36 p.
76. Ingle, J. C. Jr., 1976, Late Neogene paleobathymetry and paleo-environments of the Humboldt basin, northern California, *in* Fritzsche, A. E., Best, H. T. Jr., and Wornardt, W. W. (eds.), *The Neogene Symposium: Pacific Section*, Society of Economic Paleontologists and Mineralogists, p. 53-61.
77. Faustman, W. F., 1964, Paleontology of the Wildcat Group at Scotia and Centerville Beach: University of California Publications in Geological Sciences, v. 41, no. 2, p. 97-160.
78. Carver, G. A., 1987, Late Cenozoic tectonics of the Eel River basin region, coastal northern California, *in* Schymiczek, H., and Sushsland, R. (eds.), *Tectonics, Sedimentation and Evolution of the Eel River and Associated Coastal Basins of Northern California*: San Joaquin Geological Society Miscellaneous Paper 37, p. 61-72.
79. Sarna-Wojcicki, A. M., Lajoie, K. R., Meyer, C. E., Adam, D. P., and Rieck, H. J., 1991, Tephrochronologic correlations of upper Neogene sediments along the Pacific margin, conterminous United States: *in* Morrison, R. B., ed., *Quaternary Nonglacial Geology of the Conterminous U. S.*: Geological Society of America, *The Geology of North America*, v. K-2, p. 117-140.
80. Baksi, A. K., Hsu, V., McWilliams, M. O., and Farrar, E., 1992, Ar-40/Ar-39 dating of the Bruhnes-Matuyama geomagnetic field reversal: *Science*, v. 256, p. 356-357.
81. Sarna-Wojcicki, A. M., Meyer, C. E., Bowman, H. R., Hall, N. T., Russell, P. C., Woodward, M. J., and Slates, J. L., 1985, Correlation of the Rockland ash bed, a 400,000-year-old stratigraphic marker in northern California and western Nevada, and implications for middle Pleistocene paleogeography of central California: *Quaternary Research*, v. 23, p. 236-257.
82. Sarna-Wojcicki, A. M., 2000, Revised age of the Rockland tephra, northern California—implications for climate and stratigraphic reconstructions in the western United States: *Comment, Geology*, v. 28, no. 3, p. 286.
83. Lanphere, M. A., Champion, D. E., Clyne, M. A., and Muffler, L. J. P., 2000, Revised age of the Rockland tephra, northern California - implications for climate and stratigraphic reconstructions in the western United States: *Reply, Geology*, v. 28, no. 3, p. 287.

HUMBOLDT BAY ISFSI FSAR UPDATE

84. Carver, G. A., and Burke, R. M., 1992, Late Cenozoic deformation on the Cascadia subduction zone in the region of the Mendocino triple junction, *in* Burke, R.M., and Carver, G.A. (eds.), A Look at the Southern End of the Cascadia Subduction Zone and Mendocino Triple Junction: Pacific Cell, Friends of the Pleistocene Guidebook for the Field Trip to Northern Coastal California, p. 31-63.
85. Valentine, D. W., Vick, G., Carver, G. A., and Manhart, C. S., 1992, Late Holocene stratigraphy and paleoseismicity, Humboldt Bay, California: *in* R. M. Burke and G. A. Carver (eds.), Pacific Cell, Friends of the Pleistocene Guidebook for Field Trip to Northern Coastal California, June 5-7, 1992, p. 182-187.
86. Merritts, D. J., Chadwick, O. A., and Hendricks, D. M., 1991, Rates and processes of soil evolution on uplifted marine terraces, northern California: *Geoderma*, v. 51, p. 241-265
87. Merritts, D. J., Dunkin, T., Vincent, K., Wohl, E., and Bull, W. B., 1992, Quaternary tectonics and topography, Mendocino triple junction, *in* Burke, R.M., and Carver, G.A. (eds.), A Look at the Southern End of the Cascadia Subduction Zone and Mendocino Triple Junction: Pacific Cell, Friends of the Pleistocene Guidebook for the Field Trip to Northern Coastal California, p. 119-169.
88. Chadwick, O. A., Merritts, D. J., and Hendricks, D. M., 1992, Weathering and soil development on marine terraces along the Lost Coast of California, *in* Burke, R. M., and Carver, G. A. (eds.), A Look at the Southern End of the Cascadia Subduction Zone and Mendocino Triple Junction: Pacific Cell, Friends of the Pleistocene Guidebook for the Field Trip to Northern Coastal California, p. 199-210.
89. Lajoie, K. R., Ponti, D. J., Powell, C. L., Mathieson, S. A., and Sarna-Wojcicki, A. M., 1991, Emergent marine strandlines and associated sediments, coastal California—a record of Quaternary sea-level fluctuations, vertical tectonic movements, climatic changes, and coastal processes, *in* Morrison, R.B., ed., Quaternary Nonglacial Geology: Conterminous U. S., Decade on North American Geology, The Geology of North America, v. K-2, p. 190-214.
90. Muhs, D. R., Rockwell, T. K., and Kennedy, G. L., 1992, Late Quaternary uplift rates of marine terraces on the Pacific Coast of North America, southern Oregon to Baja California Sur: *Quaternary International*, v. 15.16, p. 121-133.
91. Hanson, K. L., Wesling, J. R., Lettis, W. R., Kelson, K. I., and Mezger, L., 1994, Correlation, ages, and uplift rates of Quaternary marine terraces: south-central coastal California, *in* Alterman, I.B., McMullen, R.B., Cluff, L.S., and Slemmons, D.B., eds., Seismotectonics of the central California Coast Ranges: Geological Society of America Special Paper 292, p. 45-71.

HUMBOLDT BAY ISFSI FSAR UPDATE

92. Berger, G. W., Burke, R. M., Carver, G. A., and Easterbrook, D. J., 1991, Test of thermoluminescence dating with coastal sediments from northern California: *Chemical Geology (Isotope Section)*, v. 87, p. 21-37.
93. Berger, G. W., 1992, Thermoluminescence dating of coastal sediments near Eureka, *in* Burke, R.M., and Carver, G.A. (eds.), *A Look at the Southern End of the Cascadia Subduction Zone and Mendocino Triple Junction: Pacific Cell, Friends of the Pleistocene Guidebook for the Field Trip to Northern Coastal California*, p. 170-175.
94. Atwater, B. F., 1992, Geologic evidence for earthquakes during the past 2000 years along the Copalis River, southern coastal Washington: *Journal of Geophysical Research*, v. 97, no. B2, p. 1901-1919.
95. Polenz, M., and Kelsey, H. M., 1999, Development of a late Quaternary marine terraced landscape during on-going tectonic contraction, Crescent City coastal plain: *Quaternary Research*, v. 52, p. 217-228.
96. Kelsey, H. M., 1990, Late Quaternary deformation of marine terraces on the Cascadia subduction zone near Cape Blanco, Oregon; *Tectonics*, v. 9, p. 983-1014.
97. McInelly, G. W., and Kelsey, H. M., 1990, Late Quaternary tectonic deformation in the Cape Arago-Bandon region of coastal Oregon as deduced from wave-cut platforms: *Journal of Geophysical Research*, v. 95, p. 6699-6713.
98. Jacyo, A. S., and Blake, M. C. Jr., 1987, Geologic terranes of coastal northern California and southern Oregon, *in* Schymiczek, H., and Sushsland, R. (eds.), *Tectonics, Sedimentation and Evolution of the Eel River and Associated Coastal Basins of Northern California: San Joaquin Geological Society Miscellaneous Paper 37*, p. 1-12.
99. McLaughlin, R. J., Silter, N. O., Frederikson, W. P., Harbert, W. P., and McCulloch, 1994, Plate motions recorded in tectonostratigraphic terranes of the Franciscan Complex and evolution of the Mendocino triple junction, northwestern California: *U. S. Geological Survey Bulletin* 1997.
100. Carver, G. A., Burke, R. M., and Kelsey, H. M., 1986, Deformation of Late Pleistocene marine terraces along the California coast north of Cape Mendocino (abs): *Geological Society of America, Abstracts with Program*, v. 18, no. 2, p. 93.
101. Carver, G. A., Burke, R. M., and Kelsey, H. M., 1986, Quaternary deformation in the region of the Mendocino triple junction: *U. S. Geological Survey National Earthquake Hazards Reduction Program, Unpublished Final Report*, 48 p.

HUMBOLDT BAY ISFSI FSAR UPDATE

102. McCrory, P. A., 2000, Upper plate contraction north of the Mendocino triple junction, northern California - Implications for partitioning of strain: *Tectonics*, v 19, no.6, p. 1144-1160.
103. Carver, G. A., 1987, Geologic criteria for recognizing individual paleoseismic events in compressional tectonic environments, *in* Crone, A. J., ed., *Directions in Paleoseismology*: U. S. Geological Survey Open File Report 87-673, p. 115-128.
104. Burke, R. M., and Carver, G. A. (eds.), 1992, A look at the southern end of the Cascadia subduction zone and the Mendocino triple junction: Guidebook for the Pacific Cell Friends of the Pleistocene Field Trip to Coastal Northern California, June 5-7, 256 p.
105. Carver, G. A., and Burke, R. M., 1988, Trenching investigation of northwestern California faults, Humboldt region: Unpublished Final Report for U. S. Geological Survey National Earthquake Hazards Reduction Program, Grant No. 14-08-0001-G1082, 53 p.
106. Carver, G. A., and Burke, R. M., 1989, Active convergent tectonics in northwestern California, *in* Aalto, K. R., and Harper, G. D., trip leaders, *Geologic Evolution of the Northwesternmost Coast Ranges and Western Klamath Mountains, California: Field Trip Guidebook T308*, 28th International Geological Congress, p. 64-82.
107. Carver, G. A., Imperato, D. T., and Nilsen, T. H., 1988, Neogene strata of the onshore Eel River basin and adjacent areas: *Field Trip Guidebook*, Applied Earth Technology, Inc., 72 p.
108. Witter, R.C., Kelsey, H.M., and Hemphill-Haley, E., in review, Great Cascadia earthquakes and tsunamis of the past 6,700 years, Coquille River estuary, southern coastal Oregon: *Geological Society of America Bulletin*, submitted May 2002.
109. LACO Associates, 1999, Site Evaluation for the Child Development Center Fault Rupture Hazard, Phase C Investigation: Prepared for College of the Redwoods, Eureka, California, by LACO Associates Consulting Engineers, Eureka, California, 24 p. plus figures.
110. LACO Associates, 1999, Final Report of Seismic Study Phase 3 at College of the Redwoods, Eureka campus: Prepared for College of the Redwoods, Eureka, California, by LACO Associates Consulting Engineers, Eureka, California, 24 p. plus figures.
111. Park, J-O., Tsuru, T., Kodaira, S., Cummins, P.R., and Kaneda, Y., 2002, Splay fault branching along the Nankai subduction zone, *Science*, v. 297, no. 5584, p. 1154-1160.

HUMBOLDT BAY ISFSI FSAR UPDATE

112. Dupre, W. R., and thirteen others, 1991, Quaternary geology of the Pacific Margin, Chapter 7 *in* Morrison, R. B., ed., Quaternary Nonglacial Geology: Conterminous U. S., Decade on North American Geology, The Geology of North America, v. k-2, p. 141-214.
113. Bickner, F. R., Vadurro, G. A., Manhart, G. L., Lindberg, D. N., Watt, C. J., and Chaney, R. C., 2000, Use of microzonation to site facility on low-angle thrust and associated fault-bend folding: Fourth International Conference on Recent Advances in Geotechnical Earthquake Engineering and Soil Dynamics, Paper No. 11.01, 6 p.
114. Carver, G. A., and Burke, R. M., 1987, Late Pleistocene and Holocene paleoseismicity of the Little Salmon and Mad River thrust systems, northwestern California - implications to the seismic potential of the Cascadia subduction zone (abs.): Geological Society of America, Abstracts with Program, v. 19, p. 614.
115. Carver, G. A., 1992, Late Cenozoic tectonics of coastal northern California, *in* Carver, G. A., and Aalto, K. R. (eds.), Field Guide to the Late Cenozoic Subduction Tectonics and Sedimentation of Northern Coastal California, GB-71. Pacific Section, American Association of Petroleum Geologists, p. 1-11.
116. Carver, G. A., and Aalto, K. R., 1992, Late Cenozoic subduction tectonics and sedimentation, northern coastal California, *in* Carver, G. A., and Aalto, K. R. (eds.), Field Guide to the Late Cenozoic Subduction Tectonics and Sedimentation of Northern Coastal California, GB-71. Pacific Section, American Association of Petroleum Geologists, p. 59-74.
117. U. S. Geological Survey (USGS), 2002. U. S. Geological Survey's Northern California Earthquake Catalog, Northern California Seismic Network (NCSN) option. Online at <http://quake.geo.berkeley.edu/ncedc/catalog-search.html>. Accessed May 9 & 22, 2002.
118. Bakun, W. H., 2000, Seismicity of California's North Coast: Bulletin of the Seismological Society of America, v. 90, no. 4, p. 797- 812.
119. Topozada, T., Branum, D., Petersen, M., Hallstrom, C., Cramer, C., and Reichle, M., 2000, Epicenters of and areas damaged by $M \geq 5$ California earthquakes, 1800-1999, California Division of Mines and Geology, Map Sheet 49.
120. Topozada, T. R., Real, C. R., and Parke, D. L., 1981, Preparation of isoseismal maps and summaries of reported effects for pre-1900 California earthquakes: California Division of Mines and Geology Open-File Report 81-11SAC, 182 p.

HUMBOLDT BAY ISFSI FSAR UPDATE

121. Bakun, W. H., and Wentworth, C. M., 1997, Estimating earthquake location and magnitude from seismic intensity data: Bulletin of the Seismological Society of America, v. 87, p. 1502-1521.
122. Ellsworth, William, 1990, Earthquake history, 1769-1989, *in* The San Andreas Fault System, U. S. Geological Survey Professional Paper 1515, Robert Wallace (ed.), p 153- 187.
123. Meltzner, A. J., and Wald, D. J., 2002. (in preparation). Aftershocks and triggered events of the great 1906 California earthquake: Paper submitted to the Bulletin of the Seismological Society of America, January 2002.
124. Toppozada, T. R., Parke, D. L., and Higgins, C. T., 1978, Seismicity of California 1900-1931, California Division of Mines and Geology, Special Report 135, 39 p.
125. Toppazada. 2002. Personal Communication
126. Council of the National Seismic System (CNSS), 2002, Council of the National Seismic System (CNSS) Worldwide Earthquake Catalog. Online at <http://quake.geo.berkeley.edu/cnss/catalog-search.html>. Accessed May 9, 2002.
127. University of California at Berkeley (UCB), 2002, Northern California Earthquake Catalog with University of California Berkeley (UCB) option: Online at <http://quake.geo.berkeley.edu/catalog-search.html>. Accessed May 22, 2002.
128. NEIC, 2002, National Earthquake Information Center (NEIC) catalog. Online at http://wwwneic.cr.usgs.gov/neis/epic/epic_rect.html. Accessed June 3, 2002.
129. Eaton, J. P., 1989, Dense microearthquake network, *in* Litehiser, J.J. (ed.), Observatory Seismology, p. 199-224.
130. Tera Corporation, 1982, Report on the November 8, 1980 Trinidad-offshore earthquake and aftershocks, B-82-219, June 1982 (Revision 1).
131. Dengler, L., Moley, K., McPherson, R., Pasyanos, M., Dewey, J., and Murray, M, 1995, The September 1, 1994, Mendocino fault earthquake: California Geology, p 43-53.
132. U. S. Geological Survey (USGS), 2002. Northern California Seismic Network seismographic station list. Online at <http://quake.geo.berkeley.edu/ftp/pub/doc/ncsn.stations>. Accessed May 24, 2002.

HUMBOLDT BAY ISFSI FSAR UPDATE

133. Engdahl, E. R., and Rinehart, W. A., 1991, Seismicity map of North America project, *in* Slemmons, D. B., Engdahl, E. R., Zoback, M. D., and Blackwell, D. D. (eds.), *Neotectonics of North America: Geological Society of America, Boulder, Colorado, Decade Map Volume 1*, p. 21-27.
134. Gee, L. 2002. Personal Communications.
135. Oppenheimmer, D. H. 2000. Personal Communications.
136. Satake, K., Wang, K., and Atwater, B., 2002, Magnitude 9 persists for the 1700 Cascadia earthquake, *Seismological Research Letters*, v. 73, No 2, p. 241.
137. Stover, C. W., and Coffman, J. L., 1993. *Seismicity of the United States, 1568-1989 (Revised)*. U. S. Geological Survey Professional Paper 1527, p. 71-186.
138. Wong, I. G., 2002. The 1873 Brookings, Oregon Earthquake and its implications for intraplate seismicity and hazard within the Central Cascadia Subduction Zone, *Seismological Research Letters*, v. 73, no. 2, p. 214-215.
139. Topozada, T. R., and Parke, D. L., 1982. Areas damaged by California Earthquakes, 1900-1949, California Division of Mines and Geology, Open File Report 82-17 SAC, 64 p.
140. Dengler, L., McPherson, R., and Carver, G., 1992. Historic seismicity and potential areas of large earthquakes in North Coast California: Pacific Cell, *Friends of the Pleistocene Guidebook for the Field Trip to Northern Coastal California*, p. 112-118.
141. Tera Corporation, 1975, Humboldt Bay Seismic Network annual report, August 1974- August 1975, Rpt. No. TR-75-4013, 23 p.
142. Pacific Gas and Electric Company (PG&E), 1975, Internal Report on June 7, 1975, Ferndale Earthquake.
143. Bechtel Power Corporation, 1975, Seismic design review, revised trip report, June 7, 1975, earthquake: Letter to Pacific Gas and Electric Company Pertaining to Humboldt Bay Power Plant Unit 3, Bechtel Job no.10373, File 0270, 0515, July 30.
144. Terra Technology Services, 1980, Records of the earthquake of November 8, 1980, as recorded on the DCA-300 system at Humboldt Bay Power Plant: Terra Technology Services, Redmond, Washington.
145. U. S. Nuclear Regulatory Commission, 1980, NRC inspection: Memo to PG&E regarding the Earthquake of November 8, 1980, November 18.

HUMBOLDT BAY ISFSI FSAR UPDATE

146. Pacific Gas and Electric Company (PG&E), 1984, Eureka Earthquake of September 20, 1984: September 21, 1984 memo from G. C. Lenfestey. Memo included with Terra Technology Services, 1980 (see reference).
147. U. S. Nuclear Regulatory Commission, 1992, Inspection-report no 50-133/92-02: Memo to G. M. Rueger, Pacific Gas and Electric Company, Regarding April 25-26, 1992, Earthquakes, May 8.
148. Pacific Gas and Electric Company (PG&E), 1992, April 25, 1992, earthquake: April 27 Memo to R. G. Domer from L. S. Cluff, Geosciences Department.
149. Pacific Gas and Electric Company (PG&E), 1992, Effects of the April 25, 1992, Cape Mendocino earthquake and aftershocks at the Humboldt Bay Power Plant: August 31 Letter to the Nuclear Regulatory Commission from G. M. Rueger: NRC docket No. 50-133, OL-DPR-7, Humboldt Bay Power Plant, Unit 3, License Event Report 3-92-002-00.
150. Pacific Gas and Electric Company (PG&E), 1992, Engineering inspection of Humboldt Bay Power Plant following the April 25, 1992, earthquake: May 27 Memo from S. Bhattacharya and M. Tressler, Civil Engineering Department.
151. Pacific Gas and Electric Company (PG&E), 1994, Response to NRC request for information regarding the earthquake of December 26, 1994: December 28 Letter HBL-94-078 to the Nuclear Regulatory Commission, Attention G. M. Vasquez, NRC Docket No. 50-133, OL-DPR-7, Humboldt Bay Power Plant Unit 3.
152. Pacific Gas and Electric Company (PG&E), 1995, Analysis of the strong motion record at Humboldt Bay Power Plant from the magnitude 5.4 Eureka, California, earthquake of December 26, 1994: February 13 Memo to L. F. Womack from L. S. Cluff, Geosciences Department.
153. Eaton, J. P., 1981, Detailed study of the November 8, 1980 Eureka, California earthquake and aftershocks (abs.): Transactions, American Geophysical Union, v. 62, no. 45, p. 959.
154. McPherson, R., and Dengler, L., 1992, The Honeydew earthquake, California Geology, p. 31-39.
155. Oppenheimer, D. H., and Magee, M. E., 1991, Untitled Subject: The 1991 M 6.0 Honeydew, California, earthquake (abs.): EOS, Transactions of the American Geophysical Union, v. 72, p. 311.
156. Pacific Gas and Electric Company (PG&E), 1991, August 16 and 17, 1991, Northern California Earthquakes: Donald Brand, August 20, 1991.

HUMBOLDT BAY ISFSI FSAR UPDATE

157. Couch, R., 1980, Seismicity of crustal structure near the north end of the San Andreas fault system, *in* Steritz, R. and Sherbourne, R. (eds.), Studies of the San Andreas Fault Zone in Northern California: California Division of Mines and Geology Special Report 140, p. 139-152.
158. Hill, D. P., Eaton, J. P., and Jones, L. M., 1990, Seismicity, 1980-1986, in Robert Wallace (ed.), The San Andreas Fault System, California: U. S. Geological Survey Professional Paper 1515, p. 115-151.
159. M. Magee, personal communication, 2000
160. Geomatrix Consultants, Inc. (Geomatrix), 1994, Seismic ground motion study for Humboldt Bay bridges on Route 255, Humboldt County, California: Final Report Prepared for California Department of Transportation, Division of Structures, Sacramento, California, Contract No. 59N722, March.
161. Earth Science Associates (ESA), 1975, Geology of the Humboldt Bay Region with Special Reference to the Geology of the Humboldt Bay Power Plant Site and Vicinity: Report Prepared for Pacific Gas and Electric Company.
162. Earth Science Associates (ESA), 1977, Humboldt Bay Power Plant site geology investigations: Report Prepared for Pacific Gas and Electric Company.
163. LACO Engineering Consultants (LACO), 1997, Reports on surface faulting potential investigations: Prepared for College of the Redwoods, Humboldt County, California.
164. Burke, R. M., Carver, G.A., and Lundstrom, S.C., 1986, Soil development as relative dating and correlation tool on marine terraces of northern California: Geological Society of America Abstracts with Programs, v. 18, no. 2, p. 91.
165. Izett, G. A., Obradovich, J. D., and Mehnert, H. H., 1988, The Bishop ash bed (Middle Pleistocene), and some older (Pliocene and Pleistocene), chemically and mineralogically similar ash beds in California, Nevada and Utah: U. S. Geological Survey Bulletin 1675, 37 p.
166. Mankinen, E. A., and Dalrymple, G. B., 1979, Revised geomagnetic polarity time-scale for the interval 0-5 m.y. B.P.: Journal of Geophysical Research, v. 84, p. 615-626.
167. Geomatrix Consultants, Inc. (Geomatrix), 2002, Data Report F - Radiocarbon Dating of Trench Sample, Humboldt Bay ISFSI Project Seismic Hazards Analysis: Data Report Prepared for Pacific Gas and Electric Company Geosciences Department, Revision 0, 14 pp.

HUMBOLDT BAY ISFSI FSAR UPDATE

168. Geomatrix Consultants, Inc. (Geomatrix), 2002, Certification of geologic data obtained by Woodward-Clyde Consultants and Earth Sciences Associates that are used in the analysis of the Humboldt Bay ISFSI site, Humboldt Bay ISFSI Project Seismic Hazards Analysis: Report Prepared for Pacific Gas and Electric Company Geosciences Department, Rev. 0, 21 p.
169. Geomatrix Consultants, Inc. (Geomatrix), 2002, Data Report A—Geologic Mapping in the ISFSI Site Area, Humboldt Bay ISFSI Project Seismic Hazards Analysis: Data Report Prepared for Pacific Gas and Electric Company Geosciences Department, May 4, Revision 0, 33 pp.
170. Carver, G. A., 2002, Seismic source characterization of the Cascadia subduction zone: Contained as Appendix 5A in Pacific Gas and Electric Company Technical Report TR-HBIP-2002-01, Seismic Hazard Assessment for the Humboldt Bay ISFSI Project, p. 5A-1 to 5A-7.
171. Cohee, B. P., Somerville, P. G., and N. A. Abrahamson (1991). Simulated ground motions for hypothesized $M_w = 8$ subduction zone earthquakes in Washington and Oregon, Bull. Seism. Soc. Am., Vol. 81, No. 1, p. 28-56.
172. Wells, D. L., and Coppersmith, K. J., 1994, New empirical relationships among magnitude, rupture length, rupture width, rupture area, and surface displacement: Bulletin of the Seismological Society of America, v. 84, p. 974-1002.
173. Abe, K., 1981, Magnitudes of large shallow earthquakes from 1904 to 1980: Physics of the Earth and Planetary Interiors, v. 27, p. 72-92.
174. Abe, K., 1984, Complements to "Magnitude of large shallow earthquakes from 1904 to 1980": Physics of the Earth and Planetary Interiors, v. 34, p. 17-23.
175. Geomatrix Consultants, Inc. (Geomatrix), 1993, Seismic margin earthquake for the Trojan site: Final Report Prepared for Portland General Electric Trojan Nuclear Plant, Rainier, Oregon.
176. Bevington, P. R. (1969). Data Reduction and Error Analysis for the Physical Sciences, McGraw-Hill. 336 pp.
177. National Geographic Society, 1995, Living on the Edge: The National Geographic Society, Washington, D. C., plate printed February 1995, published April 1995.
178. Regulatory Guide 3.73 "Site Evaluations and Design Earthquake Ground Motion for Dry Cask Independent Spent Fuel Storage and Monitored Retrievable Storage Installations" (formerly DG-3021), prepublication issue September 2003

HUMBOLDT BAY ISFSI FSAR UPDATE

179. Valera and others, "Supplemental Report No. 2, Evaluation of Liquefaction Potential, Humboldt Bay Power Plant", prepared by Dames and Moore for Pacific Gas and Electric Company, dated January 21, 1976.
180. Pacific Gas and Electric Company (PG&E), 2002, Calculation GEO.HBIP.02.04; Development of response spectra for the HBPP ISFSI, Revision 0.
181. Pacific Gas and Electric Company (PG&E), 2002, Calculation GEO.HBIP.02.06; Site amplification factors for HBIP, Revision 0.
182. Pacific Gas and Electric Company (PG&E), 2002, Calculation GEO.HBIP.02.05; Development of HBIP ISFSI spectrum compatible time histories, Revision 0.
183. Abrahamson, N. A., and Shedlock, K. M., 1997, Overview: Seismological Research Letters, v. 68, p. 9-23.
184. Abrahamson, N. A. and W. J. Silva, 1996, Empirical Ground Motion Models, Appendix A in Silva et al. (1997).
185. Somerville, P. G., Smith, N. F., Graves, R. W., Abrahamson, N. A., 1997, Modification of empirical strong motion attenuation relations to include the amplitude and duration effects of directivity: Seismological Research Letters, v. 68, p. 199-222.
186. M. Idriss, Personal Communication, 1999
187. W. Silva, Personal Communication, 1998
188. Pacific Gas and Electric Company (PG&E), 2003, Calculation GEO.HBIP.03.04; Development of Probabilistically Based Spectra for the HBIP ISFSI Site, Revision 0.
189. Geomatrix Consultants, Inc. (Geomatrix), 2002, Calculation GEO.HBIP.02.02, Determination of liquefaction potential at HBIP ISFSI site, Revision 0,
190. Geomatrix Consultants, Inc. (Geomatrix), 2002, Calculation GEO.HBIP.02.07, Determination of potential earthquake-induced displacements of critical slides at HBIP ISFSI site, Revision 1.
191. Geomatrix Consultants, Inc. (Geomatrix), 2002, Calculations GEO HBIP.02.08, Determination of potential earthquake-induced displacements of critical slides along HBIP ISFSI transport route, Revision 1.
192. Geomatrix Consultants, Inc. (Geomatrix), 2002, Data Report B–Boring Logs, Data Report Prepared for Pacific Gas and Electric Company Geosciences Department, Revision 0, May 4, 64 pp.

HUMBOLDT BAY ISFSI FSAR UPDATE

193. Geomatrix Consultants, Inc. (Geomatrix), 2002, Data Report E—Soil Laboratory Test Data, Humboldt Bay ISFSI Project Seismic Hazards Analysis: Data Report Prepared for Pacific Gas and Electric Company Geosciences Department, Revision 0, 254 p.
194. Geomatrix Consultants, Inc. (Geomatrix), 2002, Data Report C - Downhole Geophysics in ISFSI Site Area, Humboldt Bay ISFSI Project Seismic Hazards Analysis: Data Report Prepared for Pacific Gas and Electric Company Geosciences Department, Revision 0, 220 pp.
195. Seed, H. B., Tokimatsu, K., Harder, L. F., and Chung, R., 1985, Influence of SPT procedures in soil liquefaction resistance evaluations: Journal of Geotechnical Engineering Division, American Society of Civil Engineers, v. 111, no. 12, p. 1425-1445.
196. Youd, T. L., and Idriss, I. M. (eds.), 1997, Proceedings of National Center for Earthquake Engineering Research (NCEER) Workshop on Liquefaction Resistance of Soils: State University of New York, Buffalo.
197. Youd, T. L., Idriss I. M., Andrus, R. D., Arango, I., Castro, G., Christian, J., Dobry, R., Finn, W. D. L., Harder, L. F., Hynes, M. E., Ishihara, K., Koester, J. P., Liao, S. S. C., Marcuson, W. F., Martin, G. R., Mitchell, J. K., Moriwaki, Y., Power, M. S., Robertson, P. K., Seed, R. B., Stokoe, K. H. (2001), Liquefaction resistance of soils: summary report from the 1997 NCEER and 1998 NCEER/NSF workshops on evaluation of liquefaction resistance of soils, Journal of geotechnical and geoenvironmental engineering, American Society of Civil Engineers, 127(10), pp. 817-833.
198. Newmark, N. M., 1965, Effects of earthquakes on dams and embankments: Geotechnique, v. 15, no. 2, p. 139-160.
199. Makdisi, F. I., and Seed, H. B., 1978, Simplified procedure for estimating dam and embankment earthquake-induced deformations: Journal of the Geotechnical Engineering Division, American Society of Civil Engineers, v. 104, no. GT7, p. 849-867.
200. Plafker, G., Kachadoorian, R., Eckel, E. B., and Mayo, L. R., 1969, Effects of the earthquake of March 27, 1964, on various communities: U. S. Geological Survey Professional Paper 542-G, 50 p.
201. Gordon, F. R., 1971, Faulting during the earthquake at Meckering, western Australia - 14 October 1968: Royal Society of New Zealand Bulletin 9, p. 95-96.
202. Bilham, R., and Yu, T., 2000, The morphology of thrust faulting in the 21 September 1999, Chichi, Taiwan, earthquake: Journal of Asian Earth Sciences, 18, p. 351-367.

HUMBOLDT BAY ISFSI FSAR UPDATE

203. Kelson, K. I., Kang, K.-H., Page, W. D., Lee, C.-T., and Cluff, L. S., 2001, Representative styles of deformation along the Chelungpu fault from the 1999 Chi-Chi (Taiwan) earthquake—geomorphic characteristics and responses of man-made structures: *Bulletin of the Seismological Society of America*, v. 91, no. 5, p. 930-952.
204. Carver, G. A., and McCalpin, J. P., 1996, Paleoseismology of compressional tectonic environments, Chapter 5 *in* McCalpin, J. P., ed., *Paleoseismology*: Academic Press, p. 183-270.
205. Cashman, S., and Cashman, K., 1999, Cataclasis and deformation-band formation in unconsolidated marine terrace sand, Humboldt County, California: *Geology*, v. 28, no. 2, p. 111-114.
206. Suppe, J., 1983, Geometry and kinematics of fault-bend folding: *American Journal of Science*, v. 283, p. 684-721.
207. Yeats, R. S., 1986, Active faults related to folding, *in* Wallace, R. E., ed., *Active Tectonics*: National Academy Press, Washington, D. C., p. 63-79.
208. Philip, H., and Meghraoui, M., 1983, Structural analysis and interpretation of the surface deformations of the El Asnam earthquake of October 10, 1980: *Tectonics*, v. 2, p. 17-49.
209. Patton, J.R., Witter, R.C., Kelsey, H.M., Hemphill-Haley, E., Carver, G.A., and Koehler, R.D., 2002, Coseismic subsidence from combined upper-plate and subduction zone earthquakes in southern Humboldt Bay, California, over the past 3000 years (abstract): *Seismological Research Letters*, v. 73, No, 2, p. 208.
210. Pacific Gas and Electric Company (PG&E), 1966, Letter to R. L. Doan, Director of Reactor Licensing, U. S. A.E.C. from R. H. Peterson, that summarizes Dr. Wiegel's conclusions on the tsunami potential at the PG&E's Humboldt Bay Power Plant: 4 p. plus Wiegel's 1965 report, "Tsunamis at the site of the Pacific Gas and Electric Company Power Plant at Buhne Point, Humboldt Bay, California", plus figures and appendix.
211. Bourgeois, J., and Reinhart, M. A., 1989, Onshore erosion and deposition by the 1960 tsunami at the Rio Lingue estuary, south-central Chile (abs.): *EOS, Transactions of the American Geophysical Union*, v. 70, no. 43, p. 1331.
212. Benson, B. E., Grimm, K. A., and Clague, J. J., 1997, Tsunami deposits beneath tidal marshes on northwestern Vancouver Island, British Columbia: *Quaternary Research*, v. 48, p. 192-204.

HUMBOLDT BAY ISFSI FSAR UPDATE

- 213. Myers, E.P., Baptista, A.M., and Priest, G.R., 1999, Finite element modeling of potential Cascadia subduction zone tsunamis: Science of Tsunami Hazards 17, (1), 3-18.
- 214. Priest, G.R., Myers, E.P., Baptista, A.M., Fluck, P., Wang, K., and Peterson, C.D., 2000, Source simulation for tsunamis: lessons learned from fault rupture modeling of the Cascadia Subduction zone: Science of Tsunami Hazards, 18, (2), 77-106.
- 215. Bates, R.L., and Jackson, J.A., 1987, Glossary of geology (third edition): American Geological Institute, Alexandria, Virginia, 788 p.
- 216. González, F. I., 1999, TSUNAMI!: Scientific American, v. 280, no. 6, p. 56-65.
- 217. Kachadoorian, R. and Plafker, G., 1967, Effects of the earthquake of March 27, 1964 on communities of Kodiak and nearby islands, The Alaska Earthquake March 27, 1964, Effects on Communities, Kodiak Area: U.S. Geological Survey Professional Paper 542-F, 41 p.
- 218. 218. NOAA report August 22, 1984, 941-8767
- 219. Pacific Gas and Electric Company (PG&E), 1985, Memorandum report, flood hydrology, Humboldt Bay Power Plant, Unit No. 3, section 7 Tsunami, pp. 31-37.
- 220. Lander, J. F., Lockridge, P. A., and Kozuch, M. J., 1993, Tsunamis affecting the West Coast of the United States, 1806-1992: National Oceanic and Atmospheric Administration, Boulder, National Geophysical Data Center Key to Geophysical Records, Documentation No. 29, 242 p.
- 221. Darienzo, M. E., and Peterson, C. D., 1990, Episodic tectonic subsidence of late Holocene salt marshes, northern Oregon, central Cascadia margin: Tectonics, v. 9, no. 1, p. 1-22.
- 222. Carver, G. A., Abramson, H. A., Garrison-Laney, C. E., and Leroy, T., 1998, Investigation of paleotsunami evidence along the north coast of California: Final Report for Pacific Gas and Electric Company, 164 p. plus appendices.
- 223. Abramson, H.A., 1998, Evidence for tsunamis and earthquakes during the last 3500 years from Lagoon Creek, a coastal freshwater marsh, northern California: MS Thesis, Department of Geology, Humboldt State University, Arcata, 76 p.
- 224. Garrison-Laney, C. E., 1998, Diatom evidence for tsunami inundation from Lagoon Creek, a coastal freshwater pond, Del Norte County, California: M.S. thesis, Department of Geology, Humboldt State University, Arcata, California, 97 p.

HUMBOLDT BAY ISFSI FSAR UPDATE

- 225. Leroy, T.H., 1999, Holocene sand dune stratigraphy and Paleoseismicity of the north and south spits of Humboldt Bay, northern California: MS Thesis, Department of Geology, Humboldt State University, Arcata, 44 p.
- 226. Atwater, B. F., 1987, Evidence for great Holocene earthquakes along the outer coast of Washington State: *Science*, v. 236, p. 942-944.
- 227. Clague, J. J., and Bobrowsky, P. T., 1994, Evidence for a large earthquake and tsunami 100-400 years ago on western Vancouver Island, British Columbia: *Quaternary Research*, v. 41, p. 176-184.
- 228. Clague, J. J., and Bobrowsky, P. T., 1994, Tsunami deposits beneath tidal marshes on Vancouver Island, British Columbia: *Geological Society of America Bulletin*, v. 106, p. 1293-1303.
- 229. Nelson, A. R., Jennings, A. E., and Kashima, K., 1996, An earthquake history derived from stratigraphic and microfossil evidence of relative sea-level change at Coos Bay, southern coastal Oregon: *Geological Society of America Bulletin*, v. 108, no. 2, p. 141-154.
- 230. Nelson, A. R., Kelsey, H. M., Hemphill-Haley, E., and Witter, R. C., 1996b, A 7500-yr record of Cascadia tsunamis in southern coastal Oregon (abs.): *Geological Society of America, Abstracts with Programs*, v. 28, no. 5, p. 95.
- 231. Clague, J. J., Bobrowsky, P. T., and Hamilton, T. S., 1994, A sand sheet deposited by the 1964 Alaska tsunami at Port Alberni, British Columbia: *Estuarine Coastal Shelf Science*, no. 38, p. 413-421.
- 232. Hughes, J. F., Mathews, R.W., Clague, J.J., Guibault, J.-P., and Hutchinson, I., 2002, Rapid crustal rebound followed the 1700 Cascadia earthquake at Tofino, British Columbia (abstract): *Seismological Research Letters*, v. 73, No. 2, p. 241.
- 233. Kroeber, A. L., 1976, Yurok Myths, Univ. of California Press, Berkeley, CA. 488 p.
- 234. Carver, D. H., and Carver, G. A., 1996, Earthquake and thunder - native oral histories of paleoseismicity along the southern Cascadia subduction zone (abs): *Geological Society of America, Cordilleran Section, Abstracts with Program, Annual Meeting*, v.28, no. 5, p. 54.
- 235. Carver, G. A., 2002, Written communication documenting the elevation of the pebble layer at North Spit, Humboldt Bay, California: Letter from Gary Carver to William D. Page (PG&E Geosciences) dated October 28, 2002, 2 p.
- 236. Vick, G., 1989: Late Holocene paleoseismicity and relative vertical crustal movements, Mad River slough, Humboldt Bay, California: M.S. Thesis, Department of Geology, Humboldt State University, Arcata, California, 88 p.

HUMBOLDT BAY ISFSI FSAR UPDATE

- 237. Yamaguchi, D. K., Atwater, B. F., Bunker, D. E., Benson, B. E., and Reid, M. S., 1997, Tree-ring dating the 1700 Cascadia earthquake: *Nature* (London), v. 389 (6654), p. 922-923.
- 238. Garrison-Laney, C. E., Abramson, H. F., and Carver, G. A., 2002, Late Holocene tsunamis near the southern end of the Cascadia subduction zone (abstract): *Seismological Research Letters*, v. 73, No. 2, p. 248.
- 239. Wilson, B.W., and Torum, A., 1968, The tsunami of the Alaskan earthquake, 1964, U.S. Army Coastal Engineering Research Center publication, Technical Memorandum No. 25, 401 p.
- 240. Mofjeld, H. O., Foreman, M. G., and Ruffman, A., 1997, West Coast tides during Cascadia subduction zone tsunamis, *Geophysical Research Letters*, v. 24, no. 17, p. 2215-2218.
- 241. Atwater, B. F., and Moore, A. L., 1992, A tsunami about 1,000 years ago in Puget Sound, Washington: *Science*, v. 258, p. 1614-1617.
- 242. Moore, A. L., 1994, Evidence for a tsunami in Puget Sound ~1000 years ago: M. S. project, Department of Geological Sciences, University of Washington, 37 p.
- 243. Clarke, S. H., Greene, H. G., and Kennedy, M. P., 1985, Identifying potentially active faults and unstable slopes offshore: *in* J. I. Ziony (ed.), *Evaluating earthquake hazards in the Los Angeles region; an earth-science perspective*, U. S. Geological Survey Professional Paper, P 1360, p. 347-373.
- 244. Field, M. E., Clark, S.H., Jr., and White, M. E., 1980, Geology and geologic hazards of the offshore Eel River Basin, northern California continental margin, U. S. Geological Survey Open File Report 80-1080, 80 pp.
- 245. Gardner, J. V., Prior, D.B., and Field, M.E., 1999, Humboldt Slide - a large shear-dominated retrogressive slope failure, *Marine Geology*, 154, p. 323-338.
- 246. Lee, H. J., Syvitski, J. P. M., Parker, G., Orange, D., Locat, J., Hutton, W. E. H., and Imran, J., 2002, Distinguishing sediment waves from slope failure deposits: field examples, including the 'Humboldt slide' and modeling results, *Marine Geology*, in press.
- 247. Cacchione, D. A., Pratson, L. F., and Ogston, A. S., 2002, The shaping of continental slopes by internal tides, *Science*, 296, 724-727.
- 248. Garrison, C., Abramson, H. A., and Carver, G. A., 1997, Evidence for repeated tsunami inundation from two freshwater coastal marshes, Del Norte County, California: Geological Society of America, Cordilleran Section, Abstracts with Program, v. 29, no. 5, p. 15.

HUMBOLDT BAY ISFSI FSAR UPDATE

- 249. Clarke and Field, 1989, Mapping of the continental margin offshore of northern California has identified many ancient landslides on the sea floor.
- 250. Goldfinger, C., and Watts, P., 2001, Tsunamigenic mega-slides on the southern Oregon Cascadia margin: ITS 2001 Proceedings, Session 3, no. 3-3.
- 251. Plafker, G., 2002, Review of empirical data on tsunami runup versus earthquake source parameters: Report to Pacific Gas and Electric Company, 18 p. plus figures.
- 252. Plafker, G., 2002, Comparison of the southern Cascadia subduction zone with the tectonic setting of the 1964 Alaska earthquake: Report to Pacific Gas and Electric Company, 13 p. plus figures.
- 253. Brandsma, M, Divoky, D., and Hwang, L., 1979, Tsunami atlas for the coasts of the United States, "NUREG/CR-1106, TC-486, Prepared by Tetra Tech, Inc. for the U. S. Nuclear Regulatory Commission.
- 254. Camfield, F.E., 1980, Tsunami engineering: Special Report No. 6, U.S. Army Corps of Engineers, Coastal Research Center, Fort Belvoir, Virginia.
- 255. Houston, J.R., and Garcia, A.W., 1980, Type 16 flood insurance study: tsunami predictions for the West Coast of the continental United States: Technical Report H-78-26, U.S. Army Corps of Engineer Waterways Experiment Station, Vicksburg, Mississippi.
- 256. Whitmore, P. M., 1993, Expected tsunami amplitudes and currents along the North American coast for Cascadia subduction zone earthquakes: Natural Hazards, v. 8, p. 59-73.
- 257. Lamberson, R.H., Grimes, S. and Scarr, D., 1998, A tsunami simulation and shoreline inundation model for Humboldt Bay, pilot study: Report to PG&E Geosciences Department, 43 p.
- 258. Baptista, A., 2002, Personal communication – telephone memorandum by Hans Abramson (Geomatrix Consultants, Oakland, CA), July, 2002
- 259. Easterbrook, D.J., 1993, Surface Processes and landforms: McMillan Publishing Company, New York, 520 p.
- 260. Plafker, Personal Communication, 2002
- 261. Plafker, G and Kachadoorian, R., 1966, Geologic effects of the March 27, 1964 earthquake and associated seismic sea waves on Kodiak and nearby islands Alaska, The Alaskan Earthquake March 27, 1964, Regional Effects, Kodiak and Nearby Islands: U S Geological Survey Professional Paper 543-D, 46 p.

HUMBOLDT BAY ISFSI FSAR UPDATE

- 262. Valentine, D. W., 1992, Late Holocene stratigraphy as evidence for late Holocene paleoseismicity, southern Cascadia subduction zone, Humboldt Bay, California: MS Thesis, Humboldt State University, Arcata, California, 99 p.
- 263. Peterson, C. D., Barnett, E. T., Briggs, G. G., Carver, G. A., Clague, J. J., and Darienzo, M. E., 1997, Estimates of coastal subsidence from great earthquakes on the Cascadia subduction zone, Vancouver Island, B. C., Washington, Oregon, and northernmost California., Oregon Department of Geology and Mineral Industries, Open-File Report O-97-5, 44 p.
- 264. Douglas, B.C., 1991, Global sea level rise, *Journal of Geophysical Research*, vol. 96, no. C4, pp. 6981-6992.
- 265. Buwalda, J., and St. Amand, P., 1955, Geological effects of the Arvin-Tehachapi earthquake, *in* Oakeshot, G., ed., *Earthquakes in Kern County California during 1952*: California Department of Natural Resources, Division of Mines and Geology Bulletin 171, p. 41-56.
- 266. Stein, R. S., and Thatcher, W., 1981, Seismic and aseismic deformation associated with the 1952 Kern County, California, earthquake and relationship to the Quaternary history of the White Wolf fault: *Journal of Geophysical Research*, v. 86, p. 4913-4918.
- 267. Malloy, R. J., 1964, Crustal uplift southwest of Montague Island, Alaska: *Science*, v. 146, p. 1048-1049.
- 268. Gordon, F. R., and Lewis, J. D., 1980, The Meckering and Calingiri earthquakes, October 1968 and March 1970: *Geological Survey of Western Australia Bulletin* 126, 229 p.
- 269. Lenson, G. J., and Suggate, R. P., 1968, Preliminary reports on the Inangahua earthquake, New Zealand: *Department of Scientific and Industrial Research Bulletin* 193, p. 17-36.
- 270. Lenson, G. J., and Otway, P. M., 1971, Earthshift and post-earthquake deformation associated with the May 1968 Inangahua earthquake, New Zealand: *Royal Society of New Zealand Bulletin* 9, p. 107-116.
- 271. Anderson, H., Beanland, S., Blick, G., Darby, D., Downes, G., Haines, J., Jackson, J., Robinson, R., and Webb, T., 1994, The 1968 May 23 Inangahua, New Zealand, earthquake—an integrated geological, geodetic and seismological source model: *New Zealand Journal of Geophysics*, v. 37, p. 59-86.
- 272. Sharp, R. V., 1975, Displacement on tectonic ruptures: *California Division of Mines and Geology Bulletin* 196, p. 187-194.

HUMBOLDT BAY ISFSI FSAR UPDATE

- 273. Berberian, M., 1979, Earthquake faulting and bedding thrusts associated with the Tabas-Golshan (Iran) earthquake of 16 September 1978: *Seismological Society of America Bulletin*, v. 69, p. 1861-1867.
- 274. Berberian, M., 1982, Aftershock tectonics of the 1978 Tabas-Golshan (Iran) earthquake sequence—a documented active thin- and thick-skinned tectonic case: *Geophysical Journal of the Royal Astronomical Society*, v. 68, p. 499-530.
- 275. Yielding, G., Jackson, J. A., King, G. C. P., Sinvhal, H., Vita-Finzi, C., and Wood, R. M., 1981, Relations between surface deformation, fault geometry, seismicity and rupture characteristics during the El Asman (Algeria) earthquake of 10 October 1980: *Earth and Planetary Sciences Letters*, v. 56, p. 287-304.
- 276. Crone, A. J., Machette, M. N., and Bowman, J. R., 1992, Geologic investigations of the 1988 Tennant Creek, Australia, earthquakes - implications for paleoseismicity in stable continental regions: *U. S. Geological Survey Bulletin* 2031-A, 51 p.
- 277. Philip, H., Rogozhin, E., Cisternas, A., Bousquet, J. C., Borisov, B., and Karakhanian, A., 1992, The Armenian earthquake of 1988 December 7 - faulting and folding, neotectonics and paleoseismicity: *Geophysics Journal International*, v. 110, p. 141-158.
- 278. Sun, J. I., 2004, *Assessment of Vertical Ground Motions on Slope Stability*.
- 279. PG&E Letter HIL-04-007, Response to NRC Request for Additional Information for the Humboldt Bay Independent Spent Fuel Storage Installation Application, October 1, 2004.

HUMBOLDT BAY ISFSI FSAR UPDATE

TABLE 2.1-1

POPULATION TRENDS OF THE STATE OF CALIFORNIA AND OF HUMBOLDT AND TRINITY COUNTIES

<u>Year</u>	<u>California</u>	<u>Humboldt County</u>	<u>Trinity County</u>
1940	6,907,387	45,812	3,970
1950	10,586,233	69,241	5,087
1960	15,717,204	104,892	9,706
1970	19,953,134	99,692	7,615
1980	23,668,562	108,514	11,858
1990	29,760,021	119,118	13,063
2000	33,871,648	126,518	13,022

Source: State of California Department of Finance 2002

HUMBOLDT BAY ISFSI FSAR UPDATE

TABLE 2.1-2

POPULATION CENTERS WITHIN 50 MILES OF ISFSI SITE

Community	Distance and Direction from Site	2000 Population	1990 Population	1980 Population	1970 Population
Arcata	15 miles NE	16,651	15,197	12,340	8,985
Bayview	3 miles NNE	2,359	1,318	na	na
Blue Lake	16 miles NE	1,135	1,235	1,201	1,112
Cutten	5 miles ENE	2,933	1,516	2,375	2,228
Eureka	4 miles NNE	26,128	27,025	24,153	24,337
Ferndale	12 miles SSW	1,382	1,331	1,367	1,352
Fortuna	11 miles SSE	10,497	8,788	7,591	4,203
Humboldt Hill	2 miles SE	3,246	2,865	na	na
Hydesville	15 miles SSE	1,209	1,131	na	na
McKinleyville	18 miles NNE	13,599	10,749	7,772	na
Myrtletown	9 miles ENE	4,459	4,413	3,959	na
Pine Hills	3 miles NE	3,108	2,947	2,686	na
Redway	45 miles SSE	1,188	1,212	1,094	na
Rio Dell	18 miles SSE	3,174	3,012	2,687	2,817
Trinidad	30 miles N	311	362	379	300
Westhaven- Moonstone	21 miles NNE	1,044	1,109	na	na
Willow Creek	35 miles ENE	1,743	1,576	na	na
Total		94,166	85,786	67,604	45,334

Source: State of California Department of Finance
na = not available

HUMBOLDT BAY ISFSI FSAR UPDATE

TABLE 2.1-3

AGE AND SEX OF TOTAL POPULATION: 2000 HUMBOLDT COUNTY, CALIFORNIA

<u>Age Group</u>	<u>Both Sexes</u>	<u>Number</u>		<u>Percent of Total</u>		
		<u>Male</u>	<u>Female</u>	<u>Both Sexes</u>	<u>Male</u>	<u>Female</u>
Total Population	126,518	62,532	63,986	100.0	100.0	100.0
Under 5 years	7,125	3,671	3,454	5.6	5.9	5.4
5 to 9 years	7,899	4,086	3,813	6.2	6.5	6.0
10 to 14 years	8,817	4,470	4,347	7.0	7.1	6.8
15 to 17 years	5,572	2,847	2,725	4.4	4.6	4.3
18 and 19 years	4,453	2,193	2,260	3.5	3.5	3.5
20 to 24 years	11,209	5,630	5,579	8.9	9.0	8.7
25 to 34 years	16,016	8,353	7,663	12.7	13.4	12.0
35 to 44 years	18,679	9,148	9,531	14.8	14.6	14.9
45 to 54 years	19,861	9,894	9,967	15.7	15.8	15.6
55 to 59 years	6,313	3,140	3,173	5.0	5.0	5.0
60 to 64 years	4,798	2,375	2,423	3.8	3.8	3.8
65 to 74 years	8,020	3,702	4,318	6.3	5.9	6.7
75 to 84 years	5,754	2,408	3,346	4.5	3.9	5.2
85 years and over	2,002	615	1,387	1.6	1.0	2.2
Under 18 years	29,413	15,074	14,339	23.2	24.1	22.4
18 to 64 years	81,329	40,733	40,596	64.3	65.1	63.4
65 years and older	15,776	6,725	9,051	12.5	10.8	14.1

Source: US Census Bureau, 2000 Census of Population and Housing

HUMBOLDT BAY ISFSI FSAR UPDATE

TABLE 2.1-4

PERCENT OF POPULATION BY RACE FOR THE STATE OF CALIFORNIA AND FOR HUMBOLDT AND TRINITY COUNTIES

Race	Percent of Total Population		
	California	Humboldt County	Trinity County
Hispanic or Latino	32.4	6.5	4.0
White	46.7	81.6	86.6
Black or African American	6.4	0.8	0.4
Native American	0.5	5.3	4.5
Asian	10.8	1.6	0.4
Pacific Islander	0.3	0.2	0.1
Some other race	0.2	0.4	0.1
Two or more races:	2.7	3.7	3.9

Source: US Census Bureau, 2000 Census of Population and Housing

HUMBOLDT BAY ISFSI FSAR UPDATE

TABLE 2.1-5

STATE AND COUNTY PARKS AND PUBLIC LANDS WITHIN 50 MILES OF ISFSI SITE

State Parks (SP)	County Parks (CP)	Public Lands
Humboldt Lagoons SP	Mad River CP	Six Rivers National Forest
Patrick's Point SP	Moonstone Beach CP	Humboldt Bay National Wildlife Refuge
Trinidad State Beach	Table Bluff CP	Arcata Marsh and Wildlife Sanctuary
Little River SP	Centerville Beach CP	Avenue of the Giants
Grizzly Creek Redwoods SP	Freshwater CP	Samoa Dunes
Humboldt Redwoods SP	Clam Beach CP	Trinity Alps Wilderness
Fort Humboldt State Historic Park		Redwood National Park

HUMBOLDT BAY ISFSI FSAR UPDATE

TABLE 2.2-1

FIRE/EXPLOSIVE HAZARDS

Event No. ^(a)	Hazard	Size	Distance from ISFSI	Distance from Transport Route ^(b)			Mode Applicability		
							Storage – with all Vault Lids Installed	Storage – Vault Lid Removed from one Cell for Maintenance/Inspection	Transport – Cask Removed from one Cell for Maintenance/Inspection
OFFSITE HAZARDS									
N/A	Off-site Industrial Facilities – Chevron Terminal	Largest single storage tank is 30,000 barrels of either gasoline or diesel fuel oil	2 miles	2 miles			Not Applicable.	Not Applicable.	Not Applicable.
E6	Vehicles on Route 101	Equivalent 50,000 pounds of TNT	2,000 ft	1,500 ft			Not Applicable.	Not Applicable.	Applicable, but no control needed.
N/A	Railroad	N/A	1,200 ft	700 ft			Not Applicable.	Not Applicable.	Not Applicable.
F11, E8	Shipping in Bay	87,000 barrels of gasoline	4,500 ft	Spent fuel transport is not allowed when shipping is in the area			Applicable, but no controls needed. Acceptable explosion evaluation per FSAR Section 8.2.6.2.8.	Administrative controls ^c (no shipping, Coast Guard).	Administrative controls ^d (no shipping, Coast Guard).
ONSITE HAZARDS									
F1, E5	Transporter Fuel Tank ^(e)	50 – gallon capacity	0 ft	0 ft			Not Applicable, but evaluation is still valid.	Administrative controls ^d (50-gal max, fire watch with fire-fighting equipment).	Applicable. Administrative controls ^d (50-gal max, fire watch with fire-fighting equipment).
F1.1, E5.1	Mobile Crane (diesel-powered), Forklift (diesel-powered)	Administratively controlled to not exceed 50 gallons	0 ft	0 ft			Not Applicable.	Administrative controls ^d (fire watch with fire-fighting equipment).	Applicable. Administrative controls ^d (fire watch with fire-fighting equipment).
F2, E5	Vehicle Fuel Tank	20- gallon capacity	50 ft	175 ft			Applicable, bounded by F1 evaluation based on volume (50 vs 20 gal). Acceptable explosion evaluation per FSAR Section 8.2.6.2.5. Administrative controls (gas vehicle distance, vehicle gas volume).	Applicable, bounded by F1 evaluation based on volume (50 vs 20 gal). Administrative controls ^c (gas vehicle distance, vehicle gas volume).	Applicable, bounded by F1 evaluation based on volume (50 vs 20 gal). Administrative controls ^d (vehicle distance, vehicle gas volume).
F3	Fuel Oil Tanks – 1 large tank ^(b)	2,760,169 gallon capacity	322 ft Unit 1	322 ft Unit 1			Not Applicable, but evaluation is still valid.	Not Applicable, but evaluation is still valid.	Not Applicable, but evaluation is still valid.
F3	Fuel Oil Service Tanks – 2 small tanks ^(b)	120,120- gallon capacity	237 ft Unit 1 and 198 ft Unit 2	237 ft Unit 1 and 198 ft Unit 2			Not Applicable, but evaluation is still valid.	Not Applicable, but evaluation is still valid.	Not Applicable, but evaluation is still valid.

HUMBOLDT BAY ISFSI FSAR UPDATE

TABLE 2.2-1

Event No. ^(a)	Hazard	Size	Distance from ISFSI	Distance from Transport Route ^(b)			Mode Applicability		
							Storage – with all Vault Lids Installed	Storage – Vault Lid Removed from one Cell for Maintenance/Inspection	Transport – Cask Removed from one Cell for Maintenance/Inspection
F3	Diesel Oil Storage Tank – 1 large tank ^(b)	84,940- gallon capacity	232 ft	232 ft					
F4	Fuel/Diesel Oil Tanker Trucks	7,500-gallon capacity	80 ft fuel/80 ft Diesel	The fuel oil tanker truck is not allowed in area during spent fuel transport. The diesel oil tanker truck will be allowed to move on its normal route, but will be controlled to not move closer than 280 ft from the ISFSI or the transporter during transporter operations.			Applicable, but no controls needed.	Applicable. Administrative controls ^d (not allowed w/in 80 ft).	Applicable. Administrative controls ^d (tankers not allowed on HBPP site).
F5, E4	Gasoline Storage Tank and Tanker Truck ^(b)	120-gallon capacity tank and 3,000-gallon capacity tanker truck	Over 500 ft	135 ft			Not Applicable, but evaluation is still valid.	Not Applicable, but evaluation is still valid.	Not Applicable, but evaluation is still valid.
F9, E2	12 inch 30# Natural Gas Line ^(b)	12 inch line	377 ft, local detonation and vapor cloud concern	Gas line is depressurized during transport			Not Applicable, but evaluation is still valid.	Not Applicable, but evaluation is still valid.	Not Applicable, but evaluation is still valid.
F9, E2	12 inch 400# Natural Gas Line	12 inch line	1,100 ft, no line of sight to ISFSI	409 ft, local detonation and vapor cloud concern			Applicable, but no controls needed.	Applicable. Administrative controls ^d (prior leak walkdown)	Applicable. Administrative controls ^d (prior leak walkdown)
E7	Fossil Power Plant Explosion ^(b)	4 plants	2@454 ft/ 2@≥900ft	227 ft			Not Applicable.	Not Applicable.	Not Applicable.
E9	Compressed Gas Bottles	Various	Various locations. Not stored at ISFSI	Not allowed in area during transport			Applicable. Administrative controls (no storage at ISFSI).	Applicable. Administrative controls ^d (no storage at ISFSI).	Applicable. Administrative controls ^d (no storage at ISFSI).
F12	Other Combustible Materials	Various	Not allowed to be stored within ISFSI Facility	Not allowed in area during transport			Applicable. Administrative controls (no storage at ISFSI).	Applicable. Need administrative controls (no storage at ISFSI).	Applicable. Administrative controls ^d (walkdown prior).

HUMBOLDT BAY ISFSI FSAR UPDATE

TABLE 2.2-1

Event No. ^(a)	Hazard	Size	Distance from ISFSI	Distance from Transport Route ^(b)			Mode Applicability		
							Storage – with all Vault Lids Installed	Storage – Vault Lid Removed from one Cell for Maintenance/Inspection	Transport – Cask Removed from one Cell for Maintenance/Inspection
F10	Vegetation	Various	Minimum of 20 ft clear around ISFSI vault controlled by maintenance program	Maintenance program will control all vegetations growth close to transport route			Applicable, bounded by F1 evaluation based on volume and distance (non-engulfing). Administrative controls (veg height).	Applicable, bounded by F1 evaluation based on volume and distance (non-engulfing). Administrative controls (veg height).	Transport – Cask Transfer to Authorized Offsite Facility Applicable, bounded by F1 evaluation based on volume and distance (non-engulfing). Administrative controls (veg height).

HUMBOLDT BAY ISFSI FSAR UPDATE

TABLE 2.2-1

Event No. ^(a)	Hazard	Size	Distance from ISFSI	Distance from Transport Route ^(b)	Mode Applicability		
					Storage – with all Vault Lids Installed	Storage – Vault Lid Removed from one Cell for Maintenance/Inspection	Transport – Cask Removed from one Cell for Maintenance/Inspection
FA	Aqueous ammonia	54,000 gal	Greater than 900 ft	Approximately 300ft	Applicable, bounded by F3 evaluation based on volume and distance (2,760,169 gal at 322 ft. vs 54,000 gal at 900 ft.) and F4 evaluation based on volume and distance (7,500 gal at 80 ft. vs 54,000 gal at 900 ft.). No controls needed.	Applicable, bounded by F3 evaluation based on volume and distance (2,760,169 gal at 322 ft. vs 54,000 gal at 900 ft.) and F4 evaluation based on volume and distance (7,500 gal at 80 ft. vs 54,000 gal at 900 ft.). No controls needed.	Applicable, bounded by F3 evaluation based on volume and distance (2,760,169 gal at 322 ft. vs 54,000 gal at 900 ft.) and F4 evaluation based on volume and distance (7,500 gal at 80 ft. vs 54,000 gal at 900 ft.). No controls needed.
FB	Corrosion inhibitor	5,500 gal	Greater than 600 ft	Greater than 90 ft.	Applicable, bounded by F3 evaluation based on volume and distance (2,760,169 gal at 322 ft. vs 5,500 gal at 600 ft.). No controls needed.	Applicable, bounded by F3 evaluation based on volume and distance (2,760,169 gal at 322 ft. vs 5,500 gal at 600 ft.). No controls needed.	Applicable, bounded by F3 evaluation based on volume and distance (2,760,169 gal at 322 ft. vs 5,500 gal at 600 ft.). No controls needed.
FC	Diesel no. 2 tanks	634,000 gal	Greater than 900 ft	Greater than 350 ft.	Applicable, bounded by F3 evaluation based on volume and distance (2,760,169 gal at 322 ft. vs 634,000 gal at 900 ft.). No controls needed.	Applicable, bounded by F3 evaluation based on volume and distance (2,760,169 gal at 322 ft. vs 634,000 gal at 900 ft.). No controls needed.	Applicable, bounded by F3 evaluation based on volume and distance (2,760,169 gal at 322 ft. vs 634,000 gal at 900 ft.). No controls needed.
FC	Diesel no. 2 (black start and fire pump)	600 gal	Greater than 900 ft	Greater than 350 ft.	Applicable, bounded by F3 evaluation based on volume and distance (2,760,169 gal at 322 ft. vs 634,000 gal at 900 ft.). No controls needed.	Applicable, bounded by F3 evaluation based on volume and distance (2,760,169 gal at 322 ft. vs 634,000 gal at 900 ft.). No controls needed.	Applicable, bounded by F3 evaluation based on volume and distance (2,760,169 gal at 322 ft. vs 634,000 gal at 900 ft.). No controls needed.
FD	Hydraulic oil	33,000 gal (3,300 gal/engine)	Greater than 900 ft	Greater than 20 ft.	Applicable, bounded by F3 evaluation based on volume and distance (2,760,169 gal at 322 ft. vs 33,000 gal at 900 ft.). No controls needed.	Applicable, bounded by F3 evaluation based on volume and distance (2,760,169 gal at 322 ft. vs 33,000 gal at 900 ft.). No controls needed.	Applicable, bounded by F3 evaluation based on volume and distance (2,760,169 gal at 322 ft. vs 33,000 gal at 900 ft.). No controls needed.

HUMBOLDT BAY ISFSI FSAR UPDATE

TABLE 2.2-1

Event No. ^(a)	Hazard	Size	Distance from ISFSI	Distance from Transport Route ^(b)	Mode Applicability			Transport – Cask Transfer to Authorized Offsite Facility
					Storage – with all Vault Lids Installed	Storage – Vault Lid Removed from one Cell for Maintenance/Inspection	Transport – Cask Removed from one Cell for Maintenance/Inspection	
FE	Lube oil	34,500 gal	Greater than 800 ft	More than 200 ft	Applicable, bounded by F3 evaluation based on volume and distance (2,760,169 gal at 322 ft. vs 34,500 gal at 800 ft.). No controls needed.	Applicable, bounded by F3 evaluation based on volume and distance (2,760,169 gal at 322 ft. vs 34,500 gal at 800 ft.). No controls needed.	Applicable, bounded by F3 evaluation based on volume and distance (2,760,169 gal at 322 ft. vs 34,500 gal at 800 ft.). No controls needed.	Applicable, bounded by F3 evaluation based on volume and distance (2,760,169 gal at 322 ft. vs 34,500 gal at 800 ft.). No controls needed.
FF	Mineral insulating oil	15,870 gal	Greater than 550 ft	More than 50 ft	Applicable, bounded by F3 evaluation based on volume and distance (2,760,169 gal at 322 ft. vs 15,870 gal at 550 ft.). No controls needed.	Applicable, bounded by F3 evaluation based on volume and distance (2,760,169 gal at 322 ft. vs 15,870 gal at 550 ft.). No controls needed.	Applicable, bounded by F3 evaluation based on volume and distance (2,760,169 gal at 322 ft. vs 15,870 gal at 550 ft.). No controls needed.	Applicable, bounded by F3 evaluation based on volume and distance (2,760,169 gal at 322 ft. vs 15,870 gal at 550 ft.). No controls needed.
FF	Lubricating oil	12,000 gal	Greater than 600 ft	More than 20 ft	Applicable, bounded by F3 evaluation based on volume and distance (2,760,169 gal at 322 ft. vs 15,870 gal at 550 ft.). No controls needed.	Applicable, bounded by F3 evaluation based on volume and distance (2,760,169 gal at 322 ft. vs 15,870 gal at 550 ft.). No controls needed.	Applicable, bounded by F3 evaluation based on volume and distance (2,760,169 gal at 322 ft. vs 15,870 gal at 550 ft.). No controls needed.	Applicable, bounded by F3 evaluation based on volume and distance (2,760,169 gal at 322 ft. vs 15,870 gal at 550 ft.). No controls needed.
FH, EA	10 inch 60-70# natural gas line	10 inch line	Greater than 600 ft, local detonation and vapor cloud concern	30 ft, local detonation and vapor cloud concern	Applicable, bounded by F9 evaluation based on distance (377 ft. vs 600 ft.) and E2 evaluation based on fast-acting shutoff valves and non-credible vapor cloud event at ISFSI. No controls needed.	Applicable, bounded by F9 evaluation based on distance (377 ft. vs 600 ft.) and E2 evaluation based on fast-acting shutoff valves, duration of vault lid removal, and non-credible vapor cloud event at ISFSI. Administrative controls ^c (prior leak walkdown)	Applicable, bounded by F9 evaluation based on distance (377 ft. vs 600 ft.) and E2 evaluation based on fast-acting shutoff valves, duration of cask removal from cell, and non-credible vapor cloud event at ISFSI. Administrative controls ^d (prior leak walkdown)	Applicable, bounded by F9 evaluation based on distance (377 ft. vs 600 ft.) and E2 evaluation based on fast-acting shutoff valves. Administrative controls ^d (prior leak walkdown)
F3	ISFSI backup diesel generator fuel tank	Capacity does not exceed 200 gallons, administratively controlled to not exceed 50 gallons during initial loading.	> 80 ft	0 ft	Applicable, bounded by F4 evaluation based on volume (7,500 gal vs 200 gal). Administrative controls (200-gal limit)	Applicable, bounded by F4 evaluation based on volume (7,500 gal vs 200 gal). Administrative controls ^c (200-gal limit; no refilling)	Applicable, bounded by F4 evaluation based on volume (7,500 gal vs 200 gal). Administrative controls ^d (200-gal limit; no refilling)	Applicable, bounded by F1 evaluation based volume (7,500 gal vs 200 gal). Administrative controls ^d (200-gal limit; no refilling)

HUMBOLDT BAY ISFSI FSAR UPDATE

TABLE 2.2-1

Event No. ^(a)	Hazard	Size	Distance from ISFSI	Distance from Transport Route ^(b)	Mode Applicability		
					Storage – with all Vault Lids Installed	Storage – Vault Lid Removed from one Cell for Maintenance/Inspection	Transport – Cask Removed from one Cell for Maintenance/Inspection
FG	Truck transport for the supply of any of the new hazards listed above (except natural gas).	Various	Greater than 400ft	No transport trucks for any of the hazards will be allowed on site during the transport of fuel from Unit 3 to the ISFSI.	Applicable, bounded by F4 evaluation based on distance (400 ft. vs 80 ft.). No controls needed.	Applicable, bounded by F4 evaluation based on distance (400 ft. vs 80 ft.). Administrative controls ^c (prohibit travel by ISFSI).	Transport – Cask Transfer to Authorized Offsite Facility Applicable, bounded by F4 evaluation based on distance (400 ft. vs 80 ft.). Administrative controls ^d (prohibit travel by ISFSI).

Notes:

- (a) Each event is identified by a (F) for fire and (E) for explosive and an event number.
- (b) Historical
- (c) The Vault Lid Opening Hazard Control Program (under the Technical Specification 5.1.4, ISFSI Operations Program) administrative controls will be utilized to ensure these hazards do not adversely impact the ISFSI whenever a vault lid is removed.
- (d) Administrative controls will be in accordance with the CTEP (Technical Specification 5.1.5) during transfer of spent fuel and GTCC waste casks to an authorized offsite storage facility.
- (e) As discussed in Section 2.2.2.1, the transporter is equipped with a drip pan to collect any fuel tank leakage, and a hose attached to the drip pan that would drain any fuel away from the ISFSI vault. The hydraulic oil used in the onsite transporter is non-flammable, and is therefore not a concern in the fire evaluation.

HUMBOLDT BAY ISFSI FSAR UPDATE

TABLE 2.3-1

TEMPERATURE, DEW POINT TEMPERATURE, AND RELATIVE HUMIDITY (REFERENCE 2)

	Jan	Feb	Mar	Apr	May	Jun	Jul	Aug	Sep	Oct	Nov	Dec	Annual
Average Daily Temperature (°F)	47	48	48	49	52	55	56	57	56	53	50	47	51
Average of Max Daily Temperature (°F)	53	55	52	55	58	59	61	62	62	57	54	52	54
Average of Min Daily Temperature (°F)	42	42	44	46	49	51	53	52	53	48	44	39	49
Average Daily Dew Point (°F)	41	42	42	44	47	50	52	53	52	49	45	41	46
Average of Daily Max Dew Point (°F)	48	50	49	48	54	55	56	58	56	52	50	48	50
Average of Daily Min Dew Point (°F)	34	36	37	37	44	46	46	49	47	44	39	35	45
Average Daily Relative Humidity (%)	82	82	82	82	84	86	87	88	87	86	85	83	85
Average of Daily Max Relative Humidity (%)	91	90	91	90	94	94	96	96	93	97	91	90	88
Average of Daily Min Relative Humidity (%)	65	66	71	65	72	73	74	77	78	78	76	70	77

HUMBOLDT BAY ISFSI FSAR UPDATE

TABLE 2.3-2

EUREKA MAXIMUM RAINFALL STATISTICS AND SEVERAL CALCULATED RETURN PERIODS

	Measured	200-yr Return Period	1000-yr Return Period	Probable Max. Precip.
Average Annual Rainfall (inches)	38.87	n/a	n/a	n/a
Annual Maximum (inches)	67.23	67.70	74.97	189.93
Hourly Maximum (inches)	1.20	1.25	1.47	3.48
Daily Maximum (inches)	5.04	6.19	7.25	17.20

HUMBOLDT BAY ISFSI FSAR UPDATE

TABLE 2.3-3

DESIGN BASIS SNOWFALL PARAMETERS (REFERENCE 1)

Average Annual Snow (inches)	< 1	
Daily Maximum (inches)	3.4	Jan. 13, 1907
Maximum Storm Total (inches)	5.9	Jan. 12 - 15, 1907
Maximum Depth on Ground (inches)	3.4	Jan. 13, 1907
Monthly Maximum (inches)	6.9	Jan. 1907

HUMBOLDT BAY ISFSI FSAR UPDATE

TABLE 2.3-4

PEAK WIND GUSTS RECORDED AT EUREKA BETWEEN 1887 AND 1996

Record Peak Gusts by Month at Eureka												
Month	Jan	Feb	Mar	Apr	May	Jun	Jul	Aug	Sep	Oct	Nov	Dec
Peak Gust (mph)	69	60	60	62	60	60	60	42	50	50	69	60
Year	1981	1902	1898	1915	1894	1899	1897	1918	1914	1924	1981	1982

HUMBOLDT BAY ISFSI FSAR UPDATE

TABLE 2.3-5

MEAN FREQUENCY OF METEOROLOGICAL PHENOMENA

	Jan	Feb	Mar	Apr	May	Jun	Jul	Aug	Sep	Oct	Nov	Dec
Thunderstorms	1	1	(a)	(a)	(a)	(a)	(a)	(a)	(a)	(a)	1	1
Heavy Fog ^(b)	4	3	2	2	1	2	3	5	8	9	7	4

(a) Less than 1/2 day (b) Visibility less than 1/4 mile

HUMBOLDT BAY ISFSI FSAR UPDATE

TABLE 2.3-6

Sheet 1 of 7

JOINT FREQUENCY DISTRIBUTIONS OF WIND SPEED,
AND ATMOSPHERIC STABILITY CLASS^(a)

Stability Class A									
Wind Speed (mph)									
Direction	0-2	3	4-7	8-12	13-18	19-24	25-50	51-100	Row Sum
Calm	1	0	0	0	0	0	0	0	1
22.5	0	0	0	0	0	0	0	0	0
45	0	0	0	0	0	0	0	0	0
67.5	0	0	0	0	0	0	0	0	0
90	0	0	0	0	0	0	0	0	0
112.5	0	0	0	0	0	0	0	0	0
135	0	0	1	0	0	0	0	0	1
157.5	0	0	0	0	0	0	0	0	0
180	0	0	0	0	0	0	0	0	0
202.5	0	0	0	0	0	0	0	0	0
225	0	0	1	0	0	0	0	0	1
247.5	0	0	0	3	7	1	0	0	11
270	0	0	1	0	1	0	0	0	2
292.5	0	0	0	0	0	0	0	0	0
315	0	0	0	0	0	0	0	0	0
337.5	0	0	0	0	0	0	0	0	0
360	0	0	0	0	0	1	0	0	1
Col. Sum	1	0	3	3	8	2	0	0	17

HUMBOLDT BAY ISFSI FSAR UPDATE

TABLE 2.3-6

Sheet 2 of 7

Direction	Stability Class B								Row Sum
	Wind Speed (mph)								
	0-2	3	4-7	8-12	13-18	19-24	25-50	51-100	
Calm	0	0	0	0	0	0	0	0	0
22.5	0	0	0	0	0	0	0	0	0
45	0	0	0	0	0	0	0	0	0
67.5	0	0	0	0	0	0	0	0	0
90	0	0	0	0	0	0	0	0	0
112.5	0	0	0	0	0	0	0	0	0
135	0	0	0	0	0	0	0	0	0
157.5	0	0	0	0	0	0	0	0	0
180	0	0	0	0	0	0	0	0	0
202.5	0	0	0	0	0	0	0	0	0
225	0	0	0	1	2	0	0	0	3
247.5	0	0	1	3	5	0	1	0	10
270	0	0	1	3	1	0	0	0	5
292.5	0	0	1	2	0	0	0	0	3
315	0	0	0	1	0	0	0	0	1
337.5	0	0	0	0	0	0	0	0	0
360	0	0	0	0	0	0	0	0	0
Col. Sum	0	0	3	10	8	0	1	0	22

HUMBOLDT BAY ISFSI FSAR UPDATE

TABLE 2.3-6

Sheet 3 of 7

Direction	Stability Class C								Row Sum
	Wind Speed (mph)								
	0-2	3	4-7	8-12	13-18	19-24	25-50	51-100	
Calm	1	0	0	0	0	0	0	0	1
22.5	0	0	0	0	0	0	0	0	0
45	0	0	0	0	0	0	0	0	0
67.5	0	0	0	0	0	0	0	0	0
90	0	0	0	0	0	0	0	0	0
112.5	0	0	0	0	0	0	0	0	0
135	0	0	0	0	0	0	0	0	0
157.5	0	0	0	0	0	0	0	0	0
180	0	0	0	0	0	0	0	0	0
202.5	0	0	0	0	0	0	0	0	0
225	0	1	1	3	5	0	2	0	12
247.5	0	0	2	14	7	2	1	0	26
270	0	0	6	7	1	0	0	0	14
292.5	0	0	2	0	0	0	0	0	2
315	0	0	0	0	0	0	0	0	0
337.5	0	0	0	0	0	0	0	0	0
360	0	0	0	0	0	0	0	0	0
Col. Sum	1	1	11	24	13	2	3	0	55

HUMBOLDT BAY ISFSI FSAR UPDATE

TABLE 2.3-6

Sheet 4 of 7

Stability Class D									
Wind Speed (mph)									
Direction	0-2	3	4-7	8-12	13-18	19-24	25-50	51-100	Row Sum
Calm	30	0	0	0	0	0	0	0	30
22.5	0	3	9	7	7	2	0	0	28
45	0	1	6	2	1	0	0	0	10
67.5	0	1	2	0	1	0	0	0	4
90	0	0	1	1	0	0	0	0	2
112.5	0	0	2	1	0	0	0	0	3
135	0	2	3	1	3	2	0	0	11
157.5	0	2	3	6	22	8	0	0	41
180	0	0	9	37	31	11	0	0	88
202.5	0	2	12	35	20	9	1	0	79
225	1	6	33	68	57	18	15	0	198
247.5	7	4	88	114	38	11	5	0	267
270	6	9	108	82	11	3	0	0	219
292.5	3	15	57	40	5	2	0	0	122
315	1	5	44	36	5	5	3	0	99
337.5	1	2	20	18	11	12	4	0	68
360	1	2	22	16	33	25	26	0	125
Col. Sum	50	54	419	464	245	108	54	0	1394

HUMBOLDT BAY ISFSI FSAR UPDATE

TABLE 2.3-6

Sheet 5 of 7

Direction	Stability Class E Wind Speed (mph)								Row Sum
	0-2	3	4-7	8-12	13-18	19-24	25-50	51-100	
Calm	602	0	0	0	0	0	0	0	602
22.5	15	40	288	393	173	44	20	0	973
45	7	39	182	144	23	0	0	0	395
67.5	12	29	134	56	8	1	0	0	240
90	16	31	108	44	6	0	0	0	205
112.5	3	21	99	54	4	3	1	0	185
135	2	12	53	66	104	63	71	0	371
157.5	8	18	78	98	287	220	134	0	843
180	16	24	127	230	269	89	32	0	787
202.5	19	28	175	254	141	60	38	0	715
225	15	38	242	233	90	64	47	0	729
247.5	33	57	169	82	22	21	9	0	393
270	37	54	178	51	14	11	5	0	350
292.5	31	47	156	70	8	8	5	0	325
315	32	75	287	211	43	7	7	0	662
337.5	33	40	411	540	287	73	20	0	1404
360	20	61	550	988	749	340	161	0	2869
Col. Sum	901	614	3237	3514	2228	1004	550	0	12048

HUMBOLDT BAY ISFSI FSAR UPDATE

TABLE 2.3-6

Sheet 6 of 7

Stability Class F									
Wind Speed (mph)									
Direction	0-2	3	4-7	8-12	13-18	19-24	25-50	51-100	Row Sum
Calm	264	0	0	0	0	0	0	0	264
22.5	6	15	32	45	23	1	0	0	122
45	4	18	67	47	14	0	0	0	150
67.5	8	8	72	23	3	0	0	0	114
90	7	17	90	30	2	0	0	0	146
112.5	4	15	80	52	10	1	0	0	162
135	4	10	86	47	35	9	2	0	193
157.5	9	11	61	42	37	8	18	0	186
180	9	26	92	68	10	1	0	0	206
202.5	20	27	101	87	7	0	0	0	242
225	20	27	120	50	7	4	2	0	230
247.5	30	31	69	9	1	0	2	0	142
270	25	20	40	4	1	0	0	0	90
292.5	20	22	25	3	0	0	0	0	70
315	18	12	29	11	2	0	1	0	73
337.5	14	19	62	20	0	0	0	0	115
360	10	12	45	28	5	0	1	0	101
Col. Sum	472	290	1071	566	157	24	26	0	2606

HUMBOLDT BAY ISFSI FSAR UPDATE

TABLE 2.3-6

Sheet 7 of 7

Direction	Stability Class G								Row Sum
	Wind Speed (mph)								
	0-2	3	4-7	8-12	13-18	19-24	25-50	51-100	
Calm	89	0	0	0	0	0	0	0	89
22.5	5	8	7	1	0	0	0	0	21
45	0	1	19	3	5	1	0	0	29
67.5	1	4	15	7	0	0	0	0	27
90	9	12	32	6	0	0	0	0	59
112.5	2	11	39	15	1	0	0	0	68
135	2	8	32	18	3	1	0	0	64
157.5	2	3	25	9	4	0	0	0	43
180	6	9	24	7	3	0	0	0	49
202.5	8	4	26	16	1	0	0	0	55
225	7	8	29	7	0	0	0	0	51
247.5	3	12	11	0	0	0	0	0	26
270	12	5	9	1	0	0	0	0	27
292.5	5	2	9	0	0	0	0	0	16
315	2	3	3	1	0	0	0	0	9
337.5	1	5	5	3	0	0	0	0	14
360	2	1	5	2	1	0	0	0	11
Col. Sum	156	96	290	96	18	2	0	0	658

(a) Jan 1966 through Dec 1967 (Wind Speed 250 ft, Delta Temp. 250-25 ft)

HUMBOLDT BAY ISFSI FSAR UPDATE

TABLE 2.3-7

EUREKA MIXING HEIGHTS – METERS (REFERENCE 7)

<u>Season</u>	<u>Morning</u>	<u>Afternoon</u>
Winter	500	700
Spring	800	1100
Summer	500	600
Autumn	500	800
Annual	500	800

HUMBOLDT BAY ISFSI FSAR UPDATE

TABLE 2.3-8

INPUT DATA USED IN DIFFUSION MODELING

Parameter	Value	Units
Source Height Above Surface	0	Meters
Source Elevation above Sea Level	13	Meters
Area Source Dimension	10 x 30	Meters
Emission Rate	1	Grams/second or Curies/second

HUMBOLDT BAY ISFSI FSAR UPDATE

TABLE 2.3-9

RESULTS OF DIFFUSION MODELING, (χ/Q) FACTORS

Location	Distance and Direction from ISFSI to Receptor	Annual Average (χ/Q) factor ($\times 10^{-8}$ sec/m³)
Maximum at Plant Boundary	150 meters north-northeast	9.199
At Inhabited Receptor – Home 1	350 meters west	0.683
At Inhabited Receptor – Home 2	450 meters west-southwest	0.486
At Inhabited Receptor – Home 3	300 meters southwest	0.645
At Inhabited Receptor – Home 4	900 meters south	0.302
At Inhabited Receptor – School	800 meters south-southeast	0.286

HUMBOLDT BAY ISFSI FSAR UPDATE

TABLE 2.4-1

NORMAL MONTHLY PRECIPITATION AND TEMPERATURES
AT EUREKA WSO (No. 04-2910)
LATITUDE 40°48'N, LONGITUDE 124°10'W
ELEVATION 43 FT (NGVD)

Month	Precipitation (in.)	Temperature (°F)
Jan	7.42	47.3
Feb	5.15	48.4
Mar	4.83	48.3
Apr	2.95	49.7
May	2.11	52.5
Jun	0.66	55.2
Jul	0.14	56.3
Aug	0.27	57.0
Sep	0.65	56.6
Oct	3.23	54.4
Nov	5.77	51.7
Dec	5.58	48.6

HUMBOLDT BAY ISFSI FSAR UPDATE

TABLE 2.4-2

ANNUAL MAXIMUM PEAK DISCHARGES

Water Year	11-4797 Elk River Near Falk		11-4800 Jacoby Creek Near Freshwater	
	Date	Discharges (cfs)	Date	Discharges (cfs)
1955			12/30/54	1,670
1956			12/21/55	1,490
1957			12/11/56	516
1958	02/12/58	2,790	11/13/57	729
1959	02/14/59	3,220	02/14/59	749
1960	02/08/60	2,090	02/08/60	644
1961	02/11/61	2,160	02/11/61	276
1962	01/19/62	2,120	01/19/61	389
1963	04/12/63	2,220	12/02/62	446
1964	01/20/64	2,950	01/06/64	563
1965	12/22/65	3,430	12/22/64 ^(a)	1,530
1966	01/04/66	3,270		
1967	12/05/66	3,110		
1968	Record Discontinued		01/15/68	380
1969			01/13/69	626
1970			11/23/70	897
1971			11/24/70	936
1972			03/02/72	2,510
1973				
1974			01/16/74	1,170

(a) Station converted to a crest-stage partial-record station.

HUMBOLDT BAY ISFSI FSAR UPDATE

TABLE 2.4-3

ANNUAL HIGHEST TIDE LEVEL

Year	Date	Highest Tide (MLLW)	Tide Station	Adjusted Tide Elevation At Powerplant Vicinity
1920	12/25	8.1	South Jetty	8.2
1932	12/26, 11/28	8.2	South Jetty	8.3
1933	12/17	8.1	South Jetty	8.2
1934	12/8	7.8	South Jetty	7.9
1935	12/9	7.8	South Jetty	7.9
1936	12/27	7.9	South Jetty	8.0
1937	12/17	8.2	South Jetty	8.3
1939	12/10	7.6	South Jetty	7.7
1940	12/27	7.6	South Jetty	7.7
1941	12/17	8.0	South Jetty	8.1
1942	12/8	7.9	South Jetty	8.0
1943	12/27	7.7	South Jetty	7.8
1944	11/29	7.8	South Jetty	7.9
1945	12/18	8.1	South Jetty	8.2
1946	12/9	8.1	South Jetty	8.2
1947	12/27	8.1	South Jetty	8.2
1948	12/28, 12/17, 11/29	7.5	South Jetty	7.6
1949	12/18	7.9	South Jetty	8.0
1950	12/9	8.1	South Jetty	8.2
1977	12/11	8.87 (a)	North Spit	
1978	12/28	8.33 (a)	North Spit	
1979	12/30	8.86	North Spit	
1980	12/21	8.81	North Spit	
1981	11/27	12.46	North Spit	
1982	11/30	9.69	North Spit	
1983	1/26	9.96	North Spit	
1984	1 (b)	8.41 (c)	North Spit	
1985	12 (b)	8.43 (c)	North Spit	
1986	12 (b)	9.14 (c)	North Spit	
1987	1 (b)	9.11 (c)	North Spit	
1988	11 (b)	8.72 (c)	North Spit	
1989	12 (b)	8.50 (c)	North Spit	
1990	1 (b)	8.71 (c)	North Spit	
1994	12 (b)	9.08 (c)	North Spit	
1995	1 (b)	9.07 (c)	North Spit	
1996	12 (b)	9.29 (c)	North Spit	
1997	12 (b)	9.24 (c)	North Spit	
1998	1 (b)	9.14 (c)	North Spit	

(a) Record not complete for the year, but values used here are for December when highest tides usually occur.

(b) Month of highest tide.

(c) Verified historic tide values obtained from the CO-OPS database, from the National Water Level Observations Network of the National Oceanic and Atmospheric Administration.

NOTE: According to the correction table of the "Official Tide Table for Humboldt Bay and Vicinity," tides at Fields Landing are 0.3 ft higher than South Jetty Landing. Since the powerplant site is located about 1/3 of the distance between South Jetty Landing and Fields Landing, 0.1 ft is used for correcting tides recorded at South Jetty Landing for the plantsite. No correction is assumed needed for tides recorded at North Spit.

HUMBOLDT BAY ISFSI FSAR UPDATE

TABLE 2.4-4

PROBABLE MAXIMUM FLOOD PEAKS AND LEVELS HUMBOLDT BAY

PMP Event	PMP Inflow (cfs)	5-Day Volume (ac-ft)	Bay W.S. Elev. ^(a) (ft)	Freeboard ^(b) (ft)
Oct	108,070	256,150	10.05	33.95
Nov	103,920	262,350	10.05	33.95
Dec	99,460	267,060	10.04	33.96
Jan-Feb	97,670	270,940	10.03	33.97
Mar	97,490	263,180	10.03	33.97
Apr	96,030	248,280	10.03	33.97

(a) Elevation is based on National Ocean Survey Datum of mean lower low water (MLLW) level of zero at North Spit tidal gage and transposed to the ISFSI site. Antecedent Bay level was assumed equal to 9.96 ft above MLLW.

(b) Freeboard is determined from the ISFSI site elevation of 44 ft MLLW.

HUMBOLDT BAY ISFSI FSAR UPDATE

TABLE 2.4-5

ESTIMATES OF WAVE RUNUP^(a, b)

PMF Month	Design Wind (mph)		Period (sec)	Runup (ft)	Setup (ft)	Total Runup (ft)	Free- board
	Over- land	Over-water					
Oct	27	33	2.5	1.6	0.3	11.86	32.14
Nov	31	38	2.3	1.6	0.4	11.96	32.04
Dec	36	45	2.5	1.9	0.5	12.36	31.64
Jan-Feb	40	49	2.6	2.0	0.6	12.56	31.44
Mar	36	45	2.5	1.9	0.5	12.36	31.64
Apr	31	38	2.3	1.6	0.4	11.96	32.04
Windstorm 66-yr Period of Record	56	69	2.9	2.7	1.2	13.86	30.14
100-Year	62	77	3.0	3.0	1.5	18.86	25.53

(a) Based on the antecedent Bay level of 9.96 ft mean lower low water (MLLW).

(b) Determined from elevation of the ISFSI site, which is at elevation 44 ft MLLW, using PG&E survey data dated January 12, 1983.

HUMBOLDT BAY ISFSI FSAR UPDATE

TABLE 2.5-1

Sheet 1 of 5

PIEZOMETERS USED IN 1999 GROUNDWATER MEASUREMENTS IN THE
HUMBOLDT BAY ISFSI SITE AREA

Boring Number	Year	Boring Depth/ Elevation (feet)	Top Screen Elevation (feet)	Bottom Screen Elevation (feet)	Geologic/ Hydrologic Unit in screened zone	Piezometric Elevation 5/6/99 (9am-12pm) (feet)
MW-1 (BEC 84-1)	1984	49.5/ -37.6	-28.19	-32.59	upper Hookton aquifer	4.74
MW-2A (BEC 84-2A)	1984	50.0/ -39.2	-28.14	-37.54	upper Hookton aquifer	4.29
MW-4 (BEC 84-4)	1984	50.6/ -38.5	-41.00	-50.20	upper Hookton aquifer	4.43
MW-5 (BEC 84-5)	1984	45.0/ -33.3	-40.50	-44.80	upper Hookton aquifer	4.24
MW-6 (BEC 84-6)	1984	50.0/ -38.6	-32.57	-36.87	upper Hookton aquifer	4.21
MW-7 (BEC 84-7)	1984	45.0/ -20.9	-16.23	-20.53	upper Hookton aquifer	4.10
MW-8 (BEC 84-8)	1984	12.5/ 11.1	17.3	11.8	perched ground-water zone (A) in upper Hookton silts and clays	17.92
MW-9 (BEC 84-9)	1984	45.0/ -33.4	-23.58	-32.78	upper Hookton aquifer	4.76
MW-10 (BEC 84-10)	1984	60.0/ -31.9	-50.20	-59.40	upper Hookton aquifer	3.81
MW-11 (BEC 84-11)	1984	50.0/ -37.6	-35.80	-45.00	upper Hookton aquifer	4.76
1 (DER) ** (DER 85-1)	1985	38.0/ -25.8	-16.01	-26.01	upper Hookton aquifer	4.73
2 (DER) ** (DER 85-2)	1985	38.0/ -25.9	-15.91	-25.41	upper Hookton aquifer	4.78
3 (DER) ** (DER 85-3)	1985	46.5/ -34.6	-22.75	-32.25	upper Hookton aquifer	4.75
4 (DER) ** (DER 85-4)	1985	46.5/ -34.5	-22.99	-32.49	upper Hookton aquifer	4.80
5 (DER) ** (DER 85-5)	1985	41.5/-27.3	-17.35	-27.35	upper Hookton aquifer	4.20
6 (DER) ** (DER 85-6)	1985	51.5/ 37.3	-24.80	-34.30	upper Hookton aquifer	4.40
7 (DER) ** (DER 85-7)	1985	41.5/ -28.2	-10.74	-20.24	upper Hookton aquifer	4.6
8 (DER) ** (DER 85-8)	1985	38.0/ -26.0	-15.49	-24.99	upper Hookton aquifer	4.66
9 (DER) ** (DER 85-9)	1985	41.5/ -29.7	-13.17	-28.17	upper Hookton aquifer	4.76
1A (WCC) ** (WCC 85-1A)	1985	14.0/ -1.9	8.6	-1.9	perched groundwater zone (A) in upper Hookton silts and clays	8.56

HUMBOLDT BAY ISFSI FSAR UPDATE

TABLE 2.5-1

Sheet 2 of 5

Boring Number	Year	Boring Depth/ Elevation (feet)	Top Screen Elevation (feet)	Bottom Screen Elevation (feet)	Geologic/ Hydrologic Unit in screened zone	Piezometric Elevation 5/6/99 (9am-12pm) (feet)
1B (WCC) ** (WCC 85-1B)	1985	26.5/ -14.4	-7.4	-12.4	perched groundwater zone (B) in upper Hookton silts and clays	5.90
2A (WCC) ** (WCC 85-2A)	1985	14.0/ -2.3	7.6	-2.3	perched groundwater zone (A) in upper Hookton silts and clays	8.44
2B (WCC) ** (WCC 85-2B)	1985	26.5/ -14.8	-8.1	-13.1	perched groundwater zone (B) in upper Hookton silts and clays	7.30
3A (WCC) ** (WCC 85-3A)	1985	14.0/ -1.4	8.6	-1.2	perched groundwater zone (A) in upper Hookton silts and clays	8.61
3B (WCC) ** (WCC 85-3B)	1985	36.5/ -23.9	-5.7	-10.7	perched groundwater zone (B) in upper Hookton silts and clays	5.17
4A (WCC) ** (WCC 85-4A)	1985	14.0/ -2.5	7.5	-2.5	Perched groundwater zone (A) in Holocene bay deposits	9.03
4B (WCC) ** (WCC 85-4B)	1985	26.5/ -15.0	-8.4	-13.4	perched groundwater zone (B) in upper Hookton silts and clays	8.32
5A (WCC) ** (WCC 85-5A)	1985	10.0/ 3.1	8.1	3.1	Perched groundwater zone (A) in Holocene bay deposits	10.01
5B (WCC) ** (WCC 85-5B)	1985	21.5/ -8.4	3.1	-6.3	Perched groundwater zone (B) in Holocene bay deposits	9.77
6A (WCC) ** (WCC 85-6A)	1985	10.0/ 3.3	8.3	3.3	Perched groundwater zone (A) in Holocene bay deposits	10.03
6B (WCC) ** (WCC 85-6B)	1985	26.5/ -13.0	0.5	-8.9	Perched groundwater zone (B) in Holocene bay deposits	10.24
7B (WCC) ** (WCC 85-7B)	1985	22.0/ -8.3	5.5	-8.5	Perched groundwater zone (B) in Holocene bay deposits	9.1
8A (WCC) ** (WCC85-8A)	1985	10.0/ 3.5	8.5	3.5	Perched groundwater zone (A) in Holocene bay deposits	8.75

HUMBOLDT BAY ISFSI FSAR UPDATE

TABLE 2.5-1

Sheet 3 of 5

Boring Number	Year	Boring Depth/ Elevation (feet)	Top Screen Elevation (feet)	Bottom Screen Elevation (feet)	Geologic/ Hydrologic Unit in screened zone	Piezometric Elevation 5/6/99 (9am-12pm) (feet)
8B (WCC) ** (WCC 85-8B)	1985	21.5/ -7.9	7.2	-6.8	Perched groundwater zone (A) in Holocene bay deposits (intermediate, placed in zone A)	8.86
9A (WCC) ** (WCC 85-9A)	1985	10.0/ 2.1	7.1	2.1	Perched groundwater zone (A) in Holocene bay deposits	11.04
9B (WCC) ** (WCC 85-9B)	1985	21.5/ -9.1	2.4	-7.6	Perched groundwater zone (A) in Holocene bay deposits (intermediate, placed in zone A)	8.09
10B (WCC) ** (WCC 85-10)	1985	21.5/ -7.5	4.0	-6.0	Perched groundwater zone (A) in Holocene bay deposits	9.07
7A (TES) ** (DER 87-7A)	1987	12/ 8	10.97	3.97	Perched groundwater zone (A) in Holocene bay deposits	10.40
8C (TES) ** (DER 87-8C)	1987	39/ -25.5	-18.21	-23.21	Hookton sands	5.44
11B (TES) ** (DER 87-11B)		20.5/ -5.4	5.14	-4.86	Perched groundwater zone (A) in Holocene bay deposits (intermediate, placed in zone A)	9.01
12B (TES) ** (DER 87-12B)		20.5/ -5.03	5.25	-4.75	Perched groundwater zone (A) in Holocene bay deposits	9.48
13A (TES) ** (DER 87-13B)		-- /-2.0?	8.17	-1.83	perched groundwater zone (A) in upper Hookton silts and clays	8.25
14A (TES) ** (DER 87-14A)		-- /-2.0?	8.39	-1.61	perched groundwater zone (A) in upper Hookton silts and clays	8.62
15A (TES) ** (DER 87-15A)	1987	11.5/ 4	11.27	4.27	Perched groundwater zone (A) in Holocene bay deposits	8.74
15B (TES) ** (DER 87-15B)	1987	22/ -8.5	0.84	-6.16	Perched groundwater zone (A) in Holocene bay deposits (intermediate, placed in zone A)	7.09
15C (TES) ** (DER 87-15C)	1987	41.5/ -27.0	-17.86	-22.86	upper Hookton aquifer	5.15

HUMBOLDT BAY ISFSI FSAR UPDATE

TABLE 2.5-1

Sheet 4 of 5

Boring Number	Year	Boring Depth/ Elevation (feet)	Top Screen Elevation (feet)	Bottom Screen Elevation (feet)	Geologic/ Hydrologic Unit in screened zone	Piezometric Elevation 5/6/99 (9am-12pm) (feet)
16A (TES) ** (DER 87-16A)	1987	12/ 1	11.01	4.01	Perched groundwater zone (A) in Holocene bay deposits	9.41
16B (TES) ** (DER 87-16B)	1987	23/ -10	1.05	-5.95	Perched groundwater zone (B) in Holocene bay deposits	9.21
16C (TES) ** (DER 87-16C)	1987	39/ -25.5	-11.19	-16.19	upper Hookton aquifer	4.37
16D (TES) ** (DER 87-16D)	1987	51/ -38	-29.45	-34.45	upper Hookton aquifer	4.32
17A (TES) ** (DER 87-17A)	1987	13/ 1.5	10.57	3.57	Perched groundwater zone (A) in Holocene bay deposits	11.85
17B (TES) ** (DER 87-17B)	1987	24/ -9.5	0.58	-6.42	Perched groundwater zone (B) in Holocene bay deposits	7.47
17C (TES) ** (DER 87-17C)	1987	40/ -26	-12.57	-17.57	upper Hookton aquifer	4.29
17D (TES) ** (DER 87-17D)	1987	51/ -36	-25.27	-30.27	upper Hookton aquifer	4.48
18A (TES) ** (DER 87-18A)	1987	12/ 1.3	11.05	4.05	Perched groundwater zone (A) in Holocene bay deposits	9.03
18B (TES) ** (DER 87-18B)	1987	23/ -10	-0.65	-7.65	Perched groundwater zone (B) in Holocene bay deposits	5.60
101 (TES) **	1989	16.7/ -2.5	8.1	-1.9	Perched groundwater zone (A) in Holocene bay deposits	12.07
102 (TES) **	1989	16.7/ -2.8	7.8	-2.2	Perched groundwater zone (A) in Holocene bay deposits	12.14
103 (TES) **	1989	16.9/ -2.2	8.4	-1.6	Perched groundwater zone (A) in Holocene bay deposits	9.10
104 (TES) **	1989	18.0/ -2.9	7.1	-2.9	Perched groundwater zone (A) in Holocene bay deposits	9.39
105 (TES) **	1989	17.5/ -2.2	7.3	-2.2	Perched groundwater zone (A) in Holocene bay deposits	9.59
106 (TES) **	1989	17.5/ -3.9	6.7	-3.3	Perched groundwater zone (A) in Holocene bay deposits	10.03
P-1 (TES) ** (TES 87P-1)	1987	-- /-6.0?	9.45	-5.55	upper Hookton aquifer	4.17
P-2 (TES) ** (TES 87-P2)	1987	-- /-2.0?	8.51	-1.49	upper Hookton aquifer	4.95

HUMBOLDT BAY ISFSI FSAR UPDATE

TABLE 2.5-1

Sheet 5 of 5

Boring Number	Year	Boring Depth/ Elevation (feet)	Top Screen Elevation (feet)	Bottom Screen Elevation (feet)	Geologic/ Hydrologic Unit in screened zone	Piezometric Elevation 5/6/99 (9am-12pm) (feet)
OWSP-1 **		-- /-12.0?	11.82?	11.82	perched groundwater zone (A) in upper Hookton silts and clays	8.39
WEST ** (20A)		21.5/ -9.6	1.9	-8.1	perched groundwater zone (B) in intermediate Hookton silts and clays	6.36

Notes:

1. Elevations are referenced to 'Plant 0' that equals mean low water (MLLW), which is 3.6 feet below mean sea level (MSL)
2. MW-2 (BEC) = Bechtel Borings (1984) (Boring MW-3 closed prior to May 1999)
3. DER = PG&E Department of Engineering Research (1985/86)
- 4.
5. WCC = Woodward Clyde Consultants (1985)
6. TES = PG&E Department of Technical and Ecological Services (7A to 18B, P-1 & P-2: 1987; 101 to 106: 1989)
7. ** Well sealed and abandoned in September 1999
8. * = boring not plotted on map (Figure 2.5-3)

HUMBOLDT BAY ISFSI FSAR UPDATE

TABLE 2.5-2

SELECTED WATER QUALITY DATA FOR WELLS IN THE HUMBOLDT BAY ISFSI SITE VICINITY

PERCHED GROUNDWATER ZONE (A) IN UPPER HOOKTON SILTS AND CLAYS

South of Unit 3	WCC85-2A	WCC85-3A
Parameter	8/15/85	08/15/85
pH	5.9	6.4
Conductivity	2590	2830
TDS	1510	1620
Sulfate	248	87
Chloride	450	790
Sodium	430	300

PERCHED GROUNDWATER ZONE (A) IN HOLOCENE SILTS AND CLAYS

South of Unit 3	WCC85-4A	WCC85-10B
Parameter	08/15/85	08/15/85
pH	5.8	7.0
Conductivity	5220	6680
TDS	3410	3090
Sulfate	420	405
Chloride	1560	1280
Sodium	780	1000

PERCHED GROUNDWATER ZONE (B) IN HOLOCENE BAY DEPOSITS

Wastewater Pond Site	WCC85-5B	WCC85-7B	WCC85-9B
Parameter	08/15/85	08/15/85	08/15/85
pH	5.4	5.7	6.7
Conductivity	8900	11100	17300
TDS	288	358	9870
Sulfate	1450	1190	987
Chloride	1850	3500	4650
Sodium	1200	2000	1900

UPPER HOOKTON AQUIFER

Southeast of Unit 3	DER85-1	DER85-4	DER85-5	DER85-7	DER85-8	DER85-10
Parameter	04/11/85	04/11/85	04/11/85	04/11/85	04/11/85	4/11/1985
pH	7.0	6.9	7.2	7.0	7.1	7.2
Conductivity	1058	2363	5638	13022	9048	25776
TDS						
Sulfate	49	23	67	77	174	103
Chloride	200	640	1990	4550	3010	9050
Sodium	150	370	1000	2600	2000	5600

LOWER HOOKTON AQUIFER

PG&E Water Supply Wells	Well No. 1	Well No. 1	Well No. 2
Parameter	11/18/93	02/24/94	02/24/94
pH	7.4	7.8	7.7
Conductivity	140	200	150
TDS	130	130	100
Sulfate	1.9	5.8	4.3
Chloride	12	26	13
Sodium	12	18	11

Note: 1. pH is in pH units; conductivity is in micromhos/cm, and others are ppm.
2. See Figures 2.5-1, -9, -12, -13 for location of wells.

HUMBOLDT BAY ISFSI FSAR UPDATE

TABLE 2.5-3

Sheet 1 of 2

GROUNDWATER WELLS WITHIN TWO MILES OF THE HUMBOLDT BAY ISFSI

Well No.	Owner	Site Location	Township/ Range/ Section	Use	Depth (feet)	Diameter (inches)	Casing Year Completed	Casing Material
1 *	PG&E	HBPP	4N/1W/08P1	industrial	450	8	1955	steel
2	PG&E	Humboldt Hill Rd	4N/R1W/17B1	industrial	491	8	1955	steel
3 *	PG&E	HBPP	4N/R1W/08M1	domestic	55	12		
5	Dr. Stone	Spruce Pt near Bucksport School	4N/R1W/08J1	domestic	360	12	1950	
6	Fields Landing water Co	end of Princeton Dr	4N/R1W/17	municipal	176	8	1961	steel
7	Walter Eich	2035 Eich Rd. Spruce Point		commercial	180	6	1993	steel
8	Humboldt Community Services District	County Ag Site Spruce Point		public, domestic	450	12"	1988	steel
9	McMahan	Pine Hill Trailer Ct.	4N/R1W/04A	domestic	105	8	1949	
10	Glen Reed	6477 Elk River Rd		domestic			1980	plastic
11	John Giocomini		4N/R1W/16A	irrigation	160	14		
12	Gene Senistrano		4N/R1W/16H1	irrigation	210		1956	
13	John Jerome			domestic	50	6		
14	Walter Eich		4N/R1W/16N		779		1944	
15	Humboldt Community Services District		4N/R1W/17	municipal	366	6 5/8	1980	
16	Coast Guard							
17	George Reeves	5823 Humboldt Hill Rd. next to Grange Hall	4N/R1W/08	domestic-irrigation	160	14	1969	pvc
18	Evenson	Elk River Rd		domestic	95	8		kiawell
19	Laurie Cummings	5850 Elk River Rd		domestic	82	8 5/8"	1989	steel
20	Pierce Mortuary	Sunset Memorial Park		irrigation	120	12	1978	steel
21	Dale Lindholm	Berta Rd		domestic	180	8	1988	steel
22	Kenneth Evans	Berta Rd		domestic	200	8	1998	steel
23	Clinton Parks	Berta Rd		domestic	130	8	1993	steel
24	Jay Egan	2216 Burns Dr		domestic			1991	
25	Reynold Water Co	Humboldt Hill area		public domestic	400	8	1977	steel
26	Lloyd Barker	2100 Stanford Dr.		domestic	100	6	1977	pvc
27	Frank Bisio	4900 Broadway	4N/R1W/04H	monitoring (3)	7	4	1995	pvc
28	Humboldt Fire District	755 Herrick Ave		monitoring (3)	17	2	1997	pvc
29	Joan Scuri	Zazone & Elk River Rd	4N/R1W/15	domestic	60	8	1966	
30	Pacific Bell	5749 Humboldt Hill Rd	4N/R1W/08H	monitoring (4)	16.5		1995	
31	Pete Lorenzen	Elk River Rd at Elk River School	4N/R1W/16H1	irrigation	210		1956	

HUMBOLDT BAY ISFSI FSAR UPDATE

TABLE 2.5-3

Sheet 2 of 2

Well No.	Owner	Site Location	Township/Range/Section	Use	Depth (feet)	Diameter (inches)	Casing Year Completed	Casing Material
32	Reynold Water Co	Vista Dr – Humboldt Hill	4N/R1W/7H	municipal	272	8	1969	Steel
33	Jose Lopez	Elk River Road 125' E of house (address uncertain - map location approx)	4N/R1W/04	domestic		6	1977	Steel
34	H. E. Reardon	Elk River Rd 3rd house on left	4N/R1W/04H	irrigation	103	12	1960	
35	Shanahan Bros.	Spruce Pt 1 mi E of 101	4N/R1W/08H	test well (2)	205		1956	
36	Tony Dutra	Spruce Pt	4N/R1W/08H	domestic	84	8	1962	steel
37	Walter Eich	Spruce Pt btw 101 & Humboldt Hill Rd	4N/R1W/08H	domestic	190	6	1962	
38	H. E. Reardon	2 mi S Elk River Rd	4N/R1W/09H	irrigation	106	12	1967	steel
39	Frank Shanahan	Elk River Rd 2 mi E of 101	4N/R1W/15	domestic	147		1962	
40	Ann Miller	6710 Fields Landing Dr	4N/R1W/17H	monitoring	15	2	1993	pvc
41	Sun Bridge Sea View Csre Center	6400 Purdue Road	4N/R1W/17H	industrial	275	8	1968	steel
42	Humboldt County	Humboldt Hill Rd @ S. Broadway	4N/R1W/8	municipal	380	6	1988	pvc

1. Table complete as of November 1999.
2. * Indicates that well was sealed and abandoned in 2000.
3. Well number 4 referred to several monitoring wells near HBPP Unit 3; these are listed in Table 2.5-1.

HUMBOLDT BAY ISFSI FSAR UPDATE

TABLE 2.6-1

GEOLOGIC TIME SCALE AND SUBDIVISIONS OF THE MESOZOIC AND CENOZOIC ERAS

Era	Period/Epoch	Age
Cenozoic (65 million years to today)	Quaternary	1.6 million years ago to today
	Holocene	10,000 years ago to today
	Pleistocene	1.6 million to 10,000 years ago
	Tertiary	65 to 1.6 million years ago
	Pliocene	5 to 1.6 million years ago
	Miocene	23 to 5 million years ago
	Oligocene	38 to 23 million years ago
	Eocene	54 to 38 million years ago
	Paleocene	65 to 54 million years ago
Mesozoic 245 to 65 million years ago	Cretaceous	145 to 65 million years ago
	Jurassic	205 to 145 million years ago
	Triassic	245 to 205 million years ago

HUMBOLDT BAY ISFSI FSAR UPDATE

TABLE 2.6-2

COMPARISON OF THE TIMING OF EVENTS ON THE MAIN SEGMENT OF THE CASCADIA SUBDUCTION ZONE WITH EVENTS ON THE EEL RIVER SEGMENT

Main Segment of the Cascadia Subduction Zone			Eel River Segment of the Cascadia Subduction Zone
Main Cascadia Subduction Zone (years BP)	West Trace, Little Salmon Fault, Salmon Creek Site (years BP)	West Trace, Little Salmon Fault, Swiss Hall Site (years BP) ^(a)	Eel River Syncline (years BP) ^(b)
			~170 (1827 AD \pm 28) ^(c)
Event "Y," 300 (January 27, 1700)	~300	<460	
	~800		~830
Event "W," 1100		540-1230	
Event "U," 1300		1350 to 1560	~1290
Event "S," 1600	~1600	1530 to 1710	~1530
		1950 to 2300	~1930
Event "N," 2500			
Event "L," 2900			
Event "P," 3100			
Event "O," 3900			

Note: The Sixes River estuary, southern Oregon, studied by Kelsey and others is closer to Humboldt Bay than the southern Washington site studied by Atwater and Hemphill-Haley. The Sixes River record for events within the past 2,000 years is less complete, however, and only 2 events (in years before A.D. > 1950, at 250 years and 1940 to 2130 years) are recognized.

^(a) Radiocarbon dates calibrated to calendar years (2-sigma, with an error multiplier of 0.1) using CALIB 4.2.

^(b) Data regarding the carbon-14 ages are in PG&E files.

^(c) Age in calendar years using the tree-ring sequence method and high-precision radiocarbon dates calibrated to calendar years (2-sigma) using CALIB 3.0.

HUMBOLDT BAY ISFSI
SAFETY ANALYSIS REPORT

TABLE 2.6-3

Sheet 1 of 2

GEOLOGIC HISTORY OF THE HUMBOLDT BAY ISFSI SITE

Timing	Event	Evidence	Interpretation
Holocene	Continued activity in the fold-and-thrust belt in the upper plate of the Cascadia subduction zone. Timing of upper-plate earthquakes apparently coincides with great earthquakes on the Cascadia subduction zone.	Buried Holocene marsh soils	Holocene estuarine deposits deposited in upper-plate synclines record evidence for sudden subsidence during earthquakes on adjacent crustal structures. Timing of subsidence coincides with events on the Cascadia subduction zone. These upper-plate synclines include the Eel River, South Bay, and Freshwater synclines.
Late Pleistocene-Holocene	Continued late Pleistocene and Holocene activity in the fold-and-thrust belt in the upper plate of the Cascadia subduction zone	Geomorphic surfaces	Marine and fluvial terraces provide evidence for activity of upper-plate thrust faults, because they show uplift and growth of anticlines in the hanging walls of thrust faults.
Late Pleistocene-Holocene	Local fluvial deposition	Hookton Formation and related units	Coeval deposition and development of the fold-and-thrust system creates localized depocenters over synclines (the Eel River, South Bay, and Freshwater synclines) and localized erosion over anticlines.
Ca. 700 ka	Initiation of upper-plate deformation in a series of northwest-trending folds and northeast-dipping thrust faults. Uplift of Klamath Mountains, likely related to approach of Mendocino triple junction.	---- Unconformity ----	Timing of unconformity is controlled by its position above the Scotia Bluffs Formation (800 ka) and below the Hookton Formation (600 ka). Extensive erosion on upper plate of Little Salmon fault, removing the majority of the Wildcat group.

HUMBOLDT BAY ISFSI
SAFETY ANALYSIS REPORT

TABLE 2.6-3

Sheet 2 of 2

Timing	Event	Evidence	Interpretation
Late Pleistocene	Fluvial and estuarine deposition near sea level records glacio-eustatic sea level changes.	Wildcat Group, fluvial portion; Carlotta Formation	Redwood logs in the Carlotta Formation indicate it is terrestrial or very near shore. Fluvial deposits are intercalated with marine. This intercalation probably represents glacio-eustatic sea level cycles. The Carlotta Formation is derived primarily from local sources, the Eastern and Central Belt Franciscan Complex, indicating onset of uplift of the nearby Klamath Mountains.
Late Miocene to Pleistocene	Deposition and rapid submergence ca. 9 ma, then shoaling, basin filling, and gradual shallowing.	Wildcat Group, marine portion, including: Pullen, Eel River, Rio Dell, and Scotia Bluffs formations	Trace fossils and lithology at the base of the Pullen Formation indicate this unit is fluvial to littoral. Rapid submergence of the area to depths of 2 to 3 km is then recorded by the clayey deposits of the upper Pullen, Eel River, and Rio Dell formations. These deposits record gradual shoaling and basin-filling. Trace fossils in the Scotia Bluffs Formation indicate deposition in ~30 m of water. The abrupt submergence ca. 9 ma may relate to greater than normal plate convergence, or to the passing of a structure in the subducted plate that divided relatively young, warm, buoyant lithosphere from relatively old, cold, dense lithosphere. Along the Eel River at Scotia, an angular unconformity separates the tightly folded Yager turbidites from the tilted but relatively undeformed Wildcat Group.

HUMBOLDT BAY ISFSI FSAR UPDATE

TABLE 2.6-4

Sheet 1 of 14

MAGNITUDE 5 AND LARGER EARTHQUAKES WITHIN 160 KILOMETERS (100 MILES)
OF THE HB-ISFSI SITE, 1850 THROUGH APRIL 2002

Date	Origin Time (GMT)	Latitude (deg. min.)	Longitude (deg. min.)	*Depth (km)	Location References ^(a)	^s Magnitude	Magnitude References ^(a)
01/27/1700	~05:00	Cascadia	Subduction	Zone	41	~9	41
10/23/1853	11:00	40 48?	-124 12?	0	118; 119; 120	[MI] 5.5; (M _L) 5.7; <u>M</u> 5.5	118; 25; 119
11/13/1860	00:00	40 48?	-124 12?	0	118; 119; 120	[MI] 6.1; (M _L) 5.7; <u>M</u> 5.5	118; 25; 119
10/01/1865	17:15	40 48?	-124 6?	0	118	[MI] 6.2	118
		40 48	-124 12	0	119; 120	(MI) 5.4; <u>M</u> 5.5	119; 120
03/02/1871	21:05	40 18?	-124 30?	0	118	[MI] 6.3	118
		40 24	-124 12	0, 12.3	119, 122, and 34	M 6; {MI} 6.2; <u>M</u> 6.3	122; 34, 119
11/23/1873	05:00	42 12?	-124 12?	0	118	[MI] 7.3	118
		42	-124	0	120	(MI) 6.7; M 6 3/4	120, 122
		42	-124 12	0	119	<u>M</u> 6.9	119
		42 48	-124 30	0	34	{MI} 6.7	34

HUMBOLDT BAY ISFSI FSAR UPDATE

TABLE 2.6-4

Sheet 2 of 14

Date	Origin Time (GMT)	Latitude (deg. min.)	Longitude (deg. min.)	*Depth (km)	Location References ^(a)	\$Magnitude	Magnitude References ^(a)
09/30/1875	12:30	40 42	-124	0	118; 119	[MI] 5.9; <u>M</u> 5.9	118; 119
		40 06.0	-124	0	120; 34	(MI) 5.5; {M} 5.8	120; 34
05/09/1878	04:25	40 24?	-125 12?	0	118; 119	[MI] 7.0; <u>M</u> 7.0	118; 119
		40 6	-124	0	120	(MI) 5.8; <u>M</u> 6	120; 122
01/28/1884	07:30	41 6	-123 18	0	118; 119	[MI] 4.9; <u>M</u> 6.1	118; 119
		41 6	-123 36	0	120	(MI) 5.7	(Event plotted in Figures 2.6-25 to 2.6-28 as average MI 5.5) 120
07/26/1890	09:40	40 18?	-124 30?	0	118	[MI] 6.3	118
		40 30	-124 12	0	122; 119	<u>M</u> 6 1/4; <u>M</u> 6.3	122; 119
		40 30	-124 30	8.4	34	{MI} 5.9	34
09/30/1894	17:36	40 18	-123 42	0	118	[MI] 6.5; <u>M</u> 6	118; 122
		40 18	-124 30	0	120; 119	(MI) 5.9; <u>M</u> 6.5	120; 119
04/15/1898	07:07	39 18?	-123 54?	0	118	[MI] 6.8	118; 120; 119
		39 12	-123 48	0	120; 119; 34	(MI) 6.4; <u>M</u> 6.7	

HUMBOLDT BAY ISFSI FSAR UPDATE

TABLE 2.6-4

Sheet 3 of 14

Date	Origin Time (GMT)	Latitude (deg. min.)	Longitude (deg. min.)	*Depth (km)	Location References ^(a)	^s Magnitude	Magnitude References ^(a)
04/16/1899	13:40	41?	-126?	0	122	[MI] 7.0; <i>M</i> 7	118, 122
		40 30	-125 30	0	34	{MI} 6.7	34
		41	-124.4	0	120	(MI) 5.7	120
04/18/1906	13:12	37 42	-124 30	0	122	<i>M</i> 7.8; <i>M</i> 8 1/4	122; 123
04/23/1906	21:10	41	-124 30	0	119	<u><i>M</i></u> 6.4	119
		40 52.8	-125 21	0	123	<i>M</i> 6.7	123
08/11/1907	12:19	40 30	-125 30	0	119	<u><i>M</i></u> 6.4	119
08/18/1908	10:59	40 48	-124	0	119, 124	<u><i>M</i></u> 5.8; <i>MI</i> 5.0	119, 124
05/18/1909	01:19	41	-124 0	0	124	<i>MI</i> ≤ 5.5	125
		40 34.8	-124 10.2	12.9	34	<i>M_L</i> 6.1	34
10/29/1909	06:45	40 18?	-124 12?	0	118	<i>M_S</i> 5.8	118
		40 30	-124 12	14.0, 0	34, 122 & 119	<i>M_L</i> 6.0; <i>M</i> 5.8; <u><i>M</i></u> 6.0	34; 122; 119
03/19/1910	00:11	40 49.8	-124 10.2	17.7, 0	34; 24	<i>M_L</i> 6.0	34; 24
		40?	-125?	0	122; 119	<i>M</i> 6.0; <u><i>M</i></u> 6.0	122; 119

HUMBOLDT BAY ISFSI FSAR UPDATE

TABLE 2.6-4

Sheet 4 of 14

Date	Origin Time (GMT)	Latitude (deg. min.)	Longitude (deg. min.)	*Depth (km)	Location References ^(a)	^s Magnitude	Magnitude References ^(a)
12/31/1915	12:20	41	-126	0	126	M _L 6.5; M 6.5	127; 122
07/15/1918	00:23	41	-125	0	34; 126; 119	M _L 6.5; M 6.5; <u>M</u> 6.5	34 & 127; 122; 119
09/15/1919	14:07	40 48	-124 12	0	124	M _I ≤ 5.5	125
		40 49.8	-124 10.2	17.7	34	M _L 5.5	34
01/26/1922	09:31	41	-126	0	126; 122	M _L 6.0, M 6.0	126; 122
01/31/1922	13:17	41 0.0	-125 30	0	126; 122; 119	M _{G-R} 7.3; M 7.3; <u>M</u> 7.3; M _L 7.3	118; 122; & 119; 127
		40 52.2	-125 21	0	34; 31	M _L 7.0; M _L 7.3	34; 31
01/22/1923	09:04	40 30	-124 30	0	126; 122	M _{G-R} 7.2; M 7.2, M _L 7.2	118; 122; 127
		40 24	-124 54	0	119	<u>M</u> 7.2	119
		40 48	-124 3		31	M _L 7.2	31
04/29/1923	02:31	41	-125	0	126	M _L 5.0	126
06/04/1925	12:02	41 30	-125	0	126; 122; 119	M _L 6.0; M 6; <u>M</u> 6.0	127; 122; 119
12/10/1926	08:38	40 45	-126	0	126; 34; 122	M _L 6.0; M 6.0	127; 34; 122

HUMBOLDT BAY ISFSI FSAR UPDATE

TABLE 2.6-4

Sheet 5 of 14

Date	Origin Time (GMT)	Latitude (deg. min.)	Longitude (deg. min.)	*Depth (km)	Location References ^(a)	^s Magnitude	Magnitude References ^(a)
08/20/1927	20:05	41	-124 36	0, 4.8	24; 34	M _L 5.0	24; 34
09/23/1930	02:58	40 57	-124 12	0	119	<u>M</u> 5.5	119
12/11/1930	09:00	40 49.8	-124 10.2	17.7	34	M _L 5.0	34
		40 24	-124 48	0	119	<u>M</u> 5.5	119
03/10/1931	03:28	40 4.8	-124 30	0	24	[M _L] 5.0	124
		40	-125	0	119	<u>M</u> 5.6	119
08/23/1931	18:01	40 12	-125 36	0	126; 34	M _L 5.3	126; 34
09/09/1931	13:40	40 48	-125	0	126; 34; 119	M _L 5.8	126; 34; 119
06/06/1932	08:44	40 45	-124 30	0, 11.2	126; 122; 34	M _{G-R} 6.4; M _L 6.4; <u>M</u> 6.4	118; 127; 34; 122
07/06/1934	22:49	40 48	-124 18	0	119	<u>M</u> 6.4	119
		41 15	-125 45	0	122; 119	M _{G-R} 6.5; <u>M</u> 6.5	118; 122 & 119
01/02/1935	22:40	41 15	-125 25.2	0	34	M _L 5.5	34
		40 15	-125 15	0	34; 126; 119	M _L 5.7; M _L 5.8	34; 127, 119
06/03/1935	17:08	41	-124	0, 14.8	126; 34	M _L 5.0	127; 34

HUMBOLDT BAY ISFSI FSAR UPDATE

TABLE 2.6-4

Sheet 6 of 14

Date	Origin Time (GMT)	Latitude (deg. min.)	Longitude (deg. min.)	*Depth (km)	Location References ^(a)	§Magnitude	Magnitude References ^(a)
06/03/1936	09:15	40	-125 30	0	122	M _{G-R} 5.9; <u>M</u> 5.9	118; 122
		40 9.6	-126 27	0	24	M _L 5.8	24
		40 19.8	-125 24	0	34	M _L 5.9	34
10/10/1936	01:25	41	-125	0	126	M _L 5.0	127
02/07/1937	04:41	40 30	-125 15	0	34; 126; 119	M _L 5.8; <u>M</u> 5.8; M _L 5.7	127; 119; 34
07/01/1938	18:13	41	-124	0, 14.8	126; 34;	M _L 5.0	127; 34;
09/12/1938	06:10	40	-124	0	126; 119	M _L 5.5; <u>M</u> 5.5	127; 119
		40 12	-124 37	0	34	M _L 5.5	34
10/22/1940	11:00	40 30	-124 6	0, 15.8	24 34	M _L 5.5	24; 34
12/20/1940	23:40	40	-124	0	126; 119	M _L 5.5; <u>M</u> 5.5	127; 119
02/09/1941	09:44	40 42	-125 24	0	126; 122; 119	M _{G-R} 6.6; M _L 6.4; <u>M</u> 6.6; <u>M</u> 6.6	118; 127; 122; 119
		40 30	-125 21.6	0	34	M _L 6.5	34

HUMBOLDT BAY ISFSI FSAR UPDATE

TABLE 2.6-4

Sheet 7 of 14

Date	Origin Time (GMT)	Latitude (deg. min.)	Longitude (deg. min.)	*Depth (km)	Location References ^(a)	^s Magnitude	Magnitude References ^(a)
10/03/1941	16:13	40 24	-124 48	0	126; 122; 119 34	M _{G-R} 6.4; M _L 6.4; <i>M</i> 6.4; <u>M</u> 6.4	118; 126; 122 & 119 34
10/06/1941	06:59	40 24	-125	0	126	M _L 5.0	127
01/12/1944	15:02	40 18	-124 54	0	34; 126	M _L 5.1	34; 127
01/16/1944	02:20	40 18	-125 6	0	126	M _L 5.1	126
05/02/1945	19:47	41 12	-123 30	30.1, 0	34; 127	M _L 5.3; M _L 5.0	34; 127
05/27/1947	20:58	40 24	-124 42	0	126	M _L 5.2	126 34
09/23/1947	13:53	40 18	-124 13	10.0	34	M _L 5.2	126
		40 24	-125 12	0	126	M _L 5.3	34
		40 27	-125 9	0	34	M _L 5.3	126 34
08/18/1948	19:12	40 30	-124 42	0	126	M _L 5.0	126 34
		40 22.2	-124 19.8	10.4	34	M _L 5.0	126 34
04/01/1951	19:21	40 28.2	-125 18	0	126	M _L 5.0	126 34
		40 24	-125	0	34	M _L 5.0	118; 122; 119
10/08/1951	04:10	40 15	-124 30	0	122; 119	M _{G-R} 6.0; <i>M</i> 6.0; <u>M</u> 6.0	34
		40 21	-124 36	0	34	M _L 5.9	126
		40 16.8	-124 48	0	126	M _L 5.8	126; 34
09/22/1952	11:41	40 12	-124 25.2	0	126; 34	M _L 5.2	126; 34

HUMBOLDT BAY ISFSI FSAR UPDATE

TABLE 2.6-4

Sheet 8 of 14

Date	Origin Time (GMT)	Latitude (deg. min.)	Longitude (deg. min.)	*Depth (km)	Location References ^(a)	^s Magnitude	Magnitude References ^(a)
11/25/1954	11:16	40 16.2	-125 37.8	0	126; 122; 119	M _{G-R} 6.5; M _L 6.1; <i>M</i> 6.5; <u>M</u> 6.5	118; 126; 122; 119
		40 28.8	-125 27.6	0	34	M _L 6.0	34
12/21/1954	19:56	40 55.8	-123 46.8	0	122; 119	M _{G-R} 6.6; <i>M</i> 6.6; <u>M</u> 6.6	118; 122; 119
		40 56.4	-123 47.4	17.5	34	M _L 6.6	34
		40 46.8	-123 52.2	0	126		126
10/11/1956	16:48	40 40.2	-125 46.2	0	126; 125; 119	M _L 6.5	118 & 126; 122; 119
		40 35.4	-126 4.8	0	34	M _L 6.0	34
07/24/1959	01:23	41 7.8	-125 18	0	126; 119; 34	M _L 5.8; <u>M</u> 5.8	126; 34; 119
12/05/1959	08:13	40 18	-125 25.2	0	126; 34	M _L 5.1	126; 34
06/06/1960	01:17	40 49.2	-124 52.8	0	126	M _L 5.7	126
		40 52.7	-124 30	10.1	34	M _L 5.7	34
12/27/1960	10:35	41 31.2	-125 3	0, 2.0	126; 34	M _L 5.4	126; 34
04/06/1961	04:04	40 10.8	-124 45	0	126	M _L 5.0	126
04/14/1962	07:53	40 16.2	-125 19.2	0	126; 34	M _L 5.0; M _L 5.4	126; 34
07/14/1962	19:43	40 25.8	-125 31.2	0	126	M _L 5.1	126

HUMBOLDT BAY ISFSI FSAR UPDATE

TABLE 2.6-4

Sheet 9 of 14

Date	Origin Time (GMT)	Latitude (deg. min.)	Longitude (deg. min.)	*Depth (km)	Location References ^(a)	^s Magnitude	Magnitude References ^(a)
08/23/1962	19:29	40 51	-124 19.8	0	34; 126; 119 24	M _L 5.6; M _L 5.2, <u>M</u> 5.6	126; 34; 119 118
09/16/1965	04:10	41 51 40 30	-124 20 -125 48	0 0	126; 34	M _L 5.6 M _L 5.0	126; 34
12/10/1967	12:06	40 30	-124 42	0	126; 119	M _L 5.6; <u>M</u> 5.6	126; 119 34
06/26/1968	01:42	40 33.6 40 13.8	-124 34.8 -124 16.2	4.6 0	34 122; 126	M _L 5.0 M 5.4; M _L 5.9	122; 126
09/13/1970	21:10	40 21.6 40 7.8	-124 3.6 -125 4.8	14.4 0	34 127	M _L 5.7 M _L 5.4	34 127
02/27/1971	00:31	40 16.2	-124 49.8	0	127	M _L 5.2	127
03/01/1972	09:28	40 40.2	-125 15	0	127	M _L 5.2	127
06/15/1973	19:18	41 30	-125 31.8	0	127	M _L 5.0	127
08/09/1973	02:18	40 15.6	-124 14	2.0	126	Mb 5.1	126
12/21/1973	19:12	40 37.5	-124 35.8	30.0	126	Mb 5.2	126
07/03/1974	05:00	40 25.44	-125 8.16	12	126	mb 5.4	126
07/13/1974	11:09	40 20.4 40 22.3	-125 12.6 -125 10.92	0 1.00	127 126	M _L 5.1 Mb 5.0	127 126
01/28/1975	13:53	40 24.9	-125 26.76	10.0	126	Mb 5.0	126

HUMBOLDT BAY ISFSI FSAR UPDATE

TABLE 2.6-4

Sheet 10 of 14

Date	Origin Time (GMT)	Latitude (deg. min.)	Longitude (deg. min.)	*Depth (km)	Location References ^(a)	§Magnitude	Magnitude References ^(a)
06/07/1975 (Ferndale)	08:46	40 32.49	-124 16.56	23.6	126	M _L 5.3; M _C 5.3;	127; 126
		40 31.68	-124 17.88	3.27	34	M _L 5.2	34
11/26/1976	11:19	41 17.34	-125 42.5	15.0, 0	126; 119	M _S 6.8; <u>M</u> 6.8;	126; 119
		41 14.82	-125 37.08	15	34	M _L 6.0	34
12/03/1978	06:48	40 37.2	-125 50.8	98.47	126	M _C 5.0	126
02/03/1979	09:58	40 52.15	-124 19.03	23.6	126	M _L 5.2	127
04/07/1979	06:18	41 8.17	-125 2.56	5.00	126	M _C 5.4	126
03/03/1980	14:17	40 24.83	-125 07.39	11.6	126	M _L 5.1	127
11/08/1980 (Trinidad)	10:27	41 4.44	-124 36.60	15.1	126	M _S 7.2, M _C 6.7, M _L 6.9	128; 126; 127
		41 7.2	-124 40.2	0, 6	122; 119; 129	M _S 7.2, <u>M</u> 7.2, <u>M</u> 7.4	118; 122; 119
		41 2.46	-124 36.72	21.2	34	M _L 7.0	34
		41 5.84	-124 44.35	19.8	130	M _L 7.0	130
11/08/1980	11:20	40 14.8	-124 44.5	15.0	126	Mb 5.0	126
11/08/1980	22:47	40 39.0	-125 15.6	0	127	M _L 5.0	127
11/08/1980	23:07	40 32.1	-124 47.04	15.00	126	M _S 5.0	126
11/09/1980	04:09	40 30.06	-125 20.58	15.00	126	M _L 5.4	127
12/07/1980	02:56	40 54.2	-126 1.86	15	126	Mb 5.0	126

HUMBOLDT BAY ISFSI FSAR UPDATE

TABLE 2.6-4

Sheet 11 of 14

Date	Origin Time (GMT)	Latitude (deg. min.)	Longitude (deg. min.)	*Depth (km)	Location References ^(a)	^{\$} Magnitude	Magnitude References ^(a)
12/24/1980	13:29	41 17.76	-124 44.97	3.2	126	M _L 5.0	127
02/06/1982	12:02	41 04.30	-125 08.58	9.2	126	M _L 5.2	127
05/29/1983	06:55	40 27.4	-125 26.64	10.0	126	M _L 5.4; mb 5.1	127; 126
08/24/1983	13:36	40 22.39	-124 55.36	11.9	126	M _L 5.5	127
		40 22.8	-124 49.8	0	119	<u>M</u> 5.6	119
		40 21.3	-124 51.9	7.87	34	M _L 5.6	34
12/20/1983	10:41	40 25.10	-125 47.56	9.5	126	M _L 5.6	127
		40 20.16	-125 33.54	10.0	34	M _L 5.8	34
02/28/1984	15:16	40 25.59	-125 16.53	4.0	126	M _L 5.2	127
02/11/1986	01:15	41 38.04	-125 21.18	10.0	126	Mb 5.0	126
11/21/1986	23:33	40 22.39	-124 37.77	0.36	126	M _L 5.1, M 5.2	127; 118
11/21/1986	23:34	40 21.62	-124 23.72	16.0	126	M _L 5.1	127
		40 21.66	-124 25.68	7.51	34	M _L 5.9	34
07/31/1987	23:56	40 24.97	-124 23.02	17.5	126	M _S 6.0; M _L 5.6	128; 127
		40 25.2	-124 24.6	0	128; 119	M _S 6.0; <u>M</u> 6.0	128 & 118; 119
		40 25.5	-124 23.04	7.2	34	M _L 5.9	34
01/16/1990	20:08	40 14.05	-124 18.69	13.0	126	M _L 5.4	127

HUMBOLDT BAY ISFSI FSAR UPDATE

TABLE 2.6-4

Sheet 12 of 14

Date	Origin Time (GMT)	Latitude (deg. min.)	Longitude (deg. min.)	*Depth (km)	Location References ^(a)	^s Magnitude	Magnitude References ^(a)
01/18/1990	11:45	41 11.04	-123 46.08	39.9	127	M _L 5.2	127
08/16/1991	22:26	41 11.04	-123 46.2	1.58	34	M _L 5.2	34
		41 41.82	-125 23.10	10.0	126	M _S 6.3; M _L 6.0; mb 5.5	128; 127 126 119
08/17/1991 (Honeydew)	19:29	41 37.98	-125 51.66	0	119	M 6.3	
		40 16.90	-124 14.64	9.6	126	M _L 6.0; M _S 6.2	127; 128 119
		40 17.23	-124 14.28	0	119	M 6.2	
08/17/1991	22:17	41 49.26	-125 23.82	13.5	126, 119; 118	M _S 7.1, M _L 6.4, mb 6.2	118; 128; 127; 126, 119; 118
		41 42.6	-125 37.8	0	34	M 7.0, M 7.0	34
		41 36.6	-125 30.6	4		M _L 7.2	
03/08/1992	03:43	40 15.35	-124 13.98	11.1	126	M _L 5.2	127
04/25/1992 (Petrolia)	18:06	40 19.94	-124 13.69	10.6	14	M _S 7.1	14
		40 19.96	-124 13.77	0	119	M 7.2	119
		40 20.03	-124 13.78	10.3	126	m _B 6.3	127
04/26/1992	07:41	40 26.13	-124 34.43	19.3	14	M _S 6.6	128
		40 25.86	-124 34.00	19.5	119	M _L 6.5	127, 126
		40 25.63	-124 35.79	0	126	M 6.6	119

HUMBOLDT BAY ISFSI FSAR UPDATE

TABLE 2.6-4

Sheet 13 of 14

Date	Origin Time (GMT)	Latitude (deg. min.)	Longitude (deg. min.)	*Depth (km)	Location References ^(a)	§Magnitude	Magnitude References ^(a)
04/26/1992	11:18	40 23.38	-124 34.30	21.7	14, 126, 119	M _S 6.6	128
		40 25.03	-124 49.92	14.2		M _L 6.4; M _L 6.6	127; 126, 119
		40 22.51	-124 35.12	0		<u>M</u> 6.6	
09/01/1994	15:15	40 24.12	-125 40.8	10.1	126	M 7.0, mb 6.6, M _L 7.0	118; 128; 126 127
		40 26.7	-125 53.8	21.3	127	M _W 6.9	119
		40 24	-125 40.8	0	119	<u>M</u> 7.0	
12/26/1994	14:10	40 44.30	-124 18.28	23.5	126	M _W 5.4; M 5.4	127; 131
02/19/1995	04:03	40 33.36	-125 32.34	10.0	126	M _S 6.8; M _L 6.3	126; 127
01/22/1997	07:17	40 16.32	-124 23.64	0	119	<u>M</u> 5.6	119
		40 15.42	-124 29.22		126	M _W 5.6	126
10/04/1997	10:57	41 03.0	-125 21.72	7.3	132	M _L 5.1; M _W 5.6; M _W 5.5	127; 126; 132
10/26/1997	10:44	41 00.13	-125 09.85	5.7	126	M _L 5.2	127
11/26/1998	19:49	40 37.43	-122 24.39	23.4	126	M _L 5.2	127
11/27/1998	00:43	40 39.80	-125 18.68	5.4	126	M _L 5.5	127 119
		40 40.02	-125 23.04	0	119	M 5.6	
03/16/2000	15:19	40 22.96	-125 16.23	5.1	126	M _L 5.8; M _C 4.8	127; 126
01/13/2001	13:08	40 44.39	-125 17.06	5.6	126	M _L 5.2	126

^(a) Refer to the HB ISFSI Safety Analysis Report, Section 2.6.10 for references.

Notes:

Earthquakes from this table are shown on Figure 2.6-24, except the 1700 Cascadia and 18 April 1906 San Francisco earthquakes. When more than one location or magnitude is given, the first one listed is used in the figure.

*Zero (0) depths are depths that have not been calculated.

§ Magnitude symbol explanations:

M _b	Body wave magnitude
M _c	Coda magnitude
M _{G-R}	Gutenberg and Richter magnitude
M _L	Richter local magnitude
M _s	20-second surface-wave magnitude
M _w	Magnitude generally from moment tensor computation.
M	Moment magnitude (Section 2.6.10, Reference 10)
(MI)	Pre-instrument (before 1900) intensity magnitude from Topozada and others (Section 2.6.10, Reference 120) estimated from the size of the areas shaken at various levels of intensity.
[MI]	Pre-instrumental (before about 1935) intensity magnitude from Bakun (Section 2.6.10, Reference 118), calibrated to equal moment magnitude.
{MI}	Pre-instrumental (before about 1935) intensity magnitudes from Geomatrix (Reference 34, calibrated to local magnitudes, are from the Decade of North America catalog (DNAG) as described in (Section 2.6.10, Reference 133)
(M _L)	Pre-instrumental (pre-1900) local magnitude estimate reported by Dengler and others (Section 2.6.10, Reference 25).
[ML]	Local magnitude estimated using intensity data and instrumentally determined ground motion amplitudes, as described in Topozada and others (Section 2.6.10, Reference 124).
M	Summary magnitude from Ellsworth (Section 2.6.10, Reference 122). The summary magnitude characterizes the relative size of all events listed on his table of major California and Nevada earthquakes, 1769-1989. When choices are available, summary magnitudes are weighted toward long-period estimates of magnitude (e.g., reliable M _s and M _{G-R}).
M	Magnitudes from Topozada and others (Section 2.6.10, Reference 119). Magnitude types not specified.

HUMBOLDT BAY ISFSI FSAR UPDATE

TABLE 2.6-5

Sheet 1 of 3

EARTHQUAKES THAT PRODUCED GROUND MOTIONS GREATER THAN 0.10g
AT HUMBOLDT BAY POWER PLANT, 1975 THROUGH 1994
(Source parameters from Table 2.6-4)

EQ Number & Name	Date	Origin Time (GMT)	Distance (km)/ Direction from HBPP	Latitude (deg min)	Longitude (deg min)	Magnitude*	Depth (km)	Free-Field Ground Accelerations Recorded at HBPP**	Effects at HBPP
1 Ferndale	07 June 1975	846	22/ SSW	40N 32.41	124W 16.56	M _L 5.3	23.6	0.03g vert. 0.30g e/w 0.18g n/s (1)	Units 1 & 2 tripped. Unit 3 relay tripped; Unit 3 down for refueling (1). Choppy waves in spent fuel pond, 9"-12" high (1). Strong-motion duration a few seconds (1). No damage (1).
2 Trinidad	08 November 1980	1027	50/ NW	41N 4.44	124W 36.60	M _S 7.2	15.1	0.076g vert. 0.495g e/w 0.143g n/s (2.4)	No structural damage (3). Tools fell from storage rack, glassware broke, separation of paint over previous surface cracks in concrete walls (3).

HUMBOLDT BAY ISFSI FSAR UPDATE

TABLE 2.6-5

Sheet 2 of 3

EQ Number & Name	Date	Origin Time (GMT)	Distance (km)/ Direction from HBPP	Latitude (deg min)	Longitude (deg min)	Magnitude*	Depth (km)	Free-Field Ground Accelerations Recorded at HBPP**	Effects at HBPP
3 Petrolia main shock	25 April 1992	1806	55/ S	40N 19.94	124W 13.69	M _s 7.1	10.6	0.05g vert. 0.22g e/w 0.22g n/s (6)	No structural damage (5,7,8). Unit 2 offline. Water splashed out of spent fuel pond (6). New hairline cracks in walls of refueling building, caisson access shaft, and grouted areas near top of spent fuel pond (7). Cracks and leaks in water line to Unit 2 (7).
4 Petrolia aftershock	26 April 1992	0741	55/ SW	40N 26.13	124W 34.43	M _s 6.6	19.3	0.052g vert. 0.25g e/w 0.23g n/s (6).	No Damage (7). Additional electrical problems to fuse parts (6).
5 Petrolia aftershock	26 April 1992	1118	70/ SW	40N 23.38	124W 34.30	M _s 6.6	21.7	0.031g vert. 0.13g e/w 0.10g n/s (6).	No damage (6).

HUMBOLDT BAY ISFSI FSAR UPDATE

TABLE 2.6-5

Sheet 3 of 3

EQ Number & Name	Date	Origin Time (GMT)	Distance (km)/ Direction from HBPP	Latitude (deg min)	Longitude (deg min)	Magnitude*	Depth (km)	Free-Field Ground Accelerations Recorded at HBPP**	Effects at HBPP
6	26 December 1994	1410	8/ W	40N 44.30	124W 18.28	M _w 5.4	23.5	0.17g vert. 0.48g e/w 0.55g n/s (10). CSMIP recorded 0.41g to 0.56g in Eureka area (10).	Strongly felt (10). Unit 2 was offline. Unit 1 tripped offline from quake relay response (9). Fuses of startup transformer fell (9). Leak in Unit 1 stem air drip tank condensate return line to main condenser (9).

*See Table 2.6-4 for explanation of magnitude symbols.

**Component orientation: vert.= vertical; n/s= horizontal, oriented plant north-south; e/w= horizontal, oriented plant e/w.

- (1) Section 2.6.10, Reference 143
- (2) Section 2.6.10, Reference 144
- (3) Section 2.6.10, Reference 145
- (4) Section 2.6.10, Reference 146
- (5) Section 2.6.10, Reference 147

- (6) Section 2.6.10, Reference 148
- (7) Section 2.6.10, Reference 149
- (8) Section 2.6.10, Reference 150
- (9) Section 2.6.10, Reference 151
- (10) Section 2.6.10, Reference 152

HUMBOLDT BAY ISFSI FSAR UPDATE

TABLE 2.6-6

Sheet 1 of 4

DESCRIPTIONS OF SOIL PROFILES

Horizon ¹	Depth (cm)	Color ²		Texture ³	Structure ⁴	Consistence ⁵		Clay Films ⁶	Boundary ⁷
		Moist	Mottles (moist)			Moist	Wet		
PROFILE JW-11* ~ 100 M WEST OF ISFSI SITE									
A	0-35	10YR 2/2	--	L	2 f g	fr	ss, ps	N.O.	a-c, s
BAt	35-52	7.5YR 4/4	--	l-scl	2-3 m-c sbk	fi	ss-s, p	1-2 n pf & po	c, s
Bt	52-96	7.5YR 4/6	--	scl	2-3 c pr breaking to 2-3 m- c sbk	fi	s, p	2-3 n-mk po & pf	c, w
2Bt2	96-130	7.5YR 4/6	--	scl	2-3 c pr breaking to 2-3 m sbk	fi-vfi	s, p	2-3 mk-k pf & po	c-g, s
2Bt3	130-180	7.5YR 5- 6/8	c 1-2 d, 7.5YR 7/4	scl	1-2 c pr	fi	ss-s, p	1-2 n pf 3-4 mk-k po	c-g, s
3Bt	180-230	10-7.5YR 5/8	c 1-2 d-p, 10YR 7/4	sicl	1-2 c pr	fi-vfi	s, p	1-2 n pf 2-3 n-mk po	a-c, w
3Cox	230- 270+	10YR 7/4	f 2 d, 10YR 6/8 & 7.5YR 6/8	sicl	M	fi	ss-s, p	v1 n-mk po	--
PROFILE JW-12** ~130 M EAST OF ISFSI SITE									
A	0-20	10YR 2/1	--	sicl	1 m gr	fr	ss-s, p	--	c, s
A2	20-43	10YR 3/1	--	sicl	1 m sbk breaking to 2 m gr	fi	s, p	v1 n pf	c, w

HUMBOLDT BAY ISFSI FSAR UPDATE

TABLE 2.6-6

Sheet 2 of 4

Horizon ¹	Depth (cm)	Color ²		Texture ³	Structure ⁴	Consistence ⁵		Clay Films ⁶	Boundary ⁷
		Moist	Mottles (moist)			Moist	Wet		
B	43-75	7.5YR 4/6	--	sicl-sic	1-2 c-vc pr breaking to 1 m sbk	fi-vfi	s-vs, p- vp	1 n pf	c, s
2Bt	75-140	7.5YR 5- 6/8	m 2 d, 7.5YR 7/3	Sic	2 m pr breaking to 3 m sbk	fi	s-vs, vp	3 mk-k pf & po	c-g, s
2Bt	140-197	7.5YR 6/6	f 2 d, 7.5YR 7/3	sic	1 c pr breaking to 2 m abk	vfi	s-vs, p- vp	2-3 k pf & po	g, s
2BCtc	197-232	7.5YR 6/6	f-c 2 f, 7.5YR 6/4	C	1 c pr & abk	vfi-efi	vs, vp	3 k pf & po	a-c, s
3Cox	232-257	10YR 5- 6/4	--	SI	m	fi	ss, ps	--	a, s
4Cox	257- 327+	10YR 6/4	c-m 2-3 d-p, 7.5YR 5/8	sicl	m	fi	s, p	--	--
PROFILE GMX-T2*** SOUTHWEST CORNER OF ISFSI SITE									
A	0-5 mostly stripped	10YR 3/4	--	sil-sil	1 m gr	fr	ss, ps	--	a, ir
A/B	5-28	10YR 4/4	--	SI	1 m sbk	fi	so, ps	2, n, po	c-g, ir
Bt	28-75	10YR 3/6	m 2 d, 10YR 7/3 m 2 d, 10YR 3/6	scl	2 c-vc cpr breaking to 1 m sbk	fi	ss, p	3; mk; po	g, ir

HUMBOLDT BAY ISFSI FSAR UPDATE

TABLE 2.6-6

Sheet 3 of 4

Horizon ¹	Depth (cm)	Color ²		Texture ³	Structure ⁴	Consistence ⁵		Clay Films ⁶	Boundary ⁷
		Moist	Mottles (moist)			Moist	Wet		
Bt2	75-110	10YR 6/8	7.5YR 5/8 c m p, 7.5YR 8/2	scl	2 c cpr breaking to 3 m abk	fi	s, p	3 mk-k pf & po	g; ir
B/C	110-145	10YR 6/8	m 1-2, d 7.5YR 6/8 m 1-2 d, 5YR 7/1	Sc	1-2 f abk	fi	s, p	3-4 k pf	a, s
2Cox	145-213	7.5YR 4.5/8	--	s-ls	m	Fi	so, po	--	va, s
3Cox	213-235	7.5YR 5.5/8 7.5YR 6.5/2	--	sil	m	Fi	ss, p	--	a, s
4Cox	235-362	7.5YR 5.5/8 7.5YR 6.5/2	--	sil & s	m	Fi	ss, p so, po	--	va, w
4C	362-369	7.5YR N4/0	--	S	m	Fr	so, po	--	a, s
5C	369- 420+	7.5YR N4/0	--	sic	m	--	s, p	--	--

* Soil profile exposed in steep south-southwest-facing escarpment below the Buhne Point terrace. Location shown on Figure 2.6-31.

** Soil profile exposed in steep north-northwest-facing escarpment below the Buhne Point terrace. Location shown on Figure 2.6-31.

*** Soil profile exposed in northwest wall of trench GMX-T2 (station 180 ft); relict paleosol formed on the Buhne Point terrace. Location shown on Figure 2.6-31.

Explanation of Soil Descriptions

¹ Master horizons: A = a surface horizon characterized by the accumulation of organic matter and typically as a zone of eluviation of clay, sesquioxides, silica, gypsum, carbonate, and/or salts; B = a subsurface horizon characterized as having a redder color, stronger structure development, and/or accumulation of secondary illuvial materials, such as clay, sesquioxide, silica, gypsum, and/or salts; C = a subsurface horizon that may appear similar or dissimilar to the parent material and includes unaltered material and material in various stages of weathering. Modifiers of master horizons: b = buried soil horizon; c = concretions or nodules; j = used in conjunction with other modifiers to denote incipient development of that particular feature or property; ox = oxidized (for C horizon only); p = plowing or other disturbance; t = accumulation of clay; w = color or structural B horizon.

² Color: From Munsell soil color chart (Munsell Color Company, 1988); dry colors were difficult to determine given very wet weather during fieldwork; -- = not observed. Abundance: f = few, c = common, m = many. Size: 1 = fine, 2 = medium, 3 = large. Contrast: f = faint, d = distinct, p = prominent.

³ Texture: sl = sandy loam; ls = loamy sand; s = sand; l = loam; scl = sandy clay loam; sc = sandy clay; cl = clay loam; sil = silt loam; sicl = silty clay loam; sic = silty clay.

⁴ Structure: Grade: m = massive; sg = single grain; v1 = very weak; 1 = weak; 2 = moderate; 3 = strong. Size: f = fine; m = medium; c = coarse; vc = very coarse. Type: pl = platy; gr = granular; abk = angular blocky; sbk = subangular blocky; cpr = columnar; pr = prismatic.

⁵ Consistence Moist consistence: lo = loose; vfr = very friable; fr = friable; fi = firm; vfi = very firm; efi = extremely firm. Wet consistence: so = nonsticky; vss = very slightly sticky; ss = slightly sticky; s = sticky; vs = very sticky; po = nonplastic; vps = very slightly plastic; ps = slightly plastic; p = plastic; vp = very plastic.

⁶ Clay Films: Frequency: v1 = very few; 1 = few; 2 = common; 3 = many; 4 = continuous. Thickness: n = thin; mk = moderately thick. Location: br = clay bridges holding mineral grains together; pf = faces of peds; po = lining or filling tubular or interstitial pores; co = colloidal stains on mineral grains; N.O. = none observed; -- = not observed.

⁷ Boundary with lower horizon. Distinctness: va = very abrupt; a = abrupt; c = clear; g = gradual; d = diffuse. Topography: s = smooth; w = wavy; i = irregular; b = broken.

HUMBOLDT BAY ISFSI FSAR UPDATE

TABLE 2.6-7

ALTERNATIVE SEGMENT LENGTHS AND WEIGHTS FOR THE CASCADIA
INTERFACE USING THE CARVER MODEL

Rupture Extent	Segment Length (km)	Weight
Eureka to the middle of Washington	700	0.5
Eureka to the Explorer plate	1050	0.5

HUMBOLDT BAY ISFSI FSAR UPDATE

TABLE 2.6-8

DISTANCE* (KM) FROM U. S. COASTLINE TO 4 UPDIP REFERENCE
BOUNDARIES OF THE CASCADIA SUBDUCTION ZONE

N Latitude^(a)	Deformation Front (Reference 34^(b), Fig. 2-16)	Deformation Front (Reference 34, Plate 1)	Cascadia Subduction Zone (NGS)	Change in Fold Trends (Reference 34, Plate 1)
41	44	N/A	73	N/A
42	61	87	85	59
43	39	63	64	37
44	67	94	97	76
45	83	113	109	76
46	94	119	116	81
47	100	N/A	135	N/A
48	94	N/A	138	N/A

^(a) Accuracy of the distances is approximately: ± 5 km for Geomatrix Figure 2-16, ± 1 km, and ± 2 km for NGS.

^(b) Refer to Section 2.6.10

HUMBOLDT BAY ISFSI FSAR UPDATE

TABLE 2.6-9

HORIZONTAL EXTENT (KM) OF THE CASCADIA INTERFACE
USING THE CHANGE IN FOLD TRENDS (FIGURE 2-16)
AS THE UPDIP INTERFACE BOUNDARY

N Latitude (°)	Change in Fold Trends		Deformation Front	
	Zero Isobase	Transition Zone	Zero Isobase	Transition Zone
41	100	65	130	95
42	100	57	130	87
43	87	52	117	82
44	83	52	113	82
45	74	57	104	87
46	78	78	108	108
47	83	117	113	147
48	70	126	100	156
49	39	83	69	113

HUMBOLDT BAY ISFSI FSAR UPDATE

Table 2.6-10

DOWNDIP WIDTH (KM) OF THE CASCADIA INTERFACE

N Latitude (°)	Change in Fold Trends		Deformation Front	
	Zero Isobase	Transition Zone	Zero Isobase	Transition Zone
41	104	68	135	99
42	104	59	135	91
43	91	54	122	85
44	86	54	118	85
45	77	59	108	91
46	81	81	112	112
47	86	122	118	153
48	73	131	104	162
49	41	86	72	118
Average (41° to 47°)	90	71	121	102
Average (41° to 49°)	82	79	114	111

HUMBOLDT BAY ISFSI FSAR UPDATE

Table 2.6-11

MAXIMUM RUPTURE DOWNDIP WIDTH (KM) OF THE CASCADIA
INTERFACE AVERAGED ALONG THE RUPTURE LENGTH

Updip Model	Downdip Model	Rupture Model	
		Eureka to Middle of Washington	Eureka to the Explorer Plate
Deformation Front	Zero Isobase	120	115
	Thermal/Geodetic	100	110
Change in Fold Trends	Zero Isobase	90	80
	Thermal/Geodetic	70	80

HUMBOLDT BAY ISFSI FSAR UPDATE

TABLE 2.6-12

MEAN CHARACTERISTIC MAGNITUDES FOR THE CASCADIA INTERFACE USING THE CARVER SEGMENTATION MODEL

Updip Extent	Downdip Extent	Width (km)	Rupture Model	Length (km)	M(A) Model	Mag	Weights				Wt * Mag	
							Updip Extent	Downdip Extent	Length	M(A) Model		Total
Zero Isobase	Def. Front	120	Eureka to Mid Wash.	700	Geomatrix	8.69	0.3	0.6	0.5	0.5	0.045	0.39
Zero Isobase	Def. Front	115	Eureka to Expl. Plate	1050	Geomatrix	8.82	0.3	0.6	0.5	0.5	0.045	0.40
Zero Isobase	Fold Trends	90	Eureka to Mid Wash.	700	Geomatrix	8.59	0.7	0.6	0.5	0.5	0.105	0.90
Zero Isobase	Fold Trends	80	Eureka to Expl. Plate	1050	Geomatrix	8.69	0.7	0.6	0.5	0.5	0.105	0.91
Thermal-geodetic	Def. Front	100	Eureka to Mid Wash.	700	Geomatrix	8.62	0.3	0.4	0.5	0.5	0.03	0.26
Thermal-geodetic	Def. Front	110	Eureka to Expl. Plate	1050	Geomatrix	8.80	0.3	0.4	0.5	0.5	0.03	0.26
Thermal-geodetic	Fold Trends	70	Eureka to Mid Wash.	700	Geomatrix	8.50	0.7	0.4	0.5	0.5	0.07	0.60
Thermal-geodetic	Fold Trends	80	Eureka to Expl. Plate	1050	Geomatrix	8.69	0.7	0.4	0.5	0.5	0.07	0.61
Zero Isobase	Def. Front	120	Eureka to Mid Wash.	700	Abe	8.91	0.3	0.6	0.5	0.5	0.045	0.40
Zero Isobase	Def. Front	115	Eureka to Expl. Plate	1050	Abe	9.07	0.3	0.6	0.5	0.5	0.045	0.41
Zero Isobase	Fold Trends	90	Eureka to Mid Wash.	700	Abe	8.79	0.7	0.6	0.5	0.5	0.105	0.92
Zero Isobase	Fold Trends	80	Eureka to Expl. Plate	1050	Abe	8.91	0.7	0.6	0.5	0.5	0.105	0.94
Thermal-geodetic	Def. Front	100	Eureka to Mid Wash.	700	Abe	8.84	0.3	0.4	0.5	0.5	0.03	0.27
Thermal-geodetic	Def. Front	110	Eureka to Expl. Plate	1050	Abe	9.05	0.3	0.4	0.5	0.5	0.03	0.27
Thermal-geodetic	Fold Trends	70	Eureka to Mid Wash.	700	Abe	8.68	0.7	0.4	0.5	0.5	0.07	0.61
Thermal-geodetic	Fold Trends	80	Eureka to Expl. Plate	1050	Abe	8.91	9.7	0.4	0.5	0.5	0.07	0.62
												8.76

HUMBOLDT BAY ISFSI FSAR UPDATE

TABLE 2.6-13

MEAN CHARACTERISTIC MAGNITUDES FOR THE LITTLE SALMON FAULT SYSTEM

	#1	#2	#3	#4	#5	#6	#7	#8	#9	#10	#11	#12	#13
Approach	Approach Wt	Dip	Dip Wt	Thickness (km)	Downdip Width (km)	Segment Length (km)	Seg Wt	Area (km ²)	Disp (m)	Disp Wt	Mag	Total Wt	Wted Mag
Area	0.5	40	0.2	15	23.3	310	1	7223	N/A	N/A	7.85	0.10	0.79
Area	0.5	45	0.6	15	21.2	310	1	6572	N/A	N/A	7.81	0.30	2.34
Area	0.5	50	0.2	15	19.6	310	1	6076	N/A	N/A	7.78	0.10	0.78
Disp.	0.5					N/A	N/A		7	0.5	7.62	0.25	1.91
Disp.	0.5					N/A	N/A		9.3	0.5	7.72	0.25	1.93
												Mean	7.74

NOTES:

Using the dip (#2) and the thickness (#4), the downdip width (#5) is computed using eq. 2.6-6.

The area (#8) is computed by multiplying the downdip width (#5) and the segment length (#6).

The magnitude (#11) is computed using eq. 2.6-1 and the area in #8.

The total weight (#12) is the product of weights for the different approaches (#1), the segment weight (#7), and the dips (#3).

Using the displacement approach, the magnitude (#11) is computed using eq. 2.6-4 with the displacement per event value listed in #9.

The total weight (#12) is the product of the approach weight (#1) and the displacement per event weight (#10).

The magnitude is multiplied by the weight (#13).

The mean magnitude is computed using eq. 2.6-7 (sum of values in #13).

The mean weighted magnitude of 7.74 is rounded to 7.7 for defining the mean characteristic magnitude.

Equations may be found in HB ISFSI FSAR Update, Section 2.6.5.3.2.

HUMBOLDT BAY ISFSI FSAR UPDATE

TABLE 2.6-14

MCE FOR CASCADIA INTERFACE AND LITTLE SALMON FAULT

Subsource	Source Type	Moment Magnitude	Rupture Distance (km)
Little Salmon Fault Zone	Crustal Reverse	7.7	~0.5
Cascadia Interface	Subduction Interface	8.8	7

HUMBOLDT BAY ISFSI FSAR UPDATE

TABLE 2.6-15

84TH PERCENTILE MCE DESIGN SPECTRA FOR
THE FAULT NORMAL COMPONENT

Period (sec)	2% damping	4% damping	5% damping	7% damping
0.000	1.316	1.316	1.316	1.316
0.020	1.316	1.316	1.316	1.316
0.030	1.415	1.370	1.351	1.324
0.050	1.608	1.489	1.441	1.373
0.075	1.888	1.689	1.612	1.502
0.100	2.207	1.928	1.821	1.672
0.150	2.796	2.380	2.224	2.010
0.200	3.192	2.699	2.515	2.264
0.300	4.568	3.863	3.600	3.240
0.640	4.568	3.863	3.600	3.240
0.750	4.568	3.863	3.600	3.240
1.000	4.576	3.866	3.600	3.236
1.500	4.568	3.863	3.600	3.240
1.700	4.434	3.754	3.502	3.152
2.000	3.792	3.216	3.000	2.703
2.400	3.020	2.570	2.400	2.167
3.000	2.565	2.191	2.050	1.855
4.000	1.857	1.598	1.500	1.365
5.000	1.225	1.062	1.000	0.914
7.000	0.564	0.489	0.460	0.420
10.000	0.312	0.271	0.255	0.233

HUMBOLDT BAY ISFSI FSAR UPDATE

TABLE 2.6-16

84TH PERCENTILE MCE DESIGN SPECTRA FOR
THE FAULT PARALLEL COMPONENT

Period (sec)	2% damping	4% damping	5% damping	7% damping
0.000	1.316	1.316	1.316	1.316
0.020	1.316	1.316	1.316	1.316
0.030	1.415	1.370	1.351	1.324
0.050	1.608	1.489	1.441	1.373
0.075	1.888	1.689	1.612	1.502
0.100	2.207	1.928	1.821	1.672
0.150	2.796	2.380	2.224	2.010
0.200	3.192	2.699	2.515	2.264
0.300	4.552	3.849	3.587	3.228
0.640	4.114	3.479	3.242	2.918
0.750	3.934	3.326	3.100	2.790
1.000	3.559	3.007	2.800	2.517
1.500	3.122	2.640	2.460	2.214
1.700	2.784	2.357	2.199	1.979
2.000	2.275	1.930	1.800	1.622
2.400	1.510	1.285	1.200	1.083
3.000	1.001	0.855	0.800	0.724
4.000	0.557	0.479	0.450	0.410
5.000	0.331	0.287	0.270	0.247
7.000	0.159	0.138	0.130	0.119
10.000	0.085	0.073	0.069	0.063

HUMBOLDT BAY ISFSI FSAR UPDATE

TABLE 2.6-17

84TH PERCENTILE MCE DESIGN SPECTRA FOR THE VERTICAL COMPONENT

Period (sec)	2% damping	4% damping	5% damping	7% damping
0.000	1.673	1.673	1.673	1.673
0.020	1.673	1.673	1.673	1.673
0.030	2.634	2.415	2.329	2.209
0.050	4.309	3.724	3.503	3.205
0.075	5.513	4.625	4.299	3.864
0.100	5.403	4.428	4.076	3.612
0.120	5.011	4.086	3.753	3.316
0.150	4.462	3.628	3.328	2.935
0.170	4.183	3.407	3.127	2.760
0.200	3.756	3.074	2.828	2.504
0.240	3.285	2.701	2.489	2.210
0.300	2.752	2.270	2.095	1.864
0.400	2.251	1.857	1.714	1.525
0.500	1.907	1.573	1.452	1.292
0.750	1.526	1.259	1.162	1.034
1.000	1.196	0.985	0.909	0.808
1.500	0.773	0.638	0.589	0.524
2.000	0.578	0.479	0.443	0.395
3.000	0.385	0.322	0.299	0.268
4.000	0.283	0.239	0.223	0.201
5.000	0.222	0.189	0.177	0.161
7.000	0.157	0.134	0.125	0.114
10.000	0.109	0.093	0.087	0.079

HUMBOLDT BAY ISFSI FSAR UPDATE

TABLE 2.6-18

EQUAL HAZARD SPECTRA (g) FOR THE FAULT NORMAL COMPONENT
FOR SOIL SAFE CONDITIONS.

Period (sec)	1 Yr	25 yr	50 yr	100 yr	500 yr	1,000 yr	2,000 yr	5,000 yr	10,000 yr
0.01	0.0042	0.3118	0.4109	0.5294	0.7957	0.8890	0.9674	1.0798	1.1726
0.03	0.0043	0.3168	0.4175	0.5379	0.8084	0.9032	0.9829	1.0971	1.1914
0.10	0.0076	0.5219	0.6601	0.7940	1.1012	1.2304	1.3389	1.4944	1.6229
0.15	0.0088	0.6578	0.8621	1.0533	1.5286	1.6959	1.8015	1.9487	2.0767
0.20	0.0110	0.8266	1.0890	1.3608	2.0493	2.2716	2.5157	2.8337	3.1006
0.25	0.0104	0.8450	1.1837	1.5217	2.2760	2.6377	2.9280	3.2399	3.4770
0.30	0.0094	0.7644	1.1031	1.4322	2.2161	2.4778	2.7427	3.0941	3.3236
0.35	0.0087	0.6646	0.9734	1.3427	2.1535	2.4478	2.6454	2.8930	3.1113
0.40	0.0082	0.6128	0.8953	1.2384	2.0439	2.2503	2.4775	2.6986	2.8719
0.50	0.0069	0.5380	0.7870	1.0810	1.8927	2.1027	2.2800	2.5320	2.7128
0.60	0.0051	0.4335	0.6546	0.9338	1.7485	1.9607	2.1531	2.4228	2.6165
0.80	0.0040	0.3210	0.4837	0.6964	1.4445	1.6883	1.8618	2.0882	2.2517
1.00	0.0038	0.2985	0.4469	0.6452	1.3165	1.5507	1.7382	1.9419	2.1210
1.50	0.0025	0.2000	0.3196	0.4764	1.0821	1.3129	1.5282	1.8083	2.0373
2.00	0.0013	0.1205	0.1967	0.3111	0.8237	1.0551	1.2766	1.5738	1.7904
3.00	0.0001	0.0465	0.0763	0.1216	0.3356	0.5055	0.6782	0.8977	1.0571

HUMBOLDT BAY ISFSI FSAR UPDATE

TABLE 2.6-19

EQUAL HAZARD SPECTRA (G) FOR THE FAULT PARALLEL COMPONENT
FOR SOIL SITE CONDITIONS.

Period (sec)	1 Yr	25 yr	50 yr	100 yr	500 yr	1,000 yr	2,000 yr	5,000 yr	10,000 yr
0.01	0.0042	0.3118	0.4109	0.5294	0.7957	0.8890	0.9674	1.0798	1.1726
0.03	0.0043	0.3168	0.4175	0.5379	0.8084	0.9032	0.9829	1.0971	1.1914
0.10	0.0076	0.5219	0.6601	0.7940	1.1012	1.2304	1.3389	1.4944	1.6229
0.15	0.0088	0.6578	0.8621	1.0533	1.5286	1.6959	1.8015	1.9487	2.0767
0.20	0.0110	0.8266	1.0890	1.3608	2.0493	2.2716	2.5157	2.8337	3.1006
0.25	0.0104	0.8450	1.1837	1.5217	2.2760	2.6377	2.9280	3.2399	3.4770
0.30	0.0094	0.7644	1.1031	1.4322	2.2161	2.4778	2.7427	3.0941	3.3236
0.35	0.0087	0.6646	0.9734	1.3427	2.1535	2.4478	2.6454	2.8930	3.1113
0.40	0.0082	0.6128	0.8953	1.2384	2.0439	2.2503	2.4775	2.6986	2.8719
0.50	0.0069	0.5380	0.7870	1.0810	1.8927	2.1027	2.2800	2.5320	2.7128
0.60	0.0051	0.4335	0.6546	0.9338	1.7485	1.9607	2.1531	2.4228	2.6165
0.80	0.0040	0.3210	0.4838	0.6959	1.4360	1.6696	1.8373	2.0551	2.2098
1.00	0.0038	0.2985	0.4468	0.6452	1.3053	1.5272	1.7066	1.8845	2.0361
1.50	0.0025	0.2000	0.3196	0.4766	1.0630	1.2631	1.4237	1.6423	1.8033
2.00	0.0013	0.1205	0.1966	0.3114	0.7924	0.9638	1.1069	1.2808	1.4055
3.00	0.0001	0.0464	0.0763	0.1223	0.3109	0.3840	0.4744	0.5714	0.6470

HUMBOLDT BAY ISFSI FSAR UPDATE

TABLE 2.6-20

EQUAL HAZARD SPECTRA FOR THE VERTICAL COMPONENT.

Period (sec)	1 Yr	25 yr	50 yr	100 yr	500 yr	1,000 yr	2,000 yr	5,000 yr	10,000 yr
0.01	0.0011	0.0968	0.1513	0.2311	0.5338	0.6399	0.7309	0.8554	0.9419
0.03	0.0013	0.1228	0.1944	0.3035	0.7464	0.8965	1.0243	1.1988	1.3201
0.10	0.0030	0.3776	0.6004	0.9524	2.4124	2.8923	3.3594	3.9191	4.2739
0.15	0.0039	0.4189	0.6495	0.9891	2.2319	2.7238	3.1658	3.6701	4.1043
0.20	0.0040	0.3707	0.5676	0.8440	1.9088	2.3499	2.7126	3.1875	3.6014
0.25	0.0038	0.3055	0.4646	0.6784	1.5234	1.8962	2.2196	2.6067	2.9437
0.30	0.0034	0.2514	0.3805	0.5476	1.2198	1.5286	1.8102	2.1229	2.3949
0.40	0.0025	0.1746	0.2634	0.3758	0.8721	1.1024	1.3194	1.5777	1.7638
0.50	0.0020	0.1285	0.1919	0.2713	0.6513	0.8372	0.9937	1.1916	1.3193
0.60	0.0016	0.0971	0.1461	0.2076	0.5033	0.6578	0.7859	0.9464	1.0606
0.80	0.0010	0.0586	0.0885	0.1246	0.3131	0.3817	0.4281	0.4873	0.5304
1.00	0.0006	0.0378	0.0564	0.0814	0.2078	0.2557	0.2886	0.3286	0.3592
1.50	0.0002	0.0159	0.0247	0.0362	0.0913	0.1146	0.1364	0.1591	0.1763
2.00	0.0001	0.0083	0.0133	0.0196	0.0477	0.0623	0.0764	0.0916	0.1021
3.00	0.0000	0.0026	0.0045	0.0070	0.0176	0.0236	0.0296	0.0383	0.0434

HUMBOLDT BAY ISFSI FSAR UPDATE

TABLE 2.6-21

WELL-STUDIED HISTORICAL THRUST EARTHQUAKES ASSOCIATED WITH SURFACE FAULT RUPTURES

Date	Location	M	L	V	H	References ^(a)
1952	Kern County, California	7.7 M _s	57	1.2	0.8	265 266
1964	Prince William Sound	9.2 M _w	57	6-9		68 200 267
1968	Meckering, Australia	6.9 M _s	37	2	1.5	268
1968	Inanghua, New Zealand	7.1 M _s	>2	0.4	0.2	269 270 271
1971	San Fernando, California	6.5 M _s	16	2.5		272
1978	Tabas-e-Golshan, Iran	7.5 M _s	85	3		273 274
1980	El Asnam, Algeria	7.3 M _s	31. 2	6.5		208 275
1988	Tennant Creek, Australia	6.3 M _s 6.4 M _s 6.7 M _s	10. 2 6.7 16	0.1- 0.2 1.1 1.7	0.25 0.1 0.4	276
1988	Spitak, Armenia	6.8 M _s	24	2		277
1999	Chi-Chi, Taiwan	7.6 M _w	80	9	8	202

^(a) Refer to Section 2.6.10

M = magnitude; L = total length of rupture zone in kilometers, including unbroken sections;
V = maximum vertical displacement in meters; H = maximum horizontal displacement in meters.

HUMBOLDT BAY ISFSI FSAR UPDATE

TABLE 2.6-22

OBSERVATIONS OF RUNUP ELEVATIONS AT HUMBOLDT BAY
AND OTHER LOCATIONS IN NORTHERN CALIFORNIA, FROM
THE 27-28 MARCH 1964 ALASKA EARTHQUAKE (PG&E, 1966)

Location	Maximum Runup Elevation above MLLW (feet)	Tide Level at Time of Maximum Runup, Elevation above MLLW (feet)	Elevation of Maximum Runup above Tide Level (feet)	Remarks
U.S. Coast Guard Station, Humboldt Bay, North Spit	9	probably 5.9	probably 3.1	U.S. Army Engineer District, San Francisco
Municipal Marina, Eureka, Humboldt Bay	10.8 ±2	probably between 5.7 and 6.1	probably between 4.7 and 5.1 ±2	U.S. Army Engineer District, San Francisco
King Salmon (entrance to King Salmon Slough), Humboldt Bay	10.4 ±2	probably 5.9	probably 4.5 ±2	U.S. Army Engineer District, San Francisco
Humboldt Bay Power Plant Intake (0.6 mile upstream on King Salmon Slough), Humboldt Bay	9.65	5.9	3.8	Note from G. E. Altman, PG&E: Time of maximum runup, 5:00 AM, 28 March 1964
	9.6	5.2	4.4	Note from G. E. Altman, PG&E: Time, 1:30 PM, 28 March 1964
Pier at Trinidad	17.5 ±2	probably between 4.2 and 5.3	probably between 12.2 and 13.3 ±2	U.S. Army Engineer District, San Francisco
Crescent City	20 to 21	5.1	14.9 to 15.9	U.S. Army Engineer District, San Francisco
Pebble Beach, about 2 miles north of Crescent City Harbor	about 15	about 5	about 10	U.S. Army Engineer District, San Francisco
Ship Ashore Restaurant, just inside entrance of Smith River	12 ±2	probably about 5	about 7 ±2	U.S. Army Engineer District, San Francisco

HUMBOLDT BAY ISFSI FSAR UPDATE

TABLE 2.6-23

Sheet 1 of 2

EVIDENCE OF PAST TSUNAMIS AT MARSH SITES IN NORTHERN CALIFORNIA

		Freshwater Marsh Sites							Salt Marsh Sites							
	<div><div>• Present</div><div>— Not Present</div></div>	Crescent City	Lagoon Creek	High Prairie Creek	East Creek	Major Creek	Orick	Big Lagoon	Mad River Slough	Jacoby Creek Marsh	Eureka Slough	Humboldt Bay Power Plant	South Bay	HB National Wildlife Refuge	Railroad	Hookton Slough
Salt Marsh	Lithologic evidence for coseismic subsidence 1	—	—	—			•		•	•	•		•	•	•	•
	Diatom evidence for coseismic subsidence 2	—	—				•		•				•			•
	Sand present on subsided contact 3						•		—	—	—		•	—	—	•
Fresh Marsh	Muddy post-tsunami disturbance signal 4	•	•	—			•									
	Sand layer overlying freshwater deposits 5	•	•	•	•	•	•	•								
Sand Layer Characteristics	Thins inland 6	•	•				•						•			
	Fines inland 7	—	•										—			
	Rip-up clasts 8	•	•										•			•
	Sharp basal contacts 9	•	•		•	•	•	•					•			•
	Erosive basal contacts 10	•	•										•			•
	Sharp upper contacts 11	•	•		•	•	•	•					•			•?
	Well sorted 12	•	•		•	•	•	•					•			•?
	Similar grain-size distribution as beach 13	•	•		•	•	•	•					•			
	Similar lithology as beach 14	•	•				•									
	Landward transport of landslide debris 15		•													
	Woody debris mixed in 16	•	•		•	•										•
	Trash layer on top: wood, peat, mud, sand 17	•	•		•	•										•
	Normally graded 18	•	•			•	•	•					•			•
	Multiple normally graded pulses 19	•	•				•						•			•
	Pulses separated by silt partings 20	•					•									•
	Flopovers between pulses 21	•														
	Allochthonous marine diatoms 22	•	•		•	•	•						•			
	Broken, but well preserved diatoms 23		•													•
	“Beach” diatoms 24	•	•				•						•			

HUMBOLDT BAY ISFSI FSAR UPDATE

TABLE 2.6-23

Sheet 2 of 2

		Freshwater Marsh Sites							Salt Marsh Sites							
	<div><div>• Present</div><div>— Not Present</div></div>	Crescent City	Lagoon Creek	High Prairie Creek	East Creek	Major Creek	Orick	Big Lagoon	Mad River Slough	Jacoby Creek Marsh	Eureka Slough	Humboldt Bay Power Plant	South Bay	HB National Wildlife Refuge	Railroad	Hookton Slough
	Native America legends	•	•				•	•	•		•			•	•	
	Tsunami evidence	yes	yes	no	yes	yes	yes	yes	no	no	no	no	yes	no	no	yes
	Minimum number of tsunamis evident	7	6	0	1	1	3	2	0	0	0	0	3	0	0	3

Notes: See Figures 2.6-88 and 2.6-114 for locations
 Numbers in Column 2 refer to diagrams in Figures 2.6-89 and 2.6-90

HUMBOLDT BAY ISFSI FSAR UPDATE

TABLE 2.6-24

CASCADIA SUBDUCTION ZONE EVENTS

Event	Years Before Present (1950) (calibrated 2-sigma values)
“Y”	250 (January 26, 1700, 9:00 PM)
“W”	~1,100
“U”	~1,300
“S”	~1,600
“N”	~2,500
“L”	~2,900

HUMBOLDT BAY ISFSI FSAR UPDATE

TABLE 2.6-25

OPEN COAST RUNUP ESTIMATES FROM PALEOSEISMIC SITES ALONG THE NORTHERN CALIFORNIA COAST AND WORLD WIDE DATA

Site	Estimated Runup Height at Coast (feet above MLLW)	Comments
Crescent City	Higher than 28 to 31 feet	Comparison of paleotsunami deposits with deposits in Kodiak Island from the 1964 Alaska earthquake.
Lagoon Creek	18 to 52 feet Most likely 26 to 33 feet	Table 2.6-24 – values calculated using particle size and settlement velocities for “Y”, “W”, “U”, and “S” events. Most likely runup is judged to be 26 to 33 feet.
Orick	66 to 69 feet	From Native American oral history; high elevation may be anomalous local runup.
North Spit	A) Somewhat higher than 38 feet; less than 50 feet estimate 35 to 40 feet B) Less than 53 to 72 feet	A) Pebble layer at elevation of 38 ft. in dunes provides minimum estimate. Adding 12 feet depth to transport pebbles gives possible 50 feet B) Height of dunes provides maximum estimate.
South Spit	A) Higher than 18 to 23 feet B) Less than 20-40 feet	A) Height of dunes B) Height of marsh plus estimated depth of 13 to 33 ft. based on comparison with event “Y” at Lagoon Creek.
World Wide Data (Appendix A)	35 feet 30 to 40 feet	Figure 2.6-119 Empirical relationship for a tectonic runup vs. magnitude. Runup for MLLW adds 3.7 feet to MSL. A) For a 8.8 Cascadia event runup is 31 feet MSL B) For magnitude range 8.5 to 9.2 runup is 26 to 36 feet MSL

HUMBOLDT BAY ISFSI FSAR UPDATE

TABLE 2.6-26

ESTIMATED RUNUP HEIGHTS AT LAGOON CREEK FROM THE SEDIMENT TRANSPORT MODEL

Event	Maximum particle size (mm)	Most likely velocity (ft/sec) [m/sec]	Most likely depth of water above marsh surface at time of deposit (ft) [m]	Most likely depth of water referenced to MLLW (ft)
“Y”	2	6.5 – 16.3 [2 – 5]	13 – 32.5 [4 – 10]	20 – 39.5
“W”	3	6.5 – 16.3 [2 – 5]	14.5 – 36 [4.5 – 11]	21.5 – 42.5
“U”	2	6.5 – 16.3 [2 – 5]	11.5 – 29.5 [3.5 – 9]	18.5 – 36.5
“S”	10	6.5 – 16.3 [2 – 5]	16.5 – 45.5 [5 – 14]	23.5 – 52.5

Notes:

Measured from the stratigraphy at Core 4 that is 2000 feet inland from the beach berm.
Reasonable velocities based on empirical data on natural flows in rivers and tidal bores

HUMBOLDT BAY ISFSI FSAR UPDATE

TABLE 2.6-27

WIEGEL'S ESTIMATES OF TSUNAMI RUNUPS AND THEIR PROBABILITY AT HUMBOLDT BAY POWER PLANT

Maximum Tsunami Runup (feet above MLLW)	Probability Level
19	10% in 1000 years
13	10% in 100 years
11	10% in 50 years
6.5	10% in 10 years

HUMBOLDT BAY ISFSI FSAR UPDATE

TABLE 2.6-28

ESTIMATES OF MAXIMUM RUNUP ELEVATIONS AT THE ISFSI SITE

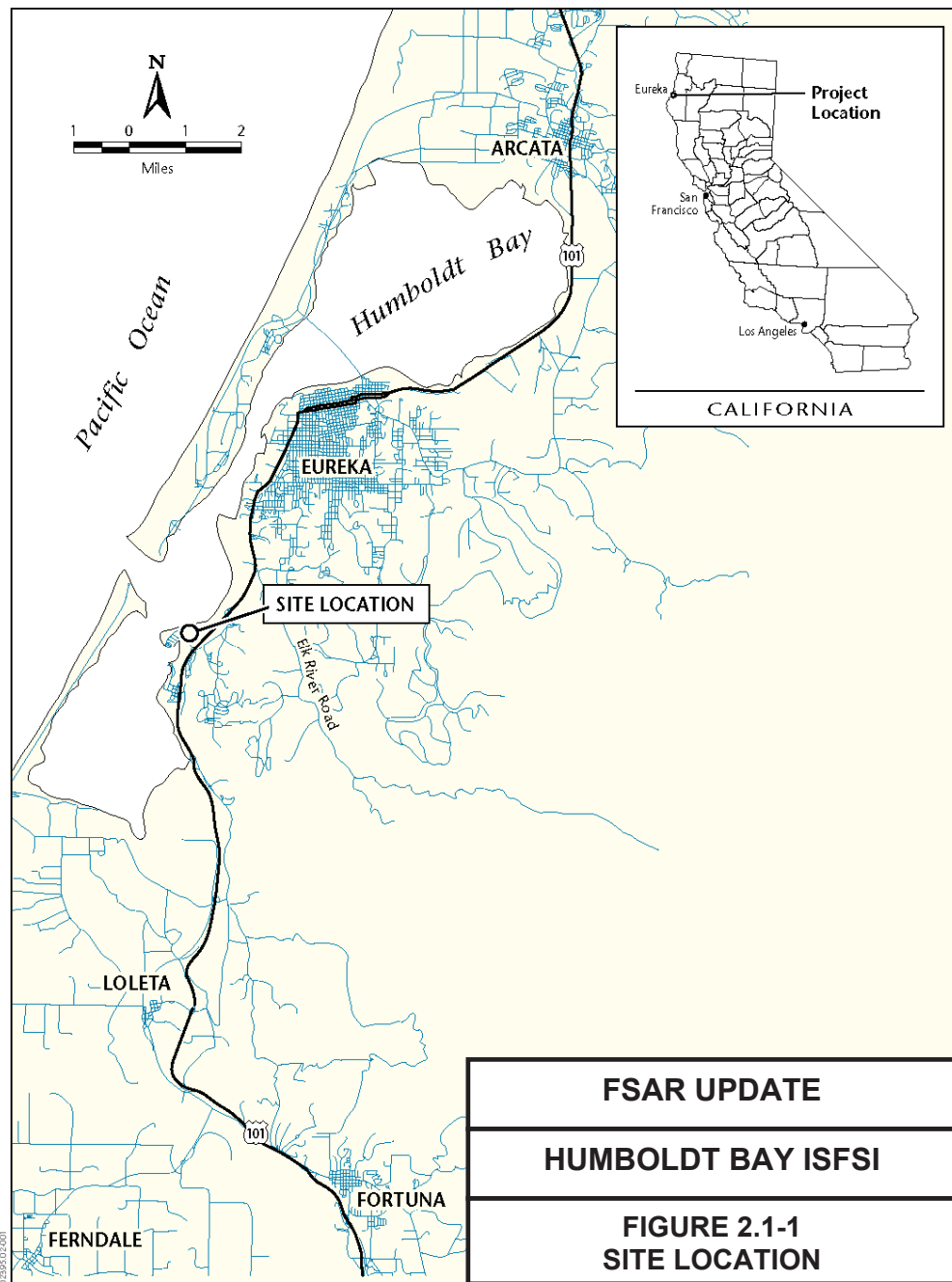
Researcher	Basis	Estimated Maximum Runup at Bay Entrance (feet above MLLW)	Estimated Maximum Runup at Humboldt Bay ISFSI Site (feet) and Attenuation (%)		
			MLLW	MHHW ^(a)	
Calculated Runups - Distant Tsunamis					
Wiegel (Reference ^(b) 210)	Calculated - 10% in 1000 years		19	26	
PG&E (Reference 219) using Brandsma & others (Reference 253) procedure	Calculated	16.1	<16.1 ^{** (c)}	<23 ^(c)	
PG&E (Reference 219), using Houston & Garcia (Reference 255) procedure	Calculated - 100-year tsunami 500-year tsunami	10.6 20.7	<10.6 ^(c) <20.7 ^(c)	<17.5 ^(c) <27.6 ^(c)	
For comparison: maximum historical distant tsunami	Observations for ~150 years	~15	9.6	16.5	
Calculated Runups - Local Tsunamis					
Wiegel (Reference 210)	Judgment	25	12.5 50%	19.4	
Whitmore (Reference 256)	Cascadia M 8.8; modeled wave amplitude that were considered equal to runup	8.7	2.8 32%	9.7	
Bernard and others (Reference 257)	Judgment for input wave amplitude (10 m) offshore; model and judgment used for inundation	33 (equal to input wave)	10 30 %	17	
Lamberson and others (Reference 257)	Wave of arbitrary amplitude (6 m) offshore of as input to model	26	16.4 63 %	23.3	
Meyer and others, (Reference 213)	Results of finite-element model for tsunami wave propagation	30	<23	<30	
Runup Estimates from Paleotsunami Studies					
Estimate from study of past tsunamis Carver and others (Reference 222)	Stratigraphy and judgment for runup at South Spit	18-40	<18-40	<18-40	
	Minimum sand-carrying water depth (13 to 17 ft) added to elevation (5 to 7 ft) of marsh	Likely depth to deposit sand (19 to 27 ft) added to elevation (5 to 7 ft) of marsh	"<35 to 85" (from back calculation using 0.3 and 0.7 from ISFSI site)	<24 to 34	

Notes: Numbers in Italics have been calculated by adding tidal range of 6.9 feet

^(a) Mean higher high tide (MHHW) is 6.9 feet higher than mean lower low tide (MLLW)

^(b) For all references, refer to Section 2.6.10.

^(c) Assumes runup at Humboldt Bay ISFSI site is less than runup at coast.

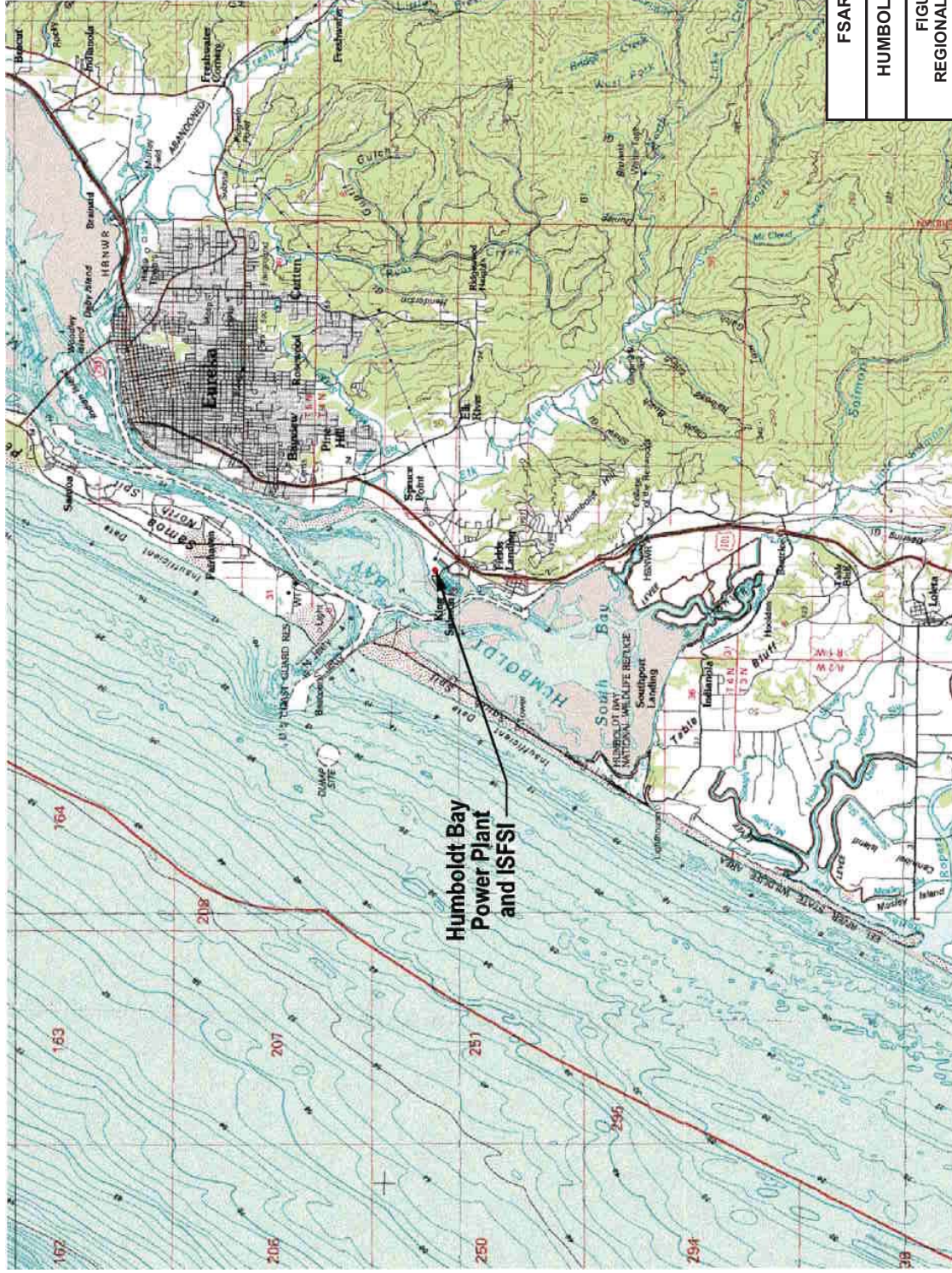


Revision 0 January 2006



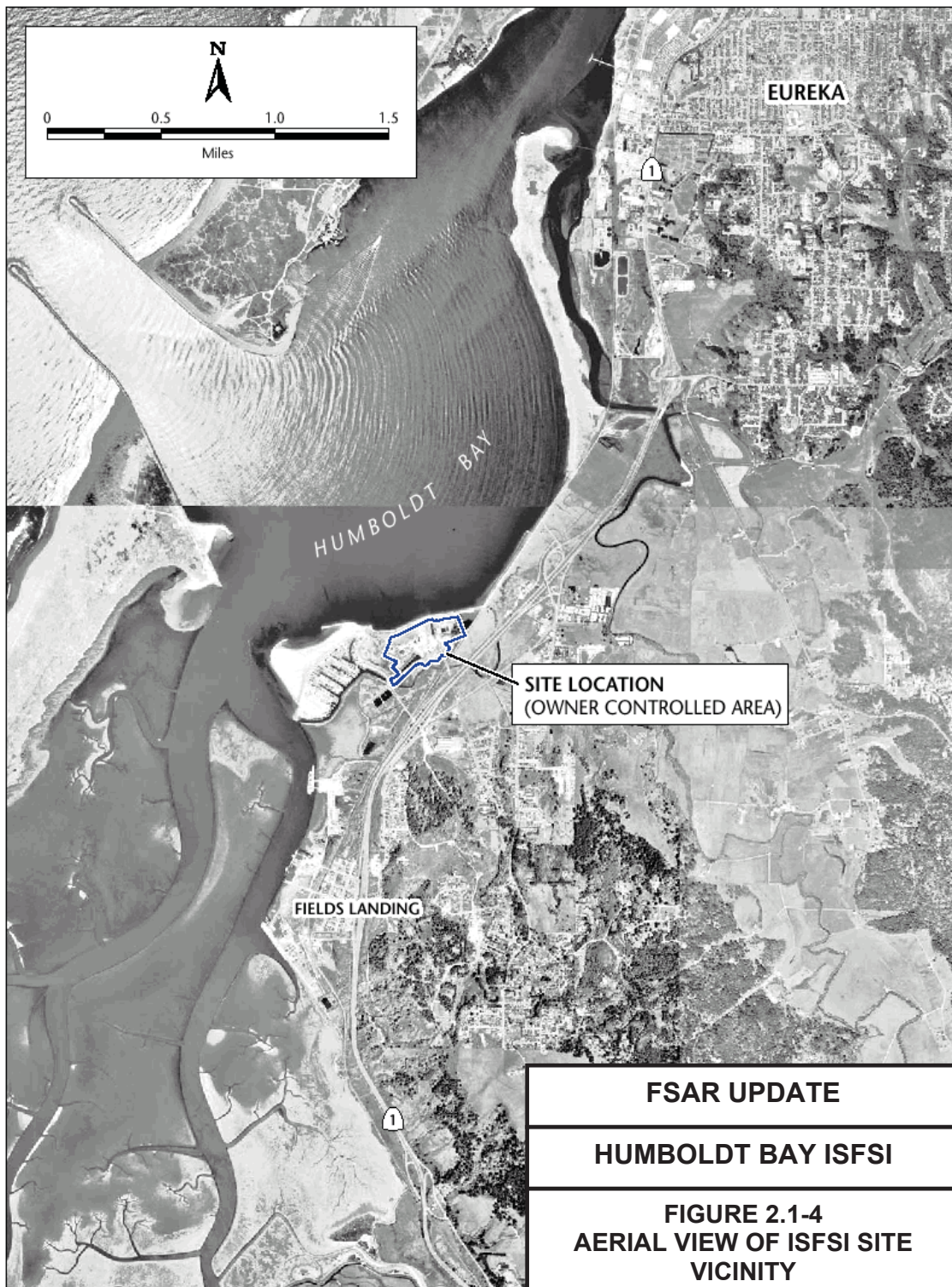
FSAR UPDATE
HUMBOLDT BAY ISFSI
FIGURE 2.1-2 PROPERTY PLAN

Revision 0 January 2006

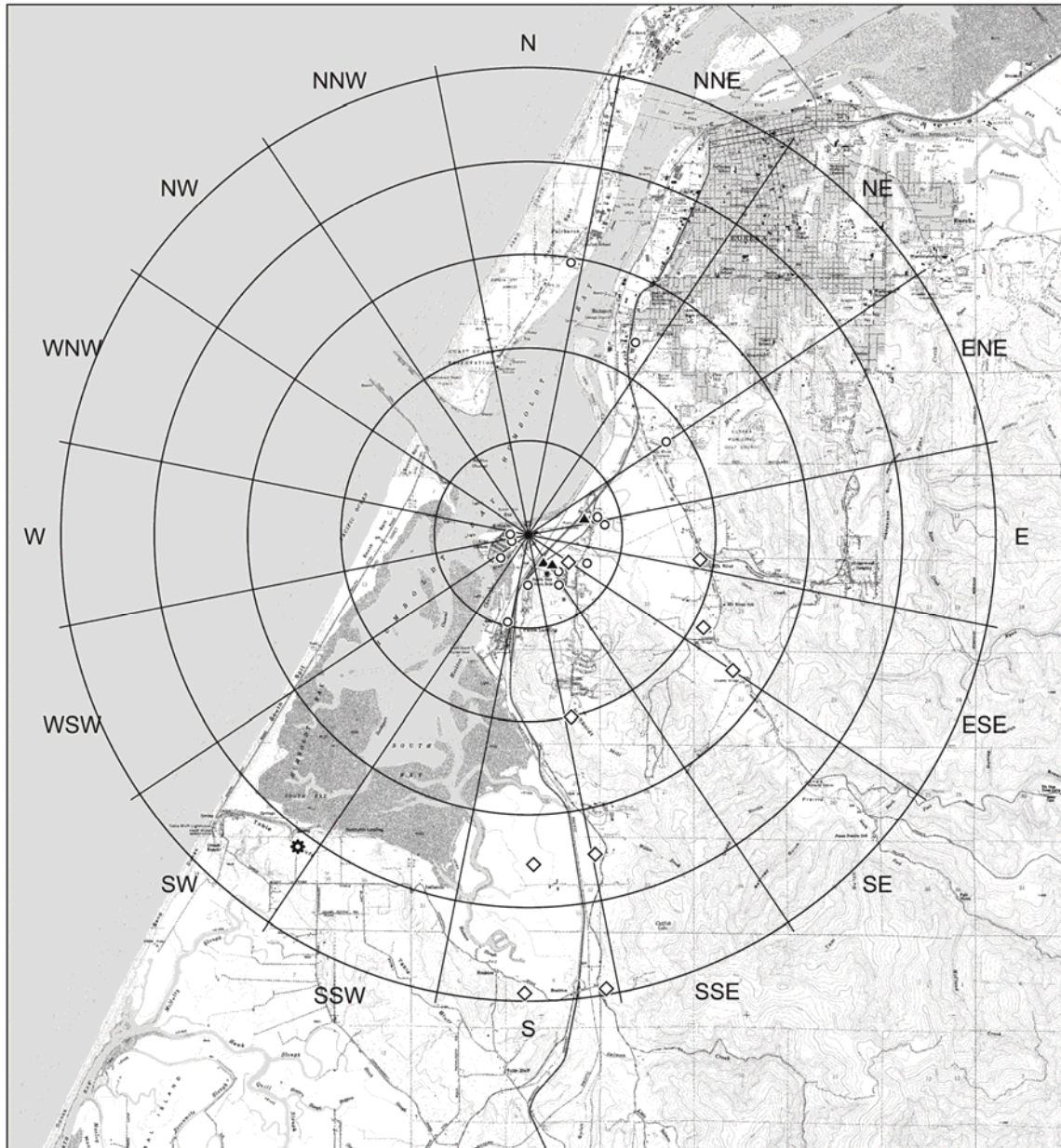


FSAR UPDATE
HUMBOLDT BAY ISFSI
FIGURE 2.1-3 REGIONAL TOPOGRAPHY

Revision 0 January 2006

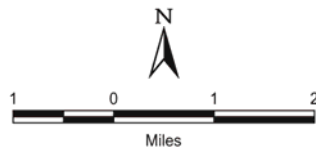


Revision 0 January 2006



LEGEND

- Nearest Residence
- ◇ Farm or Ranch
- ▲ Groundwater Well
- ⚙ Community Garden



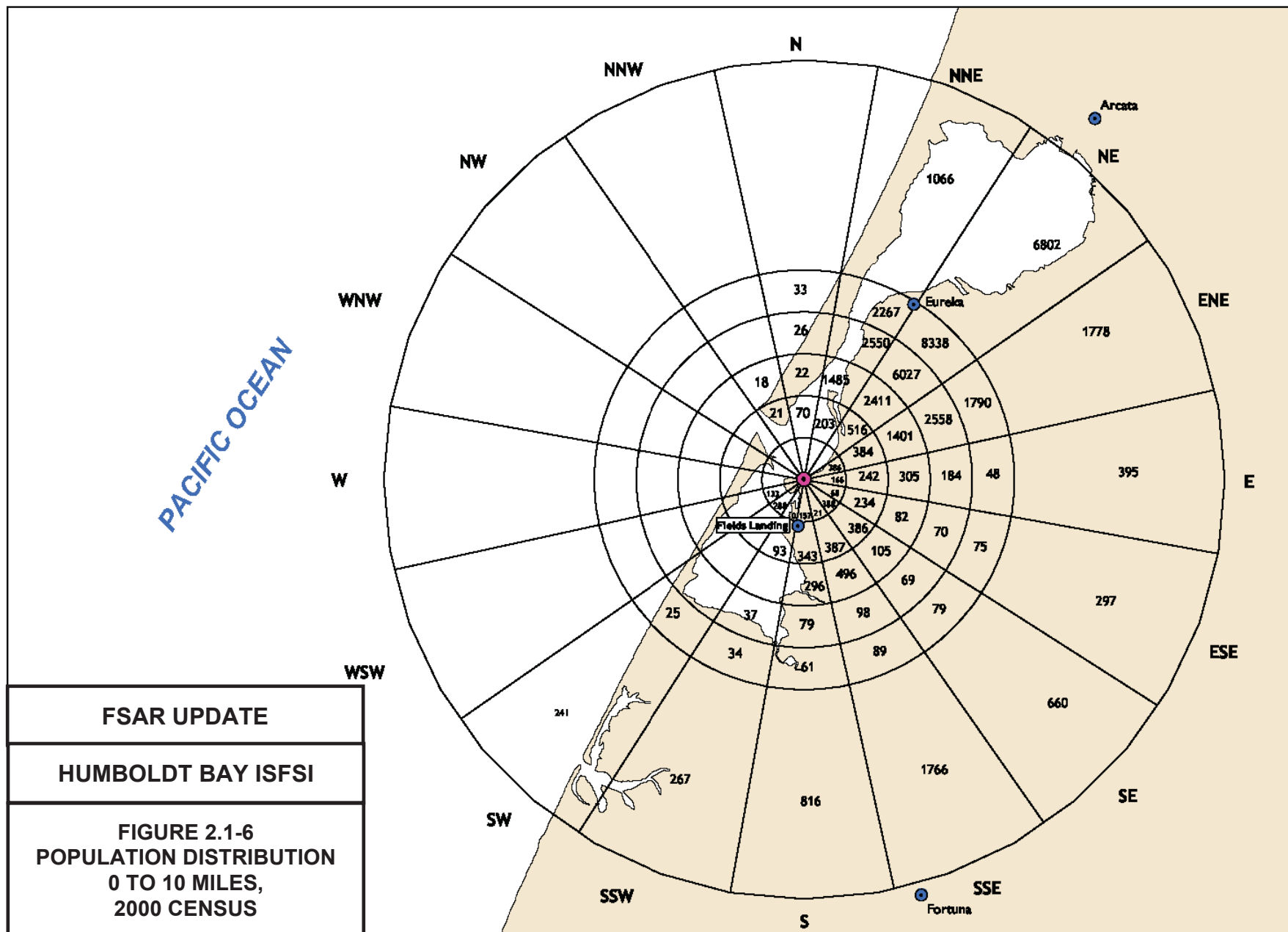
Base Map: USGS 7.5' series California quadrangles:
Arcata South, Cannibal Island, Eureka,
and Fields Landing

FSAR UPDATE

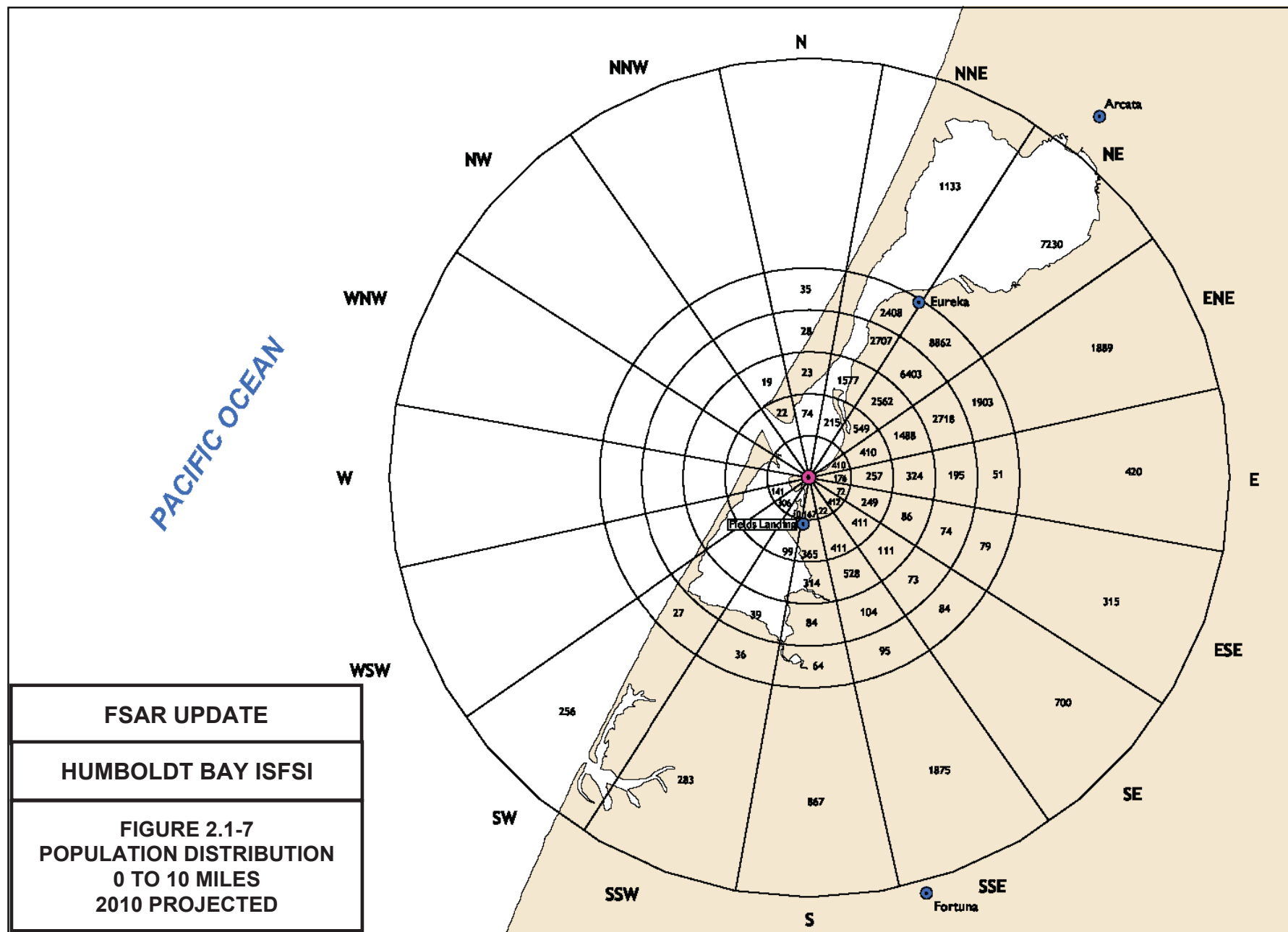
HUMBOLDT BAY ISFSI

**FIGURE 2.1-5
SENSITIVE LAND USES**

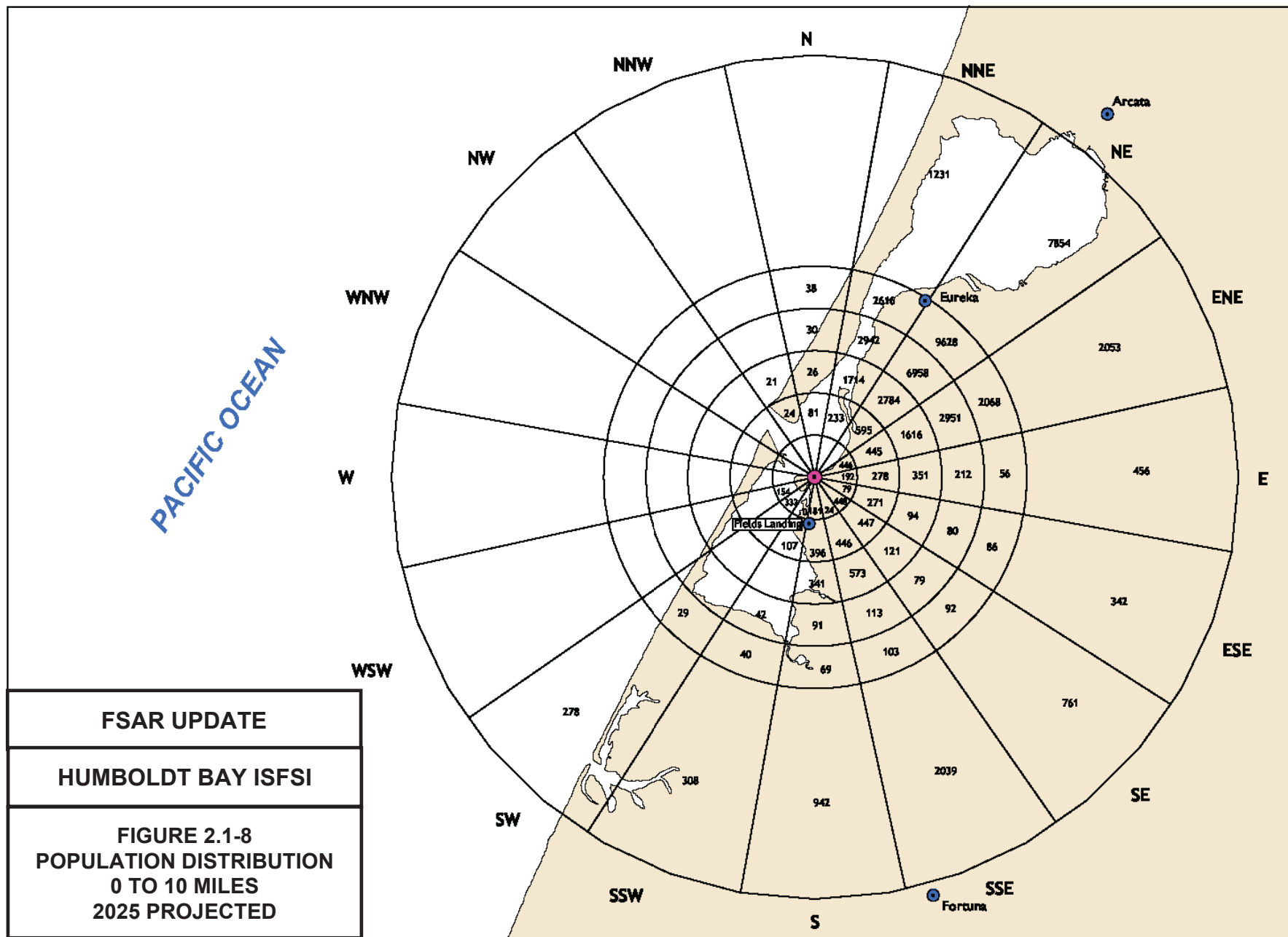
Revision 0 January 2006



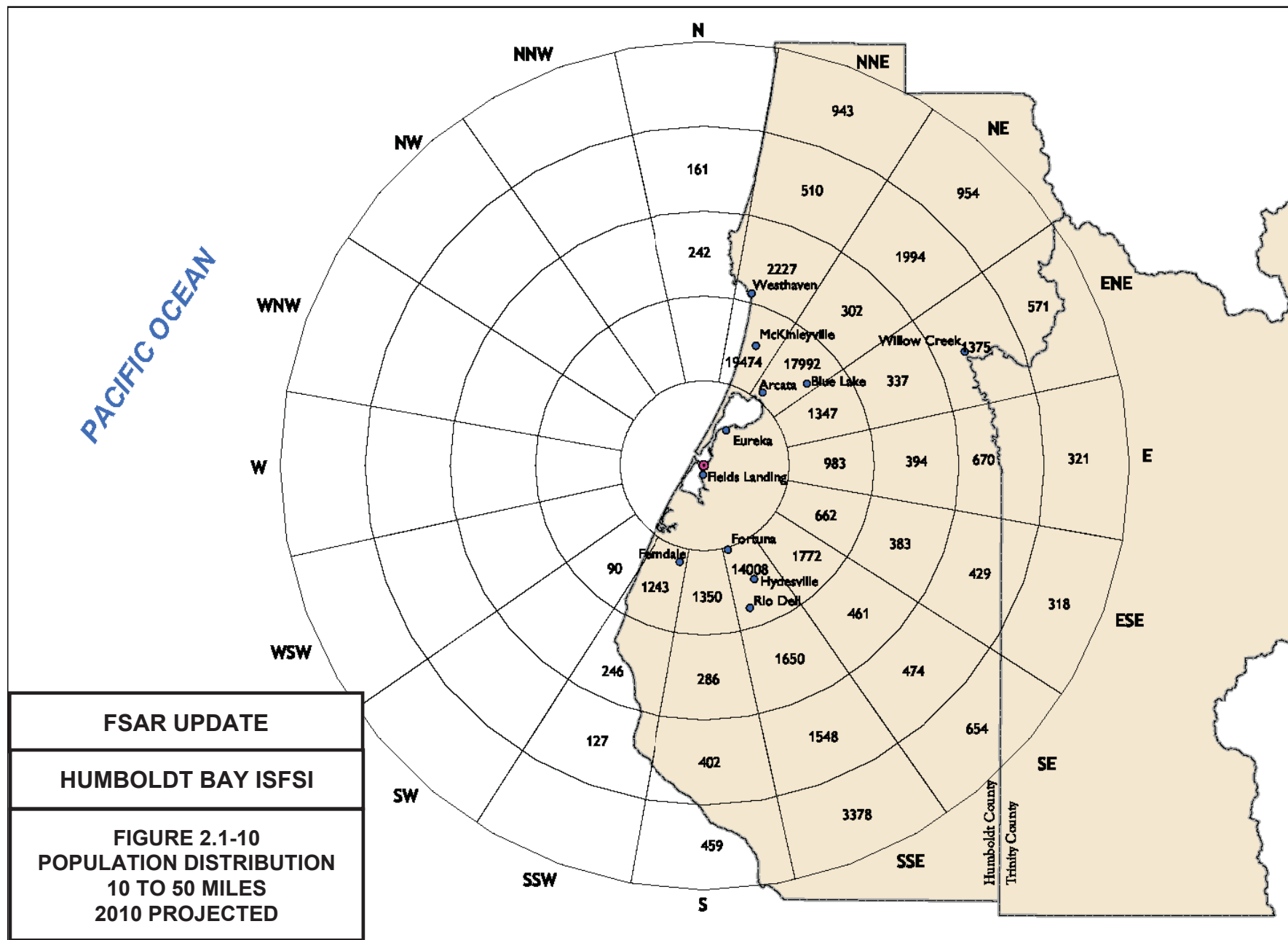
Revision 0 January 2006



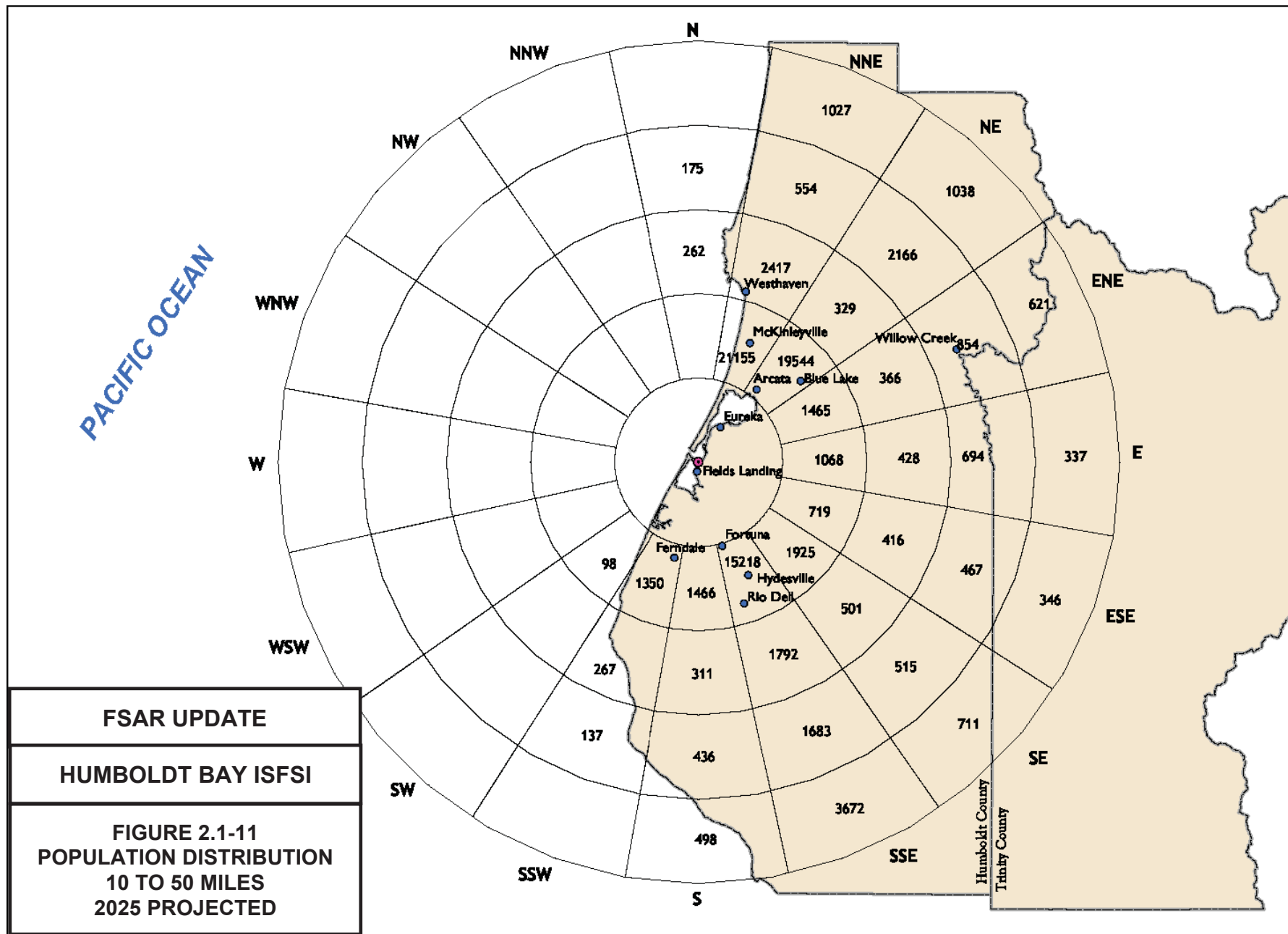
Revision 0 January 2006



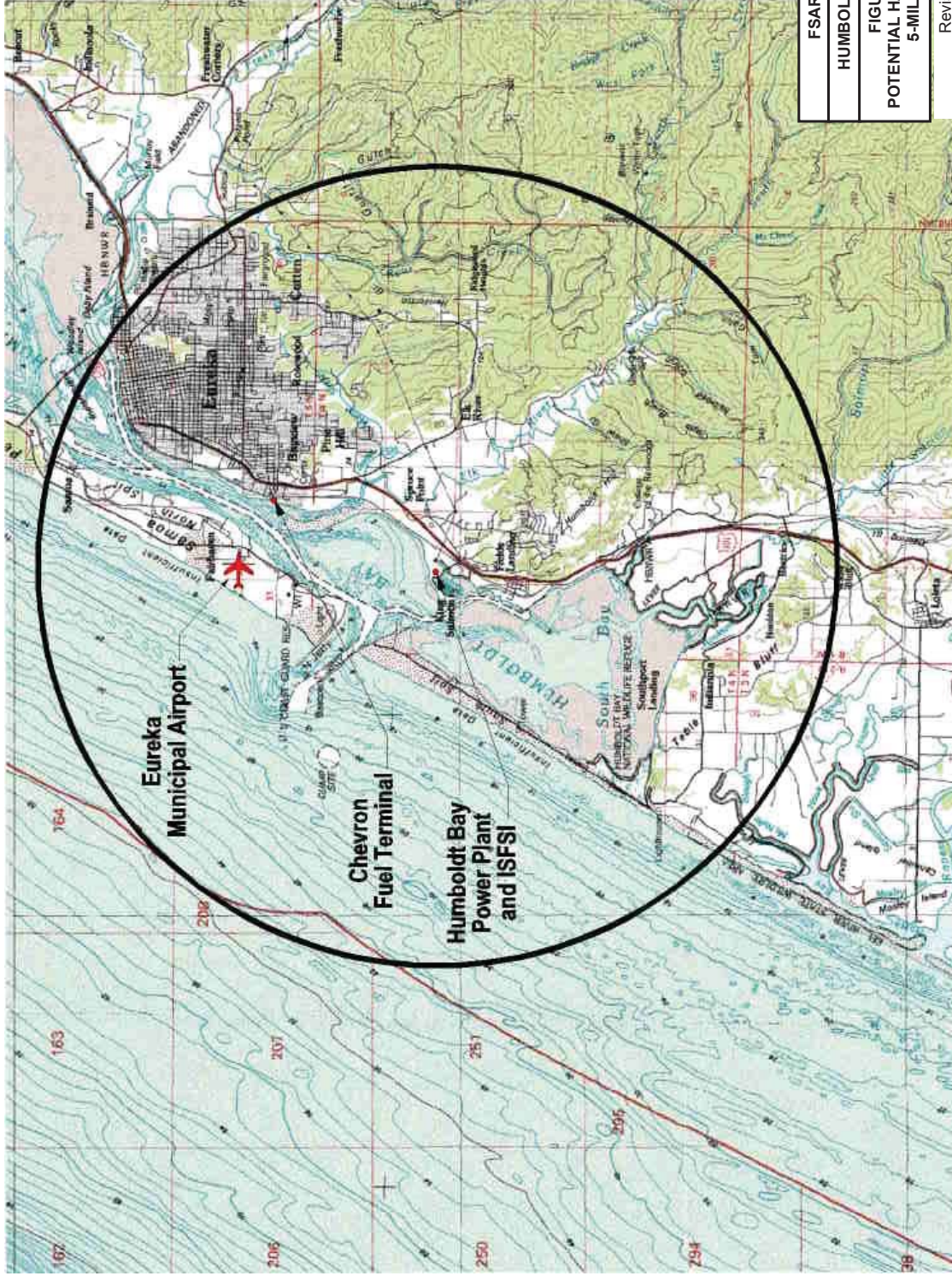
Revision 0 January 2006



Revision 0 January 2006



Revision 0 January 2006

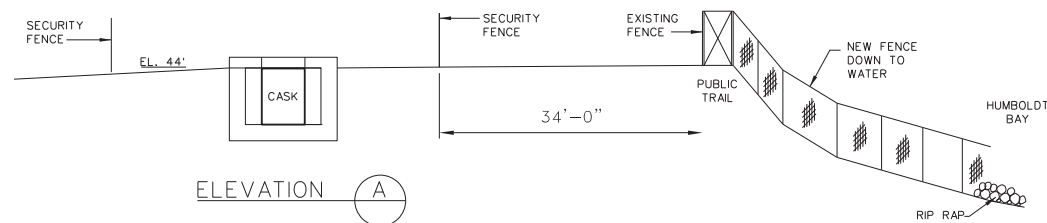
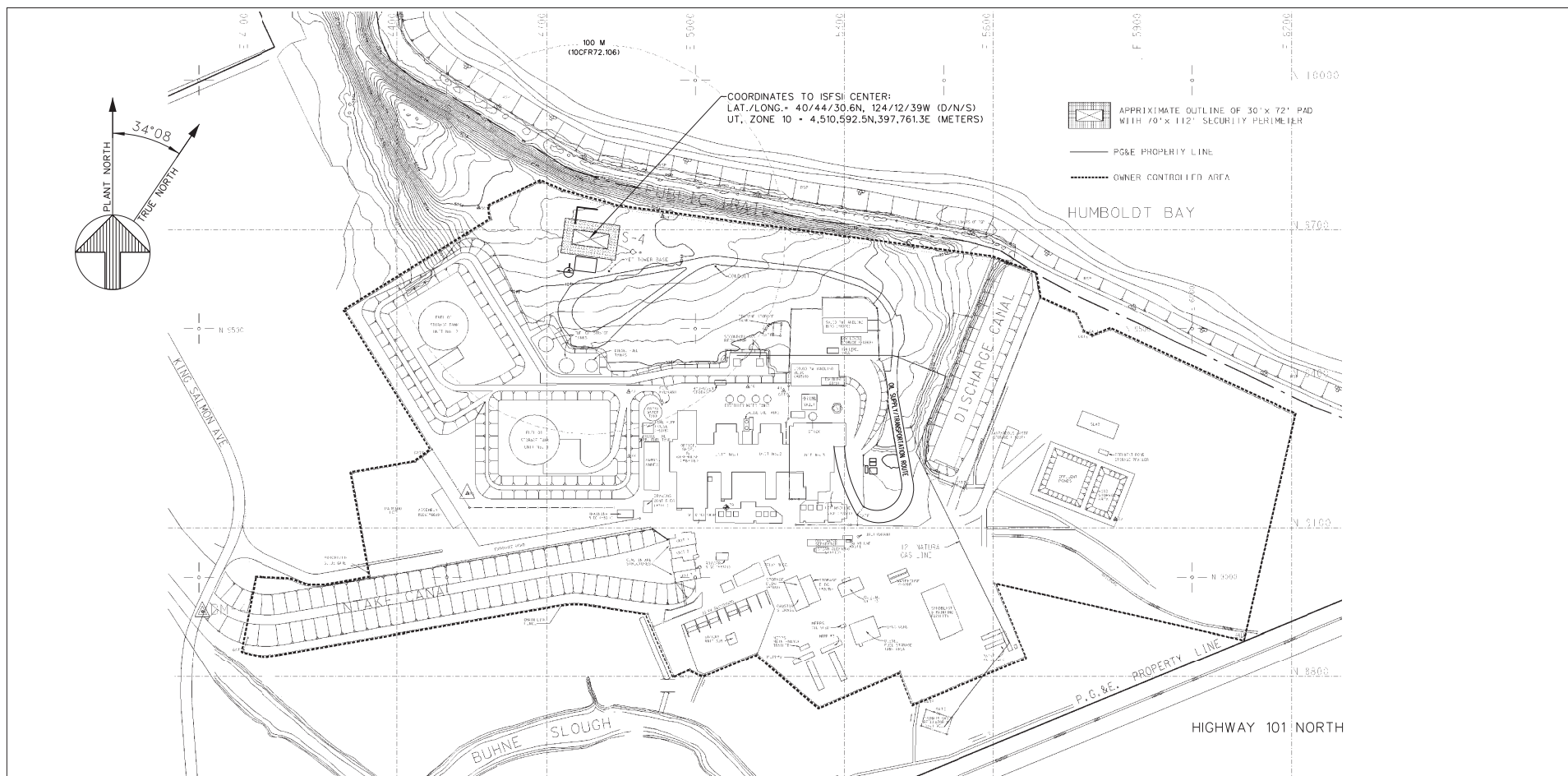


FSAR UPDATE

HUMBOLDT BAY ISFSI

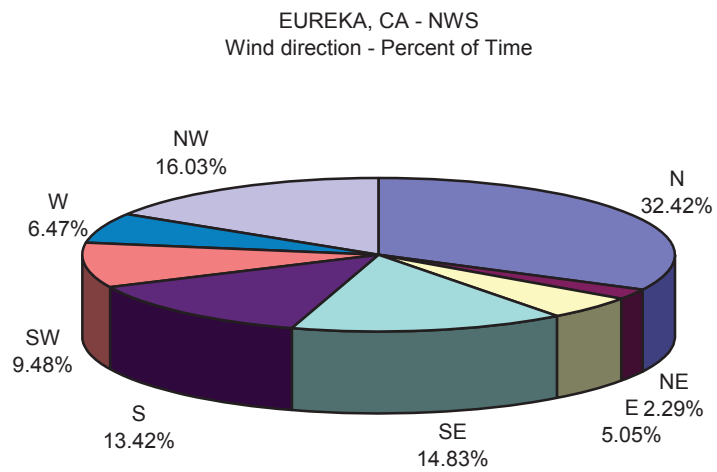
FIGURE 2.2-1
POTENTIAL HAZARDS WITHIN A
5-MILE RADIUS

Revision 0 January 2006



FSAR UPDATE
HUMBOLDT BAY ISFSI
FIGURE 2.2-2A
SITE PLAN (HISTORICAL)
Revision 9 November 2019

FSAR UPDATE
 HUMBOLDT BAY ISFSI
 FIGURE 2.2-2B
 SITE PLAN

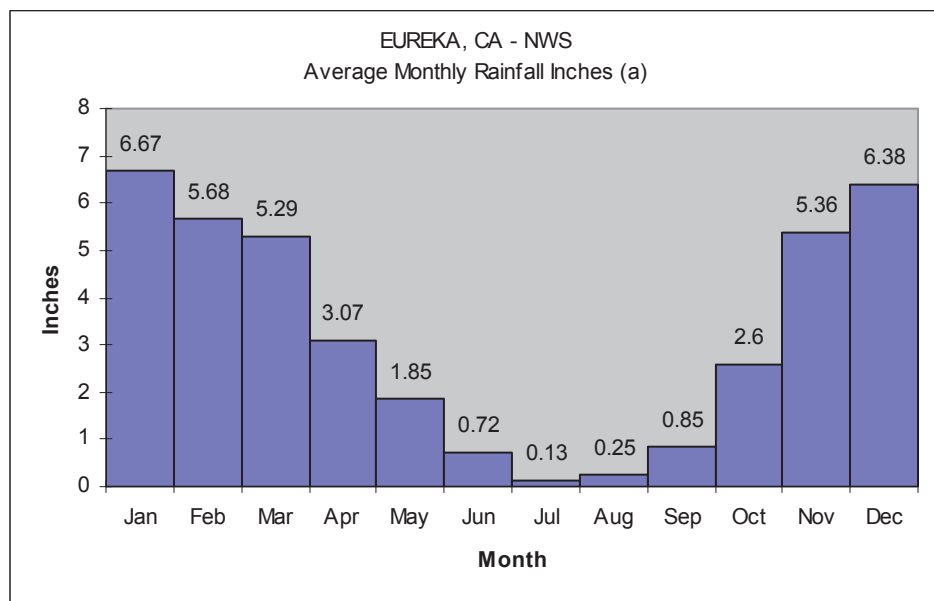


FSAR UPDATE

HUMBOLDT BAY ISFSI

**FIGURE 2.3-1
WIND DIRECTIONAL
DISTRIBUTION
1905 THROUGH 1996**

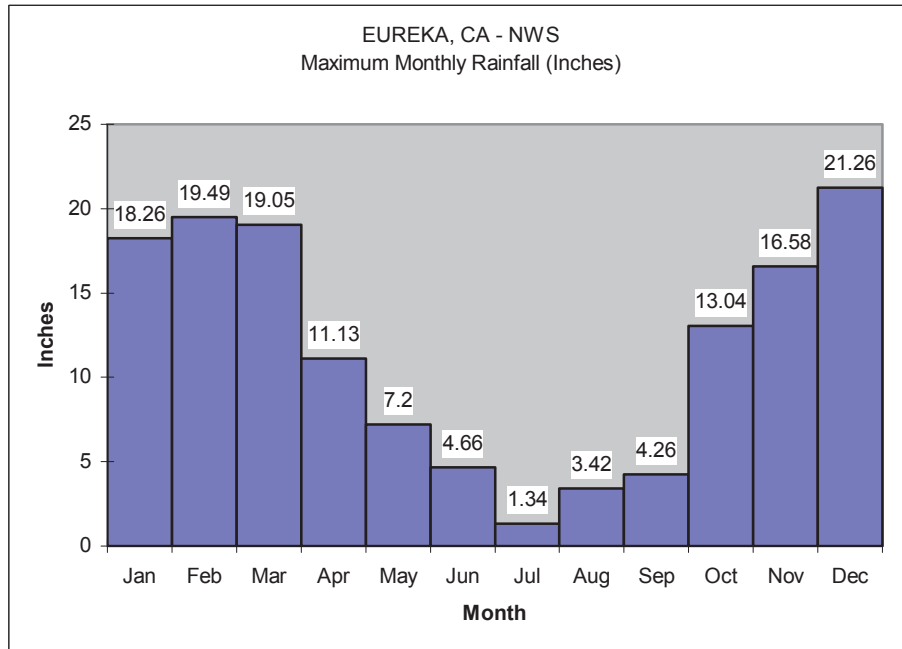
Revision 0 January 2006



(a) Shows monthly rainfall reduced to a uniform period of 30 days using Landsberg's method (Reference 1).

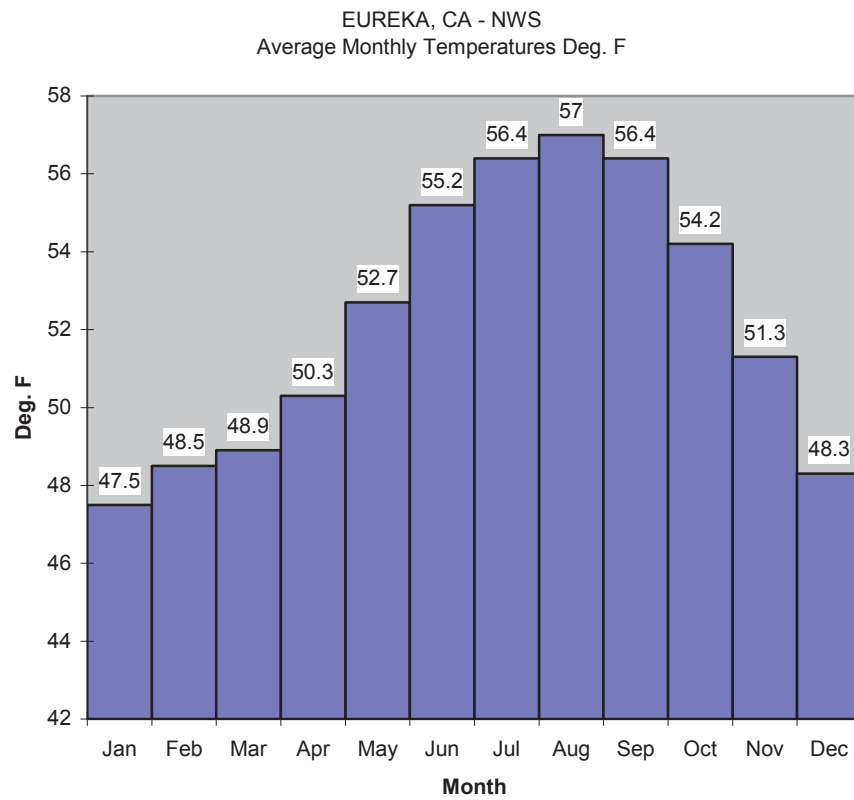
FSAR UPDATE
HUMBOLDT BAY ISFSI
FIGURE 2.3-2 AVERAGE MONTHLY RAINFALL 1887-1996

Revision 0 January 2006



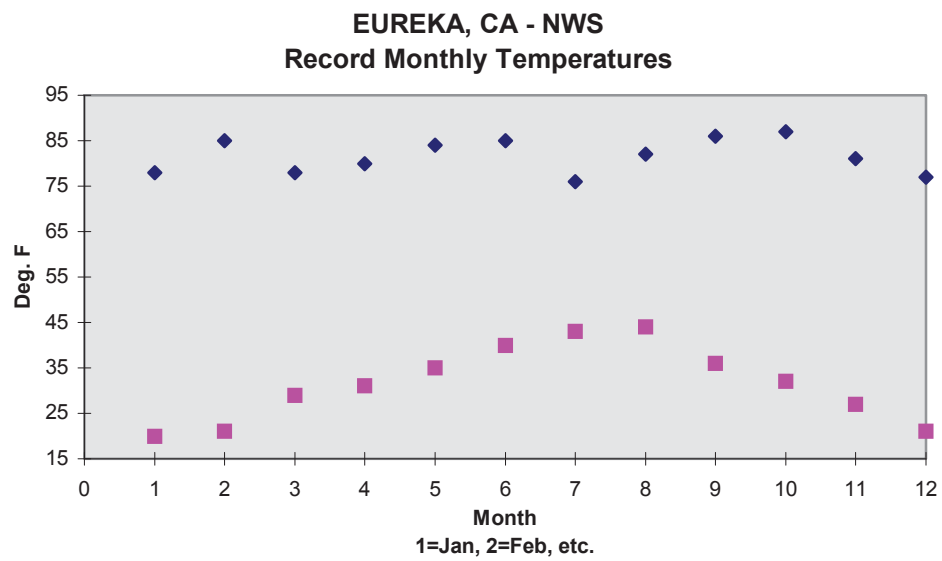
FSAR UPDATE
HUMBOLDT BAY ISFSI
FIGURE 2.3-3 MAXIMUM MONTHLY RAINFALL 1887-1996

Revision 0 January 2006



FSAR UPDATE
HUMBOLDT BAY ISFSI
FIGURE 2.3-4 AVERAGE MONTHLY TEMPERATURES 1887-1996

Revision 0 January 2006

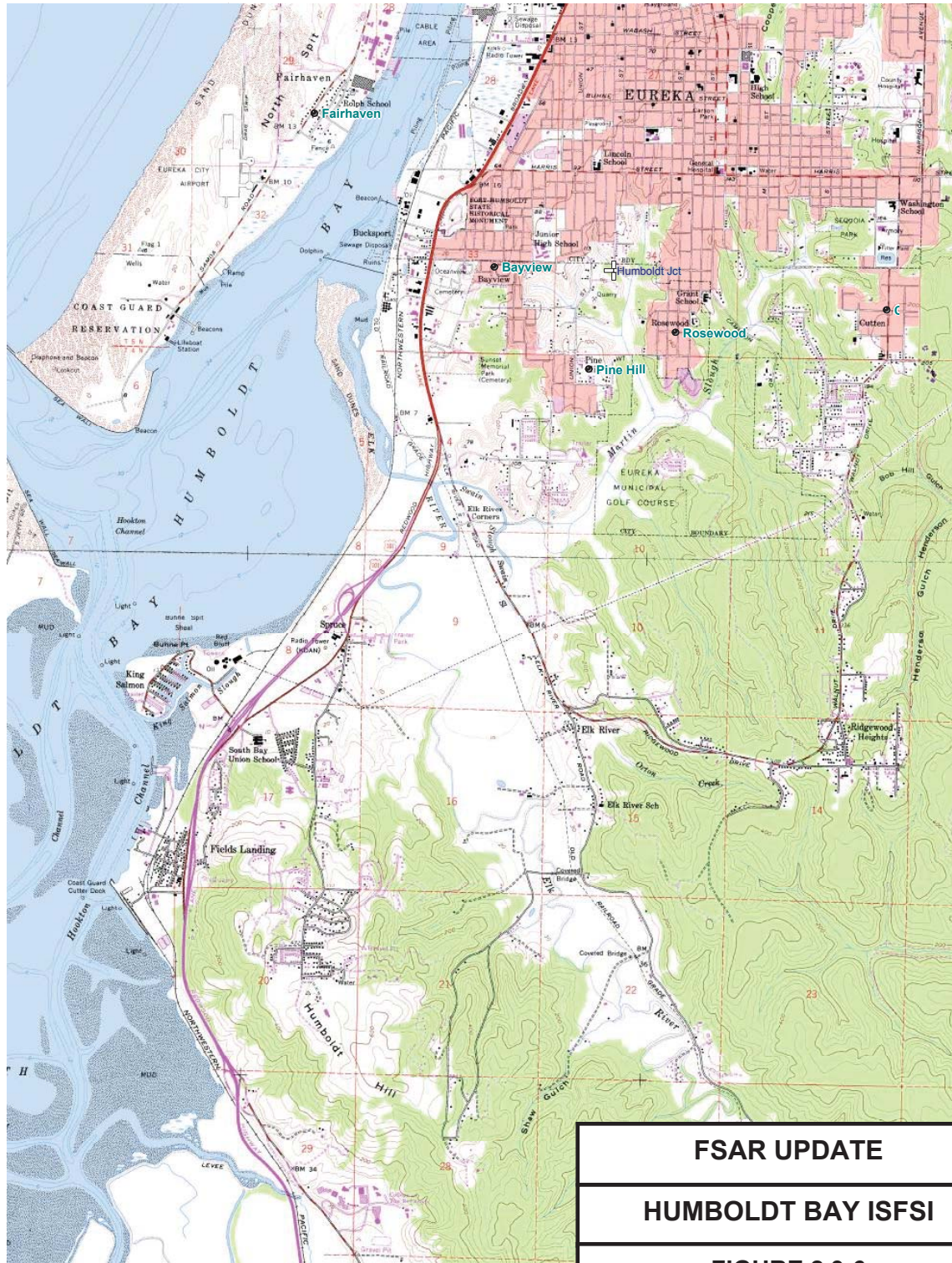


FSAR UPDATE

HUMBOLDT BAY ISFSI

**FIGURE 2.3-5
MAXIMUM AND MINIMUM
TEMPERATURES BY MONTH
1887-1996**

Revision 0 January 2006



FSAR UPDATE

HUMBOLDT BAY ISFSI

**FIGURE 2.3-6
TOPOGRAPHIC FEATURES
TO 8KM**

Revision 0 January 2006

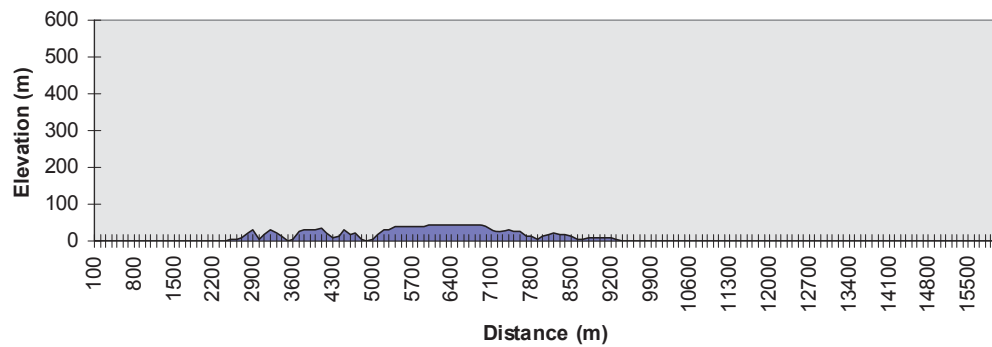


FSAR UPDATE
HUMBOLDT BAY ISFSI
FIGURE 2.3-7 TOPOGRAPHIC FEATURES TO 16 KM

Revision 0 January 2006

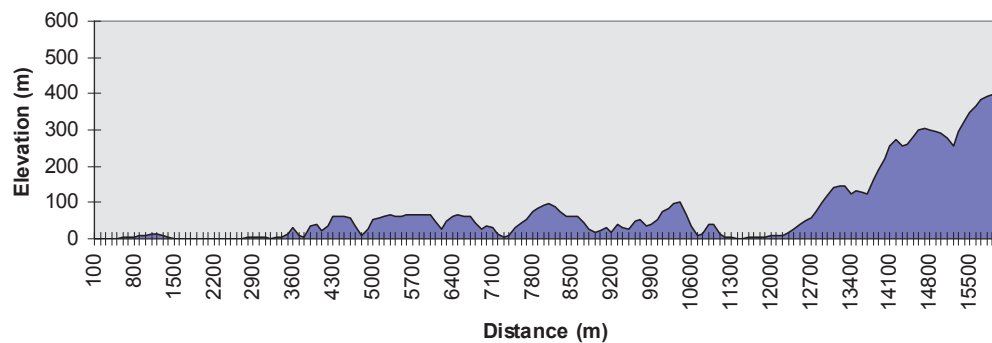
a. NE

Topographical cross sections on 045 deg radial



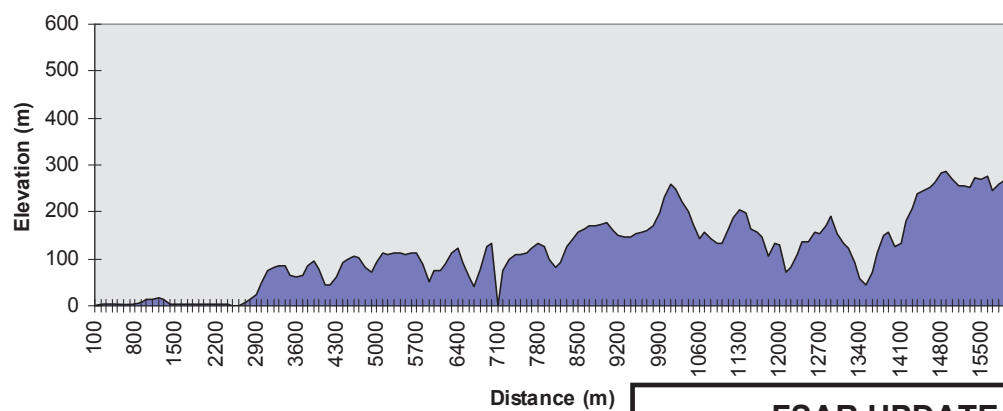
b. ENE

Topographical cross sections on 067.5 deg radial



c. E

Topographical cross sections on 090 deg radial



FSAR UPDATE

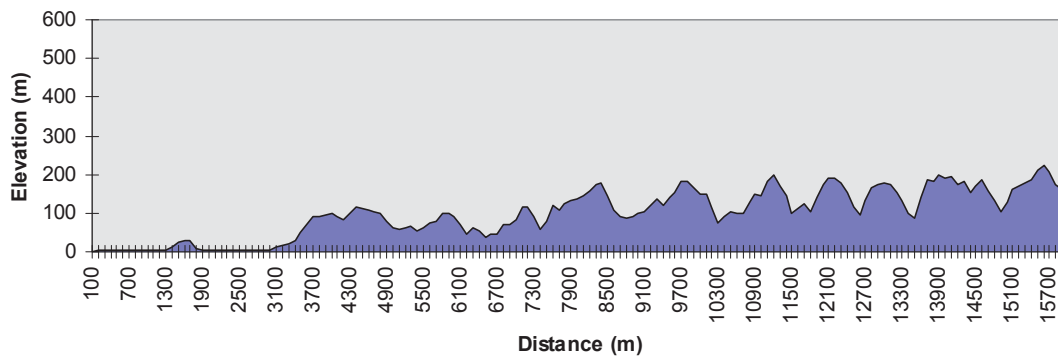
HUMBOLDT BAY ISFSI

**FIGURE 2.3-8
TOPOGRAPHICAL CROSS
SECTIONS
SHEET 1 OF 3**

Revision 0 January 2006

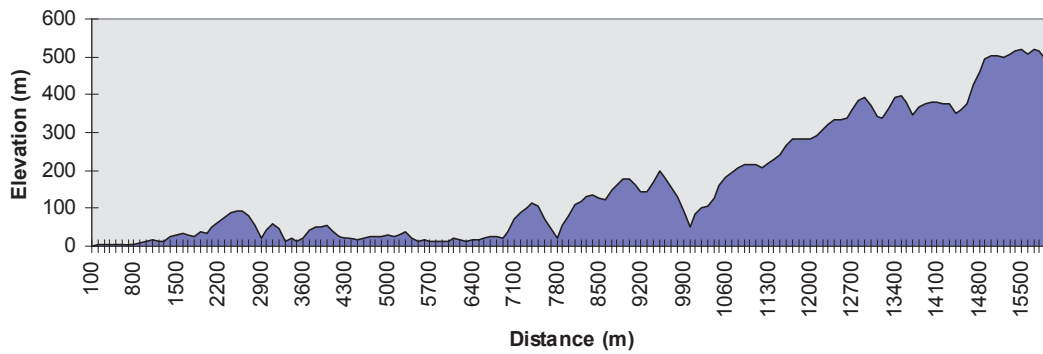
d. ESE

Topographical cross sections on 112.5 deg radial



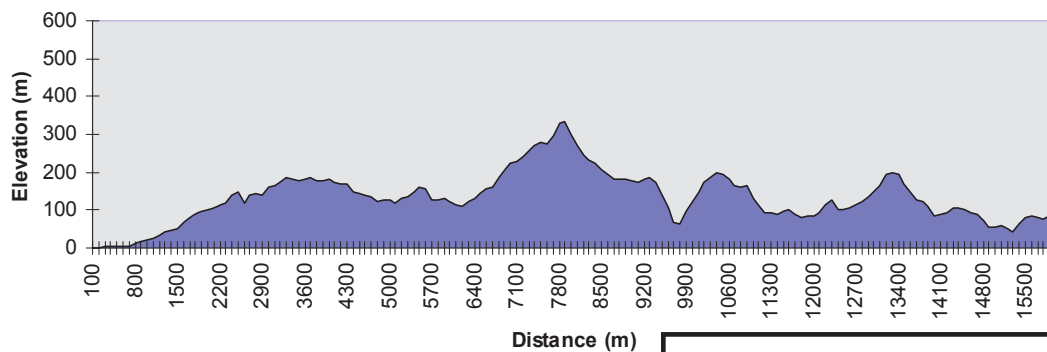
e. SE

Topographical cross sections on 135 deg radial



f. SSE

Topographical cross sections on 157.5 deg radial



FSAR UPDATE

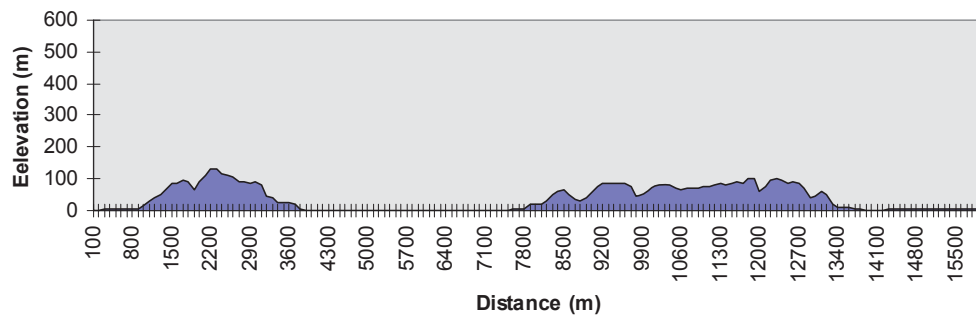
HUMBOLDT BAY ISFSI

**FIGURE 2.3-8
TOPOGRAPHICAL CROSS
SECTIONS
SHEET 2 OF 3**

Revision 0 January 2006

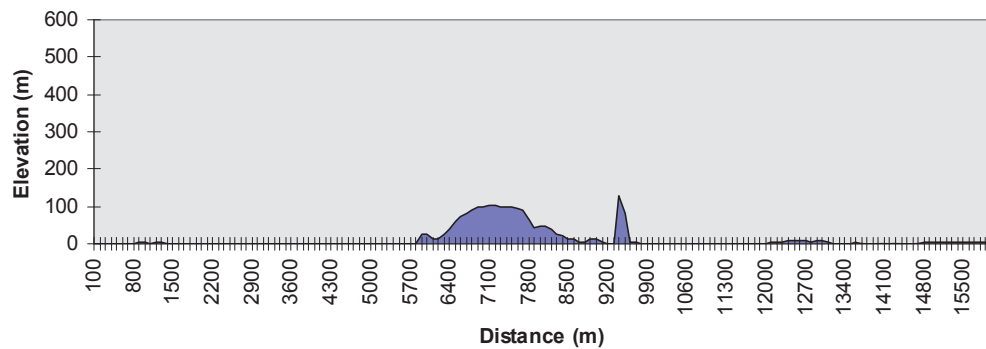
g. S

Topographical cross sections on 180 deg radial



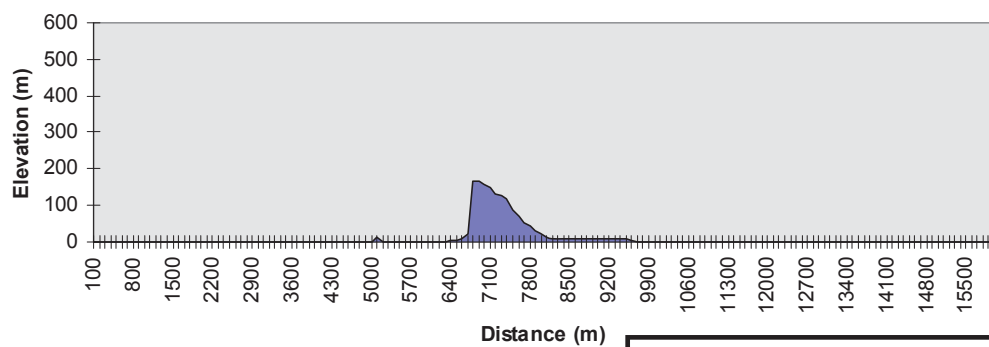
h. SSW

Topographical cross sections on 202.5 deg radial



i. SW

Topographical cross sections on 225 deg radial

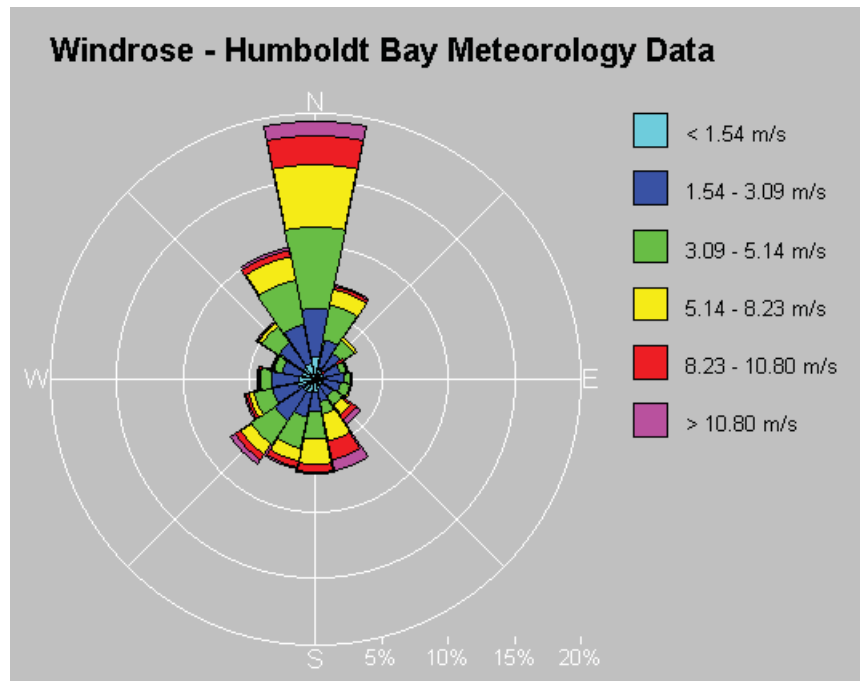


FSAR UPDATE

HUMBOLDT BAY ISFSI

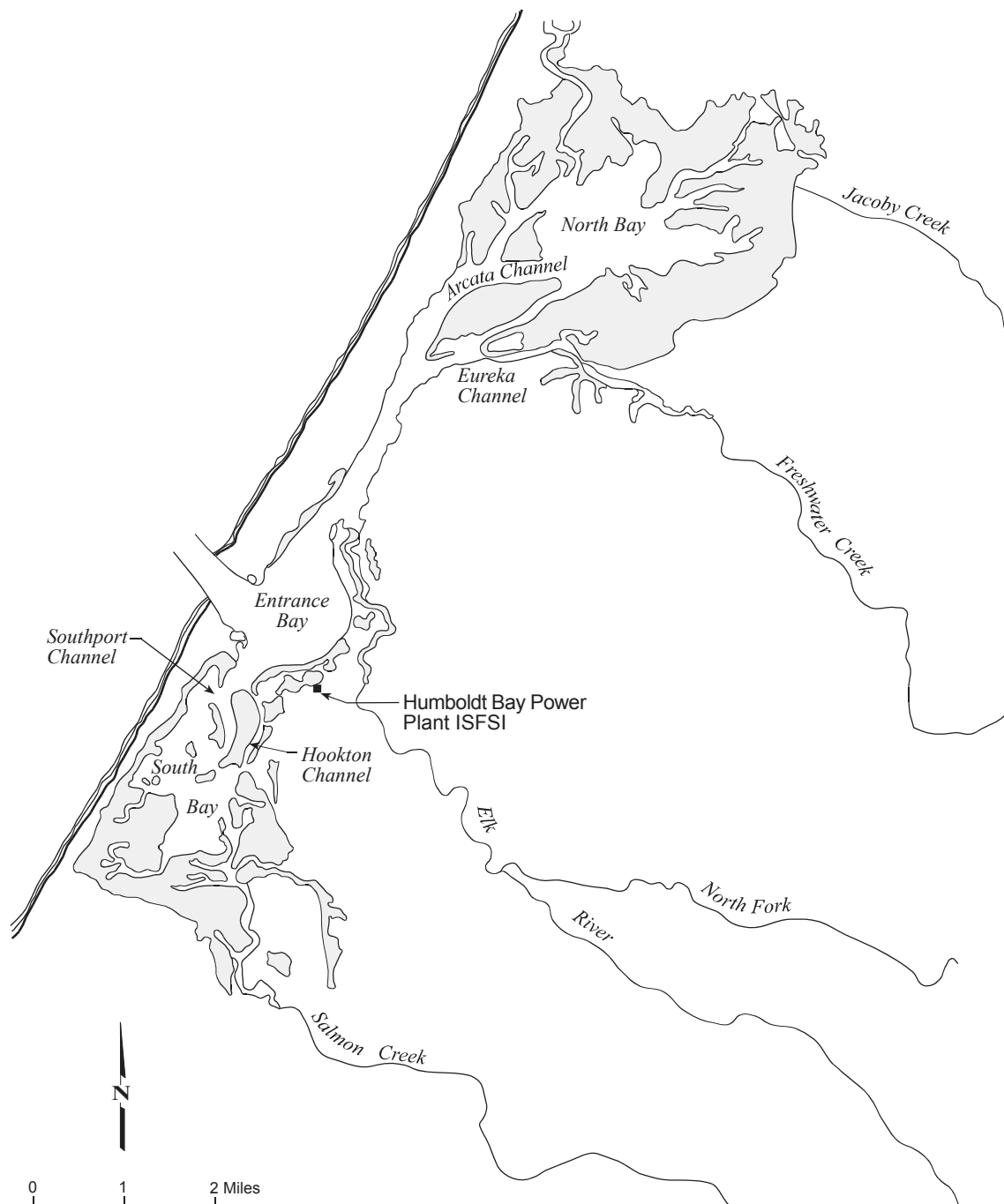
**FIGURE 2.3-8
TOPOGRAPHICAL CROSS
SECTIONS
SHEET 3 OF 3**

Revision 0 January 2006



FSAR UPDATE
HUMBOLDT BAY ISFSI
FIGURE 2.3-9 WINDROSE OF HUMBOLDT BAY METEOROLOGY DATA 1966-1967

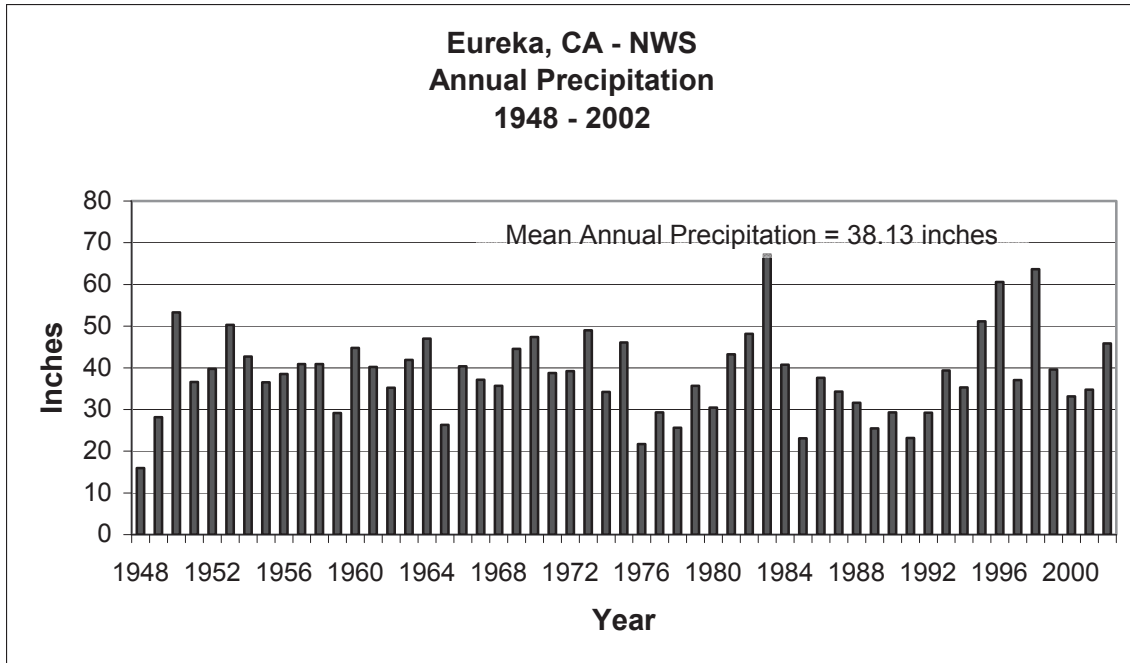
Revision 0 January 2006



 Mudflats

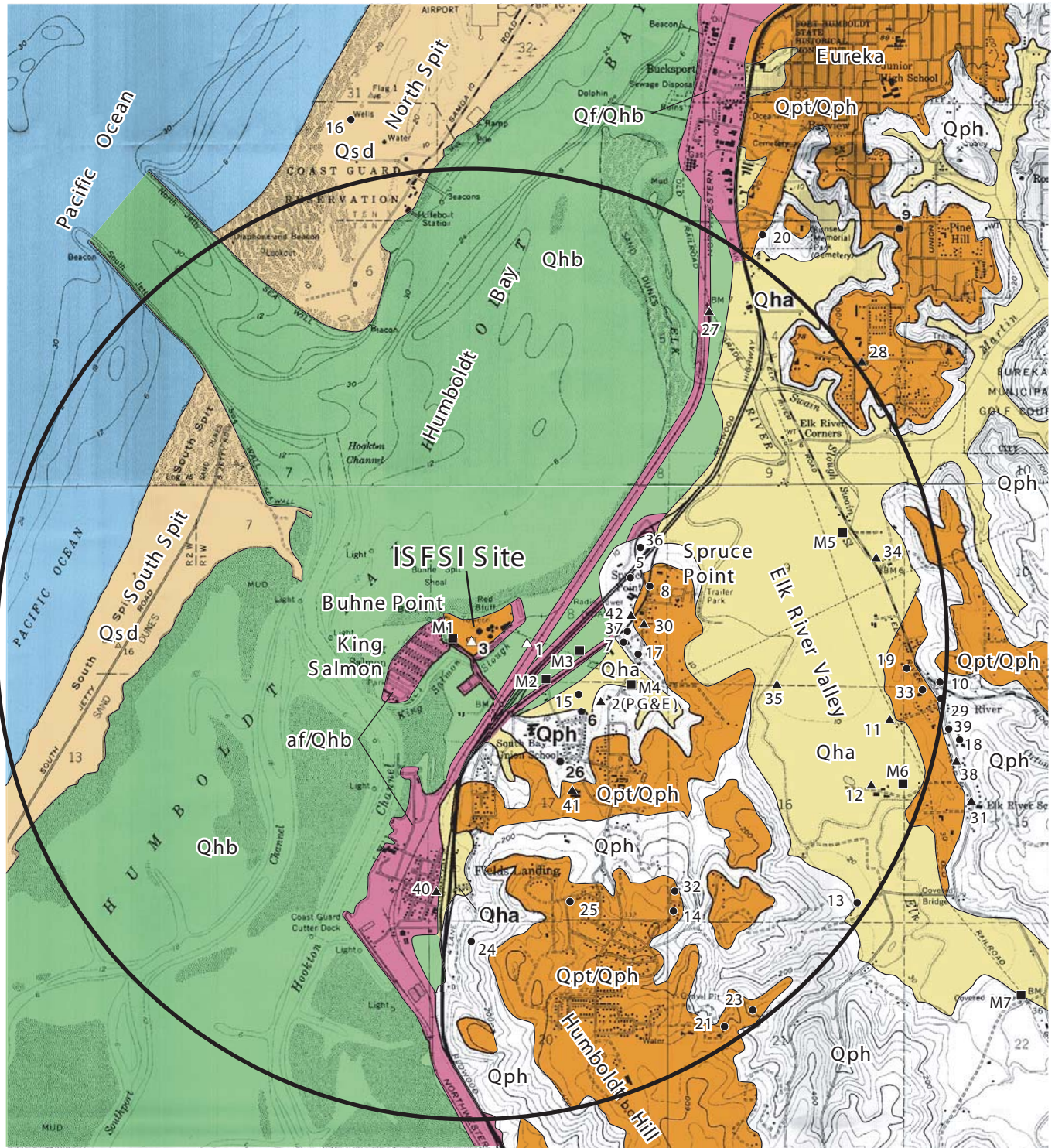
FSAR UPDATE
HUMBOLDT BAY ISFSI
FIGURE 2.4-1 WATERSHEDS OF HUMBOLDT BAY

Revision 0 January 2006

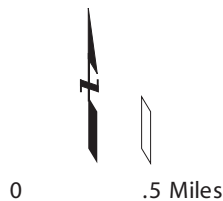


FSAR UPDATE
HUMBOLDT BAY ISFSI
FIGURE 2.4-2 MEAN ANNUAL PRECIPITATION AT EUREKA

Revision 0 January 2006

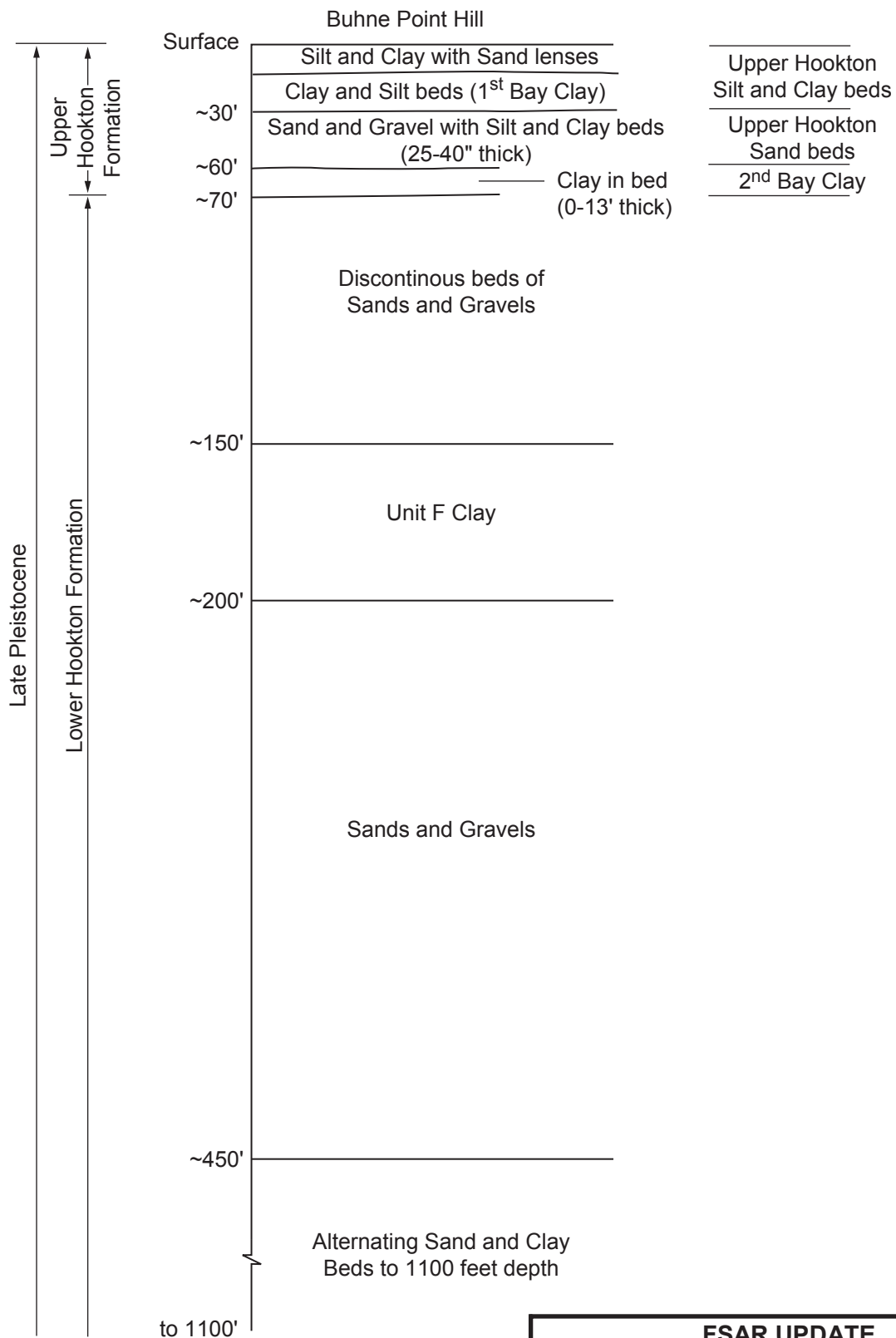


- | | |
|--|---|
| af | Fill |
| Qhb | Holocene bay deposits of Humboldt Bay |
| Qha | Holocene alluvium |
| Qsd | Holocene sand dunes |
| Qpt | Pleistocene marine/bay terrace deposits |
| Qph | Pleistocene Hookton Formation |
-
- | | |
|------|--|
| 13 ● | Domestic wells |
| 12 ▲ | Industrial/irrigation/monitoring wells |
| M1 ■ | Test wells (Marliave, 1960) |
| 1△ | Abandoned PG&E wells |

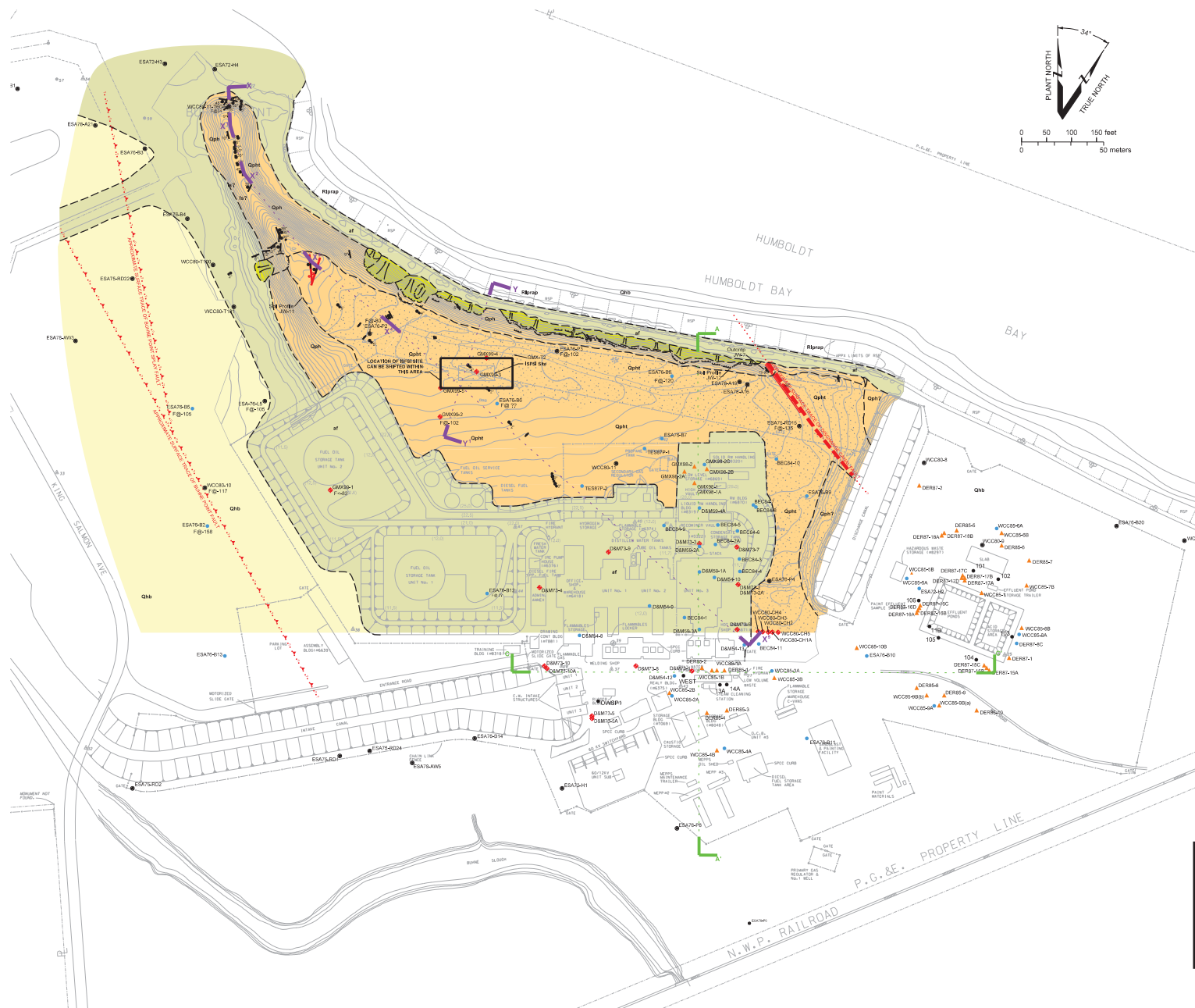


FSAR UPDATE
HUMBOLDT BAY ISFSI
FIGURE 2.5-1 GEOLOGIC MAP OF THE HUMBOLDT BAY ISFSI SITE VICINITY SHOWING WATER WELLS WITHIN 2 MILES OF THE ISFSI SITE

Revision 0 January 2006



FSAR UPDATE
HUMBOLDT BAY ISFSI
FIGURE 2.5-2 GENERALIZED STRATIGRAPHIC COLUMN IN THE HUMBOLDT BAY ISFSI SITE AREA



EXPLANATION

Map Symbols

- Lithologic contact, dashed where approximately located
- Reverse fault: dashed where approximately located; queried where uncertain; dotted where buried, barb on upper plate
- Strike and dip of normal fault: bar and ball on downthrown side
- Strike and dip of reverse fault: barb on upper plate
- Strike and dip of bedding
- Apparent dip of bedding
- Strike and dip of fractures: double bar indicates dip direction
- Apparent dip of fractures
- Vertical fractures

Lithologic Units

- af Fill, man-made fill, and disturbed areas
- Historical landslide
- Qhb Holocene bay deposits
- Qph, Qpht Pleistocene Hookton Formation
- Qph = undifferentiated
- Qpht = terrace surface
- Indicates areas where the surface is disturbed

- Rotary wash borings with SPT blow counts
- Auger borings with SPT blow counts
- Borings with no blow counts
- Other borings from geologic and groundwater investigations

- Spot elevation in feet from PG&E design/construction drawings

- Geologic cross sections shown on Figures 2.5-5 to -8

- 2-foot contour interval (elevation above mean lower low water)

NOTES:

1. Topographic survey made in 1999 and 2000.
2. Modified from Figure 2.6.4.2.

FSAR UPDATE

HUMBOLDT BAY ISFSI

FIGURE 2.5-3 GEOLOGIC MAP SHOWING BORINGS AND MONITORING WELLS IN THE HUMBOLDT BAY ISFSI SITE AREA

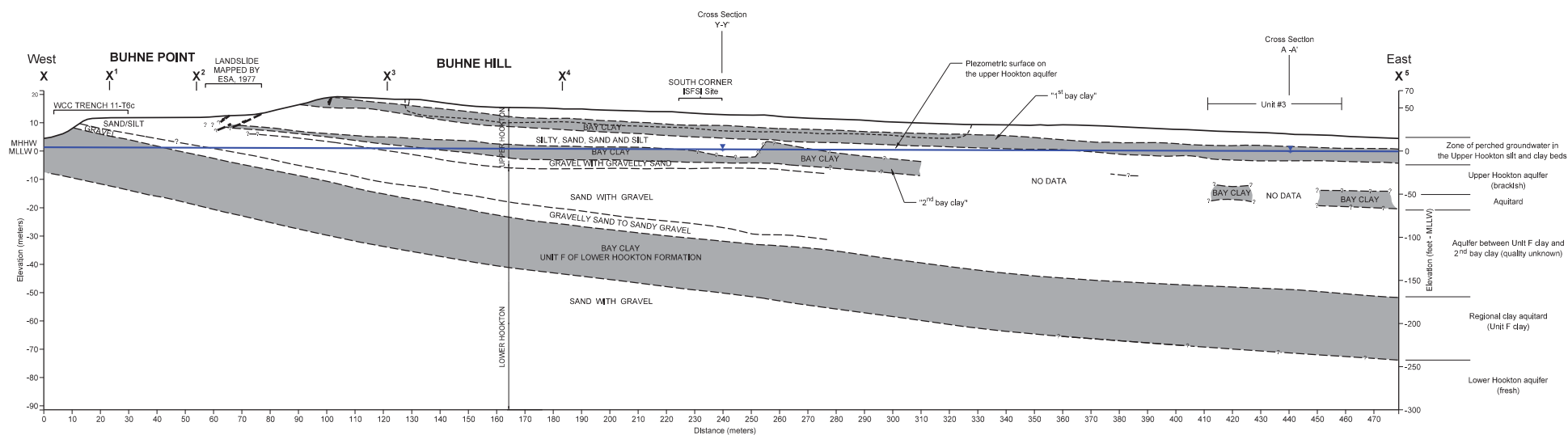
Revision 0 January 2006

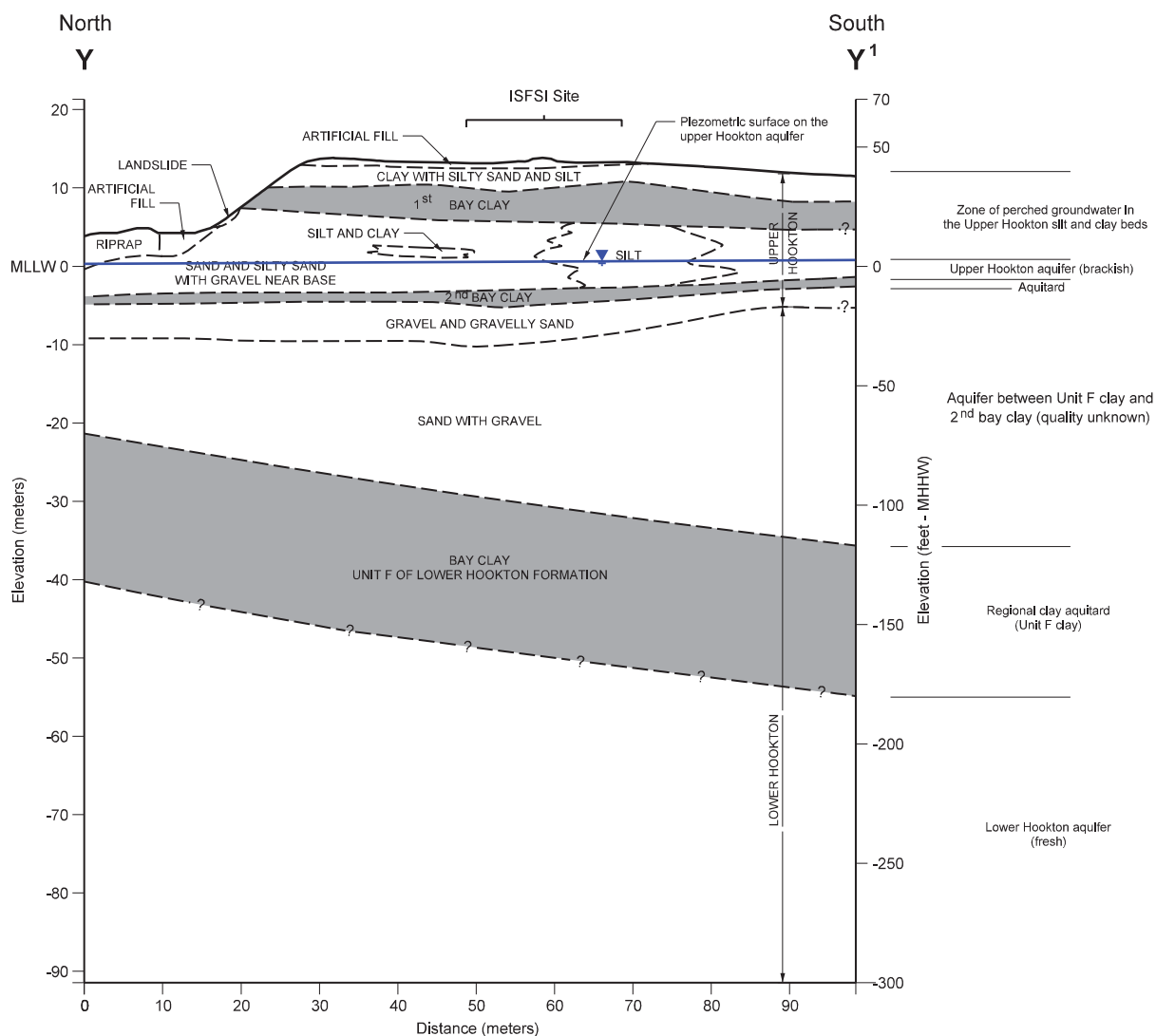
HOOKTON FORMATION		AQUIFERS INFORMATION			AQUIFERS IN HOLOCENE BAY DEPOSITS		HOLOCENE BAY DEPOSITS
Stratigraphy		This Report	Earlier Interpretations		Earlier Interpretations	This Report	Stratigraphy
Silt y sand and silt beds with sand lenses	Silt and clay beds 1 st bay clay	Zone of perched groundwater in upper Hookton clay and silt beds	A Unconfined first water bearing zone of Bower (1988) [in TES, 1988] B	1st aquifer of Bower (1988) (brackish water) [in TES, 1988]	A Unconfined first water bearing zone of Bower (1988) [in TES, 1988] B	Zone of perched groundwater in Holocene bay deposits	Silt and clay beds
Sands and gravels		Upper Hookton aquifer	C Semi-unconfined second water bearing zone of Bower (1988) [in TES, 1988] Upper sand zone of Dames and Moore (reported in WCC)				
Clay bed 2 nd bay clay		Aquitard discontinuous across site	Clay layer of Bower (1988) [in TES, 1988]				
Sands and gravels		Aquifer between Unit F clay and 2 nd bay clay					
Unit F clay		Unit F clay aquitard	Regional aquitard				
Sands and gravels		Lower Hookton aquifer	2nd aquifer of Bower 1998 [in TES, 1988] (fresh water)				

FSAR UPDATE

HUMBOLDT BAY ISFSI

FIGURE 2.5-4
GENERALIZED MODEL OF AQUIFERS IN
THE HUMBOLDT BAY ISFSI SITE AREA



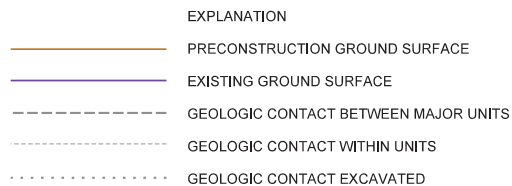


----- Lithologic contact, dashed where approximate, queried where inferred

Note:
Location of cross section is shown on Figure 2.5-3.
Figure modified from Figure 2.6.4-5.

FSAR UPDATE
HUMBOLDT BAY ISFSI
FIGURE 2.5-6 GEOLOGIC CROSS SECTION Y-Y' THROUGH THE HUMBOLDT BAY ISFSI SITE

Revision 0 January 2006



BORING
NUMBER INDICATES COMPANY OR DEPARTMENT, YEAR AND
NUMBER. NUMBER IN PARENTHESIS IS DISTANCE AND
DIRECTION BORING IS PROJECTED TO THE CROSS SECTION LINE;
SCREENED SECTION INDICATED AS NARROW BOX

SOIL DESIGNATIONS (UNIFIED SOIL CLASSIFICATION) FROM BORINGS

SOIL DESIGNATIONS (UNIFIED SOIL CLASSIFICATION) INTERPRETED FROM BORINGS

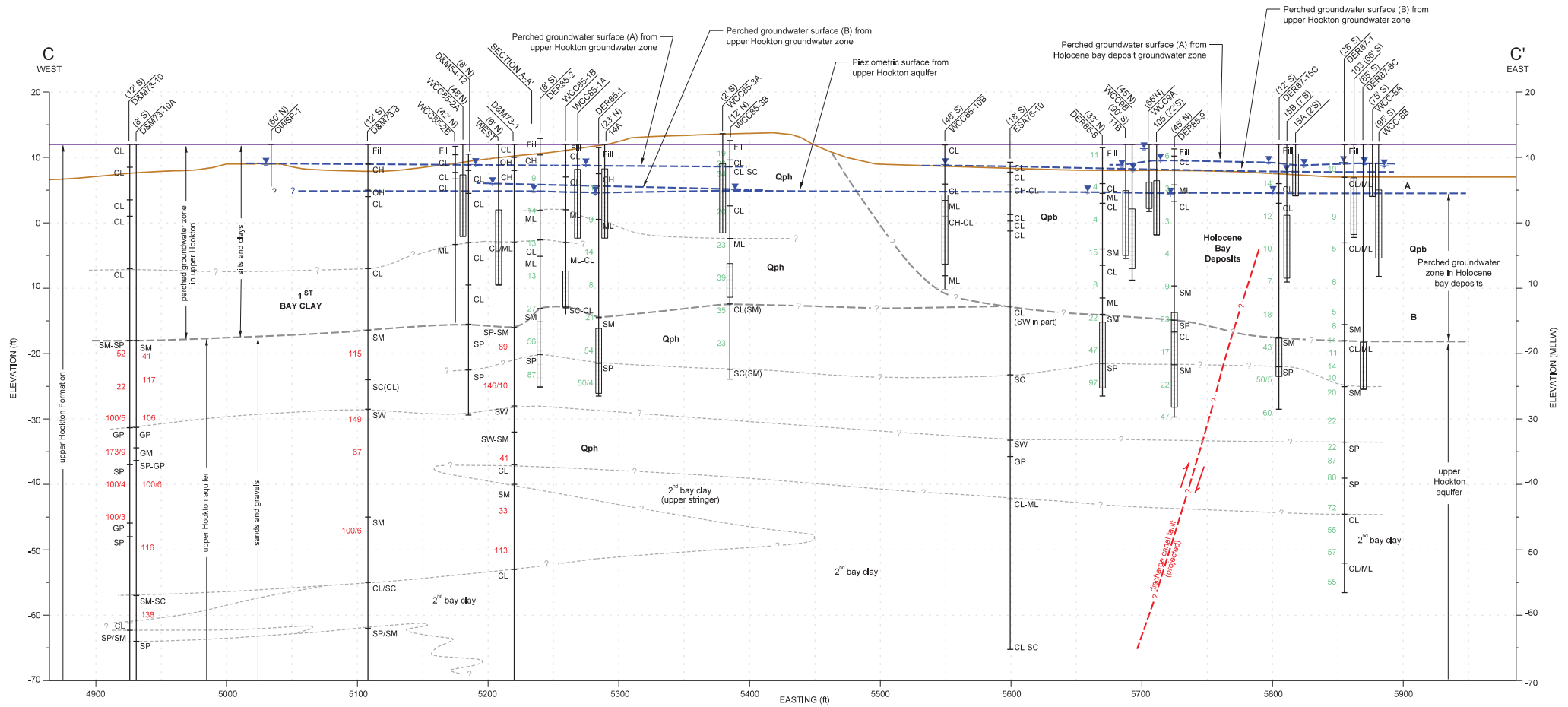
SPT BLOW COUNTS IN ROTARY WASH BORINGS

BLOW COUNTS IN AUGER BORINGS

FSAR UPDATE
HUMBOLDT BAY ISFSI

FIGURE 2.5-7
CROSS SECTION A-A'
THROUGH UNIT 3, HUMBOLDT BAY
ISFSI SITE AREA

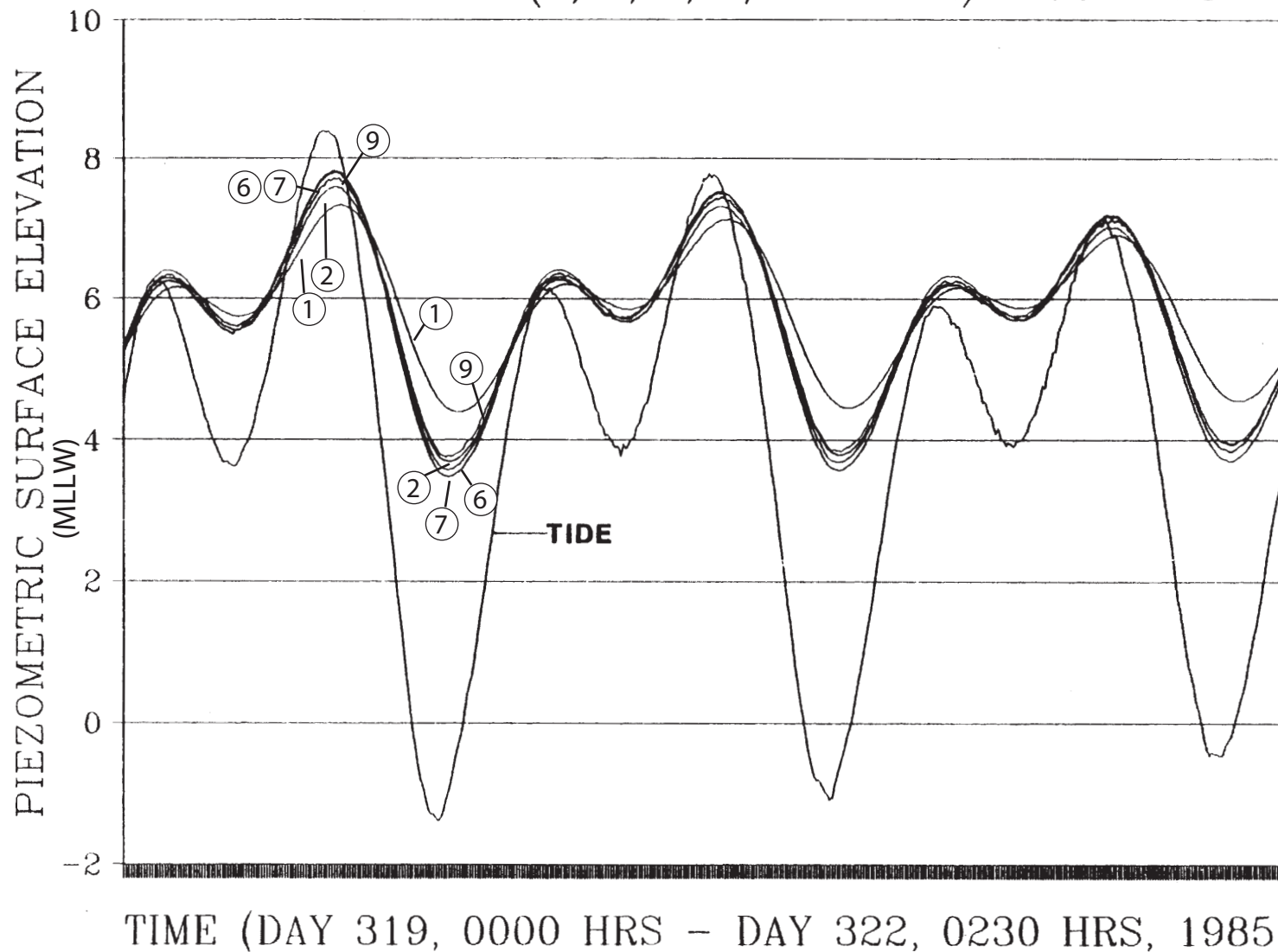
Revision 0 January 2006





HUMBOLDT BAY POWER PLANT

BECHTEL WELLS (1, 2, 6, 7, 9 & TIDE) – PHASE I

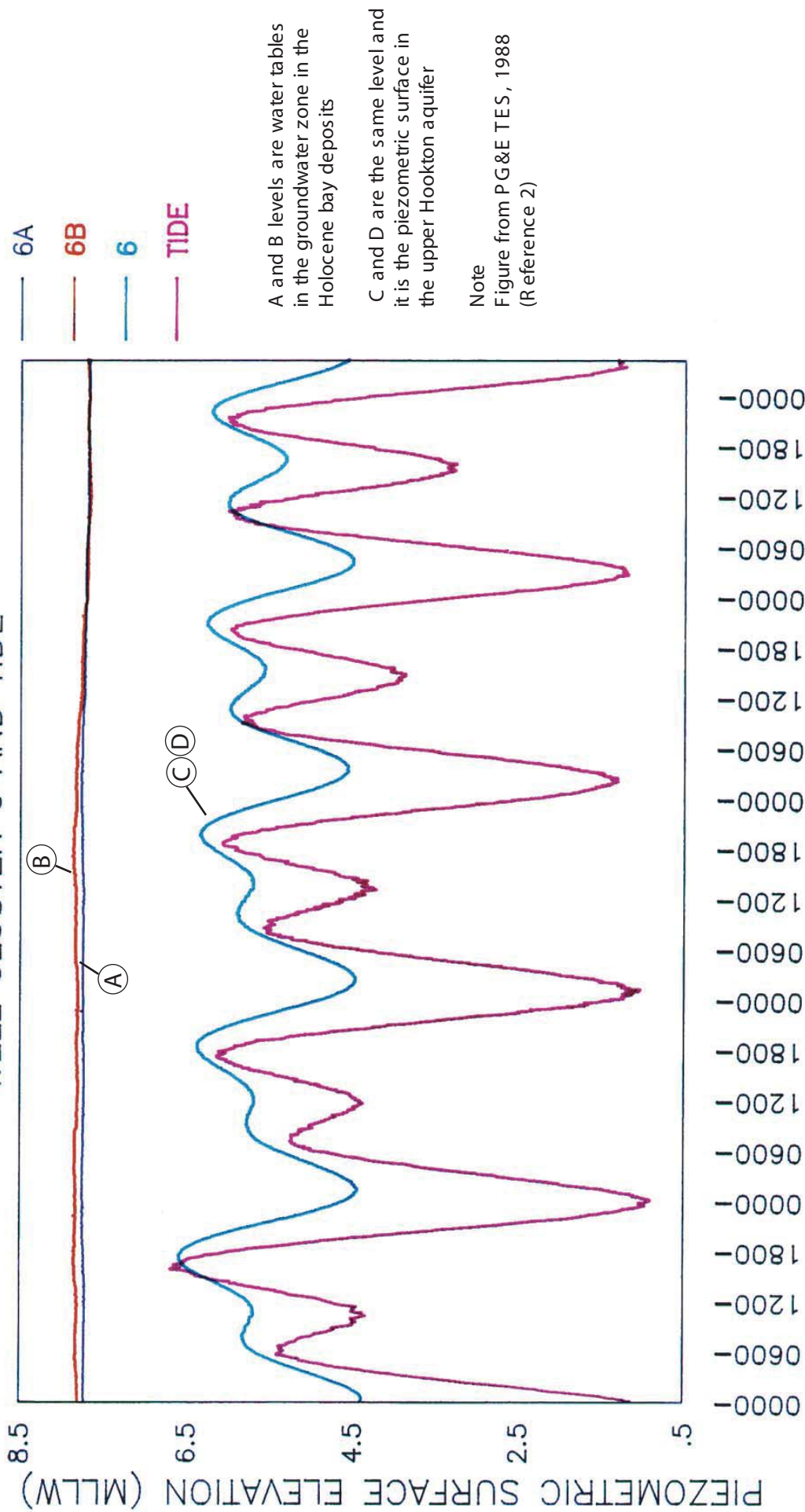


All wells measure the piezometric surface in the upper Hookton aquifer

Note
Figure from PG&E TES, 1987
(Reference 6)

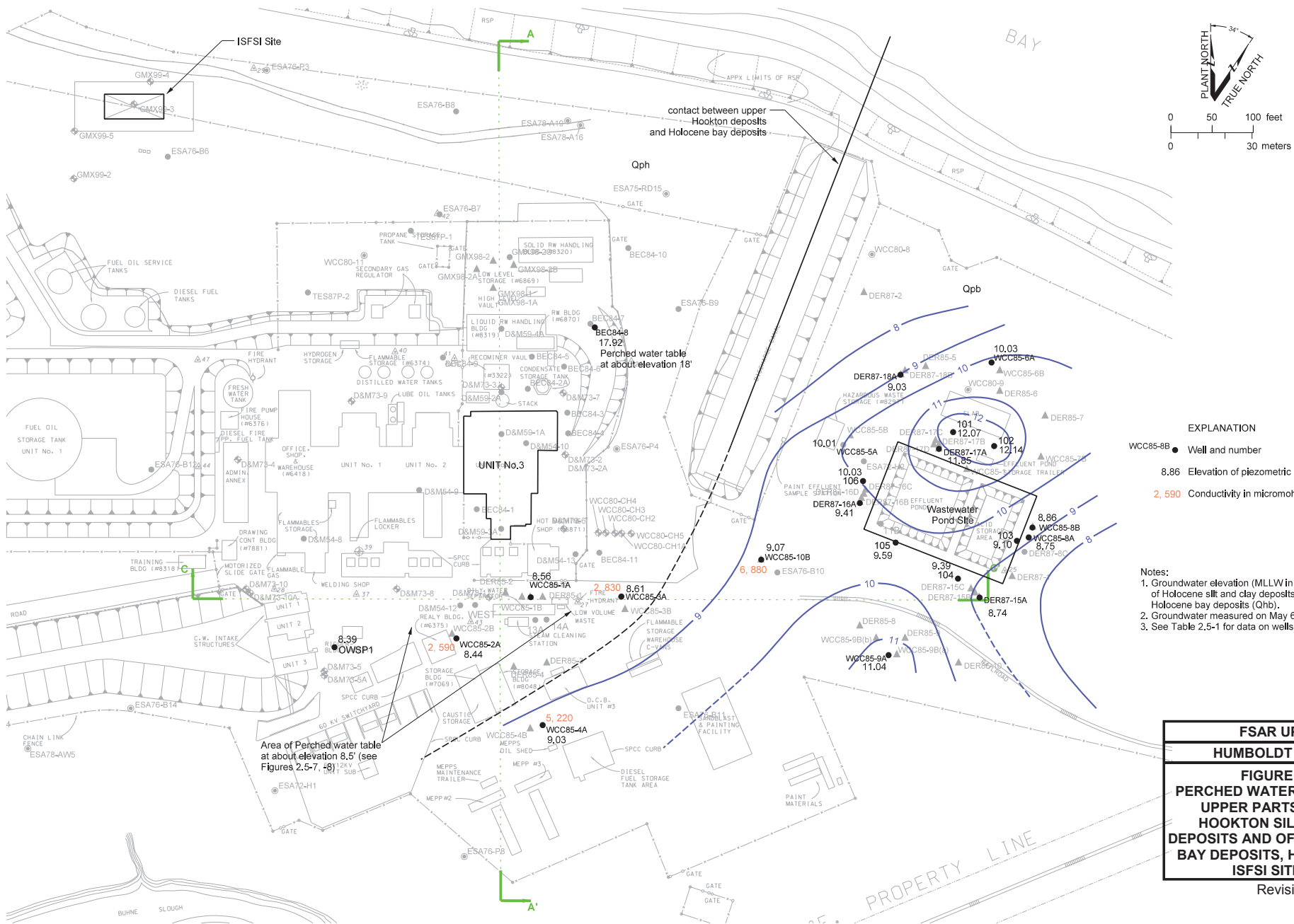
**FSAR UPDATE
HUMBOLDT BAY ISFSI
FIGURE 2.5-10
RELATIONSHIP BETWEEN THE TIDE LEVELS IN HUMBOLDT BAY AND
PIEZOMETRIC LEVELS FROM WELLS MW-1, MW-2, MW-6, MW-7, AND MW-9
(BECHTEL) NEAR UNIT 3 HUMBOLDT BAY ISFSI SITE AREA**

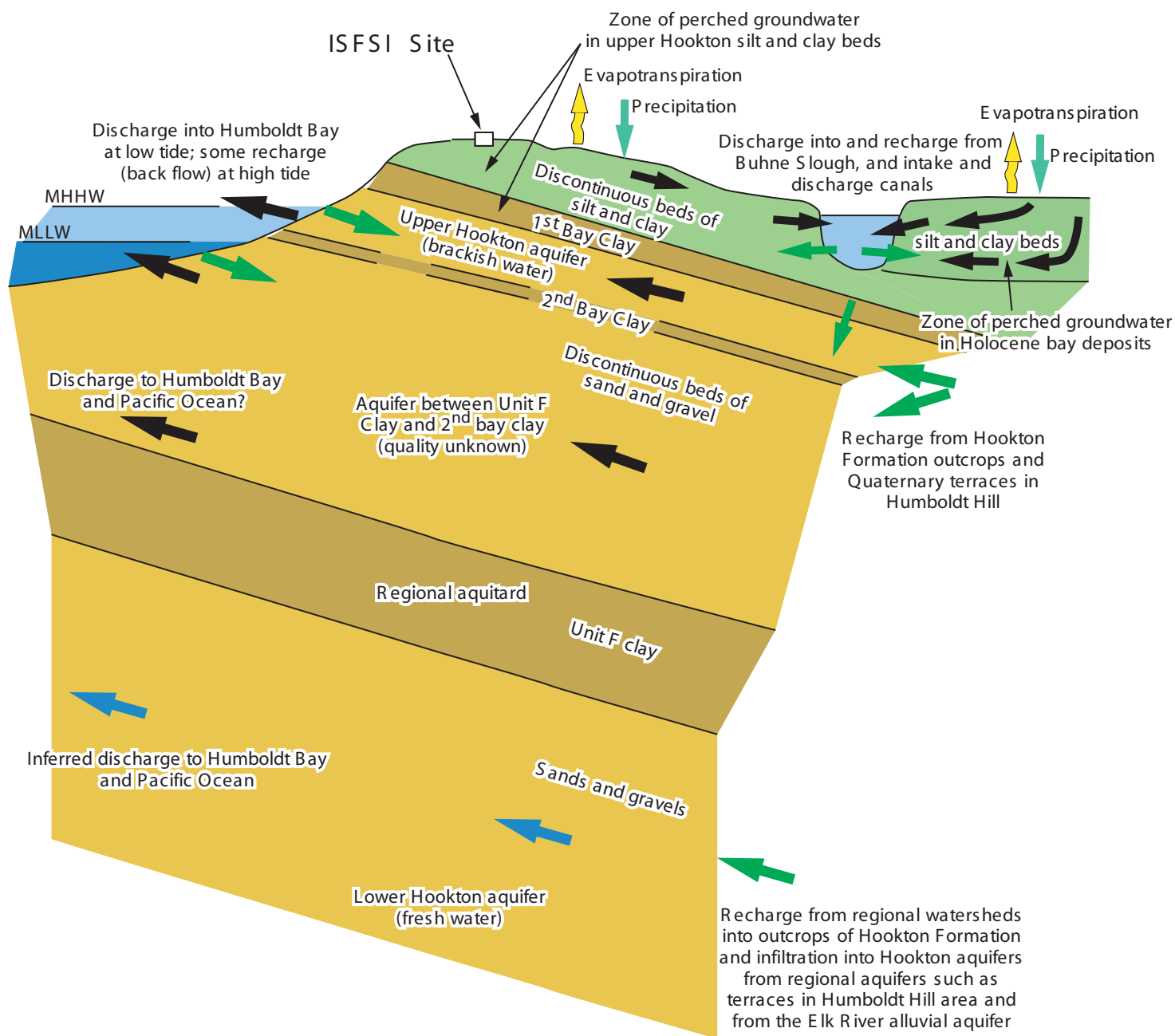
HUMBOLDT BAY POWER PLANT WELL CLUSTER 6 AND TIDE



TIME (DAY 286, 0000 HRS TO DAY 291, 0410 HRS)

FSAR UPDATE
 HUMBOLDT BAY ISFSI
 FIGURE 2.5-11
 RELATIONSHIP BETWEEN THE TIDE LEVELS IN HUMBOLDT BAY AND
 PIEZOMETRIC LEVELS FROM WELL CLUSTER 16-A, 16-B, 16-C, AND 16-D9
 (TES) IN WASTEWATER PONDS AREA, HUMBOLDT BAY ISFSI SITE AREA

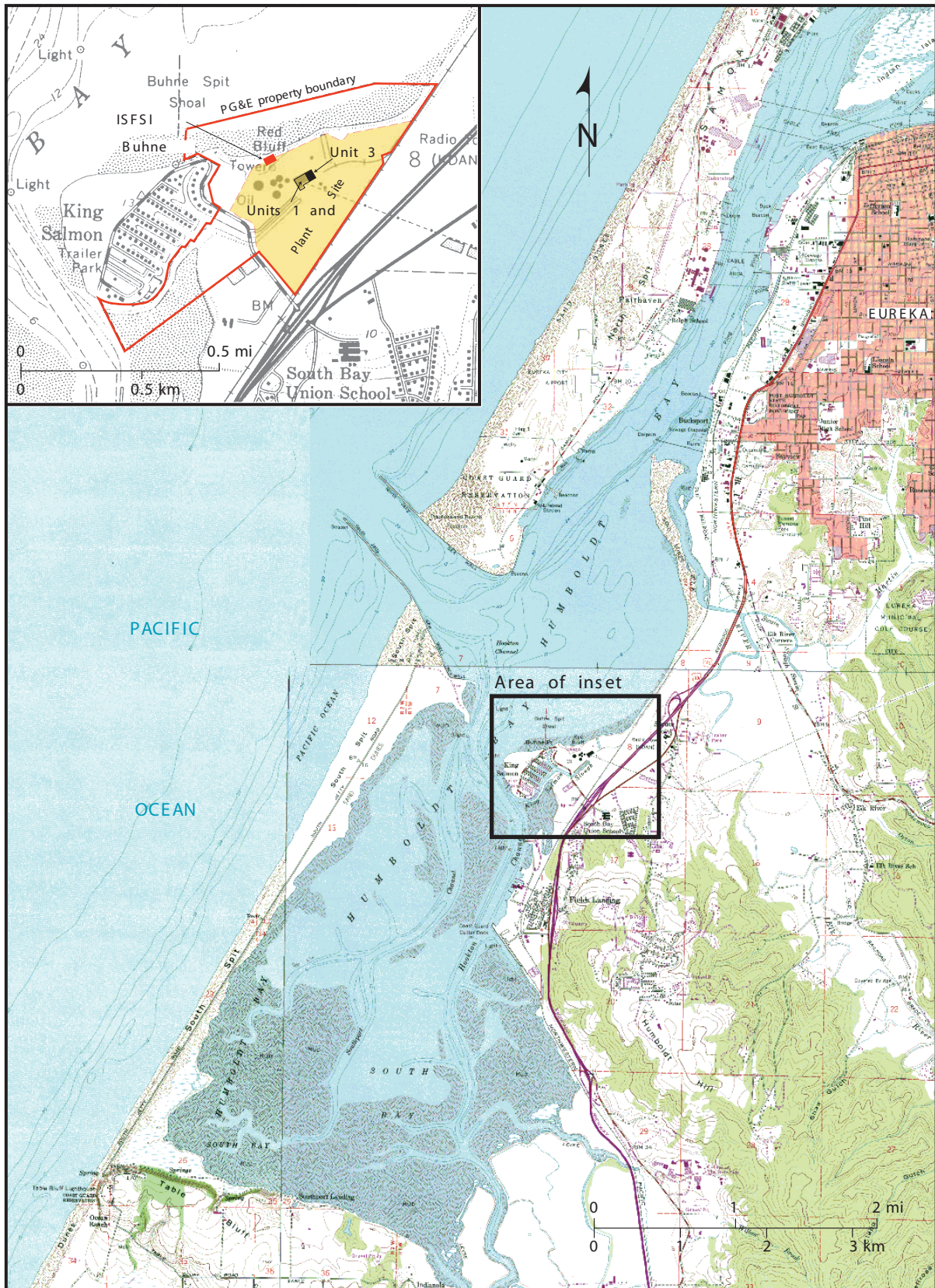




Alternating sand and clay beds to 1100 feet depth

FSAR UPDATE
HUMBOLDT BAY ISFSI
FIGURE 2.5-14 GENERALIZED MODEL SHOWING AQUIFER RECHARGE AND DISCHARGE IN THE HUMBOLDT BAY ISFSI SITE AREA

Revision 0 January 2006

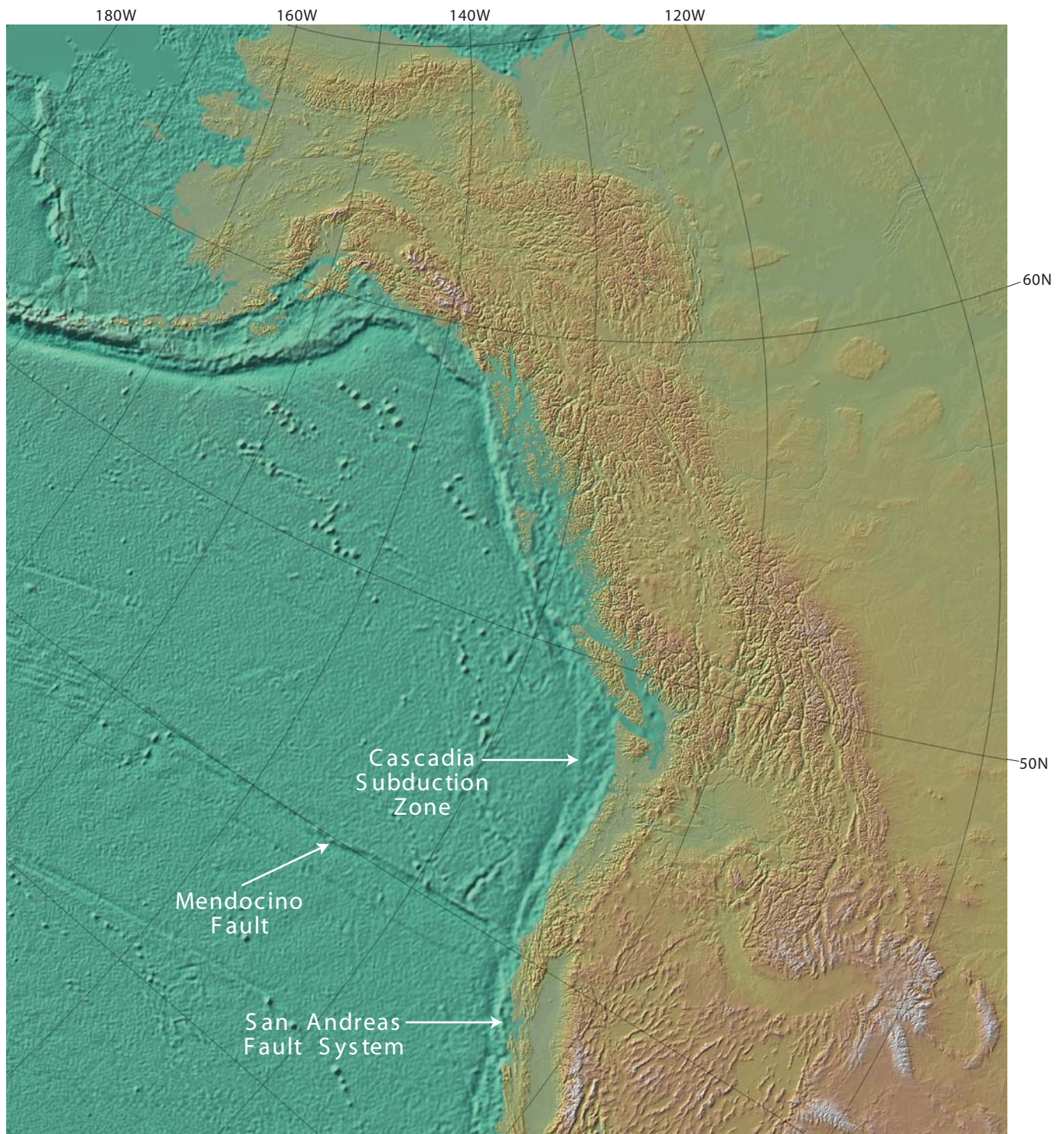


FSAR UPDATE
HUMBOLDT BAY ISFSI
FIGURE 2.6-1
TOPOGRAPHIC MAP OF HUMBOLDT
BAY SHOWING LOCATION OF THE
HUMBOLDT BAY ISFSI SITE



FSAR UPDATE
HUMBOLDT BAY ISFSI
FIGURE 2.6-2 SOUTH HUMBOLDT BAY VIEW IS SOUTHEAST

Revision 0 January 2006



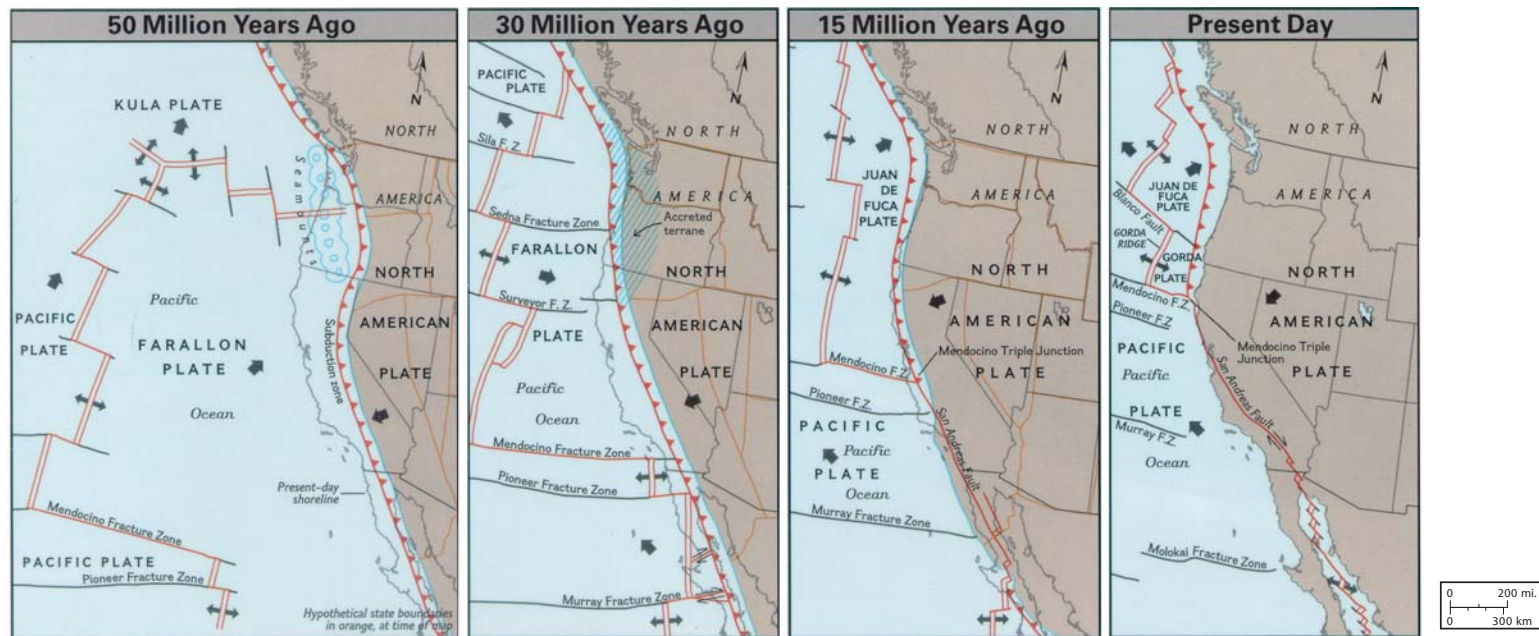
**FSAR UPDATE
HUMBOLDT BAY ISFSI
FIGURE 2.6-3**

Color shaded-relief map (oblique Mercator projection) of the Cascadia subduction zone along the northwest coast of the United States and Canada (from R.A. Haugerud, 1998, USGS Open-File Report 98-140).



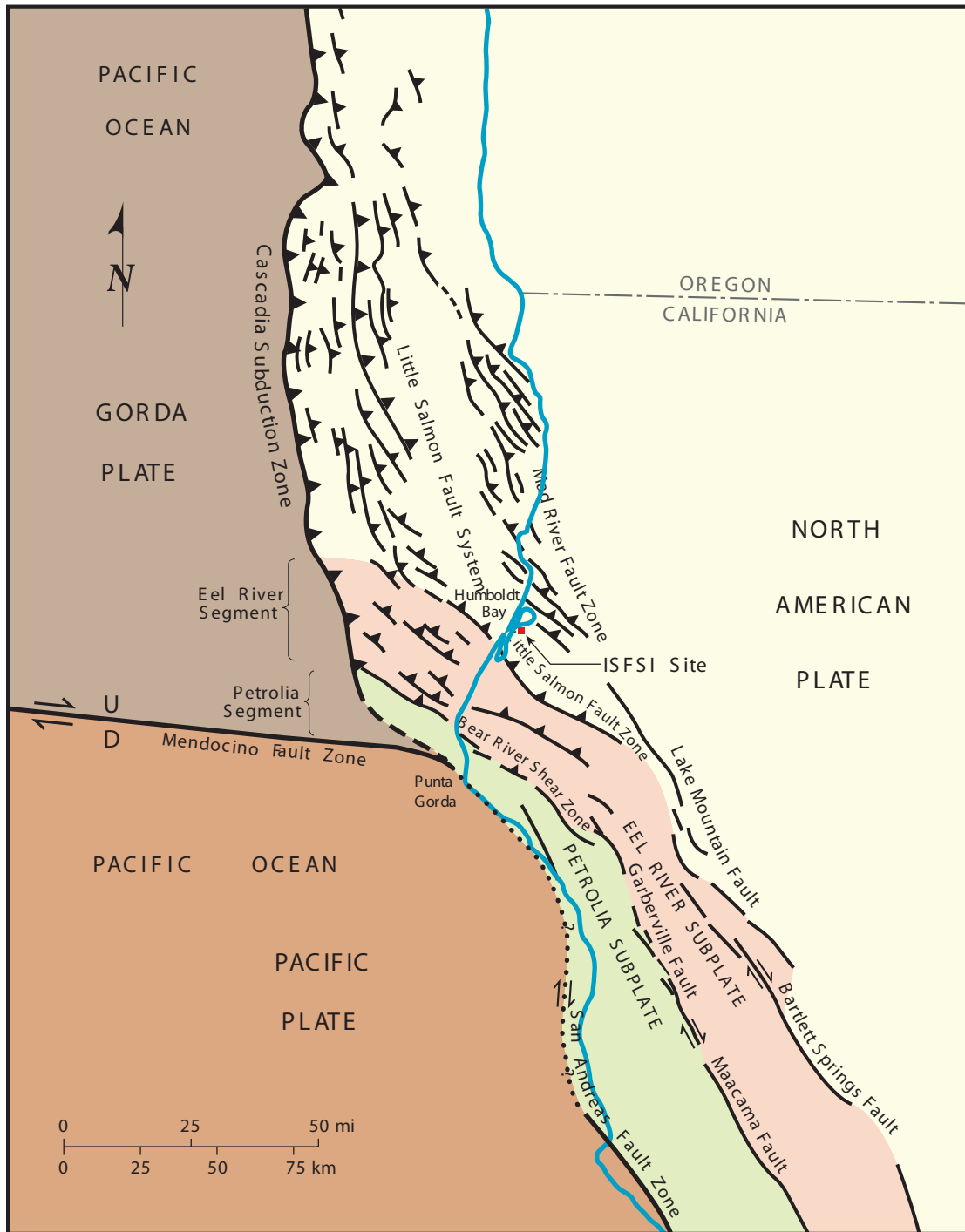
**FSAR UPDATE
HUMBOLDT ISFSI
FIGURE 2.6-4**

General plate tectonic setting of the western United States. Humboldt Bay and the proposed ISFSI site are on the western edge of the North American plate, at the north edge of the Mendocino triple junction region. Three plate-bounding fault zones, the San Andreas and Mendocino transform fault zones and the Cascadia subduction zone, intersect at the triple junction. Cross section A-A' is shown on Figure 2.6-10b.



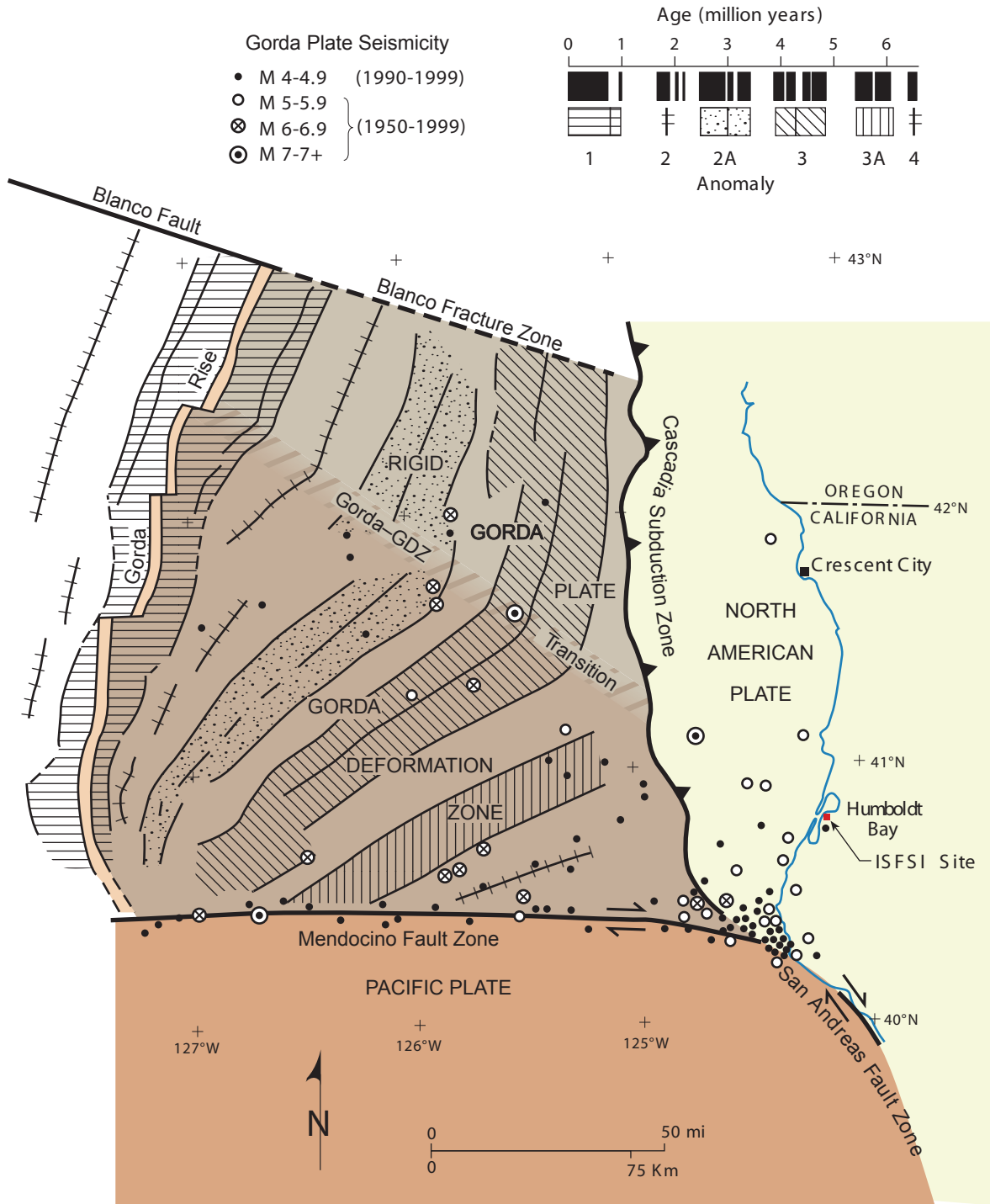
FSAR UPDATE
HUMBOLDT BAY ISFSI
FIGURE 2.6-5
TECTONIC EVOLUTION OF THE WEST COAST
UNITED STATES DURING PAST
50 MILLION YEARS
(FROM NATIONAL GEOGRAPHIC SOCIETY, 1995)

Revision 0 January 2006



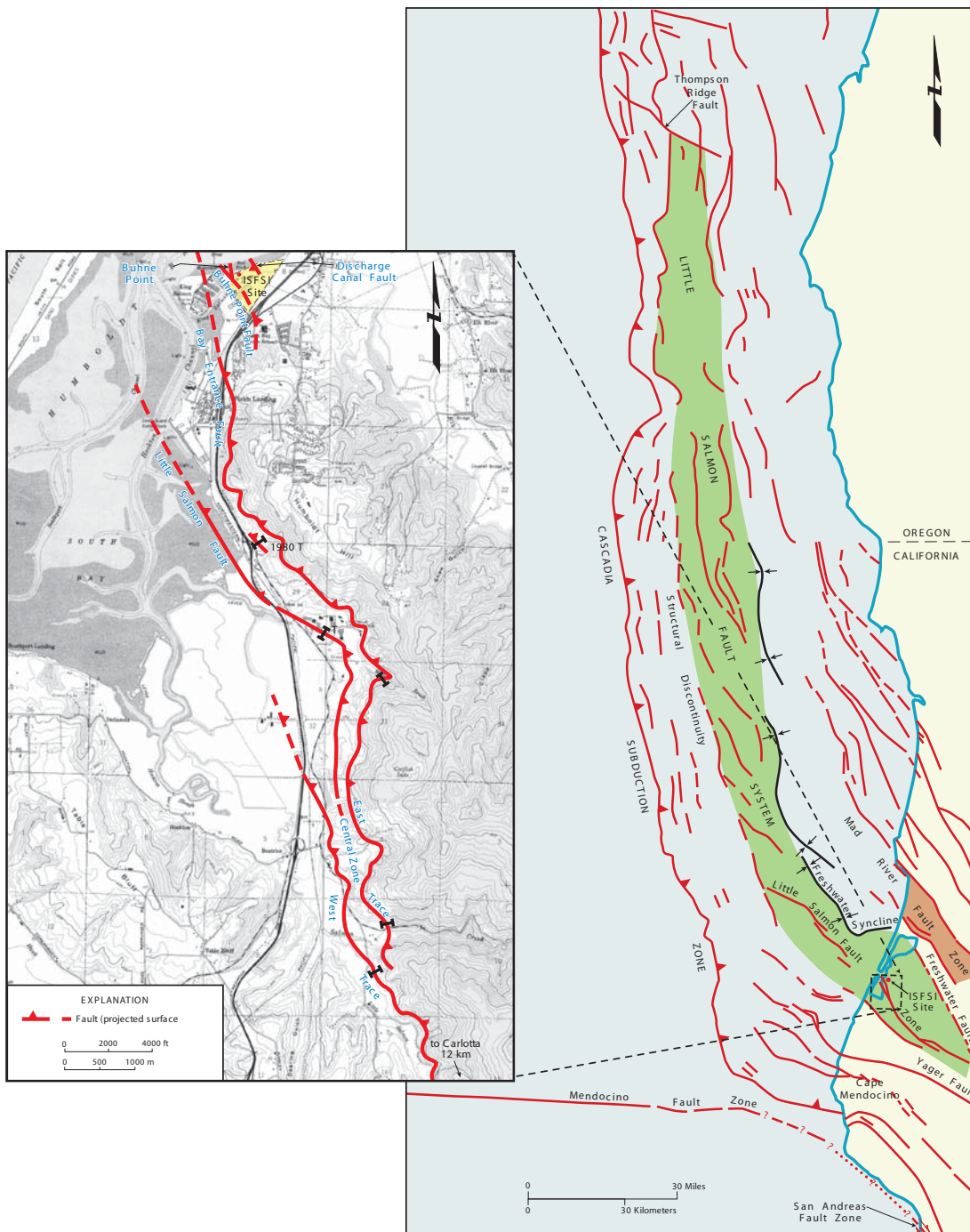
FSAR UPDATE
HUMBOLDT BAY ISFSI
FIGURE 2.6-6
MAP OF SUBPLATES IN THE NORTH AMERICAN PLATE AND MAJOR FAULTS IN NORTHWESTERN CALIFORNIA

Revision 0 January 2006



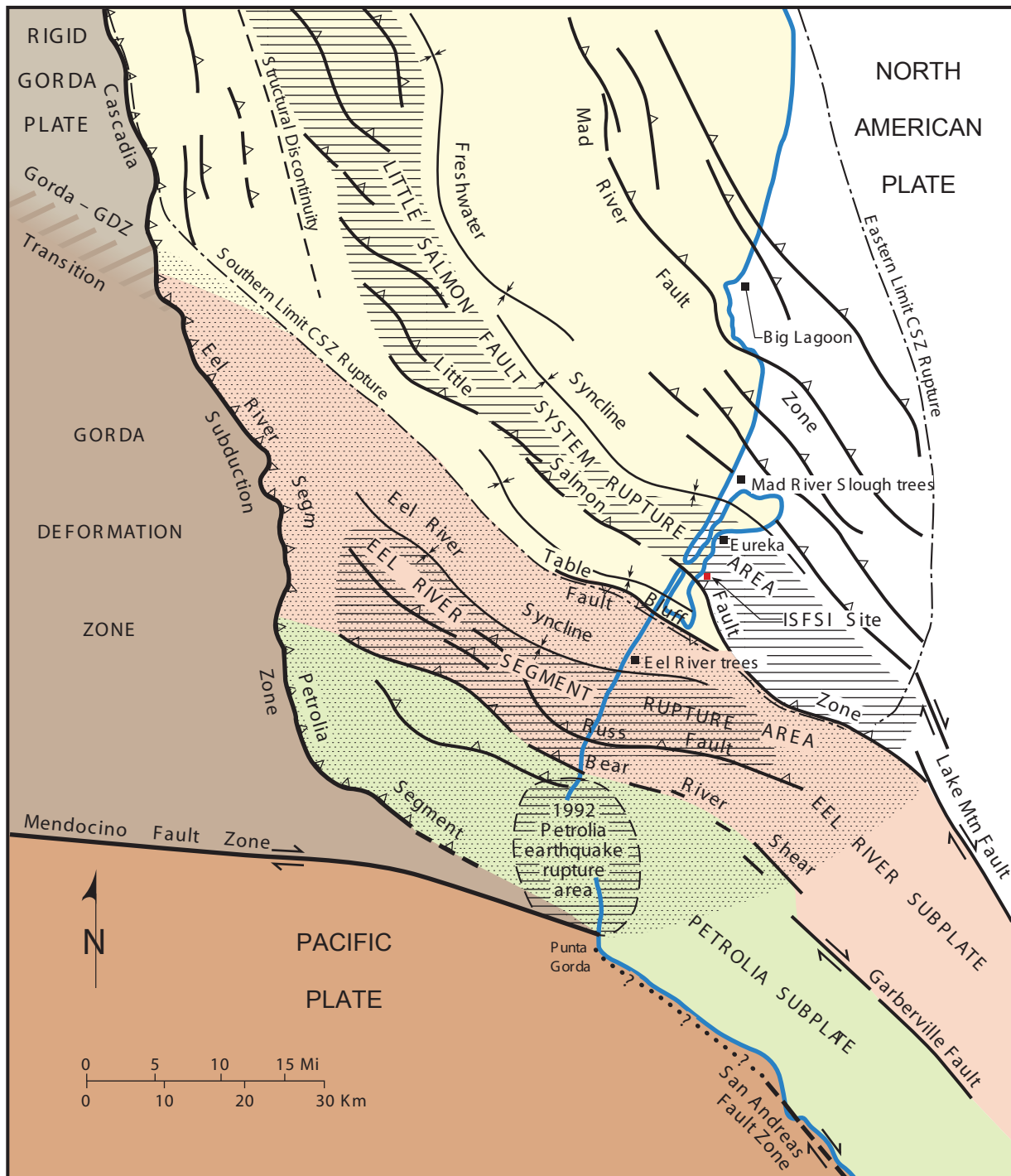
FSAR UPDATE
HUMBOLDT BAY ISFSI
FIGURE 2.6-7

Tectonics of the Gorda plate (Modified from Wilson, 1989, Figure 3). The deforming and seismically active southern part of the plate and the internally rigid northern part are separated by a narrow transition that strikes northwest and intersects the subduction zone a short distance northwest of Humboldt Bay.



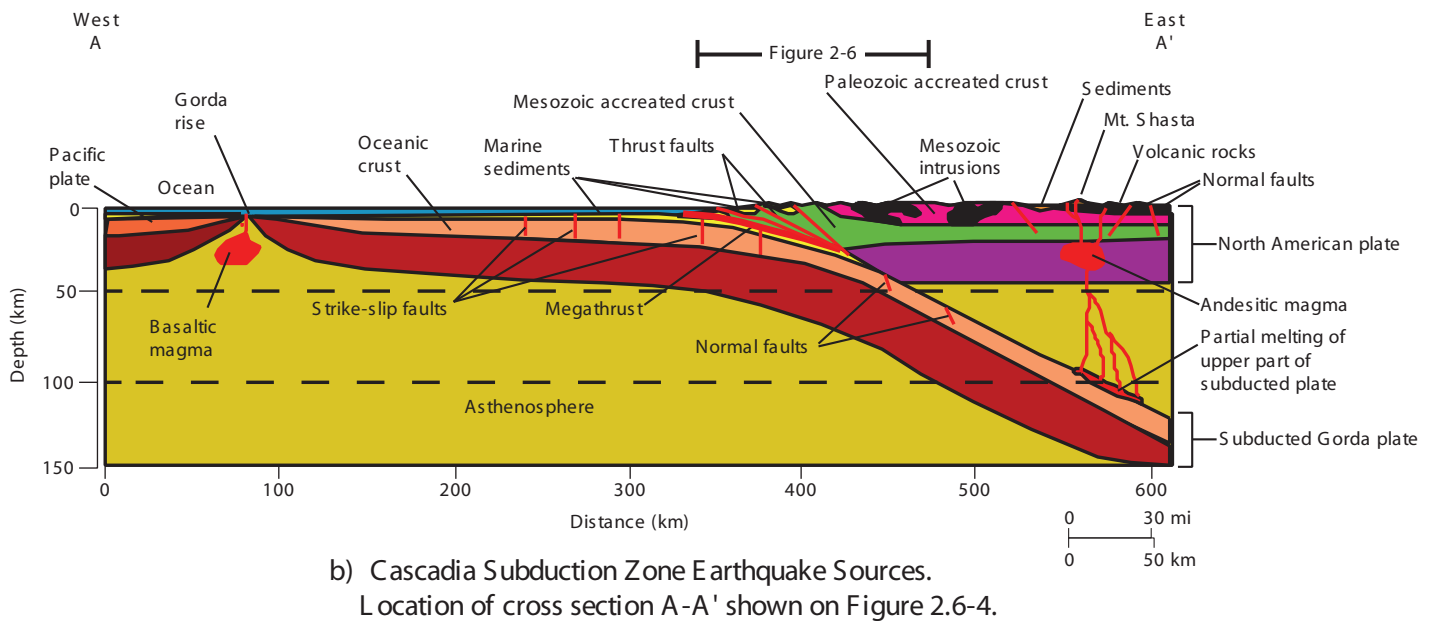
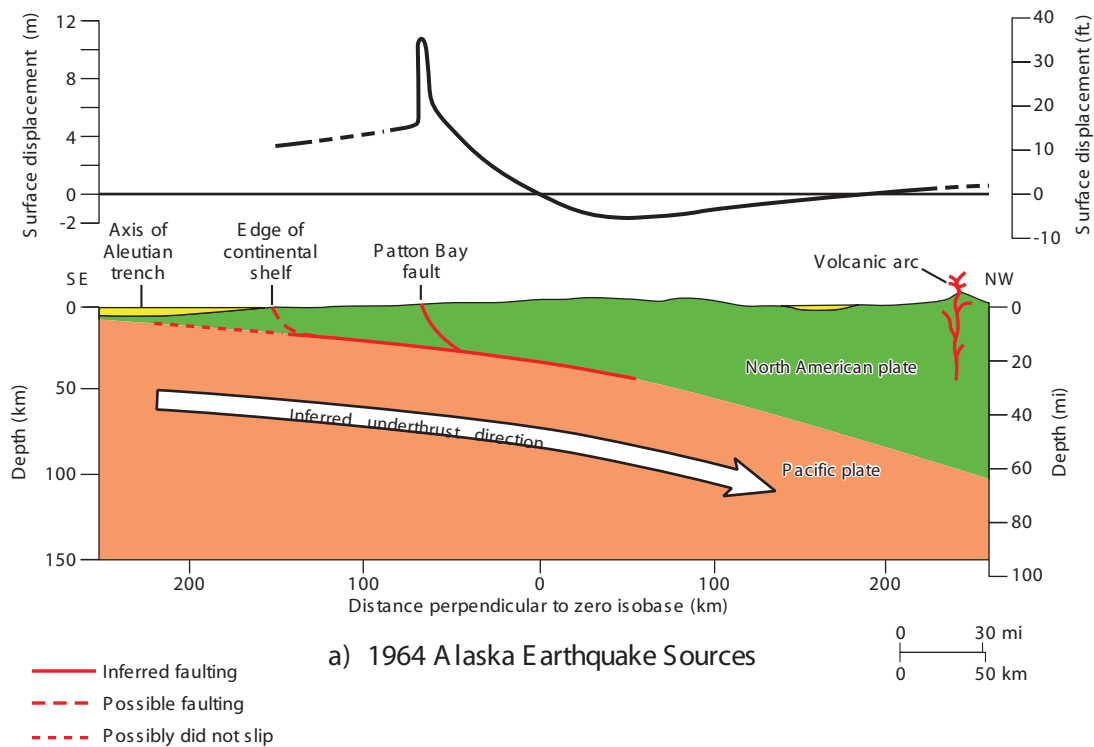
**FSAR UPDATE
HUMBOLDT BAY ISFSI
FIGURE 2.6-8**

Schematic maps showing the components of the Little Salmon fault system. The Little Salmon fault zone is part of a system of active folds and reverse faults, the Little Salmon fault system, which extends for 330 kilometers from its intersection with the Freshwater fault northwestward to its intersection with the Thompson Ridge fault off the coast of southern Oregon. The Little Salmon fault zone, which is the closest capable fault to the Humboldt Bay ISFSI site, is 95 kilometers long (including the offshore traces as mapped by Clarke (1992) and the Yager fault). The Little Salmon fault zone contains multiple subparallel surface traces. Near the Humboldt Bay ISFSI site, the Little Salmon fault zone includes two primary traces, the Little Salmon fault and the Bay Entrance fault, and three subsidiary faults in the hanging wall, the Buhne Point fault, the Buhne Point splay fault, and the Discharge Canal fault.



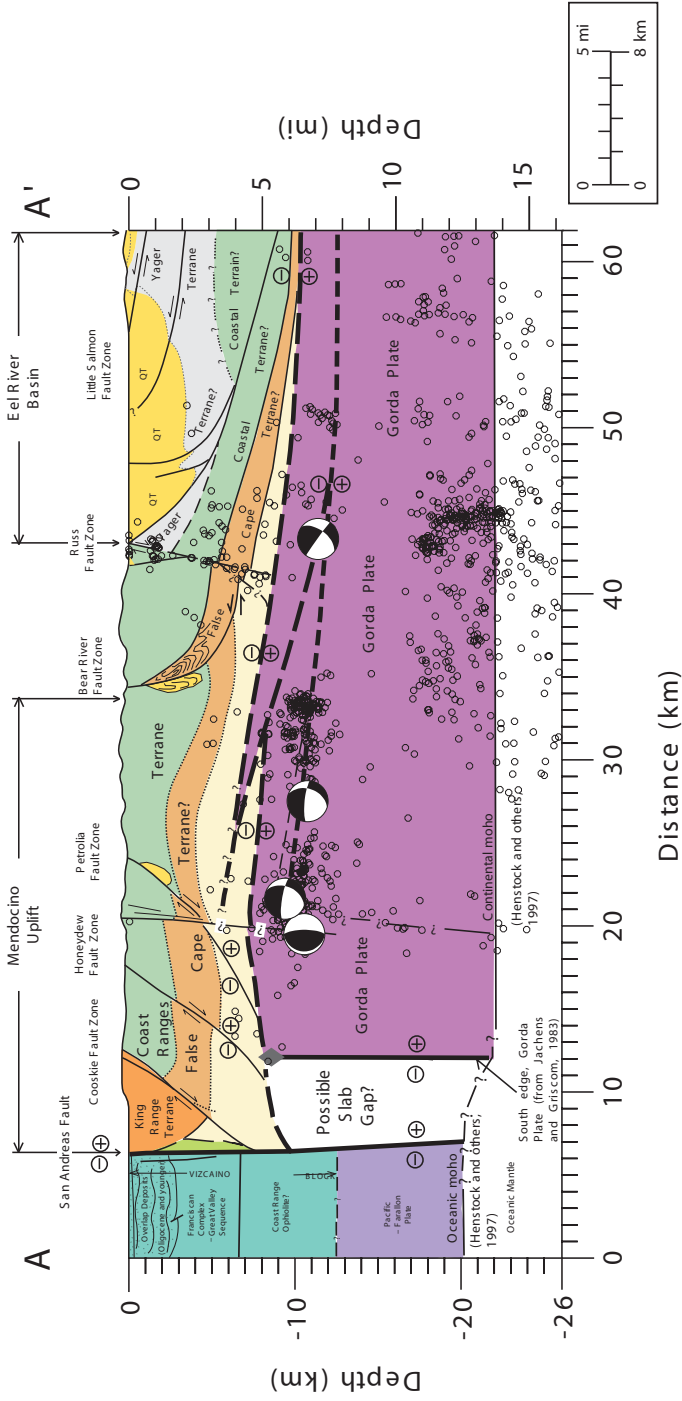
**FSAR UPDATE
HUMBOLDT BAY ISFSI
FIGURE 2.6-9**

Major active faults and known or inferred earthquake rupture areas (line pattern) in the Mendocino triple junction region (stippled area). Paleoseismic data indicate the Little Salmon fault system ruptured during a great Cascadia subduction zone (CSZ) event, which may have ruptured as far as the southern limit of the CSZ, 300 years ago, and that the Eel River segment ruptured independently less than 200 years ago.



FSAR UPDATE HUMBOLDT BAY ISFSI FIGURE 2.6-10

~Schematic cross section showing the suggested mechanisms for the 1964 Alaska earthquake (Plafker, 1972), and postulated Cascadia subduction zone earthquake sources.



Notes:
Focal mechanisms are depicted as spheres viewed from the southeast; black sectors are tensional, white sectors compressional. Location data and focal mechanisms from M. Magee, Stanford University/USGS (1994).

FSAR UPDATE HUMBOLDT BAY ISFSI FIGURE 2.6-12

Generalized regional structure section A-A' showing depth distribution of epicenters (open circles) and selected focal mechanisms (beach balls) of earthquakes from M. Magee (Stanford University and USGS), 1994 (after McLaughlin and others, 2000). The location of cross section A-A' is shown on Figure 2.6-11.

EXPLANATION

- Faults: teeth on upper plate of thrust fault; arrows indicate sense of strike slip; dashed where location uncertain; dotted where buried or concealed
- Anticline
- Anticline, overturned
- Syncline
- Location of geologic cross section (Figure 3-4)
- Location of McKinleyville trench (Woodward-Clyde Consultants, 1980)

COASTAL BELT AND OVERLYING SEDIMENTS

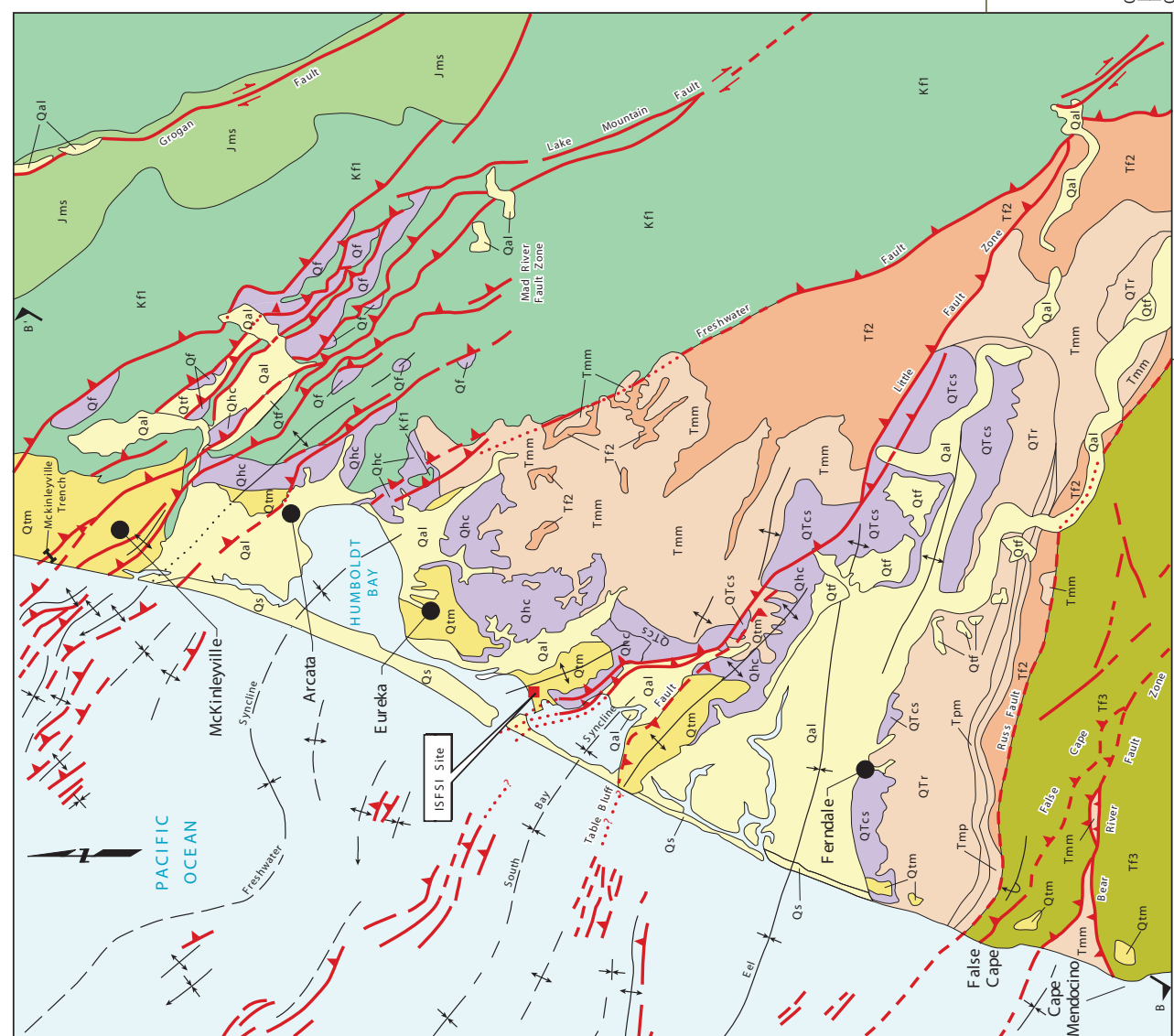
- Qs** upper Pleistocene and/or Holocene dune and beach sand
- Qal** upper Pleistocene and Holocene alluvium
- Qtf** upper Pleistocene fluvial terraces
- Qtm** middle and upper Pleistocene marine terraces
- Qf** lower and middle Pleistocene marine and nonmarine (Fabor Formation)
- Qc** Pleistocene nonmarine sediments (Carlotia Formation)

- QTcs** Plio-Pleistocene nonmarine sediments (Carlotia Formation and/or Scolia Bluffs Formation)
- QTr** upper Pliocene and lower Pleistocene marine sediments (Rio Dell Formation)
- Tpm** lower and middle Pliocene marine sediments (Eel River Formation)
- Tmm** upper Tertiary marine sediments (lower Wildcat Group)
- Tmp** upper Miocene marine sediments (Pulsen Formation)
- TF2** lower Tertiary Coastal Belt Franciscan Complex and Yager Formation

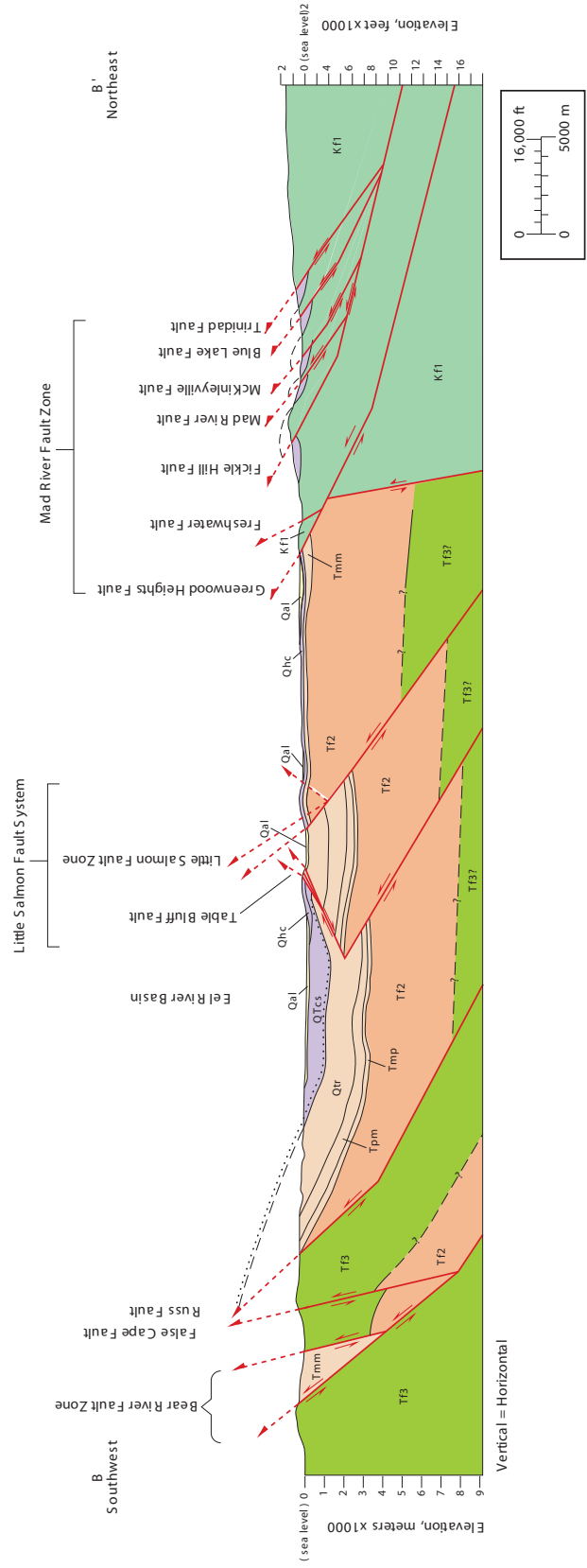
- Tmm** upper Tertiary marine sediments (lower Wildcat Group)
- TF3** lower to middle Tertiary Coastal Belt Franciscan Complex
- Kf1** Cretaceous Coastal Belt Franciscan Complex
- Jms** Pre-Cretaceous (Jurassic ?) metasedimentary rocks (South Fork Mountain Schist)

FSAR UPDATE HUMBOLDT BAY ISFSI FIGURE 2.6-13 GEOLOGIC MAP OF THE HUMBOLDT BAY REGION

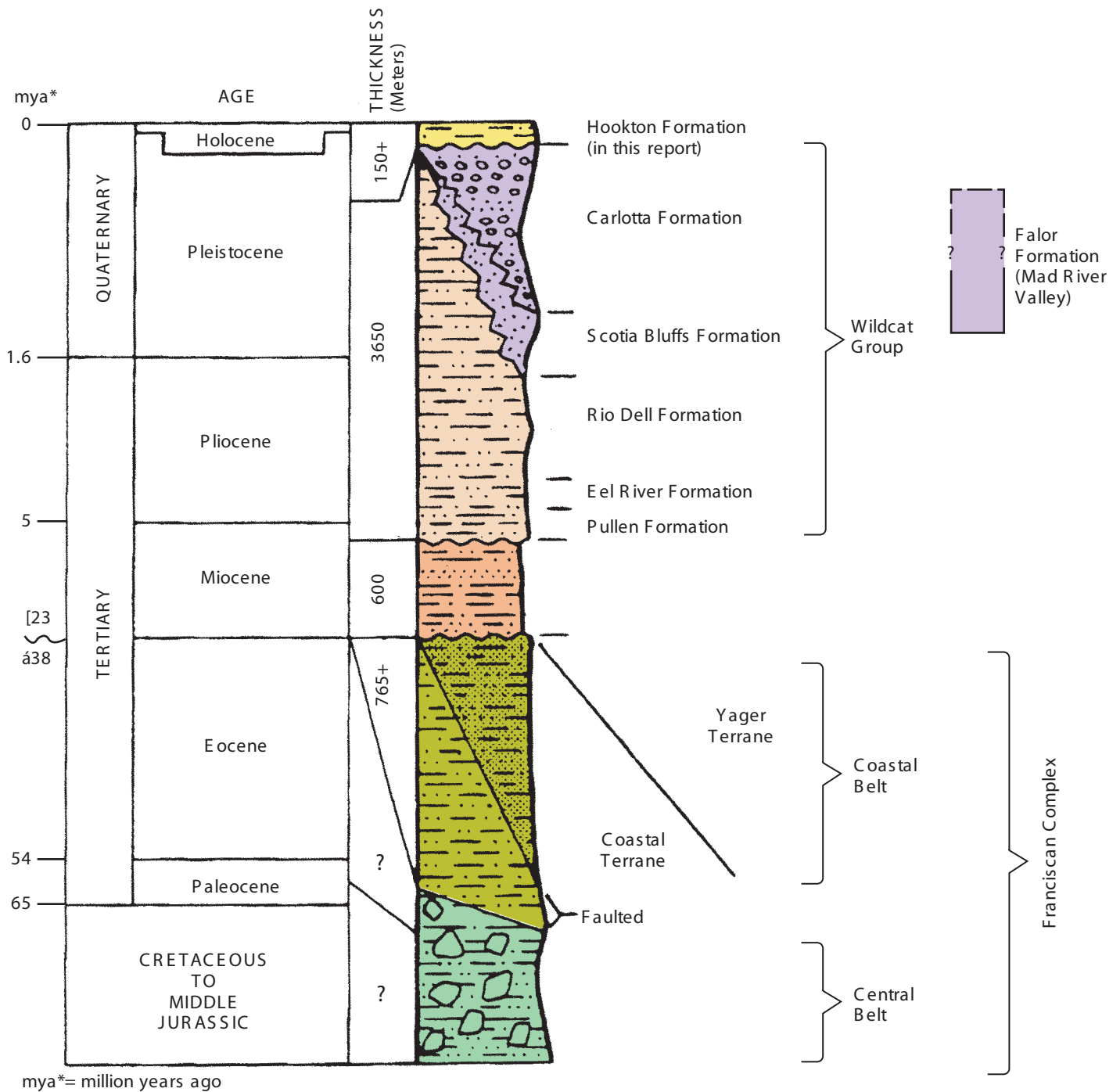
Revision 0 January 2006



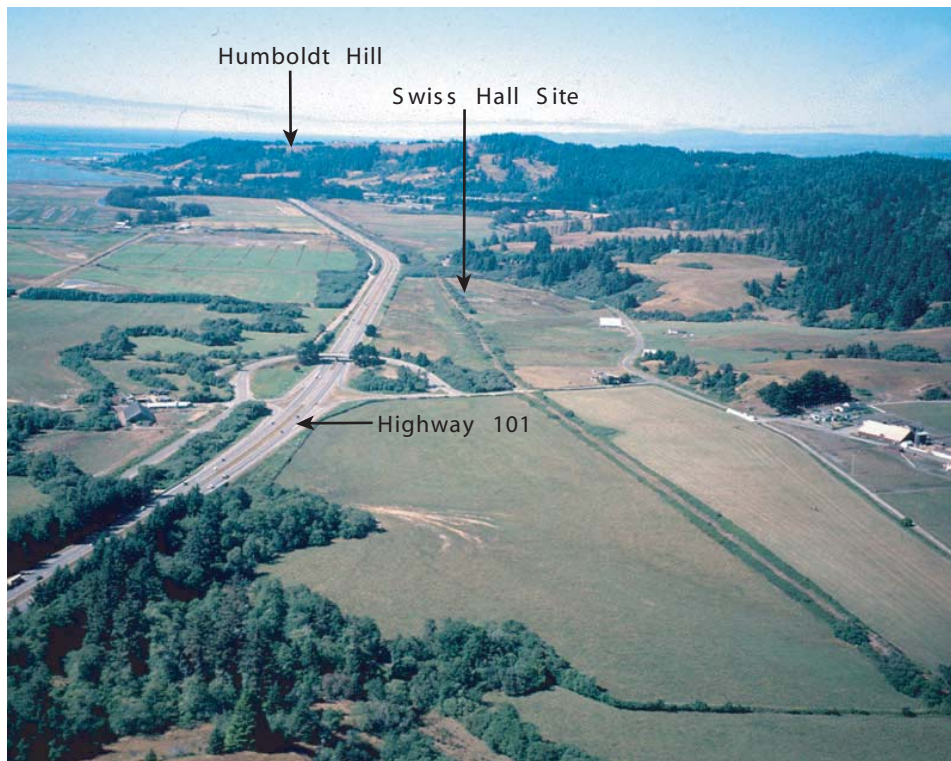
0 5.0 Miles
0 10 Kilometers



FSAR UPDATE
HUMBOLDT BAY ISFSI
FIGURE 2.6-14
Geologic cross section of the Humboldt Bay Region. See Figure 2.6-13 for description of stratigraphic units. The location of cross section B-B' is shown on Figure 2.6-13



FSAR UPDATE
HUMBOLDT BAY ISFSI
FIGURE 2.6-15
COMPOSITE STRATIGRAPHIC COLUMN, ONSHORE EEL RIVER BASIN (AFTER CLARKE, 1992)



A) View north along Highway 101 with Humboldt Hill in the distance.



B) Closer view of the Swiss Hall paleoseismic study site.

**FSAR UPDATE
HUMBOLDT BAY ISFSI
FIGURE 2.6-16**

Oblique aerial views looking north along the Humboldt Hill anticline and the Little Salmon fault zone. (Photographs taken July 25, 2000, by W.D. Page).









EXPLANATION

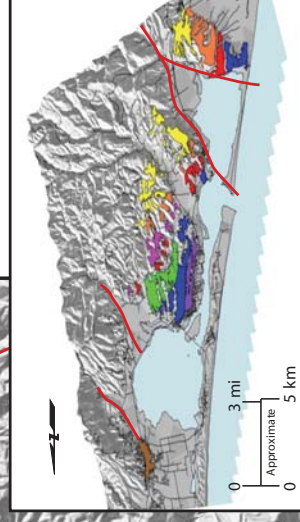
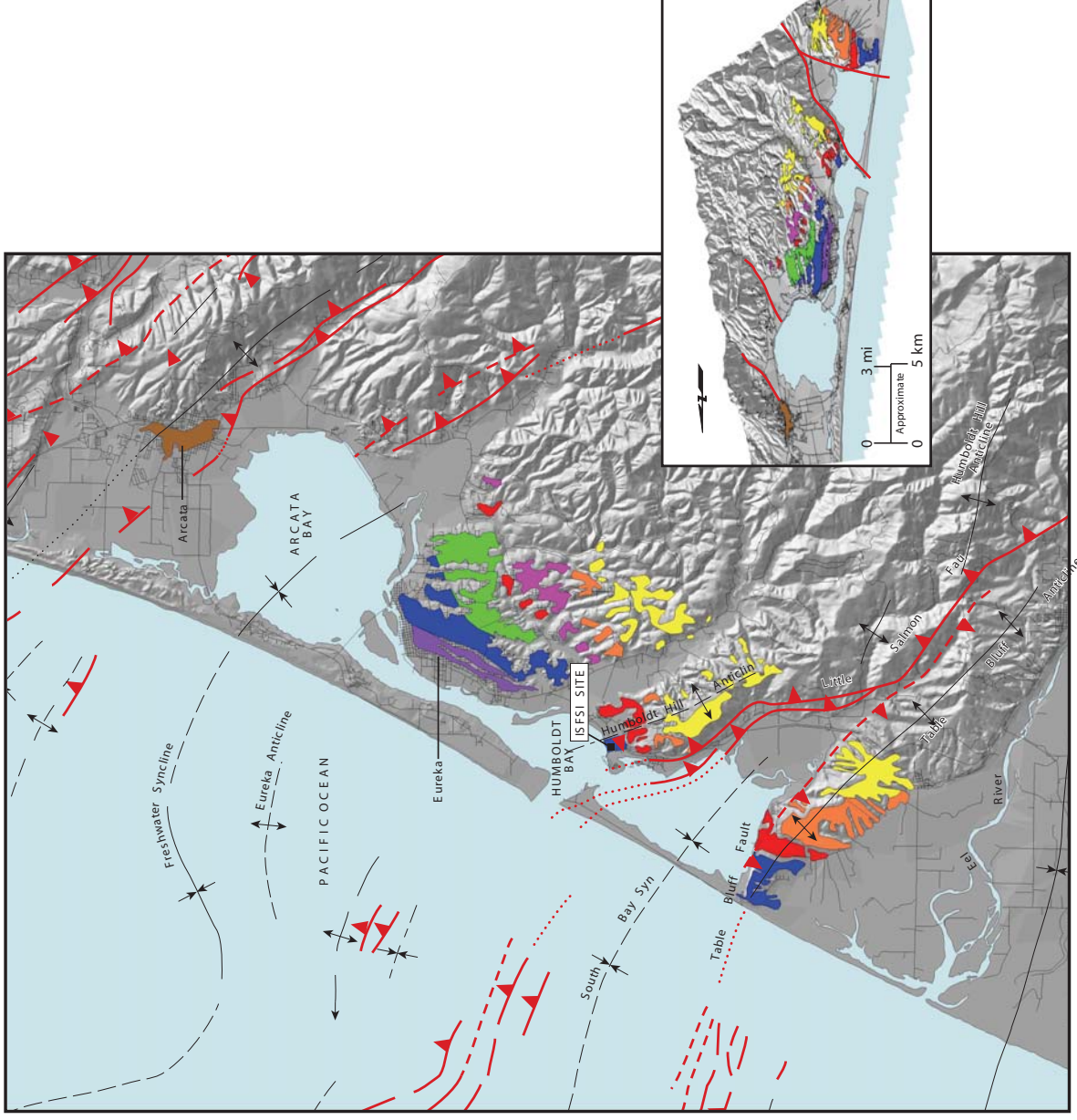
 Faults: teeth on upper plate of thrust fault; arrows indicate sense of strike slip; dashed where location uncertain; dotted where buried or concealed

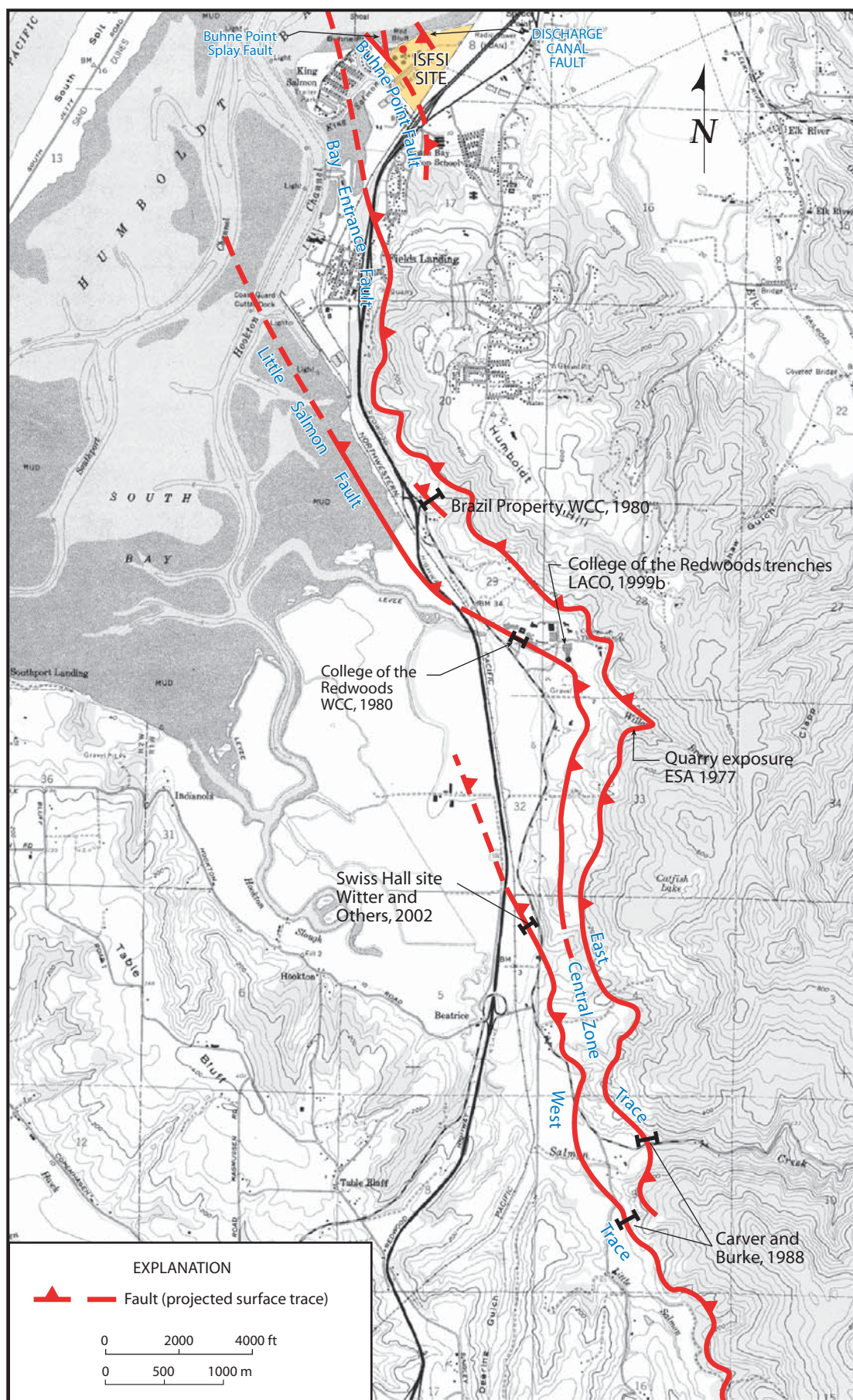
 Anticline

 Anticline, overturned

 Syncline

Terrace Name	Isotope Stage	Approximate Age (x 1000 yrs.)
 Patricks Point	4a	64
 Savage Creek	5a	83
 McKinleyville	5b	96
 Westhaven	5c	103
 Fox Farm	5d	120
 Sky Horse	5e	130
 A - Line	7a?	176
 Older and much older Terraces		200+





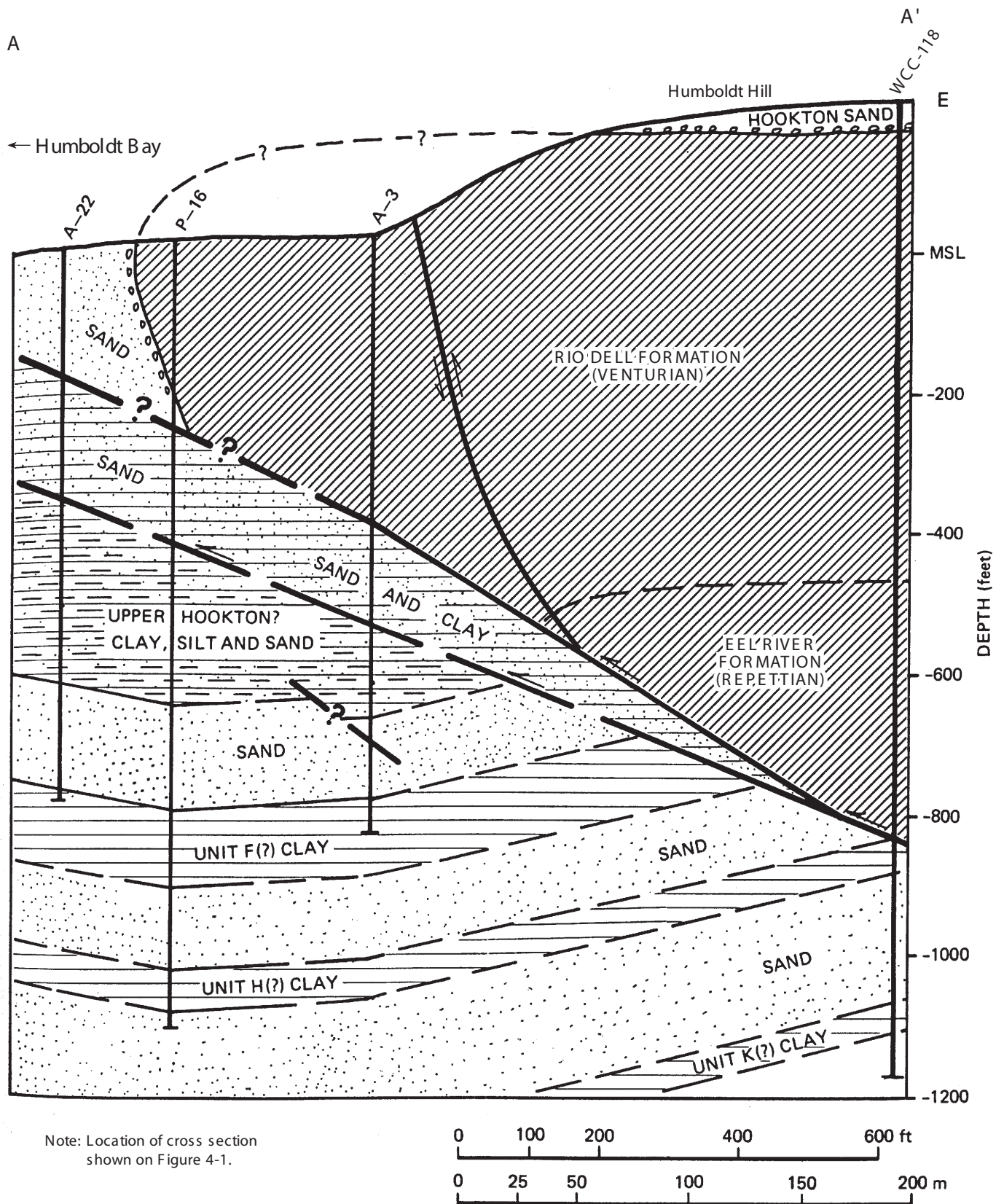
FSAR UPDATE

HUMBOLDT BAY ISFSI

FIGURE 2.6-18

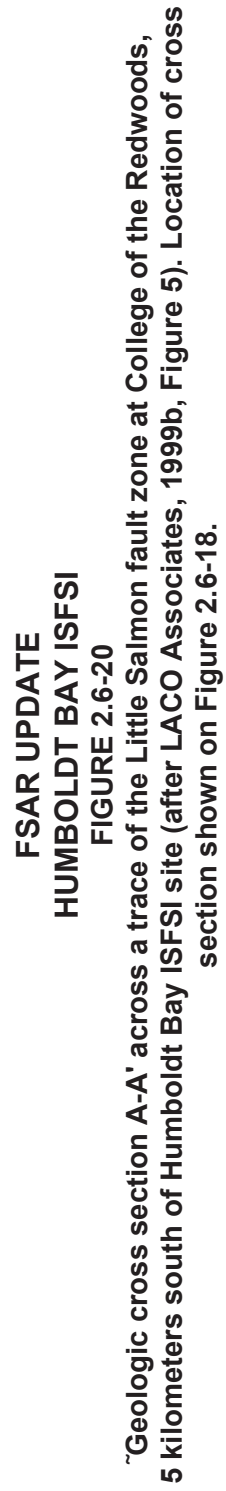
SURFACE TRACES OF THE LITTLE SALMON FAULT ZONE SOUTH OF THE ISFSI SITE

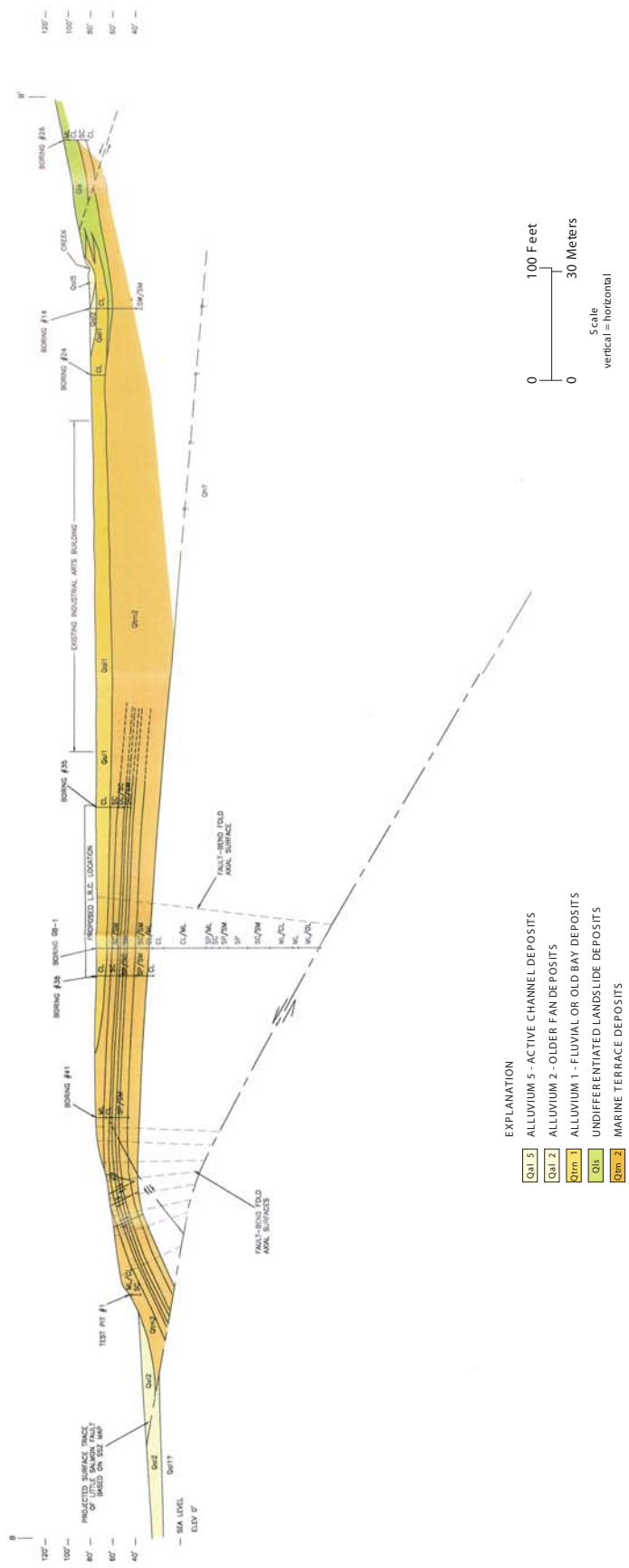
Revision 0 January 2006



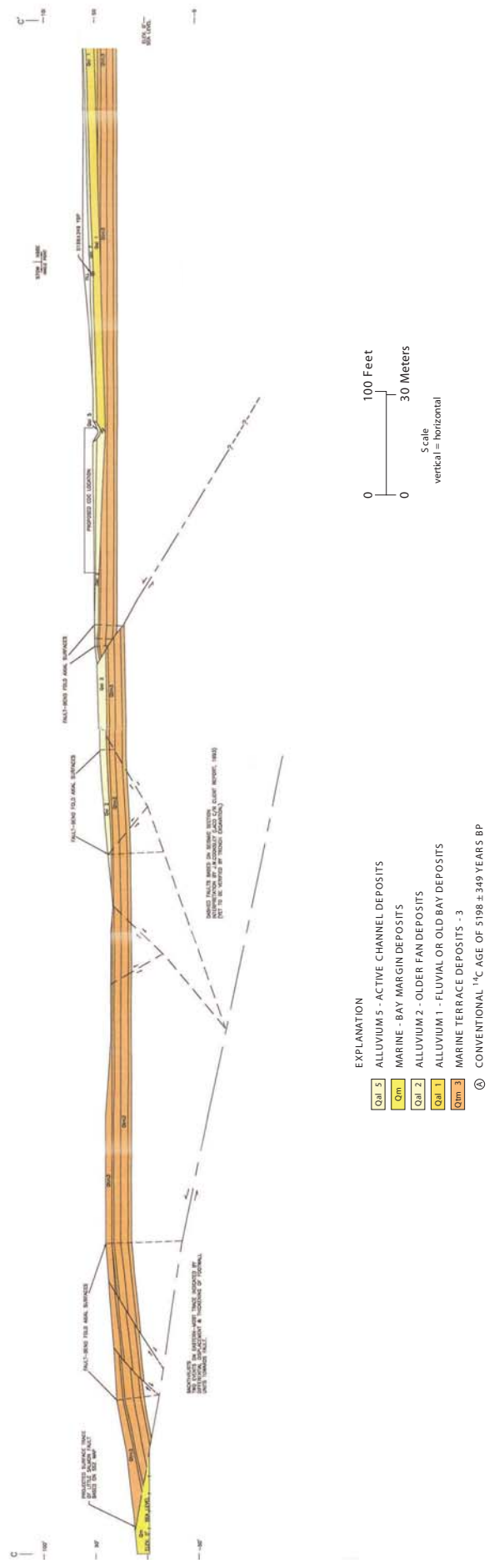
**FSAR UPDATE
HUMBOLDT BAY ISFSI
FIGURE 2.6-19**

**Cross section A-A' across the Little Salmon fault zone at Humboldt Hill
(after Woodward-Clyde Consultants, 1980, Figure C-15).**

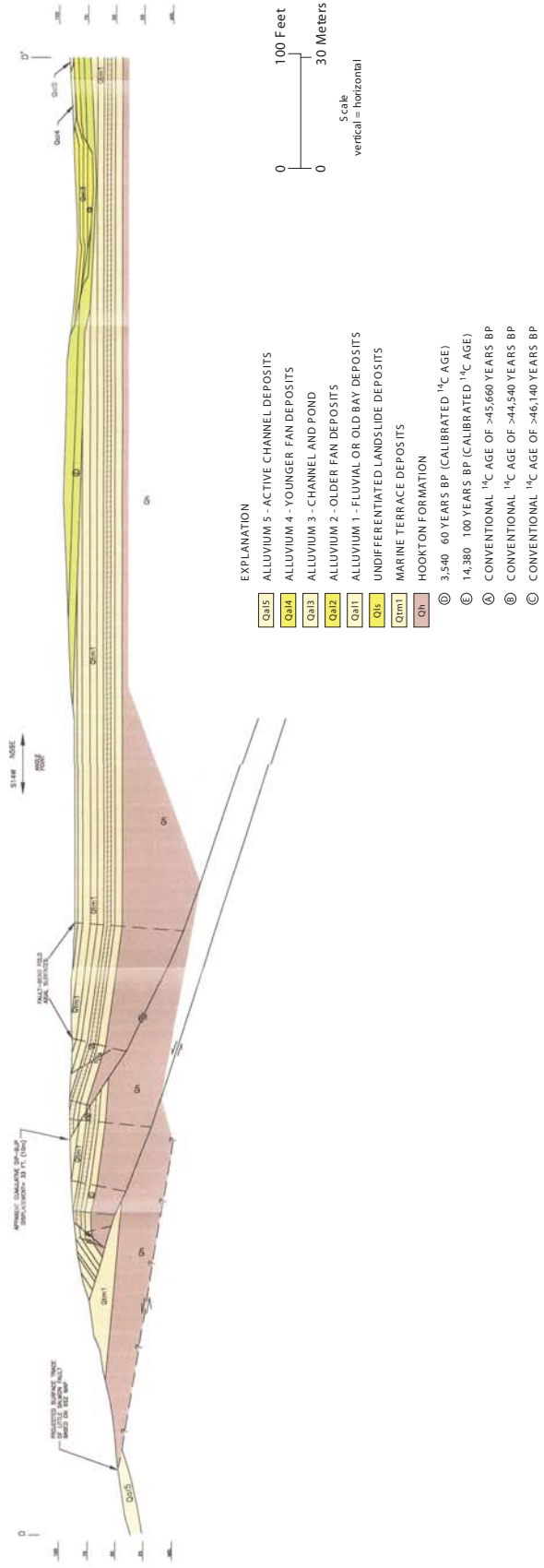




FSAR UPDATE
HUMBOLDT BAY ISFSI
FIGURE 2.6-21
Geologic cross section B-B' across a trace of the Little Salmon fault zone at College of the Redwoods, 5 kilometers south of Humboldt Bay ISFSI site (after LACO Associates, 1999b, Figure 6). Location of cross section shown on Figure 2.6-18.

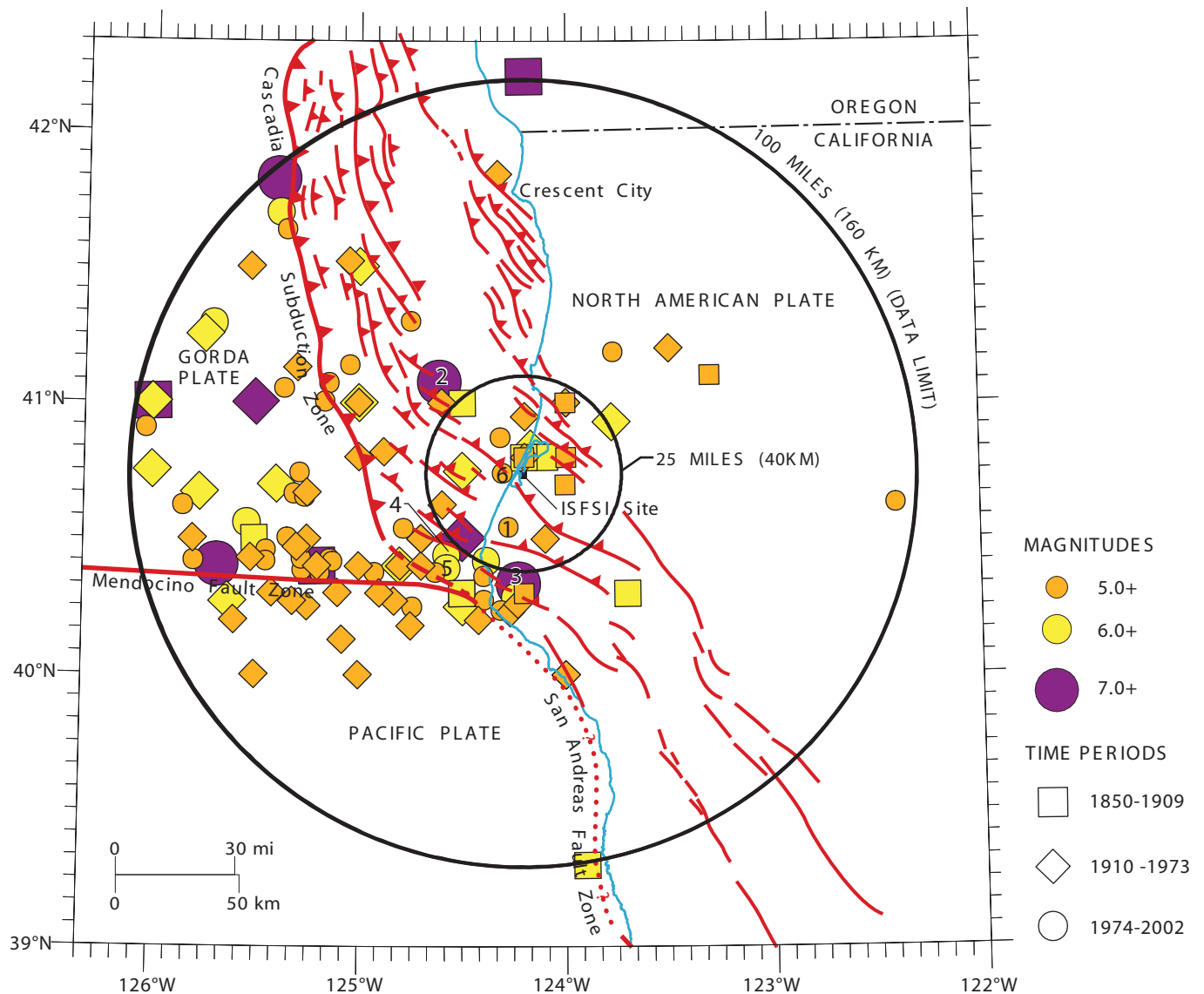


FSAR UPDATE
HUMBOLDT BAY ISFSI
FIGURE 2.6-22
Geologic cross section C-C' across a trace of the Little Salmon fault zone at College of the Redwoods,
5 kilometers south of Humboldt Bay ISFSI site (after LACO Associates, 1999b, Figure 7). Location of cross section shown on Figure 2.6-18.



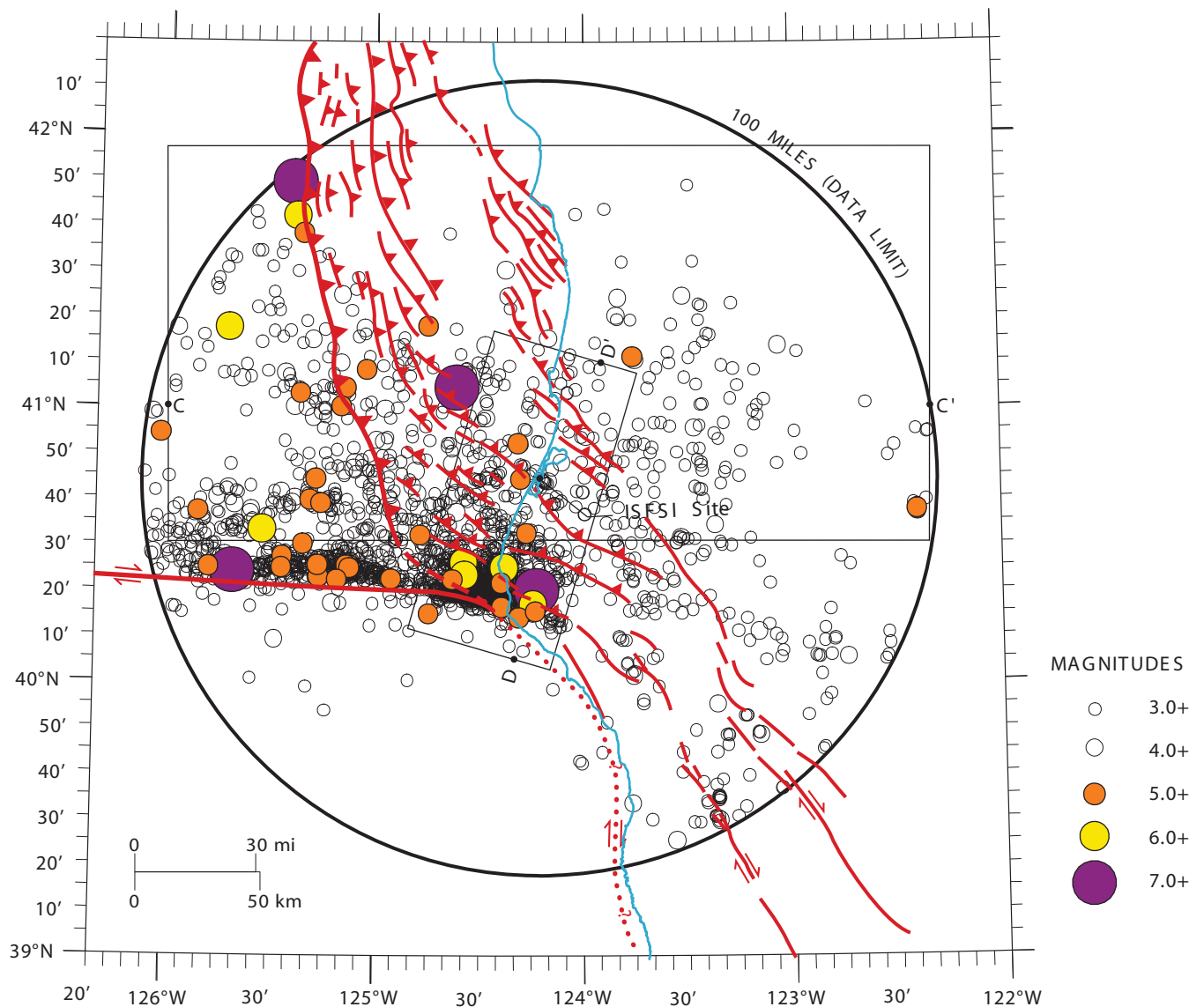
FSAR UPDATE HUMBOLDT BAY ISFSI FIGURE 2.6-23

Geologic cross section D-D' across a trace of the Little Salmon fault zone at College of the Redwoods, 5 kilometers south of Humboldt Bay ISFSI site (after LACO Associates, 1999b, Figure 8). Location of cross section shown on Figure 2.6-18.



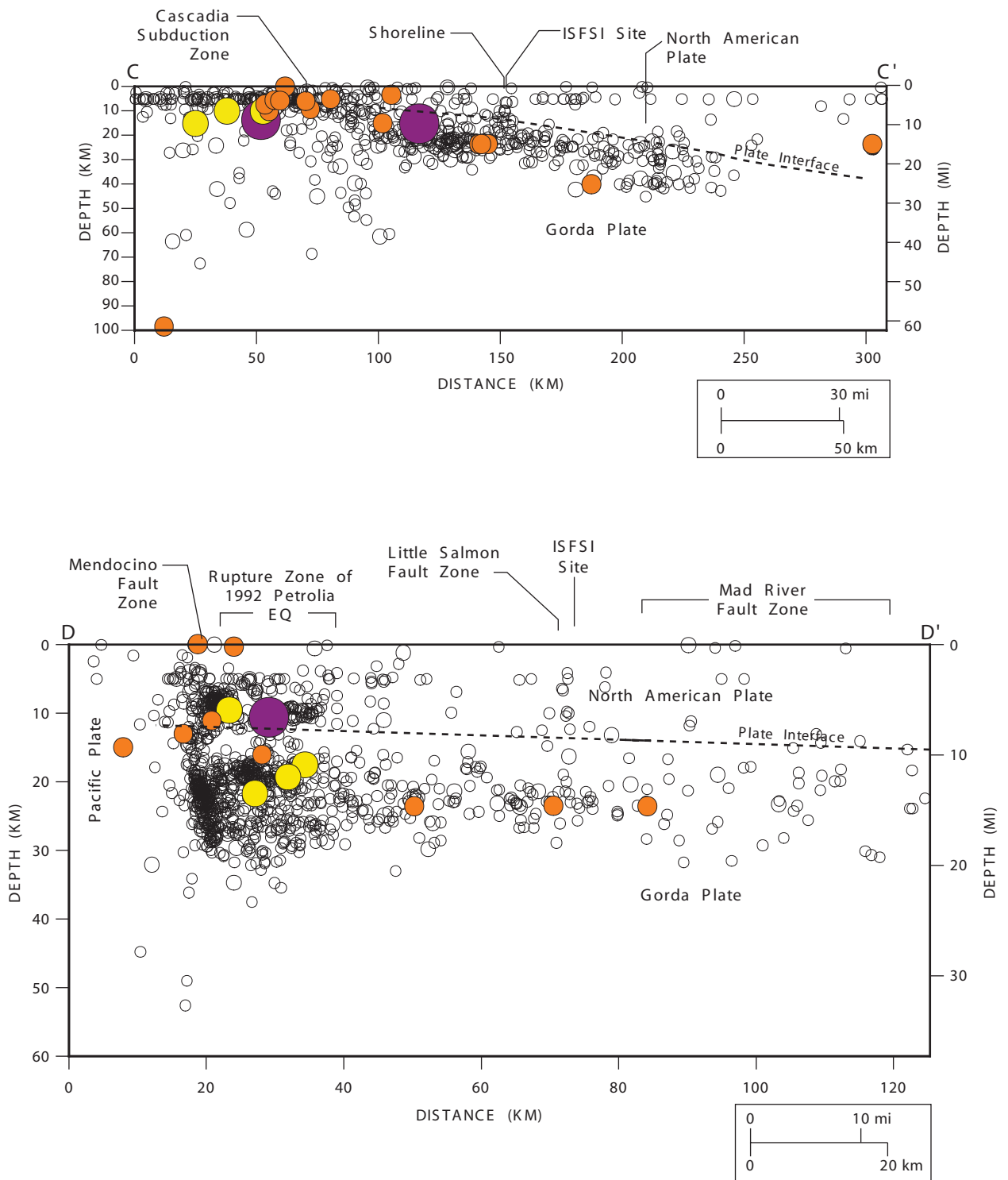
**FSAR UPDATE
HUMBOLDT BAY ISFSI
FIGURE 2.6-24**

Magnitude 5 and larger earthquakes for the period 1850 through April 2002 within 160 kilometers (100 miles) of the site. Earthquakes are scaled by magnitude and differentiated by time periods. Locations are listed in Table 2.6-4. Numbered earthquakes are included in Table 2.6-5. Earthquakes within 25 miles (40 kilometers) of the site are included in Figure 2.6-27.



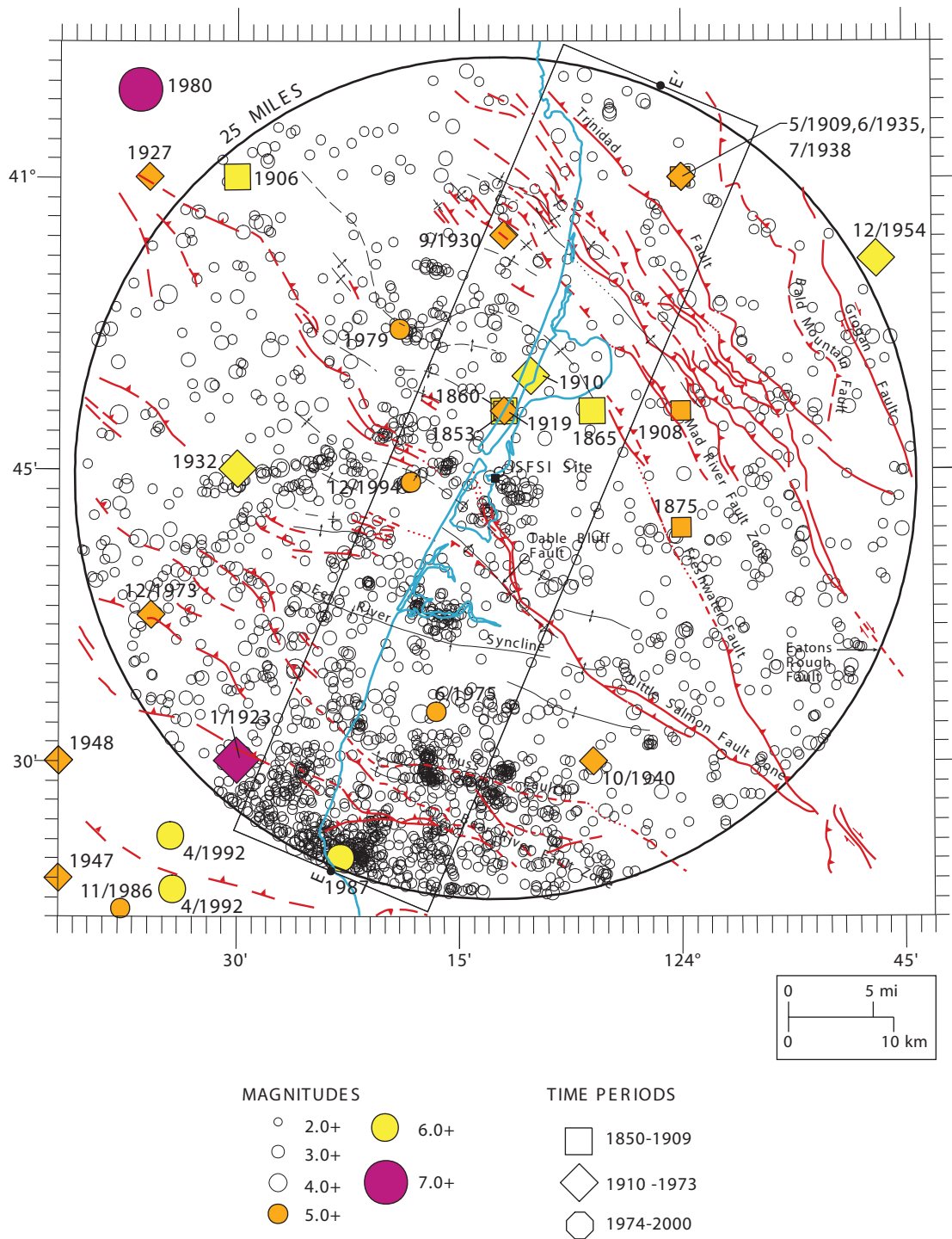
**FSAR UPDATE
HUMBOLDT BAY ISFSI
FIGURE 2.6-25**

Magnitude 3 and larger earthquakes from the period 1974 through April 2002 within 160 kilometers (100 miles) of the site. The locations of cross sections C-C' and D-D' (Figure 2.6-26) also are shown. Locations of magnitude 5 and larger earthquakes are listed in Table 2.6-12.



**FSAR UPDATE
HUMBOLDT BAY ISFSI
FIGURE 2.6-26**

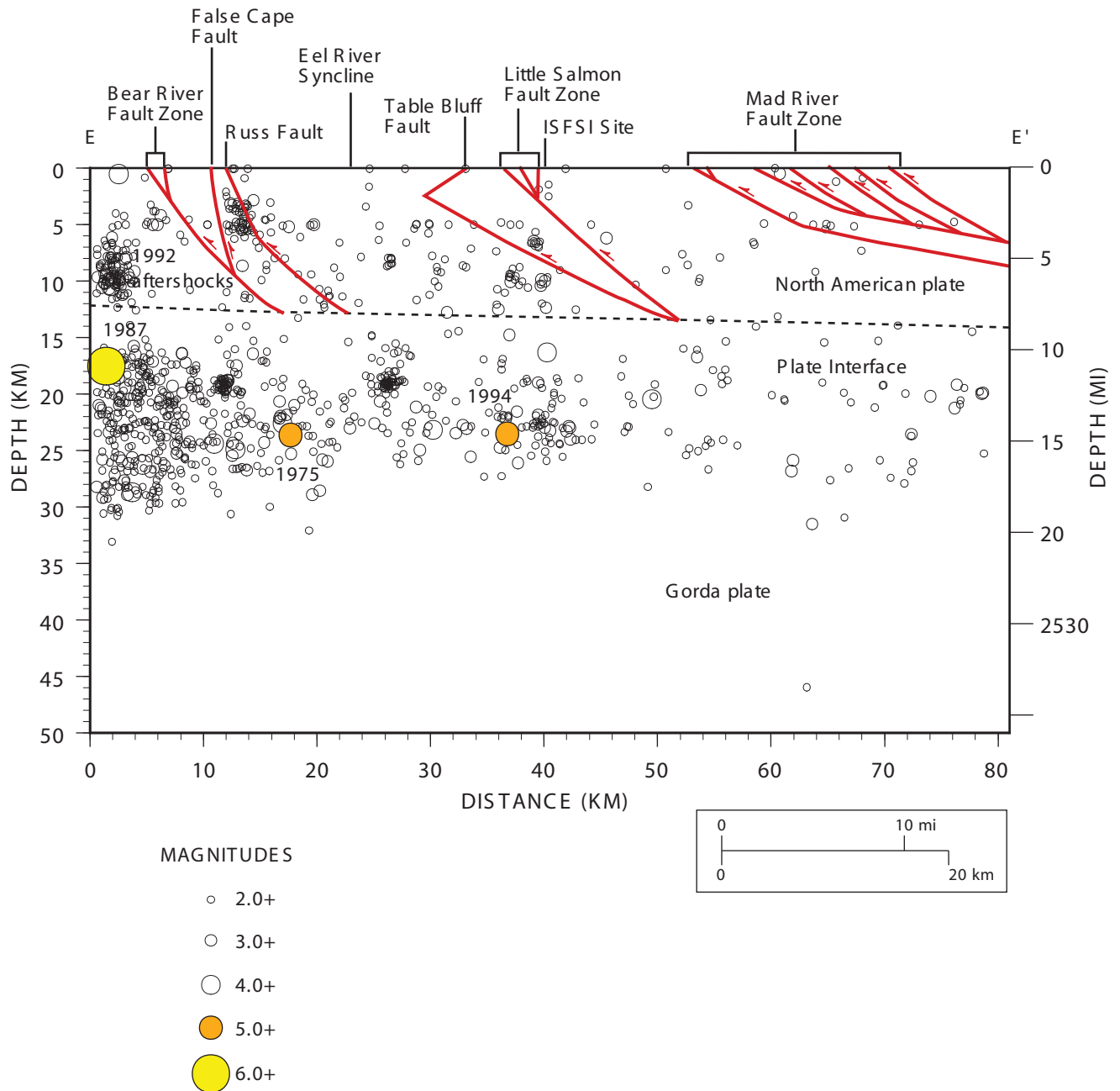
Seismic cross sections of magnitude 3 and larger earthquakes from the period 1974 through April 2002. The locations of cross sections C-C' and D-D' and earthquake symbol legend are shown on Figure 2.6-25. The location of the plate interface (dashed line) is based on Figure 2.6-12 and Geomatrix (1994).



FSAR UPDATE HUMBOLDT BAY ISFSI

FIGURE 2.6-27

Magnitude 2 and larger earthquakes from the period 1974 through April 2002, within 40 kilometers (25 miles) of the site, and earthquakes of magnitude 5 and larger from 1850 through 1973 within the map boundary. Locations of magnitude 5 and greater earthquakes are listed in Table 2.6-4.



**FSAR UPDATE
HUMBOLDT BAY ISFSI
FIGURE 2.6-28**

Seismic cross section of magnitude 2 and larger earthquakes from the period 1974 through April 2002. The location of cross section E-E' is shown on Figure 2.6-27. Fault locations are based on Figure 2.6-14; location of the plate interface (dashed line) is based on Figure 2.6-12 and Geomatrix (1994).



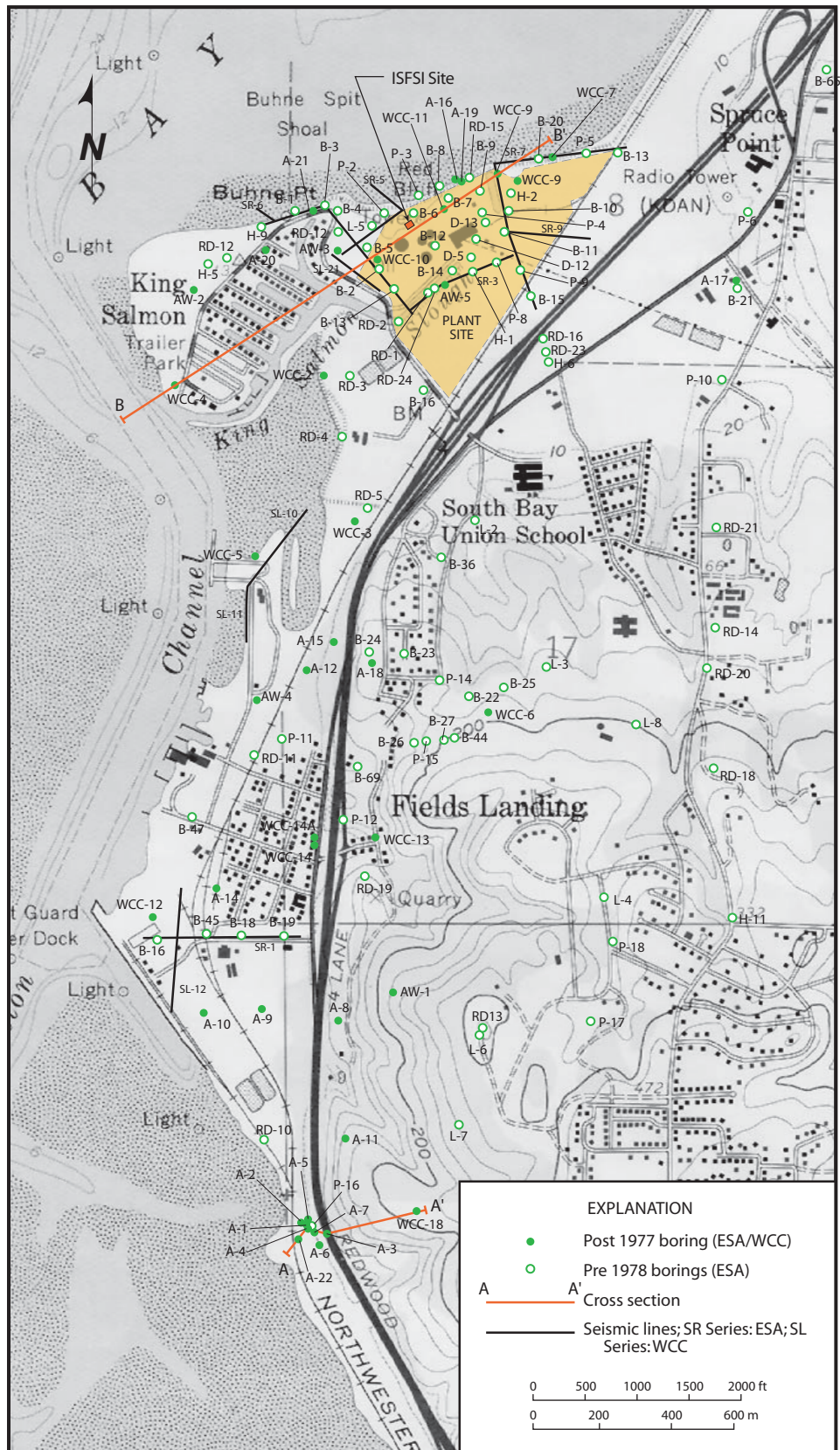
A) View toward the southwest.



B) View toward the west-southwest.

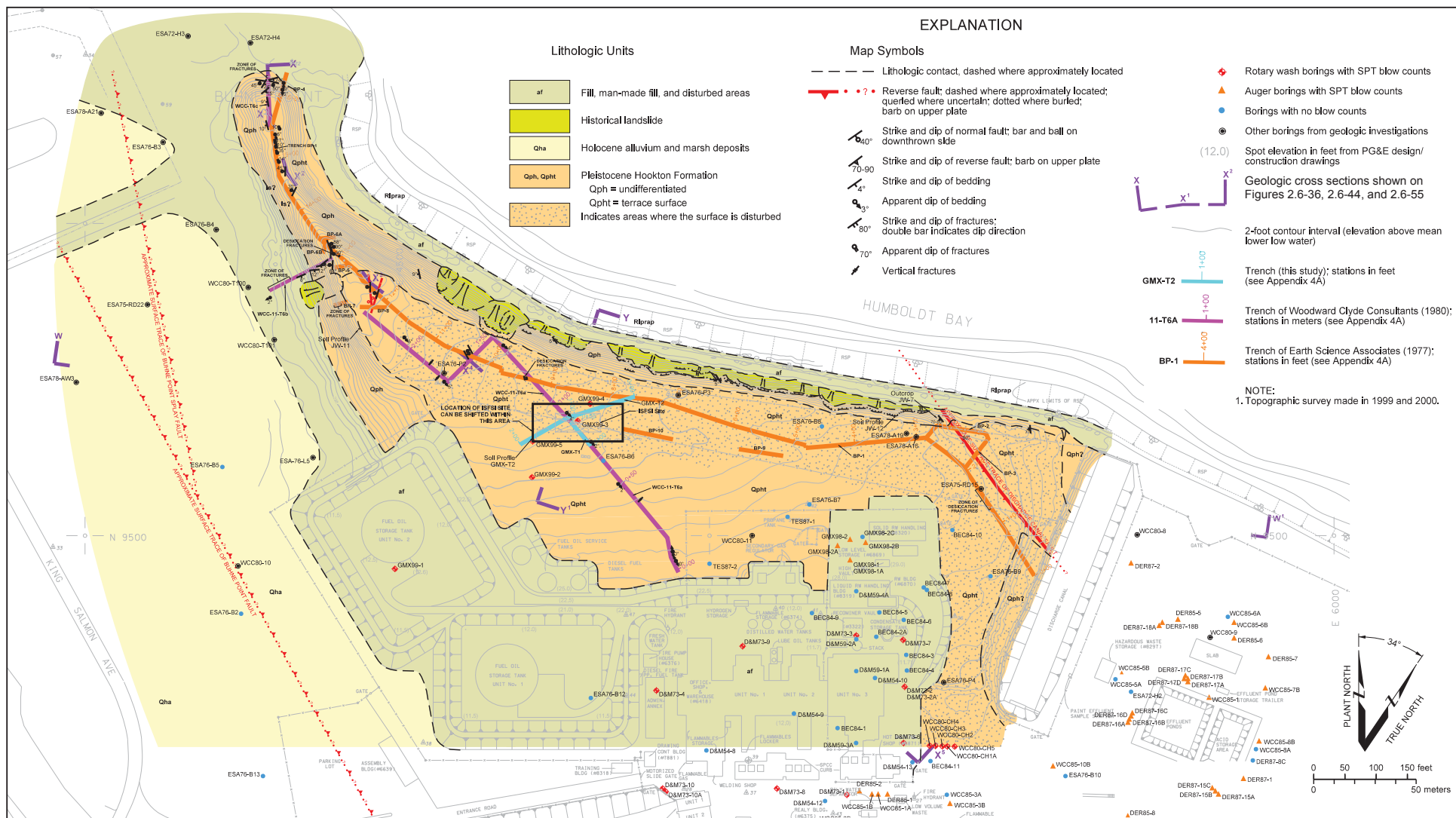
**FSAR UPDATE
HUMBOLDT BAY ISFSI
FIGURE 2.6-29**

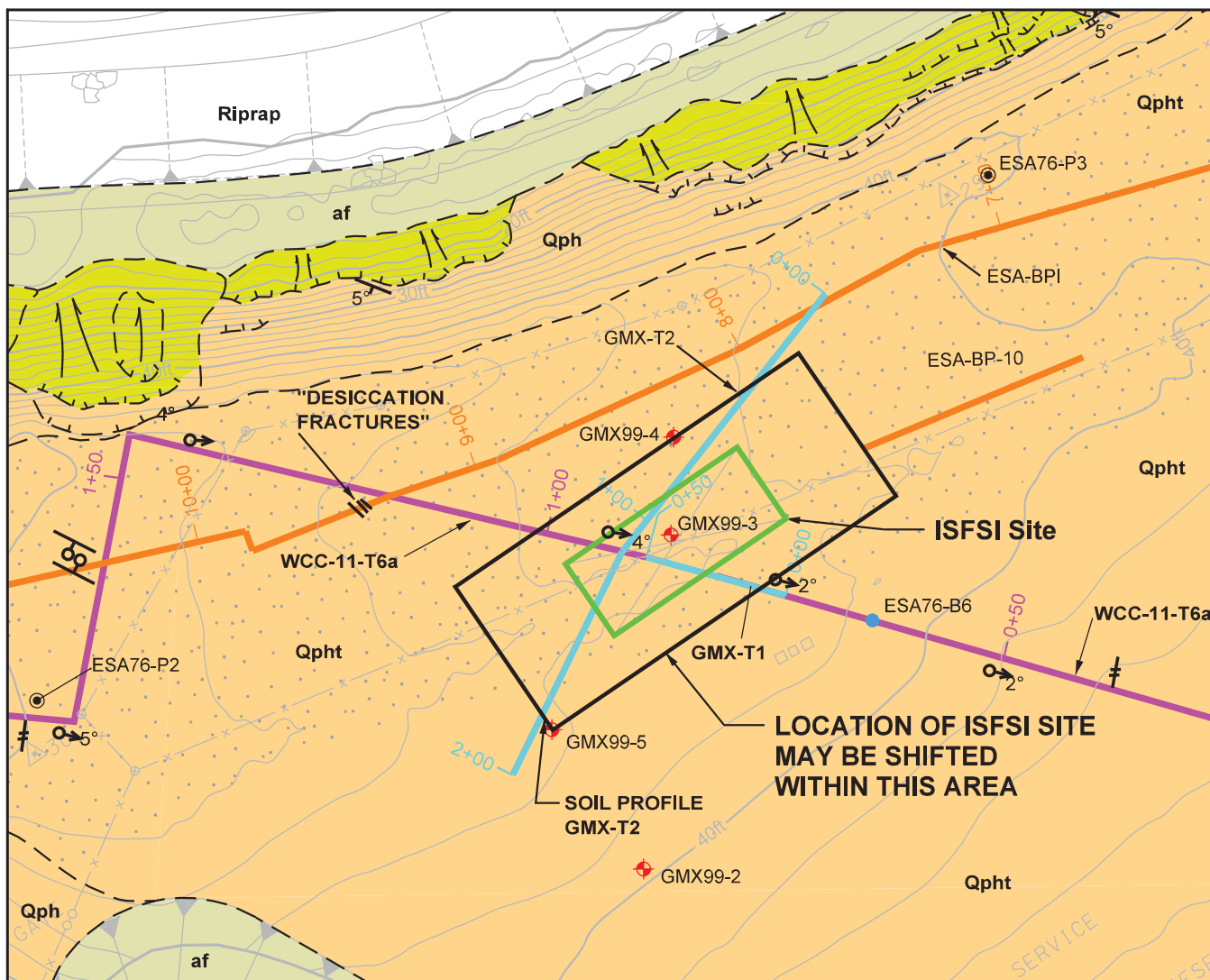
~Oblique aerial view of the Humboldt Bay ISFSI site. (Photographs taken July 25, 2000, by W. D. Page.)



**FSAR UPDATE
HUMBOLDT BAY ISFSI
FIGURE 2.6-30**

Locations of borings, cross sections, and seismic reflection lines used in the 1980 Woodward-Clyde Consultants report. (after Woodward-Clyde Consultants, 1980, Figure C-2). Cross section A-A' is shown on Figure 2.6-49 and cross section B-B' is shown on Figure 2.6-50.





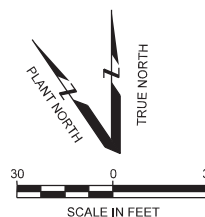
EXPLANATION

Map Symbols

- — — Lithologic contact, dashed where approximately located
- Normal fault; bar and ball on downthrown side
- Apparent dip of bedding
- Vertical fractures
- Rotary wash borings with SPT blow counts
- Borings with no blow counts
- Other borings from geologic investigations
- (12.0) Spot elevation in feet from PG&E design/construction drawings
- 2-foot contour interval (elevation above mean lower low water)
- GMX-T2 Trench excavated for this study; stations in feet
- BP-1 Trench of Earth Science Associates (1976); stations in feet
- 11-T6a Trench of Woodward Clyde Consultants (1980); stations in meters

Lithologic Units

- Fill, man-made fill, and disturbed areas
- Historical landslide
- Pleistocene Hookton Formation
 - Qph = undifferentiated
 - Qpht = terrace surface
- Indicates areas where the surface is disturbed



FSAR UPDATE

HUMBOLDT BAY ISFSI

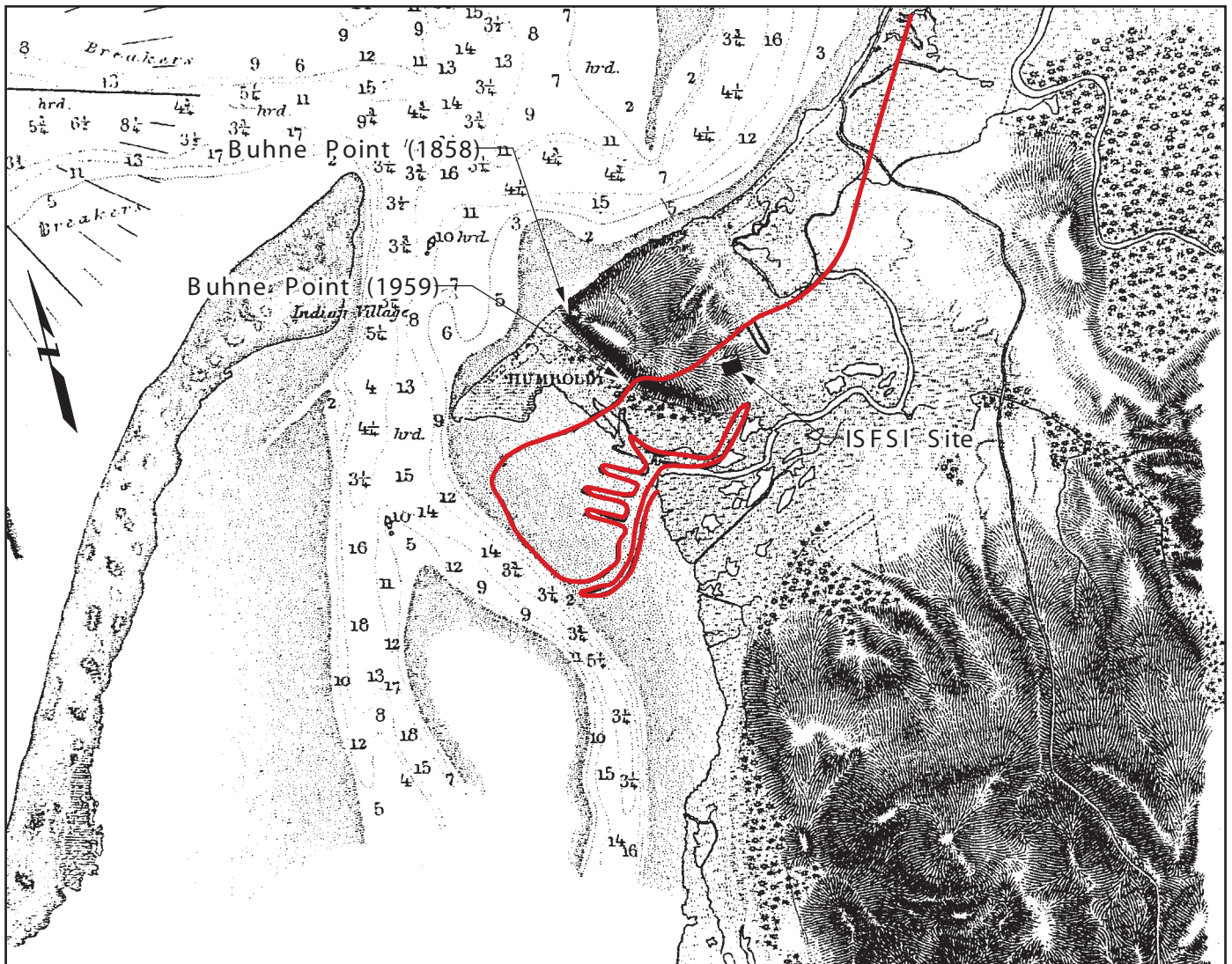
FIGURE 2.6-32 LOCATIONS OF GEOLOGIC TRENCHES AND BORINGS NEAR THE ISFSI SITE

Revision 0 January 2006



**FSAR UPDATE
HUMBOLDT BAY ISFSI
FIGURE 2.6-33**

Oblique aerial view looking northwest from above Humboldt Hill toward the entrance of Humboldt Bay. (Photograph taken July 25, 2000, by W. D. Page.)



Base map: U.S. Coast and Geodetic Survey, 1858, Preliminary survey map of Humboldt, California.

0 0.5 Mile
0 1 Kilometer

EXPLANATION

— Coastline from U.S. Geological Survey (1959) Fields Landing 7.5' Quadrangle, California

FSAR UPDATE HUMBOLDT BAY ISFSI FIGURE 2.6-34

Comparison of the shoreline shown on 1858 and 1959 surveys. The 1959 shoreline is superimposed on the 1858 map to show the extensive coastal erosion and the retreat of Buhne Point that occurred prior to placement of riprap along the shoreline of Humboldt Bay.



**FSAR UPDATE
HUMBOLDT BAY ISFSI
FIGURE 2.6-35**

View looking west from Buhne Point showing the escarpment along the north side of the Buhne Point terrace and riprap along the shoreline of Humboldt Bay. (Photograph JW-2-1 taken March 9, 2000.)



Note: Location of cross section is shown on Figure 2.6-31. Unit F location based on structure contour map (Figure 2.6-51). Stratigraphy above Unit F based on correlation boreholes (EST8-P2, GMX99-2, ESA76-6) and trenches (11-T6a, 11-T6b, 11-T6c).

FSAR UPDATE
HUMBOLDT BAY ISFSI
FIGURE 2.6-36 GEOLOGIC CROSS SECTION X-X ⁵

Revision 0 January 2006



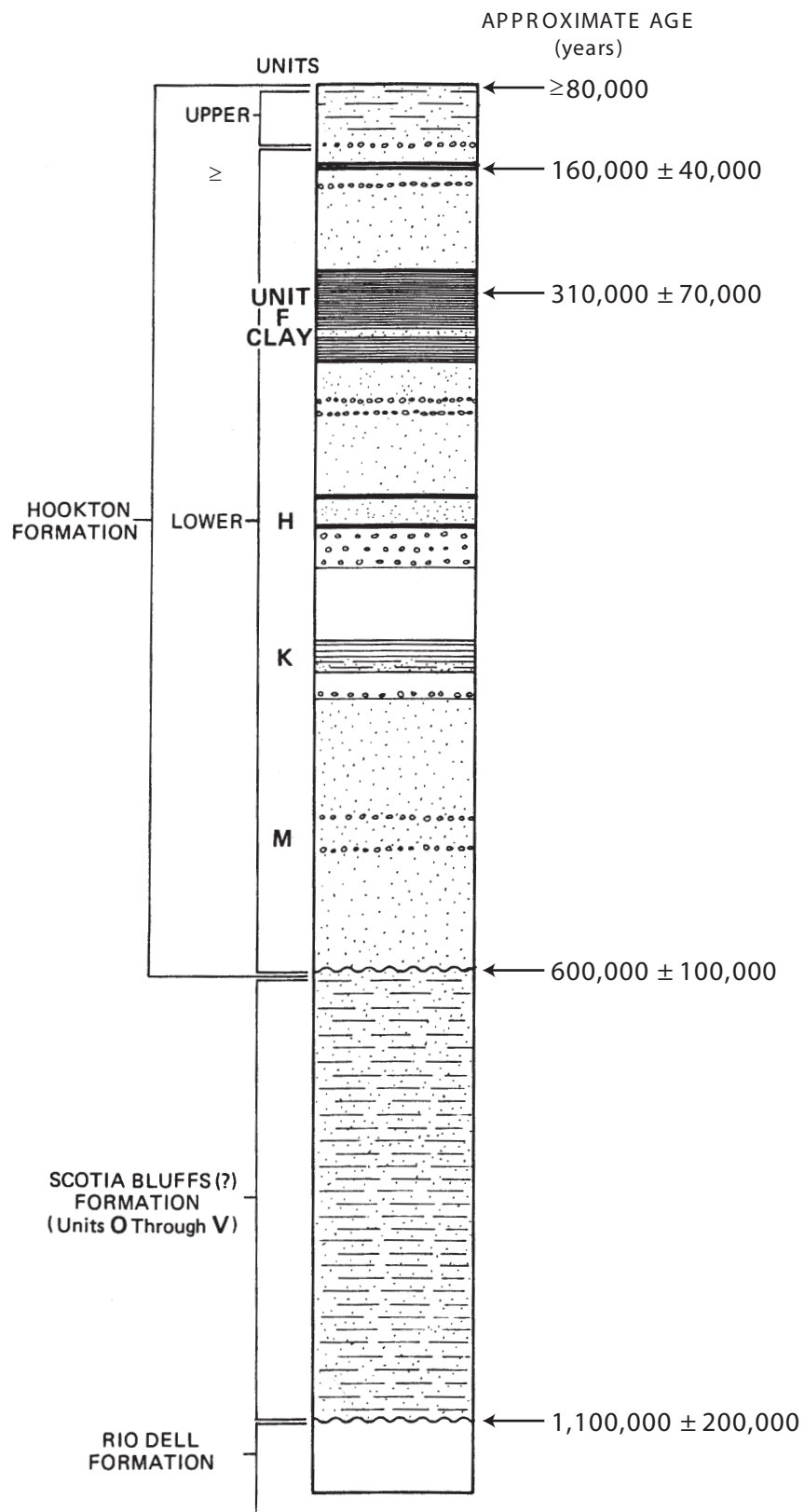
**FSAR UPDATE
HUMBOLDT BAY ISFSI
FIGURE 2.6-37**

View to east of Buhne Point terrace surface and ISFSI site. (Photographs JW-2-5 and JW-2-8 taken March 10, 2000.)



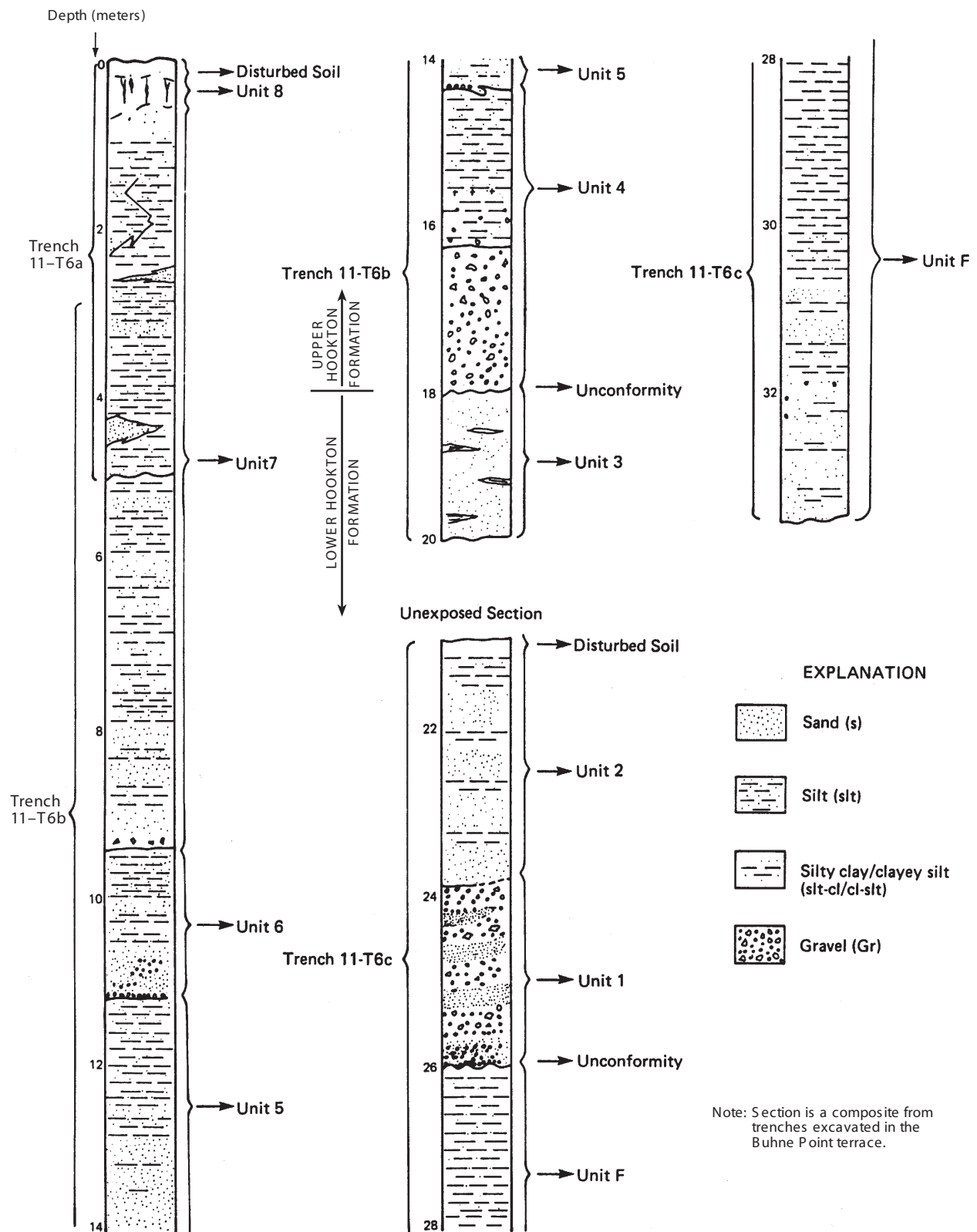
**FSAR UPDATE
HUMBOLDT BAY ISFSI
FIGURE 2.6-38**

Oblique aerial photographs showing disturbance of Buhne Point terrace during trenching activities by Earth Sciences Associates (circa 1975). (A) View to the west-southwest. (B) View to the east-southeast.



FSAR UPDATE
HUMBOLDT BAY ISFSI
FIGURE 2.6-39 GENERALIZED STRATIGRAPHIC SECTION AT THE ISFSI SITE

Revision 0 January 2006



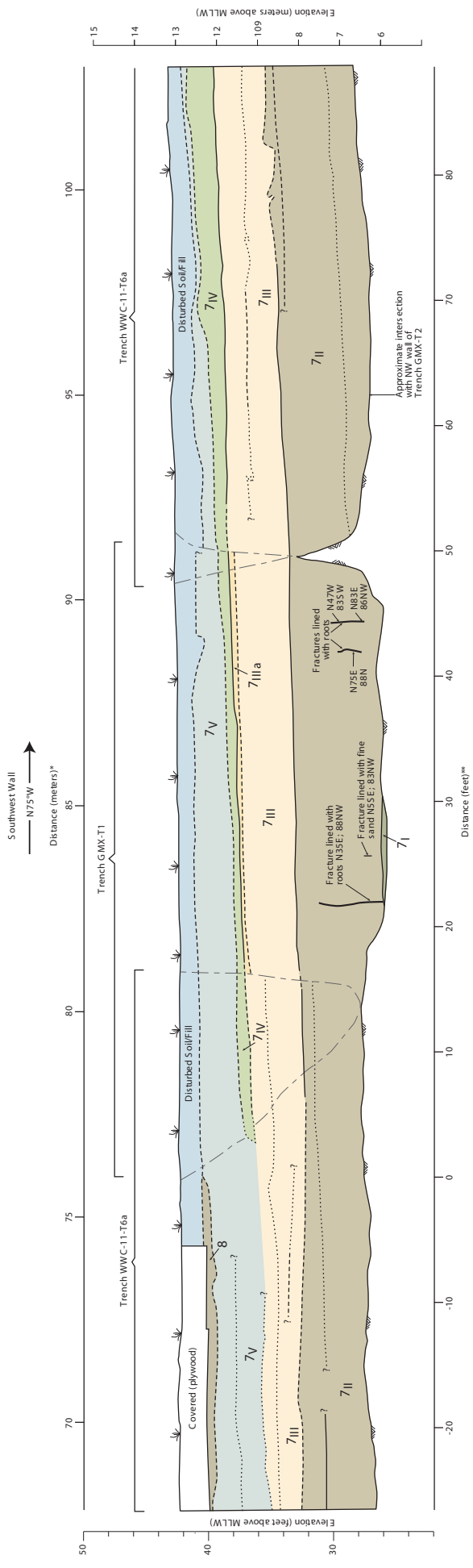
**FSAR UPDATE
HUMBOLDT BAY ISFSI
FIGURE 2.6-40**

Stratigraphic section of the uppermost lower Hookton and upper Hookton Formation exposed in Woodward-Clyde Consultants' trenches 11-T6a, 11-T6b, and 11-T6c (after Woodward-Clyde Consultants, 1980, Figure C-28).



**FSAR UPDATE
HUMBOLDT BAY ISFSI
FIGURE 2.6-41**

Outcrop of sand with interbedded silt (light layers) in sea cliff north of ISFSI site. Scale is in tenths of feet. View to the south-southeast. (Photograph JW-1-9 taken March 2, 2000.)



DESCRIPTION OF LITHOLOGIC UNITS

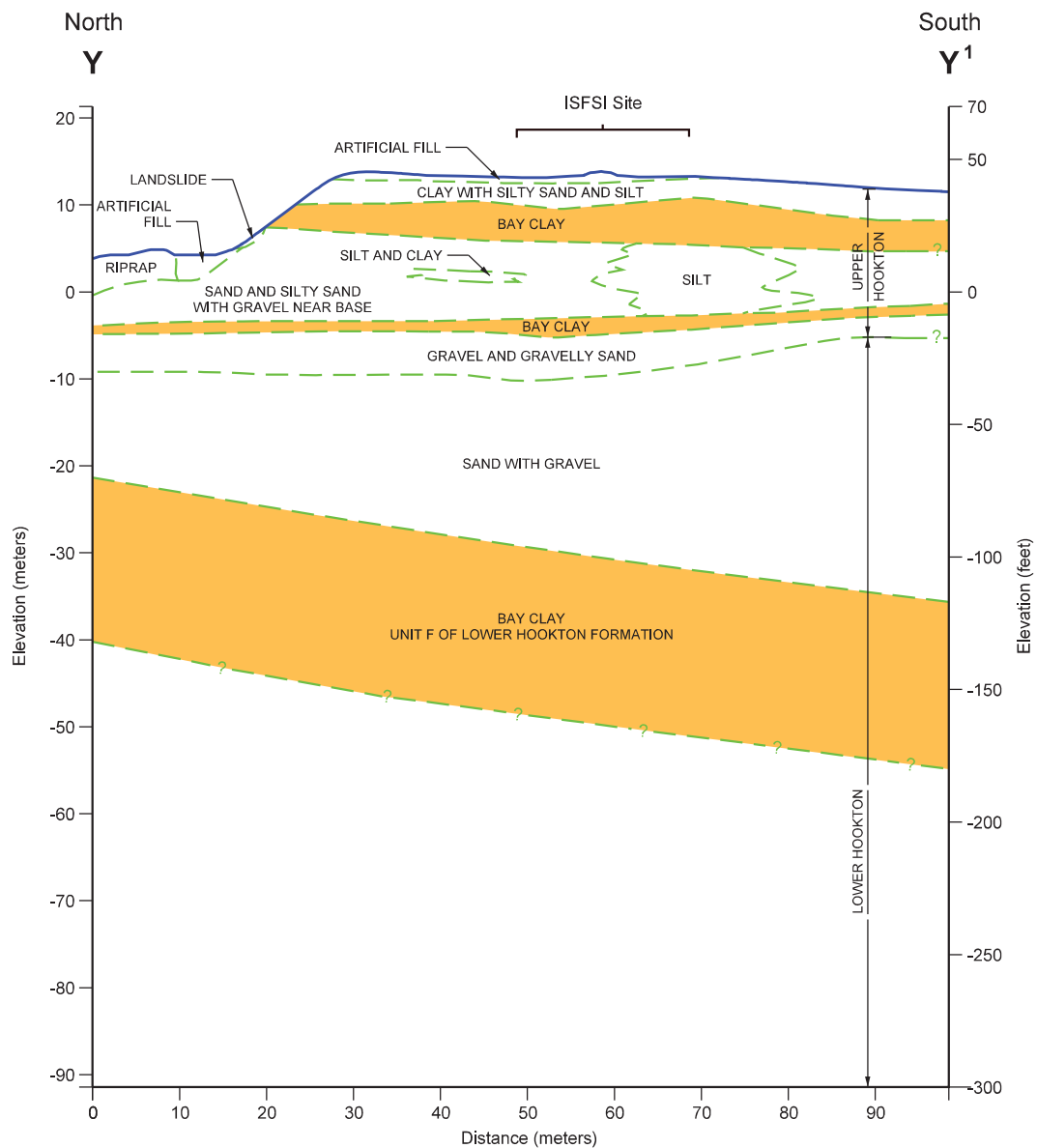
Upper Hookton Formation (Late Pleistocene)	
Unit 8:	Clayed silty and sandy clay; light gray to gray (10 YR 6/1 moist) and strong brown (7.5 YR 5/8 moist); some pebbles; moderately developed ped structure.
Unit 7:	Silty clay and clayey silt with some fine sand; strong brown (7.5 YR 5/8 dry) with pinkish white (7.5 YR 8/2 dry) coatings along columnar and blocky ped faces; sand content increases with depth; clay poorly staified to massive; strongly oxidized; locally contains manganese-oxide nodules.
7v	Moderately sorted fine sand with silt and some clay; mottled very pale brown (10 YR 7/3 dry) and reddish yellow (7.5 YR 6/8 dry) with light gray (5 Y 7/1) to gray (5 Y 6/1) coatings along ped faces; predominantly subrounded to subangular quartz sand; locally contains silty sand and silty clay; locally contains fine gravel along the basal contact; locally contains woody material.
7iv	Silt interbedded with some fine sand and clayey silt; dark gray; massive to weakly staified layers of sandy silt and clayey silt with some lenses of fine sand and silty clay; bedding is discontinuous laterally.
7iia	Silty clay; dark gray; generally massive.
7iii	
7ii	
7i	

EXPLANATION

- Lithologic contact solid line where resolution is less than 2 cm, dashed line where 2 to 5 cm; dotted line where 5 to 15 cm.
- Fracture

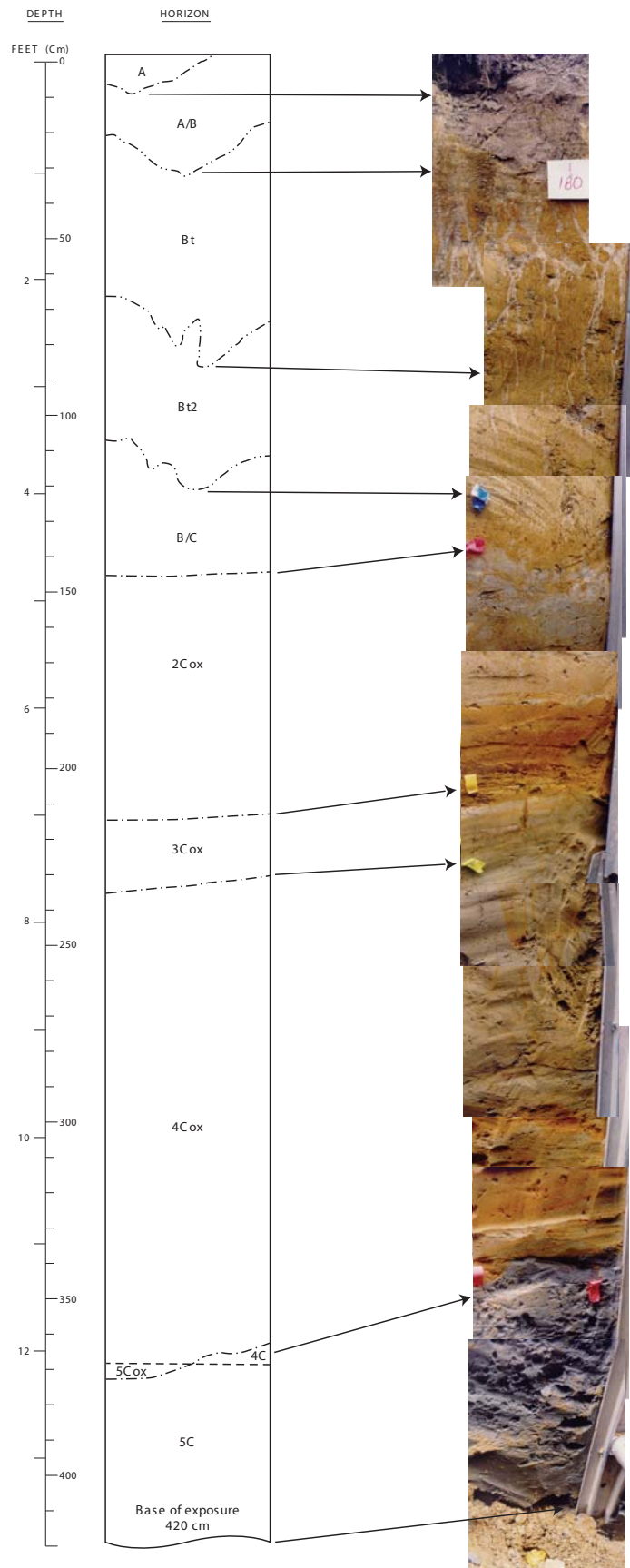
NOTES:

- *Values correspond to station numbers on original log of Trench 11-T6a (Woodward Clyde Consultants, 1980, Figure C-23, Reference 1).
- **Values correspond to station numbers on Trench GMX-T1. See Figure 2.6-31 for locations of trenches and ISFSI site.



— ? Lithologic contact, dashed where approximate, queried where inferred.

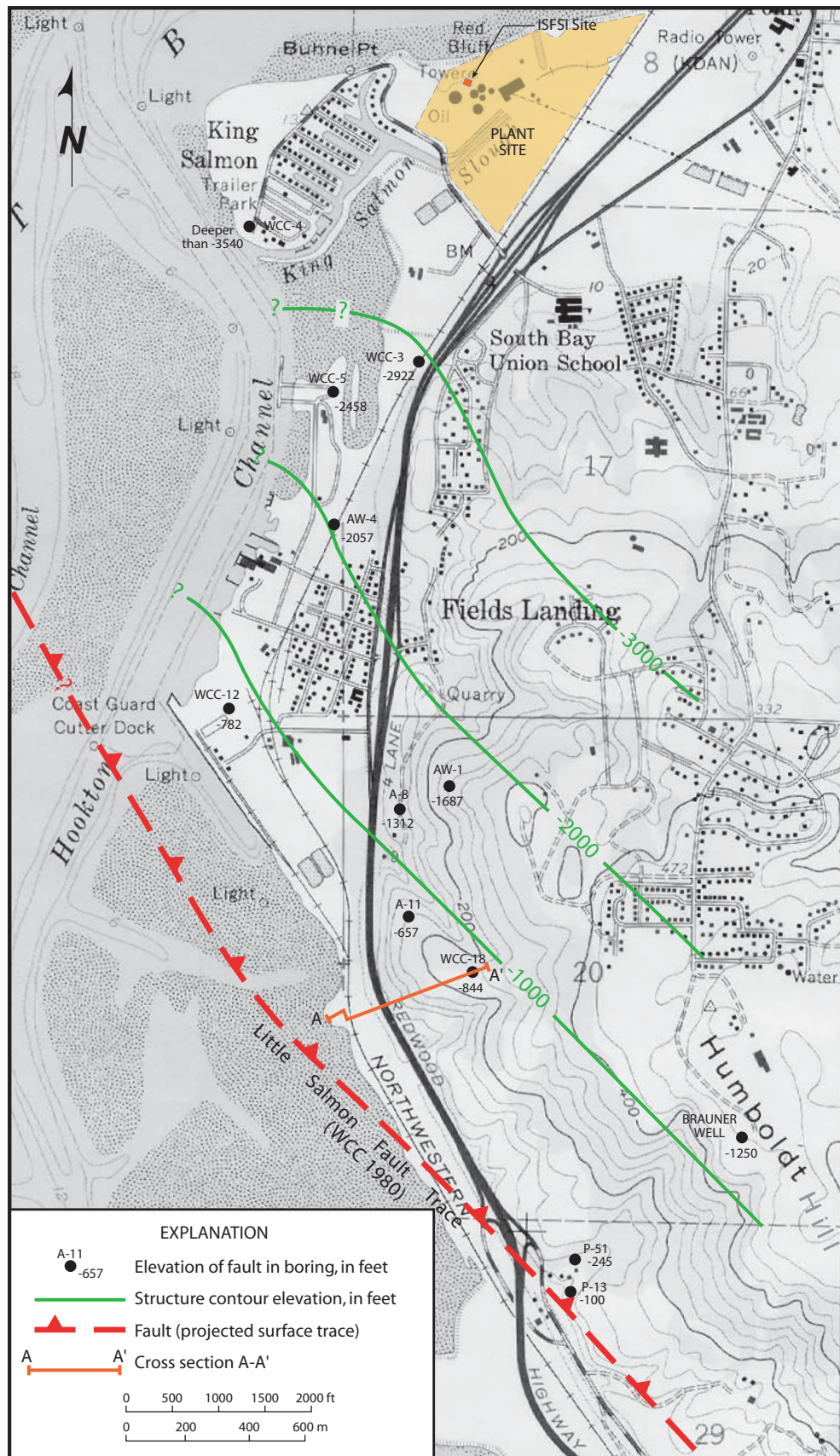
Note: Unit F location based on contour map (Figure 2.6-51).
 Stratigraphy above Unit F based on correlation of boreholes
 (GMX99-2 through -5) and trenches, and outcrop exposure in
 bluff.



See Table 2.6-6 for description of soil horizons.
(Photographs FHS00/8-2#3 through FHS00/8-2#12
taken on August 1, 2000).

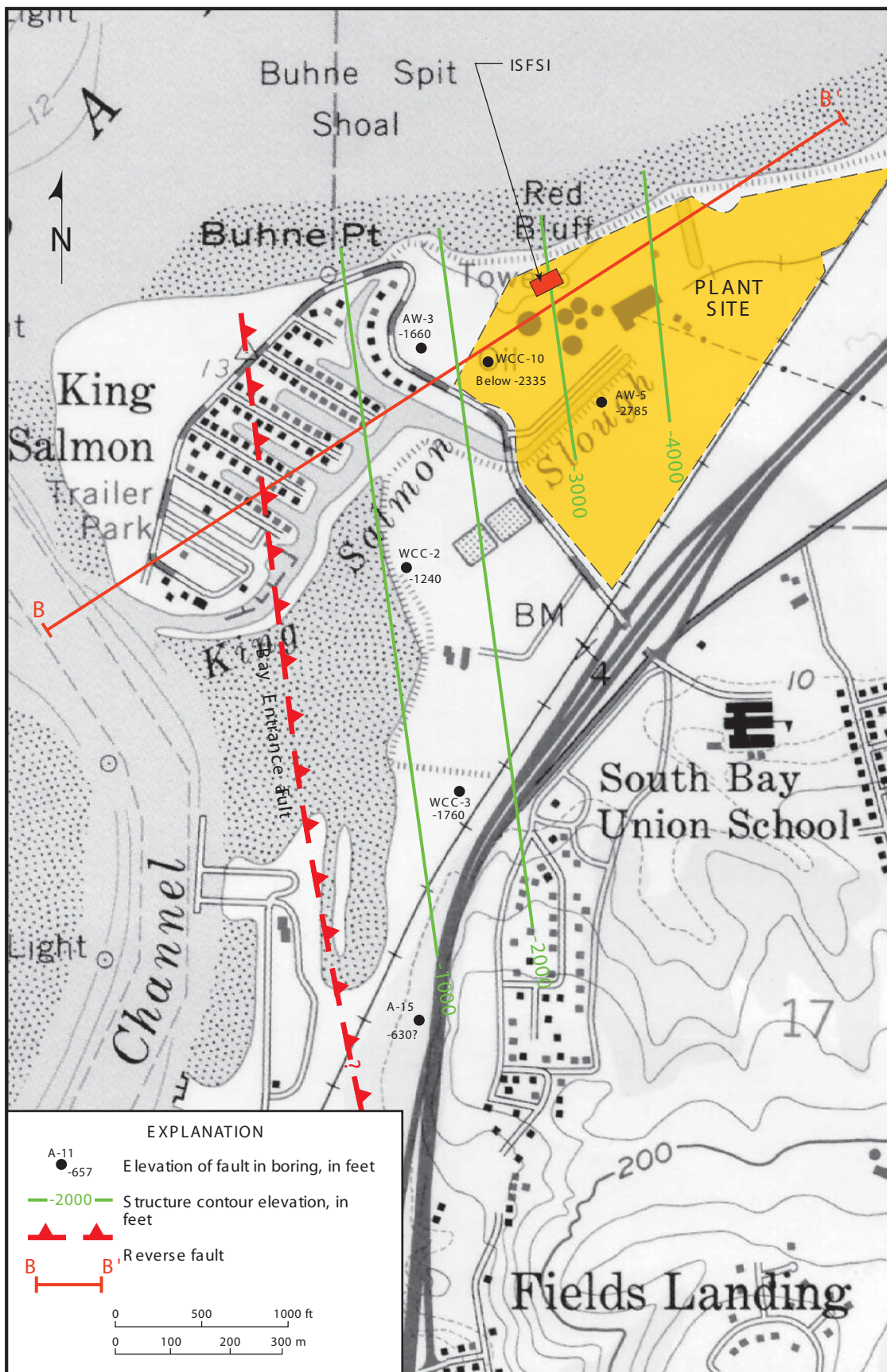
FSAR UPDATE
HUMBOLDT BAY ISFSI
FIGURE 2.6-45
RELICT SOIL AND UPPER HOOKTON
FORMATION DEPOSITS EXPOSED IN
TRENCH GMX-72
(NW WALL AT STATION 180 FT)

Revision 0 January 2006



**FSAR UPDATE
HUMBOLDT BAY ISFSI
FIGURE 2.6-46**

Structure contour map of the Little Salmon fault north of Humboldt Hill (after Woodward-Clyde Consultants, 1980, Figure C-14). Cross section A-A' shown on Figure 2.6-49.



Cross section B-B' is shown on Figure 2.6-50.
(modified from Woodward-Clyde Consultants,
1980, Figure C-18).

FSAR UPDATE

HUMBOLDT BAY ISFSI

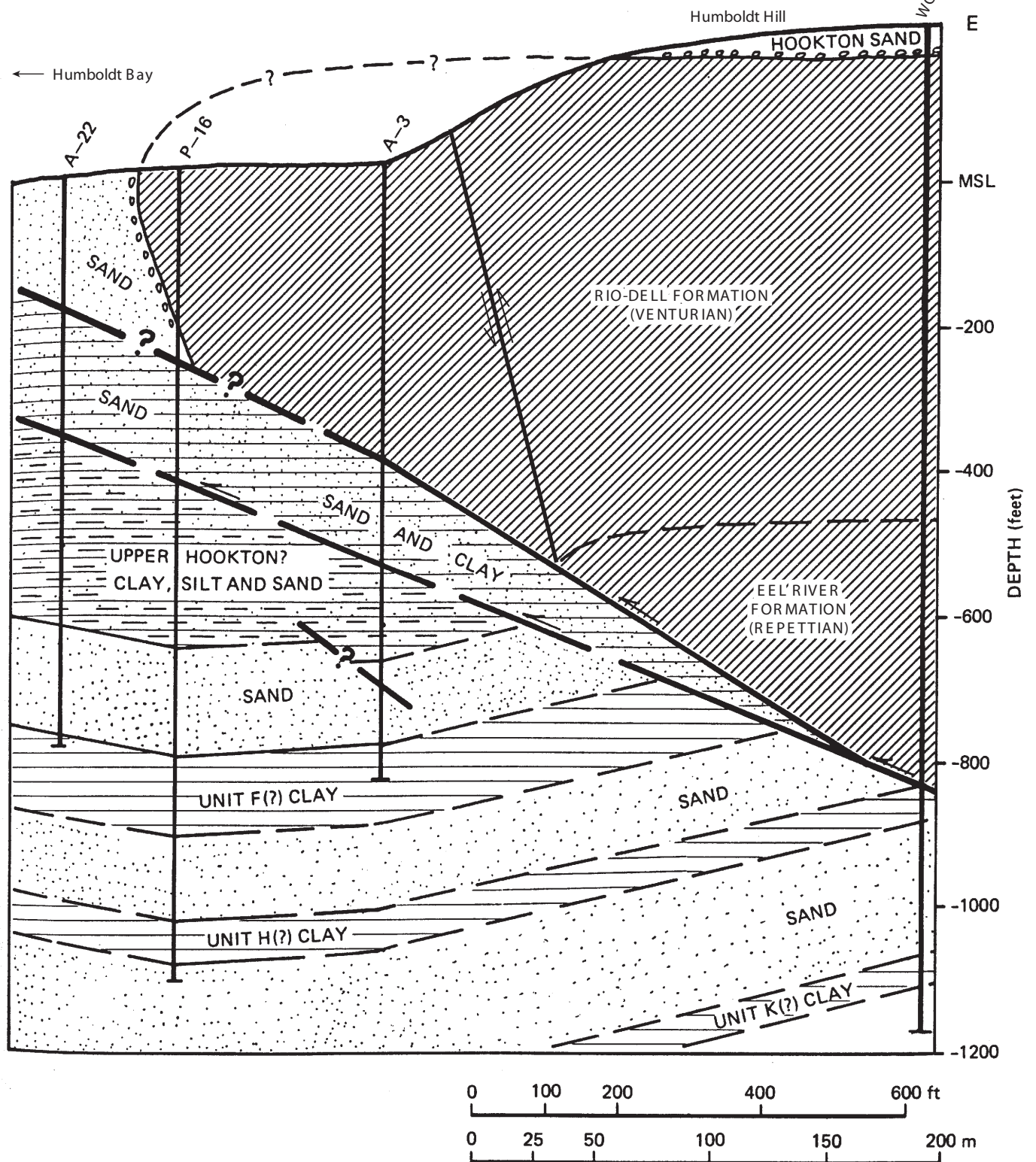
FIGURE 2.6-47 STRUCTURE CONTOUR MAP OF THE BAY ENTRANCE FAULT



FSAR UPDATE
HUMBOLDT BAY ISFSI
FIGURE 2.6-48
 Structure contour map of the Buhne Point fault (reinterpreted of data presented on Woodward-Clyde Consultants, 1980, Figure C-25). Cross section B-B' is shown on Figure 2.6-50.

A

A'

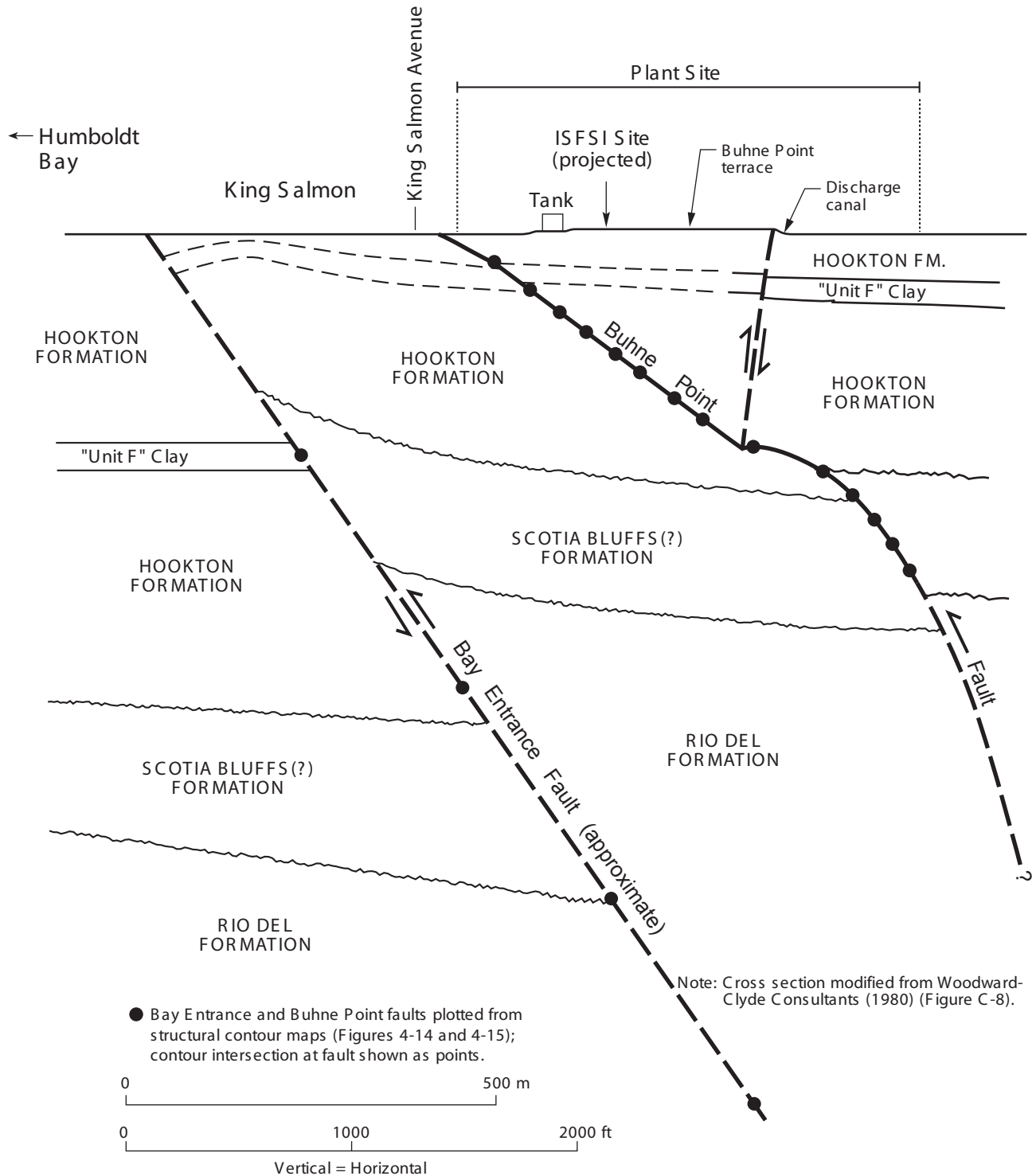


**FSAR UPDATE
HUMBOLDT BAY ISFSI
FIGURE 2.6-49**

~Cross section A-A' across the Little Salmon fault zone at Humboldt Hill (modified from Woodward-Clyde Consultants, 1980, Figure C-15). Location of cross section A-A' is shown on Figures 2.6-30 and 2.6-46.

B

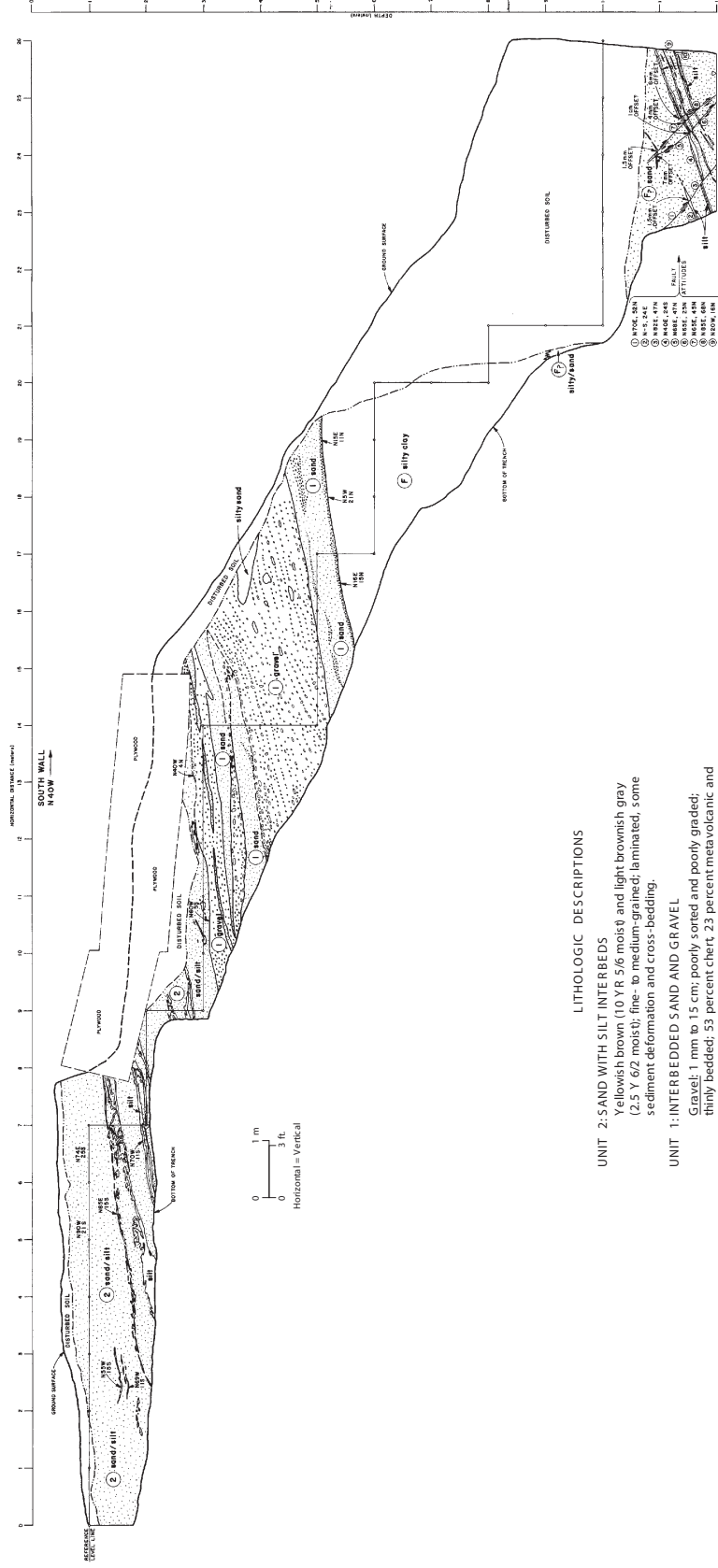
B'



**FSAR UPDATE
HUMBOLDT BAY ISFSI'
FIGURE 2.6-50**

~Cross section B-B' across the Bay Entrance and Buhne Point faults. Location of cross section is shown on Figures 2.6-30 and 2.6-47.





LITHOLOGIC DESCRIPTIONS

UNIT 2: SAND WITH SILT INTERBEDS

Yellowish brown (10 YR 5/6 moist) and light brownish gray (2.5 Y 6/2 moist); fine- to medium-grained; laminated, some sediment deformation and cross-bedding.

UNIT 1: INTERBEDDED SAND AND GRAVEL

Gravel: 1 mm to 1.5 cm; poorly sorted and poorly graded; thinly bedded; 53 percent chert, 23 percent metavolcanic and metasedimentary rocks, 11 percent quartz, 11 percent graywacke sandstone, 2 percent clay balls.

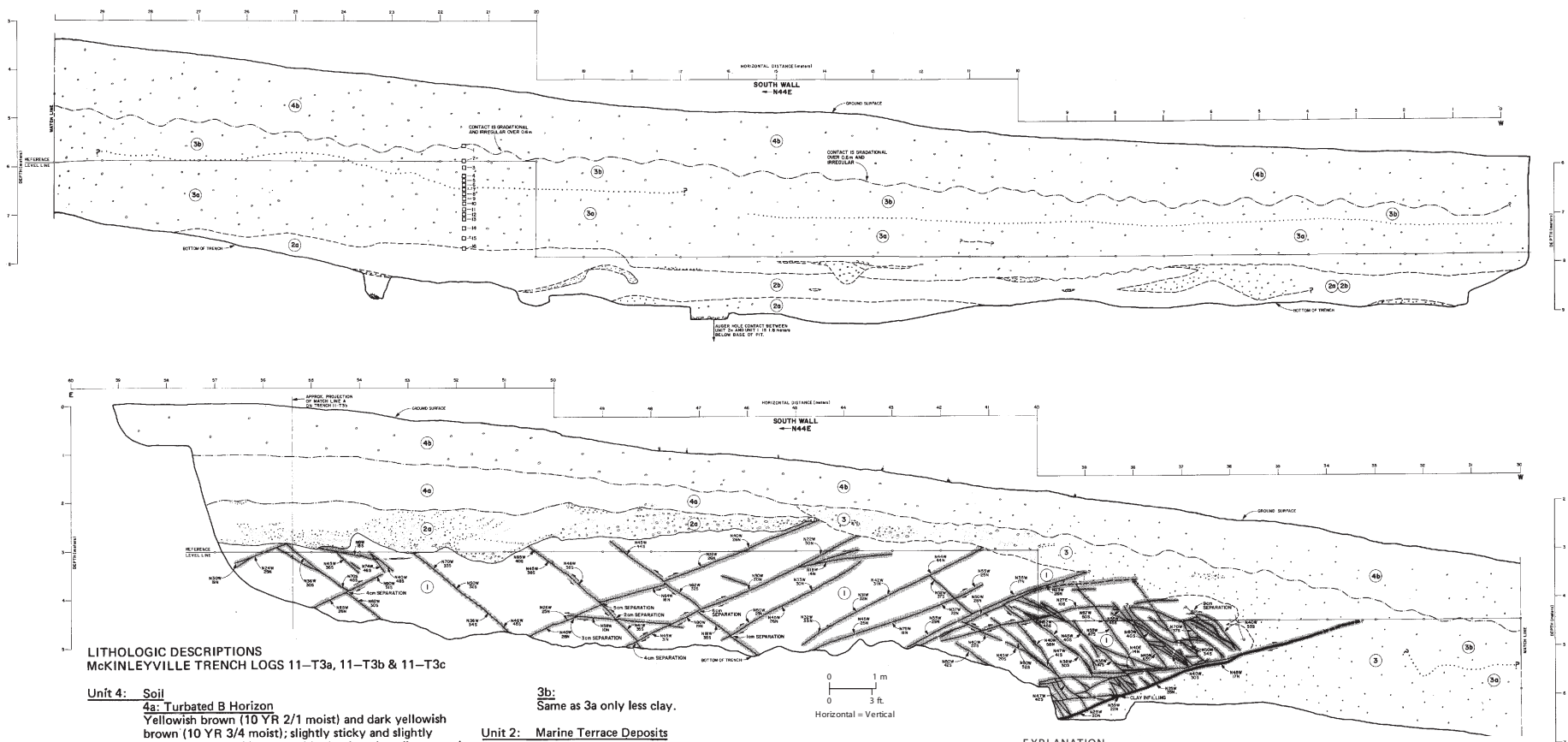
Sand: 5 strong brown (7.5 YR 4/6 moist); massive; medium-grained; subangular.

UNIT F: SILTY CLAY

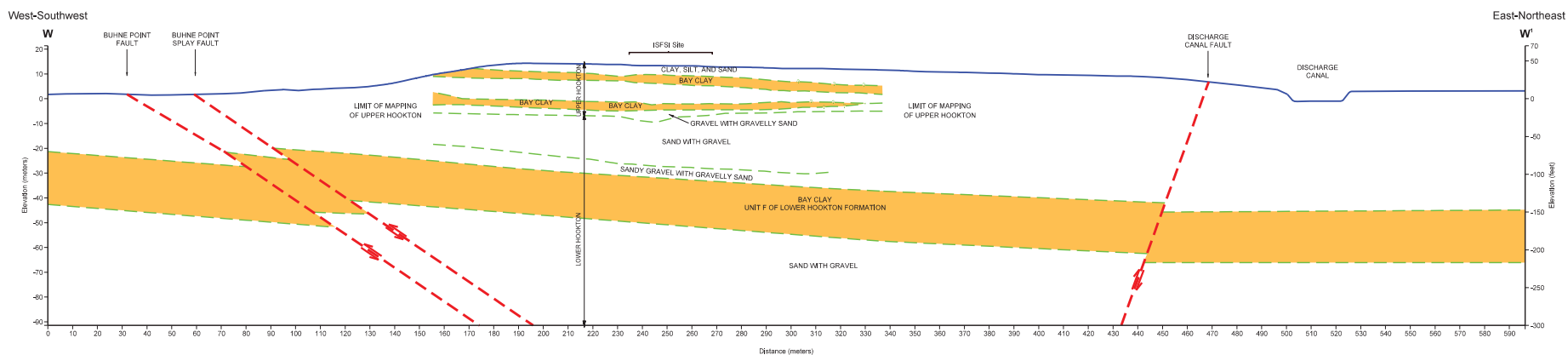
Very dark gray (10 YR 3/1 moist); slightly sticky and slightly plastic silty clay; rare shattered sea shells. Grades to interbedded and intermixed silt and sand. Unit fines upward. Interbedded and intermixed silt and sand is dark brown (7.5 YR 3/4 moist) and dark grayish brown (10 YR 4/2 moist). Sand is olive-brown (2.5 Y 4/4 moist); medium-grained; subrounded to subangular; contains some discontinuous, thin (2 mm to 4 cm) silt lenses.

FSAR UPDATE HUMBOLDT BAY ISFSI FIGURE 2.6-53

Log of trench 11-T6c showing small faults of the Buhne Point fault in the lower Hookton Formation (from Woodward-Clyde Consultants, 1980, Figure C-35). Location of trench is shown on Figure 2.6-31.



FSAR UPDATE
HUMBOLDT BAY ISFSI
FIGURE 2.6-54
McKINLEYVILLE TRENCH (FROM
WOODWARD-CLYDE CONSULTANTS,
1980, FIGURE B-19a). LOCATION OF
TRENCH SHOWN ON FIGURE 2.6-13.



- Fault, dashed where inferred, arrows show sense of displacement.
 Lithologic contact, dashed where approximate, queried where inferred.

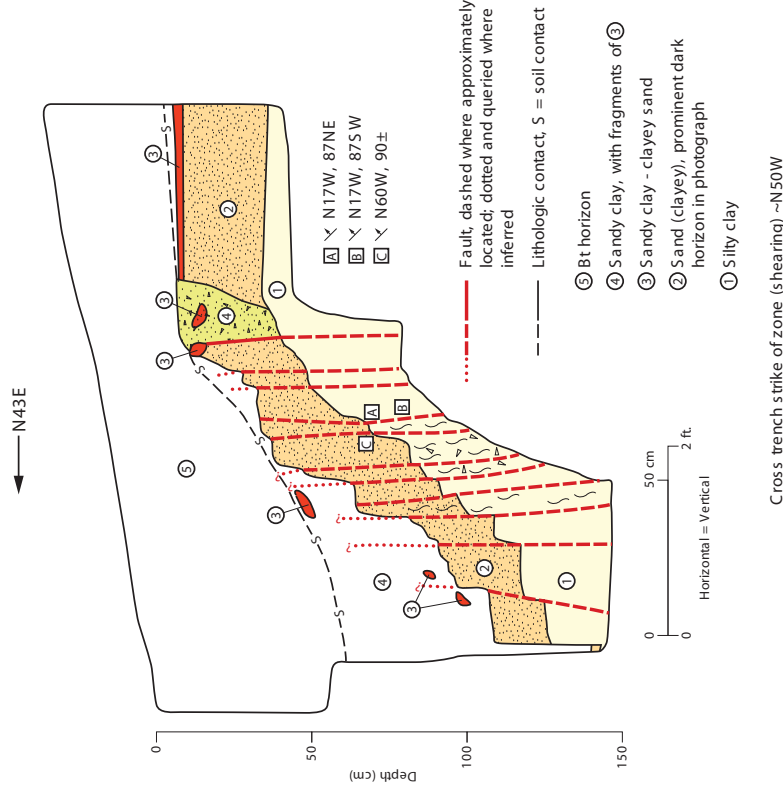
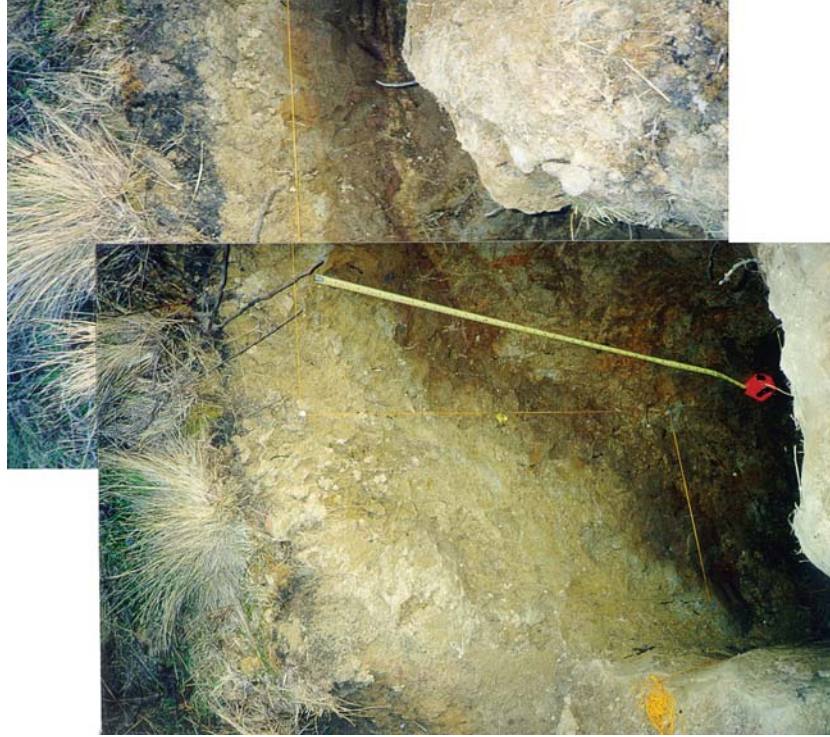
Note: Location of cross section is shown on Figure 2.6-31. Unit F location based on structure contour map (Figure 2.6-51). Stratigraphy above Unit F based on correlation of boreholes (ESA76-P2, GMX99-2, ESA76-6 through -8) and trenches. See Figure 2.6-31 for locations of boreholes.

FSAR UPDATE

HUMBOLDT BAY ISFSI

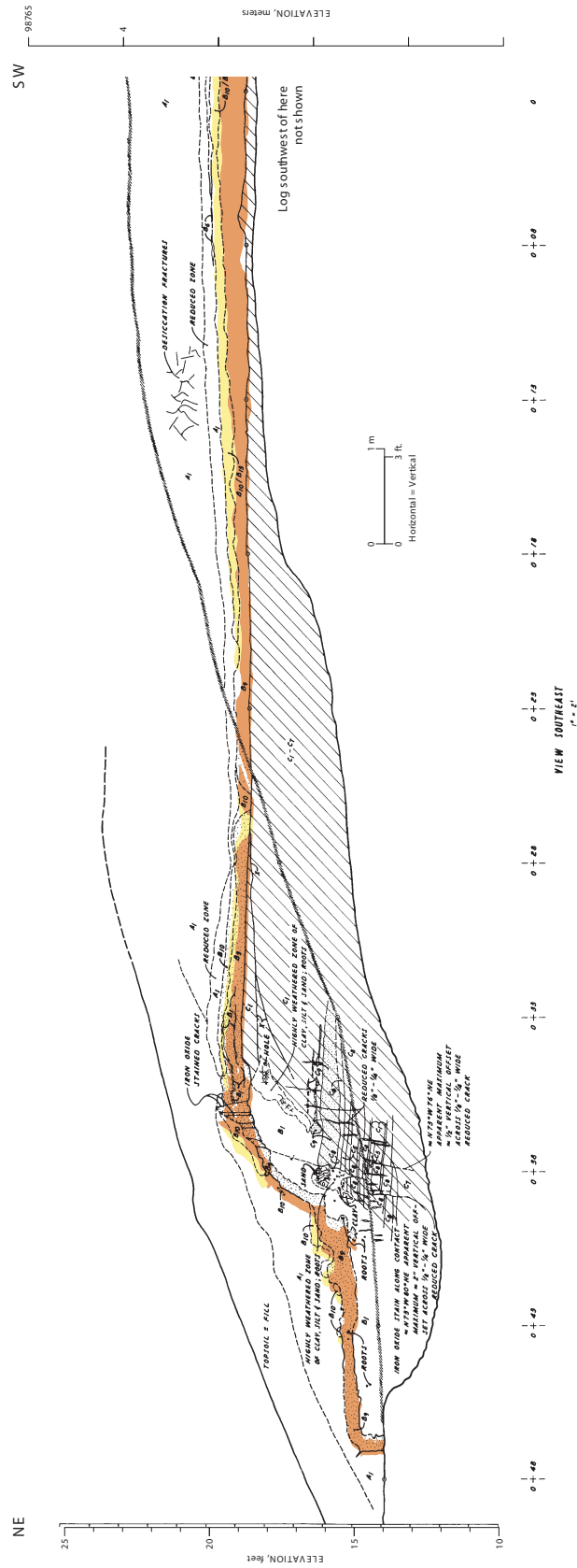
FIGURE 2.6-55
GEOLOGIC
CROSS SECTION W-W' ¹

Revision 0 January 2006



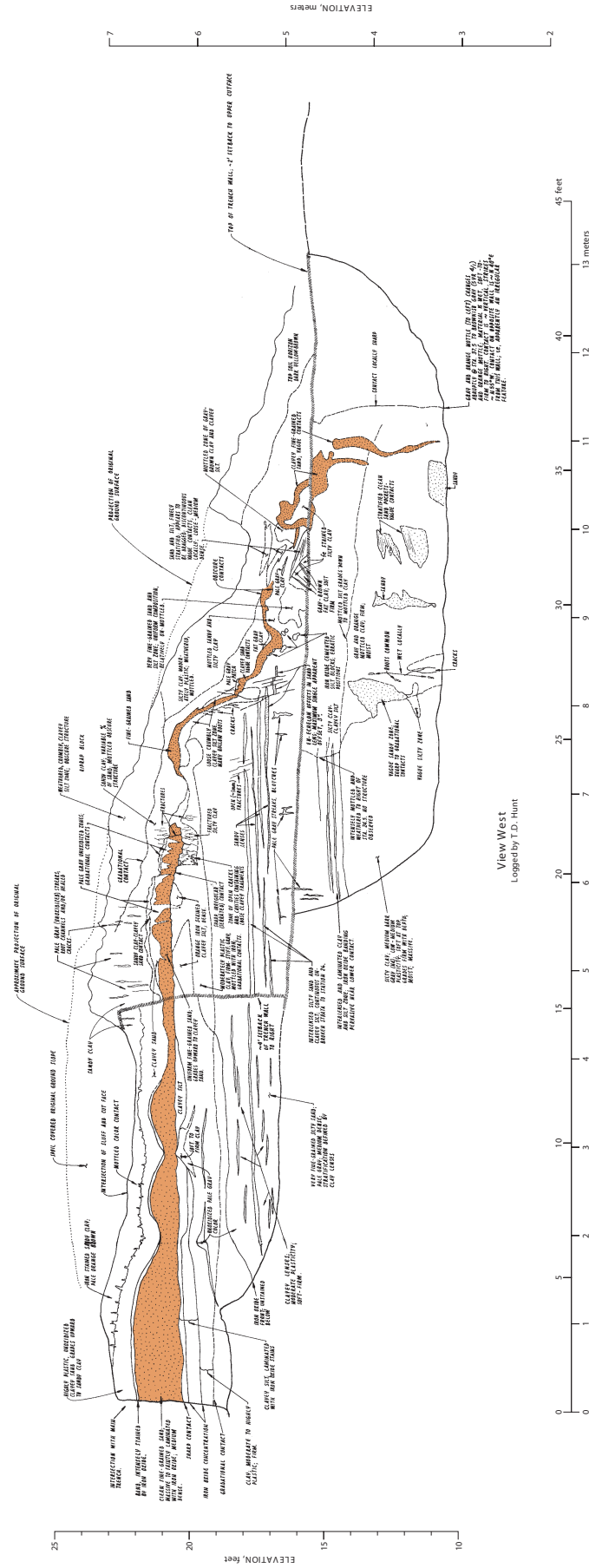
FSAR UPDATE
HUMBOLDT BAY ISFSI
FIGURE 2.6-56

Exposure of Discharge Canal fault in sea cliff west of Discharge Canal. The vertical string line in the middle of the photograph is 100 cm long. (Photographs JW-3-23 and 24; taken on March 21, 2000). Location of exposure is shown as outcrop JW-7 on Figure 2.6-31.



Log of northeastern part of trench BP-2 (from Earth Sciences Associates, 1977, Figure C37 [colors added for emphasis]). Station numbers are in feet. Location of trench is shown on Figure 2.6-31.

S spoil pile contacts not shown

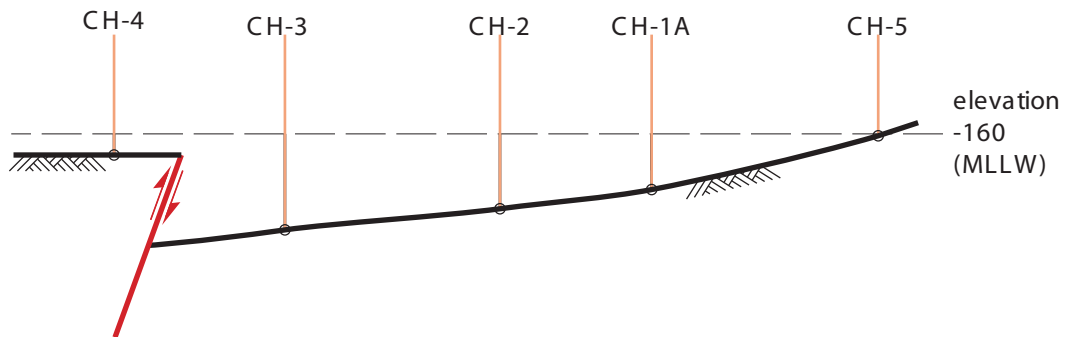


Log of trench BP-3 (from Earth Sciences Associates, 1977; Figure C37 [colors added for emphasis]). Station numbers are in feet. Location of trench is shown on Figure 2.6-31.

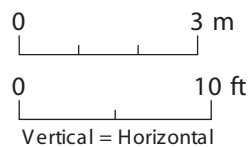
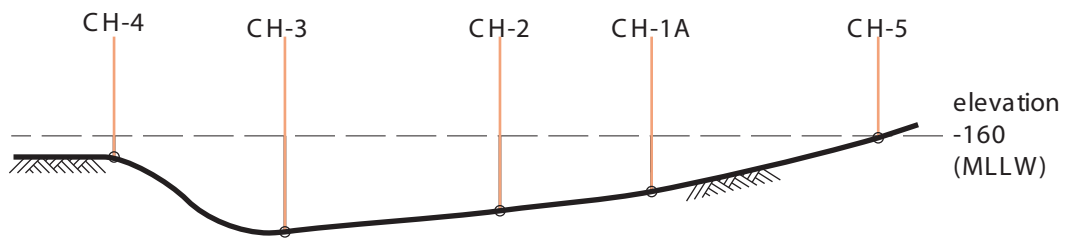
FSAR UPDATE
HUMBOLDT BAY ISFSI
FIGURE 2.6-58
LOG OF ESA (1977)
TRENCH BP-3

Revision 0 January 2006

(a) Fault



(b) Cut-and-Fill Channel



**FSAR UPDATE
HUMBOLDT BAY ISFSI
FIGURE 2.6-59**

~Alternative interpretations of the irregularities in the top of the Unit F clay between boreholes WCC80-CH4 and WCC80-CH5. Locations of boreholes shown on Figure 2.6-31.



**FSAR UPDATE
HUMBOLDT BY ISFSI
FIGURE 2.6-60**

Trench GMX-T1, view east-southeast. View along trench with Humboldt Bay Power Plant in the background. Part of trench GMX-T2 is in the foreground. (Photograph FHS-00/8-1 #29 taken August 1, 2000.)



FSAR UPDATE
HUMBOLDT BAY ISFSI
FIGURE 2.6-61 SURVEYING GEOLOGIC CONTACTS IN TRENCH GMX-T2. VIEW IS TOWARD THE SOUTH. (PHOTOGRAPH FHS-00/7-4 #9 TAKEN AUGUST 1, 2000.)

Revision 0 January 2006

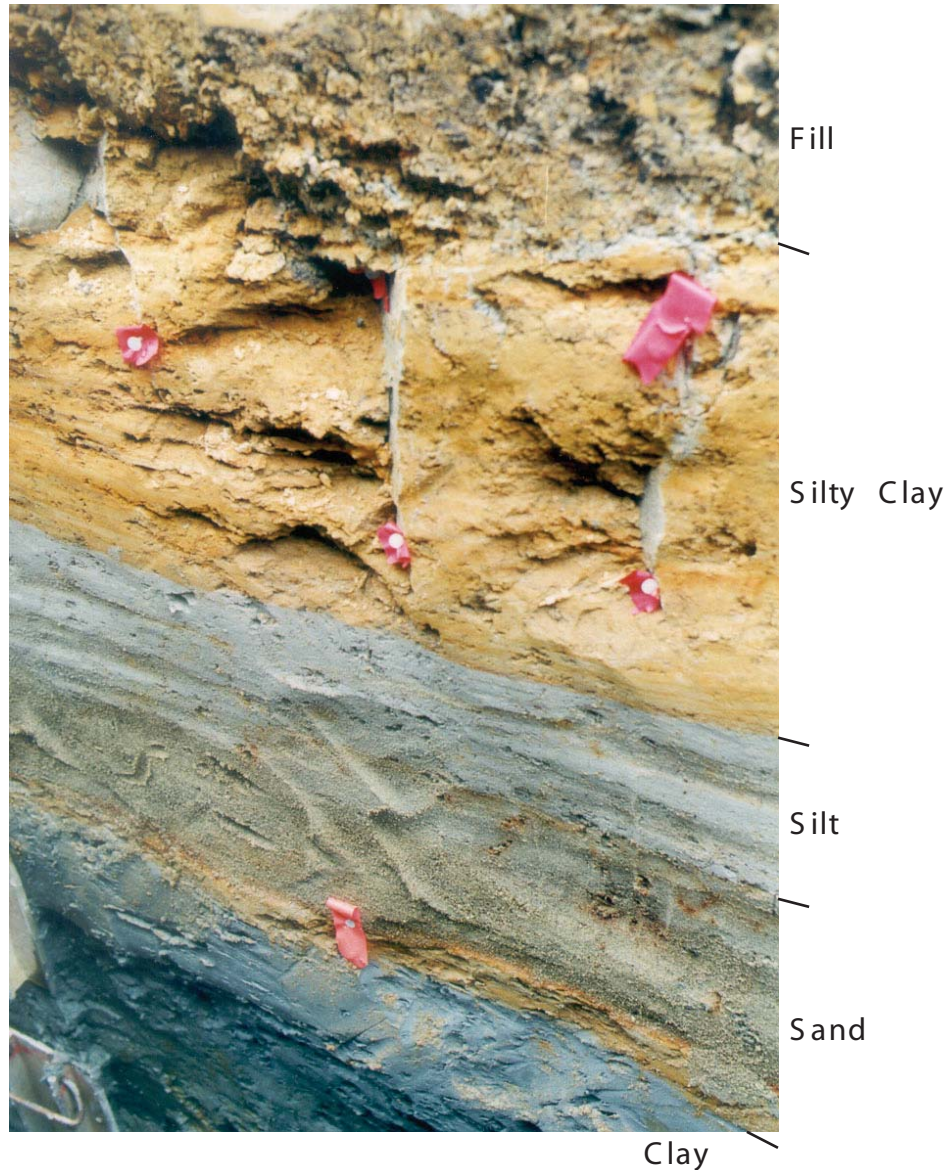


Fill

**SAFETY ANALYSIS REPORT
HUMBOLDT BAY ISFSI
FIGURE 2.6-62**

Artificial fill overlying sand and silt layers of the upper Hookton Formation in northwest wall of trench GMX-T2 between station 36 ft. and station 44 ft. (Photograph FHS-00/7-4 #19 taken August 1, 2000.)

Revision 0 January 2006



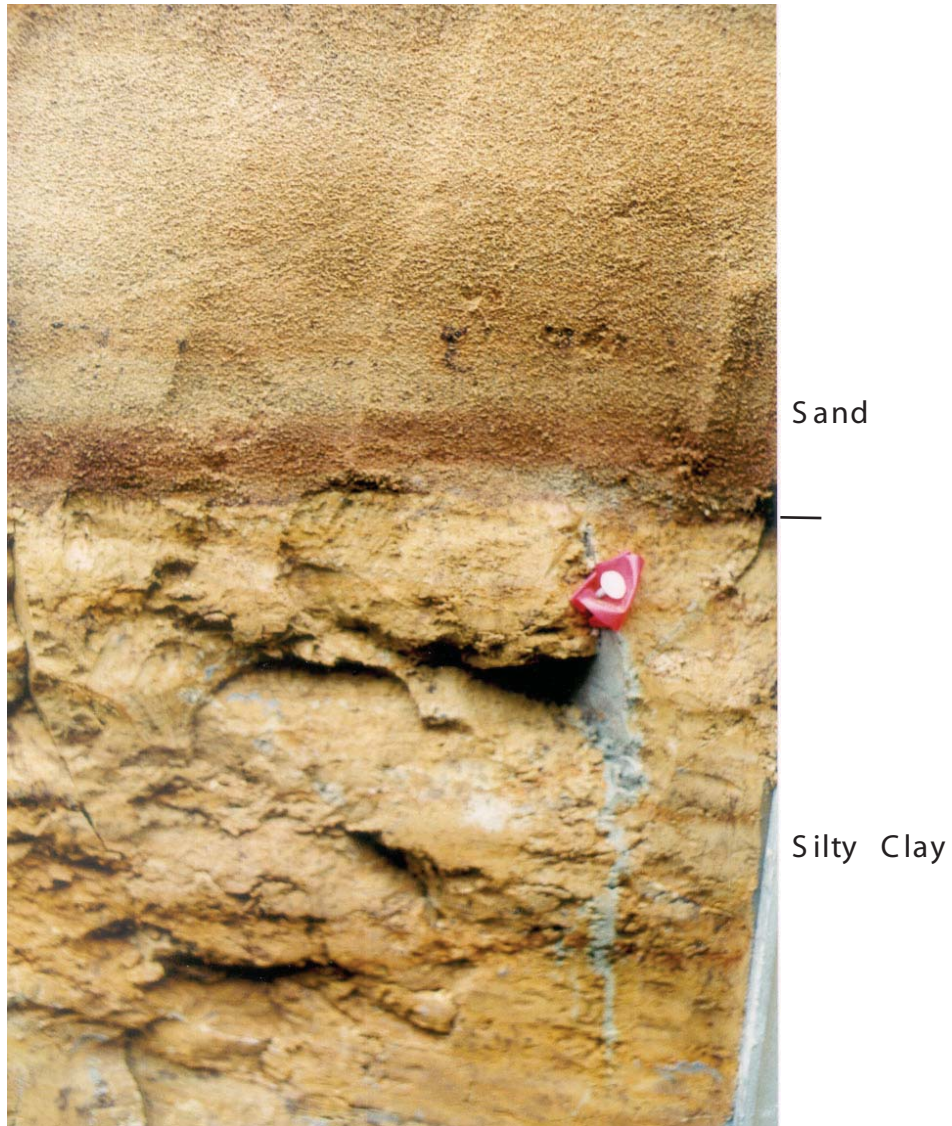
**FSAR UPDATE
HUMBOLDT BAY ISFSI
FIGURE 2.6-63**

Clay fractures in upper Hookton Formation in trench GMX-T2. Fractures are at station ~25 ft., depth ~5 ft. Note continuous bedding across fractures below where they have been bleached in the weathered silty clay. (Photograph FHS-00/8-3 #32 taken August 3, 2000.)



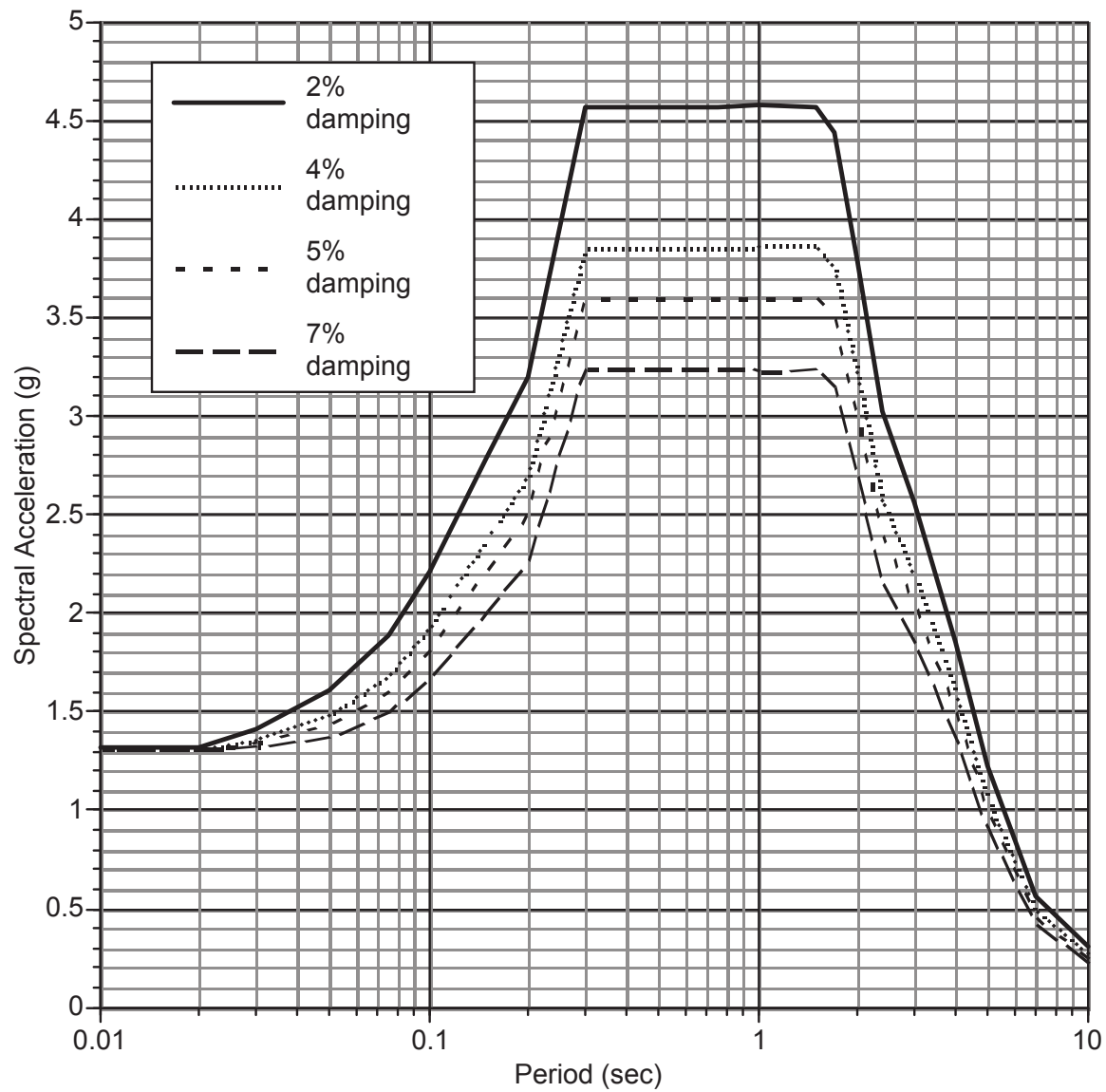
**FSAR UPDATE
HUMBOLDT BAY ISFSI
FIGURE 2.6-64**

Fracture lined with black compressed rootlets in clayey-silt bed in trench GMX-T2. Fracture is at station 40 ft., depth ~11 ft. (Photograph FHS-00/7-3 #21 taken August 3, 2000.)



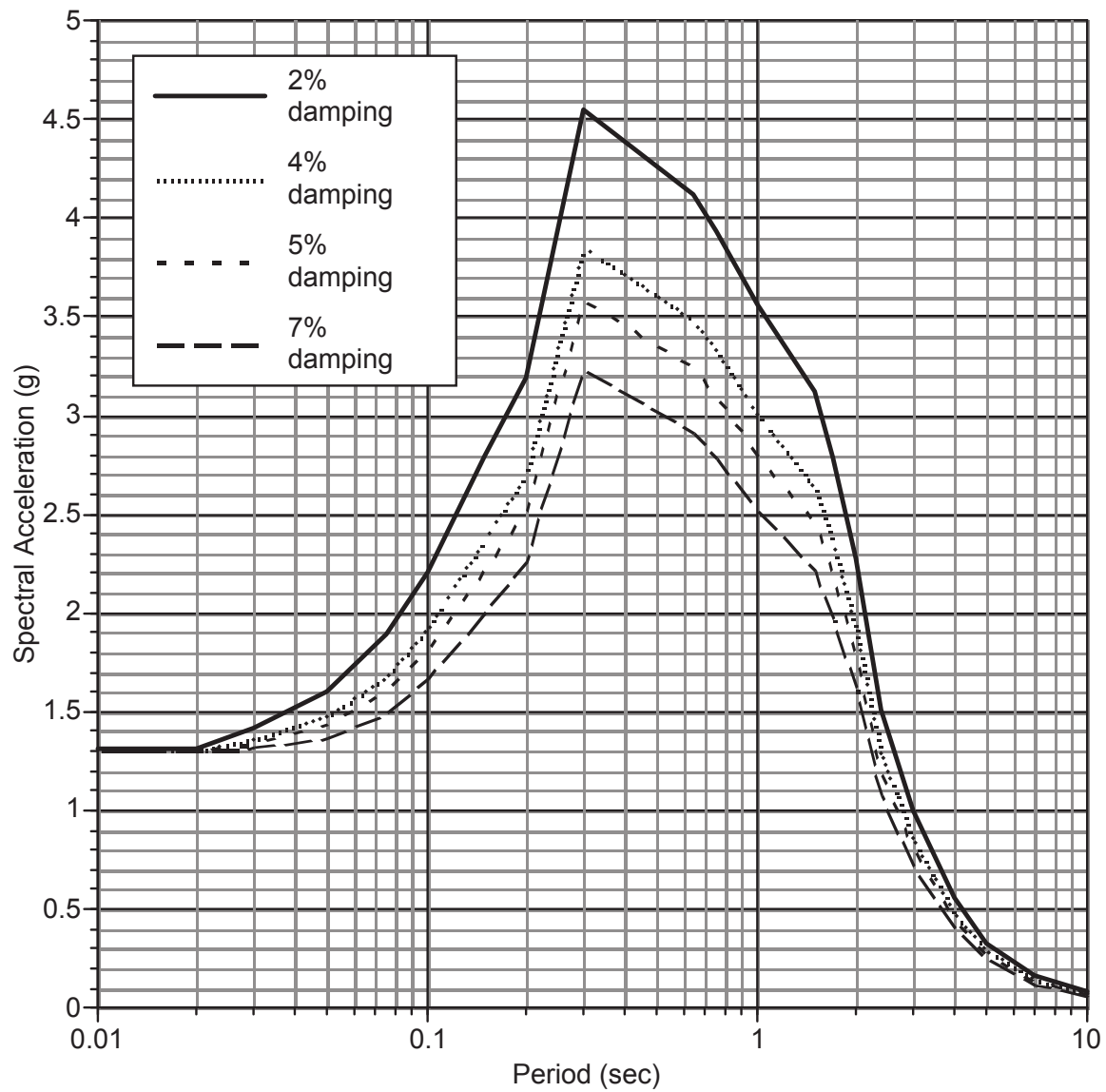
**FSAR UPDATE
HUMBOLDT BAY ISFSI
FIGURE 2.6-65**

**Continuous bedding across bleached fracture in silty clay in trench
GMX-T2. Fractures are at station 30 ft., depth ~4 ft. (Photograph
FHS-00/8-3 #26 taken August 3, 2000.)**



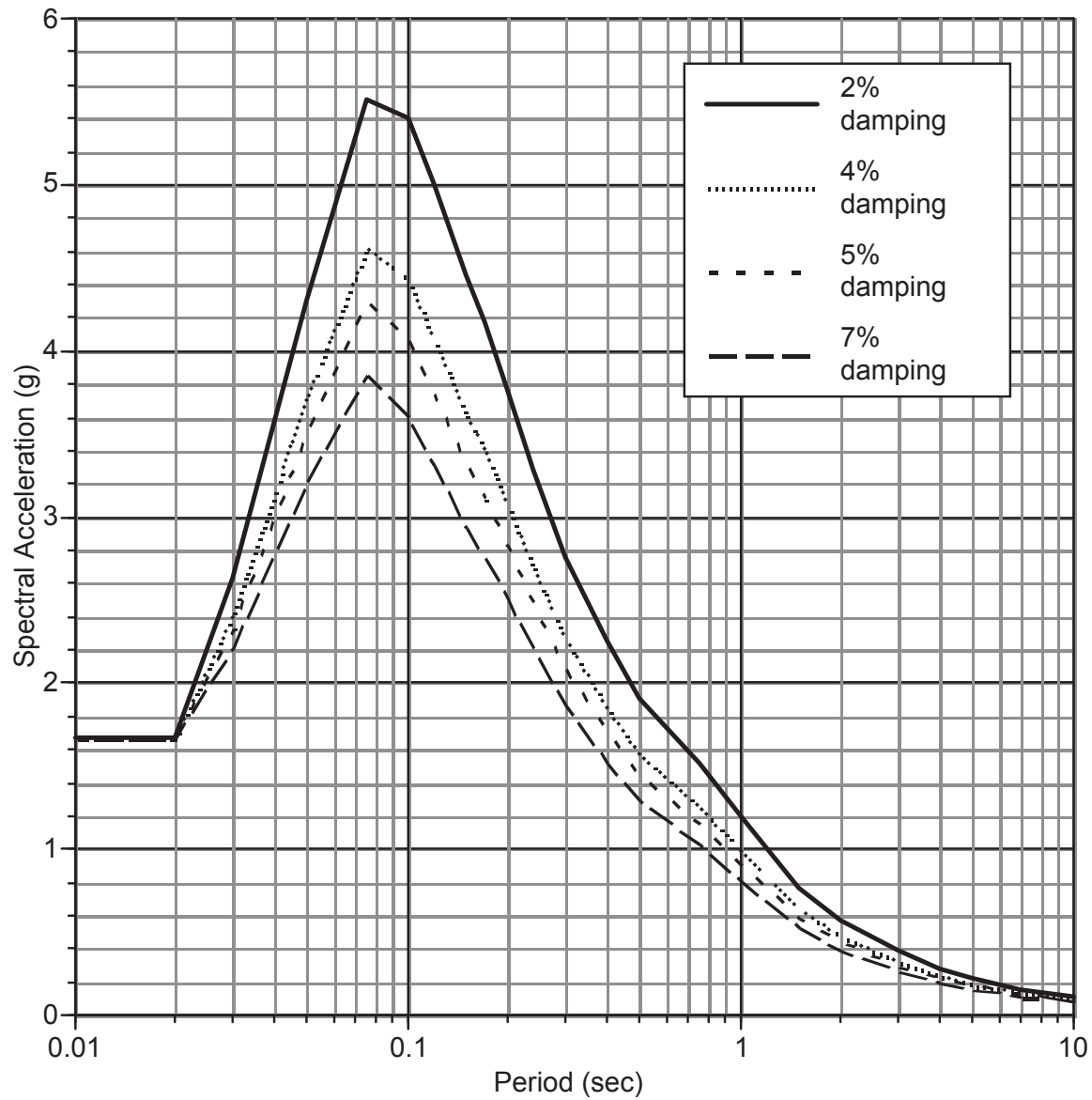
FSAR UPDATE
HUMBOLDT BAY ISFSI
FIGURE 2.6-66 FAULT NORMAL DESIGN SPECTRUM FOR DAMPING VALUES OF 2%, 4%, 5%, AND 7%

Revision 0 January 2006



FSAR UPDATE
HUMBOLDT BAY ISFSI
FIGURE 2.6-67 FAULT PARALLEL DESIGN SPECTRUM FOR DAMPING VALUES OF 2%, 4%, 5%, AND 7%

Revision 0 January 2006

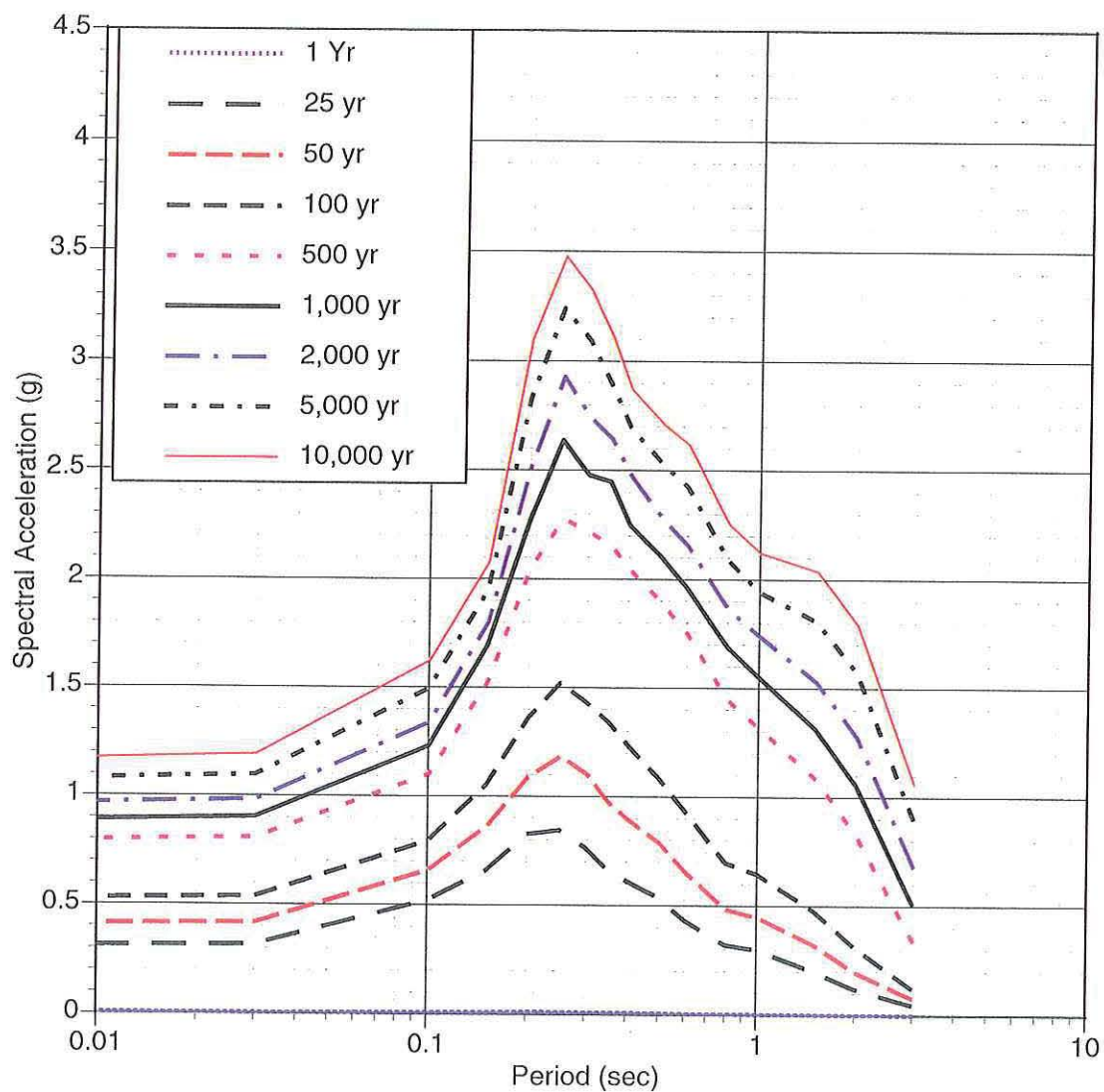


FSAR UPDATE

HUMBOLDT BAY ISFSI

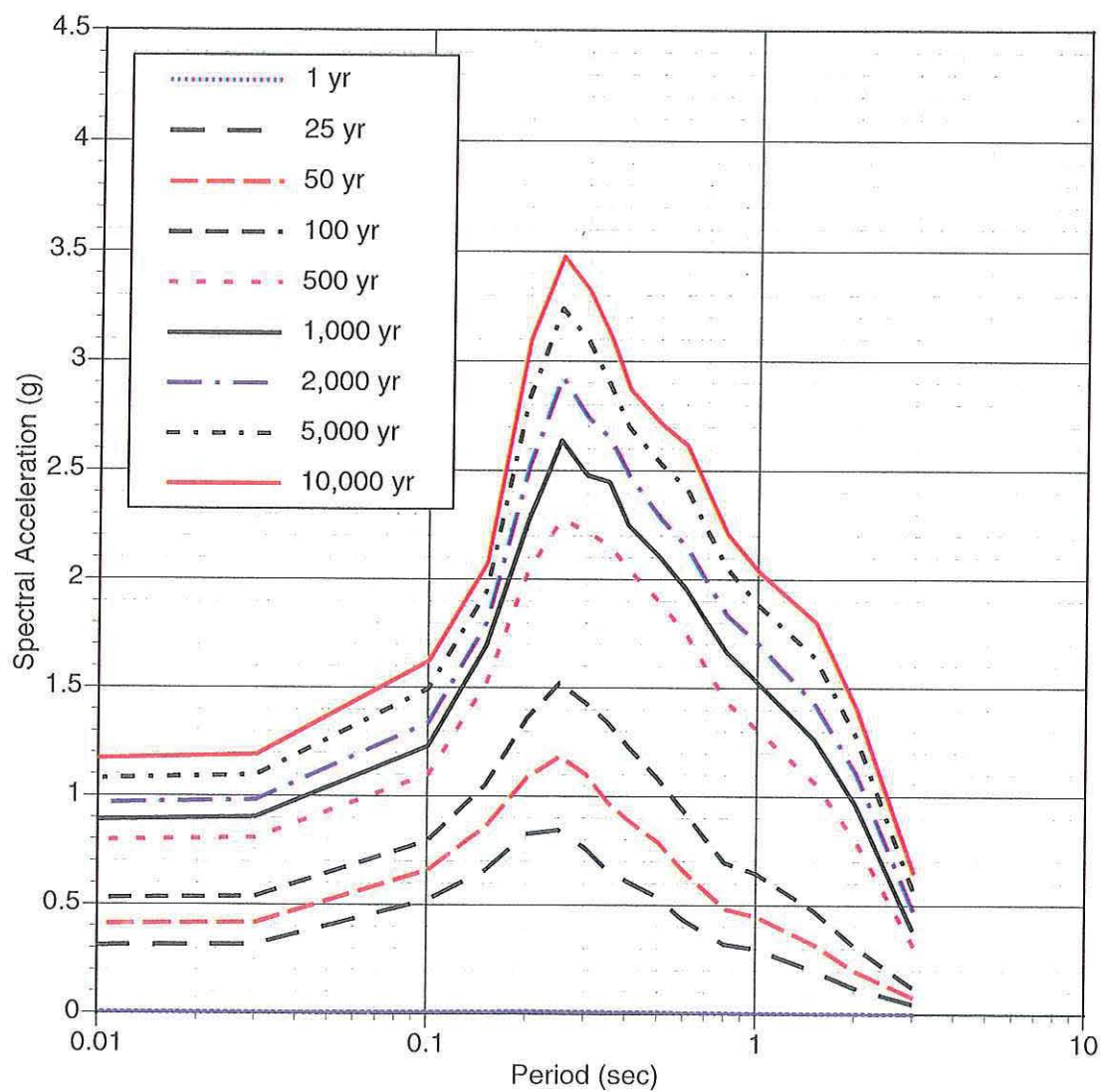
**FIGURE 2.6-68
VERTICAL SPECTRUM FOR
DAMPING VALUES OF
2%, 4%, 5%, AND 7%**

Revision 0 January 2006



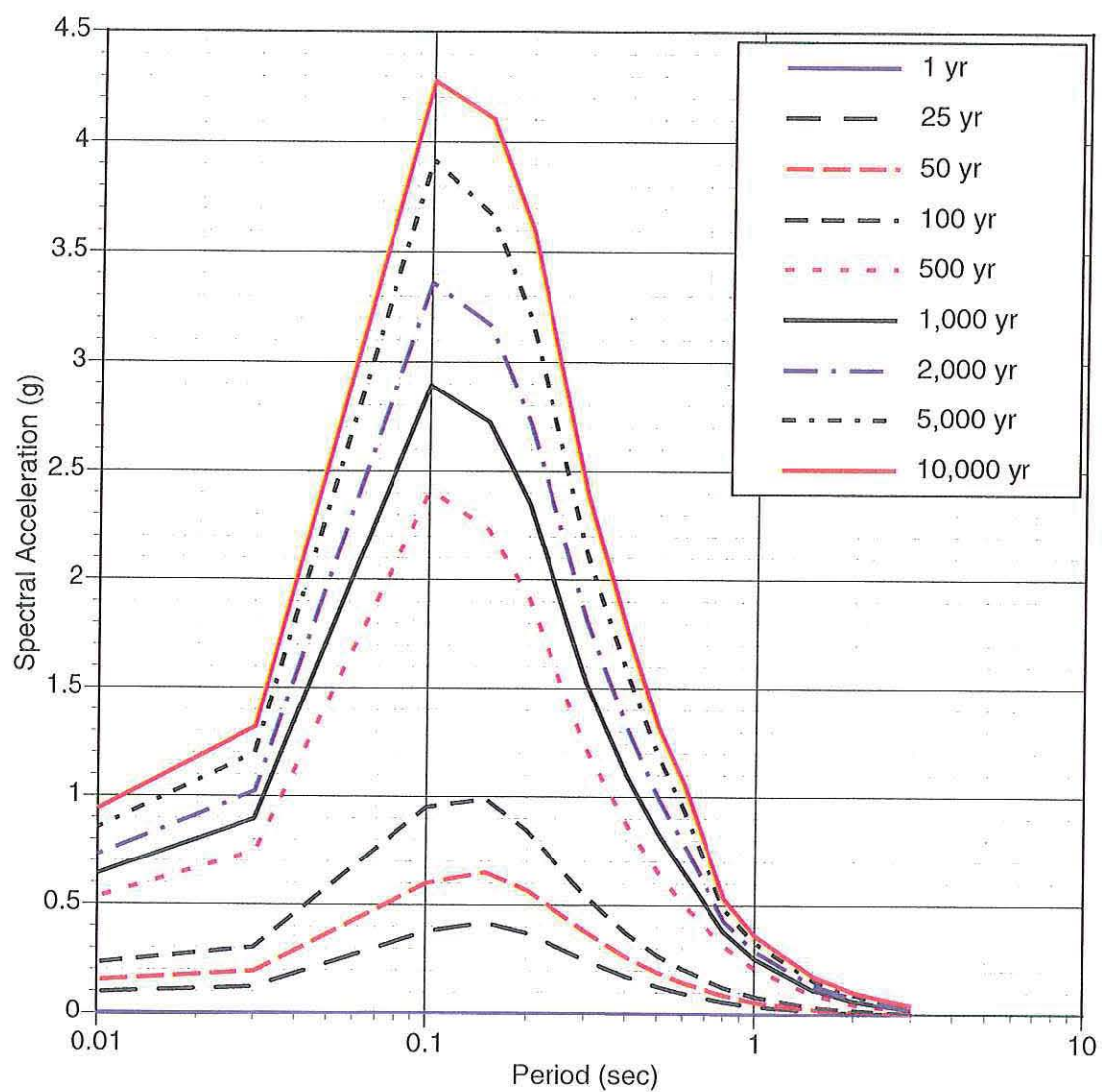
FSAR UPDATE
HUMBOLDT BAY ISFSI
FIGURE 2.6-69 EQUAL HAZARD SPECTRA FOR THE FN COMPONENT, SOIL SITE CONDITIONS

Revision 0 January 2006



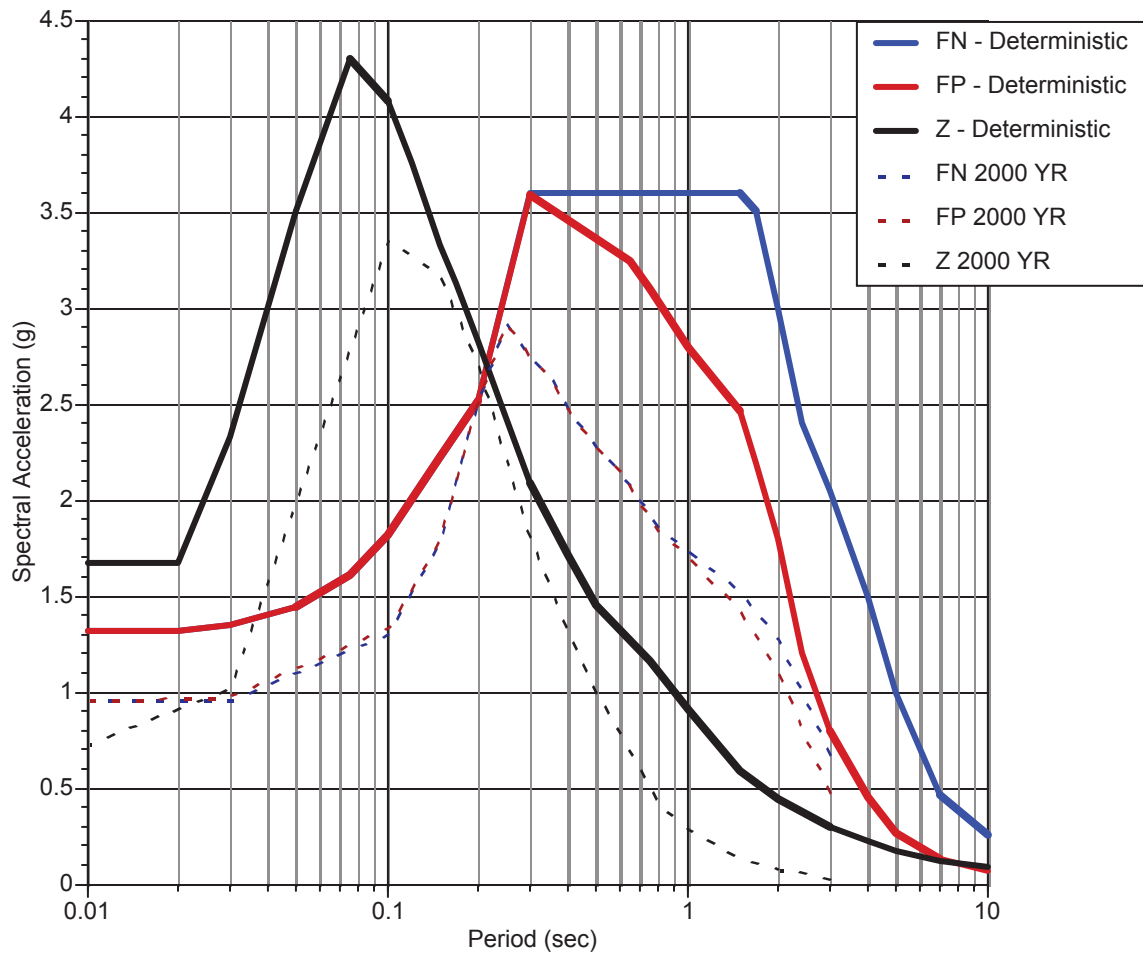
FSAR UPDATE
HUMBOLDT BAY ISFSI
FIGURE 2.6-70 EQUAL HAZARD SPECTRA FOR THE FP COMPONENT, SOIL SITE CONDITIONS

Revision 0 January 2006



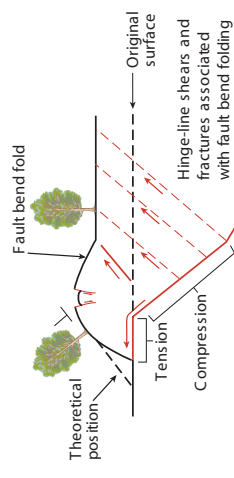
FSAR UPDATE
HUMBOLDT BAY ISFSI
FIGURE 2.6-71 EQUAL HAZARD SPECTRA FOR THE VERTICAL COMPONENTS FOR SOIL

Revision 0 January 2006

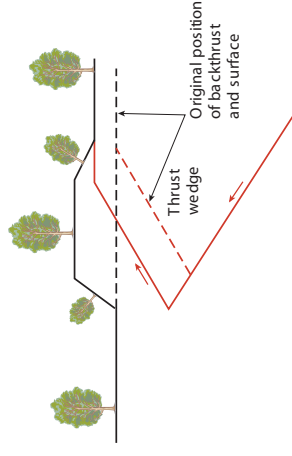


FSAR UPDATE
HUMBOLDT BAY ISFSI
FIGURE 2.6-72 COMPARISON OF DETERMINISTIC SPECTRA WITH 2000-YEAR PROBABILISTIC SPECTRA

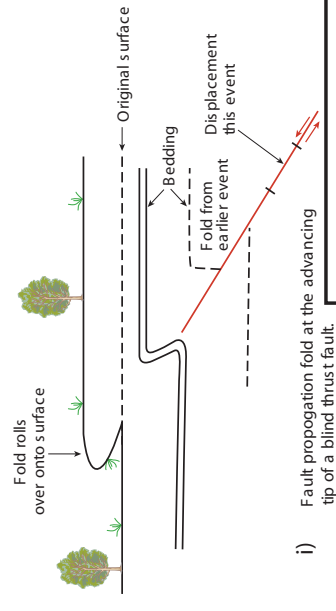
Revision 0 January 2006



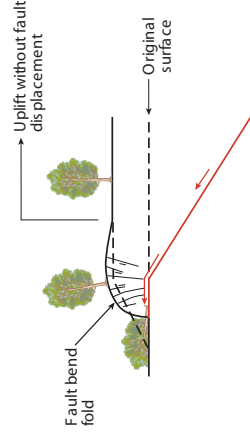
c) Uplift, compact folding at fault scarp from reverse fault that steepens dip as it approaches the surface.



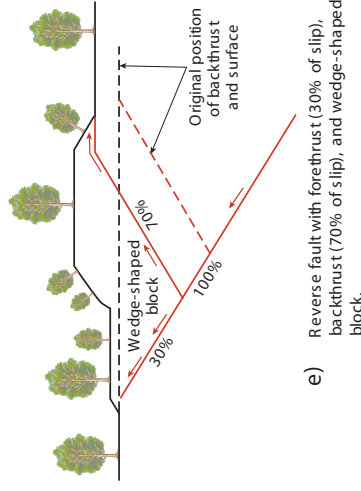
f) Reverse fault with blind forethrust and simple backthrust produced by a thrust wedge.



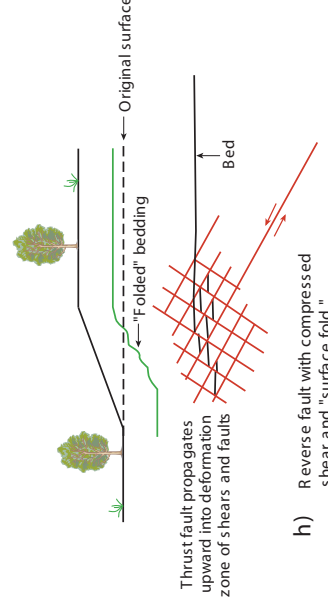
i) Fault propagation fold at the advancing tip of a blind thrust fault.



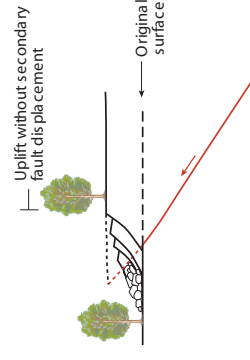
b) Uplift, folding and bulldozing at fault scarp from reverse fault having constant dip.



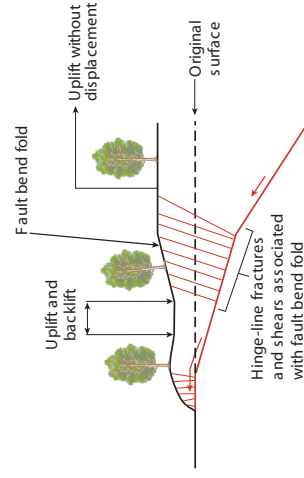
e) Reverse fault with forethrust (30% of slip), backthrust (70% of slip), and wedge-shaped block.



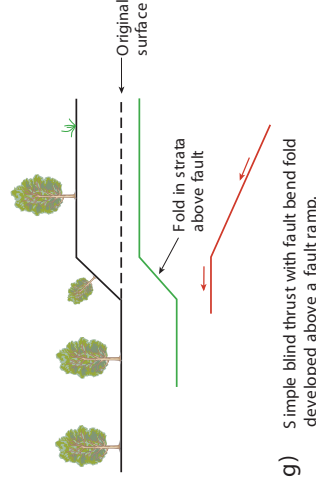
h) Reverse fault with compressed shear and "surface fold."



a) Collapsed fault scarp from reverse fault having constant dip.



d) Uplift, folding, bulldozing, and tilting from reverse fault that shallows in dip as it approaches the surface.



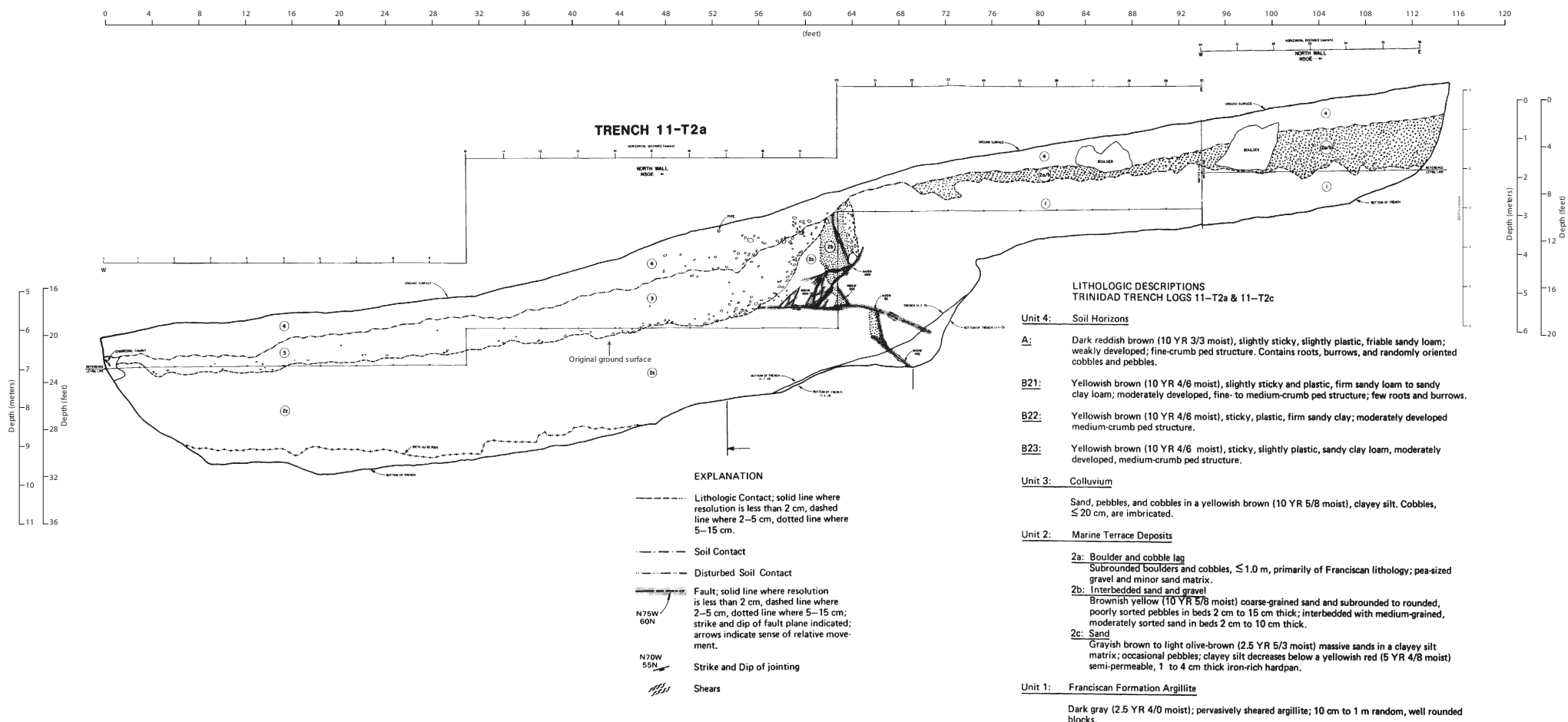
g) Simple blind thrust with fault bend fold developed above a fault ramp.

FSAR UPDATE
HUMBOLDT BAY ISFSI
FIGURE 2.6-73 TYPICAL TYPES OF SURFACE DEFORMATION ASSOCIATED WITH THRUST FAULTING



**FSAR UPDATE
HUMBOLDT BAY ISFSI
FIGURE 2.6-74**

~Collapsed fault scarp in alluvium on the Hanning Bay fault, Montague Island, Alaska. The fault dips to the left into the scarp that formed during the 1964 Alaska earthquake (from Plafker and others, 1969).



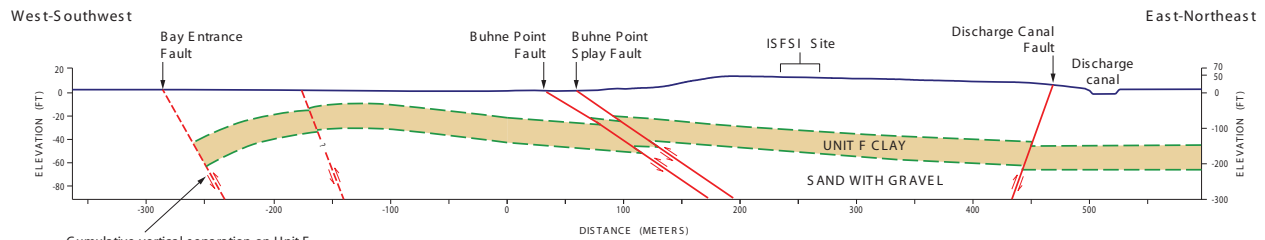
**FSAR UPDATE
HUMBOLDT BAY ISFSI
FIGURE 2.6-75**

This trench exposure near Trinidad, approximately 36 kilometers north of the ISFSI site, is an example of surface deformation produced by a displacement on a low-angle thrust fault (from Woodward-Clyde Consultants, 1980, Figure B-14). The style of deformation corresponds to Type b on Figure 2.6-73

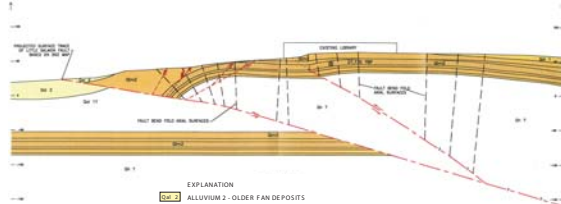


**FSAR UPDATE
HUMBOLDT BAY ISFSI
FIGURE 2.6-76**

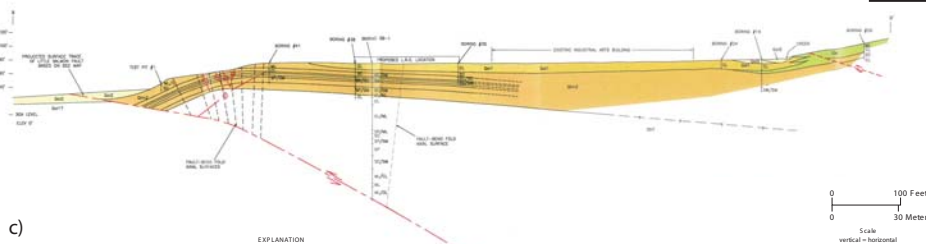
Fault scarp on the Chelungpu fault at the Kuang Fu Middle School, Taiwan. The scarp, formed during the 1999 Chi-Chi earthquake, illustrates the type of faulting in which the fault tip follows the ground surface.



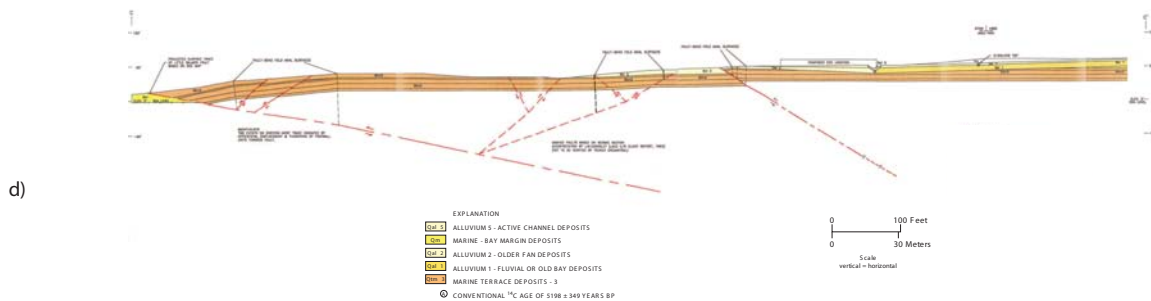
a)



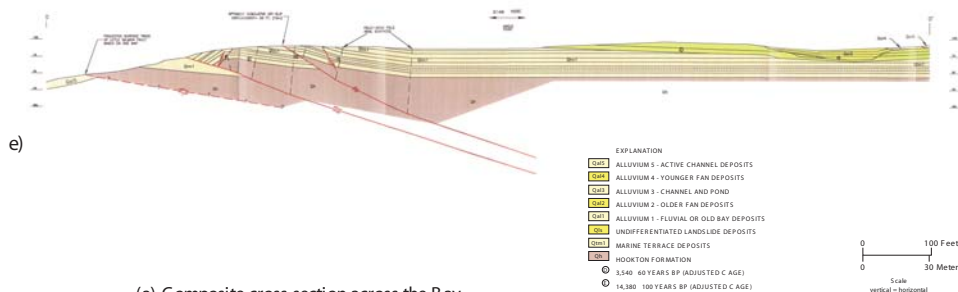
b)



c)



d)



e)

(a) Composite cross section across the Bay Entrance, Buhne Point, and Discharge Canal faults at the site (based on Figure 2.6-55 and Woodward-Clyde Consultants, 1980, Figure C-8).

(b) through (e) Geologic cross sections across a trace of the Little Salmon fault zone at College of the Redwoods (from LACO Associates, 1999b, Figures 5 through 8, respectively).

FSAR UPDATE HUMBOLDT BAY ISFSI FIGURE 2.6-77

Comparison of faulting near the Humboldt Bay ISFSI site with deformation mapped in the hanging wall of the Little Salmon fault zone at College of the Redwoods, about 5 kilometers south of the site.

← Northeast

Southwest →

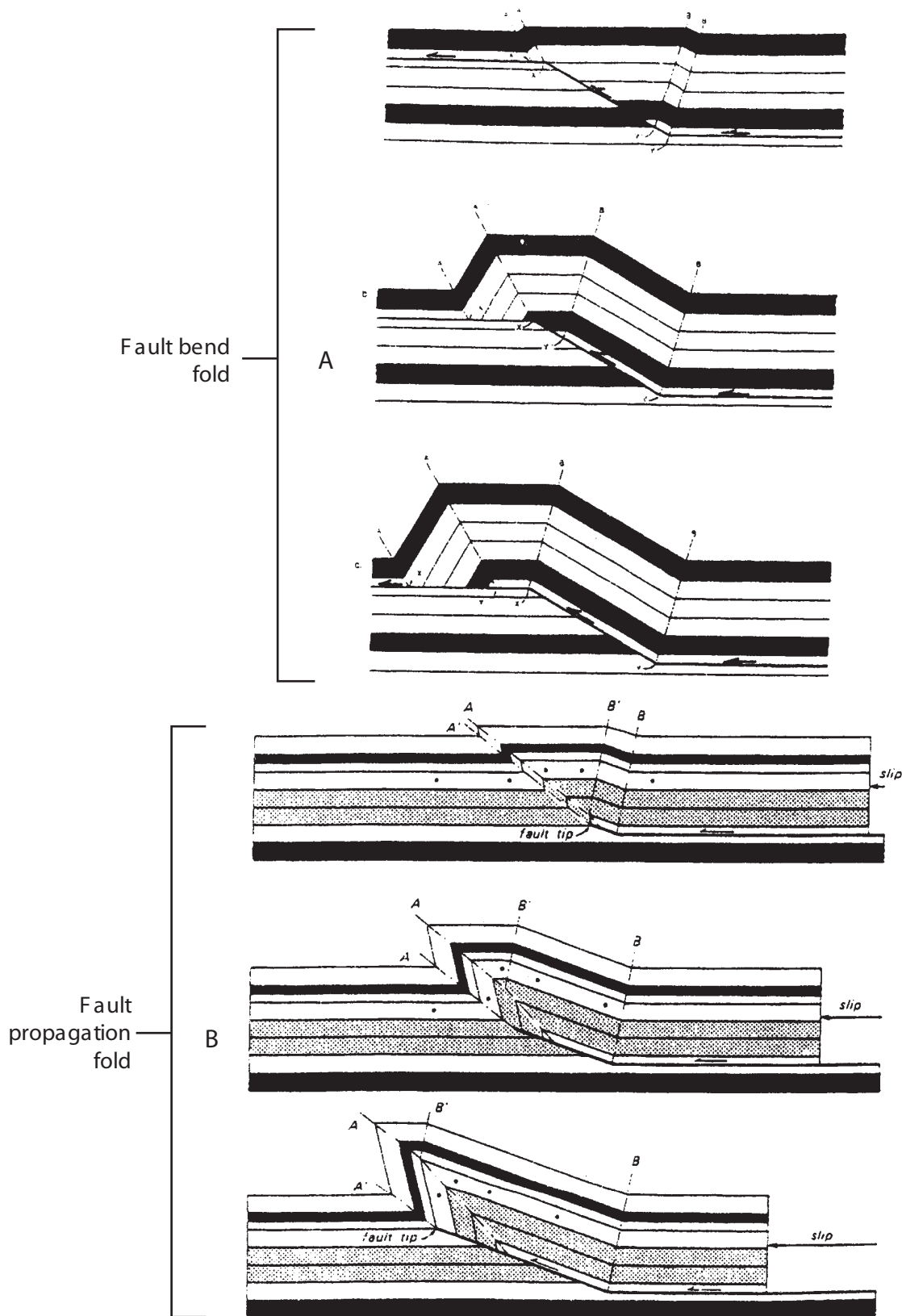


(a) Complex zones of deformation in the hanging wall of the McKinleyville fault (Mad River fault zone) exposed in the sea cliff at Clam Beach, north of Arcata (photograph by Thomas Dunklin, Arcata, California, 1999). The displacement is up to the northeast. The cliff is about 35 m high, and the photo shows a section about 150 m long.



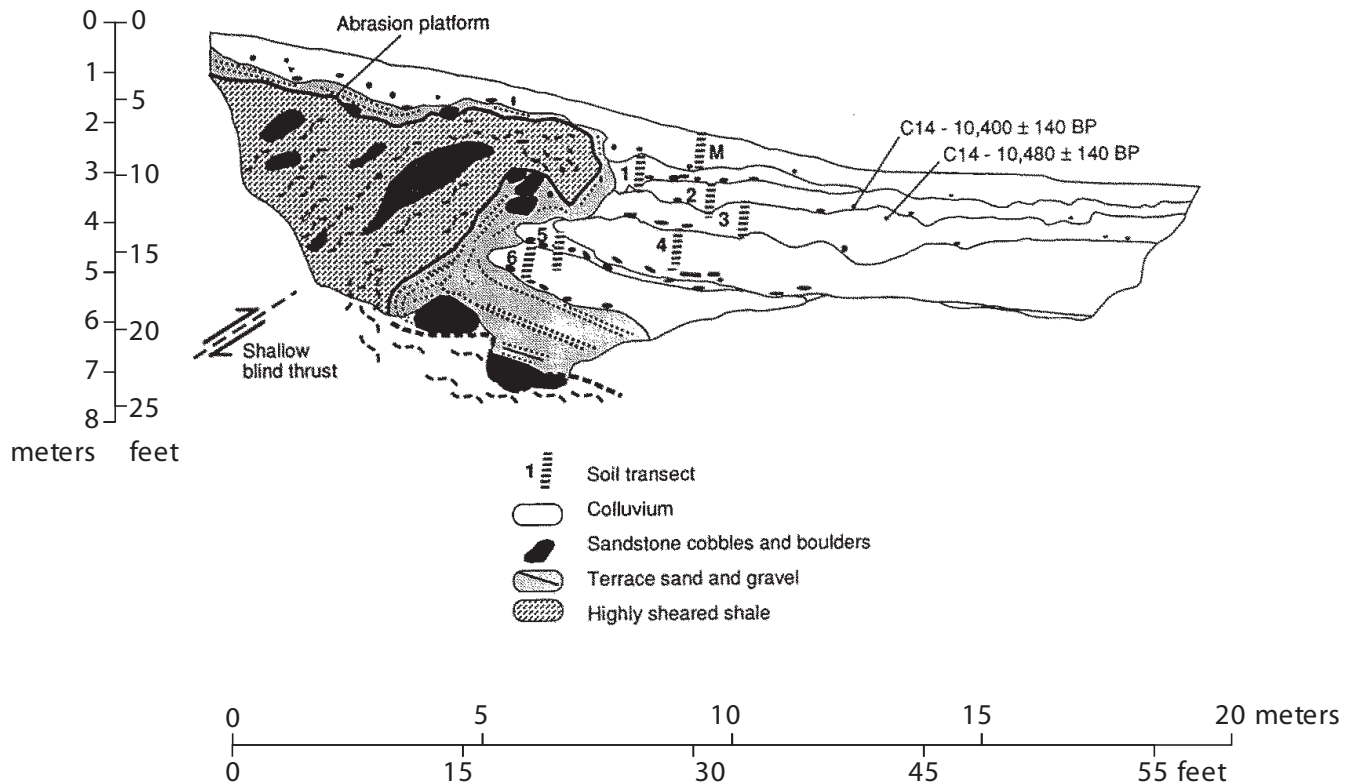
(b) The evolution of complex zones of deformation is shown sequentially with (1) initiation of faulting and development of synthetic shears and (2) continued deformation and development of antithetic shears. Repeating the process during continued movement (during either the same earthquake or subsequent earthquakes) produces a complex rhombohedral pattern of closely spaced shears (3) and (4) that individually have small displacements, but collectively can accommodate a large amount of crustal shortening.

FSAR UPDATE
HUMBOLDT BAY ISFSI
FIGURE 2.6-78
COMPLEX ZONES OF DEFORMATION WHERE CRUSTAL SHORTENING IS ACCOMMODATED BY NUMEROUS SMALL-DISPLACEMENT CONJUGATE FAULTS



**FSAR UPDATE
HUMBOLDT BAY ISFSI
FIGURE 2.6-79**

Schematic progressive development of fault bend and fault propagation folds (from Suppe, 1983). Folds develop as thrust sheet rides over a step in decollement.



The fault displaces a late Pleistocene marine terrace near Humboldt Bay (from Carver and McCalpin, 1996, Figure 5.13). The terrace deposits are underlain by very ductile, intensely sheared shaley melange. The thrust fault is blind, and displacement occurs at the surface as a sharp, overturned fault-propagation fold. The marine terrace platform (heavy line) and overlying terrace sand and gravel are overturned in the forelimb of the fold. The sequence of colluvial deposits, labeled 1 through 6 (from youngest to oldest), is interpreted to have formed on the scarp face between slip events, indicating there have been repeated surface displacements along this fault trace. The style of deformation corresponds to Type i on Figure 8-1.

FSAR UPDATE

HUMBOLDT BAY ISFSI

**FIGURE 2.6-80
LOG OF TRENCH ACROSS A
TRACE OF THE MAD RIVER
FAULT ZONE**

Revision 0 January 2006



A) Fault bend fold appears as flexure on the floor of a building destroyed by surface faulting during the 1999 Chi-Chi earthquake.

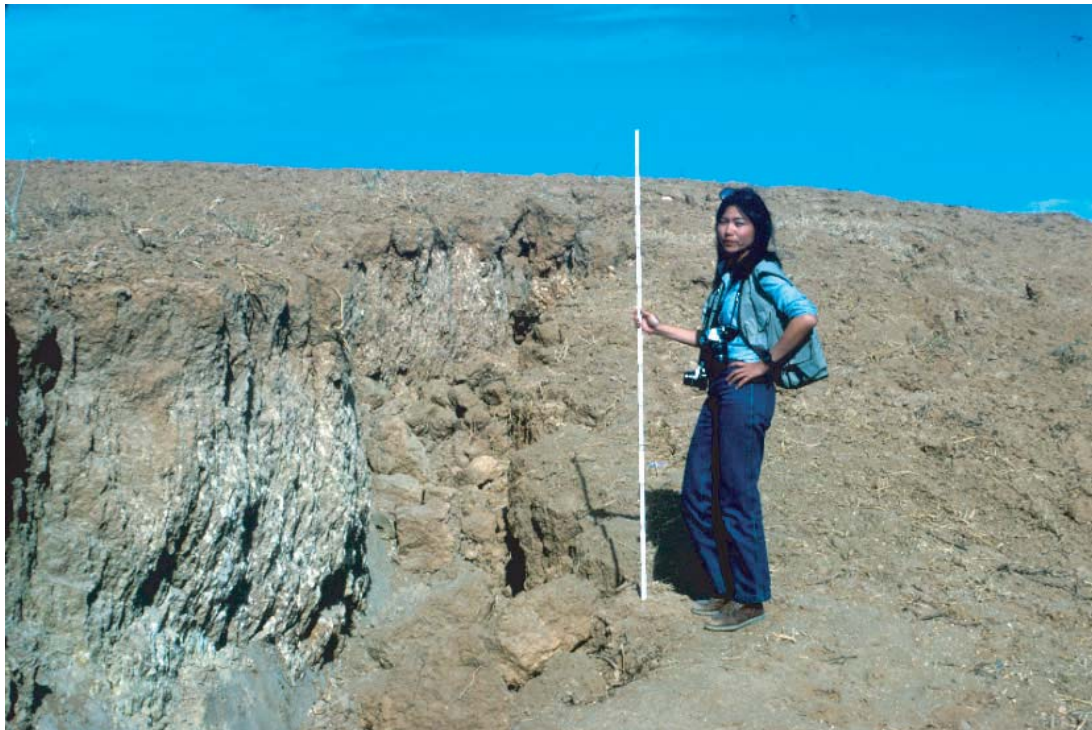


B) Shears and fractures in wall over the fault bend fold shown above.

FSAR UPDATE
HUMBOLDT BAY ISFSI
FIGURE 2.6-81
FAULT BEND FOLD AND ASSOCIATED
SHEARS AND FRACTURES ON THE
CHELUNGPU FAULT,
FENGYUAN, TAIWAN



A) Tensional cracks and normal faults that formed in the 1980 El Asnam earthquake along a secondary fault that is about 7 kilometers from the main fault trace (photograph by F. H. Swan).



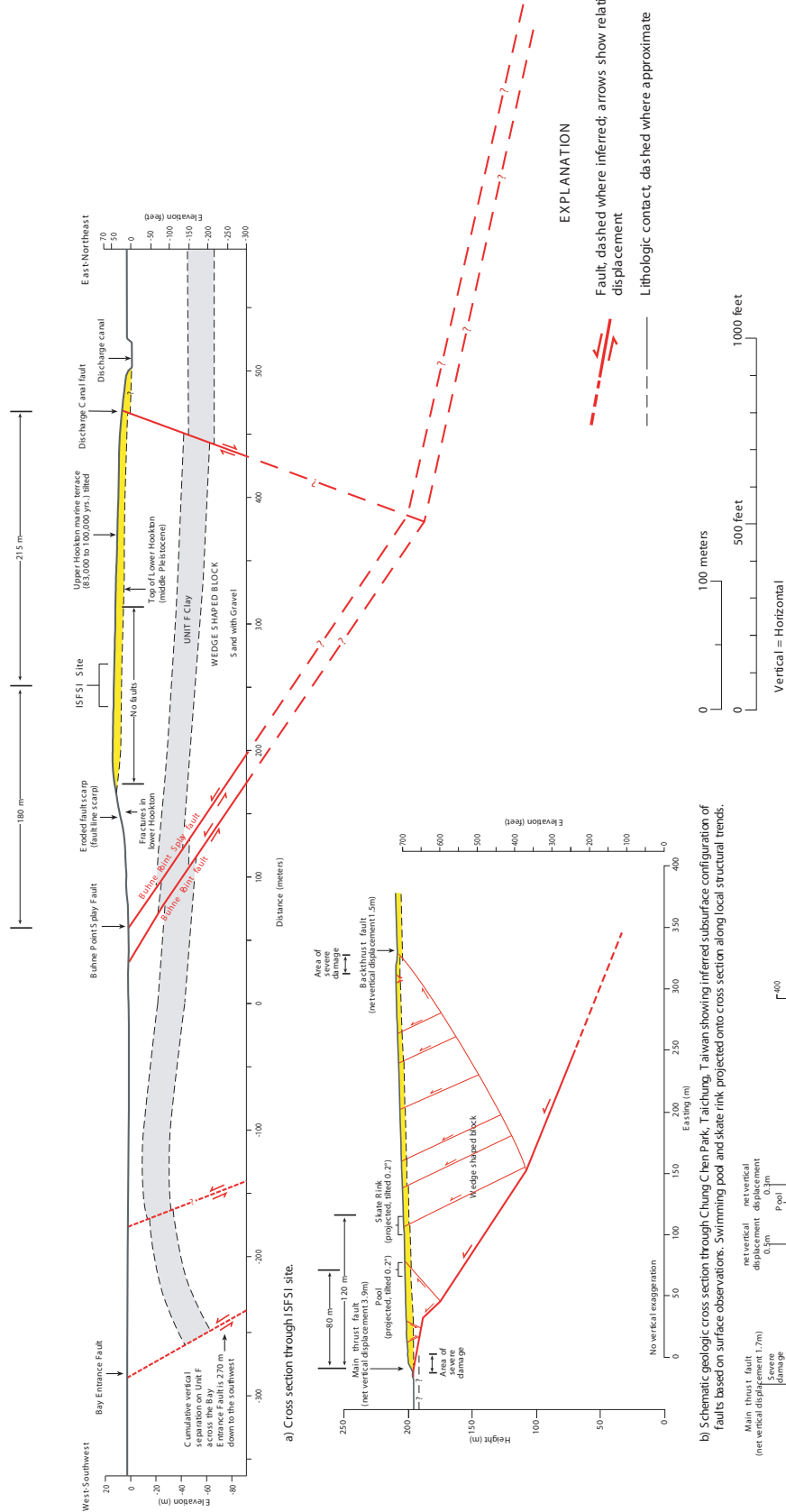
B) Normal fault scarp in the hanging wall near the same location as above.

FSAR UPDATE

HUMBOLDT BAY ISFSI

**FIGURE 2.6-82
FRACTURES AND FAULTS IN THE
HANGING WALL OF THE OUED
FODDA FAULT, ALGERIA**

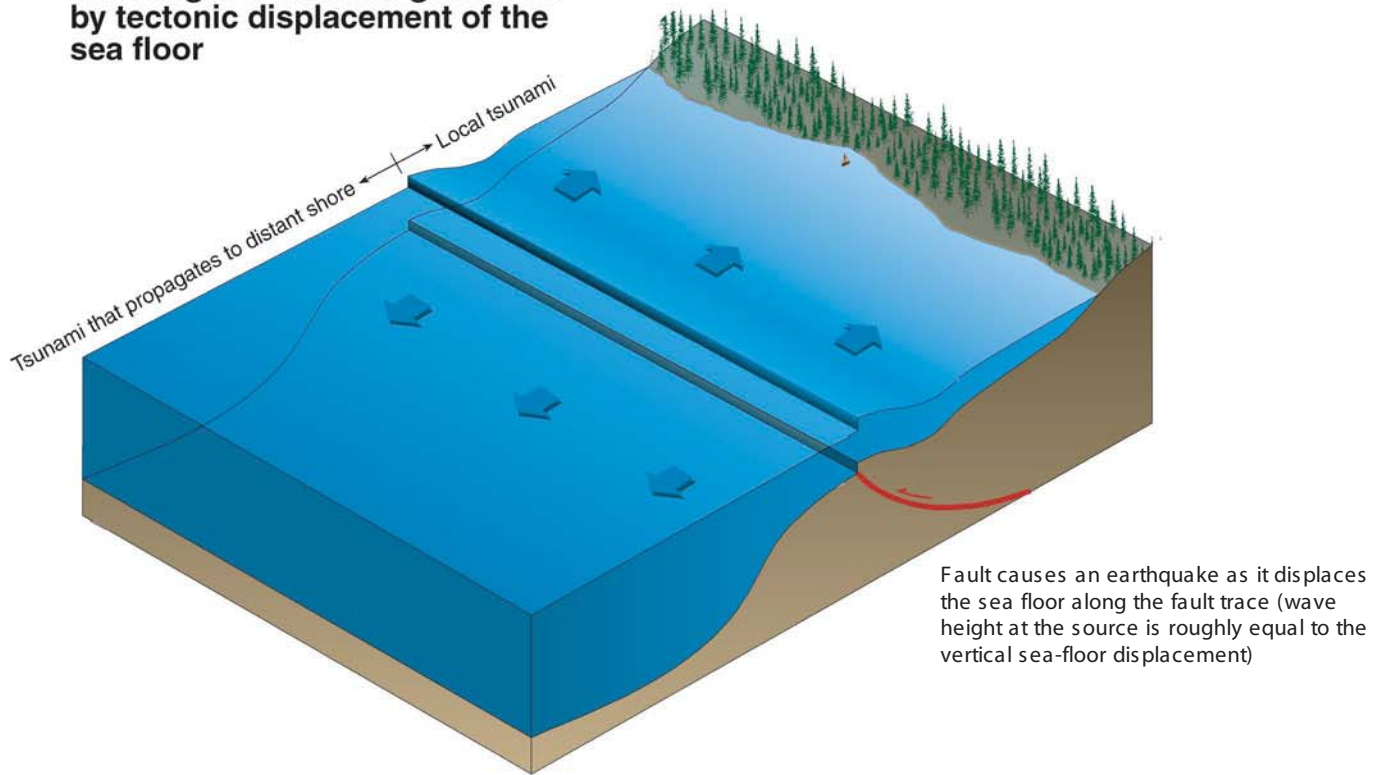
Revision 0 January 2006



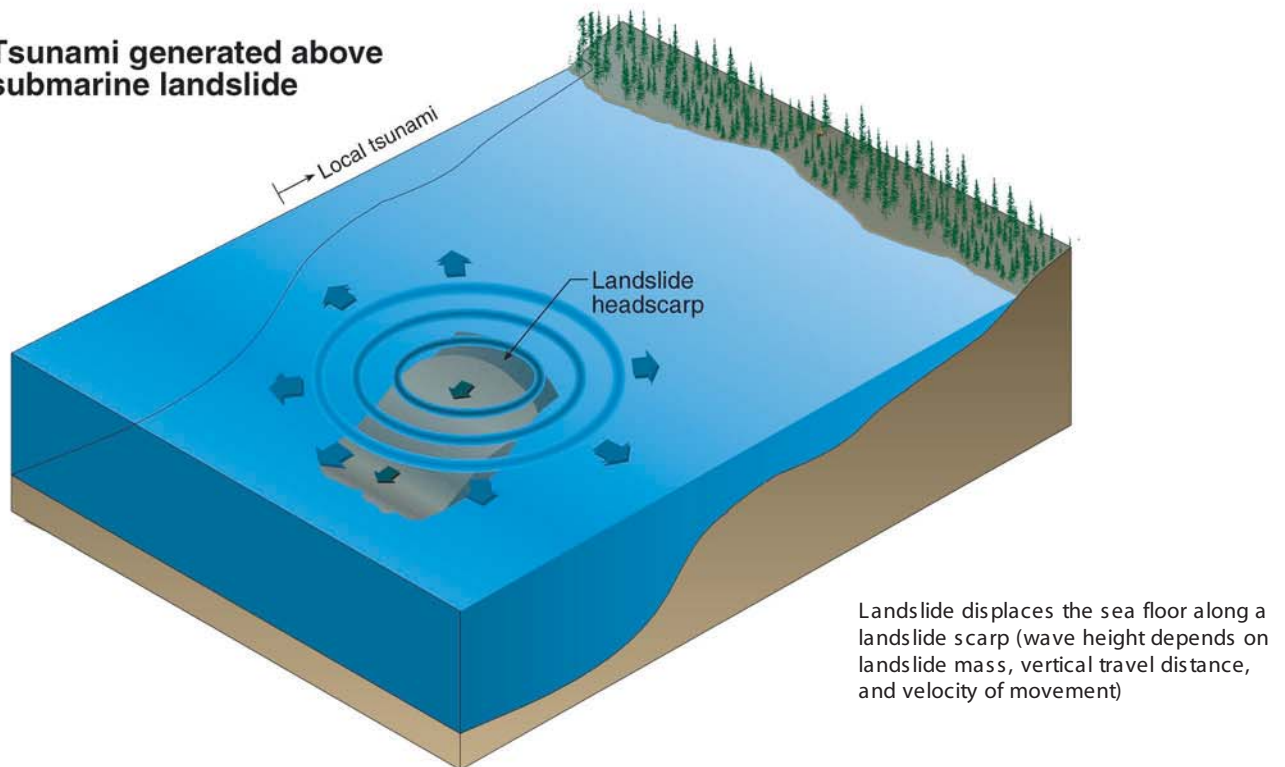
(a) Composite cross section across the Bay Entrance, Buhne Point, and Discharge Canal faults at the site (based on Figure 2.6-55 and Woodward-Clyde Consultants, 1980, Figure C-8).

(b) through d) Geologic cross sections across the 1999 Chelungpu fault rupture (from Kelson and others, 2001).

**Seismogenic tsunami generated
by tectonic displacement of the
sea floor**



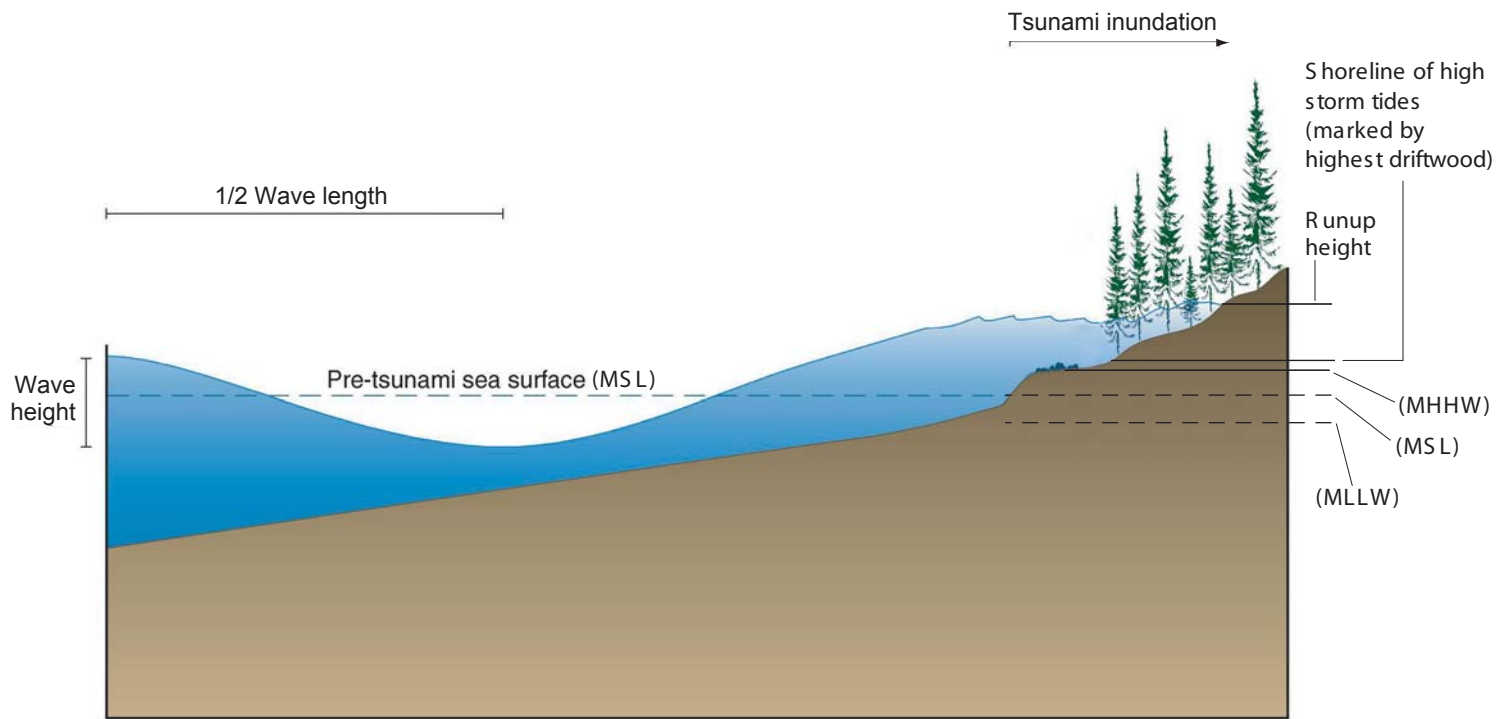
**Tsunami generated above
submarine landslide**



Vertical scale is greatly exaggerated

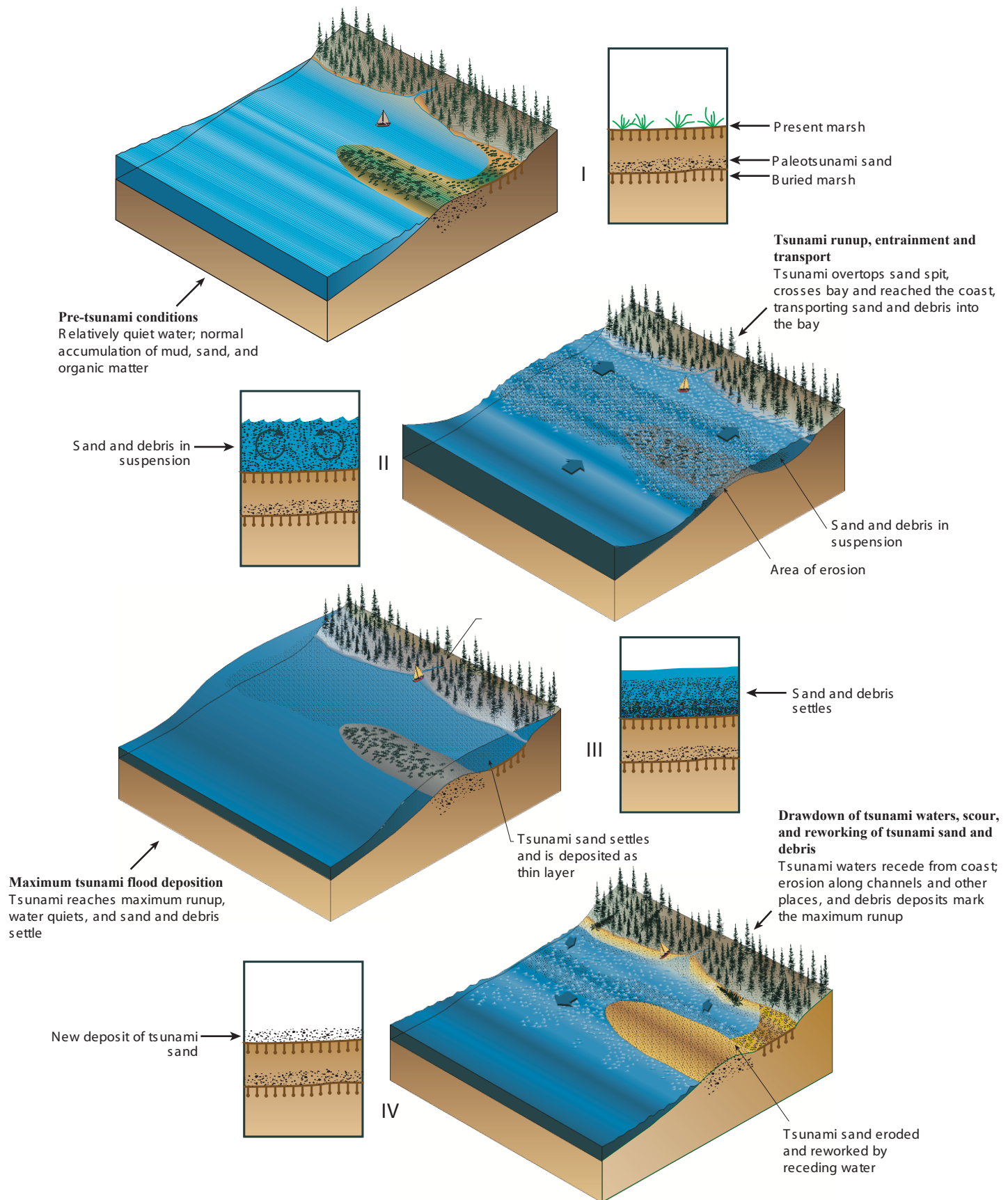
FSAR UPDATE
HUMBOLDT BAY ISFSI
FIGURE 2.6-84
SCHEMATIC DIAGRAMS OF MAJOR
TSUNAMI SOURCES

Revision 0 January 2006



FSAR UPDATE
HUMBOLDT BAY ISFSI
FIGURE 2.6-85
ILLUSTRATION OF TSUNAMI TERMS

Revision 0 January 2006



**FSAR UPDATE
HUMBOLDT BAY ISFSI
FIGURE 2.6-86**

Diagrams illustrating progression of tsunamis at the coast, and stratigraphic columns in the quiet water of bays and ponds.

Revision 0 January 2006



**FSAR UPDATE
HUMBOLDT BAY ISFSI
FIGURE 2.6-87**

North Spit, Humboldt Bay (foreground), and Arcata Bay (background). View is to the north from above the bay entrance. The Mad River Slough is located in the marshland on the north side of Arcata Bay. The Humboldt Bay Power Plant is just out of the picture to the lower right.

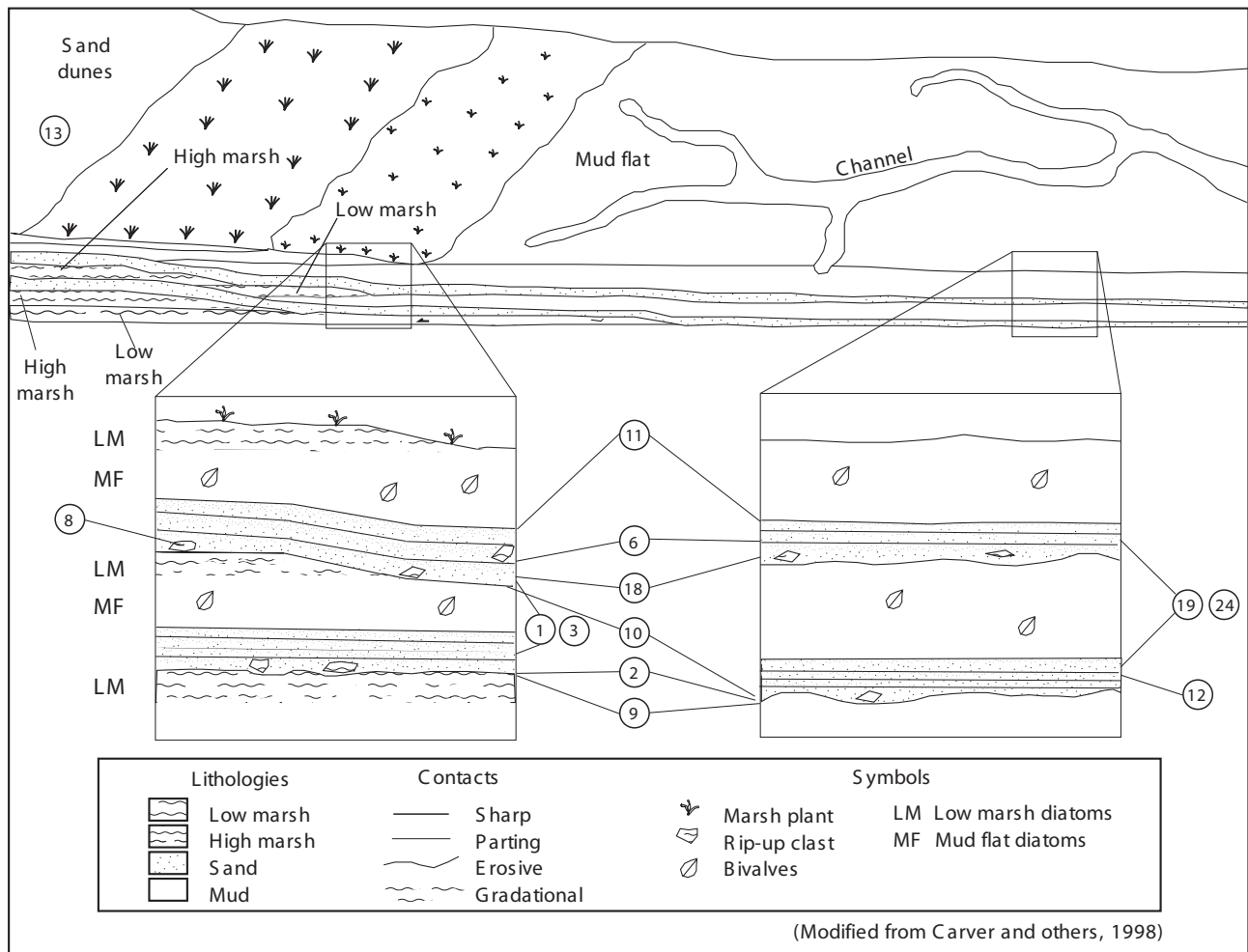


FSAR UPDATE

HUMBOLDT BAY ISFSI

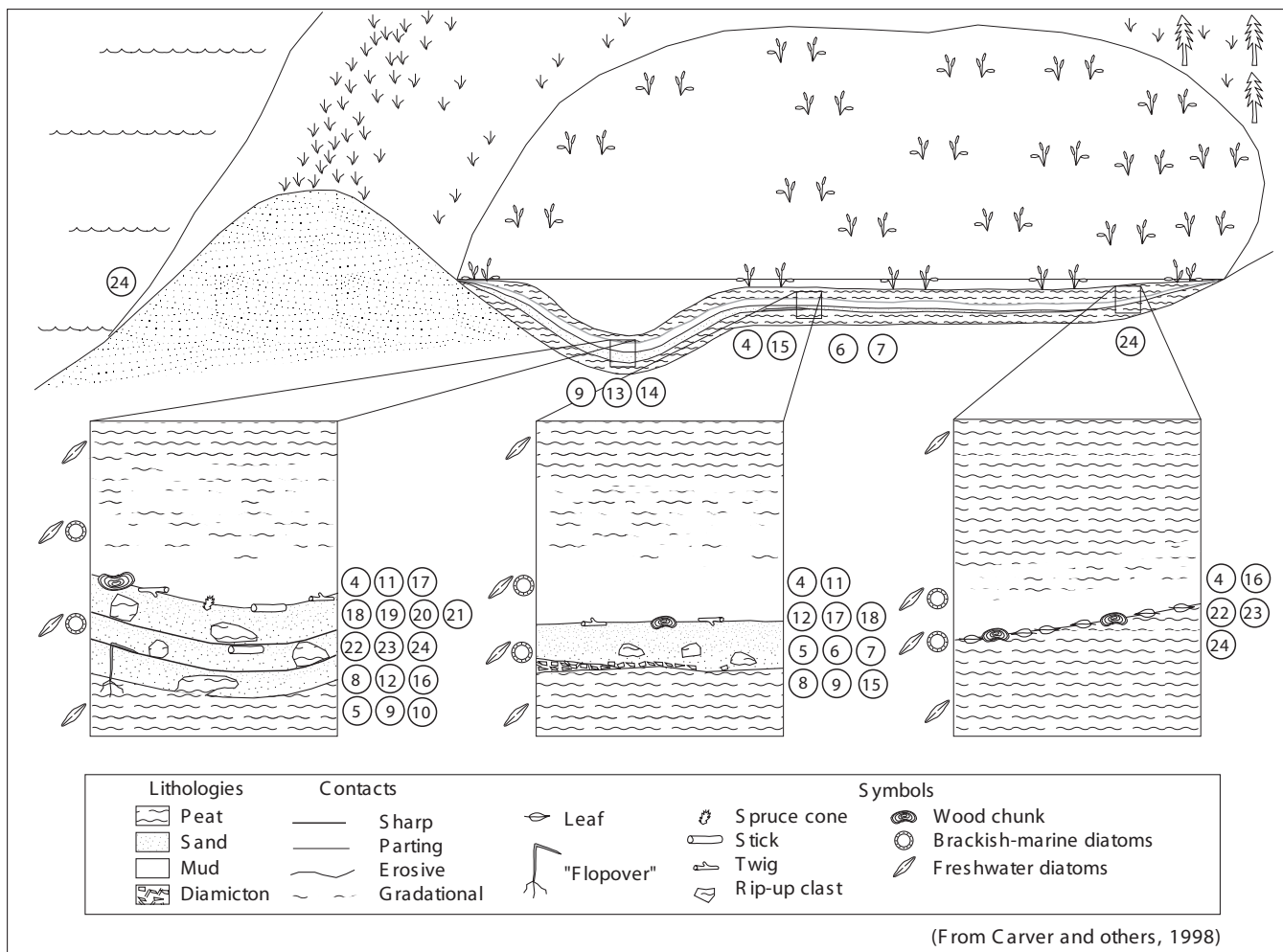
**FIGURE 2.6-88
COASTAL SITES INVESTIGATED FOR
EVIDENCE OF PALEOTSUNAMIS IN
NORTHWESTERN CALIFORNIA**

Revision 0 January 2006



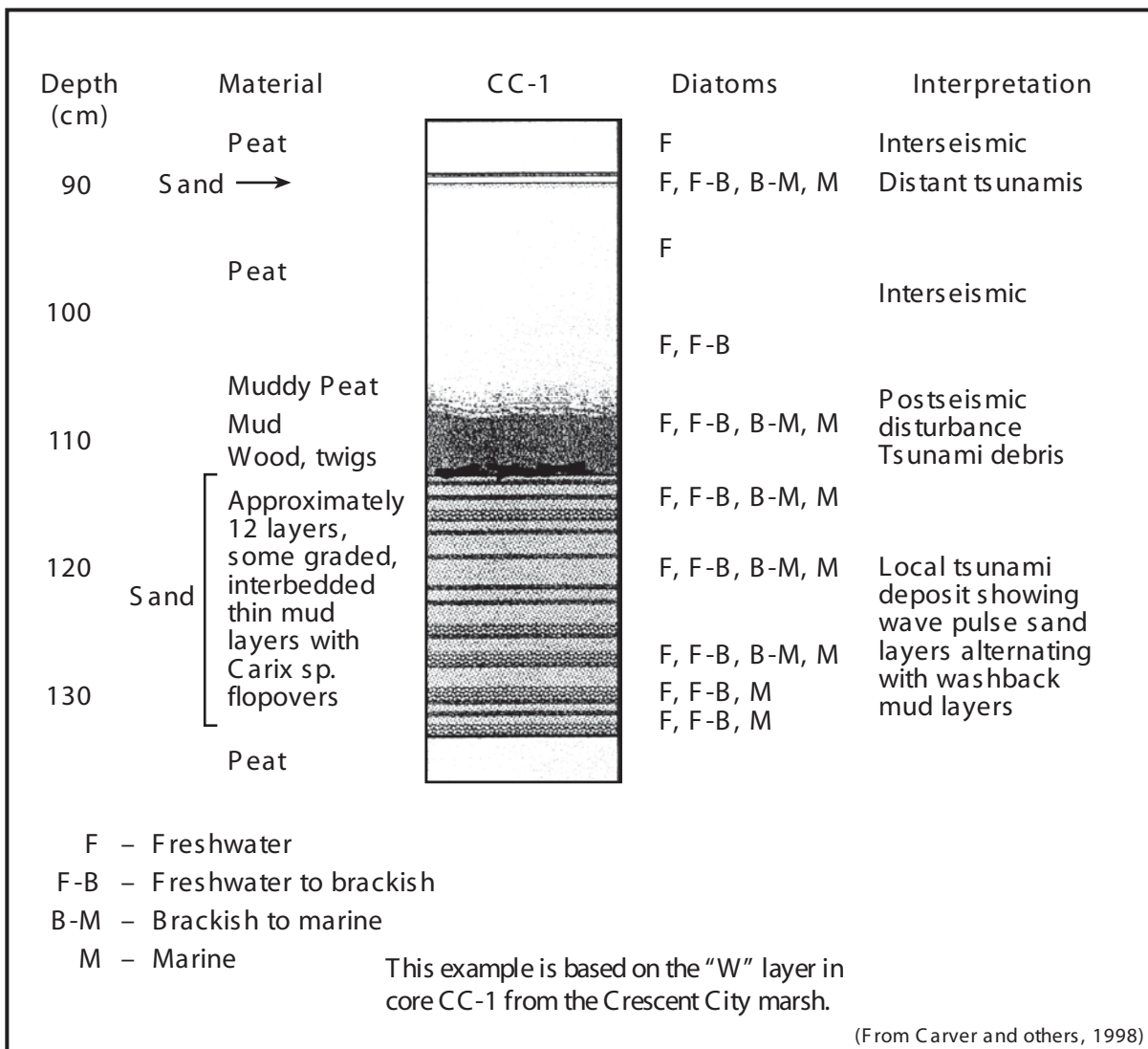
**FSAR UPDATE
HUMBOLDT BAY ISFSI
FIGURE 2.6-89**

~Cross section of a typical intertidal marsh. Figure shows the idealized relationship between tsunami sand deposits and stratigraphic and biostratigraphic features caused by coseismic subsidence. The key to the numbers is shown in Table 2.6-23.



**FSAR UPDATE
HUMBOLDT BAY ISFSI
FIGURE 2.6-90**

~Cross section of a typical coastal freshwater marsh. Figure shows an idealized tsunami sand layer interbedded with peat and mud. The key to the numbers is shown in Table 2.6-23.



FSAR UPDATE
HUMBOLDT BAY ISFSI
FIGURE 2.6-91 IDEALIZED DETAILED SECTION SHOWING MULTIPLE GRADED SANDS IN A TSUNAMI DEPOSIT



**FSAR UPDATE
HUMBOLDT BAY ISFSI
FIGURE 2.6-92**

Gouge coring at Crescent City marsh. Hans Abramson, collecting a gouge core in the marsh, is employing a typical technique for obtaining a reconnaissance core.



FSAR UPDATE

HUMBOLDT BAY ISFSI

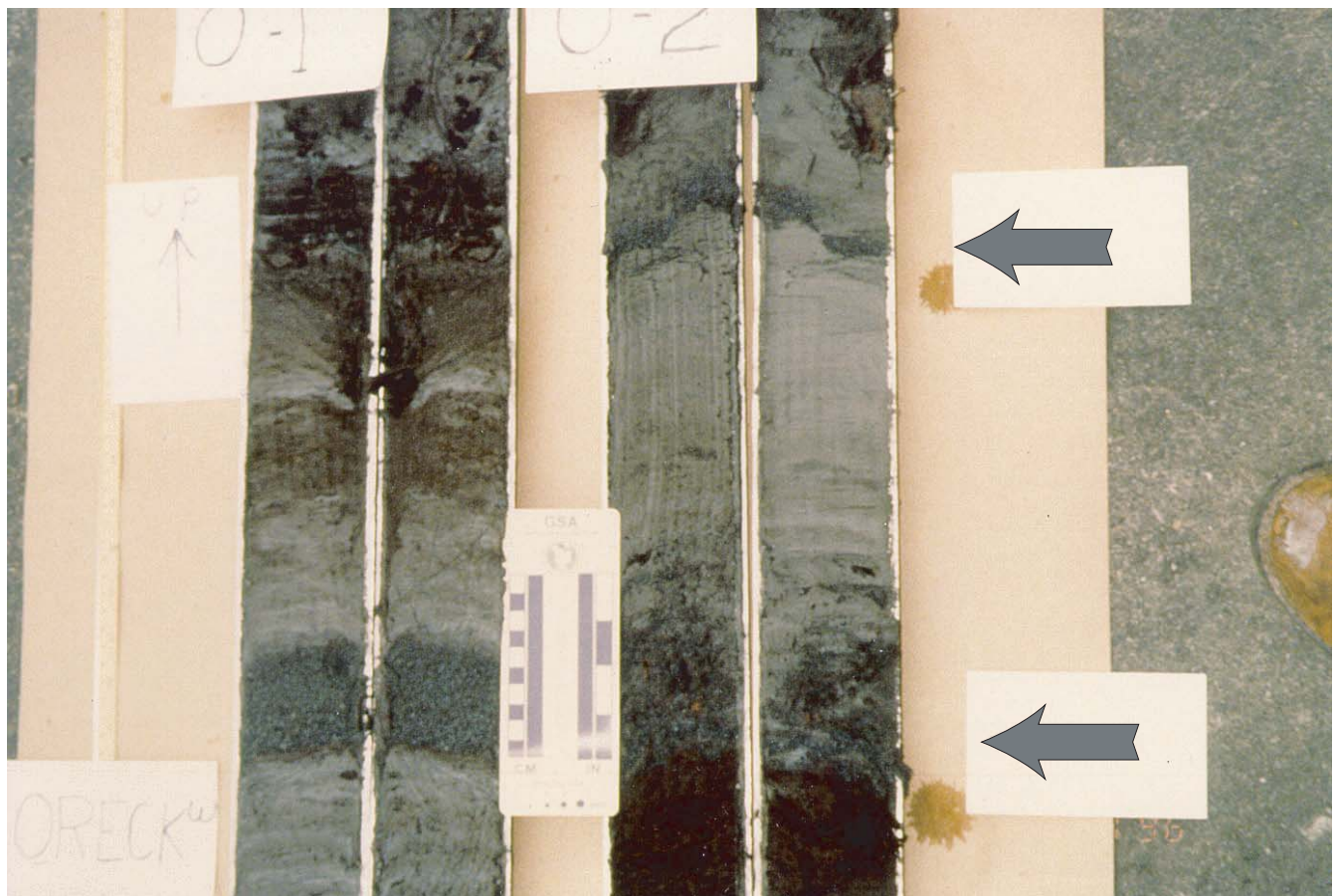
**FIGURE 2.6-93
TYPICAL GOUGE CORE. THE FINGER
POINTS TO A THIN LAYER OF FINE-
GRAINED TSUNAMI SAND, WHICH IS
INTERBEDDED WITH MARCH PEAT**

Revision 0 January 2006



**FSAR UPDATE
HUMBOLDT BAY ISFSI
FIGURE 2.6-94**

**Drilling using the Vibracore at Lagoon Creek.
The 3-inch-diameter core tube is shown in position
before being driven into marsh sediments.**

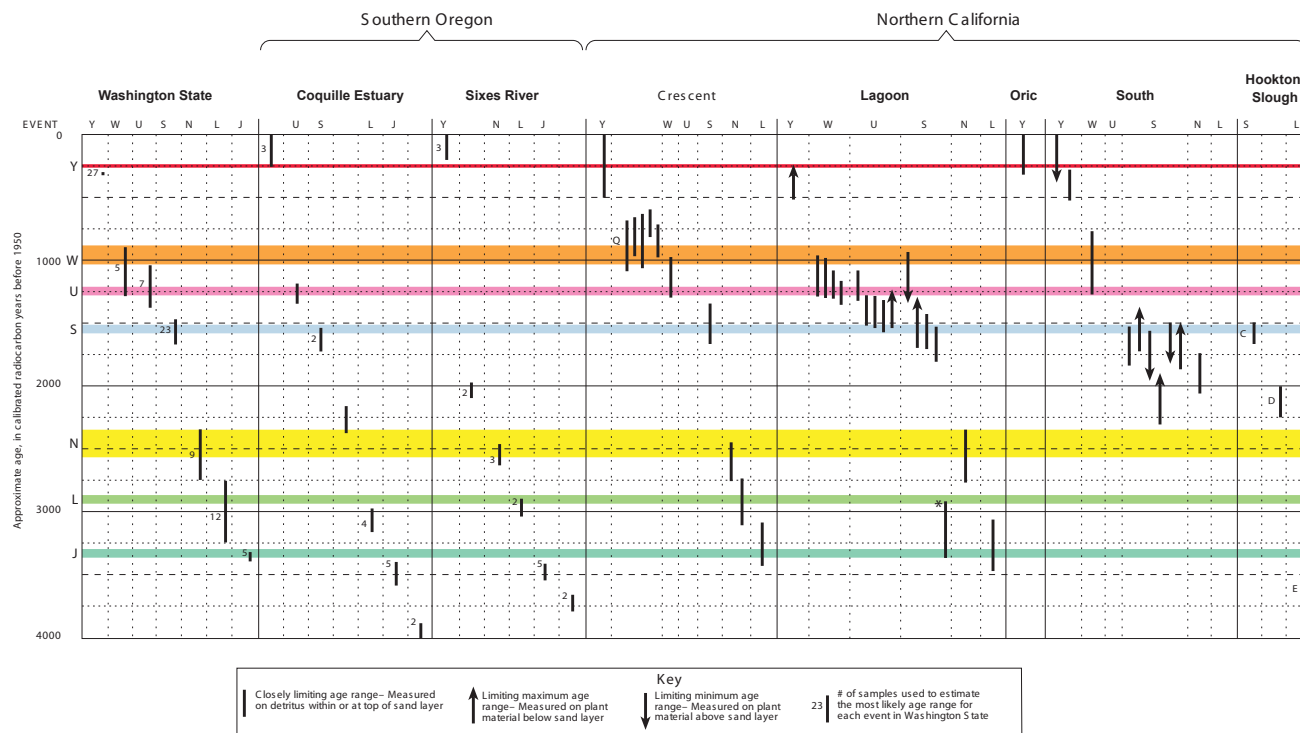


FSAR UPDATE

HUMBOLDT BAY ISFSI

**FIGURE 2.6-95
TYPICAL DRIVE CORES.
THE TWO SPLIT-SAMPLE TUBES SHOW
TSUNAMI SANDS (ARROWS) IN CORES
FROM THE ORICK MARSH**

Revision 0 January 2006

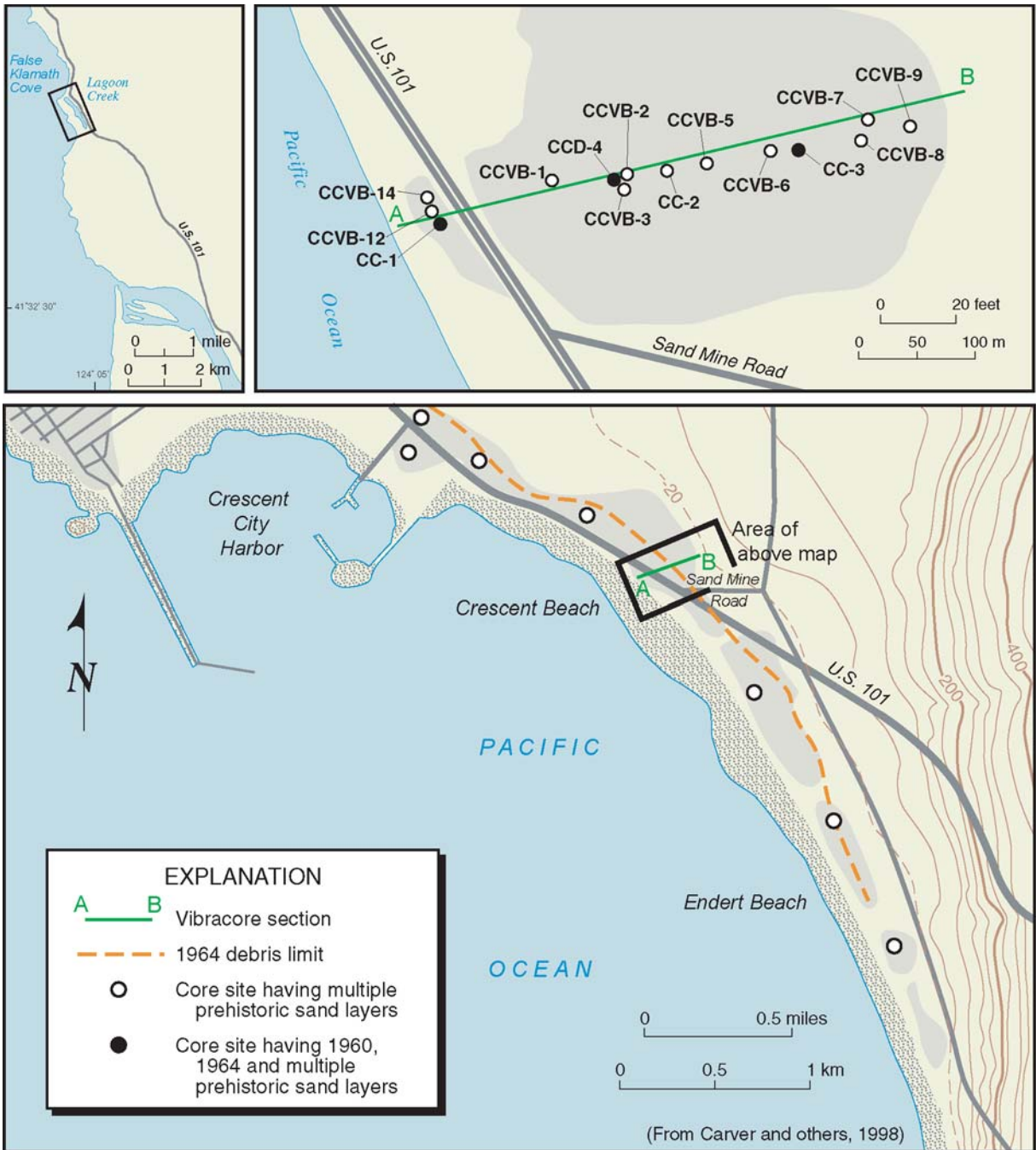


*This age, from a small seed interpreted to be reworked into sand layer S, is not considered to be a closely limiting age for the horizon

Crescent City, Orick, Lagoon Creek and South Bay data from Carver and others (1998); Washington data from Atwater and Hemphill-Haley (1997); Hookton slough data from Patton and others, (2002); and Oregon data from Kelsey and others (2002).

FSAR UPDATE HUMBOLDT BAY ISFSI FIGURE 2.6-96

"Comparison of ages for Cascadia earthquakes from tsunami data between northern California and Washington. Width of lines showing Cascadia events ("Y", "W", "U", "S", "N", "L", and "J") from Kelsey and others , 2002).



FSAR UPDATE
HUMBOLDT BAY ISFSI
FIGURE 2.6-97 LOCATION OF CORES IN CRESCENT CITY MARSH

Revision 0 January 2006



Crescent City Marsh Site

FSAR UPDATE
HUMBOLDT BAY ISFSI
FIGURE 2.6-98
CRESCENT CITY VIEW TO WEST



FSAR UPDATE
HUMBOLDT BAY ISFSI
FIGURE 2.6-99
CRESCENT CITY MARSH

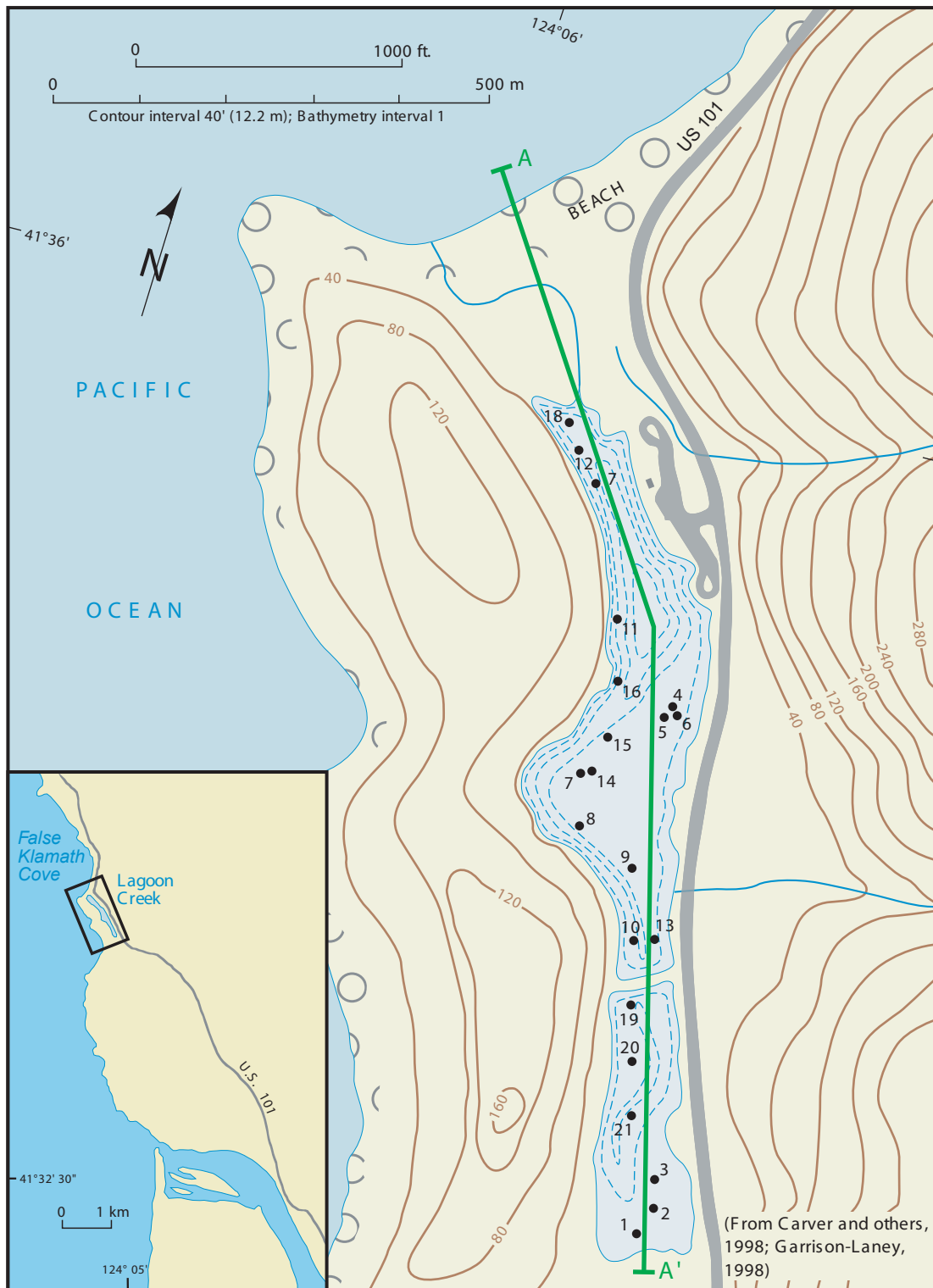
Revision 0 January 2006

[illegible]

(From Carver and others, 1998)

**FIGURE 2.6-100
CORRELATION OF TSUNAMI SANDS
IN SELECTED CORES ACROSS
CRESCENT CITY MARSH**

Revision 0 January 2006



(From Carver and others, 1998; Garrison-Laney, 1998)

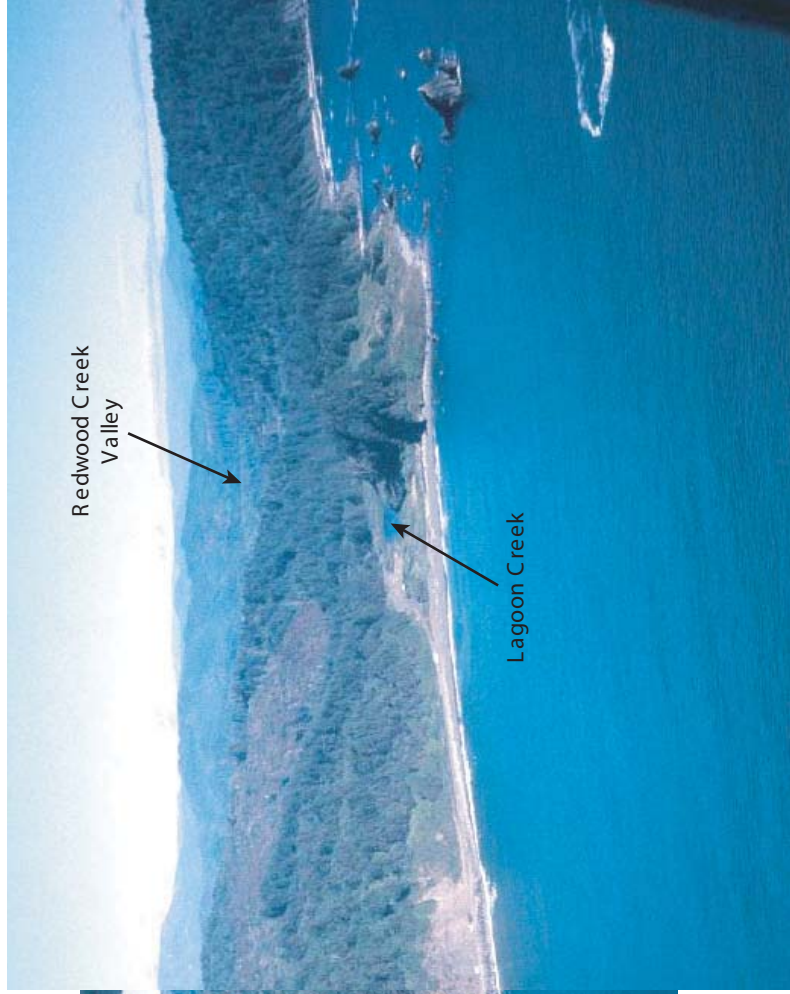
**FSAR UPDATE
HUMBOLDT BAY ISFSI
FIGURE 2.6-101**

Location of cores in the Lagoon Creek marsh. Map shows topography, bathymetry (dashed contours) and vibracore locations. Cross section A-A' is shown on Figure 2.6-105.



**FSAR UPDATE
HUMBOLDT BAY ISFSI
FIGURE 2.6-102**

The Lagoon Creek pond and marsh. View is to the south, showing the beach ridge, pond, and marsh in this narrow valley. Tsunami sand layers were found in the marsh sediments inland to the upper end of the marsh visible in this photograph.



**FSAR UPDATE
HUMBOLDT BAY ISFSI
FIGURE 2.6-103**

Wilson Creek and Lagoon Creek . Wilson creek during the Pleistocene flowed around where the sea bluffs are today and down Lagoon Creek to Redwood Creek. Sea erosion has cut off Lagoon Creek from Wilson Creek, leaving Lagoon Creek as a stable site undisturbed by stream erosion.

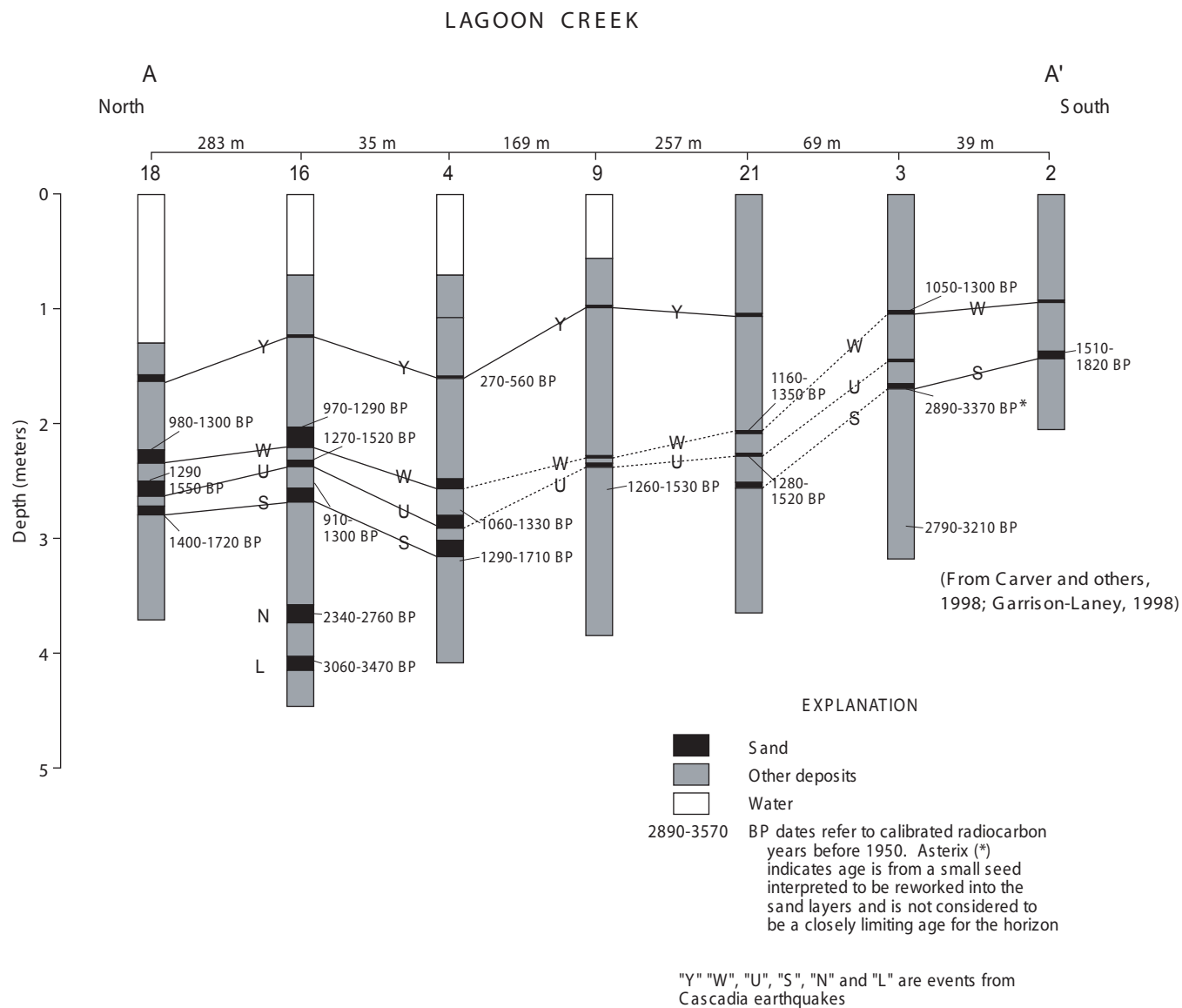


FSAR UPDATE

HUMBOLDT BAY ISFSI

**FIGURE 2.6-104
BEACH BERM AT LAGOON CREEK
23-FEET ABOVE MLLW. VIEW IS TO THE
NORTH FROM THE NORTHERN PART OF
THE LAGOON CREEK MARSH**

Revision 0 January 2006

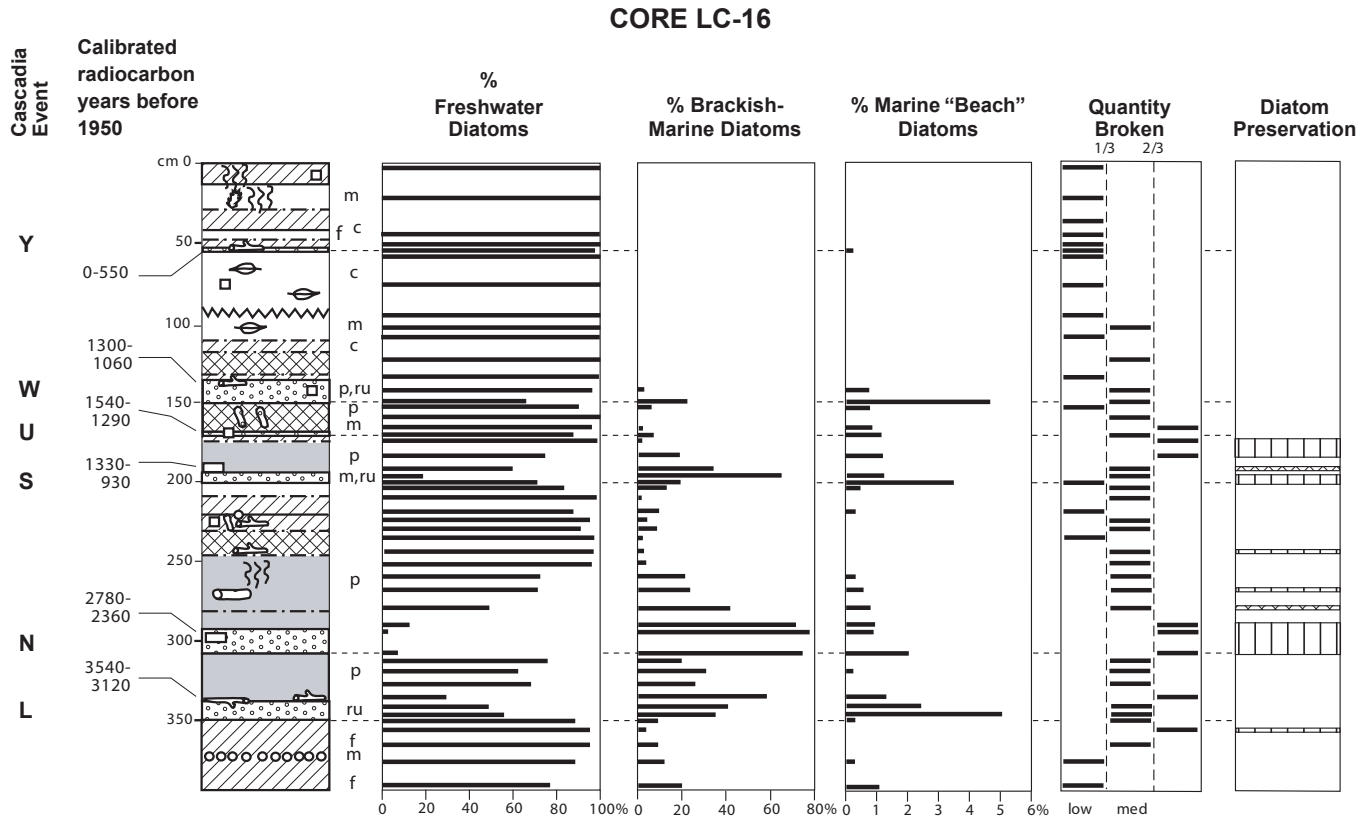


FSAR UPDATE

HUMBOLDT BAY ISFSI

FIGURE 2.6-105

**CORRELATION OF TSUNAMI SANDS IN
SELECTED CORES ACROSS LAGOON
CREEK MARSH. THE LOCATION OF CROSS
SECTION A-A' IS SHOWN IN FIGURE 2.6-101**



(From Garrison-Laney, 1998)

LITHOFACIES CODES

Lithologies

- peat
- muddy peat
- peaty mud
- mud
- sand

Lithologic Modifiers

- s sandy
- m muddy
- p peaty
- c coarse
- f fine
- d detritus
- ru rip-ups
- leaves
- wood chunks
- charcoal
- stick
- twig
- spruce cone
- roots
- sand tunnel

CONTACTS AND SYMBOLS

- Abrupt (≤ 1 mm)
- - - Sharp (1-3 mm)
- · - Gradational (4-10 mm)
- ~~~~~ Diffuse (11-20 mm)
- ~~~~~ Diffuse (≥ 50 mm)

DIATOM PRESERVATION

- Very good to excellent
- Moderate
- Fair to poor

FSAR UPDATE

HUMBOLDT BAY ISFSI

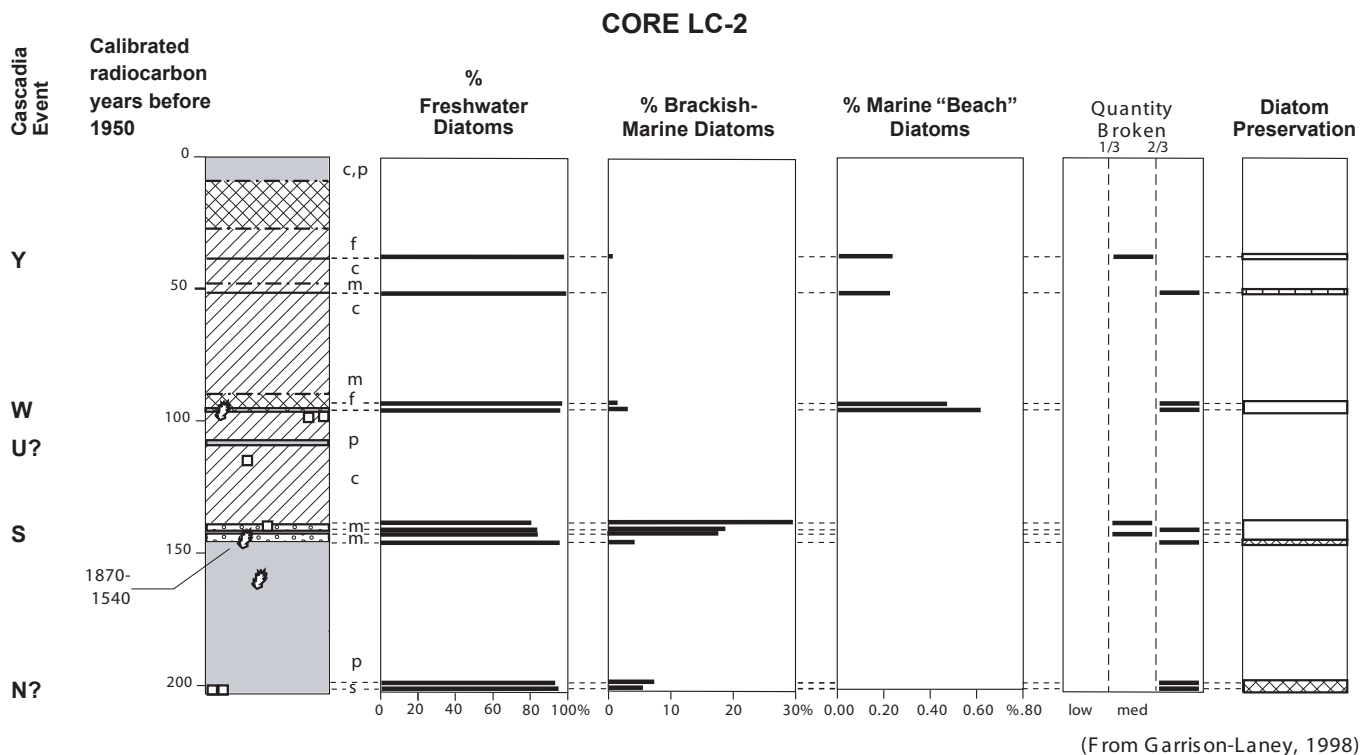
FIGURE 2.6-106

DETAILED STRATIGRAPHY OF CORE LC-16

FROM THE LAGOON CREEK MARSH.

DIAGRAM SHOWS TYPICAL MARSH, SAND

DEPOSITS AND DIATOMS NEAR THE COAST



LITHOFACIES CODES

Lithologies

peat
muddy peat
peaty mud
mud
sand

s sandy
m muddy
p peaty
c coarse
f fine

Lithologic Modifiers

d detritus	stick
ru rip-ups	twig
leaves	spruce cone
wood chunks	roots
charcoal	sand tunnel

CONTACTS AND SYMBOLS

—	Abrupt (≤ 1 mm)
- - - -	Sharp (1-3 mm)
- · - · -	Gradational (4-10 mm)
~~~~~	Diffuse (11-20 mm)
~~~~~	Diffuse ( $\geq 50$ mm)

DIATOM PRESERVATION

□	Very good to excellent
▤	Moderate
▨	Fair to poor

FSAR UPDATE

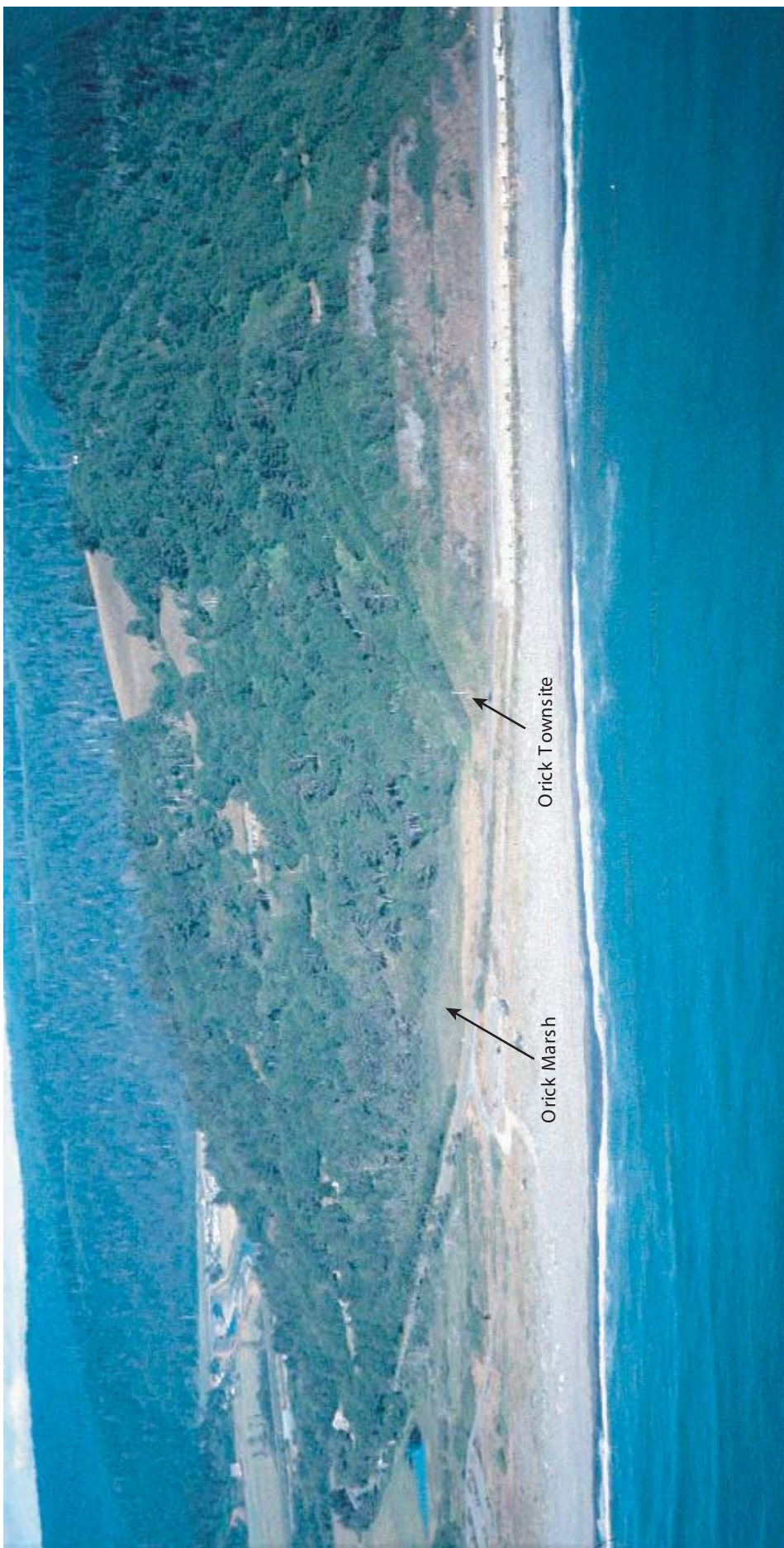
HUMBOLDT BAY ISFSI

FIGURE 2.6-107
DETAILED STRATIGRAPHY OF CORE LC-2
FROM THE LAGOON CREEK MARSH.
DIAGRAMS SHOW TYPICAL MARSH, SAND
DEPOSITS AND DIATOMS NEAR THE COAST



**FSAR UPDATE
HUMBOLDT BAY ISFSI
FIGURE 2.6-108**

Townsite of Orekw (Oreck) and location of cores in Orick marsh. Map shows the village Orekw, the site of Tskerkr's oral history, A Flood (Kroeber, 1976; Carver and Carver, 1996). Also shown is Ida's house site, where floodwaters came to "the front door." Both stories document flooding to about 66 and 69 feet elevation (MLLW). The cores from the Orick marsh record the "Y," as well as earlier tsunami intrusions, and one later tsunami.



FSAR UPDATE
HUMBOLDT BAY ISFSI
FIGURE 2.6-109 TOWNSITE OF ORICK AND THE ORICK MARSH AT THE MOUTH OF REDWOOD CREEK (ON LEFT SIDE OF PHOTO). THE TOWN WAS BUILT ON THE HILLSLOPE ABOVE THE BEACH AND MARSH

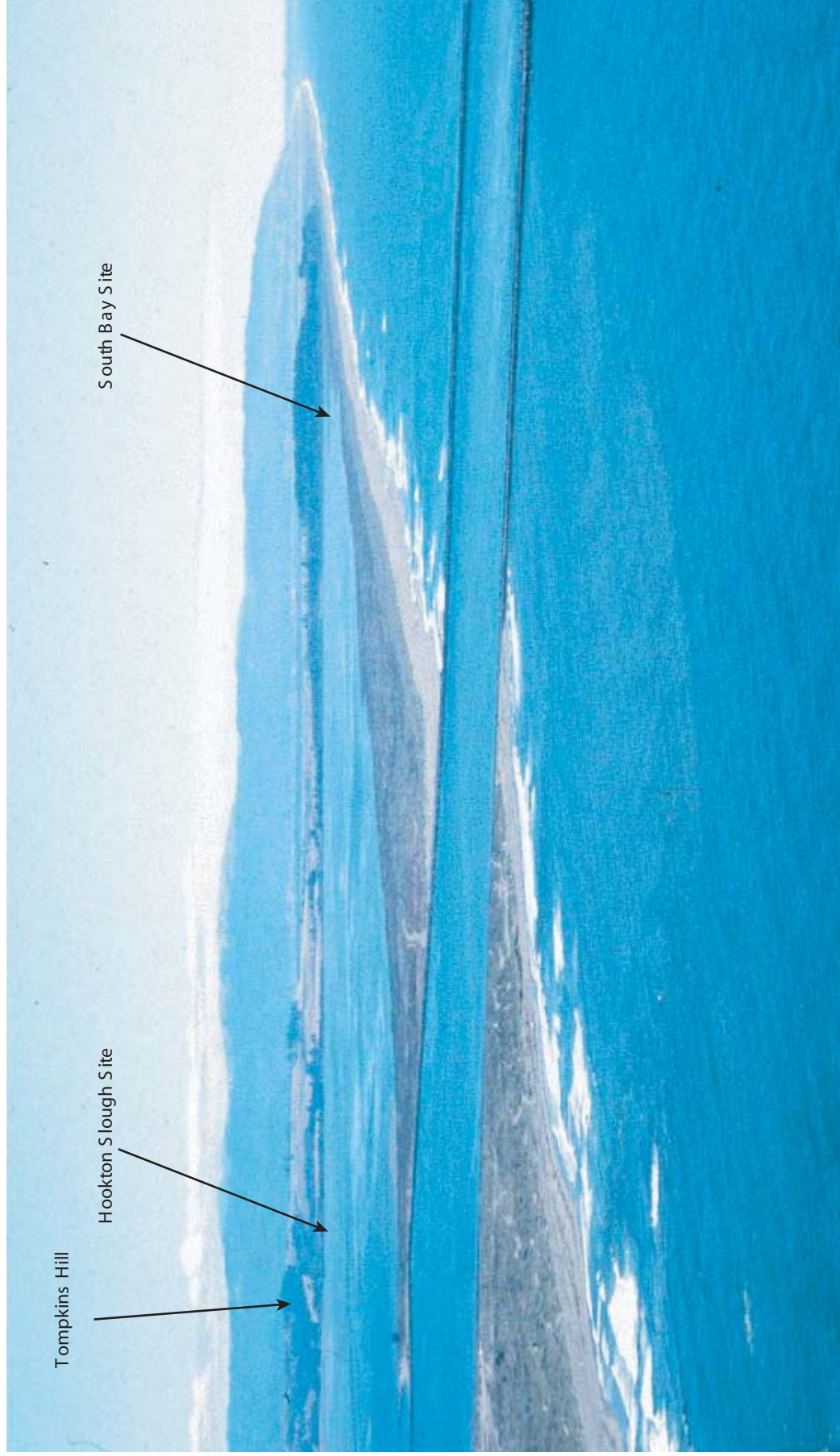


FSAR UPDATE
HUMBOLDT BAY ISFSI
FIGURE 2.6-110 GEOMORPHOLOGY OF THE NORTH AND SOUTH SPITS OF HUMBOLDT BAY

Revision 0 January 2006



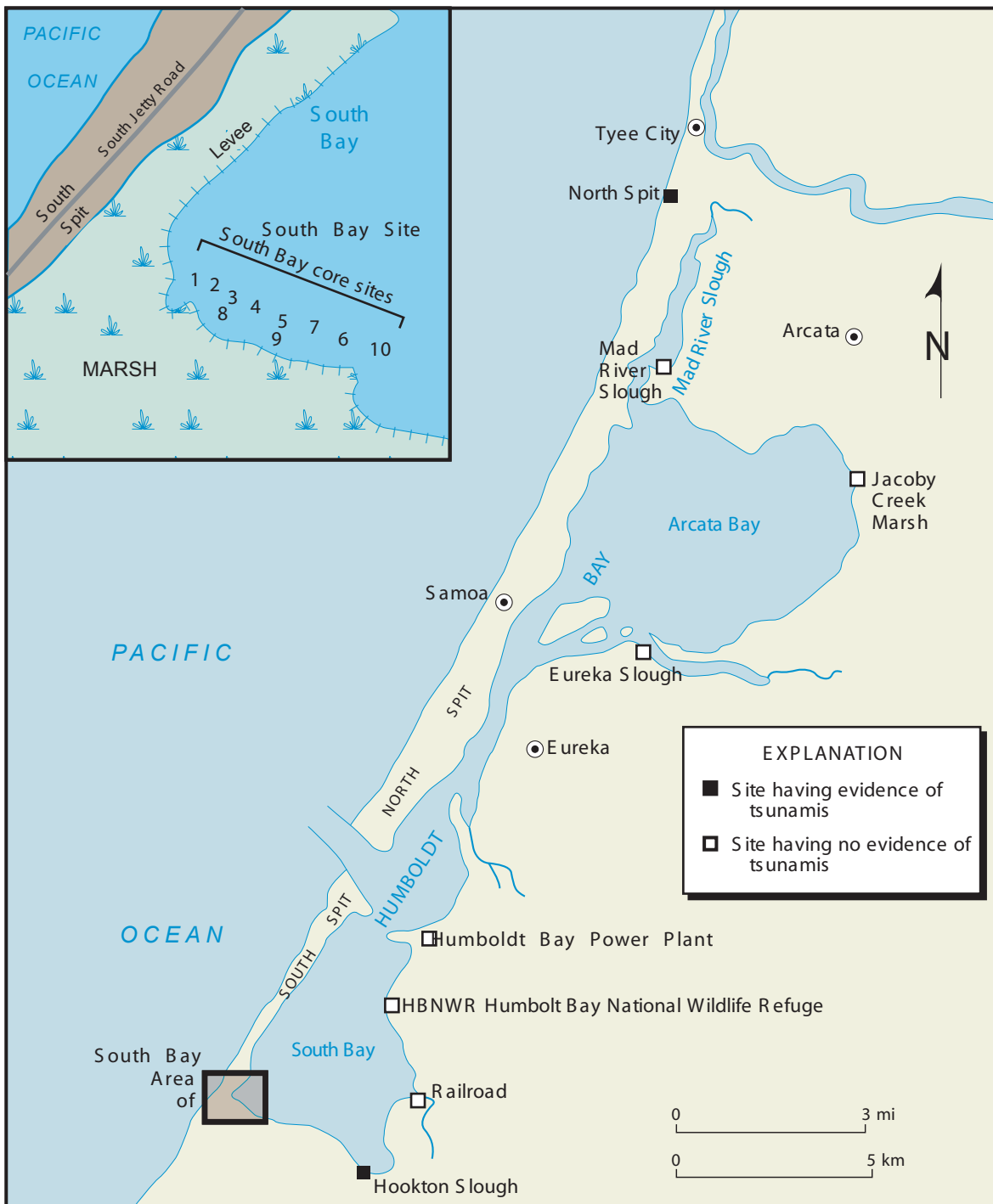
FSAR UPDATE
HUMBOLDT BAY ISFSI
FIGURE 2.6-111 SOUTH SPIT. VIEW LOOKING NORTH FROM TABLE BLUFF. SOUTHWESTERN HUMBOLDT BAY (SOUTH BAY) MARSH SITE IS IN MIDDLE RIGHT OF PHOTO



FSAR UPDATE
HUMBOLDT BAY ISFSI
FIGURE 2.6-112 MOUTH OF HUMBOLDT BAY AND THE SOUTH BAY HOOKTON SLOUGH SITES. SOUTH BAY IS SEPARATED FROM EEL RIVER VALLEY BY TOMPKINS HILL AND TABLE BLUFF



FSAR UPDATE
HUMBOLDT BAY ISFSI
FIGURE 2.6-113 LAG PEBBLES AT EL. 27 FEET (MLLW) ON THE SAND DUNES ON THE NORTH SPIT BELIEVED TO BE DEPOSITED BY A TSUNAMI THAT INUNDATED THE DUNES

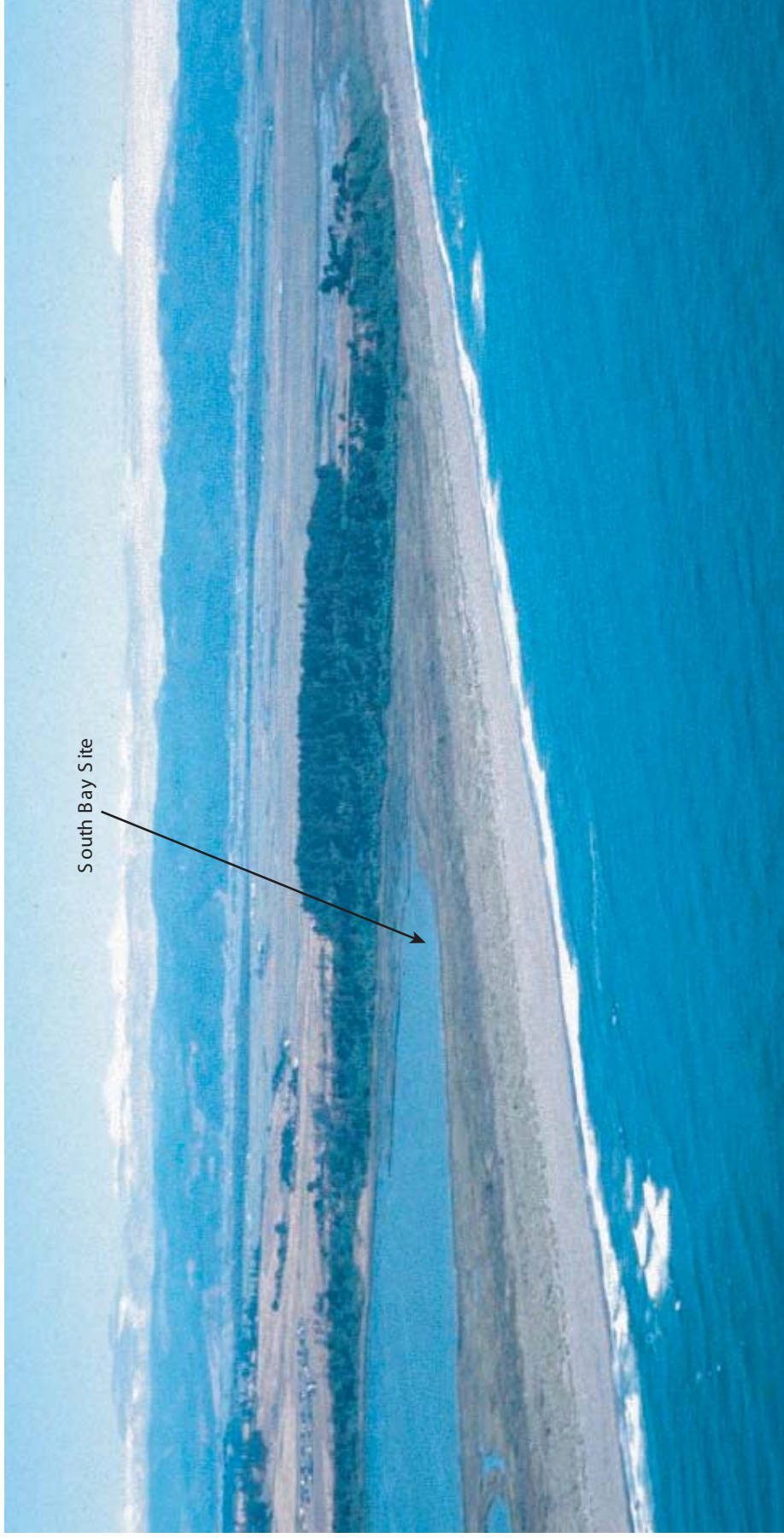


FSAR UPDATE

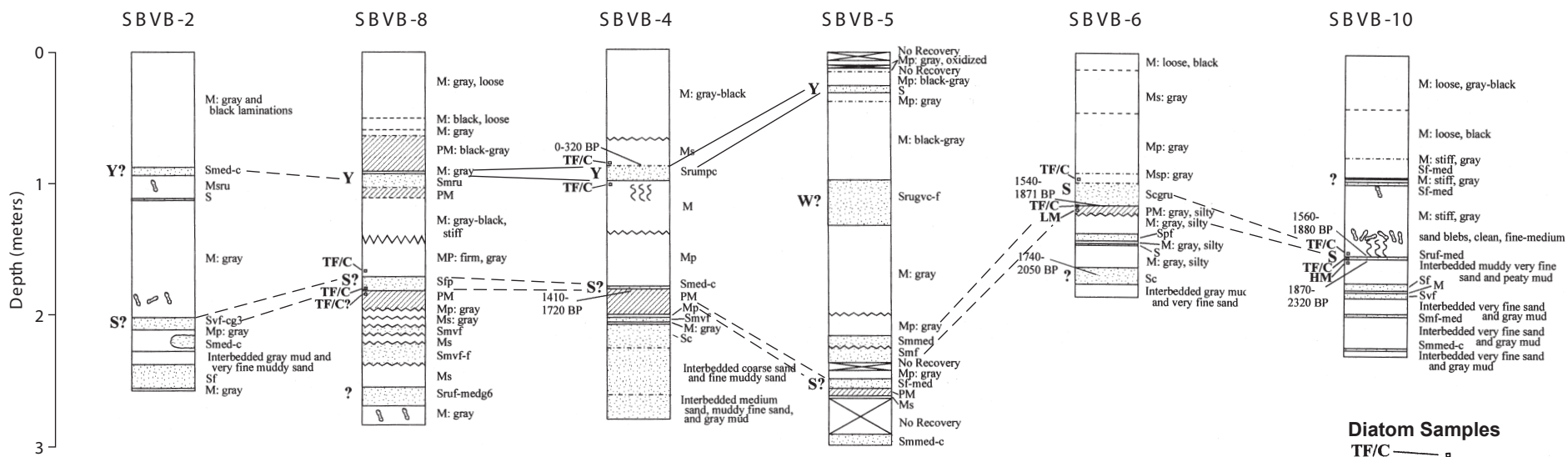
HUMBOLDT BAY ISFSI

**FIGURE 2.6-114
MAP OF THE NORTH SPIT SITE,
SOUTH BAY, AND OTHER
HUMBOLDT BAY MARSH SITES**

Revision 0 January 2006



FSAR UPDATE
HUMBOLDT BAY ISFSI
FIGURE 2.6-115 SOUTH BAY SITE. TABLE BLUFF IN THE MIDDLE OF THE PHOTO SEPARATES THE EEL RIVER VALLEY IN THE MIDDLE DISTANCE FROM SOUTH BAY ON THE LEFT



Diatom Samples
 TF/C = Tidal Flat/Channel
 LM = Low Marsh
 HM = High Marsh

Lithologies		Lithologic Modifiers and Symbols	
P	peat	s	sandy
MP	muddy peat	m	muddy
PM	peaty mud	p	peaty
M	mud	c	coarse
S	sand	med	medium
Ash		f	fine
		vf	very fine
		ru	rip-up clasts
		d	detritus
		g#	normally graded, # of normally graded sequences
		leaves	leaves
		wood chunks	wood chunks
		stick	stick
		twig	twig
		spruce cone	spruce cone
		charcoal	charcoal
		sand vein	sand vein
		pebble	pebble
		roots	roots

Contacts	
—	Abrupt (≤ 1 mm)
---	Sharp (1-3 mm)
----	Gradational (4-10 mm)
-----	Diffuse (11-20 mm)
~~~~~	Diffuse ( $\geq 20$ mm)
Radiocarbon ages reported in calibrated years before AD 1950	
BP dates refer to calibrated radiocarbon years before present.	

"Y" and "S" are events from Cascadia Earthquakes (Figure 2.6-96)

(From Carver and others, 1998)

**FSAR UPDATE**

**HUMBOLDT BAY ISFSI**

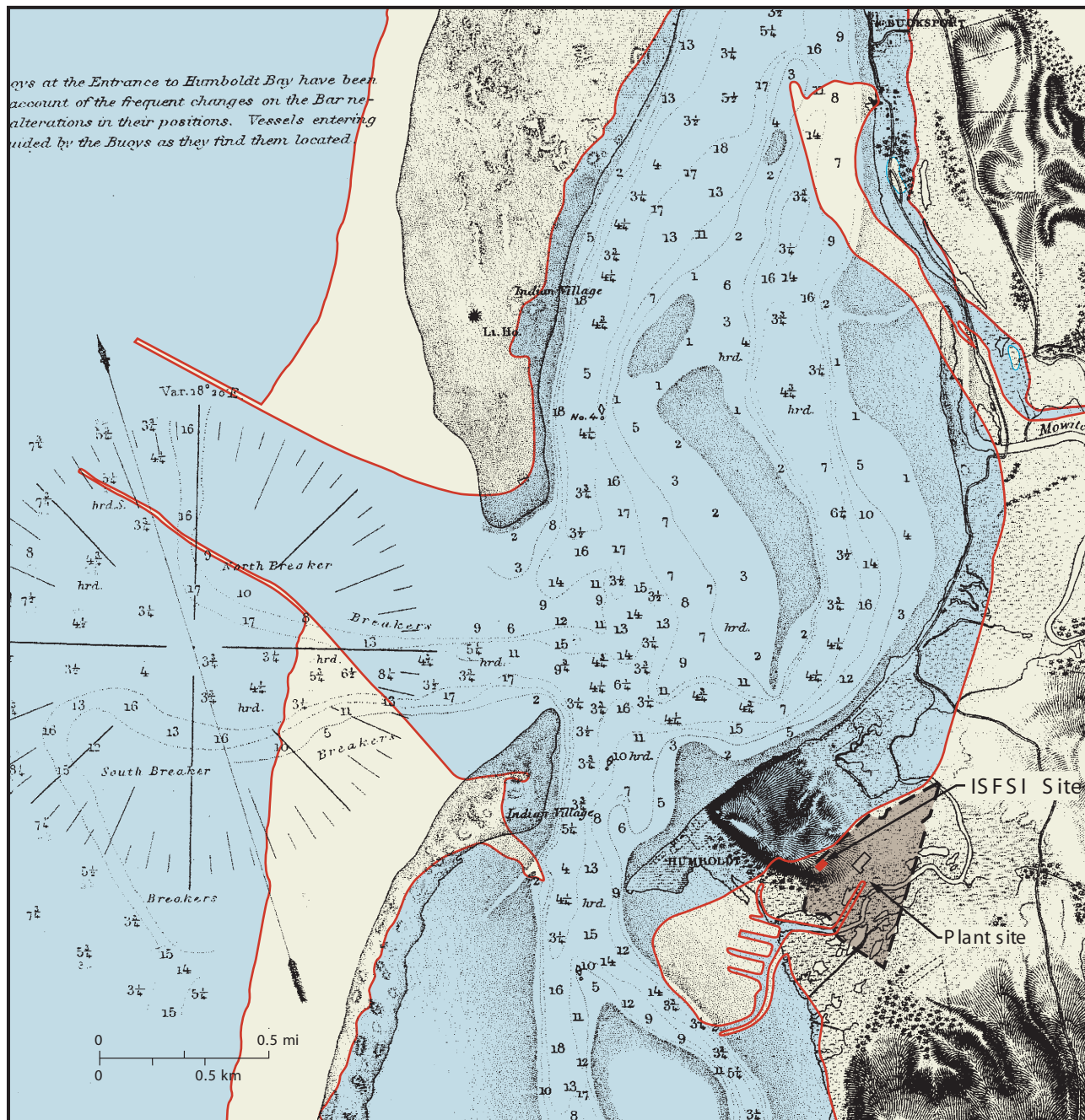
**FIGURE 2.6-116**

**CORRELATION OF TSUNAMI SANDS**

**IN SELECTED CORES ACROSS THE SOUTH**

**BAY MARSH**

Revision 0 January 2006



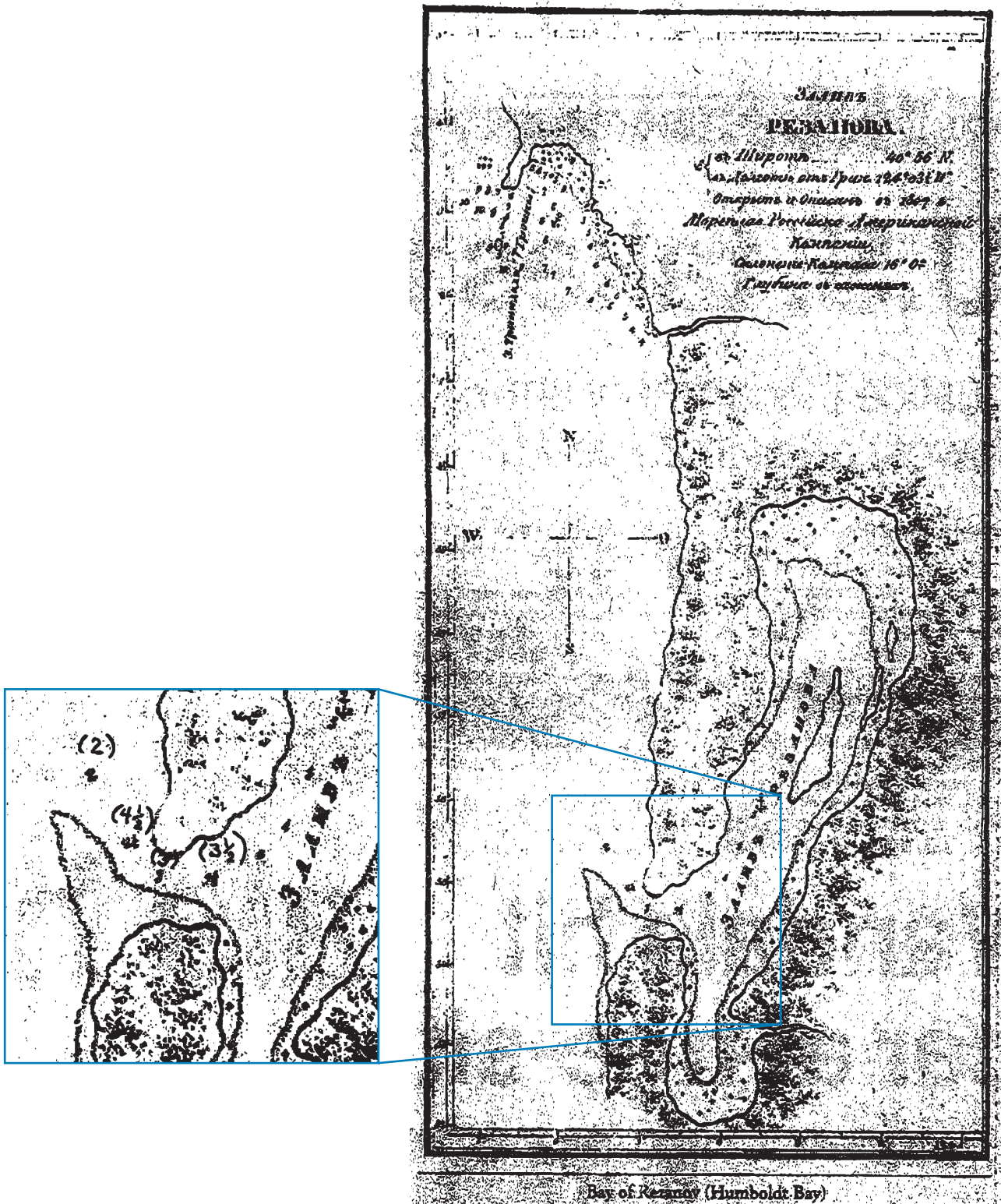
Preliminary Survey of Humboldt Bay, California, U.S. Coast Survey, 1858 (edition of 1879), (original scale 1:30,000) (aids to navigation corrected to 1885). Depths are in feet below mean lower low water to lowest dotted line, then in fathoms. Red line delineates present shoreline and jetties from USGS Fields Landing 7.5 minute Quadrangle (1989). Brown area is plant site.

## FSAR UPDATE

### HUMBOLDT BAY ISFSI

#### FIGURE 2.6-117 PRESENT COASTLINE SUPERIMPOSED ON THE 1858 MAP OF MOUTH OF HUMBOLDT BAY

Revision 0 January 2006



Soundings are in sazhen (Dr. Lydia Black, personal communication, 2001) (1 sazhen is about 7 feet); numbers in parentheses in the entrance channel clarify the original sounding. Original map in Golovnin, Vasili, undated, Voyage of Kamchatka and maps which accompany - Russian ed., Alaska State Historical Library, Juneau, Alaska

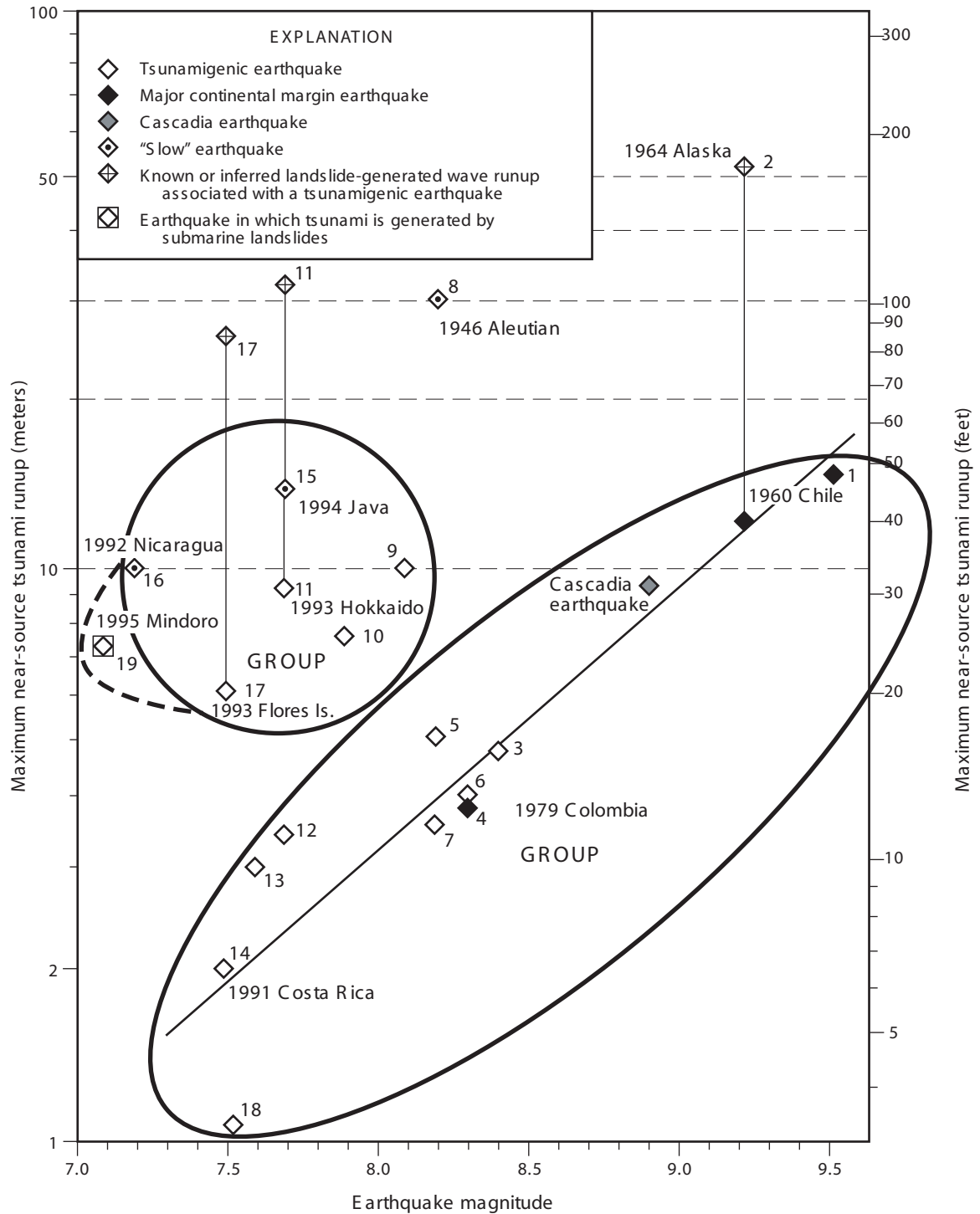
FSAR UPDATE

HUMBOLDT BAY ISFSI

FIGURE 2.6-118  
THE 1806 MAP OF HUMBOLDT BAY  
(BAY OF REZANOV) MADE BY  
RUSSIAN EXPLORERS

Revision 0 January 2006



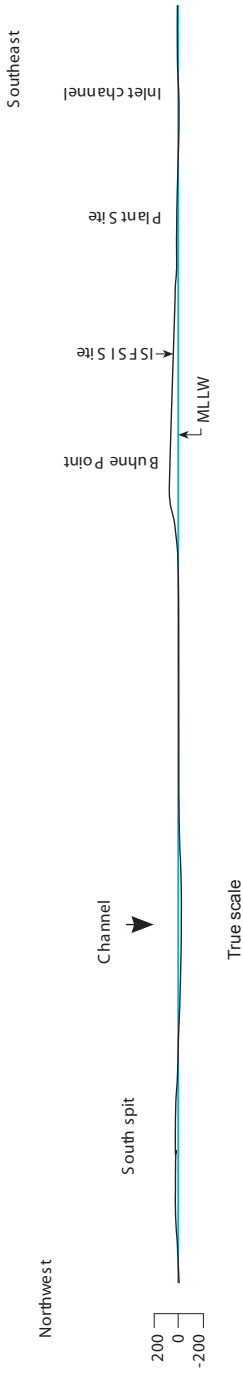


**FSAR UPDATE**

**HUMBOLDT BAY ISFSI**

**FIGURE 2.6-119**

**PLOT OF MOMENT MAGNITUDE VERSUS AVERAGE MAXIMUM TSUNAMI RUNUP FOR THE BETTER-DOCUMENTED TSUNAMIGENIC EARTHQUAKES**





# HUMBOLDT BAY ISFSI FSAR UPDATE

## CHAPTER 3

### PRINCIPAL DESIGN CRITERIA

#### CONTENTS

Section	Title	Page
3.1	PURPOSES OF INSTALLATION	3.1-1
3.1.1	Material to be Stored	3.1-1
3.1.2	References	3.1-4
3.2	DESIGN CRITERIA FOR ENVIRONMENTAL CONDITIONS AND NATURAL PHENOMENA	3.2-1
3.2.1	Tornado And Wind Loadings	3.2-2
3.2.2	Water Level (Flood) Design	3.2-4
3.2.3	Tsunami	3.2-5
3.2.4	Seismic Design	3.2-6
3.2.5	Snow and Ice Loadings	3.2-9
3.2.6	Lightning	3.2-9
3.2.7	Temperature and Solar Radiation	3.2-9
3.2.8	Combined Load Criteria	3.2-10
3.2.9	References	3.2-10
3.3	DESIGN CRITERIA FOR SAFETY PROTECTION SYSTEMS	3.3-1
3.3.1	HI-Star HB System	3.3-1
3.3.2	ISFSI Concrete Storage Vault	3.3-9
3.3.3	Cask Transporter	3.3-12
3.3.4	References	3.3-15
3.4	SUMMARY OF DESIGN CRITERIA	3.4-1
3.4.1	References	3.4-1

# HUMBOLDT BAY ISFSI FSAR UPDATE

## CHAPTER 3

### **PRINCIPAL DESIGN CRITERIA**

#### TABLES

<u>Table</u>	<u>Title</u>
3.1-1	HBPP Fuel Inspection Guidelines
3.1-2	Summary of Fuel Physical Characteristics
3.1-3	Potential Greater than Class C Waste
3.2-1	HI-STAR 100 System Tornado Design Parameters
3.2-2	HI-STAR 100 System Tornado Missile Design Parameters
3.2-3	Environmental Design Temperatures and Insolation Values for the Humboldt Bay ISFSI Site
3.4-1	Design Criteria for Environmental Conditions and Natural Phenomena Applicable to the Major ISFSI Structures, Systems, and Components
3.4-2	Principal Design Criteria Applicable to the HI-STAR HB System
3.4-3	Design Criteria for Storage Vault
3.4-4	Design Criteria for Transporter
3.4-5	List of ASME Code Alternatives for HI-STAR HB System

# HUMBOLDT BAY ISFSI FSAR UPDATE

## CHAPTER 3

### **PRINCIPAL DESIGN CRITERIA**

#### FIGURES

<u>Figure</u>	<u>Title</u>
3.2-1	Cask Vault
3.3-1	MPC-HB Enclosure Vessel
3.3-2	MPC-HB Fuel Basket
3.3-3	HI-STAR HB Overpack
3.3-4	GTCC Cask Assembly Overview
3.3-5	Process Waste Container

### **3.1 PURPOSES OF INSTALLATION**

The Humboldt Bay Independent Spent Fuel Storage Installation (ISFSI) is designed for interim, dry, and below ground vault storage of intact and damaged spent nuclear fuel assemblies, and reactor-related greater than class C (GTCC) waste from Humboldt Bay Power Plant (HBPP) Unit 3. The ISFSI uses the Holtec International HI-STAR HB storage system, as discussed in Section 1.1.

The material from the HBPP spent fuel pool is sealed in multi-purpose canisters custom-designed for HBPP fuel (MPC-HBs), and the MPCs are stored in HI-STAR HB storage/transportation overpacks in a reinforced concrete vault. The ISFSI is designed to store up to 400 spent fuel assemblies in five casks, with a sixth cask to store GTCC waste.

Each MPC-HB can store up to 80 spent nuclear fuel assemblies. Each MPC-HB is also capable of storing 80 damaged fuel containers (DFCs), of which 28 or 40, depending on the loading pattern, can contain damaged fuel as needed to store the entire HBPP spent fuel inventory at the ISFSI.

#### **3.1.1 MATERIAL TO BE STORED**

The materials to be stored at the ISFSI consist of intact fuel assemblies, damaged fuel assemblies, and GTCC waste. The fuel assemblies may be stored with, or without channels. There are 390 fuel assemblies in the HBPP inventory, and a quantity of loose debris that could constitute an equivalent of one additional assembly. Each fuel assembly contains approximately 192 pounds (87 kg) of  $\text{UO}_2$ . Damaged fuel is stored in a damaged fuel container (DFC) in an MPC-HB in accordance with ISG-1, Revision 1 (Reference 1). Damaged fuel in the form of loose fuel rods, fuel pellets, etc. can be consolidated; however, the amount of fuel debris in a single DFC is limited to the total fissile material and weight of a single intact fuel assembly. The loose debris may be stored in one or two DFCs to optimize the retrieval and handling operations.

Video inspection of the Humboldt Bay spent fuel assemblies was conducted in 2000-2001 using the guidance of ISG-1 Revision 0, Nuclear Energy Institute comments on ISG-1, and the definitions of damaged fuel and fuel debris contained in the Holtec HI-STAR 100 Certificate of Compliance (CoC). Eleven fuel assemblies were initially classified as damaged and 16 were classified as fuel debris. A supplemental evaluation of the 2000-2001 video records will be performed prior to fuel loading using the guidelines in Table 3.1-1, which meets the intent of ISG-1 Revision 1.

Discussed herein are the characteristics of these materials and how the HI-STAR HB storage system design criteria envelopes these characteristics.

### 3.1.1.1 Physical Characteristics

The spent fuel assemblies to be stored consist of General Electric Type II (a 7 x 7 array of fuel rods), General Electric Type III, Exxon Type III, and Exxon Type IV (a 6 x 6 array of fuel rods) fuel assemblies. Construction details for each type are similar (References 2 through 5). The main support structure for an assembly consists of fuel rods used as tie rods between upper and lower tie plates. All assemblies use three spacer grids attached to a single spacer capture rod to maintain fuel rod spacing. The licensing basis fuel cladding material for all assemblies is any zirconium-based alloy, consistent with the HI-STAR 100 System CoC. Fuel records indicate that all HBPP fuel cladding material for intact and damaged assemblies is Zircaloy-2. Channels are fabricated from Zircaloy material. The loose fuel debris described in Section 3.1.1 may have either Zircaloy cladding, stainless steel cladding, or may be unclad pellets. A summary of the physical characteristics of the Humboldt Bay fuel proposed for storage at the ISFSI is shown in Table 3.1-2.

Fuel records have been maintained to identify the configuration and initial enrichment of each fuel assembly. Each fuel assembly is identified with a unique identification number. Each assembly will be recorded as to its cask loading location.

### 3.1.1.2 Thermal and Radiological Characteristics

The thermal and radiological characteristics of the HBPP fuel to be stored are summarized below, and constitute limiting values for storage of fuel assemblies at the Humboldt Bay ISFSI. The values listed below were used in the analyses supporting the design and bound the actual values for these parameters for the entire HBPP spent fuel inventory to provide margin. All loose fuel debris is bounded by these parameters.

#### (1) Heat Generation

The maximum permitted heat generation rate for a single assembly that is stored at the Humboldt Bay ISFSI is 50 watts. The maximum total heat load for a single cask is 2000 watts.

#### (2) Fuel Burnup

The maximum average fuel burnup per assembly of any fuel that is stored at the ISFSI is 23,000 MWD/MTU.

#### (3) Cooling Time

The minimum cooling time of any fuel that is stored at the ISFSI is 29 years at the time of the first fuel loading in the ISFSI.



(4) Enrichment

The maximum planar-average enrichment for any one fuel assembly is 2.60 wt. %  $^{235}\text{U}$ .

The minimum planar-average enrichment for any one fuel assembly is 2.08 wt. %  $^{235}\text{U}$ .

(5) External Condition

The fuel cladding surface is fairly uniformly coated with a crud layer, which appears to be primarily oxide from the carbon steel piping system. The actual thickness of the oxide has not been determined. However, NUREG 0649 states that typically, the oxide buildup on BWR pins is on the order of 25 to 100 microns and in the form of  $\text{Fe}_2\text{O}_3$ . The NUREG further states that a calculation was made to determine whether a 100 micron buildup would affect heatup of the pins during a pool drainage accident, and found that the overall effect on pin temperature was less than one degree. There are several assemblies that have additional loose crud material attached.

### 3.1.1.3 Non-fuel Hardware and Neutron Sources

No non-fuel hardware or neutron sources are to be stored at the Humboldt Bay ISFSI.

### 3.1.1.4 Greater Than Class C Waste

Table 3.1-3 lists neutron activated components and materials at HBPP that may potentially be classified as GTCC and stored at the ISFSI. The activated metals have been placed on this list due to close proximity to the reactor core (e.g., within approximately 12 inches of active fuel) and exposure to a peak core thermal neutron flux of slightly greater than  $1 \times 10^{13}$  neutrons/sec/cm² during 13 years of reactor operation. The actual quantity of activated metals may be less than that listed, due to the conservatism used in this assumption. An accurate classification of this waste material will be performed prior to loading into the GTCC Waste Container (GWC). The process waste material was generated during cleanup of the spent fuel pool. The material consists of distributed and particulate SNM waste mixed with resins, metallic oxides, and small Stellite particles. The total activity is 4.85E+4 mCi, of which there are 18.3 grams of SNM waste. After thermal processing, the processed waste material will be in the form of dry concentrated residue.

As shown on Figure 3.3-4, the GWC is contained within HI-STAR HB GTCC Overpack. The GWC is similar to the Multi-Purpose Canister (MPC) within a spent fuel cask. Also shown is the Outer Container that is welded onto the bottom of the GWC. The process waste will be contained in a Process Waste Container (PWC), shown on Figure 3.3-5. The PWC is stainless steel, cylindrical container, approximately 12 inches in diameter and 24 inches high and will be mechanically sealed, vacuumed dried, backfilled with

9-01

## HUMBOLDT BAY ISFSI FSAR UPDATE

helium and leak tested. The PWC will be placed within the Outer Container inside the GWC. The Outer Container is designed to provide stabilization for the PWC. A lid will be placed on top of the Outer Container. The activated metals will be placed inside the GWC and outside the Outer Container. Therefore, the process waste is prevented from co-mingling with the GTCC activated metals.

After loading the GTCC waste into the GWC, a lid will be placed on top of the GWC and will be welded to the shell. The GWC will be vacuumed dried, backfilled with helium and leak tested. Then a lid will be placed on top of the HI-STAR HB GTCC Overpack and bolted shut.

The radiation dose at the surface of the HI-STAR HB GTCC Overpack is bounded by that assumed in the analysis performed for a HI-STAR HB spent fuel overpack. GTCC is stored in a separate cask from spent fuel in accordance with 10 CFR 72.120(b)(1). There are no criticality or decay heat issues associated with the storage of GTCC waste.

### 3.1.2 REFERENCES

1. Interim Staff Guidance 1, Damaged Fuel, USNRC, Revision 0, May 1999 and Revision 1, October 2002.
2. General Electric Drawing GE 731E272 (GE Type II Fuel Assembly), PG&E Drawing #6019924, Sheet 13.
3. General Electric Drawing GE 731E228 (GE Type III Fuel Assembly), PG&E Drawing #6019924, Sheet 14.
4. Exxon Nuclear (Jersey Nuclear) Drawing Nuclear R-1330 (Exxon Type III Fuel Assembly), PG&E Drawing #6019924, Sheet 15.
5. Exxon Nuclear Drawing XN 300.900 (Exxon Type IV Fuel Assembly), PG&E Drawing #6019924, Sheet 16.

### **3.2 DESIGN CRITERIA FOR ENVIRONMENTAL CONDITIONS AND NATURAL PHENOMENA**

This section summarizes the design criteria for the Humboldt Bay Independent Spent Fuel Storage Installation (ISFSI) structures, systems, and components (SSCs) that are classified as important to safety and designed to withstand the effects of site-specific environmental conditions and natural phenomena. Regulatory requirements and guidance were based upon, as applicable, 10 CFR 72 (Reference 1), Regulatory Guide (RG) 3.62 (Reference 2), the Standard Review Plan for ISFSIs (Reference 3), and the Standard Review Plan for Dry Cask Storage Systems (Reference 4). NRC Interim Staff Guidance (ISG) documents were also considered, as applicable. Humboldt Bay site-specific information for environmental conditions and natural phenomena was taken primarily from other parts of this Final Safety Analysis Report Update (FSAR). Holtec storage system generic design criteria were taken from the HI-STAR 100 System FSAR (Reference 5).

As discussed in Section 4.5, the ISFSI SSCs are classified as important-to-safety (ITS) or not important-to-safety (NITS) based on their design function. Among the SSCs classified as ITS is the multi-purpose canisters (MPC), the damaged fuel containers (DFCs), the HI-STAR HB overpack, the storage vault, and the onsite cask transporter. The ITS classification indicates that at least one subcomponent of the main component is classified as ITS. Other subcomponents may be classified as NITS, based on the function of the subcomponent. Design criteria for environmental conditions and natural phenomena for these key ISFSI SSCs are described in this section. Other design criteria for these key ISFSI SSCs are contained in Section 3.3.

Environmental conditions and natural phenomena specific to the Humboldt Bay Power Plant (HBPP) and ISFSI site are described and characterized in Chapter 2.

The storage system used at the ISFSI is the HI-STAR HB System. The HI-STAR HB System is a shortened version of the generically certified HI-STAR 100 System (Reference 6). The HI-STAR HB System is designed to ensure that fuel criticality is prevented, fuel cladding and confinement integrity are maintained, the fuel remains retrievable, and radiation shielding is maintained under all Humboldt Bay site-specific design basis loadings due to environmental conditions and natural phenomena.

The safe storage of the spent fuel assemblies depends upon the capability of the HI-STAR HB System to perform its design functions. The HI-STAR HB System is a self-contained, independent, passive system that does not rely on any mechanical systems for normal storage operations. A description of the HI-STAR HB System, including a list of differences between the HI-STAR HB and the HI-STAR 100 Systems is provided in Section 4.2.3. The text of this section refers to the HI-STAR 100 System or the HI-STAR HB System, as appropriate for the discussion.

The criteria used for the design of the HI-STAR HB System were determined for site-specific licensing under 10 CFR 72. The design criteria of the generic HI-STAR 100

## HUMBOLDT BAY ISFSI FSAR UPDATE

System were chosen for use in the design of the Humboldt Bay ISFSI and HI-STAR HB System if they were appropriate to use (i.e., if they bounded the Humboldt Bay site-specific conditions). The generic HI-STAR 100 System design criteria were chosen to ensure that most 10 CFR 50 licensees could use the HI-STAR 100 System at an onsite ISFSI under the general license provisions of 10 CFR 72. The principal design criteria for the HI-STAR 100 System meet all requirements of 10 CFR 72 and are described in Chapter 2 of the HI-STAR 100 System FSAR.

Environmental conditions and phenomena are summarized in this section for the important-to-safety SSCs, and include:

- Tornado and wind loadings, including tornado-borne missiles
- Water level (flood)
- Tsunami
- Seismic
- Snow and ice loadings
- Lightning
- Temperature and solar radiation
- Combined load criteria

The HI-STAR HB System design features are evaluated in detail for fuel handling activities in the HBPP 10 CFR 50 facilities in license amendment request (LAR) 04-02, submitted to the NRC in July 2004 (Reference 11). The LAR describes MPC fuel loading in the spent fuel pool, draining, drying, sealing, helium filling, and helium leak testing the MPC while inside the HI-STAR cask; and loading the cask onto the cask transporter for onsite transfer to the ISFSI. The NRC issued HBPP License Amendment 37 (Reference 12) to allow implementation of LAR 04-02.

### **3.2.1 TORNADO AND WIND LOADINGS**

#### **3.2.1.1 Applicable Design Parameters**

As stated in Section 2.3.2, the highest recorded peak wind gust at the HBPP site is 69 mph. For storage system design purposes, a wind velocity of 85 mph is used with a gust factor of 1.1, which envelopes the recorded, peak-gust value of 69 mph.

Over the period from 1950 through 1994, there has only been one tornado recorded in the Eureka area. This tornado occurred on March 29, 1958, and its associated intensity

## HUMBOLDT BAY ISFSI FSAR UPDATE

level, using the Fujita Scale, was estimated to be an F-2 event, i.e., tornado wind speeds between 113 and 157 mph.

The Humboldt Bay ISFSI is located in tornado intensity Region II, based on the RG 1.76 (Reference 7) classification system. RG 1.76 identifies a maximum wind speed of 300 mph for Region II. This wind speed is conservative for the Humboldt Bay ISFSI based on historical meteorological data.

The HI-STAR 100 System, (which is identical to the HI-STAR HB System with respect to its ability to withstand the effects of a tornado), is generically designed to withstand pressures, wind loads, and missiles generated by a tornado as described in Section 2.2.3.5 of the HI-STAR 100 System FSAR. The design-basis tornado and wind loads for the HI-STAR 100 System are consistent with RG 1.76, ANSI/ANS 57.9 (Reference 8), and ASCE 7-88 (Reference 9) for Region I as indicated in the HI-STAR FSAR Tables 2.2.4 and 2.2.5.

The design criteria in HI-STAR 100 System FSAR, Section 2.2.3.5 and Tables 2.2.4 and 2.2.5 for Region I wind speeds bound the applicable wind speed requirements for the Humboldt Bay ISFSI site and are considered the Humboldt Bay ISFSI design basis. Wind speeds (rotational and translational) and pressure drops established as the design basis for the Humboldt Bay ISFSI and HI-STAR HB System are taken from the HI-STAR 100 System FSAR and presented in Table 3.2-1. These values are significantly higher than the site-specific licensing basis tornado data discussed in Sections 2.2 and 2.3 and provide defense-in-depth for the design. Tornado-induced missiles are discussed in Section 3.2.1.3.

### **3.2.1.2 Determination of Forces on Structures**

Tornado wind loads include consideration of the following, as applicable: (a) tornado wind load, (b) tornado differential pressure load, and (c) tornado missile impact load. The method of combining the applicable effective tornado wind, differential pressure, and missile impact loads to determine the total tornado load is in accordance with NUREG-0800, Section 3.3.2 (Reference 10).

### **3.2.1.3 Tornado Missiles**

The HI-STAR 100 System is generically designed to withstand three types of tornado-generated missiles. The characteristics of these missiles are provided in Table 3.2-2 and are consistent with the Spectrum I missiles described in NUREG-0800, Section 3.5.1.4, and with Table 2.2.5 in the HI-STAR 100 System FSAR. The design basis for these missiles is discussed in Section 2.2.3.5 of the HI-STAR 100 System FSAR. The mass and velocity of these missiles constitute the design basis for the Humboldt Bay ISFSI site and the HI-STAR HB cask system.

Section 2.2.3.5 of the HI-STAR 100 System FSAR describes conformance with NUREG-0800, Section 3.5.1.4, which requires that postulated tornado missiles include



## HUMBOLDT BAY ISFSI FSAR UPDATE

at least three objects: a massive high kinetic energy missile that deforms on impact, a rigid missile to test penetration resistance, and a small rigid missile of a size sufficient to just pass through any openings in protective barriers. NUREG-0800 Section 3.5.1.4 suggests that these missiles should be assumed to be an 1800 kg automobile, a 125 kg eight-inch armor piercing artillery shell, and a 0.22 kg, one-inch solid steel sphere, all impacting at 35 percent of the maximum horizontal wind speed of the design basis tornado.

As discussed above, due to its similarity in design to the HI-STAR 100 System, the HI-STAR HB System can withstand impacts from the design basis tornado missiles. In addition, the vault structure provides additional defense-in-depth protection from the impact of tornado missiles on the cask during long-term storage operations at the ISFSI. Given the massive size of the reinforced concrete vault, specifically the lid thickness, tornado missiles and their impacts on the reinforced concrete structure will not produce any adverse structural effects on the vault or the HI-STAR HB cask inside the vault. While local spalling can occur on the lid and vault apron, the structural integrity of the vault will remain intact. The vault is not a target for horizontal missiles due its below-grade location. In addition, NUREG-0800, Section 3.5.1.4 indicates that vertical velocities should be considered at 70 percent of the postulated horizontal velocities, except for small missiles, which are used to test barrier openings. The HI-STAR HB system has no openings; therefore, small missiles are not required to be evaluated. The HI-STAR HB casks are designed to withstand 100 percent of the postulated horizontal missile velocities, which bounds the requirements for vertical missiles without taking credit for the vault structure.

As discussed in Section 8.2.2.2.1, during transport of the HI-STAR HB from the refueling building to the ISFSI vault and cask handling activities at the vault, the HI-STAR HB is exposed to the environment. The HI-STAR 100 System FSAR demonstrates that by comparison, the HI-STAR HB system is adequately designed for tornado missiles which bound the Humboldt Bay ISFSI tornado missile licensing basis. Additionally, the cask transporter has redundant drop protection, which makes a loss of load due to a direct missile strike on the transporter not credible.

In summary, the tornado licensing basis is that the HI-STAR HB provides adequate protection from tornado missiles during transportation, cask handling activities at the vault, and ISFSI storage conditions. The vault structure, while not relied upon to meet the tornado missile licensing basis does provide additional tornado missile protection. The vault structure missile protection capability is considered defense-in-depth and is discussed in this FSAR for information. These evaluations demonstrate that the tornado missile design criteria are in accordance with NUREG-0800 Section 3.5.1.4, 10 CFR 72.120(a) and 72.122(b).

### **3.2.2 WATER LEVEL (FLOOD) DESIGN**

The Humboldt Bay ISFSI site surface hydrology is described in Section 2.4.

## HUMBOLDT BAY ISFSI FSAR UPDATE

The ISFSI site is located on a relatively flat area on Buhne Point at elevation nominally 44 ft mean lower low water (MLLW). Surface drainage around the ISFSI area flows naturally into the existing plant drainage system. By way of the plant drain system, the surface water then discharges into the cooling water intake canal, flows through the plant, and discharges into Humboldt Bay via the cooling water discharge canal. Outside the area served by the plant drainage system, most of the surface runoff drains to the east and into the discharge canal. The remainder drains into Buhne Slough, a natural drainage for the area, which drains directly into both the intake canal and Humboldt Bay (see Figure 2.1-2). The elevation of the ISFSI is approximately 32 ft higher than the main power plant level. Thus any drainage will be away from the ISFSI area, and flooding is not a concern.

The HI-STAR HB System is designed to withstand pressure and water forces associated with flooding in the same manner as the HI-STAR 100 System. Table 2.2.8 of the HI-STAR 100 System FSAR indicates that the HI-STAR 100 overpack is capable of being submerged to a maximum depth of 656 ft. This flooding water depth is based on the submergence requirement of 10 CFR 71 for the dual purpose-certified HI-STAR 100 System.

Therefore, the HI-STAR HB System is designed to withstand the pressure and water forces associated with floods, based on the similarity in design to the HI-STAR 100 System. In conclusion, the ISFSI can withstand floods as required by 10 CFR 72.120(a) and 72.122(b).

### **3.2.3 TSUNAMI**

#### **3.2.3.1 ISFSI Storage Vault**

Section 2.6.9 describes the tsunami hazards for the Humboldt ISFSI site. The top of the ISFSI vault is at approximately elevation 44 ft above MLLW elevation. This elevation is higher than the tsunami height estimates considered in the studies for the Humboldt Bay ISFSI site, which include bounding estimates for distant tsunamis, modeling of locally generated tsunamis associated with the Cascadia subduction zone, and tsunami heights from geologic evidence of historical tsunamis inundating the region around the ISFSI site.

Using an estimate of 30 to 40 ft above MLLW elevation for the runup height of the tsunami at the bay entrance and an attenuation factor of 0.7 to 0.9, the inundation height would be 21 to 36 ft above MLLW elevation if the tsunami occurred at low tide, or 28 to 43 ft above MLLW elevation if the tsunami occurred at high tide at the ISFSI site. This maximum height is lower than the 44 ft MLLW elevation of the top of the ISFSI vault. Incorporating wave run-up for storms from Table 2.4-5, gives maximum value of 49.86 ft (including high tide and wave run-up for storms). The maximum tsunami occurring coincident with a design basis storm wave run-up and high tide is not considered credible.

Even if the tsunami flowed above the ISFSI elevation, the tsunami hazard at the ISFSI site is still considered negligible, because the HI-STAR HB System is designed to withstand the static pressure forces from submergence in 656 ft of water. Furthermore, the HI-STAR HB casks are contained in enclosed underground vaults that are designed to structurally withstand 6 ft of water head and that will protect them from damage by flowing water and water-born debris.

### **3.2.3.2 Onsite Cask Transport**

The design basis tsunami described above is a result of the design basis earthquake described in Section 3.2.4 below for the ISFSI site. As discussed in Section 3.2.4, a probabilistically determined 50 year earthquake return period spectrum is used for evaluating the onsite cask transport mode. Based on the information provided in Section 2.6.9, a 50-year return period earthquake is of insufficient size to create a tsunami that would cause flooding on the transport route. PG&E Response to NRC Question 4-1 (Reference 13) provides justification concerning using a 50-year versus a 200-year return period earthquake.

### **3.2.4 SEISMIC DESIGN**

In accordance with 10 CFR 72.103(f)(2)(i), the seismic design of the important-to-safety ISFSI SSCs, which include the HI-STAR HB overpack, the MPC-HB, the DFC, the onsite cask transporter, and the ISFSI vault, is based on design earthquake ground motions as described in Section 2.6.6. The design bases for the ISFSI SSCs, including analyses and design methods, are discussed in Sections 4.2, 4.3, 4.4.5, and 8.2.1. Seismic design for the loading and handling of the cask while in the Refueling Building are addressed as part of a 10 CFR 50 License Amendment Request (LAR) submittal to the NRC.

As discussed in Section 2.6.6, deterministic earthquake ground motion analyses were performed for the Humboldt Bay ISFSI site. Probabilistic seismic hazards analysis (PSHA) earthquake ground motion analyses were also performed in accordance with 10 CFR 72.103 and Regulatory Guide 3.73. Vibratory ground motions were considered in the design and analyses (Section 8.2.1) of the: (1) storage vault, (2) transport route/transporter, and (3) cask handling activities at the storage vault. Additional design and analyses were performed for cask handling activities in the HBPP Unit 3 Refueling Building as part of the 10 CFR 50 LAR. The approach used for developing the ground motion characteristics to be used for design and analyses of the ISFSI SSCs consisted of the following:

#### **Storage Vault Structural Analyses (Storage Mode)**

In accordance with 10 CFR 72.103, the licensing basis Design Earthquake (DE) for the ISFSI storage vault structural analyses is a probabilistically developed uniform hazard spectrum (UHS) with a 2000 year return period (reference probability of exceeding the DE is  $5E-4$ /yr). To provide additional margin, the ISFSI was analyzed to withstand a

## HUMBOLDT BAY ISFSI FSAR UPDATE

deterministically developed seismic spectra (see Figure 2.6-72) that exceeds the 2000-year return period UHS at all spectral periods.

Although not part of the Humboldt Bay ISFSI design basis, PG&E performed a supplementary evaluation to determine the potential amplifications of acceleration forces on the cask due to soil-structure interaction (SSI). The details of this supplementary evaluation are provided in PG&E Response to NRC Question 5-4 (Reference 14), and concluded the following:

There is no failure mode of the storage vault that could compromise the integrity of the overpack. The vault is conservatively designed to provide confidence that the overpacks will remain easily retrievable after a seismic event. Should the vault fail, the only consequence would be additional dose at the site boundary, but this would remain well within the 10 CFR 72.106 accident dose limits and could be mitigated by the use of temporary shielding.

Based on the results of the supplemental evaluation, the HI-STAR HB can withstand an amplification of its imposed vertical time history to a value of approximately 9.5 without exceeding its design basis deceleration limit. This magnitude of amplification as a result of SSI effects is not credible at the HB ISFSI site.

The maximum vertical excursion of the cask relative to the surrounding structure is determined to result in a vertical excursion that exceeds the cask-to-vault lid clearance, which suggests that the cask would impact the vault lid and likely lead to overstress of the lid bolts. Since maximum cask accelerations under this hypothetical amplified vertical seismic input occur if the cask is allowed to move freely within the vault, any restraint provided by the vault lid will serve to reduce the deceleration levels computed above.

Based on the above evaluation and documentation provided in Reference 14, it is concluded that the ISFSI vault lid and lid closure bolts are classified as ITS Category B, except for beyond design seismic events involving SSI, which results in vertical acceleration causing vault lid impacts. For these postulated SSI seismic events, the ISFSI vault lid and lid closure bolts are classified as NITS since they are not relied upon in the seismic design basis accident analysis. As stated above, for these postulated SSI seismic events the lid is only required for shielding purposes, and after any accident of this magnitude, temporary shielding could be emplaced prior to reaching any 10 CFR 100 limits.

### **Transport Route/Transporter Stability (Transportation Mode)**

For transient activities, the appropriate return period of the ground motion is determined by computing the return period that will result in a  $5E-4$  annual probability of being exceeded. It is given by:

## HUMBOLDT BAY ISFSI FSAR UPDATE

$$\text{Return Period (yr)} = \frac{\text{Annual Exposure Time (days)}}{365} \frac{1}{\text{DE Reference Probability}}$$

where the DE Reference Probability is 5E-4

The transport route, as discussed in Section 4.3.3, is approximately 0.238 miles long. As indicated in Table 3.4-4, the nominal transporter speed is 0.4 mph. Including rail dolly transfer time, it is conservatively assumed that each transport activity requires 0.5 days, resulting in a total of transport time, for 5 casks, of 2.5 days. Using the above equation results in a return period of 14 years for this transient activity. Conservatively, a UHS exceeding a 50 year return period is used for evaluating the transport mode.

In NRC Question 2-12 (Reference 13), the NRC requested PG&E to provide analyses for the transporter route/transport stability and storage vault cask handling activities using the design basis event loads based on the 2,000-year return period ground motions. In the PG&E response to this question, the reason for PG&E's belief that use of a 2,000-year return period is not required were explained in detail.

### **Storage Vault Cask Handling Activities (Vault Cask Handling Mode)**

As discussed in Section 5.1.1.3, the transporter will be used to lower the overpack into the vault. Bolted vault lids, base gussets, and cask alignment plates are used to secure the overpack in the vault (Figure 3.2-1). The ISFSI vault and associated cask restraints are an integral part of the seismic design of the cask system. The ISFSI vault lids are not part of the seismic restraint. They are provided for radiation shielding, prevention of unauthorized access to the vaults, and additional protection of the casks from the elements and natural phenomena. Based on information from the transporter supplier, the beam on top of the crawler moves at approximately 12 inches per minute, resulting in a total lowering time of approximately 15 minutes. The total time to lower the overpack and install all seismic restraints is conservatively estimated at 0.5 day for each overpack, resulting in a total of 2.5 days. Using the previously described method, this results in an equivalent risk earthquake return period of 14 years for this transient activity. To provide additional design margin, a UHS exceeding a 25-year return period is used for evaluating this evolution.

In NRC Question 2-12 (Reference 13), the NRC requested PG&E to provide analyses for the transporter route/transport stability and storage vault cask handling activities using the design basis event loads based on the 2,000-year return period ground motions. In the PG&E response to this question, the reason for PG&E's belief that use of a 2,000-year return period is not required were explained in detail.



### 3.2.5 SNOW AND ICE LOADINGS

As noted in Section 2.3.2, Eureka's average annual snowfall is less than 1 inch with a historic daily maximum of 3.4 inches and a historic monthly maximum of 6.9 inches. There is no published record of ice storms in the Eureka area. Therefore, even though the HI-STAR HB System is designed to bound snow and ice loadings typical of the contiguous United States, such design features are unnecessary for the Humboldt Bay ISFSI and do not need to be evaluated. In summary, the ISFSI meets the requirements of 10 CFR 72.120(a) and 72.122(b) for snow and ice loadings.

### 3.2.6 LIGHTNING

As noted in Section 2.3.1, thunderstorms at west-coast sites are rare phenomena. However, potential lightning strikes have been evaluated for the HI-STAR HB System through incorporation of the HI-STAR 100 generic evaluation by reference. This generic evaluation is described in Section 11.2.11.2 of the HI-STAR 100 System FSAR and in Section 8.2.13 of this FSAR. The HI-STAR HB System is a large, metal cask designed to be stored in an ISFSI vault. As such, it may be subject to lightning strikes during transport from the RFB to the ISFSI vault, but not after it is placed in the vault and the vault lid is installed.

The cask transporter provides protection for the HI-STAR HB from direct lightning strikes during onsite cask transport operation. The gantry and rigging metal above the cask is sufficient such that no direct lightning strike is anticipated. A lightning strike on the cask transporter would not structurally affect the transporter's ability to hold the suspended load due to the massive amount of steel in the structure. The current from a lightning strike would be transmitted to ground without significantly damaging the transporter structure. Lightning may affect the operator and/or drive and control systems of the transporter. However, the transporter is designed to shut down in a fail-safe condition. If the HI-STAR HB System overpack is struck by lightning, while in transit, the charge will travel through the steel shell of the overpack into the transporter and ultimately into the ground. The overpack outer shell is made of a conductive material (carbon steel). The MPC is protected by the overpack and not subject to direct lightning strikes, which will be absorbed by the overpack.

Therefore, the lightning design criteria meet the requirements of 10 CFR 72.122(b).

### 3.2.7 TEMPERATURE AND SOLAR RADIATION

Ambient temperature and incident solar radiation (insolation) data applicable to the ISFSI site are summarized in Section 2.3.2. Table 2.2.2 of the HI-STAR 100 System FSAR provides the design environmental temperatures for the HI-STAR 100 System. This includes ambient temperatures and the consideration of insolation, as applicable, for normal, off-normal, and extreme (accident) conditions used in the generic thermal analyses. The HI-STAR 100 design temperature for normal conditions is an annual average temperature of 80°F. The off-normal ambient temperature condition is 100°F.

## HUMBOLDT BAY ISFSI FSAR UPDATE

The extreme (three-day average) temperature limits for the HI-STAR 100 System are -40°F and 125°F. This temperature range demonstrates the margin in the HI-STAR HB System site-specific design.

For the site-specific HI-STAR HB thermal analyses with the cask inside the vault and the vault lid installed for long-term storage, values for ambient temperature, soil temperature, and insolation that are more appropriate, yet still bounding for the Humboldt Bay ISFSI site were used as the design basis. Table 3.2-3 provides these values, which bound the actual meteorological conditions for the site. The evaluations of off-normal and extreme ambient temperatures on the HI-STAR HB System located in the vault are discussed in Sections 8.1.2 and 8.2.10, respectively. The results of the evaluations show that the fuel cladding temperature remains well below the corresponding temperature limits for off-normal and accident conditions and even below the long-term normal temperature limit due to the very low decay heat of the stored fuel. In summary, the HI-STAR HB design criteria bound both the temperature and insolation values expected at the Humboldt Bay ISFSI site.

### 3.2.8 COMBINED LOAD CRITERIA

The HI-STAR 100 System is designed for normal, off-normal, and accident conditions, the definitions and design criteria for which are described in HI-STAR 100 System FSAR Sections 2.2.1, 2.2.2, and 2.2.3, respectively. The service limits, design loads, and load combinations are described in Sections 2.2.5, 2.2.6 and 2.2.7 of the HI-STAR 100 System FSAR respectively. By similarity of design, the HI-STAR HB System is also designed for these load criteria. The load combinations and the ability of the ISFSI vault and the HI-STAR HB System to withstand design loads are described in Sections 3.3.2.3 and 4.2.3, respectively.

Section 3.1.2 of the HI-STAR 100 System FSAR provides additional detail regarding the generic analyses methodologies using the design criteria, loads and load combinations. Therefore, the load combinations specified by the design criteria are appropriately considered for the design of ITS SSCs, as required by 10 CFR 72.122(b).

### 3.2.9 REFERENCES

1. 10 CFR 72, Licensing Requirements for the Independent Storage of Spent Nuclear Fuel and High-Level Radioactive Waste.
2. Regulatory Guide 3.62, Standard Format and Content for the Safety Analysis Report for Onsite Storage of Spent Fuel Storage Casks, USNRC, February 1989.
3. Standard Review Plan for Spent Fuel Dry Storage Facilities, USNRC, NUREG-1567, March 2000.
4. Standard Review Plan for Dry Cask Storage Systems, USNRC, NUREG-1536, January 1997.

## HUMBOLDT BAY ISFSI FSAR UPDATE

5. Final Safety Analysis Report for the HI-STAR 100 System, Holtec International Report No. HI-2012610, Revision 1, December 2002.
6. 10 CFR 72 Certificate of Compliance No. 1008 for the HI-STAR 100 System Dry Cask Storage System, Holtec International, Amendment 2, May 2001.
7. Regulatory Guide 1.76, Design Basis Tornado for Nuclear Power Plants, USNRC, April 1974.
8. ANSI/ANS 57.9-1992, Design Criteria for an Independent Spent Fuel Storage Installation (dry type), American National Standards Institute.
9. Standard ASCE 7-88, Minimum Design Loads for Buildings and Other Structures, American Society of Civil Engineers, 1988.
10. Standard Review Plan for the Review of Safety Analysis Reports for Nuclear Power Plants, USNRC, NUREG-0800, July 1981.
11. License Amendment Request 04-02, Spent Fuel Cask Handling, PG&E Letter HBL-04-016, July 9, 2004.
12. License Amendment 37 to DPR-7, Spent Fuel Cask Handling, Issued by the NRC, December 15, 2005.
13. PG&E Letter HIL-04-007, Response to NRC Request for Additional Information for the Humboldt Bay Independent Spent Fuel Storage Installation Application, October 1, 2004.
14. PG&E Letter HIL-05-007, Response to NRC Request for Additional Information for the Humboldt Bay Independent Spent Fuel Storage Installation Application, May 13, 2005.

### **3.3 DESIGN CRITERIA FOR SAFETY PROTECTION SYSTEMS**

The Humboldt Bay Independent Spent Fuel Storage (ISFSI) is designed for safe storage of Humboldt Bay Power Plant (HBPP) spent nuclear fuel stored with or without channels. The ISFSI is also designed for safe storage of greater than class C (GTCC) waste from HBPP. The ISFSI storage facility in general, and the HI-STAR HB System dry storage casks in particular, are designed to protect the multiple-purpose canister (MPC) contents and prevent release of radioactive material under normal, off-normal, and accident conditions in accordance with applicable regulatory requirements contained in 10 CFR 72 (Reference 1). Section 3.2 provides the design criteria for environmental conditions and natural phenomena for the HI-STAR HB System and the ISFSI storage vault. This section provides the remaining design criteria for the safety protection systems, namely, the cask system, vault, and the onsite cask transporter.

#### **3.3.1 HI-STAR HB SYSTEM**

##### **3.3.1.1 General**

The HI-STAR HB System is comprised of the all-metal HI-STAR HB overpack and its integral multi-purpose canister, known as the MPC-HB, which contains the fuel assemblies. Each of five HI-STAR HB Systems is designed to safely store up to 80 HBPP fuel assemblies. One additional cask contains GTCC waste. The GTCC cask will be certified as being designed to safely store the type of waste to be loaded (i.e., non-fuel material not requiring neutron poisons or fuel assembly-sized storage locations) while being compatible with the spent fuel cask lift devices and cask transporter. All six casks are located in individual underground storage vaults that, in total, make up the ISFSI facility. The HI-STAR HB System is a shortened version of the generally certified HI-STAR 100 System (Reference 2). Other cask dimensions, design codes, closure methods, and operating procedures for the HI-STAR HB System are essentially the same as the HI-STAR 100 System. Any differences are clearly described in the appropriate design or operating sections of this Final Safety Analysis Report Update (FSAR) and the significant physical differences between the cask system designs are summarized in Section 4.2.3.

The primary safety functions of each of the major, important-to-safety components comprising the HI-STAR HB System are summarized below, with appropriate references to the HI-STAR 100 System FSAR (Reference 3) or other sections of this FSAR for additional information.

##### **3.3.1.1.1 Multi-Purpose Canister**

The MPC-HB enclosure vessel is a cylindrical shell welded to a baseplate and lid with vent and drain ports, that contains the fuel basket. After MPC preparation, the vent and drain ports are sealed with welded cover plates. A welded closure ring provides a redundant welded boundary to the lid and vent/drain port cover plate welds. The MPC provides criticality control, decay heat removal, shielding, and acts as the confinement

boundary for the storage system. Up to 80 HBPP spent fuel assemblies may be stored in one MPC. The MPC may contain damaged fuel containers (DFCs) at prescribed fuel basket locations, which provide geometry control, structural support, and retrievability for damaged fuel assemblies. A detailed description and a summary of the design criteria for the generally certified MPCs are provided in Sections 1.2.1.1 and 2.0.1, respectively, of the HI-STAR 100 System FSAR. The MPC-HB enclosure vessel and fuel basket are shown in Figures 3.3-1 and 3.3-2, respectively, of this FSAR.

### **3.3.1.1.2 HI-STAR HB Overpack**

The HI-STAR HB overpack, a shortened version of the HI-STAR 100 overpack, is a rugged, heavy-walled, cylindrical, steel structure that houses the canister containing the spent nuclear fuel. The overpack is a bolted-lid design that contains the MPC and provides a pressure boundary that is filled with helium during normal storage operations. The bolted lid design facilitates the overpack's dual-purpose storage overpack and transportation package function. See Section 4.2 for a more detailed discussion of the design and analysis of the HI-STAR HB overpack.

The overpack provides support and protection for the MPC during normal, off-normal, and accident conditions including natural phenomena such as tornadoes and earthquakes; provides radiation shielding; and facilitates rejection of decay heat from the MPC to the environs to ensure fuel cladding temperatures remain below acceptable limits. A detailed description and a summary of the design criteria for the generally certified HI-STAR 100 overpack are provided in Sections 1.2.1.2 and 2.0.2, respectively, of the HI-STAR 100 System FSAR. The HI-STAR HB overpack is shown in Figure 3.3-3 of this FSAR.

### **3.3.1.2 Protection by Multiple Confinement Barriers and Systems**

#### **3.3.1.2.1 Confinement Barriers and Systems**

There are three confinement barriers for the radioactive contents stored in the HI-STAR HB System. Intact fuel assemblies have fuel cladding that provides the first boundary within the MPC preventing release of the fission products and fuel material. The overpack enclosure vessel provides additional confinement. However, no credit for the fuel cladding or overpack is taken in the confinement system design for storage. The MPC-HB is a strength-welded enclosure vessel that provides the confinement boundary for all normal, off-normal and accident conditions, including natural phenomena. A DFC prevents significant re-location of fuel material and the dispersal of gross particulates within the MPC for any fuel assemblies classified as damaged fuel.

The MPC-HB confinement boundary is defined by the baseplate, shell, lid, port cover plates, and the welds joining these components, as shown in Figure 4.2-4. The closure ring provides a redundant welded confinement boundary. No leakage from the confinement boundary is postulated or analyzed because the MPC-HB design and construction meets the provisions of Interim Staff Guidance (ISG) 18 (Reference 4) to



classify leakage from the MPC-HB confinement boundary non-credible. This no credible leakage designation for the Holtec MPC design has been previously submitted for NRC approval under the HI-STORM 100 System docket (Reference 5). See Figure 4.2-4 for details of the MPC confinement boundary design.

### **3.3.1.2.2 Cask Cooling**

The HI-STAR HB System provides passive decay heat removal both during processing and final storage of the MPC. The HI-STAR HB is a passively-cooled storage cask design and requires no external power or cooling systems. In its final storage configuration, the MPC and overpack annulus are backfilled with helium. Through a combination of convective, conductive, and radiative heat transfer, the decay heat from the stored contents is transferred to the ambient environment. Flow holes in the bottom of the MPC fuel basket provide for internal convection, or thermosiphon, action inside the MPC, which is appropriately modeled using techniques previously reviewed and approved under the HI-STORM 100 System docket (72-1014).

The fully welded fuel basket design provides the necessary metal continuity to provide for uninterrupted conduction of heat from the contents to the MPC shell. Heat is then transferred through the helium in the annulus between the MPC and the overpack inner shell, through the inner shell and intermediate shell layers, through the Holtite-A neutron shielding material, and finally through the outer enclosure shell to the ambient environment. The basis for the thermal design of the HI-STAR HB System (except for thermosiphon) is discussed in detail in Chapter 4 of the HI-STAR 100 System FSAR. The thermosiphon effect is discussed in Chapter 4 of the HI-STORM 100 FSAR (Reference 6). The HI-STAR HB System thermal design and analysis are discussed in detail in Section 4.2.3.3.5 of this FSAR.

### **3.3.1.3 Protection by Equipment and Instrumentation Selection**

#### **3.3.1.3.1 Equipment**

The cask transporter provides protection functions to the MPC and is discussed in Section 3.3.3.

#### **3.3.1.3.2 Instrumentation**

No instrumentation is required for storage of spent nuclear fuel and GTCC at the Humboldt Bay ISFSI. Due to the welded closure of the MPC, and the passively-cooled storage cask design, the loaded overpacks do not require continuous surveillance, monitoring or operator actions to ensure the safety functions are performed during normal, off-normal, and postulated accident conditions. Although not required for safe ISFSI operation, temperature monitoring of the vault air space will be temporarily performed for a sufficient time period (6 months) to validate information as to the actual heat rejection performance of the cask system. Monitoring the temperature of the vault air space will commence when the first cask with spent fuel is placed into the vault and

will continue for 6 months after the last cask with spent fuel has been placed into the vault.

### **3.3.1.4 Nuclear Criticality Safety**

The HI-STAR HB System is designed to ensure the stored fuel remains subcritical with  $k_{\text{eff}}$  less than 0.95 under all normal, off-normal, and accident conditions. The criticality analyses use the same methodology as described in the criticality analyses for the HI-STAR 100 System summarized in Chapter 6 of the HI-STAR 100 System FSAR. The methodology includes appropriate modifications to the criticality model to reflect the site-specific analysis of the 80-fuel assembly capacity of the HI-STAR HB System. No soluble boron or other neutron poisons other than the solid neutron absorber panels affixed to the fuel storage cell walls are credited in the analysis. Section 4.2.3.3.7 of this FSAR includes a detailed discussion of the HI-STAR HB System criticality design and analysis.

#### **3.3.1.4.1 Control Methods for Prevention of Criticality**

The design features and control methods used to prevent criticality for all MPC configurations are the following:

- (1) Favorable geometry provided by the MPC fuel basket.
- (2) Incorporation of permanent neutron absorbing material attached to the MPC fuel basket walls with a minimum required loading of the  $^{10}\text{B}$  isotope.
- (3) Use of a DFC for the storage of damaged fuel to ensure there is no significant re-location of fuel material in the MPC.

There are a number of conservative assumptions used in the HI-STAR HB System criticality analyses, including not taking credit for fuel burnup or fuel-related burnable neutron absorbers, and only crediting 75 percent of the minimum required  $^{10}\text{B}$  isotope loading in the neutron absorber. A description of the HI-STAR HB System criticality analysis, including a complete list of the conservative assumptions used is provided in Section 4.2.3.3.7.

#### **3.3.1.4.2 Error Contingency Criteria**

Provisions for error contingency are built into the criticality analyses as discussed in Chapter 6 of the HI-STAR 100 System FSAR. Because biases and uncertainties are explicitly evaluated in the analyses, it is not necessary to introduce additional contingency for error.

#### **3.3.1.4.3 Verification Analyses**

The criticality analyses for the HI-STAR HB System were performed using computer codes validated for use in this application under the Holtec International Quality Assurance Program and previously reviewed and approved in the HI-STAR 100 System and/or HI-STORM 100 System generic licensing bases. A discussion of the analyses and the applicable computer codes, including criticality benchmark experiments, is provided in Chapter 6 of the HI-STAR 100 System FSAR.

#### **3.3.1.5 Radiological Protection**

Radiation exposure due to the release of material from the storage system is precluded by the confinement boundary design, as discussed in Section 3.3.1.2. The confinement boundary is designed to maintain its integrity during all normal, off-normal, and accident conditions including natural phenomena. Radiation exposure due to direct radiation is minimized by the storage of the casks in an underground concrete vault with a shield lid. Radiation due to sky shine scatter is accounted for in the shielding analysis, as described in Section 4.2.3.3.6.

##### **3.3.1.5.1 Access Control**

The Humboldt Bay ISFSI underground storage vault is surrounded by a Security Area Fence. This Security Area Fence complies with the requirements of 10 CFR 72.180, 10 CFR 73.51 and TAC No. L23683. Only authorized personnel with a need to be in this area will be permitted entrance. This area does not require the continuous presence of operators or maintenance personnel. During normal storage operations, the HI-STAR HB System requires only infrequent, short-duration personnel activity to perform necessary checks on the material condition of the vaults. As discussed in Section 4.4.3, and 7.4, personnel will perform periodic maintenance and inspection activities. Higher occupancy times with a greater number of personnel occur when placing the loaded overpacks into the storage vault during cask loading operations, during maintenance and inspection activities requiring removal of the vault lid, and during activities that require removal of a cask from the vault or transfer activities for spent fuel and GTCC waste casks offsite. These activities will be governed by the Humboldt Bay ISFSI radiation protection program to ensure occupational radiation exposures are maintained ALARA. Chapter 7 and Section 9.6 provide additional details regarding the implementation of access control at the Humboldt Bay ISFSI.

##### **3.3.1.5.2 Shielding**

The HI-STAR HB System is designed to minimize radiation doses to HBPP personnel and the public through the use of a combination of steel and Holtite-A neutron shielding material. The HI-STAR HB System is designed to meet the annual dose limit of 25 mrem specified in 10 CFR 72.104 for annual dose at the HBPP owner-controlled area boundary by storage in an underground concrete vault.

The below-grade vault, shown in Figure 3.2-1 provides both man-made and natural shielding for the loaded HI-STAR HB casks during storage operations. The vault walls are constructed of reinforced concrete with native soil backfilled around the exterior. If the quantity of native soil is not sufficient to completely backfill the excavated area, a material with thermal conductivity greater than or equal to the native soil will be used to complete the backfill. Each vault employs a bolted lid made of steel-encased concrete.

The objective of shielding is to ensure that radiation doses/dose rates at the following locations are as low as reasonably achievable (ALARA) and below applicable regulatory limits, as applicable, for those locations:

- Immediate vicinity of the storage cask
- Immediate vicinity of the storage vault
- Controlled area (site) boundary
- Nearest resident

A detailed discussion of the HI-STAR HB System shielding evaluation, including modeling, source-term assumptions, and resultant dose rates is provided in Sections 7.2 and 7.3. Estimated occupational exposures and offsite doses for fuel loading, cask handling activities, and storage at the Humboldt Bay ISFSI have been evaluated for HBPP fuel and are discussed in Sections 7.4 and 7.5, respectively.

### **3.3.1.5.3 Radiological Alarm Systems**

The HI-STAR HB System, when used outside the refueling building (RFB), does not produce any solid, liquid, or gaseous effluents. Release of loose contamination is not a factor because the HI-STAR overpack is designed for cask decontamination after submergence in the spent fuel pool (SFP) during fuel loading. The MPC is also submerged in the SFP, but contamination of the MPC is limited to the top of the MPC lid by the annulus seal, which prevents SFP water from coming into contact with the sides and bottom of the MPC. After removal from the SFP, the overpack exterior and the top of the MPC are decontaminated to “free release” levels as described in Section 10.2. The overpack lid, which is not submerged in the spent fuel pool, is installed after the MPC is backfilled with helium and the closure ring installed. The draining, drying, and backfilling of the overpack annulus provides additional assurance that any residual low-level contamination on the MPC will not be released to the environment.

The dose rates at the Humboldt Bay ISFSI will be ALARA and decreasing over time due to the decay of the fuel sources stored inside. There is no credible event that could cause an increase in dose rate from the ISFSI.

Based on the foregoing, there is no need for either airborne or area radiological alarms at the Humboldt Bay ISFSI storage vault. Radiological alarms, if required for operations inside the RFB, will be implemented under the HBPP radiological protection program.

### **3.3.1.6 Fire and Explosion Protection**

There are no combustible or explosive materials associated with the HI-STAR HB System. The fuel contained in the cask transporter fuel tank is the only combustible material in close proximity to a loaded cask for any extended period of time during normal operations. Combustible and explosive materials are not stored within the Humboldt Bay ISFSI Security Area. The cask transporter is not parked within the ISFSI when not in use. Fires and explosion events, based on the actual quantity and location of combustion sources on site, were evaluated for potential effects on the ISFSI or on the loaded overpack during onsite transport from the RFB to the ISFSI. Those that were credible threats to the cask or ISFSI were evaluated in more detail as accident events under the Humboldt Bay ISFSI design basis. The sources of fires and explosions are discussed in detail in Section 2.2 and evaluated in Section 8.2.

Because the HI-STAR HB System is a dual purpose design, one of the fires analyzed is an engulfing fire, which is analyzed assuming a 1475°F average flame temperature and a duration of 30 minutes. This is consistent with the requirements in 10 CFR 71.73(c)(4) and bounds the actual flame temperature and duration of a fire that consumes the entire 50-gallon contents of cask transporter fuel in a pool surrounding the cask. This analysis and the evaluations of other, less severe fires are summarized in Section 8.2.5.

Overpressures on the cask system may result from accidents involving explosive materials that are stored or transported near the storage site. The magnitude of the overpressure is based on the quantity and type of explosive material, and the distance between the source of the explosion and the target being evaluated. The HI-STAR HB overpack, like the HI-STAR 100 overpack, is designed to withstand 300 psig external overpressure. This value is taken from a 10 CFR 71 requirement for transportation and corresponds to submersion in water at a depth of 656 feet. A Humboldt Bay ISFSI explosion evaluation covering the vault and the cask system during transport to the ISFSI vault is discussed in Section 8.2.6.

### **3.3.1.7 Materials Handling and Storage**

#### **3.3.1.7.1 Spent Fuel Handling and Storage**

Spent fuel is moved within the HBPP SFP and loaded into the HI-STAR HB System in accordance with Humboldt Bay ISFSI Technical Specifications (TS), HBPP 10 CFR 50 TS, and plant procedures. All fuel assemblies in the HBPP SFP meet the burnup, cooling time, decay heat, and other limits specified in Section 10.2, which were used as inputs in the safety analyses. All HBPP spent fuel in the SFP, therefore, may be loaded in the HI-STAR HB System and stored at the Humboldt Bay ISFSI. These limits, in



## HUMBOLDT BAY ISFSI FSAR UPDATE

combination with the design features of the cask system described earlier in this section, ensure that:

- The keff for the stored fuel will remain less than 0.95.
- Adequate cooling will be provided to ensure peak fuel cladding temperature limits will not be exceeded.
- Radiation dose rates and accumulated doses to plant personnel and the public will be ALARA and less than applicable regulatory limits.

Each fuel assembly is classified as intact fuel or damaged fuel in accordance with the applicable definitions in ISG-1, Revision 1. Fuel assemblies classified as damaged fuel are required to be placed in DFCs for storage in the HI-STAR HB System.

Section 3.3.1.5 discusses contamination as it relates to the operation of the HI-STAR HB System. Section 10.2 provides the necessary limits on MPC and overpack drying and helium backfill prior to declaring the system ready for storage. Section 5.1 provides operating procedures for all facets of fuel loading, MPC preparation, and cask handling. Implementation procedures are based on both generic and site-specific guidelines, as applicable.

The HI-STAR HB System is designed to allow retrievability of the fuel, as necessary, during normal and off-normal conditions as required by 10 CFR 72.122(l) as clarified in ISG-2 (Reference 7). As stated in ISG-2 and ISG-3 (Reference 8), retrievability of the fuel is not required to be demonstrated after accident events, where only post-accident recovery is required to be demonstrated. Section 5.1 of the HI-STAR FSAR describes the operational steps to unload an MPC, assuming the plant spent fuel pool is available to accommodate these activities. The HI-STAR HB system is designed to ensure that the MPC enclosure vessel will not leak or breach under all design basis loadings. There are no credible events where fuel would need to be retrieved from an MPC at the Humboldt Bay ISFSI after long-term storage operations commence. Access to the casks in the vaults is not required until such time as the overpack will be removed for transportation of the fuel to a federal repository.

As part of the decommissioning process, the HBPP SFP is being dismantled after all of the fuel has been removed and stored at the ISFSI. Therefore, unloading operations and fuel retrieval on site will only be possible until the SFP is decommissioned. Unloading operations and fuel retrieval are discussed in Sections 5.1 and 10.2 and in the HB ISFSI TS.

### **3.3.1.7.2 Radioactive Waste Treatment**

There are no radioactive wastes created by the HI-STAR HB System while in storage at the ISFSI. The vault design includes a drain system to collect water that may get into the vault and come in contact with the surface of the overpack. As the overpacks have

been decontaminated prior to being placed in the vault, this water is uncontaminated and is discharged to the storm drain system.

### **3.3.2 ISFSI CONCRETE STORAGE VAULT**

#### **3.3.2.1 General**

The ISFSI concrete storage vault is an underground, heavily reinforced concrete structure with a steel liner designed to support the static and dynamic loads imparted by the loaded overpacks under all design basis conditions of storage (see Figure 3.2-1). The vault structure is also designed to support and maintain its integrity during a postulated design basis event. The ISFSI vault has been evaluated for the effects of postulated design basis environmental events (e.g., earthquakes) and found to provide adequate protection of the HI-STAR HB casks.

#### **3.3.2.2 Natural Phenomena**

The Humboldt Bay ISFSI concrete storage vault is engineered to perform its design function under all loadings induced by design basis natural phenomena. The design criteria for the natural phenomena applicable to the Humboldt Bay ISFSI site, including seismic loadings and tornado wind loadings, are discussed in Section 3.2.

#### **3.3.2.3 Design Criteria**

The ISFSI vault design meets the applicable guidance in the ACI 349-01 (Reference 9) as clarified by Regulatory Guide 1.142 (Reference 10), and NUREG-1536 (Reference 11) including appropriate consideration of USNRC ISG documents that modify the NRC staff's review guidance. The materials of construction (for example, additives in the vault concrete) are chosen to be compatible with the environment at the Humboldt Bay ISFSI site. The ISFSI design life is 40 years.

##### **3.3.2.3.1 Load Combinations for the Concrete Storage Vault**

Load combinations for the ISFSI vault design are provided in ACI-349-01 and supplemented by the factored load combinations from Table 3-1 of NUREG-1536 (Reference 11), as applicable. The ultimate strength method described in ACI 349-01 was used to establish the acceptance criteria for the reinforced concrete structure. The ASME Boiler and Pressure Vessel Code, Section III, Subsection NF (Reference 12), was used for the structural steel acceptance criteria for the analysis of the cask alignment plates attached to the vault liner.

A discussion of the maximum stresses and displacements of the reinforced concrete vault when subjected to the required load combinations is provided in the PG&E Response to NRC Question 5-5 in Reference 14.

## HUMBOLDT BAY ISFSI FSAR UPDATE

The load combinations taken from ACI 349-01, as applicable, were modified with certain site-specific exceptions as noted below. Although RG 1.142 states that the 1997 Edition of ACI 349 is to be used, the vault structural analysis uses the ACI 349-01 Edition load cases and combinations. The load cases used in the vault structural analyses are:

Load Case 1:  $U = 1.4D + 1.7L + 1.7H$

Load Case 2:  $U = D + L + H + T_o + W_t$

Load Case 3:  $U = D + L + H + T_o + E_{ss}$

Load Case 4:  $U = 1.05D + 1.3L + 1.3H + 1.275T_o$

Load Case 5:  $U = D + L + H + T_o + A$

Where:

$U$  = required strength to resist factored load.

$D$  = dead loads including piping and equipment dead load.

$L$  = live load.

$H$  = load due to weight and pressure of soil, water in soil, or other materials.

$T_o$  = internal moments and forces caused by temperature distributions within the concrete structure occurring as a result of normal operating or shutdown conditions.

$E_{ss}$  = load effects of safe shutdown earthquake (SSE) including SSE-induced equipment reactions.

$W_t$  = load generated by the design basis tornado. These include loads due to tornado wind pressure, tornado created differential pressure, and tornado-generated missiles. (Note: As a result of the vault system being primarily below grade level and the massive structure of the vault and lid, the potential affects of tornado winds and generated missiles are considered insignificant. Only pressure differentials were factored into  $W_t$  in this analysis.)

$A$  = accident load attributable to the direct and secondary effects of an off-normal or design basis accident, as could result from and explosion, tsunami, crash, drop, impact, collapse, gross negligence, or other man-induced occurrences, or from severe natural phenomena not separately defined.

### Load Interpretations

“E_{ss}” was taken as the DBE. “A” includes the tsunami load and other man-induced events, but two unrelated accident conditions were not assumed to occur concurrently.

### Load Factor Modifications

The only applicable load with a factor to be modified is T_o. ACI 349-01, Section 9.2.1 specifies a load factor of 1.05 for Load Case 4. RG 1.142 recommends increasing the load factor from 1.05 to 1.2. NUREG 1536 suggests using a factor on T_o of 1.275. Since NUREG 1536 is bounding for the load factor on T_o, the value of 1.275 was used in the analysis. All other load factors and combinations are bounded by the ACI 349-01 code.

#### **3.3.2.3.2 Cask Alignment Plate Load Combinations**

The load combinations listed below are used in the design and analysis of the steel cask alignment plates attached to the vault liner:

Load Case 1: T_n + D

Load Case 2: DBE + T_n + D

Load Case 3: W_t + T_n + D

Load Case 4: P_a + T_n + D

Load Case 5: A + D

Where:

T_n = normal temperature

D = dead weight

DBE = design basis earthquake

W_t = tornado wind load

P_a = accident pressure

A = accident load attributable to the direct and secondary effects of an off-normal or design basis accident, as could result from an explosion, crash, drop, impact, collapse, gross negligence, or other man-induced occurrences, or from severe natural phenomena not separately defined.

### **3.3.3 CASK TRANSPORTER**

#### **3.3.3.1 General**

The cask transporter is a U-shaped tracked vehicle used for lifting, handling, and onsite transport of loaded overpacks. The cask transporter does not have a suspension system (for example, springs). The transporter consists of the vehicle main frame, the lifting towers, an overhead beam system that connects the parallel lifting towers, a cask restraint system, the drive and control systems, and a series of cask lifting attachments. The casks are individually carried in the vertical orientation within the internal footprint of the transporter tracks (Sections 4.3 and 4.4 provide more detailed descriptions of cask transportation components and operating characteristics). The cask is supported by the lifting attachments that are connected to the overhead beam. The overhead beam is supported at the ends by a pair of lifting towers. The lifting towers transfer the cask weight directly to the vehicle frame and ultimately to the tracks and the transport route surface.

#### **3.3.3.2 Design Criteria**

The key design criteria for the cask transporter are summarized in Table 3.4-4. The bases for these criteria are discussed in the sections below.

##### **3.3.3.2.1 Design Life**

The cask transporter design life of 20 years has been established based on a reasonable length of time for a vehicle of its type with normal maintenance. The cask transporter may be replaced or re-certified for continued use at the end of its design life.

##### **3.3.3.2.2 Environmental Design Criteria**

The cask transporter is an “all-weather” vehicle. It is designed to operate in both rain and snow over a temperature and humidity range that bounds the historical conditions at the HBPP site. Materials that would otherwise degrade in a coastal marine environment will be appropriately maintained.

A lightning strike on the cask transporter would not structurally affect the ability of the transporter to hold the load. Due to the massive amount of steel in the structure, the current would be transmitted to the ground without significantly damaging the transporter. However, the driver may be affected by a lightning strike. Therefore, the transporter design includes fail-safe features to automatically shut down the vehicle into a safe, stopped, and braked condition if the operator is injured or incapacitated for any reason while handling a loaded cask.

Flooding and tsunami are not a concern on the transport route as discussed in Section 2.6.9. Sources of fires and explosions have been identified and evaluated. Fixed sources of fire and explosion are sufficiently far from the transport route or are



evaluated probabilistically to not be of concern (Section 2.2). Mobile sources of fire and explosion, such as fuel tanker trucks, will be kept at a safe distance away from the transporter during cask movement through the use of administrative controls. The cask transporter is limited to carrying a maximum fuel volume consistent with that used in the HI-STAR HB System fire accident analysis.

### **3.3.3.2.3 Regulatory Design Criteria and Industry Standards**

The transporter is designed, fabricated, inspected, maintained, operated, and tested in accordance with applicable guidelines of NUREG-0612 (Reference 13), which allows the elimination of the need to establish a cask lift height limit.

### **3.3.3.2.4 Performance Design Criteria**

As described in Section 4.4, the cask transporter must lift and transport the loaded overpack, including the weight of all necessary ancillary lift devices such as lift links. The loaded overpack provides the limiting weight for the design of the transporter.

### **3.3.3.2.5 Stability Design Criteria**

The cask transporter is designed for a transport route with a maximum grade of approximately 8.5 percent. It will remain stable and will not experience structural failure, tip over, or leave the transport route should a design-basis seismic event for transient activities (see Section 3.2) occur while moving a loaded overpack from the RFB to the storage vault, or while moving a loaded overpack over the storage vault. In addition, the cask transporter is designed to withstand design-basis tornado winds and tornado-generated missiles without an uncontrolled lowering of the load or leaving the transport route. All design criteria for natural phenomena used to design the cask transporter are specific to the HBPP site (Sections 3.2 and 3.4 provide additional information).

### **3.3.3.2.6 Drop Protection Design Criteria**

In accordance with NUREG-0612, prevention of a cask drop is provided by enhancing the reliability of the load supporting systems by design, using a combination of component redundancy and higher factors of safety than would normally be used for a commercial lifting device. Load supporting components include the special lifting devices used to transfer the force of the payload to the cask transporter lift points (including attachment pins, as appropriate), the cask transporter lift points, the overhead beam, the lifting towers, and the vehicle frame.

The HI-STAR HB overpack is designed to be submerged directly in the spent fuel pool with the MPC inside for fuel loading. After MPC preparation and decontamination of the overpack, the cask is transported to the ISFSI storage vault. There is no transfer cask or associated MPC transfer operation. The overpack is lifted by its two lifting trunnions, which, along with the trunnion blocks, are designed in accordance with the applicable

guidelines of NUREG-0612. The design criteria for each of the components of the cask transporter are the following:

### Cask Transporter Lift Points, Overhead Beam, Vehicle Body and Seismic Restraints

The cask transporter lift points, overhead beam, and load supporting members of the vehicle body (whose failure would result in an uncontrolled lowering of the load) are designed to applicable guidelines of NUREG-0612.

### Lifting Towers

The lifting towers are designed with redundant drop protection features. The primary cask lifting device is the hydraulic system, which prevents uncontrolled cask lowering through the control of fluid pressure in the system. A mechanical backup load retaining device, independent of the hydraulic lifting cylinders, is provided in case of failure of the hydraulic system. This may consist of load blocks, pawl and detent, locking pins, or other suitably designed positive mechanical locking device.

#### **3.3.3.2.7 Drive System Design Criteria**

The cask transporter is capable of forward and reverse movement as well as turning and stopping. It includes an on-board engine capable of supplying enough power to perform its design functions. The cask transporter includes fail-safe service brakes (that is, brakes that automatically engage in any loss of power and/or independent emergency) and parking brakes. The brake system is capable of stopping a fully loaded cask transporter on the maximum design grade. The cask transporter is equipped with an automatic drive brake system that applies the brakes if there is a loss of hydraulic pressure or the drive controls are released. The cask transporter is not capable of coasting on a 8.5 percent downward grade with the brakes disengaged due to the resistance in the drive system.

#### **3.3.3.2.8 Control System Design Criteria**

The cask transporter is equipped with a control panel that is suitably positioned on the transporter frame to allow the operator easy access to the controls located on the control panel and, at the same time, allow an unobstructed view of the cask handling operations. The control panel provides for all-weather operation or will be enclosed in the cab. The control panel includes controls for all cask transporter operations including speed control, steering, braking, load raising and lowering, cask restraining, engine control and “dead-man” and external emergency stop switches.

The drive control system is capable of being operated by an individual from an on-board console. The control panel contains all gauges and instruments necessary for the operator to monitor the condition and performance of both the power source and hydraulic systems. A cask lift-height indicator is provided to ensure the loaded casks are lifted only to those heights necessary to accomplish the operational objective in progress.

### 3.3.3.2.9 Cask Restraint Design Criteria

The cask transporter is equipped with a cask restraint to secure the cask during movement. The restraint is designed to prevent lateral and transverse swinging of the cask during cask transport. The restraint is designed to preclude damage to the cask exterior with padding or other shock dampening material used, as necessary. The cask restraint shall be designed to sustain preload plus seismic load without exceeding its commercial rated capacity with a five to one ultimate safety factor.

### 3.3.4 REFERENCES

1. 10 CFR 72, Licensing Requirements for the Independent Storage of Spent Nuclear Fuel and High-Level Radioactive Waste.
2. 10 CFR 72 Certificate of Compliance No. 1008 for the HI-STAR 100 System Dry Cask Storage System, Holtec International, Amendment 2, May 2001.
3. Final Safety Analysis Report for the HI-STAR 100 System, Holtec International Report No. HI-2012610, Revision 1, December 2002.
4. Interim Staff Guidance 18, The Design/Qualification of Final Closure Welds on Austenitic Stainless Steel Containers as Confinement Boundary for Spent Fuel Storage and Containment Boundary for Spent Fuel Transportation, USNRC, May 2003.
5. License Amendment Request 1014-2, Holtec International, Revision 2, August 2003 (USNRC Docket 72-1014).
6. Final Safety Analysis Report for the HI-STORM 100 System, Holtec International Report No. HI-2002444, Revision 1, September 2002.
7. Interim Staff Guidance 2, Fuel Retrievability, USNRC, May, 1999.
8. Interim Staff Guidance 3, Post-Accident Recovery, USNRC, May 1999.
9. ACI-349-01, Code Requirements for Nuclear Safety Related Concrete Structures, American Concrete Institute.
10. Regulatory Guide 1.142, Safety Related Concrete Structures for Nuclear Power Plants (Other than Reactor Vessel and Containment), USNRC, November 2001.
11. Standard Review Plan for Dry Cask Storage Systems, USNRC, NUREG-1536, January 1997.
12. Boiler and Pressure Vessel Code, Section III, Division 1, Subsection NF, American Society of Mechanical Engineers, 1995 Edition including 1996 and 1997 Addenda.

## HUMBOLDT BAY ISFSI FSAR UPDATE

13. Control of Heavy Loads at Nuclear Power Plants, USNRC, NUREG-0612, July 1980.
14. PG&E Letter HIL-04-007, Response to NRC Request for Additional Information for the Humboldt Bay Independent Spent Fuel Storage Installation Application, October 1, 2004.

### **3.4 SUMMARY OF DESIGN CRITERIA**

The major ISFSI structures, systems, and components (SSCs) classified as important to safety are the HI-STAR HB System, the storage vault, and the cask transporter. The principal design criteria for these SSCs are summarized in Tables 3.4-1 through 3.4-5.

- Table 3.4-1 provides the site-specific design criteria for environmental conditions and natural phenomena.
- Table 3.4-2 provides design criteria applicable to the HI-STAR HB System. Detailed generic design criteria for the HI-STAR 100 System MPC and overpack are listed in the HI-STAR 100 System FSAR (Reference 1), Tables 2.0.1 and 2.0.2, respectively. However, certain updated generic design criteria for the MPC are taken from the HI-STORM 100 System FSAR (Reference 2)
- Table 3.4-3 provides the design criteria for the storage vault.
- Table 3.4-4 provides the design criteria for the cask transporter.
- Table 3.4-5 provides a list of ASME Code alternatives for the HI-STAR HB System.

#### **3.4.1 REFERENCES**

1. Final Safety Analysis Report for the HI-STAR 100 System, Holtec International Report No. HI-2012610, Revision 1, December 2002.
2. Final Safety Analysis Report for the HI-STORM 100 System, Holtec International Report No. HI-2002444, Revision 1, September 2002.



HBPP FUEL INSPECTION GUIDELINES

I. Intact Fuel

1. No axial crack indications with separation.
2. No secondary or branching axial crack indications that appear to propagate along the same section of tube as a primary crack is greater than 1 tube diameter in length.
3. No circumferential crack on tie rods or other rods. Circumferential cracks shall not show signs of misalignment and tube ends are captured so it cannot be displaced.
4. Must specify as not being a fuel pellet or fuel remnant.
5. Structural Damage
  - a. There shall be no loose components.
  - b. Grid straps should be intact.
  - c. Tie Plates show no signs of damage which limit ability to be handled.
6. Assembly is in good physical condition and fuel rods may have been replaced with dummy rods.

II. Damaged Fuel

1. Axial crack indications with separation.
2. Secondary or branching axial crack indications that appear to propagate along the same section of tube as a primary crack is greater than 1 tube diameter in length, but the tube appears structurally sound and is in its normal design configuration with good end connections and grid straps.
3. Circumferential crack indications on tie rods.
4. Circumferential cracks show signs of misalignment.
5. Is possibly a loose fuel pellet or fuel remnant.

6. Structural Damage
  - a. There could be loose components.
  - b. Grid straps are not intact.
  - c. Tie Plates are cut or damaged and there may be structural concerns.
7. Assembly is in good physical condition but is missing fuel rods that are not replaced with dummy fuel rods.

# HUMBOLDT BAY ISFSI FSAR UPDATE

TABLE 3.1-2

## SUMMARY OF FUEL PHYSICAL CHARACTERISTICS

Fuel Assembly Type	General Electric Type II	General Electric Type III	Exxon Type III	Exxon Type IV
Array Size	7X7	6X6	6X6	6X6
Clad Material	Zircaloy-2	Zircaloy-2	Zircaloy-2	Zircaloy-2
Design Initial U (kg/assy.)	78	78	78	78
Design Initial UO ₂ (kg/assy.)	87	87	87	87
Maximum Planar-Average Initial Enrichment (wt. % ²³⁵ U)	2.31	2.51	2.36	2.41
Initial Maximum Rod Enrichment (wt. % ²³⁵ U)	2.35	2.66 (5.5 ^(a) )	2.55	2.78
No. of Fuel Rods	49	36	36	36
Clad O.D. (in.)	0.486	0.563	0.563	0.5625
Clad I.D. (in.)	0.4205	0.499	0.499	0.4725/0.4925
Pellet Diameter (in.)	0.411	0.488	0.488	0.461/0.4810
Fuel Rod Pitch (in.)	0.631	0.740	0.740	0.740
Active Fuel Length (in.)	79.06	77.5	77.125	77.125
No. of Water Rods	0	0	0	0
Channel Thickness (in.)	0.060	0.060	0.060	0.060
Assembly Weight w/o channel (lb)	246	241	240	240
Assembly Weight w/channel (lb)	275	270	269	269

^{a)} Four assemblies contained a single high power test rod of 5.5% enrichment.

TABLE 3.1-3

## POTENTIAL GREATER THAN CLASS C WASTE

GTCC Description	Quantity	Approximate Individual Item Size	Estimated Total Volume	Material
Rollers punched from control rod blades and control rod followers	400	Cylindrical 1" dia x 1/2" h	0.09 ft ³	Stellite
Miscellaneous loose hardware from fuel assemblies - cap screws, lock washers, spring clips, spacers and compression springs	Unknown	Small	<0.10 ft ³	304 Stainless Steel, Inconel-X
Incore Thermocouple Tube	1	3/4" O.D. 16ft long	<0.03 ft ³	304 Stainless Steel
Internal removable core support plates (4 fuel assemblies each)	32	10.375" x 10.466" x 1"	2.0 ft ³	ASTM A351-58T, Grade CF-8 304 Stainless Steel
Fuel support plate - 12 holes	4	Irregular (Semi-circular) (48" largest dimension)	1 ft ³	ASTM A351-58T, Grade CF-8 304 Stainless Steel
Fuel support plate - 3 holes	4	Irregular (Semi-circular) (16" largest dimension)	0.35 ft ³	ASTM A351-58T, Grade CF-8 304 Stainless Steel
Flux monitor socket	8	2-3/4" x 4-1/2" x 6"	0.35 ft ³	304 Stainless Steel
Socket-Lower Core Support, intersection of beams and rods	37	Cylindrical 1-3/4" dia x 2-1/2" h	0.13 ft ³	304 Stainless Steel
Beam - Core Support	2	3/8" x 4-1/2" x 58"	0.12 ft ³	304 Stainless Steel

TABLE 3.1-3

GTCC Description	Quantity	Approximate Individual Item Size	Estimated Total Volume	Material
Beam - Core Support	4	3/8" x 4-1/2" x 37"	0.15 ft ³	304 Stainless Steel
Beam - Core Support	2	3/8" x 4-1/2" x 31"	0.06 ft ³	304 Stainless Steel
Beam - Core Support	4	3/8" x 4-1/2" x 20"	0.08 ft ³	304 Stainless Steel
Beam - Core Support	2	3/8" x 4-1/2" x 40"	0.08 ft ³	304 Stainless Steel
Beam - Core Support	1	3/8" x 4-1/2" x 19"	0.02 ft ³	304 Stainless Steel
Rod - Core Support	4	3/8" O.D. x 45"	0.012 ft ³	304 Stainless Steel
Rod - Core Support	2	3/8" O.D. x 40"	0.006 ft ³	304 Stainless Steel
Rod - Core Support	4	3/8" O.D. x 41"	0.011 ft ³	304 Stainless Steel
Rod - Core Support	4	3/8" O.D. x 32"	0.009 ft ³	304 Stainless Steel
Rod - Core Support)	8	3/8" O.D. x 22"	0.012 ft ³	304 Stainless Steel
Rod - Core Support)	4	3/8" O.D. x 19"	0.005 ft ³	304 Stainless Steel
Rod - Core Support	4	3/8" O.D. x 11"	0.003 ft ³	304 Stainless Steel
Miscellaneous hardware for core support assembly (u-bolts, bolts, screws, nuts, dowel pins, groove pins and safety wire)	Various	small	< 0.1 ft ³	304 Stainless Steel



TABLE 3.1-3

GTCC Description	Quantity	Approximate Individual Item Size	Estimated Total Volume	Material
Rim of Upper Shroud	1	86" O.D. x 82-1/2" I.D.	1.0 ft ³	304 Stainless Steel
Cylinder (part of core shroud - surrounds the reactor core) - includes miscellaneous associated hardware (blocks, locating pins, gussets, etc.)	1	96" O.D. x 95-3/8" h x 1/4" thick	4.5 ft ³	304 Stainless Steel
Chimney clamp and support brackets (includes all associate hardware and components)	8	Irregular 6"x12"x8"	0.93 ft ³	304 Stainless Steel, Inconel-X
Lower portion of fuel hold down at the top of the core	45	Pipe: 1-1/2" O.D. x 3 ft. Latch: 1/2" x 1-1/2" x 4-1/4"	1.8 ft ³	304 Stainless Steel
Portions of Lower Core support ring	Various	Cut to fit	2.9 ft ³	304 Stainless Steel
Upper Core Guide (Chimney base plate and grid former)	Various	Cut to fit	2.1 ft ³	304 Stainless Steel
Specimen baskets, specimens and associated hardware (RPV Shell Surveillance Program and Reactor Materials Surveillance Program	9	Various 30" to 80" long	0.45 ft ³	304 Stainless Steel
Cylinder (casing with antimony rod)	4	1-1/8" O.D. x 24" long	0.22 ft ³	304 Stainless Steel and antimony
A mixture of SNM waste, metal oxides, and stellite particles.	1	12" dia x 18" high	<1.0 ft ³	Process waste within a sealed 304 Stainless Steel container

# HUMBOLDT BAY ISFSI FSAR UPDATE

TABLE 3.2-1

## HI-STAR 100 SYSTEM TORNADO DESIGN PARAMETERS

Parameter	Value ^(a)
Rotational wind speed (mph)	290
Translational wind speed (mph)	70
Maximum wind speed (mph)	360
Pressure drop (psi)	3.0
Rate of pressure drop (psi/sec)	Instantaneous

---

^(a) Table 2.2.4 of HI-STAR 100 System FSAR, except for rate of pressure drop, which is provided in FSAR Section 3.4.8

## HUMBOLDT BAY ISFSI FSAR UPDATE

TABLE 3.2-2

### HI-STAR 100 SYSTEM TORNADO MISSILE DESIGN PARAMETERS

<b>HI-STAR 100 System^(a)</b>		
<b>Missile Description</b>	<b>Mass (kg)</b>	<b>Velocity (mph)</b>
Automobile	1,800	126
Artillery Shell (8 in. diameter)	125	126
Solid Sphere (1 in. diameter)	0.22	126

^(a) Table 2.2.5 of HI-STAR 100 System FSAR

# HUMBOLDT BAY ISFSI FSAR UPDATE

TABLE 3.2-3

ENVIRONMENTAL DESIGN TEMPERATURES AND INSOLATION VALUES FOR THE  
HUMBOLDT BAY ISFSI SITE

PARAMETER	VALUE
Normal Condition Ambient Temperature (Annual Average), (°F)	52
Off-normal Condition Ambient Temperature (72-hour average), (°F)	60
Extreme (Accident) Condition Ambient Temperature (72-hour average), (°F)	90
Soil Temperature, (°F)	52
Insolation (g-cal/cm ² /day)	602

# HUMBOLDT BAY ISFSI FSAR UPDATE

TABLE 3.4-1

Sheet 1 of 2

## DESIGN CRITERIA FOR ENVIRONMENTAL CONDITIONS AND NATURAL PHENOMENA APPLICABLE TO THE MAJOR ISFSI STRUCTURES, SYSTEMS, AND COMPONENTS

Design Criterion	Design Value	Reference Documents
Wind	85 mph with a gust factor of 1.1. Condition is bounded by tornado wind	Humboldt Bay ISFSI FSAR Section 3.2.1
Tornado	300 mph maximum speed  240 mph rotational speed  60 mph translational speed  2.25 psi pressure drop  1.2 psi/sec pressure drop rate	RG 1.76 Region II Humboldt Bay ISFSI FSAR Section 3.2.1 and Table 3.2-1
Tornado Missiles	Large: 1,800 kg @ 126 MPH  Intermediate: 125 kg @ 126 MPH  Small: 0.22 kg @ 126 MPH	Humboldt Bay ISFSI FSAR Section 3.2.1 and Table 3.2-2
Flood	Design-basis flooding event is not considered credible. Bounding evaluation provided assuming ISFSI is submerged under 6 feet of water.	Humboldt Bay ISFSI FSAR Section 3.2.2
Tsunami	Design-basis tsunami runup height maximum 43 feet MLLW elevation at high tide. Bounding evaluation provided assuming ISFSI is submerged under 6 feet of water. Tsunami during transport activities is not credible.	Humboldt Bay ISFSI FSAR Section 3.2.3
Seismic	See Humboldt Bay ISFSI FSAR Section 3.2.4	Humboldt Bay ISFSI FSAR Section 3.2.4
Snow & Ice	Design-basis snow and ice loadings are not considered credible	Humboldt Bay ISFSI FSAR Section 3.2.5
Fire	See Humboldt Bay ISFSI FSAR Sections 2.2.2.2 and 8.2.5	Humboldt Bay ISFSI FSAR Sections 2.2.2.2, 3.3.1.6, and 8.2.5 and Table 2.2-1
Explosion	See Humboldt Bay ISFSI FSAR Sections 2.2.2.3 and 8.2.6	Humboldt Bay ISFSI FSAR Sections 2.2.2.3, 3.3.1.6, and 8.2.6 and Table 2.2-1

# HUMBOLDT BAY ISFSI FSAR UPDATE

TABLE 3.4-1

Sheet 2 of 2

Design Criterion	Design Value	Reference Documents
Ambient Temperatures	<p>Annual Average = 52°F</p> <p>Minimum recorded = 20°F.</p> <p>Maximum recorded = 87°F</p> <p>Off-normal = 60°F</p> <p>Extreme Temperature Range = 15°F to 90°F</p>	Humboldt Bay ISFSI FSAR Sections 2.3.2, 3.2.7, 8.2.6, and 8.2.10
Insolation	602 g-cal /cm ² maximum for a 24-hr period	Humboldt Bay ISFSI FSAR Section 3.2.7



HUMBOLDT BAY ISFSI FSAR UPDATE

TABLE 3.4-2

Sheet 1 of 4

PRINCIPAL DESIGN CRITERIA APPLICABLE TO THE HI-STAR HB SYSTEM

Design Criterion	Design Value	Reference Documents
<b>GENERAL</b>		
HI-STAR HB System Design Life	40 years	Holtec HI-STAR 100 FSAR, Section 2.0.1 and Humboldt Bay ISFSI FSAR Section 3.3.2.3
ISFSI Storage Capacity	6 casks (5 having space for 400 spent fuel assemblies and one for GTCC)	Humboldt Bay ISFSI FSAR Section 3.1
Number of Fuel Assemblies	390 plus the equivalent of one assembly in debris form (with or without channels)	Humboldt Bay ISFSI FSAR Section 3.1
Greater than class C Waste	See Humboldt Bay ISFSI FSAR Table 3.1-3	Humboldt Bay ISFSI FSAR Section 3.1.1.4 and Table 3.1-3
<b>SPENT FUEL SPECIFICATIONS</b>		
Type of Fuel	General Electric Types II and III and Exxon Nuclear Types III and IV BWR Fuel 6x6 and 7x7 arrays	Humboldt Bay ISFSI FSAR Sections 3.1.1, 10.2.1.1, and Tables 3.1-1 and 10.2-1 through 10.2-5
Fuel Characteristics (per assembly)	Max decay heat = 50 Watts Maximum burnup = 23,000 MWD/MTU Minimum cooling time at time of first cask loading = 29 years Max enrichment = 2.60 wt.% ²³⁵ U Min Enrichment = 2.08 wt.% ²³⁵ U	See Humboldt Bay ISFSI FSAR Section 3.1.1, 10.2.1.1 and Tables 10.2-1 through 10.2-5
Fuel Classification	Intact, Damaged	Humboldt Bay ISFSI FSAR Section 3.1.1, 10.2.1.1, Tables 10.2-1 through 10.2-2, Humboldt Bay ISFSI TS, and ISG-1, Rev.1

## HUMBOLDT BAY ISFSI FSAR UPDATE

TABLE 3.4-2

Sheet 2 of 4

Design Criterion	Design Value	Reference Documents
<b>STRUCTURAL DESIGN</b>		
Design Codes	ASME III-1995, with 1996 and 1997 Addenda, Subsections NB,NG, and NF ANSI N14.6 (93)	Holtec HI-STAR FSAR Tables 2.2.6, 2.2.7, and 2.2.15
Environmental Conditions and Natural Phenomena	See Humboldt Bay ISFSI FSAR Table 3.4-1	Humboldt Bay ISFSI FSAR Sections 3.2 & 3.3
Weights	Maximum loaded overpack weight = 161,200 lb (without water in the MPC) and 171,200 (with water in the MPC) Transporter weight = 190,000 lb	Humboldt Bay ISFSI FSAR Section 4.2.3.3.2.1
MPC Internal Pressure	Normal = 100 psig Off-normal = 110 psig Accident = 200 psig	Holtec HI-STAR FSAR Table 2.0.1 Holtec HI-STORM FSAR Table 2.0.1
Cask Loads and Load Combinations	See HI-STAR 100 System FSAR	Holtec FSAR Table 2.2.14
<b>THERMAL DESIGN</b>		
Maximum Cask Heat Duty	2 kW	Humboldt Bay ISFSI FSAR Sections 3.1.1.2 and 4.2.3.3.5
Peak Fuel Cladding Temperature Limits	Long-term storage and short-term normal operations = 752°F Off-normal and accident = 1058°F	ISG-11, Revision 2
Other SSC Temperature Limits	Varies by material	Holtec FSAR, Tables 2.0.1 and 2.0.2
MPC Backfill Gas Supply	99.995% pure helium	Holtec CoC, Appendix A, Table 2-1; Humboldt Bay ISFSI FSAR Section 10.2.2.4

## HUMBOLDT BAY ISFSI FSAR UPDATE

TABLE 3.4-2

Sheet 3 of 4

Design Criterion	Design Value	Reference Documents
<b>RADIATION PROTECTION AND SHIELDING DESIGN</b>		
Dose Rate Design Objectives	$\leq 2$ mrem/hr on vault surface $\leq 15$ mrem/hr on cask surface at mid-plane	Humboldt Bay ISFSI FSAR 4.2.3.3.6
Occupational Exposure Dose Limits	5 rem/yr or equivalent	10 CFR 20.1201
Source Terms	Burnup = 23,000 MWD/MTU Minimum cooling time = 29 years Minimum enrichment = 2.08	Assumed values to bound all fuel in HBPP inventory
Controlled Area Boundary Dose Rate Limit	2 mrem/hr	10 CFR 20.1301
Normal and Off-normal Operation Dose Limits to Public	25 mrem/yr whole body 75 mrem/yr thyroid 25 mrem/yr other critical organ	10 CFR 72.104
Accident Dose Limits to Public	5 rem TEDE 50 rem DDE plus CDE 15 rem lens dose equivalent 50 rem shallow dose equivalent to skin or extremity	10 CFR 72.106
<b>CRITICALITY DESIGN</b>		
Maximum initial fuel planar average initial enrichment	$\leq 2.60\%$	Humboldt Bay ISFSI FSAR Tables 3.1-1 and 10.2-1 through 10.2-5, and the Humboldt Bay ISFSI TS
Control Method (Design Features)	MPC HB fuel storage cell pitch $\geq 5.83$ in. and B-10 loading $\geq 0.01$ g/cm ²	Humboldt Bay ISFSI FSAR Figure 3.3-2
Maximum $k_{eff}$	$<0.95$	Humboldt Bay ISFSI FSAR Section 3.3.1.4

# HUMBOLDT BAY ISFSI FSAR UPDATE

TABLE 3.4-2

Sheet 4 of 4

Design Criterion	Design Value	Reference Documents
<b>CONFINEMENT DESIGN</b>		
Confinement Method	MPC with redundant confinement boundary field welds	Humboldt Bay ISFSI FSAR Section 3.3.1.2.1 and Figure 3.3-1
Confinement Barrier Design	Multi-purpose canister: ASME III, NB	Holtec FSAR, Tables 2.2.6 and 2.2.15
Maximum Confinement Boundary Leak Rate	1.0E-7 atm-cc/sec (He)	ISG-18 HB ISFSI TS SR 3.1.1.3

# HUMBOLDT BAY ISFSI FSAR UPDATE

TABLE 3.4-3

## DESIGN CRITERIA FOR STORAGE VAULT

Design Criterion	Design Value	Reference Documents
Storage Vault Design Codes	NUREG-1536; ACI-349 (01)	Humboldt Bay ISFSI FSAR Sections 3.3.2.3 and 4.2.3.3.2
Design Life	40 years	Humboldt Bay ISFSI FSAR Section 3.3.2.3
Maximum Single Loaded Cask Weight	161,200 lb (Note 1)	Humboldt Bay ISFSI FSAR Section 4.2.3
Transporter with Loaded HI STAR HB	350,000 lb (Note 1)	Humboldt Bay ISFSI FSAR Section 4.2.3
Operating Temperature Range	15-90°F	Humboldt Bay ISFSI FSAR Section 4.2.3
Concrete Strength	4,000 psi @28 days	ACI-349(01)
Vault and Cask Alignment Plate Loads and Load Combinations	Various	NUREG-1536, Table 3-1; Humboldt Bay ISFSI FSAR Sections 3.3.2.3.1 and 3.3.2.3.2
Environmental Conditions and Natural Phenomena	See Humboldt Bay ISFSI FSAR Table 3.4-1	Humboldt Bay ISFSI FSAR Section 3.2

Note 1: The loaded cask weight is an upper bound value used for analysis. The combined transporter and cask weight is a bounding value for use in combined analyses.

# HUMBOLDT BAY ISFSI FSAR UPDATE

TABLE 3.4-4

## DESIGN CRITERIA FOR TRANSPORTER

Design Criterion	Design Value	Reference Documents
Transporter Design Codes	Purchase commercial grade and qualify by testing prior to use.	Humboldt Bay ISFSI FSAR Sections 3.3.3 and 4.3.2.1, and Humboldt Bay ISFSI TS
Design Life	20 years	Humboldt Bay ISFSI FSAR Section 3.3.3.2.1
Maximum Payload	161,200 lb	Humboldt Bay ISFSI FSAR Section 4.2.3
Transporter Weight	190,000 lb	Assumed value
Nominal Loaded Travel Speed	0.4 MPH	Assumed value
Minimum Uphill Grade Capability	8.5% (Carrying a loaded overpack)	Assumed value
Maximum On-Board Fuel Quantity	50 gallons of diesel	Humboldt Bay ISFSI TS and FSAR Sections 2.2.2.3 and 8.2.5
Maximum Hydraulic Fluid Volume	Unlimited (must be non-flammable)	Humboldt Bay ISFSI TS and FSAR Section 3.3.3.2.2
Operating Temperature Range	15-90°F	Humboldt Bay ISFSI FSAR Sections 4.2.3.3.5, 8.1.2, and 8.2.10
Redundancy and Safety Factors for Load Path Structures and Special Lifting Devices	Per the applicable guidelines of NUREG-0612	Humboldt Bay ISFSI FSAR Section 3.3.3
Hoist Load Factor	15%	CMAA 70 (94)
Position Control Maintained with Loss of Motive Power	Stops in position	Applicable Guidelines of NUREG-0612
Environmental Conditions and Natural Phenomena	For seismic see Humboldt Bay ISFSI FSAR Section 3.2.4 and Table 3.4-1.	Humboldt Bay ISFSI FSAR Sections 3.2 & 3.3



TABLE 3.4-5

## LIST OF ASME CODE ALTERNATIVES FOR HI-STAR HB SYSTEM

Component	Reference ASME Code Section/Article	Code Requirement	Alternative, Justification & Compensatory Measures
MPC	Subsection NCA	Design Specification	Not required (see Note #1).
MPC Basket Assembly		Design Report	Not required (see Note #1).
HI-STAR Overpack		Overpressure Protection Report	Not required (see Note #1).
		Data Report	Not required (see Note #3).
		Certification	Not required (see Notes #1, #2 and #3).
		Stamping	Not required (see Notes #2, #3 and #4).
		Nameplates	Not required (see Note #5).
	<u>Note #1</u> Because the MPC-HB, fuel basket assembly, and HI-STAR HB overpack are not ASME Code “N” stamped items, the Design Specifications, Design Reports, Certificates of Authorization and Over Pressure Protection Report are not required. The Humboldt Bay ISFSI FSAR and the HI-STAR 100 System FSAR, together include the design criteria, service conditions, and load combinations for the design and operation of the HI-STAR HB System. In addition, they include the stress analyses results that demonstrate that applicable Code stress limits are met.		

TABLE 3.4-5

Component	Reference ASME Code Section/Article	Code Requirement	Alternative, Justification & Compensatory Measures
			<p><u>Note #2</u> Because the MPC-HB, fuel basket assembly, and HI-STAR HB overpack cask components are not certified to the ASME Code (Section III), the term “Certificate Holder” is not applicable. To eliminate ambiguity, the responsibilities assigned in ASME Section III to the Certificate Holder shall be interpreted to apply to PG&amp;E (and, by extension, to Holtec and its fabricator) if the requirement must be fulfilled.</p> <p><u>Note #3</u> The fabricator (including the entity responsible for the final MPC-HB closure weld) is not required to have an ASME-accredited QA program. The fabricator applies an approved QA program that meets the applicable regulatory requirements to all important-to-safety items and activities. As such, ASME certification and stamping is not required. The QA documentation package for each item will be in accordance with the applicable QA program.</p> <p><u>Note #4</u> The ASME Section III term “inspector” is herein defined as the Quality Assurance personnel assigned by PG&amp;E to perform oversight (e.g., audit, inspection) of the design and manufacturing processes.</p>

TABLE 3.4-5

Component	Reference ASME Code Section/Article	Code Requirement	Alternative, Justification & Compensatory Measures
			<p><u>Note #5</u> In lieu of the requirements for nameplates, items will be marked in accordance with 10 CFR 71 and 10 CFR 72 and the Holtec QA Program.</p>
MPC	NB-1100	Statement of requirements for Code stamping of components.	MPC-HB vessel is designed and will be fabricated in accordance with ASME Code, Section III, Subsection NB to the maximum practical extent, but Code stamping is not required.
MPC basket supports and lift lugs	NB-1130	<p>NB-1132.2(d) requires that the first connecting weld of a nonpressure-retaining structural attachment to a component shall be considered part of the component unless the weld is more than 2t from the pressure-retaining portion of the component, where t is the nominal thickness of the pressure-retaining material.</p> <p>NB-1132.2(e) requires that the first connecting weld of a welded nonstructural</p>	<p>The MPC-HB basket supports (non pressure-retaining structural attachment) and lift lugs (nonstructural attachments (relative to the function of lifting a loaded MPC-HB) used exclusively for lifting an empty MPC-HB) are welded to the inside of the pressure-retaining MPC-HB shell, but are not designed in accordance with Subsection NB. The basket supports and associated attachment welds are designed to satisfy the stress limits of Subsection NG and the lift lugs and associated attachment welds are designed to satisfy the stress limits of Subsection NF, as a minimum. These attachments and their welds are shown by analysis to meet the respective stress limits for their service conditions. Likewise, non-structural items, such as shield plugs, spacers, etc. if used, can be attached to pressure-retaining parts in the same manner.</p>

TABLE 3.4-5

Component	Reference ASME Code Section/Article	Code Requirement	Alternative, Justification & Compensatory Measures
		attachment to a component shall conform to NB-4430 if the connecting weld is within 2t from the pressure-retaining portion of the component.	
MPC	NB-2000	Requires materials to be supplied by an ASME Material Organization.	Materials will be procured in accordance with an approved quality assurance (QA) program.
MPC, MPC basket assembly and HI-STAR overpack	NB-3100 NG-3100 NF-3100	Provides requirements for determining design-loading conditions, such as pressure, temperature, and mechanical loads.	These requirements are not applicable. The Humboldt Bay FSAR, serving as the Design Specification, establishes the service conditions and load combinations for the storage system.
MPC	NB-3350	NB-3352.3 requires, for Category C joints, that the minimum dimensions of the welds and throat thickness shall be as shown in Figure NB-4243-1.	The MPC shell-to-baseplate weld joint design (designated Category C) does not include a reinforcing fillet weld or a bevel in the MPC baseplate, which makes it different than any of the representative configurations depicted in Figure NB-4243-1. The transverse thickness of this weld is equal to the thickness of the adjoining shell (1/2 inch). The weld is designed as a full penetration weld that receives VT and RT or UT, as well as final surface PT examinations. Because the MPC shell design thickness is considerably larger than the minimum thickness required by the Code, a reinforcing

TABLE 3.4-5

Component	Reference ASME Code Section/Article	Code Requirement	Alternative, Justification & Compensatory Measures
			<p>fillet weld that would intrude into the MPC cavity space is not included. Not including this fillet weld provides for a higher quality radiographic examination of the full penetration weld.</p> <p>From the standpoint of stress analysis, the fillet weld serves to reduce the local bending stress (secondary stress) produced by the gross structural discontinuity defined by the flat plate/shell junction. In the MPC design, the shell and baseplate thicknesses are well beyond that required to meet their respective membrane stress intensity limits.</p>
MPC, MPC basket assembly, and HI-STAR overpack	NB-4120 NG-4120 NF-4120	NB-4121.2, NG-4121.2, and NF-4121.2 provide requirements for repetition of tensile or impact tests for material subjected to heat treatment during fabrication or installation.	<p>In-shop operations of short duration that apply heat to a component, such as plasma cutting of plate stock, welding, machining, coating, and pouring of Holiite-A are not, unless explicitly stated by the Code, defined as heat treatment operations.</p> <p>For the steel parts in the HI-STAR 100 System components, the duration for which a part exceeds the off-normal temperature limit shall be limited to 24 hours in a particular manufacturing process (such as the Holiite-A pouring process).</p>

TABLE 3.4-5

Component	Reference ASME Code Section/Article	Code Requirement	Alternative, Justification & Compensatory Measures
MPC and HI-STAR overpack	NB-4220 NF-4220	Requires certain forming tolerances to be met for cylindrical, conical, or spherical shells of a vessel.	The cylindricity measurements on the rolled shells are not specifically recorded in the shop travelers, as would be the case for a Code-stamped pressure vessel. Rather, the requirements on inter-component clearances (such as the MPC-to-overpack) are guaranteed through fixture-controlled manufacturing. The fabrication specification and shop procedures ensure that all dimensional design objectives, including inter-component annular clearances are satisfied. The dimensions required to be met in fabrication are chosen to meet the functional requirements of the dry storage components. Thus, although the post-forming Code cylindricity requirements are not evaluated for compliance directly, they are indirectly satisfied (actually exceeded) in the final manufactured components.
MPC Lid and Closure Ring Welds	NB-4243	Full penetration welds required for Category C Joints (flat head to main shell per NB-3352.3).	MPC lid and closure ring are not full penetration welds. They are welded independently to provide a redundant seal. Additionally, a weld efficiency factor of 0.45 has been applied to the analyses of these welds.
MPC Lid to Shell Weld	NB-5230	Radiographic (RT) or ultrasonic (UT) examination required.	Only UT or multi-layer liquid penetrant (PT) examination is permitted. If PT alone is used, at a minimum, it will include the root and final weld layers and each approximately 3/8 inch of weld depth.



TABLE 3.4-5

Component	Reference ASME Code Section/Article	Code Requirement	Alternative, Justification & Compensatory Measures
MPC Closure Ring, Vent and Drain Cover Plate Welds	NB-5230	Radiographic (RT) or ultrasonic (UT) examination required.	Root (if more than one weld pass is required) and final liquid penetrant examination to be performed in accordance with NB-5245. The MPC vent and drain cover plate welds are liquid penetrant examined. The closure ring provides independent redundant closure for vent and drain cover plates.
MPC Enclosure Vessel and Lid	NB-6111	All completed pressure retaining systems shall be pressure tested.	<p>The MPC enclosure vessel is seal welded in the field following fuel assembly loading. The MPC enclosure vessel shall then be pressure tested. Accessibility for leakage inspections precludes a Code compliant pressure test. All MPC enclosure vessel welds (except closure ring and vent/drain cover plate) are inspected by volumetric examination, except the MPC lid-to-shell weld shall be verified by volumetric or multi-layer PT examination. If PT alone is used, at a minimum, it must include the root and final layers and each approximately 3/8 inch of weld depth. For either UT or PT, the maximum undetectable flaw size must be demonstrated to be less than the critical flaw size. The critical flaw size must be determined in accordance with ASME Section XI methods. The critical flaw size shall not cause the primary stress limits of NB-3000 to be exceeded.</p> <p>The inspection process, including findings (indications), shall be made a permanent part of the user's records by video, photographic, or other means which provide an equivalent retrievable record of weld integrity. The video or photographic records should be taken during</p>

TABLE 3.4-5

Component	Reference ASME Code Section/Article	Code Requirement	Alternative, Justification & Compensatory Measures
			the final interpretation period described in ASME Section V, Article 6, T-676. The vent/drain cover plate and closure ring welds are confirmed by liquid penetrant examination. The inspection of the weld must be performed by qualified personnel and shall meet the acceptance requirements of ASME Code Section III, NB-5350 for PT or NB-5332 for UT.
MPC Enclosure Vessel	NB-7000	Vessels are required to have overpressure protection.	No overpressure protection is provided. The function of MPC enclosure vessel is to contain the radioactive contents under normal, off-normal, and accident conditions. The MPC vessel is designed to withstand maximum internal pressure considering 100% fuel rod failure and maximum accident temperatures.
MPC Enclosure Vessel	NB-8000	States requirements for nameplates, stamping and reports per NCA-8000.	HI-STAR 100 System to be marked and identified in accordance with 10 CFR 71 and 10 CFR 72 requirements. Code stamping is not required. QA data package to be in accordance with Holtec's approved QA program.
Overpack Pressure Boundary	NB-1100	Statement of requirements for Code stamping of components.	Overpack containment boundary is designed, and will be fabricated in accordance with ASME Code, Section III, Subsection NB to the maximum practical extent, but Code stamping is not required.
Overpack Pressure Boundary	NB-2000	Requires materials to be supplied by ASME-approved material supplier.	Materials will be supplied by Holtec approved suppliers with CMTRs per NB-2000.

TABLE 3.4-5

Component	Reference ASME Code Section/Article	Code Requirement	Alternative, Justification & Compensatory Measures
Overpack Pressure Boundary	NB-2330	Defines the methods for determining the $T_{NDT}$ for impact testing of materials.	$T_{NDT}$ shall be defined in accordance with RG 7.11 and 7.12 for the containment boundary components.
Overpack Pressure Boundary	NB-7000	Vessels are required to have overpressure protection.	No overpressure protection is provided. Function of overpack vessel is as a radionuclide containment boundary under normal and hypothetical accident conditions. Overpack vessel is designed to withstand maximum internal pressure and maximum accident temperatures.
Overpack Pressure Boundary	NB-8000	States requirements for nameplates, stamping and reports per NCA-8000.	HI-STAR 100 System to be marked and identified in accordance with 10 CFR 71 and 10 CFR 72 requirements. Code stamping is not required. QA data package to be in accordance with Holtec's approved QA program.
MPC Basket Assembly	NG-2000	Requires materials to be supplied by an ASME Material Organization.	Materials will be procured in accordance with an approved quality assurance program.
MPC Basket Assembly	NG-4420	NG-4427(a) allows a fillet weld in any single continuous weld to be less than the specified fillet weld dimension by not more than 1/16 inch, provided that the total undersize portion of the weld does not exceed 10 percent of the length	Modify the Code requirement (intended for core support structures) with the following text prepared to accord with the geometry and stress analysis imperatives for the fuel basket: For the longitudinal MPC basket fillet welds, the following criteria apply: 1) The specified fillet weld throat dimension must be maintained over at least 92 percent of the total weld length. All regions of undersized weld must be less than 3 inches long and separated from each other by at least 9 inches. 2) Areas of undercuts and porosity beyond that allowed by

TABLE 3.4-5

Component	Reference ASME Code Section/Article	Code Requirement	Alternative, Justification & Compensatory Measures
		of the weld. Individual undersize weld portions shall not exceed 2 inches in length.	<p>the applicable ASME Code shall not exceed 1/2 inch in weld length. The total length of undercut and porosity over any 1-foot length shall not exceed 2 inches. 3) The total weld length in which items (1) and (2) apply shall not exceed a total of 10 percent of the overall weld length. The limited access of the MPC basket panel longitudinal fillet welds makes it difficult to perform effective repairs of these welds and creates the potential for causing additional damage to the basket assembly (e.g., to the neutron absorber and its sheathing) if repairs are attempted. The acceptance criteria provided in the foregoing have been established to comport with the objectives of the basket design and preserve the margins demonstrated in the supporting stress analysis.</p> <p>From the structural standpoint, the weld acceptance criteria are established to ensure that any departure from the ideal, continuous fillet weld seam would not alter the primary bending stresses on which the design of the fuel baskets is predicated. Stated differently, the permitted weld discontinuities are limited in size to ensure that they remain classifiable as local stress elevators ("peak stress," F, in the ASME Code for which specific stress intensity limits do not apply).</p>
MPC Basket Assembly	NG-8000	States requirements for nameplates, stamping and reports per NCA-8000.	The HI-STAR 100 System will be marked and identified in accordance with 10 CFR 71 and 10 CFR 72 requirements. No Code stamping is required. The MPC basket data package will be in conformance with Holtec's QA program.

TABLE 3.4-5

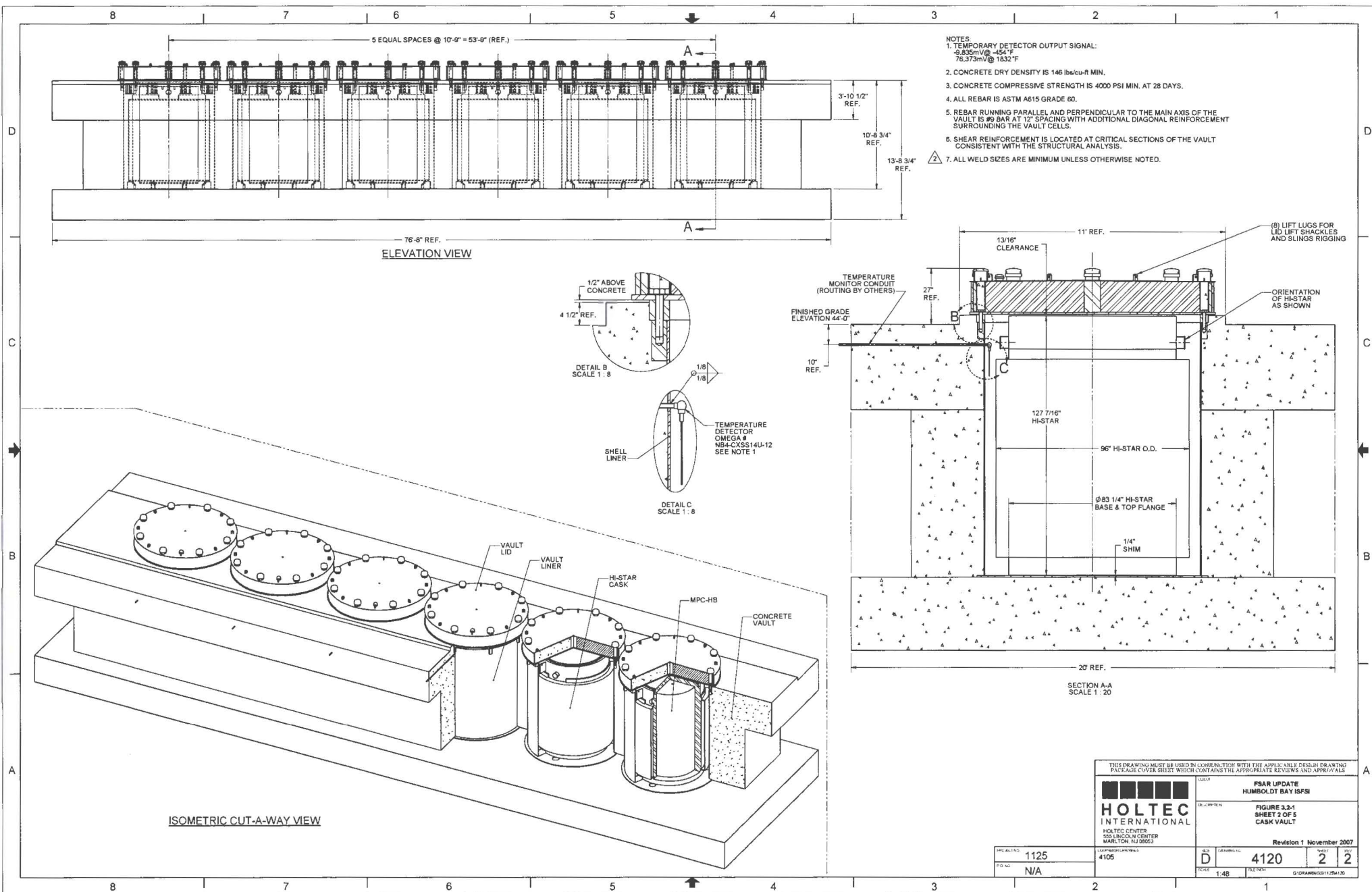
Component	Reference ASME Code Section/Article	Code Requirement	Alternative, Justification & Compensatory Measures
Overpack Intermediate Shells	NF-2000	Requires materials to be supplied by an ASME Material Organization.	Materials will be procured in accordance with an approved quality assurance program.
Overpack Containment Boundary	NF-3320 NF-4720	NF-3324.6 and NF-4720 Provide requirements for bolting.	<p>These Code requirements are applicable to linear structures wherein bolted joints carry axial, shear, as well as rotational (torsional) loads. The overpack closure plate bolted connections in the structural load path are qualified by design based on the design loadings defined in the HI-STAR 100 FSAR. Bolted joints in these components see no shear or torsional loads under normal storage conditions. Larger clearances between bolts and holes may be necessary to ensure shear interfaces located elsewhere in the structure engage prior to the bolts experiencing shear loadings (which occur only during side impact scenarios).</p> <p>Bolted joints that are subject to shear loads in accident conditions are qualified by appropriate stress analysis. Larger bolt-to-hole clearances help ensure more efficient operations in making these bolted connections, thereby minimizing time spent by operations personnel in a radiation area. Additionally, larger bolt-to-hole clearances allow interchangeability of the lids from one particular fabricated cask to another.</p>

Note: Alternatives to the above table may be used when specifically authorized by the Director of the Office of Nuclear Material Safety and Safeguards or designee in accordance with 10 CFR 72.2 and as controlled by the Humboldt Bay ISFSI Technical Specifications.

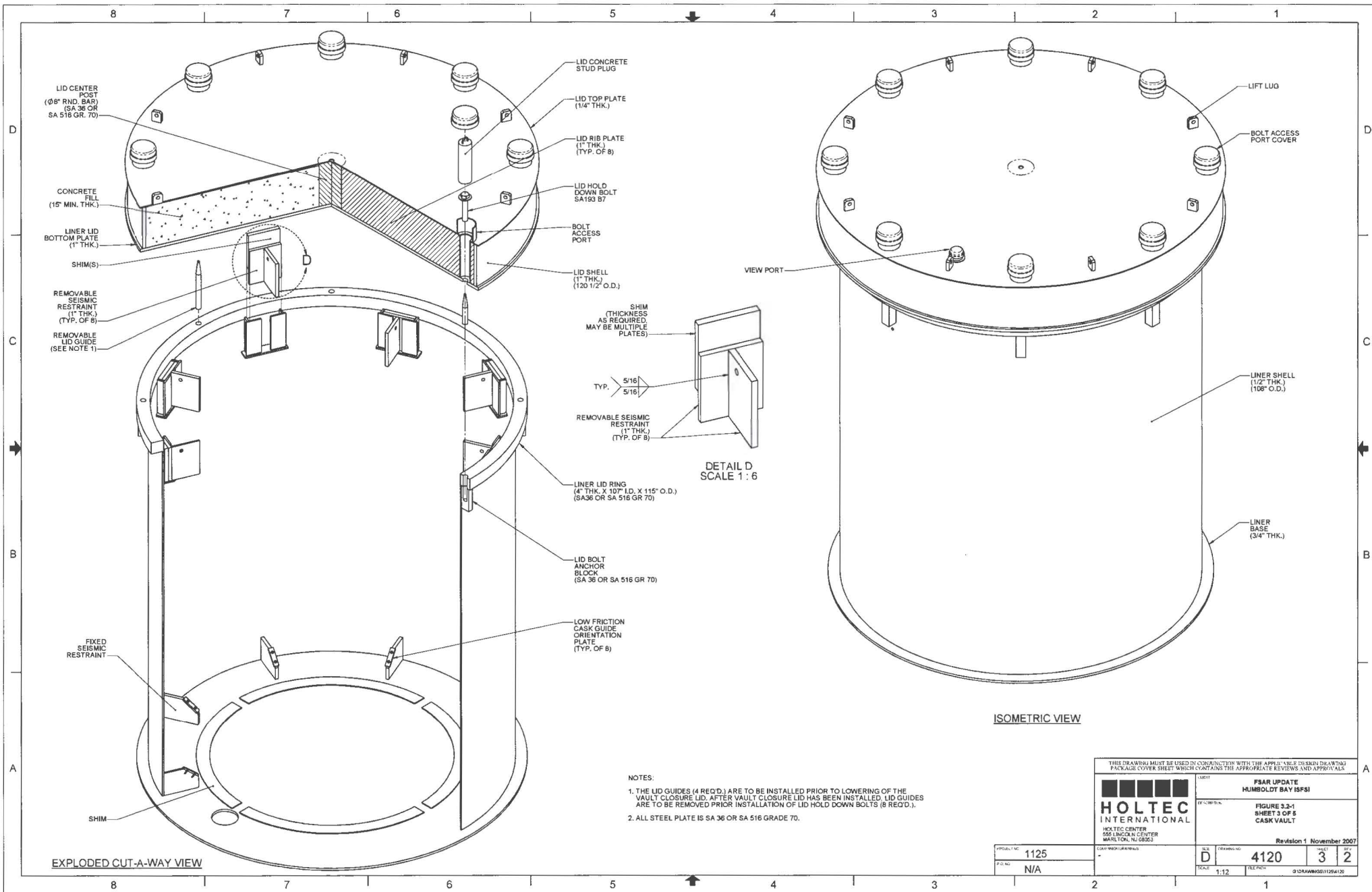






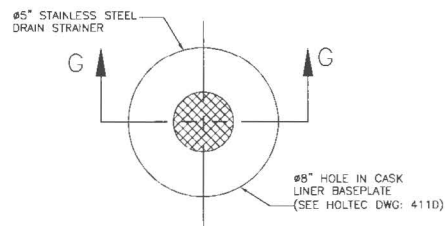


THIS DRAWING MUST BE USED IN COMBINATION WITH THE APPLICABLE DESIGN DRAWING PACKAGE COVER SHEET WHICH CONTAINS THE APPROPRIATE REVIEWS AND APPROVALS			
<b>HOLTEC INTERNATIONAL</b> HOLTEC CENTER 100 LINCOLN CENTER MARLTON, NJ 08053		PSAR UPDATE HUMBOLDT BAY ISFSI FIGURE 3.2-1 SHEET 2 OF 5 CASK VAULT Revision 1 November 2007	
PROJECT NO. 1125 P.O. NO. N/A	DRAWING NUMBER 4105	DESIGNED BY D CHECKED BY 1-4B DATE 1-4B	SCALE 1:20 SHEET NO. 2 TOTAL SHEETS 5

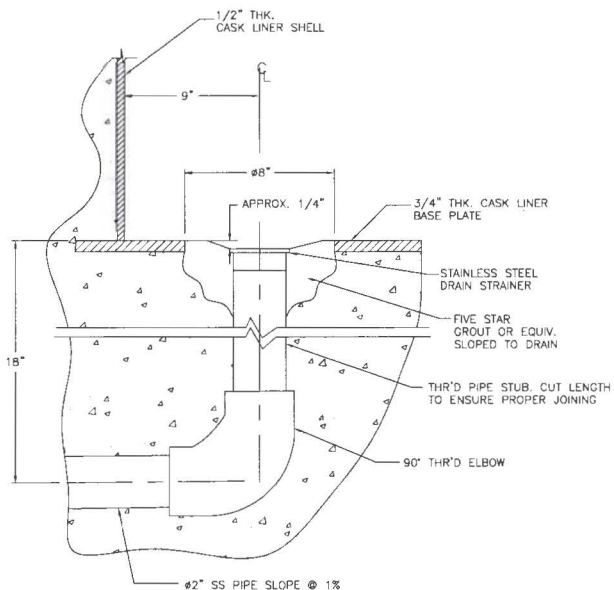




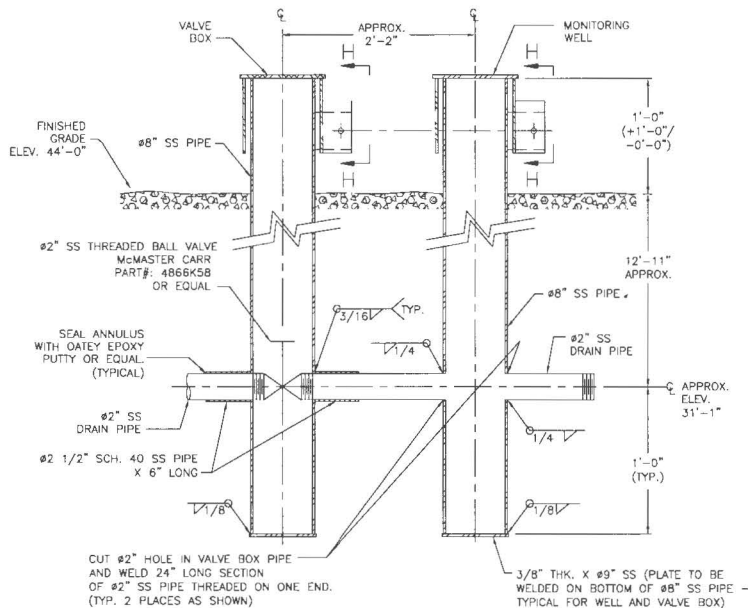
DETAIL "D"



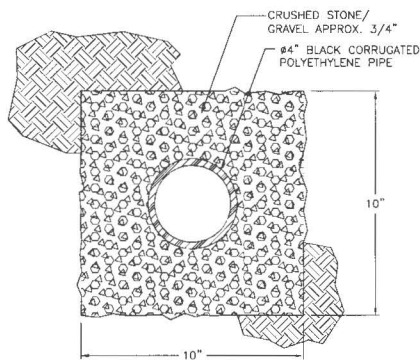
SECTION G-G



SECTION E-E

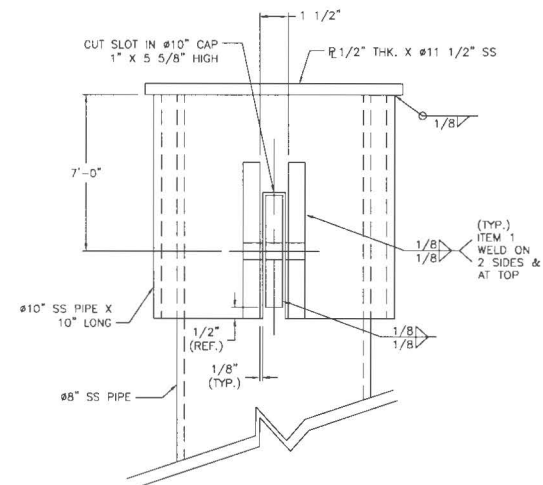


SECTION F-F



SECTION H-H

(TYPICAL CAP LOCK FOR VALVE BOX AND MONITORING WELL)



THE DRAWINGS MUST BE USED IN CONJUNCTION WITH THE APPLICABLE DESIGN DRAWING PACKAGE COVER SHEET WHICH CONTAINS THE APPROPRIATE NOTICES AND APPROVALS.		CLIENT <b>FSAR UPDATE HUMBOLDT BAY ISFSI</b>	
HOLTEC INTERNATIONAL HOLTEC CENTER 555 LINCOLN DRIVE WEST MARLTON, NJ 08053		DESCRIPTION <b>FIGURE 9.3-1 SHEETS OF 8 CASK VAULT</b>	
PROJECT NO. <b>1125</b>		Revision 1 November 2007	
P.C. NO. <b>3500120394</b>		DATE <b>D</b>	DRAWING NO. <b>4120</b>
SCALE <b>N/A</b>		FILE PATH <b>S:\DRAWINGS\1125\4120</b>	SHEET <b>5</b>
			REV <b>2</b>



PG&amp;E

P.O. NO. 3500120394

TOTAL SHEETS 4

LICENSING DRAWING PACKAGE CONTENTS:

[illegible]

# LICENSING DRAWING PACKAGE COVER SHEET

### REVISION LOG

IT IS MANDATORY AT EACH REVISION TO COMPLETE THE REVIEW & APPROVAL LOG STORED IN HOLTEC'S DIRECTORY N:\PROJECTS\WORKING\0004\B ALL RELEVANT TECHNICAL DISCIPLINES, PM AND QA PERSONNEL. EACH ATTACHED DRAWING SHEET CONTAINS ANNOTATED TRIANGLES INDICATING THE REVISION TO THE DRAWING.

[illegible]

NOTES CONT:

10. THIS COMPONENT IS CLASSIFIED AS ITS-A BASED ON THE HIGHEST CLASSIFICATION OF ANY SUBCOMPONENT. SUBCOMPONENT CLASSIFICATIONS ARE PROVIDED IN THE HUMBOLDT BAY ISFSI FSAR TABLE 4.5-1 AND HOLTEC HI-STAR SAR SUPPLEMENT 1.J FOR TRANSPORT.

11. LOCAL GRINDING OF THE MPC SHELL SHALL NOT RESULT IN GREATER THAN 10% LOSS IN BASE METAL THICKNESS OVER ANY AREA WHICH EXCEEDS 4 INCHES IN THE LONGITUDINAL OR CIRCUMFERENTIAL DIRECTION. FOR THE WELD AREA AND ADJACENT BASE METAL, AN ADDITIONAL ALLOWANCE OF 0.02" LOSS IN NOMINAL BASE METAL THICKNESS IS ALLOWED OVER THE ENTIRE LENGTH AND END OF THE WELD. THE SUM OF ALL AREAS OF LOCAL METAL LOSS SHALL NOT EXCEED 10% OF THE OVERALL INSIDE SURFACE AREA OF THE MPC SHELL. FINAL THICKNESSES IN LOCAL AREAS OF GRINDING SHALL BE CONFIRMED BY UT EXAMINATION, AS APPROPRIATE.

12. FOR NON-CODE WELDS, THE PROVISIONS OF EITHER ASME IX OR AWS MAY BE FOLLOWED.

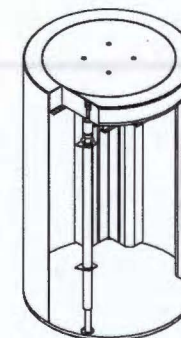
13. TOLERANCES FOR THICKNESS OF ASME CODE MPC ENCLOSURE VESSEL MATERIAL ARE SPECIFIED IN ASME SECTION II.

14. REFER TO THE COMPONENT COMPLETION RECORD (CCR) FOR THE COMPLETE LIST OF APPROVED DESIGN DEVIATIONS FOR EACH INDIVIDUAL SERIAL NUMBER.

15. DIMENSIONS NOTED AS NOMINAL ("NOM.") IN THIS DRAWING ARE FOR INFORMATION ONLY, IN ORDER TO INDICATE THE GENERAL SIZE OF THE COMPONENT OR PART. NOMINAL DIMENSIONS HAVE NO SPECIFIC TOLERANCE, BUT ARE MET THROUGH FABRICATION IN ACCORDANCE WITH OTHER DIMENSIONS THAT ARE TOLERANCED AND INSPECTED. NOMINAL DIMENSIONS ARE NOT SPECIFICALLY VERIFIED DURING THE FABRICATION PROCESS.

GENERAL NOTES:

1. THE EQUIPMENT DESIGN DOCUMENTED IN THIS DRAWING PACKAGE HAS BEEN CONFIRMED BY HOLTEC INTERNATIONAL TO COMPLY WITH THE SAFETY ANALYSES DESCRIBED IN THE SAFETY ANALYSIS REPORT.
2. DIMENSIONAL TOLERANCES ON THIS DRAWING ARE PROVIDED TO ENSURE THAT THE EQUIPMENT DESIGN IS CONSISTENT WITH THE SUPPORTING ANALYSES. HARDWARE IS FABRICATED IN ACCORDANCE WITH THE DESIGN DRAWINGS, WHICH MAY HAVE MORE RESTRICTIVE TOLERANCES, TO ENSURE COMPONENT FIT-UP. DO NOT USE WORST-CASE TOLERANCE STACK-UP FROM THIS DRAWING TO DETERMINE COMPONENT FIT-UP.
3. THE REVISION LEVEL OF EACH INDIVIDUAL SHEET IN THIS PACKAGE IS THE SAME AS THE REVISION LEVEL OF THIS COVER SHEET. A REVISION TO ANY SHEET(S) IN THIS PACKAGE REQUIRES UPDATING OF REVISION NUMBERS OF ALL SHEETS TO THE NEXT REVISION NUMBER.
4. THE ASME BOILER AND PRESSURE VESSEL CODE (ASME CODE), 1995 EDITION WITH ADDENDA THROUGH 1997 IS THE GOVERNING CODE FOR THE MPC ENCLOSURE VESSEL, WITH CERTAIN APPROVED ALTERNATIVES AS LISTED IN THE HUMBOULT BAY ISFSI FSAR TABLE 3-4-5 AND HOLTEC HI-STAR SAR TABLE 1.3-2 FOR TRANSPORTATION. THE ENCLOSURE VESSEL IS CONSTRUCTED IN ACCORDANCE WITH THE ASME SECTION II, SUBSECTION NB WITH CERTAIN APPROVED CODE ALTERNATIVES AS DESCRIBED IN THE SAR, NEW OR REVISED ASME CODE ALTERNATIVES REQUIRE PRIOR NRC APPROVAL BEFORE IMPLEMENTATION.
5. ALL MPC ENCLOSURE VESSEL STRUCTURAL MATERIALS ARE "ALLOY X" UNLESS OTHERWISE NOTED. ALLOY X IS ANY OF THE FOLLOWING STAINLESS STEEL TYPES: 316, 316L, 304, AND 304L. ALLOY X MATERIAL MUST COMPLY WITH ASME SECTION II, PART A, WELD MATERIAL COMPLIES WITH ASME SECTION II, PART A, WELD TYPE 1. ALL VESSEL WALL (I.E. CYLINDER SHELL) WILL BE FABRICATED OF PIECES MADE FROM THE SAME TYPE OF STAINLESS STEEL.
6. ALL WELDS REQUIRE VISUAL EXAMINATION (VT). ADDITIONAL NDE INSPECTIONS ARE NOTED ON THE DRAWING AS REQUIRED. NDE TECHNIQUES AND ACCEPTANCE CRITERIA ARE GOVERNED BY ASME SECTIONS V AND III, RESPECTIVELY, AS CLARIFIED IN THE APPLICABLE SAFETY ANALYSIS REPORTS.
7. UNLESS OTHERWISE NOTED, FULL PENETRATION WELDS MAY BE MADE FROM EITHER SIDE OF A COMPONENT.
8. FUEL BASKET SUPPORTS ARE ILLUSTRATIVE. ACTUAL FUEL BASKET SUPPORT ARRANGEMENTS ARE SHOWN ON THE INDIVIDUAL FUEL BASKET DRAWINGS.
9. ALL WELD SIZES ARE MINIMUMS. LARGER WELDS ARE PERMITTED. LOCAL AREAS OF UNDERSIZE WELDS ARE ACCEPTABLE WITHIN THE LIMITS SPECIFIED IN THE ASME CODE, AS APPLICABLE.



MPC-HB ENCLOSURE VESSEL  
ISOMETRIC VIEW



HOLTEC CENTER  
555 LINCOLN DRIVE WEST  
ANN ARBOR, MI 48106

PROJECT NO.

1125

P.O. NO. 35001202

CLINT	STAR UPDATE
-------	-------------

FEAR OF DATE  
HUMBOLDT BAY ISFBI

DESCRIPTIVE ... volume number ...

FIGURE 3.3-1  
SHEET 1 OF 4

L	MPC-HS ENCLOSURE YES
---	----------------------

[illegible]

Revision 1	
DATE: 01/01/2010	BY: J. J. J.

4102 1

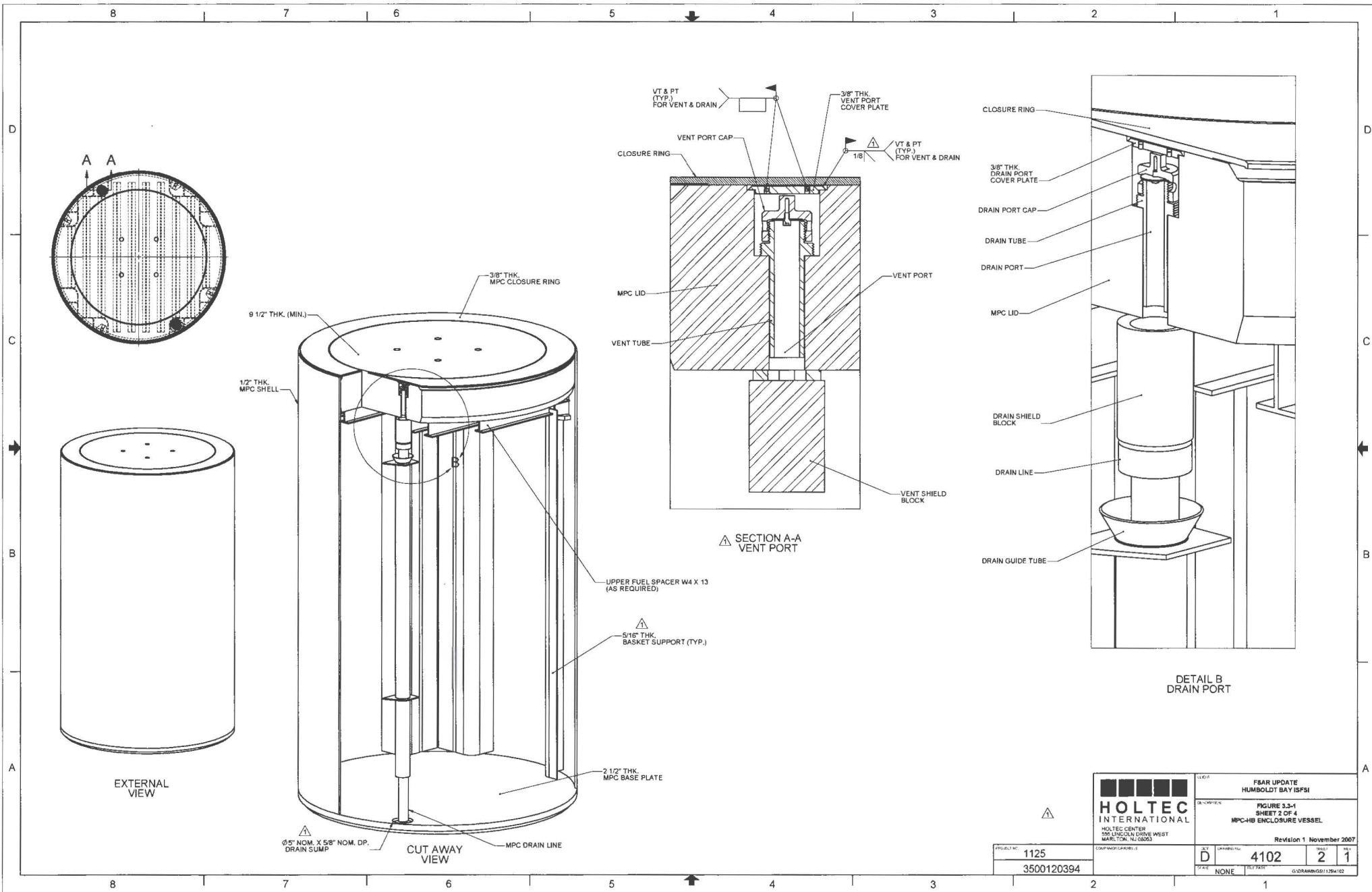
FILE NAME	FILE PATH	FILE TYPE
FILE NAME	FILE PATH	FILE TYPE

Revision 1 November 200

SHEET	TOTAL SHEETS
-------	--------------

1	4
---	---

G:\DRAWINGS\11254102



**HOLTEC**  
INTERNATIONAL

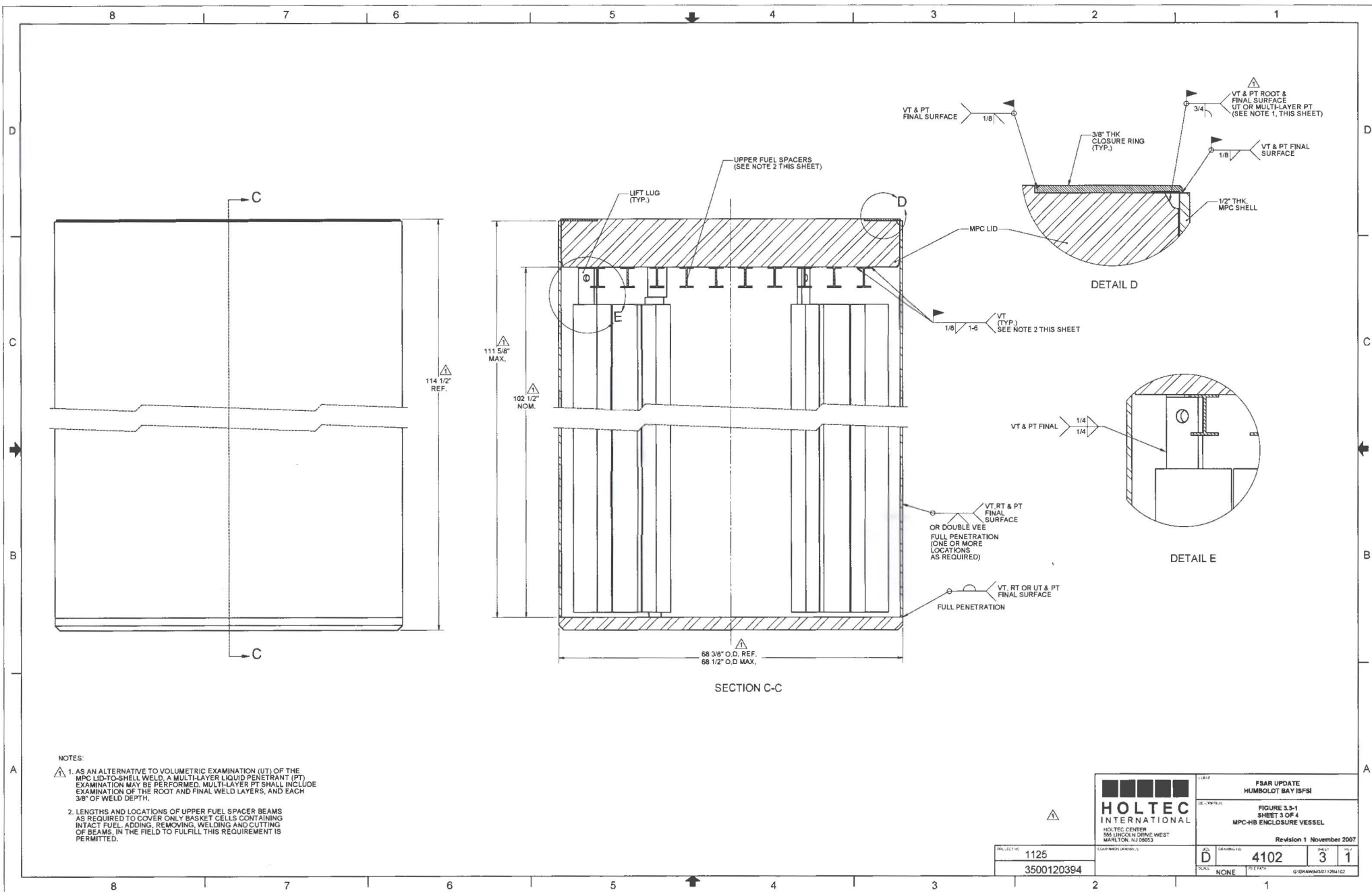
FSAR UPDATE  
HUMBOLDT BAY ISFSI

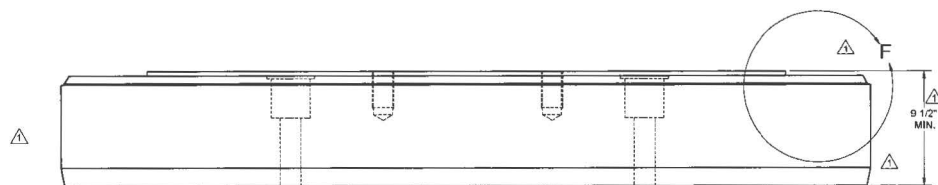
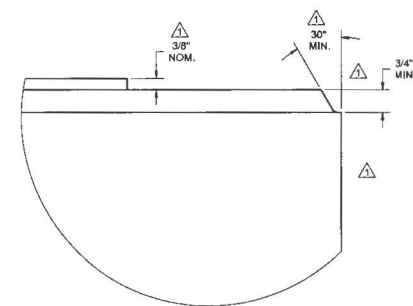
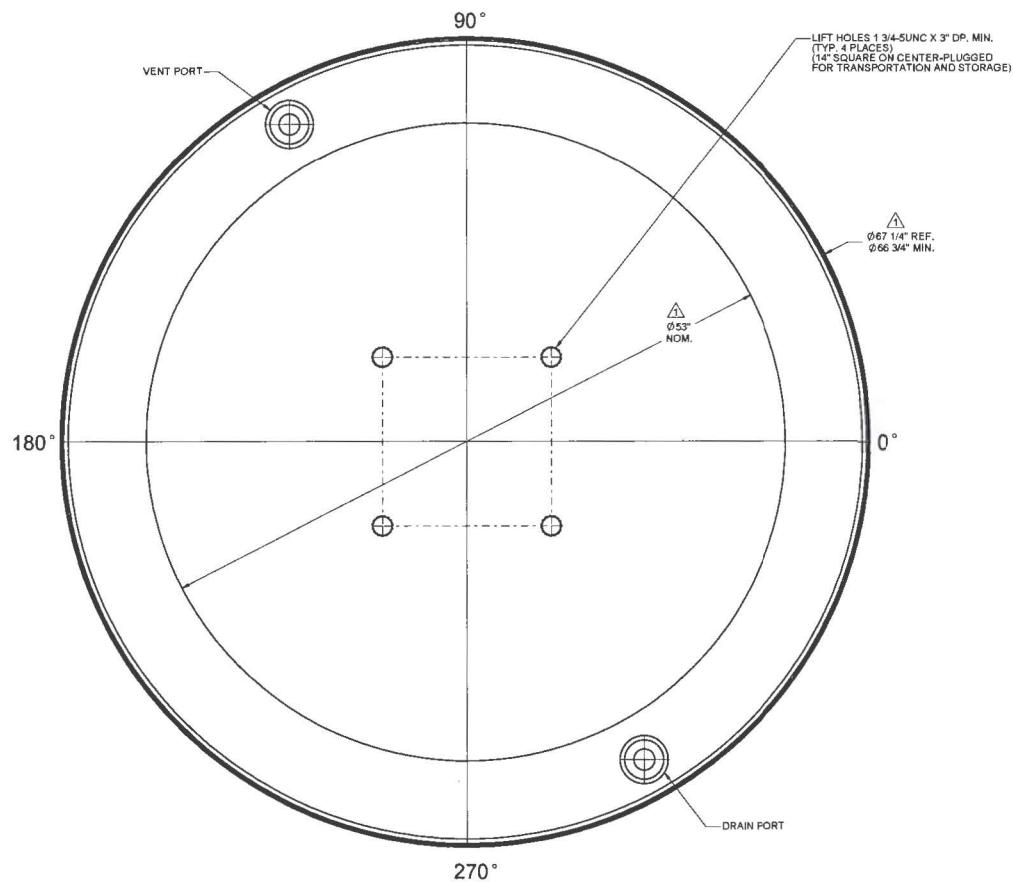
FIGURE 3.3-1  
SHEET 2 OF 4  
MPC-HB ENCLOSURE VESSEL

Revision 1 November 2007

DESIGN NO.	1125	DATE	D	REVISION NO.	4102	REV	2	REV	1
PROJECT NO.	3500120394	DATE	NONE	REV	NONE	DATE	11/29/07	REV	NONE







**HOLTEC**  
INTERNATIONAL  
HOLTEC CENTER  
500 LINCOLN DRIVE WEST  
MARTIN, NJ 08053

FSAR UPDATE HUMBOLDT BAY ISFSI			
FIGURE 3.3-1 SHEET 4 OF 4 MPC-HB ENCLOSURE VESSEL			
Revision 1 November 2007			
PROJECT NO. 1125	DESIGN NO. 4102	REVISION 4	DATE 1
3500120394	NONE	FILE PATH	GRAPHICS\11064132

PG&amp;E

P.O. NO. 3500120394

TOTAL SHEETS 3

**LICENSING DRAWING PACKAGE CONTENTS:**

[illegible]

# LICENSING DRAWING PACKAGE COVER SHEET

### REVISION LOG

[illegible]

12. TOLERANCES FOR THICKNESS OF ASME CODE MATERIAL ARE SPECIFIED IN ASME SECTION II.

13. ALL WELD SIZES ARE MINIMUMS. LARGER WELDS ARE PERMITTED. LOCAL AREAS OF UNDERSIZE WELDS ARE ACCEPTABLE WITHIN THE LIMITS SPECIFIED IN THE ASME CODE, AS CLARIFIED IN THE SAR.

14. REFER TO THE COMPONENT COMPLETION RECORD (CCR) FOR THE COMPLETE LIST OF APPROVED DESIGN DEVIATIONS FOR EACH INDIVIDUAL SERIAL NUMBER.

15. DIMENSIONS NOTED AS NOMINAL ("NOM.") IN THE DRAWING ARE FOR INFORMATION ONLY. IN ORDER TO INDICATE THE GENERAL SIZE OF THE COMPONENT OR PART, NOMINAL DIMENSIONS HAVE NO SPECIFIC TOLERANCE, BUT ARE MET THROUGH FABRICATION IN ACCORDANCE WITH OTHER DIMENSIONS THAT ARE TOLERANCED AND INSPECTED. NOMINAL DIMENSIONS ARE NOT SPECIFICALLY VERIFIED DURING THE FABRICATION PROCESS.

16. THE NEUTRON ABSORBER PANELS MAY BE A SINGLE PIECE OR TWO PIECES AS LONG AS THE TOTAL LENGTH INDICATED IS MAINTAINED AND THE GAP BETWEEN THE PANELS IS MAINTAINED AT LESS THAN 1/4".

17. THE NEUTRON ABSORBER PANELS MAY HAVE A REDUCTION IN WIDTH OF UP TO 1/32" OVER A LENGTH OF NO MORE THAN 12" PROVIDED THE AVERAGE WIDTH OF THE PANEL IS GREATER THAN THE MINIMUM SPECIFIED.

GENERAL NOTES:

1. THE EQUIPMENT DESIGN DOCUMENTED IN THIS DRAWING PACKAGE HAS BEEN CONFIRMED BY HOLTEC INTERNATIONAL TO COMPLY WITH THE SAFETY ANALYSIS DESCRIPTIONS DESCRIBED IN THE SAFETY ANALYSIS REPORT.
2. DIMENSIONAL TOLERANCES ON THIS DRAWING ARE PROVIDED TO ENSURE THAT THE EQUIPMENT DESIGN IS CONSISTENT WITH THE SUPPORT STRUCTURE. THIS FABRICATED VESSEL IS FABRICATED IN ACCORDANCE WITH THE DESIGN DRAWING, WHICH MAY HAVE MORE RESTRICTIVE TOLERANCES, TO ENSURE COMPONENT FIT-UP. DO NOT USE WORST-CASE TOLERANCE STACK-UP FROM THIS DRAWING TO DETERMINE COMPONENT FIT-UP.
3. THE REVISION LEVEL OF EACH INDIVIDUAL SHEET IN THIS PACKAGE IS THE SAME AS THE REVISION LEVEL OF THIS COVER SHEET. A REVISION TO ANY SHEET(S) IN THIS PACKAGE REQUIRES UPDATING OF REVISION NUMBERS OF ALL SHEETS TO THE NEXT REVISION NUMBER.
4. THE ASME BOILER AND PRESSURE VESSEL CODE (ASME CODE), 1995 EDITION WITH ADDENDA THROUGH 1997, IS THE GOVERNING CODE FOR THE HI-STAR 100 SYSTEM, WITH CERTAIN APPROVED ALTERNATIVES AS LISTED IN THE HUMBOLDT BAY IFSFI FSAR TABLE 3.4-5 AND HOLTEC HI-STAR SAR TABLE 1.3.2 FOR TRANSPORTATION. THE MPC FUEL BASKET IS CONSTRUCTED IN ACCORDANCE WITH ASME SECTION III, SUBSECTION NG AS DESCRIBED IN THE SAR. NEW OR REVISED ASME CODE ALTERNATIVES REQUIRE PRIOR NRC APPROVAL BEFORE IMPLEMENTATION.
5. ALL MPC BASKET STRUCTURAL MATERIALS COMPLY WITH THE REQUIREMENTS OF ASME SECTION II, PART A, WELD MATERIAL COMPLIES WITH THE REQUIREMENTS OF ASME SECTION II, PART C.
6. ALL WELDS REQUIRE VISUAL EXAMINATION (VT). ADDITIONAL NDE INSPECTIONS ARE NOTED ON THE DRAWING AS REQUIRED. NDE TECHNIQUES AND ACCEPTANCE CRITERIA ARE GOVERNED BY ASME SECTIONS V AND III, RESPECTIVELY, AS CLARIFIED IN THE APPLICABLE SAFETY ANALYSIS REPORTS.
7. FABRICATOR MAY ADD WELDS TO STITCH WELDS AT THEIR DISCRETION.
8. DO NOT MAKE A CONTINUOUS SEAL WELD BETWEEN THE SHEATHING AND THE CELL WALL.
9. ALL STRUCTURAL MATERIALS ARE "ALLOY X" UNLESS OTHERWISE NOTED. ALLOY X IS ANY OF THE FOLLOWING STAINLESS STEEL TYPES: 316, 316 LN, 304, AND 304 LN.
10. NEUTRON ABSORBER PANELS ARE INTENDED TO HAVE NO SIGNIFICANT FLAWS, HOWEVER, TO ACCOUNT FOR MANUFACTURING DEFECTS OCCURRING DURING INSTALLATION OF THE PANELS INTO THE MPC FUEL BASKET, DAMAGE OF UP TO THE EQUIVALENT OF A 1" DIAMETER HOLE IN EACH PANEL HAS BEEN ANALYZED AND FOUND TO BE ACCEPTABLE.
11. THIS COMPONENT IS CLASSIFIED AS ITS-A BASED ON THE HIGHEST CLASSIFICATION OF ANY SUBCOMPONENT. SUBCOMPONENT CLASSIFICATIONS ARE PROVIDED IN THE HUMBOLDT BAY IFSFI FSAR TABLE 4.5-1 AND HOLTEC HI-STAR SAR SUPPLEMENT 1.1 FOR TRANSPORTATION.



MPC-HB FUEL BASKET  
ISOMETRIC VIEW



HOLTEC CENTER  
555 LINCOLN DRIVE WEST  
NASHVILLE, ALABAMA

PROJECT NO. 1-10-10

1125

P.D. NO 35001203

CURRENT	FSAR UPDATE HUMBOLDT BAY ISFM
---------	----------------------------------

FIGURE 3.3-2  
SHEET 1 OF 3  
MPC-HB FUEL BASKET

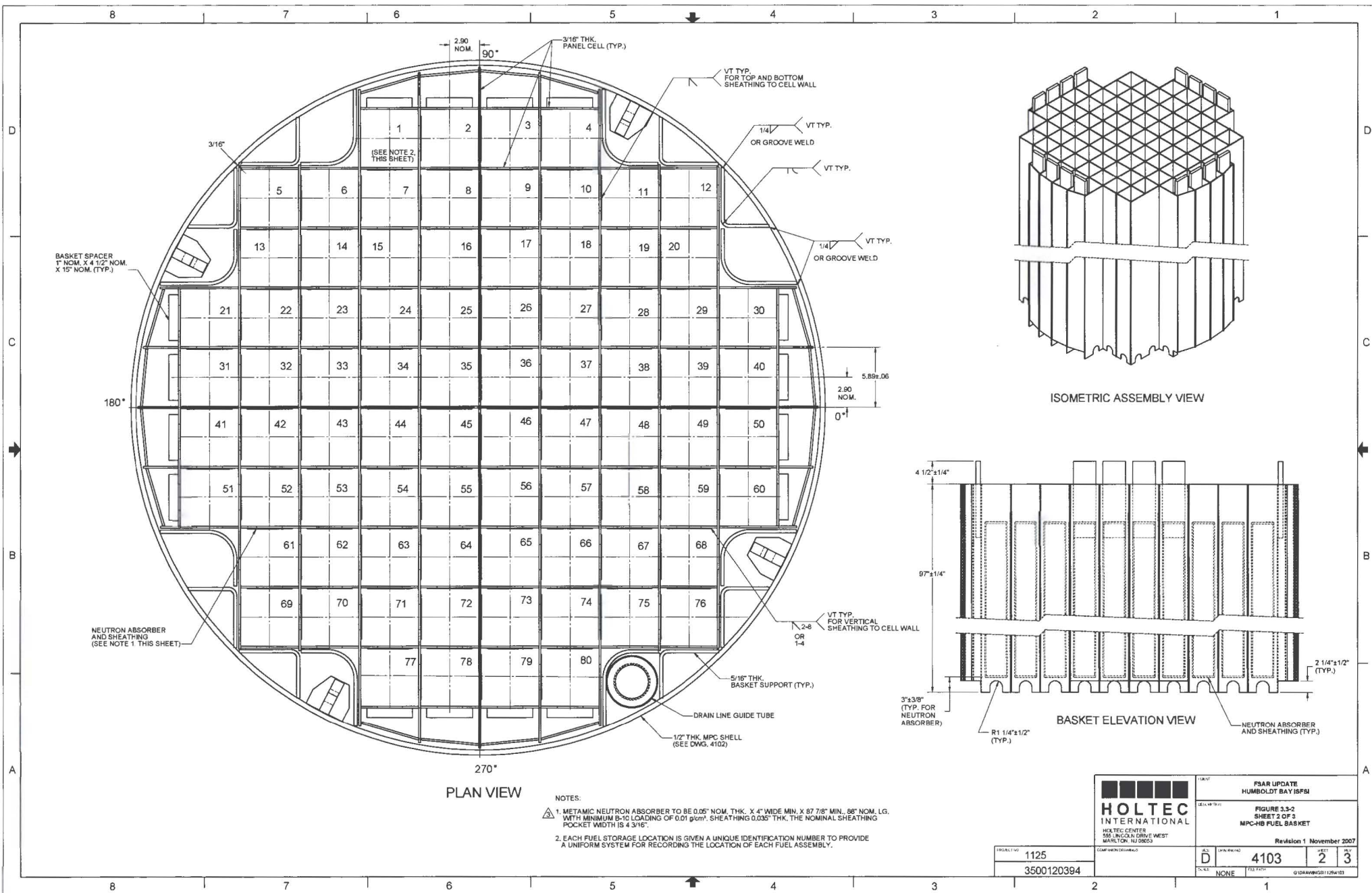
Revision 1 November 2003

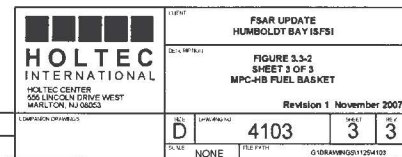
CRASHING NO.	1122	SHEET	4	TOTAL SHEETS	10
--------------	------	-------	---	--------------	----

4103	1	3
------	---	---

FILE PATH	G:\DRAWING\0211254\03
-----------	-----------------------







PROJECT NO.	1125
	3500120394

CLIENT PG&E

PROJECT NO. 1125

P.O. NO. 3500120394

DRAWING  
PACKAGE I.D. 4082

TOTAL SHEETS 7

### LICENSING DRAWING PACKAGE CONTENTS:

SHEET	DESCRIPTION
1	HI-STAR HB OVERPACK
2	ELEVATION VIEW
3	DETAIL OF TOP FLANGE AT 0° & 180°
4	DETAIL OF CLOSURE PLATE BOLT HOLE & BOLT
5	TOP PLAN VIEW "D" - "D"
6	MID-PLANE SECTION "E" - "E"
7	TEST VENT & DRAIN PORT DETAILS

### REVISION LOG

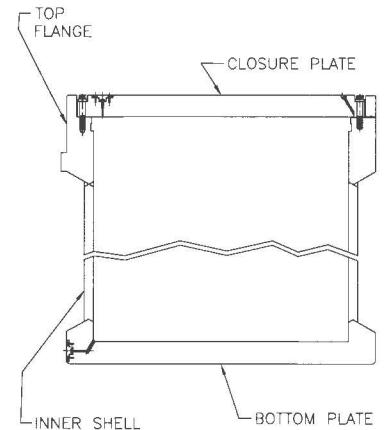
REV.	AFFECTED DRAWING SHEET NUMBERS	SUMMARY OF CHANGES/ AFFECTED ECOs	PREP. BY	APPROVAL DATE	VIR# [†]
0	INITIAL ISSUE	N/A	T.F.O.	10-03-03	85591
1	ALL SHEETS	ECO 1125-1	JJB	09-15-04	61945
2	SHEETS 1, 2, 3 & 4	ECO 1125-4 REV.0	JJB	06/05/06	80289
3	SHEETS 1,2,3,5 & 6	ECO 1125-8 REV.0	DCB	10/05/06	17458
4	SHEET 5	ECO 1125-15 REV.0	DCB	08/03/07	59612

[†] THE VALIDATION IDENTIFICATION RECORD (VIR) NUMBER IS A COMPUTER GENERATED RANDOM NUMBER WHICH CONFIRMS THAT ALL APPROPRIATE REVIEWS OF THIS DRAWING ARE DOCUMENTED IN COMPANY'S NETWORK.

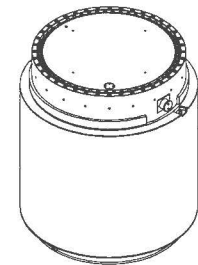
## LICENSING DRAWING PACKAGE COVER SHEET

#### GENERAL NOTES:

1. THE EQUIPMENT DESIGN DOCUMENTED IN THIS DRAWING PACKAGE HAS BEEN CONFIRMED BY HOLTEC INTERNATIONAL TO COMPLY WITH THE SAFETY ANALYSES DESCRIBED IN THE SAFETY ANALYSIS REPORT.
2. THE REVISION LEVEL OF EACH INDIVIDUAL SHEET IN THIS PACKAGE IS THE SAME AS THE REVISION LEVEL OF THIS COVER SHEET. A REVISION TO ANY SHEET(S) IN THIS PACKAGE REQUIRES UPDATING OF REVISION NUMBERS OF ALL SHEETS TO THE NEXT REVISION NUMBER.
3. ALL CATEGORY A, B, AND C JOINTS (NB-3351) IN THE CONTAINMENT BOUNDARY SHALL BE FULL PENETRATION WELDS.
4. THE ASME BOILER AND PRESSURE VESSEL CODE (ASME CODE), 1995 EDITION WITH ADDENDA THROUGH 1997 IS THE GOVERNING CODE FOR THE HI-STAR HB SYSTEM, WITH CERTAIN APPROVED ALTERNATIVES AS LISTED IN THE HUMBOLDT BAY ISFSI FSAR TABLE 3.4-5, AND HOLTEC HI-STAR SAR TABLE 1.3.2 (TRANSPORTATION). THE OVERPACK IS CONSTRUCTED IN ACCORDANCE WITH ASME SECTION III, SUBSECTION NB FOR THE CONTAINMENT BOUNDARY, AND SUBSECTION NF FOR THE BALANCE OF THE STRUCTURE, AS DESCRIBED IN THE SAR. NEW OR REVISED ASME CODE ALTERNATIVES REQUIRE PRIOR NRC APPROVAL BEFORE IMPLEMENTATION.
5. ALL WELDS REQUIRE VISUAL EXAMINATION. ADDITIONAL NDE INSPECTIONS ARE NOTED ON THE DRAWING. NDE TECHNIQUES AND ACCEPTANCE CRITERIA ARE GOVERNED BY ASME SECTIONS V AND III, RESPECTIVELY AS CLARIFIED IN THE APPLICABLE SAFETY ANALYSIS REPORTS.
6. PRESSURE (CONTAINMENT) BOUNDARY COMPONENTS SHALL MEET THE MATERIAL ACCEPTANCE CRITERIA OF NB-2000. ALL SUPPORT STRUCTURE (NON-CONTAINMENT) MATERIAL SHALL MEET THE ACCEPTANCE CRITERIA OF NF-2000.
7. WELDING PROCEDURES AND WELDER QUALIFICATIONS SHALL BE PER ASME SECTION IX AND ASME SECTION III (SUBSECTION NB FOR PRESSURE (CONTAINMENT) BOUNDARY WELDS AND SUBSECTION NF FOR NON-CONTAINMENT BOUNDARY WELDS).
8. THE NEUTRON SHIELD ENCLOSURE SHALL INCLUDE OVERPRESSURE PROTECTION. THE MAXIMUM SET PRESSURE OF THE PRESSURE RELIEF DEVICES IS 35 PSIG.
9. ALL SEALING SURFACES SHALL BE STAINLESS STEEL OVERLAID.
10. DRAWING IS NOT TO SCALE.
11. ADDITIONAL HOLES MAY BE ADDED BY THE FABRICATOR FOR LIFTING AND HANDLING WITH APPROVAL BY THE DESIGNER. HOLES NOT USED FOR TRANSPORTATION SHALL BE PLUGGED WITH STEEL.
12. DIMENSIONAL TOLERANCES ON THIS DRAWING ARE PROVIDED TO ENSURE THAT THE EQUIPMENT DESIGN IS CONSISTENT WITH THE SUPPORTING ANALYSES. HARDWARE IS FABRICATED IN ACCORDANCE WITH THE DESIGN DRAWINGS, WHICH MAY HAVE MORE RESTRICTIVE TOLERANCES, TO ENSURE COMPONENT FIT-UP. DO NOT USE WORST-CASE TOLERANCE STACK-UP FROM THIS DRAWING TO DETERMINE COMPONENT FIT-UP.
13. ALL WELD SIZES ARE MINIMUMS. LARGER WELDS ARE PERMITTED. LOCAL AREAS OF UNDERSIZE WELDS ARE ACCEPTABLE WITHIN THE LIMITS SPECIFIED IN THE ASME CODE, AS APPLICABLE.
14. THIS COMPONENT IS CLASSIFIED AS ITS-A BASED ON THE HIGHEST CLASSIFICATION OF ANY SUBCOMPONENT. SUBCOMPONENT CLASSIFICATIONS ARE PROVIDED IN THE HUMBOLDT BAY ISFSI FSAR TABLE 4.5-1 AND THE HOLTEC HI-STAR SUPPLEMENT 1.1 FOR TRANSPORTATION.
15. HOLTITE-A NEUTRON SHIELDING MATERIAL HAS CRITICAL CHARACTERISTICS OF (ALL VALUES NOMINAL): 1 WT % B4C, 6 WT % HYDROGEN, AND A SPECIFIC GRAVITY OF 1.68 GM/CC. OTHER CONSTITUENTS OF HOLTITE-A SHALL BE AS DESCRIBED IN HOLTEC PROPRIETARY REPORT HI-2002396, REV. 3.
16. OVERPACK INNER CAVITY TO BE COATED WITH THERMALINE 450 OR IDENTICAL SUBSTITUTE. OVERPACK EXTERNAL SURFACES (EXCEPT THREADED HOLES AND SEALING SURFACES) TO BE COATED WITH CARBOLINE 890 OR IDENTICAL SUBSTITUTE.
17. FOR NON-CODE WELDS, THE PROVISIONS OF EITHER ASME IX OR AWS MAY BE FOLLOWED.
18. TOLERANCES FOR THE THICKNESS OF ASME CODE OVERPACK MATERIAL ARE SPECIFIED IN ASME SECTION II.
19. REFER TO THE COMPONENT COMPLETION RECORD (CCR) FOR THE COMPLETE LIST OF APPROVED DESIGN DEVIATIONS FOR EACH INDIVIDUAL SERIAL NUMBER.
20. DIMENSIONS NOTED AS NOMINAL ("NOM.") IN THIS DRAWING ARE FOR INFORMATION ONLY. IN ORDER TO INDICATE THE GENERAL SIZE OF THE COMPONENT OR PART, NOMINAL DIMENSIONS HAVE NO SPECIFIC TOLERANCE, BUT ARE MET THROUGH FABRICATION IN ACCORDANCE WITH OTHER DIMENSIONS THAT ARE TOLERANCED AND INSPECTED. NOMINAL DIMENSIONS ARE NOT SPECIFICALLY VERIFIED DURING THE FABRICATION PROCESS.



HI-STAR HB CONTAINMENT BOUNDARY



HI-STAR HB OVERPACK ISOMETRIC VIEW

**HOLTEC**  
INTERNATIONAL  
HOLTEC CENTER  
555 LINCOLN DRIVE WEST  
MARLTON, NJ 08053

PROJECT NO. 1125  
P.O. NO. 3500120394

CLIENT FSAR UPDATE  
HUMBOLDT BAY ISFSI

DESCRIPTION FIGURE 3.3-3  
SHEET 1 OF 7  
HI-STAR HB OVERPACK

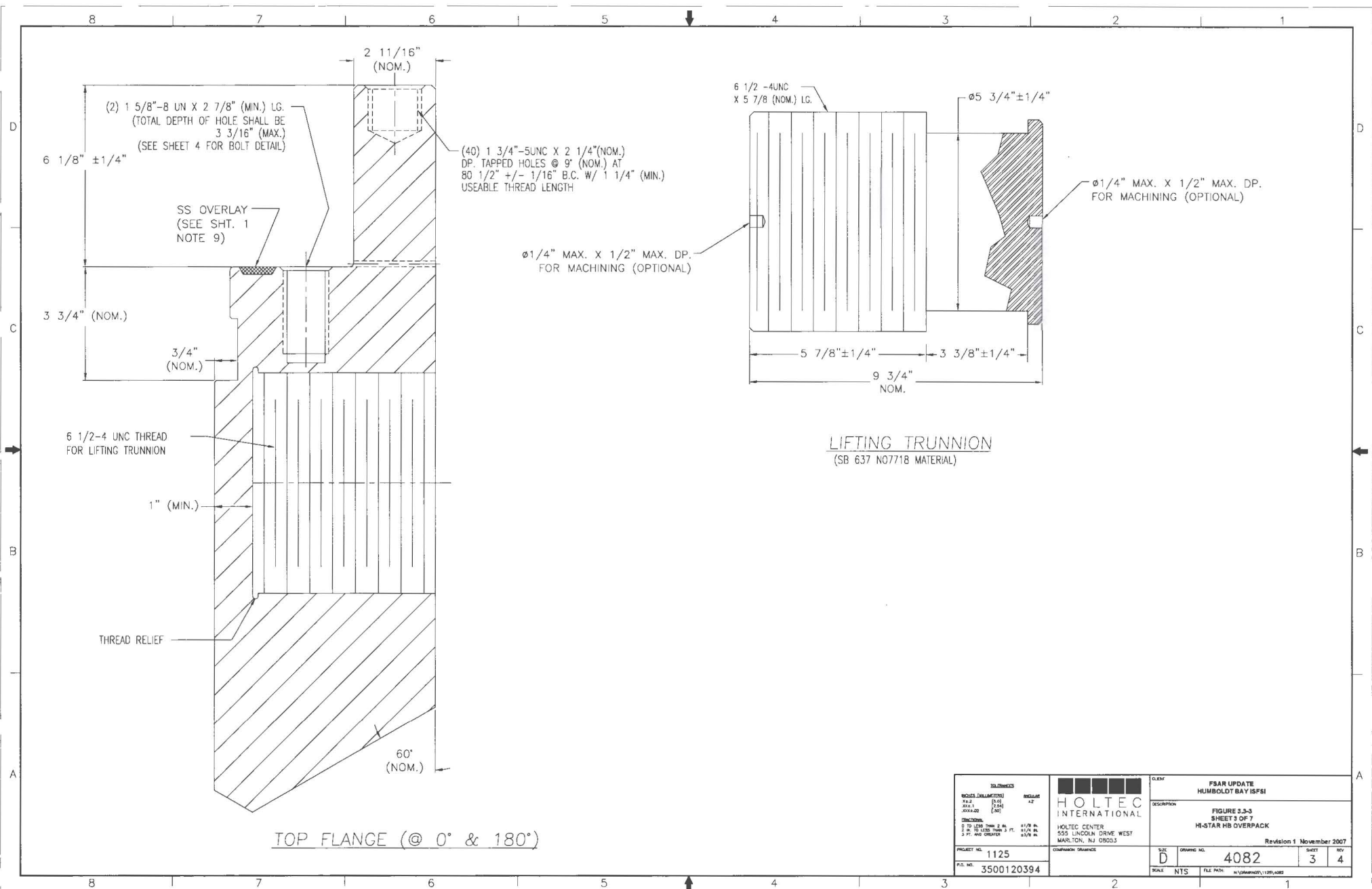
Revision 1 November 2007

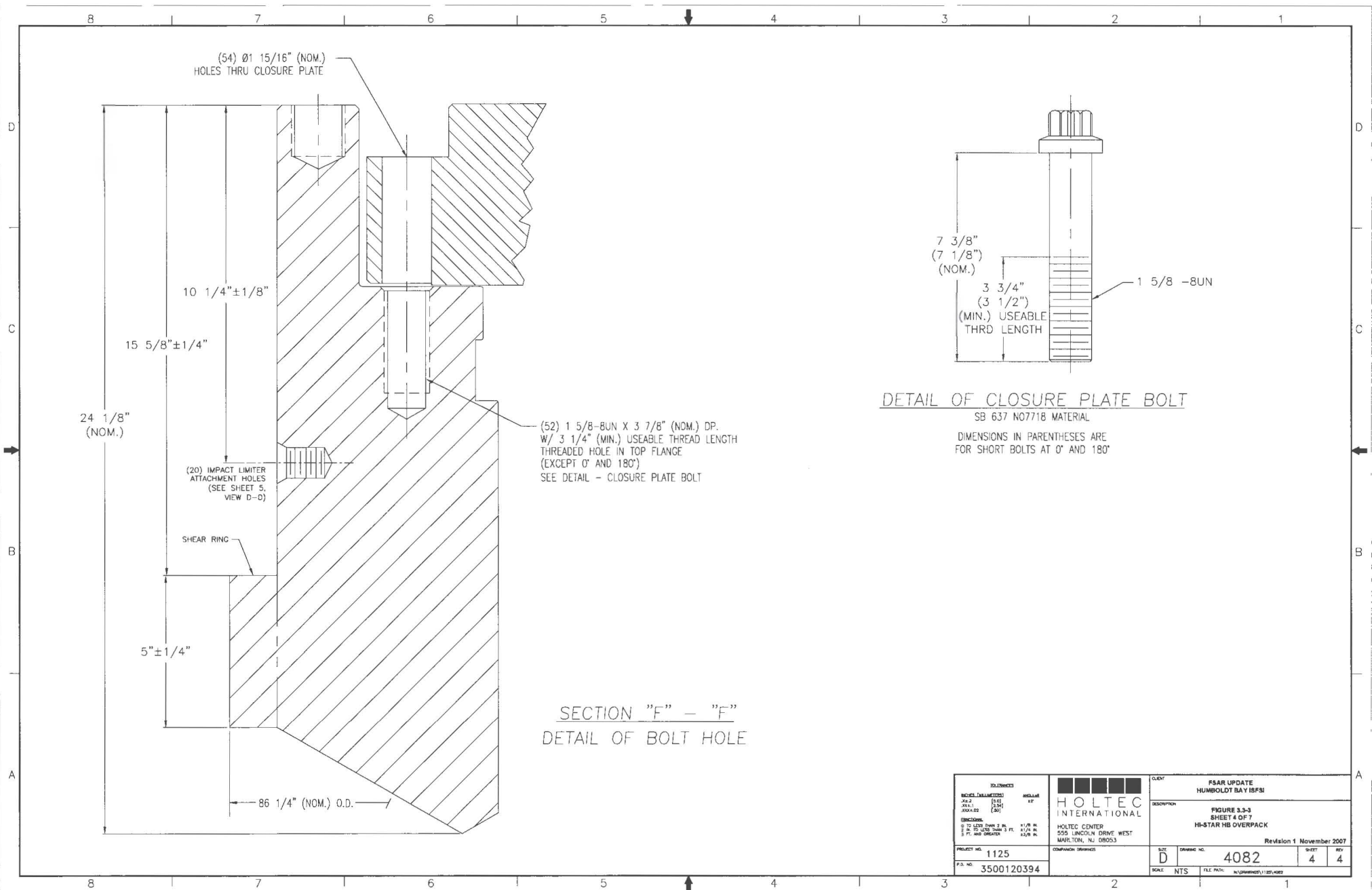
DRAWING NO. 4082  
SHEET 1 TOTAL SHEETS 7

FILE PATH: \\holtec\hds\1125\4082

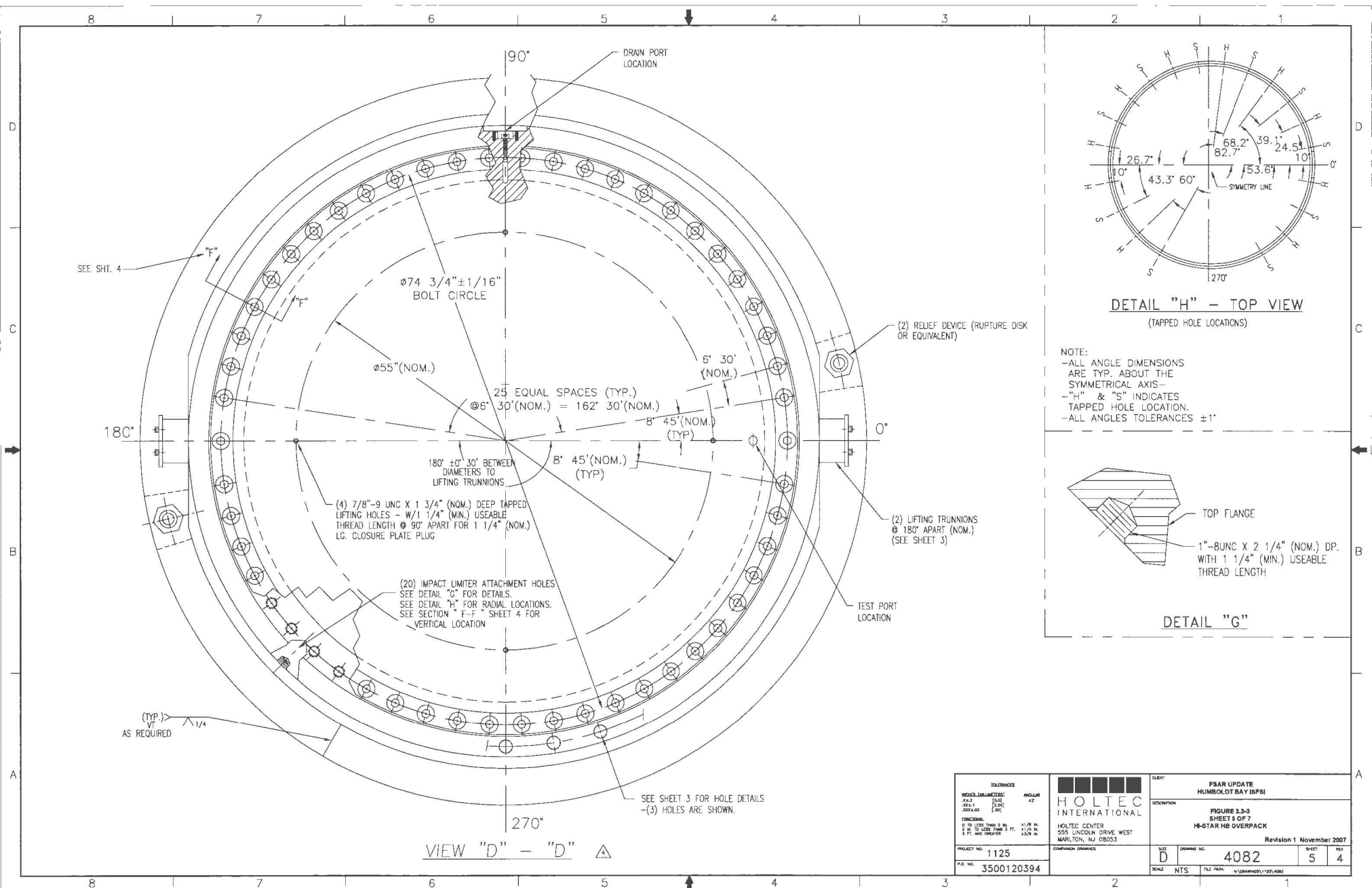




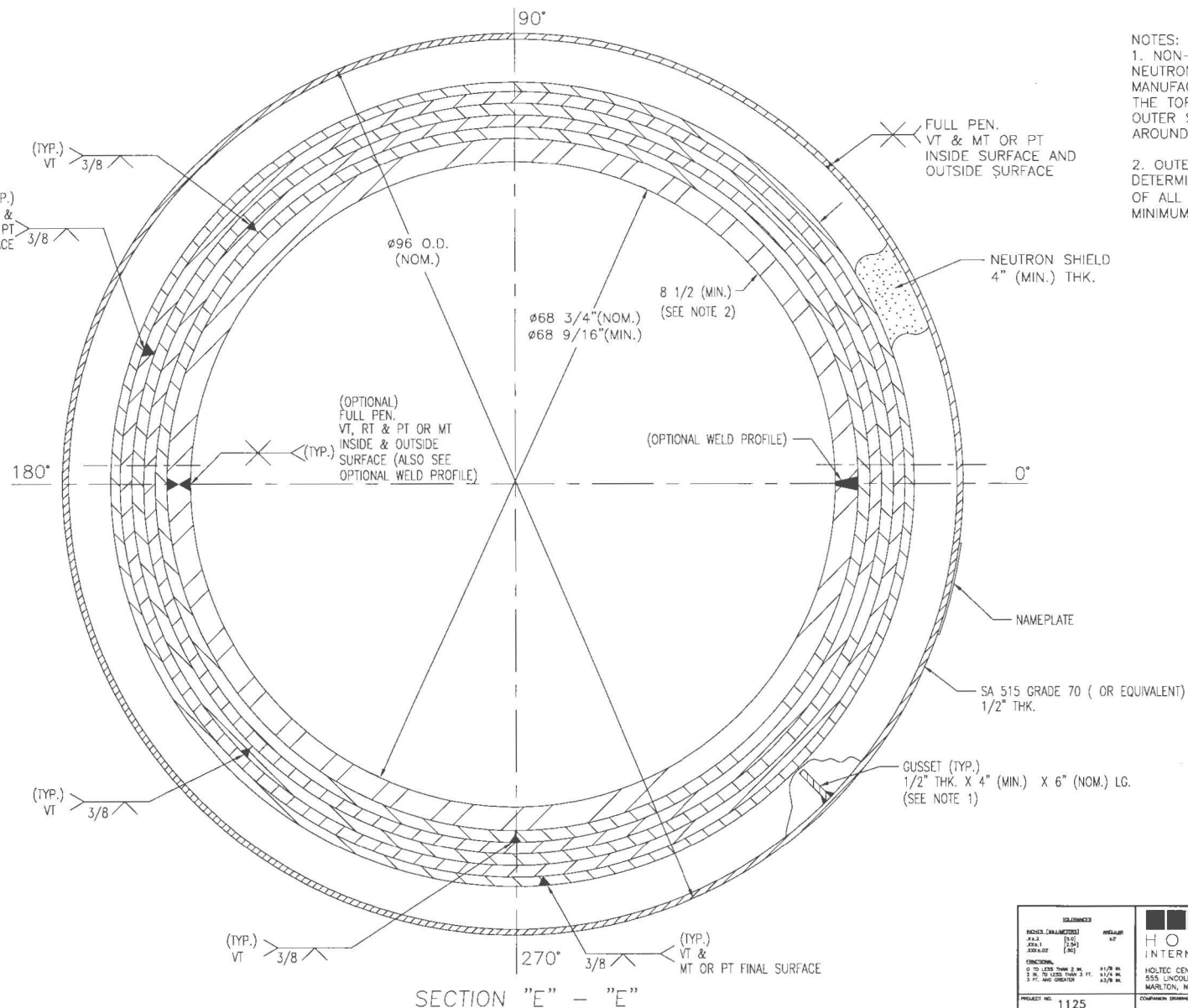




<b>REVISED</b> HOLTEC INTERNATIONAL JUL 2 2004 JUL 2 2004	<b>HOLTEC INTERNATIONAL</b> HOLTEC CENTER 555 LINCOLN DRIVE WEST MARLTON, NJ 08053	CLIENT: PSAR UPDATE HUMBOLDT BAY 18F8I DESCRIPTION: FIGURE 3.3-3 SHEET 4 OF 7 H8-STAR HB OVERPACK Revision 1 November 2007
PROJECT NO. 1125 P.O. NO. 3500120394	DRAWING NO. 4082 SCALE: NTS FILE PATH: \\HOLTEC\1125\4082	SHEET 4 REV 4

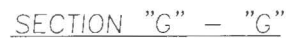


TOLERANCES		HOLTEC INTERNATIONAL		CLIENT	
HOLES (UNLESS NOTED)	MODULAR	HOLTEC INTERNATIONAL		FSAR UPDATE	
Ø 1/2	±.01	HOLTEC CENTER		HUMBOLDT BAY ISFSR	
Ø 3/4	±.01	555 LINCOLN DRIVE WEST		FIGURE 3.3-3	
Ø 1	±.01	MARLTON, NJ 08053		SHEET 5 OF 7	
Ø 1 1/2	±.01	PROJECT NO. 1125		H-STAR HB OVERPACK	
Ø 2	±.01	P.O. NO. 3500120394		Revision 1 November 2007	
Ø 2 1/2	±.01	CONFIRMATION (DATE)		SIZE D	
Ø 3	±.01	DRAWING NO. 4082		SHEET 5	
Ø 3 1/2	±.01	SCALE NTS		REV 4	
Ø 4	±.01	FILE PATH: \\100\HOLTEC\1125\4082			

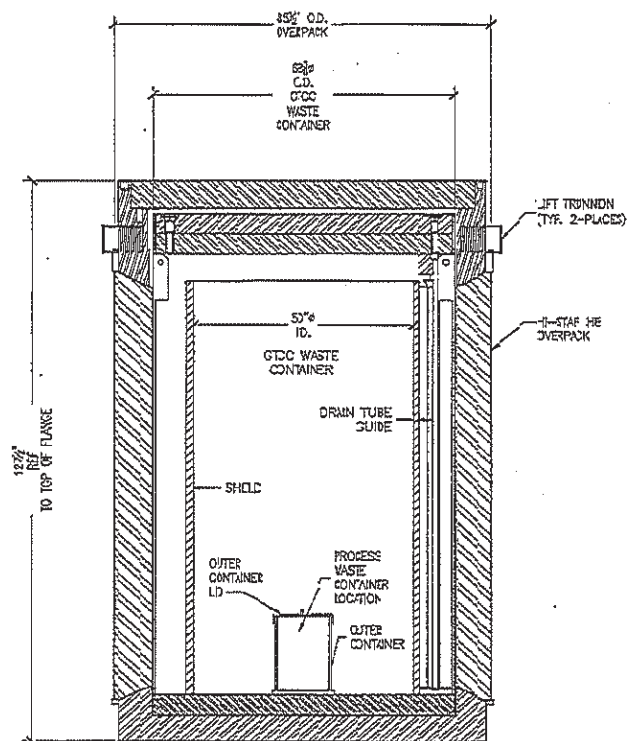


- NOTES:
1. NON-STRUCTURAL GUSSETS TO CONTROL NEUTRON SHIELD THICKNESS DURING MANUFACTURING, EIGHT GUSSETS EACH WITHIN THE TOP AND BOTTOM 10 INCHES OF THE OUTER SHELL, APPROXIMATELY EQUALLY SPACED AROUND THE CIRCUMFERENCE.
  2. OUTER LAYER SHELL THICKNESS SHALL BE DETERMINED BASED ON TOLERANCE STACKUP OF ALL INNER SHELLS SUCH THAT 8 1/2" MINIMUM TOTAL THICKNESS IS MAINTAINED.

REVISED (DATE) BY 11/25/07 (11/25/07) JAW/STJ 12/10/07 (12/10/07) JAW/STJ 01 TO LENS THIN 2 IN. 11/25/07 02 TO LENS THIN 2 IN. 11/25/07 03 TO LENS THIN 2 IN. 11/25/07		PROJECT NO. 1125 P.O. NO. 3500120394		HOLT TEC INTERNATIONAL HOLT TEC CENTER 555 LINCOLN DRIVE WEST MARLTON, NJ 08053		CLIENT FSAR UPDATE HUMBOLDT BAY 18FS1 DESCRIPTION FIGURE 1.3-3 SHEET 6 OF 7 HI-STAR HB OVERPACK Revision 1 November 2007	
SIZE D SCALE NTS		DRAWING NO. 4082 FILE PATH: \\HOLTEC\1125\4082		SHEET 6 REV 4			

[illegible]





SECTION A - A

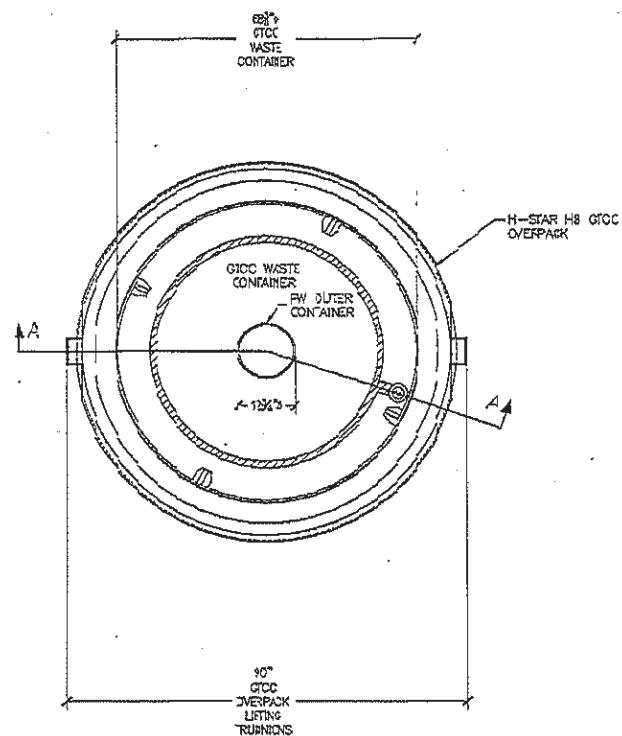
**GTCC DASK ASSEMBLY**  
N.T.S.

KEY:



STEEL

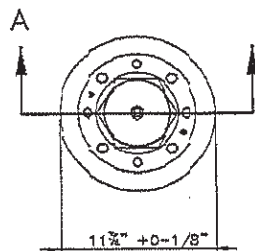
NOTE:  
*) CLOSURE LIDS NOT SHOWN IN TOP VIEW FOR CLARITY.



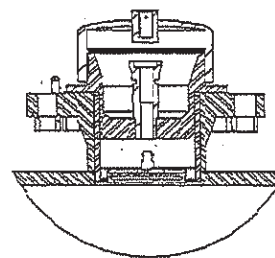
**TOP VIEW**  
N.T.S.

REVISION DESCRIPTION		HUMBOLDT BAY SFSI GTCC DASK ASSEMBLY OVERVIEW FSAR FIGURE 3.3-4		
8/21/12, REVISED FOR LAR 10-04 REVISION 1		DRAWING	SHEET	REV
		DSK-RKV-037	1 of 1	1

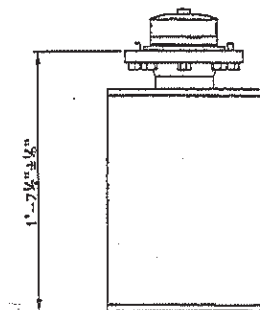
Revision 1 November 2015



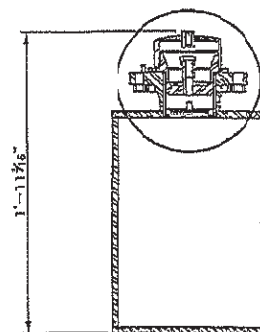
TOP VIEW  
N.T.S.



ENLARGED DETAIL B  
N.T.S.

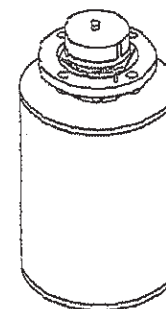


FRONT VIEW  
N.T.S.



SECTION A-A  
N.T.S.

SEE DETAIL B  
(CLOSURE  
ASSEMBLY)



PWC ISOMETRIC VIEW  
N.T.S.

REVISION DESCRIPTION	HUMBOLDT BAY POWER PLANT - FG&E CO.		
	PROCESS WASTE CONTAINER FSAR FIGURE 3.3-5		
8/23/12 REVISED FOR LAR 10-C1 REVISIONS	DRAWING DSK-RXY-042	SHEET 1 of 1	REV 1

Revision 1 November 2015

# HUMBOLDT BAY ISFSI FSAR UPDATE

## CHAPTER 4

### ISFSI DESIGN

#### CONTENTS

Section	Title	Page
4.1	LOCATION AND LAYOUT	4.1-1
4.2	STORAGE SYSTEM	4.2-1
4.2.1	Site Layout	4.2-1
4.2.2	Cask Storage Vault	4.2-1
4.2.3	HI-STAR HB Storage Cask	4.2-4
4.2.4	Instrumentation System Description	4.2-32
4.2.5	Compliance with General Design Criteria	4.2-32
4.2.6	References	4.2-32
4.3	TRANSPORT SYSTEM	4.3-1
4.3.1	Function	4.3-1
4.3.2	Components	4.3-1
4.3.3	Cask Transport Route	4.3-4
4.3.4	Design Bases and Safety Assurance	4.3-5
4.3.5	References	4.3-5
4.4	OPERATING SYSTEMS	4.4-1
4.4.1	Loading and Unloading System	4.4-1
4.4.2	Decontamination System	4.4-6
4.4.3	Storage Cask Repair and Maintenance	4.4-6
4.4.4	Utility Supplies and Systems	4.4-9
4.4.5	References	4.4-9
4.5	CLASSIFICATION OF STRUCTURES, SYSTEMS, AND COMPONENTS	4.5-1
4.5.1	Spent Fuel Storage Cask Components	4.5-2
4.5.2	Cask Storage Vault	4.5-3
4.5.3	Cask Transport System	4.5-3
4.5.4	Ancillary Equipment	4.5-3
4.5.5	Design Criteria for SSCs Not Important to Safety	4.5-3
4.5.6	References	4.5-4
4.6	MATERIALS EVALUATION	4.6-1
4.6.1	Multi-Purpose Canisters	4.6-2
4.6.2	Damaged Fuel Container	4.6-5
4.6.3	HI-STAR Overpack	4.6-6

HUMBOLDT BAY ISFSI  
SAFETY ANALYSIS REPORT

CHAPTER 4

**ISFSI DESIGN**

CONTENTS (Continued)

4.6.4	Neutron Absorber Efficacy	4.6-7
4.6.5	ISFSI Vault	4.6-7
4.6.6	Materials Summary	4.6-8
4.6.7	References	4.6-8
4.7	DECOMMISSIONING PLAN	4.7-1
4.7.1	Preliminary Decommissioning Plan	4.7-1
4.7.2	Features that Facilitate Decontamination and Decommissioning	4.7-1
4.7.3	Cost of Decommissioning and Funding Method	4.7-2
4.7.4	Long-Term Land Use and Irreversible Commitment of Resources	4.7-3
4.7.5	Recordkeeping for Decommissioning	4.7-3
4.7.6	References	4.7-3

HUMBOLDT BAY ISFSI  
SAFETY ANALYSIS REPORT

CHAPTER 4

**ISFSI DESIGN**

TABLES

Table	Title
4.2-1	Physical Characteristics of the HI-STAR MPC-HB
4.2-2	Comparison of HI-STAR 100 and HI-STAR HB System Bounding Weights
4.2-3	Comparison of Holtec MPC Design with ISG-18 Guidance for Storage
4.2-4	Physical Characteristics of the HI-STAR Overpack
4.2-5	Summary of MPC-HB Cavity Maximum Pressures for Normal Conditions
4.2-6	Finite Element Analysis Results for the MPC-HB Basket Under 60-g Loading
4.2-7	Results of Stress Calculations for Fuel Basket Spacers, Fuel Basket Spacer Welds, and Fuel Spacers
4.2-8	Results of Damaged Fuel Container Stress Analysis
4.2-9	Thermal Analysis Inputs
4.2-10	Normal Condition Thermal Analysis Results
4.2-11	Humboldt Bay ISFSI Compliance with General Design Criteria (10 CFR 72, Subpart F)
4.2-12	Interim Staff Guidance Compliance Matrix
4.3-1	Important-To-Safety Components of the Cask Transportation System
4.5-1	Quality Assurance Classification of Major Structures, Systems, and Components
4.6-1	HI-STAR HB System Materials Summary

HUMBOLDT BAY ISFSI  
SAFETY ANALYSIS REPORT

CHAPTER 4

**ISFSI DESIGN**

FIGURES

Figure	Title
4.1-1	Cask Storage Cells Layout with Surrounding Area
4.2-1	Detail View of the ISFSI Site
4.2-2	HI-STAR HB Overpack with MPC Partially Inserted
4.2-3	Damaged Fuel Container
4.2-4	MPC-HB Confinement Boundary
4.2-5	Cross-Section Elevation View of HI-STAR HB System
4.2-6	Soil Pressure Under Dead Load of Vault with Casks
4.2-7	Estimate of Volumetric Strain in Saturated Sands
4.3-1	Vertical Cask Transporter Carrying HI-STAR Outside the Humboldt Bay Fuel Building
4.3-2	HI-STAR on Rail Dolly Outside the Refueling Building
4.3-3	Vertical Cask Transporter Carrying HI-STAR at the ISFSI Vault



CHAPTER 4

**ISFSI DESIGN**

This chapter provides descriptive design information for the Humboldt Bay Independent Spent Fuel Storage Installation (ISFSI) structures, systems, and components (SSCs). Emphasized are those design features that are important to safety, are covered by the quality assurance program, and are employed to withstand environmental and accident forces. The industrial codes used in the design of these SSCs are related to their design criteria and associated bases that are presented in Chapter 3.

**4.1 LOCATION AND LAYOUT**

The locations of the Humboldt Bay ISFSI storage site and transport route from the Humboldt Bay Power Plant (HBPP) Refueling Building (RFB) are shown in Figure 2.2-2. In addition, Figure 2.2-2 shows other facilities in the vicinity of the Humboldt Bay ISFSI storage site, such as onsite roadways, buildings, water services, and transmission lines. None of these other facilities are related to the ISFSI. The Humboldt Bay ISFSI storage site and the transport route are within the HBPP owner-controlled area. Travel distance from the RFB via the transport route to the Humboldt Bay ISFSI storage site is approximately 0.24 miles (See Section 4.3.3 for a discussion of the transport route).

The HI-STAR HB casks are stored in a concrete vault identified as the Protected Area. The storage vault is designed to accommodate six casks, five casks will store spent fuel and the sixth will store greater than class C waste (GTCC), as shown in Figure 4.1-1. Each loaded spent fuel cask is approximately 8 ft in diameter, 10.5 ft high, and weighs about 160,000 lb. The vault configuration dimensions are approximately 30 ft x 70 ft within a Security Area Fence (approximately 70 ft x 112 ft).

A Security Area Fence, with a locked gate, circumscribes the storage vault. There is a minimum of 20 ft between the vault and the Security Area Fence, on all sides of the vault. A single story security building is located south of the ISFSI vault outside the Security Area Fence for the ISFSI. This building is approximately 20 ft x 40 ft.

The only utilities associated with the ISFSI are electric power for security lighting and communications and water and sewer for the security alarm station.

Loading of the multi-purpose canister takes place in the RFB. The RFB and modifications being made to facilitate cask handling are summarized in Section 4.4 and further described in License Amendment Request 04-02 to the HBPP 10 CFR 50 SAFSTOR license that was submitted in PG&E Letter HBL-04-016, dated July 9, 2004.

## **4.2 STORAGE SYSTEM**

The design and analyses of the major components of the Humboldt Bay Independent Spent Fuel Storage Installation (ISFSI), namely the cask storage vault and the HI-STAR HB System are provided in this section. Final construction design of the Humboldt Bay ISFSI facility will be completed during the detailed design phase of the project. No significant changes are anticipated from the information presented.

### **4.2.1 SITE LAYOUT**

A plan view of the ISFSI site layout is shown in Figure 2.2-2. This figure shows the functional features of the storage site, including the locations of the Security Area Fence, and the access road. A detail view of the ISFSI site is shown in Figure 4.2-1. This figure provides separation distances from the vault to nearby features.

### **4.2.2 CASK STORAGE VAULT**

The Humboldt Bay ISFSI storage vault is designed to accommodate six casks (five HI-STAR HB casks and one greater than class C (GTCC) certified cask) in individual storage vaults. Figure 4.1-1 shows the layout of the cask storage cells with the surrounding Security Area Fence and approximate dimensions. Six storage casks provide sufficient storage space for HBPP spent fuel and reactor-related GTCC waste to allow completion of plant decommissioning activities. The seismic design criteria for the cask storage vault are presented in Sections 3.2.4 and 3.3.2 and the seismic analysis of the vault is described in Section 8.2.1. The design bases, analyses, and resulting design of the cask storage vault for normal conditions is provided.

#### **4.2.2.1 Function**

The function of the cask storage vault is to provide a structurally competent facility for storage of the loaded storage casks for all design-basis conditions of storage. Each cask is stored in an individual reinforced concrete, steel-lined storage cell. The storage cells, with the lids installed, provide radiation shielding, security protection, protection from the environment, and defense-in-depth protection from tornado and explosion generated missiles. The overpack serves as the primary protection against tornado- and explosion-generated missiles. The steel storage cell liner also includes internal support attachments that provide lateral restraint during seismic events to ensure the casks continue to provide adequate structural integrity, decay heat removal, shielding, and criticality control for the stored contents. There are fixed cask alignment/seismic restraints at the bottom of the liner and removable seismic restraints at the top of the liner. The top seismic restraints are removable to allow insertion and removal of the cask. They are installed at all times during normal storage operations. The storage cells are not air or water tight, but no flow of either fluid is expected. The vault lids and closure bolts do not perform a design function with regard to restraining uplift of the cask.

#### 4.2.2.2 Design Specifications

The cask storage vault design is based on a maximum, loaded-cask weight of 161,200 lbs each. This maximum weight bounds the loaded weight of each HI-STAR HB overpack and the GTCC cask stored at the Humboldt Bay ISFSI. Each of five HI-STAR HB Systems used at the Humboldt Bay ISFSI contains one multi-purpose canister (MPC) with a fuel basket uniquely designed for HBPP fuel, known together as the MPC-HB. Nominal physical characteristics of the MPC-HB are provided in Table 4.2-1. One GTCC cask may occupy the sixth vault storage cell location. See Section 3.3.2 for more details on the storage vault design criteria.

#### 4.2.2.3 Plans and Sections

The site plan, which shows the location of the ISFSI storage vault in relation to HBPP, is shown in Figure 2.2-2.

#### 4.2.2.4 Vault and Storage Cell Components

- **Reinforced Concrete:** The steel-reinforced concrete is designed for a mix with a minimum compressive strength of 4,000 psi at 28 days curing and a minimum dry density of 146 lb/ft³. The reinforcing steel bars are deformed bars meeting ASTM A615, Grade 60 specifications. Refer to proprietary Holtec drawings 4105 and 4110 for details regarding the reinforced concrete vault rebar arrangement (Reference 23).
- **Storage Cell Steel Liner and Seismic Restraints:** The steel liner and seismic restraints are constructed of SA36 or SA516 Grade 70 carbon steel and are coated for protection against corrosion in the saline air environment of the Humboldt Bay ISFSI site. The seismic restraints include a non-steel bearing pad to prevent gouging the steel.
- **Storage Cell Lid:** The storage cell lids are constructed of SA36 or SA516 Grade 70 carbon steel plates filled with concrete with minimum dry density of 146 lb/ft³.
- **Storage Cell Lid Closure Bolts:** The storage cell lid closure bolts are constructed of SA 193 B7 material.

#### 4.2.2.5 Design Bases and Safety Assurance

The cask storage vault is classified as important to safety in order to provide the appropriate level of quality assurance in the design and construction. This classification is consistent with the overall design function of the HI-STAR HB System. Individual subcomponents may be classified as not-important-to-safety based on their design functions. See Section 4.5 for additional information on safety classification of structures, systems, and components.

#### **4.2.2.6 Storage Vault Design**

The cask storage vault is comprised of six below-grade, cylindrical storage cells that are structural units constructed of steel-reinforced concrete with a carbon steel liner. Each storage cell is approximately 9 ft in diameter by 11 ft, 7 inches deep. The vault bottom is 3 ft thick reinforced concrete. There is an approximate 7 ft thickness of concrete on each end of the vault and 5-1/2 ft on the longitudinal sides of the vault. The concrete wall thickness varies around the circumference of the storage cells and has a minimum thickness of approximately 1 foot - 9 inches of concrete between adjacent cells. Each of the storage cells accommodates one cask (either a loaded HI-STAR HB overpack or the GTCC cask). The vault top elevation (without the storage cell lids installed) is approximately flush with grade. The lids are approximately 16-1/4 inches high, not including the height of the lid bolt caps. Figure 3.2-1 provides additional details on the vault layout and design.

#### **4.2.2.7 Storage Vault Structural Analysis**

The reinforced concrete storage vault was analyzed using the ANSYS finite element analysis code (Reference 1) to determine forces and moments on critical sections of the structure. The load combinations applicable to the vault structural analysis (Reference 2) are provided in Section 3.3.2.3.1. For the normal storage condition, the combination of dead load, live load, and earth loads were considered both with, and without temperature distribution-induced internal moments and forces (Load Cases 1 and 4). Additional loads on the structure were considered, as applicable, for the onsite cask transporter and vault lid. The force and moment output was compared to the capacities of the critical section through interaction diagrams and safety factors were computed. Two loading conditions of the vault were considered. The first is a single cell loaded and the remaining five cells empty, and the second with all cells loaded with casks.

The ISFSI storage vault was modeled on a foundation of 3-dimensional finite elements to establish the proper elastic foundation using soil properties. The surrounding soil along the walls of the vault was not modeled. Its lateral pressures from self-weight were applied as pressure to the walls of the vault.

The critical section of the vault is the section between two adjacent storage cells. The capacities of critical section were calculated using the Holtec QA-validated program ShapeBuilder (Reference 3). ShapeBuilder produces axial force-bending moment interaction diagrams that were used to determine compression, tension, positive and negative pure bending moment, and positive and negative balance axial force and moment capacities. However, ShapeBuilder does not apply capacity reduction factors in accordance with ACI 349. To incorporate the ACI-349 capacity reduction factors, the capacities are modified. Then, a simpler interaction diagram (bounded by the interaction diagram produced in ShapeBuilder) is reproduced for final load versus capacity comparisons.

The thermal analysis of the storage vault is a two-step process consisting of calculating the temperature distribution, then calculating the thermal stresses. For the temperature distribution, a loaded cell was assumed to have the maximum allowable local temperature applied to its inner surface. Empty cells were assumed to have adiabatic boundary conditions (i.e., zero heat transfer across the surface) applied to their inner surface. The far-field boundary condition was set at the site annual average soil temperature. Adiabatic boundary conditions were also assumed to exist over the top surface of the soil and vault. Thermal conductivities were applied to the different materials in the model and the temperature distribution was computed for both loading conditions. A steady-state solution method was used to solve for the nodal temperatures. The nodal temperatures were then used as input to the thermal stress analysis. The resistance to expansion of the vault from the soil was conservatively neglected since it produces compressive loads in the concrete thus increasing its load carrying capacity. The steel liner is not considered in the finite element model when solving for the temperature distribution. Because the liner is relatively thin, it is expected that the temperature through the thickness will be uniform. The shell elements of the liner share common nodes with the adjacent brick elements representing the concrete. Therefore, excluding the shell elements from the thermal solution does not alter the nodal temperature distribution. When computing thermal stresses from the temperature distribution, the shell elements were included and a differential coefficient of thermal expansion between steel and concrete produces thermal stresses.

Results at limiting sections of the reinforced concrete vault are compared to the allowable limits set forth by ACI 349-01. General post-processing commands in ANSYS were used to sum the force and moment about the centroid of the concrete sections. These results were compared to the capacities of the simplified interaction diagram derived from ShapeBuilder. All results from the normal condition structural analysis of the vault are within the allowables specified in ACI-349-01.

Additional information about the criteria used for segregating cracked and uncracked concrete sections of the storage vault is provided in the PG&E Response to NRC Question 5-8 in Reference 26.

#### **4.2.2.8 Potential Settlement of Storage Vault**

An assessment of potential settlement of the reinforced concrete storage vault and a discussion of how the potential settlement could affect the internal wall of the steel liner is provided in PG&E's response to NRC Question 5-9 (Reference 26).

### **4.2.3 HI-STAR HB STORAGE CASK**

The HI-STAR HB System is an all-metal, canister-based storage system designed to store boiling water reactor spent fuel (with or without channels) from the HBPP in a dry configuration at the Humboldt Bay ISFSI. The HI-STAR HB System is a shortened version of the HI-STAR 100 System, which is generically certified under 10 CFR 72,

## HUMBOLDT BAY ISFSI FSAR UPDATE

Subpart L, for use by 10 CFR 50 license holders under the general license provisions of 10 CFR 72 (Reference 4). The HI-STAR HB System is comprised of an all-welded multi-purpose canister (MPC-HB) designed to store up to 80 HBPP fuel assemblies inside a bolted-lid steel overpack that provides physical protection of the MPC and provisions for handling. The HI-STAR HB System is similar to the HI-STAR 100 System as described in the HI-STAR 100 Final Safety Analysis Report (Reference 5). Certain differences were incorporated into the HI-STAR HB System design to take advantage of the smaller HBPP fuel, advances in the neutron absorber material state of the art, and lessons learned in the fabrication of the generic HI-STAR 100 System. The significant differences are discussed below.

- The HI-STAR HB System is approximately 76 inches shorter than the generically certified system. This eliminates the need for lower fuel spacers.
- The MPC-HB can store up to 80 HBPP fuel assemblies versus 68 BWR fuel assemblies in the generically certified system.
- The upper fuel spacer design for the MPC-HB differs from the generic design in that cross beams are welded to the bottom of the MPC-HB lid instead of each fuel storage location having an individual pipe-segment spacer threaded into the underside of the MPC lid.
- The MPC-HB fuel basket design includes longitudinal fuel basket spacers welded to the top of the basket at several locations around the periphery to prevent the fuel spacers from impacting the top of the MPC basket.
- The HI-STAR HB System may use METAMIC[®] neutron absorbers as an alternative to BORAL[®] in the MPC-HB fuel basket while the generically certified HI-STAR 100 System only uses BORAL[®]. The use of METAMIC[®] in the generic Holtec MPC design is currently under review on the HI-STORM 100 System docket (Reference 6). Details on METAMIC[®] as a suitable neutron absorber for dry storage service are provided in Section 1.2.1.3.1.2 of the HI-STORM 100 Final Safety Analysis Report Update (FSAR), as amended by license amendment request LAR 1014-2.
- The HI-STAR HB System is lighter and has a lower center-of-gravity. See Table 4.2-2 for details.
- The design of the overpack neutron shield enclosure in the HI-STAR HB overpack has been modified to provide better shielding and simplified fabrication compared to the generically certified system. See Section 4.2.3.2.3 for a detailed description of the differences.
- The HI-STAR HB overpack does not include pocket trunnions.



## HUMBOLDT BAY ISFSI FSAR UPDATE

- The Holtite-A neutron shield material utilized in the HI-STAR HB system has a minimum hydrogen density of 0.091 g/cc. Also, the HI-STAR HB shielding analysis conservatively assumes a minimum hydrogen content of 5.6 wt %.
- The HI-STAR HB lid bolts for Serial Number 12 have a site specific analysis that show that 49 bolts are adequate to perform the design basis requirements.

The Holtec MPC design is generically certified for spent fuel storage under two 10 CFR 72 Certificates of Compliance (CoCs), namely HI-STAR 100 and HI-STORM 100. While the HI-STAR HB System design bases and analysis are primarily predicated on the HI-STAR 100 System (Docket 72-1008), certain design bases and analyses are drawn from the more current work for the MPC under the HI-STORM 100 docket (72-1014). This FSAR clearly delineates which generic FSAR provides the applicable information for licensing the HI-STAR HB System. Furthermore, the HI-STAR HB System is designed as a dual purpose storage and transportation cask system that precludes the need to re-package the fuel and GTCC for shipment to another off-site storage facility or federal repository. As such, certain design features and analyses may be based upon compliance with a Part 71 analysis or load combination, which provides a bounding case for Part 72.

The HI-STAR HB System design criteria are summarized in Chapter 3 of this FSAR and the HI-STAR 100 design criteria are summarized in Chapter 2 of the HI-STAR 100 System FSAR. In addition, certain MPC design criteria incorporated by reference in this FSAR are called out in the HI-STORM 100 FSAR. Where applicable, analyses performed for the generic HI-STAR 100 System design are incorporated by reference in this FSAR. Unique, site-specific analyses are performed where the generic analyses are not applicable or are overly conservative.

### 4.2.3.1 Function

The HI-STAR HB System is designed to store spent nuclear fuel from HBPP under all normal, off-normal, and accident conditions of service applicable to the Humboldt Bay site, including the most severe design-basis natural phenomena in accordance with 10 CFR 72. A total of six casks are deployed at the Humboldt Bay ISFSI with five containing spent fuel assemblies and the sixth containing HBPP GTCC waste. The GTCC cask will be designed to accept the specific GTCC waste to be stored at the ISFSI and be compatible with all HI-STAR HB lifting and handling equipment. As applicable, analyses performed for a cask containing spent fuel (e.g., shielding) bound the GTCC cask, eliminating the need to perform any unique analyses for the GTCC cask.

The HI-STAR HB System is completely passive in providing the necessary criticality control, decay heat removal, structural, and radiation shielding features necessary for safe interim spent fuel and GTCC storage at the ISFSI. As discussed in HI-STAR

FSAR Section 9.1.4.1, relief devices on the overpack neutron shield enclosure are the only devices associated with the system that must change state to operate, and they open on an overpressure condition postulated to occur only during a hypothetical fire accident event. No HI-STAR HB System components require motive power of any kind to perform their design function.

The HI-STAR HB System is designed to permit testing, inspection, and maintenance of the systems during cask preparation and storage operations, as required. The acceptance test program for the HI-STAR HB System is the same as that used for the HI-STAR 100 System as described in Section 9.1 of the HI-STAR 100 FSAR and modified appropriately to address design differences. Because of the passive nature of the HI-STAR HB System, no planned, periodic maintenance is required during storage operations. As discussed in Section 4.4.3, PG&E will conduct periodic visual inspections of the interior of the vault cells via video camera and perform any appropriate maintenance necessary based on the inspection results. No maintenance is expected to be required.

Surveillance requirements associated with operational control and limits during cask loading are described in Chapter 10. Inspection and testing of important-to-safety components are performed in accordance with the Holtec International or PG&E Quality Assurance Program, as applicable.

Each of the HI-STAR HB System components is described in further detail in the following sections. Figures are provided to illustrate the components and their functions.

### **4.2.3.2 Description**

In its final storage configuration, the HI-STAR HB System consists of the following major components considered important to safety:

- multi-purpose canister (MPC-HB)
- damaged fuel container (DFC)
- HI-STAR-HB overpack

Figure 4.2-2 (exploded isometric view) shows the components of the HI-STAR HB System. The following sections provide a summary of the HI-STAR HB System MPC, DFC, and overpack design bases, design, and supporting analyses relative to the storage requirements of the Humboldt Bay ISFSI. The Humboldt Bay onsite cask transporter design features and applicable codes are summarized in Section 4.3. Detailed operating guidance and controls for MPC loading, onsite transport, and emplacement of the loaded overpacks in the vault storage cells is provided in Sections 5.1 and 10.2. Figures for the HI-STAR HB System components, except the

DFC, are contained in Section 3.3, Figures 3.3-1, 3.3-2, and 3.3-3. Figure 4.2-3 provides the details of the DFC design germane to performing its design function.

### 4.2.3.2.1 MPC-HB

The MPC-HB provides for confinement of radioactive materials, criticality control, and the means to dissipate decay heat from the stored spent fuel. Each MPC-HB is approximately 9-1/2 ft high with an outside diameter of approximately 68 inches, and can store up to 80 HBPP fuel assemblies. In accordance with 10 CFR 72.120(b)(1), spent fuel and GTCC are not stored together in the same cask.

The MPC-HB has the structural capability to withstand the loads imparted by all design basis accidents and natural phenomena. The MPC-HB is a totally welded structure of cylindrical profile with flat ends. It consists of a honeycomb fuel basket, baseplate, shell, lid, vent and drain port cover plates, and closure ring. The MPC-HB can accommodate intact spent fuel and damaged fuel, either with or without channels, as discussed in more detail in Sections 3.1.1 and 10.2. The MPC lid provides top shielding and is part of the confinement boundary. The MPC-HB meets all of the criteria in Interim Staff Guidance (ISG)18 (Reference 7) such that leakage of radioactive material from the MPC-HB is considered non-credible. Table 4.2-3 provides a comparison of the Holtec MPC-HB construction against the ISG-18 criteria. Therefore, no leakage from the confinement boundary is postulated for normal, off-normal, or accident conditions. Figure 4.2-4 shows a cross-section view of the MPC-HB confinement boundary and Figures 3.3-1 and 3.3-2 provide additional pertinent design details.

The MPC-HB fuel-basket assembly provides support for the fuel assemblies as well as the geometry and fixed neutron absorbers for criticality control. The MPC is constructed entirely from Alloy X stainless steel except for the neutron absorber, and an aluminum washer in the vent and drain ports. Any steel part in an MPC-HB may be fabricated from any of the acceptable Alloy X materials, except that the steel pieces comprising the MPC shell (i.e., the 1/2 inch thick cylinder) must be fabricated from the same Alloy X stainless steel type. A summary of the nominal physical characteristics of the MPC-HB is provided in Table 4.2-1.

The MPC-HB is constructed from austenitic stainless steel material in accordance with ASME Section III, Subsection NB, with certain NRC-approved alternatives to the Code. For NB-class pressure vessels, radiographic (RT) examination is required by the Code for pressure-retaining welds. However, the final closure welds for the MPC-HB are performed in the field with spent fuel in the enclosure vessel, making it impractical to perform radiography on these welds. In accordance with ISG 4 (Reference 8), the MPC lid weld receives multiple pass liquid penetrant (PT) examination in lieu of RT. PT examinations are performed after the root pass, after each approximately 3/8-inch of weld depth, and after the final pass. The 3/8-inch value is the critical flaw size calculated for the MPC-HB. This inspection protocol is the same as that licensed generically for the MPC used with the HI-STAR and HI-STORM Systems. Additional

detail pertaining to the MPC lid weld inspections may be found in Section 9.1.1.1 of the HI-STAR 100 FSAR.

### **4.2.3.2.2 Damaged Fuel Container**

The DFC is used to contain fuel assemblies classified as damaged fuel as described in Section 10.2. At PG&E's discretion, intact fuel assemblies may also be stored in DFCs. The DFC is a long, square, stainless steel container with screened openings at the top and bottom. The DFC design includes an appropriate lifting attachment at the top to allow it to be handled with the HBPP fuel handling hoist. Each DFC is inserted into a designated storage cell within the MPC, as specified in Section 10.2.

The function of the DFC is to retain the damaged fuel in its storage cell and provide the means for ready retrievability. The DFC permits gaseous and liquid media to escape into the interior of the MPC, but minimizes dispersal of gross particulates during all design basis conditions of storage, including accident conditions. The total quantity of fuel-related material permitted in a single DFC is limited to the equivalent weight and special nuclear material quantity of one intact fuel assembly. Figure 4.2-3 shows the general arrangement and pertinent design details for the DFC.

The lifting device at the top of the DFC is designed to meet the guidance of ANSI N14.6 (Reference 9). Other DFC load path components are designed to meet ASME Section III (Reference 10), Subsection NG allowables for normal handling.

### **4.2.3.2.3 HI-STAR HB Overpack**

The HI-STAR HB overpack pressure boundary is a heavy-walled, carbon steel cylindrical vessel approximately 10-1/2 ft tall and with an outer diameter of approximately 8 ft. The overpack pressure boundary is formed by an inner shell welded at the bottom to a cylindrical forging and, at the top, to a heavy main flange, with a bolted closure plate. The closure plate compresses two concentric mechanical seals to form the pressure boundary.

The inner surface of the HI-STAR HB overpack inner shell forms a cylindrical cavity for housing the MPC. The outer surface of the overpack inner shell is buttressed with five intermediate carbon steel shells for gamma shielding that are installed in a manner to ensure a significant amount of contact between adjacent layers to facilitate heat transfer. Besides serving as an effective gamma shield, these layers provide additional strength to the overpack to resist potential punctures or penetrations from external missiles.

Carbon steel radial gussets (approximately .5 inches x 4 inch x 6 inch) are longitudinally welded to the inside surface of the enclosure shell, four each within the top and bottom 10 inches of the outer shell, at approximately equal intervals around the overpack circumference (see Figure 3.3-3). These radial gussets act as pathways for heat conduction from the outer intermediate shell to the overpack outer enclosure shell

surface, and help control neutron shield thickness during manufacturing. The neutron shield enclosure shell is formed by welding a carbon steel cylinder to the gussets and to a bottom enclosure shell return. Neutron shielding material is placed into the cavity area formed by the radial gussets, the outermost intermediate shell, the enclosure shell, and the enclosure shell return. Carbon steel plate welded at the top after the neutron shield material is installed ensures a completely welded enclosure for protection of the neutron shield material. The exterior of the enclosure shell cylinder forms the overpack outer surface. Relief devices are provided for the neutron shield enclosure to provide overpressure protection for the neutron shield enclosure during a fire accident.

The generically certified HI-STAR 100 System design has a total of 40 full-length radial fins (due to the welding of 20 channels to the outermost intermediate shell) with 20 individual enclosure shell panels welded between the channel corners to form 40 neutron shield cavities (see Drawing 3913 in Section 1.5 of the HI-STAR 100 FSAR). As discussed above, the HI-STAR HB overpack has only eight partial-length radial gussets to which the outer shell cylinder is welded to form the neutron shield enclosure. The thickness of the HI-STAR HB neutron shield is the same as the generic HI-STAR 100 design and the absence of the additional radial fins eliminates nearly all neutron streaming paths through the gussets, thereby improving the overall shielding effectiveness of the overpack. This change has been appropriately modeled in the shielding and thermal analyses for the HI-STAR HB System. Due to the low heat load of the HI-STAR HB System, the impact of the change on the thermal results is inconsequential.

Figure 4.2-5 shows a cross-section elevation view of the HI-STAR HB System and Figure 3.3-3 provides additional design details. A summary of the nominal physical characteristics of the HI-STAR HB overpack is provided in Table 4.2-4.

### **4.2.3.3 Design Bases and Safety Assurance**

The governing codes used for the design and construction of the HI-STAR HB System steel components are listed in the HI-STAR 100 System FSAR, Table 2.2.6, and are summarized below. All references to the ASME Code are to the 1995 Edition with 1996 and 1997 addenda, except for Sections V (Non-destructive Examination) and IX (Welding). Activities under Sections V and IX are performed in accordance with the latest effective edition of the Code. Table 3.4-5 provides a list of ASME Code alternatives for the HI-STAR HB System.

Additional information relevant to the design and analysis requirements for the MPC-HB fuel basket spacers and basket cell walls is provided in the PG&E Response to NRC Question 5-1 in References 26 and 27.

## HUMBOLDT BAY ISFSI FSAR UPDATE

- **MPC**

Pressure boundary	ASME Code Section III, Subsection NB
Fuel Basket	ASME Code Section III, Subsection NG (core support structures)
Basket Supports (Angled Plates)	ASME Code Section III, Subsection NG (internal structures)
Fuel Basket Spacers	ASME Code Section III, Subsection NF
Fuel Spacers	ASME Code Section III, Subsection NF

- **DFC**

Lifting Bolts	ANSI N14.6 per applicable guidelines of NUREG-0612, Section 5.1.6
Steel Structure	ASME Code Section III, Subsection NG

- **Overpack**

Pressure Boundary	ASME Code Section III, Subsection NB
Intermediate Shells	ASME Code Section III, Subsection NF
Neutron Shield Enclosure	ASME Code Section III, Subsection NF
Lifting trunnions	ANSI N14.6 per applicable guidelines of NUREG-0612, Section 5.1.6

The safety classifications of the components comprising the HI-STAR HB System were determined using NUREG/CR-6407 (Reference 11) as a guide. Section 4.5 provides the safety classifications of the HI-STAR HB System components and additional detail on safety classifications of components used at the Humboldt Bay ISFSI.

### 4.2.3.3.1 System Layout

The HI-STAR HB System consists of a fully-welded MPC-HB placed inside of a vertical steel overpack. Each of five MPC-HBs can hold up to 80 HBPP BWR spent fuel assemblies in an internal basket. A sixth GTCC qualified cask holds reactor-related GTCC waste from HBPP. The specifics of the material approved for storage in the HI-STAR HB System at the Humboldt Bay ISFSI storage site are discussed in Sections 3.1.1 and 10.2.



#### **4.2.3.3.2 Structural Design**

The HI-STAR HB overpack and MPC-HB are shorter, lighter, and have lower centers-of-gravity than the corresponding HI-STAR 100 System components. Table 4.2-2 provides a comparison of the generic and site-specific cask weights and centers-of-gravity. The materials of construction of components that perform a structural design function are the same for both systems. Other significant differences in design features between the two systems are listed in Section 4.2.3.

The MPC-HB enclosure vessel (pressure boundary) is identical in design to the generic MPC except for height. The MPC-HB fuel basket is designed to store 80 HBPP fuel assemblies, while the generic BWR MPC is designed to store 68 fuel assemblies. The MPC-HB fuel basket also includes certain improvements over the generic MPC in the design of the fuel spacers and the incorporation of fuel basket spacers. Otherwise, the structural design of the baskets is the same.

As a result of these similarities, much of the structural analysis work performed for the generic MPC design is directly applicable to, or provides a bounding case for the MPC-HB design (e.g., MPC top closure analysis and shell buckling analysis). With the exception of certain analyses related to the fuel basket, the structural evaluation for the HI-STAR 100 System forms the structural licensing basis for the HI-STAR HB System. Unique structural evaluations and analyses performed specifically for the HI-STAR HB System are discussed in Section 4.2.3.3.2.10.

The HI-STAR 100 System structural evaluation is described in HI-STAR 100 System FSAR Chapter 3. Structural evaluations and analyses of the HI-STAR 100 System components have been performed for all design basis normal, off-normal, and accident conditions and for design basis natural phenomena conditions in accordance with 10 CFR 72, Subpart L.

Except for the unique analyses discussed in Section 4.2.3.3.10, the generic HI-STAR 100 System structural evaluations are incorporated by reference into this FSAR as being applicable to the HI-STAR HB System. The generic HI-STAR 100 analyses and the site-specific MPC-HB fuel basket structural analyses, together, ensure that the integrity of the HI-STAR HB System is maintained under all design-basis loads with a high level of assurance to support the conclusion that the confinement, criticality control, radiation shielding, and retrievability criteria of 10 CFR 72 are met.

The Humboldt Bay ISFSI site-specific criteria are enveloped by the HI-STAR 100 System design, as demonstrated below.

##### **4.2.3.3.2.1 Dead and Live Loads**

The dead load of the HI-STAR HB System during long-term storage operations includes the weight of the overpack steel structure, neutron shield material, and the MPC loaded with spent fuel (including a channel and DFC in each fuel storage location). The dead

## HUMBOLDT BAY ISFSI FSAR UPDATE

load of the overpack with the loaded MPC is calculated assuming the heaviest HBPP fuel assembly with a channel (300 lbs) plus 100 lbs for the DFC. The stresses calculated for the dead loads of the MPC and the overpack are shown to be within applicable Code allowables.

The overpack is generically designed and analyzed for two live loads: (a) snow loads on the overpack closure plate, and (b) lifting loads on the lifting trunnions during handling operations in the Refueling Building (RFB) and onsite transport of the cask to the ISFSI storage vault. The HI-STAR 100 overpack closure plate is designed for a snow load of 100 psi as stated in HI-STAR FSAR Table 2.2.8. However, the HI-STAR HB System will not experience a snow load because the cask will be inside the vault storage cell with the lid installed during long term storage operations.

The lifting trunnions on the HI-STAR HB system are designed identical to the lifting trunnions on the HI-STAR 100 System and the HI-STAR 100 System is significantly heavier than the HI-STAR HB System (see Table 4.2-2). The analyses for HI-STAR 100 System handling are described in Section 3.4.3.1 of the HI-STAR 100 System FSAR. Since the live loads used in the HI-STAR 100 System generic lifting analysis meet or exceed those that would be expected at the Humboldt Bay ISFSI and the trunnion design is identical, the HI-STAR 100 System FSAR analysis bounds the HI-STAR HB design.

### **4.2.3.3.2.2 Internal and External Pressure**

The MPCs are backfilled with helium during fuel loading operations to a maximum pressure of 48.8 psig at a reference temperature of 70°F. The internal pressure rises in proportion to the rise in MPC cavity gas absolute temperature due to the decay heat emitted by the stored fuel and as temperatures equilibrate to those associated with the normal condition 52°F day/night annual average ambient temperatures. The pressure rises are evaluated in the thermal analysis for the MPC design (see Section 4.2.3.3.5 and Reference 16).

As discussed in ISG 7 (Reference 12), the effect of fuel rod fill gas and fission gases leaking into the MPC cavity on cask heat transfer and internal pressure has been considered. With regard to heat transfer, the decrease in gas conductivity due to the dilution of helium with fuel rod fill and fission gases is more than offset by the increased thermosiphon effect caused by the heavier mass of the gas mixture compared to pure helium. Heavier gas promotes a more vigorous thermosiphon effect and, therefore, more heat transfer away from the fuel. The thermal analysis conservatively does not model the gas mixture, but pure helium. Pressures inside the MPC are also affected by any leaks of fuel rod fill and fission gases into the MPC cavity. The calculations assume design basis heat load and bounding maximum fuel rod fill gas and internal rod pressure for HBPP fuel.

Internal and external pressure loads are addressed for the generic MPC design in the HI-STORM 100 System FSAR, Section 3.4.4.3.1. The normal condition design

pressure for the generic MPC and the MPC-HB is 100 psig for internal pressure and 40 psig for external pressure, which is also the overpack internal design pressure (see HI-STAR FSAR, Table 2.2.1). Table 4.2-5 provides the maximum helium fill pressure and the maximum calculated MPC-HB pressures for two normal conditions; no fuel rods ruptured and 1 percent fuel rods ruptured. The resultant pressure for these two normal conditions is less than the design pressure of 100 psig.

For the off-normal condition, the MPC-HB internal design pressure is 110 psig (see HI-STORM FSAR Table 2.2.1, as amended by LAR 1014-2). An evaluation of the 10 percent rods ruptured off-normal condition is provided in Section 8.1.1 and the resultant pressure is below the 110 psig off-normal design pressure (Reference 6).

Internal and external pressures were also evaluated for postulated accident conditions, including 100 percent fuel rod cladding rupture, assuming all rod fill gas and a conservative fraction of fission product gases, are released from the failed rods into the MPC. The resultant pressure from the 100 percent fuel rod rupture is provided in Section 8.2.11 and is below the MPC accident design pressure of 200 psig (see HI-STORM FSAR Table 2.2.1). The accident external design pressure for the MPC-HB is 60 psig based on a 10 CFR 71 design criterion.

The overpack accident external design pressure is 300 psig, which is equal to submergence in 656 ft of water. This design criterion is also based on a 10 CFR 71 requirement. No accident events produce an external pressure approaching 300 psig on the overpack in storage (see Section 8.2.6). Therefore, the HI-STAR HB overpack design is bounded by the generic analysis for external pressure.

The stresses resulting from the internal and external design pressure loads were shown in the generic stress analyses to be within Code allowables. Because the MPC-HB internal and external pressures are below the values used in the generic MPC analysis and (except for height) the generic MPC and MPC-HB enclosure vessel designs are identical, the generic analysis bounds the site-specific MPC-HB design. The limits and controls described in Section 10.2 ensure that the characteristics of all of the spent fuel in the HBPP inventory fuel are bounded by the design basis fuel considered in the pressure analyses.

### **4.2.3.3.2.3 Thermal Expansion**

Thermal expansion-induced mechanical stresses due to non-uniform temperature distribution are identified in Section 3.4.4.2 of the HI-STAR 100 System FSAR. There is adequate space (gap) between the MPC basket and shell, and between the MPC shell and overpack, to ensure there will be no interference during conditions of thermally induced expansion or contraction. Due to the relatively low heat loads in the HI-STAR HB system (maximum of 2 kW per cask), differential thermal expansion loads are not significant. Table 4.4.16 of the HI-STAR 100 System FSAR provides a summary of HI-STAR 100 System component temperature inputs for the structural evaluation, consisting of temperature differences in the basket periphery and MPC shell between

the top and bottom portions of the generic MPC. The temperature gradients were used to calculate resultant thermal stresses in the MPC that were included in the load combination analysis. The stresses resulting from the temperature gradients were shown to be within Code allowables.

Section 3.4.4.2 of the HI-STAR 100 System FSAR provides a discussion of the analysis and results of the differential thermal expansion evaluation. The limits and controls discussed in Section 10.2 of this FSAR ensure that the characteristics of all of the spent fuel in the HBPP inventory are bounded by the design basis fuel characteristics used in the thermal expansion analysis. These limits are consistent with the bounding fuel limits for array/class 6x6 and 7x7 fuel assemblies in the HI-STAR 100 System CoC. Therefore, the thermal expansion evaluation, discussed above, in the HI-STAR 100 System FSAR will bound the conditions at the Humboldt Bay ISFSI.

#### **4.2.3.3.2.4 Handling Loads**

Handling loads for normal and off-normal conditions are addressed in the HI-STAR 100 System FSAR, Sections 2.2.1.2, 2.2.3.1, and 3.1.2.1.1.2. The normal handling loads that were applied included vertical lifting and handling of the overpack with a loaded MPC through all necessary operational movements. The MPC and overpack were designed to withstand loads resulting from off-normal handling assumed to be the result of a vertical drop. In the case of Humboldt Bay, however, the vertical drop during onsite transport, outside the RFB, is precluded with the use of a cask transporter that is designed, fabricated, inspected, maintained, and tested in accordance with NUREG-0612. This approach is consistent with the provisions in the HI-STAR 100 System CoC described in Section 4.2.3.3.2.5 below.

#### **4.2.3.3.2.5 Overpack Tipover and Drop**

Cask handling and movement activities inside the RFB are described and analyzed in the Humboldt Bay 10 CFR Part 50 LAR being submitted separately. Outside the RFB, cask drop is not a credible accident since the cask handling equipment is designed in accordance with the applicable requirements of NUREG-0612. Outside the RFB, tipover of a loaded overpack is a non-credible accident since the HI-STAR HB System used at the Humboldt Bay ISFSI is seismically qualified either resting on the rail dolly, suspended from the cask transporter, or resting inside its ISFSI storage cell at all times. The cask will rest on the rail dolly while being moved out of the RFB for about 50-100 ft, where it will be attached to the cask transporter. The condition of the cask resting on the rail dolly has been evaluated and it has been shown that the cask will not tipover under postulated transport seismic events. Notwithstanding this fact, and to provide added margin, analysis was performed for a tipover from the rail dolly at high seismic loadings. It was also shown that this tipover event is bounded by the 60 g drop event in the HI-STAR 100 System FSAR. See Section 8.2.1 for additional discussion. The design and analysis of the concrete storage vault is discussed in Section 4.2.1.1.7. The analysis of the cask/storage vault interface under seismic loadings is described in Section 8.2.1.

Because the cask rests on the vault bottom, and is guided by the vault, which itself bears upon the soil below, a cask drop or tip-over is not credible during normal storage operations. During onsite handling, transport to the ISFSI facility, and lowering of the cask into the vault, the loaded cask is lifted exclusively by the cask transporter. The cask transporter is designed, fabricated, inspected, operated, maintained, and tested in accordance with the applicable requirements of NUREG-0612. Thus, there is no need to postulate a cask-drop event during transport to the ISFSI. However, due to similarities of design, the HI-STAR HB System design is qualified for the loads imparted by a deceleration of 60g's, based on the bounding tipover and drop analyses described in Chapter 3 of the HI-STAR 100 System FSAR. The site-specific analysis of the HI-STAR HB fuel basket uses 60-g's as a limiting design basis recognizing the dual purpose intent of the system.

The cask lifting assembly on the transporter is a horizontal beam that is supported by towers at each end with hydraulic lifting towers. During movement of the transporter with the cask in a fixed elevation, a redundant load support system is used. During vertical movement of the cask by the transporter, design features are provided to prevent uncontrolled lowering of the load due to a loss of hydraulic pressure. These design features and the operation of the cask transporter are further described in Section 4.3 and in Chapter 5.

#### **4.2.3.3.2.6 Tornado Winds and Missiles**

Design criteria for tornado wind and missile loads are discussed in Section 3.2.1. The HI-STAR HB System is designed to withstand pressures, wind loads, and missiles generated by a tornado, based on similarity of design and the bounding analyses described in Section 3.4.8 of the HI-STAR 100 System FSAR. Although the reinforced concrete vault was not credited in these designs, it does provide additional defense-in-depth protection from missiles. In Section 8.2.2 of this FSAR, the bounding analysis of the effects of tornado winds and missiles on the HI-STAR 100 System, including pressures, wind loads, and missiles is discussed to demonstrate the defense-in-depth of the HI-STAR HB design for use at the Humboldt Bay ISFSI. The MPC confinement boundary remains intact under all design-basis tornado-wind, and missile-load combinations.

#### **4.2.3.3.2.7 Flood and Tsunami**

Flooding and tsunami are addressed in Sections 3.2.2, 3.2.3, 8.2.3, and 8.2.4 of this FSAR and in Sections 3.1.2.1.1.3 and 3.4.6 of the HI-STAR 100 System FSAR. The HI-STAR 100 System is designed to withstand hydrostatic pressure (full submergence) up to a depth of 656 ft (a 10 CFR 71 requirement) and horizontal loads due to water velocity up to 13 fps without tipping or sliding. The Humboldt Bay ISFSI storage vault is above probable maximum ISFSI design flood conditions and projected maximum tsunami runup elevation as discussed in Section 3.2.3. Furthermore, as discussed in Section 3.2.3, the ISFSI vault is designed to structurally withstand 6 ft of water head and will protect against moving flood waters. As indicated in Section 3.2.3, the



transportation mode earthquake is of insufficient size to create a tsunami that would cause flooding on the transport route. As discussed in Section 3.2.2, flooding during transportation is not a concern.

Thus, the requirements of 10 CFR 72.122(b) are met with regard to floods and tsunamis.

### **4.2.3.3.2.8 Earthquake**

Design criteria for earthquake loads at the Humboldt Bay ISFSI are discussed in Section 3.2.4. The results of the seismic analyses as an accident condition are discussed in Section 8.2.1. Analyses were performed using the ground motions discussed in Section 2.6 and 3.2.4 to verify that the Humboldt Bay ISFSI SSCs (including components of the HI-STAR HB system) meet their design requirements of 10 CFR 72.122(b) with regard to earthquakes.

### **4.2.3.3.2.9 Explosion Overpressure**

Explosion overpressure loads are addressed in Sections 3.3.1.6 and 8.2.6. The HI-STAR 100 System MPC-HB is designed for accident external pressures up to 60 psig. The HI-STAR HB overpack is designed for an overpressure of 300 psig. Both of these external design pressures are the generic values, which, by similarity of design, are also applicable to the HI-STAR HB System. As discussed in Section 8.2.6, the HI-STAR HB System was evaluated using the RG 1.91 methodology and acceptance criteria. Potentially credible explosion hazards identified in Section 2.2 were evaluated based on an acceptance criterion of 1 psia overpressure or being risk insignificant. Explosion hazards which were determined to be risk significant and exceeding the 1 psia criteria were further evaluated for potential missiles. The HI-STAR is designed for spectrum I missiles at Region 1 wind speeds and it is judged that these spectrum I missiles at Region 1 wind speeds would bound any potential missiles from potential explosions. In addition, the vault cover would provide additional protection from explosion missiles. Therefore, it is believed that the HI-STAR HB in a vault configuration is considered to be adequately protected from potential explosion missiles, as required per 10 CFR 72.122(c).

### **4.2.3.3.2.10 Humboldt Bay-Specific Structural Analyses**

#### **Fuel Basket and Fuel Basket Supports**

The 80-fuel assembly MPC-HB fuel basket was analyzed using finite element techniques and computer codes previously used in generic licensing work. The loads imparted by a 60 g deceleration were assumed in the analysis to confirm that the fuel basket will maintain structural integrity and perform its design functions under all normal, off-normal, and accident conditions of storage. Because no drop or tipover events are postulated in the 10 CFR 72 licensing basis, the 60 g deceleration provides a very conservative design basis and was chosen because of the transportation side



drop accident design requirement. A two-dimensional finite element analysis of the fuel basket was performed using the ANSYS computer code (Reference 1), which was previously used in the generic licensing of the HI-STAR 100 System.

The 60 g deceleration loads were assumed to occur as a result of a drop accident in two orientations, namely, the 0-degree and 45-degree orientations. The 0-degree orientation represents the fuel basket walls either perpendicular or parallel to the target surface. The 45-degree orientation represents the fuel basket walls impacting the target surface at a 45-degree angle. Material properties were taken from ASME Section II, Part D. The resultant computed stresses in the fuel basket were compared to the Level D stress limits in the ASME Code, Subsection NG for acceptance.

The finite element model used for this analysis is similar to the MPC model described in Subsection 3.4.4.3.1.1 of the HI-STAR FSAR. The only differences are slight variations in basket geometry and the modeling of certain welded connections.

The ANSYS model is not intended to resolve the detailed stress distributions in weld areas. For this reason, individual welds were not included in the fuel basket model. Instead the welded joints are modeled to behave in a particular fashion (e.g., clamped or pinned) and the welds are of sufficient size and strength to transfer the internal forces and moments. A separate analysis is carried out to determine the type and size of the basket welds based on the assumed behavior of the joint and the relevant loads (Reference 25).

Since the perimeter cell plates are connected to the fuel basket by a single fillet weld on their outside surface, these connections were modeled as pinned joints in ANSYS. The remaining connections are double sided fillet welds, and therefore they were modeled appropriately as clamped joints.

Where the basket welds were modeled as clamped joints, the minimum fillet weld size is calculated based on the requirement that the moment capacity of the joint be equal to the maximum bending moment in the fuel basket as determined by ANSYS. A similar approach is described in Appendix 3.M of the HI-STAR FSAR for determining the minimum weld size. At pinned connections, the minimum fillet weld size was calculated based on the maximum combined shear and tensile forces at those locations.

The bending stresses in the basket and the MPC shell at low lateral loading levels, which are too small to close the support location clearances, are secondary stresses because any additional increase in the loading will activate the overpack's support action, mitigating further increase in the stress. Therefore, to compute primary stresses in the basket and the MPC shell under lateral drop events, the gaps should be assumed closed. However, for conservatism, it is assumed that an initial gap of 0.1875 inches exists, in the direction of the applied deceleration, at all support locations between the basket and the shell and the radial gap between the shell and the overpack at the support locations is 0.01 inches. All stresses produced by the applied loading on this

## HUMBOLDT BAY ISFSI FSAR UPDATE

configuration are compared with primary stress levels, even though the self-limiting stresses should be considered secondary in the strict definition of the Code.

All calculated fuel basket stresses were less than Level D limits. Table 4.2-6 provides the results of the stress analysis. This analysis also confirmed that the minimum weld sizes specified to join the fuel basket cell plates are adequate. The hand calculations evaluated the normal and accident loads on the fuel basket spacers and the fuel spacers and compared the stresses to the applicable stress allowables in the ASME Code, Section III, Subsections NG and NF, respectively. All stresses were less than the allowables with adequate safety margins.

The minimum safety factor, including a dynamic amplification factor of 1.1 per Appendix 3.X of the HI-STAR FSAR, is 1.06 ( $= 1.17/1.1$ ), which is above the ASME Code allowable limit of 1.0.

At the pinned joints, the maximum resultant force per inch of weld is equal to 1,440.5 lb/in. Based on an allowable weld stress of 27,930 psi (per Appendix 3.M of the HI-STAR FSAR) and a weld efficiency factor of 0.35 (per ASME Subsection NG), the minimum required weld size is

$$t = \frac{\sqrt{2} \cdot (1,440.5 \text{ lb/in})}{(0.35) \cdot (27,930 \text{ psi})} = 0.208 \text{ in}$$

Thus, a 7/32 in fillet weld (single sided) is adequate to join the perimeter cell plates to the main basket structure.

The following equation, which was developed in Appendix 3.M of the HI-STAR FSAR, establishes the relationship between the weld size “t”, the fuel basket panel wall thickness “h”, and the ratio of allowable weld strength “S_w” to base metal allowable strength “S_p”.

$$h^2 = 1.698 \frac{S_w}{S_p} (ht + t^2)$$

This equation is used to determine the minimum fillet weld size to be specified for all double-sided fuel basket welds, which ensures a factor of safety of 1.0 for all normal and accident conditions. To establish the minimum permissible weld size, S_p is replaced in the above formula by (S_p × (DAF/SF)) and the ratio t/h is computed. The following results are obtained:

## HUMBOLDT BAY ISFSI FSAR UPDATE

MINIMUM WELD SIZE FOR MPC-HB FUEL BASKET					
Item	Safety Factor (SF)	Dynamic Amplification Factor (DAF)	t/h	h (inch)	T (inch)
MPC-HB	1.17	1.1	0.662	0.1875	0.124

Thus, the minimum size for all double sided fuel basket welds is 1/8 in.

### Fuel Basket Spacers and Fuel Spacers

Manual calculations were performed using strength of materials formulas to qualify the fuel basket spacer, fuel spacer, and associated weld designs for the loads imparted by the 60-g deceleration. The computed stresses are compared with the appropriate stress limits from ASME Section III, Subsection NG for acceptance. Material properties were taken from ASME Section II, Part D. Table 4.2-7 provides the results of these calculations. Safety factors are calculated using accident allowable stresses from the Code.

### Damaged Fuel Container

The DFC design was analyzed (Reference 13) to ensure it will maintain its structural integrity during normal lifting operations. A drop accident is not credible for storage, so, although the DFC is designed for such loadings because of its dual-purpose function, the stress analyses associated with drop accidents are not discussed here. The lifting bolt of the DFC and the DFC handling device are designed to meet the safety factors for special lifting devices in ANSI N14.6 (Reference 9). Other stresses computed in the DFC analysis are compared to allowables from ASME Section III, Subsection NG. Buckling of the DFC is not evaluated because the DFC is supported by the MPC-HB fuel basket walls. The design temperature during lifting operations is assumed to be 150°F to bound spent fuel pool water temperature for normal conditions. The HBPP spent fuel pool temperature is typically in the 80-90°F range.

For the normal lifting operation analysis, the container sleeve, the weld between the sleeve and the base of the container, the container upper closure, and the lifting bolt were analyzed (see Figure 4.2-3 for design details on these components). The assumed weight of the fuel, including channel, used in the analysis is 300 lbs. The weight of the DFC was assumed to be 100 lbs. A dynamic load factor of 1.15 was assumed for normal lifting, resulting in a dynamic load of 460 lbs. The results of the DFC stress analysis are shown in Table 4.2-8. A summary of the analysis for each item is provided below.

During a lift, the container sleeve is loaded axially, and the stress state is pure tensile membrane. For the stress calculation, it was assumed that the full weight of the damaged fuel container, the fuel assembly, and a channel are supported by the sleeve.

The base of the DFC supports the amplified weight of the fuel assembly. This load is carried in direct shear by the sixteen 3/16-inch spot welds (4 on each side) that connect

the base to the container sleeve. A weight of 350 lbs was used in the analysis to bound the weight of a fuel assembly, channel, and the baseplate.

The load tabs of the DFC handling device engage the DFC collar during a lift. The shear stress due to the load transferred to each engagement slot and the shear stress in the tabs were calculated.

The loaded DFC is lifted by a bolt threaded into the center of an upper closure plate. The bending stress of the upper closure plate was calculated and compared to the primary stress allowable in ASME Section III, Subsection NG. The tensile stress in the 3/8 – 16 UNC lifting bolt was compared to the two minimum allowed stresses in accordance with ANSI N14.6 for special lifting devices - one-third against yield strength and one-fifth against ultimate strength. One fifth of ultimate stress results in a lower allowable stress for the SA 193-B7 bolt material and provides the more limiting of the two safety factors, as reported in Table 4.2-8.

### Overpack Neutron Shield Enclosure Shell

The one-piece cylindrical overpack neutron enclosure shell is different from the generically licensed enclosure shell, which is fabricated from a number of channels and steel plate panels welded together to form the enclosure shell. See Section 4.2.3.2.3 for more detailed discussion of the neutron shield enclosure shell design. The cylindrical shell design was analyzed for the 30 psig internal design pressure. The hoop stress and longitudinal stress were computed and the larger of the two (hoop stress) was compared to the allowable stress from ASME III, Subsection NF, and found to yield a safety factor of 6.1.

### HISTAR lid bolting

A site specific analysis demonstrating that all design basis conditions are met with only 49 lid bolts was performed to justify the bolt damage in HI-STAR Serial Number 12. This analysis was performed using the same methodology as that used in the generic HI-STAR FSAR (Reference 5). The analysis results show that there is a factor of safety for the lid bolt preload of 1.4. This analysis is documented in SMDR 1783 (Reference 29).

#### **4.2.3.3.2.11 Turbine Missiles**

Turbine missiles are discussed in Sections 2.2.2.3 and 8.2.13. The only time that turbine missiles are required to be evaluated is when the system in question is within the low-trajectory missile strike zone, defined by  $\pm 25$ -degree lines emanating from the centers of the first and last low-pressure turbine wheels as measured from the plane of the wheels. The Humboldt Bay spent fuel will be in this strike zone for a short period of time while it is being transported in an HI-STAR HB overpack system from the RFB to the ISFSI vault. While in this strike zone, it should be noted that, there is an even shorter time period when there is a direct line of sight from the Unit 1 and 2 turbines to

the transport route. Yet for conservatism this scenario is evaluated in PRA-03-12 (Reference 14). This risk assessment conservatively assumed that the transporter carrying the loaded overpack is in the defined unfavorable orientation for approximately half of the length of the transport route and took no credit for shielding of any components by plant structures. This risk assessment concluded that the probable risk during cask transfer, due to low-trajectory turbine missiles, is below the upper limit accepted by RG 1.115 (Reference 15) as an acceptable risk rate and is therefore not considered to be a credible event.

### **4.2.3.3.3 Fire**

Design criteria for fire loads are addressed in Section 3.3.1.6. Fire is considered an accident condition for the HI-STAR HB System and the ISFSI vault. The HI-STAR HB System was analyzed site-specifically for a number of fire scenarios deemed potentially credible for the site as discussed in Section 2.2. This includes fires that fully engulf the cask and non-engulfing fires that radiate heat to the cask and the vault structure. The evaluations of potentially credible fires are discussed in Section 8.2.5. The heat imparted on the cask due to fires could cause off-gassing of the Holtite-A neutron shield material. Therefore, relief devices are provided for the neutron shield enclosure to provide overpressure protection during the fire accident. The HI-STAR 100 System design meets the Humboldt Bay ISFSI design criteria for accident-level thermal loads as required per 10 CFR 72.122(c).

### **4.2.3.3.4 Lightning**

A lightning strike of the HI-STAR 100 System at the Humboldt Bay ISFSI is addressed in Sections 3.2.6 and 8.2.12. The lightning strike accident for a free-standing cask at an outdoor ISFSI is also discussed in the HI-STAR 100 System FSAR, Sections 2.2.3.11 and 11.2.11. During normal storage in the vault, the HI-STAR HB System is not susceptible to a lightning strike because of the protection provided by the vault. However, lightning could strike the cask during transport from the RFB to the ISFSI. The analysis shows that the lightning will most likely strike and discharge through the steel structure of the cask transporter to the ground. In the unlikely event that the lightning strikes the cask directly, the generic evaluation in the HI-STAR FSAR shows that current will discharge through the steel overpack structure and will not affect the MPC, which provides the confinement boundary for the spent fuel.

The HI-STAR 100 System design bounds the HI-STAR HB design for lightning protection. Therefore, the HI-STAR HB design meets the Humboldt Bay ISFSI design criteria in Section 3.2.6 for lightning protection, as required in 10 CFR 72.122(b).

### **4.2.3.3.5 Thermal Design**

The environmental thermal design criteria for the Humboldt Bay ISFSI are discussed in Section 3.2. Thermal performance for the HI-STAR 100 System is addressed in Chapter 4 of the HI-STAR 100 System FSAR. The HI-STAR HB System is also

## HUMBOLDT BAY ISFSI FSAR UPDATE

designed to minimize internal stresses from thermal expansion caused by axial and radial temperature gradients. The HI-STAR HB System was uniquely analyzed for thermal performance at the Humboldt Bay ISFSI due to the differences in design from the generically certified system and the below-ground vault concept.

The HI-STAR HB System is designed to transfer decay heat from the spent fuel assemblies to the environment. The MPC design, which includes the all-welded honeycomb basket structure, provides for heat transfer by conduction, convection, and radiation away from the fuel assemblies, through the MPC basket structure and internal region, to the MPC shell. The internal MPC design incorporates top and bottom plenums, with interconnected downcomer paths, to accomplish convective heat transfer via the thermosiphon effect. The thermosiphon heat transfer mechanism is credited in the HB thermal calculations contained in Holtec Report HI-2033033, (Reference 16), and is consistent with prior HI-STORM licensing of heat transfer via the thermosiphon effect. The MPC is pressurized with helium, which assists in transferring heat from the fuel rods to the MPC shell by conduction and convection. The stainless steel basket conducts heat from the individual spaces for storing fuel assemblies out to the MPC shell.

The thermal analysis (Reference 16) was performed using the ANSYS (Reference 1) and FLUENT (Reference 17) computer codes, both of which were previously used in licensing the generic HI-STAR 100 System. The HI-STAR MPC-HB was evaluated to determine the temperature distribution under normal storage conditions, assuming the MPC is loaded with design basis HBPP fuel assemblies. Maximum fuel assembly decay heat generation rates for fuel to be loaded into the MPC model is specified in Section 10.2.

Ambient-temperature and incident solar radiation (insolation) values applicable to the ISFSI site are summarized in Section 2.3.2. The highest recorded hourly temperature at the Humboldt Bay site is 87°F and the lowest temperature is 20°F. The annual average temperature is approximately 52°F. The maximum insolation values for the ISFSI site are estimated to be 602 g-cal/cm² per day for a 24-hour period and 593 g-cal/cm² for a 12-hour period.

The thermal analysis (Reference 16) assumes that the HI-STAR HB overpacks are each stored in a storage cell with the lid installed, subjected to a 52°F annual average ambient temperature and full solar insolation. The annual average temperature takes into account day-and-night and summer-and-winter temperatures throughout the year. The annual average temperature is the principal design parameter in the HI-STAR HB System design analysis, because it establishes the basis for demonstration of long-term spent nuclear fuel integrity.

A maximum cask decay heat load of 2 kW and a maximum fuel assembly heat load of 50 watts were assumed as the design basis values in the thermal analysis. The 50-watt value bounds all spent fuel in the HBPP inventory time at the time of loading.



## HUMBOLDT BAY ISFSI FSAR UPDATE

References 16, 22, and 24 contain the calculation details of the Humboldt Bay thermal analysis. A summary of the Humboldt Bay thermal analysis methodology, assumptions, and results are provided below.

The normal condition thermal analysis appropriately models the portions of the HI-STAR HB System and the ISFSI vault that are germane to the transfer of decay heat from the fuel assemblies to the environment. Transport of heat from the fuel assemblies to the outside environment is analyzed broadly by three interdependent thermal models.

- The first model considers transport of heat from the fuel assembly to the basket cell walls. This model recognizes the combined effects of conduction (through helium) and radiation, and neglects heat dissipation by convection and fuel assembly grid spacers.
- The second model considers heat transfer from the fuel to the MPC shell by conduction, radiation, and internal convection. An effective thermal conductivity of the fuel-basket region is obtained from a combined fuel assembly/basket conduction-radiation model is obtained. Internal convection in the fuel-basket zone is modeled by rendering it as a porous media region zone.
- The third model deals with the transmission of heat from the MPC shell exterior surface, through the overpack and the vault structure, to the external environment (ultimate heat sink). From the MPC shell to the cask exterior surface, heat is conducted through an array of concentric shells representing the MPC-to-overpack helium gap, the overpack inner shell, the intermediate shells, the Holtite-A neutron shielding and finally the overpack outer shell. Heat rejection from the outside cask surfaces is considered by accounting for natural convection and radiation to the vault structure and ultimately to the ambient air, and conduction through the vault structure to the soil. Justifications for the assumptions that: (a) the soil thermal conductivity can be based on a soil moisture content of at least 20 percent in the vicinity of the ISFSI, and (b) that the convective heat transfer coefficients for the cask and storage vault cell cover are the same are provided in the PG&E Responses to NRC Questions 6-2 and 6-5, respectively, in Reference 26.

The mathematical models devised to articulate the temperature field in the Humboldt Bay ISFSI begins with the method to characterize the heat transfer behavior of the prismatic (square) opening referred to as the “fuel space” containing a heat emitting fuel assembly. The methodology utilizes a finite-element procedure to replace the heterogeneous fuel/fuel space region with an equivalent solid body having a well-defined temperature-dependent conductivity. This is followed by a method to replace the composite honeycomb basket walls of the fuel basket cells with equivalent “solid” walls. The method to represent the MPC cylinder, containing the fuel basket, by a mathematically equivalent cylinder, whose thermal conductivity is a function of the

spatial location and coincident temperature, was used. In using this method, the mathematical equivalents for the fuel/fuel spaces and the fuel basket walls were created. The fuel basket region is rendered as a porous media zone having effective hydraulic properties to model internal convection.

Consistent with HI-STAR/HI-STORM licensing, modeling of the Humboldt Bay ISFSI requires an evaluation of the heat dissipation characteristics of the HBPP fuel. For this purpose, a planar conduction-radiation model of the HBPP fuel rod arrays is constructed and an effective conductivity of the cell space occupied by the HBPP fuel obtained. Consistent with the HI-STAR/HI-STORM modeling process, the MPC cross-section is replaced by an equivalent two-zone model - (i) Fuel basket zone and (ii) Downcomer zone. The downcomer is a helium filled annular gap. In storage, heated helium, propelled by buoyancy forces moves down and cools by rejecting heat to the MPC shell.

In summary, appropriate finite element models are used to replace the MPC cross section with an equivalent two-region homogeneous conduction lamina whose local conductivity is a known function of coincident absolute temperature. Thus, the MPC cylinder containing discrete fuel assemblies, helium, and fuel basket walls is replaced with a right circular cylinder whose material conductivity will vary with radial and axial position as a function of the coincident temperature.

The MPC-to-overpack annular gap is modeled as stagnant helium filled space having an equivalent conductivity that reflects the conduction and radiation modes of heat transfer. No credit for convection is taken for heat transfer across the annular gap. The overpack is a radially symmetric structure readily accommodated in the modeling process by including the intermediate shell layers as concentric shells with appropriate material properties. In this manner, a HI-STAR overpack containing a loaded MPC is replaced with a right circular cylinder with spatially varying temperature-dependent conductivity.

The generic HI-STAR 100 System open-air model was augmented to include the storage vault structure, comprised of a steel liner with cover plate and reinforced concrete, buried in the soil except for the top. Heat is dissipated from the storage vault exterior surfaces to ambient air (from the top) by natural convection and radiation. Soil is modeled as an infinite half-space with conduction heat transfer from the sides and bottom. The thermal model of the HI-STAR HB overpack in the vault was constructed on the QA validated FLUENT Computational Fluid Dynamics computer code.

The key assumptions used in the thermal analysis are as follows:

- (1) The conductivity enhancement by the reinforcing steel in the vault concrete is ignored.
- (2) To maximize insolation heating, a black surface is assumed for the vault exposed surfaces.

## HUMBOLDT BAY ISFSI FSAR UPDATE

- (3) To maximize fuel temperatures, a high decay heat in the 16 innermost MPC-HB cells (50 watts/assembly) is assumed.
- (4) The fuel basket conductivity is understated (~20 percent) in the thermal models.
- (5) To maximize flow resistance, the fuel cell helium flow area outside the envelope of a fuel rod array is ignored.
- (6) Bounding hydraulic pressure loss factors are employed to overstate fuel resistance to helium flow.
- (7) Lower bound active fuel lengths were used to maximize local heat generation.
- (8) Upper bound fuel lengths were used to maximize pressure drop.
- (9) The fuel basket is assumed to be loaded with fuel stored in DFCs in all fuel cell locations. This assumption maximizes thermal and hydraulic resistances of the fuel basket.
- (10) All six cask locations in the HB vault are assumed to be loaded with casks at design heat load.
- (11) Helium and air spaces outside the MPC envelope are modeled as stagnant gaps (i.e., convection heat dissipation in these spaces is ignored).
- (12) A lower bound Holtite-A neutron shield conductivity ( $0.8 \text{ W/m}^\circ\text{K}$ ) is employed in the thermal models.

The results of the normal condition thermal analysis confirm that temperatures of all cask and vault components are within normal condition temperature limits. In particular, the spent fuel cladding remains less than the temperature limit of  $400^\circ\text{C}$  specified in ISG-11, Revision 3 (Reference 18), with a margin in excess of  $350^\circ\text{F}$ . Table 4.2-9 provides a summary of the thermal analysis inputs and assumptions. Table 4.2-10 provides a summary of the results.

The HI-STAR HB System has also been thermally evaluated for off-normal and extreme (accident) ambient temperature excursions. These evaluations are discussed in Section 8.1.2 and 8.2.10, respectively.

The thermal performance of the MPC to limit fuel cladding temperature inside the cask during welding, draining, drying, and helium backfill operations, and during transportation of the loaded cask to the ISFSI is bounded by the thermal evaluation performed for the generic MPC design under a hypothetical, complete-vacuum condition

and design basis heat load. The vacuum condition is bounding for the other transient operational conditions mentioned above, because there is a negligible level of fluid in the MPC cavity to transfer heat from the fuel to the MPC shell. In the other conditions, there is some amount of either helium or water in the MPC cavity to enhance heat transfer. Essentially all internal MPC heat transfer in the vacuum condition is through conduction and radiation.

There are two systems that can be used at Humboldt Bay to dry the MPC-HB. One of these two systems is the Forced Helium Dehydration (FHD) System, which circulates dry helium through the MPC cavity to remove any residual moisture. This helium recirculation helps promote fuel cooling while concurrently drying the MPC. The thermal analysis for vacuum conditions provides a bounding case for this short-term operation. Section 4.4.2.2 of the HI-STAR FSAR (Reference 5) shows that for vacuum dried MPCs at design heat loads (19 kW) fuel cladding temperature is limited to 950°F. As Humboldt Bay MPC decay heat is limited to a very low value (2 kW) the vacuum condition temperature reached is a small fraction of the above referenced temperature at design heat load.

The other system that can be used to dry the MPC-HB is the vacuum drying system. Once the MPC is completely drained of water using the MPC blowdown system, the last of the water is removed via evaporation through the use of a vacuum drying system (as the pressure in the MPC is reduced, the saturation temperature for the water is reduced, causing evaporation of residual water).

The above discussion demonstrates that the HI-STAR HB System as deployed at the Humboldt Bay ISFSI meets the requirements of 10 CFR 72.122(h), 72.128(a)(4), and 72.236(f) and (g) for thermal design.

#### **4.2.3.3.6 Shielding Design**

Shielding design and performance for the HI-STAR HB System is addressed in Section 3.3.1.5.2 and Chapter 7 of this FSAR specifically for the Humboldt Bay ISFSI, and in Chapter 5 of HI-STAR 100 System FSAR for the HI-STAR 100 System generically. The HI-STAR HB System is designed, along with its storage vault, to maintain radiation exposure to workers and the public as low as reasonable achievable in accordance with 10 CFR 72.126(a). The design objective is to limit the average external contact dose rates (gamma and neutron) at the vault lid to  $\leq 0.2$  mrem/hr, on the cask surface to  $\leq 10$  mrem/hr, and have the dose rate to the public be below the 10 CFR 72.104 Regulatory Limit of 25 mrem/year. The shielding analysis (Reference 19) was performed assuming that each cask contains 80 design basis HBPP fuel assemblies. Assuming the GTCC cask also contains fuel provides a bounding case for that cask. The source term of the GTCC cask will be confirmed to be less than a fuel-filled cask prior to deploying the GTCC cask at the ISFSI.

The overpack is a massive structure designed to provide gamma and neutron shielding of the spent fuel assemblies stored within the MPC. The primary HI-STAR HB shielding

is located in the overpack and consists of neutron shielding and additional layers of steel for gamma shielding. Neutron shielding is provided around the outer circumferential surface of the overpack. Gamma shielding is provided by the steel overpack inner, intermediate, and enclosure shells with additional axial shielding provided by the bottom plate and the closure plate.

The underground location of the vault reduces any side dose rates to negligible levels during normal storage operations. Credit is also taken in the shielding analysis for the shielding provided by the vault lid, which is the only accessible area of the ISFSI vault. The vault lid is comprised of a total thickness of 1-1/4-inches of steel enclosing a minimum 15-inch thickness of concrete.

Predicted Humboldt Bay ISFSI dose rates and occupational dose evaluations are presented in Chapter 7 for the HI-STAR HB System, and meet the requirements of 10 CFR 20, 10 CFR 72.104 and 10 CFR 72.106.

The above discussion and the results of the shielding analysis in Chapter 7 together demonstrate that the HI-STAR HB System as used at the Humboldt Bay ISFSI meets the requirements of 10 CFR 72.104, 72.106, 72.128(a)(2), and 72.236(d) for shielding design.

#### **4.2.3.3.7 Criticality Design**

Criticality of the HI-STAR HB System is addressed in Section 3.3.1.4 of this FSAR and Chapter 6 of the HI-STAR 100 System FSAR. The HI-STAR HB System is designed to maintain the spent fuel subcritical in accordance with 10 CFR 72.124(a) and (b) with the MPC-HB materials and geometry. The acceptance criterion for the prevention of criticality is that  $k_{\text{eff}}$  remains below 0.95 for all normal, off-normal, and accident conditions.

Criticality safety of the HI-STAR 100 System depends upon the following three principal design parameters:

- Administrative limits on the maximum fuel assembly enrichment and physical properties acceptable for storage in the MPC.
- The inherent geometry of the fuel basket designs within the MPC.
- The incorporation of permanent, fixed, neutron-absorbing panels (METAMIC[®] or BORAL[®]) in the fuel basket structure to assist in control of reactivity.

The criticality analysis performed for the HI-STAR HB System (Reference 20) assumes only fresh fuel with no credit for burnup as a conservative bounding condition. In addition, no credit is taken for fuel-related burnable neutron absorbers, and it is assumed that the Boron-10 content in the neutron absorber is only 75 percent of the

## HUMBOLDT BAY ISFSI FSAR UPDATE

manufacturer's minimum specified content. Other assumptions made to ensure the results of the analysis are conservative are identified below:

- The fuel stack density is assumed to be 96 percent of theoretical ( $10.522 \text{ g/cm}^3$ ) for all criticality analyses (The fuel stack density is approximately equal to 98 percent of the pellet density. Therefore, while the pellet density of some fuels might be slightly greater than 96 percent of theoretical, the actual stack density will still be less).
- When flooded, the moderator is assumed to be water at a temperature corresponding to the highest reactivity within the expected operating range (i.e., water density of  $1 \text{ g/cc}$ ).
- Neutron absorption in minor structural members is neglected, i.e., spacer grids, basket supports and similar structures are replaced by water.
- The worst hypothetical combination of tolerances (most conservative values within the range of acceptable values) is assumed.
- When flooded, the fuel rod pellet-to-clad gap regions are assumed to be flooded.
- Planar-averaged enrichments are assumed for BWR fuel. Analyses are presented in Appendix 6.B of the HI-STAR FSAR to demonstrate that the use of planar-average enrichments produces conservative results.
- Fuel-related burnable neutron absorbers, such as the Gadolinia, are neglected.
- For evaluation of the reactivity bias, all benchmark calculations that result in a  $k_{\text{eff}}$  greater than 1.0 are conservatively truncated to 1.0000.
- Regarding the position of assemblies in the basket, configurations with centered and eccentric positioning of assemblies in the fuel storage locations are considered.

The same computer code (MCNP4A) (Reference 21) that was used in generic licensing for the HI-STAR 100 System was used in the HI-STAR HB criticality analysis.

Benchmarking of the criticality method and a discussion of the sensitivity of certain parameters of the reactivity system as modeled are provided in Chapter 6 of the HI-STAR FSAR and are not repeated here since the same analysis method and modeling assumptions are used. In its storage configuration, the HI-STAR HB System is helium-filled (essentially no moderator), and the reactivity is very low ( $k_{\text{eff}}$  less than 0.4). At the Humboldt Bay ISFSI, the fuel will always be in a dry, helium gas environment. It is sealed within a welded MPC, and no credible accident will result in water or any other fluid entering the MPC.



## HUMBOLDT BAY ISFSI FSAR UPDATE

The limiting reactivity condition occurs in the spent fuel pool (SFP) during fuel loading, where assemblies are loaded into the MPC in close proximity to each other in unborated water. The fuel assembly parameters assumed in the criticality analysis bound all spent fuel in the HBPP inventory ensuring all fuel to be loaded is bounded by the analysis.

Accident conditions have also been considered, and no credible accidents have been identified that would result in exceeding the regulatory limit on reactivity. Section 6.1 of the HI-STAR 100 System FSAR indicates that the physical separation between overpacks due to the large diameter and the Holtite-A and steel radiation shields was adequate to preclude any significant neutronic coupling between HI-STAR HB Systems. The effect is further minimized by the below-ground, concrete vault storage system at the Humboldt Bay ISFSI.

For damaged fuel in the MPC-HB, a modeling approach was used where the damaged fuel in the DFC is represented by arrays of bare fuel rods or fuel fragments, conservatively neglecting the effect of the fuel cladding and the other structural materials of the fuel assemblies. The pitch of the fuel rods and fuel fragments, and the fuel fragment size was varied in the model to determine the optimum moderation condition. This analytical model bounds all realistic damaged fuel configurations, such as assemblies with channels, missing fuel rods, broken assemblies, or fuel pellets lost from the assembly.

Results of these analyses confirm that, in all cases, the maximum reactivity of the HI-STAR HB System with design basis damaged fuel in the most adverse condition will remain well below the regulatory limit within the enrichment range analyzed.

As discussed in Section 6.2.1 of the HI-STAR FSAR, BWR fuel assemblies with channels show a higher reactivity in the criticality model than assemblies modeled without channels. Therefore, all intact fuel assemblies are modeled with channels.

The HI-STAR HB System is designed such that the fixed neutron absorber (METAMIC[®] or Boral[®]) will remain effective for a 50-yr storage period, and there are no credible means to lose the neutron absorber's effectiveness. As discussed in Section 6.3.2 of the HI-STORM 100 System FSAR as amended by LAR 1014-2, the reduction in Boron-10 concentration due to neutron absorption from storage of design basis fuel in a HI-STAR HB overpack over a 50-year period is expected to be negligible. Further, the analysis in Appendix 3.M.1 of the HI-STAR 100 System FSAR demonstrates that the sheathing, which affixes the neutron absorber panel, remains in place during all credible accident conditions, and thus the neutron absorber panel remains fixed for the life of the Humboldt Bay ISFSI. Therefore, verification of continued efficacy of the neutron absorber is not required. This is consistent with the requirements of 10 CFR 72.124(b).

The HI-STAR design, associated procedural controls, the proposed Humboldt Bay ISFSI Technical Specifications, and Section 10.2 requirements preclude accidental criticality when the spent fuel has been properly placed in the storage cask confinement system and the confinement system has been adequately drained, dried, inerted, and sealed.

Existing analyses contained in Appendix I of the HBPP Defueled Safety Analysis Report, specifically Sections 1.1.1, 1.1.2, and 1.2.3, and Appendix IB show that the drop of a fuel assembly onto the racks, and the drop of a fuel cask in the SFP (and consequent rupture and emptying of the fuel pool) show criticality is prevented. These existing results are considered to bound any effect of the use of the HI-STAR HB system.

The above discussion demonstrates that the HI-STAR HB System as deployed at the Humboldt Bay ISFSI meets the requirements of 10 CFR 72.124 and 72.236(c) for criticality design.

#### **4.2.3.3.8 Confinement Design**

Confinement design for the HI-STAR HB System is addressed in Sections 3.3.1.2.1 and 4.2.3.2.1. The confinement vessel of the HI-STAR HB System is the MPC-HB, which provides confinement of all radionuclides under normal, off-normal, and accident conditions in accordance with 10 CFR 72.122(h). No confinement credit is taken for the HI-STAR HB overpack. The MPC-HB consists of the MPC shell, base plate, lid, vent and drain port cover plates, and the closure ring, which form a totally welded vessel for the storage of spent fuel assemblies. The MPC requires no valves, gaskets, or mechanical seals for confinement. All components of the confinement system are classified as important to safety.

The MPC-HB is a totally welded pressure vessel designed to meet the stress criteria of ASME Section III, Subsection NB. No bolts or fasteners are used for closure. All pressure boundary welds performed during fabrication are non-destructively examined as required by ASME Section III, Subsection NB and the enclosure vessel is helium leak tested in the shop to confirm weld integrity.

All field closure welds are examined using the liquid-penetrant method and pressure tested to ensure their integrity. In addition, the MPC lid-to-shell weld is subjected to multi-layer liquid penetrant examination after the root and final weld passes and each 3/8 inch of intermediate weld. Two penetrations are provided in the MPC lid for draining, drying, and backfilling during loading operations. Following loading operations, vent and drain port cover plates are welded to the MPC lid. A closure ring, which covers the penetration cover plates and welds, is welded to the MPC lid to provide redundant closure of the MPC vessel. The loading and welding operations are performed inside the HBPP RFB. There are no confinement boundary penetrations required for MPC monitoring or maintenance during storage.

The confinement features of the HI-STAR 100 System meet the requirements of 10 CFR 72.122(h) and ISG-18 such that the leakage of radioactive material from the MPC-HB is considered non-credible.

### 4.2.4 INSTRUMENTATION SYSTEM DESCRIPTION

The HI-STAR 100 System is a totally passive system. Monitoring of the loaded casks in the storage vault is not necessary to ensure that the heat transfer system for the MPC and overpack remains operable. Instrumentation used for a one-time thermal test is described in Chapter 9.

### 4.2.5 COMPLIANCE WITH GENERAL DESIGN CRITERIA

Table 4.2-11 provides a tabular presentation of the locations in this FSAR and/or the HI-STAR 100 System FSAR where compliance with the General Design Criteria of 10 CFR 72, Subpart F, is shown to be met.

### 4.2.6 REFERENCES

1. ANSYS Finite Element Modeling, ANSYS Inc., Southpointe 275 Technology Drive; Canonsburg, PA.
2. Holtec-proprietary Report HI-2033013, Humboldt Bay Cask Storage Vault Structural Analysis, Revision 3.
3. Shapebuilder 3.0, Version 3.00.002, Integrated Engineering Software, Inc., 2002.
4. 10 CFR 72 Certificate of Compliance No. 1008 for the HI-STAR 100 System Dry Cask Storage System, Holtec International, Amendment 2, May 2001.
5. Final Safety Analysis Report for the HI-STAR 100 System, Holtec International Report No. HI-2012610, Revision 1, December 2002.
6. License Amendment Request 1014-2 for the HI-STORM 100 System, Holtec International, Revision 2, August 2003 (USNRC Docket 72-1014).
7. Interim Staff Guidance 18, The Design/Qualification of Final Closure Welds on Austenitic Stainless Steel Containers as Confinement Boundary for Spent Fuel Storage and Containment Boundary for Spent Fuel Transportation, USNRC, May 2003.
8. Interim Staff Guidance 4, Cask Closure Weld Inspections, USNRC, Revision 1.
9. ANSI N14.6, Special Lifting Devices for Shipping Containers Weighing 10,000 Pounds (4,500 kg) or More, American National Standards Institute, 1993 Edition.

## HUMBOLDT BAY ISFSI FSAR UPDATE

10. Boiler and Pressure Vessel Code, Section III, Division I, American Society of Mechanical Engineers, 1995 Edition including 1996 and 1997 addenda.
11. Classification of Transportation Packaging and Dry Spent Fuel Storage System Components According to Importance to Safety, USNRC, NUREG/CR-6407, February 1996.
12. Interim Staff Guidance 7, Cask Heat Transfer, USNRC, Revision 0.
13. Holtec-proprietary Report HI-2033042, Miscellaneous Calculations for the HI-STAR HB, Revision 0.
14. Probabilistic Risk Assessment, Calculation File No. PRA03-12, Revision 0, Risk Assessment of Turbine Missiles While Transporting Loaded Casks on the Humboldt Bay Transport Route.
15. Regulatory Guide 115, Protection from Low-Trajectory Turbine Missiles, USNRC, July 1977.
16. Holtec-proprietary Report HI-2033033, Humboldt Bay Thermal Analysis, Revision 0.
17. FLUENT Computational Fluid Dynamics Software, Fluent, Inc., Centerra Resource Park, 10 Cavendish Court, Lebanon, NH 03766.
18. Interim Staff Guidance 11, Cladding Considerations for the Transportation and Storage of Spent Fuel, Revision 2, USNRC, November 2003.
19. Holtec-proprietary Report HI-2033047, ISFSI Dose Assessment for Humboldt Bay, Revision 1.
20. Holtec-proprietary Report HI-2033010, Criticality Evaluation for the Humboldt Bay ISFSI Project, Revision 2.
21. J.F. Briesmeister, Ed., "MCNP - A General Monte Carlo N-Particle Transport Code, Version 4A." Los Alamos National Laboratory, LA-12625-M (1993).
22. Holtec-proprietary Report HI-2033005, Effective Thermal Property Evaluations for HBPP Fuel Assemblies and MPC-HB, Revision 0.
23. PG&E Letter HIL-04-009 to the NRC, Submittal of Holtec Proprietary Reports, October 1, 2004.
24. Holtec-proprietary Report HI-2033023, HBPP Fuel Assembly Decay Heat Calculations, Revision 1.

## HUMBOLDT BAY ISFSI FSAR UPDATE

25. Holtec-proprietary Report HI-2033035, Structural Calculation Package for MPC-HB, Revision 2.
26. PG&E Letter HIL-04-007, Response to NRC Request for Additional Information for the Humboldt Bay Independent Spent Fuel Storage Installation Application, October 1, 2004.
27. PG&E Letter HIL-05-003, Response to NRC Request for Additional Information for the Humboldt Bay Independent Spent Fuel Storage Installation Application, April 8, 2005.
28. Holtec-proprietary Report HI-2083930, Structural Analysis of DFC Lifting Device, Revision 1.
29. Supplier Manufacturing Deviation Report (SMDR) 1783, Revision 0, Dated December 9, 2008

### **4.3 TRANSPORT SYSTEM**

The cask transporter is designed and used to safely lift, handle, and transport a HI-STAR HB overpack, loaded with spent fuel or a cask loaded with reactor-related greater than class C (GTCC) waste, between the Humboldt Bay Power Plant (HBPP) Refueling Building (RFB), and the Humboldt Bay Independent Spent Fuel Storage Installation (ISFSI) as described below. The movement is conducted exclusively on the HBPP site as shown in Figure 2.2-2. Due to its important-to-safety classification, the cask transporter is licensed under 10 CFR 72 (Reference 1). The cask transporter is designed to withstand all credible design-basis, natural-phenomena events (see Table 3.4-1) while lifting, handling, and moving the loaded transfer cask or overpack without leaving the transport route or impairing its ability to safely hold the load.

#### **4.3.1 FUNCTION**

The function of the cask transporter to transport the loaded HI-STAR HB overpack between the RFB and the Humboldt Bay ISFSI storage vault is considered to be important to safety.

The cask transporter is capable of traveling over all of the road surfaces on the transport route. The road surfaces and underground facilities (see Section 4.3.3) have been evaluated to ensure the capability to support the weight of a cask transporter plus a loaded overpack.

#### **4.3.2 COMPONENTS**

This section describes the components used to lift, handle, and transport the loaded overpack to the Humboldt Bay ISFSI storage vault. Sections 3.3.3 and 3.4 provide discussion of the design criteria for the cask transportation system. Section 8.2.1 summarizes the results of the stress analyses under seismic loading, which bound the normal operation loads. Table 4.3-1 summarizes the functions of, and applicable design codes for, the transport system components that are considered important to safety and covered by an approved 10 CFR 72 quality assurance program.

##### **4.3.2.1 Cask Transporter**

###### **4.3.2.1.1 Description**

The cask transporter, shown in Figure 4.3-1, is a self-propelled, open-front, tracked vehicle used for handling and onsite transport of a loaded HI-STAR HB overpack. It is nominally 29 ft long, 19 ft wide, and weighs approximately 95 tons, unloaded. It is designed with two steel tracks to spread out the load on the transport route surface as a distributed pressure load. These tracks provide the means to maneuver the cask transporter around the site. On top of the main structure is a lifting beam supported by two lifting towers that use hydraulic cylinders to provide the lifting force. The industrial-grade hydraulic cylinders are made of carbon steel to ensure high strength and ductility



for all service conditions. The cask transporter is diesel powered and is limited to a fuel volume of 50 gallons to ensure the assumptions in the fire analysis are bounding (see Section 8.2.5). The same cask transporter licensed for use at the Diablo Canyon ISFSI will be used at the Humboldt Bay ISFSI.

### **4.3.2.1.2 Design**

The cask transporter design is suitable for conditions at the Humboldt Bay ISFSI site, including the transport route with its maximum grade of approximately 8.5 percent. It will remain stable and will not overturn, experience structural failure, or leave the transport route should a Transportation Mode licensing basis seismic event occur (see Section 3.2.4). During cask handling activities at the storage vault, the transporter will also remain stable and will not overturn or experience structural failure should a Vault Cask Handling Mode licensing basis seismic event occur (see Section 3.2.4). In addition, the cask transporter is designed to withstand HBPP design-basis tornado winds and tornado-generated missiles without overturning, dropping the load, or leaving the transport route. Other natural phenomena, such as lightning strikes, floods and fires have been evaluated and accounted for in the cask transporter design.

A lightning strike on the cask transporter would not structurally affect the transporter's ability to hold the load. Due to the massive amount of steel in the structure, the current would be transmitted to the ground without significantly damaging the transporter. However, the driver may be affected by a lightning strike. Therefore, the transporter design includes fail-safe features to automatically shutdown the vehicle if the operator is injured or incapacitated for any reason.

Flooding and tsunami are not concerns on the transport route as discussed in Section 3.2.2. Sources of fires and explosions have been identified in Sections 2.2 and 3.3.1.6 and in Table 3.4-1, and have been evaluated with respect to cask integrity in Sections 8.2.5 and 8.2.6. Fixed sources of fire and explosion have been evaluated and are either sufficiently far from the transport route or have been probabilistically determined to be of no concern. Mobile sources of fire and explosion, such as fuel tanker trucks, will be kept at a safe distance away from the transporter during loaded cask movement through the use of administrative controls.

The cask transporter is capable of forward and reverse movement as well as turning and stopping. It includes an on-board engine that is capable of supplying enough power to perform its design functions. The cask transporter includes fail-safe service brakes (that is, setting brakes that automatically engage in any loss of power) and an independent parking brake. The brake system is capable of stopping and holding a fully loaded cask transporter on the maximum design grade. The cask transporter is also equipped with an automatic drive brake system that applies the brakes if there is a loss of hydraulic pressure or the drive controls are released. Additionally, the fully loaded cask transporter is not capable of coasting on a 10 percent downward grade with the brakes disengaged, due to the resistance in the drive system.

## HUMBOLDT BAY ISFSI FSAR UPDATE

The cask transporter is equipped with a control panel that is suitably positioned on the transporter frame to allow the operator easy access to the controls located on the control panel and, at the same time, allow an unobstructed view of the cask handling operations. The control panel provides for all-weather operation or will be enclosed in the cab. The control panel includes controls for all cask transporter operations including speed control, steering, braking, load raising and lowering, cask restraining, engine control and “dead-man” and emergency stop switches. Additional emergency stop switches are located at ground level both in the front and rear of the transporter.

Figures 4.3-1 through 4.3-3 show the cask transporter performing its required functions. The cask transporter uses steel lift links that engage the overpack lifting trunnions via connector pins to facilitate the lifting and movement of the overpack. Cask handling is performed only with the overpack in the vertical orientation using the HI-STAR HB overpack lifting trunnions.

The cask transporter, connector pins, and lift links are classified important to safety, purchased commercial grade, and qualified for MPC and overpack loading operations by testing prior to service. The connector pins and lift links are designed in accordance with ANSI N14.6 (Reference 2) per the applicable guidance of NUREG-0612 (Reference 3). Table 4.3-1 provides a summary of the design code(s) applicable to each of the lifting and handling components.

On top of the main structure of the transporter is a lifting beam supported by two lifting towers that use hydraulic cylinders to provide the lifting force. Mechanical design features and administrative controls provide a defense-in-depth approach to preventing load drops during lifting and handling. The primary load-retaining devices of the cask transporter are the hydraulic cylinders. In combination, the hydraulic system is designed to carry more than twice the rated load, including a 15 percent hoist load factor.

Once the cask is raised to its travel height by the cylinders, a redundant load support system is used. This may take the form of either locking pins and/or wedge brakes. Wedge brakes, by their shape, limit tower movement to the lift (up) direction only. Any failure of the lifting hydraulics will not result in an uncontrolled lowering of the load. Locking pins are inserted into each gantry leg to independently support the load when no vertical movement is needed. The wedge brakes are operable at all times when a load is being lifted or lowered. To remove the pins or wedge locks, the cylinder must first be extended slightly to take the load off the pin or wedge. The load may then be lowered using the lifting cylinders. Requiring the cylinders to take the load ensures that they are operational before lowering the load. Any failure of the hydraulic system at this time will be mitigated by the cylinder safety systems as described below.

The cask transporter hydraulic system wedge brake design prevents uncontrolled lowering of the load upon a loss of hydraulic fluid. A minimum amount of hydraulic fluid system pressure is required to disengage the wedge brakes to allow movement of the load. A loss of hydraulic fluid would drop the pressure in the system and engage the

wedge brakes, preventing further movement of the load until corrective actions can be implemented.

The design of the cask transporter includes a lateral cask restraining system to secure the load during transport operations. The restraint system is designed to prevent lateral and transverse swinging of the load.

#### **4.3.2.1.3 Radiation Protection**

The driver of the cask transporter and escort personnel are the only people in proximity to the overpack during onsite transportation operations who require specific radiation protection consideration. Dose rate and accumulated dose estimates for the driver during cask operations are included in Section 7.4 using HBPP design-basis spent fuel source terms. Dose estimates for the driver would also be applicable to any escort personnel. All necessary radiation protection measures will be determined by HBPP radiation protection personnel at the time of fuel loading based on the actual dose rates in the immediate vicinity of the loaded overpack.

#### **4.3.2.1.4 Functional Testing and Inspection**

The cask transporter will be inspected for operating conditions prior to each ISFSI loading campaign. During the operational testing of this equipment, procedures are followed that will affirm the correct performance of the cask transporter features that provide for safe fuel-handling operations.

#### **4.3.2.2 Cask Transfer Rail Dolly**

The cask transporter is unable to gain access to the RFB due to its size. Therefore, a cask transfer rail dolly is used to move the cask to and from the cask preparation area under the davit crane. The rail dolly is a plate of steel fitted with two rows of heavy capacity rollers underneath to allow movement of the overpack in and out of the RFB along a rail system. The rail system is fabricated from standard railroad track. Rails currently exist in the RFB and will be augmented with new rails outside the RFB, extended out to the distance necessary to allow the cask transporter to gain access to the cask. Use of the rail dolly for movement of the cask within the RFB, until picked up by the transporter, is addressed as part of a 10 CFR 50 license amendment request submittal to the NRC (Reference 5).

### **4.3.3 CASK TRANSPORT ROUTE**

The cask transport route between the RFB and the Humboldt Bay ISFSI storage vault is shown in Figure 2.2-2. The route begins in the radiological control area (RCA) at the south side of the RFB, proceeds past the hot machine shop, and out of the RCA through a gate, turns northward and uphill past the discharge canal, then continues west along the RCA fence to the ISFSI. This route consists of a 26 ft wide compacted gravel roadway. The transport route is essentially level in transverse slope. The

## HUMBOLDT BAY ISFSI FSAR UPDATE

transport route is built to USACE Technical Manual EM 1110-3-141 standards (Reference 4). The underground utilities and structures have been evaluated and found suitable to withstand the load from the loaded cask transporter and rail dolly, as appropriate. The following is a discussion of underground utilities along the transport route.

Underground utilities and concrete pipeways were originally designed for H-20 traffic loads.

None of the water lines or drains to be crossed are safety related for the 10 CFR 50 power plant. Firewater lines are 10 CFR 50 nonsafety-related, but they are subject to prescribed quality assurance requirements.

Immediately south of the RFB, the rail dolly will cross an underground pipe chase outside the RFB railroad doors and parts of the fire system. The pipe chase is approximately 4 ft wide. After transferring the cask from the rail dolly, the transporter will cross over the following items:

- 12-inch Steel natural gas pipe
- 4-inch Steel Radwaste Drain Line
- 6-inch Transite fresh water line
- 6-inch Steel fire water line
- 21-inch Corrugated Metal Drainage Pipe
- Reinforced Concrete Pipes (conduits) for the Circulating Water System

### 4.3.4 DESIGN BASES AND SAFETY ASSURANCE

The design criteria and associated design bases for the transporter are presented in Section 3.3.3. The components of the transportation system in the direct load support path while the load is suspended (lifting points) are considered important to safety. The design and construction of important-to-safety items are conducted under an approved 10 CFR 72 quality assurance program. The design approach to classify certain load path members as important to safety with enhanced safety factors is taken to render all hypothetical overpack drop events outside the RFB not credible. Section 8.2.7 describes this approach in more detail. As a defense-in-depth measure, however, the transportation system design and administrative controls are such that the overpack will be lifted only to those heights necessary for cask handling operations. These transporter design bases and administrative controls are in compliance with 10 CFR 72.128 (a) with regard to ensuring adequate safety under normal and accident conditions.

### 4.3.5 REFERENCES

1. 10 CFR 72, Licensing Requirements for the Independent Storage of Spent Nuclear Fuel and High-Level Radioactive Waste.

## HUMBOLDT BAY ISFSI FSAR UPDATE

2. ANSI N14.6, Special Lifting Devices for Shipping Containers Weighing 10,000 Pounds (4,500 kg) or More, American National Standards Institute, 1993 Edition.
3. Control of Heavy Loads at Nuclear Power Plants, USNRC NUREG-0612, July 1980.
4. Technical Manual EM 1110-3-141, Airfield Flexible Pavement, Mobilization Construction, U.S Army Corps of Engineers, April 1984.
5. PG&E Letter HBL-04-016 to the NRC, License Amendment Request 04-02, Spent Fuel Cask Handling, July 9, 2004.

## **4.4 OPERATING SYSTEMS**

### **4.4.1 LOADING AND UNLOADING SYSTEM**

The dry storage cask handling systems are provided to lift, move, handle, and otherwise prepare a multi-purpose canister (MPC) loaded with Humboldt Bay Power Plant (HBPP) spent fuel for storage at the Humboldt Bay Independent Spent Fuel Storage Installation (ISFSI). Equipment is also available to unload an MPC in the unlikely event this becomes necessary. This section provides an overview of the functions and design of the equipment used to deploy the HI-STAR HB System at the Humboldt Bay ISFSI for normal, off-normal, and accident conditions. Regulatory Guide 3.62 uses the term “emergency conditions.” This Final Safety Analysis Report Update (FSAR) uses the term “accident conditions” for consistency with the more recent regulatory guidance of NUREG-1567. Movement of spent fuel assemblies between the spent fuel racks and the MPC is conducted in accordance with existing plant equipment and procedures, which will be modified as necessary, to meet handling requirements and commitments as described in Pacific Gas and Electric Company’s (PG&E) License Amendment Request 04-02 on Docket 50-133 submitted in PG&E Letter HBL-04-016 dated July 9, 2004, and is not specifically addressed here. Chapter 5 provides a detailed operating guidance regarding use of the structures, systems, and components to perform the various cask handling activities.

Personnel radiation exposures occurring as a result of dry storage operations will be planned and monitored in accordance with the HBPP radiation protection program (Section 7.1).

#### **4.4.1.1 Function**

The function of the loading system is to safely accomplish the following major objectives while maintaining occupational doses as low as reasonable achievable (ALARA):

- Place the empty MPC-HB and HI-STAR HB overpack into the HBPP Spent Fuel Pool (SFP) using the davit crane.
- Load the MPC-HB using 10 CFR 50 fuel handling equipment.
- After fuel loading, place the MPC-HB lid on the MPC.
- Remove the loaded MPC-HB and HI-STAR overpack from the SFP and place the assemblage down on the rail dolly in the cask washdown area of the Refueling Building (RFB). Install the lid retention device prior to releasing the HI-STAR HB from the davit crane.
- Remove MPC-HB lid retention device after sufficient welding is performed on the MPC lid (Reference 1).



## HUMBOLDT BAY ISFSI FSAR UPDATE

- Complete welding the MPC-HB lid to the MPC shell.
- Pressure test the MPC-HB.
- Drain, dry, and backfill the MPC-HB with helium.
- Weld the vent and drain port cover plates and closure ring to the MPC-HB lid and shell.
- Install the HI-STAR HB overpack closure plate.
- Vacuum dry the HI-STAR HB overpack annulus.
- Helium leak test the HI-STAR HB overpack closure plate inner seal and the vent and drain port plugs.
- Move the loaded HI-STAR HB overpack out of the RFB using the rail dolly.
- Lift loaded overpack using the cask transporter.
- Move the loaded overpack out of the Unit 3 yard and to the ISFSI storage vault using the cask transporter and place it in its designated position.
- Perform the same operations, as applicable, for the greater than Class C cask.

The same lifting and handling equipment is used in reverse order to return the loaded MPC to the truck bay area in the RFB in the unlikely event that an MPC needs to be unloaded. Loading and unloading operations are summarized below, including descriptions of the equipment used in performing these operations.

### **4.4.1.2 Major Components and Operating Characteristics**

Detailed operational guidance is provided in Section 5.1. The following discussion provides an overview of the cask loading and unloading operations, including normal, off-normal, and accident conditions.

#### **4.4.1.2.1 Component Arrival and Movement to the Preparation Area**

The MPC is a cylindrical, stainless steel pressure vessel containing an internal honeycomb fuel basket that is designed to house the spent fuel assemblies chosen for storage at the Humboldt Bay ISFSI. The nominal thicknesses of the MPC shell, lid, and baseplate are 1/2 inch, 9-1/2 inches, and 2-1/2 inches, respectively. See Section 4.2.3.2.1 for detailed description of the MPC.

The MPC is shipped to the HBPP site with the fuel basket having been installed at the fabrication facility. Upon arrival at the site, the MPC is removed from the delivery vehicle, receipt inspected, and cleaned as necessary, prior to being declared ready for installation into the overpack. The MPC is upended and removed from its transport frame.

A HI-STAR overpack is used to lift and move the MPC located inside it. It is used both before and after the MPC has been loaded with spent fuel assemblies. The overpack is designed to provide radiation shielding while maintaining the total weight of the loaded MPC and overpack within the load rating of the davit crane (95 tons). Most surfaces exposed to the SFP water are coated with materials compatible with the SFP water chemistry and any uncoated items (e.g., stainless steel materials) are compatible with the SFP water chemistry (see Section 4.6).

Upon arrival onsite, the overpack is removed from the delivery vehicle, inspected, cleaned as necessary, and upended to the vertical position with a lifting device such as a mobile crane. The overpack lid is removed and the empty MPC is lifted and placed inside the overpack using the four lift lugs welded to the inside of the shell.

#### **4.4.1.2.2 Cask Preparation and Fuel Loading**

Section 5.1 provides detailed procedural guidance. A summary of major operational steps is provided here to describe the operational systems. The rail dolly is positioned outside the RFB on the rails, where the overpack, with an empty MPC inside can be placed on the dolly. The overpack and MPC are rolled on the rail dolly into the RFB and positioned under the davit crane. Once positioned in the RFB, the MPC-to-overpack annulus is filled with clean (uncontaminated) water, the inflatable annulus seal is installed, and the annulus overpressure system is connected. The annulus overpressure system is a defense-in-depth measure to ensure that any breach of the annulus seal will force leakage of clean water into the SFP, and not contaminated SFP water into the annulus. The lift yoke is attached to the overpack lifting trunnions and is lifted, by the davit crane, into position over the cask loading area in the SFP. The annulus overpressure system supply is opened and the cask is then lowered using the lift yoke until the overpack rests on the bottom of the cask loading area.

The lift yoke is disconnected and the selected fuel assemblies are loaded and verified in the MPC in accordance with plant procedures. After fuel loading, the MPC lid is installed. The davit crane and lift yoke are then used to lift the loaded overpack out of the SFP and place it onto the rail dolly in the cask washdown area. The lid retention device is attached prior to releasing the HI-STAR HB from the davit crane.

#### **4.4.1.2.3 MPC and HI-STAR Preparation for Storage**

Once the loaded overpack and MPC are lowered onto the cask transfer rail dolly in the cask wash down area, the MPC lid is welded to the MPC. After MPC-lid welding, a pressure test is performed on the MPC welds. Upon successful pressure test

completion, the MPC is drained of water and dried using either forced helium dehydration or vacuum drying to reduce oxidizing gases to a residual level. The drying acceptance criteria for the MPC are provided in Section 10.2. After meeting the drying acceptance criteria, the MPC is backfilled with 99.995 percent pure helium gas supply to within a range of pre-calculated volumes as defined by Section 10.2.

When the MPC has been satisfactorily drained, dried, and backfilled with helium, the MPC vent and drain port cover plates are welded on and inspected. Then, the MPC closure ring is welded in place and inspected. The inner diameter of the closure ring is welded to the MPC lid and the outer diameter is welded to the top of the MPC shell. The overpack closure plate is installed and the overpack annulus, if not previously drained, is drained and then vacuum dried. The vacuum drying criteria are specified in Section 10.2. After successful vacuum drying, the annulus is backfilled with helium in accordance with the acceptance criteria in Section 10.2. The closure plate inner mechanical seal and the vent and drain port plugs are then helium tested. Upon completion of successful helium testing, the overpack is ready to be transported to the ISFSI.

The davit crane is used to place the loaded overpack on the rail dolly. The overpack is moved on the rail dolly with a winch or other similar device to a point outside the RFB, where the cask transporter picks it up and transports it to the ISFSI.

#### **4.4.1.2.4 Off-Normal and Accident Conditions**

For off-normal and accident conditions, the necessary response is a function of the nature of the event. Chapter 8 describes the off-normal and accident events for which the cask system is designed and provides suggested corrective actions. The HI-STAR 100 System is designed to maintain confinement integrity under all design-basis, off-normal, and accident conditions, including natural phenomena and drop events. For Humboldt Bay, there are no credible drops as described in Sections 4.4.1.3.1 and 4.4.1.3.2. Based on the circumstances of an actual event, plant personnel will take appropriate action ranging from inspections of the affected cask components to movement of the cask back into the SFP and unloading of the spent fuel assemblies.

#### **4.4.1.2.5 Unloading Operations**

To unload a HI-STAR HB System, the loading operations are essentially performed in reverse order, using the same lifting and handling equipment. Once the overpack is returned to the cask washdown area in the RFB, the MPC closure ring and vent and drain port cover plates are removed by cutting their attachment welds. Fuel cooldown is performed, if necessary, using the vent and drain and the helium cooldown system until the helium temperature is reduced to the maximum temperature specified in Section 10.2. Helium cooldown is required prior to re-flooding the MPC with water to prevent flashing of the water and the associated pressure excursions. Once the fuel is sufficiently cool, the MPC is flooded with water and the lid weld is removed using the weld removal system. Then, the lid retention system is installed, and the overpack and

MPC are lowered into the SFP using the lift yoke and davit crane. Finally, the lid retention system and MPC lid are removed, and the fuel assemblies are transferred from the MPC to the spent fuel racks.

### **4.4.1.3 Safety Considerations and Controls**

The MPC shell is designed in accordance with ASME Section III (Reference 2), Subsection NB, with certain Nuclear Regulatory Commission (NRC)-approved alternatives to the Code (see Table 3.4-5). The MPC fuel basket is designed in accordance with ASME Section III, Subsection NG, with certain NRC-approved alternatives to the Code (see Table 3.4-5). As discussed in Reference 3, the MPC is designed to retain its confinement boundary integrity under all normal, off-normal, and accident conditions. The MPC is a fully welded vessel that does not require the use of mechanical seals or leakage monitoring systems. The cask system is completely passive by design and does not require the operability of any supporting systems to safely store the spent nuclear fuel in the ISFSI storage vaults. The design features that ensure safe handling of the fuel are described in Section 4.4.1.2 and the ISFSI operations are provided in Section 5.1.

The HI-STAR HB overpack pressure boundary is designed in accordance with ASME Section III, Subsection NB, with certain NRC-approved alternatives to the Code (see Table 3.4-5). The overpack is designed to withstand the design-basis normal, off-normal, and accident loadings (including natural phenomena) for the Humboldt Bay ISFSI. The overpack design includes shielding design features that keep dose rates ALARA during fuel loading operation and transport of the loaded cask to the storage vaults.

The overpack shielding is optimized to provide the maximum practicable protection from radiation while staying within the size and weight limits necessary for compatibility with the HBPP facility and the capacity of the davit crane. Additionally, the design of the overpack includes as few pockets and crevices as practicable in the design to minimize the amount of radioactive crud that could be retained in these areas. The paint on the overpack is suitable for ready decontamination and removal of loose particles through the use of a standard decontamination practices. The overpack provides the maximum shielding possible while keeping the cask at a reasonable size and weight, compatible with commercially available crawler vehicles. Details of the overpack shielding design features are provided in Chapter 5 of the HI-STAR 100 System FSAR and Section 7.3.1 of this FSAR.

#### **4.4.1.3.1 Considerations Inside the 10 CFR 50 Facility**

NUREG-0612 provides guidelines to licensees to ensure the safe handling of heavy loads. The guidelines define acceptable alternatives for heavy load movements, which include using a single failure proof handling system or analyzing the effects of a load drop.

Inside the RFB, the cask and any ancillary components are lifted, handled, and moved in accordance with HBPP procedures for lifting heavy loads. The davit crane will be used with an integral lift yoke to perform all lifts of the cask inside the RFB. The overpack lifting trunnions and the lift yoke are designed, fabricated, inspected, maintained, and tested in accordance with NUREG-0612 as applicable to ensure that structural failures of these items are not credible. The redundancy provides the requisite temporary, single-failure proof protection during these operations. The complete description of the load handling in the RFB is described in HBPP 10 CFR 50 LAR 04-02.

#### **4.4.1.3.2 Considerations Outside the 10 CFR 50 Facility**

Cask drop events are precluded during transport of the loaded cask from the RFB to the storage vault, through the design of the cask transport system, including the cask transporter (Section 4.3). Drop events are precluded by lift devices designed, fabricated, operated, inspected, maintained, and tested in accordance with NUREG-0612 as applicable. The cask transport system is designed in accordance with these requirements and appropriate design codes and standards to preclude drop events on the transport route. The cask transporter is also designed to withstand applicable, site design-basis natural phenomena, such as seismic events, without dropping the load or leaving the transport route. The load-path parts of the cask transporter are designed as specified in Section 4.3.2.1. The cask transporter is procured commercial grade and is qualified by functional testing prior to service for overpack traversing operations. Uncontrolled movement of the cask transporter is prevented by setting the brakes, an emergency stop switch, and a dead-man switch, as discussed in Section 4.3.2.1.2; these components also are procured commercial grade and are qualified by functional testing prior to service.

#### **4.4.2 DECONTAMINATION SYSTEM**

Standard decontamination methods will be used to remove surface contamination, to the extent practicable, from the overpack and accessible portions of the MPC (that is, the lid) resulting from their submersion in the SFP. The cask and MPC lid will be rinsed with clean water while over the SFP. Final decontamination of the overpack and MPC lid will be performed in the drip catch tray in the cask washdown area on the RFB. Decontamination will typically be performed manually. While the entire MPC is submerged in the SFP during fuel loading, the annulus seal and annulus overpressure system prevent contaminated water from coming in contact with the sides of the MPC.

#### **4.4.3 STORAGE CASK REPAIR AND MAINTENANCE**

The HI-STAR HB overpack does not require any periodic maintenance during storage operations in the vault, which provides protection from the elements. Provisions for visual inspection of the vault interior are included in the design. Although unexpected, if these visual inspections reveal the need for repairs or maintenance, these activities will be performed by maintenance personnel either in-situ or in another appropriate location,

based on the nature of the work to be performed. Radiation protection personnel will provide input to and monitor as necessary these maintenance work activities through the work control process.

### **4.4.3.1 Structural and Pressure Parts**

PG&E anticipates that it will use a cask loading campaign where the entire set of storage casks will be loaded in an essentially continuous work effort. Prior to each overpack fuel loading, a visual examination is performed on the overpack lifting trunnions. The examination consists of inspections for indications of overstress such as cracking, deformation, or wear marks. Repair or replacement is required if unacceptable conditions are identified. The overpack trunnions are maintained and inspected in accordance with ANSI 14.6.

As described in the HI-STAR 100 System FSAR, Chapters 7 and 11, there are no credible normal, off-normal, or accident events that can cause the structural failure of the MPC. Therefore, periodic structural or pressure tests on the MPCs, following the initial acceptance tests, are not required as part of the storage maintenance program.

### **4.4.3.2 Leakage Tests**

There are no seals or gaskets used on the fully welded MPC confinement system. Therefore, confinement boundary leakage testing is not required as part of the storage system maintenance program. Leakage testing of the overpack closure plate inner seal and the vent and drain port plugs occurs at initial closure. Any required overpack leakage testing prior to transportation will be governed by the 10 CFR 71 certificate of compliance for the HI-STAR HB System.

### **4.4.3.3 Subsystem Maintenance**

The HI-STAR 100 System does not include any subsystems that provide auxiliary cooling during loading operations or in its final storage configuration. Normal maintenance and calibration testing is required on the vacuum drying, FHD, helium backfill, and leakage testing systems. Rigging, remote welders, cranes, and lifting beams are inspected prior to each loading campaign to ensure this equipment is ready for service.

### **4.4.3.4 Relief Devices**

The relief devices on the overpack neutron shield enclosure shell are provided only for the fire event, where off-gassing of the heated Holtite-A neutron shield material could cause pressurization of the enclosure shell. During normal storage operations, no fires are postulated inside the vault and normal storage conditions do not produce off-gassing of the neutron shield material since the temperature of the material remains within its design temperature. Therefore, periodic replacement of the relief devices is not required (Reference 5, Appendix A). If degradation of the relief devices is identified



during aging management inspections, then replacement of the relief devices will be evaluated. The relief devices will be replaced as a matter of good practice if the cask is removed from the vault for maintenance purposes if it has been over 5 years since last replacement. In accordance with the HI-STAR Part 71 FSAR, Section 7.1.5, prior to shipping the cask offsite, the relief devices will be replaced if it has been over 5 years since the last replacement.

### **4.4.3.5 Shielding**

The gamma and neutron shielding materials in the overpack and MPC degrade negligibly over time or as a result of usage. Radiation monitoring of the ISFSI provides ongoing evidence and confirmation of shielding integrity and performance. If the monitoring program indicates increased radiation doses, additional surveys of the overpacks will be performed to determine the cause of the increased dose rates.

### **4.4.3.6 Criticality Control**

Criticality control is provided primarily by the geometric spacing provided by the MPC-HB fuel basket and the fixed neutron absorber affixed to the basket walls. The METAMIC[®] or Boral[®] neutron absorber panels installed in the MPC baskets are not expected to degrade in the dry, inert-gas environment inside the MPC during normal storage operations. The use of METAMIC[®] as the fixed neutron absorber is discussed in Section 4.2.3.3.5 with additional detail provided in Section 1.2.1.3.1.2 of the HI-STORM FSAR, as amended by LAR 1014-2. No periodic verification testing of neutron poison material or other maintenance is required to assure criticality control for the HI-STAR HB System.

### **4.4.3.7 Thermal Performance**

The HI-STAR HB System is a totally enclosed cask design. The thermal performance of the HI-STAR HB System is confirmed by analysis. No periodic surveillance is required to verify heat removal. A one-time thermal test, performed after initial loading, will confirm the heat removal capability of the system. See Chapter 9 for details of this one-time test.

### **4.4.3.8 Vault Inspections**

The vault is essentially weather tight, and is not subject to any expected degradation. As described in the PG&E Response to NRC Question 3-2 in Reference 4, a periodic inspection of the vault drain system will be performed to detect any evidence of water intrusion. If any water is found, additional visual inspection of the vault cells will be performed to determine the source, and corrective action will be taken. Upon any significant dynamic load (i.e., large earthquake) an inspection to determine any damage will be performed.

The inspection for water in the vault drain system will be performed initially on a monthly basis. The subsequent inspection interval will be selected based on the results obtained during the initial 12-month period (selected to bound all seasons). The inspection method will be visual inspection of the drain collection point, combined for this initial period with remote camera inspection through the vault viewports. The vault cells are closed and no significant water is expected to be found in the vault cells even after 20 years of operation. Also, the HI-Star overpack and the vault liner are coated with a paint that would allow for substantial resistance to corrosion even when exposed to water. The coating material used is Carboline 890 for the outer surfaces of both the overpack and the liner as is licensed for the HI-STAR 100 overpack. This material is suitable for extended exposure to moisture without any detrimental effects. No extended exposure is expected.

9-01

#### 4.4.4 UTILITY SUPPLIES AND SYSTEMS

Electric power is provided for the storage vault area lighting and the storage vault area security system. As the HI-STAR HB System is a passive system, no other utilities are required for ISFSI operation.

##### 4.4.4.1 Electrical Systems

Electric power is not required to support functions of the Humboldt Bay ISFSI important-to-safety SSCs. Power is supplied from the site 12-kV distribution system. There are no motorized fans, dampers, louvers, valves, pumps, electronic monitoring systems, and no electrically operated cranes. In the event of a HBPP loss of offsite power, power will not be supplied to the ISFSI components, except for certain security loads. A discussion of the normal and emergency power for security equipment is provided in the Physical Security Plan. **FSAR** Section 8.1.5 describes recovery actions to mitigate the loss of electrical power event.

9-01

##### 4.4.4.1.1 Grounding

The ISFSI storage vault area, perimeter fencing, lighting and poles, and security equipment will be provided with a ground grid, and it will be connected to the existing station ground grid. Each storage cask will be grounded to the ISFSI area ground grid.

#### 4.4.5 REFERENCES

1. Holtec-proprietary Report HI-2033042, Miscellaneous Calculations for the HI-STAR HB, Revision 0.
2. Boiler and Pressure Vessel Code, Section III, Division 1, Subsection NF, American Society of Mechanical Engineers, 1995 Edition including 1996 and 1997 addenda.

## HUMBOLDT BAY ISFSI FSAR UPDATE

3. Final Safety Analysis Report for the HI-STAR 100 System, Holtec International Report No. HI-2012610, Revision 1, December 2002.
4. PG&E Letter HIL-04-007, Response to NRC Request for Additional Information for the Humboldt Bay Independent Spent Fuel Storage Installation Application, October 1, 2004.
5. Holtec Report HI-2167476, Response Package for Humboldt Bay ISFSI License Renewal, Revision 2.

#### **4.5 CLASSIFICATION OF STRUCTURES, SYSTEMS, AND COMPONENTS**

The structures, systems, and components (SSCs) comprising the Humboldt Bay Independent Spent Fuel Storage Installation (ISFSI) are classified as important to safety (ITS) or not important to safety (NITS). The criteria for selecting the classification for particular SSCs are based on the following definitions:

- Important to Safety

A classification from 10 CFR 72.3 for any SSC whose function is to maintain the conditions required to safely store spent fuel; prevent damage to the spent fuel or spent fuel container during handling and storage; or provide reasonable assurance that spent fuel can be received, handled, packaged, stored, and retrieved without undue risk to the health and safety of the public.

- Not Important to Safety

A classification for SSCs that do not meet the criteria for classification as ITS.

Major Humboldt Bay ISFSI SSCs are classified as ITS if at least one subcomponent comprising the major component is classified ITS. SSCs classified ITS are subject to the Humboldt Bay ISFSI Quality Assurance (QA) Program described in Chapter 11. The importance to safety for each ITS SSC is further refined into three QA classification categories based on the guidance contained in NUREG/CR-6407 (Reference 1). The categories are intended to standardize the QA control applied to activities involving spent fuel storage systems. These classifications are defined as follows:

- Classification Category A – Critical to Safe Operation

Category A items include SSCs whose failure or malfunction could directly result in a condition adversely affecting public health and safety. The failure of a single item could cause loss of containment leading to release of radioactive material, loss of shielding, or unsafe geometry compromising criticality control.

- Classification Category B – Major Impact on Safety

Category B items include SSCs whose failure or malfunction could indirectly result in a condition adversely affecting public health and safety. The failure of a Category B item, in conjunction with the failure of an additional item, could result in an unsafe condition.

- Classification Category C – Minor Impact on Safety

Category C items include SSCs whose failure or malfunction would not significantly reduce the cask system effectiveness and would not be likely to create a situation adversely affecting public health and safety.

The major SSCs that are classified ITS are discussed in the following sections. A safety classification for these SSCs establishes the requirements that satisfy the 10 CFR 72.122(a) general design criteria, which specify that SSCs that are classified ITS be designed, fabricated, erected, and tested to quality standards. The safety classification of the subcomponents and the determination of the ITS category of each item is administratively controlled by Pacific Gas and Electric Company (PG&E) via design and procurement control procedures with input from the storage cask vendor.

### **4.5.1 SPENT FUEL STORAGE CASK COMPONENTS**

The major ITS components comprising the HI-STAR HB System are described below with a brief description as to why each is classified as ITS. Table 4.5-1 lists the major storage cask components by QA Category, based on the highest QA category of any subcomponent comprising the major component.

#### **4.5.1.1 Multi-Purpose Canister and Fuel Basket**

The multi-purpose canister (MPC-HB) is classified ITS because it serves as the primary confinement structure for the fuel assemblies and is designed to remain intact under all normal, off-normal, and accident conditions. The fuel basket inside the MPC-HB is classified ITS, because it ensures the correct geometry of the stored fuel assemblies and provides the fixed neutron absorber between fuel cells to prevent criticality.

#### **4.5.1.2 Damaged Fuel Container**

The damaged fuel container (DFC) is classified ITS because it maintains fuel classified as damaged fuel or fuel debris in a safe geometry and enables retrieval of the damaged fuel assembly or fuel debris. The DFC also prevents the gross dispersal of particulates, including loose fuel pellets.

#### **4.5.1.3 Overpack**

The overpack is classified ITS because it is designed to remain intact under all normal, off-normal, and accident conditions and serves as the primary component for protecting the MPC during storage. It provides structural protection to prevent damage to the spent fuel and ensures fuel retrievability. It also provides radiation shielding and allows for MPC heat rejection to the environment.

#### **4.5.2 CASK STORAGE VAULT**

The cask storage vault is classified ITS (see Table 4.5-1) because it provides the necessary protection for the overpack to prevent sliding and tipover during a design basis seismic event and also provides protection from tornado- and explosion-generated missiles.

#### **4.5.3 CASK TRANSPORT SYSTEM**

The cask transport system is classified ITS because the load-bearing components prevent damage to the spent fuel and spent fuel storage cask system components during onsite transport, lifting, and lowering operations under all normal, off-normal, and accident conditions. The cask transporter “dead-man” and emergency stop features and the setting brakes are classified as ITS. The transport system was designed to prevent uncontrolled lowering of the load. In addition, the cask transporter was designed to maintain stability on the transport route between the Refueling Building (RFB) and the cask storage vault. The cask transporter was purchased commercial grade and qualified by functional testing prior to use.

#### **4.5.4 ANCILLARY EQUIPMENT**

Ancillary equipment is comprised of those SSCs, not described above, that are used to lift, handle, and move the cask and prepare the MPC for storage operations. Table 4.5-1 lists the major ancillary equipment. Any additional ancillary equipment not included on the list will be classified and categorized in accordance with the PG&E design and procurement control procedures with input from the storage cask vendor.

#### **4.5.5 DESIGN CRITERIA FOR SSCs NOT IMPORTANT TO SAFETY**

The design criteria for SSCs classified as NITS, but which have security or operational importance, are addressed in other sections of this Final Safety Analysis Report Update (for example, security systems, and portions of the cask transport system, and ancillary equipment systems). These SSCs are designed in accordance with applicable commercial codes and standards to ensure, where interfaces exist, that there is compatibility with SSCs that are ITS.

The Humboldt Bay ISFSI security system is classified as NITS because it does not have a design function directly related to the protection of public health and safety due to operation of the Humboldt Bay ISFSI. The primary function of the security system is to prevent and detect unauthorized access to the Humboldt Bay ISFSI. The Humboldt Bay ISFSI security system design meets the requirements of 10 CFR 72, Subpart H.

The electrical power system is classified as NITS because it is not ultimately relied upon to support a function necessary for the safe operation of the dry cask storage system. The HI-STAR HB System is completely passive in design and requires no electric power to ensure safe, long-term storage of the spent nuclear fuel.



## HUMBOLDT BAY ISFSI FSAR UPDATE

Portions of the cask transporter, cask storage vault, and ancillary equipment not having design functions directly related to protecting public health and safety, as defined by the ITS classification categories in Reference 1, are classified as NITS. Major NITS equipment of this type are provided in Table 4.5-1. New equipment and subcomponents of existing equipment not included in Table 4.5-1 will be classified in accordance with the PG&E administrative control process with input from the storage cask vendor.

### 4.5.6 REFERENCES

1. Classification of Transportation Packaging and Dry Spent Fuel Storage System Components According to Importance to Safety, USNRC, NUREG/CR-6407, February 1996.

#### 4.6 **MATERIALS EVALUATION**

In accordance with NRC Bulletin 96-04 and consistent with Interim Staff Guidance (ISG) 15 (References 1 and 2), a review of the potential for adverse chemical, galvanic, or other reactions among the materials of the HI-STAR HB dry storage system, its contents, and the operating environments has been performed. The ISG-15 regulatory requirements and acceptance review criteria were grouped into ten major categories as shown below. A summary of the materials used is provided in Table 4.6-1. Compliance with the regulatory requirements covered by each category is discussed with references to the discussions of each HI-STAR HB component that follows, as appropriate.

- Adequate Description – Important-to-safety (ITS) components comprising the cask system and the Independent Spent Fuel Storage Installation (ISFSI) are identified in Section 4.5. The materials of construction for the Multi-purpose Canister (MPC)-HB, damaged fuel container, overpack, and ISFSI vault are described in detail in the sections that follow.
- Quality Standards – ITS Structures, Systems, and Components (SSCs) are designed, built, inspected, and tested in accordance with appropriate design codes, under quality assurance programs that meet 10 CFR 72, Subpart H. Section 3.4 discusses the applicable design criteria and codes that govern the construction/fabrication of ITS SSCs and the Humboldt Bay ISFSI.
- Design Life – The design life of the Cask System SSCs is 40 years, which is twice the licensed life of the ISFSI of 20 years.
- Environmental Capability – In the following sections, the various environments in which each component must operate during all modes of ISFSI operation are discussed. Potential galvanic and chemical reactions among components and between components and their environments are discussed, as applicable. All components are suitable for service in the various anticipated environmental conditions.
- Cladding Integrity – The licensing basis for the Humboldt Bay ISFSI includes adoption of a peak fuel cladding temperature (PCT) limit of 400°C (752°F) for normal operations, including short term operations during cask preparation and long-term storage at the ISFSI. For off-normal and accident conditions, the PCT limit of 570°C (1058°F) is used. These limits are consistent with the guidance in Interim Staff Guidance (ISG) 11, Revision 2 (Reference 3). The analyses supporting the design confirm that these PCT limits are not exceeded during any normal, off-normal, or accident conditions and, therefore, fuel cladding degradation leading to rupture is precluded. The helium-filled environment inside the MPC-HB together with the design of the cask and vault assure that the actual

## HUMBOLDT BAY ISFSI FSAR UPDATE

condition of the fuel is maintained consistent with the analysis bases.

- Fire Protection – There are no materials used in the cask or vault design that will ignite at the service temperatures expected. The primary materials of construction used in the cask and vault are stainless steel, carbon steel, and concrete. Exposed carbon steel surfaces are coated. The materials of construction are discussed in further detail in the sections that follow. No combustible materials are to be permanently stored inside the ISFSI-controlled area. Credible fires potentially affecting the cask during onsite cask transportation and long-term storage at the ISFSI are evaluated in Section 8.2.5. All fire consequences meet applicable acceptance criteria.
- Nuclear Control – All materials used for criticality control and shielding have known performance characteristics, either through actual use or through test. Radiation shielding is provided by steel and concrete. Criticality control is provided through geometric spacing of the fuel in the basket and fixed neutron absorber panels on the fuel basket walls.
- Confinement – The structural and thermal analyses discussed in Chapter 4 demonstrate that the austenitic stainless steel confinement boundary maintains its integrity under all normal, off-normal, and accident conditions. Further, the MPC-HB meets all of the criteria in ISG-18 (Reference 4) such that leakage from the final closure welds is not deemed credible (see Section 4.2.3.2.1). No confinement credit is taken for the bolted, sealed overpack closure.
- Offsite Shipment – The HI-STAR HB System design is based upon the dual purpose HI-STAR 100 System design, which is certified for transportation of spent fuel under 10 CFR 71. The HI-STAR HB System is therefore designed to be shipped offsite to another spent fuel storage facility or the federal repository without repackaging.
- Operating Conditions – The cask and vault materials of construction have been evaluated for the expected normal service conditions and certain credible off-normal and accident conditions, including environmental phenomena. The technical evaluations discussed in Chapter 4 confirm that the materials are suitable for service and will perform their design function for the design life of the cask system.

### 4.6.1 MULTI-PURPOSE CANISTERS

The passive, non-cyclic nature of dry storage conditions does not subject the MPC-HB to conditions that might lead to structural fatigue failure. Ambient temperature and insolation cycling during normal dry storage conditions and the resulting fluctuations in the MPC thermal gradients and internal pressure is the only mechanism for fatigue.

## HUMBOLDT BAY ISFSI FSAR UPDATE

These low-stress, high-cycle conditions cannot lead to a fatigue failure of the MPC enclosure vessel or fuel basket structural materials, that are made from austenitic stainless steel, known as “Alloy X.” “Alloy X” is a fictitious stainless steel designation used in the design basis analyses of the MPC to ensure any of the permitted austenitic stainless steels used in MPC fabrication are bounded by the analyses. “Alloy X” is defined as any of the following austenitic stainless steel types:

- 304
- 304LN
- 316
- 316LN

Any steel part in the MPC-HB may be fabricated from any of the above stainless steel types, except that the steel pieces comprising the MPC shell (i.e., the ½-inch thick cylinder) must be fabricated from the same type of stainless steel. See HI-STAR 100 Final Safety Analysis Report Update (FSAR) Section 1.2.1.1 for a detailed discussion of Alloy X.

A typical MPC construction material specification, ASME SA240-304 stainless steel, has a fatigue endurance limit well in excess of 20,000 psi. All other off-normal or postulated accident conditions are infrequent or one-time occurrences, which cannot produce fatigue failures. The MPC also uses materials that are not susceptible to brittle fracture.

The MPC-HB enclosure vessel and fuel basket are in contact with air, helium, and unborated spent fuel pool (SFP) water during various stages of use at the Humboldt Bay Power Plant (HBPP) and ISFSI. The MPC enclosure vessel and fuel basket, with the exception of the neutron absorber panels, and aluminum seal washers used in the vent and drain port caps, is fabricated entirely of austenitic stainless steel. Aluminum heat conduction elements, offered as optional equipment in the HI-STAR 100 System generic MPC design (Section 1.2.1.1 of the HI-STAR FSAR), will not be used in any of the MPCs deployed at the Humboldt Bay ISFSI. There are no significant chemical or galvanic reactions of stainless steel with air or helium. The aluminum seal washers used with the vent and drain port caps never are in contact with water, so combustible gas generation is not a concern. There are no coatings of any kind used in or on the MPC. The control of combustible gases generated by the interaction of the neutron absorber with the SFP water is discussed in Section 4.6.1.1.

The moisture in the MPC is removed during loading operations to a point where oxidizing liquids and gases are at insignificant levels. The MPC cavity is then backfilled with dry, inert helium at the time of closure to maintain an atmosphere in the MPC that provides corrosion protection for the fuel cladding and MPC materials throughout the dry storage period. Insofar as corrosion is a long-term time-dependent phenomenon, the inert gas environment in the MPC minimizes the incidence of corrosion during storage on the ISFSI to an insignificant amount. The external surface of the MPC is also protected from adverse chemical or galvanic reactions because the annulus

between the MPC and the HI-STAR HB overpack is drained, dried, and backfilled with helium for long-term storage operations.

### 4.6.1.1 METAMIC® Neutron Absorber

METAMIC® is a neutron absorber material developed by the Reynolds Aluminum Company in the mid-1990s for spent fuel reactivity control in dry and wet storage applications. Metallurgically, METAMIC® is a metal matrix composite (MMC) consisting of a matrix of 6061 aluminum alloy reinforced with Type 1 ASTM C-750 boron carbide ( $B_4C$ ). METAMIC® is characterized by extremely fine aluminum and boron carbide powder. The use of METAMIC® as a neutron absorber material in spent fuel storage applications has been evaluated by the Electric Power Research Institute (Reference 5) and found to be acceptable. In addition, use of METAMIC® in the Holtec MPC design is currently under NRC review as part of License Amendment Request 1014-2 for the HI-STORM 100 System (Reference 6). Previous approval for use of an aluminum alloy metal matrix composite, such as METAMIC®, in a dry storage cask may be found on Docket 72-1004 for the Standardized NUHOMS® Dry Storage System.

The one difference between the METAMIC® design for the generic Holtec MPC and the MPC-HB is that the amount of boron carbide required for criticality control is much less. Due to the low reactivity of the HBPP fuel to be stored, the METAMIC® used in the MPC-HB has a minimum  $^{10}B$  areal density of  $0.01 \text{ g/cm}^2$  compared to the generic Holtec MPC design value of  $0.0310 \text{ g/cm}^2$ .

The METAMIC® neutron absorber panels are submerged in unborated water during fuel loading operations in the SFP, and during MPC lid welding and cutting (in the unlikely event the MPC needs to be unloaded). The aluminum on the surface of the as-manufactured METAMIC® panels reacts with water to produce an aluminum oxide on the panel surface. A byproduct of that chemical reaction is a small amount of hydrogen gas. For the most part, the oxidation process happens early in the exposure of the neutron absorber panel to air, and then to water during loading operations, and the oxide layer prevent any significant additional hydrogen generation. However, some trace amounts of hydrogen may continue to be produced thereafter while water is in MPC. While in the SFP with the MPC lid not yet installed, any hydrogen produced will either remain entrained in the SFP water or rise out of the SFP and be released to the environment by the HBPP SFP ventilation system before any combustible concentration can accumulate.

After the point in fuel loading operations where the MPC lid is installed, any hydrogen produced could accumulate in the MPC in the space above the water surface and below the lid. The rate and total amount of hydrogen produced is not able to be accurately predicted, but is expected to be insignificant since METAMIC® is not a porous material and the surfaces of the panels will be substantially protected from further aluminum-water reaction by the layer of aluminum oxide that will have formed from the reaction itself earlier in the loading process. To preclude hydrogen ignition during welding or cutting, the operating procedures for the Humboldt Bay ISFSI require that the

## HUMBOLDT BAY ISFSI FSAR UPDATE

space beneath the MPC be purged or exhausted before and during MPC lid welding or cutting operations. In addition, appropriate combustible gas monitoring is performed during these operations. These controls are consistent with the controls discussed in Sections 8.1.5 and 8.3.3 of the HI-STAR 100 System FSAR, Revision 1, for loading and unloading operations, respectively.

Galvanic reaction between the stainless steel of the MPC and aluminum in METAMIC[®] is minimized to an insignificant amount by the rapid oxidation of the aluminum surfaces of the neutron absorber panel. The aluminum oxide layers acts as an insulator against current flow in the electric couple comprised of the aluminum, steel, and SFP water. Further, the MPC is submerged in water only during fuel loading in the SFP through MPC lid welding operations, which together last anywhere from one to three days, based on previous experience. This short duration minimizes the extent of any galvanic corrosion that may be occurring between dissimilar metals with water in the MPC. After lid welding, the MPC is drained of water in preparation for drying and helium backfilling operations, eliminating galvanic corrosion as a concern.

After the MPC-HB has been drained of water and dried, it is backfilled with helium to create the inert gas environment required for long term storage operations at the ISFSI. There are no adverse chemical or galvanic reactions between METAMIC[®] and helium, nor does helium act as an electrolyte for galvanic coupling between METAMIC[®] and other materials in the MPC-HB.

### **4.6.1.2 BORAL[®] Neutron Absorber**

Information on the characteristics of the Boral neutron absorbing material possibly used in the MPC fuel basket is provided in Subsection 1.2.1.3.1 of the HI-STORM 100 System FSAR. The relatively low neutron flux, which will continue to decay over time, to which this borated material is subjected, does not result in significant depletion of the material's available boron to perform its intended safety function. An evaluation discussed in Section 6.3.2 of the HI-STORM 100 System FSAR demonstrates that the boron depletion in the Boral is negligible over a 50-year duration. Thus, sufficient levels of boron are present in the fuel basket neutron absorbing material to maintain criticality safety functions over the 40-year design life of the MPC.

### **4.6.2 DAMAGED FUEL CONTAINER**

The damaged fuel container (DFC) is constructed of all stainless steel material. Stainless steel has no significant reactions in spent fuel pool water or in a helium environment as discussed above. Therefore, there are no significant chemical or galvanic reaction issues with the DFC used at the Humboldt Bay ISFSI.



#### 4.6.3 HI-STAR OVERPACK

The HI-STAR HB overpack combines low-alloy and nickel alloy steel, carbon steels, neutron shielding material, and bolting materials as shown in Table 4.6-1. All of these materials are the same as previously licensed for the HI-STAR 100 System overpack (see Table 3.4.2 in the HI-STAR 100 FSAR). There are no significant galvanic or chemical reactions among the materials of construction for the overpack. The internal and external steel surfaces of the overpack are coated to minimize any chemical reactions with the SFP water during loading operations and to preclude surface oxidation of the steel during long term storage. Threaded holes, lifting trunnions, and stainless steel sealing surfaces are not coated. The coating materials are Thermaline 450 for the inner overpack surfaces and Carboline 890 for the outer surfaces as are licensed for the HI-STAR 100 overpack. Chemically identical coating materials under different names are also acceptable for use. Thermaline 450 is chosen for use on the inner surfaces due to its high temperature resistance features. Data sheets for both of these materials are provided in Appendix 1C of the HI-STAR 100 FSAR.

The annulus between the overpack and the MPC is filled with clean water during loading operations in the SFP, which is a short-term evolution where no significant corrosion of the steel is likely, even if there was a blemish in the coating that exposed the steel underneath the coating material to water. During long-term storage, the annulus is filled with helium to preclude any deleterious material interaction.

The external surfaces of the overpack are exposed to unborated water during loading operations. The coating material precludes any chemical or galvanic interaction between the carbon steel of the overpack and the water. In its long-term storage configuration, the overpack external surfaces are exposed to the saline air environment inside the ISFSI vault storage cell. The coating material on the carbon steel protects the steel from adverse chemical or galvanic reactions with the air in the vault storage cell. Because the overpack is not handled or moved in any way during long-term storage operations, it is highly unlikely that the overpack coating could be damaged, exposing the carbon steel to the air environment. Uncoated threaded holes and sealing surfaces are not directly exposed to environment due to the installation of the overpack closure plate with its closure bolts or plugs in unused holes. The lifting trunnions are made from a non-ferrous nickel alloy and are not coated because of the interface with the lift links, which would damage any coating during lifting evolutions. The nickel-based alloy is resistant to corrosion in the spent fuel pool and the saline air environment.

The Holtite-A neutron shielding material in the overpack is completely sealed inside the welded steel neutron shield enclosure shell. The enclosure shell separates the neutron shield material from the ambient environment during all modes of operation, eliminating any potential for adverse chemical or galvanic reactions with the SFP water or storage vault air.

In summary, the materials of construction of the overpack design are compatible with the environment in which the overpack will operate. These design features ensure that the overpack can perform its design functions for the life of the ISFSI.

### **4.6.4 NEUTRON ABSORBER EFFICACY**

The effectiveness of the fixed borated neutron absorbing material used in the MPC-HB fuel basket design requires that sufficient concentrations of boron be present to assure criticality safety during worst case design basis conditions over the 40-year design life of the MPC. Information on the characteristics of the METAMIC[®] and BORAL neutron absorbing material used in the MPC fuel basket is provided in Subsection 1.2.1.3.1.2 of the HI-STORM 100 System FSAR, as amended by License Amendment Request (LAR) 1014-2. The relatively low neutron flux, which will continue to decay over time, to which this borated material is subjected, does not result in significant depletion of the material's available boron to perform its intended safety function. In addition, the boron content of the material used in the criticality safety analysis is conservatively based on the minimum specified boron areal density (rather than the nominal), which is further reduced by 25 percent for analysis purposes, as described in Section 4.2.3.3.7 of this Safety Analysis Report. An evaluation discussed in Section 6.3.2 of the HI-STORM 100 System FSAR, as amended by LAR 1014-2 demonstrates that the boron depletion in the METAMIC[®] and BORAL is negligible over a 50-year duration. Thus, sufficient levels of boron are present in the fuel basket neutron absorbing material to maintain criticality safety functions over the 40-year design life of the MPC. Based on this evaluation and consistent with 10 CFR 72.124(b), no continued verification of neutron absorber efficiency is required.

### **4.6.5 ISFSI VAULT**

The ISFSI vault is a below grade structure constructed of reinforced concrete with carbon steel liners in each of the six cells. The concrete mix is designed to provide durability in the environment, and the reinforcement has at least the minimum cover specified in ACI-349. The vault is surrounded by a French drain to preclude buildup of localized subsurface water. The carbon steel liner and other exposed carbon steel materials will be coated with a material suitable for the saline air service conditions to prevent corrosion. Threaded holes will either be plugged or filled with their mating bolts during long-term storage operations to prevent corrosion of the threads. The vault structure is lightly loaded under normal storage conditions, and is not expected to have any stress induced cracking which could allow the environment to approach the reinforcement. Similar type structures have a service life well in excess of the license term of this facility.

Additional information describing the cement and aggregate types used in construction of the vault is provided in the PG&E Response to NRC Question 5-7 in Reference 7.

#### 4.6.6 MATERIALS SUMMARY

Table 4.6-1 provides a listing of the materials of fabrication for the HI-STAR HB dry storage system and summarizes the performance of the material in the expected operating environments during short-term loading/unloading operations and long-term storage operations. As a result of this review, no operations were identified that could produce adverse reactions beyond those conditions already generically evaluated and approved in the licensing of the HI-STAR 100 System.

#### 4.6.7 REFERENCES

1. Bulletin 96-04, Chemical, Galvanic, or Other Reactions in Spent Fuel Storage and Transportation Casks, USNRC, July 1996.
2. Interim Staff Guidance Document 15, Materials Evaluation, USNRC, January 2001.
3. Interim Staff Guidance 11, Cladding Considerations for the Transportation and Storage of Spent Fuel, Revision 2, USNRC, July 2002.
4. Interim Staff Guidance 18, The Design/Qualification of Final Closure Welds on Austenitic Stainless Steel Containers as Confinement Boundary for Spent Fuel Storage and Containment Boundary for Spent Fuel Transportation, USNRC, May 2003.
5. Qualification of METAMIC® for Spent Fuel Storage Applications, EPRI, 1003137, Final Report, October 2001.
6. License Amendment Request 1014-2, Holtec International, Revision 2, August 2003 (USNRC Docket 72-1014).
7. PG&E Letter HIL-04-007, Response to NRC Request for Additional Information for the Humboldt Bay Independent Spent Fuel Storage Installation Application, October 1, 2004.

## **4.7 DECOMMISSIONING PLAN**

### **4.7.1 PRELIMINARY DECOMMISSIONING PLAN**

At the end of the Humboldt Bay Independent Spent Fuel Storage Installation (ISFSI) life, Multi-purpose Canisters (MPCs) loaded with spent fuel will be transported offsite. Since the MPCs are designed for storage and transport of spent fuel, the fuel assemblies will remain sealed in the MPCs such that decontamination of the MPCs is not required. Following shipment of the HI-STAR HB casks/MPCs offsite, the ISFSI will be decommissioned by identification and removal of any residual radioactive material, and performance of a final radiological survey. Details on decommissioning are provided in the ISFSI License Application, Attachment F, "Preliminary Decommissioning Plan." A brief summary is provided herein.

### **4.7.2 FEATURES THAT FACILITATE DECONTAMINATION AND DECOMMISSIONING**

The design features of the HI-STAR HB storage/transportation casks, plus a "start clean/stay clean" philosophy, will facilitate decommissioning the Humboldt Bay ISFSI. Radioactive materials associated with spent fuel assemblies are contained within MPCs, which will be seal welded before leaving the Refueling Building (RFB). The MPC conforms to the requirements of Section III of the ASME code and provides assurance that radioactive material will not be released from the MPC over the life of the ISFSI. Health physics measures to ensure MPC external surfaces are maintained in a clean condition are implemented during MPC loading operations. These measures minimize contaminated fuel pool water from contacting the external surfaces of the MPC. Following fuel loading operations, a swipe survey is performed on the MPC lid and HI-STAR HB cask. Using administrative controls, transport of the HI-STAR HB cask and MPC to the storage vault is not permitted if removable contamination levels exceed Nuclear Regulatory Commission (NRC) requirements. Since the MPCs are sealed to preclude release of radioactive material inside the MPCs, minimizing contamination on external surfaces of the MPCs transported to the ISFSI vault minimizes the quantity of radioactive waste and contaminated equipment.

The interior design of the HI-STAR HB casks facilitates decommissioning, if necessary. The interior of the casks are made of coated steel thereby making them relatively easy to decontaminate.

Minimal non-radioactive hazardous materials may be used or stored at the Humboldt Bay ISFSI and any that are needed to support the ISFSI operations will be identified and controlled in accordance with procedures. Strict measures will be applied to prevent any hazardous materials from contacting radioactive contamination, so that mixed hazardous and radioactive waste will not be generated at the Humboldt Bay ISFSI.

## HUMBOLDT BAY ISFSI FSAR UPDATE

As shown in the HI-STAR 100 System Final Safety Analysis Report, the overpack would be expected to have only minimal interior or exterior radioactive surface contamination. Any neutron activation of the metal cask walls and neutron shielding is expected to be extremely small, and the assembly would qualify as Class A waste in a stable form based on definitions and requirements in 10 CFR 61.55. As such, the material would be suitable for burial in a near-surface disposal site as Low Specific Activity (LSA) material.

It is also likely that both the overpack and MPC, or extensive portions of both, can be further decontaminated to allow recycle or reuse options. After decontamination, the only radiological hazard the HI-STAR 100 system may pose is slight activation of the HI-STAR 100 materials caused by irradiation over a 40-year storage period.

### **4.7.3 COST OF DECOMMISSIONING AND FUNDING METHOD**

10 CFR 72.30(b) requires that the proposed decommissioning plan include a decommissioning cost estimate, a funding plan, and a method of ensuring the availability of decommissioning funds.

The philosophy of operating the Humboldt Bay ISFSI is “start clean/stay clean.” Thus, the intention is to maintain the facility free of radiological contamination at all times. During the operational phase of the facility, all radioactive contamination will be removed, if possible, immediately upon its discovery.

A cost estimate has been performed by TLG Services, Inc for HBPP Unit 3. This detailed estimate is contained in the 2002 Nuclear Decommissioning Cost Triennial Proceeding (NDCTP) submitted to the CPUC (Application No 02-03-020) on March 15, 2002. As shown therein, it is estimated that decommissioning the Humboldt Bay ISFSI will cost about \$878,000 in 2002 dollars. The major cost contributors are cost of labor and radiological surveys. The costs are based on several key assumptions, including regulatory requirements, estimating methodology, contingency requirements (a 30 percent contingency was assumed), and site restoration requirements.

Pacific Gas and Electric (PG&E) has established external sinking fund accounts for decommissioning HBPP Unit 3, as discussed in the Preliminary Decommissioning Plan and PG&E’s Letter HBL-03-002 dated March 27, 2003, Decommissioning Funding Report to the NRC (Reference 1), pursuant to the requirements of 10 CFR 50.75(f). With collection of additional funding that was approved by the CPUC in the 2002 NDCTP filing these accounts will contain adequate monies for any required nuclear decommissioning activities for the Humboldt Bay ISFSI.

#### **4.7.4 LONG-TERM LAND USE AND IRREVERSIBLE COMMITMENT OF RESOURCES**

Following removal of all storage casks from the ISFSI and decontamination of the storage vault, as necessary, these structures and associated areas can be released for unrestricted use.

The security-related structures could be dismantled and removed. The concrete structure above the ISFSI vault could be sectioned and removed, or alternatively, left in place. In either case, the storage vault area could be demolished or covered with topsoil and replanted with native vegetation, thus returning the land to its original condition.

The long-term plan will be addressed further in a final decommissioning plan that will be submitted prior to ISFSI license termination.

#### **4.7.5 RECORDKEEPING FOR DECOMMISSIONING**

The following records will be maintained until the Humboldt Bay ISFSI is released for unrestricted use, in accordance with 10 CFR 72.30(d), and will be used to plan the actual decommissioning efforts:

- Records of spills or other unusual occurrences involving the spread of contamination in and around the facility, equipment, or site. These records will include any known information on identification of nuclides, quantities, forms, and concentrations.
- As-built drawings and modifications of structure and equipment in restricted areas.
- A document, which is updated a minimum of every 2 years, containing:  
(a) a list of all areas designated at any time as restricted areas as defined in 10 CFR 20.1003; and (b) a list of all areas outside of restricted areas involved in a spread of contamination as required by 10 CFR 72.30(d)(1).
- Records of decommissioning cost estimates and the funding method used.

These records will be stored as part of the PG&E Records Management System.

#### **4.7.6 REFERENCES**

1. Decommissioning Funding Reports for Humboldt Bay Power Plant, PG&E Letters HBL-03-002 to the NRC, March 27, 2003.



# HUMBOLDT BAY ISFSI FSAR UPDATE

TABLE 4.2-1

## PHYSICAL CHARACTERISTICS OF THE MPC-HB

PARAMETER	NOMINAL VALUE
Outside Diameter	68-3/8 inches
Length	114 ½ inches
Maximum Heat Load	2.0 kW
Material of Construction	Stainless Steel (except neutron absorber and aluminum washer in vent and drain ports)
Maximum Weight with Fuel (dry/wet)	59,000 lb/70,000 lb
Internal Atmosphere	Helium

# HUMBOLDT BAY ISFSI FSAR UPDATE

TABLE 4.2-2

## COMPARISON OF HI-STAR 100 AND HI-STAR HB SYSTEM BOUNDING WEIGHTS

Component	Value	
	HI-STAR 100	HI-STAR HB
MPC weight, loaded with fuel, dry	90,000 lb	59,000
Overpack weight, empty	158,000 lb	102,200
Overpack weight, with loaded MPC, dry	250,000	161,200
Center-of-gravity of loaded, dry MPC	103.2 inches	61 inches
Center-of-gravity of empty overpack	99.7 inches	61.8 inches

# HUMBOLDT BAY ISFSI FSAR UPDATE

TABLE 4.2-3

## COMPARISON OF HOLTEC MPC DESIGN WITH ISG-18 GUIDANCE FOR STORAGE

DESIGN/QUALIFICATION GUIDANCE	HOLTEC MPC DESIGN
The canister is constructed from austenitic stainless steel	The MPC enclosure vessel is constructed entirely from austenitic stainless steel (Alloy X). Alloy X is defined as Type 304, 304LN, 316, or 316LN material
The canister closure welds meet the guidance of ISG-15 (or approved alternative), Section X.5.2.3	The MPC lid-to-shell (LTS) closure weld meets ISG-15, Section X.5.2.3 for austenitic stainless steels. UT examination is permitted and NB-5332 acceptance criteria are required. An optional multi-layer PT examination is also permitted. The multi-layer PT is performed at each approximately 3/8" of weld depth, which corresponds to the critical flaw size. A weld quality factor of 0.45 (45% of actual weld capacity) has been used in the stress analysis.
The canister maintains its confinement integrity during normal conditions, anticipated occurrences, and credible accidents, and natural phenomena	The MPC is shown by analysis to maintain confinement integrity for all normal, off-normal, and accident conditions, including natural phenomena. The MPC is designed to withstand 60 g deceleration.
Records documenting the fabrication and closure welding of canisters shall comply with the provisions 10 CFR 72.174 and ISG-15. Record storage shall comply with ANSI N45.2.9.	Records documenting the fabrication and closure welding of MPCs meet the requirements of ISG-15 via controls required by this FSAR, Holtec QA program, and implementing procedures. Compliance with 10 CFR 72.174 and ANSI N.45.2.9 is achieved via Holtec QA program and implementing procedures.
Activities related to inspection, evaluation, documentation of fabrication, and closure welding of canisters shall be performed in accordance with an NRC-approved quality assurance program.	The NRC has approved the Holtec quality assurance program under 10 CFR 71. That QA program approval has been adopted for activities governed by 10 CFR 72 as permitted by 10 CFR 72.140(d)

## HUMBOLDT BAY ISFSI FSAR UPDATE

TABLE 4.2-4

### PHYSICAL CHARACTERISTICS OF THE HI-STAR HB OVERPACK

PARAMETER	VALUE
Height	127-7/16 inches
Outside Diameter	83-1/4 inches (bottom baseplate) 96 inches (enclosure shell)
Capacity	One loaded MPC-HB
Material of Construction	Carbon steel (except neutron shield and seal surfaces) Stainless steel (seal surfaces) Holtite-A (neutron shield)
Maximum Weight, including MPC, and fuel (dry/wet)	161,200 lb/172,200 lb
Design Life	40 years

# HUMBOLDT BAY ISFSI FSAR UPDATE

TABLE 4.2-5

SUMMARY OF MPC-HB CAVITY MAXIMUM PRESSURES FOR NORMAL CONDITIONS

<b>Condition</b>	<b>Pressure (psig)</b>
Maximum initial backfill pressure (at 70°F)	48.8
Normal condition with no rod rupture	70.58
Normal condition with 1% rods ruptured	70.89

# HUMBOLDT BAY ISFSI FSAR UPDATE

TABLE 4.2-6

## FINITE ELEMENT ANALYSIS RESULTS FOR THE MPC-HB FUEL BASKET UNDER 60-g LOADING

<b>Stress Result</b>	<b>0-Degree Event Stress (psi) (Safety Factor)</b>	<b>45-Degree Event Stress (psi) (Safety Factor)</b>
Fuel Basket – Primary Membrane ( $P_m$ )	15,523 (2.38)	12,316 (3.00)
Fuel Basket – Local Membrane Plus Primary Bending ( $P_L + P_b$ )	27,511 (2.02)	47,518 (1.17)
Enclosure Vessel – Primary Membrane ( $P_m$ )	6,066 (7.16)	5,801 (7.49)
Enclosure Vessel – Local Membrane Plus Primary Bending ( $P_L + P_b$ )	19,252 (3.39)	16,904 (3.86)
Fuel Basket Supports – Primary Membrane ( $P_m$ )	8,397 (5.17)	6,948 (6.25)
Fuel Basket Supports – Local Membrane Plus Primary Bending ( $P_L + P_b$ )	50,294 (1.30)	39,659 (1.64)



## HUMBOLDT BAY ISFSI FSAR UPDATE

TABLE 4.2-7

### RESULTS OF STRESS CALCULATIONS FOR FUEL BASKET SPACERS, FUEL BASKET SPACER WELDS, AND FUEL SPACERS

<b>Item Evaluated</b>	<b>Safety Factor</b>
Fuel Basket Spacer – Direct Compression	1.49
Fuel Basket Spacer - Buckling	13.55
Weld Between Fuel Basket Spacers and Fuel Basket Walls	1.34
Fuel Spacer Web Yielding	1.86
Fuel Spacer to MPC Lid Weld Shear Stress	12.1

# HUMBOLDT BAY ISFSI FSAR UPDATE

TABLE 4.2-8

## RESULTS OF DAMAGED FUEL CONTAINER STRESS ANALYSIS

Item Analyzed	Stress Result (psi)	Factor of Safety
Sleeve – Tensile, Primary Membrane	376	53.2
Base-to-Sleeve Spot Welds - Shear	787	15.2
Container Collar – Tensile	19,042	1.6
Collar Engagement Slots - Shear	1245	9.6
Upper Locking Device Load Tabs - Shear	350	34.2
Upper Closure Plate - Bending	3,680	8.2
Lifting Bolts - Tensile	5,936	1.2 (Note 1)
DFC Handling Device	4,293	1.03 (Note 2)

- 
1. For SA 197-B7 bolt material, the minimum required stress of 1/10th against ultimate stress per ANSI N14.6 provides the governing case.
  2. For DFC handling device, the minimum required stress of 1/6th against yield stress per ANSI N14.6 provides the governing case.

# HUMBOLDT BAY ISFSI FSAR UPDATE

TABLE 4.2-9

## THERMAL ANALYSIS INPUTS

<b>Input</b>	<b>Value</b>
Maximum Cask Heat Load	2 kW
Maximum Fuel Assembly Heat Load	50 Watts
Minimum Helium Backfill Pressure (@ 70°F)	45.2 psig
Annual Average Air Temperature	52°F
Annual Average Soil Temperature	52°F
Maximum Solar Insolation	602 g-cal/cm ² over 24 hours
Carbon Steel Conductivity	20 Btu/ft-hr-°F
Reinforced Concrete Conductivity	1.0 Btu/ft-hr-°F
Soil Conductivity	0.833 Btu/ft-hr-°F
Upper Bound Active Fuel Length	96.91 inches
Lower Bound Active Fuel Length	77.125 inches

# HUMBOLDT BAY ISFSI FSAR UPDATE

TABLE 4.2-10

## NORMAL CONDITION THERMAL ANALYSIS RESULTS

<b>Component</b>	<b>Calculated Temperature (°F)</b>	<b>Normal Condition Limit (°F)</b>
Fuel Cladding	373	752
Holtite-A Neutron Shield	195	300
MPC Shell	203	450
Local Concrete	175	300
Bulk Concrete	145	150

# HUMBOLDT BAY ISFSI FSAR UPDATE

TABLE 4.2-11

Sheet 1 of 7

## HUMBOLDT BAY ISFSI COMPLIANCE WITH GENERAL DESIGN CRITERIA (10 CFR 72, SUBPART F)

10 CFR 72 REQUIREMENT	REQUIREMENT SUMMARY	FSAR SECTION WHERE COMPLIANCE IS DEMONSTRATED
72.122 (a) Quality standards	Structures, systems, and components (SSCs) important to safety must be designed, fabricated, erected, and tested to quality standards commensurate with the importance to safety of the function.	<ul style="list-style-type: none"> <li>Section 4.5 provides the classification for SSCs important to safety.</li> <li>Chapter 4 describes the ISFSI design features of SSCs that are important to safety.</li> <li>HI-STAR 100 SYSTEM FSAR Tables 2.2.6 and 8.1.4 provide the safety classifications of cask and ancillary components, respectively.</li> <li>Chapter 11 describes the Humboldt Bay ISFSI QA Program</li> </ul>
72.122 (b) Protection against environmental conditions and natural phenomena	SSCs important to safety must be designed to accommodate the effects of and be compatible with site characteristics and environmental conditions and to withstand postulated accidents.	<ul style="list-style-type: none"> <li>Section 3.2 provides the design bases and criteria for environmental conditions and natural phenomena for the Humboldt Bay ISFSI.</li> <li>Section 4.2 describes the design for the ISFSI vault structure for normal, off-normal and accident conditions, and environmental conditions and natural phenomena.</li> <li>Section 3.3 describes the design criteria for the cask transporter and ISFSI vault.</li> <li>Section 4.2.3.3.2.10 describes the site-specific structural analyses of the MPC-HB fuel basket, basket spacers, and fuel spacers.</li> <li>Section 4.3 describes the design for the cask transport system.</li> <li>HI-STAR FSAR Chapters 3 and 11 describe the details of the cask structural design, including normal, off-normal, and accident conditions of storage.</li> </ul>

# HUMBOLDT BAY ISFSI FSAR UPDATE

TABLE 4.2-11

Sheet 2 of 7

10 CFR 72 REQUIREMENT	REQUIREMENT SUMMARY	FSAR SECTION WHERE COMPLIANCE IS DEMONSTRATED
72.122 (c) Protection against fires and explosions	SSCs important to safety must be designed and located so that they can continue to perform their safety functions under credible fire and explosion exposure conditions.	<ul style="list-style-type: none"> <li>Section 3.3.1.6 describes the fire and explosion protection design criteria.</li> <li>Sections 4.2.3.3.2.9 and 4.2.3.3.3 discuss cask design features as they relate to the capability of the cask system to withstand explosions and fires.</li> <li>Sections 8.2.5 and 8.2.6 describe the evaluations and analyses related to fires and explosions.</li> </ul>
72.122 (d) Sharing of SSCs	SSCs important to safety must not be shared between the ISFSI and other facilities unless it is shown that such sharing will not impair the capability of either facility to perform its safety functions.	<ul style="list-style-type: none"> <li>Section 1.2 discusses the shared SSCs between the Humboldt Bay ISFSI and HBPP. No important to safety SSCs are shared between the ISFSI and HBPP.</li> </ul>
72.122 (e) Proximity of sites	An ISFSI located near other nuclear facilities must be designed and operated to ensure that the cumulative effects of their combined operations will not constitute an unreasonable risk to the health and safety of the public.	<ul style="list-style-type: none"> <li>Sections 2.1 and 4.1 discuss the location and layout of the Humboldt Bay ISFSI.</li> <li>Chapter 7 discusses the combined radiation doses to the public from the concurrent operation of the ISFSI and HBPP.</li> </ul>
72.122 (f) Testing and maintenance of systems and components	Systems and components that are important to safety must be designed to permit inspection, maintenance, and testing.	<ul style="list-style-type: none"> <li>Section 3.3.1.5.1 describes the expected need for access to the ISFSI to conduct maintenance and inspection activities.</li> <li>Section 4.2 describes the design features of the ISFSI that accommodate inspection, maintenance, and testing.</li> <li>Chapter 9 of the HI-STAR 100 FSAR and Section 4.3.4 of this FSAR describes the limited amount of maintenance expected to be required for the cask system.</li> </ul>



# HUMBOLDT BAY ISFSI FSAR UPDATE

TABLE 4.2-11

Sheet 3 of 7

10 CFR 72 REQUIREMENT	REQUIREMENT SUMMARY	FSAR SECTION WHERE COMPLIANCE IS DEMONSTRATED
72.122 (g) Emergency capability	SSCs important to safety must be designed for emergencies. The design must provide accessibility to the equipment by onsite and available offsite emergency facilities and services.	<ul style="list-style-type: none"> <li>Section 1.2 describes how the Humboldt Bay ISFSI is designed for accessibility during emergencies.</li> <li>Section 9.5 summarizes the Emergency Plan for the ISFSI.</li> </ul>
72.122 (h) Confinement barriers and systems	The spent fuel cladding must be protected during storage against degradation that leads to gross ruptures or the fuel must be otherwise confined. Ventilation systems must be provided, where necessary, to ensure confinement of airborne particulates. Periodic monitoring is sufficient, consistent with cask design requirements.	<ul style="list-style-type: none"> <li>Section 3.3.1.2.1 describes the HI-STAR HB System confinement barriers and systems.</li> <li>Sections 3.3.1.5.3, 3.3.1.7.2, 7.3.3, and 7.7 discuss the absence of radioactive effluents from the HI-STAR HB System, which eliminates the need for ventilation systems.</li> <li>Section 4.2.3.3.6 describes how the design of the HI-STAR HB System maintains confinement integrity under all normal, off-normal, and accident conditions of storage.</li> <li>Chapter 3 of the HI-STAR 100 System FSAR describes the structural evaluations performed to demonstrate confinement integrity under all conditions of storage.</li> </ul>
72.122 (i) Instrumentation and control systems	Instrumentation and control systems must be provided in accordance with cask design requirements to monitor normal, off-normal, and accident conditions.	<ul style="list-style-type: none"> <li>Section 3.3.1.3.2 discusses the fact that the HI-STAR HB System requires no instrumentation for normal or off-normal operation or for accidents.</li> </ul>
72.122 (j) Control room or control area	A control room or control area, if appropriate, must be designed to permit occupancy and actions to be taken to monitor the ISFSI safely under normal conditions, and to provide safe control of the ISFSI under off-normal or accident conditions.	<ul style="list-style-type: none"> <li>Section 3.3.1.5.1 discusses why access to the ISFSI may periodically be required.</li> <li>Section 5.2 discusses why a dedicated ISFSI control room/area is not required.</li> <li>The ISFSI Physical Security Plan provides the details for ISFSI access control. Section 9.6 provides a brief non-safeguards summary.</li> </ul>

# HUMBOLDT BAY ISFSI FSAR UPDATE

TABLE 4.2-11

Sheet 4 of 7

10 CFR 72 REQUIREMENT	REQUIREMENT SUMMARY	FSAR SECTION WHERE COMPLIANCE IS DEMONSTRATED
72.122 (k) Utility or other services	Each utility service system must be designed to meet emergency conditions. The design of utility services and distribution systems that are important to safety must include redundant systems to maintain the ability to perform safety functions assuming a single failure. An ISFSI located on the site of another facility may share common utilities and services provided the sharing or physical connection does not significantly increase the probability or consequences of an accident or malfunctions of equipment important to safety; or reduce the margin of safety as defined in the technical specification bases for either facility.	<ul style="list-style-type: none"> <li>Section 1.2 discusses shared utility services between the ISFSI and HBPP. No important to safety services are shared.</li> <li>Section 8.1.5 discusses the evaluation of a loss of electrical power to the Humboldt Bay ISFSI.</li> </ul>
72.122 (l) Retrievability	Storage systems must be designed to allow ready retrieval of spent fuel for further processing or disposal.	<ul style="list-style-type: none"> <li>Section 5.1 discusses unloading of the HI-STAR HB System and ready fuel retrievability for return to the HBPP spent fuel pool.</li> </ul>
72.124 (a) Design for criticality safety	Spent fuel handling, packaging, transfer, and storage systems must be designed to be maintained subcritical.	<ul style="list-style-type: none"> <li>Sections 3.3.1.4, 3.3.1.7, and 4.2.3.3.7 summarize the design features and administrative controls used to ensure subcriticality of the spent fuel is maintained during all phases of fuel loading, cask preparation, and storage.</li> <li>Chapter 6 of the HI-STAR 100 System FSAR provides a detailed discussion of the benchmarking of the criticality method and sensitivity of changes to the reactivity system.</li> <li>Section 4.2.3.3.7 describes the criticality analyses performed for the HI-STAR HB System.</li> </ul>

# HUMBOLDT BAY ISFSI FSAR UPDATE

TABLE 4.2-11

Sheet 5 of 7

10 CFR 72 REQUIREMENT	REQUIREMENT SUMMARY	FSAR SECTION WHERE COMPLIANCE IS DEMONSTRATED
72.124 (b) Methods of criticality control	When practicable, the design of an ISFSI must be based on favorable geometry, permanently fixed neutron absorbing materials (poisons), or both. The continued efficacy of the neutron absorbing material may be confirmed by demonstration or analysis before use, showing significant degradation over the life of the facility cannot occur.	<ul style="list-style-type: none"> <li>Sections 3.3.1.4 and 4.2.3.3.7 discuss the combination of geometry and fixed neutron poisons as the means of subcriticality control.</li> <li>Section 6.3.2 and 1.2.1.3.1.2 of the HI-STORM 100 System FSAR, as modified by LAR 1014-2 describe the METAMIC® neutron absorber to be used in the Holtec generic MPCs and MPC-HB, and provides information showing that significant degradation over the life of the facility will not occur and verification of continued efficacy is not required.</li> </ul>
72.124 (c) Criticality monitoring	A criticality monitoring system shall be maintained in each area where special nuclear material (SNM) is handled, used, or stored which will energize clearly audible alarm signals if accidental criticality occurs. Monitoring of dry storage areas where SNM is packaged in its stored configuration under a 10 CFR 72 license is not required.	<ul style="list-style-type: none"> <li>Section 4.2.3.3.7 discusses criticality monitoring based on compliance with 10 CFR 50.68(b).</li> </ul>
72.126 (a) Exposure control	Radiation protection systems must be provided for all areas and operations where onsite personnel may be exposed to radiation or airborne radioactive materials.	<ul style="list-style-type: none"> <li>Section 3.3.1.5 provides the radiological protection design criteria and the key cask system components relied upon for shielding.</li> <li>Chapter 7 discusses the radiation protection program.</li> </ul>

# HUMBOLDT BAY ISFSI FSAR UPDATE

TABLE 4.2-11

Sheet 6 of 7

10 CFR 72 REQUIREMENT	REQUIREMENT SUMMARY	FSAR SECTION WHERE COMPLIANCE IS DEMONSTRATED
72.126 (b) Radiological alarm systems	Radiological alarm systems must be provided in accessible work areas as appropriate to warn operating personnel of radiation and airborne radioactive material concentrations above a given set point and of concentrations of radioactive material in effluents above control limits.	<ul style="list-style-type: none"> <li>Section 3.3.1.5.3 discusses the requirements for radiological alarm systems.</li> <li>Section 7.3.4 describes the radiological monitoring program.</li> </ul>
72.126 (c) Effluent and direct radiation monitoring	As appropriate for the handling and storage system, means to measure effluents must be provided for normal and accident conditions. Areas containing radioactive materials must be provided with systems for measuring the direct radiation levels in and around these areas.	<ul style="list-style-type: none"> <li>Section 3.3.1.5.3 describes how the HI-STAR HB System emits no solid, gaseous, or liquid effluents under normal or off-normal conditions of storage.</li> <li>Section 4.2.3.3.8 describes how confinement integrity is maintained under normal, off-normal, and accident conditions.</li> <li>Section 7.3.4 describes the radiological monitoring program.</li> </ul>
72.126 (d) Effluent control	The ISFSI must be designed to provide means to limit to ALARA levels, the release of radioactive materials in effluents during normal operations and control the release of radioactive materials in effluents under normal conditions and to control the release of radioactive materials under accident conditions.	<ul style="list-style-type: none"> <li>Section 3.3.1.5.3 describes how the HI-STAR HB System emits no gaseous or liquid effluents under normal or off-normal conditions of storage.</li> <li>Section 4.2.3.3.8 describes how confinement integrity is maintained under normal, off-normal, and accident conditions.</li> </ul>

# HUMBOLDT BAY ISFSI FSAR UPDATE

TABLE 4.2-11

Sheet 7 of 7

10 CFR 72 REQUIREMENT	REQUIREMENT SUMMARY	FSAR SECTION WHERE COMPLIANCE IS DEMONSTRATED
72.128 (a) Spent fuel storage and handling systems	Spent fuel storage and other systems that might contain or handle radioactive materials associated with spent fuel must be designed to ensure adequate safety under normal and accident conditions.	<ul style="list-style-type: none"> <li>Section 4.2 describes the design of SSCs that contain or handle radioactive material for normal and accident conditions.</li> </ul>
72.128 (b) Waste treatment	Radioactive waste treatment facilities must be provided.	<ul style="list-style-type: none"> <li>Sections 3.3.1.5.3, 3.3.1.7.2, 7.3.3, and 7.7 discuss how no radioactive waste is produced by the HI-STAR HB System.</li> <li>Sections 4.4.2 and 6.2 describes the decontamination process during loading operations and the treatment of and waste that is created.</li> </ul>
72.130 Criteria for decommissioning	The ISFSI must be designed for decommissioning. Provisions must be made to facilitate decontamination of structures and equipment, minimize the quantity of radioactive wastes and contaminated equipment, and facilitate the removal of radioactive waste at the time of decommissioning.	<ul style="list-style-type: none"> <li>Section 4.7 summarizes the ISFSI preliminary decommissioning plan.</li> <li>Section 2.4 of the HI-STAR 100 System FSAR describes the cask design features as they relate to decommissioning.</li> <li>The Humboldt Bay Preliminary Decommissioning Plan presents an overall description of the decommissioning requirements.</li> </ul>

# HUMBOLDT BAY ISFSI FSAR UPDATE

TABLE 4.2-12

Sheet 1 of 4

## INTERIM STAFF GUIDANCE COMPLIANCE MATRIX

ISG Number and Title	Guidance Summary	FSAR Section where Guidance is Addressed
1, Rev. 1: Damaged Fuel	This Interim Staff Guidance (ISG) provides the staff position on damaged fuel, including a definition of damaged fuel. It also outlines how damaged fuel is considered in storage or transportation analyses, and provides guidance for classifying spent fuel as either damaged or intact prior to placing the fuel into storage or transportation casks.	3.1.1 and 10.2
2, Rev. 0: Fuel Retrievability	This ISG provides the staff position on the interpretation of 10 CFR 72.122(l) (fuel retrievability) and the relationship of this regulation to the licensing of dry storage casks in general, and dual purpose casks in particular. It reemphasizes that on-site Independent Spent Fuel Storage Installation (ISFSIs) are interim storage facilities with limited license terms and not “defacto” repositories.	3.1, 3.3.1.7.1, and 4.2.3.2.2
3, Rev. 0: Post-Accident Recovery and Compliance with 10 CFR 72.122(l)	This ISG further clarifies the staff position on 10 CFR 72.122(l) by stating that retrievability of fuel applies to normal and off-normal conditions, but not to accidents. It also provides the staff position on consideration of credible versus non-credible accidents in the ISFSI design and the focus of credible accident analysis should be the protection of the confinement boundary. Accident analysis should focus on the requirements of 10 CFR 72.106 (dose to the public) and §72.122(b) (protection against environmental conditions and natural phenomena.	3.2, 4.2.3, 8.1, and 8.2
4, Rev. 1: Cask Closure Weld Inspections	This ISG provides the staff position on the examination requirements for cask closure welds. Austenitic stainless steel designs may be inspected using either volumetric or multiple pass dye penetrant techniques subject to the various conditions listed in the ISG.	4.2.3.2.1



HUMBOLDT BAY ISFSI FSAR UPDATE

TABLE 4.2-12

Sheet 2 of 4

ISG Number and Title	Guidance Summary	FSAR Section where Guidance is Addressed
5, Rev. 1: Confinement Evaluation	This ISG provides the staff position on containment (Part 71) and confinement (Part 72) dose analyses and associated fuel rod release fractions. The analysis portions of this ISG are not applicable to the Humboldt Bay ISFSI (See ISG-18).	8.1.1
6, Rev. 0: Establishing Minimum Initial Enrichment for the Bounding Design Basis Fuel Assembly(s).	This ISG provides the staff position on specifying a minimum enrichment limit for the design basis fuel assembly used in the shielding analysis.	3.1.1.2, 7.2, and 10.2
7, Rev. 0: Potential Generic Issue Concerning Cask Heat Transfer in a Transportation Accident	This ISG provides the staff position pertaining to the effect of fission gases released from the fuel rods on canister pressurization and the thermal analysis.	4.3.3.2.2 and 4.2.3.3.5
8, Rev. 2: Burnup Credit in The Criticality Safety Analyses of PWR Spent Fuel in Transport and Storage Casks	This ISG provides the staff position on the assumptions and methodology used in criticality analyses that incorporate credit for fuel burnup. This ISG is not applicable to the Humboldt Bay ISFSI since fresh fuel is assumed in the criticality analysis.	3.3.1.4.1 and 4.2.3.3.7
9, Rev. 1: Storage Of Components Associated With Fuel Assemblies	This ISG provides the staff position on the types of materials that may be licensed for storage with a fuel assembly in a dry storage cask. Boiling water reactor fuel channels may be stored with the fuel assemblies, but control blades may not.	3.1.1 and 10.2
10, Rev. 1: Alternatives to the ASME Code	This ISG provides the staff position on the use of the ASME Code for the construction of dry storage casks and how to identify and control NRC-approved alternatives to the Code.	4.2.3.3

## HUMBOLDT BAY ISFSI FSAR UPDATE

TABLE 4.2-12

Sheet 3 of 4

ISG Number and Title	Guidance Summary	FSAR Section where Guidance is Addressed
11, Rev. 2: Cladding Considerations for the Transportation and Storage of Spent Fuel	This ISG provides the staff position on peak fuel cladding temperature limits and technical guidance pertaining to high burnup ( $\geq 45,000$ MWD/MTU) fuel.	3.4 and 4.2.3.3.5
12, Rev. 1: Buckling of Irradiated Fuel Under Bottom End Drop Conditions	This ISG provides the staff position on the methodology used to determine the fuel assemblies' resistance to buckling in a bottom-end drop event. This ISG is not applicable to the Humboldt Bay ISFSI because a bottom-end drop is not a credible accident.	3.3.3.2.6, 4.2.3.3.2.5, and 8.2.7
13, Rev. 0: Real Individual	This ISG provides the staff position on: (1) the meaning of "real individual" as used in 10 CFR 72.104, (2) how ISFSI dose evaluations may be performed considering the real individual, and (3) clarify standard review plan text regarding dose calculations.	7.5 and 7.7
14, Rev. 0: Supplemental Shielding	This ISG provides the staff position on supplemental shielding that may be installed at an ISFSI to meet the requirements of 10 CFR 72.104(a). This applies to the Humboldt Bay ISFSI vault.	3.3.1.5.2, 4.2.1.1, 4.5.2, 7.3, 7.4, and 7.5
15, Rev. 0: Materials Evaluation	This ISG provides the staff position on the evaluation of materials to be used in the design of the ISFSI, including the storage cask.	4.6
16, Rev. 0: Emergency Planning	This ISG provides the staff position on the review of emergency plans for facilities licensed pursuant to 10 CFR part 72. Specifically, it removes the reference to Regulatory Guide 3.67 and restores the guidance published in the draft version of NUREG-1567 pertaining to emergency planning.	9.5
17, Rev. 0: Interim Storage of Greater Than Class "C" Waste	This ISG provides the staff position on the storage of greater-than-class-C waste at an ISFSI.	3.1, 3.1.1.4, 4.2.3.1, 7.2, and 10.2

HUMBOLDT BAY ISFSI FSAR UPDATE

TABLE 4.2-12

Sheet 4 of 4

ISG Number and Title	Guidance Summary	FSAR Section where Guidance is Addressed
18, Rev. 0: The Design/Qualification of Final Closure Welds on Austenitic Stainless Steel Canisters as the Confinement Boundary for Spent Fuel Storage and Containment Boundary for Spent Fuel Transportation	This ISG provides the staff position on the design/qualification of final closure welds on austenitic stainless steel canisters as confinement boundary for spent fuel storage and containment boundary for spent fuel transportation. It provides the criteria for designating austenitic stainless steel, welded confinement vessels as having no credible leakage.	3.3.1.2.1, 4.2.3.1, and 4.2.3.3.8
19, Rev. 0: Moderator Exclusion Under Hypothetical Accident Conditions and Demonstrating Subcriticality of Spent Fuel Under the Requirements of 10 CFR 71.55(e)	This ISG provides the staff position on moderator exclusion under hypothetical accident conditions applicable to spent fuel transportation under 10 CFR 71. This ISG is not applicable to the Humboldt Bay ISFSI.	Not applicable

## HUMBOLDT BAY ISFSI FSAR UPDATE

TABLE 4.3-1

### IMPORTANT-TO-SAFETY COMPONENTS OF THE CASK TRANSPORTATION SYSTEM

<b>Component</b>	<b>Function</b>	<b>Applicable Design Codes</b>
Cask Transporter	Lift, handle, and transport a loaded HI-STAR 100 HB overpack	Purchased commercial grade and tested prior to use in accordance with NUREG-0612
Overpack Lift Links	Transmit the force of the lifted load from the overpack lifting trunnions to the cask transporter lift points	ANSI N14.6 per NUREG-0612, Section 5.1.6
Connector Pins	Connect the overpack lift links to the cask transporter lift links	ANSI N14.6 per NUREG-0612, Section 5.1.6
Cask Restraint	Prevent lateral movement and transverse swinging of the cask during cask transport.	Purchased commercial grade and tested prior to use to confirm its commercial rated capacity with a 5 to 1 ultimate safety factor.

# HUMBOLDT BAY ISFSI FSAR UPDATE

TABLE 4.5-1

## QUALITY ASSURANCE CLASSIFICATION OF MAJOR STRUCTURES, SYSTEMS, AND COMPONENTS

IMPORTANT TO SAFETY ^(a)	NOT IMPORTANT TO SAFETY
<p>Classification Category A</p> <p>Multi-Purpose Canister</p> <p>Fuel Basket and Basket Spacers</p> <p>Damaged Fuel Container</p> <p>HI-STAR 100 HB Overpack</p> <p>HI-STAR HB GTCC Overpack</p> <p>Transporter Lift Links</p> <p>GTCC Waste Container</p> <p>Classification Category B</p> <p>ISFSI Storage Vault^(c)</p> <p>Fuel Spacers</p> <p>Transporter Connector Pins</p> <p>Helium Fill Gas^(b)</p> <p>Lid Retention Device</p> <p>Process Waste Container</p> <p>Cask Transporter^(b)</p> <p>Classification Category C</p>	<p>Security Systems</p> <p>Fencing</p> <p>Lighting</p> <p>Electrical Power</p> <p>Communications Systems</p> <p>Automated Welding System (AWS)</p> <p>MPC Forced Helium Dehydration System</p> <p>Overpack Vacuum Drying System</p> <p>Rail Dolly</p> <p>ISFSI Storage Vault Drainage Pipe^(d)</p>

- (a) Major cask system components are listed according to the highest QA category of any subcomponent comprising the major component. The safety classification of the subcomponents and the determination of the ITS category of each item is administratively controlled by PG&E via design and procurement control procedures with input from the storage cask vendor.
- (b) Purchased commercial grade and qualified by testing prior to use.
- (c) ISFSI storage vault lid, lid closure bolts, and vault plugs are classified as ITS Category B except for beyond design basis soil structure interaction seismic events. For these postulated SSI seismic events, the ISFSI storage vault lid, lid closure bolts, and vault plugs are classified as NITS since they are not relied upon in the seismic accident analysis. Refer to Section 3.2.4 and PG&E Letter HIL-05-007, dated June 3, 2005, for details of the classification.
- (d) The storage vault drainage pipe is classified as NITS because the drainage system is only one of several design features relied upon to ensure adequate performance of the cask and storage vault system in the event of standing water in the vault cells. Details of the assessment performed are provided in PG&E Response to NRC Question 5-10 in PG&E Letter HIL-04-007, dated October 1, 2004.

# HUMBOLDT BAY ISFSI FSAR UPDATE

Sheet 1 of 4

TABLE 4.6-1

## HI-STAR HB SYSTEM MATERIALS SUMMARY

Material/Component	Fuel Pool (Unborated Water) ^(a)	ISFSI Vault (Open to Environment)
<p><u>Alloy X (Type 304, 304LN, 316, or 316LN Stainless Steel):</u></p> <p>MPC fuel basket and fuel basket spacers</p> <p>MPC baseplate</p> <p>MPC shell</p> <p>MPC lid</p> <p>MPC fuel spacers</p>	<p>Stainless steels have been extensively used in spent fuel storage pools with both borated and unborated water with no significant adverse reactions or interactions with spent fuel. Galvanic reactions between stainless steel and aluminum in the neutron absorber is insignificant because the aluminum oxide on the neutron absorber panel surface acts as a insulator inhibiting current flow.</p>	<p>The MPC internal and external environment will be an inert (helium) atmosphere.</p>
<p><u>METAMIC®</u></p> <p>Neutron absorber in MPC fuel basket</p>	<p>The METAMIC® will passivate in air and water during fabrication and loading operations to minimize the amount of hydrogen released from the aluminum-water reaction to an insignificant concentration during MPC lid welding or cutting operations. See Chapter 5 for additional requirements for combustible gas monitoring and actions for control of combustible gas accumulation under the MPC lid.</p>	<p>The MPC internal environment will be an inert (helium) atmosphere.</p>
<p><u>BORAL®</u></p> <p>Neutron absorber in MPC fuel basket</p>	<p>The BORAL® will passivate in air and water during fabrication and loading operations to minimize the amount of hydrogen released from the aluminum-water reaction to an insignificant concentration during MPC lid welding or cutting operations. See Chapter 5 for additional requirements for combustible gas monitoring and actions for control of combustible gas accumulation under the MPC lid.</p>	<p>The MPC internal environment will be an inert (helium) atmosphere.</p>



# HUMBOLDT BAY ISFSI FSAR UPDATE

TABLE 4.6-1

Sheet 2 of 4

Material/Component	Fuel Pool (Unborated Water) ^(a)	ISFSI Vault (Open to Environment)
<p><u>Carbon Steels:</u></p> <p>Overpack closure plate, top flange, inner shell, bottom plate, intermediate shells, and neutron shield enclosure</p> <p>SA350-LF3</p> <p>SA515 Grade 70</p> <p>SA516 Grade 70</p> <p>SA193 Grade B7</p>	<p>All exposed steel surfaces (except seal areas, lifting trunnions and threaded holes) are coated with material specifically selected for performance in the operating environments. Lid bolts are plated and the threaded portion of the bolt holes are plugged or otherwise covered to seal the threaded area from exposure to water.</p>	<p>Exposed surfaces of the overpack will be coated and protected from the environment by the storage vault.</p>
<p>Stainless Steels (Misc.):</p> <p>SA240 304</p> <p>MPC Basket and Fuel Spacer</p> <p>SA193 Grade B8</p> <p>Vent, drain, and test port plugs</p> <p>Alloy X750</p> <p>Port plug seals</p>	<p>Stainless steels have been extensively used in spent fuel storage pools with borated and unborated water with no adverse reactions.</p>	<p>Stainless steel has a long proven history of corrosion resistance when exposed to the atmosphere. These materials are used for washers.</p>

HUMBOLDT BAY ISFSI FSAR UPDATE

TABLE 4.6-1

Sheet 3 of 4

Material/Component	Fuel Pool (Unborated Water) ^(a)	ISFSI Vault (Open to Environment)
<u>Nickel Alloy:</u> SB637-NO7718 Overpack lifting trunnions	No adverse reactions with unborated water.	Long-term exposure to saline air environment. Non-ferrous steel not susceptible to corrosion
<u>Brass/Bronze:</u> Neutron shield enclosure pressure relief device	Small surface of pressure relief device will be exposed. No significant adverse impact identified.	Long-term exposure to saline air environment. Normal inspection and replacement assures operability of valves.
<u>Holtite-A:</u> Solid neutron shield in overpack	The neutron shield is fully encapsulated in the neutron shield enclosure. The neutron shield material is not wetted by the SFP water. No adverse reactions.	The neutron shield is fully encapsulated in the neutron shield enclosure. Therefore, Holtite-A is not exposed to the environment. No adverse reactions.
<u>Coatings:</u> Carboline 890 Thermaline 450 Exterior overpack carbon steel surface coatings	Carboline 890 used for overpack surfaces other than the inner shell for good decontamination properties and acceptable temperature resistance for the application. Acceptable performance for short-term exposure in unborated SFP water.  Thermaline 450 selected for overpack inner shell surfaces for excellent high temperature resistance properties. Will be exposed to clean, unborated water during in-pool operations as annulus is filled with clean water prior to placement in the spent fuel pool, and the inflatable seal prevents contaminated fuel pool water in-leakage.  Manufacturer's data confirms that these coatings will perform adequately in these environments.	Coating products are used in a variety of corrosive external environments, including chemical industry. Good for resistance to oceanside saline environment.  Thermaline 450 for overpack inner surfaces exposed to helium environment and suitable for high temperature resistance.  Carboline 890 used on exposed overpack outer surfaces (except lifting trunnions) and is suitable for saline air environment.

HUMBOLDT BAY ISFSI FSAR UPDATE

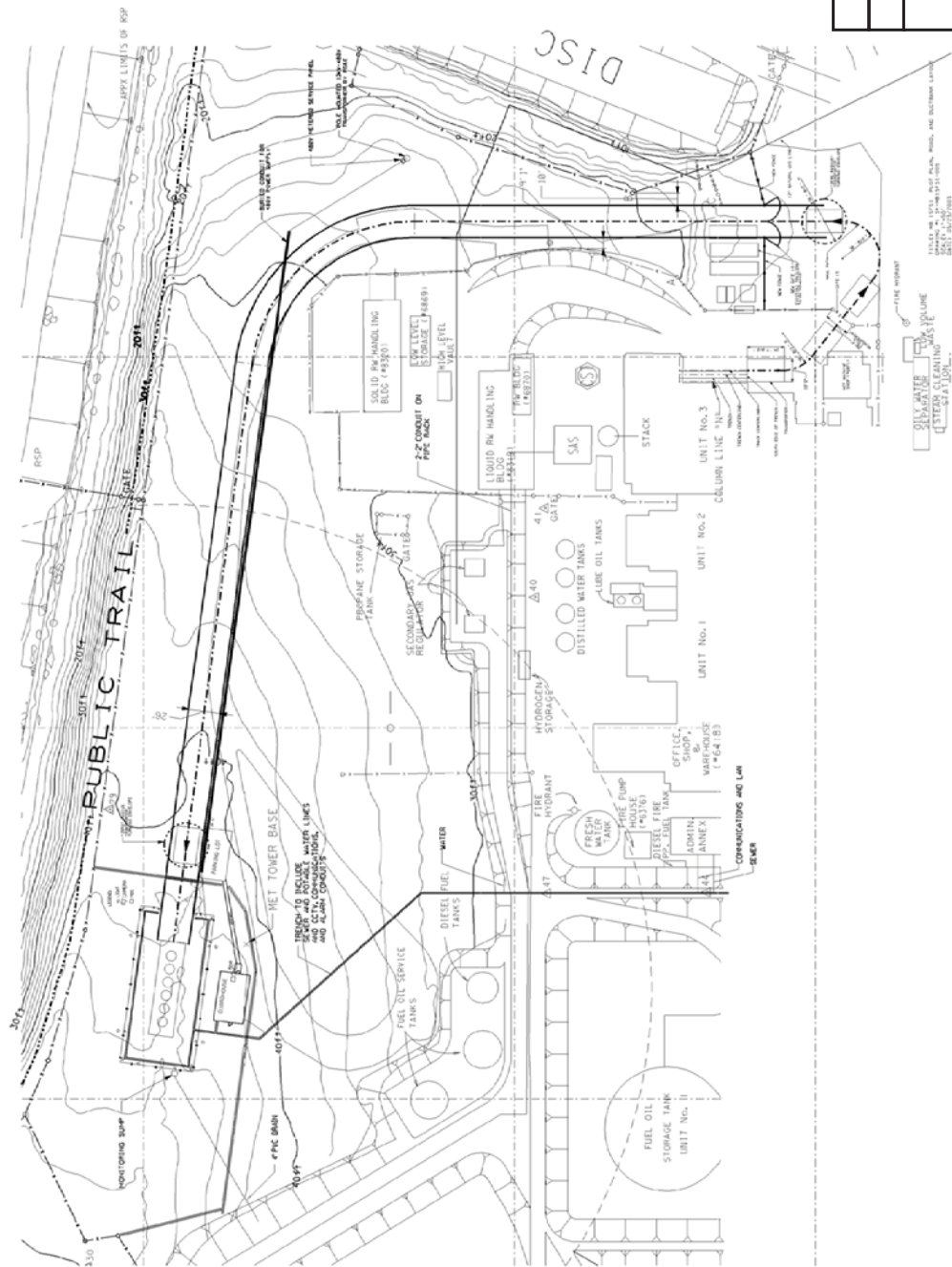
TABLE 4.6-1

Sheet 4 of 4

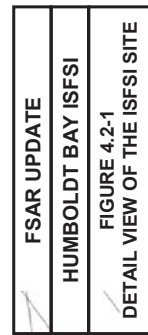
Material/Component	Fuel Pool (Unborated Water) ^(a)	ISFSI Vault (Open to Environment)
		Manufacturer's data confirms that these coatings will perform adequately in these environments.
<u>Mechanical Seals:</u> Transfer cask pool	Gasket is compressed between pool lid and transfer cask bottom flange to prevent spent fuel pool water inleakage. Gasket will be inspected periodically and replaced as necessary.	Leakage prevention function not required after the transfer cask is removed from the spent fuel pool and the annulus is drained.

---

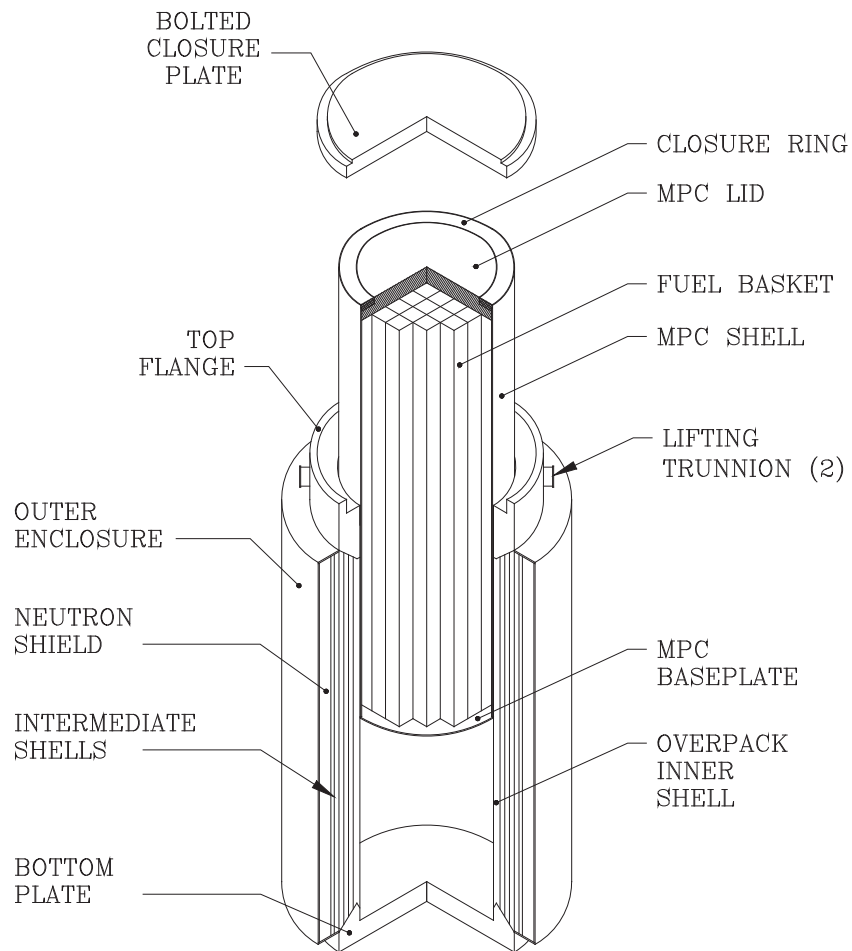
^(a) HI-STAR HB System short-term operating environment during loading and unloading.



Revision 0 January 2006



Revision 0 January 2006



**FSAR UPDATE**

**HUMBOLDT BAY ISFSI**

**FIGURE 4.2-2  
HI-STAR HB OVERPACK WITH  
MPC PARTIALLY INSERTED**

Revision 0 January 2006



# LICENSING DRAWING PACKAGE COVER SHEET

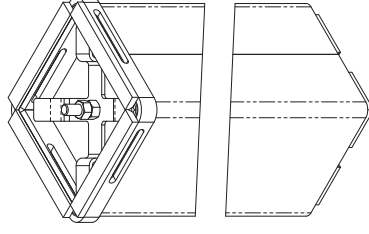
## REVISION LOG

[illegible]

+ THE VALIDATION IDENTIFICATION RECORD (VIR) NUMBER IS A COMPUTER GENERATED RANDOM NUMBER WHICH CONFIRMS THAT ALL APPROPRIATE REVIEWS OF THIS DRAWING ARE DOCUMENTED IN COMPANY'S NETWORK.

## GENERAL NOTES:

1. THE EQUIPMENT DESIGN DOCUMENTED IN THIS DRAWING PACKAGE HAS BEEN CONFIRMED BY HOLTEC INTERNATIONAL TO COMPLY WITH ALL APPLICABLE CODES AND STANDARDS.
2. THE REVISION LEVEL OF EACH INDIVIDUAL SHEET IN THIS PACKAGE IS THE SAME AS THE REVISION LEVEL OF THIS COVER SHEET. A REVISION TO ANY SHEET(S) IN THIS PACKAGE REQUIRES THE REVISION NUMBERS OF ALL SHEETS TO THE NEXT REVISION NUMBER.
3. THE ITS CATEGORY OF A SUB-COMPONENT IS THE HIGHEST SUB-COMPONENT CATEGORY OF ANY SUB-COMPONENT. SUB-COMPONENT CLASSIFICATIONS ARE PROVIDED IN THE SAFETY ANALYSIS REPORT.
4. THE ASME BOILER AND PRESSURE VESSEL CODE (ASME CODE), 1905 EDITION WITH ADDENDA THROUGH 1997, IS THE GOVERNING CODE FOR THE HI-STAR 100 SYSTEM, WITH CERTAIN APPROVED ALTERNATIVES AS LISTED IN APPENDIX 3. THE DESIGN OF THE SUB-COMPONENTS CONSTRUCTED IN THE HI-STAR 100 SYSTEM SHALL BE IN ACCORDANCE WITH THE CODES AND STANDARDS LISTED IN APPENDIX 3. SUB-COMPONENTS NOT DESCRIBED IN THE SAR NEW OR REQUIRING AN ASME CODE ALTERNATIVE REQUIRE PRIOR NRC APPROVAL BEFORE IMPLEMENTATION.
5. WELDING PROCEDURES AND WELDER QUALIFICATIONS SHALL BE PER ASME SECTION IX AND ASME SECTION III, SUBSECTION NG.
6. MATERIAL USED IN ASME SECTION III SHALL MEET THE REQUIREMENTS OF ASME SECTION II, PART 2. WELD MATERIAL SHALL MEET THE REQUIREMENTS OF ASME SECTION II, PART 2.
7. ALL WELDS REQUIRE VISUAL EXAMINATION (VT).
8. ALL WELD SIZED ARE MINIMUMS. LARGER WELDS ARE PERMITTED. LOCAL AREAS OF OVERSIZED WELDS ARE ACCEPTABLE WITHIN THE LIMITS OF THE ASME CODE.



THIS COVER SHEET MUST BE MAINTAINED WITH THE LATEST REVISIONS OF THE DRAWINGS IDENTIFIED HEREIN

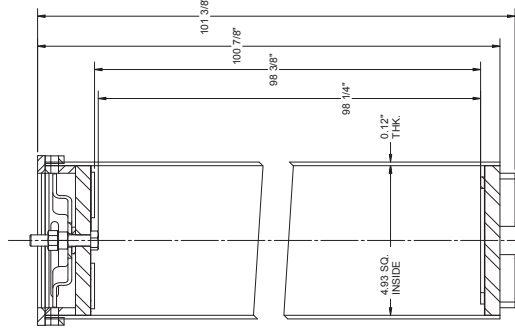
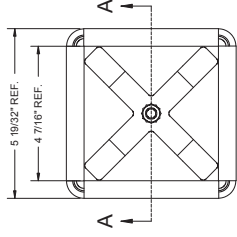
 <b>HOLTEC</b> INTERNATIONAL HOLTEC CENTER 500 LINCOLN DRIVE, WEST PALM BEACH, FL 33411		SAFETY ANALYSIS REPORT HUMBOLDT BAY/ISFSI FIGURE 4.2-3 SHEET 1 OF 2 DAMAGED FUEL CONTAINER Revision 0 January 2006	
CLASS	CLASSIFICATION	DATE	REVISION
13-00007	13-00007	4/11/03	1
PROJECT NO.	PROJECT NO.	DATE	REVISION
1125	3500120394	4/11/03	2
PROJECT NO. 3500120394 PROJECT NO. 3500120394		DATE 4/11/03 REVISION 2	

[illegible]

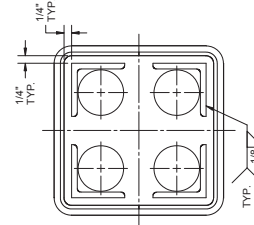
LICENSE DRAWING PACKAGE CONTENTS:

NOTES:

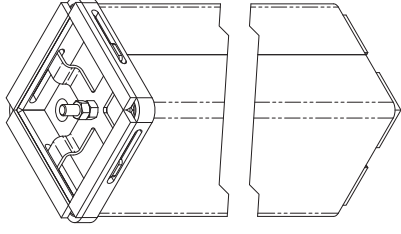
1. ALL DIMENSIONS ARE IN INCHES AND ARE NOMINAL.
2. ALL MATERIALS TYPE 304 STAINLESS STEEL EXCEPT BOLTS (ANY TYPE SS), HEX NUTS (SA 194 OR 6), AND WASHERS (ANY TYPE SS).



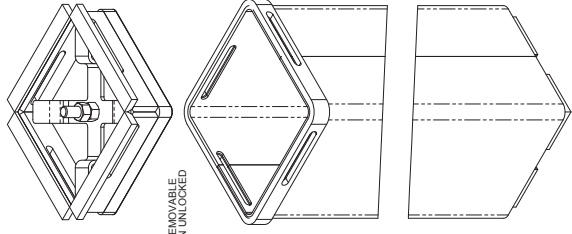
SECTION AA



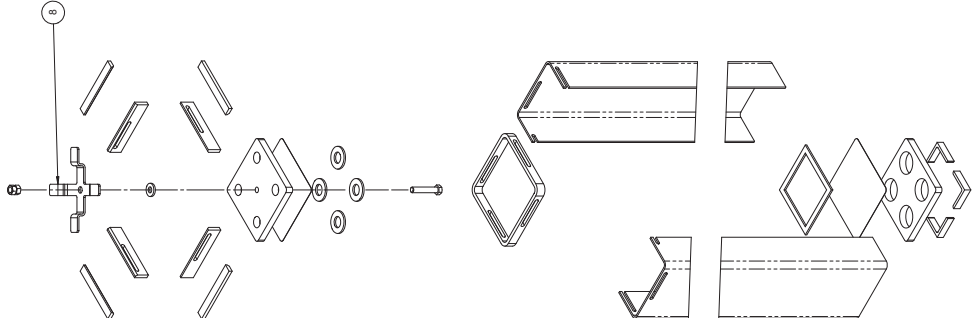
BOTTOM VIEW



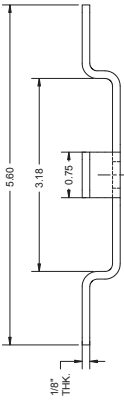
LOCKED VIEW



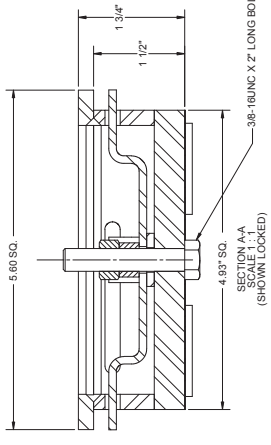
UNLOCKED VIEW



WELDMENT



ITEM 8



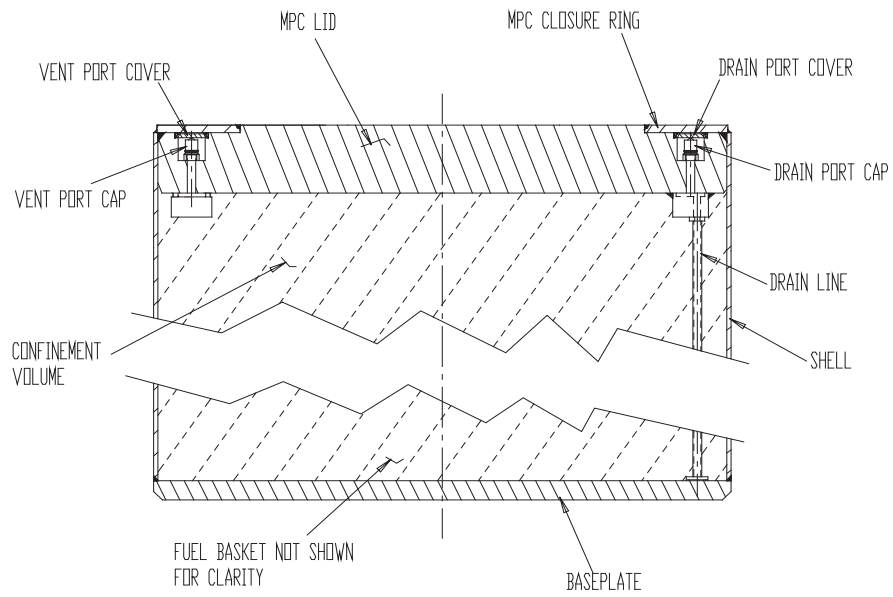
SECTION AA  
SCALE: 1:1  
(SHOWN LOCKED)

**HOLTEC**  
INTERNATIONAL  
HOLTEC CENTER WEST  
MARTIN, NJ 08053

**SAFETY ANALYSIS REPORT**  
**HUMBOLDT BAY/FSI**  
**FIGURE 4.2-3**  
**SHEET 2 OF 2**  
**DAMAGED FUEL CONTAINER**

Revision 0 January 2006

PROJECT NO.	1125	3500120394	DATE	1/2	FIGURE	2	0
REV.			SCALE	1:2	FIGURE	2	0
DATE	1/2	3500120394	FIGURE	2	0	0	0

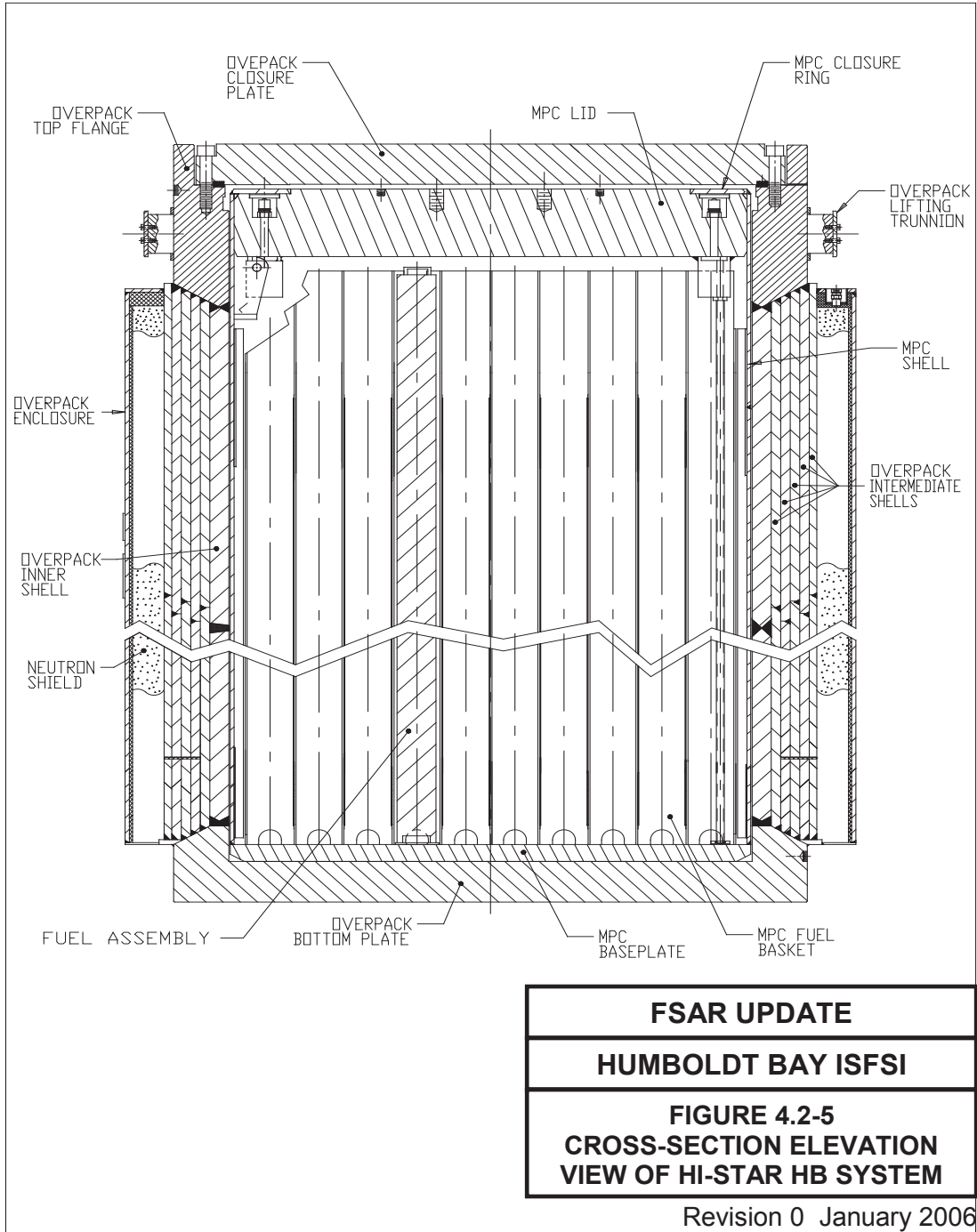


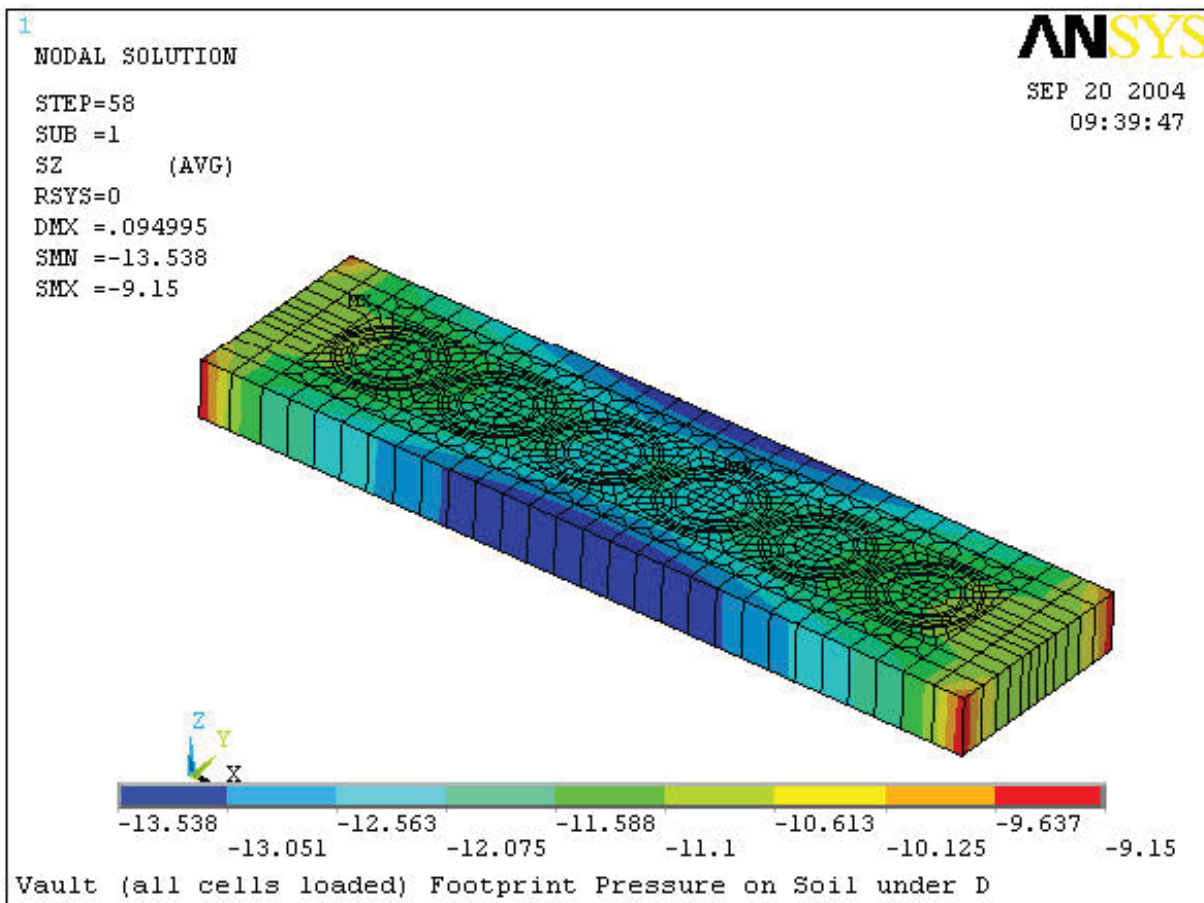
**FSAR UPDATE**

**HUMBOLDT BAY ISFSI**

**FIGURE 4.2-4  
MPC-HB CONFINEMENT  
BOUNDARY**

Revision 0 January 2006



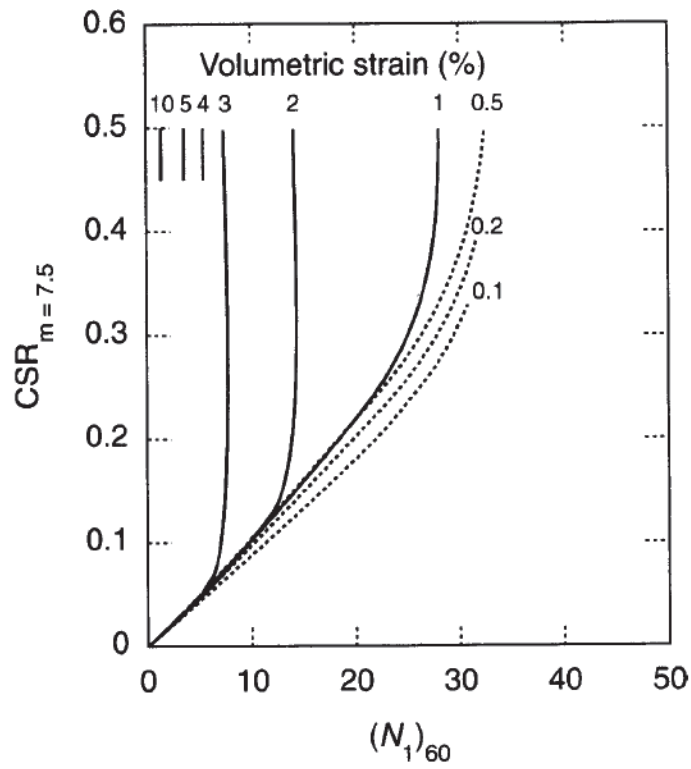


FSAR UPDATE

HUMBOLDT BAY ISFSI

FIGURE 4.2-6  
SOIL PRESSURE UNDER DEAD  
LOAD OF VAULT WITH CASKS

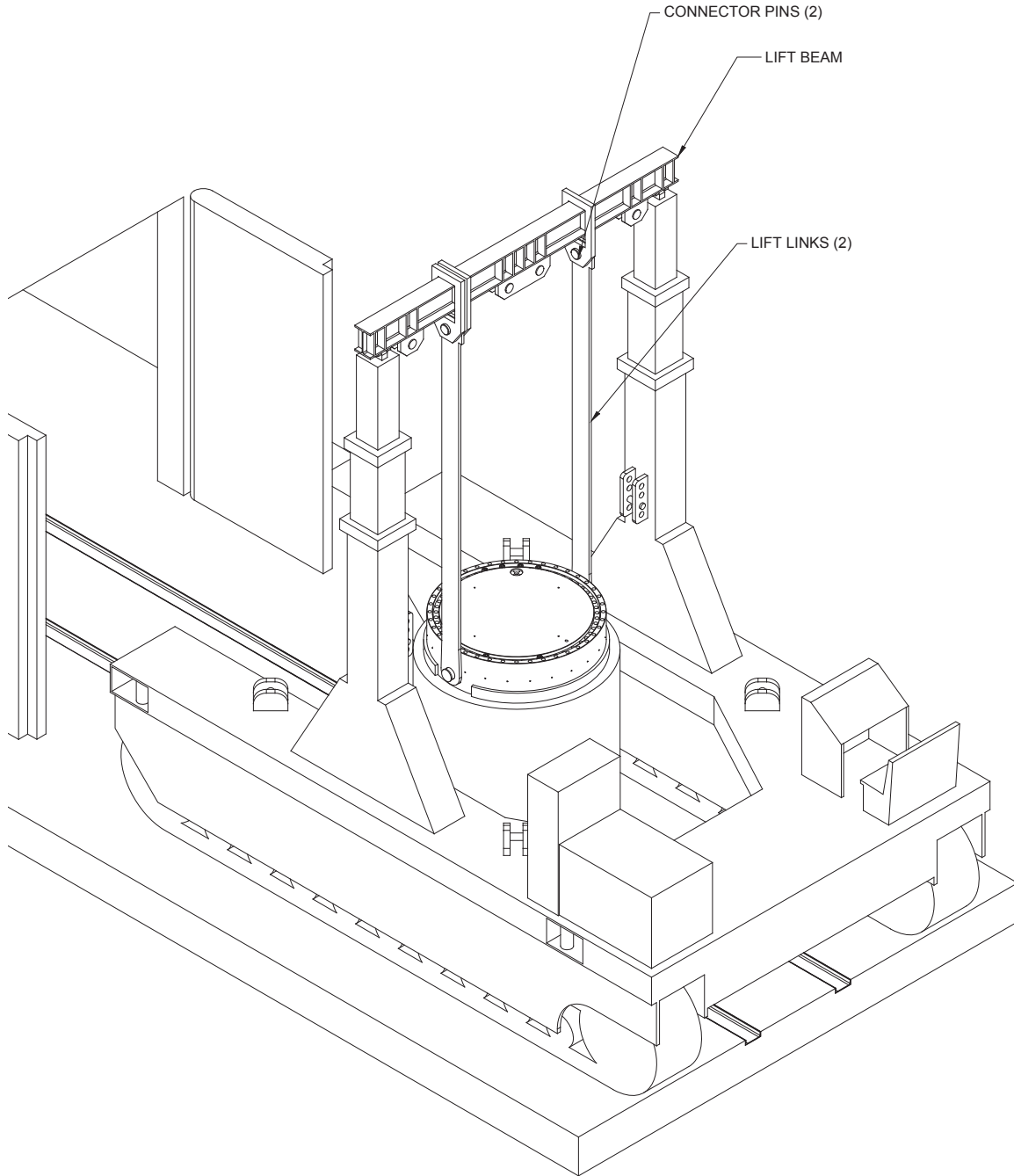
Revision 0 January 2006



FSAR UPDATE
HUMBOLDT BAY ISFSI
FIGURE 4.2-7 ESTIMATE OF VOLUMETRIC STRAIN IN SATURATED SANDS

Revision 0 January 2006



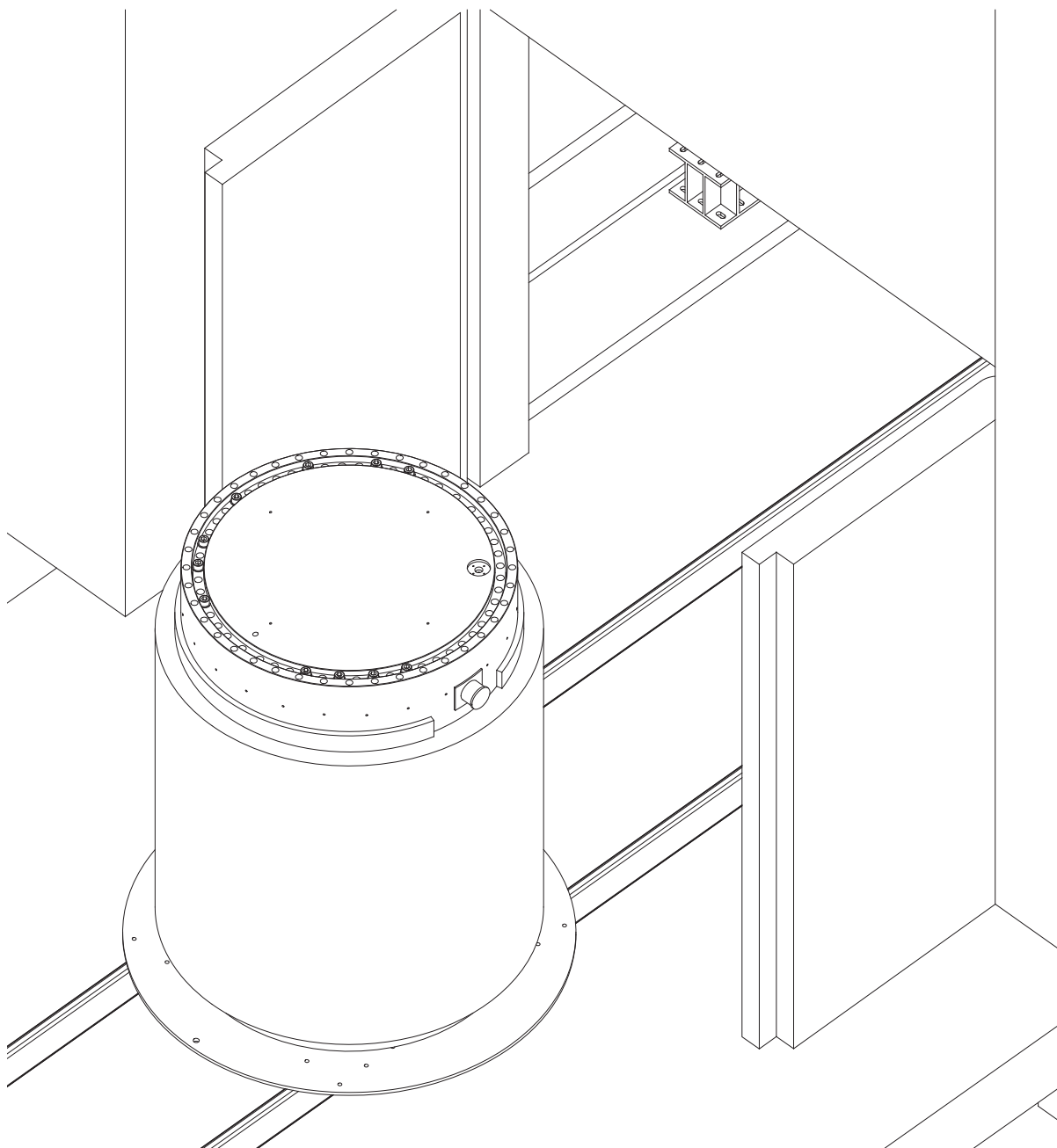


**FSAR UPDATE**

**HUMBOLDT BAY ISFSI**

**FIGURE 4.3-1  
VERTICAL CASK TRANSPORTER  
CARRYING HI-STAR OUTSIDE THE  
HUMBOLDT BAY FUEL BUILDING**

Revision 0 January 2006

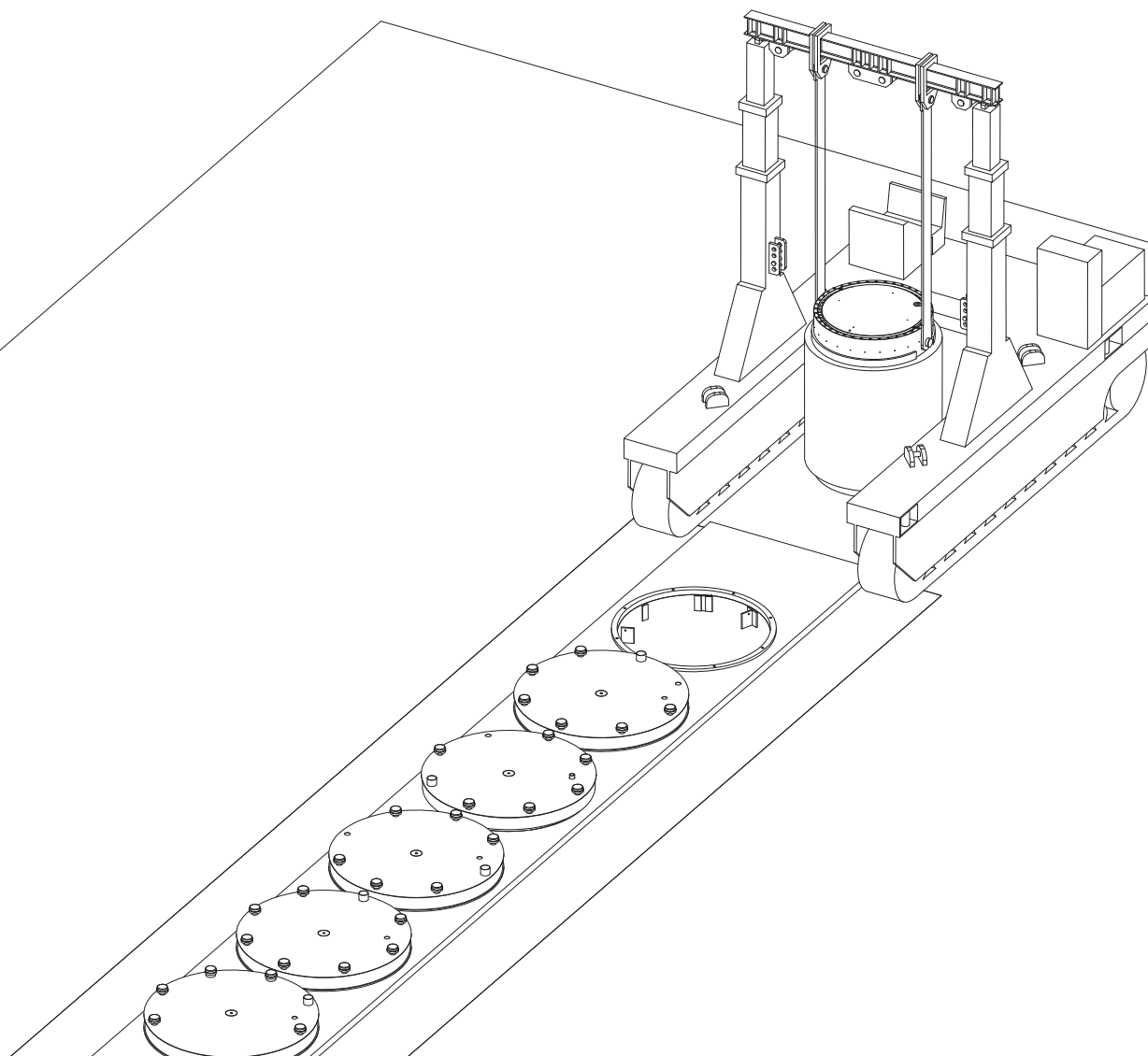


**FSAR UPDATE**

**HUMBOLDT BAY ISFSI**

**FIGURE 4.3-2  
HI-STAR ON RAIL DOLLY OUTSIDE  
THE REFUELING BUILDING**

Revision 0 January 2006



**FSAR UPDATE**

**HUMBOLDT BAY ISFSI**

**FIGURE 4.3-3  
VERTICAL CASK  
TRANSPORTER CARRYING  
HI-STAR AT THE ISFSI VAULT**

Revision 0 January 2006

# HUMBOLDT BAY ISFSI FSAR UPDATE

## CHAPTER 5

### **ISFSI OPERATIONS**

#### CONTENTS

<u>Section</u>	<u>Title</u>	<u>Page</u>
5.1	OPERATION DESCRIPTION	5.1-1
5.1.1	Narrative Description	5.1-2
5.1.2	Identification of Subjects for Safety and Reliability Analysis	5.1-10
5.1.3	References	5.1-11
5.2	CONTROL ROOM AND CONTROL AREAS	5.2-1
5.3	SPENT FUEL ACCOUNTABILITY PROGRAM	5.3-1
5.4	SPENT FUEL TRANSPORT	5.4-1

# HUMBOLDT BAY ISFSI FSAR UPDATE

## CHAPTER 5

### **ISFSI OPERATIONS**

#### TABLES

<u>Table</u>	<u>Title</u>
5.1-1	Measuring and Test Equipment

# HUMBOLDT BAY ISFSI FSAR UPDATE

## CHAPTER 5

### **ISFSI OPERATIONS**

#### FIGURES

<u>Figure</u>	<u>Title</u>
5.1-1	Deleted in Revision 1.
5.1-2	Deleted in Revision 1.



## CHAPTER 5

### ISFSI OPERATIONS

This chapter describes the operations associated with the Humboldt Bay Independent Spent Fuel Storage Installation (ISFSI). Fuel movement and cask handling operations in the Humboldt Bay Power Plant (HBPP) Refueling Building (RFB) are performed in accordance with the HBPP 10 CFR 50 license. On-site cask handling outside the RFB and storage activities associated with the ISFSI are performed in accordance with the 10 CFR 72 Humboldt Bay ISFSI license. As indicated in previous chapters, the Humboldt Bay ISFSI, in its final storage configuration, is a totally passive installation. Periodic surveillance is required only to check the material condition of the casks and vault interior. No degradation of the cask or vault interior is expected.

The operations described in this chapter relate to the loading and preparation of the multi-purpose canisters (MPCs) and the overpacks and transport of the loaded overpacks from the RFB to the ISFSI storage vault. Also described is the process for off-normal event recovery, including unloading of fuel from a loaded overpack. An overview of activities occurring in the HBPP RFB is provided. Specific licensing of the components and activities is provided in the 10 CFR 50 license amendment request (LAR) associated with dry spent fuel storage.

#### 5.1 OPERATION DESCRIPTION

The methods and sequences described below provide an overview of the operational controls that the personnel performing spent fuel loading, MPC and overpack preparation for storage, cask transfer, onsite handling, and storage activities implement to ensure safe, reliable, long-term spent fuel storage at the ISFSI storage site. Site-specific procedures are used to implement these activities, including the use of existing procedures, revision of existing procedures, and the creation of new procedures, as necessary. The specific number, wording, and sequence of site procedural steps may vary from the guidance provided here as long as the steps comply with assumptions and inputs in the governing, design-basis analyses.

Operations to load and place the HI-STAR HB System at the storage location in the ISFSI vault are performed both inside and outside the HBPP RFB. MPC fuel loading and handling operations are performed inside the RFB using existing HBPP systems and equipment for radiation monitoring, decontamination, and auxiliary support, augmented as necessary by ancillary equipment specifically designed for MPC fuel loading and handling functions. This includes the use of the davit crane and cask transfer rail dolly for heavy lifts and other cask movements. The implementing procedures incorporate applicable 10 CFR 50 license conditions and commitments, such as those governing heavy loads and fuel movements in the spent fuel pool (SFP). MPC installation in the overpack and movement of the loaded overpack to the storage location are performed using procedures developed specifically for these operations.

### 5.1.1 NARRATIVE DESCRIPTION

The following discussion describes the specifics of the integrated operation, including fuel loading, MPC closure operations, overpack closure operations, HI-STAR HB System handling, and placement of the loaded overpack in the ISFSI vault. To the extent practicable, the same operations as used in deploying the generic HI-STAR 100 System are used with the HI-STAR HB System. Certain operating procedures have been customized for site-specific licensing at HBPP and the Humboldt Bay ISFSI.

The MPC is loaded, while in the HI-STAR HB overpack, in the SFP. The MPC is welded and prepared for storage while in the RFB. The MPC is sealed inside the overpack in the RFB and is then transported to the ISFSI vault for storage.

Section 5.1.1.1 describes loading operations for damaged fuel. Section 5.1.1.2 describes cask fuel loading and sealing operations. Section 5.1.1.3 describes the operations for transferring the loaded HI-STAR HB System to the ISFSI storage site for storage. Section 5.1.1.4 describes off-normal event recovery operations. Section 5.1.1.5 describes greater-than-class C (GTCC) cask loading and sealing operations, and section 5.1.1.6 describes HI-STAR HB GTCC Overpack transfer to the ISFSI storage site.

Specific procedures identify and control the selection of fuel assemblies and greater than Class C waste (GTCC) for loading into the HI-STAR HB System or GTCC qualified casks, as appropriate. Fuel and GTCC will not be loaded in the same MPC. All HBPP fuel is acceptable for storage in the HI-STAR HB System based on a comparison of the fuel assemblies' physical characteristics against the limits specified in Section 10.2. The selected fuel assemblies are classified as intact fuel or damaged fuel in accordance with the definitions in Section 10.2, and the classification criteria described in Section 3.1.

Fuel assemblies chosen for loading are assigned a specific storage location in the MPC in accordance with the Humboldt Bay ISFSI TS and Section 10.2. The classification of the assembly (that is, intact or damaged) is used to determine the acceptable fuel storage locations for each assembly. Records are kept that track the fuel assembly, its assigned MPC, and its specific fuel storage location. Videotape (or other visual record) is used during fuel loading operations in the SFP to record fuel assembly serial numbers and to provide an independent record of the MPC inventory.

The loading, unloading, and handling operations described in this section were developed based on the Holtec International field experience in loading HI-STORM 100 and HI-STAR 100 dry cask storage systems at other ISFSIs. The equipment and operations used at these sites were evaluated and modified, as necessary, based on this experience to reduce occupational exposures and further enhance the human factors involved in performing the activities needed to successfully deploy the HI-STAR HB System at the Humboldt Bay ISFSI.

#### **5.1.1.1 Damaged Fuel Loading**

Damaged fuel containers (DFCs) are used to store damaged fuel assemblies in the MPC-HB in accordance with the requirements of the Humboldt Bay ISFSI TS and Section 10.2. Any qualified fuel assembly that is classified as damaged fuel must be stored in a DFC and be loaded into specific fuel storage locations in an MPC-HB. Two patterns for loading DFCs containing damaged fuel are permitted (see Section 10.2):

- Up to 28 DFCs around the basket periphery, or
- Up to 40 DFCs in a checkerboard pattern throughout the basket.

In both cases, the balance of fuel stored in an MPC must be intact fuel assemblies, optionally stored in DFCs themselves. Storage of damaged fuel in the HI-STAR HB System is discussed in Section 4.2.3.2.2 and the structural analysis of the containers is described in Section 4.3.2.2.10. Figure 4.2-3 shows the pertinent design details of the Humboldt Bay DFC.

#### **5.1.1.2 Fuel Cask Loading and Sealing Operations**

This section describes the general sequence of operations to load and seal the fuel cask, including the movement of the HI-STAR HB overpack within the RFB. Site-specific procedures control the performance of the operations, including inspection and testing. At a minimum, these procedures control the performance of activities and alert operators to changes in radiological conditions around the cask. These sequences are controlled by Humboldt Bay ISFSI TS and Section 10.2.

Several components (e.g., the davit crane and cask transfer rail dolly) are used during the cask loading process. A discussion of these items is provided for the sole purpose of describing the loading process. These items, along with their design and use, are described in the HBPP 10 CFR 50 LAR to support ISFSI operations in the RFB.

Placement of loaded HI-STAR HB overpacks in the ISFSI vault is a cyclical process involving the movement of a loaded overpack to the ISFSI and returning the empty cask transporter to the RFB for the next loading process. The operations described herein start at the time the empty MPC is loaded into the overpack and is ready for movement into the RFB.

Prior to bringing the HI-STAR HB overpack into the RFB, the overpack is visually verified to be free of foreign materials and the top lid sealing surface is visually inspected for potential damage. Also, an empty MPC has been cleaned, inspected, and inserted into the overpack. Alignment marks are checked to ensure correct rotational alignment between the MPC and the HI-STAR HB overpack.

## HUMBOLDT BAY ISFSI FSAR UPDATE

The HI-STAR HB overpack containing an empty MPC is brought into the RFB in the vertical orientation through the railroad door on the cask transfer rail dolly that runs from inside the RFB to the Unit 3 yard. The cask transfer rail dolly is used because dimensional limitations of the RFB door prevent access of the cask transporter inside the RFB. After bringing the overpack into the RFB, the overpack is positioned under the davit crane that is configured with the lift yoke and the overpack annulus overpressure system is connected.

The overpack-to-MPC annulus is filled with clean water and the inflatable annulus seal is installed in the top part of the annulus to minimize the risk of contaminating the external shell of the MPC. The MPC internal cavity is filled with SFP water or water from another suitable source to prevent splash-back when the cask is lowered into the SFP. The lift yoke engages the overpack lifting trunnions and is used to raise and lower the overpack during loading operations inside the RFB.

The HI-STAR HB overpack is raised by the davit crane, positioned over the cask loading area of the SFP, and lowered using the davit crane hoist until the top the overpack is nearly level with the water level in the annulus overpressure system. The annulus overpressure system supply line to the overpack is opened and the overpack is lowered to the bottom of the SFP. The annulus overpressure system applies a slight overpressure to the annulus to protect the MPC external shell from contamination from the SFP water in the event there is a leak in the annulus seal. When the cask is fully lowered to the bottom of the cask loading area in the SFP, the lift yoke is remotely disconnected from the overpack and moved out of the way to allow fuel loading into the cask.

Fuel-loading and post-loading verification of correct fuel assembly placement in the MPC (i.e., assembly identification and storage cell location) is conducted in accordance with approved fuel-handling procedures. For damaged fuel assemblies, the assembly is loaded into the DFC, and the DFC is loaded into the MPC. Optionally, an empty DFC may be first loaded into the appropriate fuel storage location in the MPC and then the damaged fuel assembly may be loaded into the DFC. Intact fuel assemblies may be stored in DFCs at Pacific Gas and Electric's (PG&E) discretion.

The MPC lid, with the drain line attached, is placed in position in the MPC after the completion of fuel loading and verification, while the HI-STAR HB overpack is in the SFP. The lift devices are detached from the MPC lid allowing the lift yoke, which is attached to the davit crane, to be lowered to the overpack to engage the lifting trunnions. The overpack and lift yoke are raised until the top of the MPC and overpack break the water surface. The annulus overpressure supply line is closed and the overpressure system is disconnected. Initial decontamination of the overpack may be performed as the overpack emerges from the SFP or in any other manner approved by the Radiation Protection (RP) Department. The overpack is raised completely out of the SFP. The overpack is placed onto the cask transfer rail dolly in the cask washdown

area. The lid retention device is attached. The lift yoke is disconnected and removed from the area.

The MPC water volume is reduced to provide enough space between the water surface and the lid to avoid a water-weld interaction. The inflatable annulus seal is removed and the annulus water level is lowered. Once the top edge of MPC shell is surveyed and found to be in satisfactory condition, the annulus shield is installed. The lid retention device remains in place until a sufficient number of tack welds are applied, and is then removed to allow room for the automatic weld system to be installed.

The space under the MPC lid is exhausted or purged during welding operations to prevent combustible gas concentrations that may result from the oxidation of the neutron absorber panels in the water. Appropriate monitoring for combustible gas concentrations is performed prior to and during MPC lid welding operations. The MPC lid-to-shell weld, including liquid penetrant inspections after the root pass, each approximately 3/8-inch of weld depth, and after the final pass, is then completed.

Once the lid-to-shell weld is complete, the MPC undergoes a pressure test for leaks in accordance with the ASME Code. The lid-to-shell weld is liquid penetrant inspected after the pressure test. Either prior to, or following successful completion of the pressure test (depending on whether a hydrotest or pneumatic test is performed), the RVOAs are installed and the remaining MPC water is displaced from the MPC by pumping or blowing pressurized nitrogen or helium gas into the MPC. The water may be drained from the overpack annulus and vacuum drying or the Forced Helium Dehydration (FHD) System is used to remove the remaining liquid water from the MPC and to ultimately reduce the moisture content of the MPC cavity to an acceptable level.

Following the successful completion of moisture removal from the MPC, the MPC is backfilled with helium to within the required pressure range. Helium backfill to the required pressure range ensures that the conditions for heat transfer inside the MPC are consistent with the thermal analyses and provides an inert atmosphere to ensure long-term fuel integrity. After successful helium backfill operations, the RVOAs are removed and the MPC vent and drain port cover plates are installed, welded, and examined. The MPC closure ring is then installed, welded, and examined.

The HI-STAR HB overpack and accessible portions of the MPC are checked to ensure any removable contamination is within applicable limits. Additional decontamination and surveys may be performed throughout the loading process. The closure plate is installed on the HI-STAR HB with the redundant mechanical seals, and the bolts are tightened to seat the seals. The overpack annulus is drained, if not previously completed, and dried using the vacuum drying system and the annulus is backfilled with helium in accordance with the Humboldt Bay ISFSI TS and Section 10.2.

The integrity of the closure plate mechanical seals is verified by performing a helium leakage test between the seals using the overpack test port. Upon successful completion of the seal leakage test, a test port plug and cover plate are installed. The



overpack vent and drain ports are then sealed with port plugs and the port plugs are helium leakage tested. Upon successful testing of the port plugs, the vent and drain port covers are installed and the cask is ready for transport to the ISFSI storage vault. The loaded overpack is moved out of the RFB along the rail dolly using a winch system or similar device and positioned under the lift beam of the cask transporter with the lift links attached.

### 5.1.1.3 Fuel Cask Transfer to the ISFSI Storage Site

The cask transporter is positioned outside the RFB doors to receive the HI-STAR HB overpack from the cask transport rail dolly. The transporter will have undergone preoperational testing and maintenance and is operated in accordance with the Cask Transportation Evaluation Program, which evaluates and controls the transportation of loaded overpacks between the HBPP RFB and ISFSI vault. The cask transporter lift links engage the HI-STAR HB lifting trunnions and the overpack is lifted off of the rail dolly. A restraining strap is used to secure the overpack to the transporter. The overpack is transported to the ISFSI vault along the approved transportation route using appropriate administrative controls as described in Section 4.3.3 and shown in Figure 2.2-2.

The cask transporter centers the HI-STAR HB overpack over the open vault storage cell. The restraining strap is released from the overpack. The cask transporter towers are used to lower the overpack down into the vault and the lift links are removed. The cask transporter is driven away from the ISFSI vault, the seismic shims are installed, and the storage cell lid is installed.

### 5.1.1.4 Off-Normal Event Recovery Operations

The evaluations of off-normal and accident events, as defined in ANSI/ANS-57.9 (Reference 1) and as applicable to the Humboldt Bay ISFSI, are presented in Chapter 8. Each postulated off-normal and accident event evaluated and discussed in Chapter 8 addresses the event cause, analysis, and consequences. Suggested corrective actions are also provided for off-normal events. The actual cause, consequences, corrective actions, and actions to prevent recurrence (if required) will be determined through the HBPP corrective action program on a case-specific basis. All corrective actions will be taken in a timely manner, commensurate with the safety significance of the event. Of primary importance in the early response to any event will be the verification of continued criticality prevention, the protection of fuel cladding integrity (that is, heat removal), and the adequacy of radiation shielding while longer-term corrective actions are developed. This may also involve the need for temporary shielding or cask cooling in accordance with the recommendations of PG&E technical staff personnel, based on the event conditions.

Should the need arise during the loading campaign, the MPG can be returned to the SFP for unloading. To unload a HI-STAR HB overpack, the operations described above are effectively executed in reverse order from the point in the operation at which the



event occurred. Once the overpack is back in the RFB, the overpack closure plate is removed, and preparations are made to re-open the MPC in the SFP. This involves first installing the annulus shield and cutting or grinding out the welds to remove the MPC closure ring and vent and drain port cover plates.

Then, the bulk temperature of the gas in the MPC cavity is ensured to be below the maximum value to allow re-flooding. Given the age of the fuel at the time of loading, it is unlikely that the cavity gas will require cooling prior to re-flooding. Nevertheless, the bulk gas temperature will be determined and cooled using appropriate means, if necessary. Appropriate means could include recirculating water in the overpack annulus and/or helium recirculation with the FHD system to cool the MPC to a temperature at or below the maximum allowed temperature for re-flooding in accordance with the Humboldt Bay ISFSI TS and Section 10.2.

Ensuring the MPC cavity bulk gas temperature to be below the maximum allowed temperature allows the MPC to be re-flooded with water with a minimal amount of flashing and the associated undesirable pressure spikes in the MPC cavity. The weld removal system is used to cut the MPC lid weld. Once the lid weld is removed, the lid retention device is installed.

After re-flooding, appropriate monitoring for combustible gas concentrations shall be performed prior to, and during, MPC lid cutting operations to prevent the build-up of combustible mixtures caused by oxidation of neutron absorber panels contained in the MPC. In addition, the space below the MPC lid shall be exhausted prior to, and during, MPC lid welding operations to provide additional assurance that explosive gas mixtures will not develop in this space.

When the lid weld has been successfully cut, the annulus shield is removed. The annulus is filled with clean water and the annulus overpressure system and annulus seal are installed. The lift yoke is installed on the davit crane and attached to the overpack. The davit crane moves the overpack and MPC over the cask loading area of the SFP and lowers it to the SFP floor. As the top of the HI-STAR HB reaches a level approximately equal to the SFP level, the supply line from the annulus overpressure system is connected and opened. Once in the SFP, the lid retention device and the MPC lid are removed and the spent fuel assemblies are removed from the MPC and placed back into the wet storage racks as necessary.

### 5.1.1.5 GTCC Cask Loading and Sealing Operations

This section describes the general sequence of operations to load and seal the GTCC cask, including the movement of the HI-STAR HB GTCC Overpack within the RFB. Site-specific procedures control the performance of the operations, including inspection and testing. At a minimum, these procedures control the performance of activities and alert operators to changes in radiological conditions around the cask. These sequences are controlled by Humboldt Bay ISFSI TS and Section 10.2.

## HUMBOLDT BAY ISFSI FSAR UPDATE

Several components (e.g., the RFB crane and cask transfer rail dolly) are used during the cask loading process. A discussion of these items is provided for the sole purpose of describing the loading process.

Prior to bringing the HI-STAR HB GTCC Overpack into the RFB, the overpack is visually verified to be free of foreign materials or physical damage. Also, the empty GTCC Waste Container (GWC) has been cleaned, inspected and inserted into the overpack. Alignment marks are checked to ensure correct rotational alignment between the GWC and the overpack. The GWC is similar to the Multi-Purpose Canister (MPC) within a spent fuel cask and has an outer container welded to the bottom of the GWC. The GWC is shown in Figure 3.3-4.

The overpack containing an empty GWC is brought into the RFB in the vertical orientation through the railroad door on the cask transfer rail dolly that runs from inside the RFB to the Unit 3 yard. The cask transfer rail dolly is used because dimensional limitations of the RFB door prevent access of the cask transporter inside the RFB. After bringing the overpack into the RFB, the overpack is positioned under the RFB crane that is configured with the lift yoke and the overpack annulus overpressure system is connected.

The overpack-to-GWC annulus is filled with clean water and the inflatable annulus seal is installed in the top part of the annulus to minimize the risk of contaminating the external shell of the GWC. The GWC internal cavity is filled with SFP water or water from another suitable source to prevent splash-back when the cask is lowered into the SFP. The lift yoke engages the overpack lifting trunnions and is used to raise and lower the overpack during loading operations inside the RFB.

The overpack is raised by the RFB crane, positioned over the cask loading area of the SFP, and lowered using the RFB crane hoist until the top of the overpack is nearly level with the water level in the annulus overpressure system. The annulus overpressure system supply line to the overpack is opened and the overpack is lowered to the bottom of the SFP. The annulus overpressure system applies a slight overpressure to the annulus to protect the GWC external shell from contamination from the SFP water in the event there is a leak in the annulus seal. When the cask is fully lowered to the bottom of the cask loading area in the SFP, the lift yoke is remotely disconnected from the overpack and moved out of the way to allow loading GTCC waste into the cask.

Loading GTCC waste (including the process waste container and the irradiated hardware pieces) is conducted in accordance with approved procedures. The GTCC process waste contained in the PWC will be thermally processed offsite at a vendor's facility. A dry heating process known as dry-ashing will be used to remove organics and other hydrogen bearing components from the process waste to produce a dry concentrated residue. The residue will have sufficiently low hydrogen content to mitigate the formation of hydrogen gas from radiolytic decomposition in long term storage casks. This is needed to maintain hydrogen at less than 5 percent by volume of the PWC void space [USNRC Information Notice 84-72, Clarification of Conditions for

## HUMBOLDT BAY ISFSI FSAR UPDATE

Waste Shipments Subject to Hydrogen Gas Generation]. After the dry-ashing process is complete, the vendor will vacuum dry the PWC, install a mechanical seal and backfill the PWC with helium and conduct a leak test. The PWC will be returned to HBPP and stored in the spent fuel pool (SFP), a wet environment; however, the process waste contained in the PWC will remain dry. The PWC will eventually be loaded into the GWC in the SFP.

After the PWC has been loaded into the GWC, the activated metals will be loaded into the GWC. The GWC will be moved out of the SFP, drained, vacuum dried and backfilled with helium.

The GWC lid, with the drain line attached, is placed in position in the GWC after the completion of loading GTCC waste, while the overpack is in the SFP. The lift devices are detached from the GWC lid allowing the lift yoke, which is attached to the RFB crane, to be lowered to the overpack to engage the lifting trunnions. The overpack and lift yoke are raised until the top of the GWC and overpack break the water surface. The annulus overpressure supply line is closed and the overpressure system is disconnected. Initial decontamination of the overpack may be performed as the overpack emerges from the SFP or in any other manner approved by the Radiation Protection (RP) Department.

The overpack is raised completely out of the SFP. The overpack is placed onto the cask transfer rail dolly in the railroad bay. The lift yoke is disconnected and moved from the area.

The GWC water volume is reduced to provide enough space between the water surface and the lid to avoid a water-weld interaction. The inflatable annulus seal is removed and the annulus water level is lowered. Once the top edge of GWC shell is surveyed and found to be in satisfactory condition, the annulus shield is installed if required by Radiation Protection personnel for dose considerations.

Although no combustible gas is expected, the space under the GWC lid is exhausted or purged during welding operations to prevent combustible gas concentrations from accumulating. Appropriate monitoring for combustible gas concentration is performed prior to and during GWC lid welding operations. The GWC lid-to-shell weld is then completed, including liquid penetrant inspections after the root pass, each approximately 3/8-inch of weld depth, and after the final pass.

Once the lid-to-shell weld is complete, the GWC undergoes a pressure test for leaks in accordance with the ASME Code. The lid-to-shell weld is liquid penetrant inspected after the pressure test. Either prior to, or following successful completion of the pressure test (depending on whether a hydrotest or pneumatic test is performed), the Removable Valve Operating Assemblies (RVOAs) are installed and the remaining GWC water is displaced from the GWC by pumping or blowing pressurized nitrogen or helium gas into the GWC. The water may be drained from the overpack annulus and vacuum

## HUMBOLDT BAY ISFSI FSAR UPDATE

drying is used to remove the remaining liquid water from the GWC and to ultimately reduce the moisture content of the MPC cavity to an acceptable level.

Following the successful completion of moisture removal from the GWC, the GWC is backfilled with helium to a nominal pressure range of 10 to 15 psig. Helium backfill provides an inert atmosphere to ensure long-term waste integrity. After successful helium backfill operations, the RVOAs are removed and GWC vent and drain port cover plates are installed, welded, and examined. The GWC closure ring is then installed, welded, and examined.

The overpack and accessible portions of the GWC are checked to ensure any removable contamination is within applicable limits. Additional decontamination and surveys may be performed throughout the loading process. The closure plate is installed on the overpack and the bolts are tightened as specified by the cask manufacturer.

The overpack annulus is drained, if not previously completed, and the cask is ready for transfer to the ISFSI storage vault. The loaded overpack is moved out of the RFB using the cask transport rail dolly and positioned under the lift beam of the cask transporter with the lift links attached.

### 5.1.1.6 GTCC Cask Transfer to the ISFSI Storage Site

The cask transporter is positioned outside the RFB doors to receive the HI-STAR HB GTCC overpack from the cask transport rail dolly. The cask transporter lift links engage the HI-STAR HB lifting trunnions and the overpack is lifted off of the rail dolly. A restraining strap is used to secure the overpack to the transporter. The overpack is transported to the ISFSI vault along the approved transportation route using appropriate administrative controls as described in Section 4.3.3 and shown in Figure 2.2-2.

The cask transporter centers the HI-STAR HB GTCC overpack over the open vault storage cell. The restraining strap is released from the overpack. The cask transporter towers are used to lower the overpack down into the vault and the lift links are removed. The cask transporter is driven away from the ISFSI vault, the seismic shims are installed, and the storage cell lid is installed.

## 5.1.2 IDENTIFICATION OF SUBJECTS FOR SAFETY AND RELIABILITY ANALYSIS

### 5.1.2.1 Criticality Prevention

A summary description of the principal design features, procedures, and special techniques used to preclude criticality in the design and operation of the HI-STAR HB System is provided in Section 3.3.1.4. Additional detail on the criticality design of the storage cask is provided in Section 4.2.3.3.7.

### 5.1.2.2 Instrumentation

Examples of measuring and test equipment (M&TE) used during the preparation of the cask for storage operations are listed in Table 5.1-1. Additional, or different M&TE, may be used as determined through the development of site-specific operating procedures, including the revision of those procedures as experience in cask loading operations is gained and the state of the art evolves.

No instrumentation is required to detect off-normal operations of the HI-STAR HB System while in its final storage configuration at the ISFSI storage site. The cask system is designed to maintain confinement integrity under all design-basis normal, off-normal, and accident conditions.

### 5.1.2.3 Maintenance Techniques

No periodic maintenance is required to ensure the safe, long term operation of the Humboldt Bay ISFSI. Any required corrective maintenance will be completed under the work control process.

### 5.1.3 REFERENCES

1. ANSI/ANS-57.9-1992, Design Criteria for an Independent Spent Fuel Storage Installation (dry type), American National Standards Institute.

## HUMBOLDT BAY ISFSI FSAR UPDATE

### 5.2 **CONTROL ROOM AND CONTROL AREAS**

Due to the welded closure of the HI-STAR cask, the passively-cooled HI-STAR cask design, and the Independent Spent Fuel Storage Installation (ISFSI) vault design features, the Humboldt Bay ISFSI does not require continuous surveillance and monitoring or operator actions to ensure that its safety functions are performed during normal, off-normal, or postulated accident conditions. Therefore, a control room or control area is not considered necessary, as allowed by 10 CFR 72.122(j).

Normal loading and unloading operations will take place in the Humboldt Bay Power Plant (HBPP) refueling building under local control and in coordination with the HBPP staff and subject to the controls established under the HBPP 10 CFR 50 license.



## HUMBOLDT BAY ISFSI FSAR UPDATE

### 5.3 SPENT FUEL ACCOUNTABILITY PROGRAM

Accountability and control of spent fuel will be maintained at all times during loading, transfer, and storage operations. Existing Humboldt Bay Power Plant (HBPP) procedures for control and accountability of special nuclear material will be revised to document loading and transfer records for spent fuel moved from the HBPP spent fuel pool to the Independent Spent Fuel Storage Installation (ISFSI). The Humboldt Bay ISFSI will be treated as a separate material balance area from HBPP.

As required by 10 CFR 72.72, records are maintained showing the receipt, inventory (including location), disposal, acquisition, and transfer of all spent fuel and radioactive waste in storage. In addition, accountability records for all fuel assemblies transferred to, stored at, or removed from the Humboldt Bay ISFSI are maintained for as long as fuel assemblies are stored at the ISFSI and retained for a period of 5 years after the fuel is transferred out of the ISFSI. PG&E requested an exemption from 10 CFR 72.72(d), which requires that spent fuel and high-level radioactive waste records in storage be kept in duplicate. The NRC granted the exemption, and, as specified in Humboldt Bay ISFSI License SNM-2514, License Condition 16, the exemption allows PG&E to maintain records of spent fuel and high-level radioactive waste in storage either in duplicate, as required by 10 CFR 72.72(d), or, alternatively, a single set of records may be maintained at a records storage facility that satisfies the standards of ANSI N 45.2.9-1974. All other requirements of 10 CFR 72.72(d) must be met.

Material status reports will be completed and submitted to the Nuclear Regulatory Commission as specified in 10 CFR 72.76. Nuclear material stored at the ISFSI will not be received from foreign sources nor transferred from Pacific Gas and Electric to other ownership until eventual transfer to Department of Energy for offsite transportation and storage. Therefore, Nuclear Transaction Reports (DOE/NRC Form-741) required by 10 CFR 72.78 will not be needed until that time.

#### **5.4 SPENT FUEL TRANSPORT**

Spent fuel transport from the Humboldt Bay Power Plant Unit 3 refueling building to the Independent Spent Fuel Storage Installation vault is accomplished using a specifically designed transporter. Design criteria for the transporter are presented in Sections 3.2 and 3.3.3. A description of the transporter is provided in Section 4.3. Operation of the transporter is described in Sections 4.4.1, 4.5.4 and 5.1.1.3. The location and construction features of the transport route are described in Section 4.3.3.

# HUMBOLDT BAY ISFSI FSAR UPDATE

TABLE 5.1-1

## MEASURING AND TEST EQUIPMENT

<b>Instrument</b>	<b>Function</b>
Contamination Survey, Radiation Monitoring	Measures contamination levels and dose rate levels on HI-STAR HB overpack, MPC lid, and ancillaries.
Dew Point Sensor	Measures moisture content of helium stream during Forced Helium Dehydrator (FHD) operations.
Pressure Gauge	Measures fluid pressure during pressure testing of MPC lid-to-shell weld.
Vacuum Gauge	Measures vacuum during overpack annulus drying.
Flow Meter and Totalizer	Measures amount of helium inserted into the MPC during helium backfill operations.
Temperature Gauge	Measures helium temperature to ensure MPC dryness during FHD System operations.

# HUMBOLDT BAY ISFSI FSAR UPDATE

## CHAPTER 6

### **WASTE MANAGEMENT**

#### CONTENTS

<u>Section</u>	<u>Title</u>	<u>Page</u>
6.1	MPC CONFINEMENT BOUNDARY DESIGN	6.1-1
6.2	RADIOACTIVE WASTES	6.2-1
6.3	REFERENCES	6.3-1

CHAPTER 6

**WASTE MANAGEMENT**

**6.1 MPC CONFINEMENT BOUNDARY DESIGN**

.The multi-purpose canister (MPC) is designed to endure normal, off-normal, and accident conditions of storage with maximum decay heat loads without loss of confinement. The MPC confinement boundary ensures that there will be no release of radioactive materials from the cask storage system under all postulated loading conditions and meets the criteria of Interim Staff Guidance-18. Therefore, leakage of radioactive material from the MPC is considered non-credible. Refer to Chapter 3 for additional details regarding confinement barriers and systems.

## **6.2 RADIOACTIVE WASTES**

No radioactive wastes are expected to be generated due to transport or storage of the loaded multi-purpose canister (MPC) at the Independent Spent Fuel Storage Installation. Radioactive wastes generated during MPC loading operations in the refueling building (RFB) will be treated using the existing HBPP radioactive waste treatment systems.

Contaminated water from loaded MPCs will normally be drained back into the spent fuel pool (SFP) and be subject to the normal treatment for the SFP water. A small amount of liquid waste will result from decontamination of the exterior surfaces of the transfer cask and MPC. The decontamination waste will be demineralized water, which may contain a small amount of detergent (limited in order to avoid problems with waste treatment and NPDES analysis requirements). Liquid wastes from decontamination activities in the RFB are directed to the liquid radwaste treatment system.

The MPC loading operation will take place in the RFB, with all RFB ventilation exhaust air routed through the stack filtration system before release. To the extent practical, potentially contaminated air and helium vented from the MPC during loading operations will be directly routed to the RFB ventilation system, rather than being released into the general RFB work area.

A small quantity of low-level solid waste may be generated during MPC loading operations. The solid waste may include disposable anti-contamination garments, paper, rags, tools, etc., and will be processed as described in the HBPP procedures.



**6.3    REFERENCES**

1.    None

# HUMBOLDT BAY ISFSI FSAR UPDATE

## CHAPTER 7

### **RADIATION PROTECTION**

#### CONTENTS

Section	Title	Page
7.1	ENSURING THAT OCCUPATIONAL RADIATION EXPOSURES ARE AS LOW AS IS REASONABLE ACHIEVABLE	7.1-1
7.1.1	Policy Consideration and Organization	7.1-1
7.1.2	Design Considerations	7.1-2
7.1.3	Operational Considerations	7.1-4
7.1.4	References	7.1-5
7.2	RADIATION SOURCES	7.2-1
7.2.1	Characterization of Sources	7.2-1
7.2.2	Airborne Radioactive Material Sources	7.2-4
7.2.3	References	7.2-5
7.3	RADIATION PROTECTION DESIGN FEATURES	7.3-1
7.3.1	Storage System Design Features	7.3-1
7.3.2	Shielding	7.3-2
7.3.3	Ventilation	7.3-3
7.3.4	Area Radiation and Airborne Radioactivity Monitoring Instrumentation	7.3-4
7.3.5	References	7.3-4
7.4	ESTIMATED ONSITE COLLECTIVE DOSE ASSESSMENTS	7.4-1
7.5	OFFSITE COLLECTIVE DOSE	7.5-1
7.5.1	Direct Radiation Dose Rates	7.5-1
7.5.2	Offsite Dose from Overpack Loading Operations	7.5-1
7.5.3	Total Offsite Collective Dose	7.5-2
7.5.4	References	7.5-3
7.6	HEALTH PHYSICS PROGRAM	7.6-1
7.6.1	Organization	7.6-1
7.6.2	Equipment, Instrumentation, and Facilities	7.6-1
7.6.3	Policies and Procedures	7.6-2
7.6.4	References	7.6-5
7.7	ENVIRONMENTAL MONITORING PROGRAM	7.7-1
7.7.1	References	7.7-1

# HUMBOLDT BAY ISFSI FSAR UPDATE

## CHAPTER 7

### **RADIATION PROTECTION**

#### TABLES

Table	Title
7.2-1	Description of Design Basis Fuel Assembly
7.2-2	Description of the Axial Shielding Model of the Design Basis Fuel Assembly
7.2-3	Normalized Distribution Based on Burnup Profile
7.2-4	Calculated Gamma Source Term per Assembly for a Burnup of 23,000 MWD/MTU
7.2-5	Calculated Neutron Source Term per Assembly for a Burnup of 23,000 MWD/MTU
7.2-6	Calculated $^{60}\text{Co}$ Source Term per Assembly for a Burnup of 23,000 MWD/MTU
7.3-1	Surface and 1 Meter Dose Rates for the Overpack 23,000 MWD/MTU and 29-Year Cooling
7.4-1	Deleted in Revision 1.
7.4-2	Deleted in Revision 1.
7.4-3	Deleted in Revision 1.
7.5-1	Normal Operation Dose Rates and Annual Doses at the Site Boundary and Nearest Resident from Direct Radiation from the Humboldt Bay ISFSI
7.5-2	Dose Rates at the Site Boundary from Overpack Loading Operations
7.5-3	Maximum Total Annual Offsite Collective Dose (MREM/YEAR) at the Site Boundary and Nearest Resident from the Humboldt Bay ISFSI

# HUMBOLDT BAY ISFSI FSAR UPDATE

## CHAPTER 7

### **RADIATION PROTECTION**

#### FIGURES

<u>Figure</u>	<u>Title</u>
7.3-1	Overpack with Dose Rate Locations Marked
7.3-2	ISFSI Filled with Fuel-Filled HI-STAR HB Overpacks
7.3-3	Side View of Single Storage Cell in the ISFSI Vault with Parallel Reflective Boundary Conditions
7.3-4	Top View of Single Storage Cell in the ISFSI Vault with Parallel Reflective Boundary Conditions

CHAPTER 7

**RADIATION PROTECTION**

This chapter provides information regarding the radiation protection design features of the Independent Spent Fuel Storage Installation (ISFSI) and the estimated onsite and offsite doses expected due to operation of the Humboldt Bay ISFSI. The HI-STAR HB System deployed at Humboldt Bay is a shortened version of the generic HI-STAR 100 System, described in the HI-STAR 100 System FSAR (Reference 1). In certain cases, references may be made to more current information described in the HI-STORM 100 Final Safety Analysis Report (Reference 2) or HI-STORM License Amendment Request 1014-2 (Reference 3). The generic shielding analyses, including methodology, computer codes, and modeling were performed and licensed in accordance with NUREG-1536. These same, previously-licensed techniques were used in performing the site-specific analyses described in this chapter.

**7.1 ENSURING THAT OCCUPATIONAL RADIATION EXPOSURES ARE AS LOW AS IS REASONABLY ACHIEVABLE**

**7.1.1 POLICY CONSIDERATION AND ORGANIZATION**

It is the policy of Pacific Gas and Electric Company (PG&E) to design, operate, and maintain the Humboldt Bay ISFSI in a manner that maintains personnel radiation doses as low as is reasonably achievable (ALARA).

The Health Physics Program used for operating the Humboldt Bay ISFSI is described in Section 7.6 and implements the requirements of 10 CFR 20, 10 CFR 72, and the HB ISFSI policy for implementation of the ALARA philosophy. The Radiation Protection Manager is responsible for administering, coordinating, planning, and scheduling all radiation protection activities involving the ISFSI.

The primary objective of the Health Physics Program is to maintain radiation exposures to workers, visitors, and the general public below regulatory limits and ALARA.

The Holtec HI-STAR HB System, chosen for use at the Humboldt Bay ISFSI, is designed with the principles of ALARA considered for the operation, inspection, maintenance, and repair of the cask system. PG&E provides the facilities, equipment, and the trained and qualified staff to ensure that any radiation exposures due to ISFSI operations are ALARA. Direct radiation from the ISFSI storage vault will be measured and evaluated on a routine basis to ensure that radiation exposures from the ISFSI to unrestricted areas are ALARA.

Specific design and operations-oriented ALARA considerations are described in the following sections.

### 7.1.2 DESIGN CONSIDERATIONS

The Humboldt Bay ISFSI storage vault is located as shown in Figure 2.2-2 in near proximity to an unrestricted area. The location was chosen based on factors described in the Humboldt Bay ISFSI Environmental Report, Section 8.1. ALARA considerations associated with this location are as follows:

- The edge of the ISFSI vault is located approximately 53 ft from a public access trail. The use of a vault minimizes radiation exposure to members of the public that occasionally use this trail.
- The use of a vault for the ISFSI minimizes doses to onsite personnel.

Regulatory Position 2 of Nuclear Regulatory Commission (NRC) Regulatory Guide 8.8 (Reference 4) provides guidance regarding facility and equipment design features. This guidance has been followed in the design of the Humboldt Bay ISFSI and the HI-STAR HB System as described below:

- Regulatory Position 2a, regarding access control, is met by the use of a vault for the purpose of protecting individuals against undue risks from exposure to radiation and radioactive materials, and by the use of a perimeter fence with a locked gate that surrounds the ISFSI storage vault to prevent unauthorized access.
- Regulatory Position 2b, regarding radiation shielding, is met by the vault and HI-STAR HB cask biological shielding that minimizes personnel exposure to the extent practicable. Fundamental design considerations that directly influence occupational exposures and which have been incorporated into the HI-STAR HB System design include:
  - minimization of the number of handling and transfer operations for each spent fuel assembly;
  - minimization of the number of handling and transfer operations for each multi-purpose canister (MPC) loading;
  - maximization of fuel capacity; thereby taking advantage of the self-shielding characteristics of the fuel and the reduction in the number of MPCs that must be stored at the ISFSI;
  - minimization of planned maintenance requirements;



## HUMBOLDT BAY ISFSI FSAR UPDATE

- minimization of decontamination requirements at ISFSI decommissioning;
  - optimization of the placement of shielding with respect to anticipated worker locations and fuel placement during loading and transfer operations;
  - a thick-walled overpack that provides gamma and neutron shielding;
  - a thick MPC lid that provides effective shielding for operators during MPC loading and transfer operations;
  - multiple welded barriers to confine radionuclides;
  - smooth surfaces to reduce decontamination times;
  - MPC penetrations located and configured to reduce streaming paths;
  - overpack designed to reduce streaming paths;
  - MPC vent and drain ports, with remotely operated valves, to prevent the release of radionuclides during loading and unloading operations and to facilitate draining, drying, and backfill operations;
  - use of an annulus overpressure system to minimize contamination of the MPC shell outer surfaces during loading operations;
  - minimization of maintenance to reduce doses during storage operation; and
  - use of a dry environment inside the MPC cavity to preclude the possibility of release of contaminated liquids.
- Regulatory Position 2c, regarding process instrumentation and controls, is met since there are no radioactive systems at the ISFSI.

## HUMBOLDT BAY ISFSI FSAR UPDATE

- Regulatory Position 2d, regarding control of airborne contaminants, is met since the HI-STAR HB System is designed to withstand all normal, off-normal, and accident design-basis conditions without loss of confinement function, as described in Chapter 7 of the HI-STAR 100 System FSAR. Therefore, no gaseous releases are anticipated. No significant surface contamination is expected since the exterior of the MPC is kept clean by using clean water in the overpack annulus and by using an inflatable annulus seal to preclude spent fuel pool (SFP) water contacting the exterior surface of the MPC. The HI-STAR HB overpack coating material minimizes the accumulation of contamination, and is relatively easy to decontaminate.
- Regulatory Position 2e, regarding crud control, is not applicable to the Humboldt Bay ISFSI since there are no radioactive systems at the ISFSI that could transport crud.
- Regulatory Position 2f, regarding decontamination, is met since the exterior of the loaded HI-STAR HB cask is decontaminated prior to being removed from the HBPP refueling building. The exterior surface of the cask is designed with a minimal number of crud traps and a smooth, painted surface for ease of decontamination. In addition, an inflatable annulus seal and annulus overpressure system are used to prevent SFP water from contacting and contaminating the exterior surface of the MPC.
- Regulatory Position 2g, regarding monitoring of airborne radioactivity, is met since the MPC provides confinement for all design basis conditions. Airborne radioactivity monitoring equipment is provided for greater than design basis events.
- Regulatory Position 2h, regarding resin treatment systems, is not applicable to the Humboldt Bay ISFSI since there are no treatment systems containing radioactive resins.
- Regulatory Position 2i, regarding other miscellaneous features, is met by the use of an underground ISFSI storage vault which provides substantial shielding for onsite personnel and the general public. In addition, the MPC is constructed from stainless steel. This material is resistant to corrosion and the damaging effects of radiation, and is well proven in spent nuclear fuel storage cask service.

### 7.1.3 OPERATIONAL CONSIDERATIONS

Operating procedures planned for the Humboldt Bay ISFSI, including cask loading, unloading, and movement to the ISFSI storage vault are summarized in Chapter 5.

## HUMBOLDT BAY ISFSI FSAR UPDATE

The operating procedures will be developed with an underlying ALARA philosophy and will be modified, as appropriate, to incorporate lessons learned from actual loading campaigns conducted at other nuclear power plant ISFSIs.

ISFSI personnel will follow site-specific implementing procedures consistent with the philosophy of Regulatory Guides 8.8 and 8.10. Personnel radiation exposure during ISFSI operations will be minimized through the incorporation of the following concepts:

- Fuel loading procedures that follow accepted practice and build on lessons learned from operating experience.
- Preparation of the loaded MPC and HI-STAR HB cask inside the RFB using existing plant equipment and procedures, where possible.
- Filling of the annulus between the MPC and the HI-STAR HB cask with clean water and using the inflatable annulus seal and annulus overpressure system to minimize contamination of the outer surface of the MPC.
- Performance of as many MPC preparation activities as possible with water in the MPC cavity.
- Use of temporary portable shielding, as appropriate.
- Use of power-operated tools, when possible, to install and remove bolts on the overpack.
- Consideration of the ALARA philosophy in job briefings prior to fuel movement, cask loading, and MPC preparation.
- Use of classroom training, mock-ups, and dry-run training to verify equipment operability, procedure adequacy, and efficiency.

### 7.1.4 REFERENCES

1. Final Safety Analysis Report for the HI-STAR100 Cask System, Holtec International Report No. HI-2012610, Revision 1, December 2002.
2. Final Safety Analysis Report for HI-STORM 100 System, Holtec International Report No. HI-2002444, Revision 1, September 2002.
3. License Amendment Request 1014-2, Holtec International, Revision 2, August 6, 2003.
4. Regulatory Guide 8.8, Information Relevant to Ensuring that Occupational Radiation Exposures at Nuclear Power Stations will be As Low As Is Reasonably Achievable, USNRC, June 1978.

## 7.2 **RADIATION SOURCES**

The source terms presented in this section were developed specifically for use in the Humboldt Bay Independent Spent Fuel Storage Installation (ISFSI) shielding analyses. Development of the source terms was performed using the same method as previously approved for the generic HI-STAR 100 System as described in Chapter 5 of the HI-STAR 100 Final Safety Analysis Report (FSAR) (Reference 1).

### 7.2.1 **CHARACTERIZATION OF SOURCES**

Shielding analyses for dose rates from direct radiation were performed assuming that the overpacks contain multi-purpose canisters (MPC) completely loaded with fuel assemblies having identical burnup and cooling times. The burnup was assumed to be 23,000 megawatt-days per metric ton of uranium (MWD/MTU) with an initial cooling time of 29 years.

Humboldt Bay Power Plant (HBPP) Unit 3 was shut down in July of 1976. For analysis purposes, a cask loading date of July 2005 was chosen, providing a minimum cooling time of 29 years. However, the vast majority of the fuel assemblies will have considerably longer cooling time. The burnup of 23,000 MWD/MTU was chosen because it is a bounding burnup for all fuel assemblies in the HBPP spent fuel pool (SFP) inventory. An enrichment of 2.09 wt. %  $^{235}\text{U}$  was used for the shielding analysis. This enrichment is the lowest initial assembly planar average enrichment for any single cask containing HBPP fuel, and is a conservative value because lower enrichments result in slightly higher neutron source terms.

The principal sources of direct radiation in the HI-STAR HB System are:

- Gamma radiation originating from the following sources
  - Decay of radioactive fission products
  - Secondary photons from neutron capture in fissile and nonfissile nuclides
  - Hardware activation products generated during power operations
- Neutron radiation originating from the following sources
  - Spontaneous fission
  - Alpha, neutron ( $\alpha$ , n) reactions in fuel materials
  - Secondary neutrons produced by fission from subcritical multiplication
  - Gamma, neutron ( $\gamma$ , n) reactions (this source is negligible)

The foregoing can be grouped into three distinct sources: fuel-gamma source, fuel-neutron source, and non-fuel activation source, each of which will be discussed later in this chapter. The source terms for the analyses presented in this FSAR were calculated using the same methods described in the HI-STAR 100 System FSAR. The neutron and gamma source terms were calculated with the SAS2H and ORIGEN-S modules of

the SCALE 4.4 system (References 2 and 3, respectively). The SCALE 4.3 system was used for the HI-STAR 100 System generic analysis.

### **7.2.1.1 Design-Basis Fuel Assembly**

The physical characteristics of the fuel used at HBPP Unit 3 are summarized in Table 3.1-2 and Section 10.2.

The fuel assembly chosen as the design basis fuel assembly for the shielding analysis was the GE Type III fuel assembly because it has the highest uranium mass loading and therefore will have a higher source term for the same burnup and cooling time than the other HBPP fuel designs. In addition, this fuel assembly comprises the largest fraction of the HBPP Unit 3 spent fuel inventory. Table 7.2-1 provides a physical description of the design basis fuel assembly and Table 7.2-2 describes the axial configuration of this fuel assembly as it was modeled in the shielding analysis. The axial burnup profile used in these analyses is identical to that described in Chapter 2 of the HI-STAR 100 System FSAR for boiling water reactor fuel. Table 7.2-3 presents the axial burnup profile used in this analysis.

The HI-STORM 100 System FSAR (Reference 4) describes the shielding analysis to qualify generic damaged fuel assemblies. The discussion in Section 5.4.2 of the HI-STORM 100 System FSAR describes the effect of damaged fuel assemblies on the external dose rates. This discussion indicates that the change in dose rate associated with the storage of damaged fuel assemblies is not significant. Based on that analysis, a specific evaluation of HBPP damaged fuel assemblies was not performed. Rather, all assemblies in all casks were assumed to be intact at the design basis burnup and cooling times. The basis for the validity of this approach is further explained in the PG&E Response to NRC Question 7-2 in Reference 8.

The Humboldt Bay ISFSI vault can house six storage casks. Five of these will be HI-STAR HB Systems containing spent fuel from HBPP and the sixth will contain greater than class C (GTCC) waste from HBPP. For the purposes of the shielding analysis, all six vault storage cells were assumed to contain spent fuel in HI-STAR HB overpacks. Pacific Gas and Electric will characterize the GTCC waste as part of the preparation activities for ISFSI operations, and ensure that the calculated radiation dose rate from the GTCC material does not exceed the calculated radiation dose rate from the spent fuel casks. Assurance that the dose rate at the controlled area boundary remains bounded by the calculations will be achieved through dose rate measurements. The surface dose rate from the cask loaded with GTCC will be compared to the GTCC cask calculations performed using the methodology of Section 7.3 and the validity of the calculations will be confirmed by measuring the loaded GTCC cask surface dose rate prior to placing the GTCC cask in the ISFSI. This provides reasonable assurance that the ISFSI will meet the regulatory requirements once the cask with GTCC waste is placed in the ISFSI.

### 7.2.1.2 Fuel-Gamma Source

Table 7.2-4 presents the gamma source terms that were used for the active fuel portion of the design basis assembly. The source is presented in both MeV/sec and photons/sec for an energy range of 0.45 MeV to 11.0 MeV. The lower bound of 0.45 MeV is consistent with the HI-STORM 100 System FSAR (the HI-STAR 100 System FSAR used a lower bound of 0.7 MeV) and was chosen because gammas with energies below 0.45 MeV are too weak to penetrate the HI-STAR HB overpack. The upper bound of 11.0 MeV was chosen to ensure the contribution of the higher energy photons was accounted for, since they may contribute a higher fraction of the total dose rate than in the generic analysis, given the additional shielding provided by the vault compared to just the cask system.

### 7.2.1.3 Fuel-Neutron Source

Table 7.2-5 presents the neutron source term used for the active fuel portion of the design-basis fuel assembly. The neutron source term is presented in neutrons/sec. Section 5.2.2 of the HI-STAR 100 System FSAR provides additional discussion on the calculation of the neutron source term.

The neutron source term increases as the  $^{235}\text{U}$  enrichment decreases for the same burnup and cooling time. Therefore, as discussed earlier in this section, a bounding low enrichment was chosen for the source term calculations. The neutron source strength also varies with burnup, by the power of 4.2 (Reference 1). Since this relationship is nonlinear and since burnup in the axial center of a fuel assembly is greater than the average burnup, the neutron source strength in the axial center of the assembly is greater than the relative burnup multiplied by the average neutron source strength.

In order to account for this effect, the neutron source strength in each of the 10 axial nodes listed in Table 7.2-3 was determined by multiplying the average source strength by the relative burnup level raised to the power of 4.2, resulting in a total neutron source strength factor of 1.369, which would increase the neutron source strength listed in Table 7.2-5 by 36.9 percent. This increase in neutron source term is not reflected in the data presented in Table 7.2-5, but is accounted for in the shielding analysis.

### 7.2.1.4 Non-fuel Sources

The non-fuel portions of a fuel assembly (e.g., steel and Inconel in the end fittings) activate during in-core operations to produce a radiation source. The primary radiation from these portions of the fuel assembly is  $^{60}\text{Co}$  activity. The activity from other isotopes within the steel and Inconel has a negligible impact on the radiation dose rate compared with the  $^{60}\text{Co}$  activity. Therefore,  $^{60}\text{Co}$  was the only isotope considered in the analysis. The method used to calculate the activity in the non-fuel regions of the assembly is the same as that described in Section 5.2.1 of the HI-STAR 100 System FSAR. The  $^{59}\text{Co}$  impurity level assumed in the steel and Inconel of the fuel assembly was 1.0 gm/kg or 1000 ppm and 4.7 gm/kg or 4700 ppm, respectively. These values,



which are consistent with Reference 5, are more conservative than those used in the HI-STAR 100 System FSAR. It was also assumed for this analysis that the fuel assemblies contained non-Zircaloy grid spacers with a  $^{59}\text{Co}$  impurity level of 4.7 gm/kg or 4700 ppm.

Table 7.2-6 lists the  $^{60}\text{Co}$  source that was used in the non-fuel portions of the fuel assemblies. Table 7.2-1 describes the mass and dimensions of these non-fuel portions of the fuel assembly.

The HBPP fuel may be stored in the HI-STAR HB System with or without channels. The channels are made of Zircaloy material and their activation gamma source is not significant in comparison with the fuel. Therefore, the channels are not modeled in the shielding analysis, which also conservatively neglects any shielding of the fuel source that they would provide. This approach is consistent with the approach used to address Zircaloy channels in the HI-STAR 100 generic shielding analysis.

Crud on the fuel assemblies is not explicitly accounted for in the source term. A conservative estimate of the crud deposition on a fuel assembly has been determined to be 112 milligram per square cm. Analysis in early 2000 determined the activity level of the crud in the bottom of the spent fuel pool. This crud is representative of the crud on the fuel assembly. The majority of the activity was from  $^{60}\text{Co}$ . Decay correcting the activity for an additional 5 years of cooling time produces a total activity level of less than 17.7 micro-curie/gm crud. Using the activity level, the mass of crud per sq cm, the diameter and number of fuel rods, and total length of the fuel assembly (this is conservative), the gamma source strength from crud is estimated to be  $6.87\text{E}+9$  gammas/sec. Comparing this value to the fuel assembly source term,  $5.98\text{E}+11$  gammas/sec, in the 1.0-1.5 MeV range (the range for Co-60 gammas) demonstrates that the crud is less than 1.2 percent of the source in this energy range and therefore is insignificant compared to the fuel assembly source term and as a result was not included in the dose analysis. This minimal source term from crud is considered to be especially insignificant when it is noted that the MPC source term is based on the assumption that all fuel assemblies in the MPC are at the maximum burnup for any single assembly rather than the average burnup for the MPC. Additional information describing the method for estimating the amount of crud on a fuel assembly is provided in the PG&E Response to NRC Question 7-1 in Reference 9.

### **7.2.2 AIRBORNE RADIOACTIVE MATERIAL SOURCES**

Loading of spent fuel into the MPC, in the overpack, is performed under water in the SFP cask loading pit, which prevents the spread of effluent radioactivity during fuel loading. The MPC is sealed and dried within the Refueling Building (RFB), allowing the liquid and gaseous waste released from the MPC during the draining and drying to be processed by the appropriate HBPP systems. Therefore, no airborne releases to the environment from the spent nuclear fuel assemblies are expected to occur during loading and handling operations.

The MPC enclosure vessel, which provides the confinement boundary for the HI-STAR HB System, is a welded pressure vessel and has no bolted closures or mechanical seals. Chapter 3 of the HI-STAR 100 System FSAR describes the structural analyses that demonstrate that all confinement boundary components are maintained within Code-allowable stress limits under all design-basis normal, off-normal, and accident conditions. The all-welded construction of the MPC in conjunction with the extensive inspections and testing performed during closing operations ensures that no release of radioactive effluents will occur from the HI-STAR HB System. The all-welded construction of the MPC meets the criteria contained in Interim Staff Guidance (ISG) 18 (Reference 7) providing justification that leakage from the confinement boundary is not credible. Therefore, no confinement analysis is required or performed. See Section 4.2.3.2.1 for details on the MPC construction compared to the ISG-18 criteria.

### 7.2.2.1 External Contamination Control

The external surface of the MPC shell and the internal surface of the HI-STAR HB are protected from contamination by preventing it from coming into contact with the SFP water. Prior to submergence in the SFP, an inflatable seal is installed at the top of the annulus formed between the MPC shell and the overpack cavity. This annulus is filled with clean, uncontaminated water, and the seal is inflated. An annulus water overpressurization system is used to maintain the water behind the inflated seal at a slight positive pressure. This system, in the unlikely event of a leak in the inflated seal, will preclude the entry of contaminated water into the annulus. These steps ensure that the MPC shell surface and the internal surface of the HI-STAR HB are free of contamination that could become airborne during storage. Additionally, following fuel-loading operations and removal from the SFP, the MPC lid, the upper end of the MPC shell, and the exterior surfaces of the HI-STAR HB are decontaminated, and then surveyed for any remaining, loose surface contamination. No contaminated surfaces will have removable contamination that exceeds normal release criteria.

### 7.2.3 REFERENCES

1. Final Safety Analysis Report for the HI-STAR 100 Cask System, Holtec International Report No. HI-2012610, Revision 1, December 2002.
2. O.W. Hermann, C.V. Parks, SAS2H: A Coupled One-Dimensional Depletion and Shielding Analysis Module, NUREG/CR-0200, Revision 6, (ORNL/NUREG/CSD-2/V2/R6), Oak Ridge National Laboratory, September 1998.
3. O.W. Hermann, R.M. Westfall, ORIGEN-S: SCALE System Module to Calculate Fuel Depletion, Actinide Transmutation, Fission Product Buildup and Decay, and Associated Radiation Source Terms, NUREG/CR-0200, Revision 6, (ORNL/NUREG/CSD-2/V2/R6), Oak Ridge National Laboratory, September 1998.

4. Final Safety Analysis Report for the HI-STORM 100 System, Holtec International Report No. HI-2002444, Revision 1, September 2002.
5. A.G. Croff, M.A. Bjerke, G.W. Morrison, L.M. Petrie, Revised Uranium-Plutonium Cycle PWR and BWR Models for the ORIGEN Computer Code, ORNL/TM-6051, Oak Ridge National Laboratory, September 1978.
6. Interim Staff Guidance 18, The Design/Qualification of Final Closure Welds on Austenitic Stainless Steel Containers as Confinement Boundary for Spent Fuel Storage and Containment Boundary for Spent Fuel Transportation, USNRC, May 2003.
7. PG&E Letter HIL-04-007, Response to NRC Request for Additional Information for the Humboldt Bay Independent Spent Fuel Storage Installation Application, October 1, 2004.
8. PG&E Letter HIL-05-003, Response to NRC Request for Additional Information for the Humboldt Bay Independent Spent Fuel Storage Installation Application, April 8, 2005.

### 7.3 RADIATION PROTECTION DESIGN FEATURES

#### 7.3.1 STORAGE SYSTEM DESIGN FEATURES

The Humboldt Bay Independent Spent Fuel Storage Installation (ISFSI) and the HI-STAR HB System are described in Chapters 1 through 4. Six dry storage casks are stored in the storage cells of the ISFSI vault. Five of the storage cells contain HI STAR HB Systems filled with Humboldt Bay Power Plant (HBPP) spent fuel. The sixth storage cell contains a greater than class C (GTCC) waste certified cask. The storage cells are arranged in a single row. Figures 2.2-2 and 4.1-1 illustrate the ISFSI location and pad layout. The storage cells/casks are positioned on a 10 ft, 9 inch, center-to-center pitch. As discussed in Section 4.1, a Security Area Fence, surrounds the ISFSI.

The ISFSI and dry cask storage system has a number of design and administrative control features that ensure that radiation exposures are as low as is reasonably achievable (ALARA).

- There are no radioactive systems at the ISFSI other than the GTCC cask and the overpacks containing multi-purpose canister (MPCs).
- The fuel is stored dry inside the MPC so that no radioactive liquid is available for leakage.
- The MPC-HB is prepared for storage and decontamination activities occur in the HBPP Refueling Building (RFB) prior to being moved to the ISFSI.
- Fuel is not removed from the MPCs at the ISFSI.
- The MPCs are heavily shielded by the overpack, the vault, including the vault lid while in place and the surrounding soil.
- A locked fence surrounds the ISFSI storage vault to prevent unauthorized access.
- The ISFSI Security Area within the fence is typically not occupied.
- The MPC design includes a 9.5-inch thick steel lid for shielding of workers.
- The MPC-HB is designed such that leakage from the confinement boundary is not credible.

The HI-STAR 100 System Final Safety Analysis Report (FSAR) (Reference 1) describes the HI-STAR 100 overpack in detail. Section 4.2.3 of this FSAR describes the HI-STAR HB System and lists the significant differences between the generic design and the HI-STAR HB System. The design features of the HI-STAR HB overpack that ensure radiation exposures are ALARA follow:

## HUMBOLDT BAY ISFSI FSAR UPDATE

- The overpack has a large mass of steel encasing the MPC in the radial direction (8.5 inches). This material provides primarily gamma shielding.
- A radial neutron shield (minimum of 4 inches thick) is provided for neutron shielding.
- The bottom forging of the HI-STAR overpack provides 6 inches of steel for shielding.
- The top lid of the HI-STAR overpack is also 6 inches thick of steel, which provides substantial shielding and protection for the MPC.
- The number of penetrations in the overpack has been minimized and the overpack surface is painted to minimize decontamination time.
- The overpack is a bolted, sealed pressure vessel that is leak tested.
- Neutron streaming paths created by the channel-based design of the neutron shield enclosure shell have been eliminated in the HI-STAR HB neutron shell enclosure design, which has no channels and four small gussets at the top and bottom of the enclosure (see Figure 3.3-3).

### 7.3.2 SHIELDING

The design of the generic HI-STAR 100 System as it relates to the shielding evaluation is described in Section 5.3 of the HI-STAR 100 System FSAR. Unlike the free-standing, generically certified HI-STAR 100 System, the HI-STAR HB System is stored in an underground vault with a thick, steel-encased concrete lid, which adds a significant amount of shielding. Design criteria for dose rates are given in Table 3.4-2 of this FSAR. Besides the overpack and the vault, no other radiation shielding features are required for the Humboldt Bay ISFSI.

The Humboldt Bay ISFSI is located in an area where the adjacent terrain is essentially flat. Therefore, the shielding models assume flat ground surrounding the ISFSI vault. The details of the calculations are described in Sections 7.4 and 7.5.

#### 7.3.2.1 Surface and One Meter Dose Rates

As described in Section 7.2, the design-basis fuel assembly used in the shielding analysis has a burnup and cooling time of 23,000 megawatt-day per metric ton of uranium and 29 years, respectively. All fuel assemblies in the MPC-HB are assumed to have this bounding burnup and cooling time in the shielding model. Figure 7.3-1 shows the overpack with dose rate locations numbered 1 through 5. The dose locations for the HI-STAR HB are similar to the dose locations for which values were reported in the HI-STAR 100 System FSAR. Table 7.3-1 presents the surface and 1-meter dose rates

for the overpack. The dose contributions from the individual source components (neutron, photon, and cobalt) are explicitly listed. The dose rate at all locations adjacent to a single storage cell in the ISFSI vault with the lid installed is less than 0.15 mrem/hr. No breakdown of dose rate is provided since this dose rate is extremely low.

### **7.3.2.2 Dose Versus Distance**

The dose rate versus distance from both a single overpack and the Humboldt Bay ISFSI as a whole were calculated using the Monte Carlo N-Particle (MCNP) transport code (Reference 2). Figure 7.3-2 provides a pictorial representation of the ISFSI with all 6 storage cells completely filled with fuel-filled HI-STAR HB overpacks. Modeling the GTCC cask as a fuel-containing cask provides a bounding approach. Based on the size of the ISFSI, it was decided not to model the entire ISFSI in MCNP. Instead, a simplified and conservative modeling approach was used. Figure 7.3-3 and Figure 7.3-4 show side and top views of a single storage cell in the ISFSI vault with parallel reflective boundary conditions positioned on both sides of the storage cell. These reflective boundary conditions are located at a distance midway between storage cells and have the effect of representing an infinite line of storage cells. Therefore, the dose rate at the public access trail is conservatively calculated from an infinite line of casks rather than the six casks that are actually present.

The models assumed a flat terrain surrounding the ISFSI vault and the ISFSI vault was assumed to be embedded in an infinite slab of soil. The MCNP models used 700 meters of air in altitude above the vault and 1,050 meters of air in the radial direction above the vault. The results of the dose rate calculations are discussed in Sections 7.4 and 7.5.

### **7.3.3 VENTILATION**

10 CFR 72.122(h)(3) requires that ventilation systems and offgas systems be provided where necessary to ensure the confinement of airborne radioactive particulate materials during normal and off-normal conditions. However, the HI-STAR HB System is designed to prevent the release of radioactive materials and gases during normal and off-normal conditions. Thus, there are no offgas systems required once the spent fuel is enclosed in the welded MPCs.



#### **7.3.4 AREA RADIATION AND AIRBORNE RADIOACTIVITY MONITORING INSTRUMENTATION**

Permanent area radiation and airborne radioactivity monitors are not needed at the Humboldt Bay ISFSI since the storage system is passive. Portable, hand-held radiation protection instruments are available during routine maintenance at the ISFSI storage area. Environmental thermoluminescent dosimeters at fixed locations will be used to record and trend area gamma doses at appropriate locations along the ISFSI Security Area Fence.

#### **7.3.5 REFERENCES**

1. Final Safety Analysis Report for the HI-STAR 100 Cask System, Holtec International Report No. HI-2012610, Revision 1, December 2002.
2. J.F. Briesmeister, Ed., MCNP - A General Monte Carlo N-Particle Transport Code, Version 4A., Los Alamos National Laboratory, LA-12625-M (1993).

#### 7.4 **ESTIMATED ONSITE COLLECTIVE DOSE ASSESSMENTS**

The results presented in this section are based on the shielding analysis of the HI-STAR HB overpack assuming design basis fuel with a burnup and cooling time of 23,000 megawatt-days per metric ton of uranium (MWD/MTU) and 29 years in every multi-purpose canister (MPC)-HB fuel storage location.

The estimated occupational exposures to Humboldt Bay Power Plant (HBPP) personnel during the following phases of Independent Spent Fuel Storage Installation (ISFSI) operation is approximately 568 millirem for each cask.

- (1) Loading of fuel into the MPC contained in the overpack.
- (2) Decontamination of the overpack and MPC in preparation for storage.
- (3) Transport of the overpack from the Refueling Building to the ISFSI vault.
- (4) Transfer of the overpack and MPC from the crawler into the storage cell of the ISFSI vault.
- (5) Closing of the storage cell in the ISFSI vault.

The estimated occupational exposures during the unloading of an overpack and MPC-HB (the reversal of the steps listed above) is approximately 328 millirem.

The estimated exposure is based on industry experience with the Holtec HI-STAR and HI-STORM casks and casks from other vendors. The dose rates used for this analysis are conservatively estimated using design-basis fuel, yet are still very low due to the long cooling time of the fuel. Humboldt Bay radiation protection personnel will assure that the appropriate radiation monitoring is performed and that all operations are performed in a manner consistent with ALARA.

The estimated annual occupational exposure as a result of ISFSI walkdowns and occasional maintenance/inspections is approximately 112 millirem for those years where a license renewal inspection is performed with a vault lid removed (on a 5-year frequency). The estimated dose is based on a total occupancy time of 79 hours per year, with 9 hours being with a vault lid removed. The dose rates used in the vault lid removal estimate are based on the measured dose rate over background exposure for the ISFSI vault of 1000 microrem/hour. The dose rates used in the estimate for non-lid removal activities are based on the measured dose rate over background exposure for the ISFSI vault of 2 microrem/hour. (Reference 1)

For those years where a license renewal inspection is not performed with a vault lid removed, the estimated annual occupational exposure as a result of ISFSI walkdowns and occasional maintenance/inspections is approximately 0.153 millirem. The estimated dose is based on a total occupancy time of 60 hours per year. The dose rates used in

## HUMBOLDT BAY ISFSI FSAR UPDATE

the estimate are based on the measured dose rate over background exposure for the ISFSI vault of 2 microrem/hour. (Reference 1)

The estimated annual occupational exposure as a result of overpack repairs is approximately 0.0036 REM. The doses for the repair operations assume one repair operation per month of one-hour duration with two people performing the operation. The dose rates were conservatively based on the contact dose rate for the ISFSI vault of 0.015 mrem/hour.

The conservative dose rates demonstrate that the estimated occupational exposures from the Humboldt Bay ISFSI meet the regulatory requirements of 10 CFR 20. The actual doses from the ISFSI are expected to be considerably less than the conservatively estimated values.

### 7.4.1 REFERENCES

1. Annual Occupancy Exposure Estimates Evaluation for Humboldt Bay ISFSI, May 23, 2017, RLOC 90102-5075.

## **7.5 OFFSITE COLLECTIVE DOSE**

This section addresses doses for normal conditions. Off-normal and accident analyses are provided in Sections 8.1 and 8.2, respectively.

The multi-purpose canister (MPC) is welded and designed to maintain confinement integrity under all normal, off-normal, and accident conditions of storage, thereby, precluding any release of radioactivity and any offsite dose from radioactive effluents. Therefore, the annual offsite dose from the Humboldt Bay Independent Spent Fuel Storage Installation (ISFSI) was calculated for only direct radiation (neutrons and gammas).

Since the loading of the HI-STAR HB into the ISFSI vault occurs outside the Refueling Building (RFB), the offsite dose due to those loading operations was also calculated and included in the total annual dose estimate.

The public trail at the controlled area boundary is located 53 ft from the edge of the ISFSI, and the nearest resident is located 811 ft from the center of the ISFSI. Although the public trail at the controlled area boundary has only occasional use, the occupancy time for the dose calculation was conservatively assumed to be 2,080 hours per year, based on a 40-hour work week and 52 weeks per year. The occupancy for the dose calculation at the nearest resident location was assumed to be continuous (8,760 hours per year), consistent with Interim Staff Guidance-13 (Reference 1).

### **7.5.1 DIRECT RADIATION DOSE RATES**

Table 7.5-1 presents the dose rate and annual doses at the site boundary and the nearest residence from direct radiation from the Humboldt Bay ISFSI after it is completely filled with six casks, five of which are HI-STAR HB overpacks loaded with Humboldt Bay Power Plant (HBPP) fuel at design-basis burnup and cooling times. The sixth cask, which contains greater than class C (GTCC) waste, is modeled as a sixth spent fuel cask to provide a bounding case for the ISFSI, since the spent fuel provides a stronger radiation source than the GTCC. As described in Section 7.3.2.2, these dose rates and doses were conservatively calculated for an infinite row of HI-STAR HBs rather than the six casks that will be present at the ISFSI.

### **7.5.2 OFFSITE DOSE FROM OVERPACK LOADING OPERATIONS**

The transfer of the HI-STAR HB into the final storage configuration at the ISFSI vault will occur outside the RFB. As a result, the offsite dose for transferring the HI-STAR HB from the RFB to the ISFSI was considered. Table 7.5-2 presents the results of this analysis. The analysis assumes that access to the public trail will be controlled to keep members of the public beyond a 100-meter boundary during cask transport and vault loading operations. Refer to Section 2.1.2 for additional information regarding control of the public access trail to the 100-meter controlled area.

### 7.5.3 TOTAL OFFSITE COLLECTIVE DOSE

Table 7.5-3 presents the maximum annual direct radiation dose from normal ISFSI operations for the site boundary and for the nearest resident. The typical annual offsite radiation dose from the other uranium fuel cycle operation within the region (that is, HBPP) is normally less than 0.1 mrem/year for any internal exposure pathway as well as for direct radiation. Note that the HBPP direct radiation dose is calculated from public access boundary thermoluminescent dosimeters measurements with the assumption (from US Nuclear Regulatory Commission (NRC) Regulatory Guide 1.109) that the annual occupancy time for access to the public trail is 67 hours/year. If the ISFSI occupancy time assumed above (2080 hours/year) is used to calculate the HBPP direct radiation dose, the typical HBPP direct radiation dose would be less than 2 mrem/year. Further, the location for the highest annual dose from HBPP does not correspond to the location for the highest annual dose from the ISFSI. This means that adding the two values overestimates the appropriate value for any intermediate location. Therefore, Table 7.5-3 demonstrates that the normal combination of HBPP and the ISFSI will be in compliance with 10 CFR 72.104.

Changing the fuel storage location from spent fuel pool to ISFSI is not expected to have a significant effect on offsite direct radiation dose rates from HBPP Unit 3. However, for some periods during the future decommissioning of HBPP Unit 3, large component removal and/or radioactive waste shipping could produce higher than usual direct radiation dose rates at portions of the site boundary for limited time periods. Generally, the potentially affected locations are sufficiently distant from the ISFSI so that such activities would not significantly increase the combined direct radiation dose rate at the limiting location. Nevertheless, such activities will be administratively controlled so that the combined dose rates comply with the HBPP Off-site Dose Calculation Manual (Reference 2) Specification 2.10, 10 CFR 72.104 and 49 CFR 100.

The actual dose from the ISFSI will be considerably less than the values presented in Table 7.5-3. The following are some of the conservative assumptions used in the calculating the dose rates.

- The design basis fuel assembly, the design basis operating exposure (burnup), and the design basis post-operation decay (cooling) time were conservatively chosen.
- All fuel assemblies in the MPC are assumed to be identical with the design basis burnup and cooling time.
- The analyzed ISFSI pattern was conservatively chosen to result in the highest offsite dose rate.
- The dose rate was calculated at the most conservative location around the ISFSI.

## HUMBOLDT BAY ISFSI FSAR UPDATE

### 7.5.4 REFERENCES

1. Real Individual, USNRC, Interim Staff Guidance Document-13, Revision 0, June 2000.
2. HBPP Off-site Dose Calculation Manual, Revision 9, April 2003.



## **7.6 HEALTH PHYSICS PROGRAM**

The organization, equipment, instrumentation, facilities, and policy and procedures described below will comprise the health physics program during the ISFSI operations phase.

The following health physics program will be used when casks are stored in the ISFSI.

### **7.6.1 ORGANIZATION**

The organization that will implement the Health Physics Program is described in Section 9.

### **7.6.2 EQUIPMENT, INSTRUMENTATION, AND FACILITIES**

The various equipment and instrumentation for performing radiation surveys and measuring and maintaining personnel exposure, and the facilities for radiation protection activities are summarized in this section. The radiation protection equipment, instrumentation, and facilities are highly simplified because the HI-STAR HB radiological hazard is limited to gamma and neutron radiation.

#### **7.6.2.1 Radiation Protection Instrumentation**

Radiation protection instruments to comply with the Emergency Plan (EP) and EP implementing procedures are maintained on site. Calibration and maintenance of this equipment is coordinated through the radiation protection organization at Diablo Canyon Power Plant.

#### **7.6.2.2 Area Radiation Monitoring Instrumentation**

Refer to Section 7.7.

### **7.6.2.3 Radiation Protection Facilities**

Radiation protection instrumentation and equipment to detect and mitigate potential releases are maintained on site in accordance with the Emergency Plan.

### **7.6.3 POLICIES AND PROCEDURES**

The purpose of this section is to summarize how ISFSI policies and procedures implement the Health Physics Program to maintain radiation exposure ALARA while spent nuclear fuel and Greater Than Class C waste are stored in the ISFSI.

It is the policy of PG&E to design, operate, and maintain the Humboldt Bay ISFSI in a manner that maintains personnel radiation doses ALARA and in accordance with this program and implementing procedures. The Director, Security and Emergency Services ensures that the content and implementation of the health physics program is reviewed at least annually.

#### **7.6.3.1 Control of Radiation Exposure to the Public**

Monitoring, analyzing, and reporting radiation levels in the environment is performed as described in Section 7.7 to demonstrate that the dose to the public is below regulatory limits and ALARA.

Radiation monitoring will be accomplished as described in Section 7.6.2.2.

Because of the HI-STAR HB design, no gaseous, liquid, or solid radioactive effluents are produced. Therefore, routine monitoring for effluents is not performed.

#### **7.6.3.2 Control of Personnel Radiation Exposure (Occupational)**

Personnel radiation exposure is maintained ALARA by the ISFSI design, access control, surveys and monitoring, work planning, training, and sound radiation protection practices implemented by procedures. The procedures for personnel radiation protection are prepared consistent with the requirements of 10 CFR 20 and are approved, maintained, and adhered to for activities involving personnel radiation exposure.

##### **7.6.3.2.1 Shielding**

The ISFSI design provides radiation shielding, which in conjunction with a program for controlling personnel access and occupancy in the Restricted Area, reduces external doses to personnel to levels that are both ALARA and within regulations defined in 10 CFR 20. Radiation protection implementing procedures provide for evaluation of the use of temporary shielding in the planning of any activities involving high dose rates.

### **7.6.3.2.2 Access Control and Area Designations**

The Security Area Fence restricts physical access to the ISFSI. Access into the Restricted Area is controlled by Radiation Protection Program procedures for the purpose of protecting individuals from exposure to radiation. Procedures describe the requirements for radiological postings, advising workers of potential radiological hazards at the entrance and boundaries of the posted Restricted Area.

### **7.6.3.2.3 Facility Contamination Control**

As described in Section 7.2.2.1, no external surfaces will have removable contamination that exceeds normal release criteria, and radioactive contamination of the ISFSI is not anticipated. Following fuel-loading operations and removal from the spent fuel pool, the MPC lid, the upper end of the MPC shell, and the exterior surfaces of the HI-STAR HB are decontaminated, and then surveyed to verify that any remaining, loose surface contamination is below release criteria.

### **7.6.3.3 Personnel Contamination Control**

As stated above, no external surfaces will have removable contamination that exceeds normal release limits. In addition, there is no credible accident that would cause radioactive contamination of the ISFSI. However, surveys for contamination are routinely performed to confirm that contamination is not present.

### **7.6.3.4 Area Surveys**

Surveys are performed in the accessible areas of the ISFSI. These surveys consist of periodic contamination surveys and external radiation measurements in appropriate areas. Additionally, specific surveys are performed as needed for operational and maintenance functions involving potential exposure of personnel to radiation or radioactive materials.

#### **7.6.3.5 Personnel Monitoring**

Personnel assigned to the HB ISFSI are not expected to exceed the individual monitoring threshold as described in 10 CFR 20.1502.

#### **7.6.3.6 Work Planning**

Work in the ISFSI Restricted Area is planned prior to performance. Consideration is given to dosimetry requirements, personnel protective equipment, monitoring requirements, and special cautions pertinent to the work. The planning also considers the maximum radiation level that will be encountered by and allowed by a worker.

#### **7.6.3.7 Training**

Training commensurate with the radiological hazards within the HB ISFSI controlled area is provided to HB ISFSI unescorted access personnel.

#### **7.6.4 REFERENCES**

1. None

## **7.7 ENVIRONMENTAL MONITORING PROGRAM**

No radioactive gas, liquid, or solid waste effluents are released from the Humboldt Bay Independent Spent Fuel Storage Installation (ISFSI) during operation. Therefore, a radioactive effluent monitoring system is not required, routine monitoring for effluents is not performed, and the reporting requirements of 10 CFR 72.44(d)(3) do not apply. The radioactive effluents released during fuel loading operations, which is a 10 CFR 50 licensed activity, are monitored and controlled by existing plant systems as explained in Chapter 6.

The ISFSI will emit direct radiation that will be monitored in the environment. The Environmental Monitoring Program will be implemented by posting thermoluminescent dosimeters (TLDs) in the vicinity of the Owner-Controlled Area fence and on the Security Area Fence. TLDs will be read quarterly to monitor direct radiation from the ISFSI.

In accordance with ISG-13 (Reference 1), the environmental monitoring program will reevaluate potential increases in exposure to real individuals during the term of the license. Compliance with the dose limits in 10 CFR 72.104 will be verified by the environmental program using direct radiation measurements.

### **7.7.1 REFERENCES**

1. Real Individual, USNRC, Interim Staff Guidance Document-13, Revision 0, June 2000.



# HUMBOLDT BAY ISFSI FSAR UPDATE

TABLE 7.2-1

## DESCRIPTION OF DESIGN BASIS FUEL ASSEMBLY

Assembly type	GE Type III
Active fuel length (in.)	77.5
No. of fuel rods	36
Rod pitch (in.)	0.740
Cladding material	Zircaloy-2
Rod diameter (in.)	0.563
Cladding thickness (in.)	0.032
Pellet diameter (in.)	0.488
Pellet material	UO ₂
Pellet density (gm/cc)	10.3
Enrichment (wt.% 235U)	2.08
Burnup (MWD/MTU)	23,000
Cooling time (years)	29
Specific power (MW/MTU)	17.836
Lower tie plate mass (kg)	5.73 304 SST
Grid spacer mass (kg)	0.16 Inconel 0.84 Zircaloy (neglected)
Plenum springs mass (kg)	0.027 Inconel
Compression / expansion springs mass (kg)	0.11 Inconel
Upper tie plate mass (kg)	1.55 304 SST

# HUMBOLDT BAY ISFSI FSAR UPDATE

TABLE 7.2-2

## DESCRIPTION OF THE AXIAL SHIELDING MODEL OF THE DESIGN BASIS FUEL ASSEMBLY

Region	Start (in.)	Finish (in.)	Length (in.)	Material Modeled (MCNP)
Lower tie plate	0	7.23	7.23	SS 304
Active Fuel	7.23	84.73	77.5	UO ₂ and Zircaloy
Plenum springs	84.73	90.14	5.41	SS 304
Compression / expansion springs	90.14	90.7	0.56	SS 304
Upper tie plate	90.7	96.91	6.21	SS 304

# HUMBOLDT BAY ISFSI FSAR UPDATE

TABLE 7.2-3

## NORMALIZED DISTRIBUTION BASED ON BURNUP PROFILE

Interval	Axial Distance from Bottom of Active Fuel (% of Active Fuel Length)	Normalized Distribution
1	0% to 4-1/6%	0.2200
2	4-1/6% to 8-1/3%	0.7600
3	8-1/3% to 16-2/3%	1.0350
4	16-2/3% to 33-1/3%	1.1675
5	33-1/3% to 50%	1.1950
6	50% to 66-2/3%	1.1625
7	66-2/3% to 83-1/3%	1.0725
8	83-1/3% to 91-2/3%	0.8650
9	91-2/3% to 95-5/6%	0.6200
10	95-5/6% to 100%	0.2200

# HUMBOLDT BAY ISFSI FSAR UPDATE

TABLE 7.2-4

CALCULATED GAMMA SOURCE TERM PER ASSEMBLY  
FOR A BURNUP OF 23,000 MWD/MTU

Lower Energy	Upper Energy	29-Year Cooling	
(MeV)	(MeV)	(MeV/s)	(Photons/s)
4.5E-01	7.0E-01	6.31E+13	1.10E+14
7.0E-01	1.0	7.96E+11	9.37E+11
1.0	1.5	7.47E+11	5.98E+11
1.5	2.0	5.26E+10	3.01E+10
2.0	2.5	5.67E+08	2.52E+08
2.5	3.0	1.94E+07	7.04E+06
3.0	4.0	1.21E+06	3.46E+05
4.0	6.0	7.41E+05	1.48E+05
6.0	8.0	1.19E+05	1.70E+04
8.0	11.0	1.86E+04	1.96E+03
Totals		6.47E+13	1.12E+14

# HUMBOLDT BAY ISFSI FSAR UPDATE

TABLE 7.2-5

CALCULATED NEUTRON SOURCE TERM PER ASSEMBLY  
FOR A BURNUP OF 23,000 MWD/MTU

Lower Energy (MeV)	Upper Energy (MeV)	29-Year Cooling (Neutrons/s)
1.0E-01	4.0E-01	1.27E+05
4.0E-01	9.0E-01	6.48E+05
9.0E-01	1.4	6.06E+05
1.4	1.85	4.66E+05
1.85	3.0	8.85E+05
3.0	6.43	7.41E+05
6.43	20.0	6.17E+04
Total		3.53E+06

# HUMBOLDT BAY ISFSI FSAR UPDATE

TABLE 7.2-6

CALCULATED  $^{60}\text{Co}$  SOURCE TERM PER ASSEMBLY  
FOR A BURNUP OF 23,000 MWD/MTU

Location	29-Year Cooling (curies)
Lower Tie Plate	2.218
Active Fuel Zone (grid spacers)	4.107
Plenum Springs	0.065
Compression / Expansion Springs	0.133
Upper Tie Plate	0.400



# HUMBOLDT BAY ISFSI FSAR UPDATE

TABLE 7.3-1

## SURFACE AND 1 METER DOSE RATES FOR THE OVERPACK 23,000 MWD/MTU AND 29-YEAR COOLING

Dose Point Location	Fuel Gammas (mrem/hr)	⁶⁰ Co Gammas (mrem/hr)	Neutrons (mrem/hr)	Totals (mrem/hr)
Surface Dose Rate				
1	1.2	12.4	14.7	28.3
2	6.5	0.05	1.8	8.3
3	0.7	4.9	6.1	11.7
4	0.04	0.02	9.9	9.9
5	1.5	8.8	18.6	28.9
1 Meter Dose Rate				
1	1.0	2.2	1.9	5.1
2	2.6	0.3	0.9	3.8
3	0.5	2.2	1.8	4.6
4	0.02	0.01	2.8	2.8

Notes:

- Refer to Figure 7.3-1 for the dose locations.
- Gammas generated by neutron capture are included with fuel gammas.

# HUMBOLDT BAY ISFSI FSAR UPDATE

TABLE 7.4-1 DELETED

# HUMBOLDT BAY ISFSI FSAR UPDATE

TABLE 7.4-2 DELETED

# HUMBOLDT BAY ISFSI FSAR UPDATE

TABLE 7.4-3 DELETED

## HUMBOLDT BAY ISFSI FSAR UPDATE

TABLE 7.5-1

NORMAL OPERATION DOSE RATES AND ANNUAL DOSES AT  
THE SITE BOUNDARY AND NEAREST RESIDENT FROM  
DIRECT RADIATION FROM THE HUMBOLDT BAY ISFSI

<b>Location</b>	<b>Dose Rate (mrem/hr)</b>	<b>Occupancy (hours/year)</b>	<b>Annual Dose (mrem)</b>
Site Boundary (53 ft / 16.2 m)	8.16E-03	2080	17.0
Nearest Resident (0.15 mi / 811 ft / 247 m)	5.11E-04	8760	4.48

## HUMBOLDT BAY ISFSI FSAR UPDATE

TABLE 7.5-2

### DOSE RATES AT THE SITE BOUNDARY FROM OVERPACK LOADING OPERATIONS

<b>Condition</b>	<b>Dose Rate (mrem/hr)</b>	<b>Event Duration (hours)</b>	<b>Total Loadings</b>	<b>Total Dose (mrem)</b>
HI-STAR HB movement to ISFSI	0.051	8	6	2.45

Note: During overpack loading operations access of any individual outside the HBPP Controlled Area boundary will be restricted to a minimum distance of 100 meters from the transport path (see Section 7.5.2).



# HUMBOLDT BAY ISFSI FSAR UPDATE

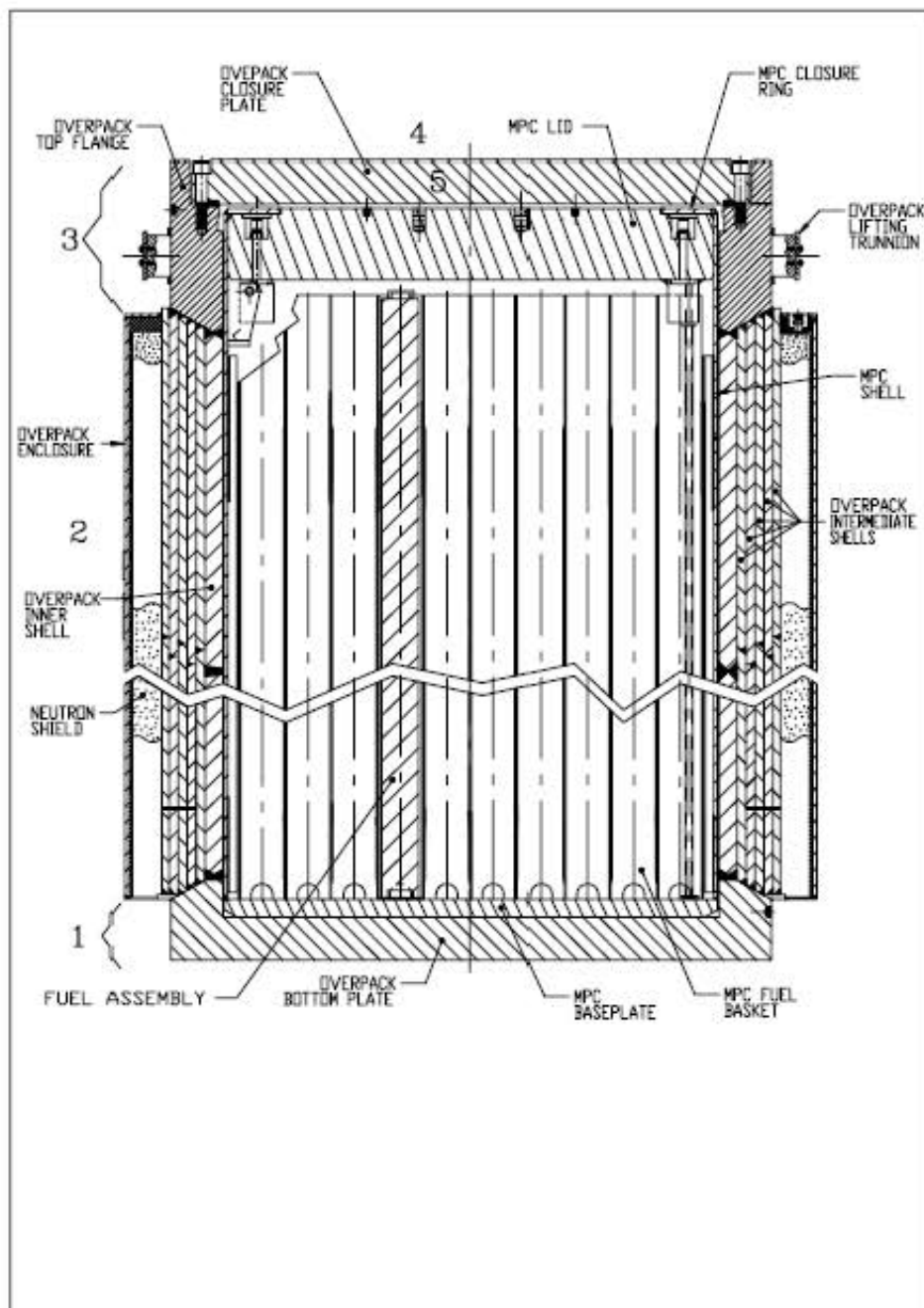
TABLE 7.5-3

MAXIMUM TOTAL ANNUAL OFFSITE COLLECTIVE DOSE (MREM/YEAR)  
AT THE SITE BOUNDARY AND NEAREST RESIDENT  
FROM THE HUMBOLDT BAY ISFSI

Direct Radiation	Overpack Loading Operations	Other Uranium Fuel Cycle Operations	10 CFR 72.104 Regulatory Limit
Site Boundary (53 ft / 16.2 m)			
17	2.45	<2	25
Nearest Resident (0.15 miles / 811 ft / 247m) to center of ISFSI			
4.48	1.83	<0.1	25

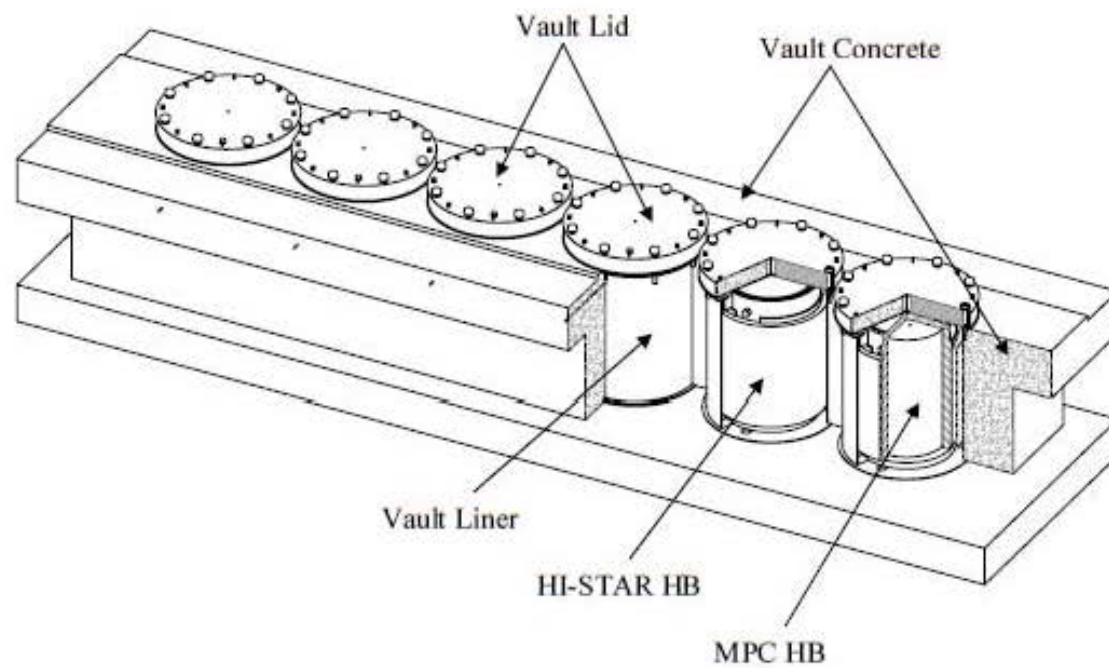
NOTES:

- (1) There will be a maximum of 6 loading operations; thereafter the annual offsite dose will be limited to the direct radiation and other uranium fuel cycle operations.
- (2) During overpack loading operations access of any individual outside the HBPP Controlled Area boundary will be restricted to a minimum distance of 100 meters from the transport path. Therefore, the dose from loading operations is calculated at 100 meters rather than 53 ft/16.2 m.



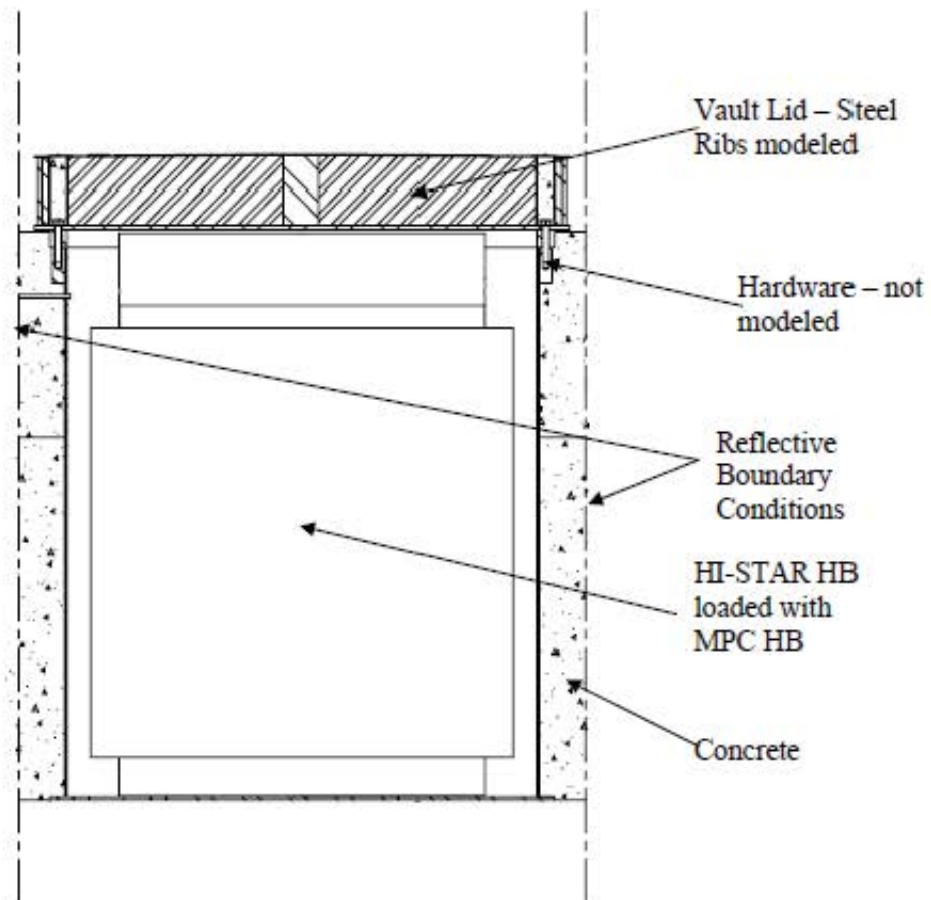
<b>FSAR UPDATE</b>
<b>HUMBOLDT BAY ISFSI</b>
<b>FIGURE 7.3-1</b>
<b>OVERPACK WITH DOSE RATE</b>
<b>LOCATIONS MARKED</b>

Revision 0 January 2006



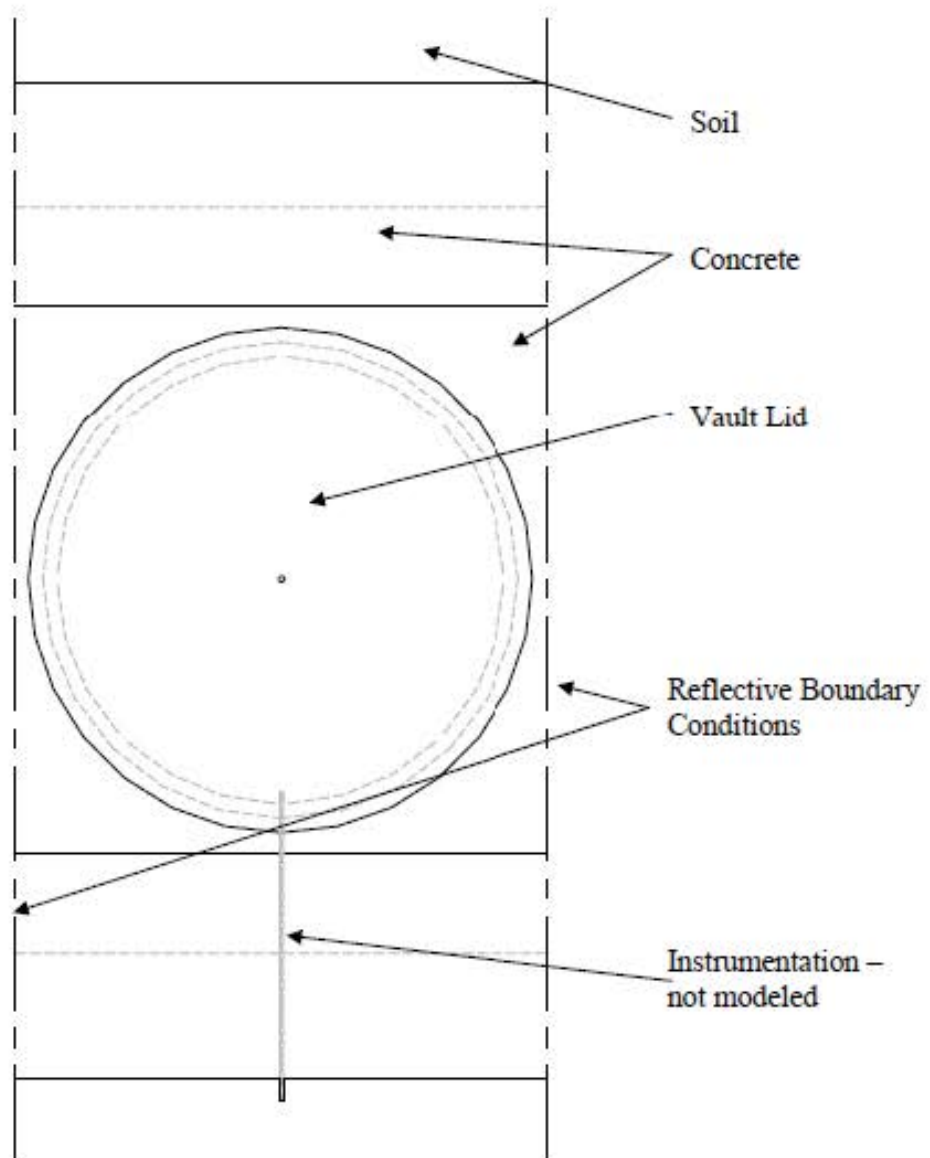
FSAR UPDATE
HUMBOLDT BAY ISFSI
FIGURE 7.3-2 ISFSI FILLED WITH FUEL-FILLED HI-STAR HB OVERPACKS

Revision 0 January 2006



<b>FSAR UPDATE</b>
<b>HUMBOLDT BAY ISFSI</b>
<b>FIGURE 7.3-3</b> <b>SIDE VIEW OF SINGLE</b> <b>STORAGE CELL IN THE ISFSI</b> <b>VAULT WITH PARALLEL</b> <b>REFLECTIVE BOUNDARY</b> <b>CONDITIONS</b>

Revision 0 January 2006



<b>FSAR UPDATE</b>
<b>HUMBOLDT BAY ISFSI</b>
<b>FIGURE 7.3.4</b> <b>TOP VIEW OF SINGLE</b> <b>STORAGE CELL IN THE ISFSI</b> <b>VAULT WITH PARALLEL</b> <b>REFLECTIVE BOUNDARY</b> <b>CONDITIONS</b>

Revision 0 January 2006

# HUMBOLDT BAY ISFSI FSAR UPDATE

## Chapter 8

### **ACCIDENT ANALYSES**

#### CONTENTS

<u>Section</u>	<u>Title</u>	<u>Page</u>
8.1	OFF-NORMAL OPERATIONS	8.1-1
8.1.1	Off-Normal Pressures	8.1-2
8.1.2	Off-Normal Environmental Temperatures	8.1-3
8.1.3	Confinement Boundary Leakage	8.1-5
8.1.4	Cask Drop Less Than Allowable Height	8.1-5
8.1.5	Loss of Electric Power	8.1-6
8.1.6	Cask Transporter Off-Normal Operation	8.1-6
8.1.7	References	8.1-8
8.2	ACCIDENTS	8.2-1
8.2.1	Earthquake	8.2-1
8.2.2	Tornado	8.2-13
8.2.3	Flood	8.2-15
8.2.4	Tsunami	8.2-16
8.2.5	Fire	8.2-17
8.2.6	Explosion	8.2-25
8.2.7	Drops and Tip-Over	8.2-36
8.2.8	Leakage from Confinement Boundary	8.2-36
8.2.9	Mis-Loading of a Damaged Fuel Assembly	8.2-37
8.2.10	Extreme Environmental Temperature	8.2-37
8.2.11	100 Percent Fuel Rod Rupture	8.2-38
8.2.12	Lightning	8.2-39
8.2.13	Turbine Missiles	8.2-40
8.2.14	Blockage of MPC Vent Holes	8.2-40
8.2.15	Aqueous Ammonia Release from the HBGS	8.2-43
8.2.16	References	8.2-44
8.3	SITE CHARACTERISTICS AFFECTING SAFETY ANALYSIS	8.3-1



**ACCIDENT ANALYSES**

TABLES

<u>Table</u>	<u>Title</u>
8.2-1	Key Input Data for Transporter Stability
8.2-2	Transporter Simulations
8.2-3	Maximum Transporter Excursions
8.2-4	Peak Impact Load From Dynamic Analysis of HI-STAR HB in Vault
8.2-5	Effective Design Loads and Amplification Factor for Vault Structural Integrity Analysis
8.2-6	Reinforced Concrete Properties
8.2-7	Properties of Carbon Steel Shell Liner, ASME SA-36
8.2-8	Soil Properties
8.2-9	Deleted
8.2-10	Deleted
8.2-11	Results of Cask Engulfing Fire Analysis
8.2-12	Results of Non-Engulfing Fire Analyses
8.2-13	Result from Explosion Analyses
8.2-14	Extreme Environmental Temperature Results
8.3-1	Summary of Site Characteristics Affecting Safety Analysis

## **ACCIDENT ANALYSES**

### FIGURES

<u>Figure</u>	<u>Title</u>
8.2-1	VN Simulation Model Showing HI-STAR HB Carried by Transporter
8.2-2	Visual Nastran Simulation Model of Vault Liner Containing Loaded HI-STAR HB
8.2-3	Vault Finite Element Model
8.2-4	Vault and Subgrade Finite Element Model
8.2-5	Global Cross Sections Evaluated for Capacity/Demand Ratio

CHAPTER 8

**ACCIDENT ANALYSES**

This chapter describes the accident analyses for the Humboldt Bay Independent Spent Fuel Storage Installation (ISFSI). Sections 8.1 and 8.2 evaluate the safety of cask transportation and lowering activities, and long-term ISFSI storage operations under applicable off-normal operations and accident conditions, respectively. Off-normal events and accidents associated with movement of the HI-STAR HB within the RFB are considered within the scope of 10 CFR 50 and are addressed in PG&E's License Amendment Request 04-02 on Docket 50-133 in PG&E Letter HBL-04-016 dated July 9, 2004. For each event, the postulated cause of the event and the evaluation of the event's effects and consequences, including radiological impact, are presented. The results of the evaluations described herein demonstrate that the HI-STAR HB System can withstand the effects of off-normal events and accidents without affecting function and the consequences of the events are in compliance with the applicable acceptance criteria. Section 8.3 summarizes site characteristics that affect the safety analysis.

**8.1 OFF-NORMAL OPERATIONS**

This section addresses events designated as Design Event II, as defined by ANSI/ANS-57.9 (Reference 1). The following are considered off-normal events for the Humboldt Bay ISFSI:

- Off-normal pressures
- Off-normal environmental temperatures
- Confinement boundary leakage
- Cask drop less than allowable height
- Loss of electric power
- Cask transporter off-normal operation

For each event, the postulated cause of the event, detection of the event, an evaluation of the event effects and consequences, corrective actions, and radiological impact are presented. The following sections present the evaluation of the HI-STAR HB System and the Humboldt Bay ISFSI for the design-basis, off-normal conditions that demonstrate that the requirements of 10 CFR 72.122 are satisfied and that the corresponding radiation doses satisfy the requirements of 10 CFR 72.104(a).

### **8.1.1 OFF-NORMAL PRESSURES**

The confinement pressure boundary for the HI-STAR HB System is the multi-purpose canister (MPC). Internal pressure in the MPC is a function of the initial helium fill pressure, variations in the helium temperature, and leakage of any gases contained within the fuel rods. The MPC off-normal pressure evaluation addresses the hypothetical rupture of a certain number of fuel rods, which subsequently release the gases contained in the fuel rods (initial fill gas and fission gases) into the MPC cavity. This evaluation assumes that 10 percent of the fuel rods rupture, allowing 100 percent of the fill gas and 30-percent of the fission gases from these fuel rods to be released to the MPC cavity. This assumption is consistent with the guidance in NUREG-1536 for the review of dry storage cask designs (Reference 2), as clarified by Interim Staff Guidance (ISG) 5 (Reference 3).

#### **8.1.1.1 Postulated Cause of Off-Normal Pressure**

After fuel assembly loading, the MPC is drained, dried, and backfilled with helium to ensure long-term fuel cladding integrity during dry storage. The pressure of the gas in the MPC cavity is affected by the initial fill pressure, the MPC cavity volume, the decay heat emitted by the stored fuel, fuel-rod gas leakage, ambient temperature, and solar insolation. Of these, the initial fill pressure and MPC cavity volume do not vary with time in storage and can be ignored as a cause of off-normal pressure. The decay heat emitted by the stored fuel decreases with time and is conservatively accounted for in the analysis by using the highest rate of decay heat. Temperature-induced internal MPC pressure increases are addressed in Section 8.1.2.

Off-normal MPC internal pressure is caused by the release of fuel rod gases into the MPC cavity. However, there is no credible off-normal condition that can cause the fuel rods of an intact fuel assembly to rupture. Fuel assemblies classified as damaged fuel due to fuel rod damage will likely have already released their fission gases prior to loading into the MPC-HB. Nevertheless, the off-normal pressure event is conservatively evaluated considering a non-mechanistic rupture of ten percent of the maximum permitted number of total stored fuel rods in the MPC-HB (i.e., eight fuel assemblies).

#### **8.1.1.2 Detection of Off-Normal Pressure**

The HI-STAR HB System is a fully welded pressure vessel designed to withstand the MPC off-normal internal pressure without any effects on its ability to perform its design safety functions. The MPC has no pressure relief design features. No personnel actions or equipment are required to respond to an off-normal pressure event. Therefore, no detection instrumentation is required and the event, if it occurred, would be undetectable.

#### **8.1.1.3 Analysis of Effects and Consequences of Off-Normal Pressure**

In analyzing the off-normal pressure event, the initial conditions are that the MPC is at its normal steady-state long-term storage temperature and pressure. Normal ambient temperature and solar insolation are assumed. The internal gas volume from ten percent of the fuel rods is assumed to be added to the helium in the MPC cavity and the resultant pressure is calculated using the Ideal Gas Law.

The resulting pressure was computed to be 73.63 psig. This value is an increase of 2.74 psig above the computed normal internal MPC pressure (which conservatively assumes 1 percent rod rupture) and is below the MPC off-normal design pressure of 110 psig and the normal design pressure of 100 psig. Therefore, the HI-STAR HB System meets the acceptance criterion for this off-normal event.

#### **8.1.1.4 Corrective Action for Off-Normal Pressure**

The HI-STAR HB System is designed to withstand the off-normal pressure without any effect on its ability to maintain safe storage conditions. The confinement boundary of the MPC is maintained for this event. Therefore, there are no corrective actions associated with off-normal pressure.

#### **8.1.1.5 Radiological Impact from Off-Normal Pressure**

The off-normal pressure event has no radiological impact because the confinement boundary and shielding integrity are not affected.

### **8.1.2 OFF-NORMAL ENVIRONMENTAL TEMPERATURES**

The off-normal temperature evaluation addresses a potential low magnitude, short-term elevation of ambient temperature above the annual average value used in the thermal analysis for normal storage conditions. This off-normal event is of a short duration and is postulated to occur during long-term storage operations with the cask in the vault and the vault lid installed. Therefore, the resultant fuel cladding temperature for the cask evaluations is compared against the accident condition (short-term) temperature limit.

#### **8.1.2.1 Postulated Cause of Off-Normal Environmental Temperatures**

The off-normal environmental temperature is postulated as a constant ambient temperature caused by unusual weather conditions. To determine the effects of off-normal temperature, it is conservatively assumed that these temperatures persist for a sufficient duration to allow the HI-STAR HB System to achieve thermal equilibrium. Because of the large mass of the HI-STAR HB System with its corresponding large thermal inertia and the limited duration for the off-normal temperatures, this assumption is conservative.

#### **8.1.2.2 Detection of Off-Normal Environmental Temperatures**

The HI-STAR HB System is designed to withstand off-normal environmental temperatures without any effects on its ability to maintain safe storage conditions. There are no personnel actions or equipment required for mitigation of an off-normal temperature event. Deleterious effects of off-normal temperatures on the cask transporter and concrete storage vaults are precluded by design. Ambient temperature is available from thermometers used at the Humboldt Bay Power Plant (HBPP) site. Due to the benign climatic conditions at HBPP and the conservative nature of the evaluation of the off-normal temperature event, no administrative controls for temperature monitoring are required for onsite cask transportation operations.

#### **8.1.2.3 Analysis of Effects and Consequences of Off-Normal Environmental Temperatures**

There are no adverse safety effects on the cask transporter or concrete storage vault resulting from off-normal environmental temperatures because they are designed for these temperature ranges.

The off-normal event, considering an off-normal ambient temperature of 60°F, has been evaluated for the HI-STAR HB System. This ambient temperature value exceeds the annual average site ambient temperature of 52°F used for the normal condition thermal analysis. The evaluation was performed for the loaded overpack, assuming design-basis fuel with the maximum decay heat and the most restrictive thermal resistance. The 60°F environmental temperature was applied with peak solar insolation applicable to the HBPP site.

Due to the low decay heat load in the casks at the Humboldt Bay ISFSI, a simplified, very conservative approach was used to evaluate this event. That is, the difference between the normal condition ambient air temperature and the off-normal ambient air temperature, 8°F, was simply added to the computed normal long-term fuel cladding and component temperatures. This is conservative because an increase in ambient temperature will not cause a degree-for-degree increase in the fuel cladding and component temperatures. The resulting fuel cladding temperature for this off-normal event is 381°F, which is well below the temperature limit of 1058°F for off-normal events and is also well below the normal condition fuel cladding temperature limit of 752°F. Likewise, all component temperatures remain well below their respective temperature limits.

The off-normal event, considering a limiting low environmental temperature of -40°F and no insolation for a duration sufficient to reach thermal equilibrium, has been evaluated for the generic HI-STAR system with respect to overpack material brittle fracture at this low temperature. The overpack and MPC are conservatively assumed to reach -40°F throughout the structure. This evaluation is discussed in Section 3.1.2.3 of the HI-STAR 100 System Final Safety Analysis Report (FSAR) (Reference 4). These results are applicable to the HI-STAR HB System because the same materials are used in the two



designs. Due to the benign climatic conditions at HBPP, no administrative controls are required for cask transport operations.

### **8.1.2.4 Corrective Action for Off-Normal Environmental Temperatures**

The HI-STAR HB System is designed to withstand the off-normal environmental temperatures without any effects on its ability to maintain safe storage conditions. The integrity of the MPC confinement boundary is maintained. The cask transporter and ISFSI vault are designed for temperature ranges consistent with the dry storage cask components used at these facilities. Therefore, no corrective actions are required for off-normal environmental temperature conditions.

### **8.1.2.5 Radiological Impact of Off-Normal Temperatures**

Off-normal environmental temperatures have no radiological impact as the integrity of the confinement barrier and shielding effectiveness are unaffected by off-normal ambient temperatures.

## **8.1.3 CONFINEMENT BOUNDARY LEAKAGE**

The MPC has a welded confinement boundary to confine radioactive material under all design-basis normal, off-normal, and accident conditions. The confinement boundary is defined by the MPC shell, baseplate, MPC lid, and vent and drain port cover plates. The closure ring provides a redundant welded confinement boundary. As described in Section 4.2.3.1, the MPC meets all of the criteria in ISG 18 (Reference 5). Therefore, leakage of radioactive material from the MPC is considered non-credible and no confinement dose analysis is necessary.

Since this event is applicable only to the MPC, the evaluation is applicable for all locations (i.e., during onsite cask transportation, lowering activities, and long-term storage at the ISFSI vault). No cause, consequences, or corrective actions are discussed for this event.

## **8.1.4 CASK DROP LESS THAN ALLOWABLE HEIGHT**

Cask drops outside the Refueling Building (RFB) are not credible due to the design of the cask transporter and the ISFSI storage vaults, as discussed in Section 8.2.7. The structural load path members of the HI-STAR HB overpack (the lifting trunnions) and the cask transporter (lift links, connector pins, and lift beam) used in Humboldt Bay ISFSI operations are designed, operated, fabricated, tested, inspected, and maintained in accordance with the applicable guidelines of NUREG-0612 (Reference 6). The loaded MPC is never lifted separately from the overpack (i.e., there are no MPC transfer operations required with the HI-STAR HB System). Therefore, a drop of the loaded HI-STAR HB during cask operations is not a credible event. No cause, consequences, or corrective actions are discussed for this event.

### **8.1.5 LOSS OF ELECTRIC POWER**

A total loss of external AC electric power is postulated to occur as a result of either a disturbance in the offsite electric supply system or the failure of equipment in the electrical distribution system feeding the ISFSI storage site.

#### **8.1.5.1 Postulated Cause of Loss of Electric Power**

Loss of the external power supply may occur as the result of natural phenomena, such as lightning strike or high winds, or as a result of undefined factors causing a disturbance in the offsite electrical grid. Loss of electrical power may also result from an electrical system fault or the failure of electrical distribution equipment such as a transformer.

#### **8.1.5.2 Detection of Loss of Electrical Power**

Loss of electrical power would be detected by the failure of electric-powered equipment.

#### **8.1.5.3 Analysis of Effects and Consequences of Loss of Electrical Power**

A loss of electric power does not affect the cask transporter because all active functions of the transporter, such as cask lifting, are driven from the onboard engine. There is no effect on the ability of the HI-STAR HB System to safely continue storing the spent fuel at the ISFSI storage site during a loss of electric power event because the dry storage system is a completely passive design. No electric-powered equipment is used with the storage overpack while it is in its storage configuration in the concrete storage vaults.

#### **8.1.5.4 Corrective Action for Loss of Electric Power**

There are no corrective actions required for the assumed loss of electric power. The ability of the HI-STAR HB System to safely store spent fuel at the ISFSI storage site is not compromised.

#### **8.1.5.5 Radiological Impact of Loss of Electric Power**

The off-normal event of loss of electric power has no radiological impact because the MPC confinement barrier is not breached and shielding is not affected.

### **8.1.6 CASK TRANSPORTER OFF-NORMAL OPERATION**

Off-normal operation of the cask transporter includes postulation of the following human performance and active component failures during transport of the loaded overpack:

- Driver error
- Driver incapacitation

- Transporter engine failure
- Loss of hydraulic fluid

#### **8.1.6.1 Postulated Cause of Cask Transporter Off-Normal Operation**

Cask transporter driver error may be caused by poor training or any of several human performance-related causal factors. Driver incapacitation would be most likely caused by a sudden medical emergency. Transporter engine failure may be caused by a variety of mechanical problems typical of combustion engines. A loss of hydraulic fluid may be caused by a leak anywhere in the hydraulic system.

#### **8.1.6.2 Detection of Cask Transporter Off-Normal Operation**

Driver error or driver incapacitation would be detected by the support staff walking along with the transporter on the transport route observing the driver in distress or erratic transporter motion. Transporter engine failure would be detected by the halt of any engine-driven activity taking place at the time. A hydraulic fluid leak would be detected by the pressure instrumentation in the hydraulic system and possibly by visual observation of leaking fluid.

#### **8.1.6.3 Analysis of Effects and Consequences of Cask Transporter Off-Normal Operation**

In addition to the transporter driver, transport operations will be conducted with a support team consisting of security and other personnel affiliated with the fuel movement walking along with the transporter to ensure a safe and efficient move of the loaded cask from its point of origin to its destination. These personnel will be observing the movement of the transporter to ensure the designated travel path is being followed. Should the transporter start to veer from the travel path, the transporter will be stopped (either by the driver or by a support team member using either of two external stop switches mounted on the outside of the transporter), the cause investigated, and corrective actions taken to get the vehicle back on the correct path.

Incapacitation of the driver will be addressed by the design of an automatic shutoff control where the vehicle will stop whenever the control is released. The same control is used to move the transporter vehicle and operate the cask lifting apparatus integral to the transporter. A selector switch is used to ensure only one function can be performed by the transporter at a time. Also, either of two emergency stop switches, mounted on the outside of the transporter, can be operated to stop the transporter.

A transporter engine failure will result in the vehicle stopping or the hydraulic brakes engaging to stop any lift operations in progress.

A loss of hydraulic fluid will cause a loss of pressure in the hydraulic system that will engage the hydraulic brakes and stop movement of the lifting apparatus.

Based on the above evaluation, there are no unacceptable consequences caused by cask transporter off-normal operation.

### **8.1.6.4 Corrective Action for Cask Transporter Off-Normal Operation**

The corrective actions for cask transporter off-normal operation would be developed and implemented based on the nature and safety significance of the problem at the time it occurs. Corrective actions may include additional training for the driver, replacement of the driver, improved operating procedures, and repair or replacement of failed mechanical parts. The transporter is designed “fail-safe” to preclude uncontrolled lowering of the loaded overpack if a failure of an active component occurs, so no corrective actions related to the cask are necessary. If necessary, cribbing could be used to support the loaded overpack if the transporter needs to be replaced or detached from the load for repairs.

### **8.1.6.5 Radiological Impact of Cask Transporter Off-Normal Operation**

The cask transporter off-normal event has no radiological impact since the confinement barrier is not breached and shielding is not affected.

### **8.1.7 REFERENCES**

1. ANSI/ANS 57.9-1992, Design Criteria for an Independent Spent Fuel Storage Installation (dry type), American National Standards Institute.
2. Standard Review Plan for Dry Cask Storage Systems, USNRC, NUREG-1536, January 1997.
3. Interim Staff Guidance 5, Confinement Evaluation, USNRC, Revision 1.
4. Final Safety Analysis Report for the HI-STAR 100 System, Holtec International Report No. HI-2012610, Revision 1, December 2002.
5. Interim Staff Guidance 18, The Design/Qualification of Final Closure Welds on Austenitic Stainless Steel Containers as Confinement Boundary for Spent Fuel Storage and Containment Boundary for Spent Fuel Transportation, Revision 0, USNRC, May 2003.
6. Control of Heavy Loads at Nuclear Power Plants, USNRC, NUREG-0612, July 1980.

## **8.2 ACCIDENTS**

### **8.2.1 EARTHQUAKE**

An earthquake is classified as a natural phenomenon Design Event IV as defined in ANSI/ANS-57.9 (Reference 1). The effects of seismic events on cask loading operations inside the refueling building (RFB) are discussed in the 10 CFR 50 License Amendment Request submitted in support of Humboldt Bay Independent Spent Fuel Storage Installation (ISFSI). This section addresses the effect of a seismic event on the operations related to the Humboldt Bay ISFSI that occur outside the RFB. Cask handling activities outside the RFB were reviewed to identify potential risk significant configurations during a seismic event. The seismic evaluations address the following potentially risk significant configurations (all configurations are analyzed with a multi-purpose canister (MPC) loaded with spent fuel):

- (1) HI-STAR HB cask oriented vertically on the rail dolly while traversing the Humboldt Bay Power Plant (HBPP) Unit 3 yard prior to being picked up by the transporter.
- (2) HI-STAR HB cask being transported to the ISFSI storage vault, suspended vertically from the cask transporter.
- (3) HI-STAR HB cask being lowered into the ISFSI storage vault, suspended vertically from the cask transporter.
- (4) HI-STAR HB cask stored in the ISFSI storage vault

Additionally, the slopes around the ISFSI and transport route were analyzed for stability during a seismic event as described in Section 2.6.7.

#### **8.2.1.1 Cause of Accident**

Earthquakes are natural phenomena caused by the movement of large geological plates under the earth's surface.

#### **8.2.1.2 Earthquake Accident Analysis**

Two methods were used for seismic analysis of structures, systems, and components (SSCs), that is, equivalent static analysis method and dynamic analysis method. These methods were used as follows:

##### **Equivalent Static Analysis Method**

- (1) Design of the reinforced concrete vault.

The concrete vault structure was subject to the load combinations of ACI-349-01 (Reference 2). Loadings considered were dead weight of the vault structure plus the contained casks, lateral soil static pressures, thermal loads from temperature gradients arising from the presence of the casks, seismic loading from the vault inertia, and seismic loads arising from the seismic restraint of the casks. The peak values from individual loadings were oriented in directions providing maximum combined demand on the vault structure. Static finite element analyses of the concrete vault structure were performed under individual loads and the results combined to form the Code load combinations

### Dynamic Analysis Method

- (1) Determination of slope stability.
- (2) This analysis is described in detail in Section 2.6.7.
- (3) Determination of transporter stability while carrying a loaded overpack. Transporter stability is evaluated by integrating the equations of motion describing the transporter and the loaded HI-STAR HB. The computer code Visual Nastran (VN) (Reference 3), capable of simulating the dynamic behavior of bodies, which may make or break contact with the ground surface, and which are subject to nonlinear time history load inputs in the form of inertia forces proportional to the design basis earthquake ground acceleration time histories. This computer code has previously been used in licensing the HI-STAR 100 System as described in the HI-STAR 100 System Final Safety Analysis Report (FSAR) (Reference 4). The results from the dynamic simulations were used to demonstrate that the transporter, carrying the loaded cask, would not overturn, and would not depart from the roadway. Simulations were performed for the loaded transporter on level ground and on the design basis grade for the path from the yard to the ISFSI vault. Analysis details are presented in Section 8.2.1.2.2.
- (4) Determination of storage cask loads on the vault. Loads from the restraint of movement of the storage casks during a design basis seismic event are transmitted to the walls of the vault through seismic restraint shims. The loads are determined by modeling a loaded cask, the cylindrical walls and the floor of a cask pit in the vault, and the top and bottom shims. The vault is driven by the time history of ground accelerations associated with the design basis earthquake and the resulting equations of motion solved using direct integration in the time domain. The computer code VN (Reference 3) is used as the simulation engine; the results for the shim loading at each of the shims (8 each, top and bottom) used to restrain the cask in a vault cask pit are determined at each instant of time during the simulation and include the effect of the



clearance gap between the shims and the cask body. Analyses details are presented in Section 8.2.1.2.4.

- (5) Determination of storage cask response while on the dolly. The response of the storage cask/dolly system while in the yard (after exiting the RFB but prior to the cask being attached to the transporter), was evaluated using the time history method with the cask and dolly modeled in the computer code VN (Reference 3). Large motions of the dolly relative to ground and of the cask relative to the dolly and to ground, were expected to occur under the design basis earthquake up to and including overturning of the cask. The results from the dynamic simulation were focused on the prediction of maximum decelerations of the cask to demonstrate that HI-STAR design basis limits (Reference 4) remained valid. A summary of the analyses performed is presented in Section 8.2.1.2.1.

Information relevant to validation of the Visual Nastran[®] finite element analysis program for use in performing cask drop and tip-over analyses is provided in the PG&E Response to NRC Question 5-3 in Reference 27.

As discussed in Sections 2.6.6 and 3.2.4, there are three licensing basis earthquake ground motions corresponding to the specific evolution. These are: storage (a 2000-year return period), transport (14-year return period) and handling at the vault (also 14-year return period). For each of these earthquake scenarios, there is a corresponding design basis earthquake (DBE) that exceeds the required licensing basis for added conservatism. In these analyses there are four earthquakes used to bound the requirements. These are termed the DBE, the 50 percent DBE, the 25 percent DBE and the 1978 Safe Shutdown Earthquake Evaluation RFB Spectra (SSEERFB). The DBE spectra are defined for periods up to 10 seconds. Four sets of spectrum compatible time histories were generated containing a range of characteristics of the near fault effects (Reference 5). The regenerated DBE time histories meet the NRC Standard Review Plan spectral matching criteria, Section 3.7.1 of NUREG-0800, (Reference 6) and the three components of the time-histories for each earthquake were verified to be statistically independent in accordance with ASCE 4-98 (Reference 7).

### **8.2.1.2.1 Seismic Evaluation of Operations Involving the Rail Dolly – Seismic Configuration 1**

This section discusses the seismic stability evaluation of the spent fuel cask on the rail dolly used at the Humboldt Bay ISFSI.

The HI-STAR HB cask, containing a loaded MPC, exits the RFB on the rail dolly in a vertical orientation. The rail dolly traverses approximately 100 ft in a southerly direction from the RFB on a level surface. Figure 4.3-2 shows the rail dolly and cask during this operational mode.

While this evolution is expected to take less than one hour per cask, one half day per cask is conservatively used, which would equate to a required return period of 14 years as described in Section 3.2.4. To add defense in depth, this evolution is conservatively analyzed for both the full DBE as well as the SSEERFB ground motions, which equates to nearly a 50-year return period earthquake in order to impose the maximum demand load on the cask contents. This analysis is contained in calculation HI-2033046 (Reference 8). The dynamic simulation was performed using VN (Reference 3). The analyses determined that the cask and dolly were stable and the cask did not slide off the dolly or tip over under the SSEERFB condition. Under the full DBE event, the dolly would tilt and the HI-STAR cask would slide off the dolly and overturn. However, even under this conservatively predicted demand, the decelerations experienced by the contained fuel during the overturning and subsequent ground impact did not exceed the HI-STAR design basis limit of 60 g. Therefore, the contained fuel and the cask meet all of the design basis requirements of the HI-STAR FSAR (Reference 4) even under a most conservative seismic loading that would ensure cask overturning.

### **8.2.1.2.2 Seismic Evaluation of Cask Transport to the ISFSI - Seismic Configuration 2**

This section discusses the seismic stability evaluation of the spent fuel cask transporter used at the Humboldt Bay ISFSI.

After the HI-STAR HB cask exits the RFB on the rail dolly, the cask transporter lifts the HI-STAR and carrying the cask in a vertical orientation, moves along the transport route approximately 0.24 miles to the ISFSI storage site, in the process traversing an incline grade that does not exceed 8.5 percent (nominal). Figure 4.3-1 shows the cask transporter and cask during this operational mode.

While this evolution is expected to take less than one hour per cask, one half day per cask is conservatively used, which would equate to a required return period of 14 years as described in Section 3.2.4. To add defense in depth, this evolution is conservatively analyzed for both the full DBE as well as 50 percent of the DBE ground motions, which equates to greater than a 50-year return period earthquake. The analysis determined that the transporter would not overturn under any of the events, or leave the roadway under the 50 percent event. The seismic stability analysis of the transporter on the transport route is provided in calculation HI-2033036 (Reference 9).

The transport route is located on surficial deposits similar to those forming the ISFSI vault foundation (Section 2.6.4). As described in Section 2.6.7, Calculation GEO.HBIP.02.08 (Reference 10) shows that the transport route is free from uncontrolled ground movement. At the 50 percent ground motion, the subsidence is expected to be nearly zero.

In summary, the transporter will remain stable under seismic conditions while the transporter is traversing the entire transport route.

### **Methodology**

The DBE seismic events for the Humboldt Bay ISFSI, described in Section 8.2.1.2, were evaluated and applied as inputs for the transporter stability analysis. Four sets of DBE time-histories were used to demonstrate transporter stability as it carries a loaded cask on the transport route. As discussed in Section 2.6.6, the DBE spectra and associated time histories are appropriate for use along the transport route.

VN 4-D (Reference 3) serves as the simulation engine to obtain the response to the 3-dimensional seismic events. The time-domain dynamic simulations model the cask transporter, and the HI-STAR HB cask, including contents, as rigid bodies. The mass and inertia of the MPC and the contained spent fuel is lumped with the mass and inertia of the overpack.

The cask transporter sits on a grade that is subjected to a ground acceleration time history appropriate to the free field DBE event. The simulations use the model of the cask transporter with a track width and length identical to that planned for the Humboldt Bay cask transporter. Figure 8.2-1 shows the VN model of the cask and transporter as imported from a CAD program with mass and inertia properties. The cask and transporter are two separate rigid bodies with the cask held to the transporter by two vertical flexible links. Side-to-side and fore-to-aft restraints are not shown.

### **Acceptance Criteria**

The cask transporter plus its carried load must remain stable (not overturn) and remain on the travel path under all seismic events applicable to the Humboldt Bay ISFSI site. The minimum roadway width is 26 ft, and an allowable transporter lateral sliding distance of 70 inches is used. The maximum acceptable sliding movement along the roadway is not limited, as there are no consequences of longitudinal movement.

### **Assumptions**

The following key assumptions were employed to construct the models for the simulations:

- (1) The time domain dynamic analyses of the transporter seismic stability simulate the modeled components (cask transporter and loaded overpack) as rigid bodies with specified geometry and bounding mass. These are conservative assumptions for the seismic analysis since energy dissipation in the dynamic system from rattling of the cask contents is neglected.
- (2) The analyses in time domain are simplified by assuming the rigid bodies to have uniform mass density when calculating their mass moments of inertia and mass center locations. Any shift in the centroid due to this assumption has a negligible effect on the results of the analysis.

## HUMBOLDT BAY ISFSI FSAR UPDATE

- (3) The coefficient of restitution for the internal contact surfaces (MPC/overpack) is set to zero. The coefficient of restitution between the transporter treads and the ground was set to 0.5 (the exact value has no influence on the solution when sliding movements predominate). For the coefficient of friction at the transporter tread/ground interface, an upper bound value of 0.8 was conservatively assumed to emphasize tipping action. A lower bound value for the tread/roadway surface of 0.4 was assumed to emphasize any sliding behavior of the transporter.
- (4) The time domain dynamic simulations use a generic model of the cask transporter with a track length that is equal to the length of the Humboldt Bay cask transporter tracks. The analyses considered the stability of the cask transporter when on both a horizontal ground surface and an 8.5 percent grade.
- (5) In all stability analyses, the positioning of the cask in the cask transporter is set at 36 inches, which is higher than the maximum anticipated carry height, to ensure that overturning moments are conservatively computed at each time point during the dynamic simulations.
- (6) All bodies are assumed to be rigid for the global analysis. The cask transporter design specification includes a requirement that the transporter be designed such that its lowest global natural frequency is in the rigid range. To account for any vertical flexibility of the attachment of the cask to the transporter, suitable linear springs were used to simulate the connection of the cask to the transporter.

### **Key Input Data**

The key input data used in the cask transporter seismic analyses are shown in Table 8.2-1. Input time histories used for the dynamic simulations are the four sets of DBE design earthquake excitations discussed above. The case of these four sets giving the greatest displacement is subsequently used for the 50 percent case.

### **Results of Analyses**

A series of nonlinear dynamic simulations were performed using the VN 4-D computer code to assess the seismic stability of the cask transporter during the four DBE earthquakes. Table 8.2-2 lists the simulations performed for the stability evaluation. The combinations of grade, coefficient of friction, and seismic events have been chosen to be bounding for the site-specific conditions.

Table 8.2-3 summarizes the estimates of the maximum transporter horizontal excursions in the transverse and longitudinal direction for each of the dynamic simulations performed. The reported maximum excursions are at the top of the transporter relative to the ground.

The maximum value of 61 inches reported for the transverse excursion with a friction coefficient of 0.4 demonstrates that in the event of transport earthquake, the transporter will not leave the road while moving from the RFB to the Humboldt Bay ISFSI. The small relative movements reported for the case with friction coefficient of 0.8 demonstrate that overturning of the loaded cask transporter is not a credible event under either the DBE seismic event or the transport earthquake. The values presented in Table 8.2.3 for the DBE may be considered as upper bound values; more realistic values may be obtained by averaging the peak results from the four sets of DBE events.

The time domain dynamic simulations of the cask transporter demonstrate that the cask transporter, carrying a loaded HI-STAR HB cask in the vertical orientation, will not overturn during a seismic event and will not leave the road while moving from the RFB to the storage vault.

### **Cask Drop during Transport (Seismic)**

As discussed in Section 8.2.4, the load path portions of the cask transporter and the lifting devices attached to the cask components will be designed to preclude drop events, either through redundancy or enhanced safety factors. The transporter design will include consideration of seismic loads. Therefore, a seismic event occurring during transport would not result in a cask drop. As additional defense in depth, Holtec has qualified the HI-STAR with an MPC for a vertical cask drop of 21 inches (Section 3.4.9 of Holtec's HI-STAR 100 System FSAR (Reference 4)).

#### **8.2.1.2.3 Seismic Evaluation of Lowering the Cask into the Vault – Seismic Configuration 3**

This section discusses the seismic stability evaluation of the spent fuel cask transporter when lowering the overpack into the storage vault at the Humboldt Bay ISFSI.

At the end of the transport evolution, the overpack must be lowered into the storage vault. Figure 4.3-3 shows the cask transporter and cask during this operational mode. This mode also includes installing the seismic lateral shims and installing the vault lid. This evolution is performed by the cask transporter, and is conservatively estimated to take less than half a day per cask. As stated in Section 3.2.4, the vault cask handling earthquake must be at least a return period of 14 years. The actual analysis is performed with a time history equal to 25 percent of the DBE, which is a return period in excess of 25 years. The analysis is performed using the methodology described above for Configuration 2. This analysis shows that the transporter slides no more than 1.6 inches (Table 8.2-3), which is less than the clearance in the vault cells.

#### **8.2.1.2.4 Seismic Analyses of the HI-STAR HB Overpack Restrained in the ISFSI Storage Vault in its Long-Term Storage Configuration - Seismic Configuration 4**

##### **8.2.1.2.4.1 Cask Seismic Analysis**

Analysis of this configuration is performed in HI-2033014 (Reference 11) using the DBE seismic event (four sets). The DBE is characterized by four sets of free-field acceleration time-histories, in each of three orthogonal directions, with durations of 40 seconds or longer. Therefore, the results from these events are bounding and the dynamic simulations to obtain time-history behavior of the system are performed using the VN simulation code described previously. The HI-STAR HB overpack design difference of significance from the HI-STAR 100 is that it is shorter and lighter. Figure 3.2-1 shows the loaded HI-STAR HB overpack in the ISFSI vault.

##### **Methodology**

Figure 8.2-2 shows the dynamic model used by VN to develop the solutions. Shown in the figure is the vault liner and the HI-STAR HB. The loaded MPC inside the cask is not shown in the figure nor are the top and bottom seismic restraints (lateral shims that restrain the seismic movement of the cask relative to the liner).

The dynamic model of the HI-STAR HB overpack in VN consists of the following major components:

- The HI-STAR HB overpack is modeled as a six-degree of freedom (rigid body) component.
- The loaded MPC is also modeled as a six degree-of-freedom (rigid body) component that is free to rattle inside the overpack shell. Gaps between the two bodies reflect the nominal dimensions from Figures 3.3-1 and 3.3-3.
- The vault cavity is modeled as a rigid cylindrical shell with lid and baseplate attached. The vault cylinder is assumed fixed and the overpack and the contained MPC are driven by known forces, applied at the respective mass centers, which are proportional to their masses multiplied by the appropriate component of the input free-field acceleration
- Shims are simulated by four compression-only linear spring elements at the top of the vault cylinder (initial clearance gap approximately equal to 0.125 inch) and four compression-only elements at the base of the vault cylinder (initial clearance gap approximately equal to 0.875 inch). The top shims are installed after the cask has been lowered into the vault



## HUMBOLDT BAY ISFSI FSAR UPDATE

cavity. The coefficient of friction at the shim locations is conservatively set to zero.

- The contact between the MPC and the overpack is simulated by a classical impulse-momentum equation. The coefficient of restitution is set to 0.254 (reflecting the expected behavior between rattling surfaces) and the coefficient of friction is set to 0.5, which is representative of steel-on-steel.
- The interface contact between the base of the overpack and the ISFSI storage vault is modeled by compression-only linear spring elements together with a coefficient of friction of 0.5.
- Bounding weights are used for the HI-STAR overpack and for the contained MPC. Inertia properties are computed based on these bounding weights.

The simulation model is subject to the four sets of DBE events and the time history of loads in the shim restraints archived for use in the vault structural analysis.

### **Acceptance Criteria**

Two requirements for the shims between the vault and the HI-STAR HB are defined as follows:

- The final shim design must behave as a linear elastic body with the stiffness specified in the simulations.
- The shim will respond in the elastic range to a load level of 1.5 times the actual calculated load.

In addition to the above restraint criteria, it is required to demonstrate that the seismic events do not induce acceleration levels in the body of the cask that exceed the cask design basis (60 g) as defined in the HI-STAR 100 System FSAR (Reference 4).

### **Assumptions**

The key assumptions used in the dynamic model are listed and explained within the methodology description given above.

### **Key Design Inputs**

Bounding weights of 161,200 lb for a loaded HI-STAR HB and 59,000 lb for a loaded MPC are used in the analyses (Reference 11). Dimensions for the two cask bodies are taken from Figures 3.3-3 and 3.3-1, respectively. Mass moment of inertia properties are

determined based on cylindrical body assumptions with the specified mass uniformly distributed.

Seismic inputs for the dynamic analyses are obtained from acceleration time histories developed from the response spectra for the DBE earthquake.

### **Results of Analyses**

The restrained HI-STAR HB overpacks do not exceed the generic cask design basis deceleration limit of 60g under any of the seismic events. The maximum computed cask deceleration is 14g (Reference 11). Therefore, the state of stress in the cask, in the MPC, and in the fuel basket, is assured to remain below the design basis limits of the HI-STAR FSAR (Reference 4) while the loaded HI-STAR HB is in the vault.

The peak interface loads in the shim restraints and on the base of the vault cavity are summarized in Table 8.2-4 for each of the four DBE events. Table 8.2-5 provides the bounding input loads that are used for the vault structural design.

The dynamic simulations also showed that the HI-STAR HB vertical displacement, relative to the vault liner, did not exceed 0.5 inch. This is less than the initial clearance between the top of the HI-STAR HB and the bottom of the vault lid. Therefore, HI-STAR HB will not impact the vault lid during a DBE seismic event.

#### **8.2.1.2.4.2 Storage Vault Seismic Analyses**

The objective of the seismic analyses of the concrete vault is to:

- Ensure that the concrete maintains shielding under normal factored dead and live loads
- Ensure that cask spacing is maintained and the cask-to-vault liner shims maintain their ability to transfer load under applicable load combinations that include seismic events

Static analyses were performed and subsequently combined into applicable load combinations to ensure that the storage vault resisted dead and live loads, the loads resulting from seismic accelerations applied to the vault, and the resultant loads from the cask dynamic analysis (Section 8.2.1.2.4.1).

### **Vault Static Analysis**

#### **Methodology**

The reinforced concrete cask storage vault was analyzed using the finite element method to determine forces and moments on critical sections of the structure. The computer code used was ANSYS (Reference 12) and the modeling and calculations are

documented in calculation HI-2033013 (Reference 13). All sections are designed to provide safety factors greater than 1.0 for the reinforced concrete structure against bending and shear in accordance with ACI 349-01 (Reference 2). Two loading conditions of the vault were considered. The first condition assumed a single loaded cask in the vault and the remaining five cells empty, and the second condition assumed all cells loaded with casks. Figure 8.2-3 shows the finite element model of the vault.

Information about the structural adequacy of the removable seismic restraint gussets, specifically the potential failure due to buckling, is provided in the PG&E Response to NRC Question 5-11 in Reference 27.

The cask storage vault rests on a foundation of 3-D soil finite elements to establish the proper elastic foundation using soil properties. The surrounding soil along the walls of the vault is not modeled. Rather, soil lateral pressures from self-weight and seismic conditions are applied as pressure to the walls of the vault. Figure 8.2-4 shows the vault finite element model resting on the soil subgrade.

Inertial loads due to vault self-weight are computed based on the zero period acceleration (ZPA) of the DBE. The three orthogonal ZPAs are applied in the vault coordinate system and conservatively their effects are combined by absolute sum. Peak loads from HI-STAR HB restraints are applied in directions that correspond to the assumed seismic loads from vault self-weight to assure that all seismic effects conservatively add together. These seismic loads from the contained casks are applied at the shim locations and have the values given in Table 8.2.5.

The thermal analysis of the cask storage vault is a two-step process consisting of calculating: (1) the temperature distribution, and (2) the thermal stresses. For the temperature distribution, a loaded cell has the maximum allowable local temperature applied to its inner surface. Empty cells are considered with adiabatic boundary conditions (i.e., zero heat transfer across the surface) applied to their inner surface. The far-field boundary condition is set at the site annual average soil temperature. Adiabatic boundary conditions also exist over the top surface of the soil and vault. Thermal conductivities are applied to the different materials in the model and the temperature distribution is computed for both loading conditions. A steady-state solution method is used to solve for the nodal temperatures. The nodal temperatures are then used as input to the thermal stress analysis. The resistance to expansion of the vault from the soil is conservatively neglected since it produces compressive loads in the concrete thus increasing its load carrying capacity. The steel liner is not considered in the finite element model when solving for the temperature distribution. Since the liner is thin, it is expected that the temperature through the thickness will be uniform. The shell elements of the liner share common nodes with the adjacent brick elements representing the concrete. Therefore, the nodal temperature distribution is not altered by not including the shell elements in the thermal solution. When computing thermal stresses from the temperature distribution, the shell elements are included and a differential coefficient of thermal expansion between steel and concrete produces thermal stresses.

### **Acceptance Criteria**

Applicable load combinations and capacity limits are those from ACI-349-01 (Reference 2). From all combinations in Reference 2, the following are considered as limiting and are evaluated.

$$U = 1.4D + 1.7L + 1.7H$$

$$U = D + L + H + T_o + W_T$$

$$U = D + L + H + T_o + E_{ss}$$

$$U = 1.05D + 1.3L + 1.3H + 1.275T_o$$

$$U = D + L + H + T_o + A$$

In the above, the following definitions apply:

U = Required strength to resist factored loads

D = Internal forces and moments from dead loads

L = Internal forces and moments from live loads

H = Internal forces and moments due to weight and pressure of surrounding soil

T_o = Internal forces and moments generated by temperature distributions within the concrete structure as a result of normal operating conditions

E_{ss} = Internal forces and moments generated by the DBE seismic event

A = Internal forces and moments from explosion and other similar events.

### **Assumptions**

Normal engineering assumptions associated with developing FEA models (for example, boundary conditions, modeling techniques).

### **Key Input Data**

Tables 8.2-6 to 8.2-8 summarize the material properties used for the vault analysis.

Soil elastic properties for the analyses were obtained from Reference 14.

### **Results**

Capacity evaluations were performed for global sections of the vault (based on diametral sections through the vault cavities. Figure 8.2-5 shows the global sections which were considered. Capacity calculations were also performed for locally loaded areas near shim locations and the vault base at the bottom of a vault cavity. The maximum vault stresses and the embedded steel ductility requirements meet the ACI 349 code requirements.

### **Earthquake Accident Dose Calculations**

The HI-STAR HB overpack and MPC confinement boundary were explicitly analyzed for, and shown to withstand, the seismic ground motion during transport to the storage vaults, and during storage operations, as applicable. The seismic ground motion does not cause stresses above allowable limits in the MPC confinement boundary, or the storage overpack during transport or storage operations. No radioactivity would be released in the event of an earthquake and there would be no resultant dose.

#### **8.2.2 TORNADO**

A tornado is classified as a natural phenomenon Design Event IV, as defined in ANSI/ANS-57.9 (Reference 1). This event involves the potential effects of tornado-induced wind, differential pressure, and missile impact loads on the ISFSI SSCs that are important to safety.

##### **8.2.2.1 Cause of Accident**

The cause of this event is the occurrence, at or near the ISFSI site, of meteorological conditions that are favorable to the generation of a tornado. The HI-STAR 100 System is generically designed to withstand pressures, wind loads, and missiles generated by a tornado as described in Section 2.2.3.5 of the HI-STAR 100 System FSAR (Reference 4). The design-basis tornado and wind loads for the HI-STAR 100 System are consistent with Regulatory Guide (RG) 1.76 (Reference 15), ANSI/ANS 57.9 (Reference 1), and ASCE 7-98 (Reference 16) for Region I as indicated in the HI-STAR FSAR Tables 2.2.4 and 2.2.5. The HI-STAR 100 System is generically designed to withstand three types of tornado-generated missiles. The characteristics of these missiles are provided in Table 3.2-2 and are consistent with Spectrum I missiles described in NUREG-0800, Section 3.5.1.4 and with Table 2.2.5 in the HI-STAR 100 System FSAR.

As discussed in Section 3.2.1.1, the Humboldt Bay ISFSI is located in tornado intensity Region II, based on the RG 1.76 classification system. The design criteria in the HI-STAR 100 System FSAR for Region I wind speeds bound the Humboldt Bay ISFSI tornado licensing basis.

##### **8.2.2.2 Accident Analysis**

The accident analysis for tornado effects involves evaluation of the loaded cask during transport to the ISFSI, transfer operations at the ISFSI, and long-term storage at the ISFSI.

###### **8.2.2.2.1 Transport to the ISFSI**

During transport of the HI-STAR HB System from the RFB to the ISFSI vault, the loaded cask is carried in a vertical orientation and is exposed to the environment. HI-STAR

100, FSAR Section 3.4.8, analyzes and concludes that there are no radiological releases associated with any tornado missile impacts on the HI-STAR 100 System. By similarity of design with the HI-STAR 100 System, the HI-STAR HB System is capable of withstanding impacts due to tornado missiles without loss of the confinement boundary or any significant damaged to the cask. The cask transporter has redundant drop protection by design (Section 3.3.3). Therefore, a drop of the load due to a direct strike on the transporter is not credible.

### **8.2.2.2.2 Transfer Operations at the ISFSI Vault**

During lowering of the HI-STAR HB into the ISFSI vault, the HI-STAR HB is exposed to the environment. The lowering operation will be a short duration (nominally less than two hours). Therefore, a tornado missile impact during cask lowering into the vault is not considered credible. Although a tornado missile during the lowering is not considered credible, the cask transporter has redundant drop protection and therefore a drop of load due to a direct tornado missile strike is not credible.

The basis for concluding that a tornado missile impact during cask lowering is not credible is further explained in the PG&E Response to NRC Question 15-4 in Reference 27. The response to Question 15-4 also notes that ISFSI TS 5.1.5 includes requirements to evaluate the weather conditions projected to be present during transport and lowering activities to ensure that no severe weather is projected for the area.

Nevertheless, by similarity of design with the HI-STAR 100 System, the HI-STAR HB System is capable of withstanding impacts due to tornado missiles without loss of the confinement boundary or any significant damaged to the cask.

### **8.2.2.2.3 Long-Term Storage in the ISFSI Vault**

Given the massive size of the reinforced concrete vault, specifically the steel-encased concrete lid, tornado missiles and their impacts on the structure will likely not produce any significant adverse structural effect on the vault. Because the cask system is designed to absorb tornado missile impacts without significant damage, no tornado missile analyses were performed for the vault structure. While localized denting of the lid steel and spalling of the vault apron may occur, the structural integrity of the vault will be preserved and the cask protected from tornado missile impacts.

The vault is not a target for horizontal missiles due its below-grade location. In addition, NUREG-0800, Section 3.5.1.4, indicates that vertical missile velocities required to be considered are 70 percent of the postulated horizontal velocities, except for small missiles that are used to test barrier openings. The ISFSI vault has no openings; therefore, small missiles are not required to be evaluated.

The HI-STAR 100 System has been analyzed to withstand tornado missiles impacting the side and top of the cask at 100 percent of the postulated horizontal velocities, which



bounds the requirements for vertical missiles without taking credit for the vault structure. However, localized denting of the vault concrete lid from a vertical tornado missile may slightly decrease the shielding effectiveness of the lid in the local area around the point of impact. This effect is addressed in Section 8.2.2.4.

### **8.2.2.3 Conclusions**

The HI-STAR HB overpack provides an effective tornado missile barrier for the MPC. No potential tornado missile strike would cause tip over of the cask, compromise the integrity of the confinement boundary, cause a cask drop, or jeopardize retrievability of the MPC. In addition, global stress intensities arising from the missile strikes satisfy ASME Code, Section III, Level D limits for an accident condition. Therefore, the requirements of 10 CFR 72.122(b) are met with regard to tornados.

### **8.2.2.4 Accident Dose Calculations**

Extreme winds in combination with tornado missiles are not capable of damaging an MPC located within a HI-STAR HB overpack. Therefore, no radioactivity would be released due to tornado effects on the HI-STAR HB cask. If there is local reduction of shielding provided by the vault lid due to denting and/or loss of concrete, the local dose rates could increase. However, there should be no noticeable increase in the ISFSI site or controlled-area boundary dose rate, because the affected area will likely be small. In the event of such an accident occurring, the 100-meter controlled area will be maintained as described in Section 2.1.2, and an ISFSI operator will first perform a radiological and visual inspection to determine the extent of the damage to the vault. As appropriate, temporary shielding would be placed around the affected area to reduce dose rates.

## **8.2.3 FLOOD**

A flood is classified as a natural phenomenon Design Event IV in accordance with ANSI/ANS 57.9.

### **8.2.3.1 Cause of Accident**

The probable maximum flood is classified as a severe natural phenomenon. Floods are generally predictable events caused by extended periods of rainfall, storm surges, or structural failures, such as a dam break.

The ISFSI site is located on a relatively flat area on Buhne Point at elevation 44 ft mean lower low water (MLLW). Surface drainage around the ISFSI area flows naturally into the existing plant drainage system. The plant drain system then discharges the surface water into the cooling water intake canal, which flows through the plant, and discharges into Humboldt Bay via the cooling water discharge canal. Outside the area served by the plant drainage system, most of the surface runoff drains to the east and into the discharge canal. The remainder drains into Buhne Slough, a natural drainage for the

area, which drains directly into both the intake canal and Humboldt Bay. The elevation of the ISFSI is approximately 32 ft higher than the main power plant level. Thus, any drainage will be away from the ISFSI area, and flooding is not a concern.

### **8.2.3.2 Accident Analysis**

The HI-STAR HB System is designed to withstand pressure and water forces associated with flooding in the same manner as the HI-STAR 100 System. Table 2.2.8 of the HI-STAR FSAR indicates that the HI-STAR 100 overpack is capable of being submerged to a maximum depth of 656 ft. This flooding water depth is based on the submergence requirement of 10 CFR 71 for the dual purpose-certified HI-STAR 100 System.

As shown in Section 2.4, the maximum flood level will not impact the transport route. Therefore, flooding during transport is not considered credible.

In addition, the HI-STAR HB System is designed to withstand the pressure and water forces associated with floods, based on the similarity in design to the HI-STAR 100 System. Also, the Humboldt Bay ISFSI vault is designed for a six-ft static head of water. In conclusion, the ISFSI can withstand floods as required by 10 CFR 72.120(a) and 72.122(b).

### **8.2.3.3 Accident Dose Calculations**

Flooding has no significant effect on the Humboldt Bay ISFSI based on the above considerations. There will be no releases of radioactivity, no effect on shielding effectiveness, and no resultant doses.

### **8.2.4 TSUNAMI**

A tsunami is classified as a natural phenomenon Design Event IV in accordance with ANSI/ANS 57.9.

#### **8.2.4.1 Cause of Accident**

Tsunamis are water waves caused by earthquakes with epicenters located under water whose pressure waves propagate through the water and eventually make landfall. The tsunami accident bounds the condition of water run-up due to storm surges.

#### **8.2.4.2 Accident Analysis**

The accident analysis for tsunami effects involve evaluation of the loaded HI-STAR HB cask during transport from the RFB to the ISFSI vault, cask handling activities at the vault, and long-term storage in the ISFSI vault. Section 2.6.9 describes the tsunami hazards for the Humboldt ISFSI site. The top of the ISFSI vault is at elevation 44 ft above mean lower low water (MLLW). This elevation is higher than the tsunami height

estimates at MLLW elevation considered in the studies for the Humboldt Bay ISFSI site, which include bounding estimates for distant tsunamis, modeling of locally generated tsunamis associated with the Cascadia subduction zone, and tsunami heights from geologic evidence of tsunamis inundating the region around the ISFSI site.

Using the estimate of 30 to 40 ft above MLLW for the runup height of the tsunami at the bay entrance, and an attenuation factor of 0.7 to 0.9, the inundation height would be 21 to 36 ft above MLLW if the tsunami occurred at low tide. Incorporating wave run-up for storms from Table 2.4-5, gives maximum value of 49.86 ft (including high tide and wave run-up for storms). The maximum tsunami occurring coincident with a design basis storm wave run-up and high tide is not considered credible. Even if the tsunami flowed above the ISFSI elevation, the tsunami hazard at the proposed ISFSI site is negligible because the HI-STAR HB System is designed to withstand the static pressure forces from submergence in 656 ft of water. Furthermore, the HI-STAR HB casks will be contained in an enclosed underground vault that is designed to structurally withstand 6 ft of water head and will protect them from damage by flowing water and water-born debris.

The design basis tsunami described above is a result of the design basis earthquake described in Section 3.2.4 for the ISFSI site. As discussed in Section 3.2.4, a probabilistically determined spectrum exceeding a 50-year return period is used for evaluating the transport mode. This earthquake is of insufficient size to create a tsunami that would cause flooding on the transport route or during handling activities at the ISFSI vault.

### **8.2.4.3 Accident Dose Calculations**

As discussed above, tsunamis will not cause any releases of radioactivity, or reduce shielding effectiveness.

### **8.2.5 FIRE**

Fires are classified as human-induced or natural phenomena design events in accordance with ANSI/ANS 57.9 Design Events III and IV. Section 2.2.2 identifies all potential fire hazards on site.

During the original licensing of the HB ISFSI, there were the fossil-fueled (HBPP Units 1 and 2, and mobile emergency power plants), one shutdown nuclear unit (HBPP Unit 3), and two mobile emergency power plants (MEPPs) within the HBPP owner controlled area. The original licensing analyses evaluated potential fire hazards associated with these units. The fossil-fueled Units and the MEPPs were removed and replaced with the new HBGS subsequent to the completion of the original licensing. In addition, decommissioning activities commenced and are still in progress. The ISFSI FSAR was updated to reflect the revised fire and explosion hazards and additional evaluations were performed for the new hazards associated with new HBGS and decommissioning activities. The fire and explosion hazards associated with Units 1, 2, and 3 and the

## HUMBOLDT BAY ISFSI FSAR UPDATE

MEPPs were labeled with numeric event identifiers. The fire and explosion hazards for the new HBGS were identified with alphabetical identifiers. The descriptions of many of the Units 1, 2, and 3, and MEPPs fire hazard evaluations are identified as historical in Section 2.2.1.1 since they are no longer present onsite. The evaluations for the Units 1, 2, and 3, and MEPPs fire hazards are still valid and were determined to be bounding for the new HBGS hazards. Table 2.2-1 identifies fire and explosion hazards that presently have the potential to impact the ISFSI vault and also those which are historical. Table 2.2-1 also identifies the original licensing fire hazard evaluations that bound the presently existing fire hazards.

The following are the original licensing basis credible fire sources that warranted further evaluation to establish a conservative design basis. Unless noted, each of these events are currently applicable to the ISFSI:

- F1 Onsite cask transporter fuel tank
  - F1.1 Mobile crane or forklift
- F2 Other onsite vehicle fuel tank
- F3 On-site stationary fuel oil and diesel fuel storage and service tanks (historical)
- F4 Fuel oil and diesel fuel tanker truck
- F5 Gasoline tanker truck and 120 gallon gasoline storage tank (historical)
- F6 Combustion of propane storage tank (historical)
- F7 Combustion of propane tanker truck (historical)
- F8 Fire from mineral oil from the Unit 3 main bank transformers (historical)
- F9 Natural gas pipeline
- F10 Surrounding vegetation
- F11 Barge in bay carrying fuel
- F12 Other local combustible materials

Fires are categorized in one of two classes: (1) engulfing, and (2) non-engulfing fires. Engulfing fires are characterized by flames that completely surround the cask such that convection heat transfer from the fire is a significant contributor to the heat up of the cask and contents. The cask transporter and onsite vehicle fuel fires (Events F1, F1.1,

and F2 above), where the burning of the fuel in a pool around the base of the cask is postulated, are the only engulfing fires considered for the Humboldt Bay ISFSI.

Non-engulfing fires occur at some distance away from the cask or the ISFSI vault such that the convection mode of heat transfer is negligible in the fire analysis. The balance of the fires listed above (Events F3 through F12) is non-engulfing fires.

The potential for fire is addressed for onsite cask transportation from the RFB (historical), maintenance activities that involve removal and reinstallation of a cask from the storage vault, transfer of the spent fuel and GTCC waste casks to an authorized offsite storage facility, a vault lid removal for maintenance/inspections and long-term storage in the storage vault, as applicable to the source of combustible material. The evaluations performed for these postulated fire events are discussed in the following sections.

### **8.2.5.1 Cause of Accident**

Multiple causes, both human-induced and natural, are assumed for each of the fire events postulated above. For the purposes of this FSAR, all conservatively postulated fire events are classified as ANSI/ANS 57.9, Design Event IV, events because they establish a conservative design basis for important-to-safety SSCs.

### **8.2.5.2 Accident Analysis**

Site-specific fire evaluations were performed for the Humboldt Bay ISFSI using methods and assumptions documented in Reference 17 demonstrate that the results of the fire evaluations meet the accident acceptance criteria for the Humboldt Bay ISFSI. The Humboldt Bay ISFSI site-specific fire evaluations are discussed below.

#### **8.2.5.2.1 Engulfing Fires**

The engulfing fire provides a bounding fire case for the HI-STAR HB cask components and the spent fuel. In the storage vault structure, the source fuel is postulated to be burning in a pool surrounding the cask. Therefore, the vault concrete short-term temperature limit may be exceeded and is an expected consequence of the event. If a fire does occur, recovery from a fire event on the ISFSI vault will require an inspection and technical evaluation of the ISFSI vault structure, in the affected area, to perform its design function. Appropriate compensatory and corrective actions will be taken as necessary.

##### **8.2.5.2.1.1 Fire Surrounding a Cask Outside the ISFSI Vault**

For the evaluation of the onsite cask transporter and other onsite vehicle fuel tank fires (Events F1 and F2), it is postulated that the fuel accumulates in a pool around the periphery of the cask. The fuel is ignited and burns in a fire located adjacent to the cask outer surface.

The HI-STAR HB System is designed as a dual-purpose cask system for spent fuel storage under 10 CFR 72 and for transportation under 10 CFR 71. The transportation regulations (10 CFR 71.73(c)(4)) require a transportation package to be able to withstand a 30-minute engulfing fire with a flame temperature of 1475°F. A post-fire duration of 12 hours is also considered to ensure peak component temperatures are considered. This transportation fire provides a bounding case for the historical cask transporter fire and onsite vehicle fuel fire. The results of this fire analysis are shown in Table 8.2-11. The spent fuel cladding and all steel component temperatures remain less than their short-term temperature limits and are acceptable. The temperature of the Holtite-A neutron shield material exceeds its short-term design temperature of 350°F and will result in higher, but acceptable dose rates for the accident condition (see Section 8.2.5.3).

### **8.2.5.2.1.2 Fire Inside the ISFSI Vault**

Because the on-site transporter must enter the ISFSI to place the loaded casks into the vault, an evaluation was completed for a ruptured fuel tank to leak fuel into the vault and create a source of fire inside the vault during, or after the cask has been lowered into the storage cell. This event is bounded by the results of the open-air engulfing fire presented above. The heat input to the cask from the engulfing fire comes from both thermal radiation and convection. With respect to thermal radiation, the relatively small clearance between the vault internal diameter and the cask outer diameter precludes flames of sufficient optical thickness to emit a significant amount of heat by this mechanism. With respect to convection, the lack of a low-resistance air inlet to the bottom of the vault requires that combustion air be drawn in from above the vault through the annulus between the cask and the cell wall. This constricts the air flow into the vault and the flow of combustion products out of the vault, precluding flame velocities of the magnitude that occur in open pool fires and limiting the heat input from this mechanism. As a result, the engulfing fire outside the ISFSI vault is considered the bounding event for a fire inside the ISFSI vault.

As discussed in Section 2.2.2.2.1, Event F1.1 is bounded by the F1 event for a 50-gallon onsite transporter diesel fuel tank fire. Administrative controls will be used consistent with the Humboldt Bay ISFSI Technical Specification CTEP to ensure the crane is limited to a maximum of 50 gallons of diesel fuel and a fire watch is employed during a cask being removed from the vault during maintenance or transfer of spent fuel and GTCC waste casks to an authorized offsite storage facility. The administrative controls of the Vault Lid Opening Hazard Control Program will be utilized to ensure the crane is limited to a maximum of 50 gallons of diesel fuel and a fire watch is employed whenever a vault lid is removed for maintenance/inspections so it is not considered a hazard to these activities and is only a hazard to the ISFSI storage vault.

### **8.2.5.2.2 Non-engulfing Fires**



The set of non-engulfing fires (Events F3 through F12) were evaluated for their effect on the cask during onsite historical cask transportation to the ISFSI and on the ISFSI vault structure during long-term storage operations, as applicable. Once the casks are moved to the ISFSI and stored below ground in an enclosed vault system, there is no direct effect of non-engulfing fires on the casks. Therefore, the analyses address the effect of these fire events on the vault structure, not the cask itself. The applicability of each fire event to the cask and/or the ISFSI vault structure is discussed under each fire event listed below. A common methodology was used to determine the cask surface temperature rise and the vault surface temperature rise.

If a flammable material fire occurs at some distance from the target such that the convection heat transfer mode is negligible compared to the thermal radiation mode, the fire is termed non-engulfing. For a fire that does not engulf a cask, heat transfer from the fire to the cask is dominated by thermal radiation. This is due to the high flame temperatures associated with fires and the fourth-power relationship between the flame temperature-to-target temperature difference, and the radiation heat flux.

The rate of heat input to a cask or the ISFSI vault structure during these fires can, therefore, be conservatively estimated by using the following relationship:

$$q_{in} = \sigma \times \epsilon \times A_{fire} \times F_{view} \times (T_{fire}^4 - T_{target}^4)$$

where:

$q_{in}$  is the rate of heat input during the fire

$\sigma$  is the Stefan-Boltzmann constant

$\epsilon$  is the emissivity of the cask or ISFSI surfaces

$A_{fire}$  is the projected area of the fire flame front

$F_{view}$  is the fire-to-cask or fire-to-ISFSI geometric view factor

$T_{fire}$  is the average flame temperature

$T_{target}$  is the initial surface temperature of the cask or ISFSI

The fire-to-cask geometric view factor ( $F_{view}$ ) can be estimated by modeling the cask as a cylinder and the fire as a planar wall of flame, while the fire-to-ISFSI geometric view factor can be estimated by modeling the ISFSI as a rectangular area and the fire as a perpendicular planar wall of flame. The basis for the view factor equations is provided in the PG&E Response to NRC Question 6-6 in Reference 27. The surface temperature of the cask or ISFSI ( $T_{target}$ ) will rise during the duration of any fire event, so the maximum rate of heat input will occur at the start of the event.

At some point in the fire event, a steady state will be reached where the additional heat input to the cask or ISFSI will be completely rejected from the surface to the ambient air. Once the steady state rate of heat input to the cask or ISFSI is obtained, the maximum temperature of the exposed surface can be determined. Table 8.2-12 provides the fuel

types for each of the sources of fire, the distances to the targets, and the computed cask and vault lid surface temperature increases due to non-engulfing fires. Fuel volumes are not required for the fire analyses since a continuously burning fire is conservatively assumed.

During the transport of casks (historical) for all of the non-engulfing fire events, except for the Holtite-A neutron shield material, all cask component temperature increases are less than the increase in the temperature limit from normal conditions to accident conditions, and is therefore acceptable. The effect on dose rates due to the loss of all Holtite-A neutron shielding material is addressed in Section 8.2.5.3 and results in acceptable dose level increases. For long-term cask storage with the vault cell lids in place only the vault cover is directly susceptible to the effects of the fire and, although there could be some minor concrete deterioration, no damage to the casks will result from any of the non-engulfing fires. During removal and reinstallation of casks during maintenance activities and vault lid removal for maintenance/inspections, appropriate compensatory measures will be taken as discussed in Section 2.2.2.2.1 and Table 2.2-1 to ensure that these activities are bounded by the fire analyses shown in Table 8.2-12.

#### **8.2.5.2.2.1 Stationary Fuel Oil and Diesel Oil Storage and Service Tanks (historical)**

Event F3 evaluated the onsite stationary fuel oil tanks associated with HBPP Units 1, 2, and 3, and MEPPs, which have been removed and are listed in Table 2.2-1 as historical, except for the ISFSI backup diesel generator fuel tank. Descriptions of the Event F3 fuel oil and diesel oil storage tanks and associated fire evaluations are provided below. The Event F3 evaluation methodology and hazard analysis are relied upon as a bounding evaluation for the onsite stationary diesel tanks associated with the HBGS and the ISFSI as discussed in Section 2.2.2.6.1, Events FA-FF.

Onsite stationary fuel oil or diesel tanks larger than 50 gallons (Event F3) are at least 198 ft from the storage vault and the historical transport route, and are surrounded by berms. The HBPP site has one Number 6 fuel oil storage tank and two Number 6 fuel oil service tanks. There is also a diesel fuel storage tank on the HBPP site and a diesel fuel tank for the ISFSI backup generator that is no larger than 200 gallons, and that is located over 100 feet from the nearest cask. The backup generator diesel fuel tank storage is limited to no more than 50 gallons during historical transport operations. During removal and reinstallation of the casks from the storage vault for maintenance, during the vault lid removal for maintenance/inspections, and future removal and transport activities for transferring the spent fuel and GTCC waste casks to an authorized offsite storage facility, refueling of the backup generator tank will be prohibited by the use of administrative controls. Both the Number 6 fuel oil and diesel fuel oil have a moderate fire hazard rating of two and are not considered to be significant fire hazards. The flash points of Number 6 fuel oil and diesel fuel are greater than the average ambient temperature for the site and there is a lack of ignition sources in the area. However because of this moderate hazard rating, fires from each of these

tanks were analyzed uniquely due to the different fuels and different distances between the fire sources and the targets.

A 200 gallon ISFSI backup diesel generator fuel tank fire during historical transport operations or during spent fuel and GTCC waste casks transfer to an authorized offsite storage facility is not considered credible and is not uniquely analyzed. This is based on the short time during each transport operation that the cask is exposed to the detonation source and the low likelihood of a tank fire occurring simultaneously. This event is bounded by the 50 gallon engulfing fire (Event F1) during historical transport operations when the tank storage limit was administratively controlled to 50 gallons. The 200 gallon ISFSI backup diesel generator fuel tank is not uniquely analyzed for the vault lid being removed for inspection/maintenance and removal and reinstallation of a cask from the vault during maintenance, as its location and size is bounded by the diesel fuel tank truck fire (Event F4).

The other fuel oil tanks and the diesel fuel storage tank were assumed to be fire threats to the cask during the historical onsite cask transportation and to the ISFSI vault structure. In addition, during the historical transport of the casks there is only a very small distance on the transport route that has a direct line of sight to these tanks. Therefore, the potential for these fires to even affect the transportation of the cask is minimal.

### **8.2.5.2.2.2 Fuel Oil and Diesel Fuel Tanker Trucks**

Event F4 evaluated the fuel oil and diesel oil tanker trucks associated with HBPP Units 1, 2, and 3. Descriptions of the Event F4 fuel oil and diesel oil tanker trucks and associated fire evaluations are provided below. The Event F4 evaluation methodology and hazard analysis are relied upon as a bounding evaluation for the fuel oil and diesel oil tanker trucks associated with the HBGS and the ISFSI as discussed in Section 2.2.2.6.1, Event FG.

Fuel oil and diesel fuel tanker trucks (Event F4) require periodic access to the site to replenish the storage tanks discussed in Section 8.2.5.2.2.1. During a cask being removed from the vault during maintenance or during spent fuel and GTCC waste casks transfer to an authorized offsite storage facility, all activities will be controlled under a Humboldt Bay ISFSI Technical Specification CTEP as discussed in Section 2.2.2.2.1 and Table 2.2-1. In addition, the Vault Lid Opening Hazard Control Program administrative controls will be utilized to ensure these hazards do not adversely impact the ISFSI whenever a vault lid is removed for maintenance/inspections. Therefore, fires due to fuel oil and diesel fuel tanker trucks are not considered threats to the cask during these activities.

During long-term ISFSI operations, when these trucks make periodic deliveries of fuel oil and diesel fuel, the threat of fire to the ISFSI vault does exist. When the tanker truck is moving on the roadway past the ISFSI, the roadbed is below the level of the ISFSI pad, which ensures that even if there was a tanker truck accident resulting in a tank

rupture and fuel spill, the fuel would not flow toward the ISFSI. This ensures that the location of truck represents the shortest distance between the fuel and the ISFSI during fuel deliveries on site. Fires consuming the contents of these trucks have been analyzed for their effect on the ISFSI vault cover temperature. The analysis (Reference 17) shows that the temperature rise of the vault lid is insignificant and acceptable in all cases, as summarized in Table 8.2-12.

#### **8.2.5.2.2.3 Gasoline Tanker Truck and Gasoline Storage Tank (historical)**

Event F5 evaluated the onsite gasoline storage tank and associated tanker truck associated with HBPP Units 1, 2, and 3, and MEPPs, which have been removed and are listed in Table 2.2-1 as historical. Descriptions of the historical Event F5 gasoline storage tank and associated tanker truck and associated fire evaluations are provided below.

A gasoline tanker truck (Event F5) requires periodic access to the east side of the HBPP site to fill a 120-gallon storage tank. The storage tank is on the east side of the site and the HBPP Unit 1 and 2 power blocks do not allow a direct line of sight between the tank and the ISFSI vault. Therefore, it is not considered a significant hazard to the ISFSI vault.

Gasoline tanker trucks are prohibited from the site during onsite cask transportation and lowering activities by the CTEP. Therefore, this fire is not considered a risk during onsite transport and cask lowering operations. Because of the long distance between the gasoline storage tank and the closest point on the transport route, the limited time that there is a line of sight from the cask in transport to the storage tank (less than one hour per transport operation), and the limited volume of fuel, the gasoline tank fire is not considered a significant hazard during these activities. Even if it was a threat, a gasoline storage tank fire at this distance and fuel volume is considered bounded by the engulfing fire as discussed in Section 8.2.5.2.1.1.

A fire from a gasoline tanker truck is considered a credible threat to the ISFSI vault. The effect of a fire from the gasoline tanker truck on the ISFSI vault is shown in Table 8.2-12.

#### **8.2.5.2.2.4 Propane Tanker Truck and Propane Storage Tank (historical)**

This item was deleted during 2010 since the hazard is no longer present.

#### **8.2.5.2.2.5 Mineral Oil from the Unit 3 Main Bank Transformers (historical)**

This item was deleted during 2010 since the hazard is no longer present.

#### **8.2.5.2.2.6 Natural Gas Pipeline**

Event F9 evaluated the natural gas pipeline hazards associated with Humboldt Units 1, 2, and 3, and MEPPs. The low pressure portion of the natural gas pipeline (30 psi) has been removed and is listed in Table 2.2-1 as historical. The high pressure portion of the natural gas pipeline (400 psi, upstream of the regulating station) supplies the new HBGS natural gas pipeline and is an existing hazard. Descriptions of the historical Event F9 low pressure natural gas pipeline and existing high pressure natural gas pipeline and associated fire evaluations are provided below. The Event F9 evaluation methodology and hazard analysis are relied upon as a bounding evaluation for the natural gas pipeline associated with the HBGS as discussed in Section 2.2.2.6.1, Event FH.

Humboldt Bay Units 1 and 2 (historical) are capable of operating with fuel oil or natural gas (see Section 2.2 for details). A main supply line delivers gas to the site at high pressure (approximately 400 psig). The pressure is reduced at a pressure regulating station to approximately 30 psig and fed through distribution piping to the units. Just downstream of the pressure regulating station is a manual isolation valve. Administrative controls are used to isolate and depressurize the gas distribution line during onsite cask transportation and lowering activities. These controls are implemented through the CTEP.

Two fire scenarios for the natural gas supply lines (Event F9) are evaluated. The first is during onsite cask transportation (historical) and lowering activities, where a fire is assumed to occur on the high pressure side of the pressure regulating station, with the low pressure side isolated. The second is during long-term storage operations, when the gas distribution line (historical) that feeds Unit 1 and 2 may be in service and is a source of fire that could affect the ISFSI vault. The analysis (Reference 17) shows that both scenarios result in insignificant effects that are acceptable. See Table 8.2-12. The new HBGS natural gas pipeline is equipped with automatic gas shutoff valves.

#### **8.2.5.2.2.7 Surrounding Vegetation**

The native vegetation (Event F10) surrounding the ISFSI storage vault is primarily grass, with no significant brush, and no trees as discussed in Section 2.2. Maintenance programs prevent uncontrolled growth of the surrounding vegetation. A conservative fire model was established for the evaluation of grass fires on the ISFSI vault (Reference 17) and results in effects that are acceptable. A vegetation fire is not assumed during onsite cask transportation and lowering activities, during the vault lid removal for maintenance/inspections, or removal of the cask from the vault for maintenance since it is not credible to assume a vegetation fire starts suddenly with no forewarning during these activities.

**8.2.5.2.2.8 Barge in Bay Carrying Fuel**

Event F11 concerns the effects of a fire from a barge that contains a maximum of 87,000 barrels of fuel as it moves up the North Bay to the Chevron Fuel Terminal. As discussed in Section 2.2.1.2, the barge is not considered to be a hazard to onsite cask transportation and lowering activities, transport of the spent fuel and GTCC waste casks to an authorized offsite storage facility, removal of a cask from the vault for maintenance activities, or removal of a vault cell lid for maintenance/inspections because administrative controls ensure that no related activities take place when the barge is moving through the bay. These controls are implemented through the Cask Transport Evaluation Program or Vault Lid Opening Hazard Control Program, as applicable. However, as stated in Section 2.2.1.2, the barge needed to be further evaluated when considering potential effects on the ISFSI vault during long-term storage operations.

This barge holds a maximum of 87,000 barrels of liquid fuels in 12 separate tank compartments. Normally the barge carries gasoline in eight compartments and diesel fuel in the other four compartments. Each compartment holds approximately 7,250 barrels of fuel and is separated from the other compartments by steel walls. This barge is not motorized and requires a tug boat for motion. Because of the lack of onboard motive force, there are a limited number of ignition sources on the vessel. When the barge is moving through the bay, the shipping company and the U.S. Coast Guard control its motion and the motion of other vessels in the area. These controls include requiring good weather and low vessel traffic.

The edge of the North Bay channel is approximately 1,500 yards from the ISFSI. Outside of that channel (i.e., closer to the ISFSI), the water depth is limited and will not support the movement of the barge with the tug boats. A fire that included the complete volume of the barge at the 1,500 yards distance would not have an effect on the cask greater than the design basis engulfing fire. However, the shore of the North Bay does run up to approximately 200 ft of the ISFSI facility at its closest point. As a result, it is possible that if a barge leak occurred in the channel, a portion of the leaked fuel could float to within approximately 200 ft of the ISFSI facility and, at that point, ignite.

This floating fuel scenario has limitations, including the natural limited depth of unconfined floating fuel and the limited volume of fuel from a barge, which would likely be a break or crack in a single fuel compartment. As a result of the design of the barge and its separated compartments, the amount of fuel would likely never include more than the volume of one or two compartments at any one time. In addition, the fuel would have to stay together in a concentrated pool, move together as close to the ISFSI facility as possible, and then ignite from some unknown ignition source. Also, in this scenario the barge would have to be leaking for an extended time. Because of the controls on the movement of this barge, it is not credible that a leak or break large enough to empty these tanks would not be identified early and mitigation undertaken to control the movement of the fuel toward the ISFSI facility. As a result of the limitations on this potential hazard, its effects are considered to be limited and bounded by the design basis engulfing fire analysis (Event F1).



#### **8.2.5.2.2.9 Other Local Combustible Materials**

As discussed in Section 2.2.2.2.1, administrative controls are imposed to ensure no combustible materials are stored within the security fence around the ISFSI storage vault (Event F12). Prior to onsite cask transportation activities, a vault lid being removed for inspection/maintenance, a cask being removed from the vault during maintenance, or during transfer of spent fuel and GTCC waste casks to an authorized offsite storage facility, a walkdown is performed to ensure all local combustible materials, including transient combustibles, are removed or otherwise controlled in accordance with ISFSI fire protection requirements.

#### **8.2.5.3 Accident Dose Calculations**

The analyses of the effects of fires on the cask during transport and storage reveal that all materials, except the neutron shield in the overpack remain below their short-term temperature limits. Therefore, the MPC confinement boundary remains intact after a design basis fire and there is no release of the contained radioactive material from the MPC-HB. The seals on the overpack will be exposed to short-term high temperature excursions that remain below the maximum design accident temperature limits listed in HI-STAR FSAR Table 2.2.3. However, as no radioactive materials are present in the annulus, the loss of the helium retention boundary will have no radiological impact. Fire consequences during storage in the vault were evaluated and were determined to not cause any significant loss of shielding because the vault lid temperatures remain below the short-term limits. Therefore, a fire during storage has no radiological dose consequences.

The complete loss of the HI-STAR overpack's radial neutron shield is assumed in the shielding analysis for the post-fire condition of the HI-STAR HB System during onsite transport and cask lowering activities (Reference 19). The shielding effectiveness provided by the steel structure is not significantly diminished in a fire event. The accident condition dose rate at 100 meters, for the complete loss of the radial neutron shield, was very conservatively estimated to be 0.45 mrem/hr. This estimate is based on a 1/R attenuation for the dose rate calculated in Reference 19, which is 45 mrem/hr at a distance of 1 meter from the cask. At this level, the total accumulated dose in a 30 day period would be 324 mrem. Therefore, the HI-STAR HB System fulfills the 5 Rem dose requirement of 10 CFR 72.106. In the event of a fire accident occurring, the 100-meter controlled area will be maintained and a radiological and visual inspection will be performed to determine the extent of the damage to the overpack and the vault. As appropriate, temporary shielding shall be placed around the affected area to reduce dose rates. Recovery operations to restore the dose rates to acceptable levels should easily be accomplished within the 30-day duration assumed above.

### **8.2.6 EXPLOSION**

## HUMBOLDT BAY ISFSI FSAR UPDATE

Explosions are classified as human-induced or natural phenomena design events in accordance with ANSI/ANS 57.9, Design Events III and IV.

During the original licensing of the Humboldt ISFSI, there were the fossil-fueled units (HBPP Units 1 and 2, and MEPPs) and one shutdown nuclear unit (HBPP Unit 3) within the HBPP owner controlled area. The original licensing analyses evaluated potential explosion hazards associated with these units. The fossil-fueled Units and MEPPs were removed and replaced with the new HBGS subsequent to the completion of the original licensing. In addition, decommissioning activities commenced and are still in progress. The ISFSI FSAR was updated to reflect the revised explosion hazards and additional evaluations were performed for the new hazards associated with new HBGS and decommissioning activities. The explosion hazards associated with Units 1, 2, and 3 were labeled with numeric event identifiers. The explosion hazards for the new HBGS were identified with alphabetical identifiers. The evaluations for the Units 1, 2, and 3 explosion hazards are still valid and were determined to be bounding for the new HBGS hazards. Table 2.2-1 identifies explosion hazards that presently have the potential to impact of the ISFSI vault and also those which are historical. Table 2.2-1 also identifies the original licensing explosion hazard evaluations that bound the presently existing explosion hazards.

Section 2.2.2 identifies the potential explosion hazards that could affect the HI-STAR HB System during onsite transportation and lowering activities, and during long-term storage at the ISFSI vault. The following are the explosion sources that warranted further evaluation to establish a conservative design basis. Unless noted, each of these events are currently applicable to the ISFSI:

- E1 Propane storage tank (historical)
- E2 Natural gas pipeline
- E3 Propane tanker truck (historical)
- E4 Gasoline tanker truck and day tank (historical)
- E5 Other site vehicle fuel tanks
  - E5.1 Detonation of a mobile crane or forklift fuel tank
- E6 Vehicles on Route 101
- E7 Fossil power plant explosion (fixed or mobile units) (historical)
- E8 Barge in bay carrying fuel
- E9 Explosive decompression of compressed gas bottles

Table 2.2-1 identifies the events that are applicable to the ISFSI, the onsite historical transport route, or both. The following is an evaluation of the explosion hazards in Section 2.2 that were determined to require further evaluation. In those cases where administrative controls are used to preclude the threat of explosion, those controls are implemented through either the CTEP during a cask being removed from the vault during maintenance or during spent fuel and GTCC waste casks transfer to an authorized offsite storage facility, or the Vault Lid Opening Hazard Control Program whenever a vault lid is removed for maintenance/inspections or during removal and reinstallation of a cask from the vault for maintenance.

### **8.2.6.2 Accident Analysis**

#### **8.2.6.2.1 Propane Storage Tank (historical)**

There are two explosion scenarios in Event E1 that have been identified and evaluated for the propane storage tank. These include a detonation at the tank site and its effect on the cask during onsite transportation, lowering activities, and long-term storage at the ISFSI. The other scenario is the possibility of a vapor cloud forming due to a tank leak, with the cloud moving to a position over the cask during transportation, lowering, or long-term storage at the ISFSI vault. In evaluating all of these scenarios, consideration was given to the following assumptions:

- Propane is heavier than air and does not disperse readily.
- The normal wind direction on the site is from west to east away from the transport route and the ISFSI vault.
- The propane tank is significantly lower in elevation than the ISFSI vault and a motive force would be required to push a vapor cloud uphill.
- The range of concentration allowing ignition is very limited (from approximately 2.1 percent to a maximum of 9.5 percent).
- Because of the wind force required to move the vapor cloud toward the vault, and the fact that there are no structures at the vault site to hold a vapor cloud in a position for any significant period of time, the cloud would have no means of organizing itself strictly over vault. It would continue to mix with air and move upward and past the vault, spreading out (diluting) rather than becoming concentrated at or near the vault.
- There are limited ignition sources at the ISFSI vault.
- There are no vents in the vault to allow the propane to easily enter the vault.

## HUMBOLDT BAY ISFSI FSAR UPDATE

- For explosions away from the vault, the only significant effect would be to the vault lids.

### Local Detonation of Propane Tank

Ignition of the propane tank at its location is not considered to be credible when considering the RG 1.91 (Reference 20) criteria and methodologies. RG 1.91 suggests a model where the entire propane tank volume, dispersed at a flammable concentration would have an instantaneous, 100 percent, ignition of the fuel. This type of explosion is not supported by industry data. Most tank ignitions are the result of either a catastrophic rupture caused by an outside source or a leak over time into an area where the gas can be partially confined, (i.e., by structures), and then ignited.

For the HBPP site propane tank, the catastrophic rupture scenario is not credible because there are no outside sources that can reasonably be expected to come in contact with the tank. With the exception of the tanker truck that fills the tank, site procedures prohibit vehicular traffic in the vicinity of the propane facility at any time. The tanker truck does not get closer than 20 ft from the tank. In addition, there are barriers around the facility to keep any vehicle from accidentally rolling into the tank. For the tank leakage scenario, there are no structures at the propane facility that would allow partial confinement of the gas. The facility is in an open area of the site with the only structures to the east of the facility and farther away from the transport route and the ISFSI vault area.

During onsite cask transportation and lowering operations, administrative controls implemented by the CTEP do not permit the propane tanker truck on the HBPP site and no vehicles other than the transporter are permitted to be moving in the vicinity of the propane tank. These administrative controls preclude the catastrophic rupture event, as the cask transporter moves very slowly, is under constant watch during onsite transportation and lowering, and there are no failure modes to cause a runaway transporter (see Section 4.3).

In addition, propane gas contains a significant odor that is easily detectable at concentrations well below the allowable ignition concentration level. As a part of the CTEP, the transport route is walked down for all existing hazards, including leaks at the propane facility. No cask transportation activities are permitted with any indication of a leak at the propane facility. Also, there are only a maximum of five scheduled operations involving transport of spent fuel from the RFB to the ISFSI over the life of the ISFSI. As such, the potential exposure of the transport operation to this hazard is very limited (a maximum of 15 hours). Based on this limited exposure, the pre-transport inspections and the administrative controls on external hazards to the propane tank during transport and lowering operations, the probability of an explosion at the propane facility is considered to be extremely low.

For storage at the ISFSI the probability is also very low based on the limited potential for tank rupture, as discussed above. However, an analysis was performed (Reference 21)

for the potential effects of a local detonation on the ISFSI vault cover. Given the massive size of the reinforced concrete vault, specifically the lid thickness, the impacts from the calculated overpressure on the reinforced concrete structure will not produce any adverse structural effects on the vault or the HI-STAR HB cask inside the vault. The resulting overpressure is shown in Table 8.2-13. This overpressure is much lower than the HI-STAR HB overpack external design pressure.

However, this calculated overpressure exceeds the RG 1.91 acceptance criteria of 1 psi. Following the guidance of RG 1.91, when the 1 psi overpressure criterion is exceeded an analysis of missile effects is required. This analysis is discussed in Section 8.2.6.2.9.

### Vapor Cloud Detonation

In addition to the local detonation of the propane tank, a scenario is postulated where a vapor cloud from a propane tank leak could drift directly over a cask in transport or the ISFSI vault and detonate. Based on the limited exposure time, pre-transport inspections of all hazards, and the administrative controls on external hazards to the propane facility during transport and lowering operations, the propane vapor cloud is not considered to be a credible event for transport and lowering operations. However, the potential for a propane vapor cloud to move over the ISFSI vault was evaluated further.

As stated in prior discussion, propane is heavier than air, the normal wind direction is from west to east, away from the ISFSI vault, and the change in elevation between the propane facility and the ISFSI vault would require the cloud to move uphill. Although movement up the hill in the direction of the ISFSI vault would be possible given the right motive force, accumulation of the propane in a concentrated cloud over the ISFSI vault is not considered a likely scenario because there are no structures or enclosures to retain the vapor cloud over the ISFSI for more than a few seconds.

Based on the above discussion and the fact that there are a very limited number of ignition sources at or near the vault, the probability of this event is considered very low. However, an analysis was performed (Reference 21) for the potential effects of a vapor cloud detonation over the ISFSI vault. The peak calculated overpressure due to the detonation of a 20 ft x 80 ft x 40 ft propane gas cloud over the ISFSI vault is shown in Table 8.2-13. Given the massive size of the reinforced concrete vault, specifically the lid thickness, the impacts from the calculated overpressure on the reinforced concrete structure will produce minimal adverse structural effects on the vault cover and will not adversely affect the HI-STAR HB cask inside the vault. This overpressure is much lower than the HI-STAR HB overpack external design pressure.

However, this calculated overpressure exceeds the RG 1.91 acceptance criteria of 1 psi. Following the guidance of RG 1.91, when the 1 psi overpressure criterion is exceeded, an analysis of missile effects is required. However, in a vapor cloud explosion scenario there are no missiles from the detonation and no further analysis is required.

### 8.2.6.2.2 Natural Gas Pipeline

Event E2 evaluated the natural gas pipeline explosion hazards associated with Humboldt Units 1, 2, and 3. The low pressure portion of the natural gas pipeline (30 psi) has been removed and is listed in Table 2.2-1 as historical. The high pressure portion of the natural gas pipeline (400 psi, upstream of the regulating station) supplies the new HBGS natural gas pipeline and is an existing hazard. Descriptions of the Event E2 natural gas pipeline and associated explosion evaluations are provided below. The Event E2 evaluation methodology and hazard analysis for the low pressure portion of the natural gas pipeline are relied upon as a bounding evaluation for the natural gas pipeline associated with the HBGS as discussed in Section 2.2.6.2, Event EA.

Event E2 involves the detonation of a 12-inch natural gas distribution line that supplies fuel to Units 1 and 2. For this gas line, there are four scenarios identified as potential hazards. The first is a break and local detonation of the high pressure gas supply line upstream of the pressure regulating station, which reduces the gas pressure for use in the boilers from approximately 400 psi to approximately 30 psi. The second scenario is a leak in the high pressure supply line causing a vapor cloud, which moves over the transporter or vault and detonates. The third is a break and local detonation of the gas distribution line downstream of the regulating station. The fourth scenario is a vapor cloud from a leak in the distribution line, which moves over the ISFSI vault and detonates.

#### Local Detonation of the Gas Supply Line Upstream of the Pressure Regulating Station

The local detonation of the gas supply line upstream of the pressure regulating station was evaluated as a potential explosion event. This explosion event is not considered credible for several reasons, and is not analyzed. The regulating station is inside the owner-controlled area of the HBPP site and there is no vehicular traffic or threat in the vicinity of the regulating station that could cause a rupture of the supply line or ignition. In addition, seismic studies of the upstream supply line, which feeds the HBPP site supply line, have shown that in a seismic event, and if the gas line ruptured, it would fail at several points well upstream of the line that supplies the HBPP site. This would effectively eliminate the supply to HBPP and depressurize the line. These predicted break points are several miles from the HBPP site and are not a hazard to the site.

For onsite cask transportation and lowering activities this event is not considered credible and is not analyzed. This is based on the limited number of onsite transportation and lowering operations (5 maximum) and the short time during each transport operation that the cask is exposed to the detonation source (less than 3 hours). In addition, prior to onsite transportation operations, the CTEP requires a walkdown to identify and evaluate any hazards. The gas distribution line shall be verified to be free of leaks. The regulating station itself is monitored to assure that there are no leaks or potential for detonation. If any leaks are identified, the CTEP prohibits onsite cask transportation operations to take place until the leaks are eliminated.



### Vapor Cloud Detonation from a Leak of the Gas Supply Line Upstream of the Pressure Regulating Station

The potential for a vapor cloud from a leak in the gas supply line upstream of the pressure regulating station has been evaluated as a potential explosion source. This event is not considered credible and is not analyzed. This is based on the low potential of a line leak or break, the short duration of transport operation exposure, the prevailing winds being from west to east away from the transport route, and the pre-transport walkdowns required by the CTEP, during transport activities to transfer spent fuel and GTCC waste casks to an authorized offsite storage facility and during removal and reinstallation of a cask from the storage vault for maintenance, that identify any leaks and preclude onsite cask transportation operations if a leak is detected.

The potential for a vapor cloud from this leak to move across the site and over the vault is also not considered credible. This is based on the lower potential of a line break, and the prevailing winds being from west to east away from the ISFSI vault. In addition, because the vault is below ground with only the lids of the vault structure exposed vertically above ground, detonation from anywhere other than directly over the vault would have insignificant effects on the vault and no effects on the HI-STAR cask inside the vault.

### Local Detonation of the Gas Distribution Line Downstream of the Regulating Station

The original licensing Event E2 scenario where the supply line ruptures and detonates locally downstream of the regulating station was evaluated for effects on the ISFSI vault. During the historical initial ISFSI loading, onsite cask transportation and lowering activities, this scenario is not considered a hazard because the CTEP administrative controls require that this supply line be isolated and depressurized back to the regulating station during these operations. However, the line will be in service during long-term storage operations and has been evaluated for its effect on the ISFSI vault.

Gas lines are normally not prone to catastrophic rupture except during a seismic event. As discussed above for the gas supply line, the seismic studies show that in an earthquake large enough to rupture this line, the predicted breaks would take place miles away from HBPP and the supply line to HBPP would be depressurized immediately. Therefore the probability of a catastrophic rupture of this line downstream of the regulating station is very low. However, an analysis (Reference 21) was performed for this explosion scenario and the peak overpressure at the vault is reported in Table 8.2-13. The computed overpressure is much less than the 300 psig design overpressure of the HI-STAR HB overpack. Given the massive size of the reinforced concrete vault, specifically the lid thickness, the impacts from the calculated overpressure on the reinforced concrete structure will not produce any adverse structural effects on the vault or the HI-STAR HB cask inside the vault.

## HUMBOLDT BAY ISFSI FSAR UPDATE

This computed overpressure exceeds the RG 1.91 acceptance criteria of 1 psi. Following the guidance of RG 1.91, when the 1 psi overpressure criterion is exceeded an analysis of missile effects is required. This analysis is discussed in Section 8.2.6.2.9.

Local detonation of a gas pipeline leak is not credible due to the new HBGS gas pipeline being equipped with automatic gas shutoff valves, distance from the ISFSI vault, and the prevailing winds being from west to east away from the ISFSI vault, which further reduce the probability of this event. In addition, Table 8.2-13 shows that a natural gas distribution line vapor cloud explosion would result in a cask overpressure with acceptable results.

### Detonation of a Vapor Cloud Due to a Leak from the Gas Distribution Line Downstream of the Pressure Regulating Station

The original licensing Event E2 scenario where a leak in the gas line, downstream of the pressure regulating station, creates a vapor cloud that moves over the cask, during onsite transportation and lowering activities, is not credible because the CTEP ensures the line is isolated and depressurized during these operations. However, the new HBGS gas pipeline is equipped with automatic gas shutoff valves.

A vapor cloud detonation due to a leak in the gas distribution line, where the cloud moves to the ISFSI vault, is also not considered likely, but has been analyzed. Underground gas lines are normally not prone to catastrophic rupture and most gas line breaks are leak-before-break scenarios, especially at the low 70 psi pressure level in this line. This type of leak would significantly limit the available volume of gas available for cloud formation. If there was a large leak or rupture in the distribution line, automatic gas shutoff valves would isolate the source.

However, small gas leaks may go unidentified for some period. This low flow leakage could, over time, lead to the formation of a vapor cloud. However, the vapor cloud would only collect over the ISFSI vault if there was some enclosed or partially enclosed area where the lighter-than-air gas could collect. This situation does not exist at the ISFSI vault and the properties of natural gas would not support a concentrated vapor cloud formation over time, which moves to the ISFSI vault and detonates. As a result, this is not a likely event.

Nevertheless, a conservative analysis (Reference 21) was performed for the original licensing Event E2 (30 psi pipe line) to determine the effect on the ISFSI vault of the detonation of a cloud of natural gas above the vault surface. This analysis is bounding to the new 70 psi HBGS gas pipe line because (1) the analysis did not include use of an automatic shutoff valve, and thus, the volume of gas released would be less than the analysis, and (2) the analysis assumed the gas line leak occurred at a distance of 377 ft. from the ISFSI vault instead of the new 600 ft. distance. Table 8.2-13 shows the resulting overpressure calculated for the detonation of a 20 ft. x 80 ft. x 40 ft. natural gas cloud located directly over the ISFSI vault. This overpressure is below the HI-STAR HB overpack external design pressure. Given the massive size of the reinforced concrete

vault, specifically the lid thickness, the impacts from the calculated overpressure on the reinforced concrete structure will produce minimal adverse structural effects on the vault cover and will not adversely affect the HI-STAR HB cask inside the vault.

However, this calculated overpressure exceeds the RG 1.91 acceptance criteria of 1 psi. Following the guidance of RG 1.91, when the 1 psi overpressure criterion is exceeded, an analysis of missile effects is required. However, in a vapor cloud explosion scenario there are no missiles from the detonation and no further analysis is required.

In summary, the new HBGS gas pipeline is equipped with automatic gas shutoff valves. Therefore a leak in the 70 psi distribution line causing a significant gas vapor cloud which could migrate over the storage vault in the event of adverse weather conditions during transport activities to transfer spent fuel and GTCC waste casks to an authorized offsite storage facility, removal and reinstallation of a cask from the storage vault for maintenance, or opening of a vault lid for maintenance/inspections is not credible. In addition, Table 8.2-13 shows that a natural gas distribution line vapor cloud explosion would result in a cask overpressure with acceptable results.

### **8.2.6.2.3 Propane Tanker Truck (historical)**

Event E3 concerns the detonation of a propane tanker truck. Administrative controls implemented through the CTEP prohibit propane deliveries by tanker truck during onsite cask transportation and lowering activities. Therefore, an explosion of a propane tanker truck is not considered a credible hazard during these activities and is not analyzed.

When the tanker truck is allowed onsite to fill the propane storage tank, the filling process is performed under the propane industry's standard practices and the tanker truck is only in the area for less than one hour per year. An analysis was performed to determine the overpressure from a tanker truck detonation at its closest point to the ISFSI vault on the route that the tanker truck takes to and from the propane facility. Table 8.2-13 shows the computed overpressure at the ISFSI for this event. The computed overpressure is much less than the HI-STAR HB overpack design external pressure. Given the massive size of the reinforced concrete vault, specifically the lid thickness, the impacts from the calculated overpressure on the reinforced concrete structure will not produce any adverse structural effects on the vault or the HI-STAR HB cask inside the vault.

This computed overpressure exceeds the RG 1.91 acceptance criteria of 1 psi. Following the guidance of RG 1.91, when the 1 psi overpressure criterion is exceeded, an analysis of missile effects is required. This analysis is discussed in Section 8.2.6.2.9.

### **8.2.6.2.4 Gasoline Tanker Truck and Gasoline Storage Tank (historical)**

Event E4 concerns the detonation of gasoline tanker truck and a 120-gallon gasoline storage tank associated with HBPP Units 1, 2, and 3, and MEPPs, which have been removed and are listed in Table 2.2-1 as historical. Descriptions of the historical Event E4 gasoline storage tank and tanker truck and associated explosive evaluations are provided below.

Administrative controls implemented through the CTEP prohibit gasoline deliveries by tanker truck during onsite cask transportation and lowering activities, and an explosion of a 3000-gallon gasoline tanker truck is, therefore, not considered a credible hazard to the cask during these activities. During long-term storage operations, when the tanker truck is periodically permitted onsite, it remains on the eastern side of the owner-controlled area for the HBPP site and does not approach the ISFSI vault. When the tanker is onsite filling the storage tank, there is no line of sight to the ISFSI vault because of the Units 1 and 2 power blocks and other structures. As a result, neither the detonation of the gasoline tanker truck nor the gasoline storage tank is considered to be credible hazards for the ISFSI vault.

An explosion of the gasoline storage tank during onsite transportation (historical) operations has been evaluated and found to be not credible and is not analyzed. The onsite cask transport route allows a line of sight to the cask for a short period of time. Prior to the transport of spent fuel to the ISFSI vault, the CTEP requires walkdowns to be performed of all potential hazards to the transport operation. These walkdowns will include verifying that the gasoline storage tank is intact and that there is no leakage or potential for detonation. During transport operations (a maximum of 5) the transported cask is in the line of sight of the storage tank for less than 15 minutes.

### **8.2.6.2.5 Other Onsite Vehicle Fuel Tanks**

Event E5 involves the detonation of onsite vehicles. Because of its physical properties, diesel fuel does not pose any real explosion hazard. The pertinent material property for this determination, the flash point, is defined as the lowest temperature at which the vapor pressure of a liquid is sufficient to produce a flammable vapor/air mixture at the lower limit of flammability. A combustible liquid cannot vaporize sufficiently to detonate if the ambient temperature is below the flash point. Such materials could conceivably burn, but would be incapable of detonation.

The flash point of diesel fuel is 125°F. To be classified as flammable, the flash point of a liquid must be less than 100°F, as discussed in the National Fire Protection Association Handbook (Reference 18). The highest ambient temperature recorded for the Humboldt Bay ISFSI site is 87°F. This temperature is considerably less than the flash point of diesel fuel. Therefore, under ambient or normal operating temperature, this material does not represent a credible explosion hazard. Therefore, vehicles containing diesel fuel are excluded from further consideration as an explosion hazard.

Onsite vehicle explosions are reduced to the explosion of gasoline powered vehicles. Administrative controls implemented through the CTEP during historical original cask

transport, transport activities to transfer spent fuel and GTCC waste casks to an authorized offsite storage facility, and during removal and reinstallation of a cask from the storage vault for maintenance are used to (a) keep onsite gasoline powered vehicles either at a sufficient distance from the transport route during cask transport to ensure the total explosion overpressure is less than 1 psi, (b) perform a risk assessment using RG 1.91 risk acceptance criteria, or (c) allow only diesel-powered vehicles to be used.

As shown in the original licensing basis, the onsite vehicles can approach the ISFSI vault to a minimum distance of 50 ft when there are no onsite cask transportation or lowering operations in progress. Administrative controls during long-term storage and in the Vault Lid Opening Hazard Control Program require that no gasoline is allowed within the vehicle barrier system which ensures that all vehicles are greater than 50 ft from the storage vault. This minimum distance will be administratively controlled along with the cumulative volume of gasoline in vehicles allowed at that distance. As a result, the detonation of the gasoline tank of an onsite vehicle has been evaluated (Reference 21) for its overpressure effect on the ISFSI vault. Table 8.2-13 shows the computed overpressure at the ISFSI for this event. The computed overpressure is much less than the HI-STAR HB overpack design external pressure. Given the massive size of the reinforced concrete vault, specifically the lid thickness, the impacts from the calculated overpressure on the reinforced concrete structure will not produce any adverse structural effects on the vault or the HI-STAR HB cask inside the vault.

This computed overpressure exceeds the RG 1.91 acceptance criteria of 1 psi. Following the guidance of RG 1.91, when the 1 psi overpressure criterion is exceeded, an analysis of missile effects is required. This analysis is discussed in Section 8.2.6.2.9.

Event E5.1 is a variation of E5 and evaluated a diesel-powered mobile crane that may be used to remove or reinstall a vault lid. Event F1.1 also includes a fire associated with related equipment needed to mobilize the crane in the ISFSI area, such as a diesel-powered forklift. Detonation of diesel fuel used in any onsite vehicle is not considered credible because of its high flash point.

### **8.2.6.2.6 Vehicles on Route 101**

Event E6 involves a potential vehicle crash on Route 101 that is approximately 2000 ft east of the ISFSI site at its closest point, and runs north and south. Event E6 is not a threat to the ISFSI facility itself as it is more than 2000 ft away and meets the acceptance criteria RG 1.91, based on that distance. However as discussed in Section 2.2.1.2, it may be a hazard to the cask during onsite transportation to the ISFSI facility or during transfer of the spent fuel and GTCC waste casks to an authorized offsite storage facility. At its closest point the historical transport route is approximately 966 ft from Route 101, which does not meet the RG 1.91 criteria and requires further review. As a result, a probabilistic risk assessment was performed (Reference 22) and it was determined, based on distance, traffic flow, and national truck crash data that the



risk of exceeding the RG 1.91 overpressure criteria is  $8.85\text{E-}8/\text{year}$ , which is less than the  $1\text{E-}6/\text{year}$  acceptance criteria in RG 1.91. Therefore, no explosion analysis was performed.

#### **8.2.6.2.7 Fossil Power Plant Explosion (historical)**

Event E7 involves a fossil power plant explosion (fixed or mobile units). There are safety provisions at HBPP Units 1 and 2, as well as in the mobile generators, that are designed to prevent explosions and to avoid undetected leakage. Similarly, explosions of steam boilers at power plants are precluded by design requirements as required by codes and standards. A fossil plant boiler explosion was analyzed (Reference 21) for effects on a cask in transport and during storage at the ISFSI. The resultant overpressures on the cask during transport and the ISFSI vault were calculated. Table 8.2-13 shows the computed overpressures on the cask during onsite transportation and at the ISFSI for this event. The computed overpressure is much less than the HI-STAR HB overpack design external pressure. Given the massive size of the reinforced concrete vault, specifically the lid thickness, the impacts from the calculated overpressure on the reinforced concrete structure will not produce any adverse structural effects on the vault or the HI-STAR HB cask inside the vault.

During transport, the transit time is very small, and an explosion in that interval is not considered credible. However, the resulting pressure is still well within the design pressure of the HI-STAR cask.

This computed overpressure exceeds the RG 1.91 acceptance criteria of 1 psi. Following the guidance of RG 1.91, when the 1 psi overpressure criterion is exceeded an analysis of missile effects is required. This analysis is discussed in Section 8.2.6.2.9.

#### **8.2.6.2.8 Barge in Bay Carrying Fuel**

Event E8 concerns the detonation of a barge that contains a maximum of 87,000 barrels of fuel as it moves up the North Bay to the Chevron Fuel Terminal. As discussed in Section 2.2.1.2, the gasoline barge is not considered to be a hazard to the transport of spent fuel because administrative controls will ensure that fuel is not transported when the barge is moving through the bay. However as stated in Section 2.2.1.2, the barge needed to be further evaluated when considering potential effects on the ISFSI facility itself.

This barge holds a maximum of 87,000 barrels of liquid fuels in 12 separate tank compartments. Normally the barge carries gasoline in eight compartments and diesel fuel in the other four compartments. Each compartment holds approximately 7,250 barrels of fuel and is separated from the other compartments by steel walls. This barge is not motorized and requires a tug boat for motion. Because of the lack of onboard motive force, there are a limited number of ignition sources on the vessel. When the barge is moving through the bay, the shipping company and the U.S. Coast



Guard control its motion and the motion of other vessels in the area. These controls include requiring good weather and low vessel traffic.

The edge of the North Bay channel is approximately 1500 yards from the ISFSI. Outside of that channel (i.e., closer to the ISFSI), the water depth is limited and will not support the movement of the barge with the tug boats. The ISFSI facility is a vault system that is built underground, with the exception of the vault cover. The actual vault is embedded in a hill and the top of the vault cover is approximately 44 ft above sea level.

The configuration of the barge and its separated tanks would not credibly support an explosion of the total volume of fuel on the barge at one time. The likely scenario would be an explosion of a single tank as a result of a fire or vessel collision. If this tank was to explode, then additional tanks might rupture and secondary explosions might result. However, the largest single explosion would not involve more than one tank at any time (additional information supporting this assumption is provided in PG&E Responses to NRC Question 15-16 in References 27 and 28). Based on this assumption, an evaluation was performed that showed that for the single tank volume the setback distance to ensure that the blast pressure wave was less than the RG 1.91 criteria of 1 psi would be approximately 4,338 ft. As the setback for the barge in the channel is approximately 4,500 ft, the effect of the blast would meet the RG 1.91 criteria and is considered acceptable.

### **8.2.6.2.9 Missile Evaluations**

The following is a discussion of missile evaluations for Events E1, E2, E3, E5, E7, and E9.

An evaluation of potential missiles from explosions in accordance with RG 1.91 concluded that the HI-STAR HB overpack is designed for Spectrum 1 missiles at Region I wind speeds (see Section 8.2.2). These missiles at, Region I wind speeds, would bound any potential missiles from any potential explosions. In addition, given the massive size of the reinforced concrete vault, specifically, the lid thickness, missiles, and their impacts on the reinforced concrete structure will not produce any adverse structural effects on the vault or the HI-STAR HB cask inside the vault. While local spalling can occur on the lid and vault apron, the structural integrity of the vault will remain intact. Most of the vault, with the exception of approximately 18 inches, is not a target for horizontal missiles due its below-grade location. In addition, NUREG-0800 Section 3.5.1.4 indicates that vertical velocities should be considered at 70 percent of the postulated horizontal velocities, except for small missiles, which are used to test barrier openings. The ISFSI vault has no openings; therefore, small missiles are not required to be evaluated. The HI-STAR HB casks are designed to withstand 100 percent of the postulated horizontal missile velocities, which bounds the requirements for vertical missiles without taking credit for the vault structure.

The PG&E Response to NRC Question 15-18 in Reference 27 justifies why the characteristics of explosion-generated missiles would be bounded by tornado-generated missile characteristics. The response also justifies why the methodology for estimating the effects of tornado-generated missiles on an item important to safety is applicable to estimate the effects of explosion-generated missiles.

### **8.2.6.2.10 Explosive Decompression of Compressed Gas Bottles**

Various buildings at the HBPP site also store a limited quantity of compressed gas cylinders, such as oxygen, nitrogen, and acetylene for use in various maintenance activities. During storage, proper restraint of the compressed gas bottles is controlled by administrative controls. Event E9 involves the missile created by the explosive decompression of a gas cylinder assuming that a compressed gas cylinder under high-pressure is damaged such that the valve assembly located at the top of the cylinder breaks off. While explosive decompression of these compressed gas cylinders were not explicitly evaluated for the HB ISFSI, this was evaluated for the Diablo Canyon (DC) ISFSI HI-TRAC (DC ISFSI FSAR, Section 8.2.6.2.2). The HI-TRAC (DCPP ISFSI FSAR, Table 3.2-2) and the HI-STAR HB (see Table 3.2-2) both utilize the same tornado missile design criteria. Both systems have been licensed by the NRC. Therefore, the HI-STAR HB design would preclude damage to the MPC confinement boundary due to a compressed gas bottle missile.

### **8.2.7 DROPS AND TIP-OVER**

The hypothetical drop/tip-over of a storage cask is classified as Design Event IV, as defined by ANSI/ANS-57.9. The design for the Humboldt Bay ISFSI, as explained below, eliminates the need to postulate and analyze cask drop and non-mechanistic tip-over events. The load path portions of the cask transporter and the lifting devices attached to the cask components (i.e., the HI-STAR HB overpack lifting trunnions) are designed to preclude drop events, either through redundancy or enhanced safety factors. Section 4.2.3.3 discusses the design codes and standards applicable to the HI-STAR HB System. Sections 3.3.3 and 4.3 discuss the design criteria, applicable codes and standards, and design features of the cask transporter that demonstrate that the transporter will not leave the transport route, tip over, or drop the loaded HI-STAR HB cask under all credible design basis conditions, including natural phenomena.

Section 8.2.1 describes the analysis of a seismic event, verifying that the cask transporter will not slide, tip over, or drop a loaded HI-STAR HB overpack, and the cask transporter will remain stable on the transport route for the duration of a credible earthquake. During long-term storage operations, the overpack is located in the ISFSI vault, which makes drops and tipover events non-credible. Therefore, HI-STAR HB cask drop events are not analyzed, nor are maximum lift heights established for handling the casks. Administrative controls in operation procedures will ensure the casks are lifted only to those heights necessary to complete the required activities for cask loading and unloading.

### **8.2.8 LEAKAGE FROM CONFINEMENT BOUNDARY**

The MPC-HB has a reliable seal-welded confinement boundary in accordance with Interim Staff Guidance (ISG) -18 (Reference 23) to contain radioactive fission products under all design basis normal, off-normal, and accident conditions. Therefore, in accordance with ISG-18, leakage of the MPC confinement boundary is not credible for the Humboldt Bay ISFSI and is not analyzed.

### **8.2.9 MIS-LOADING OF A DAMAGED FUEL ASSEMBLY**

This accident involves the potential for three mis-loading events involving damaged fuel assemblies. They are:

- Loading a damaged fuel assembly, in a damaged fuel container (DFC), in a fuel storage location not authorized for damaged fuel, or
- Loading a damaged fuel assembly into a fuel storage location without a DFC, or
- Loading more damaged fuel assemblies in an MPC than authorized

Any one of these events would place the MPC-HB in a condition not consistent with the criticality analysis. The criticality analysis assumes all damaged fuel is in DFCs and in certain authorized fuel storage locations in the MPC. This accident is precluded by the use of administrative controls, as described in Section 10.2.1.1, to ensure all fuel is correctly loaded into the MPC. Procedures are used to document and verify the fuel identification, classification, presence of a DFC, and the fuel storage location for all fuel assemblies in the MPC-HB. Therefore, this accident is not considered credible and is not analyzed.

### **8.2.10 EXTREME ENVIRONMENTAL TEMPERATURE**

Extreme environmental temperature is classified as a natural phenomenon Design Event IV, as defined in ANSI/ANS-57.9. Unlike the off-normal high temperature evaluated in Section 8.1.2, the postulated, extreme-high temperature is, based on historical temperature data, beyond what can be reasonably expected to occur over the life of the ISFSI and represents a bounding, worst-case scenario.

#### **8.2.10.1 Cause of Accident**

The extreme environmental temperature accident is caused by weather conditions that result in unusually high ambient temperature at the Humboldt Bay ISFSI site.

#### **8.2.10.2 Accident Analysis**

An extreme ambient temperature of 90°F is postulated at the ISFSI site. This value bounds the highest value for ambient air temperature ever recorded at the HBPP site

(see Section 2.3). Due to the low decay heat load of the stored fuel, a simplified evaluation was performed to determine a bounding estimate of the fuel cladding temperature, the cask, and vault component temperatures resulting from this event. The difference between the normal condition ambient temperature (52°F) and the extreme ambient temperature is 38°F. This difference is simply added to the normal condition fuel cladding and component temperatures for comparison against the accident temperature limits. The actual temperatures of the fuel cladding and components will be less due to the heat dissipation provided by the vault structure and heat loss to the ambient environment. The results listed in Table 8.2-14 show that the fuel cladding temperature and all component temperatures are below their respective temperature limits.

The effect of extreme environmental temperature on MPC internal pressure was also evaluated. The normal condition MPC internal cavity temperature of 251.8°F was conservatively increased by 38°F and the resultant pressure is calculated using the Ideal Gas Law. The resultant pressure is 75.1 psig (Reference 24), which is below the accident design pressure of 200 psig, and is therefore acceptable.

### **8.2.10.3 Dose Consequences for Extreme Environment Temperature Event**

The extreme environmental temperature event for the HI-STAR HB System was evaluated and the MPC confinement boundary remains intact. The margins between the accident temperatures and the accident temperature limits show that no radioactive releases will occur and the shielding effectiveness of the cask is not degraded. Therefore, dose rates remain at the normal level and no unique radiological analyses are necessary for this event.

### **8.2.11 100 PERCENT FUEL ROD RUPTURE**

This accident event postulates that all of the fuel rods in a sealed MPC rupture and that fission-product gases and fill gas are released from the fuel rods into the MPC cavity.

#### **8.2.11.1 Cause of Accident**

Through all credible accident conditions, the HI-STAR 100 System maintains the spent nuclear fuel in an inert environment while maintaining the peak fuel-cladding temperature below the short-term temperature limits; thereby, ensuring fuel-cladding integrity. Although rupture of all the fuel rods is assumed, there is no credible cause for 100 percent fuel rod rupture. This accident is postulated to evaluate the MPC confinement boundary for the maximum possible internal pressure based on the non-mechanistic failure of 100 percent of the fuel rods.

#### **8.2.11.2 Accident Analysis**

The 100 percent fuel rod rupture accident has no significant thermal, criticality, or shielding consequences. The event does not change the reactivity of the stored fuel,

the magnitude of the radiation source that is being shielded, the shielding capacity, or the criticality control features of the HI-STAR 100 System. The most significant thermal consequence of a postulated 100 percent fuel rod rupture accident is the increase in MPC confinement boundary pressure to 101.1 psig (Reference 24). The generic structural evaluation of the MPC for the accident condition internal pressure (200 psig) presented in Section 3.4 of the HI-STORM 100 FSAR demonstrates that the MPC shell stresses are well within the allowable values. By similarity of design, this analysis is applicable to the MPC-HB.

### **8.2.11.3 Accident Dose Calculations**

There is no effect on the shielding performance, confinement function, or criticality control features of the system as a result of this event. All MPC stresses remain within allowable values, ensuring confinement boundary integrity. Since there is no degradation in shielding or confinement capabilities as discussed above, there is no effect on occupational or public exposures as a result of this event.

The MPC confinement boundary maintains its integrity for this postulated event. There is no effect on the shielding effectiveness, and the magnitude of the radiation source is unchanged. However, the radiation source could redistribute within the sealed MPC cavity causing a slight increase in the radiation dose rates at the bottom of the cask. Since the cask is always handled vertically and access to the bottom of the cask is unnecessary for loading operations, increased bottom dose rates have no significant effect on personnel or off-site dose.

### **8.2.12 LIGHTNING**

A lightning strike is classified as natural phenomena, Design Event IV, in accordance with ANSI/ANS 57.9. A lightning strike can occur during cask transport or storage. HI-STAR 100 FSAR Section 11.2.11 discusses the effects of a lightning strike on a HI-STAR cask and concludes there is no degradation in shielding or confinement capabilities and there is no effect on occupational or public exposures as a result of lightning.

Section 3.2.6 of this FSAR discusses the potential for lightning strikes at the Humboldt Bay ISFSI. Section 3.2.6 indicates the HI-STAR HB may be subject to lightning strikes while in transport from the RFB to the ISFSI vault, but not after it is placed in the vault and the vault lid is installed. The cask transporter provides protection for the HI-STAR HB from direct lightning strikes. The gantry and rigging metal above the cask is sufficient such that no direct lightning strike is anticipated. A lightning strike on the cask transporter would not structurally affect the transporter's ability to hold the suspended load, due to the massive amount of steel in the structure. The current from a lightning strike would be transmitted to ground without significantly damaging the transporter structure. Lightning may affect the operator and/or drive and control systems of the transporter. However, the transporter is designed to shut down in a fail-safe condition.

In addition, the HI-STAR 100 FSAR lightning evaluation is applicable to the HI-STAR HB.

Based on this evaluation, it is concluded that the lightning accident does not affect the safe operation of the HI-STAR HB.

### **8.2.13 TURBINE MISSILES (Historical)**

The only time that turbine missiles are required to be evaluated is when the target in question is within the low-trajectory missile strike zone, defined by  $\pm 25$ -degree lines emanating from the centers of the first and last low-pressure turbine wheels as measured from the plane of the wheels. The loaded HI-STAR HB cask will be in this strike zone for a short period of time while it is being transported from the RFB to the ISFSI vault. While in this strike zone, it should be noted that there is an even shorter time period when there is a direct line of sight from the Unit 1 and 2 turbines to the transport route. Yet, for conservatism, this scenario is evaluated in PRA-03-12 (Reference 25).

This risk assessment conservatively assumed that the transporter carrying the loaded overpack is in the defined unfavorable orientation for approximately half of the length of the transport route and took no credit for shielding of any components by plant structures. This risk assessment concluded that the probability of a missile strike during onsite cask transportation operations, due to low-trajectory turbine missiles, is below the upper limit accepted by RG 1.115 (Reference 26), as an acceptable risk rate. Therefore, a turbine missile strike on the cask is not considered to be a credible event and no analysis was performed.

### **8.2.14 BLOCKAGE OF MPC VENT HOLES**

Each MPC basket fuel cell wall has elongated vent holes at the bottom. The blockage of the MPC basket vent holes event analyzes the effect on the HI-STAR HB System due to the restriction or full blockage of helium flow through the vent holes. These holes facilitate the natural circulation of helium inside the MPC for convection heat transfer. The partial blockage of the MPC basket vent holes accident has been evaluated generically to determine the effects on the HI-STAR 100 System due to the reduction in the size of the vent openings. This accident condition is discussed in Section 11.2.4 of the HI-STAR 100 System FSAR and the method of evaluation is applicable to the HI-STAR HB System.

#### **8.2.14.1 Cause of Blockage of MPC Vent Holes**

After the MPC is loaded with spent nuclear fuel, the MPC cavity is drained, dried, and backfilled with helium. Fuel cladding, fuel pellets, and crud are the only three possible sources of material that could block the MPC basket vent holes. Gross fuel cladding rupture is precluded by design in accordance with 10 CFR 72.122(h)(1). Due to the maintenance of relatively low cladding temperatures during storage, it is not credible



that the fuel cladding would rupture and that fuel cladding and fuel pellets would fall to block the basket vent holes. Damaged fuel is stored in damaged fuel containers, which have screens to minimize the dispersal of gross particulates. However, it is conceivable that a percentage of the loose crud deposited on the external surfaces of the fuel rods may fall away and deposit at the bottom of the MPC.

Crud can be made up of two types of layers, namely, loosely-adherent and tightly-adherent. The fuel assembly movement from the fuel racks to the MPC, and subsequent movement of the MPC during cask loading and transport operations, may cause a portion of the loosely-adherent crud to fall away. The tightly-adherent crud remains in place during ordinary fuel handling operations.

#### **8.2.14.2 Analysis of Partial Blockage of MPC Vent Holes**

The MPC vent holes that act as the bottom plenum for the MPC internal helium circulation are of an elongated, semi-circular design to ensure that the flow passages will remain open under a hypothetical shedding of the crud on the fuel rods (see Figure 3.3-2). Two evaluations are provided. The first is a qualitative evaluation based on the generic HI-STAR 100 work that demonstrates that it is unlikely that enough crud would deposit at the bottom of the MPC to block any portion of the semi-circular flow hole area assumed to be available in the thermal analysis. The second evaluation discusses the impact of full blockage of the MPC vent holes by crud and/or other fuel-related debris in the MPC.

In the generic evaluation discussed in Section 11.2.4 of the HI-STAR 100 FSAR, the maximum amount of crud was assumed to be present on all fuel rods within the MPC-68, assuming a standard boiling water reactor (BWR) fuel assembly with an active fuel length on the order of 150 inches. Both the tightly- and loosely-adherent crud was conservatively assumed to fall off of the fuel rods. The maximum crud depth calculated generically for the MPC-68 is listed in Table 2.2.8 of the HI-STAR 100 System FSAR (0.85 inch). Since the generic MPC-68 design and the MPC-HB design have the same internal diameter, the generically evaluated MPC-68 crud depth can be scaled up by the ratio of the number of fuel assemblies in each basket (80/68) to conservatively estimate the crud depth for the MPC-HB as 1.0 inch. This is a conservative approach to estimating the MPC-HB crud depth for the following reasons:

- The HBPP fuel assemblies are approximately half the length of the design basis BWR fuel assembly used to estimate the crud depth in the generic evaluation.
- The design basis burnup of the HBPP fuel is 23,000 megawatt-days per metric ton of uranium, which is less than typical burnups of BWR fuel of more recent vintage, meaning crud creation is less on the HBPP fuel.

## HUMBOLDT BAY ISFSI FSAR UPDATE

- Drop events for the HI-STAR HB System are not credible; therefore, the driving force for the accumulation of crud at the bottom of the MPC is not as high as the generic design.

The cross-sectional flow area of the vent holes assumed in the thermal analysis is a semi-circle of radius 1-1/4 inch. The elongation of the holes is another one inch. Because the estimated depth of the crud is one inch, the crud does not block the semi-circular area of the vent holes, there is no effect on the thermal analysis and the results of this accident evaluation are acceptable.

In the unlikely event that enough crud accumulated in the bottom of the MPC to completely block the vent holes and halt the circulating flow of helium (thermosiphon effect), adequate heat transfer from the fuel to the MPC shell would still occur. This is based on the HI-STAR 100 System thermal analysis described in Chapter 4 of the HI-STAR 100 System FSAR. The current licensing basis thermal analysis for the HI-STAR 100 System suppresses the thermosiphon effect and relies solely on the conduction and radiation modes of heat transfer to remove the decay heat generated by the fuel. The peak fuel cladding temperature computed in the generic analysis is 741.5°F, which is less than the normal temperature limit of 752°F and much less than the accident temperature limit of 1058°F. While the generic BWR MPC holds 68 fuel assemblies and the MPC-HB holds 80, the generic analysis is applicable and provides a bounding case for the following reasons:

- The effective thermal properties for the two MPC designs are of the same order.
- The heat load used in the generic analysis (18.5 kW) is nearly an order of magnitude higher than the maximum heat load permitted in any one HI STAR HB System (2 kW).

The blockage of the MPC basket vent holes has no unacceptable effect on the structural, confinement, and thermal analysis of the MPC. There is no significant effect on the shielding analysis because the source term from the crud is enveloped by the source term from the fuel and the activated nonfuel hardware of the fuel assemblies. Because the MPC basket vent holes are either not completely blocked or will not be blocked with enough material to prevent water flow between fuel cells, preferential flooding of the MPC fuel basket is not possible during draining operations and, therefore, the criticality analyses are not affected.

### **8.2.14.3 Dose Calculations for Blockage of MPC Vent Holes**

Blockage of MPC basket vent holes will not result in a compromise of the confinement boundary because the thermal model accounts for the blockage. Therefore, there will be no loss of confinement or radioactive material release.

Any increase in dose rate through the bottom of the cask due to crud accumulation is inconsequential for several reasons. The total amount of source in the cask is not increased; it is simply relocated by the distance between where the crud particle was located on the fuel assembly and the bottom of the MPC. Any minimal dose increase at the bottom of the cask is inconsequential while the cask is in the ISFSI vault because the bottom of the cask (being flush against the vault bottom surface) is not a source of exposure during storage operations. During vertical handling operations, operations do not require personnel access to the bottom of the cask and the cask is lifted only to those heights necessary to facilitate required cask movements. These heights are typically low enough to physically prevent personnel access. Therefore, the cask is carried very close to the ground such that access is physically restricted and any additional dose to personnel is negligible.

## 8.2.16 REFERENCES

1. ANSI N57.9-1992, Design Criteria for an Independent Spent Fuel Storage Installation (dry type), American National Standards Institute.
2. ACI-349-01, Code Requirements for Nuclear Safety Related Concrete Structures, American Concrete Institute.
3. Visual Nastran Desktop Code, Version 2001, MSC Software Corp., 2001.
4. Final Safety Analysis Report for the HI-STAR 100 System, Holtec International Report No. HI-2012610, Revision 1, December 2002.
5. Calculation No. GEO.HBIP.02.05, Seismic Time Histories for DBE, Revision 0.
6. Standard Review Plan for the Review of Safety Analysis Reports for Nuclear Power Plants, USNRC, NUREG-0800, July 1981.
7. ASCE 4-98, Seismic Analysis of Safety-Related Nuclear Structures and Commentary on Standard for Seismic Analysis of Safety-Related Nuclear Structures, American Society of Civil Engineers, September 1998.
8. Calculation No. HI-2033046, Seismic Response of HI-STAR HB in RFB and Yard in RFB, Revision 0.
9. Calculation No. HI-2033036, Seismic Response of the HI-STAR HB and Transporter to the DBE Event, Revision 0.
10. Calculation No. GEO.HBIP.02.08, Stability of Transport Route, Revision 1.

## HUMBOLDT BAY ISFSI FSAR UPDATE

11. Calculation No. HI-2033014, Seismic Response of HI-STAR HB in Vaults Subject to DBE, Revision 1.
12. ANSYS Version 7.0, ANSYS, INC., 2003.
13. Calculation No. HI-2033013, Humboldt Bay Cask Storage Vault Structural Analysis, Revision 3.
14. Calculation No. GEO.HBIP.02.07, Stability of ISFSI Site, Revision 1.
15. Regulatory Guide 1.76, Design Basis Tornado for Nuclear Power Plants, USNRC, April 1974.
16. Standard ASCE 7-98, Minimum Design Loads for Buildings and Other Structures, American Society of Civil Engineers, 1998.
17. Calculation No. HI-2033006, Evaluation of Fires for the HBPP ISFSI, Revision 3.
18. National Fire Protection Association Fire Protection Handbook, 16th Edition, 1986.
19. Calculation No. HI-2033047, ISFSI Dose Assessment for Humboldt Bay, Revision 1.
20. Evaluations of Explosions Postulated to Occur on Transportation Routes Near Nuclear Power Plants, USNRC, Regulatory Guide 1.91, Revision 1, February 1978.
21. Calculation No. HI-2033041, Evaluation of Explosions for the HBPP ISFSI, Revision 1.
22. Calculation PRA-03-13 Risk Assessment of Explosive Hazards to the Dry Cask/Spent Fuel Transportation and Storage at the Humboldt Bay ISFSI, Revision 0, December 2003.
23. Interim Staff Guidance 18, The Design/Qualification of Final Closure Welds on Austenitic Stainless Steel Containers as Confinement Boundary for Spent Fuel Storage and Containment Boundary for Spent Fuel Transportation, USNRC, May 2003.
24. Calculation No. HI-2033033, Humboldt Bay Thermal Analysis, Revision 0.
25. Calculation PRA 03-12 Risk Assessment of Turbine Missiles While Transporting Loaded Casks on the Humboldt Bay Transport Route, Revision 0, December 2003

## HUMBOLDT BAY ISFSI FSAR UPDATE

26. Regulatory Guide 115, Protection from Low-Trajectory Turbine Missiles, USNRC, July 1977.
27. PG&E Letter HIL-04-007, Response to NRC Request for Additional Information for the Humboldt Bay Independent Spent Fuel Storage Installation Application, October 1, 2004.
28. PG&E Letter HIL-05-003, Response to NRC Request for Additional Information for the Humboldt Bay Independent Spent Fuel Storage Installation Application, April 8, 2005.
29. PG&E Application for Certification to Construct the Humboldt Bay Repowering Project to the California Energy Commission, September 29, 2006.
30. Ground-Level Aqueous Ammonia Concentration, Worst-Case Release Scenario, Humboldt Bay Generating Station, results: Figure 2-1

### **8.3      SITE CHARACTERISTICS AFFECTING SAFETY ANALYSIS**

The Humboldt Bay Independent Spent Fuel Storage Installation (ISFSI) storage site is located as shown in Figure 2.2-2. The nearby transportation facilities are described in Section 2.2. Sections 2.2 and 8.2 evaluate the onsite and offsite industrial, transportation, or military facilities that could potentially have a significant adverse impact on the ISFSI. Site characteristics that affect the safety analysis, and how they have been considered in developing suitable margins of safety for the storage of Humboldt Bay Power Plant's spent fuel, are summarized in Table 8.3-1.



## HUMBOLDT BAY ISFSI FSAR UPDATE

TABLE 8.2-1

### KEY INPUT DATA FOR TRANSPORTER STABILITY

ITEM	VALUE
Weight of HI-STAR with MPC (lb.)	161,200
Weight of Transporter (lb.)	190,000
Transporter/Ground Interface Coefficient of Restitution	0.5
Transporter/Ground Coefficient of Friction	0.8, 0.4
Travel Path Grade for Analyses	0%, 8.5% (bounds actual grade)

# HUMBOLDT BAY ISFSI FSAR UPDATE

TABLE 8.2-2

## TRANSPORTER SIMULATIONS

<b>SEISMIC EVENT</b>	<b>REMARKS</b>
DBE 1	COF=0.4, Grade=0%, 8.5%
DBE 2	COF=0.4, Grade=0%, 8.5%
DBE 3	COF=0.4, Grade=0%, 8.5%
DBE 4	COF=0.4, Grade=0%, 8.5%
DBE 3	COF=0.4, Grade=8.5%, Horizontal Earthquakes Rotated 90 degrees
DBE3	COF=0.8, Grade=8.5%
0.5 x DBE3	COF=0.4, Grade=0%
0.25 x DBE3	COF=0.4, Grade=0%

# HUMBOLDT BAY ISFSI FSAR UPDATE

TABLE 8.2-3

## MAXIMUM TRANSPORTER EXCURSIONS

Seismic Event	Level Ground – Max. Excursion Perpendicular to Track (inch)	8.5% Grade – Max. Excursion Parallel to Track (inch)	8.5% Grade – Max. Excursion Perpendicular to Track (inch)	Remarks
DBE 1	108	289	81	COF=0.4
DBE 2	175	297	20	COF=0.4
DBE 3	258	449	63	COF=0.4
DBE 4	213	341	42	COF=0.4
DBE 3	-	215	282	COF=0.4 with FN perpendicular to roadway
DBE3	136 (base of transporter) 136.40 (top of transporter)	-	-	COF=0.8
0.5 x DBE3	60.8	-	-	COF=0.4
0.25 x DBE3	1.59	-	-	COF=0.4

## HUMBOLDT BAY ISFSI FSAR UPDATE

TABLE 8.2-4

PEAK IMPACT LOAD FROM DYNAMIC ANALYSIS OF HI-STAR HB IN VAULT

<b>Seismic Event</b>	<b>Lateral Impact Force At Base (kip)</b>	<b>Lateral Impact Force at Top (kip)</b>	<b>Vertical Impact Force at Base of Vault Liner (kips)</b>
DBE 1	476.8	573.6	810.6
DBE 2	750.9	294.2	653.6
DBE 3	799.0	457.5	853.3
DBE 4	750.0	525.0	515.0

# HUMBOLDT BAY ISFSI FSAR UPDATE

TABLE 8.2-5

## EFFECTIVE DESIGN LOADS AND AMPLIFICATION FACTOR FOR VAULT STRUCTURAL INTEGRITY ANALYSIS

Upper Impact Location (kips)	Lower Impact Location (kips)	Vertical Load (kips)
$500 \times 1.5 = 750$	$800 \times 1.5 = 1,200$	854

# HUMBOLDT BAY ISFSI FSAR UPDATE

TABLE 8.2-6

## REINFORCED CONCRETE PROPERTIES

Property	Value
Compressive Strength	4,000 psi
Modulus of Elasticity*	$3.6 \times 10^6$ psi
Poisson's Ratio	0.17
Reinforcement Yield Strength**	60,000 psi
Thermal Conductivity	1.0 Btu / ft-hr-°F
Coefficient of Thermal Expansion	$5.5 \times 10^{-6}$ in / in / °F
Density	150 lb / ft ³

*  $57,000 \times \sqrt{f_c}$  , where  $f_c$  is the compressive strength of concrete

** ASTM A 615 Grade 60



# HUMBOLDT BAY ISFSI FSAR UPDATE

TABLE 8.2-7

## PROPERTIES OF CARBON STEEL SHELL LINER, ASME SA-36*

Property	Value
Modulus of Elasticity**	$28.8 \times 10^6$ psi
Poisson's Ratio	0.3
Thermal Conductivity	20.0 Btu / ft-hr-°F
Coefficient of Thermal Expansion***	$5.89 \times 10^{-6}$ in / in / °F
Density	0.283 lb / in ³

* Property values at 200°F

** Carbon steel with C < 0.30%

*** Mean coefficient of thermal expansion for Material Group C, C-Mn-Si steels

# HUMBOLDT BAY ISFSI FSAR UPDATE

TABLE 8.2-8  
SOIL PROPERTIES

Property	Value
Static Shear Modulus	33,952 psi
Static Modulus of Elasticity	90,311 psi
Seismic Shear Modulus	11,875 psi
Seismic Modulus of Elasticity	32,000 psi
Poisson's ratio	0.3
Density	130 lb / ft ³
Thermal Conductivity*	0.833 Btu / ft-hr-°F

# HUMBOLDT BAY ISFSI FSAR UPDATE

TABLE 8.2-11

## RESULTS OF CASK ENGULFING FIRE ANALYSIS

<b>CASK SYSTEM COMPONENT</b>	<b>MAXIMUM TEMPERATURE (°F)</b>
Fuel Cladding	813.6
Fuel Basket Periphery	587.7
MPC-HB Enclosure Vessel Inner Surface	259.2
MPC-HB Enclosure Vessel Outer Surface	258.9
Overpack Inner Shell Inner Surface	251.1
Overpack Inner Shell Outer Surface/ Intermediate Shells Inner Surface	250.5
Overpack Intermediate Shells Outer Surface/Neutron Absorber Inner Surface	249.5
Overpack Neutron Absorber Outer Surface/Enclosure Shell Inner Surface	1189.4
Overpack Enclosure Shell Outer Surface	1208.7

# HUMBOLDT BAY ISFSI FSAR UPDATE

TABLE 8.2-12

## RESULTS OF NON-ENGULFING FIRE ANALYSES

<b>Fire Event</b>	<b>Distance from Cask (ft.)</b>	<b>Distance from ISFSI (ft.)</b>	<b>Cask Surface Temp. Rise (°F)</b>	<b>Vault Lid Temp. Rise (°F)</b>
Unit 1 Residual No. 6 Fuel Oil Storage Tank 1	322	322 (Note 1)	165.1	103.9
Unit 1 Residual No. 6 Fuel Oil Service Tank 2	237	237 (Note 1)	75.2	29.8
Unit 2 Residual No. 6 Fuel Oil Service Tank 1	243	243 (Note 1)	229.6	182.8
Unit 2 Residual No. 6 Fuel Oil Service Tank 2	198	198 (Note 1)	98.9	47.5
Diesel Fuel Storage Tank	232	232 (Note 1)	56.9	9.5
Diesel Fuel North Service Tank	123	N/A	237.9	N/A
Diesel Fuel South Service Tank	123	N/A	237.9	N/A
Gasoline Tanker Truck	N/A	80	N/A	149.3
Propane Storage Tank	113	370	43.1	0.2
Unit 3 Transformers	52	N/A	169.0	N/A
Natural Gas Distribution Pipeline	N/A	377	N/A	1.0
Natural Gas Main Supply	409	N/A	8.6	N/A
Site Vegetation	N/A	20	N/A	93.2
Fuel Oil Tanker Truck	N/A	80	N/A	149.3
Diesel Fuel Tanker Truck	N/A	80	N/A	149.3
Propane Tanker Truck	N/A	394	N/A	2.3

### NOTES:

1. The closest approach of the cask transporter to these tanks is at the ISFSI.

# HUMBOLDT BAY ISFSI FSAR UPDATE

TABLE 8.2-13

## RESULT FROM EXPLOSION ANALYSES

<b>Explosion Event</b>	<b>Distance to Cask (ft)</b>	<b>Distance to Vault (ft)</b>	<b>Cask Overpressure (psig)</b>	<b>Vault Overpressure (psig)</b>
Propane Tank	113	414	16.0	1.8
Propane Vapor Cloud	N/A	20 (Note 1)	N/A	82.0
Natural Gas Distribution Line	N/A	377	N/A	6.3
Natural Gas Distribution Line Vapor Cloud	N/A	20 (Note 1)	N/A	199.1
Propane Tanker Truck	N/A	394	N/A	2.3
Gasoline Tanker Truck	N/A	562	N/A	2.2
Other Site Vehicles	N/A	50	N/A	7.2
Unit 1 or 2 Boiler	227	454	16.8	4.6

### NOTES:

1. This distance is from the vault surface to the center of a 40-ft high cloud.

# HUMBOLDT BAY ISFSI FSAR UPDATE

TABLE 8.2-14

## EXTREME ENVIRONMENTAL TEMPERATURE RESULTS

<b>Component</b>	<b>Accident Temperature (°F)</b>	<b>Accident Temperature Limit (°F)</b>
Fuel Cladding	411	1058
Neutron Shield Material	233	300
MPC Shell	241	775
Vault Concrete	213	350

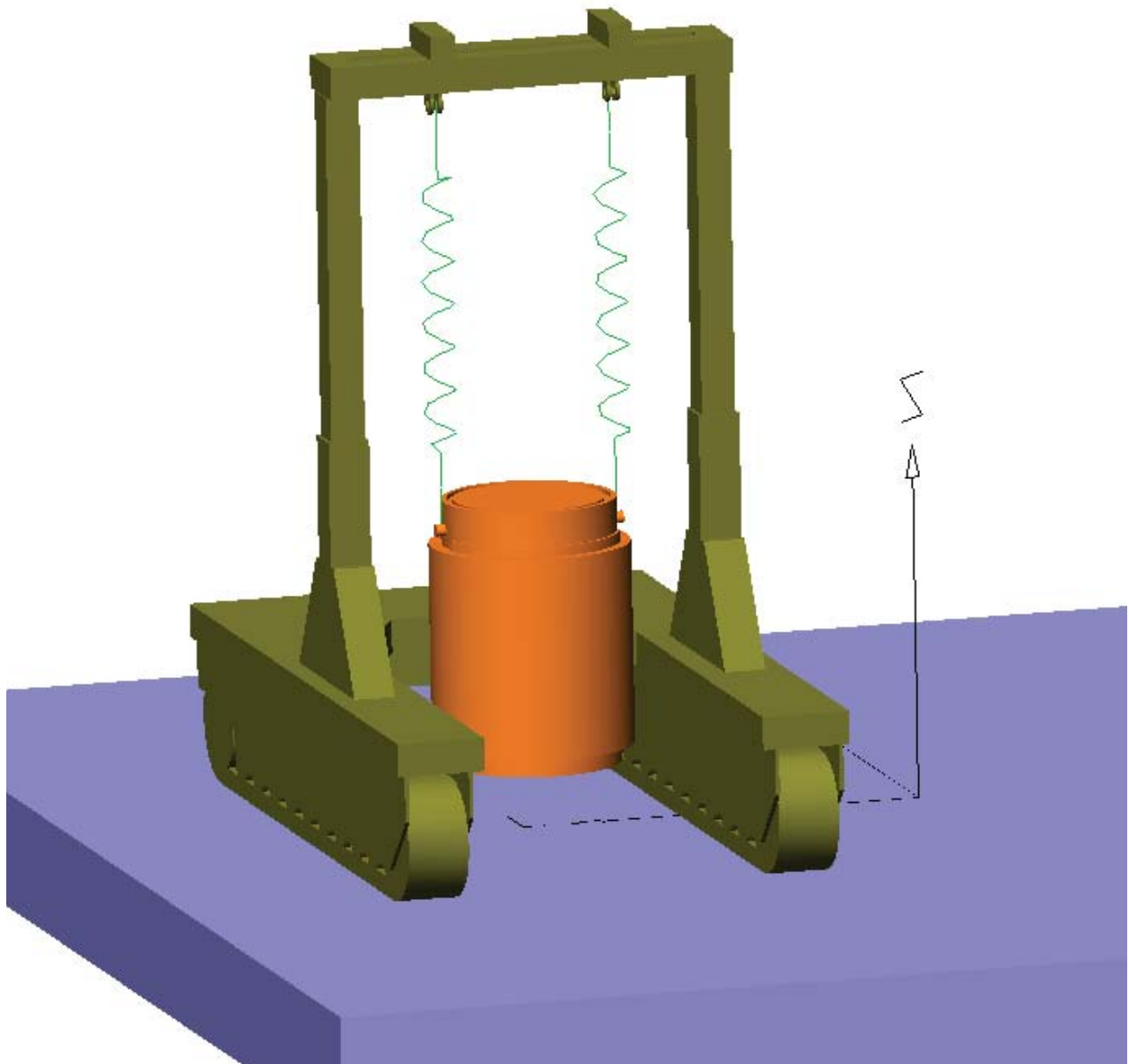


# HUMBOLDT BAY ISFSI FSAR UPDATE

TABLE 8.3-1

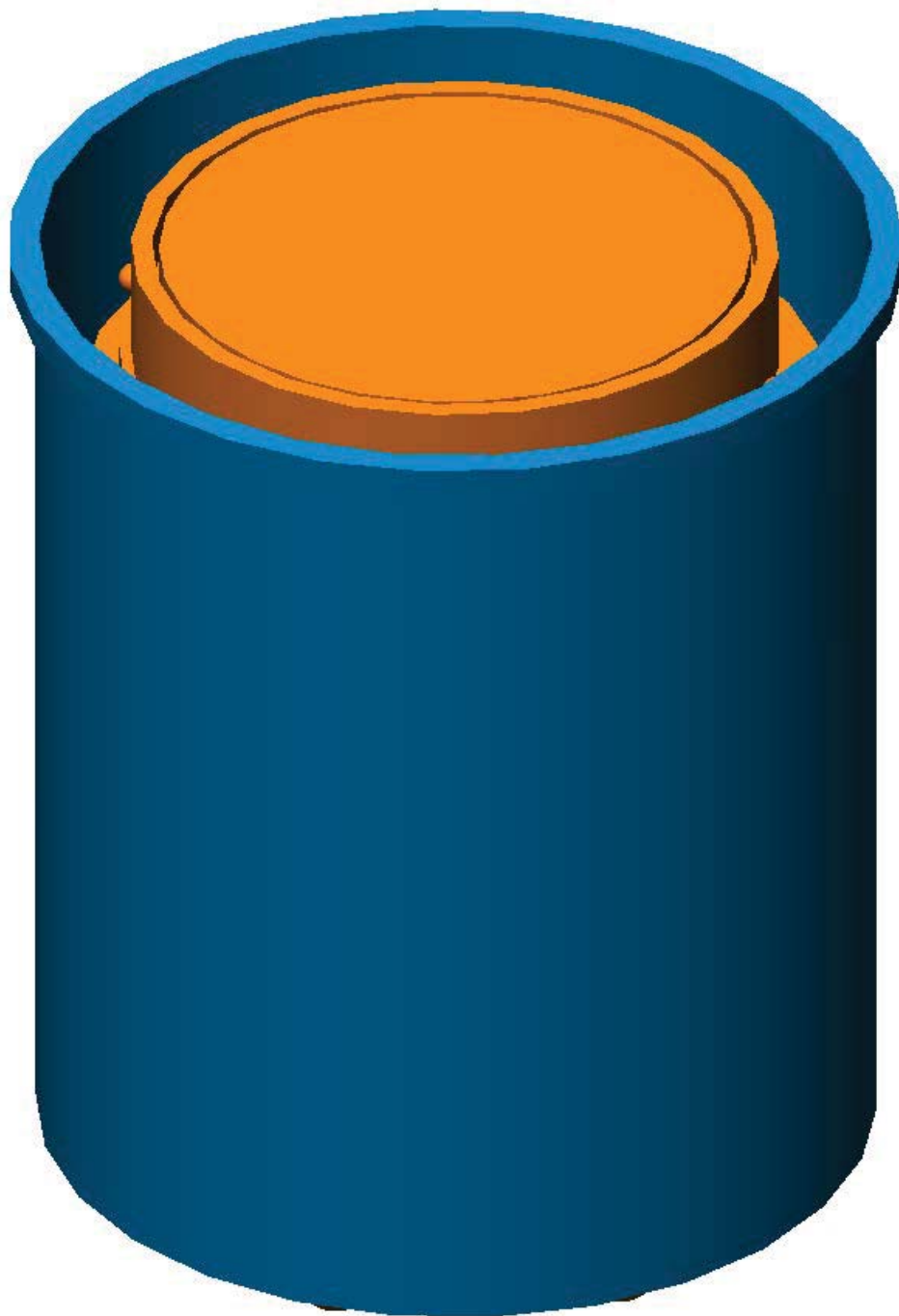
## SUMMARY OF SITE CHARACTERISTICS AFFECTING SAFETY ANALYSIS

Site Characteristic	Effect on ISFSI Safety Analysis
Earthquakes	Regional and site geology and seismology were used to define the design basis ground motion. (Sections 3.2 and 8.2.1)
Tornado winds and missiles	Regional meteorology and plant conditions were considered in the determination of the design basis tornado maximum wind and missile parameters. (Sections 3.2 and 8.2.2)
Flooding	ISFSI evaluated and determined to be acceptable. (Sections 3.2 and 8.2.3)
Tsunami	Even though the maximum estimated tsunami runup may flow above the ISFSI elevation, the tsunami hazard at the proposed ISFSI site is negligible, because the casks can be temporarily wetted without harm and they will be contained in underground vaults which protect them from damage by flowing water and damage from water-born debris. (Sections 2.6 and 8.2.4)
Fires	The evaluation of fire potential was based on the site characteristics and equipment. (Sections 2.2, 3.3, and 8.2.5)
Explosions	Site-specific conditions were evaluated and bounded by the cask design. Administrative controls are used to limit the risk. (Sections 2.2, 3.3, and 8.2.6)
Severe environmental conditions in summer and winter	Thermal analyses of the effects of abnormally high ambient temperatures on the storage system considered climatic conditions of the area. Design temperatures were selected to bound day/night average maximum temperatures that could occur over a significantly long period of time. (Sections 3.2 and 8.2.10)
Lightning	Evaluation determined cask design acceptable. (Sections 3.2 and 8.2.12)
Turbine Missiles	This event is not considered to be credible for the ISFSI facility because of the configuration and location of the turbines in relation to the ISFSI. However, this event could potentially affect the transport of spent fuel. This event is evaluated in Section 8.2.13. (Sections 2.2 and 8.2.13)
Site location	A public trail to access a breakwater for fishing traverses the ISFSI controlled area (Figure 2.1-2). Public access to and recreation activities on the breakwater will be restricted by PG&E during ISFSI activities that require limited access within the 100-meter controlled area. (Section 2.1.2)



<b>FSAR UPDATE</b>
<b>HUMBOLDT BAY ISFSI</b>
<b>FIGURE 8.2-1 VN SIMULATION MODEL SHOWING HI-STAR HB CARRIED BY TRANSPORTER</b>

Revision 0 January 2006



<b>FSAR UPDATE</b>
<b>HUMBOLDT BAY ISFSI</b>
<b>FIGURE 8.2-2</b> <b>VISUAL NASTRAN SIMULATION</b> <b>MODEL OF VAULT LINER</b> <b>CONTAINING LOADED HI-STAR HB</b>

Revision 0 January 2006

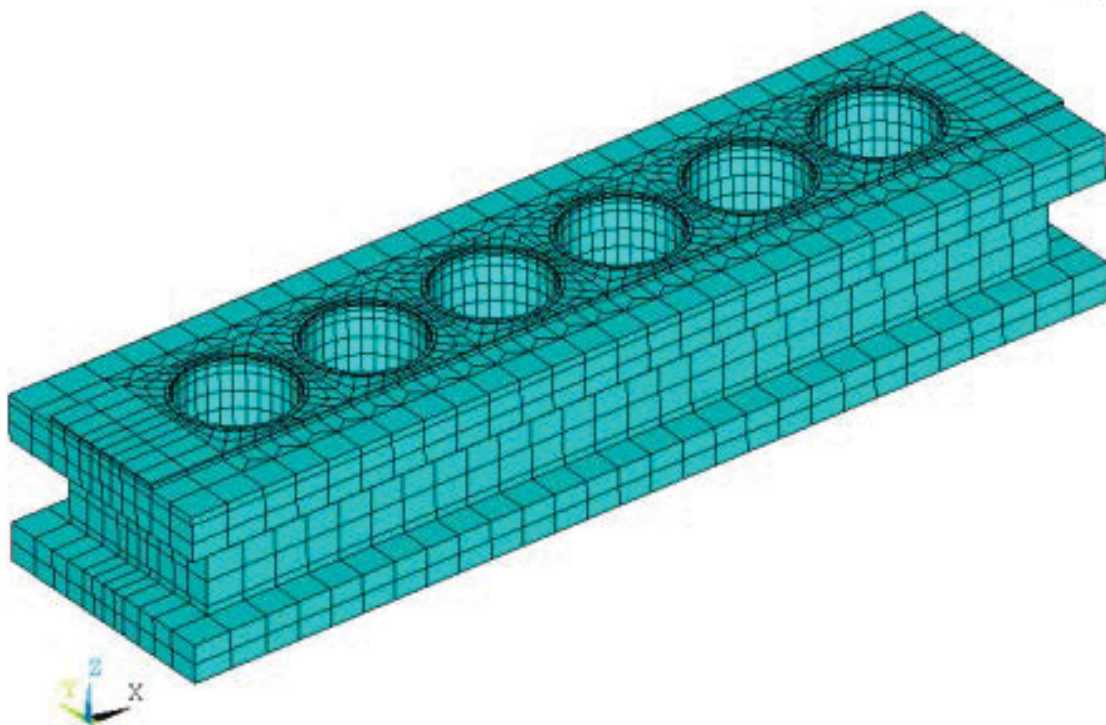
1

ELEMENTS

ANSYS

JUN 5 2003

09:16:44

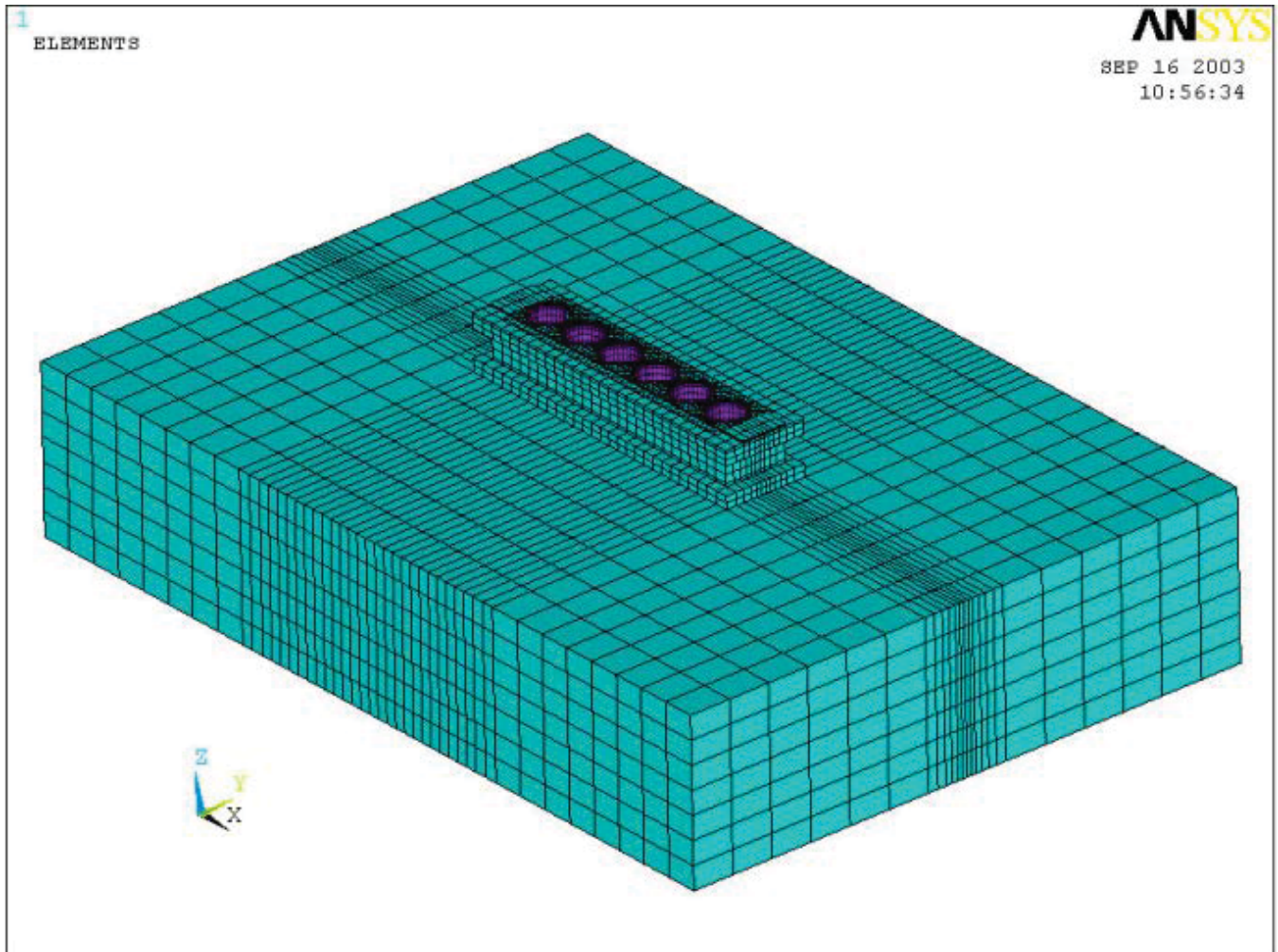


FSAR UPDATE

HUMBOLDT BAY ISFSI

FIGURE 8.2-3  
VAULT FINITE ELEMENT MODEL

Revision 0 January 2006

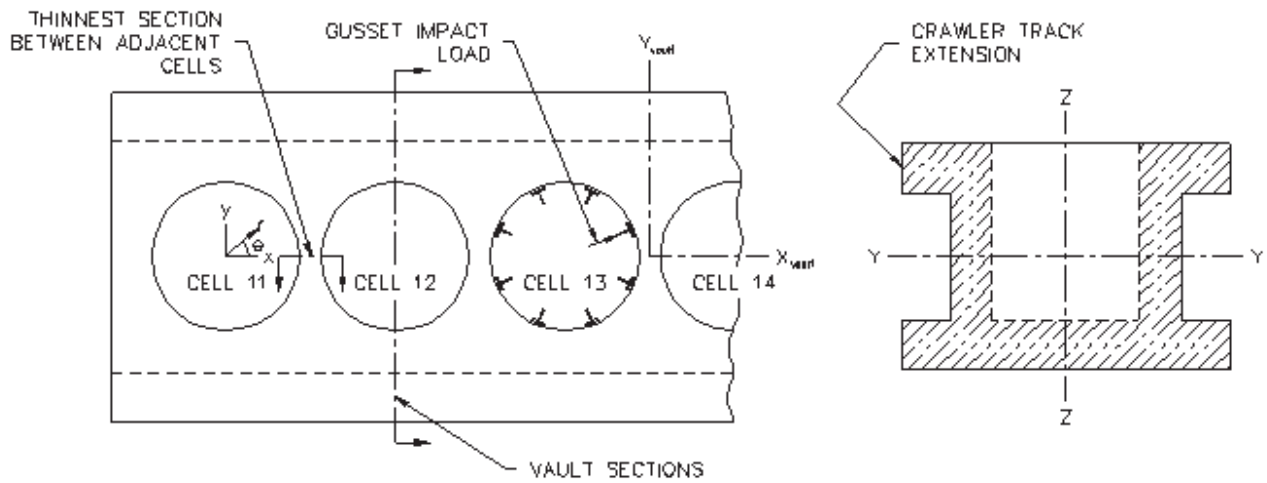


**FSAR UPDATE**

**HUMBOLDT BAY ISFSI**

**FIGURE 8.2-4  
VAULT AND SUBGRADE FINITE  
ELEMENT MODEL**

Revision 0 January 2006



<b>FSAR UPDATE</b>
<b>HUMBOLDT BAY ISFSI</b>
<b>FIGURE 8.2-5 GLOBAL CROSS SECTIONS EVALUATED FOR CAPACITY/DEMAND RATIO</b>

Revision 0 January 2006



# HUMBOLDT BAY ISFSI FSAR UPDATE

## CHAPTER 9

### CONDUCT OF OPERATIONS

#### CONTENTS

<u>Section</u>	<u>Title</u>	<u>Page</u>
9.1	ORGANIZATIONAL STRUCTURE	9.1-1
9.1.1	Corporate Organization	9.1-1
9.1.2	Corporate Functions, Responsibilities, and Authorities	9.1-2
9.1.3	In-House Organization	9.1-2
9.1.4	Relationships with Contractors and Suppliers	9.1-2
9.1.5	Technical Staff	9.1-2
9.1.6	Operating Organization, Management, and Administrative Control System	9.1-2
9.1.7	Personnel Qualification Requirements	9.1-3
9.1.8	Liaison With Outside Organizations	9.1-4
9.1.9	References	9.1-4
9.2	ISFSI TEST PROGRAM	9.2-1
9.2.1	Administrative Procedures for Conducting Test Program	9.2-1
9.2.2	Test Program Description	9.2-1
9.2.3	Preoperational Testing	9.2-2
9.2.4	Startup Test Plan	9.2-2
9.2.5	Operational Startup Testing	9.2-3
9.2.6	Operational Readiness Review Plan	9.2-3
9.3	TRAINING PROGRAM	9.3-1
9.3.1	Humboldt Bay Power Plant and ISFSI General Employee Training	9.3-1
9.3.2	Supplemental ISFSI Training	9.3-2
9.3.3	ISFSI Certification	9.3-3
9.3.4	Continuing ISFSI Training	9.3-3
9.3.5	Job Specific	9.3-4
9.3.6	Administration and Records	9.3-4
9.4	NORMAL OPERATIONS	9.4-1
9.4.1	Procedures	9.4-1
9.4.2	Records	9.4-3
9.5	EMERGENCY PLANNING	9.5-1
9.6	PHYSICAL SECURITY PLAN	9.6-1

CHAPTER 9

**CONDUCT OF OPERATIONS**

CONTENTS

This chapter discusses the Pacific Gas and Electric Company (PG&E) organization for the operation, modification, and decommissioning of the Humboldt Bay Independent Spent Fuel Storage Installation (ISFSI) during the operations phase after the spent fuel casks were loaded into the ISFSI. Included are descriptions of organizational structure, personnel responsibilities and qualifications, and PG&E interface with contractors and other outside organizations.

Programs under 10 CFR 50 Appendix B, such as radiation protection, environmental monitoring, emergency preparedness, quality assurance (QA), and training will be adopted to ensure the safe operation and maintenance of the Humboldt Bay ISFSI under 10 CFR 72. PG&E submitted the following plans that support the conduct of ISFSI operations: a Physical Security Plan, a Safeguards Contingency Plan, a Security Training and Qualification Plan, an Emergency Plan, a Preliminary Decommissioning Plan, a QA Program, and a Training Program.

Following completion of HBPP Unit 3 decommissioning milestones, or termination of the 10 CFR 50 license, these programs will be revised in accordance with 10 CFR 72 to ensure continued compliance with 10 CFR 72 license requirements. This process will result in stand-alone ISFSI programs that implement the 10 CFR 72 license. PG&E will maintain the appropriate administrative and managerial controls at the ISFSI until the Department of Energy (DOE) takes title to and assumes responsibility for the spent fuel.

**9.1 ORGANIZATIONAL STRUCTURE**

**9.1.1 CORPORATE ORGANIZATION**

Relationships between corporate personnel and Humboldt Bay ISFSI personnel are identified in the Humboldt Bay Quality Assurance Plan (HB QAP).

The costs for operation, and decommissioning of the Humboldt Bay ISFSI will be funded from the HBPP Decommissioning Trust, as approved by the California Public Utilities Commission (CPUC). All costs are monitored and controlled by PG&E.

Humboldt Bay ISFSI organization changes will be dependent on current risk and regulatory requirements. PG&E will notify the Nuclear Regulatory Commission (NRC) of changes as required.

### **9.1.2 CORPORATE FUNCTIONS, RESPONSIBILITIES, AND AUTHORITIES**

The corporate positions, functions, responsibilities, and authorities are identified in the HB QAP, procedures, and organization charts.

The Director, Security and Emergency Services reports to the corporate organization, and is responsible for providing engineering and design services, safety assessments, licensing services for the ISFSI and is responsible for ISFSI operations.

Throughout the ISFSI lifetime, legal support will be available from PG&E corporate headquarters; technical support will be available from DCPD personnel and outside consultants. This support will be provided, when needed, for licensing, QA, engineering, radiation protection, maintenance, testing, emergency planning, security, and decommissioning.

The Quality Assurance (QA) and quality control functions will be performed by personnel independent of the ISFSI line organization. The reporting relationships, responsibilities and qualifications of the QA organization, and audit requirements, are contained in the HB QAP.

### **9.1.3 IN-HOUSE ORGANIZATION**

During Humboldt Bay ISFSI operations, the Director, Security and Emergency Services will be responsible for the day- to-day management of ISFSI activities, cost control, and overall safety.

### **9.1.4 RELATIONSHIPS WITH CONTRACTORS AND SUPPLIERS**

All activities associated with the ISFSI are managed and approved by PG&E. Qualified vendors may be selected to provide services and/or equipment as needed.

### **9.1.5 TECHNICAL STAFF**

The functions, responsibilities, and authorities of the Humboldt Bay ISFSI personnel are described in procedures. The qualifications of ISFSI personnel are specified in Section 9.1.7.

### **9.1.6 OPERATING ORGANIZATION, MANAGEMENT, AND ADMINISTRATIVE CONTROL SYSTEM**

#### **9.1.6.1 Onsite Organization**

Lines of authority, responsibility, and communication will be defined and established for all ISFSI organization positions. These relationships will be documented and updated, in organization charts, functional descriptions of departmental responsibilities and relationships, and job descriptions for key personnel positions.

#### **9.1.6.2 Personnel Functions, Responsibilities and Authorities**

The Director, Security and Emergency Services is responsible for the safe operation, maintenance, radiation protection, training and qualification, and security of the ISFSI.

The ISFSI Manager, or equivalent position, reports to the Director, Security and Emergency Planning and is responsible for administering, coordinating, planning, and scheduling ISFSI operating activities including maintenance and work planning; ensuring that appropriate operating procedures are available; and that personnel performing operations functions, are familiar with the procedures.

The DCCP Radiation Protection Manager supports the Director, Security and Emergency Services and is responsible for the health physics program.

Functions such as engineering, design, construction, QA, radiation protection, testing, operations, and security will be overseen by PG&E personnel.

ISFSI personnel and security staff will be responsible for the day-to-day operation of the ISFSI. They will perform their activities in accordance with the requirements of the Humboldt Bay ISFSI license, technical specifications, QA program, physical security plan, security Interim Compensatory Measures issued by the NRC procedures, and applicable state and federal regulations. Security staff personnel will be responsible for ISFSI site security during routine, emergency, and contingency operations.

In order to ensure continuity of operation and organizational responsiveness to off-normal situations, a formal order of succession and delegation of authority will be established. The Director, Security and Emergency Services will designate in writing personnel who are qualified to act as the Director, Security and Emergency Services in his absence.

#### **9.1.6.3 Administrative Control**

Planned and scheduled internal and external quality assurance audits of the ISFSI program in accordance with the HB QAP will be performed to evaluate the application and effectiveness of management controls, procedures, and other activities affecting nuclear safety. The audit program will describe audit frequency, methods for documenting and communicating audit findings, resolution of issues, and implementation of corrective actions.

#### **9.1.7 PERSONNEL QUALIFICATION REQUIREMENTS**

The DCCP Radiation Protection Manager will meet or exceed the qualifications of Regulatory Guide 1.8 (Reference 1). In addition, the Director, Security and Emergency Services ISFSI personnel and security staff are qualified as described below:

- The Director, Security and Emergency Services shall have a minimum of 8 years of power plant experience, of which a minimum of 3 years shall be nuclear power plant experience. A maximum of 2 years of the remaining 5 years of power plant experience may be fulfilled by satisfactory completion of academic or related technical training on a one-for-one basis.
- The ISFSI personnel and security staff, at the time of appointment to their positions, shall have a high school diploma or successfully completed the General Education Development test. Consistent with the assigned duties, ISFSI personnel will be trained and qualified in accordance with the Humboldt Bay Training Program described in Section 9.3. Security staff that supports the ISFSI will be trained and qualified in accordance with the HBPP Security Training and Qualifications Plan requirements.
- During ISFSI operations, operation of equipment and controls that are identified as important to safety for the ISFSI will be limited to personnel who are trained and qualified in accordance with the Humboldt Bay ISFSI Training and Certification Program described in Section 9.3.3, or personnel who are under the direct visual supervision of an individual who is trained and qualified in accordance with the Humboldt Bay ISFSI Training and Certification Program.

### 9.1.8 LIAISON WITH OUTSIDE ORGANIZATIONS

All activities associated with ISFSI operations are managed and approved by PG&E. These activities will be performed in accordance with approved procedures. Qualified vendors may be selected to provide specialty services and/or equipment. Interface with DOE, cask vendor, and other outside organizations is performed in accordance with contractual agreements.

### 9.1.9 REFERENCES

1. Regulatory Guide 1.8, Qualification and Training of Personnel for Nuclear Power Plants, USNRC, Revision 2, April 1987
2. Humboldt Bay ISFSI Training and Certification Program

## **9.2 ISFSI TEST PROGRAM**

This section describes the test program for the storage system, including necessary equipment and facility testing. Prior to the loading of any spent fuel for placement in the Independent Spent Fuel Storage Installation (ISFSI) storage vault, preoperational and startup tests will be performed and satisfactorily completed to verify that individual components and the storage system function as described in this Final Safety Analysis Report Update (FSAR). Maintenance and surveillance tests will be accomplished during ISFSI operations.

### **9.2.1 ADMINISTRATIVE PROCEDURES FOR CONDUCTING TEST PROGRAM**

Test procedures will be prepared, reviewed, approved, performed, and revised in accordance with HBPP administrative procedures which meet the requirements of the Humboldt Bay ISFSI Quality Assurance (QA) Program. Test procedures will be reviewed to determine if there is any negative impact on existing HBPP Unit 3 or ISFSI structures, systems, and components.

Preoperational test procedures prepared and performed by outside vendors (at their facilities) will meet the requirements of a Pacific Gas and Electric Company (PG&E) approved QA Program. PG&E will review and approve vendor test procedures prior to use in accordance with established procedures. PG&E personnel will witness the performance of preoperational tests performed by vendors.

### **9.2.2 TEST PROGRAM DESCRIPTION**

The test program is defined by procedures for: (a) preoperational testing, (b) startup testing, (c) operational testing.

The objective of preoperational testing is to verify that the individual components of the storage system, facilities, and equipment meet respective functional requirements as described in this FSAR. Successful preoperational testing will be completed before commencing with startup testing. Section 9.2.3 discusses the preoperational testing.

The objective of startup testing is to verify that the complete loading and unloading sequence, using the storage system components, facilities, and equipment work together as a complete system in accordance with the requirements of this FSAR. Successful startup testing will be completed prior to handling spent nuclear fuel. Section 9.2.4 discusses startup testing.

Section 9.4 addresses testing during normal ISFSI operation.

Discrepancies between FSAR requirements and preoperational and startup tests will be resolved in accordance with corrective action procedures.



### **9.2.3 PREOPERATIONAL TESTING**

Preoperational tests will be performed to demonstrate the ability of the ISFSI systems, structures, and components to meet functional requirements.

#### **9.2.3.1 Component and System Testing**

Component testing will be performed on the davit crane, the transporter, the storage system ancillaries, and the ISFSI security system to verify they are in compliance with the requirements of the FSAR and respective functional specifications.

#### **9.2.3.2 Construction Tests**

Tests associated with construction will be completed as required by construction specifications.

#### **9.2.3.3 Calibration of Measuring and Test Equipment**

Measuring and test equipment with an important-to-safety or security function will be controlled in accordance with procedures which satisfy the requirements of the Humboldt Bay QA Program.

### **9.2.4 STARTUP TESTING**

Startup testing will verify the performance of the storage system; ensure that plant equipment complies with the requirements of this FSAR, and validate the ISFSI operation procedures. Startup testing will be implemented with approved procedures.

Actual storage system components will be utilized for startup testing to the greatest extent possible. One or more MPC mock-ups may be used to validate the automated welding process.

The following operations will be included in startup testing for the Humboldt Bay ISFSI:

- (1) Preparing the HI-STAR HB cask for movement into the spent fuel pool (SFP).
- (2) Placing the HI-STAR HB cask into the SFP, and simulating movement of fuel using a dummy fuel assembly, into the cask.
- (3) Removing the HI-STAR HB cask from the SFP, and installing the MPC lid retention device.
- (4) Decontaminating the HI-STAR HB cask.

## HUMBOLDT BAY ISFSI FSAR UPDATE

- (5) Removing the MPC lid retention device, welding the MPC lid, moisture removal, and filling the MPC with helium.
- (6) Installing the HI-STAR HB cask top lid.
- (7) Loading the HI-STAR HB cask onto the rail dolly using the davit crane and removal from the refueling building.
- (8) Transporting the loaded HI-STAR HB cask from the RFB to the storage vault using the transporter.
- (9) Positioning and lowering the HI-STAR HB into the storage vault.
- (10) Unloading activities; MPC cooldown and MPC lid weld removal.

Personnel performing startup testing will have completed applicable ISFSI training program requirements (Refer to Section 9.3).

Discrepancies between the requirements of this FSAR and startup test results will be resolved in accordance with the HBPP corrective action process.

### **9.2.5 OPERATIONAL STARTUP TESTING**

Operational startup testing may be performed during the initial loading of an MPC. These tests will be limited to gathering information available only when nuclear fuel is in the MPC; or when final verification of data obtained in previous startup testing is required.

One such test is a six-month monitoring program for the vault temperature. Each vault cell is monitored via a temperature probe placed near the top of the cell air space. The temperature will be recorded periodically during the six month period to validate that the temperature is within design basis.

### **9.2.6 OPERATIONAL READINESS REVIEW PROGRAM**

PG&E will perform an operational readiness review prior to the commencement of ISFSI operations. The readiness review will verify all appropriate actions have been completed prior to initial MPC loading. As a minimum, the operational readiness review program will ensure:

- Results of preoperational and startup testing are satisfactory; that all corrective actions and lessons learned have been incorporated into the approved ISFSI operations procedures.
- Radiation protection procedures and controls are in place.

## HUMBOLDT BAY ISFSI FSAR UPDATE

- Operations procedures including surveillance, operating security, and emergency response procedures are approved and in place.
- All engineering issues relating to the storage system are resolved.
- Fire protection procedures are approved and in place.
- Maintenance procedures are approved and in place, and all storage system and related plant components are ready for use.
- Cask Transportation Evaluation Program is in place.

### **9.3 TRAINING PROGRAM**

Pursuant to 10 CFR 72.190 and 10 CFR 72.192, personnel (including supervisory personnel who personally direct the operation of important-to-safety equipment and controls), receive training and indoctrination designed to provide and maintain a well-qualified work force for safe and effective operation of the ISFSI.

With the ISFSI fuel and greater than Class C material loading completed, changes to the following training programs were made commensurate with reduced hazards.

#### **9.3.1 HUMBOLDT BAY GENERAL EMPLOYEE TRAINING**

Humboldt Bay maintains a general employee training (GET) program for unescorted Pacific Gas and Electric (PG&E) and contractor employees who work at the ISFSI. Topics in the GET include radiation protection, site emergency plans, safety, fire protection, security, and quality assurance as applicable. Training may be accomplished through the use of formal classroom lecture(s), multimedia, computer based training, and/or handouts.

#### **9.3.2 SUPPLEMENTAL ISFSI TRAINING**

Supplemental training is provided to personnel assigned duties associated with the ISFSI, as needed. This supplemental training includes training modules developed under the Humboldt Bay ISFSI training program.

### **9.3.2.1 ISFSI ESSENTIALS**

The ISFSI fundamentals element of supplemental training provides a general overall of the ISFSI and includes the following training modules:

- (1) HI-STAR HB System design overview.
- (2) ISFSI facility design overview.
- (3) ISFSI licensing basis (e.g., ISFSI Technical Specifications and FSAR).
- (4) Operational topics related to ISFSI operations and maintenance.

### **9.3.2.2 ISFSI LOADING**

The ISFSI loading element of supplemental training has been discontinued and archived. The elements of ISFSI Fundamentals and Operations training that are applicable in storage configuration have been combined into ISFSI Essentials.

### **9.3.2.3 ISFSI OPERATIONS**

The ISFSI operations element of supplemental training will be provided to those personnel involved with the operation of the ISFSI. This element provides personnel with the job specific knowledge to implement the procedures for the ISFSI operations and includes modules in the following areas:

- (1) ISFSI operations procedure overview.
- (2) Instrumentation and controls.
- (3) Emergency Plan and procedures.
- (4) Security Plan and procedures.
- (5) ISFSI Radiological Control procedures and practices.
- (6) Environmental protection.
- (7) Administrative procedures.

### **9.3.3 ISFSI CERTIFICATION**

Personnel who operate ISFSI equipment and controls that have been identified as important-to-safety must be trained and certified. Supervisory personnel who direct the operation of equipment and controls that are important-to-safety must also be certified. After satisfactory completion of the supplemental training described in Section 9.3.2, the trainee is eligible for ISFSI Certification. The ISFSI Certification process is controlled by administrative procedures.

The physical condition and general health of ISFSI certified personnel are subject to the requirements of 10 CFR 72.194. The individual's physical condition and general health must not be such as might cause operational errors that could endanger other personnel or the public health and safety. Any condition that might cause impaired judgment or motor coordination must also be considered in the selection of personnel for ISFSI certification. These conditions need not categorically disqualify a person if appropriate provisions are made to accommodate such limitation.

Data collected from test results, job performance results, instructor and trainee critiques will be evaluated and necessary adjustments made to ensure program effectiveness.

### **9.3.4 CONTINUING ISFSI TRAINING**

All ISFSI personnel will receive retraining at a frequency of not more than every two years. The topics selected for retraining will include, at a minimum, the subjects covered in initial GET. Job specific and certification retraining will be provided at a frequency of not more than every two years. Topics for this continuing training may be selected from initial training, NRC bulletins and



information notices, major equipment and procedure changes, relevant industry events, and topics designated by the HB ISFSI Manager or requested by other site personnel.

### **9.3.5 JOB SPECIFIC**

Job specific training, or training for other tasks that require special training prior to implementation, shall be developed and implemented as required.

### **9.3.6 ADMINISTRATION AND RECORDS**

The HB ISFSI Manager is responsible for administration of the training program and for maintaining training records. Qualified instructors will be available to conduct all training activities.

Training records will be maintained as required by the ISFSI quality assurance program.

## **9.4 NORMAL OPERATIONS**

This section describes the administrative controls and conduct of operations associated with activities considered important to safety. Also described in this section is the management system for maintaining records related to the operations of the Independent Spent Fuel Storage Installation (ISFSI).

### **9.4.1 PROCEDURES**

ISFSI activities that are important to safety will be conducted at the Humboldt Bay ISFSI in accordance with detailed written approved procedures. The activities include but are not limited to, operations identified in the Humboldt Bay ISFSI Technical Specifications (TS) and Chapter 10. Pre-operational, normal operating, maintenance and surveillance testing will be in effect prior to commencing loading operations. These procedures are briefly described in Section 9.4.1.1. These procedures, and any subsequent revisions, will be reviewed and approved in accordance with the Humboldt Bay Quality Assurance (QA) Program. Procedures will contain sufficient detail to allow qualified and trained personnel to perform the actions without incident or abnormal event.

#### **9.4.1.1 Categories of Procedures**

##### **9.4.1.1.1 Administrative Procedures**

Administrative procedures will provide directions and instructions to all Humboldt Bay ISFSI personnel to provide a clear understanding of operating philosophy and management policies. These procedures include instructions pertaining to personnel conduct and procedures to prepare, review, approve, and revise procedures. Administrative procedures include actions to ensure that personnel safety, the working environment, procurement, and other general ISFSI activities are carried on at a high degree of readiness, quality, and success.

##### **9.4.1.1.2 Radiation Protection Procedures**

Radiation protection procedures are used to implement the radiation protection program. These procedures will assure compliance with 10 CFR 20 and As Low as Reasonably Achievable (ALARA) principles. Information contained in these procedures include the acquisition of data, use of equipment, and qualifications and training of personnel to perform radiation surveys, measurements, and evaluations for the assessment and control of radiation hazards associated with the Humboldt Bay ISFSI.

The operation and use of radiation monitoring instrumentation at the Humboldt Bay ISFSI, along with measurement and sampling techniques, will be described in written procedures.

#### **9.4.1.1.3 Maintenance and Surveillance Testing Procedures**

Procedures will be established for performing preventive and corrective maintenance, and for surveillance testing on Humboldt Bay ISFSI equipment and instrumentation. Preventive maintenance and surveillance testing, including calibrations, will be performed on a periodic basis to verify operability and to preclude the degradation of Humboldt Bay ISFSI systems, equipment, and components. Corrective maintenance will be performed to rectify any unexpected system, equipment, or component malfunction, as the need arises.

Important-to-safety structures, systems, and components (SSCs) that are purchased commercial grade will be qualified by test prior to use. Testing will verify functionality and, for structural SSCs, the ability to carry full-rated load without degradation. Subsequent to the qualification testing, preventative maintenance, surveillance testing, and corrective maintenance will be as described above.

#### **9.4.1.1.4 Operating Procedures**

The operating procedures will provide the instructions for routine and projected contingency (off-normal) operations, including handling, loading, sealing, transporting, storing, and unloading the SSCs and for all other operations important to safety. Operating procedures will include off-normal occurrences and operations identified in the Humboldt Bay ISFSI TS and Chapter 10. The requirements for certification of personnel operating equipment and controls important to safety will be specified in the operating procedures.

#### **9.4.1.1.5 Procedures Implementing the QA Program**

Procedures will be established for important-to-safety activities to ensure that the operation and maintenance of the ISFSI is performed in accordance with the Humboldt Bay QA Program, applicable regulations, the Humboldt Bay ISFSI TS and the radiation protection program. The requirements for qualification of personnel operating important-to-safety equipment and controls will be specified in procedures. The QA procedures will clearly communicate that the responsibility for quality rests with each individual employee or visitor who enters the facility.

### **9.4.2 RECORDS**

Humboldt Bay ISFSI records will be maintained in accordance with the Humboldt QA Program.

Pacific Gas and Electric (PG&E) was granted an exemption from 10 CFR 72.72(d), which requires that spent fuel and high level radioactive waste records in storage be kept in duplicate. As specified in License Condition 16 of the Humboldt Bay ISFSI License SNM-2514, the exemption allows PG&E to maintain records of spent fuel and high level radioactive waste in storage either in duplicate, as required by 10 CFR 72.72(d), or alternatively; a single set of records may be maintained at a records storage facility that satisfies the standards of ANSI N45.2.9-1974. All other requirements of 10 CFR 72.72(d) must be met.

## **9.5    EMERGENCY PLANNING**

The Humboldt Bay Site Emergency Plan complies with the provisions of 10 CFR 72.32 (a), and describes the organization, assessment actions, conditions for activation of the emergency organization, notification procedures, emergency facilities and equipment, training, provisions for maintaining emergency preparedness, and recovery criteria used for any radiological emergencies that may arise at the ISFSI.

The Humboldt Bay Site Emergency Plan and implementing procedures reflect the conditions and indications that require entry into the Emergency Plan. Response actions and notifications are contained in the Emergency Plan.

## **9.6    PHYSICAL SECURITY PROGRAM**

The purpose of the physical security program for the Humboldt Bay Independent Spent Fuel Storage Installation (ISFSI) is to establish and maintain physical protection for the stored spent fuel. The physical security program is described in the Humboldt Bay ISFSI Physical Security Plan, the Safeguards Contingency Plan, and the Security Training and Qualification Plan. This program meets the requirements contained in 10 CFR 72, Subpart H, "Physical Protection," and the applicable portions of 10 CFR 73.51.

Because the ISFSI security program contains information that is to be withheld from the public in accordance with 10 CFR 2.790(d) and 10 CFR 73.21, it was submitted as a separate document to the Nuclear Regulatory Commission (NRC). The program as described therein will be implemented as necessary to support the ISFSI operation schedule as discussed in Chapter 5. A summary of physical protection features that does not include safeguards information follows.

The Humboldt Bay ISFSI security force controls access through the Vehicle Barrier System (VBS), into the Primary Alarm Station (PAS) and to the ISFSI Security Area. Access is limited to individuals who require access to perform work-related activities. The Humboldt Bay security force maintains a list of approved individuals authorized for access. Individuals granted access to the ISFSI Security Area and PAS are required to display badges indicating authorization and identification. Personnel, hand-carried articles, and vehicles are searched prior to entry through the VBS, into PAS and to the ISFSI Security Area to detect the presence of explosives.

The ISFSI Security Area has an intrusion detection system to detect attempted unauthorized entry. Manned alarm stations support the security program by monitoring intrusion detection system alarms, coordinating security communications, and performing closed circuit television surveillance and alarm assessment.

In accordance with 10 CFR 72.184, the Humboldt Bay ISFSI Safeguards Contingency Plan addresses responses to potential threats. The plan contains a responsibility matrix that provides guidance for corresponding security force actions. Contingency planning involves detailed response procedures and assistance from local law enforcement agencies when requested.

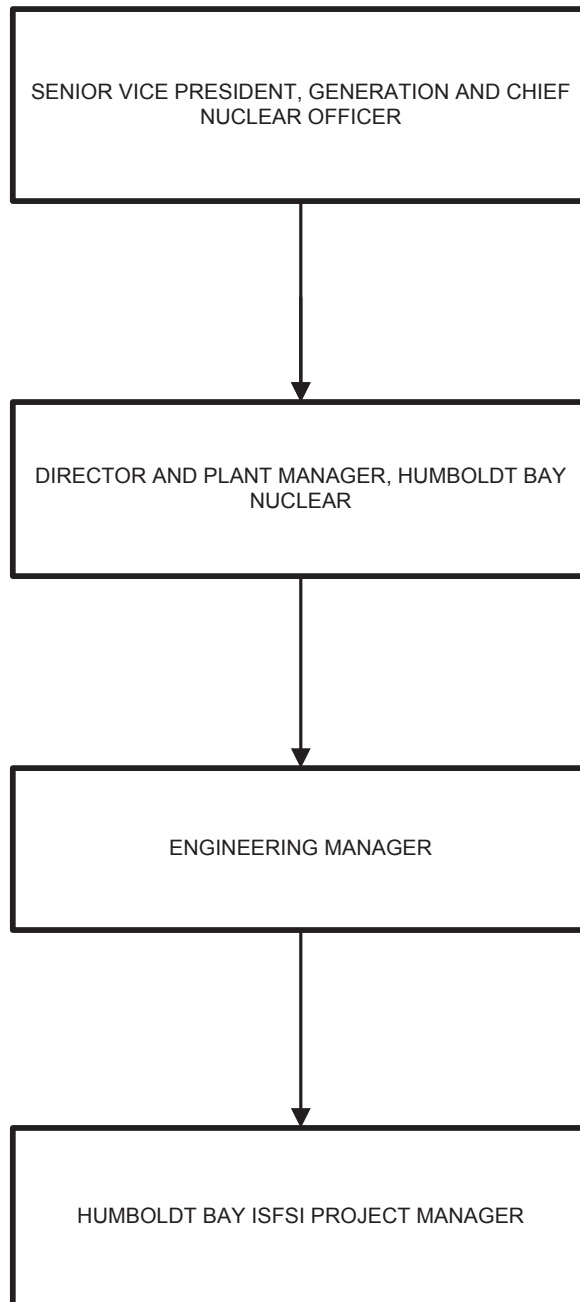
Provisions for training and qualifying security force members are contained in the Humboldt Bay ISFSI Security Training and Qualification Plan. This plan identifies security tasks and the associated positions that must be trained in these tasks. The plan also describes initial and recurring training requirements and a screening program used to determine that security force members meet prescribed background, physical, and mental qualification criteria.

Each commitment made in the Humboldt Bay ISFSI Physical Security Plan, the Humboldt Bay ISFSI Safeguards Contingency Plan, and the Humboldt Bay ISFSI Security Training and Qualification Plan is implemented via written procedures in



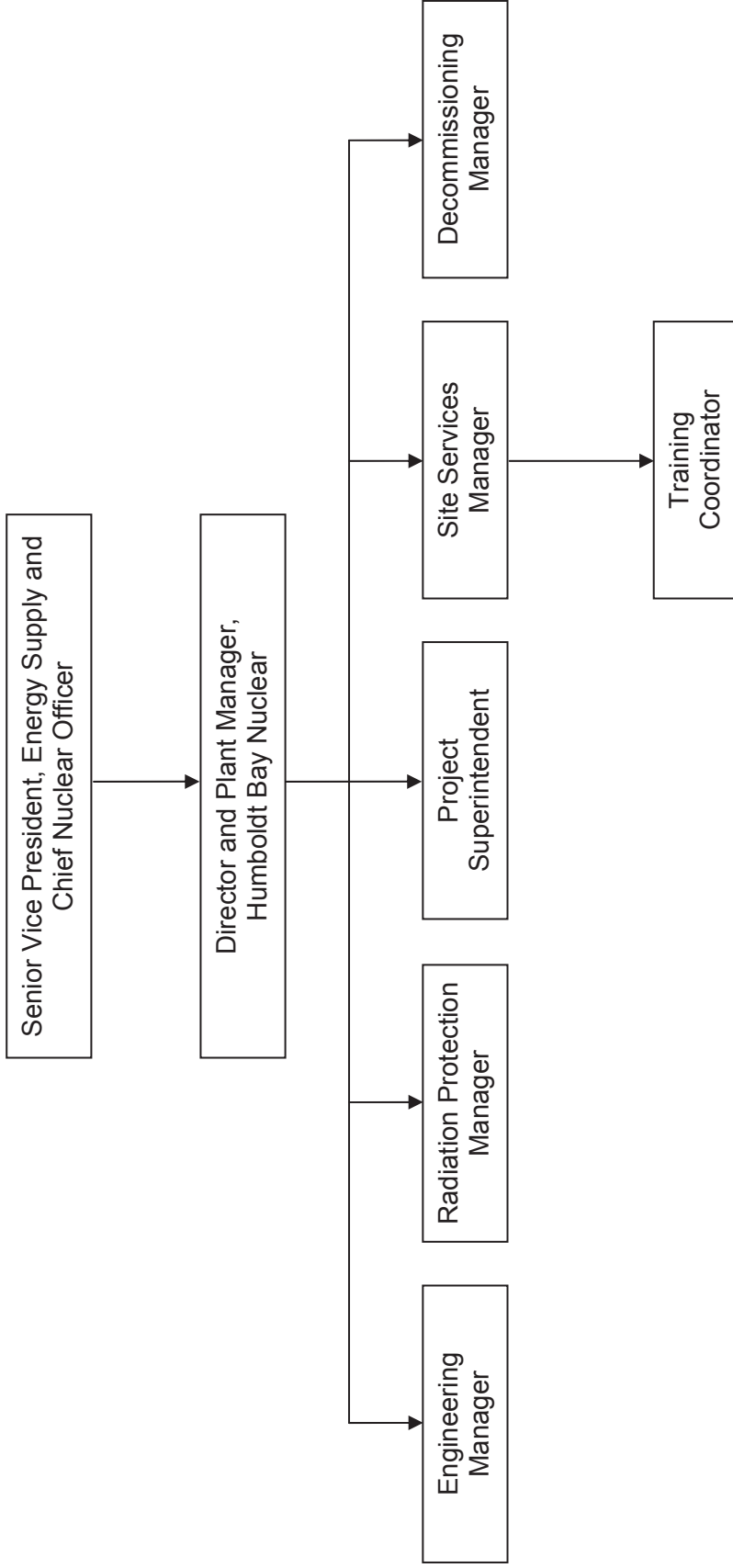
## HUMBOLDT BAY ISFSI FSAR UPDATE

accordance with 10 CFR 73.51(d)(10). These implementing procedures, which are developed, approved, and maintained by security management, ensure accurate and organized day-to-day security operations.



<b>FSAR UPDATE</b>
<b>HUMBOLDT BAY ISFSI</b>
<b>FIGURE 9.1-1 PRE-OPERATION ORGANIZATION</b>

Revision 1 November 2007



FSAR UPDATE
HUMBOLDT BAY ISFSI
FIGURE 9.1-2 OPERATIONAL PHASE ORGANIZATION

Revision 2 November 2009

# HUMBOLDT BAY ISFSI FSAR UPDATE

## CHAPTER 10

### **OPERATING CONTROLS AND LIMITS**

#### CONTENTS

<u>Section</u>	<u>Title</u>	<u>Page</u>
10.1	PROPOSED OPERATING CONTROLS AND LIMITS	10.1-1
10.2	DEVELOPMENT OF OPERATING CONTROLS AND LIMITS	10.2-1
10.2.1	Functional and Operating Limits, Monitoring Instruments, and Limiting Control Settings	10.2-1
10.2.2	MPC Loading Characteristics	10.2-4
10.2.3	MPC Unloading Characteristics	10.2-7
10.2.4	Overpack Operating Controls and Limits	10.2-8
10.2.5	Vault Operating Controls and Limits	10.2-9
10.2.6	Limiting Conditions For Operation	10.2-9
10.2.7	Surveillance Requirements	10.2-11
10.2.8	Design Features	10.2-11
10.2.9	Administrative Controls	10.2-11
10.2.10	Operating Control and Limit Specifications	10.2-12
10.2.11	References	10.2-12

# HUMBOLDT BAY ISFSI FSAR UPDATE

## CHAPTER 10

### **OPERATING CONTROLS AND LIMITS**

#### TABLES

Table	Title
10.1-1	Operating Controls and Limits
10.2-1	MPC-HB Fuel Assembly Limits
10.2-2	Fuel Assembly Characteristics

# HUMBOLDT BAY ISFSI FSAR UPDATE

## CHAPTER 10

### **OPERATING CONTROLS AND LIMITS**

#### FIGURES

Figure	Title
10.2-1	Configuration 1: Damaged Fuel in Peripheral Cells of Basket
10.2-2	Configuration 2: Checkerboard of Damaged Fuel
10.2-3	Schematic Diagram of the Forced Helium Dehydration System



CHAPTER 10

**OPERATING CONTROLS AND LIMITS**

**10.1 PROPOSED OPERATING CONTROLS AND LIMITS**

The Humboldt Bay Independent Spent Fuel Storage Installation (ISFSI), in general, and the HI-STAR HB storage system in particular, are totally passive and require minimal operating controls. The Humboldt Bay ISFSI and the HI-STAR HB System employ proven technologies, stringent codes of construction, and comprehensive quality assurance measures. As a result, they have substantial design and safety margins. The areas where controls and limits are necessary to ensure safe operation of the Humboldt Bay ISFSI are provided in Table 10.1-1.

The items in this chapter that are to be controlled are selected based on the design criteria and safety analyses for normal, off-normal, and accident conditions.

## **10.2 DEVELOPMENT OF OPERATING CONTROLS AND LIMITS**

This section provides an overview of, and the general bases for, the operating controls and limits specified for the Humboldt Bay Independent Spent Fuel Storage Installation (ISFSI).

### **10.2.1 FUNCTIONAL AND OPERATING LIMITS, MONITORING INSTRUMENTS, AND LIMITING CONTROL SETTINGS**

This section provides requirements for the controls or limits that apply to operating variables that provide verification that an important-to-safety design function is being accomplished and are observable and measurable. The operating variables required for the safe operation of the Humboldt Bay ISFSI are:

- Spent fuel characteristics
- Multi-purpose canister (MPC) exit gas dew point during forced helium dehydration
- MPC vacuum drying pressure
- Overpack vacuum drying pressure
- Helium purity
- MPC and overpack helium backfill pressures
- Overpack helium leakage
- MPC cavity helium gas bulk temperature of an MPC prior to re-flooding

Each of the specifications for these characteristics is provided below. The Technical Specifications (TS) and bases also provide Limiting Conditions for Operation and bases applicable during cask preparation that ensure the integrity of the MPC and overpack during storage operations.

#### **10.2.1.1 Fuel Characteristics**

The Humboldt Bay ISFSI is designed to provide interim storage for up to 400 Humboldt Bay Power Plant (HBPP) fuel assemblies in five casks, with a sixth cask to store greater-than-class-C (GTCC) waste. The design storage capacity of 400 fuel assemblies is sufficient to accommodate the entire HBPP spent fuel inventory and allow decommissioning of the spent fuel pool.

The Humboldt Bay ISFSI employs the Holtec International HI-STAR HB System, which is a variation of the generically certified HI-STAR 100 System (Reference 1). The

## HUMBOLDT BAY ISFSI FSAR UPDATE

HI-STAR HB System is comprised of the MPC-HB, damaged fuel containers (DFCs), and the HI-STAR HB storage/transport overpack. The design and operation of generic versions of these components are described in detail in the HI-STAR 100 System Final Safety Analysis Report (Reference 2). Holtec developed the modified MPC and overpack specifically for use at Humboldt Bay due to the shorter fuel assembly length. The smaller fuel cross-section allowed the capacity of the MPC-HB to be 80 fuel assemblies instead of the standard 68.

The fuel stored at the ISFSI consists of intact fuel assemblies and damaged fuel assemblies. The fuel assemblies may be stored with or without channels. Damaged fuel is stored in a DFC in the MPC. The damaged fuel can be consolidated; however, the amount of material contained in a single DFC is limited to the equivalent of a single intact fuel assembly.

Fuel qualification is based on the requirements for criticality control, decay heat removal, radiological protection, and structural integrity. The analyses presented in Chapters 4, 7, and 8 of this FSAR document the qualification of the entire HBPP inventory of spent fuel assemblies for storage in the HI-STAR HB System at the Humboldt Bay ISFSI.

Video inspection of the Humboldt Bay spent fuel assemblies was conducted in 2000-2001 using the guidance of Interim Staff Guidance (ISG)-1 Revision 0, Nuclear Energy Institute comments on ISG-1, and the definitions of damaged fuel and fuel debris contained in the Holtec HI-STAR 100 Certificate of Compliance. Eleven fuel assemblies were initially classified as damaged and 16 were classified as fuel debris. A supplemental evaluation of the 2000-2001 video records will be performed prior to fuel loading using the guidelines in Table 3.1-1, which meet the intent of ISG-1 Revision 1. ISG-1, Revision 1, does not define the term “fuel debris.” Therefore, all HBPP fuel is classified as either intact fuel or damaged fuel to be consistent with the revised guidance.

HBPP fuel loading is conducted in accordance with administrative controls, including an MPC loading plan, to ensure proper loading of all fuel assemblies. This loading plan ensures that all damaged fuel assemblies are loaded into a DFC for storage in the MPC-HB. The damaged fuel may be placed in the DFC prior to putting the DFC in the MPC or, if the damaged fuel assembly is capable of being handled by normal means, an empty DFC may first be placed in the MPC and then the damaged fuel loaded into the DFC. This loading plan is referenced in Humboldt Bay ISFSI operating procedures.

The following controls ensure that each fuel assembly is correctly loaded:

- The cask-loading plan is independently verified and approved.
- The fuel movement sequence is in accordance with the written loading plan. All fuel movements from any wet storage rack location is performed

under controls that ensure strict, verbatim compliance with the fuel movement sequence of the loading plan.

- Prior to placement of the MPC lid, all fuel assemblies are either video taped or visually documented by other means, by identification number, to match the fuel movement sequence.
- Upon completion of the visual documentation, an independent verification of the fuel loading pattern is performed by a member of the loading crew.
- A cognizant engineer is responsible for performing an additional independent verification to ensure that the fuel assemblies in the MPCs are placed in accordance with the original MPC loading plan.

Based on the qualification process of the spent fuel and the administrative controls (i.e., MPC loading plan) provided, incorrect loading of an MPC is not considered to be a credible event.

### **10.2.1.2 Fuel Specification and Loading Conditions (Allowable Contents)**

Intact fuel assemblies and damaged fuel assemblies meeting the limits specified in Tables 10.2-1 and 10.2-2, may be stored in the HI-STAR HB system. These tables and specifications are duplicated in Tables 2.2-1 and 2.2-2 of the Humboldt Bay ISFSI TS.

Section 4.2 summarizes the technical evaluations applicable to the Humboldt Bay ISFSI and the HI-STAR HB System for normal operations. Evaluations are described for the structural, thermal, criticality, and shielding disciplines. As defined in Section 4.2, the technical evaluations are a combination of Humboldt Bay-specific analyses and generic HI-STAR 100 analyses that were determined to bound the HI-STAR HB System. Sections 8.1 and 8.2 describe the off-normal and accident evaluations, respectively, which are applicable to the Humboldt Bay ISFSI and the HI-STAR HB System. The limits specified in Tables 10.2-1 and 10.2-2 preserve the assumptions used in the technical evaluations and ensure the entire HBPP spent fuel inventory is bounded. The technical evaluations for the HI-STAR HB System and for the vault demonstrate that all HBPP spent fuel may be loaded in HI-STAR HB casks and stored at the ISFSI with adequate safety margins.

### **10.2.1.3 GTCC Waste (Allowable Contents)**

GTCC waste meeting the description in Section 3.1 may be stored in one cask at the ISFSI. The source strength of the GTCC cask contents shall be verified to be less than the source strength of one MPC and HI-STAR HB overpack containing a maximum load of authorized spent fuel.

#### **10.2.1.4 Functional and Operating Limits Violations**

If any fuel specifications or loading conditions above are violated, the actions required by Humboldt Bay ISFSI TS 2.2 and 10 CFR 72.75(d) shall be completed.

#### **10.2.2 MPC LOADING CHARACTERISTICS**

The confinement of radioactivity during the storage of spent fuel in the MPC-HB is ensured by the structural integrity of the strength-welded MPC enclosure vessel. However, long-term integrity of the fuel and cladding depends on storage in an inert heat removal environment inside the MPC. This environment is established by removing water from the MPC and backfilling the cavity with an inert gas.

The loading process of an MPC-HB involves placing a HI-STAR HB cask with an empty MPC in the SFP and loading it with fuel assemblies that meet the specifications for allowable contents discussed above. Once this is complete, the lid is then placed on the MPC and the cask is moved to the cask washdown area for preparation for storage. See Section 5.1 for details of loading operations. After the water is drained from the MPC cavity, moisture removal is performed using either vacuum drying or the Forced Helium Dehydration (FHD) system. The MPC cavity is then backfilled with helium. Additional dose rates are measured and the MPC vent and drain cover plates and closure ring are installed and welded. Nondestructive examination inspections are performed on the welds.

During the loading process there are several characteristics vital to ensuring that the resulting MPC internal environment is conducive to long-term heat removal and maintaining the integrity of the fuel cladding. These characteristics are: reducing the level of oxidizing gases in the MPC cavity to trace amounts and backfilling the MPC with high quality inert gas (helium). The dry, inert and sealed MPC atmosphere is required to be in place during loading, transport, and storage operations.

##### **10.2.2.1 MPC Water Temperature**

During operations with fuel and water in the MPC, maintaining the integrity of the fuel in the MPC is the critical activity. As a result of decay heat produced by the spent fuel assemblies, providing a coolant source is important in maintaining control of cladding temperature and the fuel integrity. During processes when there is water and fuel in the MPC, the water is considered the coolant source. As long as there is water in the MPC it will continue to perform the coolant function. This water will continue to perform its function as long as it does not boil off. As a result, the parameter that best indicates the potential reduction of water would be the temperature of the water in the MPC. However, since monitoring the water temperature in the MPC directly may not always be possible, an analysis of the time it would take for the water to reach the boiling temperature was performed to ensure that appropriate actions are taken before the boiling temperature is reached. This analysis was based on the maximum permitted cask decay heat level, the MPC cavity being full of water, and various initial

temperatures of the water in the MPC. The results of this analysis, considering an initial water temperature of 90°F (greater than the typical temperature of the fuel pool water) shows that the MPC water temperature will achieve a steady state maximum below the boiling point of water.

While there is water in the MPC, there will be adequate assurance through analysis that the temperature of the water in the MPC will not reach the boil-off level and that the volume of water in the MPC is not allowed to decrease significantly.

### 10.2.2.2 MPC Drying Characteristics

After the bulk water is drained from the MPC, the moisture in the cavity is reduced to an acceptably small amount by using either vacuum drying or a FHD system. See Figure 10.2-3 for a schematic diagram of the FHD system. The Standard Review Plan acceptance criterion for dryness is  $\leq 1$  gram-mole per cask of oxidizing gases. This has been translated by the industry to be 3 torr for vacuum drying. For the recirculation drying process using the FHD system, measuring the temperature of the gas exiting the demister of the FHD system provides an indication of the amount of water vapor entrained in the helium gas in the MPC. Maintaining a demister exit temperature of less than or equal to 21°F for 30 minutes or more during the recirculation drying process ensures that the partial pressure of the entrained water vapor in the MPC is less than 3 torr.

In the vacuum drying process, any water that has not drained from the MPC cavity evaporates from the MPC cavity due to the vacuum. This drying is aided by the temperature increase due to the decay heat of the fuel. To ensure adequate drying the vacuum drying pressure in the MPC must be verified to be at  $\leq 3$  torr for  $\geq 30$  minutes. This low vacuum pressure is an indication that the cavity is dry and the moisture level in the MPC is acceptable.

The FHD system can be used to remove the remaining moisture in the MPC cavity after all of the water that can practically be removed through the drain line using a hydraulic pump has been expelled in the water blowdown operation. The recirculation process using the FHD involves introducing dry gas into the MPC cavity that absorbs the residual moisture in the MPC. This humidified gas exits the MPC and the absorbed water is removed through condensation and/or mechanical drying. The dried gas is then forced back through the MPC until the gas exit temperature from the FHD demister is  $\leq 21^\circ\text{F}$  for at least 30 minutes. Meeting these temperature and time criteria ensures that the cavity is dry and the moisture level in the MPC is acceptable. The FHD system shall be designed to ensure that during normal operation (that is, excluding startup and shutdown ramps) the following criteria are met:

- (1) The temperature of helium gas in the MPC shall be at least 15°F higher than the saturation temperature at coincident pressure.



## HUMBOLDT BAY ISFSI FSAR UPDATE

- (2) The pressure in the MPC cavity space shall be less than or equal to 60.3 psig (75 psia).
- (3) The recirculation rate of helium shall be sufficiently high (minimum hourly throughput equal to ten times the nominal helium mass backfilled into the MPC for fuel storage operations) so as to produce a turbulated flow regime in the MPC cavity.
- (4) The partial pressure of the water vapor in the MPC cavity will not exceed 3 torr if the helium temperature at the demister outlet is  $\leq 21^{\circ}\text{F}$  for a period of 30 minutes.

In addition to the above system design criteria, the individual modules shall be designed in accordance with the following criteria:

- (1) The condensing module shall be designed to devaporize the recirculating helium gas to a dew point of  $120^{\circ}\text{F}$  or less.
- (2) The demister module shall be configured to be introduced into its helium conditioning function after the condensing module has been operated for the required length of time to ensure that the bulk moisture vaporization in the MPC has been completed.
- (3) The helium circulator shall be sized to effect the minimum flow rate of circulation required by the system design criteria described above.
- (4) The preheater module shall be engineered to ensure that the temperature of the helium gas in the MPC meets the system design criteria described above.

At the completion of the drying operation using the vacuum drying or FHD system, helium backfill operations may commence.

### **10.2.2.3 MPC Helium Backfill Characteristics and Purity**

Having the proper helium backfill pressure ensures adequate heat transfer from the fuel to the fuel basket and surrounding structure of the MPC. During the loading operation, once the dryness limits are met, the MPC cavity is backfilled with helium to provide the inert environment required for long-term storage. Due to the low decay heat, there is no time limit specified for this evolution, but it should be completed expeditiously. To ensure the proper environment is established, the helium supply used in the backfill process shall have a purity of  $\geq 99.995$  percent. The proper backfill is ensured by verifying helium within the pre-calculated volume range for each MPC in standard cubic feet (scf).

#### **10.2.2.4 MPC Leakage Characteristics**

Leakage of radioactive material from the MPC-HB is considered non-credible based on the criteria in ISG-18 (Reference 4). Section 4.2.3.2.1 provides a detailed discussion of the construction of the MPC confinement boundary and a comparison against the ISG-18 criteria. Therefore, no leak rate testing of the MPC lid closure weld in the field after final closure welding is required.

#### **10.2.2.5 Returning MPC to Safe Condition**

If, for a loaded MPC, the fuel cavity dryness or backfill pressure cannot be successfully met or maintained for any reason during loading operations, the fuel must be ensured to be in a safe, analyzed condition, which may ultimately require the fuel to be placed back in the SFP. The completion time for this effort shall be based on the safety significance of the condition. The completion time shall consider the time required to ensure the MPC cavity gas is at a sufficiently low enough temperature; re-flood the MPC; remove the MPC closure ring; vent and drain cover port; and lid welds; move the SFSC into the SFP; remove the MPC lid; and remove the spent fuel assemblies in an orderly manner and without challenging personnel. Such a scenario is considered a contingency for a beyond-design-basis situation.

### **10.2.3 MPC UNLOADING CHARACTERISTICS**

In the event that an MPC must be unloaded during the loading campaign, the MPC and HI-STAR HB overpack are returned to the refueling building to begin the process of fuel unloading. The overpack is vented of helium, and the overpack lid is removed. The MPC closure ring, and vent and drain port cover plates are then removed. An evaluation is made to estimate the bulk temperature of the gas in the MPC cavity. If the bulk gas temperature is estimated to be above 200°F, means to cool the gas must be determined. This may include air or water cooling of the MPC shell, a recirculating cooling system or any other appropriate means.

Once the cool-down process is complete, the MPC is reflooded with water and the MPC lid weld is removed leaving the MPC lid in place. The SFSC is placed in the SFP and the MPC lid is removed. The contents are removed from the MPC and the MPC and HI-STAR HB overpack are removed from the SFP and decontaminated.

#### **10.2.3.1 MPC Cavity Gas Bulk Temperature Prior To Reflooding**

The integrity of the MPC depends on maintaining the internal cavity pressures within design limits. During the unloading process, the MPC cavity bulk helium gas temperature must be low enough to preclude flashing of the water when the cavity is re-flooded. This may be monitored directly or based on the decay heat of the fuel in the specific MPC, the bulk gas temperature can be estimated via a thermal evaluation. If cooling is required, any appropriate means (e.g., external forced air or water cooling or recirculation of the MPC gas through a cooler) may be used to reduce the gas

temperature to below the maximum permitted value. Reducing the MPC cavity bulk gas temperatures eliminates the risk of high MPC pressure due to sudden generation of steam during re-flooding. The bulk gas temperature limit of  $\leq 200^{\circ}\text{F}$  was selected to be lower than the boiling temperature of water with additional margin to eliminate the possibility of flashing to steam during re-flooding.

### **10.2.4 OVERPACK OPERATING CONTROLS AND LIMITS**

The HI-STAR HB System is a dual-purpose spent nuclear fuel storage and transportation system. During transportation and storage, the HI-STAR HB overpack functions as the containment boundary for radioactive material. As such, there are certain operations that must be implemented to ensure the overpack internal space is prepared in accordance with the supporting design analyses.

After the MPC has been loaded and prepared for storage, the overpack closure plate is installed to create the pressure boundary that eventually contains the helium in the annulus between the overpack and the MPC. The overpack closure design includes two concentric mechanical seals that fit into the top flange and are compressed by the installation of the bolted closure plate. The overpack is designed with a vent port in the closure plate and a drain port in the bottom flange that allow for removal of the water from the annulus, vacuum drying, and backfilling of the annulus with helium. The closure plate also includes a test port to allow for helium leakage testing of the inner mechanical seal.

#### **10.2.4.1 Overpack Drying Characteristics**

Maintenance of a helium environment in the overpack annulus is necessary to preserve the assumptions of the thermal analysis (which models helium in that space) and to ensure an inert, non-corrosive environment around the MPC enclosure vessel. Once the bulk water is drained from the overpack annulus, the overpack closure plate is bolted in place, the drain port plug is installed, and the vacuum drying system (VDS) is connected to the overpack vent port via the backfill tool. The VDS is used to reduce pressure in the annulus space. The pressure is lowered from approximately atmospheric pressure (760 torr) to 3 torr. The annulus is considered adequately dried when the pressure of 3 torr or less can be held for at least 30 minutes. The backfill tool allows for vacuum drying and subsequent helium backfill without losing the vacuum in the annulus.

#### **10.2.4.2 Overpack Helium Backfill Characteristics**

After successful vacuum drying, 99.995% pure helium is used to backfill the overpack annulus to between 10.0 and 14.0 psig. The thermal analysis assumes a helium atmosphere in the annulus, but no particular value is required because, except at very low pressures (less than approximately 10 torr), thermal conductivity does not vary significantly with pressure. The range is chosen to provide appropriate operating guidance to the operations staff.

#### **10.2.4.3 Overpack Helium Leakage Characteristics**

When the overpack annulus is successfully backfilled, helium leakage testing of the vent and drain port plugs and the closure plate inner mechanical seal is performed. Leakage from the overpack annulus is limited to a cumulative value of  $4.3 \times 10^{-6}$  atm-cc/sec (He) from all leakage paths. This value is based on the containment boundary leakage rate licensed for the HI-STAR 100 System for transportation under 10 CFR 71. For storage, no credit is taken for any confinement function provided by the overpack and leakage from the MPC is not credible.

The vent and drain port plugs are designed with mechanical seals under the plug head. The plugs are threaded into place and a port test cover is installed. A mass spectrometer leak detector (MSLD) is attached to the vent or drain port and a vacuum is drawn. Any leakage through the port plug seals is detected by the MSLD. Upon successful completion of testing of each port plug, the test cover is removed and the permanent port cover plates are bolted in place.

The closure plate mechanical seals are tested via the test port in the closure plate. The test port provides a test flow path between the concentric mechanical seals under the closure plate to the MSLD. Drawing a vacuum between the mechanical seals allows the detection of leakage either through the inner seal (helium) or the outer seal (air). The test is considered successful if a vacuum can be held and helium leakage through the inner seal, when combined with the measured vent and drain port plug leakage is less than the acceptance criterion. The outer mechanical seal is required to maintain a vacuum during the test, but is not required to meet a particular leak rate since only the inner seal represents the containment boundary.

#### **10.2.5 VAULT OPERATING CONTROLS AND LIMITS**

The ISFSI storage vault is a passive design and there are no operating controls and limits.

#### **10.2.6 LIMITING CONDITIONS FOR OPERATION**

##### **10.2.6.1 Equipment**

All important-to-safety Humboldt Bay ISFSI equipment is passive in nature; therefore, there are no limiting conditions regarding minimum available equipment or operating characteristics. The MPC and HI-STAR HB overpack have been analyzed for all credible failure modes and extreme environmental conditions. No credible postulated event results in damage to fuel, release of radioactivity above acceptable limits, or danger to the public health and safety. All operational equipment is to be maintained, tested, and operated according to the implementing procedures developed for the ISFSI. The failure or unavailability of any operational equipment can delay the transfer of an MPC to the HI-STAR HB overpack, but would not result in an unsafe condition.

### 10.2.6.2 Technical Conditions and Characteristics

The following technical conditions and characteristics are required for the Humboldt Bay ISFSI:

- Spent fuel characteristics
- Water temperature of a flooded MPC after the MPC lid is installed
- Overpack vacuum pressure
- MPC recirculation gas exit dew point
- MPC vacuum drying
- Helium purity
- MPC and overpack helium backfill pressures
- Gas bulk temperature of an MPC prior to reflooding
- Overpack helium leak rate

The spent fuel specifications for allowable contents for storage in the ISFSI and their bases are detailed in Section 10.2.1. In addition, the spent fuel specifications are also contained in Humboldt Bay ISFSI TS Section 2.0. A description of the bases for selecting the above remaining conditions and characteristics are detailed in Sections 10.2.2 through 10.2.4. Although provided in the above sections, the Humboldt Bay ISFSI TS and TS Bases also provide Limiting Conditions for Operations and bases applicable during loading operations to ensure integrity of the MPC during long-term storage at the ISFSI. TS and bases are also provided for the unlikely condition where the MPC needs to be unloaded. These include overpack vacuum pressure, MPC recirculation gas exit dew point, MPC vacuum drying pressure, backfill pressure, and overpack leak rate during loading, and MPC bulk gas temperature during unloading.

The technical and operational considerations are to:

- Ensure proper internal MPC atmosphere to promote heat transfer, minimize oxidation, and prevent an uncontrolled release of radioactive material.
- Ensure that dose rates in areas where operators must work are ALARA and that all relevant dose limits are met.

## HUMBOLDT BAY ISFSI FSAR UPDATE

- Ensure that the fuel cladding is maintained at a temperature sufficiently low enough to preclude cladding degradation during normal storage conditions.

Through the analyses and evaluations provided in Chapters 4, 7, and 8, this FSAR demonstrates that the above technical conditions and characteristics are adequate and that no significant public or occupational health and safety hazards exist.

### 10.2.7 SURVEILLANCE REQUIREMENTS

The analyses provided in this FSAR show that the Humboldt Bay ISFSI and the storage system fulfill its safety functions during all accident conditions as described in Chapter 8. Surveillance requirements are provided in the Humboldt Bay ISFSI TS for loading operations. No continuous surveillance of the HI-STAR HB System is required during storage in the ISFSI vault. Periodic inspections are described in Section 4.4.3.

### 10.2.8 DESIGN FEATURES

The following storage system design features are important to the safe operation of the Humboldt Bay ISFSI and require design controls and limits:

- Material mechanical properties for structural integrity, confinement, and shielding.
- Material composition and dimensional control for subcriticality.

Component dimensions are not specified here since the combination of material types, dose rates, criticality safety, and component fit-up define the operable limits for dimensions (that is, thickness of shielding materials, MPC plate thicknesses, etc.). The values for these design parameters are specified on the drawings (see Figures 3.2-1, 3.3-1, and 3.3-3).

The combination of the above controls and limits, and those discussed previously in Section 10.2, define requirements for the Humboldt Bay ISFSI storage system components that provide radiological protection, decay heat removal, criticality control, and structural integrity during normal storage and postulated accident conditions.

### 10.2.9 ADMINISTRATIVE CONTROLS

Use of the existing HB ISFSI organizational and administrative systems and procedures, record keeping, review, audit, and reporting requirements coupled with the requirements of this FSAR ensure that the operations involved in the storage of spent fuel at the ISFSI are performed in a safe manner. This includes both the selection of assemblies qualified for ISFSI storage and the verification of assembly identification numbers prior to and after placement into individual MPCs. The spent fuel qualification, identification, and control are discussed in Sections 10.2.1 through 10.2.4 above. Other



administrative programs will control revisions to the Humboldt Bay ISFSI TS Bases, radioactive effluents, MPC loading and unloading processes, ISFSI operations, and transportation route conditions, including control of the 100-meter area. These other programs are defined in the Humboldt Bay ISFSI TS.

### 10.2.10 OPERATING CONTROL AND LIMIT SPECIFICATIONS

The operating controls and limits applicable to the Humboldt Bay ISFSI, as documented in this FSAR, are delineated in the Humboldt Bay ISFSI TS and the TS Bases. These include:

- MPC dryness and backfill pressure
- MPC bulk gas temperature limitation for re-flooding
- Overpack dryness, backfill pressure, and leak rate

### 10.2.11 REFERENCES

Detailed information describing the HI-STAR 100 System is provided in the following reference:

1. 10 CFR 72 Certificate of Compliance No. 1008 for the HI-STAR 100 System Dry Cask Storage System, Holtec International, Amendment 2, May 2001.
2. Final Safety Analysis Report for HI-STAR 100 System, Revision 1, December 2002.
3. Interim Staff Guidance 1, Damaged Fuel, USNRC, Revision 0, May 1999 and Revision 1, October 2002.
4. Interim Staff Guidance 18, The Design/Qualification of Final Closure Welds on Austenitic Stainless Steel Containers as Confinement Boundary for Spent Fuel Storage and Containment Boundary for Spent Fuel Transportation, USNRC, May 2003.

TABLE 10.1-1  
OPERATING CONTROLS AND LIMITS

<b>Areas For Operating Controls and Limits</b>	<b>Conditions Or Other Items To Be Controlled</b>
Fuel characteristics	Physical condition
Multi-Purpose Canister	Exit gas dew point during drying with forced helium dehydration system Vacuum drying pressure MPC gas bulk temperature prior to reflooding Helium backfill pressure
Overpack	Vacuum drying pressure Helium backfill pressure Helium leakage
Administrative Controls	Fuel loading verification including assembly location

TABLE 10.2-1

## MPC-HB FUEL ASSEMBLY LIMITS

## A. Allowable Contents (Notes 1, 2, and 4)

Uranium oxide, INTACT FUEL ASSEMBLIES and DAMAGED FUEL ASSEMBLIES, with or without channels, meeting the criteria specified in Table 10.2-2 and the following specifications.

Cladding type	ZR (Note 3)
Planar-Average Initial enrichment	$\leq 2.60$ and $\geq 2.08$ wt% $^{235}\text{U}$ .
Post-irradiation cooling time per assembly	$\geq 29$ years
Average burnup per assembly	$\leq 23,000$ MWD/MTU
Decay heat per assembly	$\leq 50$ Watts (Note 4)
Decay heat per SFSC	$\leq 2000$ Watts
Fuel assembly length	$\leq 96.91$ inches (nominal design)
Fuel assembly width	$\leq 4.70$ inches (nominal design)
Fuel assembly weight	$\leq 400$ lb (including channel and Damaged Fuel Container)

## B. Quantity per MPC-HB: Up to 80 fuel assemblies.

C. DAMAGED FUEL ASSEMBLIES must be stored in a DAMAGED FUEL CONTAINER. Allowable Loading Configurations: Up to 28 DAMAGED FUEL ASSEMBLIES in DAMAGED FUEL CONTAINERS, can be stored in the peripheral fuel storage locations as shown in Figure 10.2-1, or up to 40 DAMAGED FUEL ASSEMBLIES in DAMAGED FUEL CONTAINERS, can be stored in a checkerboard pattern as shown in Figure 10.2-2. The remaining fuel storage locations may be filled with INTACT FUEL assemblies meeting the above applicable specifications, or INTACT FUEL assemblies optionally stored in DFCs.

NOTE 1: Fuel assemblies with channels may be stored in any fuel cell location.

NOTE 2: The total quantity of damaged fuel permitted in a single DAMAGED FUEL CONTAINER is limited to the equivalent weight and special nuclear material quantity of one intact fuel assembly.

NOTE 3: ZR means any-zirconium-based fuel cladding material authorized for use in a commercial nuclear power plant reactor.

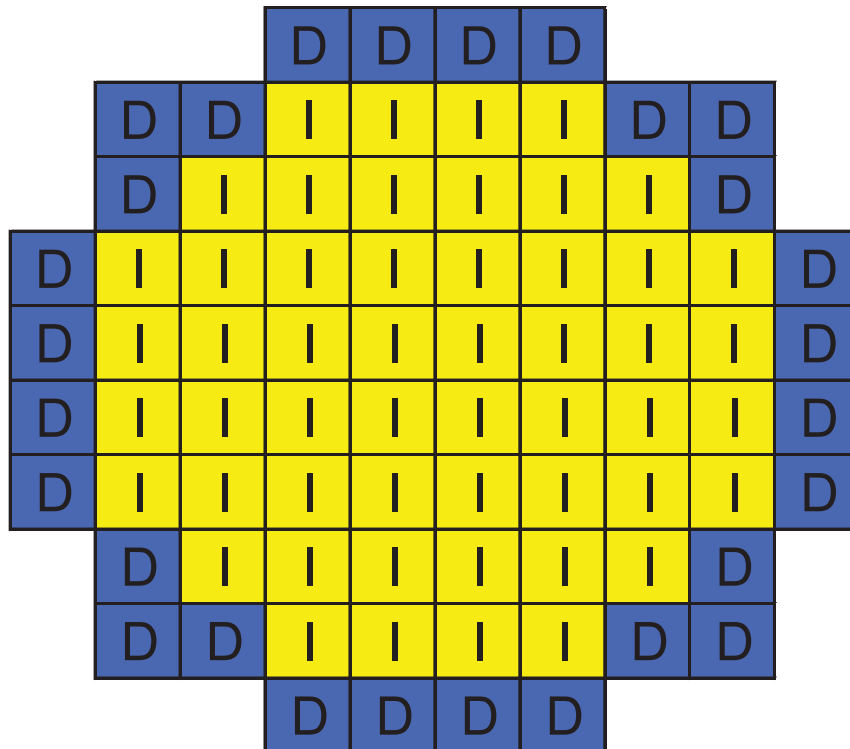
NOTE 4: Storage of DAMAGED FUEL in the form of fuel debris that consists of zirconium clad pellets, stainless steel clad pellets, or unclad pellets up to a maximum of one equivalent fuel assembly is allowed.

TABLE 10.2-2

## FUEL ASSEMBLY CHARACTERISTICS (Note 1)

Fuel Assembly Type	GE Type II	GE Type III, Exxon Type III & IV
Design Initial U (kg/assy.)	$\leq 78$	$\leq 78$
No. of Fuel Rods	49	36
Fuel Rod Cladding O.D. (in.)	$\geq 0.486$	$\geq 0.5585$
Fuel Rod Cladding I.D. (in.)	$\leq 0.426$	$\leq 0.505$
Fuel Pellet Dia. (in.)	$\leq 0.411$	$\leq 0.488$
Fuel Rod Pitch (in.)	$\leq 0.631$	$\leq 0.740$
Active Fuel Length (in.)	$\leq 80$	$\leq 80$
No. of water rods	0	0
Channel Thickness (in)	0.060	0.060

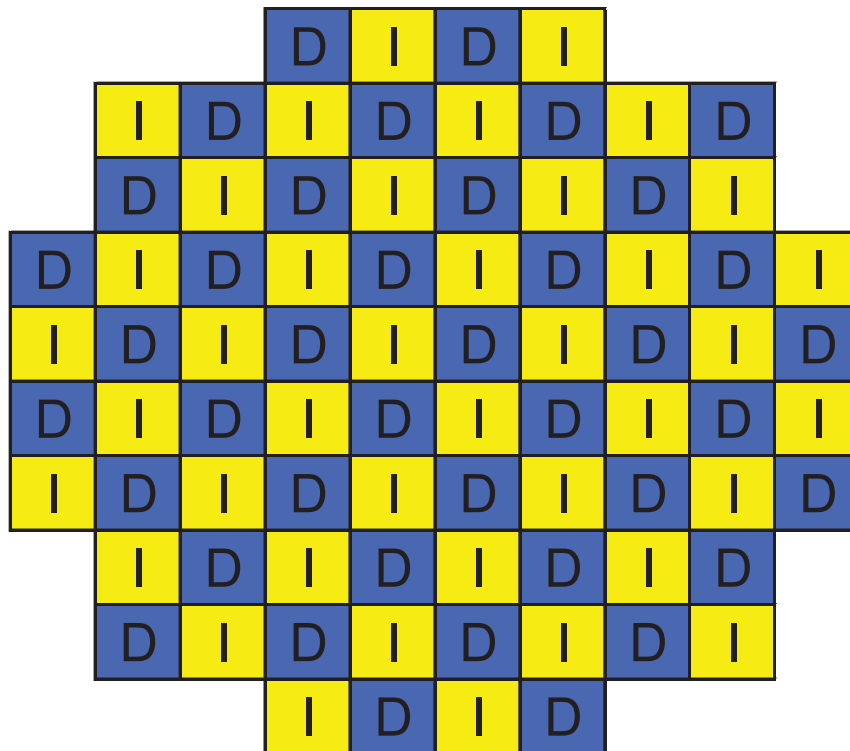
NOTE 1: All dimensions are design nominal values. Maximum and minimum dimensions are specified to bound variations in design nominal values among fuel assemblies.



I	Intact Assembly (with or w/o DFC)
D	Damaged Fuel in DFC

<b>FSAR UPDATE</b>
<b>HUMBOLDT BAY ISFSI</b>
<b>FIGURE 10.2-1 CONFIGURATION 1: DAMAGED FUEL IN PERIPHERAL CELLS OF BASKET</b>

Revision 0 January 2006

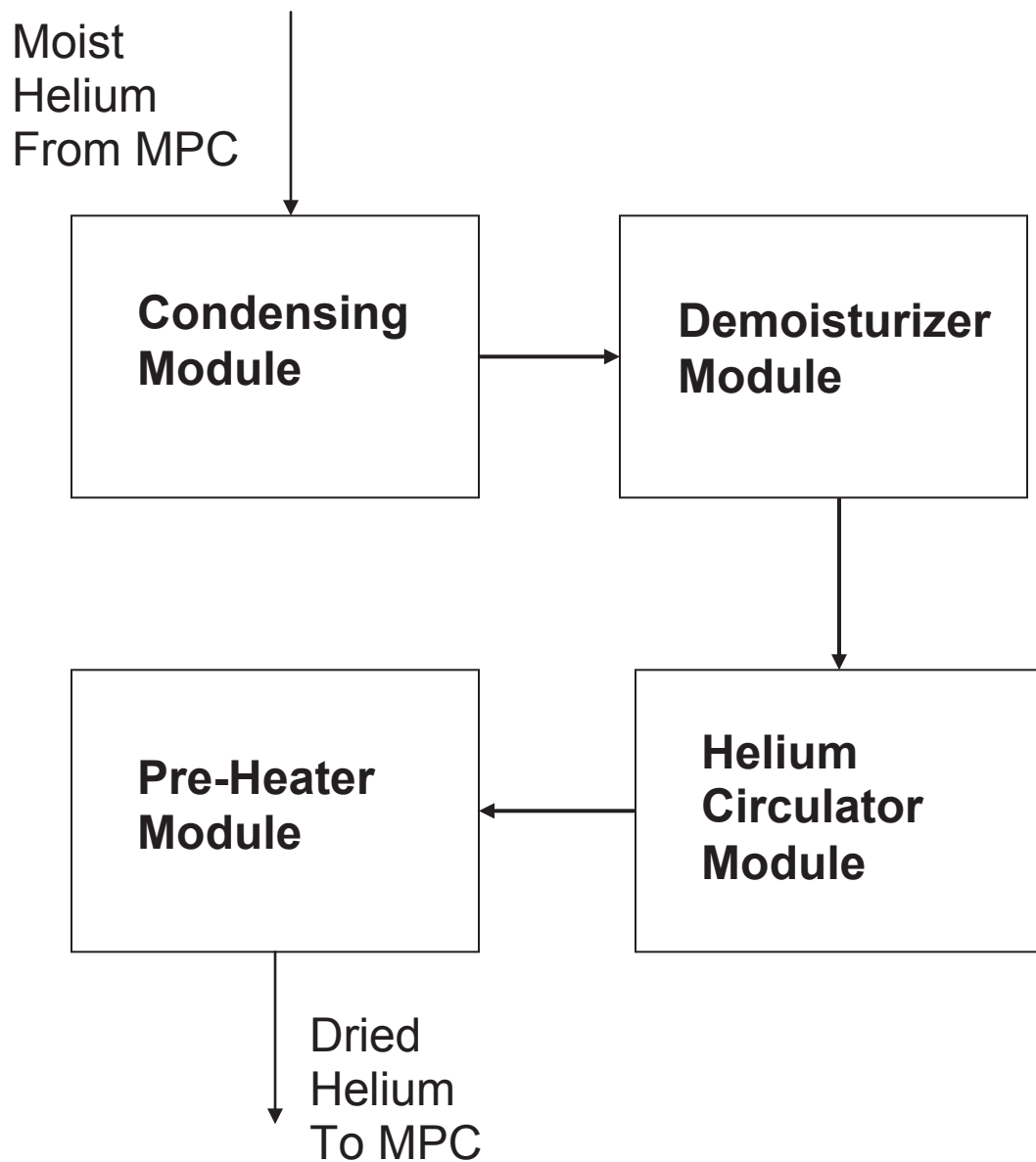


I	Intact Assembly (with or w/o DFC)
D	Damaged Fuel in DFC

FSAR UPDATE
HUMBOLDT BAY ISFSI
<p>FIGURE 10.2-2 CONFIGURATION 2: CHECKERBOARD OF DAMAGED FUEL</p>

Revision 0 January 2006





<b>FSAR UPDATE</b>
<b>HUMBOLDT BAY ISFSI</b>
<b>FIGURE 10.2-3</b> <b>SCHEMATIC DIAGRAM OF THE</b> <b>FORCED HELIUM DEHYDRATION</b> <b>SYSTEM</b>

Revision 0 January 2006

# HUMBOLDT BAY ISFSI FSAR UPDATE

## CHAPTER 11

### **QUALITY ASSURANCE**

#### CONTENTS

<u>Section</u>	<u>Title</u>	<u>Page</u>
11.1	QUALITY ASSURANCE	11.1-1
11.2	REFERENCES	11.2-1

CHAPTER 11

**QUALITY ASSURANCE**

**11.1 QUALITY ASSURANCE**

10 CFR 72.140(b) states that each licensee shall establish, maintain, and execute a quality assurance program (QAP) satisfying each of the applicable criteria of Subpart G. Paragraph (d) of 10 CFR 72.140 states that a Commission-approved quality assurance program that satisfies the applicable criteria of Appendix B of Part 50 and which is established, maintained, and executed with regard to an ISFSI will be accepted as satisfying the requirements of 10 CFR 72.140(b).

Since PG&E is currently licensed under 10 CFR 50 to maintain a nuclear power facility, a Commission-approved QAP meeting the requirements of 10 CFR 50, Appendix B, is already in place. The governing document for this program is the Humboldt Bay (HB) QAP that is included in the Humboldt Bay Power Plant (HBPP) Plant Manual. The QAP requirements for the HB ISFSI, described in the HB QAP, comply with the requirements set forth in the code of federal regulations. The HB QAP (originally called HBPP QAP) was first submitted to the NRC on July 30, 1984 (HBL-84-027) and was approved on April 29, 1987 in an NRC Safety Evaluation Report. Changes to the HB QAP will continue to be made in accordance with 10 CFR 50.54 requirements. The NRC is periodically notified of the changes to the document as required by 10 CFR 50.71.

PG&E will apply this QAP to the design, purchase, fabrication, handling, shipping, storing, cleaning, assembly, inspection, testing, operation, maintenance, repair, modification, and decommissioning of HB ISFSI structures, systems, and components to an extent that is commensurate with the importance to safety. Section 4.5 identifies systems and components that are important to safety. The program also applies to managerial and administrative controls used to ensure safe HB ISFSI operation.

QAP implementation is accomplished through separately issued procedures, instructions, and drawings. The objective of the QAP for the HB ISFSI is to comply with the criteria established in 10 CFR 50, Appendix B, as amended, and with applicable QAP requirements for nuclear power plants as referenced in regulatory guides and ANSI standards. The applicable guides and standards are identified in the HB QAP.

Procurement documents are reviewed prior to approval to ensure that the proper criteria have been specified. During the HB ISFSI design phase, vendor information (drawings, specifications, procedures, etc.) is reviewed to ensure compliance with HB ISFSI technical and quality requirements. During design, licensing, and fabrication of the cask storage system, PG&E's vendor surveillance representative will visit the suppliers' and fabricators' facilities to ensure compliance with PG&E's requirements.

Vendors and contractors that provide important-to-safety items and services will work to a PG&E-approved QAP that meets the requirements of 10 CFR 72.140.

## **11.2 REFERENCES**

None